

post-carbon

Proceedings of the 27th International Conference on Computer-Aided
Architectural Design Research in Asia (CAADRIA 2022)

Volume 2

Edited by

Jeroen van Ameijde

The Chinese University of Hong Kong

Nicole Gardner

University of New South Wales

Kyung Hoon Hyun

Hanyang University

Dan Luo

University of Queensland

Urvi Sheth

CEPT University

Post-Carbon

27th International Conference on Computer-Aided Architectural Design
Research in Asia (CAADRIA 2022)

9-15 April 2022

Hosted By:

University of New South Wales
The University of Sydney
University of Technology Sydney

©2022 *All rights reserved and published by*

The Association for Computer-Aided Architectural Design Research in Asia
(CAADRIA), Hong Kong

ISBN: 978-988-78917-8-9

ISSN: 2710-4257 (print)

2710-4265 (online)

Printed in Sydney, Australia

TABLE OF CONTENTS

Robotics & Digital Fabrication in Construction	9
Rapid Assembly of Masonry Structures with Ad-Hoc Material Attributes, Computer Vision and SCARA Robots. <i>Adam Fingrut, Carson Ka Shut Leung</i>	11
Hybrid Digital Crafts With Collaborative Robotics <i>Alan Burden, Jared Donovan, Glenda Caldwell, Müge Belek Fialho Teixeira</i>	21
Development of an Affordable On-Site Wood Craft System: Interactive Fabrication via Digital Tools <i>Arastoo Khajehee, Taisei Yabe, Xuanyu Lu, Jia Liu, Yasushi Ikeda</i>	31
In-Situ Robotic Fabrication of Spatial Glulam Structures <i>Hua Chai, Zhixian Guo, Hans Jakob Wagner, Tim Stark, Achim Menges, Philip F. Yuan</i>	41
(e)mulate AEC: A Gestural Pedagogy and Cloud-based Collaborative Management Paradigm for On-site Robotics in Construction <i>Vishal Vaidhyanathan, Twisha Raja</i>	51
Robotic 3D Printing of Mineral Foam for a Lightweight Composite Concrete Slab <i>Patrick Bedarf, Anna Szabo, Michele Zanini, Alex Heusi, Benjamin Dillenburger</i>	61
Digital Design and Fabrication of a 3D Concrete Printed Funicular Spatial Structure <i>Hao Wu, Ziyang Li, Xinjie Zhou, Xinyu Wu, Dingwen Bao, Philip F. Yuan</i>	71
Additive Formwork in Precast Construction - Agent-based Methods for Fabrication-aware Modularization of Concrete Building Elements <i>David Stieler, Tobias Schwinn, Achim Menges</i>	81
Robotic Fabrication of Topology Optimized Concrete Components With Reusable Formwork <i>Yiyao Guo, Yang Luo, Sihan Wang, Ying Yi Tan, Kenneth Tracy</i>	91
Topology Optimization for 3D-Printable Large-Scale Metallic Hollow Structures With Self-Supporting <i>Qiang Cui, Huikai Zhang, Siddharth Suhas Pawar, Chuan Yu, Xiqiao Feng, Song Qiu</i>	101
Robotic Assembly of Modular Multi-Storey Timber-Only Frame Structures Using Traditional Wood Joinery <i>Matthias Helmreich, Hannes Mayer, Matteo Pacher, Tadahiro Nakajima, Mitsuhiro Kuroki, Shinya Tsubata, Fabio Gramazio, Matthias Kohler</i>	111

Timber De-Standardized 2.0 : Mixed Reality Visualizations and User Interface for Processing Irregular Timber <i>Leslie Lok, Jiyeon Bae</i>	121
Smart Hand for Digital Twin Timber Work -The interactive procedural scanning by industrial arm robot <i>Chika Sukegawa, Arastoo Khajehee, Takuma Kawakami, Syunsuke Someya, Yuji Hirano, Masako Shibuya, Koki Ito, Yoshiaki Watanabe, Qiang Wang, Tooru Inaba, Alric Lee, Kensuke Hotta, Mikita Miyaguchi, Yasushi Ikeda</i>	131
Vizor, Facilitating Cyber-physical Workflows in Prefabrication through Augmented Reality <i>Xiliu Yang, Felix Amtsberg, Lior Skoury, Hans Jakob Wagner, Achim Menges</i>	141
A Collaborative Workflow to Automate the Design, Analysis, and Construction of Integrally-Attached Timber Plate Structures <i>Nicolas Rogeau, Aryan Rezaei Rad, Petras Vestartas, Pierre Latteur, Yves Weinand</i>	151
Adaptive Robotic Fiber Winding System for Multiple Types of Optimized Structural Components <i>Zhuoyang Xin, Guanqi Zhu, Eryu Ni, Chongyi Tang, Dan Luo</i>	161
Forming Strategies for Robotic Incremental Sheet Forming <i>Qiang Cui, Siddharth Suhas Pawar, Mengxi He, Chuan Yu</i>	171
Augmented Active-Bending Formwork for Concrete, A Manufacturing Technique for Accessible Local Construction of Structural Systems <i>Alvaro Lopez Rodriguez, Pablo Isaac Jaramillo Pazmino, Igor Pantic</i>	181
Augmented Reality for Construction From Steam-Bent Timber <i>Gwyllim Jahn, Cameron Newnham, Nick van den Berg</i>	191
Training a Vision-Based Autonomous Robot From Material Bending Analysis to Deformation Variables Predictions With an XR Approach <i>Chi-Fu Hsiao, Ching-Han Lee, Chun-Yen Chen, Yu-Cyuan Fang, Teng-Wen Chang</i>	201
Innovative Material Systems and 3D Printing	211
Robotic Fabrication Process of Glued Laminated Bamboo for Material Efficient Construction <i>Chung-Chieh Cheng, Yu-Ting Sheng, Shih-Yuan Wang</i>	213
Digital Construction of Bamboo Architecture Based on Multi-Technology Cooperation: Constructing a New Parameterized Digital Construction Workflow of Bamboo Architecture From Traditional Bamboo Construction Technology <i>Ke Nan Sun, Tian Tian Lo, Xiangmin Guo, Jinxuan Wu</i>	223

Softness and Hardness: What Does Concrete Want? Concrete Physical Form Finding Based on Computational Combined Formwork <i>Ce Li, Zhe Guo, Chengzhi Cai, Junyi Miao, Xiaoyu Cao, Cong Li, Yefei Guo, Qingning Cao, Zifei Zheng, Yuchen Guo, Wanling Wu, Zhiyan Xu, Xinyan Zhou</i>	233
S.n.o.w_Sintering TPU via Nichrome Wire <i>Tsung-Han Tsai, Ting-Chia Chen, Ching-Wen Huang, Yen-Cheng Lu, Shih-Yuan Wang</i>	243
Autonomous Transhumance <i>Tushar Mondal</i>	253
Sustainable Rapid Prototyping with Fungus-Like Adhesive Materials <i>Stylianios Dritsas, Jian Li Hoo, Javier Fernandez</i>	263
Extrusion-Based 3d Printing for Recyclable Gypsum <i>Lei Gong, Yifan Zhou, Lang Zheng, Philip F. Yuan</i>	273
Droop – An Iterative Design Tool for Material Draping <i>Gabriella Perry, Jose Luis García del Castillo y López</i>	283
Bio-Synthetic Assemblages: Computational Assembly of Synthetic Bio-Sand Units Made From Dune Sand <i>Marcus Farr</i>	293
Robotically Printed Seaweed as a Biomaterial within Architecture and Design <i>Ilaena Mariam Napier</i>	303
Computational Design Education, Theory and Methodology	313
Exploring the Effect of Immersive VR on Student-Tutor Communication in Architecture Design Crits <i>Hadas Sopher, Julie Milovanovic, John S. Gero</i>	315
Cockroach: an Open-source Tool for Point Cloud Processing in CAD <i>Andrea Settini, Petras Vestartas, Julien Gamberro, Yves Weinand</i>	325
Towards AI-Assisted Design Workflows for an Expanded Design Space <i>Shermeen Yousif, Emmanouil Vermisso</i>	335
Learning Timber Tectonics through Digital Collaboration <i>Nancy Cheng, Mariapaola Riggio</i>	345
Learning from Logs: Introductory Analog and Digital Pedagogy Addressing Material Irregularity <i>Kyle Schumann</i>	355
Optimization of Partition Wall Infilled Pattern for Minimizing Carbon Footprint: A Method That Integrates Parametric Design Tool With FEA Analysis Engine <i>Hanmo Wang, Abhimanyu Goel, Alexander Lin</i>	365

Complex Shape Modelling by Tessellation. Advanced Geometry Control for Variably Curved Surfaces <i>Alessandro Zomparelli, Roberto Naboni</i>	375
Robust Attributed Adjacency Graph Extraction Using Floor Plan Images <i>Jielin Chen, Rudi Stouffs</i>	385
A Remote Sharing Method of 3D Physical Objects Using Instance-Segmented Real-Time 3D Point Cloud for Design Meeting <i>Ryo Onishi, Tomohiro Fukuda, Nobuyoshi Yabuki</i>	395
On-site Holographic Building Construction: A Case Study of Aurora <i>Sijie Liu, Ziru Wei, Sining Wang</i>	405
Architecture Value Change in Response to the Anthropocene: The Contribution of Digital Innovation <i>Dermott McMeel, Emina K. Petrovic</i>	415
The Spatial Environment Affects Human Emotion Perception-Using Physiological Signal Modes <i>Xinyue Ding, Xiangmin Guo, Tian Tian Lo, Ke Wang</i>	425
The What, Why, What-If and How-To for Designing Architecture, Explainability for Auto-Completion of Computer-Aided Architectural Design of Floor Plan Layouting During the Early Design Stages <i>Jessica Bielski, Christoph Langenhan, Christoph Ziegler, Viktor Eisenstadt, Frank Petzold, Andreas Dengel, Klaus-Dieter Althoff</i>	435
Designing a Framework for Metaverse Architecture <i>Sheng Kai Tang, June-Hao Hou</i>	445
Net Zero Game: A Pilot Study of Game Development for Green Building Education in Rural Schools <i>Jong Bum Kim, Danielle Oprean, Laura Cole, Laura Zangori</i>	455
Co-presence in Remote VR Co-design: Using Remote Virtual Collaborative Tool Arkio in Campus Design <i>Shuva Chowdhury, Johan Hanegraaf</i>	465
Exploring Users' Visual Impression of a Japanese Streetscape by Correlating Attention With Speech. Utilizing eye-tracking technology for computer-aided architectural planning <i>Khang Nguyen-Tran, Yuval Kahlon, Takuya Oki, Naya Marsatyasti, Ryo Murata, Haruyuki Fujii</i>	475
PlacemakingAI : Participatory Urban Design with Generative Adversarial Networks <i>Dongyun Kim, George Guida, Jose Luis García del Castillo y López</i>	485
Continuous Adaptability: Web-Based Residential Participatory Design Using Modular Prefabricated Construction <i>Huiyao Hu, Do Phuong Tung Bui, Patrick Janssen</i>	495
Participatory Planning: Heritage Conservation Through Co-design and Co-decision <i>Siew Leng Leong, Patrick Janssen</i>	505

Building Information Modelling	515
DfD-based Design, Assembly, High-Accuracy Real-time Monitoring and Levelling Calibration for Large-scale Prefabricate Structure with Multiple Measuring Systems <i>Xiang Wang, Ziqi Zhou, Xueyuan Lv, Philip F. Yuan, Lei Chen</i>	517
UnityRev - Bridging the gap between BIM Authoring platforms and Game Engines by creating a Real-Time Bi-directional Exchange of BIM data <i>Kieran May, James Walsh, Ross Smith, Ning Gu, Bruce Thomas</i>	527
Building Information Modelling based Transparent Envelope Optimization Considering Environmental Quality, Energy and Cost <i>Dian Zhuang, Xing Shi</i>	537
Interactive Virtual Construction – A Case Study of Building Component Assembly towards the adoption of BIM and VR in Business and Training <i>Hassan Anifowose, Wei Yan, Manish Dixit</i>	547
Revit Add-In for Documenting Design Decisions and Rationale, a Bim-Based Tool to Capture Tacit Design Knowledge and Support Its Reuse <i>Ata Zahedi, Frank Petzold</i>	557
Implementation of Point Cloud and BIM Technologies in a Construction Workflow: A Case Study of a Building Project in Yuecheng District, China <i>Andre Li, Hong Zhang, Weiwen Cui, Jie Huang</i>	567
Enabling Component Reuse from Existing Buildings through Machine Learning, Using Google Street View to Enhance Building Databases <i>Deepika Raghu, Areti Markopoulou, Mathilde Marengo, Jacopo Neri, Angelos Chronis, Catherine De Wolf</i>	577
Data, Stakeholders, and Environmental Assessment: A BIM-Enabled Approach to Designing-out Construction and Demolition Waste <i>Gabriela Dias Guimaraes, Ning Gu, Vanessa Gomes da Silva, Jorge Ochoa Paniagua, Rameez Rameezdeen, Wolfgang Mayer, Ki Kim</i>	587
Development of Technology for Automatic Extraction of Architectural Plan Wall Lines for Concrete Waste Prediction Using Point Cloud <i>Taehoon Kim, Soonmin Hong, David Stephen Panya, Hyeongmo Gu, Hyejin Park, Junghye Won, Seungyeon Choo</i>	597
How a Flooded City Can Be Visualized from Both the Air and the Ground with the City Digital Twin Approach, System Integration of Flood Simulation and Augmented Reality with Drones <i>Naoki Kikuchi, Tomohiro Fukuda, Nobuyoshi Yabuki</i>	607

Environmental Performance Based Design and Sustainability	617
Considering Energy, Materials and Health Factors in Architectural Design, Two Renovation Strategies for the Portuguese Building Stock <i>Adrian Krezlik</i>	619
Sensitivity and Uncertainty Analysis of Combined Building Energy Simulation and Life Cycle Assessment, Implications for the Early Urban Design Process <i>Roland Reitberger, Farzan Banihashemi, Werner Lang</i>	629
How to Prevent a Passive House from Overheating: An Industry Case Study Using Parametric Design to Propose Compliance Strategies <i>Max Marschall, Pablo Sepulveda</i>	639
Computational Design with Myco-Materials <i>Phillip Gough, Anastasia Globa, Dagmar Reinhardt</i>	649
Modular Formwork Techniques for Funicular Slabs <i>Mayank Singh</i>	659
Compiling Open Datasets to Improve Urban Building Energy Models with Occupancy and Layout Data <i>Ayca Duran, Orcun Koral Iseri, Cagla Meral Akgul, Sinan Kalkan, Ipek Gursel Dino</i>	669
Investigating Urban Heat Island and Vegetation Effects Under the Influence of Climate Change in Early Design Stages <i>Farzan Banihashemi, Roland Reitberger, Werner Lang</i>	679
AD-Based Surrogate Models for Simulation and Optimization of Large Urban Areas <i>Goncalo Araujo, Luis Santos, António Leitão, Ricardo Gomes</i>	689
Climate-Driven Architectural Design Optimization and Exploration, A Reverse Passive Building Design Approach <i>Tong Shao, Likai Wang, Guohua Ji</i>	699
Tactile Oceans - Enabling Inclusive Access to Ocean Pools for Blind and Low Vision Communities <i>Dagmar Reinhardt, Leona Holloway, Sue Silveira, Nicole Larkin</i>	709
Quantification of the Thermal Environmental Value of Urban Pores: A Case Study of Nanjing <i>Zihao Wu, Yunsong Zhang, Ziyu Tong</i>	719
Outdoor Thermal Environment Assessment of Existing Residential Areas Supported by UAV Thermal Infrared and 3D Reconstruction Technology <i>Yongjie Pan, Tong Zhang</i>	729
Designing Out Heat – Developing a Computer-Aided Street Layout Tool to Address Urban Heat in Existing Streets and Suburbs <i>Daniel Yu, Matthias Irger, Alex Tohidi, Matthias Hank Haeusler</i>	739

- Building Resilience - Using Parametric Modelling and Game Engines to Simulate the Impacts of Secondary Structures in Bushfire Events 749
Anastasia Globa, Dagmar Reinhardt, Adrienne Keane, Peter Davies
- Decentralised Solar Economy: Unattended and Smart Solar Energy Urban System (UnSSEUS) 759
Provides Ng, David Doria, Baha Odaibat, Alberto Fernandez, Nikoletta Karastathi

Robotics & Digital Fabrication in Construction

RAPID ASSEMBLY OF MASONRY STRUCTURES WITH AD-HOC MATERIAL ATTRIBUTES, COMPUTER VISION, AND ROBOTS

ADAM FINGRUT¹ and CARSON KA SHUT LEUNG²

^{1,2}*The Chinese University of Hong Kong.*

¹*adam.fingrut@cuhk.edu.hk, 0000-0002-8898-8863*

²*kashutleung@cuhk.edu.hk, 0000-0003-2936-0344*

Abstract. This paper discusses the design and development of scale masonry structures using robot arms, computer vision hardware and bespoke computational workflows. In parallel to the development of full-scale masonry solutions using a Cable Driven Parallel Robot (CDPR), a faster method for testing large numbers of brick elements is needed to verify buildability, mitigate collisions, and think differently about recycled materials during real-world construction activities. Additionally, by incorporating scanning and analysis technology, materials can be digitized, and their attributes translated into variables for placement within an intended structure.

Keywords. Automation in Construction; Masonry; Computational Design; Discrete Element Assemblies; Reuse; SDG 9; SDG 12.

1. Introduction

The automated assembly of masonry structures is becoming an increasingly popular area of research in the fields of computational design, structural, and mechanical automation engineering. From Gramazio and Kohler Research's project Flight Assembled Architecture to Mamou Mani's POLIBOT, teams have been developing and deploying systems using cable robotics, drone technology, and stationary arms for this purpose as a means toward further exploring the potential of automation in construction with dexterous work fundamentally calibrated to human scale and traditional craftsmanship. Robotic arms and computer vision is commonplace within industrial automation and are ideal for “pick and place” operations. They are also ideal for emulating brick laying activities due to their two-link arm layout which is similar human ergonomics.

UN Sustainable Development Goal 12 declares the need to substantially reduce waste generation through prevention, reduction, recycling, and reuse. There is great need for the construction industry to consider its relationship to waste, material use, and the carbon footprint associated with creating new materials rather than upcycling. Bricks and masonry are robust materials that offer an opportunity for reuse in new building assemblies. One consideration when recycling any material is the energy

required to sort and/or clean into a usable state. This paper considers new methods for reducing some of those processes by considering the possibilities of unsorted masonry, of various dimensions and attributes, for further integration into construction assemblies.

2. Research Question and Objective

This research asks the following questions: 1) What is the potential for automation systems typically found in the manufacturing industry to be transposed to building construction? 2) Can irregular block materials be integrated into an automated structure assembly without pre-sorting? 3) Can this setup be linked with standard architectural tools using computational design, computer vision and collaborative robotics?

To answer to these questions, the following activities needed to occur: 1) Develop and configure communications between a computer model, robotics, and computer vision systems for accurate scanning, design integration and execution of pick and place operations; 2) Populate the system with materials containing unpredictable and randomized material dimensions; 3) Test the system and proof of concept using scale equipment for assembly of small structures using above.

3. Background

The above questions follow a series of research projects that examine the integration automation equipment for building construction, and for teaching and learning among higher learning and architecture students. Those projects linked standard “off the shelf” robotic arms with customized GH and PY components that allowed for seamless one-way communication between standard design tools found in architecture, and automation hardware that could carry out instructions – under the assumption that the scale brick materials were predictable and known ahead of the design. The preliminary design methods are also based upon automation and construction projects using long spanning cable robotics for masonry applications (Fingrut, 2019). This shows the scalability and transferability of the system into live construction contexts.

4. Hardware Overview

4.1. ROBOT ARM AND END EFFECTOR

The experimental setup is developed around the Dobot Magician robot arm. It consists of a base, rear arm, forearm, and end-effector. The 3 degrees of freedom (DoF) robot has three stepper motors to actuate its joints and generates a maximum payload capacity of 500 grams. The end-effector utilizes a servo motor and a pneumatic pump to operate with its payload. The maximum distance that can be reached by the equipment is 320 mm with 180° rotational capability. It is attached to a sliding rail that has an effective travel distance of 1000mm, allowing the robot arm to operate long distance pick and place tasks with a total volumetric working area of 320mm X 320mm X 1110mm. The setup up is mounted onto a custom platform to explicitly define the build area and to optimize travel distances of the setup. An identical 3D model (digital twin) of the custom build platform and all associated robotic hardware aids in the planning of design output and allows for the translatability of physical and digital data.

4.2. CONVEYOR BELT AND SCANNING HARDWARE

The system works in conjunction with an image processing system that extracts the characteristics of brick elements by calibrating the range of hue, saturation, value, and pixel area of the imageries obtained from the computer vision kit. The image processing system includes a HIKROBOT (MVL-HF1228M-6MP) 1/1.8" 12mm F2.8 manual iris C-mount lens mounted to a HIKROBOT (MV-CE050-30UC) 5 mega pixel colour camera, 2.2 micrometre narrow field of view, 1/2.5" CMOS, Rolling Shutter, 31 fps, and connects to a workstation via a USB 3.0 Output. A white 40000 lux ring shaped auxiliary light source is mounted around the camera to provide consistent ambient lighting condition and intensity. It is important to note that any varying and inconsistent external source of lighting (skylight) or complex multidirectional lighting (interior lighting) will affect the image processing system. Therefore, consistent ambient room conditions were necessary, to avoid recalibration.

The camera points vertically downwards from a camera mounting kit 300-350mm above the target brick picking location and analyses the XY plane image which it transforms pixels into Cartesian coordinates. The system temporarily stores that data for potential collection by a robot, or other system via PY-API. An automated conveyor belt makes it possible to enlarge the pick-up area without requiring the camera to move. This has an added proximity sensor to ensure the visible zone is populated with material, or to advance the belt forward.

4.3. AD HOC DELIVERY OF BRICK MATERIALS

Based upon the system scale, reach, and limited payload, a series of scaled wooden and acrylic bricks measuring roughly 10mm at width were used for the experiment. The

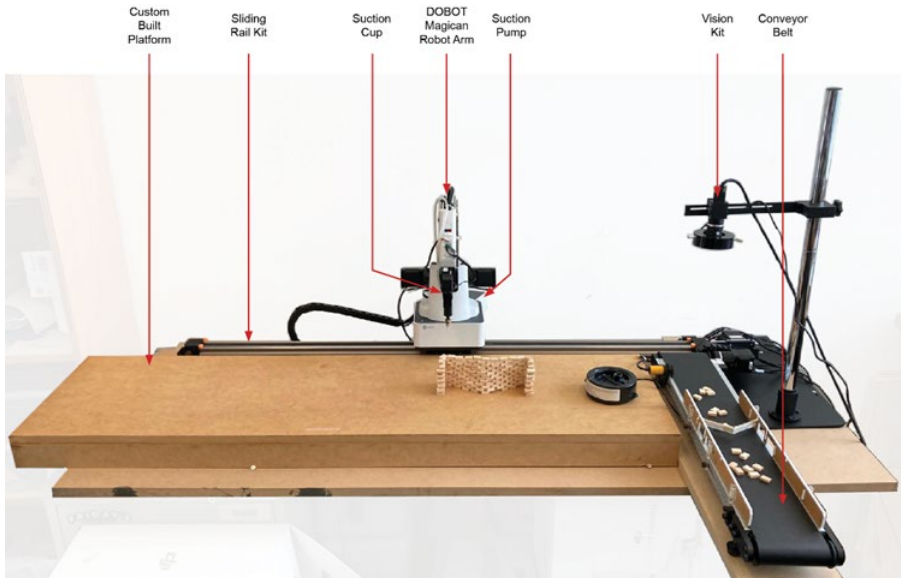


Figure 1. Robot and Computer Vision Setup

length of the bricks ranged from 15mm to 30mm in a randomized manner. The stock material also has a variable wood grain. Materials were randomly placed only the conveyor belt, and guiding rails helped to align or discard any units that may have been placed along the wrong edge. This physical pre-filter helped to maintain clear boundaries between adjacent bricks that may be processed as single units.

5. Control System Overview

The control system uses Rhinoceros 3D (RH) and Grasshopper (GH) as a central platform for design, communications, and coordination between the scanning and robotic assembly process. This is carried out using custom PY tools that were embedded as GH components and allowed for real-time data feedback loops to automate the design process based on data collected from the computer vision system.

While traditional fabrication process sees design and production as two distinctive tasks which involve design data output from RH and input to the robotic control software, the workflow of this setup conceives the system as one singular workflow. Robotic control functionalities are added to RH via its plugin database and its API. This streamlines the connectivity of different software (such as the computer vision modules) and creates stable, looped communications between hardware and software without crashes or unexpected behaviour.

This is achieved with the computational modelling plugin GH for RH. The node-based editor formulates the main interface, in which data is passed in a unidirectional manner between components from start to endpoint with connecting links. Input data can be defined locally as a constant and can also be imported from the modelling space of RH or from a saved comma separated value (CSV) file. Data is always stored in parameters, which can either be free-floating or attached to a component as input and outputs objects. Within the algorithm, data is free floating as parameters.

5.1. DESIGN MODELLING

A curve that represents the building path of the bricks is modelled within the design software. Curve data is then defined as the input data of the GH/PY definition which automatically populates the curve with brick bounding box dimensions based on attributes extracted from the computer vision system.

The computational definition parses brick attributes, such as length, width, colour, and sorts into list. It then selects the desired brick by comparing the unbuilt length of the curve input to the list of brick. Based on this the model selects the longest possible brick (best/biggest fit) until the remaining built length is shorter than any available bricks returned from the computer vision input. The brick spacing is also specified as a local input within the definition.

Base curve design requires design decision making relying upon external contexts. The rest of the definition is designed in a recursive manner, for which autonomous design decisions are made upon the beginning of the construction process. While the overall massing of the assembly can be predicted, the specific layout of brick units will only be fully visualized and known upon completion of its construction. This feedback loop (Figure 3) within the definition aids in real time construction process by using recursion. The outcomes achieved are the possibility of defining an infinite set of

objects by a finite statement (Wirth, 1985).

Besides the default scripting components native to the GH environment, the GH/PY components allow RhinoScriptSyntax functions to instantiate modelled geometry inside of GH. PY nodes can expand upon the functionality of RH to become a communication device between different tools, hardware, and software programmes working together on a singular task. Custom built PY tools were embedded in the GH definition to create real-time links to the computer vision and the hardware control API. They also store and display project specific information beyond the default data manipulation capability of GH. Two custom PY tools were created for this setup, namely the Vision_PY (passing variables from the computer vision modules to the computational design setup) and Robot_PY (passing instructions from the computational design setup to hardware for assembly).

The function libraries used within the GH/PY environment includes RhinoScriptSyntax that provided functionality relating to geometry modelling, and DobotDIIType that provided robotics control commands and methods. To specify a brick placement coordinates, the robotic arm read a set of (x, y, z) coordinates generated from the GH definition via the Robot_PY which then allowed the robotic arm and vacuum gripper to reach the specified location while observing pre-programmed movement rules.

5.2. COMPUTER VISION

To specify a brick pickup location, the Vision_PY relays data from the computer vision module via a bi-directional Transmission Control Protocol (TCP) Network Socket. The Vision_PY communicates brick width, height, (x, y) coordinates, rotation angle, RGB data to the GH/PY component. This is triggered by an 'image update' controlled from within GH and a trigger component.

The data generation process of the machine vision setup starts with camera calibration, which is carried out within the Dobot Vision Studio environment which uses a node-based interface for custom definitions that operates on and organize feedback on data processing. The first node inputs the camera imagery with exposure calibration and cropping functionality. This step is crucial to the construction accuracy as a calibration computer vision module definition is used to calculate the geometric image transformation. The HIKROBOT (MVL-HF1228M-6MP) lens and HIKROBOT (MV-CE050-30UC) camera is a pre-set in the vision software, compensating through pre-calibration for lens distortion. However, the distance and angle between the camera and the target XY plane is defined in physical setup, therefore, a sequential N- point calibration node is needed to construct a calibration file using the imagery data that passes through the checkerboard pre-sets in the CalibBoard Calib node. This step correlates the real word coordinates of a checkerboard image and the relative pixel coordinates.

The calibration file is then used to undistort the image received from the camera lens. The connected camera image exposure, pixel format is adjusted according to the environmental condition. The image then passes through a colour extraction node, in

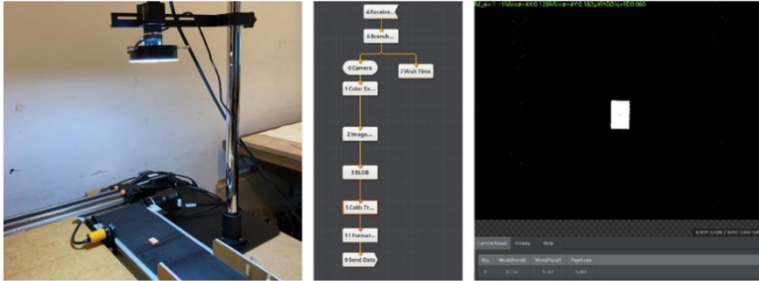


Figure 2. LS: Brick under Computer Vision; M: Computer Vision Definition; RS: Brick parameter detection

which the colour making attribute, (hue, saturation, lightness) HSV parameter is calibrated by of limiting the attribute range to create a figure ground style binary image (Figure 2). The binary image is then morphed to define the perimeter of an object by locating the edges of the outer extremities. The process goes through a dilated convolution which expands the boundary (kernel input) by skipping pixels to cover a larger area of the input. In morphological dilation operations, the state of any given pixel in the output image is determined by applying a rule to the corresponding pixel and its neighbours in the input image (Bishop, 1995).

During system testing, the interaction time is set to 0 to avoid dilation of unwanted white points detected, while the kernel matrix width and height set to facilitate the feature extraction process. Once a boundary line is established, the blob detection node returns the area, perimeter length, centroid XY, rotation angle, rectangularity rate and long, short axis length. The set of data is then filtered according to area range and rectangularity range pre-sets. The resulting verified data is compiled and sent to the custom PY tool in GH.

The setup of this system comprises of four components: 1) assortment of brick units delivered via conveyor belt; 2) computer vision processing material ad attributes; 3) design software that probes for the ‘best fit’ location of that item and communicates those details; 4) automation hardware that carries out instructions set in 3.

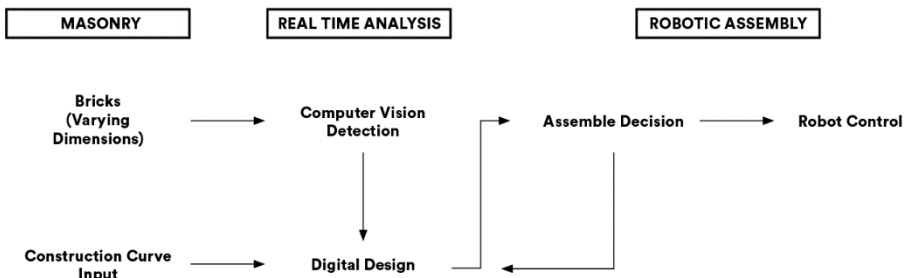


Figure 3. Scan-Analysis-Loop

6. System Testing

From this setup, a series of experiments were conducted to test different methods of optimized pick and place operations for small scale testing and assembly. Three cases were tested to supply sufficient diversity in brick type, guide curve setup, and approach to guide curve population. While the brick input is limited to 5 per input, each case added an additional variable of 5mm linear spacing along the curve variable between elements, to ensure no collisions would occur during assembly. Each type of test was conducted and repeated a minimum of five times with randomized input materials to establish insight into the success, accuracy of the equipment, and predictability of the design weaknesses.

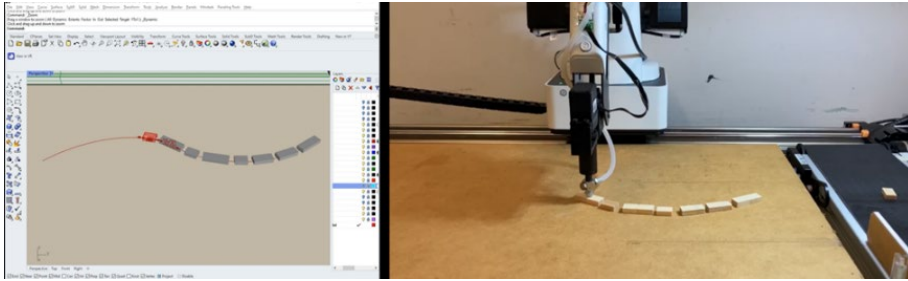


Figure 3. LS: Simulation; RS: Automated Assembly

6.1. LINEAR DEPLOYMENT (LD)

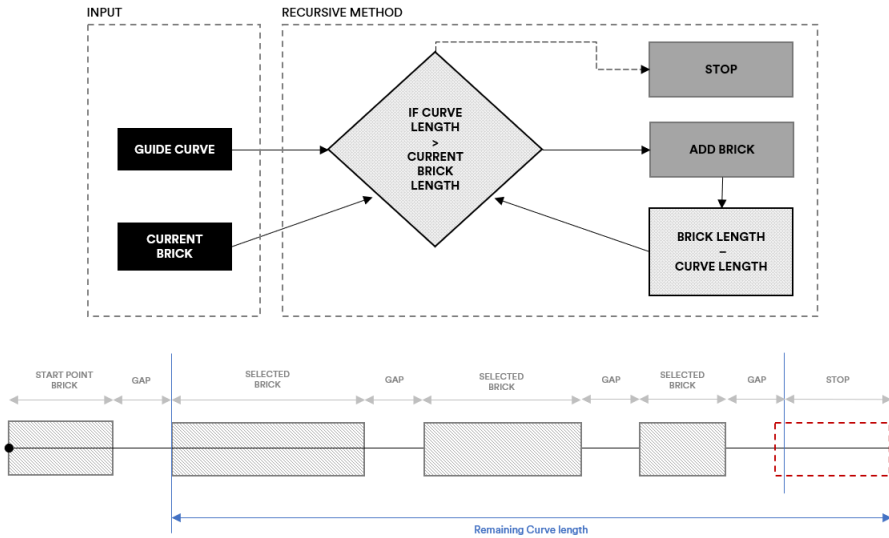


Figure 4. Linear Deployment

In this, the simplest of three tests, ad-hoc brick units were deployed in a linear

fashion from a starting point toward an endpoint of the guide curve (Figure 5). For each iteration of the system loop, a brick that meets sufficient criterion (set as variables) would be added along the curve in both the design model, and simultaneously executed by the robotic hardware. This recursive process was repeated until brick units were too large to fit into the remainder of the guide curve. The advantages of this test were a highly predictable starting point, and regulated placement of units – however an unpredictable end condition that could vary widely depending on the lengths of brick units.

6.2. MIDPOINT-OUT (MO)

MO describes a deployment process whereby the midpoint of the guide curve is established for the first brick unit placement (Figure 6). Once this is in place, the system selects best fit based on the remaining curve length in either direction against the available best-fit scanned materials. This recursive algorithm bifurcates the problem into two separate guide curves, that are then treated similarly to the LD setup. The advantages of this, are the highly predictable midpoint placement, however, end conditions suffer from similar irregularities as the LD, with uncontrollable end conditions.

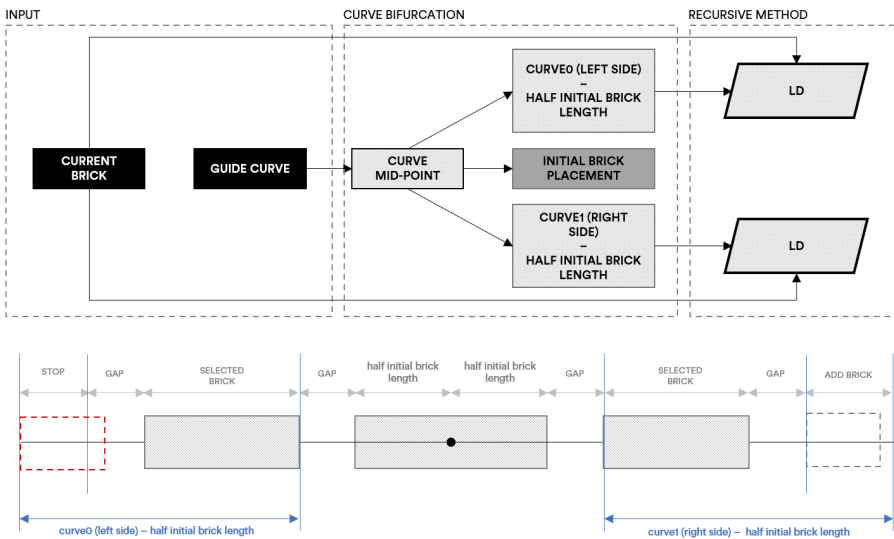


Figure 5. Midpoint-Out ERD

6.3. ENDPOINT-IN (EI)

EI describes a deployment process whereby guide-curve end conditions are established as the first, and second brick units for placement. This is critical as it prioritizes end conditions as being the most accurately placed, and subsequently selects the best fit for the remaining curve length while populating internal spaces (Figure 7). This recursive algorithm continuously evaluates new ‘end conditions’ on smaller sub-curves until no brick unit can be safely fit into the assembly without collision. The advantages of this,

are the highly predictable endpoints, and spacing of units, however, final brick placement suffers from the potential for collisions based on the attributes of brick units in the supply chain.

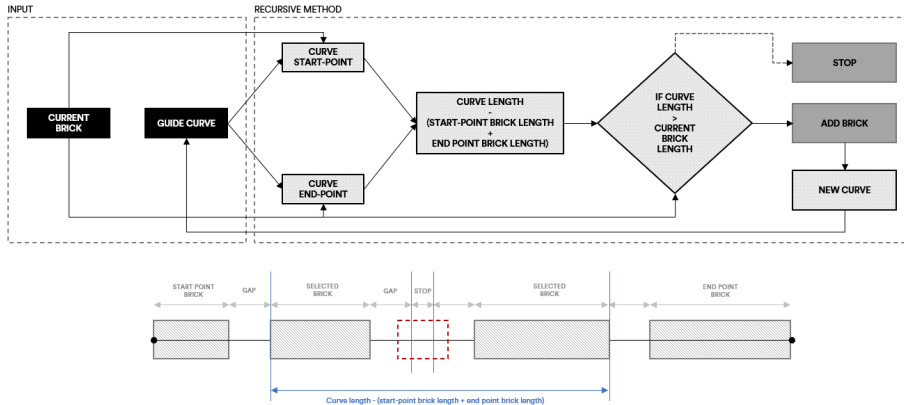


Figure 6. Endpoint-In

7. Findings and Results

The above testing and experiments have shown that there is potential or automation systems to be transposed into building construction, when less “predictable” variables, such as tolerances related to building materials, or recycled and unsorted materials are integrated into assemblies. Although there are many refinements that will need to be incorporated into the setup, the preliminary findings positively conclude that ad-hoc masonry materials can be considered as part of an automated robotic assembly system.

The key aspect of this research project is to determine how computer vision can carefully digitize materials, parse their attributes into usable variables in a 3D design model, and subsequently execute automated assembly based on that model. Discrete assemblies, such as those found in masonry are typically based on regular, sorted patterns. Laborers are often using their experience to modify and fine-tune placement based on minute and large differences in material attributes, site conditions, and design elements. The above preliminary tests have shown that this process can be digitized and automated to some degree (Figure 4).

By linking this setup to standard architectural tools, such as RH, it provides access to a broad range of users without requiring specialist computer programming skills and gives designers the flexibility of designing without having any knowledge of material specifics. This leaves the potential for automated masonry to reconsider a position of pattern design based on material availability, rather than a typical more top-down approach.

8. Future Directions

Further computational dexterity and specificity is needed to advance this line of

research into more deployable construction contexts. Particularly, more complex subroutines that can more flexibly consider local unit rotation as part of a best fit algorithm. The current setup only allows for bricks to be placed in parallel to the curvature normal, however, rotating bricks (under certain conditions) would increase the potential fitness of units based on their width instead of length alone.

The above tests only consider two-dimensional placement sensitivity. Although 3D structures were assembled, they were calculated as discrete layers within a system. Needed is a method to consider the placement of new brick units onto previously placed brick layers, ensuring that each unit is sufficiently placed on a stable foundation via intersecting surface area.

Scanning conducted in this setup is only considered in a 2D setup, and the height of all units is assumed to be the same. In future iterations, scanning should include a Z(height) factor that can increase the complexity of material assemblies. This type of configuration may require a mortar or adhesive layer to assist in the fine differences between material layers and levelling.

With the revisions, the system may be sufficiently prepared to scale up toward more realistic architectural material testing, using a stronger hardware such as a cable robotic system. This would allow for a broadening of the research and system into structural engineering.

References

- Bonwetsch, T. (2012). Robotic Assembly Processes as a Driver in Architectural Design. *Nexus Network Journal*, 14(3), 483-494.
- Dakhli, Z., & Lafhaj, Z. (2017). Robotic mechanical design for brick-laying automation. *Cogent Engineering*, 4(1), DOI: 10.1080/23311916.2017.1361600.
- Fingrut, A., Crolla, K., & Lau, D. (2019). Automation Complexity-Brick By Brick. In *24th International Conference on Computer-Aided Architectural Design Research in Asia: Intelligent and Informed, CAADRIA 2019* (pp. 93-102). The Association for Computer-Aided Architectural Design Research in Asia (CAADRIA).
- Kohler, M., Gramazio, F., & Willmann, J. (2014). *The robotic touch: how robots change architecture*.
- Mora, R., Rivard, H., & Bédard, C. (2006). Computer representation to support conceptual structural design within a building architectural context. *Journal of Computing in Civil Engineering*, 20(2), 76-87.
- Pritschow, G., Dalacker, M., Kurz, J., & Gaenssle, M. (1996). Technological aspects in the development of a mobile bricklaying robot. *Automation in Construction*, 5(1), 3-13.
- Sousa, J. P., Varela, P. A., & Martins, P. F. (2015). Between manual and robotic approaches to brick construction in architecture. In *33rd eCAADe Conference* (pp. 361-370). Education and research in Computer Aided Architectural Design in Europe (eCAADe).
- Wu, Y., Cheng, H. H., Fingrut, A., Crolla, K., Yam, Y., & Lau, D. (2018, May). CU-brick cable-driven robot for automated construction of complex brick structures: From simulation to hardware realisation. In *2018 IEEE International Conference on Simulation, Modeling, and Programming for Autonomous Robots (SIMPAR)* (pp. 166-173). IEEE.

HYBRID DIGITAL CRAFTS WITH COLLABORATIVE ROBOTICS

New Methods in Artisan Patternmaking Using Collaborative Robots and Augmented Reality

ALAN BURDEN¹, JARED DONOVAN², GLENDA CALDWELL³
and MÜGE BELEK FIALHO TEIXEIRA⁴

^{1,2,3,4}*Queensland University of Technology (QUT), Australia.*

¹*alan.burden@qut.edu.au, 0000-0002-1734-1077*

²*j.donovan@qut.edu.au, 0000-0002-8025-1947*

³*g.caldwell@qut.edu.au, 0000-0003-0837-9310*

⁴*muge.teixeira@qut.edu.au, 0000-0003-0593-9597*

Abstract. Bespoke manufacturers that fabricate for architecture and design rely on skill artisans such as patternmakers to remain profitable. Collaborative robotics and augmented reality (AR) offer new technological options and approaches that integrate with existing artisan techniques. Can these technologies provide productive and practical assistance to skilled handcraft artisans? This research presents an original approach to robotic fabrication using AR robot control, and artisan techniques to fabricate an original design. The method includes documenting artisan ethnography, designing a custom cutting end effector and an AR control interface, utilising the capabilities of the robot fabricating system. The research outcome is a hybrid digital craft approach to collaborative robotic patternmaking and handcrafting. The fabrication system reduced the amount of time and physical exertion of designing and cutting out patterns from various materials. This demonstrates that robotic tools can expand rather than replace the capability of existing artisan occupations, helping to strengthen resilience in local industries and promote new innovations.

Keywords. Collaborative Robotic Fabrication; Hybrid Digital Craft; Artisan Manufacturing; Augmented Reality; SDG9.

1. Introduction

Industries that design and manufacture bespoke, one-of-a-kind products must adopt work practices that allow them to be agile and adaptable. Small-scale, bespoke, and artisan-driven modes of production are a feature of many small to medium-sized enterprise (SME) manufacturers, therefore supporting this kind of manufacturing will be vital to achieving the UN's sustainable development goals. SMEs that fabricate bespoke items rely on skilled artisans to remain profitable hence have high costs per

unit, due to the need for specific manufacturing requirements, specialised resources, and skilled labour (Stepputat et al., 2021). The use of robotic fabrication promises to alleviate some of these pressures with a need for approaches that are adaptable for small scale manufacture to retain the skilled input of human artisans. Crucially, robotics should not be seen as a simple technology-fix to replace existing artisan skill but should be approached as means by which human work can be assisted and supported. Compared to large scale industrial robotic arms, emerging collaborative robot platforms are an attractive proposition for bespoke manufacturing because they are typically less expensive, can be adapted to different tasks with the addition of custom end effectors, and are easier to integrate into human workflows. To achieve sustainable industrialization (SDG9), it is imperative that researchers working at the intersection of design, manufacturing, and robotics engage with end-users to understand existing practices and design processes to appropriate to end-user needs for robotic adoption.

In this research, a local art manufacturer, UAP, that produces art and architectural fabrications was analysed for retrofitting technology innovations within an existing workflow of their patternmaking department. The company manufactures custom-designed products and employs many skilled local craftspeople, including patternmakers who primarily produce templates and moulds for a metal foundry. Patternmaking as a profession is changing – with less reliance on trade-based apprenticeship for learning skills and towards an exploratory ‘hands-on’ craft-based practice that includes mixed techniques from sculptors and artisans. A component of the exploratory approach shows that craft-based activities like patternmaking are poised to quickly evolve from predominately analogue workflows into a hybridised digital craft that includes emerging technology (Loh et al., 2016; Xia, 2017).

This paper argues that industries and professions based around creative fabrication methods have the expertise, skills, and agility in practice to customise collaborative robot arms and augmented reality (AR) as assistive tools. Instead of diminishing as an industry, patternmaking – like similar artisan industries – will continuously evolve by including emerging technology into new hybrid and digital crafts (Bernabei & Power, 2018). As these professions evolve, they will create new relationships between humans, technology as a tool, and application upon physical materials (Gramazio et al., 2014; Kolarevic, 2003).

These new factors can aid in supporting the United Nations’ Sustainable Development Goals by developing new digital infrastructure that supports traditional manual activities in design and fabrication. The long-term effects promote and sustain local manufacturing development and help innovation when using new digital tools that can be retrofit into established industries. This paper contributes to the CAADRIA 2022 conference theme of Post Carbon by examining the UN Sustainable Development Goal #9 to build resilient infrastructure, promote inclusive and sustainable industrialization and foster innovation. We present a 4-step framework for conceptualising the design of collaborative robotic fabrication and illustrate this with a novel solution for robotic support of patternmaking practices, thus promoting sustainable industrialisation and resilient infrastructure by retrofitting a local industry.

2. Robotic Fabrication and Augmented Reality in Hybrid Digital Craft

There is a growing body of research into robotic fabrication in craft-related

manufacturing that traditionally uses highly skilled artisans. Past theories proposed that increased industrialisation creates increased automation in design (Kolarevic, 2003; Negroponete, 1995). However, there is evidence that digital fabrication methods can also form new links between robotic tools, craftsmanship, and local building traditions (Shaked et al., 2020). Digital fabrication, when implementing industrial robotics and AR can shift the focus from automation towards opportunities for human and robot interactions in assisting or augmenting daily work tasks such as making manufacturing patterns (Lavallee et al., 2011; Verma & Epps, 2013).

An industrial robot can transfer a digital design into physical material (Gramazio et al., 2014). Furthermore, other capabilities of industrial robots are demonstrated through manipulating rigid materials (Verma & Epps, 2013), precision in robot construction (Bonwetsch, 2012), and data-driven robotic fabrication to produce complex forms (Gandia et al., 2019; Menges & Knippers, 2015).

Studies have also demonstrated the practicality of using AR in design and construction that provides assembly documentation to visualise where to place components (Jahn et al., 2019). Further research has used AR to guide analogue skills such as points for welding and helping assembly of fabrication components (Bottani & Vignali, 2019). Studies have also analysed human skillsets have used motion capture, force sensors, and robotic vision to establish how robots can replicate human actions through force, speed, and motion (Brugnarò & Hanna, 2017; Shaked et al., 2020). However, analysis of traditional craft techniques has often been undertaken for aiding robotic automation, rather than providing insight into how the technology can be used as a part of the crafting process (Brugnarò & Hanna, 2017; Schwarzmans, 2020). In this study, we are using the robot as a tool for digital craft fabrication to replicate a precise transfer of digital patterns into the material at various scales.

3. Research Method

This paper presents a novel method of using a collaborative industrial robot to assist in cutting and perforating materials into 2D patterns. The research study utilises an AR head-mounted device (or headset) as a method of interaction between the digital pattern, the customised robot tool, and the materials used. In the context of patternmaking and robotic fabrication, this paper uses an ethnographically informed case study to investigate suitable craft techniques to augment and design a proof of concept with the capacity to use a robotic tool and an AR headset as part of a workflow to create an original design. This research is presented in four stages: Ethnography & Case Study, Robotic Tool, AR Headset Interaction, Fabricating a Design.

3.1. ETHNOGRAPHY AND CASE STUDY

At its core, a patternmaker's job is to create the original 'patterns' that are used in later fabrication processes such as metal casting of sculptures. However, at UAP the patternmaking department is also involved in final fabrication of elements for sculptural artworks and is involved in researching and developing new fabrication processes. An ethnography was undertaken within the UAP patternmaking department over a period of three months to observe the patternmaker's work and identify potential opportunities for developing robotic fabrication techniques to support them. The

patternmaking technique identified for analysis was used in cutting patterns for a public art installation designed by Richard Sweeney, who is renowned for folded papercraft designs. Sweeney produced a small-scaled maquette of the intended final design in cardstock as seen in Figure 1.



Figure 1. (left) Maquette of folded cardstock, and the final Installation for the artwork 'Cloud' (image credit: Richard D'Souza/UAP).

The challenge for the patternmakers was to recreate the aesthetic of thin, lightweight paper with a robust material suitable for public display. The UAP patternmakers settled on using compressed PVC foam sheets. The cutting technique transferred the flattened forms onto the PVC material. The 2D patterns of Sweeney's maquettes were used as the reference and scaled up to the dimensions of the installation

Patterns were hand cut and scored referenced from design documents. Metal rulers and templates guided craft knives that cut directly into the foamed PVC sheets. The knives also marked dimensions as pen and pencil would smudge. The patternmaker attempted to make curved cuts in one motion, requiring focus and steady application of force to cut accurately into the material. Shortcomings of the technique required the PVC to be debossed or perforated so it would not crack and split when the material was manipulated by hand.

The observations revealed a physically demanding and focussed approach to cutting materials - with the motto of 'measure twice, cut once' applied to precisely measuring and making patterns. Cutting the PVC remained a manual task as digital tools like CNC laser cutters burn the PVC releasing hydrochloric acid and toxic fumes. In contrast, waterjet cutters soften and disintegrate the material and change its composition. The shortcomings of recreating analogue patterns while rescaling included introducing potential inaccuracies and the amount of time, concentration, and physical exertion of cutting rigid materials – particularly with patterns that measured metres in their dimensions.

The ethnographic observations revealed the identified workflow for creating the pattern, that is summarised as creating an analogue 2D pattern from an unfolded 3D pattern, digitising the 2D pattern for documenting and reference, manually rescaling and applying the 2D pattern to the material. Individual elements of the art installation took up to a week to complete – with transferring the pattern, debossing, and creasing

required days per item. Within this workflow, an opportunity was identified from this analysis that robotic fabrication could be applied via an assistive system that a solo person could operate to rescaling and cut patterns into the foamed PVC. The workflow variations are shown in Figure 2.

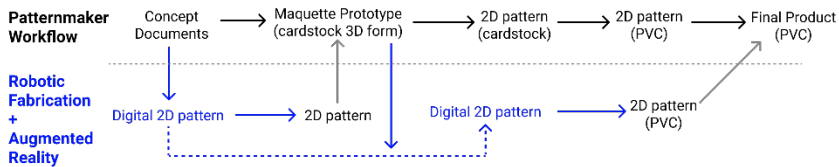


Figure 2. Diagram showing workflow between handcrafted techniques (black) and techniques using robotic fabrication and the AR interface (blue).

3.2. DESIGN TO ROBOTIC FABRICATION WORKFLOW

Based on the ethnographic observations, the research produced a proof-of-concept system of robotic fabrication that would assist patternmakers in cutting and perforating cardstock and compressed foamed PVC. A custom-designed and fabricated end effector tool was made for the robot, a Universal Robots UR10. The tool consisted of a utility knife with replaceable blades and a ‘spiked’ tracing wheel, shown in Figure 3, which is common in clothes patternmaking to transfer patterns to cloth. A modified workbench allowed the patternmaker to position cardstock for the robot and access to the material, also shown in Figure 3.

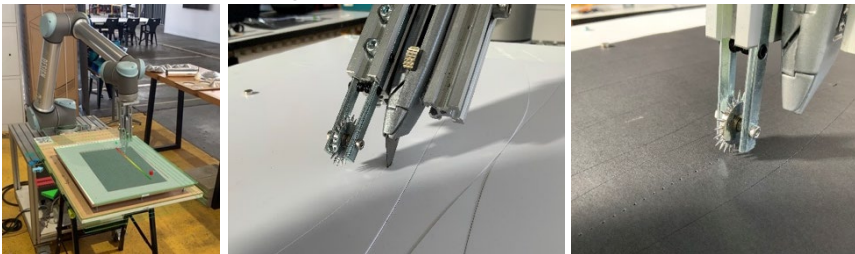


Figure 3. (left) Workbench and UR10 robot set up for fabrication (AR interface visible), (middle) craft knife end effector cutting into foamed PVC, (right) tracing wheel end effector perforating 600gsm cardstock).

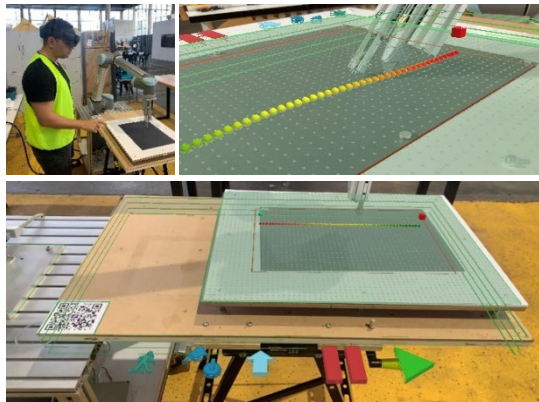
The objective of the custom robot tool was to replicate the cutting technique and introduce a perforation technique that allowed the material to be creased on either side of the sheet material. The robot tool cutter used craft knives with blades that can easily be replaced – like those already used by patternmakers. A tracing wheel was also attached to make perforations on the material, which meant the material could be folded in either direction, unlike debossed folds that favour one direction. The UR10 robot was controlled using Grasshopper components and the Robots plugin. The patternmaker’s approach was followed to place and nest the location of the patterns on the material, and experimental prototype forms were made using cardstock (250 and 600gsm) and a compressed PVC sheet (1mm). A user interface for interacting with the

robot was designed using Fologram (Jahn et al., 2019) (see next section). The final set up was arrived at through a process of iterative design where problems with the fabrication technique were progressively uncovered and resolved.

3.3. AR HEADSET INTERACTION

To enhance the patternmaker's perception of visualising, placing, and controlling action pathways for robot action, an AR user interface was implemented using a Microsoft HoloLens2 headset or an Apple iPad tablet. The patternmaker could use these devices to visualise and interact with the projected pathways via the AR user interface buttons displayed next to the workbench and within the work environment. In this context, AR provides a bridge for supplementing digital craft skills by allowing the patternmaker to visualise, plan and control the cutting and perforating toolpaths close to the material.

The development of an AR interface aimed to encourage easy adoption of robot fabrication techniques for patternmakers or craftspeople to make 2D patterns. The AR interface minimised the need for the patternmaker to access the Grasshopper application to control the pattern or robot and allowed direct human contact to the work area and material being cut and perforated. Figure 4 shows the frequently used robot tool commands implemented in making the patterns were designed to be accessible via the HoloLens2 AR headset, or Apple iPad. The advantage of the headset device freed both human hands to interact with material or environment. Rhinoceros 3D and Grasshopper used the Fologram plugin to create the user interface and display the AR



visualisations as presented in Figure 4.

Fabricating Figure 4. (top left) Setup configured to use the HoloLens2 with the UR10 robot, (top right) AR display of the toolpath projected over the cutting surface. (bottom) Interface buttons to command the UR10 located along the edge of the workbench, from left to right: (a) switch toolpath direction, (b) swap tools, (c) cycle to next toolpath, (d) pause, and (e) start task.

Commands necessary for controlling the robot tool were designed as buttons located parallel to the edge of the workbench. The AR button locations was customised to suit the patternmaker's approach. The button commands included: changing the toolpath, flipping toolpath direction, switching between cut or perforate tools, starting,

and pausing the robot action. The AR interface used a QR code marker to calibrate and anchor the projected visuals to the environment and toolpath to the cutting bed of the workbench and aid the patternmaker in aligning the robot, workbench, and the material. A physical safety 'e-stop' button was kept close to user as per safety protocol.

3.4. THE TEST DESIGN

A lampshade was designed and created as an object that would reflect complexity in form and assembly and that would prove difficult to recreate completely by hand. Design sketches created a form reminiscent of a segmented seashell requiring curved adjoining panels. Two shell forms, similar in pattern shape, but with different sizes would require eight panels each to complete the shell forms.

Early prototypes were hand-made with cardstock to develop a method of adjoining panels. Once an approach was established, forms were developed as 3D CAD drawings in Rhinoceros 3D and were then unrolled into 2D patterns. Initially the patterns were made as adjoining panels, but these occasionally produced unwanted and unpredictable creases in the denser materials. Therefore, a decision was made to separate panels, as shown in Figure 5. The edges of the panel pattern took an elliptical form and used perforation toolpaths along one or two edges to allow for guidance in panel curving, and creation of creased tabs for affixing neighbouring panels.

Patterns were input to grasshopper as NURBS for the toolpaths along a 2D plane. Multiple iterations of card maquettes were produced to find a form that combined rigidity and uniformity in curve, along with aesthetics of each panel within the assembled form. The panels were assembled first by hand using 600gsm cardstock maquettes to test the final designed form. The final design was cut, perforated and hand assembled using 1mm foamed PVC sheets within three days, and required minimal finessing or recutting by hand.



Figure 5. (top left) Partially assembled shells for fabricated panels, (bottom left) completed shells joined with Kevlar fibre and tested for maintaining structure, (right) Finished lamp design.

4. Discussion and Conclusion

This paper explored the potential of using robot fabrication and AR in an evolving, niche patternmaking industry for bespoke products. Despite the industry showing capacity for increasing use of digital technology as assistive tools – custom, skilled, physical tasks are still frequently performed by hand. Even though prevalent assumptions that digital fabrication methods will replace human activities such as skilled craftwork, this study presents that there are aspects of handcrafting that can integrate with digital tools. Elements of handcrafting are time-consuming, repetitive, fatiguing, and as shown in patternmaking, require focus and precision for the best production outcomes. Using robot tools can create a disconnect between the crafting person and the material – physical touching of material is diminished as humans are always removed from the active robot for safety reasons. Collaborative robots reduce that barrier by allowing a human closer to the material, and with enough safeguards applied, could allow a human to touch the material while the robot is acting upon it. Providing visual data via AR also reduces the barrier further by trading interaction and robot control from behind a computer screen, towards a level of interaction and communication taking place to the point of action in the work environment.

To produce a tool that allows a sole practicing patternmaker to utilise robotic fabrication, this paper presented a four-step framework which included: (a) an ethnographic case study, to document and specify a patternmaking technique that could be augmented, (b) designing a custom end-effector and cobot workflow to cut and perforate material, (c) a AR user interface to provide visual data and interaction to the patternmaker in their working environment, (d) a workflow that integrates robotic fabrication with handcrafting skills to design and make a customised novel product.

This research highlights the need for ethnographic case study observations when developing robot fabrication systems to assist and augment custom, high-skill industries. The experience gained by patternmakers on the job develops with their exposure to different materials and design outcomes. In parallel to this knowledge are the skills in using different tools and sometimes customising existing equipment or making new tools for specific activities. The shift from manual analogue work to digital techniques poses a query about how humans can maintain a physical link to materials which is a key element of crafting (Pye, 2008; Sennett, 2008).

Allowing the user to closely monitor the robot acting on the material minimised errors, but also initiated explorations for a better flow of work. Alterations to patterns, and predicting material curling helped with the outcome quality of panels and allowed for easier assembly. The patterns could be accurately cut by the UR10 robot and perforations would provide guidelines to aid with handcrafted assembly and finessing. Future research will document other professions, techniques, materials, and other augmented interactions with collaborative robots in 3D environment, not limited to 2D planar actions.

Industries with a foundation in creative and practical skillsets are well positioned to adopt and customise new technologies. The capacity of such innovation displays a positive approach for SMEs that are early adopters of technology and can promote agile and sustainable support to reaching United Nation Sustainable Development Goals. The effects of fostering innovation are not only received locally but interconnected

globally. While full economic impact analysis is beyond the scope of this paper, we know from research regarding the implementation of industrial robots in UAP's manufacturing process led to additional jobs, savings in time and material consumption, and returns based on 'localising' the manufacturing process. Therefore, we believe that the process using cobots for patternmaking would create efficiencies in terms of time savings, economic costs, human health and job satisfaction. More research is required to quantify these figures, examine the financial aspects and human benefits of cobotics in manufacturing.

Acknowledgements

This study was supported by a Department of Industry, Innovation and Science (Innovative Manufacturing CRC Ltd.) UAP Australia Pty Ltd Co-funded project grant "Design Robotics for Mass Customisation Manufacturing" (IMCRC/UAP/25072017).

References

- Bernabei, R., & Power, J. (2018, March 1). Hybrid design: Combining craft and digital practice. https://doi.org/info:doi/10.1386/crr.9.1.119_1
- Brugnaro, G., & Hanna, S. (2017). Adaptive Robotic Training Methods for Subtractive Manufacturing. 6.
- Bottani, E., & Vignali, G. (2019). Augmented reality technology in the manufacturing industry: A review of the last decade. *IISE Transactions*, 51(3), 284–310. <https://doi.org/10/gh64mq>
- Envision2030 *Goal 9: Industry, Innovation and Infrastructure* | United Nations Enable. (2021).
- Flavián, C., Ibáñez-Sánchez, S., & Orús, C. (2019). The impact of virtual, augmented and mixed reality technologies on the customer experience. *Journal of Business Research*, 100, 547–560. <https://doi.org/10.1016/j.jbusres.2018.10.050>
- Gandia, A., Parascho, S., Rust, R., Casas, G., Gramazio, F., & Kohler, M. (2019). Towards Automatic Path Planning for Robotically Assembled Spatial Structures. In J. Willmann, P. Block, M. Hutter, K. Byrne, & T. Schork (Eds.), *Robotic Fabrication in Architecture, Art and Design*, 2018 (pp. 59–73). Springer International Publishing. https://doi.org/10.1007/978-3-319-92294-2_5
- Gramazio, F., Kohler, M., & Willmann, J. (2014). *The robotic touch: How robots change architecture*. Park Books.
- Jahn, G., Newnham, C., Berg, N., & Beanland, M. (2019, January 5). *Making in Mixed Reality*.
- Kaasinen, E., Schmalfuß, F., Öztürk, C., Aromaa, S., Boubekour, M., Heilala, J., Heikkilä, P., Kuula, T., Liinasuo, M., Mach, S., Mehta, R., Petäjä, E., & Walter, T. (2020). Empowering and engaging industrial workers with Operator 4.0 solutions. *Computers & Industrial Engineering*, 139, 105678. <https://doi.org/10.1016/j.cie.2019.01.052>
- Kolarevic, B. (2003). *Architecture in the Digital Age: Design and Manufacturing*. Taylor & Francis.
- Latour, B. (1994). *On technical mediation*. *Common Knowledge*, 3(2).
- Lavallee, J., Vroman, R., & Keshet, Y. (2011). Automated Folding of Sheet Metal Components with a Six-axis Industrial Robot. *ACADIA 11: Integration through Computation Proceedings of the 31st Annual Conference of the Association for Computer Aided Design in Architecture*. Banff, 13-16 October, 2011, pp. 144-151.

- Loh, P., Burry, J., & Wagenfeld, M. (2016). Reconsidering Pye's theory of making through digital craft practice: A theoretical framework towards continuous designing. *Craft Research*, 7(2), 187–206. https://doi.org/10.1386/crre.7.2.187_1
- Longo, F., Nicoletti, L., & Padovano, A. (2017). Smart operators in industry 4.0: A human-centered approach to enhance operators' capabilities and competencies within the new smart factory context. *Computers & Industrial Engineering*, 113, 144–159. <https://doi.org/10.1016/j.cie.2017.09.016>
- Menges, A., & Knippers, J. (2015). Fibrous Tectonics: Fibrous Tectonics. *Architectural Design*, 85(5), 40–47. <https://doi.org/10.1002/ad.1952>
- Michaelis, J. E., Siebert-Evenstone, A., Shaffer, D. W., & Mutlu, B. (2020). Collaborative or Simply Uncaged? *Understanding Human-Cobot Interactions in Automation. Proceedings of the 2020 CHI Conference on Human Factors in Computing Systems*, 1–12. <https://doi.org/10.1145/3313831.3376547>
- Negroponte, N. (1995). *Being Digital*. Knopf.
- Romero, D., Bernus, P., Noran, O., Stahre, J., & Fast-Berglund, Å. (2016). The Operator 4.0: Human Cyber-Physical Systems & Adaptive Automation Towards Human-Automation Symbiosis Work Systems. In I. Nääs, O. Vendrametto, J. Mendes Reis, R. F. Gonçalves, M. T. Silva, G. von Cieminski, & D. Kiritsis (Eds.), *Advances in Production Management Systems. Initiatives for a Sustainable World* (pp. 677–686). Springer International Publishing. https://doi.org/10.1007/978-3-319-51133-7_80
- Schwarzmann, W. (2020). Traditional Knowledge on Modern Milling Robots—How CNC-joinery machines promote a renaissance to lost techniques in the profession of a carpenter. Werner, L and Koering, D (Eds.), *Anthropologic: Architecture and Fabrication in the Cognitive Age - Proceedings of the 38th ECAADe Conference - Volume 2*, TU Berlin, Berlin, Germany, 16-18 September 2020, Pp. 597-604.
- Shaked, T., Bar-Sinai, K. L., & Sprecher, A. (2020). Autonomous in Craft—Embedding Human Sensibility in Architectural Robotic Fabrication. D. Holzer, W. Nakapan, A. Globa, I. Koh (Eds.), *RE: Anthropocene, Design in the Age of Humans - Proceedings of the 25th CAADRIA Conference - Volume 2*, Chulalongkorn University, Bangkok, Thailand, 5-6 August 2020, Pp. 243-252.
- Stepputat, M., Beuss, F., Pfletscher, U., Sender, J., & Fluegge, W. (2021). Automated one-off production in woodworking by Part-to-Tool. *Procedia CIRP*, 104, 307–312. <https://doi.org/10.1016/j.procir.2021.11.052>
- Verma, S., & Epps, G. (2013). Curved Folding: Design to Fabrication. *ACADIA 13: Adaptive Architecture [Proceedings of the 33rd Annual Conference of the Association for Computer Aided Design in Architecture]*. Cambridge 24-26 October, 2013), Pp. 453-454.
- Xia, T. (2017). Form-finding with Robotics—Fusing Physical Simulation and Digital Fabrication. P. Janssen, P. Loh, A. Raonic, M. A. Schnabel (Eds.), *Protocols, Flows, and Glitches - Proceedings of the 22nd CAADRIA Conference*, Xi'an Jiaotong-Liverpool University, Suzhou, China, 5-8 April 2017, Pp. 893-902.

DEVELOPMENT OF AN AFFORDABLE ON-SITE WOOD CRAFT SYSTEM: INTERACTIVE FABRICATION VIA DIGITAL TOOLS

ARASTOO KHAJEHEE¹, TAISEI YABE², XUANYU LU³, JIA LIU⁴
and YASUSHI IKEDA⁵

^{1,2,3,4,5}*Keio University, Japan.*

¹*arastookhajehee@keio.jp, 0000-0001-5381-7784*

²*tai@sfc.keio.ac.jp, 0000-0002-3166-3232*

³*luxuanyu@keio.jp, 0000-0001-6826-8642*

⁴*liujia66@sfc.keio.ac.jp, 0000-0002-0895-1711*

⁵*yasushi@sfc.keio.ac.jp, 0000-0002-2016-4083*

Abstract. This research aims to develop a craft system that simplifies the transition between design and fabrication. One of the main purposes of this system is to allow non-professionals to engage in craft with the aid of affordable digital fabrication tools. By removing the technical hurdles that prevent beginners from engaging in digital fabrication, the system aims to enable those who are interested in making things as a hobby or DIY projects to enjoy digital craft. The developed craft system provides a comprehensive workflow, starting from the initial shape to the final CNC milling machine G-Code generation. It is developed through Object-Oriented Programming, resulting in an interactive system that provides information about the fabricability of the final shelf structure to user/designer. The real-time design-to-fabrication aspect allows for some degree of simultaneous design changes, making the craft experience more enjoyable. In line with the UN Sustainable Development Goals, this research is an attempt to provide more opportunities for individuals to get into digital fabrication, enabling them to acquire skills within the rapidly growing industry. Furthermore, as demonstrated by other digital fabrication tools like 3D printers, DIY builds can potentially be economically beneficial for the users.

Keywords. Digital Fabrication; Real-Time Design to Fabrication; Affordable On-Site Craft; SDG 8; SDG 9.

1. Introduction

Authors Over the past 2 to 3 decades researchers and designers have been exploring how to build increasingly complex shapes and forms. The Buga Wood Pavilion and the Landesgartenschau Exhibition Hall, designed by the team of Oliver David Krieg and Achim Menges at Stuttgart university, are great example that demonstrates how robotic fabrication tools can build incredibly intricate structures with amazing accuracy (Alvarez et al., 2019; Menges et al., 2015). Similar to Gilles Retsin's timber installation and Gramazio & Kohler's robotic fabrication projects, it is quite evident that these

structures require incredible precision and complicated tools and techniques (Burry et al., 2020). These achievements demonstrate how our ability to build performative enclosures have evolved via digital fabrication. However, this level of complexity requires meticulous preparation, which can become a major hurdle for those who want to get into digital fabrication. It makes it extremely hard for beginners and non-professionals to engage in the production of such structures. By non-professionals, this paper refers to individuals who may not have specific skills in crafts and fabrication but wish to enjoy making things as a hobby or as "Do It Yourself" (DIY) solutions. Rather than exploring how complex of a structure we can build, this paper focuses on developing a system that facilitates enthusiasts to enter the realm of digital fabrication. As digital fabrication tools become more affordable, we see more people getting interested in DIY builds. Such builds are not only engaging for the user, but also economically beneficial. As Emily E. Petersen and Joshua Pearce have calculated, investing in a 3D printer can have a return value of over 100% for low-cost items in 5 years; as for high-cost items, it can produce a 986% return of investment in less than 6 months (Petersen & Pearce, 2017).

While this might be the case with plastic 3D prints, larger scale productions still are quite difficult to manage as they require more expertise and sophisticated tools. With the aid of affordable digital fabrication tools, this research tries to provide a system that produces timber shelf structures that can be assembled by hand and have as much flexibility as possible in terms of shape, scale and size. Having "Decent Work and Economic Growth" and "Industry, Innovation and Infrastructure" as guidelines, this paper attempts to create an innovative system that allows easy entry for individuals to the digital fabrication industry. As mentioned previously, DIY projects and digital fabrication tools can have great economic potentials. By enabling more people to get engaged in such technologies, this research hopes to foster more innovation in the field by enthusiastic individuals. Consequently, it aims to help people gain new skills that would in turn create more opportunities for growth. In fact, this research was established to create an interior design solution for a small art gallery renovation project located in Tokyo, Japan. The developed craft system in this paper provides a comprehensive workflow, starting from the initial shape to the final CNC milling machine G-Code generation. Figure 1 shows a 2m*1m built example of the structure that was fabricated in multiple stages, with two different ShopBot CNC machines. The design of the shelves also was slightly changed during the fabrication stage.



Figure 1. Fabricated shelf structure

2. Object-Oriented Programming and Agent-Based Design

Invented in the early 1960s, Object-Oriented Programming (OOP) refers to a programming paradigm that relies on the creation of "objects" with properties and capabilities. OOP relies on custom type objects that have a lot of functionalities and properties built in them. These objects can interact with other objects of the same type or other types (Object-Oriented Programming, n.d.). Closely related to OOP, Agent-Based Design (ABD) can be thought of as a paradigm that is suitable for building systems that involve large numbers of geometrically unique elements. ABD can allow internal interactions between a structure's members and external user inputs (Groenewolt et al., 2018). As an example, Achim Menges et. al used ABD to enable designers to move structural timber plates, while the system dealt with all the joint geometries and structural considerations (Menges et al., 2015).

The craft system developed in the paper generates straight members with unique lengths and joint configurations that as a whole would shape the final curved shelf structure. Since these members need to interact with one another to create notch joints, conventional McNeel Rhinoceros 3D (Rhino) and Grasshopper (GH) visual programming proved quite limiting. Thus, the system was developed through ABD based on the Microsoft .NET Framework, using the C# language. The aim of the development has been to reduce as much technical hurdles as possible to allow creative individuals enjoy craft with the aid of digital fabrication tools.

The developed program generates linear objects that represent real-life structural members. These members have inherent properties, such as their dimensions, ID number, list of joints and so on. In terms of interactions, they generate notch joints with other members in the system. They also record their joint count with other members. Identifying and removing redundant members is another example of the ADB interactive implementation. Redundant Member removal refers to an algorithm implemented in the system that would remove extra members with too many joints while making sure all members have a minimum number of joints. Figure 2 shows how these functionalities and properties can be retrieved in a scripting environment.

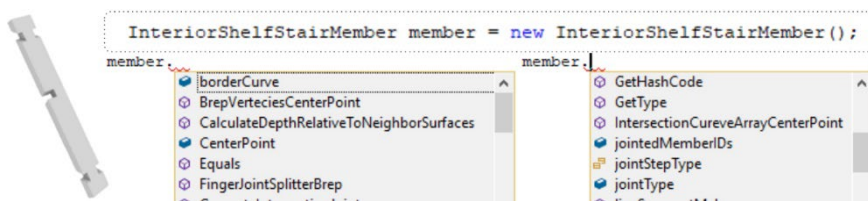


Figure 2. Creating of a shelf member class instance and accessing its properties

While Achim Menges et. al.'s ADB implementation enabled changes up to the fabrication stage starts. This paper, on the other hand, tries to keep the interactive design capability even during the fabrication stage. Once a part of the structure is built, the developed system in this paper still allows for some constrained design changes, including introducing holes in the shelf, or changing the curvature of the structure, as long as the previously built joints are not affected drastically.

3. Material and Joint System

3.1. WOOD AS A MATERIAL

Wood is among the most sustainable construction materials that is available in the building industry. Compared to other available building materials, wood has a very low embodied energy foot prints (Alcorn et al., 1996; Gordon, 2003). Rather than having huge carbon foot prints like steel and concrete, it is actually considered to be carbon absorbent since it traps large amount of carbon in its growth phase (Gold & Rubik, 2009). In addition to energy considerations, wood can be shaped into different forms with hand tools and digital fabrication tools. Assembly and disassembly as a sustainable solution is another aspect that is being explored by designers. Kengo Kuma's KODAMA permanent pavilion for Arte Sella Foundation, and Atsushi Kitagawara's design for Japan's pavilion at Expo Milano 2015 are great examples of this approach (Kitagawara et al., 2019; Kuma et al., 2019). With the aid of digital fabrication tools, buildings and structures that have disassembly in mind in their design can have much less of an energy footprint. This approach can also decrease landfill waste to a great degree (Shannon Hosey et al., 2015). Particularly, the re-usability of wood can increasingly contribute to this reduced energy footprint. The system described in this paper creates small notch joints as a means of maximizing the material's re-usability in other builds at the same time as reducing fabrication waste.

One-by-four (1*4) timber bars are the material of choice for this system because of accessibility, affordability, and the fact that they can be easily processed with a ShopBot CNC mill. In addition, by limiting the type of material for the system, it became possible to develop and build additional tools to improve the CNC milling process, resulting in better cost and material efficiency.

3.2. JOINT SYSTEM DESIGN AND FABRICATION TOOL

Interlocking jointing is one of the most commonly used joint systems in timber structures. These joint systems allow structures to be assembled without the need for nails, glue, or other fasteners as much as possible. However, depending on the function of the structure and regulations extra fastening measures need to be implemented. Since notches can be easily milled using CNC mills and other digital fabrication tools, interlocking joints offer great flexibility in terms of shape and size. As the shape of the structure gets more complex the joints also become more complex and irregular Kengo Kuma's KODAMA pavilion's simple 2D joints, Schwinn et. Al.'s Landesgartenschau pavilion robotically fabricated finger joints, and Nabei et. al.'s interlocking joints in a reciprocal panel structure are great example of the versatility of interlocking joints in wooden structures (Kuma et al., 2019; Schwinn et al., 2014; Nabaei et al., 2011).

4. Shape and Structure Design

4.1. SYSTEM FRAMEWORK SUMMERY

The shelf structure is generated based on two inputs: 1. A 2D reciprocal pattern, and 2. A curved 3D surface. The initial 2D line pattern can be changed for the desired shape, size, and functions of the final shelf. The 3D surface can be altered to change the overall

curvature and shape of the structure. The system can generate structures form a variety of 2D patterns. However, 2D reciprocal patterns are recommended for this system as they have inherent structural characteristics that contributes to the stability of the structure. Figure 3 Shows the workflow of the system from the input patterns to the final CNC G-Code generation. Each step will be explained in the following sections.

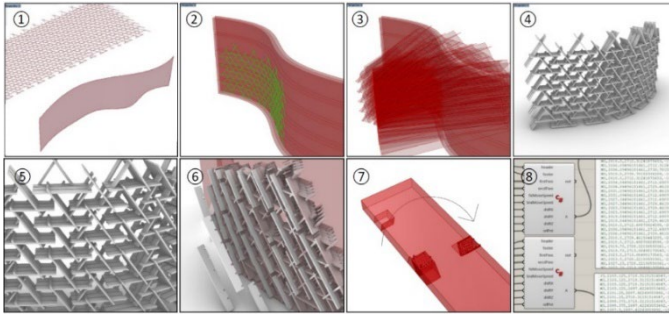


Figure 3. (1) Pattern generation and target input surface, (2) Generation of the multiple surface layers and transformation of the pattern, (3) Extrusion of the pattern based on the input surface normal vectors, (4) Generation of all the members, (5) Redundant Member Removal (6) Notch joint generation, (7) Generation of geometry required for a double-side milling operation, (8) CNC G-Code compilation ready to be used on the ShopBot CNC milling machine

4.2. 2D PATTERN DESIGN

The system uses 2D patterns to generate shelf structures. This 2D pattern does not necessarily need to be completely repeatable. By adding empty spots in the pattern, it's possible to change the shape. Figure 4 showcases the use of empty spots in the structure as a means of creating bigger shelves and change the final shape.

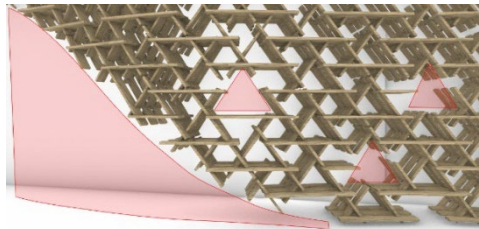


Figure 4. Use of empty space to add larger shelves and to change the shape of the structure

4.3. 3D MEMBER GENERATION

Alignment of the 3d structures is achieved by extruding the first layer's pattern according to the normal vectors of the input surface. These extrusions are then intersected with the other layers to create the subsequent 3D transformed patterns. In earlier iterations of the system, other methods of generating members were explored. However, those methods proved to create structurally unstable results, or joints that did not align. Figure 5 showcases the previous and the current iteration of the system. In the current system, the diagonal members are shifted by half of their width inside to create the bonding joints between the different layers.

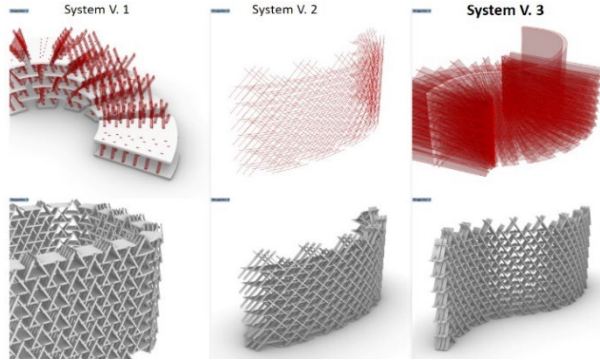


Figure 5. (left) first iteration of the system: structural integrity problems, (middle) transforming patterns on surface layers individually: joint alignment problems (right) current system version

4.4. REDUNDANT MEMBER REMOVAL

Fabrication time presented one of the biggest challenges in the development. When all of the generated members were kept in the final shelf structure, a lot of extra joints were also created. More than half of the members in the structure would have up to 12 joints. These extra joints drastically increased the fabrication time while not contributing so much to the structure's stability. The purpose of the Redundant Member Removal Algorithm (RMRA) is to remove as many extra members as possible up to the points where all members are necessary to keep the structure stable. The criteria for the developed algorithm were to keep removing members until all members have at least 3 joints with other members. It was discovered during the algorithm's development that less than 3 joints per member would result in unstable structures. The RMRA is developed via the core OOP system. It intersects all the members together in a recursive manner until all members become necessary for the structure:

- Removing one member and checking how many joints other members have left
- If the removal of a member would violate the 3-joint criteria, then that member and all connected members would be marked as necessary and be kept
- The recursive algorithm continues until all members are deemed necessary

The redundant member removal algorithm reduced the member count resulting in less material needed for the structure. Table 1 shows the result of the member removal for 3 different shelf structure (The average fabrication time for each joint was 1.5 minute):

Structure Size (L * H)	Layer Count	Member Count Before RMRA	Joint Count before RMRA	Member Count After RMRA	Joint Count After RMRA	Estimated Time Saved (Hours)
6m*2.5m	3	630	3888	512	2784	27.6hrs
4m * 2.5m	3	450	2724	368	2028	17.4hrs
2.7m*2m	3	219	1134	184	714	10.5hrs

Table 1. Comparison of fabrication time saving before and after RMRA

4.5. JOINT GEOMETRY AND GENERATION ALGORITHM

Every Joint in the system is generated as a result of intersecting two members. Going through all of the members after the RMRA, the system detects the 3D intersections between two-member sets. It divides each intersection volume into two parts and removes half of the joint from each one. The resulting joint is an angled volume that needs to be milled out. During fabrication experiments, some problems were discovered regarding the volume of the joints. Sometimes the it was not sufficient enough to be divided into two parts. In such cases, the intersection volume is removed only from one of the members. Another issue was that the length was sometimes so small that the joint became ineffective. As a result, an Intersection Length Checker Algorithm (ILCA) was developed to check for these problematic joints and intersections while designing. The ILCA highlights the members and joints that cause issues, prompting the user to change the initial shape to avoid fabrication errors. In other words, the system offers feedback to the designer regarding the fabricability of the structure. Figure 6 shows the joint generation method and a joint problem example detected by the ILCA.

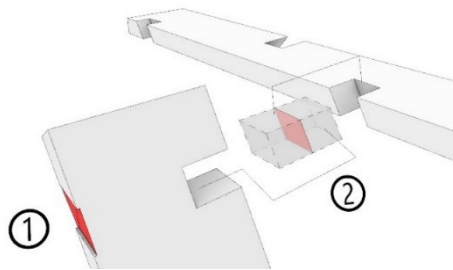


Figure 6. (1) ILCA joint problem detection, (2) Joint generation method

4.6. CNC FABRICATION AND G-CODE COMPILER

ShopBot CNC machines were selected as the fabrication tool for this research mainly because of their affordability and ease of use. In order to use a ShopBot for CNC milling, a software named VCarve Pro (Vectric Ltd, n.d.) is commonly used to convert CAD models to machine-readable commands "G-Code" (G-Code, n.d.). VCarve is a powerful tool for different methods of milling, including regular XYZ milling, double-sided milling, additional axes such as angle milling tools. However, the learning curve for the software is steep, which can become a hurdle for new users. Regardless of the skill level, the amount of time that is required for CAD to G-Code conversion is another issue that this paper addresses. Since this paper attempts to simplify fabrication, a custom G-Code compiler is developed that automatically generates the machine-readable commands. An example of custom G-Code compilers is the work of Bae et. al. that uses custom control of 3D printers to create novel objects that were impossible to make using regular 3D printing software and slicers (Bae et al., 2020). Developing the custom compiler in this paper removes the necessity to use VCarve Pro altogether, resulting in a real-time CAD to G-Code workflow. Table 2 provides a time comparison between VCarve Pro and the custom compiler. The average time spent for preparing files using VCarve was measured around 5 minutes.

Structure Size	Member Count	VCarve Geometry Preparation time	Custom Compiler Preparation Time
6m*2.5m*3layers	512	42.6hrs	None
4m*2.5m*3layers	368	30.6hrs	None
2.7m*2m*3layers	184	15.3hrs	None

Table 2. Time comparison of G-Code generation between VCarve Pro and the custom Compiler

As mentioned, the custom compiler reduced the tool path generation time to virtually none, making it real-time. This real-time aspect affords the user to make design changes even during the fabrication stage. In fact, the design of the fabricated example shelf structure was slightly changed during fabrication to test this real-time design/fabrication concept by adding some extra empty spaces in the structure. The real-time aspect actually allows the users to fabricate members based on the assembly sequence that they want to go through. Figure 7 showcases the virtual model that was used during the fabrication.

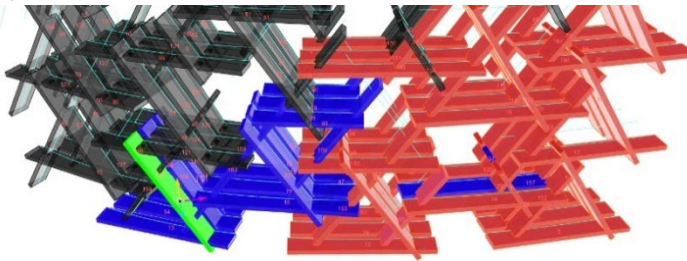


Figure 7. (Black) Not yet fabricated, (Green) Selected member to be fabricated, (Blue) Fabricated but not yet assembled, (Red) Fabricated and assembled

In terms of fabricability, the resulting joints are volumes with an angle. They cannot be milled out with conventional 2D CNC tool paths. Since regular CNC machines can only move in the XYZ axes, they can only remove material from above. As a result, an algorithm was developed to convert the joint geometries into two parts that can be milled in two steps: milling the top part of the joint, and then milling the bottom part after flipping the material. The ShopBot's approach toolpath was also incorporated in the compiler. It was seen that when the milling bit carves material from inside towards the edges of the 1*4 material, in many cases the timber would break. This was in part because of the speed of the ShopBot, but more importantly because of the milling tool path. Accordingly, a tool path system was developed that would first carve the edges of the material from the outside towards the inside. This prevented the timber's edges from breaking and chipping off. The Tool path was also divided into two phases of material removal and surface smoothing. All of these tool path optimizations resulted in a drastic reduction in milling time and much cleaner result. The time required for each joint on average was reduced from 10 minutes to 1.5 minutes in the latest tool path generator script. Cutting each member in length after the joints also reduced material use. Figure 8 displays how the joint milling operation from the geometry to the final milling operation.

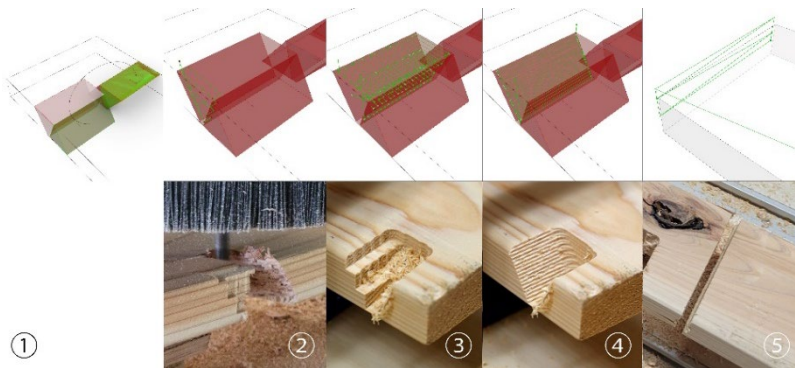


Figure 8. (1) Dividing the joint geometry to 2-side s, (2) Cutting the edge from outside, (3) Material Removal, (4) Smoothing one needed surface, (5) Cutting the member in length

5. Discussion and Conclusion

Digital Fabrication, as an industry, has great space to for growth and offers so many economic opportunities that can significantly improve lives. The aim of this paper is to develop a system that enables non-professionals to engage in making things with CNC machines as the easier to use and affordable fabrication tool. It tries to remove some of the hurdles of using digital fabrication tools that prevent those who wish to engage in digital craft as a hobby, or DIY solutions.

Time and material costs are two of most immediate constraints that beginners face in this field. The development of the Real-Time Geometry to G-Code compiler was an attempt to solve this issue and enable individuals to design and build structures without having the need to think about the technical aspects of file and geometry preparation. By reducing the design to machine code preparation time to virtually zero, it facilitates the fabrication experience for beginners and enthusiasts quite well. Of course, Further research can explore how this Real-Time design/fabrication aspect can be applied to more complex shapes using CNC machines. The developed craft system here generates curved-shaped shelf structures that are fabricable with the aid of affordable CNC machines. Curve-shaped structures have been addressed here since they offer more flexibility for the user. At the same time, they present fabrication challenges quite vividly, making the fabrication experience more engaging for the user. The system is developed in a way that shows the results of the design, along with information about its fabricability. It also incorporates optimization algorithms. For instance, the Redundant Member Removal Algorithm substantially reduces material and time costs before the fabrication starts. While it may not be as effective during fabrication, further research on similar algorithms that incorporate the produced waste material, resulting from the current fabrication, can improve time and cost efficiency even further.

Digital fabrication tools have enabled architects and designers to build incredibly complex structures that answer to questions of structure, design, aesthetics, and so on simultaneously. As mentioned earlier in this paper, the robotic fabrications of Gramazio & Kohler at ETH Zurich and timber structures by the team of Oliver David Krieg and Achim Menges at Stuttgart University (Alvarez et al., 2019; Burry et al.,

2020; Menges et al., 2015) have demonstrated the amazing possibilities of digital fabrication in Architecture and Design. Inspired by the "Decent Work and Economic Growth" and the "Industry, Innovation and Infrastructure" of the UN Sustainable Development Goals, this research tries to develop a system that democratizes digital fabrication and enable less skilled individuals to benefit from this industry as well. While the aforementioned researches have demonstrated the great possibilities of the field, this research tries to develop a craft system that simplifies the transition from design to fabrication not just for experts but also for beginners in the field.

References

- Alcorn, A. (1996). *Embodied Energy Coefficients of Building Materials*. Centre for Building Performance Research, Victoria University of Wellington.
<https://books.google.co.jp/books?id=NiKdbwAACAAJ>
- Alvarez, M., Wagner, H., Groenewolt, A., Krieg, O., Kyjanek, O., Aldinger, L., Bechert, S., Sonntag, D., Menges, A., & Knippers, J. (2019, October). The BUGA Wood Pavilion – Integrative Interdisciplinary Advancements of Digital Timber Architecture. *39th ACADIA Conference 2019*.
- Burry, J., Sabin, J., Sheil, B., & Skavara, M. (2020). *Fabricate 2020: Making Resilient Architecture*. UCL Press. <https://doi.org/10.2307/j.ctv13xpsvw>
- Gold, S., & Rubik, F. (2009). Consumer attitudes towards timber as a construction material and towards timber frame houses – selected findings of a representative survey among the German population. *Journal of Cleaner Production*, 17(2), 303–309.
<https://doi.org/10.1016/j.jclepro.2008.07.001>
- Gordon, J. E. (2003). *Structures: Or Why Things Don't Fall Down*. Da Capo Press.
<https://books.google.co.jp/books?id=QrLvsWEACAAJ>
- Groenewolt, A., Schwinn, T., Nguyen, L., & Menges, A. (2018). An interactive agent-based framework for materialization-informed architectural design. *Swarm Intelligence*, 12(2), 155–186. <https://doi.org/10.1007/s11721-017-0151-8>
- Kitagawara, A., Imperadori, M., Kuwabara, R., Brunone, F., & Matsukawa, M. (2019). Wooden Byobu. From Architectural Façade to Sculpture. In F. Bianconi & M. Filippucci (Eds.), *Digital Wood Design*, 24, 1287–1315. Springer International Publishing.
https://doi.org/10.1007/978-3-030-03676-8_52
- Kuma, K., Imperadori, M., Clozza, M., Hirano, T., Vanossi, A., & Brunone, F. (2019). KODAMA: A Polyhedron Sculpture in the Forest at Arte Sella. In F. Bianconi & M. Filippucci (Eds.), *Digital Wood Design*, 24, 1255–1286. Springer International Publishing. https://doi.org/10.1007/978-3-030-03676-8_51
- Menges, A., Schwinn, T., & Krieg, O. (2015). *NAWT Balloons*. Landesgartenschau Exhibition Hall. Retrieved from <https://doi.org/10.4324/9781315678825-9>
- Nabaei, S., Weinand, Y., & Bayerel, O. (2011). Geometrical description and structural analysis of a modular timber structure. *Proceedings of the IASS Annual Symposium 2016*.
 Wikipedia. *Object-oriented programming*. (n.d.). Retrieved from https://en.wikipedia.org/wiki/Object-oriented_programming#cite_ref-alanKayOnOO_5-0
- Petersen, E., & Pearce, J. (2017). Emergence of Home Manufacturing in the Developed World: Return on Investment for Open-Source 3-D Printers. *Technologies*, 5(1), 7.
<https://doi.org/10.3390/technologies5010007>
- Schwinn, T., Krieg, O., & Menges, A. (2014, October). Behavioral Strategies: Synthesizing design computation and robotic fabrication of lightweight timber plate structures.
- Shannon Hosey, Beorkrem, C., Damiano, A., Lopez, R., & McCall, M. (2015). Digital Design for Disassembly. *Proceedings of the 33rd ECAADe Conference*, Volume 2, 371–382.
http://cumincad.scix.net/cgi-bin/works/Show?_id=ecaade2015_265

IN-SITU ROBOTIC FABRICATION OF SPATIAL GLULAM STRUCTURES

HUA CHAI¹, ZHIXIAN GUO², HANS JAKOB WAGNER³, TIM STARK⁴, ACHIM MENGES⁵ and PHILIP F. YUAN^{6*}

^{1,6}*College of Architecture and Urban Planning, Tongji University.*

²*Shanghai Fab-Union Technology Co., Ltd.*

^{3,4,5}*Institute for Computational Design and Construction, University of Stuttgart*

^{1,3,4,5}*DFG Cluster of Excellence 2120 – Integrative Computational Design and Construction for Architecture, University of Stuttgart*

¹*chaihua@tongji.edu.cn, 0000-0002-7816-1280*

²*guozhixian@fab-union.com, 0000-0002-3844-9378*

³*hans.jakob.wagner@icd.uni-stuttgart.de, 0000-0001-8600-8481*

⁴*tim.stark@icd.uni-stuttgart.de, 0000-0002-4179-1887*

⁵*achim.menges@icd.uni-stuttgart.de, 0000-0001-9055-4039*

⁶*philipyuan007@tongji.edu.cn, 0000-0002-2871-377X*

Abstract. While current approaches in timber construction stress the advantages of off-site prefabrication, glued laminated timber (glulam) structures is limited to the constraints of standardized, prefabricated mostly linear elements, which also lends itself only to building typologies that offer an increased level of standardization and regularity. The design freedom of timber structures is incomparable to that of reinforced concrete structures, which mostly gains from the in-situ fabrication process. An in-situ robotic timber fabrication platform allows the on-site construction of glulam structures with highly differentiated networks of beams composed of robotically assembled discrete linear elements. Based on the possibilities of such mobile robotic fabrication process, this paper explores novel architectural typologies of spatial glulam structures. The research is conducted from several aspects including joint tectonics, design method, and robotic fabrication process. A large-scale pavilion is designed and fabricated to verify the feasibility of the proposed system. This research could provide a novel mode of in-situ robotic timber fabrication and corresponding glulam structure system for timber construction.

Keywords. Mobile Robot; Timber Structure; In-situ Fabrication; Computational Design; SDG 9.

1. Introduction

Current timber construction benefits from off-site prefabrication approaches, the efficiency and economy of which gain mostly from the standardized design and

production of the building system (Thomas et al., 2004). As the prefabricated components need to be assembled on site, timber construction still suffers from the constraints of transportation, connection system and assembly process, despite the many advantages. The monolithic nature of on-site cast steel-reinforced concrete structures plays out its main benefits: the material can be formed flexibly into almost any shape, while the rebar allows for the reinforcement of the structures in various directions. For timber construction, there is no on-site fabrication system for large-scale structures that could be comparable and competitive with the flexibility of such steel-reinforced concrete structures.

In this work we are aiming to tackle exactly this problem of large-scale timber construction with a customized mobile robotic fabrication platform that allows on-site construction of timber frames composed of robotically assembled discrete wooden elements. Based on the possibilities of such mobile robotic construction process, novel design opportunities for timber construction are developed through the contextualization of a spatial glulam building system involving the intricate negotiations of material tectonics, structure optimization and fabrication constraints. This paper will show how a robot platform (Wagner, Chai, et al., 2020) could be employed in a fabrication system that integrates aspects of in-situ construction robotics and architectural building system design. The development of the proposed system and its evaluation through a large-scale case-study structure will be presented in this paper.

2. Background

2.1. IN-SITU ROBOTIC CONSTRUCTION

State of the art concepts for in-situ mobile robotics have shown great potentials in mastering complexity within and beyond existing building typologies. Mobile robots that are used to automate existing construction processes have appeared on the market, such as the Ceiling drilling robot HILTI Jaibot BIM (Xu et al., 2021), wall painting robot Pictobot (Asadi et al., 2018) and OKibo (okibo, 2021). The “In-situ fabricator” developed by ETH Zürich is a typical case that promotes the development of new construction systems such as Mesh Mould (Dörfler et al., 2019). Despite all the technological challenges facing In-situ mobile robotics, it can be expected that in-situ mobile robotics will become increasingly integrated in the construction site.

2.2. GLULAM STRUCTURES

Glulam is one of the most important structural materials in the practice of modern wood architectures. Currently, efficient production lines to produce ordinary glulam components have been formed through reasonable organization of the production workflow (Chai et al., 2021). Combined with the processing capabilities of computer-aided manufacturing equipment such as timber CNC-machining centres, the size and form of the prefabricated glulam components can be almost unlimited, regardless of cost. The past decade has witnessed the emergence of a series of complex glulam structures, such as the French Pavilion for Milan Expo (Scheurer et al., 2015), and La Seine Musicale (Stehling et al.). Nevertheless, due to transportation constraints, it's normally necessary to segment the glulam components in the factory then transport

them to the site for connection. Therefore, the joint systems are particularly challenging for the structural integrity. While broadly successful in linear and standardized building applications, the main challenge for glulam structure at present comes from the disproportional loss of economic and efficiency benefits in customized designs with complex spatially differentiated components and connectors. Studies in how robotic timber construction can become more flexible and offer advanced manufacturing also for non-standard structures, will be paramount in order to enable broad application of sustainable wood architecture (Wagner, Alvarez, Groenewolt, et al., 2020).

2.3. ROBOTIC TIMBER ASSEMBLY

Robotic timber assembly with both linear sawn timber and wood panels has been extensively studied during the last 15 years (Willmann et al., 2016). The assembly process of timber structures has been automated through the development of robotic assembly tools such as grippers and automatic nail guns (Apolinarska et al., 2016). The assembly of the DFAB project explore dual-robot fabrication of timber frame structures (Graser et al., 2021). The assembly of tenon-and-mortise joints-based timber structures through the flexible use of robotic grippers and tool changers have also been recently explored (Leung et al., 2021), as well as the off-site robotic glue-pressing of timber assemblies (Wagner, Alvarez, Kyjanek, et al., 2020). Currently, the research of robotic timber assembly is mainly carried out in laboratories and factories. What remains to be explored is the adaptability of robot assembly technology to complex conditions on site and the corresponding timber system for in-situ construction.

3. Robotic Platform for in-situ Timber Construction

A mobile robotic platform was developed to be flexibly deployable for various on-site timber construction tasks, which have been introduced in previous research (Wagner, Chai, et al., 2020). An ABB IRB 4600 industrial robot arm is installed on a track platform, with a customized tool station for timber processing equipped. To ensure ideal productivity in fabrication scenarios, the reach envelope of the platform could cover both typical ceiling and floor heights. A gripper with automated nail gun is mounted on the robot to conduct assembly tasks. A gluing station is fixed on the platform to apply glue during assembly. An Intel RealSense D415 RGB-D camera is rigidly mounted on the robot flange to localize the robot root in the environment by identifying pre-embedded markers. With real-time communication via ABB EGM, a cyber-physical system linking the design software and the robotic construction process can be established (Menges, 2015). With this setup, timber structures could be robotic assembled on-site from discrete timber elements through a continuous repetition of a series of fabrication tasks: gripping-gluing-placing-nailing.

4. Design of Spatial Glulam Structures

4.1. SPATIAL GLULAM STRUCTURE

As one of the most cost-effective fasteners, nail connections are usually employed in robotic timber assembly using automatic nail guns to shoot the nails. However, nails do not provide large resistance (Johnsson, 2001). In timber construction, Glue bonding

is the only connection method that could establish continuous stiffness at the interface (Ramage et al., 2017). Normally, the high strength of glue bonding is obtained through maintaining certain pressure for several hours. The on-site mobile construction robot could assemble the discrete timber sticks into an integrated spatial structure through gluing and nailing which blurs the clear distinction between components and joints, avoids the customization of complicated components and connectors. This kind of nail-glue hybrid connections obtains its performance mainly from nail assisted glue interface. In this regard, the on-site construction system of integrated spatial timber structure with nail-press-glue connection can be regarded as a custom glulam structure, and as an extension of the common concept of glued laminated timber.

As a robot-fabricated building system, the design of such spatial glulam structures is subject to several constraints of the robotic construction process. For example, the use of standardized or simple materials is more conducive to the robot assembly process. The component size is constrained by the tool parameters such as the size of the gripper, the length of the nail, and operational space of glue application station. The robot assembly sequence of the components also needs to be defined in the design process of the construction system.

4.2. TECTONICS SYSTEM

The tectonics system-how joints and structures are formed with timber components-is essential for spatial glulam structure, which should allow multi-directional growth of the structure while meeting the fabrication requirements of the robot platform. In this research, the building system is conceived taking wood frame structure as a prototype. Wood frame structures, especially in multi-story construction, usually employs orthogonal spatial grids with prefabricated columns and beams. The orthogonal frame structure is conducive to the standardized production of components and connection joints, reducing the difficulty of processing and installation. However, what is lost in the standardization process is the freedom of structural design and the flexibility of architectural space. If the axes of the frame structure do not conform to an orthogonal grid, the processing difficulty of components and connectors will be significantly increased, which will in turn increase the workload and cost.

The design of the Spatial Glulam Structure pavilion explores innovative construction system of wood frame structures by introducing 45-degree oblique members into the orthogonal frame. The different combinations of oblique members and orthogonal grids will greatly increase the diversity of the structure system. By limiting the components to orthogonal ones and 45-degree oblique ones, the complexity of the structure itself is also limited to a certain range, which is more conducive to the robotic fabrication process.

Typological study is first carried out on the tectonics system of frame structure after the introduction of oblique members. Starting from a single linear axis, the tectonic system of different joints is defined with the same logic, including planar orthogonal axis, spatial orthogonal axis, planar oblique axis, and spatial oblique axis. The assembly sequence and nailing positions of the components are also defined at this stage, so that the robot assembly logic can be clarified (Figure 1).

The construction system is designed with straight sticks with a uniform square section. With a 3*3 square grid defined at the cross-section of the axis, three sticks are arranged on the three corner cells of the grid, spacing one cell in between to accommodate the intersecting sticks. if axes are intersecting, the axes will maintain one cell spacing at the intersection to avoid collisions between sticks. Using three sticks as a group instead of four, could make the organization of the assembly sequence much easier, simplifying the robotic assembly process. The joints at both ends of the same axis can be connected by adding sticks in the vacant cells. Therefore, for a given axis frame, a spatial glulam structure can be formed by first classifying the axis by different intersecting type, then calling the corresponding joint definition, fitting different situations through parameter adjustment.

Joint types	Axes	Stick Model	Assemble Sequence
Single axis			
Planar orthogonal			
Spatial orthogonal			
Planar oblique			
Spatial oblique			

Figure 1 Tectonics for spatial glulam structure

4.3. STRUCTURAL DESIGN STRATEGY

This research makes a preliminary attempt on the integrated design process of spatial frame structures through the design and construction of a large-scale pavilion (Figure 2). The pavilion is designed around a concrete column, with the structure completely independent from the column, which provides shelter and seating for visitors with a dominant structural cantilever on the top.

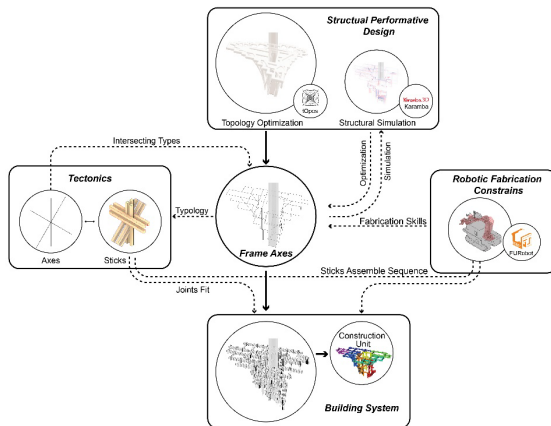


Figure 2 Integrated design of spatial glulam structure

Topology optimization is used for form-finding, which provides a basis for the high-performance layout of the timber sticks. Grasshopper plug-in tOpos is employed to perform topology optimization calculations. With a given roof profile and support area as a starting point, uniformly distributed vertical and horizontal loads are applied to the design range for optimization (Figure 3). After optimization, a series of curves are obtained by extracting the medial axes of the mesh model output by the topology optimization. The curves are then transformed into a series of polylines composed of only horizontal, vertical, and 45-degree diagonal segments. For functional considerations, the polylines were further optimized with two benches added at the bottom of the structure.

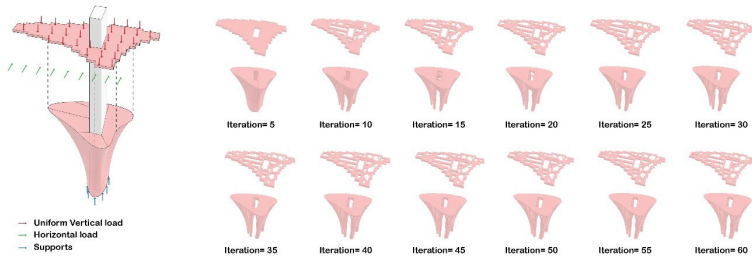


Figure 3 Topology optimization-based form-finding process

Due to the difference in lengths of the obtained frame axes, three types of sticks are adopted here with three different lengths 300 mm, 500 mm and 800 mm, and a uniform square section of 50 mm*50 mm. In order to arrange the sticks on the spatial frame obtained from topology optimization, the axis intersecting at each joint are first analysed. Then the corresponding tectonics are selected from the joint library and positioned on the axis, with appropriate stick lengths endowed according to the length of the axis. After all the axes are fitted with the joint system, additional connecting sticks are added to connect different joints to form a complete spatial frame structure.

5. On-site Robotic Fabrication

Taking use of the on-site mobile construction platform, the structure is gradually assembled through the processes of stick picking, gluing, placing, and nailing. The structure is first divided into a series of construction units according to the robot's reach, with the range of the corresponding robotic fabrication position roughly clarified. The robot platform assembles the structure on-site by repeating the following process: move the robot to the construction area of a certain unit, robot localization, robot programming, robotic fabrication.

5.1. ROBOT LOCALIZATION

At the construction site, the robot platform locates itself by recognizing markers pre-laid on the steel foundation with the camera. The robot collects three to four markers each time it moves and uses the results of multiple markers to calculate a relatively accurate root of the robot. The markers are laid on the steel foundation at an interval of 1-1.5m to make sure that the robot can recognize at least three markers at each location.

A KTS-462R4L total station is used to calibrate the position of all the markers by identifying the reflectors attached to the corner of the markers. At the same time, the total station is also used to calibrate the corners of the steel foundation to clarify the relative position relationship between the markers and the steel foundation, as well as the timber structure to be built. After hand-eye calibration, the camera is used to identify the markers and transform the coordinate frame of the markers into the root of the robot. The entire structure will be assembled by the robot platform through multiple movements and repositions following the construction sequence mentioned above.

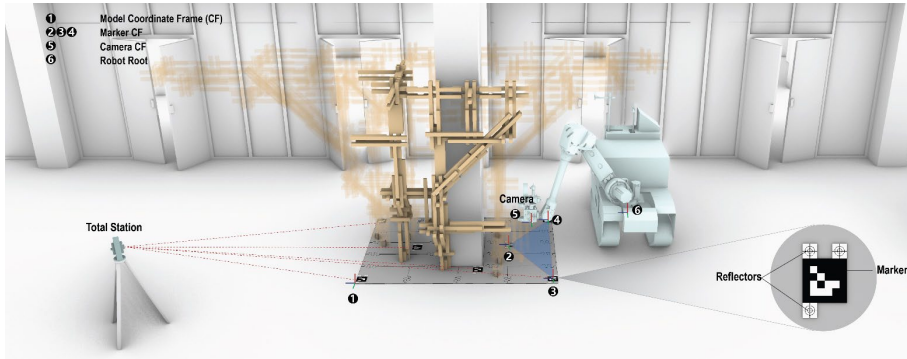


Figure 4 localization system of the mobile robot

5.2. ROBOT PROGRAMMING

After localizing the robot in the environment, the robot path for corresponding construction unit will be programmed. After being picked by the robot, the stick needs to be glued and nailed, the gluing and nailing position of which corresponds to the intersecting area of this stick and sticks that have been built. Due to the complex relationship between sticks, spatial glulam structure must be assembled in strict accordance with a specific order. With the assembly sequence of each joint type defined in the tectonics design stage, the robot path is mainly extracted from the intersecting relationship between the sticks. Therefore, when programming the robot, it is necessary to first determine the intersection relationship between each stick to be built and ones that have been built. Then a plane could be generated at the interface, which serves as a reference for the robot target (Figure 5). It is worth mentioning that there are no intersecting sticks for the first or first few sticks at the beginning of each construction unit. Additional sticks need to be added to determine the robot's grasping position.

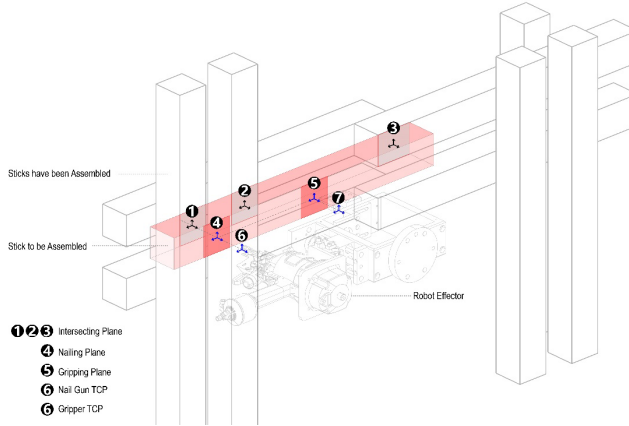


Figure 5 Robotic assembly process of a typical joints

5.3. ON-SITE ROBOTIC FABRICATION

When constructing on site, the prefabricated steel foundation is first installed in place, with steel connectors that connect the foundation and the timber structure pre-welded on the plate. Then the markers and the reflectors for total station measurement are laid on the steel plate, with the reflectors attached to the corners of the markers and the corners of the steel foundation. The total station measures the relative position between the markers and the steel foundation to establish a global environment model for the robotic construction.

The structure is split into 8 construction units for construction, with the corresponding location of the platform roughly determined in advance through the robotic simulation (Figure 6). After the robot moves in place, the camera recognizes three to four markers within the reach zone of the robot arm to obtain the root of the robot in the global model. Then the robotic fabrication process will be simulated, outputting the robot program for execution. The program instructs the robot to grab the sticks, apply glue, and place sticks in place, while an operator holds the nail gun to fix the sticks. Each construction unit could be assembled by simply repeating this process.

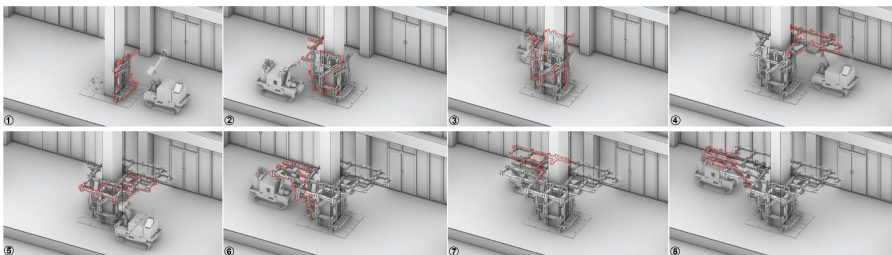


Figure 6 simulation of on-site robotic construction sequence of 8 construction units

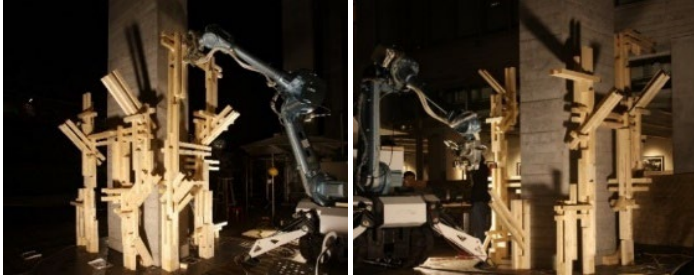


Figure 7 on-site robotic fabrication

6. Result and Evaluation

The structure is composed of 937 members, including 328 members with 800 mm length, 302 members with 500 mm length, and 307 members with 300 mm length. The on-site robot construction process of all sticks took roughly 10 days. The completed Spatial Glulam Structure presents unique aesthetic characteristics under the combined effect of structural performance design and robotic fabrication.



Figure 8 Robotic fabricated Spatial Glulam Structure

7. Conclusion

A spatial glulam structure system is developed in this paper based on a custom mobile robotic timber fabrication platform, the feasibility and potential of which have been verified through the construction of a large-scale pavilion. Although the technology has yet to be improved, this research has opened a novel mode of in-situ fabrication for timber construction. Subsequent research will focus on the mechanical properties of the proposed system to further improve its practicality.

Acknowledgement

The work was supported by the National Key R&D Program of China (Grant No. 2018YFB1306903), Shanghai Science and Technology Committee (Grant No.21DZ1204500, 16DZ2250500), the State of Baden - Wuerttemberg, the European Regional Development Fund and was partially supported by the German Research Foundation under Germany's Excellence Strategy – EXC 2120/1 - 390831618. We'd like to thank Jiahao Zhao, Jiayu Feng, Ken Cheng, Zhenyang Yin, Zhuo Zhang for their contribution to the design and fabrication of the pavilion.

References

- Apolinarska, A. A., Bärtschi, R., Furrer, R., Gramazio, F., & Kohler, M. (2016). Mastering the Sequential Roof. In *Advances in architectural geometry 2016* (pp. 240-258). Advances in Architectural Geometry (AAG).
- Asadi, E., Li, B., & Chen, I.-M. (2018). Pictobot: A cooperative painting robot for interior finishing of industrial developments. *IEEE Robotics & Automation Magazine*, 25(2), 82-94.
- Chai, H., So, C., & Yuan, P. F. (2021). Manufacturing double-curved glulam with robotic band saw cutting technique. *Automation in Construction*, 124(4), 103571.
- Dörfler, K., Hack, N., Sandy, T., Gifftthaler, M., Lussi, M., Walzer, A. N., Buchli, J., Gramazio, F., & Kohler, M. (2019). Mobile robotic fabrication beyond factory conditions: case study Mesh Mould wall of the DFAB HOUSE. *Construction Robotics*, 1-15.
- Graser, K., Adel, A., Baur, M., Pont, D. S., & Thoma, A. (2021). Parallel Paths of Inquiry: Detailing for DFAB HOUSE. *Technology| Architecture+ Design*, 5(1), 38-43.
- Herzog, T., Natterer, J., Schweitzer, R., Volz, M., & Winter, W. (2004). *Timber construction manual*. Birkhäuser Architecture.
- Johnsson, H. (2001). *Systematic design of glulam trusses*. Luleå tekniska universitet.
- Leung, P. Y. V., Apolinarska, A. A., Tanadini, D., Gramazio, F., & Kohler, M. (2021). Automatic Assembly of Jointed Timber Structure using Distributed Robotic Clamps. In *Proceedings of CAADRIA 2021* (pp. 583-592). The Association for Computer-Aided Architectural Design Research in Asia (CAADRIA).
- Menges, A. (2015). The new cyber-physical making in architecture: Computational construction. *Architectural Design*, 85(5), 28-33.
- Okibo. (2021). *The Autonomous Wall Plastering Robot*. Retrieved September 23 2021, from <https://okibo.com/>
- Ramage, M. H., Burrige, H., Busse-Wicher, M., Fereday, G., Reynolds, T., Shah, D. U., Wu, G., Yu, L., Fleming, P., & Densley-Tingley, D. (2017). The wood from the trees: The use of timber in construction. *Renewable and Sustainable Energy Reviews*, 68, 333-359.
- Scheurer, F., Simonin, L., & Stehling, H. (2015). “Energy for life”—the timber structure of the French Pavilion at the EXPO 2015. In *Proceedings of the International Association for Shell and Spatial Structures (IASS) Symposium 2015*.
- Stehling, H., Scheurer, F., Roulier, J., Geglo, H., & Hofmann, M. From Lamination to Assembly--Modelling the Seine Musicale. In, R. Sheil, A. Menges, R. Glynn, & M. Skavara (Ed.), *Fabricate 2017* (pp. 258-263). UCL Press.
- Wagner, H. J., Alvarez, M., Groenewolt, A., & Menges, A. (2020). Towards digital automation flexibility in large-scale timber construction: integrative robotic prefabrication and co-design of the BUGA Wood Pavilion. *Construction Robotics*, 1-18.
- Wagner, H. J., Alvarez, M., Kyjanek, O., Bhiri, Z., Buck, M., & Menges, A. (2020). Flexible and transportable robotic timber construction platform—TIM. *Automation in Construction*, 120, 103400.
- Wagner, H. J., Chai, H., Guo, Z., Menges, A., & Yuan, P. F. (2020). Towards an On-site Fabrication System for Bespoke, Unlimited and Monolithic Timber Slabs. In *2020 IEEE/RSJ International Conference on Intelligent Robots and Systems (IROS) - Workshop on Construction and Architecture Robotics*.
- Willmann, J., Knauss, M., Apolinarska, A. A., Gramazio, F., & Kohler, M. (2016). Robotic timber construction — Expanding additive fabrication to new dimensions. *Automation in Construction*, 61, 16-23.
- Xu, X., Holgate, T., Coban, P., & Soto, B. G. d. (2021). Implementation of a Robotic System for Overhead Drilling Operations: A Case Study of the Jaibot in the UAE. In *38th International Symposium on Automation and Robotics in Construction, ISARC 2021* (pp. 661-668), The International Association for Automation and Robotics in Construction (IAARC)

(E)MULATE AEC: A GESTURAL PEDAGOGY AND CLOUD-BASED COLLABORATIVE MANAGEMENT PARADIGM FOR ON-SITE ROBOTICS IN CONSTRUCTION

VISHAL VAIDHYANATHAN¹ and TWISHA RAJA²

¹*Harvard University Graduate School of Design,*

²*Carnegie Mellon University School of Architecture.*

¹*vishalvaidhyathan@gsd.harvard.edu, 0000-0001-5389-5723*

²*traja@andrew.cmu.edu, 0000-0001-7553-0338*

Abstract. With about \$10 trillion in annual revenue – contributing to almost 6% of the global GDP, construction is one of the largest industries. However, with “Industry 4.0” causing paradigm shifts in other industries, construction has failed to be as efficient and technologically fluent. There have been issues of deteriorating labour productivity. This calls for on-site technological task automation to increase efficiency and abate workforce requirements. Robots in construction can be a great way to expedite and automate this process, as robotic construction is much more efficient in terms of operation and cost. They can complement and augment conventional construction methods and craft-based fabrication with a high level of efficiency. Robots in construction are being increasingly and ubiquitously used in large scale construction sites for performing several, different tasks in tandem, with humans. Programming these robots to perform specific tasks, however, is a highly skill demanding process, necessitating expertise in robotic coding and path planning. It is also impossible to robotically replicate specialized tasks with the same craftsmanship through conventional robot programming methods, as it is a mode of tacit knowledge transfer. Using several robots on-site for different tasks also calls for an efficient network and management system. This paper discusses a new paradigm of teaching industrial robots with natural gestures, and a cloud-based management system to synchronize all robots on-site. A prototype was built to teach simple toolpaths to robots of different scales using gestures. All taught toolpaths were synchronized to all robots through the cloud-based interface. Scalability of toolpaths between two different robots (ABB IRB6640 and ABB IRB120) after cloud synchronization was demonstrated. It was experimentally concluded that gestural robot programming with cloud-sync, enabled expedited teaching times, and no skill-gap in programming robotic tool paths.

Keywords. Architectural Robotics; Gesture Based Programming; Human Computer Interaction; Cloud Computing; SDG 9.

1. Introduction

One of the issues in the construction industry is its shortage of skilled labour. While this demonstrates a reduction in vocational training in the United States and indicates the need for more training and retaining, it is also an opportunity for more automation to fill the gap. (Adam Higgins, 2019) The degree of automation in construction is far less than in other industries, such as manufacturing. This results in both poor productivity and risky working conditions. Thus, by way of example, the authors have developed a robotic workflow for demonstrating how automation and robotic applications are opportunities to cater to such issues in the construction industry. (Jeong Kim et al. 2015)

Construction activities like bricklaying, surface finishing, painting etc. form the essential domain in the architectural and construction practice, which require skilled workers and demand precise quality control procedures. (Siciliano and Khatib 2016) Based on scientific research, it has been established that improved quality of construction processes is achieved through precise control of functions and operation. The working conditions are improved by removing workers from dangerous environments and reducing the amount of heavy physical work. Such practices are also sustainable because of the reduced material consumption through precise control of material delivery, and collection and reuse of unused material. (Saidi, Bock, and Georgoulas 2016) Most of the on-site construction processes where robots are used can be grouped into three predominant types of functional operators as follows:

Materials handling, Materials shaping, Structural joining. (Bard et al., n.d.)

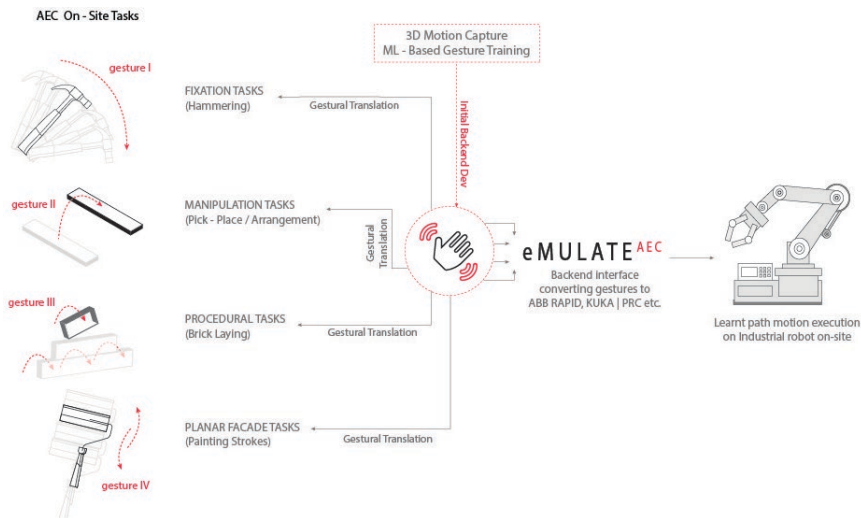


Figure 1. Conceptual Overview of Project- Gestural Translation of Tasks

The degree of automation in construction is far less than in other industries, such as manufacturing. This results in both poor on-site productivity and risky working conditions. Automation and robotics applications are thus, opportunities to solve such

issues in the construction industry. Apart from the customary on-site construction tasks, quite a few of the most highly skilled building trades are dying out. This is noted because a lot of the most highly skilled hands have little digital literacy and most of the digitally literate lack the dexterity gained from sustained interaction with physical material. This suggests that soon an increasing number of digital/physical workflows will reward practice. (Bidgoli 2015)

In this research, we set a consideration that individuals in the construction industry may not be well-versed with text-based programming which relies exclusively on the expertise of the human programmer. Robotic control is hard to grasp for unexperienced users, but motion in space is a tangible phenomenon. (Siciliano and Khatib 2016) Through this project, we propose a system that works with the combination of the precision of machines with human cognitive skills, thus developing an interface that is not just for the cognoscenti. Our research is based on construction processes that are not possible by human skill alone wherein building a symbiotic relationship between the human body and robotic machines becomes integral. Here, human dexterity and robotic precision are choreographed in the production of innovative on-site construction workflows.

Even though industrial development has been explicitly described in prior Millennium Development Goals, SDG 9 is the first independent development goal to include industrialization in its aims, as well as some aspects of infrastructure and technology development. (UN, 2019) Industrial growth, according to the United Nations, is critical for both generating income and improving living conditions. Suitable infrastructures, in turn, provide facilities for industry and society, while innovation boosts technological capabilities and leads to the creation of new talents. (Cheryl and Leurent, 2017)

The results of a recent study indicate that, the US construction industry does not realise approximately 15 billion US dollars per year in potential savings due to inadequate interoperability related to information exchange and management practices. (Bard et al., n.d.) Embedding robotic processes that have a capability of scaling up/down increase the modularity of the robot on site. Seamless data transfer facilitated through cloud-based management is a prompt for significant gains and productivity in construction processes, preventing further fragmentation within the AEC industry. (C Howard et al., n.d.)

2. Methodology

This exploration is an effort towards seeing how human skills can be transferred directly to generate informed robotic motion control, eliminating any third interface between these two processes. It separates craftsmen and designers from offline and textual programming to movements and sensor-integrated cognitive devices to communicate with robot collaborators in highly skilled building applications, seamlessly. (Menges 2013)

2.1. APPARATUS SETUP

The software setup unifies the system and forms an integral part of the system whereas the hardware setup is variable, i.e., task specific. These site-level tasks that

are taught individually to robots, are synchronised onto a cloud server through this proposed interface. These tasks can be inherited by any other robot on the same network to perform these taught tasks from cloud-based storage system.

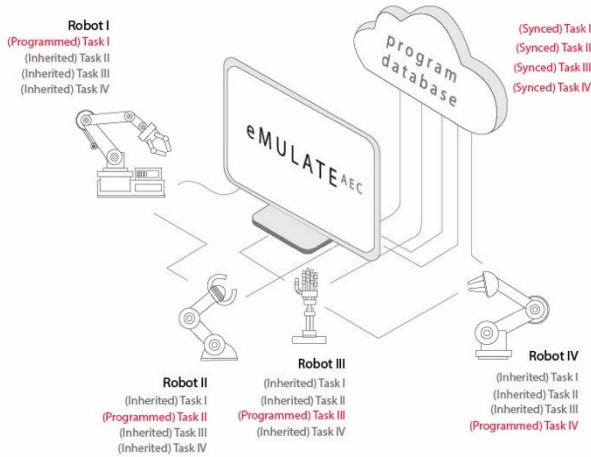


Figure 2. Synchronous Task Upload on Cloud

2.2. SOFTWARE

In the entire course of this workflow, software integration happens at two major stages - gesture recognition through ‘Wekinator’, a platform for image classification, and secondly - while translating these gestures into robotic actions.

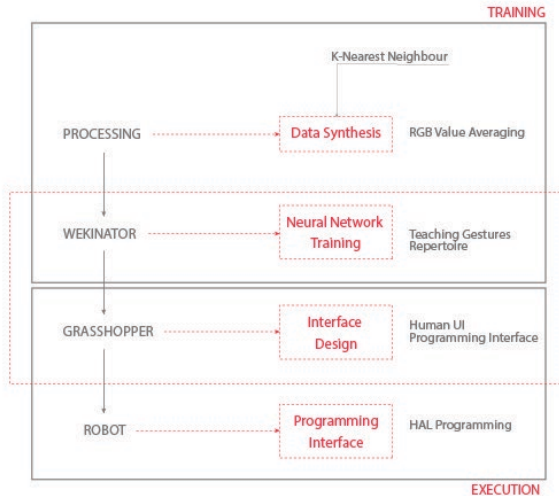


Figure 3. Stages of Software Integration

The first step in the backend process is where relational value-based pixel clustering (an implementation of the KNN algorithm for supervised learning) is used for gesture detection and recognition. A workflow executed using Processing pixelates the video camera stream and detected colour values are averaged out using this logic. The next step in the process is the training of the gestures.

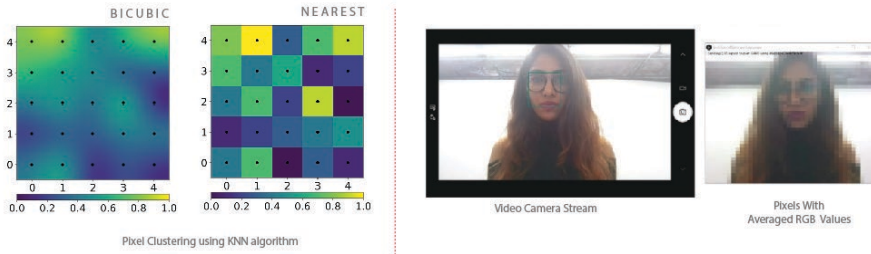


Figure 4. Pixel Clustering using KNN algorithm

Basic gestures such as- Move Up, Move Down, Move Left, Move Right and Stop (as seen in Figure 5) were recorded. Customisation of gestures is always an option at the user's disposal.

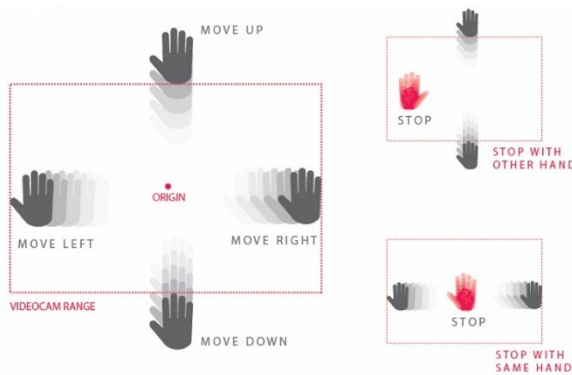


Figure 5. Examples of Taught Gestures

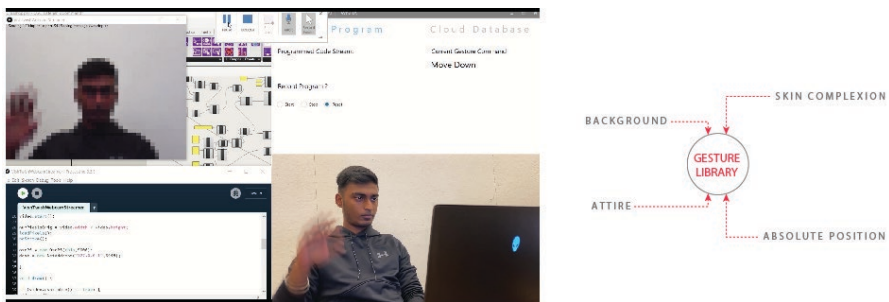


Figure 6. Parameter Considerations for building Gesture-Library

The library is built by taking into consideration factors like the colour of the background, attire of the user, skin complexion of the user, absolute position of user with respect to the camera and the position of gesture within the recording screen.

2.3. INTERFACE DEVELOPMENT

The two parts of the interface include creating a new program and execution of this created program. The interface gives the user an option to save the recorded program with a custom name.

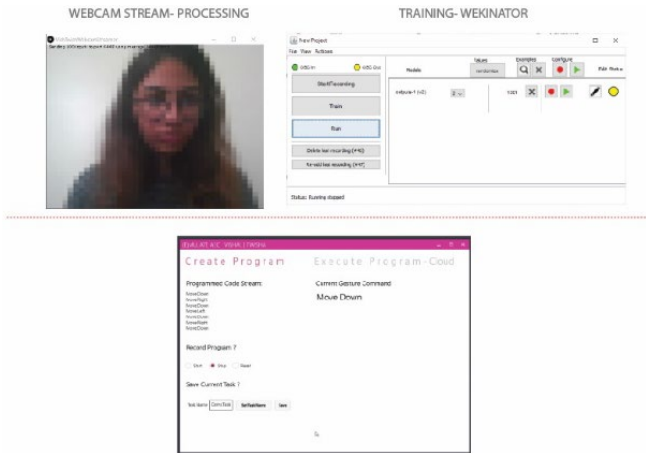


Figure 7. Webcam- Wekinator- Interface Interplay

The latter includes selection of the pre-saved tasks and selection of the robot for task execution. Once the model is trained for gestures, the interface detects the gestures from the library/repository and displays the same.

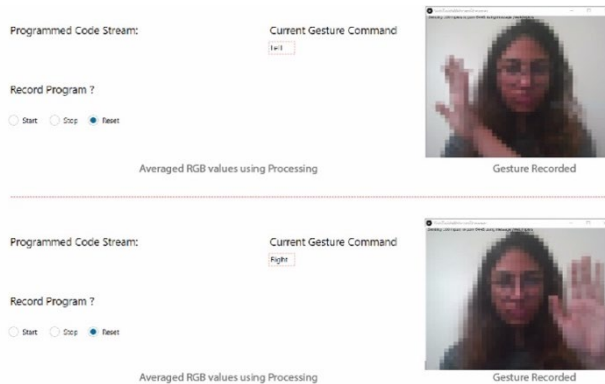


Figure 8. Testing recorded gestures on interface

(E)MULATE AEC: A GESTURAL PEDAGOGY AND CLOUD-BASED COLLABORATIVE MANAGEMENT PARADIGM FOR ON-SITE ROBOTICS IN CONSTRUCTION

A list of these recorded gestures is generated when a routine of gestures is performed by the user. The interface also generates RAPID scripts (a programming language for ABB industrial robot), which are simulated in the RobotStudio environment to check for execution errors.

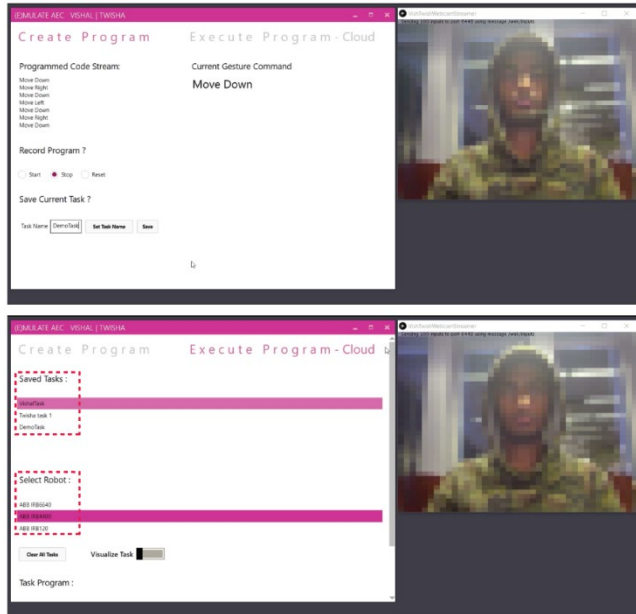


Figure 9. Gesture Recording within interface

The robotic motion is simulated using ‘HAL’, developed by Thibault Schwartz, a plugin for controlling industrial robots manufactured by KUKA, ABB and UR.

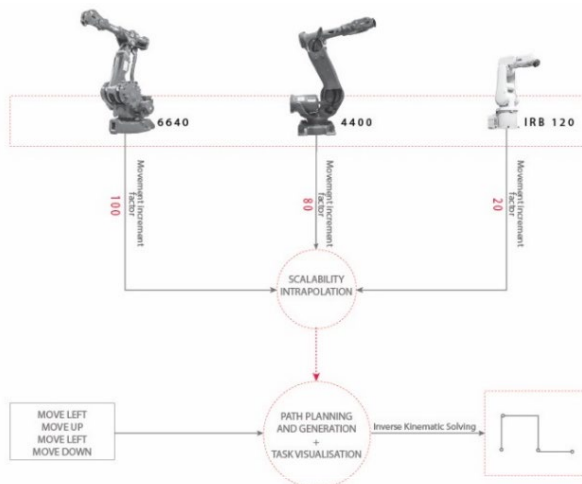


Figure 10. Tool path porting/ Scalability on Robots of Various Payloads

The interface prompts available robots for execution of the routine. All robots are differently configured and thus the path for each robot needs to be precisely scaled. The scalability interpolation feature integrated in the interface allows this kind of information exchange.

The scalability feature also facilitates the same task being replicated by different robots (six axis robots with varying payloads), as spatial and usability restrictions may be applicable to on-site robots. Network based web sockets and OSC based data streaming allows this interoperability of robots.

The robot simulations from RobotStudio are streamed onto the interface and once the desired simulation results are achieved, the files are transferred to the robot for actuation. This workflow makes it possible for the user to use interactions at the frontend which are developed on JavaScript, while leveraging Grasshopper developed scripts on the back end. Users thus interact with the robot through the gestural interface for motion commands, triggering the image processing workflow (explained earlier).

An interactive environment of this kind provides the opportunity to visually understand the relationship between changes in users' parameters, motion of the robot, and produced actions in real-time. An interactive environment of this kind provides the opportunity to visually understand the relationship between changes in users' parameters, motion of the robot, and produced actions in real-time. An interactive environment of this kind provides the opportunity to visually understand the relationship between changes in users' parameters, motion of the robot, and produced actions in real-time.

2.4. HARDWARE

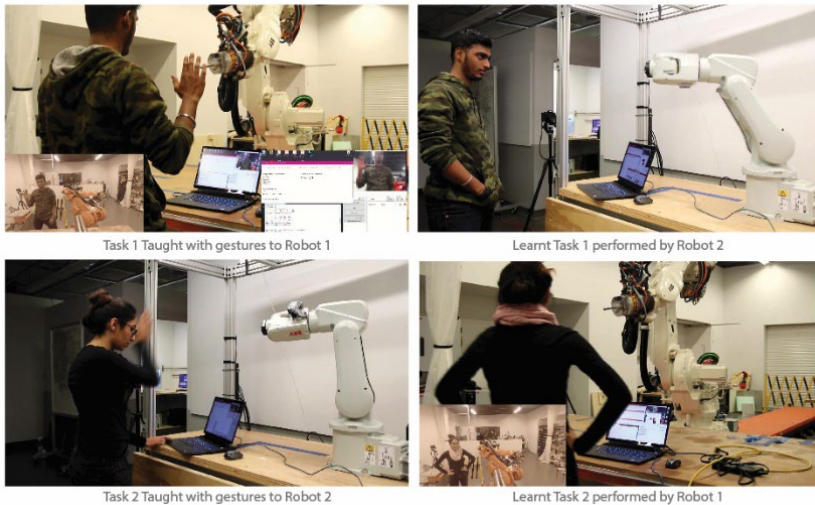


Figure 11. Robotic Telepresence: executing the (e)mulate framework.

Having task-specific end-effectors adds on to the complexity of managing and controlling the tool. Thus, an attempt to transition from job-specific, computer-controlled machinery to more generic production robots has been done. This generic character of the basic robotic hardware — that only becomes specific when equipped with a particular effector and tool — enables the design of new fabrication processes prior or in parallel to a specific project, and thus potentially challenges the conventional hierarchy and sequences still predominant in design and fabrication in today's architectural practice.

3. Discussion

As we look to develop this concept, we anticipate extending the application of the proposed model to different scenarios in the construction process. This approach can also be useful for fabrication workflows, such as additive manufacturing, complex pick-place workflows constituting a variety of components etc. This concept showcases a transition from job-specific computer-controlled machinery to more generic production robots. (Menges 2013) The machine only becomes specific when equipped with a specific effector and thus making a move towards a new way of looking at construction in architecture. The challenges inherent to the facilitation of more complex operations could be included as an added complexity and variety to the repository. These gestures could be task-specific or generalised, pertaining to operator-needs.

United Nations' Sustainable Development Goal 9 is "Build resilient infrastructure, promote inclusive and sustainable industrialization and foster innovation". While this research directly attempts to let the craftspeople and designers in the AEC industry benefit from the affordances of six axis robots, the larger idea is to contribute towards innovation and development by making technology accessible to all.

Acknowledgements

We thank Ardavan Bidgoli for giving us this opportunity and guiding us throughout the project. We are also grateful for resources provided at Carnegie Mellon University.

References

- Adam Higgins. (2019). *Robotics in Construction: A Brief History of Automation in the Industry*. Retrieved on 08-Feb-2020 from [:// connect.bim360.autodesk.com/robotics-in-constructionhistory](://connect.bim360.autodesk.com/robotics-in-constructionhistory).
- Bard, J., Gannon, M., Jacobson-Weaver, Z., Jeffers, M., Smith, B., & Contreras, M. (2014). *Seeing is doing: synthetic tools for robotically augmented fabrication in high-skill domains*.
- Bechthold, M. (2010). The return of the future: a second go at robotic construction. (pp. 116-121). *Architectural Design*, 80(4).
- Bidgoli, Ardavan, Daniel Cardoso-Llach. (2015). Towards A Motion Grammar for Robotic Stereotomy. (pp. 723-732.) The Association for Computer-Aided Architectural Design Research in Asia (CAADRIA).

- de Soto, B. G., Agustí-Juan, I., Hunhevicz, J., Joss, S., Graser, K., Habert, G., & Adey, B. T. (2018). *Productivity of digital fabrication in construction: Cost and time analysis of a robotically built wall*. (pp. 92, 297-311). Automation in Construction.
- Gerbert, P., Castagnino, S., Rothballer, C., Renz, A. and Filitz, R. (1992). Digital in Engineering and Construction: The Transformative Power of Building Information Modeling. (pp. 453-469.) Anderson, R.E. Social impacts of computing: Codes of professional ethics. *Social Science Computing Review* 10, 2.
- Howard, H. C., Levitt, R. E., Paulson, B. C., Pohl, J. G., & Tatum, C. B. (1989). Computer integration: reducing fragmentation in AEC industry. (pp. 18-32) *Journal of computing in civil engineering*, 3(1).
- Kim, M. J., Chi, H. L., Wang, X., & Ding, L. (2015). Automation and robotics in construction and civil engineering. *Journal of Intelligent & Robotic Systems*, 79(3-4), 347.
- Martin, C., & Leurent, H. (2017). *Technology and innovation for the future of production: Accelerating value creation*. In World Economic Forum, Geneva Switzerland.
- Menges, A. (2013). Morphospaces of robotic fabrication. In *Rob | Arch 2012* (pp. 28-47). Springer, Vienna.
- Saidi, K. S., Bock, T., & Georgoulas, C. (2016). *Robotics in construction*. In Springer handbook of robotics (pp. 1493-1520). Springer, Cham.
- Seventy Percent of Contractors Have a Hard Time Finding Qualified Craft Workers to Hire Amid Growing Construction Demand, National Survey Finds | Associated General Contractors of America. Retrieved from: <https://www.agc.org/news/2017/08/29/seventy-percentcontractors-have-hardtime-finding-qualified-craftworkers-hire-am-0>. Retrieved on 04-Feb-2020.
- Siciliano, B., & Khatib, O. (2016). *Robotics and the handbook*. In Springer Handbook of Robotics (pp. 1-6). Springer, Cham.

ROBOTIC 3D PRINTING OF MINERAL FOAM FOR A LIGHTWEIGHT COMPOSITE CONCRETE SLAB

PATRICK BEDARF¹, ANNA SZABO², MICHELE ZANINI³, ALEX HEUSI⁴, and BENJAMIN DILLENBURGER⁵

^{1,2,5} *Digital Building Technologies, ETH Zurich*

^{3,4} *FenX AG*

¹*bedarf@arch.ethz.ch, 0000-0003-2893-6743*

²*szabo@arch.ethz.ch, 0000-0002-8665-3779*

³*michele.zanini@fenx.ch* ⁴*alex.heusi@fenx.ch*

⁵*dillenburg@arch.ethz.ch, 000-0003-1229-9647*

Abstract. This paper presents the design and fabrication of a lightweight composite concrete slab prototype using 3D printing (3DP) of mineral foams. Conventionally, concrete slabs are standardized monolithic elements that are responsible for a large share of used materials and dead weight in concrete framed buildings. Optimized slab designs require less material at the expense of increasing the formwork complexity, required labour, and costs. To address these challenges, foam 3D printing (F3DP) can be used in construction as demonstrated in previous studies for lightweight facade elements. The work in this paper expands this research and uses F3DP to fabricate the freeform stay-in-place formwork components for a material-efficient lightweight ribbed concrete slab with a footprint of 2 x 1.3 m. For this advancement in scale, the robotic fabrication and material processing setup is refined and computational design strategies for the generation of advanced toolpaths developed. The presented composite of hardened mineral foam and fibre-reinforced ultra-high-performance concrete shows how custom geometries can be efficiently fabricated for geometrically complex formwork. The prototype demonstrates that optimized slabs could save up to 72% of total concrete volume and 70% weight. The discussion of results and challenges in this study provides a valuable outlook on the viability of this novel fabrication technique to foster a sustainable and resourceful future construction culture.

Keywords. Robotic 3d-printing; Mineral Foam; Stay-in-place Formwork; Concrete Composite; SDG 12.

1. Building Better with Less

The global status report for buildings and construction of the UN environment programme estimates that production emissions of building materials such as cement, steel, and glass are increasing and make up 10% of global carbon emissions (UN Environment Programme 2020). Approximately 7% originate from cement

production. Therefore, it is imperative to reduce the amount of cement in concrete construction for supporting the sustainable development goal of responsible consumption and production (SDG12).

Most concrete in construction is used today for standardized flat cast floor slabs that are oversized, monolithic elements for the favour of fabrication simplicity and cost-efficiency (Georgopoulos & Minson 2014). However, this emphasis on costs is short-sighted: slabs are not only the largest material consumers in buildings with the highest associated amount of embodied carbon, but also account for the highest mass concentration in structures. This in turn requires a stronger load-bearing structure of buildings and thus increases the energy and costs required for construction logistics.

Fortunately, there are many ways to optimize slabs for using less materials and being lighter. A standardized approach bases on the placement of hollow forms in areas of the slab where no structural strength is required; subsequently the remaining area is filled with a concrete cast (“BubbleDeck” 2021; “Cobiax” 2021). For non-standard slabs this is more challenging because custom geometrically complex concrete formwork is typically manufactured by means of wasteful subtractive processes, they are not reusable and require more material and labour which results in higher costs.

Additive manufacturing (AM) in construction has changed these sustainability relationships because complex shapes can be manufactured without moulds, production-specific tooling, and additional workforce. Thus, several studies used AM techniques to produce the formwork for innovative, material-efficient, lightweight concrete slabs (Jipa and Dillenburger 2021; Hansemann et al. 2021).

This paper presents the design and fabrication of a lightweight composite concrete slab prototype using 3D printing (3DP) of mineral foams combined with concrete casting. It is the next step in the body of research investigating foam 3D printing (F3DP) for architectural scale applications. This line of reasoning has been already explored in a preliminary study using sintered mineral foams for a composite facade shading panel (Bedarf, Martinez Schulte, et al. 2021).

The current study advances the material and robotic fabrication system and demonstrates the fabrication of 24 freeform stay-in-place formwork elements that are used with fibre-reinforced ultra-high-performance concrete (UHPFRC) to create a 2 x 1.3 m ribbed concrete slab. Computational design workflows and advanced toolpath generation are presented along with the fabrication documentation. The resulting prototype shows a high degree of material-efficiency with 72% savings in concrete and 70% savings in weight when compared to monolithic slabs. The advantages and challenges of this novel fabrication method are discussed and complemented with strategies for future improvements.

2. Additive Foam Construction

Foams are particularly suitable materials for formwork applications due their high strength-to-weight ratio and good machinability. Conventionally, blocks of foam are cut or milled into complex shapes for custom formwork with high amounts of waste from chipping and offcuts. In contrast, F3DP enables the use of porous construction materials for automated, waste-free materialization of geometrically complex building parts (Bedarf, Dutto, et al. 2021).

This facilitates the fabrication of stay-in-place formwork for custom geometrically optimized building components. Additionally, the excellent heat and sound insulating properties of foams can improve the functionality of wall and slab elements. Thus, F3DP enables the production of innovative composite structures that are lightweight, easier to transport and handle, and use less material while increasing labour efficiency and work safety.

Several studies previously investigated F3DP for stay-in-place formwork. Expanding polyurethane spray foam was used to build the stay-in-place formwork for a dome prototype (Keating et al. 2017) and a single-storey residential house (Furet, Poullain, and Garnier 2019). However, more sustainable, cement-free, and inherently non-flammable mineral foams are available for F3DP and were used in this research.

3. Material and 3D Printing System

The main component of the sustainable mineral foam used in this project is fly ash, an industrial by-product of coal combustion. In an alkaline environment fly ash sets and hardens like cement developing its final strength after mild thermal curing (no need of sintering) (Palomo, Grutzeck, and Blanco 1999; Fernández-Jiménez and Palomo 2005; Xu and Van Deventer 2000).



Figure 1. The robotic F3DP setup with the stationary foam generator in the foreground connected to the industrial robot in the background.

The material preparation for printing starts with mixing fly ash, water, and admixtures in a planetary mixer (up to 40L of slurry). Then the slurry and the hardener are pumped continuously at a specific ratio into the foam generator that intermixes and foams these components. The resulting hardening foam travels in a flexible hose from the foam

generator to the ABB IRB 1600 robotic arm which performs the printing on rigid wooden plates as print beds with 55 x 95 cm footprint (Fig. 1). The robotic trajectory and the speed for printing is defined with the digital path generator tool that is described in the next section.

At each experiment, the setup allows for producing 100 L foam with $< 500 \text{ kg/m}^3$ wet densities. The foam is deposited with 110 mm/s robotic printing speed with an extrusion rate of 2.1 L/min. After printing, the elements are stored at 40 °C for the first day in high humidity (~70%RH) and for an additional 6 days at low humidity (~45%RH).

4. Design of Geometry and Print Path

This study focuses on the application of F3DP for a non-standardized building element that is tailored to a specific building context. Therefore, the generic geometry of the slab prototype is generated using methods based on the ribbed floor slab systems of Pier Luigi Nervi (Halpern, Billington, and Adriaenssens 2013). More specifically, isostatic lines derived from the principal stress pattern occurring in a specific boundary and loading condition are used to define the location of structural floor ribs. This approach uses ribs in tension in contrast to other studies that target optimized vaulted slabs as compression-only structures (Jipa et al. 2019).

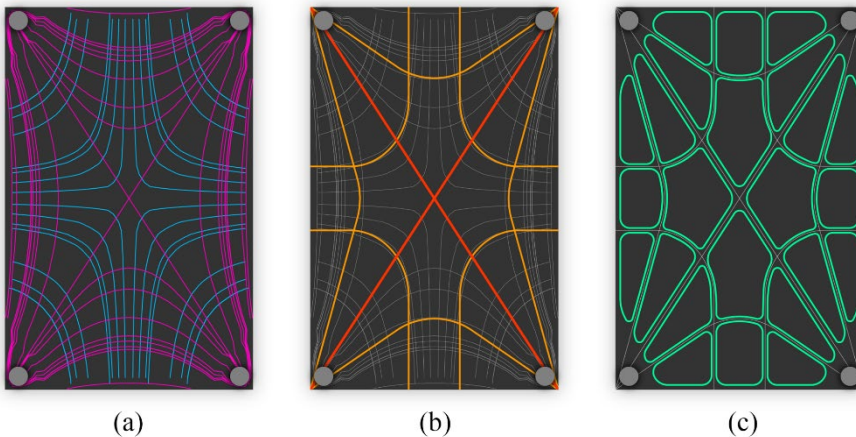


Figure 2. Slab layout design stages: a) principal stress pattern derived from FE analysis, b) simplified hierarchical rib lines, c) final formwork elements.

The Finite Element (FE) analysis is conducted using the Millipede Plugin for Rhino3D/Grasshopper. The FE model resembles a rectangular 2 x 1.3m concrete slab with a thickness of 14 cm. The load case is defined with an evenly distributed area load of 2 kN/m², the estimated dead load, and 4 point supports, one in every corner. Simplified hierarchical rib lines are derived from the resulting principal stress pattern and define the final stay-in-place formwork geometry (Fig. 2). They segment the slab into equal sized regions that fit into the robotic F3DP fabrication space.

The formwork for the ribs consists of 24 foam elements with 12 pairs of identical geometry due to the symmetric load case and stress pattern. All formwork elements are 10 cm high and are covered with 4 cm of concrete, which results in 14 cm overall thickness of the slab prototype. Their outline curvature is optimized for the resolution of the F3DP process and sharp corners are reduced to avoid potential over-extrusion. The ribs are articulated in a hierarchy of 25 and 40mm thickness.

For printing all 24 formwork elements, their geometry needs to be processed, usually referred to as “slicing”, which generates the print paths for the specific 3DP process. In the case of the presented F3DP process, this is computed with python scripts within the Rhino/Grasshopper environment using the COMPAS framework (“Compas” 2020). Thus, formwork geometries can be selected within the CAD environment, processed, and the resulting print path and fabrication metrics visualized (Fig. 3).

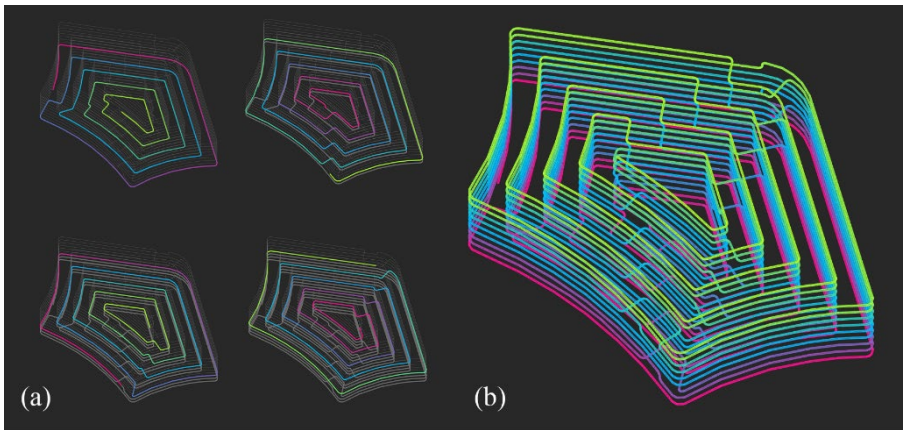


Figure 3. Print path visualization showing (a) sequence of different layers and (b) all layers of sliced print geometry.

The print path generator calculates the printing speed as a function of the input parameters layer height, layer width, and material flow rate. A vertical pre-scaling factor of 1.2 is applied to the print geometries, which was established empirically to improve dimensional accuracy (Bedarf, Szabo, et al. 2021). Based on the input variables, several infill patterns can be selected. Since this study aims to print solid formwork elements, a direction-continuous connected Fermat spiral (Zhao et al. 2016) is used. It extends the work of Zhao et al. for layered 3DP with a direction-continuous approach that minimizes changes of the print path trajectory when transitioning between layers.

The fabrication data is generated in the JSON file format consisting of robot targets and robot speed information. Robot operation is executed using the COMPAS framework and the COMPAS_RRC extension. During fabrication the F3DP processing equipment is operated manually, and the material flow rate assumed constant. In case deviations occur, minor adjustments can be tuned by the operator in scaling the programmed speed values.

5. Fabrication of the Prototype

Fabricating the demonstrator as a ribbed concrete slab prototype required 4 major steps: printing the foam elements, preparing a formwork with the foam elements, casting concrete, and removing the formwork (Fig. 4).

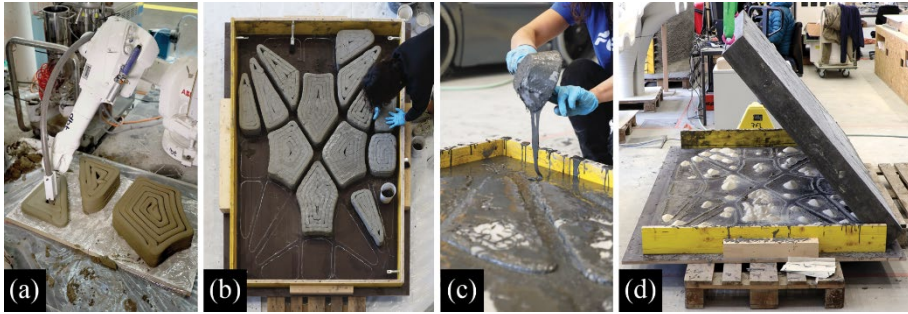


Figure 4. Fabrication steps: (a) printing foam elements, (b) preparing temporary timber formwork and stay-in-place foam elements, (c) casting UHPFRC, and (d) removal of temporary formwork

First, the 24 custom-shaped foam elements were printed during 3 sessions, in less than 10 hours (deadtimes not considered). The smallest prototype with 5.5 l volume required 2:45 min printing time while the largest of 13.2 L took 6:05 min to fabricate. In total, 8 print beds were used accommodating a set of 3 prototypes each. For each print bed a clean hose was installed. The fresh foam prototypes were put into the oven immediately after production to cure and dry for a week resulting in ~ 350 kg/m³ density. The dimensional accuracy assessment of the elements has been presented in a previous publication (Bedarf, Szabo, et al. 2021).

Second, a simple wooden formwork was built with the inner dimensions of the concrete slab prototype, 2 x 1.3 X 0.14 m. Next, the layout of the foam elements was projected onto the bottom surface of the formwork and transferred with chalk as an outline. Then, the cured foam elements were positioned one-by-one and sealed at the perimeter of their bottom plane. The sealing was applied manually with a mixture of sand, water, and fly ash with the goal to prevent the lightweight foam elements from floating during casting. At last, dry sand is poured onto the foam elements to fill any potential gap where the concrete could creep in. Each foam element required 15 minutes of manual work, which resulted in 6 hours of preparation time for all 24 parts.

Third, an UHPFRC mix was used for the casting with the formulation and mixing procedure described in (Jipa and Dillenburger 2021). The concrete was prepared in 30 l batches and gradually filled into the formwork with a team of 6 people. First, the space between the foam elements was filled at a low and spatially consistent casting rate and only subsequently the elements were covered with a continuous layer of concrete. The prototype was covered with a plastic foil and left curing for 3 weeks in the unheated fabrication hall.

Finally, the wooden formwork was removed, and the slab prototype was turned upside down to display the ribbed geometry defined by the printed formwork. The dried sealing and the loose sand around the foam elements were flushed out with

compressed air to create the final appearance.

6. Evaluation, Challenges, and Future Improvements

The slab prototype (Fig. 5) demonstrates the novel fabrication technology combining conventional concrete casting and F3DP of formwork. The custom printed sustainable mineral foam elements define the material-efficient ribbed geometry of the concrete. Typical rib thicknesses were chosen along with the use of UHPFRC, a high-performance load-bearing material in the construction industry. The structural performance of the slab prototype is expected to be similar to the ribbed slabs that are produced with conventional formwork made from timber or polystyrene (Liew et al. 2017). Therefore, no structural assessment was conducted in this study. Instead, the F3DP process and the consecutive fabrication steps of the slab prototype were evaluated.

Although no structural assessment was conducted in this study, using F3DP for custom stay-in-place formwork is highly relevant. It enables the feasibility of building material-efficient ribbed slab geometries through a fabrication method that significantly reduces material waste in the production process. The resulting prototype shows that 72% of the concrete can be substituted with sustainable mineral foam and the total mass can be reduced by 70%.

The F3DP system presented in this study used alkali activation to harden the foam. This approach is less energy-intensive than consolidation via sintering and allows to fabricate larger elements with lower densities saving material in the slab prototype. Additionally, both the foam production and the printing were faster compared to any syringe foam extrusion setup. Thus, it provides a major improvement compared to the previous study (Bedarf, Martinez Schulte, et al. 2021).

The robustness of the printing process was sufficient to produce a significant number of foam elements for a real-scale demonstrator. The printing was reliable for different element sizes and layer times. However, the weak point of the setup was the hose connecting the foam generator with the robot. It had to be changed regularly during production due to the accumulation of hardening material on its inner surfaces. Furthermore, the hose constrained the robot movements, thus limiting the building area. Future improvements of the setup include the development of an integrated robotic print head and an optimized tempered environment for curing larger prints.

The foam elements showed enough strength to be easily handled and sufficient precision to fulfil the requirements of concrete construction. Although the freshly hardening material presents an early-age shrinkage, dimensional deviations to the target geometry could be minimized through the implementation of sensing routines and a geometrical pre-scaling factor (Bedarf, Szabo, et al. 2021). Further improvements on dimensional accuracy could be possible through live feedback for process supervision and correction.

The preparation for the casting started with the fast and simple assembly of the wooden frame and positioning the printed foam. However, sealing the foam elements with wet sand was labour and time intensive. Additionally, this manual step increases the risk of possible inaccuracies for the final formwork layout. This could be improved with further detailing the printed geometries and the addition of alignment details, such

as peripheral notches. Moreover, the integration of subsystems would be possible with printed installation details such as cavities and tunnels.

At last, the environmental impact of the resulting composite element could be further reduced by using a more sustainable concrete mix than UHPFRC as structural filler. Cement-free mineral foams with high density and compressive strength could be used as structural material. Assessing the thermal and structural properties of the cured foams will help to inform the distribution of different densities within one printed part. The resulting mono-material building component with hierarchically graded porosity would facilitate circular construction through simplified recycling. Additionally, graded mono-material systems contain no sudden material interfaces and feature smooth thermal gradients, which is beneficial for building enclosures such as slabs and walls.

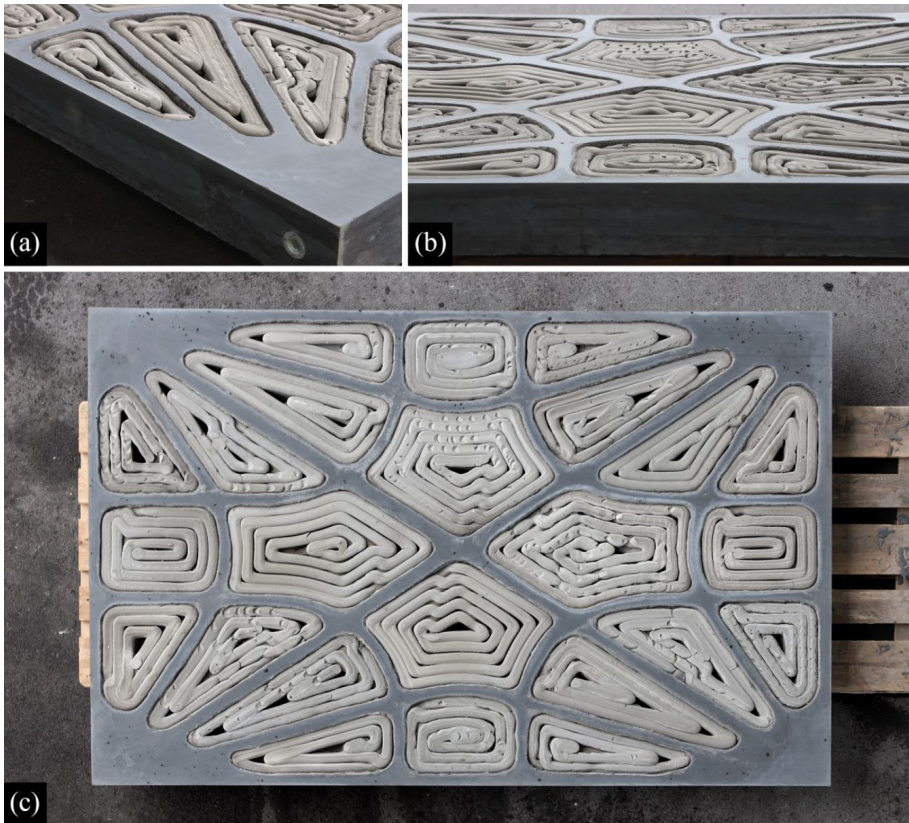


Figure 5. The finished slab prototype flipped with exposed underside. (a-b) detail closeups, (c) birds eye view

7. Conclusion

This paper presents a novel fabrication technique based on F3DP for producing functional stay-in-place formwork of a lightweight composite concrete slab. The

resulting prototype is an innovative combination of sustainable mineral foams and UHPFRC that shows great potential for saving materials and embodied carbon emissions. A robust procedure for F3DP, material processing, and environment control could be achieved. As a result, construction-scale objects can be fabricated with accuracy suitable for concrete construction. The digital workflow for print geometry processing and path generation for robotic F3DP produces reliable results for various formwork shapes.

This novel fabrication approach is envisioned to significantly impact the responsible and sustainable consumption of resources and energy. It enables the manufacturing of geometrically complex foam elements that were previously unfeasible and wasteful to produce with conventional methods. As shown in this study, these foam elements are suitable for stay-in-place formwork applications for building elements with shapes optimized for low mass, low material consumption, and thus low embodied carbon. This reduces the amount of required resources twofold: i) the building element itself needs less material and ii) the entire load-bearing structure as well, since less weight must be supported. Furthermore, this has a positive impact on logistical efforts for construction.

Moreover, custom foam elements produced with F3DP can be used as insulating building elements directly. Applications can cover the entire spectrum of building enclosures: from slabs, to roofs, walls, and transitional elements. F3DP would significantly save material for those elements that feature complex geometries, such as curved facade panels and thermo-structurally optimized walls. Additionally, to the material-savings, this application could further contribute to the construction of energy-efficient buildings.

Consequently, the proposed combination of innovative materials, novel fabrication techniques, and geometrically optimized building elements addresses the responsible consumption of both - energy and resources - for future sustainable construction.

Funding

This research was supported by the Innosuisse Impulse programme (Grant number 41905.1 IP-EE), the ETH Research Commission (Grant number ETH-01 19-2), and the NCCR Digital Fabrication (Grant number 51NF40-141853).

References

- Bedarf, P., Dutto, A., Zanini, M., & Dillenburger, B. (2021). Foam 3D printing for construction: A review of applications, materials, and processes. *Automation in Construction*, 130, 103861. <https://doi.org/10.1016/j.autcon.2021.103861>
- Bedarf, P., Martinez Schulte, D., Senol, A., Jeoffroy, E., & Dillenburger, B. (2021). Robotic 3D Printing of Mineral Foam for a Lightweight Composite Facade Shading Panel. In *26th International Conference of the Association for Computer-Aided Architectural Design Research in Asia, CAADRIA 2020* (pp. 603–612). The Association for Computer-Aided Architectural Design Research in Asia (CAADRIA).
- Bedarf, P., Szabo, A., Zanini, M., & Dillenburger, B. (2021). Machine Sensing for Mineral Foam 3D Printing. In *International Conference on Intelligent Robots and Systems: Workshop Robotic Fabrication, IROS 2021*. <https://doi.org/10.3929/ethz-b-000506097>

- BubbleDeck. (2021). *The Original Voided Slab*. Retrieved May 11 2021, from <https://www.bubbledeck.com>
- Cobiax. (2021). *Voided flat plate slab technologies available worldwide*. Retrieved May 11 2021, from <https://www.cobiax.com/intl/en/>
- Compas. (2020). Retrieved May 11 2021, from <https://compas.dev/index.html>
- Fernández-Jiménez, A., & Palomo, A. (2005). Composition and microstructure of alkali activated fly ash binder: Effect of the activator. *Cement and Concrete Research*, 35(10), 1984–1992. <https://doi.org/10.1016/j.cemconres.2005.03.003>
- Furet, B., Poullain, P., & Garnier, S. (2019). 3D printing for construction based on a complex wall of polymer-foam and concrete. *Additive Manufacturing*, 28, 58–64. <https://doi.org/10.1016/j.addma.2019.04.002>
- Georgopoulos, C., & Minson, A. (2014). *Sustainable concrete solutions*. Wiley-Blackwell.
- Halpern, A. B., Billington, D. P., & Adriaenssens, S. (2013). The Ribbed Floor Slab Systems of Pier Luigi Nervi. *Proceedings of the International Association for Shell and Spatial Structures (IASS)*, 7. http://formfindinglab.princeton.edu/wp-content/uploads/2011/09/Nervi_ribbed_floors.pdf
- Hansemann, G., Schmid, R., Holzinger, C., Tapley, J. P., Peters, S., Trummer, A., & Kupelwieser, H. (2021). Lightweight Reinforced Concrete Slab: 130 different 3D printed voids. *CPT Worldwide - Construction Printing Technology*, 2021(2), 68.
- Jipa, A., Calvo Barentin, C., Lydon, G., Rippmann, M., Chousou, G., Lomaglio, M., Schlüter, A., Block, P., & Dillenburger, B. (2019). 3D-Printed Formwork for Integrated Funicular Concrete Slabs. *Proceedings of the IASS Annual Symposium 2019*, 10. https://www.researchgate.net/publication/335175125_3D-Printed_Formwork_for_Integrated_Funicular_Concrete_Slabs
- Jipa, A., & Dillenburger, B. (2021). 3D Printed Formwork for Concrete: State-of-the-Art, Opportunities, Challenges, and Applications. *3D Printing and Additive Manufacturing*, 00, 24. <https://doi.org/10.1089/3dp.2021.0024>
- Keating, S. J., Leland, J. C., Cai, L., & Oxman, N. (2017). Toward site-specific and self-sufficient robotic fabrication on architectural scales. *Science Robotics*, 2(5), 1-15. <https://doi.org/10.1126/scirobotics.aam8986>
- Liew, A., López, D. L., Van Mele, T., & Block, P. (2017). Design, fabrication and testing of a prototype, thin-vaulted, unreinforced concrete floor. *Engineering Structures*, 137, 323–335. <https://doi.org/10.1016/j.engstruct.2017.01.075>
- Palomo, A., Grutzeck, M. W., & Blanco, M. T. (1999). Alkali-activated fly ashes: A cement for the future. *Cement and Concrete Research*, 29(8), 1323–1329. [https://doi.org/10.1016/S0008-8846\(98\)00243-9](https://doi.org/10.1016/S0008-8846(98)00243-9)
- UN Environment Programme. (2020). Global Status Report for Buildings and Construction. Retrieved May 11 2021, from https://globalabc.org/sites/default/files/inline-files/2020%20Buildings%20GSR_FULL%20REPORT.pdf
- Xu, H., & Van Deventer, J. S. J. (2000). The geopolymerisation of alumino-silicate minerals. *International Journal of Mineral Processing*, 59(3), 247–266. [https://doi.org/10.1016/S0301-7516\(99\)00074-5](https://doi.org/10.1016/S0301-7516(99)00074-5)
- Zhao, H., Gu, F., Huang, Q.-X., Garcia, J., Chen, Y., Tu, C., Benes, B., Zhang, H., Cohen-Or, D., & Chen, B. (2016). Connected fermat spirals for layered fabrication. *ACM Transactions on Graphics*, 35(4), 1–10. <https://doi.org/10.1145/2897824.2925958>

DIGITAL DESIGN AND FABRICATION OF A 3D CONCRETE PRINTED FUNICULAR SPATIAL STRUCTURE

HAO WU¹, ZIYAN LI², XINJIE ZHOU³, XINYU WU⁴, DINGWEN BAO⁵ and PHILIP F. YUAN⁶

^{1,3,6}*College of Architecture and Urban Planning, Tongji University*

^{2,4,5}*School of Architecture and Urban Design, RMIT University*

¹*2032186@tongji.edu.cn, 0000-0002-0503-1696*

²*S3764754@student.rmit.edu.au, 0000-0002-2027-9227*

³*xinjie_zhou@tongji.edu.cn, 0000-0002-2543-2307*

⁴*S3701802@student.rmit.edu.au, 0000-0002-0616-6787*

⁵*nic.bao@rmit.edu.au, 0000-0003-1395-8747*

⁶*philipyuan007@tongji.edu.cn, 0000-0002-2871-377X*

Abstract. In recent years, additive manufacturing (AM) and 3D concrete printing technologies have been increasingly used in the field of construction engineering. Several 3D concrete printing bridges were built with post-tensioning technology. However, the current post-tensioned 3D concrete printing projects are mostly in a single direction of force. There are fewer cases of concrete printing funicular spatial structures, and most funicular spatial structures are currently manufactured by casting-in-place in formwork. This paper presents a case of manufacturing spatial 3D concrete printed structure using post-tensioned technology with multiple force direction. The design of the non-parallel printing path, the joints between single units, and the post-tensioned steel cable system in the design and research process are discussed. A funicular spatial structure is built, and a method of manufacturing 3DCP funicular spatial structure is proposed.

Keywords. 3D concrete printing; Robotic fabrication; Prestressed concrete; Funicular spatial structure; Structural optimization; SDG 9; SDG 11; SDG 13.

1. Introduction

In the last decade, 3D concrete printing has demonstrated its potential to change the traditional construction way by printing concrete walls without conventional formworks (Le et al., 2012), which creates new possibilities in both architectural design and environmental protection. The application strategies for 3D concrete printing in building construction can be generally divided into on-site printing (Scott, 2020) (Mechtcherine, 2019) and prefabricated assembly. For prefabricated assembly 3DCP project, post-tensioned technology is widely applied to make separated printed units become a whole. The past five years have seen the completion of several post-tensioned 3D concrete printing bridge projects (Vantighem et al., 2020) (Salet et al.,

2018) (Zhan et al., 2021). However, these projects are tensioned in a single direction, which is why all are beam-like structures, namely bridges.

Typically, elements printed in concrete are achieved by extruding wet paste-material in layers which eventually build up the desired shape, which is first described as Contour Crafting in 2004 (Khoshnevis et al., 2004) and has been popular still now. However, the CC technology is limited to vertical extrusion, hence yielding 2.5D topologies (vertical extension of a planar shape) (Gosselin et al., 2016). Concrete units printed in this way are best stressed in the vertical direction, which is why many 3D printed structures are tensioned in one direction.

From the research of Gosselin, the method of non-parallel printing is described, which makes it possible to realize multi-angle printing (Gosselin et al., 2016). The arched masonry structure from BRG et al. (2021) fully demonstrates the advantages of this printing method in building funicular spatial structure. Separated units are printed in layers orthogonal to the main structural forces and they compress each other to form a compression-only funicular structure. In this arched masonry structure, there are no joints connecting the separate units, yet joint design is important in post-tensioned spatial structures.

The research project described in this paper is committed to exploring how to achieve post-tensioned 3DCP funicular spatial structure. Macroscopically, post-tensioning technology has been applied to achieve the efficiency and rationality of the structure. At the micro-level, non-parallel printing technology is applied to realize the printing of all separated units. A set of steel plate system for positioning and a set of post-tensioned pre-stressed steel bar system were applied. Finally, an experimental funicular spatial structure with a range of about 6m*6m*3m was built. The project discussed the rationality of the structural design of large-scale concrete printing funicular spatial structure and how to use these techniques to achieve the complexity of the printing structure.

2. Research and Prototyping

2.1. PROTOTYPING DESIGN

In order to verify the feasibility of prestressed 3D concrete printed spatial structure and to discover potential problems during installation, a simple small-scale experimental prototype was designed, and the printing and installation tests were carried out.

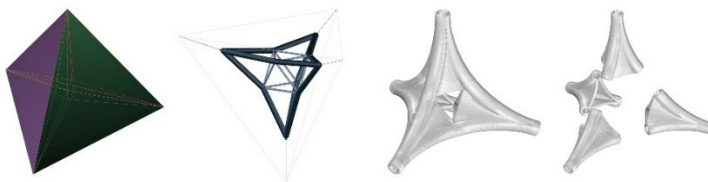


Figure 1. The development of the prototyping design

This simple funicular spatial structure is designed using PolyFrame (Masoud et al. 2019), a Grasshopper plugin based on 3D graphic statics. This plug-in is good at

constructing purely compressed space structures. While in this prototype, prestressed steel bars can be used to simulate this compressed state. It is designed into a uniform structure composed of four identical units and four curved steel bars. The four concrete members are compressed tightly together to form a stable structure that presses and restrains each other. Figure 1 shows the development of the prototyping design.

2.2. PRINTING AND ASSEMBLY TEST

The segmented units are geometries with multiple direction, which means that they are non-developable curved surface. In Lim et al.'s (2020) work, a method of printing a non-developable curved surface is described (Lim et al., 2020). Compared to traditional method, it required temporary fabric formwork supported by height-adjustable rods. Lim has proposed in his theory within this technology, which is to print with saddle and dome surface on the temporary fabric formwork. The limitation of this kind of method is that a specific height-adjustable system is required, and each piece of printing will consume one piece of fabric. In addition, the temporary fabric formwork has relatively low accuracy and hard to control, which will increase the printing error and may eventually lead to the failure of the entire structure when assembly.

In prototype design, a method of printing the base with concrete material is proposed. As shown in Figure 2, a triangular base was designed according to the shape of the printed segment in this experiment. This base has three inclined surfaces that need to be printed with a specific printing path. After base printing, a piece of plastic film was in use to separate the unit from the base that it attaches to. With this technique, four identical structural segments are printed.

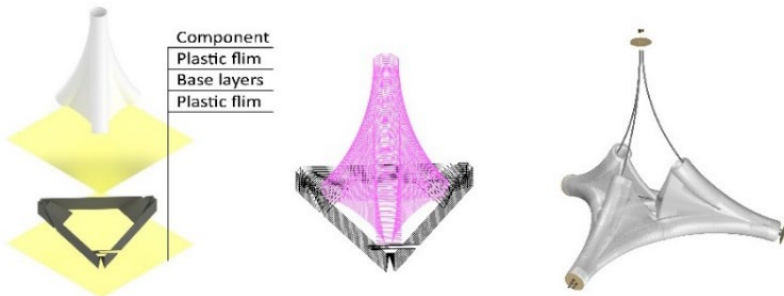


Figure 2. Left: printing process, Mid: toolpath, Right: steel bar system

2.3. PROBLEM

Although the printed base can ensure that the inclinations of the three slope surfaces of each unit are accurate. However, from a micro perspective, as it's shown in Figure 3, the inclined surface of the printed base is stepped. The bottom of the final printed object cannot fit this inclined curved surface completely, which makes the connecting surface of the prints uneven.

Figure 3 shows that because the nozzle has an unchangeable size, the printing height of the first layer needs to be raised to prevent the print head from rubbing against the inclined surface of the base. Therefore, the first layer of the printed component is obviously wider, and the layer height is also different from others.

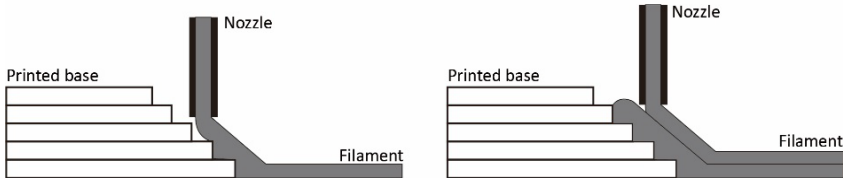


Figure 3. A micro view of the filament

Due to the superposition of the previous two reasons, the stability and accuracy of the entire prototype structure were declined from expectation. When the printed components were assembled, the connecting surface could not be fully attached. This leads to insufficient assembly accuracy of the printed parts and affects structural stability. Figure 4 describes the printing process and the assembly process.

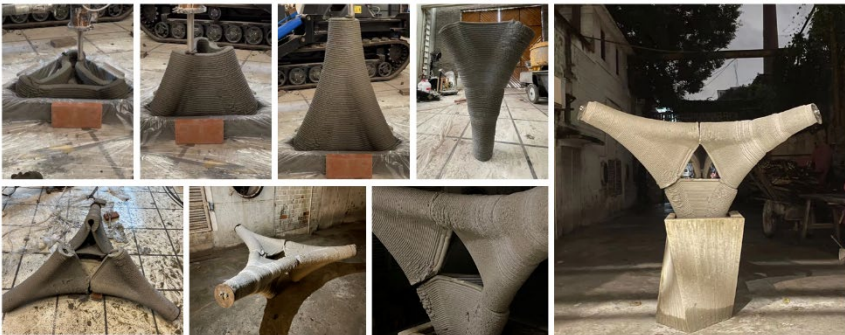


Figure 4. Record of printing and assembly process

3. Computation design

3.1. MULTI-TOOL COLLABORATIVE DESIGN

The design result is attributed to the collaboration of two software, Polyframe, which generates a purely compressed frame, and Ameba (Xie et al. 2016), which calculates the volume through topological optimisation. With the help of PolyFrame, a system of purely compressed funicular spatial structure is created upon the basis of 3D graphical statics. Then optimization based on Ameba was introduced into the design. Some members were set as non-designed regions under the same boundary conditions, and then the Ameba algorithm was used, followed by 90 iterations. Figure 5 shows the development of the design process. As a result, an efficient spatial structural system based on mesh optimization was obtained, which predicts the basic material distribution of the final pavilion shape and improves the feasibility of concrete 3D printing.

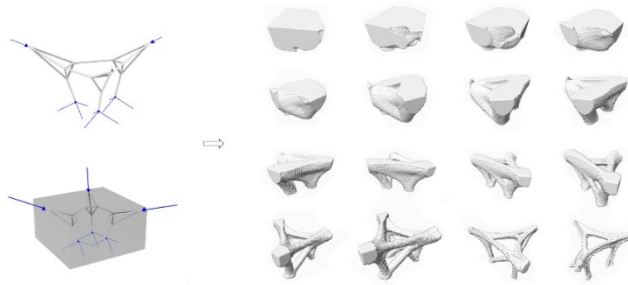


Figure 5. Iterations in Ameba

3.2. SEGAMENTATION

The final structure design needs to be divided into small pieces for printing. The direction of the force, the maximum printing height, and the maximum printable inclination are 3 main factors that need to be considered during the segmentation process. Finally, the whole structure is divided into 18 segments, each of which is less than 1500mm in height. To meet the requirements of reliable printing, every segment has at least one horizontal surface, with a maximum inclination angle no more than 45 degrees. Each column and beam are divided into two and three segments respectively. The remaining three outward heads each become an independent piece. Each segment is attached with one or two steel plates, which are used for positioning in assembly process. The division of the segments, the position and the serial number of steel plates are shown in Figure 6.

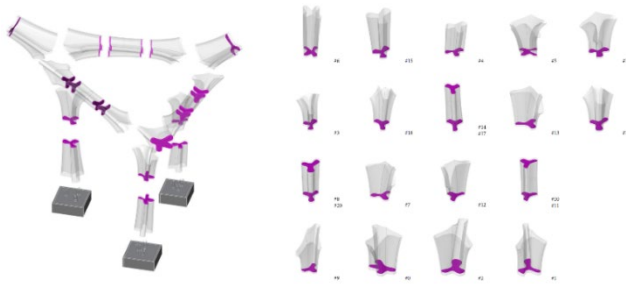


Figure 6. Segmentation

3.3. PRESTRESSED STEEL BAR

To simulate the calculation results of PolyFrame, 9 steel bars were added to this system. Three of them are connected to the column foundation from the overhanging ends and each beam has two steel bars. All steel bars are pre-stressed by post-tensioning.

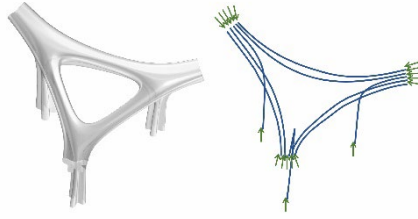


Figure 7. Nine steel bars

3.4. POSITIONING STEEL PLATE

This funicular structure is post-tensioned in multiple force direction, which create another difficulty in accurate positioning. The joints between single units need to be specially designed. 3D printing concrete ink usually has good fluidity during movement and satisfying standing behavior at static state (Zhang et al. 2018). The printing filament is in a wet-state and maintains a certain degree of plasticity for a certain period of time after extrusion. Exploit this property of 3DCP filaments, some scholars have demonstrated the feasibility of implanting micro cable during filaments deposition process (Ma et al. 2019) (Li et al. 2020). In this study, a method of implanting steel plates as positioning joints between the units during the printing process was employed.

Each segment has at least one steel plate, the segment in the middle of the beam has two steel plates. The printing of a single unit is paused during the printing process and the steel plates are then manually placed. After inserting steel plate, the printing process is continued. The concrete and the steel plates will become a whole when concrete gain strength.

The thickness of the steel plate processed by CNC milling machine is 4mm. There are two kinds of holes with diameters of 20mm and 50mm on the steel plate. 20mm holes are used for steel pipe welding during assembly. It plays the role of positioning between segments. The 50mm hole is where the steel bar passes through. The edge of the steel plate is designed to be zigzag, as shown in Figure 8, so that the steel plate and the concrete printing filament can be combined more firmly. The jagged edges make the filaments on both sides have a larger contact area. This is because, through the early printing experiments, it was found that the steel plate with a smooth edge will cause poor connection of the filaments separated by the steel plate. The printing segment brokes easily at where the smooth steel plate was placed.



Figure 8. Steel plates with zigzag edges

4. Robotic fabrication

4.1. TRAJECTORY DESIGN

The final structure is a multi-directional pre-stressed structure. The segmented unit is a multi-directional block, which cannot be printed by the traditional horizontal printing path. As shown in Figure 9, three sets of non-parallel planes are used to cut the printed units and then the intersected curves are connected to form the final path. Filaments are printed in non-uniform and non-parallel layers. The printing layers are orthogonal to the prestressed tensile direction so that the printing filaments within the structural unit can be tightly compressed together.



Figure 9. Toolpath generation

4.2. PRINTING PROCESS

In the prototype experiment, the bottom of the printing segments was uneven which will cause poor integrity when assembly. The accuracy of the connecting faces is not only an important factor but also an essential guarantee for the structure stability.

To achieve good connectivity, the contact surface of each unit must be flat. Thus, the printing strategy with the multi-directional side down in the experiment is abandoned. Every unit is printed with one-direction side down to obtain a rational flat surface connected with the base. This contact surface allows the unit to be stressed evenly during the printing process to ensure stability of the final structure.

The printing process is described in Figure 10:

- Place the tray (for the convenience of subsequent transportation)
- Lay the plastic film
- Print the base and pause for a horizontal surface)
- Lay the plastic film (for the subsequent separation of the base and the unit)
- Print the first 4 layers of the unit and pause
- Manually place the steel plate
- Print the remaining part
- Manually place the 2nd steel plate (for units in the middle of the beam)
- Print the remaining part (for units in the middle of the beam)

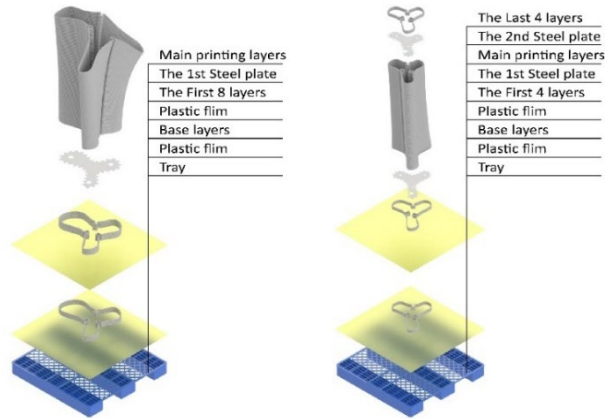


Figure 10. Printing process

4.3. ASSEMBLY

After all the printing work is completed, each unit has been cured for at least 14 days to ensure that it has obtained sufficient early yield strength. The installation process is as follows:

- What installed first is three pillars. The steel bars inside the three pillars are welded to the foundation. Inside the three pillar legs, 300mm-thick mortar is poured to connect the pillars with the embedded steel components.
- Install the second section of the column.
- The three beams are assembled on the ground respectively, and then the three beams are hoisted up.
- The three overhanging units are put on last.

The connections between the units are installed with anti-collision strips with a width of 30mm. The steel pipes are welded to the steel plate in the 20mm hole, and then assembled with the other segment whose steel plate they go through to achieve

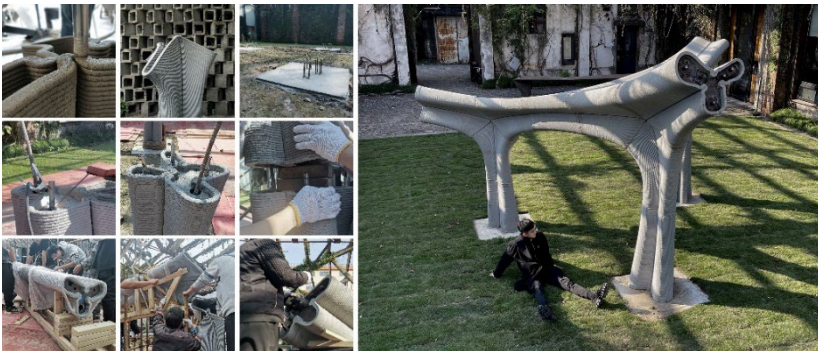


Figure 11. Record of the assembly process and final outcome

precise positioning between the units. Pre-stressed steel bars with a diameter of 15mm pass through the 50mm hole in the steel plate and reach three overhang ends respectively. At the end of each overhang end, 9 steel bars are tightened with nuts to realize the post-tension of the entire structure.

5. Result and discussion

The final structure presents a relatively good surface quality. Although there are some discordant seams in some connections, but the overall quality is within the acceptable range of the architectural scale. The reasons for this may be:

- The error of non-parallel 3D printing is larger than that of traditional 3D printing.
- The deviation of the position of the pillars.

The method of placing the steel plate during the printing process needs to be optimized. It is found that the filament where holds the steel plate will slightly bulge, which declare that the method of embedding the steel plate in the concrete need further investigation. Methods such as optimizing the zigzag design, reducing the size or thickness of the steel plate deserve further exploration.

At present, the mainstream concrete 3d printing construction is divided into two categories: on-site printing and prefabricated assembly. The on-site printing technology is relatively mature and there is no segmentation problem. When it comes to prefabricated assembly, however, there are more issues to be settled.

In general, the concrete printing segments are relatively heavy and fragile, which leads to lots of difficulties in assembly period. In this project and the arched masonry structure from BRG et al. (2021), although each unit was manufactured using template-free 3D printing technology, a large amount of supports were used for positioning, including wood scaffold, during the assembly process, which led to a significant increase in both construction and environmental costs. Recent years, non-parallel concrete printing becomes popular and further eliminates the limitations of complex shapes. It is foreseeable that more large-scale 3DCP funicular spatial structures will emerge in the near future, which will also mean more complex scaffolds are needed. In this context, perhaps 3DCP technology needs to be re-evaluated, because the best option for these complex scaffolds is wooden waffle scaffold.

Acknowledgements

This spatial structure is part of the result of RMIT master studio "Intelligent Force Printing", studio leaders and all students of the studio have made great contributions to this project.

Studio leaders: Philip F. YUAN (RMIT Visiting Professor), Dingwen 'Nic' Bao (RMIT lecturer)

Teaching Assistants: Hao Wu, Xinjie Zhou, Xiang Wang

Students: Bowen Li, Da Wang, Guowei Xia, Jingyi Liu, Ruoxing Wang, Wenjie Gai, Xinyu Wu, Yuhan Bao, Zengwei Wang, Zhangxizhi Wang, Zhengqian Peng, Zhuohua Tan, Ziyang Li, Ziyu Zhou (Sorted by initial letter)

This research was supported by National Key R&D Program of China (Grant

No.2018YFB1306903), National Natural Science Foundation of China (Grant No. U1913603), and Shanghai Science and Technology Committee (Grant No. 21DZ1204501).

References

- Block Research Group (BRG), Zaha Hadid Architects Computation and Design Group (ZHACODE), Incremental3D (in3D), Striatus - 3D concrete printed masonry bridge, Venice, Italy, 2021. from <https://block.arch.ethz.ch/brg/project/striatus-3d-concrete-printed-masonry-bridge-venice-italy-2021>
- Gosselin, C., Duballet, R., Roux, P., Gaudillière, N., Dirrenberger, J., & Morel, P. (2016). Large-scale 3D printing of ultra-high performance concrete—a new processing route for architects and builders. *Materials & Design*, 100, 102-109. <https://doi.org/10.1016/j.matdes.2016.03.097>
- Khoshnevis, B. (2004). Automated construction by contour crafting—related robotics and information technologies. *Automation in construction*, 13(1), 5-19. <https://doi.org/10.1016/j.autcon.2003.08.012>
- Le, T. T., Austin, S. A., Lim, S., Buswell, R. A., Gibb, A. G., & Thorpe, T. (2012). Mix design and fresh properties for high-performance printing concrete. *Materials and structures*, 45(8), 1221-1232. <https://doi.org/10.1617/s11527-012-9828-z>
- Li, Z., Wang, L., Ma, G., Sanjayan, J., & Feng, D. (2020). Strength and ductility enhancement of 3D printing structure reinforced by embedding continuous micro-cables. *Construction and Building Materials*, 264, 120196. <https://doi.org/10.1016/j.conbuildmat.2020.120196>
- Lim, J. H., Weng, Y., & Pham, Q. C. (2020). 3D printing of curved concrete surfaces using Adaptable Membrane Formwork. *Construction and Building Materials*, 232, 117075. <https://doi.org/10.1016/j.conbuildmat.2019.117075>
- Ma, G., Li, Z., Wang, L., & Bai, G. (2019). Micro-cable reinforced geopolymer composite for extrusion-based 3D printing. *Materials Letters*, 235, 144-147. <https://doi.org/10.1016/j.matlet.2018.09.159>
- Masoud Akbarzadeh. Andrei Nejur. (2019). Polyframe. From <https://psl.design.upenn.edu/polyframe/>
- Mechtcherine, V., Nerella, V. N., Will, F., Näther, M., Otto, J., & Krause, M. (2019). Large-scale digital concrete construction—CONPrint3D concept for on-site, monolithic 3D-printing. *Automation in Construction*, 107, 102933. <https://doi.org/10.1016/j.autcon.2019.102933>
- Salet, T. A., Ahmed, Z. Y., Bos, F. P., & Laagland, H. L. (2018). Design of a 3D printed concrete bridge by testing. *Virtual and Physical Prototyping*, 13(3), 222-236. <https://doi.org/10.1080/17452759.2018.1476064>
- Scott, C. (2020, March 17). Chinese construction company 3D prints an entire two-story house on-site in 45 days. from <https://3dprint.com/138664/huashang-tengda-3d-print-house/>.
- Vantghem, G., De Corte, W., Shakour, E., & Amir, O. (2020). 3D printing of a post-tensioned concrete girder designed by topology optimization. *Automation in Construction*, 112, 103084. <https://doi.org/10.1016/j.autcon.2020.103084>
- Xie, Y. M. (2016). Ameba. From <https://ameba.xieym.com/>
- Zhan, Q., Zhou, X., & Yuan, P. F. (2021). Digital Design and Fabrication of a 3D Concrete Printed Prestressed Bridge.
- Zhang, Y., Zhang, Y., Liu, G., Yang, Y., Wu, M., & Pang, B. (2018). Fresh properties of a novel 3D printing concrete ink. *Construction and building materials*, 174, 263-271. <https://doi.org/10.1016/j.conbuildmat.2018.04.115>

ADDITIVE FORMWORK IN PRECAST CONSTRUCTION

Agent-based Methods for Fabrication-aware Modularization of Concrete Building Elements

DAVID STIELER¹, TOBIAS SCHWINN² and ACHIM MENGES³
^{1,2,3}*Institute for Computational Design and Construction (ICD), University of Stuttgart, Germany*
¹*david.stieler@icd.uni-stuttgart.de, 0000-0002-3854-0016*

Abstract. This paper presents the geometric foundations for an agent-based modeling (ABM) approach to modularize concrete building elements for prefabrication via additive formwork. The method presented extends the functionality of existing planning tools for concrete prefabrication to address the manufacturing characteristics of additive formwork production using fused deposition modeling (FDM), and negotiates these with the structural requirements of its underlying building geometry. First, a method to classify building components according to fabrication methods using a probabilistic feature-based Naive Bayes classifier is presented. This classification allows to automatically assign the most suitable production method to every individual building element within a given building model. Following this classification, elements identified for the production using additive formwork are modularized in an automated, agent-based process. The modularization process utilizing a voxel-representation of the initial building element geometry is described in detail. An agent-based method to simulate multiple modularization variants is presented and the integration of feedback from iterative negotiation processes between fabrication expenditures and structural behaviour outlined. The approach presented fosters material-saving construction and production processes in planning and therefore directly addresses crucial issues of the agenda for global Sustainable Development Goals (SDGs).

Keywords. Agent-based Modeling; Modularization; Prefabrication; ABM; Volumetric Modeling; Additive Formwork; SDG 9; SDG 12.

1. Introduction

In construction, twice as much concrete is used as all other building materials combined. In comparison to the amount of all materials used in general, concrete is second only to water (Gagg, 2014). While fluid concrete can take almost any shape, it needs formwork to support it during its curing process. In many cases, the cost of formwork itself can exceed the combined total cost of labour, reinforcement materials

and concrete used (Robert H., 2007). This imbalance between the cost distribution of the temporary formwork and permanent concrete structure leads to a paradoxical approach on how to design and build with concrete. To keep the construction process cheap and quick, concrete elements often follow the formal dictate of simple formwork and thereby the actual cost of built structures is reduced by using more material than needed (Jipa & Dillenburger, 2021).

For concrete construction to achieve the Global Sustainable Development Goals (SDGs) (UN, 2020), formwork plays a crucial role on two levels. On the one hand, formwork that allows for a variety of geometries enables targeted differentiation of building components and thus material savings in concrete; on the other hand, the use of recyclable materials for the production of formwork itself can avoid the disposal of building component-specific formwork. This directly addresses the goal of sustainable consumption and production. A promising fabrication method to overcome formal and thereby performative limitations imposed by traditional formwork construction is 3d printing (Han et al., 2020). While current research both in academia (Naboni & Breseghello, 2019) and practice (Roschli et al., 2020) explores the potential of 3d printed formwork (3DPF) from a formal, performative, and fabrication point of view, the integration of this fabrication method into planning processes and design to manufacturing workflows is less explored. To avoid shifting the manual labour needed to construct physical freeform formwork to digital drafting processes, the potential to automate and simulate the still-discrete steps of building modularization, formwork planning, and respective print path generation needs to be addressed. Existing Building Information Modeling (BIM) software include features that allow designers and planners to modularize planar building elements into standardized building modules of given dimension and mass (Peticila, 2017). While these features enable the modularization of standard geometries and building elements, they are unable to modularize freeform geometries. Yet, it is exactly these freeform and load-adapted geometries that have the potential to reduce material usage of concrete and offer a promising field of application for 3DPF (Jipa et al., 2018). In combination with prefabrication in a controlled environment, and, therefore error-free production, this can significantly reduce the negative impact of construction activities on the environment (Mark et al., 2021).

Within this paper, we therefore present a method that classifies building elements according to suitable fabrication method and that allows for the simulation and evaluation of modularization results early on in the design process. The method thereby extends the functionality of current planning tools for the modularization of buildings geometries for prefabrication. To integrate feedback from later fabrication stages into early design steps, we present an agent-based approach to the modularization of freeform concrete building elements. In agent-based modeling (ABM), a system is modeled from the perspective of its constituent units, where each individual agent assesses its situation and makes decisions and interacts based on a set of rules (Bonabeau, 2002). Therefore, ABM has become a popular method to model and understand complex and non-linear systems, used across a variety of disciplines whenever individuals interact with each other and their environment (Macal, 2016). Previous research investigated such behaviour-based strategies to facilitate the synthesis of computational design and fabrication aspects with regards to performative

lightweight timber plate structures (Schwinn et al., 2014) and façade elements (Gerber et al., 2017). Within the research presented in this paper, ABM is used to similarly synthesize computational design and fabrication aspects, but with a focus on fabrication-informed segmentation of non-standard concrete elements. In the model, pairs of agents represent single concrete modules following specific and adjustable behaviours to extract solid modules from hollow design input models. To make the modularization process independent of the boundary representation type of its input geometry, we present a voxel-based approach using constructive solid geometry (CSG) techniques to decompose an input design model into non-intersecting, space filling modules.

2. Method

2.1. WORKFLOW INTEGRATION

To demonstrate our approach, we use a section of an early design stage model as shown in Figure 3 (1). Within the concept of the six levels of model development (LOD) in BIM, ranging from 100 (symbolic or generic representation) to 500 (model has been validated with constructed building) (Borrmann et al., 2015), this model is situated at LOD 200. Size, dimension, form, position and orientation of elements are approximately known, what is yet to be defined is the precise modularization of building elements and semantic information regarding production, assembly and installation. Situating our classification and modularization approach early in the design process, aims to visualize and understand better the consequences of early design decisions on later production expenditures. Current formwork classifications focus on the architectural function of the element they are intended to form, e.g., a slab, a wall, a column and are thereby unable to address non-standard geometries and 3DPF as production type (Hickert & Knaack, 2016). Therefore, we propose a geometry-based classification of building elements that automates the process of assigning the most suitable production process to each building element based on its geometric features. We consider production types for three different kinds of elements (Figure 1, from left to right):

- Standard elements: Planar hollow-core elements, elements from planar shuttering tables, or cylindrical elements with standardized cross-sections.
- Combinatorial elements: One or more sides consist from printed elements (center).
- Custom elements: Formwork is fully printed.

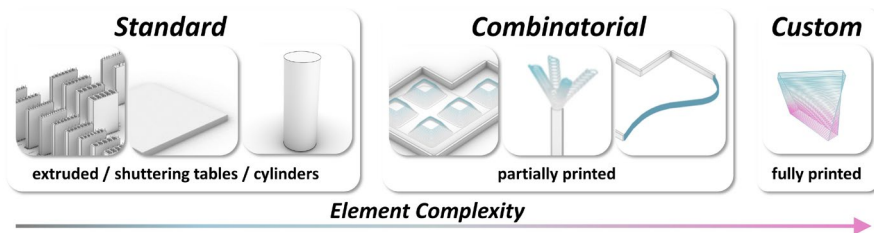


Figure 1. Production types considered for building element classification

2.2. ELEMENT CLASSIFICATION

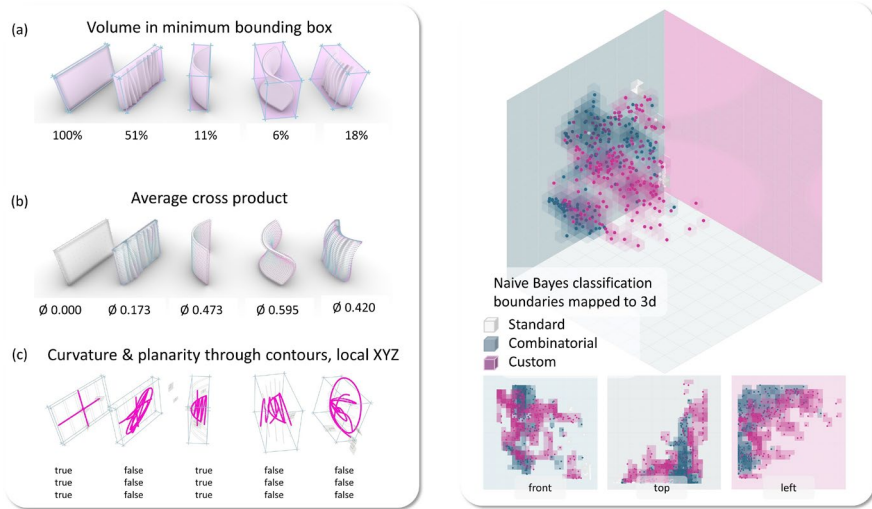


Figure 2. Feature extraction, Naive Bayes Classification and mapped decision boundaries

While an intuitive approach to classify elements to standard and custom production methods would be to measure curvature, either in mesh or NURBS geometries, this would not allow the categorization of elements to the class of combinatorial formworks, where building elements are described by a variable number of planar and non-planar sides. Here, not only curvature is a factor that impacts the choice of a suitable production method, but also the question how many sides of an object are curved, how much the deviation is from its bounding box, and if the objects cross-section is constant or not. To be able to evaluate these factors and thereby universally classify models independent of the geometry type used to model design inputs, we use a retopologized mesh representation of each respective input model. The following three features shown in Figure 2 (left) are used to numerically describe the properties mentioned above and form the basis for the probabilistic classification utilizing a Naive Bayes Classifier (Cluster, 2015):

- (a) Ratio between the volume of the input model and its minimum bounding box (MBB) volume as an indicator for object planarity and variations in cross section.
- (b) Average of the cross product of all face normals to the local coordinate system derived from the building element's MBB X, Y, or Z vector, measuring the vector which is closest in direction. This serves as an indicator for surface texture and relief-like structures.
- (c) Contours are extracted from the input model in MBB X, Y, and Z directions. The center points of contours for each direction are interpolated with a curve. Planarity of the resulting curves serve as a rough indicator for the overall element curvature.

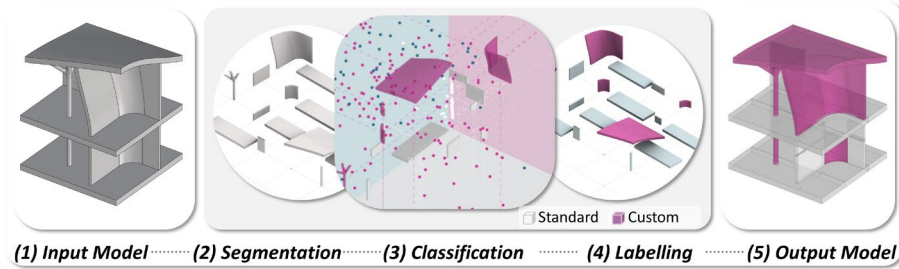


Figure 3. Classification applied to sample model

The Naive Bayes classifier is an efficient approach to calculate class probabilities given a set of features (Sammut & Webb, 2017). Figure 2 (right) shows the distribution of data points from 500 manually labelled input geometries that served as training data for this supervised classification. The labelled input data is used to make a prediction about the likelihood of any new, unlabelled building element being a member of one of the categories shown in Figure 1. Figure 3 shows the integration of the classifier into the modularization workflow starting from the input design model (1), applying the modularization possible in given BIM software (2), classifying the resulting elements (3), and transferring the production information back into the initial model (5). The output model in Figure 3 (5) serves as the basis for the modularization of non-standard building geometries.

2.3. VOXEL BASED MODULARIZATION

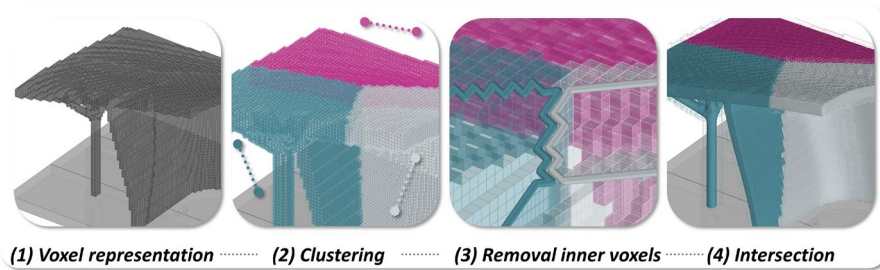


Figure 4. The use of voxel clusters as input independent cutting proxies to define modules

In the next step, building elements identified suitable for 3DPF are prepared for further modularization. Previous research highlights the strength of quadrilateral meshes to rationalize freeforms to be built from planar elements (Pottmann, 2013). However, the modularization of freeform concrete elements without altering the surface of the initial design geometry requires a different geometric approach. This approach should be able to create solid, space-filling, non-intersecting geometries from hollow design models, regardless of input geometry type and form.

Therefore, we propose a geometric approach that relies on a voxel representation of the initial design geometry, where voxel clusters serve as proxy geometries to

generate cutting elements and subsequently extract modules from the input geometry. Figure 4 shows the voxel representation of the building elements identified for 3DFP (1), three voxel clusters formed by grouping the closest voxels based on the distance to three randomly distributed lines (2), the hollow representation of the clusters (3), and the resulting element geometry after intersecting the voxel clusters with the initial building geometry (4). For preview purposes, the voxel resolution at this step is kept low, which leads to jagged module interfaces, in the following section voxel resolution is increased.

2.4. MODEL DESCRIPTION AND SIMULATION

The goal of this simulation approach is the evaluation of multiple modularization variants and the negotiation of fabrication expenditures, structural impact of modularization, and the adherence to a certain size of resulting modules. The computational foundation for this model is formed by the ABM framework developed at the Institute for Computational Design and Construction (ICD) at the University of Stuttgart (Groenewolt et al., 2018). While the process of clustering voxels and their intersection with the input geometry forms the geometric basis for modularization, locomotion behaviour mechanisms as described by Reynolds (Reynolds, 1999) form the conceptual basis for simulating different modularization variants and their evaluation.

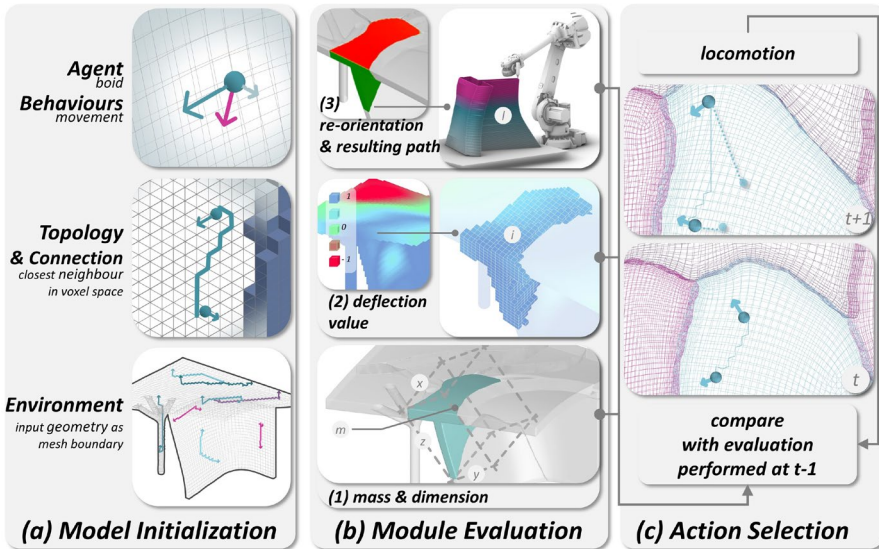


Figure 5. Model constituents, module evaluation and action selection

The initial model by Reynolds was built to simulate the flocking behaviour of birds in computer graphics. Reynolds decomposes the task of constructing motion behaviours into a three level hierarchy of: Action selection, steering, and locomotion. Here, actions are mainly based on distances between single individual agents. Therefore, in the context of modularization, we augment the layer of action selection with information about the current state of the concrete module each agent is associated

with:

- Action selection: Agents observe the state of the module they are associated with and perceive changes in module mass, dimension, deflection value, and resulting print path length for the module's formwork. These perceptions form the basis for the respective goal selection.
- Steering: Goals selected from the previous step are coordinated with the agents' internal rules and translated to steering signals.
- Locomotion: steering signals are converted into motion parameters.

Figure 5 shows the model constituents (a), the analysis for one module at a given timestep (b), and a zoom in on two consecutive iterations with resulting agent positions, locomotion vectors, their connection in voxel space, and resulting module boundaries (c). The initial state of the model at $t = 0$ starts from the distribution of a given number of agents from random starting points within the given geometry that serves as environment for the agents to move in. At initialization, for each agent its nearest neighbouring agent in voxel space is found. Their connecting graph within the voxel space functions as reference curve to measure voxel distances to. Voxel clusters are formed by the closest distance from voxel position to connecting graph. By using voxel space, not euclidean distances, it is ensured that for each agent pairing, exactly one module, and not multiple, can be created. From this initialization step, the first modularization variants are evaluated and the following parameters stored in the action selection layer:

- (1) Mass & dimension: Mass is directly derived from each modules volume, dimension considers the longest side of each module's MBB.
- (2) Deflection value: Derived from a deflection analysis of the unsegmented input model. Deflection values are stored in the voxels forming the clusters and the average value considered for each module's deflection value at every timestep.
- (3) Print path length: Due to fabrication constraints of FDM, modules are automatically oriented to reduce surface areas with overhangs larger than 45 degrees. For areas over 45 degrees, print supports are generated and the additional material needed is considered in the module evaluation.

Instead of studying the dynamic movement of swarms, we seek to achieve a dynamic equilibrium, meaning that no agents are moving once all set requirements are met and the model converges to a steady-state. Behaviours described by Reynolds include cohesion and separation which can be used to create an even distribution of agents in their environment. While an even distribution in size is desirable, the control over size to stay within a given domain should be ensured. Therefore, the larger the module size, the larger the attraction force between two agents composing one module, resulting in smaller module sizes. Conversely, with decreasing module size, separation force between agent pairings helps to keep spacing consistent. Figure 5 shows the resulting locomotion vectors for different timesteps (right). While the behaviour affecting module size is directly influenced by the steering directions resulting from agent positions, the behaviours affecting deflection value and print path length rely on a metaheuristic approach, meaning a comparison of each module's evaluation from

previous timesteps and their current state. Locomotion direction is stored and results from the evaluation at timestep $t-1$ is compared with evaluation at timestep t . An improvement, meaning less print path or a lower deflection value, results in no modification of the steering vector. If the values deteriorate, the direction is adjusted to steer towards the last position with better values. Conceptually, this approach is known from particle swarm optimization (PSO), which is used to search for a solution to an optimization problem by iteratively moving a population of candidate solutions through a search space (Eberhart & Sixth, 1997). The final locomotion vector results from the addition of cohesion and separation behaviours amongst all neighbouring agents, the directed cohesion between agent pairings, and the memory-based approach to steer towards previous positions. On the system level, this allows for the observation of multiple modularization variants, their effect on fabrication expenditures and their influence on structural behaviour.

Figure 6 shows the modularization of the non-standard area within the initial building design model (a), the oriented modules to reduce overhangs (b), and respective information for each resulting module (c).

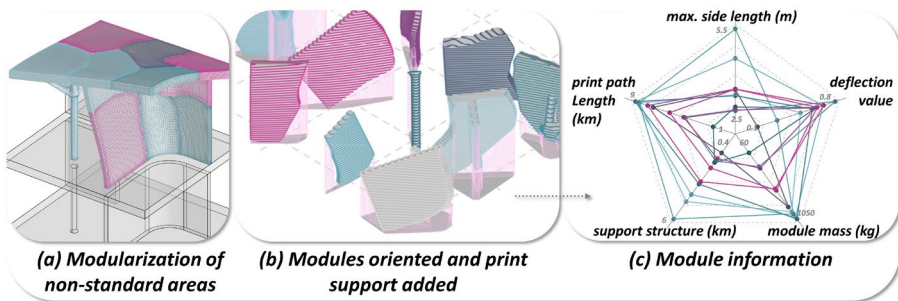


Figure 6. Non-standard modules within the initial building geometry, resulting modules oriented for printing, and module information

3. Discussion, Limitations, Outlook

Within this paper, we presented an automated workflow to identify building elements where 3DPF is applicable. We demonstrated the decomposition of hollow input models into solid, space-filling modules using voxels as proxy geometry and embedded this geometric approach into an agent-based model.

Since it is a common goal to reduce overhangs in 3d printing processes (Luo et al., 2012), the model presented could also be used to modularize geometries for concrete 3d printing. While this universality of the presented method presents an addition to planning tools also for other production processes, some main aspects of formwork planning remain unaddressed at this stage. So far, formwork is conceived as a monolithic shell around building modules. Some research has shown the successful demoulding of thin monolithic formwork (Burger et al, 2019), However, this is the exception rather than the rule. Therefore as the next step, formwork segmentation, the connection of single formwork elements, and general demouldability of building elements need to be addressed.

The voxel-based segmentation approach is in itself independent from the constituents of the input design model. In the research presented, the voxel structure was also used to transport analysis results from an initial deflection analysis performed on the input model to resulting modules. For now, this deflection value is simply mapped to a domain between 1, largest deflection detected, to -1, least deflection detected. Values from the input mesh are stored in each voxel based on spatial proximity and serve as indicator for expected stresses on module interfaces. While we demonstrate the transfer, storage, and analysis of values obtained from an input model to resulting modules, the analysis itself needs further refinement to adequately inform position and design of module interfaces and the requirements for connecting elements. So far, the design of module interfaces is not addressed. However, module interfaces can clearly be identified in voxel space, and therefore the voxel unit could potentially be beneficial in locally defining variable interfaces between modules. To test connections and interfaces and consider production tolerances in the modularization process, physical prototypes directly resulting from the proposed approach are part of ongoing research.

3DPF offers the potential to combine the efficiency of prefabrication with the formal freedom and performance of freeform concrete structures. This research presents a modularization approach to address the vast field of geometric solutions enabled by 3DPF, therefore addressing planning methods that show a possible path for concrete construction to meet the SDGs. On the simulation level, the approach allows for further refinement of agent behaviours to better understand the effects different modularization variants have on the building system level. By automating the steps necessary for modularization, this research seeks to make freeform modularization more accessible and thereby widening the design space of prefabricated concrete.

Acknowledgements

This research has been supported by the Deutsche Forschungsgemeinschaft (DFG, German Research Foundation) under the Special Priority Programme SPP 2187 - 424070949 and Germany's Excellence Strategy – EXC 2120/1 – 390831618.

References

- Bonabeau, E. (2002). Agent-based modeling: Methods and techniques for simulating human systems. *Proceedings of the National Academy of Sciences of the United States of America*, 99(SUPPL. 3), 7280–7287.
- Borrmann, A., Koch, C., König, M., Beetz, J. (2015), *Foundations & Practice in Building Information Modeling*.
- Claster, W. B. (2015). Naïve Bayes classifier. In *Data Mining Algorithms* (pp. 118–133). John Wiley & Sons, Ltd.
- Eberhart, R., & Sixth, J. K. (1997). A new optimizer using particle swarm theory. In: *Proceedings of the IEEE Symposium on Micro Machine and Human Science*, Nagoyo, Japan, 39–43.
- Gagg, C. R. (2014). Cement and concrete as an engineering material: An historic appraisal and case study analysis. *Engineering Failure Analysis*, 40, 114–140.
<https://doi.org/10.1016/j.engfailanal.2014.02.004>

- Gerber, D. J., Pantazis, E., & Wang, A. (2017). A multi-agent approach for performance based architecture. *Automation in Construction*, 76, 45–58. <https://doi.org/10.1016/j.autcon.2017.01.001>
- Groenewolt, A., Schwinn, T., Nguyen, L., & Menges, A. (2018). An interactive agent-based framework for materialization-informed architectural design. *Swarm Intelligence*, 12(2), 155–186. <https://doi.org/10.1007/s11721-017-0151-8>
- Han, D., Yin, H., Qu, M., Zhu, J., & Wickes, A. (2020). Technical Analysis and Comparison of Formwork-Making Methods for Customized Prefabricated Buildings: 3D Printing and Conventional Methods. *Journal of Architectural Engineering*
- Hickert, S., & Knaack, U. (2016). Evaluation of free-form concrete architecture, moulding systems and their technical potentials. *Journal of Facade Design and Engineering*, 3(3–4), 273–288.
- J. Burger, E. Lloret-Fritschi, F. Scotto, T. Demoulin, L. Gebhard, J. Mata-Falcón, F. Gramazio, M. Kohler, R.J. Flatt. (2019). Eggshell: Ultra-thin 3D Printed Formwork for Concrete Structures. *3D Printing and Additive Manufacturing*. <https://doi.org/10.1089/3dp.2019.0197>
- Jipa, A., Aghaei Meibodi, M., Giesecke, R., Shammass, D., Leschok, M., Bernhard, M., & Dillenburger, B. (2018). 3D-Printed Formwork for Prefabricated Concrete Slabs. *1st International Conference on 3DCP, 2018*. <https://doi.org/10.13140/RG.2.2.26722.89280>
- Jipa, A., & Dillenburger, B. (2021). 3D Printed Formwork for Concrete: State-of-the-Art, Opportunities, Challenges, and Applications. *3D Printing and Additive Manufacturing*. <https://doi.org/10.1089/3dp.2021.0024>
- Luo, L., Baran, I., Rusinkiewicz, S., & Matusik, W. (2012). Chopper: Partitioning models into 3D-printable parts. *ACM Transactions on Graphics*, 31(6). <https://doi.org/10.1145/2366145.2366148>
- Macal, C. M. (2016). Everything you need to know about agent-based modelling and simulation. *Journal of Simulation*, 10(2), 144–156. <https://doi.org/10.1057/jos.2016.7>
- Mark, Peter and Lanza, Gisela and Lordick, Daniel and Albers, Albert and König, Markus and Borrmann, Andre and Stempniewski, Lothar and Forman, Patrick and Frey, Alex Maximilian and Renz, Robert and Manny, Agemar (2021). Vom Handwerk zur individualisierten Serienfertigung. *Bautechnik*. <https://doi.org/10.1002/bate.202000110>.
- Naboni, R., & Breseghello, L. (2019). Additive Formwork for Concrete Shell. *IASS Annual Symposium – Structural Membranes 2019*.
- Peticila, D. (2017). *Structural Precast for Revit – Fast and Accurate Modeling in a Single BIM Model*.
- Pottmann, H. (2013). Architectural Geometry and Fabrication-Aware Design. *Nexus Network Journal*, 15(2), 195–208.
- Reynolds, C. W. (1999). Steering Behaviors For Autonomous Characters. *Proceedings of Game Developers Conference*, 763–782.
- Robert H. (2007). Think formwork – reduce costs. *Structure Mag.*, April, 14.
- Roschli, A., Post, B. K., Chesser, P. C., Sallas, M., Love, L. J., & Gaul, K. T. (2020). Precast concrete molds fabricated with BAAM. *Proceedings of the 29th Annual International Solid Freeform Fabrication Symposium, SFF 2018*, 568–579.
- Sammut, C., & Webb, G. I. (Eds.). (2017). *Encyclopedia of Machine Learning and Data Mining (2nd ed.)*. Springer.
- Schwinn, T., Krieg, O. D., & Menges, A. (2014). Behavioral Strategies: Synthesizing design computation and robotic fabrication of lightweight timber plate structures. *Proceedings of the 34th ACADIA*, 177–188. http://cumincad.scix.net/cgi-bin/works/Show?acadia14_177
- UN (2020). *The Sustainable Development Goals Report 2020* (pp.48-49). ISSN: 2518-3915

ROBOTIC FABRICATION OF TOPOLOGY OPTIMISED CONCRETE COMPONENTS WITH REUSABLE FORMWORK

A design-to-fabrication workflow to manufacture freeform multi-branching concrete structures

YIYAO GUO¹, YANG LUO², SIHAN WANG³, YING YI TAN⁴ and KENNETH TRACY⁵

^{1,2}Zhejiang University, ^{3,4,5}Singapore University of Technology and Design.

¹guoyiyaoelina@163.com, 0000-0002-6346-6612

²3170105017@zju.edu.cn, 0000-0001-5449-5799

³sihan_wang@alumni.sutd.edu.sg, 0000-0003-1383-6790

⁴yingyi_tan@sutd.edu.sg, 0000-0003-0545-7061

⁵kenneth_tracy@sutd.edu.sg, 0000-0002-5143-6053

Abstract. In this paper, we introduce a design-to-fabrication workflow to create topology optimised concrete components by clay printing a temporary mould and simultaneously casting concrete into it. Our fabrication approach addresses the United Nation's Sustainability Development Goal (SDG) 12 of reducing waste in construction by employing the phase changing properties of clay, allowing this natural resource to be broken down and reused for subsequent projects. We implemented our workflow in the design and fabrication of a resilient infrastructure that responds to SDG 9 - an urban furniture that braces large trees during high-speed typhoon winds and serving as a bench for locals to rest under the tree. This paper documents our workflow with considerations of its overall workability, material properties and fabrication efficiency. We showcase our final prototype and discuss the feasibility and challenges of this approach in fabricating complex freeform components on a large scale.

Keywords. Robotic Fabrication; Topology Optimisation; Freeform Concrete; Reusable Formwork; SDG 9; SDG 12.

1. Introduction

Rapid urbanisation over the past few decades has led to construction waste becoming an increasingly prominent problem. In response, both practice and academia have moved towards adopting algorithmically driven modelling and robotic fabrication to design structurally efficient building components that can be manufactured with less resultant waste respectively (Hauschild & Karzel, 2011). These strategies echo United

Nation's Sustainability Development Goal (SDG) 12 in reducing waste in our modern-day construction industry (United Nations, 2022).

The subject of this research is the manufacture of concrete which has often been used to make building components. Although it serves as a low-cost and structurally viable building material, fabricating concrete is conventionally a high waste process. Each component requires a sacrificial mould, typically made from timber or foam, that attributes 46.7%-73% of costs of the total building project (Agusti-Juan et al., 2017). These moulds get discarded after the project ends which inevitably leads to significant wastage.

In this paper, we investigate how concrete building components, that have their geometries derived from topology optimisation, can be fabricated in a sustainable manner. This research tackles the challenge of creating geometrically complex 3D forms that are often the result of topology optimisation algorithms. It advances our previous work that has explored using clay as a temporary mould for concrete casting (Wang et al., 2016, 2019). This combination of additive and formative manufacturing capitalises on the phase changing properties of clay as a natural resource, allowing it to be: (i) robotically extruded as a viscous material; (ii) stiffen to resist lateral pressure and broken off and (iii) recycled for future prints.

This edition of our research incorporates simultaneous casting in this fabrication workflow – a technique inspired from traditional slipforming (Lachemi et al., 2007). Our new approach involves pouring wet concrete at certain periodic intervals of the mould printing process, allowing both concrete and clay to harden and gain stiffness together as the mould is being built up. This brings about various benefits such as: (a) faster manufacturing speeds; (b) reduction of moisture loss from concrete when in contact with wet clay; (c) facilitating the creation of more complex geometries such as low cantilevers and overhanging branching elements without risking concrete not entirely filling up the mould.

We test our fabrication approach on designs created as part of an undergraduate design-and-build studio, with this paper documenting a multi-branching urban furniture shaped by topology optimisation. We describe the steps taken from design to fabrication to produce this prototype on 1:1 scale and later discusses its advantages and limitations on using this method.

2. Motivation

The design of the urban furniture responds to SDG 9 (United Nations, 2022), specifically focusing on creating resilient infrastructure in regions that experience typhoons – tropical storms with wind speeds greater than or equals to 33 m/s (Neumann, 1999). These strong winds can break large branches or even uproot trees which then injure the nearby pedestrians and/or damage buildings and infrastructure. Thus, it is vital to reinforce trees in anticipation of high wind loads from all directions during a typhoon (Kamimura et al., 2016).

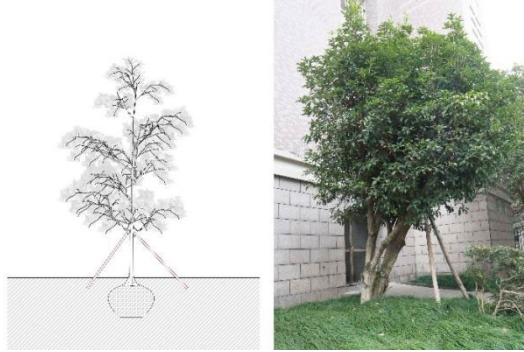


Figure 1. Traditional manual support structure made of timber poles.

Traditionally, trees are manually affixed with several timber poles at different orientations to stabilise them during the multi-directional typhoon (Figure 1). While this is a straightforward and efficient method that can be easily implemented, it faces several limitations: (I) the tree supporting structures are mostly constructed based on the workers' experience which makes the structural performance unpredictable; (II) wood poles tend to decay in high humidity in these typhoon-hit areas and require regular maintenance or replacement; (III) the supporting structure makes the area under the tree canopy inaccessible and unusable, which could have been used as a natural sunshades.

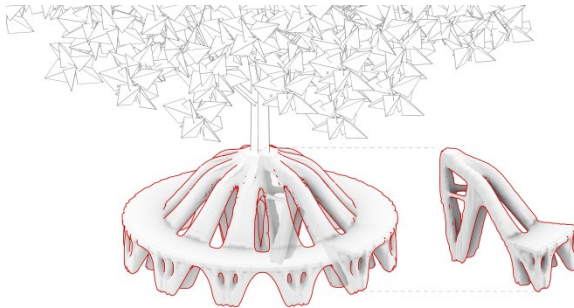


Figure 2. Conceptual design of the tree supports.

As such, our design strategy proposes a radial concrete bench positioned around the tree which can withstand multi-directional high wind loads reliably without needing constant maintenance. This also serves as a public seating area where locals can relax during regular weather conditions (Figure 2).

The support system is designed as a series of modular concrete benches that are polar arrayed around the bottom half of the tree to resist wind loads from all directions. These prefabricated benches would be assembled as a series of individual components connected to each other using concrete anchors bound by steel wires and with rubber suspensions between the trunk and the modules. Thus, this mechanism allows the

individual modules to be adjusted or replaced, enabling the overall structure to adapt to different heights and girths of the tree as it grows over time, as depicted in Figure 3.

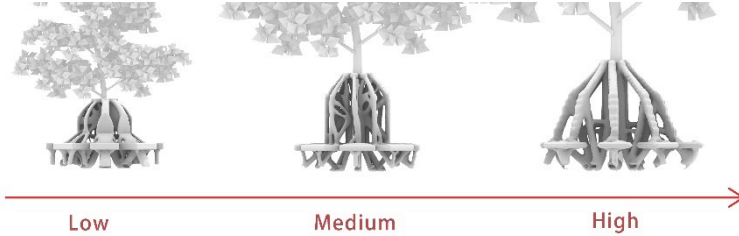


Figure 1. Supports applied on various heights and girths of the trunks.

3. Design of Components

The geometry generated by topology optimisation is dependent on the magnitudes, positions and directions of the forces that are acting on the bench. In this investigation, we defined two types of loading scenarios: (A) The load exerted by the people who sit on the flat bench surface, which is set as 2000N; (B) The wind load that the support structure can undergo to prevent breakage which should be greater than the maximum bending moment that a tree trunk can withstand:

$$M_{sb} = \frac{\pi}{32} \times MOR \times B^3 \times K_{not}$$

Equation 1. The equation of wind load on surface.

In the above equation, M_{sb} refers to the critical bending moment for trunk breakage. This is derived from the multiplication of the modulus of rupture (MOR), trunk diameter (B) and knot factor (Knot) to account for reductions in the capacity due to imperfections and defects in the wood (Mohamed et al., 2020). Here, the tree used was Wutong, a common species in East Asia and considered as medium to tall tree standing at a height of 8-12 meters. Using equation 1, the load applied was approximately 3600 N.

The supports were designed as 12 polar arrayed individual components around the tree that each occupied a 30-degree circular sector. As the wind loads would be applied from all directions, every component would have an identical structure and is able to withstand a wind load of approximately 2000 N.

Topology optimisation was executed in tOpos - a Grasshopper plugin which uses GPU to accelerate the iterative algorithm. The optimisation boundary was set as two adjacent volumetric blocks as seen in the grey zone of Figure 4a. The loads were assigned as red surfaces which represent the (A) human sitting load and (B) wind load, while the blue indicated the boundary support area of this structure. Once the optimisation was completed, a meshed model of the ideal distribution of material was created in Figure 4b. Lastly, the mesh was smoothed for fabrication in Figure 4c.

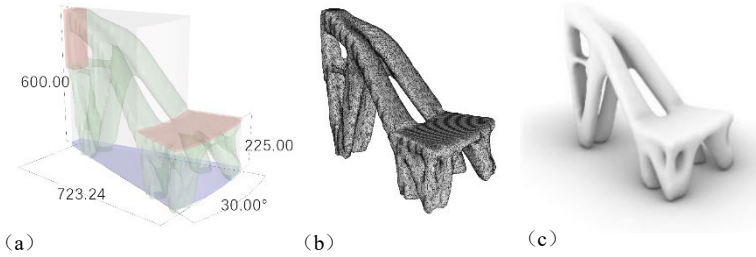


Figure 2. Design of the tree support component: (a) topology optimisation parameters for the support structure; (b) the meshed model generated from the optimisation; (c) the finalised model for fabrication.

4. Fabrication

4.1. HARDWARE AND SOFTWARE

Our 3D clay printing system has two sub-systems: (a) the extrusion end effector which includes a pump that feeds material into a cavity extruder; and (b) the positioning apparatus that allows precise control of location and motion of deposition. We used a Kuka KR120 R2500 six-axis industrial robot placed 1.6m apart from the centre points of the printing platform. Other parts of the work cell include a clay mixing sector, a concrete mixing sector and a reloading sector.

A customised end-effector was employed with a clay-feeding pump and a dispenser made of a cavity pump (Figure 5). This used a direct extrusion mechanism for the material feeder, utilising a plunger impulse by a step motor-driven reduction gearbox to push the clay out. A second phase extruder made of cavity pump was attached to the main body of the clay pump. This cavity pump can dispense 1.69 litres of clay per

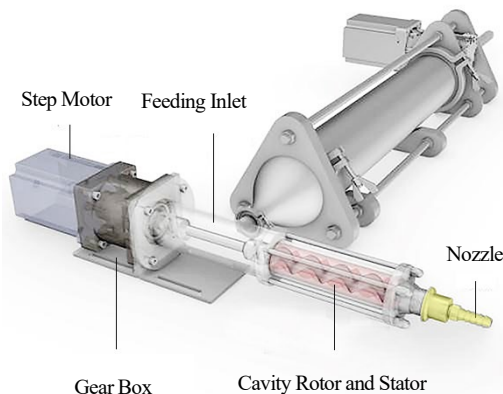


Figure 5. Schematic of the clay extrusion end effector.

minute at 300 rpm. The system also allowed the clay pump to store a large quantity of clay and generate enough torque to feed this viscous material to the extruder for precise extrusion and distribution at a rapid speed.

4.2. PRINTING WORKFLOW

The printing paths were based on the contours of global shape, sliced by the x-y plane at increments along the z-axis. We obtained these paths by offsetting the contours by half of the nozzle diameter. A double layered mould strategy was employed to create a wall thickness sufficient to resist the lateral pressure from the poured concrete and prevent leakage. Subsequently, the offset contoured paths were sorted and grouped in ascending order to assign transitions between the paths.

The planning of our approach had to consider not only the 3D printing strategy but also the casting processes, with special care to prevent the printing nozzle from colliding with the mould as it was printed. This was especially challenging as sectional contours with branches were discontinuous paths and printing these contours would cause the nozzle to travel from branch to branch without depositing material, making the printing process inefficient. Our solution was to print each branch separately so that the travel distance could be reduced. Another consideration was limiting the path length of each segment so that the amount of extruded clay was within one cylinder to avoid running out of clay before the segment was completed.

Factoring all these constraints, the component was sliced horizontally into several chunks of 300mm in height as seen in Figure 6a. This slicing also considered the large overhanging seat top surface of the mould which generated large cantilever angles. Thus, this wide area had to be split into 4 separate print paths (6-1 to 6-4) to be printed successfully.

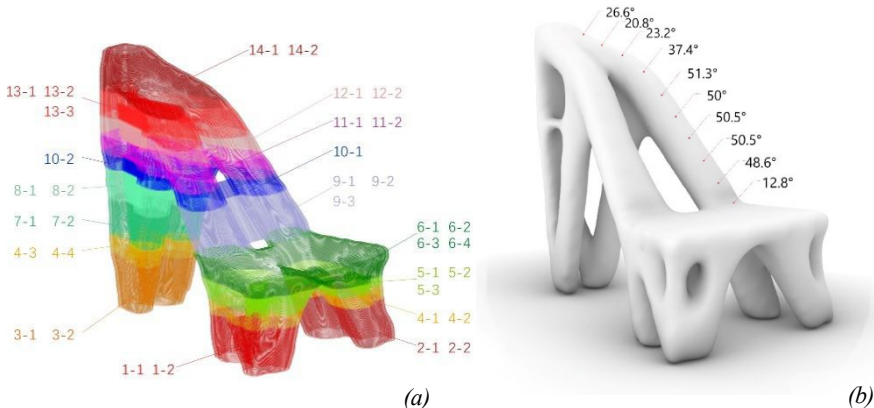


Figure 6. Fabrication challenges: (a) the segmentation of the printing paths; (b) cantilever angles along the branch.

4.3. FABRICATION METHOD & SEQUENCE

Our fabrication approach is inspired by slipforming, where a mobile formwork moves vertically upwards incrementally while concrete being poured in simultaneously. This method is useful for constructing monolithic structures and has been recently customised to fabricate geometrically complex structures (Lloret-Fitschi, et. al., 2020).

For our scenario, we print an adequately thick clay mould that resists the lateral pressure exerted by the concrete poured at specific intervals during the printing process. This gives several benefits of: (i) concurrent setting of both concrete and clay, allowing both materials to stiffen together to support the next segment, enabling larger cantilevers to be created incrementally; (ii) reducing the drying shrinkage of both materials as the concrete almost instantly fills the wet clay mould; (iii) ensure that the poured concrete entirely fills all the gaps of the mould, which is problematic for moulds with complex geometries.

The main challenge of such an approach is to identify the appropriate timing of pouring the concrete into the clay mould during the printing process. In this scenario, we consider three critical objectives: 1. The neighbouring segments of concrete must be well connected to ensure structural stability by avoiding delamination at these regions; 2. The clay printing must finish before the setting of the preceding segment of concrete; 3. The concrete has to be fast setting so that preceding segments of concrete no longer exert pressure on the clay mould and can sustain the incoming weight of the next segment of concrete. Thus, each segment of concrete must be cast before the initial setting of the former portion and must be given enough time to hydrate and solidify.

Our concrete mixture is designed to reduce its setting time and be sufficiently stiff for our application. The ingredients and their quantities are listed in Table 1, with the mix including: Calcium Sulfoaluminate (CSA), sand (S), water (W), superplasticiser (Sp), glass fibre with strands of 6 mm (GF6) and 12 mm (GF12) in length, deformer (D) and Dihydroxysuccinic acid (Da).

Table 1. Proportion of the concrete mix.

Component	CSA	S	W	Sp	GF6	GF12	D	Da
Amount(g)/Litre	812	988	295	6.5	12	12	0.9	0.5

Moreover, to guarantee the success of the print, several areas of the mould were manually supported using foam blocks that were cut to s, small clay chunks or a thin stick. These were positioned directly under the cantilevering areas with higher than 35-degree angles, such as under the seat top and at the branches at the back of the chair seat. This combination of automated and manual methods helped to reduce the chance of deformations of the clay mould when concrete was added and further sped up the overall fabrication process. In total, this combination of simultaneous robotic printing and casting allowed this urban furniture to be completed in a short duration of 5 hours.

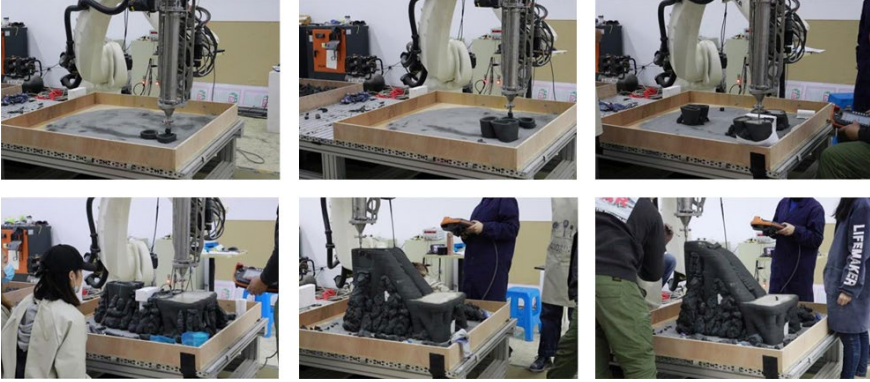


Figure 7. Fabricating the prototype

Subsequently, the concrete was left to cure within the clay mould for a total of five days before demoulding. On the first day, many cracks around the cantilever branches were observed at the regions where the segments were bonded (Figure 8a). This could be due to the smaller bonding area per layer due to the smaller sizes of the branches and larger shifts of printing paths to form the target cantilever angle. As for other areas, the cracking was distributed evenly in the cross-layer direction and along-layer direction.

On the final day, the clay mould was removed and recycled without much effort as the dried clay had already cracked and peeled off, making it easy to remove by hand. The demoulded clay was then recycled by mixing with water to filter off the concrete dust and settle as a slurry. The uncontaminated clay can be recycled for the next print job, closing the loop to this material cycle.

5. Discussion

This paper demonstrates our improved design-to-fabrication workflow to create a geometrically complex branching concrete urban furniture intended to brace trees during typhoon weathers. It showcases how our method can fabricate this topology optimised component with large cantilever angles and overhangs within a short duration. Such an approach can also facilitate the fabrication of not only structurally optimised components like our previous truss structure (Wang, et. al., 2019) or ribbed floor slabs, but also geometrically complex decorative components such as doubly curved facade panels or bifurcating non-load bearing columns.

Moreover, this approach responds to SDG 12 by considering the entire material cycle of using clay from extrusion, casting, demoulding to recycling. This closed-loop material consideration provides ecological benefits by ensuring that the clay material always returns to the first mould-making step after demoulding. This method contrasts with typical concrete formwork construction which usually ends up discarding its formwork or mould materials. Thus, this encourages a sustainable take on how a sacrificial mould material can be recycled for future prints and minimise waste.

Although this prototype uses a largely automated process in its fabrication, there still are geometric limitations where we used manual procedures. Thus, our future work aims to investigate how we can fully automate this fabrication process to minimise human intervention and make the printing and casting steps more efficient.



Figure 8. The final artifact of the tree support: (a) the clay mould a day after the final cast (before demoulding); (b) the concrete prototype (after demoulding).

Acknowledgements

This design project was one of many created during an option studio conducted in collaboration with the Zhejiang University and the Singapore University of Technology and Design. The prototyping was carried out in the Robotic and AI lab of the architectural department of Zhejiang University. The conceptual design was created by Guo Yiyao and Luo Yang with further refinements to the model and printing path generation implemented by the tutor, Wang Sihan. The fabrication sequence was planned by Guo Yiyao, Luo Yang, and Zheng Liquan. In addition to the first two authors, the fabrication process was assisted by several other students in the studio, namely Zheng Liquan, Chen Xinchang, Huang Jiale, Gu Sijia, Xu Qian, Zhu Yijiang, and Yufan.

References

- Agustí-Juan, I., Müller, F., Hack, N., Wangler, T., and Habert, G. (2017) Potential benefits of digital fabrication for complex structures: Environmental assessment of a robotically fabricated concrete wall, *Journal of Cleaner Production*, vol. 154, 330-340, 06/15 2017, doi: 10.1016/j.jclepro.2017.04.002.
- Akhnoukh, A. K. (2020). Advantages of Contour Crafting in Construction Applications. *Recent Patents on Engineering*, 14. <https://doi.org/10.2174/1872212114666200218111631>.

- Gramazio, F., Kohler, M., Willmann, J., & Eidgenössische Technische Hochschule Zürich. Chair of Architecture and Digital Fabrication. (2014). *The robotic touch: how robots change architecture*. Park Books.
- Hauschild, M. and Karzel, R. (2011). *Digital Processes: Planning, Designing, Production*. Birkhäuser. <https://doi.org/10.11129/detail.9783034614351>.
- Kamimura, K., Gardiner, B., Dupont, S., Guyon, D., & Meredieu, C. (2016). Mechanistic and statistical approaches to predicting wind damage to individual maritime pine (*Pinus pinaster*) trees in forests. *Canadian Journal of Forest Research*, 46(1), 88-100. <https://doi.org/10.1139/cjfr-2015-0237>.
- Lachemi, M., Hossain, K. M. A., Anagnostopoulos, C., and Sabouni, A. R. (2007) Application of maturity method to slipforming operations: Performance validation, *Cement and Concrete Composites*, vol. 29, no. 4, pp. 290-299.
- Lloret-Fritschi, E., Wangler, T., Gebhard, L., Mata-Falcón, J., Mantellato, S., Scotto, F., ... & Flatt, R. (2020). From smart dynamic casting to a growing family of digital casting systems. *Cement and Concrete Research*, 134, 106071.
- Mansour, M. A., Rhee, D. M., Newson, T., Peterson, C., & Lombardo, F. T. (2020). Estimating Wind Damage in Forested Areas Due to Tornadoes. *Forests*, 12(1), 17. <https://doi.org/10.3390/fl2010017>.
- Neumann, C. J., National Climatic Data Center (U.S, National Hurricane Center (1965-1995, United States. National Weather Service, & United States. National Environmental Satellite, Data, And Information Service. (1993). *Tropical cyclones of the North Atlantic Ocean, 1871-1992*. National Oceanic And Atmospheric Administration, National Weather Service, National Environmental Satellite, Data, And Information Service.
- Reinhardt, D., Saunders, R., & Burry, J. (2016). *Robotic Fabrication in Architecture, Art and Design 2016*. Cham Springer International Publishing.
- United Nations. (2022). *Build resilient infrastructure, promote inclusive and sustainable industrialization and foster innovation*, Retrieved January 22, 2022, from <https://sdgs.un.org/goals/goal9>.
- United Nations. (2022). *Ensure sustainable consumption and production patterns*. Retrieved January 22, 2022, from <https://sdgs.un.org/goals/goal12>.
- Vantyghe, G., De Corte, W., Shakour, E., & Amir, O. (2020). 3D printing of a post-tensioned concrete girder designed by topology optimization. *Automation in Construction*, 112, 103084. <https://doi.org/10.1016/j.autcon.2020.103084>.
- Wang, S.H., Morel, P., Ho, K., & Dritsas, S. (2016). Clay robotics: A hybrid 3D printing casting process, In *Proceedings of the International Conference on Sustainable Smart Manufacturing (S2M)*, Lisbon, pp. 83-88.
- Wang, S.H., Huang, K.S., Huang, Z.X., Sodano, M., Xu, W.S., Raspall, F. (2019). Fabrication of Topology Optimized Concrete Components Utilizing 3D Printed Clay Mould, In *Proceedings of the International Association for Shell and Spatial Structures (IASS)*, Barcelona.

TOPOLOGY OPTIMIZATION FOR 3D-PRINTABLE LARGE-SCALE METALLIC HOLLOW STRUCTURES WITH SELF-SUPPORTING

QIANG CUI¹, HUIKAI ZHANG², SIDDHARTH SUHAS PAWAR³,
CHUAN YU⁴, XIQIAO FENG⁵ and SONG QIU⁶

^{1,6}*Academy of Arts and Design, Tsinghua University.*

^{2,5}*Department of Engineering Mechanics, Tsinghua University.*

^{3,4}*PIX Moving Inc.*

¹*cui-q18@mails.tsinghua.edu.cn, 0000-0002-0876-5054*

²*zhk19@mails.tsinghua.edu.cn, 0000-0003-4792-6356*

³*smsusi@pixmoving.com, 0000-0002-6917-9489*

⁴*angelo@pixmoving.com, 0000-0001-6269-064X*

⁵*fengxq@tsinghua.edu.cn, 0000-0001-6894-7979*

⁶*qiusong@mail.tsinghua.edu.cn, 0000-0002-5230-1011*

Abstract. Design for Additive Manufacturing (DfAM), is a one of the most commonly used and foundational techniques used in the development of new products, and particularly those that involve large-scale metallic structures composed of hollow components. One such AM technique is Wire Arc Additive Manufacturing (WAAM), which is the application of robotic welding technology applied to Additive Manufacturing. Due to the lack of a simple method to describe the fabricating constraint of WAAM and the complex hollow morphology, which difficultly deploys topology optimization structural techniques that use WAAM. In this paper, we develop a design strategy that unifies ground-structure optimization method with generative design that considers the features of hollow components, WAAM overhang angle limits and manufacturing thickness limits. The method is unique in that the user can interact with the design results, make changes to parameters, and alter the design based on the user's aesthetic or specific manufacturing setup needs. We deploy the method in the design and 3D printing of an optimized Electric Vehicle Chassis and successfully test in under different loading conditions.

Keywords. Topology Optimization; Generative Design; Self-supporting; Hollow Structures; Metallic 3D Printing; SDG 12.

1. Introduction

Additive manufacturing technology has greatly been used in the fields of architecture, material science, vehicle and aircraft. It is a great challenge to manufacture low cost, short design cycle, strong reliability and integrated large-scale metallic structures. First of all, low cost requires us to use as few materials as possible to meet the design requirements. Many structures in nature have hollow tubular structures, which can not

only meet the nutrient transfer requirements of plants and animals with small materials but also maintain the stiffness and strength of tissues to a certain extent. Therefore, it is favored in the design of some energy-absorbing materials and large truss structures.

Secondly, the short design cycle requires an automated design process to select different tubular structures for optimization and integration. Therefore, the two problems to be faced here are that what kind of automatic topology optimization method should choose and how to describe tubular geometry. In terms of optimization methods, there are many topology optimization methods to find material distribution, including continuum (Aage, et al., 2017) and discrete ground structure (He, et al., 2017) topology optimization method. It is very difficult to describe hollow tubular geometry in a continuum optimization model, especially for three-dimensional and complex structures. A transformation continuum optimization models named a moving morphable components model (MMC) (Guo et al., 2014) try to design hollow vehicle hollow frames (Bai, et al., 2020), but the results are not ideal. It is relatively easy to describe hollow tubular structures in a discrete optimization model. The geometry of hollow tubular structures can be expressed by a few simple parameters.

Moreover, metallic additive manufacturing technology can greatly shorten the manufacturing cycle, and compared with traditional manufacturing technology, it can print some more complex shapes and structures; However, different additive manufacturing technologies have some geometric printing constraints on the internal details of the printed structure (Liu et al., 2018; Zhu et al., 2021); Therefore, it is important to consider specific printing constraint in the topology optimization process. Most of the previous researchers tried to consider some printing constraints into mathematical language, and then use them as constraints of optimization methods, to restrict the optimized structure to meet the geometric constraints of printing methods. It is difficult to achieve this goal in a continuum optimization model, especially in a three-dimensional complex model. Although some optimized structures can meet certain angle and size constraints in the ground topology optimization, they cannot satisfy the industrial aesthetics.

To sum up, motivation, the author of this paper, based on the traditional ground structure topology optimization framework, develop a new design method named generation design strategy, this method not only can satisfy WAAM (Xia et al., 2020) manufacturing constraints of a large-scale metallic hollow structure but at the same time also allows engineers to locally modify the structure of fast post-processing; Outdoor experiments verify that our designed products are high in structural safety and structural reliability.

2. Chassis of electric vehicle and load analysis

The design of the electric vehicle chassis (Figure 1a) is based on PIXBOT, a fully electric, four-hub motor drive, a four-wheel steered vehicle that is used as a platform for autonomous vehicles development by many companies and universities. Defining the design domain (Figure 1c) is the first step in our workflow. As shown in Figure 1c, the design domain geometry is constructed according to the shape of the original chassis and the layout of necessary components installed on the chassis (Figure 1b). To leave the maximum freedom to the optimization algorithm in search of the most optimal structure, the domain is made as large as possible. The battery pack, controller

and steering parts are defined as obstacle areas, while the other parts, such as holes for the electrical wires that supply power to the hub-motors, and holes for the steering rods, are defined as preserved areas. In addition, the wheelbase and the track of the vehicle are fixed. According to the actual size of the chassis, the design domain of the chassis is 2500mm in length, 1400mm in width and 400mm in height.

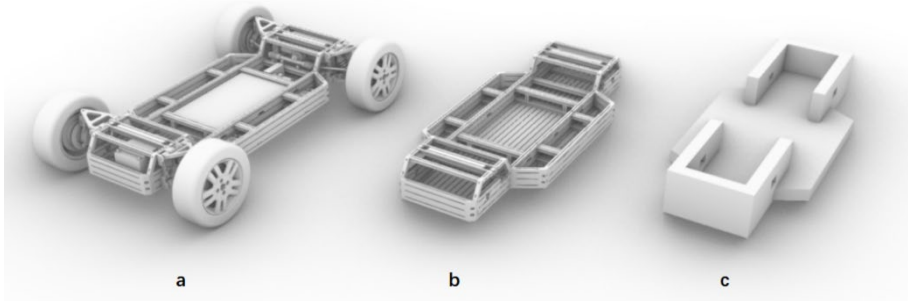


Figure 1. (a) The chassis with components; (b) The basic chassis structure; (c) Design domain of the chassis

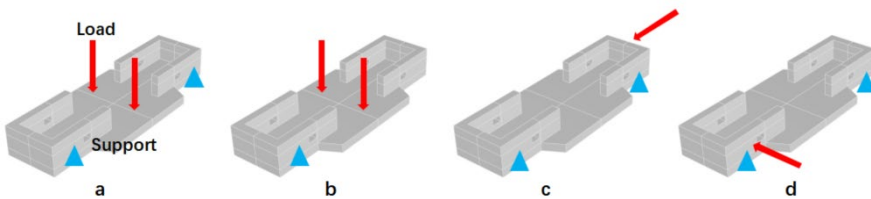


Figure 2. (a) Landing on four wheels; (b) Landing on three wheels; (c) Acceleration or deceleration; (d) Turning

The static load of the chassis is mainly composed of the weight of the chassis, the weight of the components and the weight of the cargo. The typical conditions should be analysed because of the complicated terrain encountered in the process of electric vehicle driving. There are four main types of load cases. The main working condition of an electric vehicle is landing on four wheels (Figure 2a). Under the condition of applying full load, the electric vehicle can land on four wheels and travel at a constant speed in good road conditions. The main load of the chassis includes its self-weight, weight of chassis components and cargo weight. In this case, the chassis is subjected to a vertical load and bending load. For landing on three wheels or the suspension system load (Figure 2b), one of the wheels of an electric car may leave the ground during rough roads. In this case, the chassis structure is subjected to severe torsional load. When the electric vehicle accelerates or decelerates (Figure 2c), the inertial force exerts a longitudinal load on the chassis structure. Its magnitude can be determined by the acceleration and the overall mass of the electric vehicle. When an electric vehicle turns (Figure 2d), the chassis structure tilts to one side under centrifugal force. The force is determined by the turning radius and driving speed.

When building a complex optimization model, secondary factors should be

ignored, which makes it easier to solve the model. There are many components of the chassis, and some components with a small load are omitted to reduce the number of stress points, such as computers, transformers, etc. In addition, because the structure of the frame is symmetric with the force, we only calculate a quarter of the model to speed up the calculation.

During the analysis, the weight of the chassis is applied by attaching a vertical downward gravitational acceleration. A load of each component is simply distributed to the stress point of the corresponding structure. For example, the total weight of the cargo 800kg is applied to the points at which the cargo rack is connected to the chassis. So, the points need to support at least 8000N of force downward (Figure 2). The influence of dynamic load on the chassis of the electric vehicle is considered by introducing a dynamic load factor and applying the load times to the dynamic load factor to the corresponding position during the finite element analysis of the chassis. According to the actual test, the dynamic load coefficient is selected to be 1.5.

3. Topology optimization and fabrication constraint

Topology optimization provides an efficient inverse analysis tool to design engineering structures with specific mechanical or other functions by using a minimal volume (or mass) of materials. For the continuous topology optimization method, the designed domain is discretized into many continuous and finite meshes. Various optimization methods, such as the solid interpolation of material penalty (SIMP) model (Aage et al., 2017), the level set model (Wang et al. 2003), and a moving morphable components model (MMC) (Guo et al., 2014), use a different framework to describe the design variables.

3.1. HOLLOW TUBULAR STRUCTURE

It is difficult for the continuous topology optimization method, such as the SIMP model and level-set method, to design the tubular structures (Clausen et al., 2015). In this method, the boundary of the tubes needs to be described by the complex mathematical formula, and they are not easily performed in large-scale structures and commercial software. Recently, the feature-driven MMC method (Bai et al., 2020) has been used to design the hollow tube framework of the vehicle, but the optimized results are too complex, and lose the aesthetics of the industrial products.

A discrete topology optimization method starts with a ground-structure model and produces optimized truss-like structures. For the stiffness problem, the optimization formula is written as (He et al, 2017; Ye et al., 2021; Zhang et al., 2017)

$$\begin{aligned} \min_{\mathbf{r}}: V &= 2\pi t \mathbf{I}^T \mathbf{r} \\ \text{subject to: } \mathbf{B}\mathbf{q} &= \mathbf{f}, \\ -2\pi t \sigma_0 r_i &\leq q_i \leq 2\pi t \sigma_0 r_i, \\ (0 \leq r_i &\leq r^*), \quad i = 1, 2, \dots, N, \end{aligned}$$

where V is the structural volume, $\mathbf{I} = [l_1, l_2, \dots, l_N]^T$ is a vector of hollow tube length, N is the number of the hollow tube. We assume that all hollow tubes have a uniform wall thickness with $t = 2\text{mm}$, $\mathbf{r} = [r_1, r_2, \dots, r_N]^T$ is the vector of all hollow

tube radii and design variable, \mathbf{f} and \mathbf{q} are the vectors of the external nodal loads and internal force of hollow tube, respectively. The area of i -th hollow tube is approximate $a_i = 2\pi r_i \cdot \sigma_0 = 350.7\text{MPa}$ is the limiting tensile strength for the additive manufacturing material 7075 aluminum alloy. This discrete optimization process has three steps. In this model, the tube is easy to present by small geometrical parameters.

First, the design domain, load and supporting conditions are specified (Figure 3a). Next, the discrete nodes are generated inside the design domain and all possible members are created by interconnecting these nodes, forming a ground structure (Figure 3b). Then the problem can be solved by the optimization algorithm (e. g. the convex optimization) and the design variables are also be updated through mathematical iterations (Figure 3c). Finally, the discrete structures are transformed into a continuum of organic forms (Figure 3d). While, owing to the constraints of overhang, the optimized results generally cannot be fabricated through WAAM.

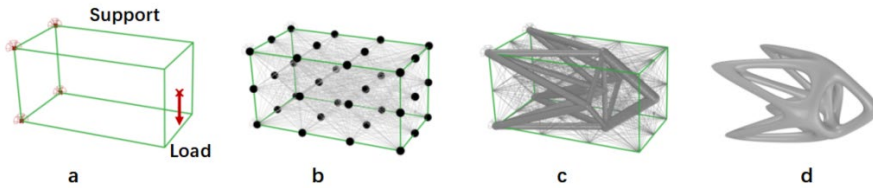


Figure 3: The schematic of the ground structure topology optimization. (a) Design domain; (b) Ground structure; (c) Optimization result; (d) Organic forms

3.2. FABRICATION CONSTRAINTS

Self-supporting 3D printing is a frontier fields for the manufacturing techniques and structural optimization. Recent attempts were made to study these geometric constraints in continuous topology optimization framework. However, these methods, containing complex mathematical descriptions of geometric constraints (Guo et al., 2017.) are too cumbersome for engineers and were found to not work well, especially for the design of large structures with complex loads. In addition, current topology optimization software cannot take manufacturing constraints into account at the design stage. For example, in our continuous topology optimization process, the optimized structure (Figure 4a) does not satisfy the manufacturing constraints of WAAM, as the resulting structures have sharp overhangs and the feature thickness at some locations is too low. To make the optimized results be manufacturable for the WAAM, manual and auto modification of these results were carried out as shown in Figure 4b-c, and the final results were still not promising.

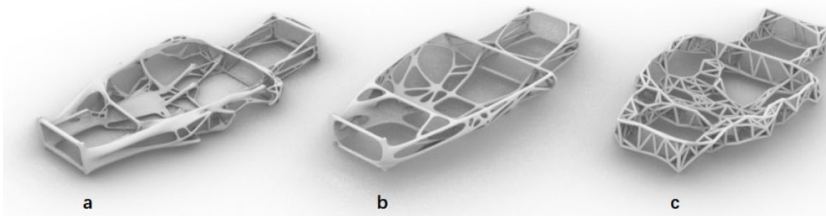


Figure 4: (a) Continuous topology optimization; (b) Manual modelling; (c) Auto modelling

3.3. GENERATIVE STRATEGY

Our initiative strategy to overcome this problem is to generate many possible results under one kind of load and boundary condition. There are three parameters in the topology optimization framework which we choose to vary:

$M \in \{3, 5, 7, 9, 11\}$: where M is the number of the discretizing parts on each edge of the design domain, and $M = 3$ denotes that the three-dimensional design domain is divided with $3 \times 3 \times 3$ nodes.

$J \in \{0, 0.1, 0.2, 0.5, 1\}$: The length of the i -th member is modified as $l_i + 2J$, J is the nodal penalizing factor that is used to reduce the number of short members in the optimized structures (Parker et al., 1975). The larger the value, the fewer the short members in the structure.

$R \in \{0, 1, 2, 5, 10\}$: $R_i = \max(r_{i,j}), j = 1, 2, \dots, n_i$, is the nodal merging radius of i -th node, and $r_{i,j} = ((\sum_{k=1}^{n_i} (1 + l_{i,j} \cdot l_{i,k}) a_{i,k}) / (2\pi))^{1/2}$ (He et al., 2019).

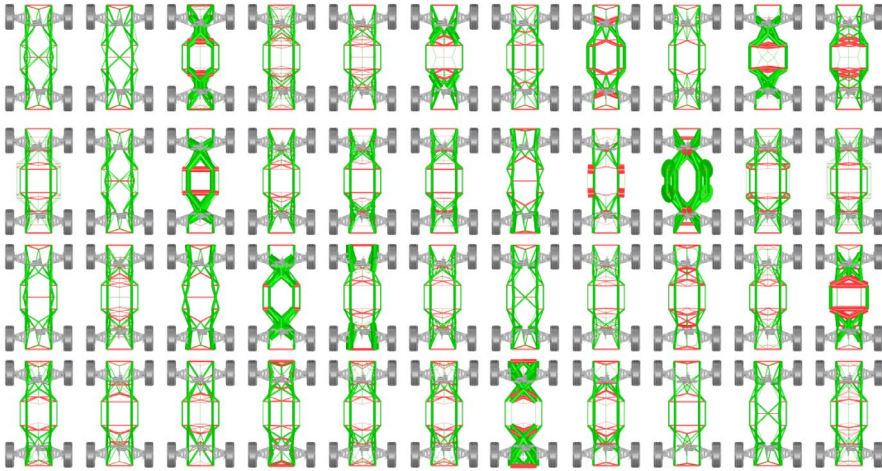


Figure 5. Part of the generated results. (Components greater than 60 degrees are marked in red)

By default, combining these factors leads to 1200 total chassis designs. Figure 5 represents part of the generated results, where green parts can be WAAM printed while red parts cannot. Each design takes an average of 2 seconds to calculate, requiring 40 minutes total. In order to get manufacturable and lightweight solutions, our generated results also should satisfy the following expectations:

$$\text{minimize: } \{V_{\min}^{(j)} \mid j \in \Omega\}, \text{ and } \{n_j \mid j \in \Omega, \text{ in which } \theta_i \leq 60^\circ, i \in N\},$$

where Ω is the sets of generated results, $V_{\min}^{(j)}$ is the minimum material volume of the j -th result in Ω ; n_j is the number of tubes in the j -th generated structure with an inclination θ_i to the horizontal plane.

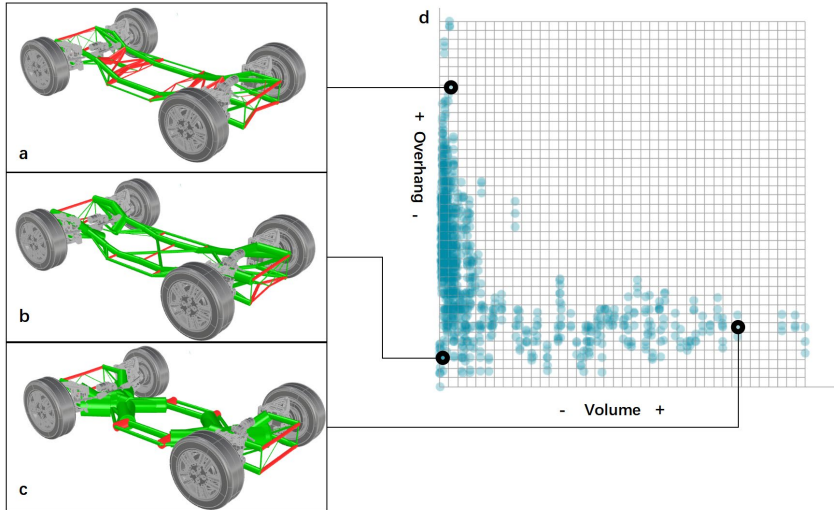


Figure 6. Objective space

We chose the final solution in an interactive way rather than an automatic optimization. In order to clearly understand the attributes of all solutions, we can visualize the results by plotting a Pareto front of the two objective function values. Figure 6d shows each chassis design as a point on a scatter plot where the x-axis represents the weight of the chassis, the y-axis represents the number of overhang hollow components. The performance values of each design are mapped to the coordinate system. Fig 6a shows one of the obtained design results of a lightweight chassis with a large number of overhang hollow components. Fig 6b shows a lightweight chassis with a low number of overhang hollow components, therefore having much greater manufacturability. Fig 6c shows a very heavy chassis with a large number of overhang hollow components.

Once the result is determined, the user has a further choice to locally edit the final results to meet the aesthetic and manufacturing constraint of WAAM, without fundamentally altering the design. For instance, the user can go into the edit mode, click on the element that needs to be changed and rebuild its size or change the position of the joint nodes. Manual modification is useful when the structural complexity of obtained results is relatively low. It has a high dependency on the artistic skill of the designer or engineer and cannot be scaled to highly complex structures.

To get a continuous, smooth and organic structure, we apply the SubD algorithm to our optimized result (Figure 7a). In Rhino7.0, MultiPipe can make a smooth piped surface out of a network of curves with a smooth joint at each curve intersection, at the same time adhering to the optimized cross-sectional area values obtained after optimization. In Figure 7b, the optimized hollow structure can be directly imported in the commercial finite element software Abaqus. The 7075 aluminum alloy with its material density, Young's modulus and Poisson's ratio 2810 kg/m^3 , 71 GPa and 0.33 , is taken in our simulations and the printed structures, and the von-Mises stress and

lower-frequency modes of the optimized hollow structures are calculated using shell model in the software Abaqus, and the results (Figure 7c) show that the optimized structures have great strength and reliability.

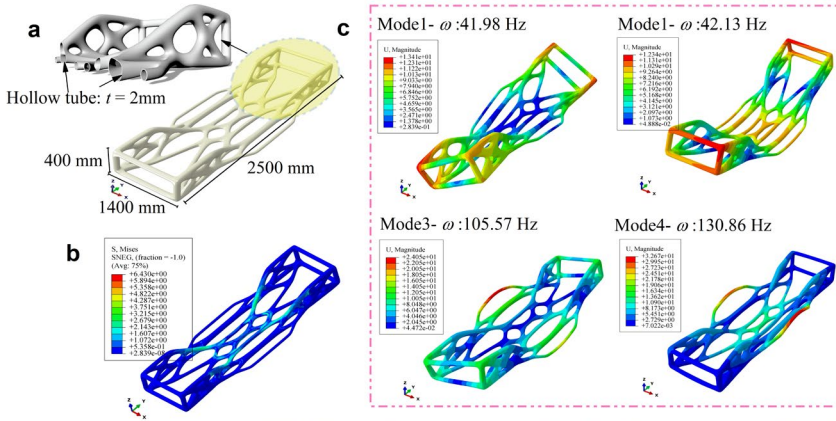


Figure 7: (a) Smoothed hollow structure; (b) von-Mises stress of the optimized structure; (c) Modal analysis

4. Fabrication

WAAM is an emerging AM technology that uses a combination of an electric arc as a heat source and a metal wire as feedstock. The hardware included a KUKA six-axis robot, a Fronius CMT welding equipment. No part-rotator was used.

A key factor that allows the model to be manufactured is path planning. The model is sliced into horizontal layers and each layer is further broken down into a list of points with their respective orientation for the robot to reach. The orientation of each point is defined by a unit normal vector that is normal to the surface of the optimized final result geometry at that point. This is the orientation the robotic end-effector will be aligned in the 3D printed object and is critical because it allows the weld bead to have a maximum area of contact with the weld pool. The method is different from the traditional desktop 3D printing process wherein the printing head is always aligned vertically, thereby reducing its ability to print at sharp overhang angles without a support structure.

The final designed chassis has a dimension of 2500 mm × 1400 mm × 400 mm, made from high specific strength aluminium alloy 7075, was printed in 80 hours, and weighs about 60kg (Figure 8). The 3D printing chassis is half as heavy as the previous chassis (PIXBOT). The cost of aluminium filament wire used for 3D printing is about 10 US dollars/kg, and for the final designed 60kg chassis, this amounts to a cost of 600 dollars. If we do not consider the initial investments made in acquiring the robot and the welding equipment, the only other cost is that of electricity.

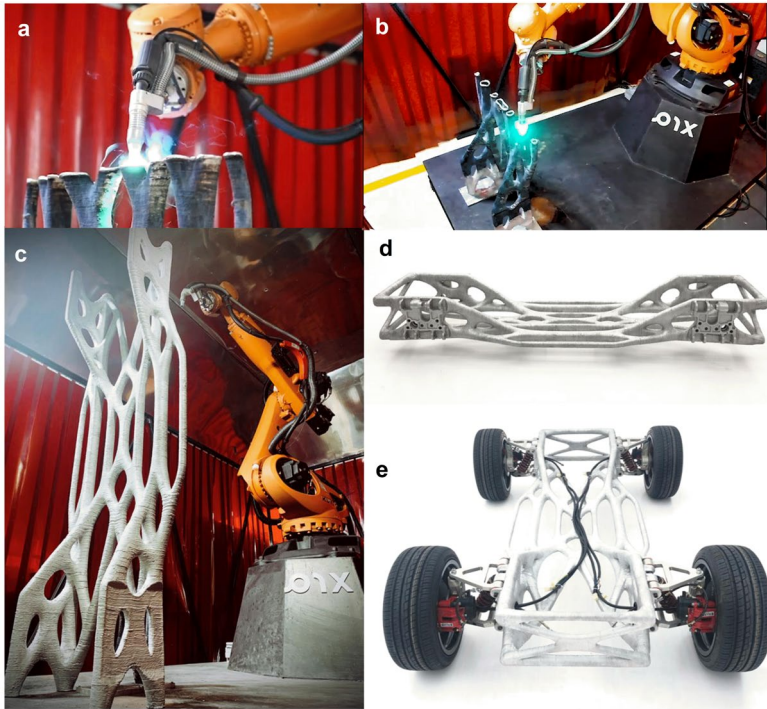


Figure 8: (a), (b) and (c) Manufacturing process; (d) Chassis printing part; (e) Chassis assembly

5. Discussion

Our work contributes to the development of a method that allows user to fabricate large-scale structurally optimized results for a given load-case while considering WAAM manufacturability simultaneously. To the best of the authors' knowledge, no computational tools currently exist that perform structural optimization design while considering WAAM manufacturing constraints and our work addresses this problem. We first justify the use of WAAM as an extremely economical and production-scalable AM technique due to its low running costs and high metal deposition rates. We then address the problem through a unification of truss-network based continuous layout optimization, hollow model of tube, aesthetics and further manufacturing consideration of the user through user-interaction with the model, creation of a final organic shape with a smooth transition of the hollow tube network at the joints. The method is used to design and fabricate the world's first metal 3D-printed full-scale Electric-Vehicle chassis that has been successfully tested for strength and durability in real-road conditions.

References

Aage, N., Andreassen, E., Lazarov B. S., & Sigmund, O. (2017). Giga-voxel computational morphogenesis for structural design.

- Nature*, 550, 84-86.
<https://doi.org/10.1038/nature23911>
- Bai, J. T., & Zuo, W. J. (2020). Hollow structural design in topology optimization via moving morphable component method.
Structural and Multidisciplinary Optimization, 6, 187-205.
<https://doi.org/10.1007/s00158-019-02353-0>
- Clausen, A., Aage, N., Sigmund, O. (2015). Topology optimization of coated structures and material interface problems.
Computer Methods in Applied Mechanics and Engineering, 290, 524-541.
<https://doi.org/10.1016/j.cma.2015.02.011>
- Guo, X., Zhou, J. H., Zhang, W. S., Du, Z. L., Liu, C., Liu, Y. (2017). Self-supporting structure design in additive manufacturing through explicit topology optimization.
Computer Methods in Applied Mechanics and Engineering, 323, 27-63.
<https://doi.org/10.1016/j.cma.2017.05.003>
- Guo, X., Zhang, W. S., & Zhong, W. L. (2014). Doing topology optimization explicitly and geometrically-a new moving morphable components based framework.
Journal of Applied Mechanics, 81, 081009.
<https://doi.org/10.1115/1.4027609>
- He, L. W., Matthew, G., & Song, X. Y. (2019). A python script for adaptive layout optimization of trusses.
Structural and Multidisciplinary Optimization, 60, 835-847.
<https://doi.org/10.1007/s00158-019-02226-6>
- Liu, J. K., Gaynor A. T., Chen, S. k., Kang, Z., Suresh, K., Takezawa, A., Li, L., Kato, J. J., Tang, J. Y., Wang, Charlie C. L., Cheng, L., Liang, X., & To, A. C. (2018). Current and future trends in topology optimization for additive manufacturing.
Structural and Multidisciplinary Optimization, 57, 2457–2483.
<https://doi.org/10.1007/s00158-018-1994-3>
- Parkes, E. W. (1975) Joints in optimization frameworks.
International Journal of Solids and Structures, 11, 1017-1022.
- Wang, M. Y., Wang, X. M., Guo, D. M. (2003). A level set method for structural topology optimization.
Computer Methods in Applied Mechanics and Engineering, 192, 227-246.
- Xia, C. Y., Pan, Z. X., Polden, J., Li, H. J., Xu, Y. L., Chen, S. B., Zhang, Y. M. (2020). A review on wire arc additive manufacturing: Monitoring, control and a framework of automated system.
Journal of Manufacturing Systems, 57, 31-45.
<https://doi.org/10.1016/j.jmsy.2020.08.008>
- Ye, J., Kyvelou, P., Gilardi, F., Lu, H. J., Gilbert, M., & Gardner L. (2021) An end-to-end framework for the additive manufacture of optimized tubular structures. *IEEE Access*.
<https://doi.org/10.1109/access.2021.3132797>
- Zhang, X. J., Ramos, A. S., Paulino, G. H. (2017). Material nonlinear topology optimization using the ground structure method with a discrete filtering scheme.
Structural and Multidisciplinary, 55, 2045–2072.
- Zhu, J. H., Zhou, H., Wang, C., Zhou, L., Yuan, S. Q., Zhang, W. H. (2021) A review of topology optimization for additive manufacturing: Status and challenges.
Chinese Journal of Aeronautics, 34, 91-110.
<https://doi.org/10.1016/j.cja.2020.09.020>

ROBOTIC ASSEMBLY OF MODULAR MULTI-STOREY TIMBER-ONLY FRAME STRUCTURES USING TRADITIONAL WOOD JOINERY

MATTHIAS HELMREICH¹, HANNES MAYER², MATTEO PACHER³, TADAHIRO NAKAJIMA⁴, MITSUHIRO KUROKI⁵, SHINYA TSUBATA⁶, FABIO GRAMAZIO⁷ and MATTHIAS KOHLER⁸

^{1,2,3,7,8} *ETH Zurich.*

^{1,2,3,7,8} {helmreich|mayer|pacher|gramazio|kohler}@arch.ethz.ch

^{1,2,3,7,8} {0000-0003-4312-9456|0000-0001-8683-4732|0000-0002-8519-4005|0000-0002-3761-7675|0000-0002-4111-4122}

^{4,5,6} *Shimizu Corporation.*

^{4,5,6} {nakajimat|s.tsubata|m.kuroki}@shimz.co.jp

^{4,5,6} {0000-0001-8100-1731|0000-0001-6630-8858|0000-0002-5436-0269}

Abstract. This paper presents a novel approach to computationally designed and robotically assembled modular timber-only structures with traditional wood joinery methods. We geometrically adapt and parametrize five traditional joint typologies to compensate for robotic placement inaccuracies and comply with modern structural requirements. The force-locking capacity of the connections is utilised to support the robotic assembly of five unique timber frame modules of 5.5 by 2.2 by 2.5 metres, each with a unique timber lattice pattern. For each major joint typology we conduct a series of structural load-tests to evaluate the structural performance. We develop a custom software to enable architects and engineers to interactively design with those principles, taking into account both structural and production feasibility constraints. As a demonstration of our design approach, the five modules were robotically assembled using the described methods.

Keywords. Robotic Assembly; Wood Joints; Spatial Timber Structures; Timber-only; SDG 9; SDG 11; SDG 12.

1. Introduction

Timber construction plays a critical role in pursuing a more sustainable alternative to carbon-intensive concrete and steel buildings (Herzog et al., 2003). Recent advances in the timber industry as well as updates to building codes have enabled architects and engineers to design and construct multi-storey buildings, but these designs focus mostly on light wood stud framing or mass timber construction methodologies, such as cross-laminated timber (CLT) panels (Deplazes, 2000). In contrast, traditional timber framing and wood joints, which were widely applied construction methods in Europe between the 6th and 19th century and have a long tradition in Japan (Togashi,

2013), are rarely applied despite their ingenuity, durability and in these regions, cultural embedding.

This paper presents an approach to rejuvenating traditional timber frame construction methods through computational design and robotic fabrication – positioning it as an alternative to mass timber construction or light wood stud framing. Here we analyse and digitally adapt five major traditional wood joints within the architectural design context of a three-storey timber lattice structure focusing on and expanding the following research topics:

- **Design parametrization of traditional wood joints.** The complexity of timber connections varies from simple butt joints to geometrically complex scarf joints composed of multiple subparts, like wedges and dowels. Nowadays only a limited number of timber connection types and parametrization functionalities are available in common timber CAD software's like Cadwork or SEMA. It is hardly possible to define parametric interdependencies of timber connections composed of multiple parts.
- **Robotic assembly of geometrically complex wood joints.** The assembly of wood joints requires high accuracy in machining and in assembly. Traditionally they were handcrafted and manually assembled by the builder on site in an iterative fitting process. While nowadays the Computer Numerical Control (CNC) machining of the individual parts is sufficiently accurate, robotic assembly on large scale structures can still only achieve low positioning accuracy, especially in a non-repetitive placement process (Stadelmann et al., 2019).
- **Structural evaluation of traditional wood joints.** Traditional wood joints greatly influence the performance of the whole structure. The evaluation of their capacity (strength and stiffness) remains a big challenge. There is little scientific data on, or knowledge of their structural behaviour and performance (Japanese Guidelines for timber-timber connections), although historical European and Asian timber-only constructions like the Hōryūji temple (built in 747) showcase the durability and structural integrity of the building method.

2. State of the Art

Today's timber construction methods are mainly classified into light wood stud framing, glue-laminated timber (i.e. glulam), traditional heavy timber, and construction methods using mass timber such as CLT or dowel-laminated timber (DLT). Wood frame construction elements usually consist of a simple timber frame with braces or plates for lateral stiffness. Screws, nails and other metal connectors join the different layers and materials into one almost inseparable component making the recycling process cumbersome. Mass timber methods involve fitting CLT plates or dimensional lumber into a solid timber wall or ceiling component, e.g. a board plywood deck or a board stack wall (Herzog et al., 2003). Yet in a large and upscaling market the material demand of solid timber buildings will quickly exceed the supply of sustainably sourced timber (Kromoser et al., 2021). Thus material-efficient, optimised timber structures are required to avoid exploitation of natural resources.

Current building code standards (such as Eurocode 5 and The Building Standard

Law of Japan) offer little guidance for engineers and architects on how to design with traditional timber-only joints in practice. For structural analysis, connections between timber parts are abstracted into simple geometries (e.g. contact areas), which are then calculated by hand.

Limited research has been conducted on the spatial robotic assembly of wood joints. Apolinarska et al. (2020) utilised reinforcement learning models to control the robotic assembly of tight fit timber joints. However, their method only demonstrated the assembly of a few small sized elements with a simple lap joint geometry. Leung et al. (2021) used distributed high force clamps to assemble structures also with simple tight-fitting lap joints.

3. Modern Timber-only Connections

In contrast, the authors tackle the challenge of robotic placement inaccuracies by introducing CNC-milled geometric guiding features, which render special robotic tools obsolete. In addition the developed wood joints fulfil the structural and legal requirements of a three-storey timber lattice frame structure in Japan and Switzerland.

First, the traditional joint geometry was refined based on the expertise of roboticists and engineers. Second, tapering and chamfering (Figure 1) were included at the engaging edges of the joint to guide the robotic insertion process. Third, the density and layout of the diagonal lattice members was modified until the structure met the required joint strength and stiffness. The parametrization of the timber joint geometry allows us to vary the joint incident angles within a given range, thus giving the designer more freedom in designing the timber lattice layout.

Our ambition was to not use any adhesives. However, due to regulatory requirements regarding the long-term durability of the joint's outdoor weather exposure, epoxy glue has been applied to certain joint faces to guarantee compliance with the Japanese Building Code for structures.

3.1. JOINT TYPOLOGIES

In total our structure is composed of five unique modules (Figure 2f). Figure 1 exemplifies the location of each joint typology in a module.

- **Tapered dovetailed lap joint for diagonal members' ends (Joint 1, Figure 1a).** This connection type is called 'ari-tsugi' in Japan and has been used since ancient times. The dovetailed end allows the connection to transfer high compression and tension forces to the lower and upper chords. The dovetail is tapered to compensate for the robotic placement inaccuracy. The oak dowel locks the position of the connection.
- **Dovetailed joint for hanging floor and ceiling joists (Joint 2, Figure 1b)** is a standard European dovetail connection in floor and ceiling joists with variable connection angles and a chamfer of 5 mm at the engaging edge.
- **Tabled splice joint for intermodule diagonals (Joint 3, Figure 1c).** This connection originates from the European 'Hackenblatt,' similar to the traditional Japanese 'kanawa-tsugi' or 'okkake-daisen-tsugi,' and connects two or three

collinear and coplanar diagonals spanning through multiple modules (Figure 2e). It consists of a connecting timber plate, six alternating dowels, and four wedges. After the plate has been placed, wedges are put in place to ensure contact pressure.

- **Corner lap joint for lower and upper chords (Joint 4, Figure 1d).** The corner lap joint originates from the European ‘Eckblatt’, which is still a widely used corner connection for floor and ceiling joists that end at 90°. In order to improve the resistance against cross-sectional forces, the mating sides are interlocked.
- **Cross lap joint for crossing-diagonals (Joint 5, Figure 1e).** Standard half-lap joint, which is reduced from $\frac{1}{2}$ to $\frac{1}{4}$ of the cross-section height to maintain the structural capacity of the member. Known as ‘ai-kaki’ in Japanese. This joint connects two intersecting diagonals at various angles.

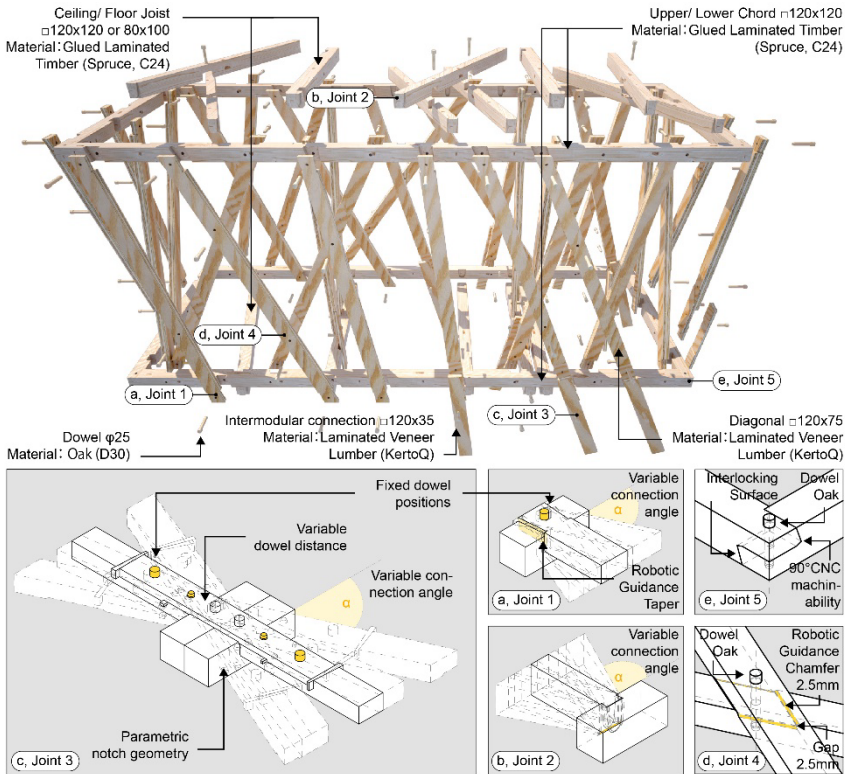


Figure 1. Exploded visualisation of one timber module showing the joint typologies 1-5 applied in one module (above) and their parametric variations (below)

4. Computational Design and Fabrication Framework

The volumetric starting point is a rectangular parallelepiped module of 5.5 by 2.2 by 2.5 metres (Figure 2b) designed to fit in standard 40' high cube containers. The topology of the timber lattice is initially drawn by the architect (Figure 2d). To reduce buckling behaviour, the diagonals need to intersect at least one or multiple other diagonals. Extended intermodular diagonals are added to ensure the structural integrity

of the aggregation of the different modules (Figure 2e).

4.1. INTERACTIVE COMPUTATIONAL DESIGN

The overall parametric design was generated with a custom Grasshopper/ Python script within the CAD software Rhinoceros 6. The design tool allows the designer to input boxes as volumetric envelopes of each module, and lines representing the timber lattice elements.

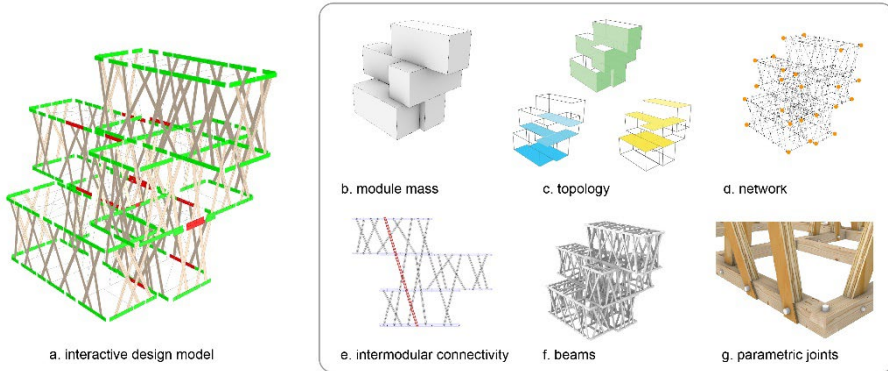


Figure 2. Computational design data structure

Lines are classified according to the surface topology (wall, ceiling, floor), which allows elements to be generated automatically (joist, diagonal, chord). In this process global parameters, such as the timber element cross-sections and the dowel diameters, are predefined and applied to the specific type of elements.

Lines intersections define the resulting joint type (e.g. when two lines of the type diagonal meet, Joint 5 is geometrically generated by the element intersections).

The data structure of the lattice (Figure 2d) uses functionalities of the COMPAS framework (Mele et al., 2017), such as the network class where edges represent lattice elements and nodes represent their connections. The network and its associated information also serve as a serializable unified model, which through custom implementation is exported to structural engineering software.

The wood joint geometries are parametrically generated (Figure 2g) by subtractive boolean operations. The structurally constraining parameters of each connection, such as the distance between the dowel drill holes or the notch depth, are predefined. The connecting lines meeting angle is the most impactful parameter (Figure 1a-e).

4.1.1. Interactive Design and Structural Feedback

Timber-only connections require a minimum distance between their notches to allow forces to flow through the member. The notch depth and distance is derived from the dowel diameter: neighbouring diagonals minimum distance = notch depth*7; notch depth = dowel diameter*2.

The design tool colour-codes structural members to illustrate the distance between diagonal joints, which provides real-time feedback about the fulfilment of

requirements. The feedback is indicated in Figure 2a as a green rectangular surface which turns red when the requirement is not met. Using this information, the user can interactively adjust the input lines.

4.2. ROBOTIC FABRICATION SIMULATION AND MOTION PATH PLANNING

The computational design model also embeds information required for the robotic assembly. This includes the assembly sequence, element gripping poses, insertion vectors, and inputs for the robotic motion planning solver.

The robotic assembly sequence is manually evaluated and defined, taking into account the multi-robot collaborative assembly strategy. Based on the given sequence, collision-free gripping poses and insertion vectors are automatically computed for each assembly element. Path-planning, both for placing and retraction motion paths, was carried out using COMPAS FAB (Rust et al., 2018), relying on MoveIt as backend. The robotic set-up, consisting of an external overhead gantry system and two robots, was described as a Unified Robot Description Model (URDF) and implemented as part of the MoveIt package. To enhance the speed and success rate of the robotic motion planning, the user can input in-between robot configurations to guide and speed up path planning computation for hard-to-reach targets (Figure 3c). The kinematic paths are pre-computed and executable on the real robot exploiting the COMPAS RRC (Fleischmann et al., 2020) communication library.

5. Robotic Fabrication of Timber Modules

The fabrication process was subdivided into six steps: (1) manually placing a member on the pick up station, (2) robotic pick-up of the member, (3) robotically manoeuvring the member to the insertion position, (4) robotic insertion of the member in its final position, (5) manually inserting the dowel and applying epoxy (optional) and (6) retracting the robot from the insertion position. Each module has 52-57 members, 107-143 dowels and was assembled in an average time of under 48 work hours.

5.1. ROBOTIC ASSEMBLY PROCESS

The assembly strategy (Figure 3) is derived from (1) the interlocking connectivity and (2) the interdependencies between the collaborating robots.

The **floor joists** are simultaneously assembled by both robots to speed up the assembly process. The dovetail connection is designed to force (pull/ push) the lower chord into position, helping to accommodate the tolerances.

The **long side wall segments** (Figure 3g-h) are assembled collaboratively by the two robots: one robot supports the upper chord while the other is placing the diagonal chords (Figure 3a-b). After the first diagonal layer is completed, the robots switch their assembly tasks. After completion, the interlocking joints allow the wall to stand upright without additional support.

All diagonals of the **short side walls** are positioned by one robot from one side. The motion planning of the members is particularly challenging due to the limited manoeuvrability of the robot in between the two long walls and the complex rotational

insertion movements of the arm.

The **ceiling joists** were simultaneously assembled by both robots moving at the same time to speed up the fabrication process. Both the dense lattice layout and the half-lap joints reduced the number of feasible gripping poses.

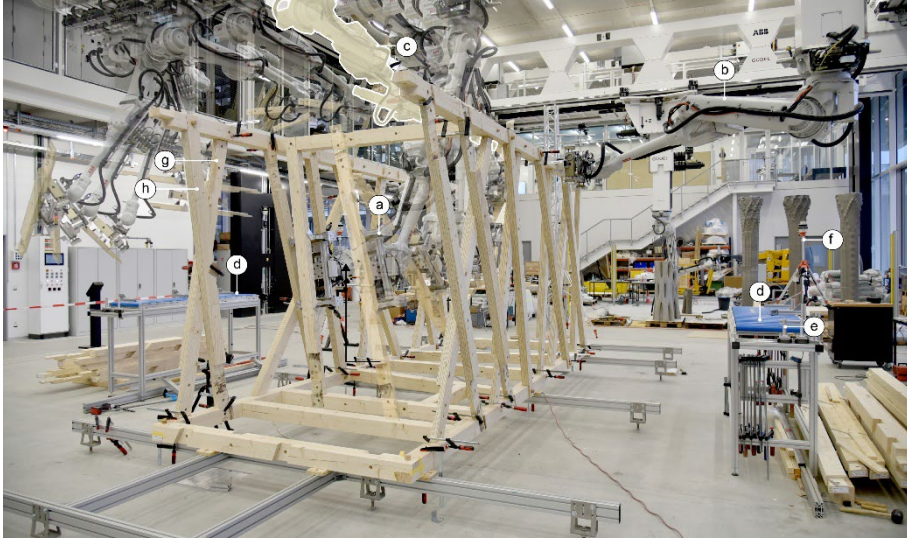


Figure 3. (a) Robot placing beam. (b) Robot supporting structure. (c) Intermediate robot configuration. (d) Pick-up stations. (e) Reference pin. (f) Absolute correction system. (g) Outer diagonal layer. (h) Inner diagonal layer.

6. Structural Analysis

Timber frame structures are dynamic spring-loaded structures that continuously adjust to the current load situation, i.e. wind from different sides. It is important to allow the joints to move slightly and adjust to the different load direction so as to not overstress a single member. Therefore, all joints have a gap of 0.5 mm to ensure this spring flexibility. The location of the continuous braces (Figure 2e) connecting the different modules are determined through semi-parametric structural analyses aiming to balance the member and joint stresses. The structural analysis model description was performed with the software SNAP 8.0.

6.1. STRUCTURAL EVALUATION OF WOOD JOINTS

The member stresses are primarily determined by the design forces, which are self-weight (ca. 700 kg per module), wind (wind speed 34m/s) and seismic force (seismic shear coefficient 0.5). Applying traditional joints to the structural system involves several structural engineering challenges: (1) traditional interlocking joints have elaborate details, which result in complicated load transfer mechanisms, (2) the design methods in calculation are not clearly stated in structural engineering guidelines, and (3) the robotic fabrication requires additional gaps among the surfaces of interlocking joints. To overcome these challenges, the authors decided to adopt performance-based

approaches in structural engineering and conduct experimental studies to evaluate joint strengths and stiffnesses.

6.2. STRUCTURAL LOAD TESTS

To evaluate the joint strength and stiffness of the connections, load tests have been conducted on six specimens of each of the three major joint typologies, Joint 1-3.

6.2.1. Description of Test Set-Up

The test for the tensile performance of the joints is conducted using two different methods of force application. In the first test, we examine Joint 1 and Joint 2 (Figure 4). Here, the tensile performance of joints can be examined by anchoring the transverse members to the steel frame and pulling the longitudinal members with the hydraulic jack. In the second test, we examine Joint 3. In the experiment, the lower part of the longitudinal member is fixed to the frame, and the upper part is pulled by the hydraulic jack (Figure 4).

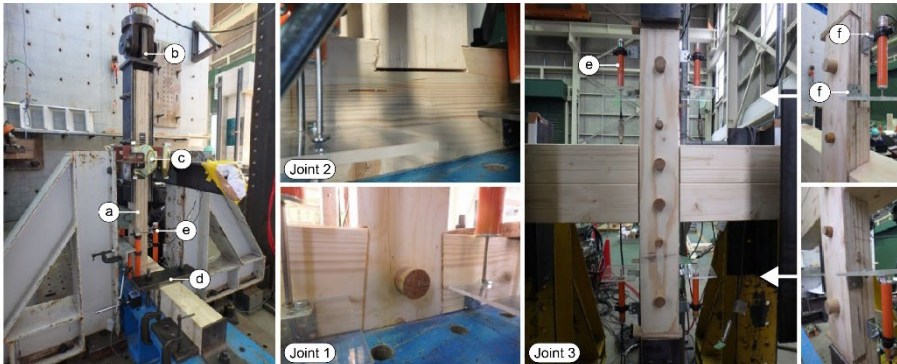


Figure 4. (a) Specimen. (b) Hydraulic jack. (c) Clamp for lateral guidance. (d) Clamp. (e) Displacement gage. (f) Sensor reference.

6.2.2. Summary of results

Figure 5a-c show the load-displacement relationship and Figure 5d-h the failure patterns of each joint.

In **Joint 1** the relation between load and displacement was generally the same among the specimens. However, the initial stiffness of specimens 1 to 3 was low and became high in the middle. Since there was no visual change in the surface of the specimen when the stiffness changed, it is inferred that there were gaps inside the specimen, and the stiffness increased as the gaps closed due to the joint deformation. Although the maximum tensile capacity of specimen 1 was lower than that of the others, the breakage was the same as that of the other specimens, which is attributed to variation in material characteristics.

In **Joint 2** the maximum tensile capacity varied greatly among the specimens and various joint failure patterns were observed. In particular, the specimen with the lowest bearing capacity showed early cracking on the back of the transverse material, which

is attributed to variation in material characteristics.

In **Joint 3** the load-displacement relationship showed generally the same behaviour among all specimens. However, the maximum tensile capacity of specimen 1 was lower than that of the other specimens. In Joint 3, adhesive was applied to the joint surface of the longitudinal material and the joint plate. In specimen 1, gaps in the joint surface were observed from the initial loading stage, which was attributed to the peel-off of adhesive in the early loading stage. The specimens without gaps were generally stable until the final stage, and the fracture was caused by cracks in the base member and wedge at the end.

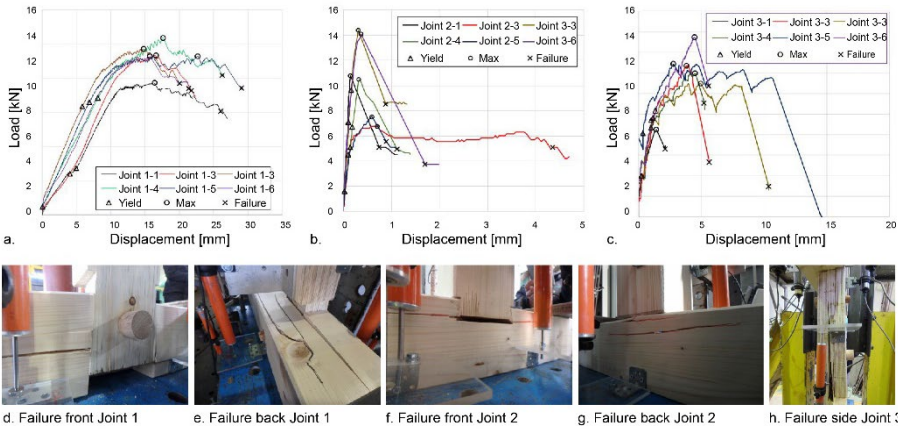


Figure 5. Load/displacement graph of six specimens for each joint typology (a-c). Images of failure at the end-state of Joint 1-3 (d-h)

In general, the test results showed similar structural behaviour in all joint specimens. However, the performance of some specimens in all joints was lower due to the tolerance gaps that were needed to compensate for robotic fabrication and construction tolerances. In accordance with these findings, the safety factor on the member calculation is to be defined based on experimental results.

7. Conclusion and Outlook

The research demonstrates how traditional knowledge about timber joints can be combined with interactive computational design, structural analysis, and digital/robotic fabrication methods to achieve high-performance timber constructions. We have demonstrated and verified the design and structural applicability of modern timber-only joints within a modular multifaceted three-storey lattice timber structure, while also considering the extreme wind and earthquake conditions in Japan. The interactive design feedback enables the planner to design with the complex interdependent structural constraints of timber-only joints, while maintaining a high level of design freedom. Further explorations of the method could go beyond a modular box system and investigate more complex geometric arrangements. This would then require further research into the proposed joint typologies with respect to structural and robotic fabrication constraints.

This study has further demonstrated that geometrical adjustments of the joint design can overcome robotic placement inaccuracies. The extensive load testing carried out in this study, constitutes a viable reference for engineers and architects seeking to understand the structural behaviour of modern timber-only joints. Using only wood materials improves both the carbon footprint and circularity of structures and thus this research contributes to reaching sustainable development goals. In the next phase of our project, the structure will be erected in Japan to complete the research of this paper.

Acknowledgements

This research project is supported by Presence Switzerland/ Swiss Federal Department of Foreign Affairs (FDA), Shimizu Corporation, ERNE Holzbau AG, Kalt AG, SJB Kempter Fitze AG, Holzwerke Bullinger, Cypress Sunadaya Co., Ltd.. We would like to thank Steffen Hermann, Adrian Gredig, Lukas Ehrle, Michael Lyrenmann, Philippe Fleischmann, Dr. Aleksandra Anna Apolinarska, Victor Y. P. Leung and Gonzalo Casas for their technical assistance, and Stephen P. Maher and Dylan M. Wood for reviewing this publication.

References

- Apolinarska, A. A., Pacher, M., Li, H., Cote, N., Pastrana, R., Gramazio, F., & Kohler, M. (2021, May). Robotic assembly of timber joints using reinforcement learning. *Automation in Construction*, 103569. <https://doi.org/10.1016/j.autcon.2021.103569>
- Deplazes, A. (2000, January). Diskussion: Holz: indifferent, synthetisch - *DETAIL inspiration*. <https://inspiration.detail.de/diskussion-holz-indifferent-synthetisch-107263.html>
- Fleischmann, P., Casas, G., & Lyrenmann, M. (2020). *COMPAS RRC: Online control for ABB robots over a simple-to-use Python interface*. Retrieved from <https://doi.org/10.5281/zenodo.4639418>
- Herzog, T., Natterer, J., Schweizer, R., Volz, M., Hauser, G., Winter, W., Zeitler, F., Draeger, K., & Institut für Internationale Architektur-Dokumentation. (2003). *Holzbau Atlas*. Birkhäuser.
- Kromoser, B., Braun, M., & Ortner, M. (2021). Construction of All-Wood Trusses with Plywood Nodes and Wooden Pegs: A Strategy towards Resource-Efficient Timber Construction. *Applied Sciences*, 11(6), 2568. <https://doi.org/10.3390/app11062568>
- Leung, P. Y. V., Apolinarska, A., Tanadini, D., Gramazio, F., Kohler, M. (2021). Automatic Assembly of Jointed Timber Structure using Distributed Robotic Clamps. In the *26th International Conference of the Association for Computer-Aided Architectural Design Research in Asia: Reflections, CAADRIA 2021* (Volume 1, pp. 583-592). The Association for Computer-Aided Architectural Design Research in Asia (CAADRIA).
- Mele, T. V., et al. (2017). COMPAS: A framework for computational research in architecture and structures. <https://doi.org/10.5281/zenodo.2594510>
- Rust, R., Casas, G., Parascho, S., Jenny, D., Dörfler, K., Helmreich, M., Gandia, A., Ma, Z., Ariza, I., Pacher, M., Lytle, B., & Huang, Y. (2018). *COMPAS FAB: Robotic fabrication package for the COMPAS Framework*. <https://doi.org/10.5281/zenodo.3469478>
- Stadelmann, L., Sandy, T., Thoma, A., & Buchli, J. (2019). End-Effector Pose Correction for Versatile Large-Scale Multi-Robotic Systems. *IEEE Robotics and Automation Letters*, 4(2), 546–553. <https://doi.org/10.1109/lra.2019.2891499>
- Togashi, S. (2013). *Fittings and Joints of Wooden Buildings*. Omusha.
- Traditional Construction Method Database (2021). *Japanese Guidelines for timber-timber connections*. Retrieved May 4, 2021, from <https://www.denmoku-db.jp/publics/index/18>.

TIMBER DE-STANDARDIZED 2.0

Mixed Reality Visualizations and User Interface for Processing Irregular Timber

LESLIE LOK¹ and JI YOON BAE²

^{1,2}*Cornell University.*

¹*wll36@cornell.edu, 0000-0002-6948-3544*

²*jb2672@cornell.edu, 0000-0001-9182-554X*

Abstract. Timber De-Standardized 2.0 is a mixed reality (MR) user interface (UI) that utilizes timber waste produced by manufacturing dimensional lumber, suggesting an expanded notion for “material usability” in timber construction. The expanded notion of designing with discarded logs not only requires new tools and technologies for cataloguing, structuring, and fabricating. It also relies on new methods and platforms for the visualization and design of these structures. As a MR UI, Timber De-Standardized enables professionals and non-professionals alike to seamlessly design with irregular logs and to create viable structural systems using an intuitive MR environment. In order to develop a MR environment with this level of competency, the research aims to finesse the visualization techniques in the immersive full-scale 3D environment and to minimize the use of alternative 2D UI(s). The research methodology focuses on (1) cataloguing and extracting basic properties of various tree logs, (2) refining mesh visualization for better user interaction, and (3) developing the MR UI to increase user design agency with custom menu lists and operations. This methodology will extend the usability of MR UI protocols to a broader audience while democratizing design and enabling the user as co-creator.

Keywords. Irregular Tree Logs; Wood Construction; Augmented and Mixed Realities; Mixed Reality User Interface; Digital Representation and Visualization; SDG 9; SDG 12; SDG 13.

1. Introduction

Timber can be considered as one of the most common and most sustainable construction materials. However, it requires socio-economic responsibility of industries, ethical forest management, and sustainable harvesting practices to further reduce its carbon footprint and energy use. Without sustainable practices, the manufacturing process of timber products produces carbon emissions and affects the surrounding environment (Adhikari and Ozarska, 2018). Dimensional lumber products

are widely used in building construction in the US. Specifically, 87.6 million m³ of softwood lumber are annually used for residential building construction in the US (Spelter et al., 2007). Therefore, timber production entails significant energy consumption and carbon emissions in auxiliary manufacturing, including sawing, gluing, planing, and the transportation process (Bergman and Bowe, 2010).

Additionally, many countries do not have access to source local materials used for dimensional lumber and are reliant on imports for timber construction. According to the US Department of Agriculture (USDA), US import of softwood and plywood has increased 346% between 2010 and 2019, related to the growth of housing construction markets and increased lumber prices during 2017 (Howard and Liang, 2019). Furthermore, the shortage of domestic access to specific types of wood can be another factor that accelerates the lumber trade and potentially affects the environment. Thus, to combat these issues and further utilize timber as a localized resource, there must be an expanded notion of usable timber for structural and architectural applications.

This expanded notion of designing with unused logs requires new tools and technologies for cataloguing, structuring, and fabricating. It also relies on new methods and platforms for the visualization and design of these new structures. The Timber De-standardized research project leverages mixed reality technology to utilize regular and irregular logs, minimizing waste and unnecessary energy use during auxiliary manufacturing. As an MR user interface (UI), Timber De-Standardized 2.0 allows professionals and non-professionals to experience seamless design workflows using tree logs. This paper presents the following methodologies: (1) Mesh visualization studies, (2) cataloguing and extracting the basic properties of sourced tree logs, (3) refining the MR environment with menu lists and operations to visualize a manipulated geometry next to the original element. The live feedback from the MR environment and ability to work at a 1:1 scale provides the user with an informed, intuitive, and educational platform that is non-deterministic. A series of visualization strategies were developed to test the applicability of the MR UI features mentioned above. Timber De-Standardized is a design tool and an educational device using localized timber logs.

2. State of the Art

2.1. IRREGULAR LOGS IN DIGITAL FABRICATION

Recent academic research, including Wood Chip Barn (2016), Limb (2018), and Digital Workflows for Natural Wood in Constructions (2020), demonstrate the potentiality of discarded logs as a usable construction material. Wood Chip Barn at the Architectural Association utilizes inherent characteristics of non-linear logs like forks to construct a truss structure. It demonstrates a research pipeline from extracting basic information of irregular logs such as geometry centerlines and cross-sections to manage the harvested materials for construction (Devadass et al., 2016). Limb uses discarded tree forks that are not harvested due to their low economic value to build a full-scale reticulated shell by replacing mortise and tenon joinery methods (Von Buelow et al. 2018). Digital Workflows for Natural Wood in Constructions transforms irregular natural logs into digital information to rationalize the geometry and to inform the fabrication process using an advanced laser scanner and bespoke algorithm (Larsen et al., 2020). These projects enable the possible implementation of irregular tree logs

as an added resource for building construction. However, there are limitations to the direct user engagement with material information such as geometric properties or structural analysis feedback.

2.2. IMPLEMENTATION OF MIXED REALITY IN CONSTRUCTIONS

During the 2018 CAADRIA conference, the workshop Making in Mixed Reality, introduced Fologram, a software platform that enables designers to generate an interactive holographic instruction within a MR environment (Jahn et al., 2018). During the workshop, a pavilion made of bent steel tubes was constructed by leveraging this MR platform which assisted and guided fabrication, and assembly. In a prior investigation by this research team, Timber De-standardized 1.0 is a framework that salvages irregular and regular logs by utilizing a MR interface for the design, fabrication, and assembly of a structurally viable tree log assembly (Figure 1). The process engages users through a direct, hands-on design approach with an embedded structural analysis feedback loop to modify and design irregular geometry at full scale within an immersive MR environment without altering the original material (Lok et al., forthcoming). Although both projects focused on a MR workflow design practice, advanced skills for multiple 2D & 3D computational UI platforms are still required. Moreover, the projects revealed the necessity for more intuitive UI for users.



Figure 1. Physical Components, Composite of Mixed Reality, and Structural Analysis

3. 3. Methodology

3.1. MIXED REALITY WORKFLOW

The research in this paper is built upon the above-mentioned prior investigation. A digital archive of 3D scanned logs constitute the building elements from which users, designing in the MR environment, can digitally harvest log parts (through slicing) and place the elements into a digitally constructed whole. The constructed whole is structurally analysed and optimized through recursive feedback loops to preserve the user's predetermined design. This iterative toggling between the physical and virtual emancipates the use of irregular tree log structures while informing and prioritizing the user's design intent. To test this approach, a scaled prototype was developed and fabricated in MR. The interactive workflow provides greater design agency to users as

co-creators in processing material parts. However, the process has an entry barrier due to the requirement of advanced expertise in different computational software. Hence, the main goal of this current research is to embed the entire processing of and designing with irregular log members in an immersive MR environment.

This paper improves upon previous research with an MR design workflow without using supplementary 2D UI platforms. The UI is improved by providing users with specific visualization of the log parameters and design operation menu in a full-scale 3D workspace. The refinements enable users to seamlessly design iterations of wood components or structural systems with one single MR protocol menu (Figure 2).

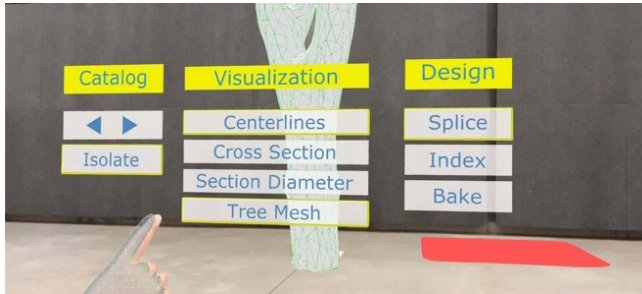


Figure 2. MR Implemented User Interface Menu

The UI menu is developed in the following phases. (1) Users can select and isolate a certain log geometry among the digital log library in the full-scale 3D environment. (2) The visualization categories allow users to choose the mesh option and toggle the geometric information such as centerline, cross-section, and diameter. (3) Users can slice geometries by moving and rotating slicing planes to generate wood components. The index will be automatically created for material cataloguing. (4) Users can bake the timber components by tapping the original geometries (Figure 3).

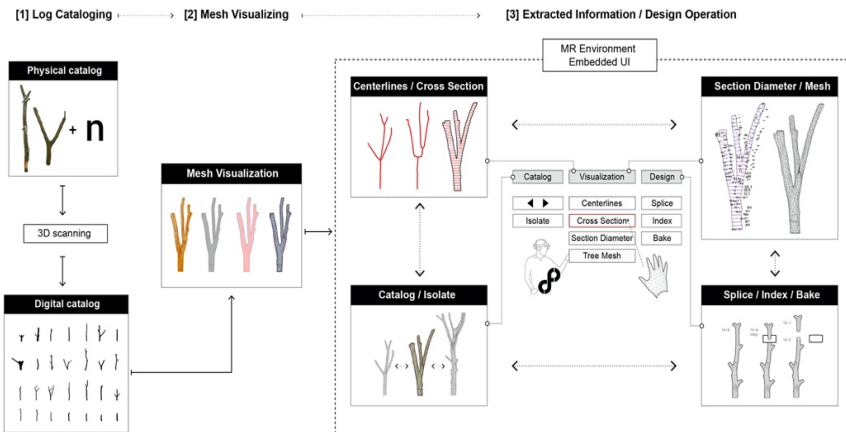
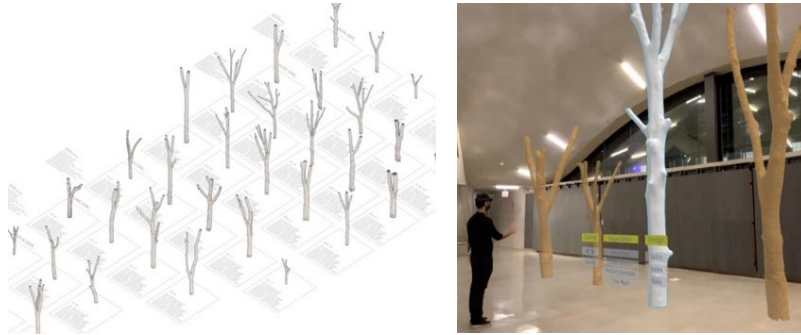


Figure 3. Overall Workflow of Timber De-standardized 2.0

3.2. DIGITAL TREE LIBRARY

The workflow begins with collecting logs and converting the physical elements into digital data. For the digital tree library, irregular logs were sourced from a local groundskeeping entity, catalogued and indexed using a 3D scanner. Then, the digital logs were used as ‘building blocks’ for design iterations (Figure 4). In the MR space, users can see this digital log library on a 1:1 scale. The virtual catalogue menu allows users to browse and to select proper forms and scales for further operations. The visualization of the selected log geometry is differentiated from the other log elements. The user can turn off the rest of the logs by tapping the isolate menu (Figure 5).



[left] Figure 4. Digital Log Library, [right] Figure 5. Log Library Visualized in an MR environment

3.3. VISUALIZATION

3.3.1. Mesh Visualization Studies

Mesh, the geometric discretization of surfaces, plays a significant role in various fields of computation. For example, establishing high-quality mesh data is considered a success factor in determining computing performance (Baker, 2005). In computational fluid dynamics (CFD) for instance, mesh quality significantly affects the convergence and accuracy of CFD solutions (Katz and Sankaran, 2011). In the case of additive manufacturing, the optimization of mesh resolution is also essential to achieve suitable physical outcomes (Wang et al., 2016). Alternatively, a mesh can be a visual medium in computer graphics that viewers can visually interact with (Sorkine, 2006).

This paper investigates mesh visualization options as the visual medium, which interacts with users rather than retaining the high resolution of the geometric data. First, irregular log pieces were 3D scanned as digital mesh data. Then, the following mesh visualization options, (1) photogrammetry, (2) solid mesh, (3) transparent mesh surface with the outline, (4) triangulated mesh edges, and (5) Mesh edges with surfaces, are generated in Grasshopper and transferred into the MR environment. Each mesh visualization option was assessed based on evaluation factors, including visibility, materiality, informativeness, and computing speed. (Figure 6) This assessment has informed the selection of mesh visualization settings for the MR environment in which users can intuitively experience both visualization and design processes using irregular log geometries. Photogrammetry, for example, has conspicuous visibility and materiality since the texture of the original log is mapped onto the mesh surfaces.

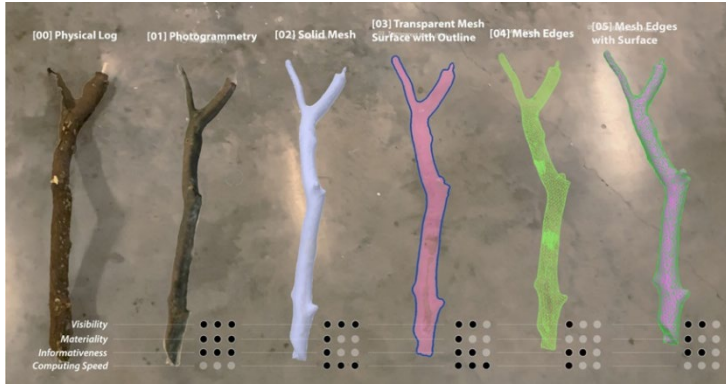


Figure 6. Mesh Visualization Studies for Further Implementation.

It also delivers the visual information of the natural logs such as bark or tree-knots. However, photogrammetry was not chosen because of the computational overhead that significantly delays the MR processing. Alternatively, mesh surfaces with an outline are used as a default mesh visualization setting. The surface colour and transparency can be adjusted to increase visibility. Mesh Edges are also selected as one of the visualization options. Even though significant computing time is required to transfer high-resolution mesh edges into the MR environment, mesh edges effectively illustrate the natural log's arbitrary geometry and visually highlight subtracted information of the logs such as centerlines and cross-section. Moreover, the proposed UI allows users to toggle on and off this option according to their preference.

3.3.2. Centerline

It is crucial to extract the geometric properties to understand the non-standardized logs due to their irregularity. The abstracted centerline works as a simple but powerful information. Furthermore, the discarded forks can be exploited to create idiosyncratic architectural structures such as trusses or joinery (Devadass et al., 2016). Hence, centerline as a design parameter allows users to identify the overall shape of irregular log geometry and gauge the approximate angle of tree forks. Centerlines are extracted by interpolating the subdivided cross-sections of the log (Figure 7).

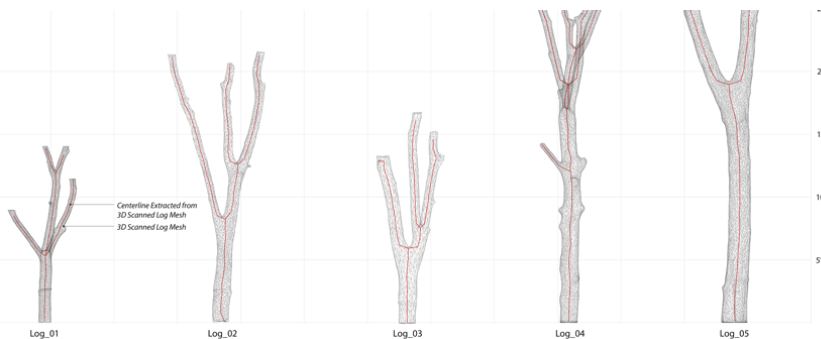


Figure 7. Centerlines Extracted from 3D Scanned Log Meshes.

The research illustrates the UI, enabling the user to toggle on and off the centerline throughout the pre-design process (visualization). Thus, users can understand the abstracted properties of irregular tree logs such as the formation of tree forks, approximate fork angle, and scale solely through 3D holographic view without using the supplementary 2D proxies, including *Rhinoceros* or *Grasshopper*.

3.3.3. Cross Section and Dimension

Cross-sections are also one informative factor extracted from the scanned irregular log geometry. Wood Chip Barn, for example, extracted the cross-sections of the log by contouring them along with one direction (Devadass et al., 2016). In our previous project, Timber De-standardized 1.0, cross-sections were used more closely throughout the design process as essential design parameters. In regular roundwood processing, the cross-section can also become a parameter for straightening the log without excessive material waste. Cross-sections of the irregular log establish the primary subdivision of the longitudinal dimension of the material (Lok et al., forthcoming). Rather than cutting the sections horizontally, a log geometry is discretized using the planes perpendicular to the vector of each subdivision point of the centerline at the optimized distance, 2.5". Moreover, the dimensional information of the cross-sections is computationally measured and visualized. Both maximum and minimum diameters are displayed due to a log's natural asymmetrical and multi-axis form. The text size of each diameter is displayed relative to the values of diameters to make dimensions discernible and interactive (Figure 8).

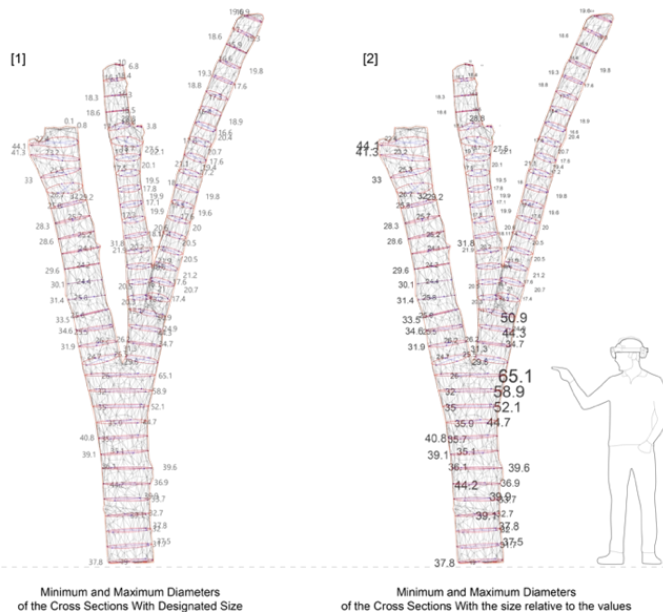


Figure 8. Minimum and Maximum Diameters of Cross Sections and Visualization Options.

Within the MR environment, users can toggle cross-section and section diameter buttons via holographic UI to utilize this abstracted information as a visual reference to decide the primary subdivision of the irregular log geometries (Figure 9). In doing so, the MR UI empowers designers to visualize the information without using 2D platforms. The visualization schemes and operating methods are expected to enable users to visually interact with the geometric data in the full-scale 3D environment.

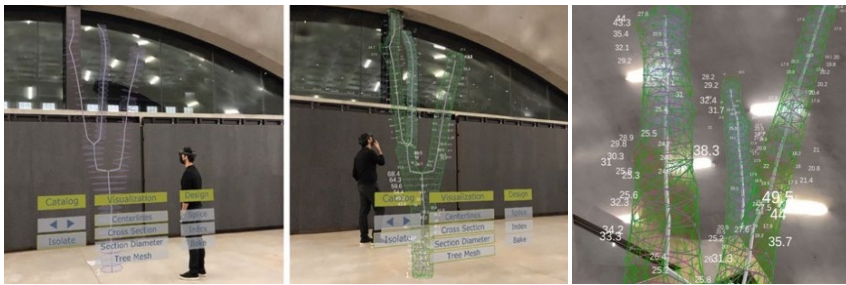


Figure 9. Holographic UI and Visualized Cross Sections and Diameters.

3.4. DIGITAL HARVESTING: SLICING, INDEXING AND BAKING

The workflow in this paper includes a virtual log processing protocol that digitally harvests the discrete log elements from the digital tree library. This process enables users to have a direct impact on the design of discretized tree logs that would otherwise have been discarded in standardized manufacturing. The 'slicer,' a plane for slicing the digital tree log, is used to determine the cut locations for each log. This process previously required the toggling between the MR UI and operations in Grasshopper.

In this paper's refinement, the entire design operations are implemented and visually optimized within the MR UI for digital harvesting: (1) Slicing, (2) Indexing, and (3) Baking. Users can subdivide the log geometry by moving, placing, and rotating slicing planes. The extracted log information such as cross-section or section diameter can be turned on as a visual guide to aid user's decision-making. After pre-placing all slicing planes, the indexing operation automatically catalogues the material parts with indices organized in the Z direction (Figure 10). Lastly, the sliced log can be harvested with the bake button. The baked logs are copied with the index alongside the original log geometry. The harvested discrete members can be distinguished by different mesh visualization such as surface colour and outline (Figure 11).

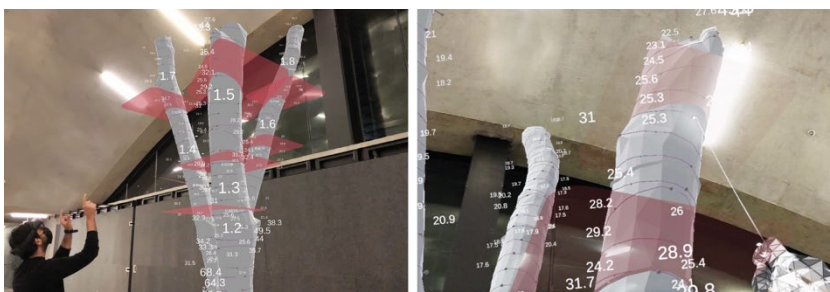


Figure 10. Slicing and Indexing for Digital Harvesting

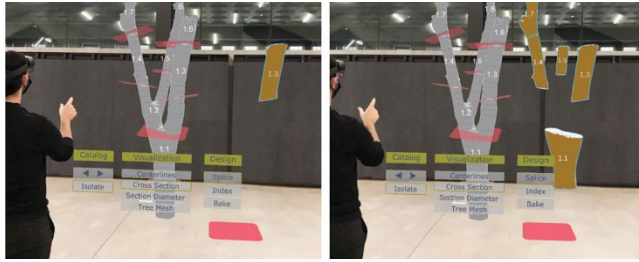


Figure 11. Baking the Digitally harvested Timber.

4. 4. Results

This paper demonstrates that this immersive process motivates the user to work iteratively according to their own design exploration. The mixed reality workflow enables users to modify and make unique parts without altering any of the discretized physical tree logs until the final design is set. The following research methodologies are illustrated to enhance the interactivity and work efficiency for user experience. (1) Mesh visualization studies that investigate options for optimizing visibility and the computing process. (2) Cataloguing and extracting the essential properties of non-standard log geometries such as centerlines, cross-sections, and section diameters. This information enables the user to evaluate the irregularity of the natural logs for further design processes. (3) Finetuning the MR environment with custom UI, design operation process including indexing, slicing, and baking allow users to toggle on and off the UI buttons to manipulate the digitally harvested timber elements. By leveraging this MR framework, users can seamlessly manage the irregular construction material and generate innovative timber structures in 1:1 scale (Figure 12).

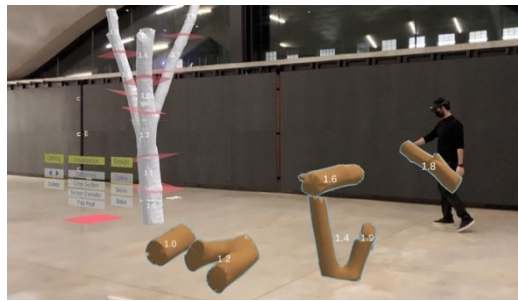


Figure 12. Cataloguing the Baked Timber Products and Generating the Design Iterations.

5. 5. Discussion

Timber De-Standardized 2.0 highlights a mixed reality (MR) user interface (UI) that rethinks how we interpret and utilize timber in our current design and construction models. More importantly, it presents a viable minimum-infrastructure solution to our environmental crisis regarding the manufacturing and processing of lumber-based products. The research started by focusing on defining the expanded notion of “usable” timber and questioning how we might re-purpose the discarded logs as a renewable

construction material by leveraging emerging technologies and platforms. While this paper focused on development of digital cataloguing, visualizing, and design protocols, further investigation will tackle integrating the visualization of structural analysis and similarly minimizing the toggling between computational platforms for fabrication and assembly. Regarding further application and material usage, the workflow can be applied towards creating viable conventional structural systems such as trusses using both irregular logs and standard round wood members. For the user experience, the hands-on workflow presents a small learning curve and provides the user with a greater sense of design authorship. Moving forward, there is potential in exploring how the workflow can engage multiple users to coordinate and work together as a team in the MR environment. A team dynamic would restructure and introduce new variables to the current framework.

References

- Adhikari, S., Ozarska, B. (2018). Minimizing environmental impacts of timber products through the production process “From Sawmill to Final Products”. *Environmental Systems Research*, 7(6). <https://doi.org/10.1186/s40068-018-0109-x>
- Baker, T. J. (2005). Mesh Generation: Art or science? *Progress in Aerospace Science*, 41(1).
- Bergman, R. D., Bowe, S. A. (2010). Environmental Impact of Manufacturing Softwood Lumber in Northeastern and North Central United States. *Wood and Fiber Science*. 42(1).
- Buelow, P. V., Torghabehi, O. O., Mankouche, S, Vilet, K. (2018). Combining Parametric Form Generation and Design Exploration to Produce a Wooden Reticulated Shell Using Natural Tree Crotches. In *Proceedings of IASS Annual Symposia, IASS 2018 Boston Symposium: Timber Spatial Structures* (pp. 1-8).
- Devadass, P., Dailami, F., Mollica, Z., Martin S. (2016). Robotic Fabrication of Non-Standard Material. In *Proceedings of the 36th Annual Conference of the Association for Computer Aided Design in Architecture, ACADIA 2016, Posthuman Frontiers: Data, Designers, and Cognitive Machines* (pp 206 – 213).
- Howard, J. L., Liang, S. (2019). U.S. timber production, trade, consumption, and price statistics. *Department of Agriculture, Forest Service, Forest Products Laboratory*.
- Jahn, G., Newnham, C., Berg, N.V.D., Beanland, M. (2018). Making in Mixed Reality: Holographic Design, Fabrication, Assembly, and Analysis of Woven Steel Structures. In *Proceedings of the 38th Annual Conference of the Association for Computer Aided Design in Architecture, 2016, Recalibration on Imprecision and Infidelity* (pp 88 – 97).
- Katz, A., Sankaran, V. (2011). Mesh Quality Effects on the Accuracy of CFD Solutions on Unstructured Meshes. *Journal of Computational Physics*. 230(20). 7670-7686.
- Larsen, N. M., Aagaard, A, K., Kieffer, L.H. (2020). Digital Workflow in Constructions. In *25th International Conference on Computer-Aided Architectural Design Research in Asia, RE: Anthropocene, Design in the Age of Humans, CAADRIA 2020* (pp. 125-134).
- Lok, L., Samaniego, A., Spencer, L. (Forthcoming). Timber De-Standardize. In *Proceedings of the 41th Annual Conference of the Association for Computer Aided Design in Architecture, ACADIA, 2021*.
- Spelter, H., McKeever, D., Toth, D. (2009). *Profile 2009: softwood sawmills in the United States and Canada*. USDA, Forest Service, Forest Products Laboratory.
- Sorkine, O. (2006). Differential Representations for Mesh Processing. *Computer Graphics Forum*. 25(4), 789-807.
- Wang, W. M., Zanni, C., Kobbelt, L.(2016). Improved Surface Quality in 3D Printing by Optimizing the Printing Direction. *Computer Graphics Forum*. 35(2), 59-70.

SMART HAND FOR DIGITAL TWIN TIMBER WORK

The interactive procedural scanning by industrial arm robot

CHIKA SUKEGAWA¹, ARASTOO KHAJEHEE², TAKUYA KAWAKAMI³, SYUNSUKE SOMEYA⁴, YUJI HIRANO⁵, MASAKO SHIBUYA⁶, KOKI ITO⁷, YOSHIAKI WATANABE⁸, QIANG WANG⁹, TOORU INABA¹⁰, ALRIC LEE¹¹, KENSUKE HOTTA¹², MIKITA MIYAGUCHI¹³ and YASUSHI IKEDA¹⁴
^{1,2,6,7,11,12,14}Keio University ^{3,4,5,8,9,10,13} Takenaka Corporation
{¹c.sukegawa²arastookhajehee⁶m.shibuya⁷k.ito¹¹l.alric¹²hottak-ensuke¹⁴y.ikeda}@keio.jp, ¹³kawakami.takuma⁴someya.shun-suke⁵hirano.yuuji⁸watanabe.yoshiaki⁹qi-ang.Wang¹⁰inaba.tooru¹³miyaguchi.mikita¹@takenaka.co.jp
²0000-0001-5381-7784, ¹²0000-0003-3507-570X, ¹⁴0000-0002-2016-4083

Abstract. This paper describes a 3D automated scanning method for building materials, namely “*The Interactive Procedural Scanning*”, in a collaborative environment composed of a human worker and a CNC robot. This procedure aims to translate the observation skill of an experienced carpenter into an intelligent robotic system. The system frames its function on the first stage of a traditional timber examination process, called ‘*Kidori*’, in which observations and findings are marked on the timber surface to provide hints for the subsequent cutting process. This paper aims to recreate the procedures using an industrial robotic arm, computer vision, and a human worker. A digital twin model of the timber is created with a depth camera serving as a base map to exchange information and receive instruction from the human worker. The margin of a discrepancy between the original processing location and the location of the actual end effector, where the tools are, is minimised in this system.

Keywords. 3D Scanning; Computer Vision; Traditional Technique; Phycology; Machine Learning; SDG 9.

1. Introduction

This research aims to reduce the technical threshold required for a human worker to perform advanced wood processing procedures. In this framework, a human worker with little wood processing knowledge or skill collaborates with a robotic arm to examine and acquire properties information of the material. The robot must be robust enough to function in a dynamic environment with unforeseeable disruptions and

encourage interaction with its workers. Disruptions are unpredictable circumstances that include human misjudgement, accidental moves of the material in the middle of the process, or the heterogeneity of materials that will affect the final product's performance. The human worker has two cognition tasks in a traditional CNC machinery workflow. Firstly, they must carefully select an appropriate material suitable for the design purpose, considering the factor of sizing and natural material defects; for example, wood knots should be avoided. Secondly, the human worker must determine the best orientation and location for the material's placement on the processing table and assign a local-material origin point to confirm the coordinates of CAD/CAM and physical space.

This premise is translated into two predetermined conditions in this demonstration; i) the material is placed at an arbitrarily selected orientation and location within a workable area; ii) the individual materials would have heterogeneous materiality, e.g., the presence of knots wood grain direction. The two conditions reproduce the realistic scenario of a primitive collaboration between a human and robot where cognition tasks are highly dependent on the human counterpart.

The research aims to utilise the unspoiled aspects of human workers' input to robotic behaviour. We research with a skilled carpenter called '*Miya-daiku*' in his observation process on a piece of timber, then the procedures and the embedded techniques are translated into our system. The procedural steps are not copied because machines and humans work require different thinking. However, this deconstruction of a human observation and action process enables us to analyse the behavioural pattern of specialists and provide hints on how to implement the principles in a robotic setting. Our team assumes that machines can perform more efficiently when given implications by conventional human wisdom.

2. Background

In 2021, there are many examples of computer vision or machine vision applications in the market, such as object detection in autonomous driving or image recognition in industrial robots (Klette, 2014). Most carmakers attempt to improve the scanning capacity by utilising multiple sensors, distance-related sensors include radar, laser rangefinder 3D-lider, RGB camera, other sensors are geography-based such as GPS and gyrocompass. In recent years, there have been the following three trends. The first is the development of cognitive image processing by machine learning. In the 2010s, most automakers used multiple sensors to make up for their weaknesses, but tech companies have begun to develop camera-only technology again (Mobileye, 2020). The second is the utilisation of digital twins. Some companies are training in virtual space to quickly acquire the results of the above-mentioned geometric learning, which is dozens of times more efficient than in real space. (Ohnsman, 2018). Virtual space is useful for training robot too. (Matsas and Vosniakos, 2017.)The third is cooperative: automobiles have become connected to the network with infrastructure development. There is a flow of sharing information and synchronising with a conventionally operating system for everyone, with each other, or with a central concept such as a global map, in some companies such as Honda, Komatsu, Google. Also, there is an example of training robotic arm by using virtual and physical environment. (Luis et al., 2019)

3. Limit of Current Research and Problem Statement

There are two problem statements: 1) Similar to applications in other industries, the role of robots will shift from executing monotonous, repetitive commands to more intelligent ones that involve cognitive and decision making in the construction field. This paper suggests an adaptive setup for a robotic arm on-site that accommodates accidental occurrence and heterogeneous materials. The use of computer vision is the first step in understanding the situation in front of the robot on-site. 2) A few examples of transferring human specialist skills to a robotic system (Madhura et al., 2021). The mechanical resemblance of a robotic arm and that of a human arm provides a good starting point on adapting the experience and wisdom of a skilled specialist to a computer-assisted robotic system.

4. Aim of This Paper

The first aim is to dissect and understand the workflow of skilled Japanese carpenters; The subject of this research, specialist carpenters, are also known as palace carpenters in Japan. It is not easy to replace their implicit knowledge with a robotic system because a significant part of the knowledge is embedded into the specialists' intuition developed from years of experience (Nishioka, 1984). As the author of this paper possesses no carpentry knowledge, a documentary of a palace carpenter's workflow was filmed for further investigation. We extracted points of interest from an amateur's point of view and studied the unique abilities of a palace carpenter. Initially, we tried to replicate the entire wood process but later restricted the scope to only the "wood inking" stage, where the most exciting features have been observed in experiment 1.

The second aim is to reconstruct a human's workflow into a robot. There are a few examples of robotic applications in wood processing for construction. Some robotic arms are fitted with sensors on the end-effector to provide a feedback loop. The accuracy of the industrial robotic arm ensures the precision of coordinates interpolated by the computer vision program. Secondly, the idea of digital twins is applied to wood processing robots. The virtual twin space is used for obtaining training data for machine learning engines through simulation. The physical space counterpart is used to conduct interactive experiments with human agents. As this study aims to synchronise knowledge between all agents, global information obtained from the sensors of other robots and even human operators is to be shared. We envision a system that can share experiences through connections. The authors have chosen a case study in which a robotic arm processes a wood part. Machine vision technology may be used to its full potential as most of the wood process has been replaced by electrically driven tools. Thus, two experiments will prove the concept for the above two points.

5. Hypothesis and Research Questions

The overall hypothesis is that by closely observing the working process of palace carpenters, hints can be obtained to design an autonomous and adaptive control system to handle non-homogeneous materials with a robotic arm and computer vision.

- **Hypothesis for experiment 1:** From the palace carpenters' work analysis and linguistic analysis, the skilful points for observing their trees (raw parts) can be

extracted. Also, what kind of information is being read, what resolution is being read, etc., can be extracted and used when implementing them in computers and robots?

- **Hypothesis for experiment 2** (implementation on a robot): Is it possible to increase the accuracy of the computer vision of the robotic arm and the accuracy of machining by dividing the scan into different stages?

6. Experiment-1: Observation of Well-skilled Carpenter

6.1. INTRODUCTION

One of the most critical parts of a palace carpenter's working process is 'inking', in which they inspect the timber and makes markings on the surface for further processing. To design a parallel mechanism for the robot to acquire the characteristics of the subject material in collaboration with an amateur human worker. To determine the necessary knowledge, it is essential to understand the thinking process of palace carpenters. Table 1 shows how an experienced carpenter looks at their subject.

	What to look for	What can be understood
Pattern/Grain	Distance of lines, Comparing the pattern of each surface	Tree species / weak direction / dry deformation direction / creep direction
Annual Ring	Distance of ring, Pattern, Centre direction	Tree species / address (weak direction) / original up / down / expected dry shrinkage / natural tree or tree planting
Colour	Sapwood, Heartwood	Heartwood / Sapwood, Compression / Tension material, Internal stress, Bottom/ End of log
Knot	The density of fibre, Texture	Top and bottom, Brittleness, appearance, Knots appear.

Table 1. Observed Items Respectively



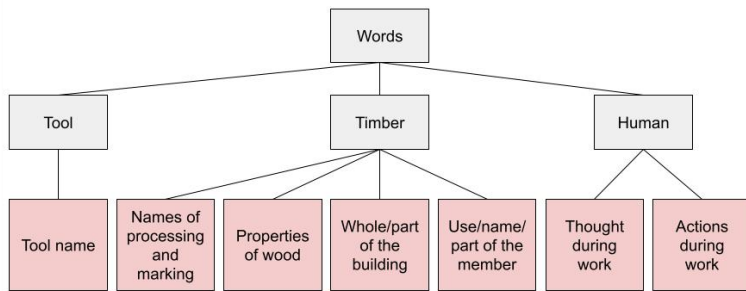
Figure 1. (left) Work environment (centre) Screenshot of the head-mounted camera for Experiment-1. (right) the place carpenter explained what he was thinking while watching the video

6.2. METHOD

The proficiency of the carpenters is based on implicit thinking. Protocol Analysis is a way to analyse their thoughts and existing physiological methods to reveal the process of intellectual action (Suwa and Barbara, 1997), (Ericsson, K and Simon, H. A, 1984). Here, we recorded the process of 'inking' as part of the construction of a small temple.

To document the eye movements of an experienced palace carpenter, a camera is mounted to the palace carpenter's forehead, and a first-person view video is recorded. After that, while watching the video, the carpenter was asked to explain what they were thinking of. The video footage of the explanation is transcribed, keywords were extracted and categorised. Finally, the number of appearances is graphed in chronological order for each category— to understand the logistics of the thinking flow. The video recorded is about the inking work for four pillars in the small temple (Figure 1).

Since no existing quantitative method can systematically classify the terms, the carpenter explained his working process. Yet hierarchy and the level of abstraction is essential (Suwa, 2016). Then here, we classified key terms into three categories: 'tools', 'lumpers', and 'humans'. Languages related to 'timber' have been categorised into “processing / marking names”, “wood properties”, “whole/part of members”, and “uses/names of members/parts of members”. Determine the "classification of inking" after having "the function (pillar) of the result". 'Human' was also fixed in the hierarchy of "thinking at work" and "behaviour at work".



Classification of Words	Explanation of Words, and examples	The number of appearances
① Name of tools	Toolbox · Carpenter's square · Long measure · Inking parallel ruler	58
② Feature of Timbers	Knot · Straight-grain · Sapwood · Swirl · Straight	66
③ The name of the process, and Inking	Grid · Mortise · Inking reference line etc.	57
④ usage, the name/part of the building,	Column · Horizontal interior timber · Front side of building · bottom part of wood · Top part of the wood	43
⑤ the whole building, part	Building · Foundation · a side of facade people pass by most	27
⑥ action in operation	Roll (wood) · draw (inking) lines · look (drawing)	201
⑦ thought, related words	To think (about the arrangement of buildings and parts) · To decide (to replace the arrangement)	94

Figure 2 & Table 2. Classification of words and their number of appearances

6.3. RESULT

The verbal explanation was then transcribed. Its length was about 15,200 words,

including the experimenter's remarks. Based on the transcripts, we classified the words into seven categories according to their contents and analysed the transition of thoughts. Thus, from the first-person video of the palace carpenter and the analysis of his remarks, it turned out that there are 3 phases following: 1) the period of observing multiple surfaces while rolling multiple pieces of wood, 2) the period of observing while rolling one piece of wood, 3) the period of inking. In this paper, each period is tentatively named '*overall observation period*', '*individual observation period*', and '*inking period*', respectively.

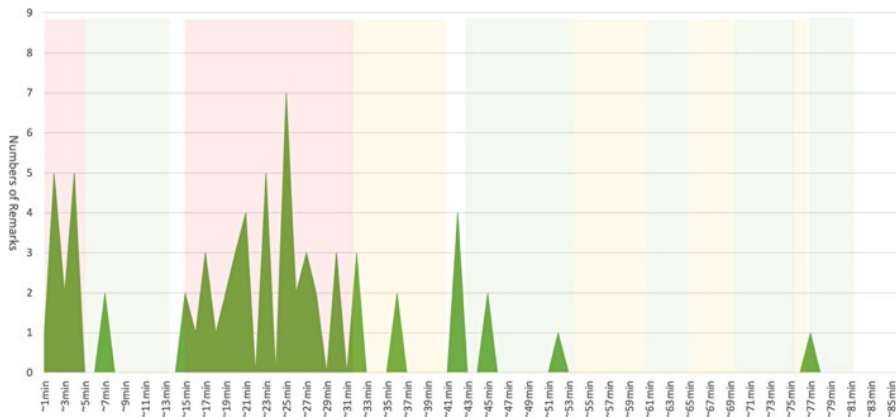


Figure 3. The number of remarks regarding 'Feature of Timbers' on the table in the working period; the number of remarks about 'Feature of Timbers' peaks immediately after the beginning of work and between 15 and 30 min from the start. On the contrary, the number of times decreases significantly after 35 min, and there are almost no remarks after 55 min.

To sum up from experiment 1: protocol analysis reveals two phases within the observation stage, called 'Sumitsuke' in which the timber is prepared for further processing. The first phase is "comprehensive inspection". All material sides are quickly inspected visually, sometimes by rotating the wood. Then the carpenter decides on the final orientation of the material based on the inspection result. The second phase is the "local observation" period, where material parts are scrutinised, and precise cutting location is decided. From the above, human observe of wood, there is a "period to compare multiple timbers and roughly grasp their characteristics" and a "period to determine detailed processing based on the rough observations".

7. Three Directions of Utilising the Human Analogy into a Robot

The above conclusion implies the potential to 1) utilise the reductionistic analysis approach to reconfigure the workflow. 2) Prepare various sensors, depending on an interview that reveals implicit knowledge. Moreover, the mechanical resemblance between robot and the human eye, and the human hand can now combine into one device as an end-effector. Concretely, 3) the relative position of the eye (camera) and material helps effectively detect and recognise features of the material and simultaneously can move to an operation that the hand does.

8. Experiment-2; The Implementation for Robot and its Precision

8.1. INTRODUCTION

From the behavioural analysis of the palace carpenter in Experiment 1, the purpose of each observational action had been linked to a specific piece of information. This experiment constructs the input and output logic of an automated program like the set of activities performed by the carpenter. Depending on the subject, the robotic arm's end-effector, the scanning method, and the workflow must be designed accordingly. The following is an account of the necessary functional requirements of the system; 1) The system recognises the location and shape of the object that is placed arbitrarily on the table. 2) Determine if the object has been registered in the database. 3) Recognize and identify material parts that may cause performance problems in the final product (limited to timber knots in this study). 4) With computer vision, the end-effector's position can be controlled with an accuracy of a millimetre for machining. 5) Perform a scan of the object with a resolution optimised for quick inspections inside the computer environment.

8.2. CONCEPT OF PROCEDURAL SCANNING

Attempts to scan the timber without a plan had encountered several difficulties. The depth sensor had involuntarily acquired data irrelevant to the wood in the subject, unnecessarily increasing the computational time since the algorithm cannot distinguish the object from the immediate environment; hence, a low-resolution map that provides an overview of the material is to be obtained first, then the scanning resolution can be increased for areas of interest for closer inspection. Different scanning scales can yield a comprehensive understanding of the working environment. Getting useful information from the environment selectively and quickly will be an essential subject for future development in computer vision.

STEP	Title	Entry	Sensor/Device	Purpose
0	Pre-training for ML	Image (RGB)	RGB-camera	ML training
1	Surrounding Scan	Geometry (very rough)	HoloLens, (+Lider)	Human safety
2	Rough Scan	Geometry, location	D-camera	Workable area, Material position, - axis
3	Individual-Timber Recognition	Image (RGB, Outline enhancement)	RGB-camera + ML(cloud)	To pull information from DB
4	Individual's Surface-recognition	RGB Image (Outline enhancement)	RGB-camera + ML(cloud)	To recognise which side is up and down
5	Detailed Scan	Geometry (high resolution)	D-camera + robot arm (arbitrary position)	To get the latest geometry
6	Re-calibration for process	Points and their line	D-camera + robot arm (arbitrary position)	Minimise physical deviation

Table 3. Seven procedures of Scanning

8.3. TOOLS AND SETTINGS

Microsoft HoloLens2® as a data communication tool for human workers, Intel Relasense® as a composite computer vision for the robot, and an RGB-D camera was used in this experiment. Since the digital twin model is projected and placed in the MR, the human workers can superimpose virtual objects on the physical space and perform a real-time evaluation. In addition, a mapping is projected from the robot's end-effector onto the material surface to display its properties in a visually intuitive way. In other words, both the human and the robot are equipped with a channel to generate input and obtain output in the system. All the scan stages are used to gradually achieve an increasingly accurate representation of the material in the computer. The level of detail achievable using each scan stage corresponded with what was required by the next step. The resulting system can operate on a given timber block with a repeatable coordination accuracy of the timber's local origin point, the deviation between the end of milling and scanned timber 5mm to 10mm. The projection mapping function can also instruct and interact with the robot to increase the accuracy to the desired degree. In addition, human has a role in authenticating whether the robot's understanding of the material is correct.

8.4. PERFORMANCE AND EVALUATION METHOD

The purpose of experiment 2 is to confirm if the proposed system works effectively to satisfy the required performance. Various factors work effectively, but here we set the accuracy of the entire robot arm system using computer vision tentatively (potentially it can be the amount of data, time, labour of humans). Precisely, the difference between the ideal target point and the tip of the mill of the end effector was measured (Figure 3). We also indirectly justify the above by saying that this difference is exacerbated when the "step scan" known below is not used.

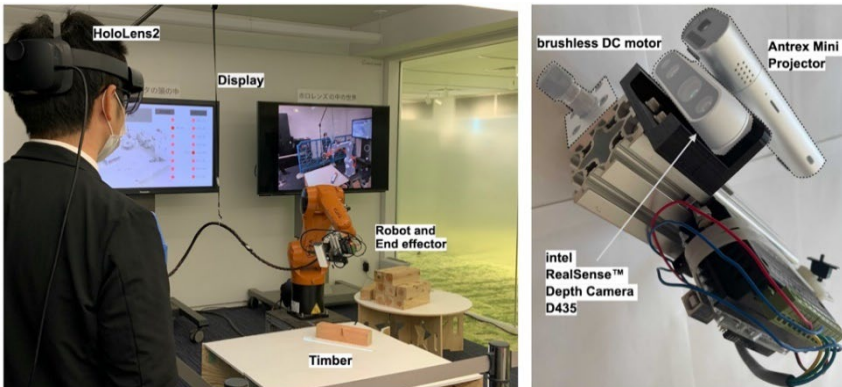


Figure 4. Developed end effector consists of milling, computer vision, projector. The design of this end-effector is made an aiming with lightweight and small size. Our team used kinectV2 and KinectAzure, but Intel Realsense® is used mainly because of size and weight.

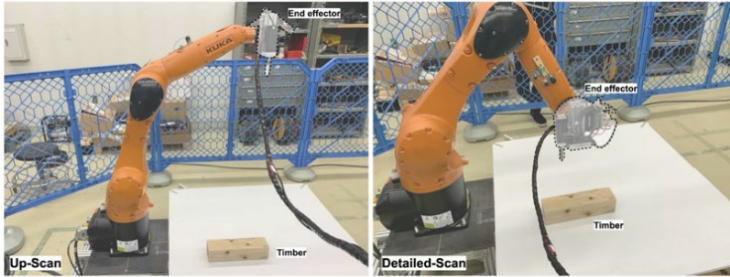


Figure 5. The screenshot of each scanning moment and robot attitude ;(case-1) Up-scan is the rough scan of the procedure following 0, 1, 2, (see table 3) ;(case-2) Detailed-Scan is the procedure following 0,1,2,(3,4), 5 (see table 3)

8.5. STATISTICAL METHOD

Experiments were performed ten times for each timber. In addition, five pieces of wood called A, B, C and D were used to smoothen the differences between individuals. As for scanning, the above cases 1 and 2 were tried, so 40 samples were obtained. Here, we wanted to see the effectiveness of the procedural scanning method, so the difference distribution was taken separately for case-1 and case-2 (figure5).

The below boxplot (Figure6), The left side (blue) of each table is the scanning method of case 1 ('Up-scan'), and the plot (orange) on the right is an example of performing a stepwise scan in case 2 ('Detailed-scan') to some extent. Case- 2 has a more negligible average difference at any point. For points 1 and 2, the average difference is about 12 mm or less, but for points 3 and 4, the absolute value of the difference is 18 mm or less. It is inferred that this is due to the poor accuracy of the peripheral edge of the angle of view of the depth camera. Again, the benefits of stepped scanning come out.

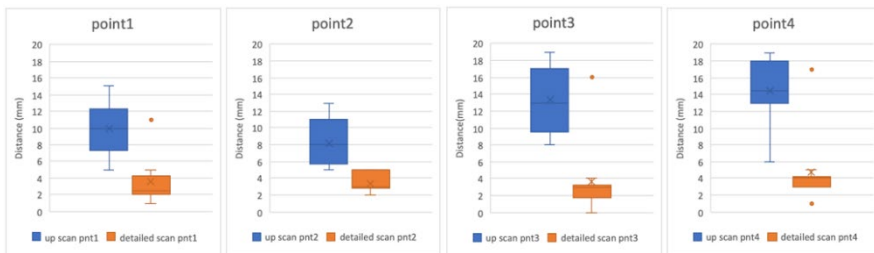


Figure6. The result of the experiment. Comparison of the error between the ideal position of timber and physical place.pt1~4 indicates four corners of timber's top surface.

8.6. SUMMARY

To realise the concept of 'Procedural Scanning', it is necessary to properly design the scanning method and its order in consideration of LOD. From experiment-2, the accuracy tends to improve with this scanning method, but other evaluation criteria must be considered to measure the multifaceted effectiveness. The concept has been proven valid, but the methodology still must be refined. To evaluate the system's practicality, it is necessary to meet the requirement inaccuracy and realistic criteria such as time for

system execution, amount of human labour, power consumption, and data size. As the system has gone through rounds of iterations, issues that would likely arise in practical applications have been noticed and rectified. For example, in the initial game, the amount of data obtained from scanning had exceeded the processing computer's capacity and crashed the system. It is essential to ensure the data is lightweight enough for rapid computation for real-time processing.

9. Conclusion

The contribution of this research is the development of an effective scanning system for half automated and interactive CNC robotic arms as a part of wood processing. The system reduces the time and resources usually required to create a meaningful digital information profile of the material, with an adaptive scanning resolution in parts of interest determined by the human user during the interactive process. In conclusion, the computer vision system developed in this paper creates an interactive workflow in which the robotic movement is visualised beforehand and presents a current understanding of the material to the user in real-time with gradually increasing accuracy, demonstrating the potential of machine vision in the AEC industry, not as a replacement for human workers but as a complementary counterpart.

Acknowledgements

Takenaka Corporation and Keio University hold this co-research, also thank the master carpenter firm, Hakuo-syaji.

Selected References

- Ericsson, K. A., & Simon, H. A. (1984). *Protocol analysis: Verbal reports as data*. US; The MIT Press.
- Klette, R. (2014). *Concise Computer Vision*. Springer. ISBN 978-1-4471-6320-6.
- Luis Perez, Eduardo Diez, Ruben Usamentiaga, & Daniel F. Garcia. (2019). Industrial robot control and operator training using virtual reality interfaces, *Computers in Industry*, 19, 114-120.
- Madhura Jayaratne, Daminda Alahakoon, & Daswin de Silva.(2021). Unsupervised skill transfer learning for autonomous robots using distributed Growing Self Organizing Maps, *Robotics and Autonomous Systems*, 144, 103835.
- Matsas, E., Vosniakos, GC. (2017). Design of a virtual reality training system for human-robot collaboration in manufacturing tasks, *Int J Interact Des Manuf*, 11, 139-153. <https://doi.org/10.1007/s12008-015-0259-2>
- Mobileye. (2020). *CES2020* and Retrieved December 1, 2021, from <https://www.mobileye.com/>
- Nishioka, Y (1984). 木に学べ[*Lean from Tree*]. 1st ed. Tokyo, Japan; Shogakukan publish.
- Ohnsman, A., (2018). *Waymo Is Millions Of Miles Ahead In Robot Car Tests; Does It Need A Billion More?* Retrieved December 1, 2021, from <https://www.forbes.com/sites/alanohnsman/2018/03/02/waymo-is-millions-of-miles-ahead-in-robot-car-tests-does-it-need-a-billion-more/?sh=7a7f080b1ef4>
- Suwa M. (2016). 「こつ」と「スランプ」の研究 身体知の認知科学[*Research on Tip and Slump Cognitive Science of Embodied knowledge*], Tokyo, Japan; Kodan-Sya.
- Suwa, M., Barbara, T.(1997). What do architects and students perceive in their design sketches? A protocol analysis, *Design Studies*, 18(4), pp385-403.

VIZOR: FACILITATING CYBER-PHYSICAL WORKFLOWS IN PREFABRICATION THROUGH AUGMENTED REALITY

XILIU YANG¹, FELIX AMTSBERG², LIOR SKOURY³, HANS JAKOB WAGNER⁴ and ACHIM MENGES⁵
^{1,2,3,4,5}*Institute for Computational Design and Construction, Cluster of Excellence Integrative Computational Design and Construction for Architecture University of Stuttgart, Germany.*
¹*xiliu.yang@icd.uni-stuttgart.de, 0000-0002-5835-9898*

Abstract. This research presents Vizor, a software framework to facilitate Human Robot Collaboration (HRC) in fabrication using Augmented Reality (AR), specifically within the environment of high Level of Automation (LoA) prefabrication for the AEC industry. The framework supports skill set extensions of fabrication setups via the integration of human craft and automation through AR and improves the accessibility and adaptability of these fabrication setups. It features a *Grasshopper* plugin for low-barrier-to-entry prototyping and an integrated *HoloLens* application for operation. The tool is demonstrated through three use case examples and validated in a proof-of-concept case study involving a craftsman and a 14-Axis robotic setup, which demonstrates a novel interactive task-sharing process. Vizor opens new opportunities to extend robotic prefabrication with craftspeople who are skilled yet untrained in robotic control and provides greater access to tools for prototyping HRC workflows.

Keywords. Augmented Reality; Human Robot Collaboration; Cyber-physical Fabrication; SDG 8; SDG 9; SDG 12.

1. Introduction

Industrial prefabrication brings benefits such as higher productivity and reduced waste production (SDG 12) to the construction industry. While sustainable industrialisation fosters job creation and economic growth (SDG 9), automation also changes the profile of human labour. Technological progress has catalysed major shifts in the labour landscape, such as industrialisation in the 1800s that saw a decline in the crafts profession, yet many factory jobs created. Ensuring productive employment and decent work for all (SDG 8) thus calls for a better understanding and integration of traditional labour and skilled craft in high Level of Automation construction processes.

Augmented Reality (AR) has shown promising potential in bolstering human capacity in non-standard fabrication tasks in the Architecture Engineering and Construction (AEC) context. It aids in the extension of craft-based fabrication procedures by enabling collective assembly of complex structures (Jahn et al., 2018),

achieving higher geometric complexity with manual labour (Mitterberger et al., 2020), and utilising unpredictable, unconventional materials in large-scale fabrication (Yoshida et al., 2015). In combination with machines and robotic tools, AR has been applied towards creating intuitive interfaces for interactive fabrication, which leverages unique human and machine capacities to build novel structures (Mueller et al., 2019).

This research proposes a software framework for AR integration in Cyber-physical fabrication, to not only extend manual procedures, but also facilitate interaction between human and other fabrication units on a network, such as industrial robots. Incorporating the human in the loop allows the sharing and transfer of human skills into automated systems (Garcia et al., 2019) and can be an effective strategy to increase process flexibility (Amstberg et al., 2021). This is particularly relevant in the project-based construction industry, where the high precision and standardisation of prefabrication methodologies alone are not sufficient to address the variety of building geometries and processes necessary (Wagner et al., 2020).

Existing tool sets for Mixed-Reality fabrication (Jahn et al., 2018) and real-time robot control (Garcia del Castillo y López, 2019) streamline important elements of AR-integrated robotic fabrication. However, a bridge is required for a system to combine humans and robots in a single workflow. For instance, while Fologram offers rich features for Mixed Reality experimentation (Fologram, 2021) it provides little integration with robotic fabrication tools. Projects that combine the two are often based on one-off setups, which limits the reusability and accessibility of such workflows to a wider audience, as well as their adaptability to new production scenarios. Vizer aims to address this by proposing a reusable and extensible framework that incorporates humans and machines in a joint fabrication workflow, to adapt and extend high LoA prefabrication setups.

2. Context

2.1. BACKGROUND

Augmented Reality head-up displays have been proposed towards enhancing manufacturing and assembly tasks since the 1990s (Caudell & Mizell, 1992). In addition to visual cues, non-visual AR assistance has also been applied for task execution in construction, such as haptics-based robotic teleoperation.

Cyber-physical Systems (CPS) are relevant for industrialised prefabrication as they involve physical processes with a high level of digital integration and networking capabilities (Ruiz Garcia et al., 2019). The translation of CPS into architecture has also opened novel design possibilities that 'unfold in the material realm through explorative processes' (Menges, 2015).

Application of AR in CPS in the environment of high Level of Automation (LoA) prefabrication brings the benefits of 1) **flexibility & collaboration**: coordination, skill extension and integration between human (e.g., decision-making, adaptability, flexibility, mobility) and robots (e.g., speed, precision, payload, endurance); and 2) **transparency & connectivity**: keeping people informed and integrated within the highly networked, automated processes.

2.2. STATE OF THE ART

Recent work in Human Robot Collaboration for AEC fabrication has explored many exciting possibilities using various interaction modalities and custom architectures. On an abstract level, we consider AR-integrated HRC systems to generally require four components: AR client, information generation, process management, and machine control. On an implementation level, the four components can be executed using a variety of tools and frameworks.

Augmented Materiality (Johns, 2017) uses projection-based AR interface for interactive fabrication with highly stochastic material properties. Information generation occurs on the fly based on depth information, topological optimisation, and user inputs. RoMA (Peng et al., 2018) proposes an interactive 3D printer using a custom AR goggle with Oculus controllers as the AR client, a Rhino plugin for information generation and process management, and a printer sub-module for robotic control. CROW (Kyjanek et al., 2019) demonstrates a HRC process for timber prefabrication using a NoSQL database to store CAD information and ROS-based process manager connected directly to a KUKA Sunrise controller, and human interacts through a HoloLens. Prototype as Artefact (Atanasova et al., 2020) showcases a live HRC assembly process using a custom mobile application. Assembly information is generated on the fly while as-built structures are registered through visual-inertial tracking on the AR device.

Vizor presents an architecture that leverages the visual programming tool Grasshopper to generate and operate Human-Robot collaborative tasks. It enables designers and architects with little software development experience to build and run such workflows and facilitates runtime orchestration and participation by a human worker or craftsman who is unskilled in programming robots.

3. Methodology

Introducing human labour in high LoA prefabrication opens new opportunities to rethink traditional robotic fabrication workflows. Human and machine tasks should be considered in conjunction during planning and design phases, and a higher level of information integration at run-time is necessary.

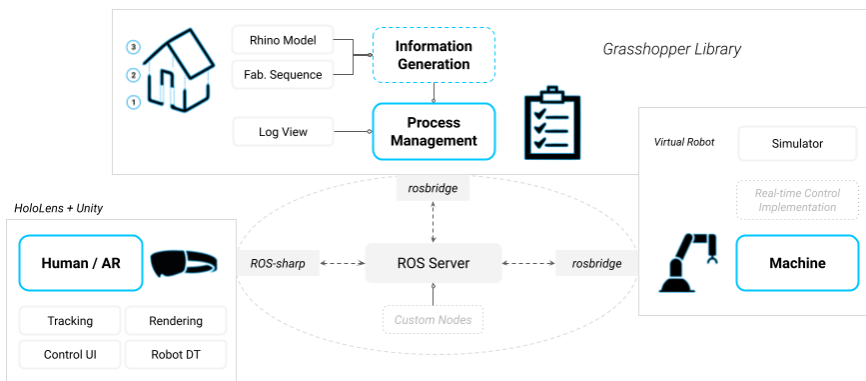


Figure 1. Augmented Reality Human Robot Collaboration System

The prototyping environment is accessible to designers via a Grasshopper plugin, which integrates with a HoloLens application that supports a user interface and Process Digital Twin for both the robot and work tasks. The overall system architecture is shown in Figure 1, and the main design considerations are summarised below:

- Information generation and process management are encapsulated in Grasshopper's visual programming environment, allowing direct access to Rhino geometries.
- AR client is built on the all-in-one device, *HoloLens*, and equipped with a modular interface to simplify interaction with key system components.
- Communication framework is built on the Robot Operating System, allowing easy integration with robotic tools and resources available from the ROS ecosystem.
- Message and topic structures related to HRC workflows are defined in a general way, allowing potentially different, enhanced implementations of system elements. (e.g., HoloLens can be replaced with mobile devices, or statically determined task information can be replaced by adaptive, procedurally generated information based on real-time sensor inputs.)

3.1. AR CLIENT

The HoloLens application is developed using Unity. Its modular interface allows users to control important system elements, namely: marker detection and tracking, robot digital twin and simulation, human task information, 3D model access, and system status overview. These UI elements make use of simple interaction widgets available on *HoloLens 1*, shown in Figure 2.

A Digital Twin of the robot platform, TIM (Wagner et al., 2020), allows fast robotic visualisation through robot joint values streamed through the network. Relevant work geometries are also updated during execution to support visualisation of the Process Digital Twin. Marker-based localisation for workpieces and robots is implemented using the Vuforia Engine, which handles marker detection and tracking. ROS-sharp is used to integrate message publication and subscription with other system elements.

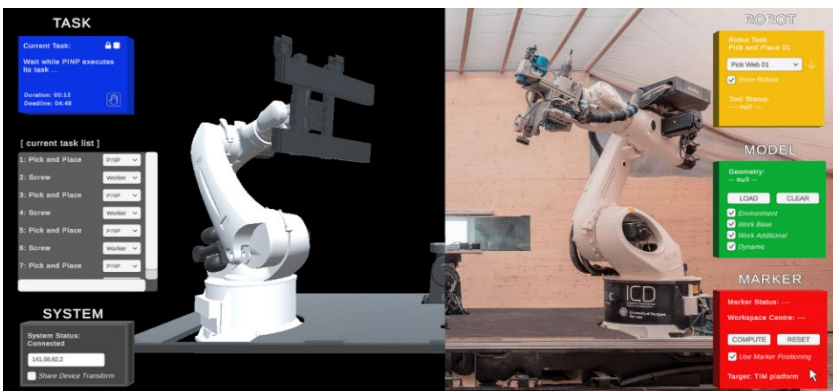


Figure 2. AR Client Interface allowing User Control for Marker Detection (red), 3D Model Access (green), Robot Simulation (yellow), System and Task Overview (grey), Task Information (blue) and the Digital Twin of the Robot Platform TIM in Unity

3.2. GRASSHOPPER PLUGIN

By providing bidirectional information between the AR device and the Grasshopper environment, prototyping Mixed Reality workflows is more rapid and accessible to an audience with little programming or application development experience (Jahn et al., 2018). In addition to supporting the basic exchange of geometry and marker information between Grasshopper and the AR device, Vizor provides components for task definition, process control, and robot simulation to facilitate human-robot collaboration in high LoA prefabrication environments.

An overview of the plugin library at the current stage of development is shown in Figure 3. Controller components are key to running and managing the task execution process, as they respond to inputs and update the Digital Twin as the fabrication process unfolds, in addition to providing a text-based log output. The respective use cases of these elements are elaborated in Workflow Examples.

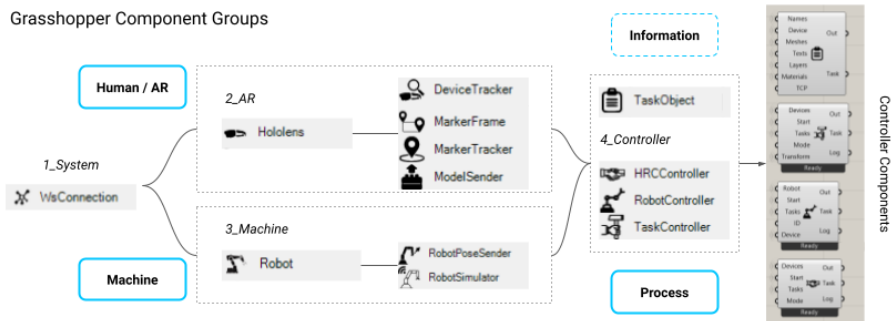


Figure 3. Component Library

3.3. COMMUNICATION STRUCTURE

The ROS-based communication framework allows integration with other system elements through rosbriidge. For instance, to facilitate the orchestration of multiple AR clients, a custom ROS node is implemented to manage the process based on the 'sharing mode' defined in 'Task Controller'. This is relevant when multiple units share the same work process, and their task assignment and completion logic need to be tailored to needs of the relevant processes.

To support the basic information flow necessary for human robot collaboration, pre-defined topics and message structures are incorporated in the main nodes of the system. Shown in Figure 4, these topics encompass three main categories: Process/System-initiated (red), AR/Human-initiated (orange), and Machine/Robot-initiated (green). The participating elements subscribe to the relevant topics, and the list of topics can be extended when more system elements are added.

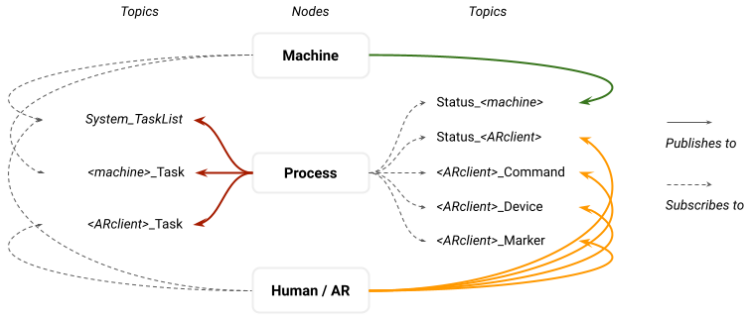


Figure 4. Topic and Communication Structure

4. Workflow Examples for Illustration

Vizor's Grasshopper library is the cornerstone on which three proof-of-concept workflows are shown. They demonstrate the use of the framework in Human-System, Robot-System, and Human-Robot interaction to adapt to different use cases in prefabrication scenarios.

4.1. HUMAN - SYSTEM (TASK CONTROLLER)

Human-System interaction allows work tasks that are difficult, or impractical to achieve by robotic prefabrication to be executed manually with AR (i.e., extending the fabrication space of the robot through the flexibility of human craft).

As an example, consider a robotic setup without an end effector for screw insertion and a worker needs to complete the task. First, the designer inputs a list of CAD geometries and auxiliary information such as rendering options to create a 'Task Object'. The objects feed into the 'Task Controller' component, which becomes active when the 'Start' toggle is triggered. As the AR client detects markers in physical space, their positions are streamed to 'Marker Frame' which automatically computes the transform matrix to localise the workpiece. The task controller supplies necessary visual and text assistance as the worker signals task completion with the Task panel on *HoloLens*, and the designer sees a real-time overview of the task progress (Figure 5).

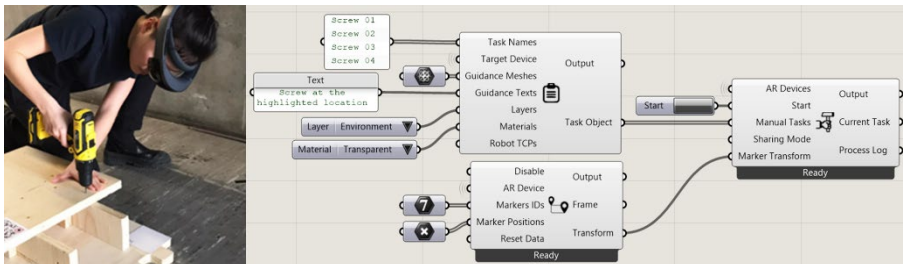


Figure 5. Task Controller Workflow (Screw Insertion)

4.2. ROBOT - SYSTEM (ROBOT TASK CONTROLLER)

Robot-System interaction allows robot planning to be augmented by the AR system,

which helps designers visualise robot paths in situ (e.g., to account for unplanned obstacles missing from the digital model). At the current stage, the component serves as a 'virtual' controller for simulation while physical robot control is not integrated.

The robot object is defined using an existing robot library for kinetic simulation. The library is a custom in-house development independent of the developments described in this paper. Robotic tasks are defined using frames along the programmed trajectory, together with an optional programme name for each action (Figure 6). The 'Robot Simulator' runs a given task virtually, by looping through each point on the trajectory, converting it to joint values using an Inverse Kinematics function in the robot object, and triggering updated visualisations of the Digital Twin on HoloLens. The list of robot tasks is sent to HoloLens in a dropdown menu, allowing the operator to select and visualise selected simulations as needed.

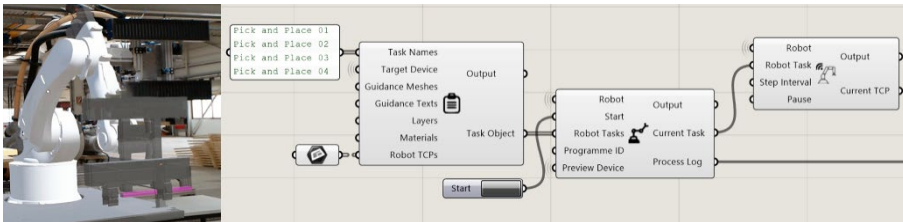


Figure 6. Robot Controller Workflow (Pick and Place Simulation)

4.3. HUMAN - ROBOT (HRC CONTROLLER)

Human-Robot collaboration combines the two mechanisms above and allows both units to collaborate in a task series. The workspace is not oriented around the workpiece, but around a shared workspace with the robots. The 'HRC Controller' converts the task objects defined generically for both humans and robots and dispatches the information to either the AR device or the robot for execution.

As an example, we imagine a scenario in which a human and a robot collectively disassemble a structure where the blocks are in known locations, but the screws are not. Since the robot cannot be programmed for unknown locations and angles, a sequence can be built with the HRC component (Figure 7), where the human unscrews while the robot first holds and subsequently removes the block at pre-programmed positions. Each human task ends when the AR client signals completion; each robotic task ends when every point on the path has been looped through. The human and robot take turns to execute in a sequential manner.

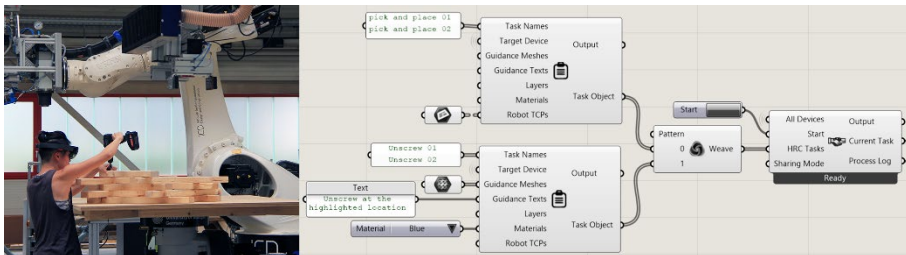


Figure 7. HRC Task Controller Workflow (Sequential Task Sharing)

5. Case Study

The Vizor framework is tested in a case study, where a human craftsperson, two 6-axis KUKA KR500 industrial robots, and one 2-axis tilt-turn table collaboratively assemble timber slats into clusters. It presents a dynamic, instructive Human Robot Collaboration (iHRC) process, where the sequential task sharing described in 4.3 is augmented with objects that implement real-time physical robot control, as well as a task reassignment mechanism for humans to interact with the fabrication process on the fly.

5.1. SETUP

One KUKA robot executes pick and placing the timber slats. The second robot inserts nails at the slat intersections with an automatic nail gun. The tilt-turn table adjusts its orientation to ensure the robots can reach target locations. The human is equipped with a *HoloLens* and an electric screwdriver. The craftsperson within the high LoA production setup carries out the following activities:

- Overseeing the execution of the task sequence through the task list
- Inspecting the timber slats, such that, when the nailing position has a knot hole (where a loose connection would likely result), he/she intervenes by reassigning the task from robotic to manual execution and inserts a 4x60mm screw
- Inspecting and potential manual intervention of the robot execution, where, if unpredictable contingencies occur, he/she intervenes by reassigning a robotic task to manual execution

5.2. SUMMARY

Vizor is applied to a collaborative fabrication process where humans are put in the driving seat of the robotic platform's operation. Each human-executed task is assisted with AR-rendered geometry to indicate location of the operation, as well as details of task description and timing. Each robotic task is executed with a human in the loop, accompanied by information on the robot's next movement, task information and timer (Figure 8). Geometric deviation between the robotically placed and manually placed slats should be better addressed in future studies.

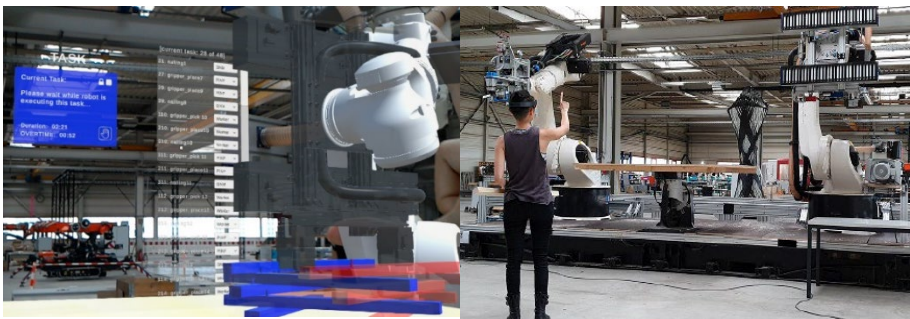


Figure 8: AR interface showing the task information panel, task list, robot digital twin, and work geometries overlaid on the physical workspace (Left) and Craftsman wearing HoloLens (Right)

6. Discussion and Future Work

This research presents Vizer, a software framework developed with the aim of introducing human craft in high LoA prefabrication and streamlining the creation of HRC workflows integrating Augmented Reality. Its main design considerations, architecture, components, and their usage are presented. Its application in robotic prefabrication in both planning and execution phases are illustrated through use case examples and a case study.

The framework is the first step towards a more accessible, adaptable, and intuitive AR-integrated human machine collaboration workflow, which can be augmented with additional hardware, control, sensing, tracking, and AR client implementations. For instance, human-robot interaction modalities can be expanded to include haptics, voice, or more sophisticated gestural inputs available on *HoloLens 2*. The robotic execution module can be developed further and integrate higher sensing capabilities e.g., using depth cameras to capture structures as they are built.

Though the system has only been demonstrated in prototyping environments in this paper, it is currently used in a pavilion construction project under more realistic conditions for prefabrication. To further validate and improve the framework, workshops and seminars are also relevant avenues to test the use of the system with a wider audience, from workflow design, simulation, through to the fabrication stage.

Acknowledgements

The research has been supported in part by the Deutsche Forschungsgemeinschaft (DFG, German Research Foundation) under the Excellence Strategy - EXC 2120/1 - 390831618. The work presented in this paper was partially developed within the ITECH (Integrative Technologies and Architectural Design Research) Master's program at the University of Stuttgart.

Additionally, the authors would like to thank Long Nguyen for the development of the robot kinematics solver 'VirtualRobot' at the Institute for Computational Design and Construction (ICD).

References

- Amtsberg, F., Yang, X., Skoury, L., Wagner, H., & Menges, A. (2021). IHRC: An AR-Based Interface for Intuitive, Interactive and Coordinated Task Sharing Between Humans and Robots in Building Construction. *38th International Symposium on Automation and Robotics in Construction (ISARC 2021)*, 25–32.
- Atanasova, L., Mitterberger, D., Sandy, T., Gramazio, F., Kohler, M., & Dörfler, K. (2020). Prototype As Artefact. *Proceedings of the 40th Annual Conference of the Association of Computer Aided Design in Architecture (ACADIA)*, 350–359.
- Caudell, T. P., & Mizell, D. W. (1992). Augmented reality: An application of heads-up display technology to manual manufacturing processes. *Proceedings of the Twenty-Fifth Hawaii International Conference on System Sciences* (pp. 659–669). <https://doi.org/10.1109/HICSS.1992.183317>
- Fologram. (2021). *Computer software*. Retrieved from <https://fologram.com/>
- García del Castillo y López, J. L. (2019). Robot Ex Machina. *Proceedings of the 39th Annual Conference of the Association for Computer Aided Design in Architecture*. Ubiquity and Autonomy.

- Garcia, M. A. R., Rojas, R., Gualtieri, L., Rauch, E., & Matt, D. (2019). A human-in-the-loop cyber-physical system for collaborative assembly in smart manufacturing. *Procedia CIRP*, 81, 600–605. <https://doi.org/10.1016/j.procir.2019.03.162>
- Jahn, G., Newnham, C., van der Berg, N., & Beanland, M. (2018). Making in Mixed Reality. *Proceedings of the 38th Annual Conference of the Association for Computer Aided Design in Architecture*. Recalibration: On Imprecision and Infidelity, Mexico City.
- Johns, R. L. (2017). Augmented Materiality: Modelling with Material Indeterminacy. *Negotiating Design & Making, Fabricate 2014: Negotiating Design & Making*, 216–223. <https://doi.org/10.2307/j.ctt1tp3c5w>
- Kyjanek, O., Al Bahar, B., Vasey, L., Wannemacher, B., & Menges, A. (2019). Implementation of an Augmented Reality AR Workflow for Human Robot Collaboration in Timber Prefabrication. *36th International Symposium on Automation and Robotics in Construction*, Banff, AB, Canada. <https://doi.org/10.22260/ISARC2019/0164>
- Menges, A. (2015). The New Cyber-Physical Making in Architecture: Computational Construction. *Architectural Design*, 85(5), 28–33. <https://doi.org/10.1002/ad.1950>
- Mitterberger, D., Dörfler, K., Sandy, T., Salveridou, F., Hutter, M., Gramazio, F., & Kohler, M. (2020). Augmented bricklaying: Human–machine interaction for in situ assembly of complex brickwork using object-aware augmented reality. *Construction Robotics*, 4(3–4), 151–161. <https://doi.org/10.1007/s41693-020-00035-8>
- Mueller, S., Seufert, A., Peng, H., Kovacs, R., Reuss, K., Guimbretière, F., & Baudisch, P. (2019). FormFab: Continuous Interactive Fabrication. *Proceedings of the Thirteenth International Conference on Tangible, Embedded, and Embodied Interaction* (pp. 315–323). <https://doi.org/10.1145/3294109.3295620>
- Peng, H., Briggs, J., Wang, C.-Y., Guo, K., Kider, J., Mueller, S., Baudisch, P., & Guimbretière, F. (2018). RoMA: Interactive Fabrication with Augmented Reality and a Robotic 3D Printer. *Proceedings of the 2018 CHI Conference on Human Factors in Computing Systems*, 1–12. <https://doi.org/10.1145/3173574.3174153>
- Wagner, H. J., Alvarez, M., Groenewolt, A., & Menges, A. (2020). Towards digital automation flexibility in large-scale timber construction: Integrative robotic prefabrication and co-design of the BUGA Wood Pavilion. *Construction Robotics*, 4(3–4), 187–204. <https://doi.org/10.1007/s41693-020-00038-5>
- Yoshida, H., Igarashi, T., Obuchi, Y., Takami, Y., Sato, J., Araki, M., Miki, M., Nagata, K., Sakai, K., & Igarashi, S. (2015). Architecture-scale human-assisted additive manufacturing. *ACM Transactions on Graphics*, 34(4), 1–8. <https://doi.org/10.1145/2766951>

A COLLABORATIVE WORKFLOW TO AUTOMATE THE DESIGN, ANALYSIS, AND CONSTRUCTION OF INTEGRALLY-ATTACHED TIMBER PLATE STRUCTURES

NICOLAS ROGEAU¹, ARYAN REZAEI RAD², PETRAS VESTARTAS³, PIERRE LATTEUR⁴ and YVES WEINAND⁵

^{1,2,3,5}*Ecole Polytechnique Fédérale de Lausanne*

⁴*Université Catholique de Louvain*

¹*nicolas.rogeau@epfl.ch, 0000-0003-1329-0177*

²*aryan.rezaeirad@epfl.ch, 0000-0003-1149-7617*

³*petras.vestartas@epfl.ch, 0000-0002-4428-1110*

⁴ *pierre.latteur@uclouvain.be, 0000-0002-4608-3732*

⁵*yves.weinand@epfl.ch, 0000-0002-8088-6504*

Abstract. This paper introduces a computational framework that fosters collaboration between architects, engineers, and contractors by bridging the gap between architectural design, structural analysis, and digital construction. The present research is oriented toward the formulation of an automatic design-to-construction pipeline for Integrally-Attached Timber Plate Structures (IATPS). This construction system is based on assembling timber panels through the sole interlocking of wood-wood connections inspired by traditional Japanese joinery. Prior research focused on developing distinct computational workflows and dealt with the automation of 3D modelling, numerical simulation, fabrication, and assembly separately. In the current study, a single and interactive design tool is presented. Its versatility is demonstrated through two case studies, as well as the assembly of a physical prototype with a robotic arm. Results indicate that efficiency in terms of data flow and stakeholder synergy is considerably increased. The proposed approach contributes to the Sustainable Development Goal (SDG) 11 by facilitating the collaborative design of sustainable timber structures. Besides, the research also contributes to SDG 9 as it paves the way for sustainable industrialisation of the timber construction sector through streamlined digital fabrication and robotic assembly processes. This reduces manufacturing time and associated costs while leveraging richer design possibilities.

Keywords. Timber Plate Structures; Timber Joints; Collaborative Design; Interdisciplinary Design; Structural Performance Assessment; Robotic Assembly; SDG 11; SDG 9.

1. Introduction

1.1. INTERDISCIPLINARITY AS A DRIVER OF SUSTAINABILITY

In 2020, the construction sector was responsible for 37% of energy-related CO₂ emissions. A decrease in economic activities due to the COVID-19 pandemic has led to temporary improvements. However, the decarbonisation of buildings is currently not on track to reach the goals of the Paris Agreement (United Nations Environment Programme, 2021). While there is a clear reduction trend in life cycle greenhouse gas emissions due to improved operational energy performance, researchers have reported an increase in embodied emissions arising from the manufacturing and processing of building materials (Röck et al., 2020) (Zimmermann et al., 2021). Given the high demand for new housing, the entire life cycle of buildings should be taken into consideration during the design phase to mitigate the environmental impact of construction.

Digitisation can enhance the productivity of the construction sector and help deliver the required building stock. However, automating existing workflows without a paradigm shift would only increase the environmental impact of building activities. To reach United Nations Sustainable Development Goal 11 – Making cities and human settlements inclusive, safe, resilient, and sustainable – it is necessary to both rethink standard design workflows and develop more sustainable construction processes. On the one hand, given the increasing complexity of architectural projects, interdisciplinary collaboration needs to be strengthened (Knippers et al., 2021). Physical considerations such as material properties, structural performance, and prefabrication constraints need to be included upstream in the design process. On the other hand, low carbon materials and efficient manufacturing techniques need to be more broadly adopted.

This research focuses on Integrally-Attached Timber Plate Structures (IATPS) – an innovative building system relying on the interlocking of engineered timber panels. Drawing inspiration from traditional Japanese craftsmanship, the elements are connected solely by wooden joints (i.e. mortises and tenons), reducing the need for additional metallic fasteners (Figure 1). The advantages of IATPS are double. Firstly, this construction technique offers the possibility of creating complex shapes out of flat standard wooden panels. It therefore provides a low-carbon alternative for creating architecturally appealing structures, relying mainly on a natural and renewable resource. Secondly, recent advances in digital timber construction allow a high degree of automation for IATPS. Panels can be cut with a Computer Numerical Control (CNC) machine and assembled into larger modules with an industrial robotic arm (Rogeanu et al., 2021). The main objective of this research is to ease the design of IATPS by facilitating the data flow from architectural design to structural analysis and automated construction. To enable reciprocal feedback between the different fields of expertise involved in the project (i.e. architecture, engineering, and robotics), a collaborative computational design tool has been developed and is presented in this paper.



Figure 1. Two examples of IATPS: the theatre of Vidy in Lausanne (left, © Ilka Kramer) and the multipurpose hall of Annen in Manternach (right, © Valentin Bianchi).

1.2. INTERACTIVE COMPUTATIONAL WORKFLOWS

Despite the progressive adoption of Computer-Aided Design (CAD) software that increased drafting productivity in architectural and engineering offices, standard design-to-construction workflows have barely changed and remained very linear (Carpo, 2017). However, as design teams keep getting bigger and their members more and more specialised, collaboration is both more essential and more complex than ever (Dalla Valle, 2021). One major challenge lies in the diversity of digital tools used by architects, engineers, and contractors, as proprietary file formats lack interoperability to enable a real collaborative design workflow (Oti & Tizani, 2010). Indeed, most professional software focuses on one part of the design process (drafting, analysing, manufacturing...) and ensures that its functionalities are generic enough to accommodate all building typologies (Figure 2, left).

As developing custom software, applications, and plugins become more accessible, collaborative design workflows tailored for specific building typologies (Figure 2, right) have been elaborated and tested by different researchers. So-called “Interactive co-design methods” have been used to realise the BUGA wood (Wagner et al., 2020) and fibre (Dambrosio et al., 2019) pavilions. Computational developments consisted notably in integrating physical constraints linked to the robotic prefabrication of the elements into the 3D design model. This was achieved by allowing designers to simulate fabrication toolpath and assembly sequences inside the design interface.

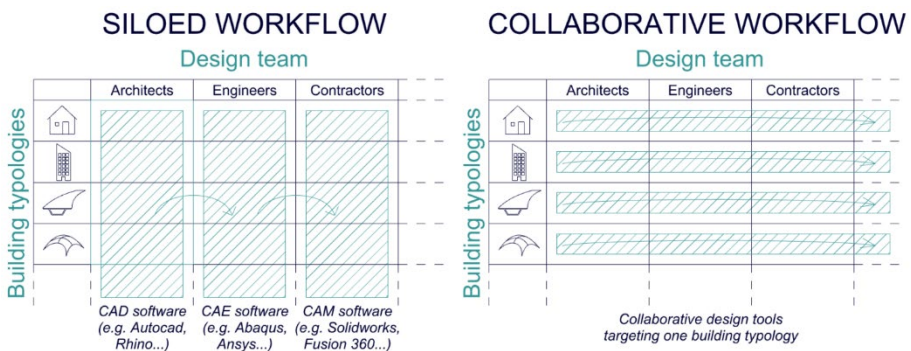


Figure 2. Standard software focuses on one part of the design process leading to siloed workflows. Collaborative design workflows focus instead on one building typology.

2. Method

2.1. DEVELOPING A COLLABORATIVE DESIGN INTERFACE

The methodology builds on previous work on Integrally-Attached Timber Plate Structures (IATPS) conducted at the laboratory for timber constructions (IBOIS, EPFL). An integrated design tool to generate joint geometry, fabrication toolpath, and robot trajectories (Rogea et al., 2021), as well as a framework for the structural analysis of IATPS (Rezaei Rad et al., 2020), were separately introduced. The novelty of this contribution lies in the integration of the structural engineering feedback directly into the design interface. This is achieved through the systematic conversion of architectural 3D models to Finite Element (FE) meshes and will be further detailed in the next sections.

The collaborative design workflow was implemented in Grasshopper – the parametric interface of Rhinoceros 3D software and released as an open-source plugin named Manis. The algorithm automatically outputs visual information on the structural performance and the construction feasibility of a timber plate structure based on an initial 3D model (Figure 3). Interdisciplinary collaboration is thereby made possible by following an iterative design process. The collection of 3D panels that composes the structure is converted to a *plate model object*. This custom python class instance automatically generates an additional layer of data based on the order of the elements (assembly sequence) and the way they are connected (adjacency graph). A set of components that operate on the plate model is then available to: (1) simulate the computed assembly sequence, (2) generate parametric timber joints between the pieces, (3) generate a FE model and run a FE analysis, (4) generate, simulate, and execute CNC fabrication toolpath, (5) generate, simulate, and execute robotic trajectories.

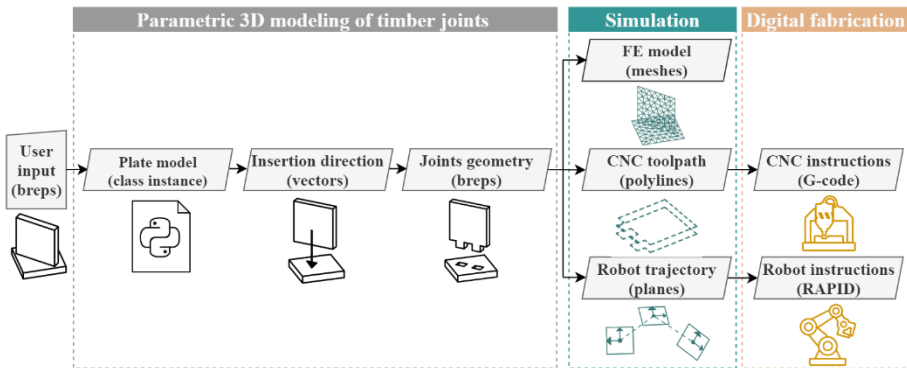


Figure 3. The algorithm enables collaboration by integrating structural performance as well as fabrication and assembly constraints into the design process.

2.2. INTEGRATING NUMERICAL SIMULATION

The integration of the numerical simulation is achieved through COMPAS – an open-source python-based platform developed at the NCCR Digital Fabrication to enhance code reusability and facilitate the development of collaborative design workflows (Van

Mele et al., 2017). The COMPAS_FEA extension aims to provide a smooth interface between CAD and FEA. First, this Python package creates a *structure* object associated with the 3D model. It includes geometric information, element, section, and material properties. Then, it enables the user to specify loads and boundary conditions for structural analysis. The construction of the *structure* object is performed using various modules that exist in the core COMPAS library (i.e., data structure, mesh) and the FEA extension. Accordingly, the majority of the repetitive scripting tasks are eliminated while streamlined data post-processing and visualisation support are provided. Once the *structure* object is constructed, COMPAS_FEA writes the native input file for the FE software. In this case, the model is generated in either ABAQUS or OpenSees. It is then sent to the original solver for analysis. Lastly, the data from the analysis results are extracted and returned to the collaborative design interface (Figure 4).

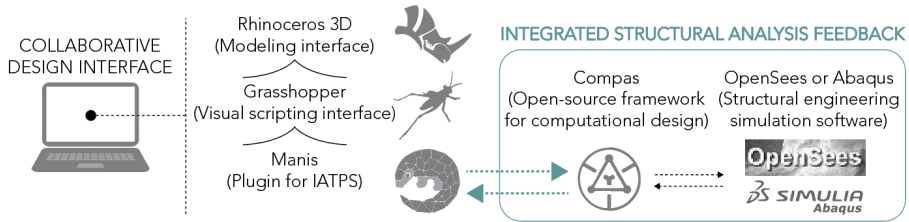


Figure 4. Integrating engineering feedback from Abaqus and OpenSees into the collaborative design plugin "Manis" via COMPAS open-source platform.

In detail, each plate is simulated using a conventional shell element with a homogeneous section property. The thickness, the integration rule (i.e. Simpson's rule), and the number of integration points are also specified in this step. General-purpose thin shell elements are used to account for finite membrane strains, as well as large rotations. In particular, a finite-strain shell element with four nodes (S4R), which uses lower-order integration to compute the element stiffness, is employed. This type of shell element has six degrees of freedom and enables thickness changes, which will lead to a realistic evaluation of the performance of the structure. Also, a free meshing technique is used to convert each plate mid-surface to a triangular mesh while line segments are created to represent the connections between the plates (Figure 5). Those connection links are integrated into the simulation by defining Spring elements between the Shell elements. The algorithm ensures that the nodes of each connection link correspond to vertices of the plate meshes. Finally, mesh data and connection links are added to the *structure* object to perform the analysis.

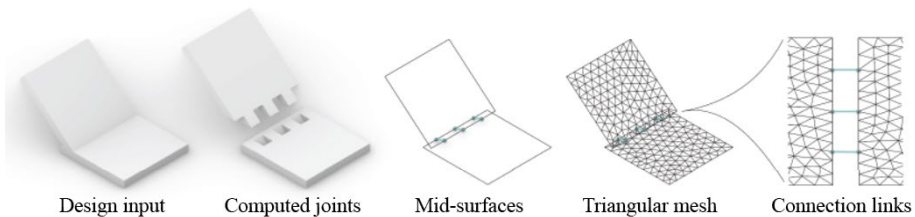


Figure 5. Automated conversion of architectural 3D models to Finite Element models.

3. Results

3.1. FIRST CASE STUDY: ORTHOGONAL TIMBER SLAB

Our collaborative design workflow has first been tested on a piece of timber slab consisting of 4 panels connected by through tenon joints (Figure 6). This construction system was initially developed with the idea of shipping flat packs of timber panels to be assembled on-site (Gamerro et al, 2020). Using our parametric tool, timber joints are automatically generated between the panels. The influence of the number of tenons, their dimensions, and spacing on the structural performance is systematically visualised through the integrated numerical simulation module. Load and support points for the analysis are parametrically defined through a complementary script. The deformation of the structure is displayed in the design interface. In addition, von Mises stresses are computed to evaluate yield and failure states near the connections. The simulation of the CNC toolpath, as well as the robotic trajectory, is performed in the same environment. This allows modifying the design at any time while ensuring compliance with fabrication and assembly constraints.

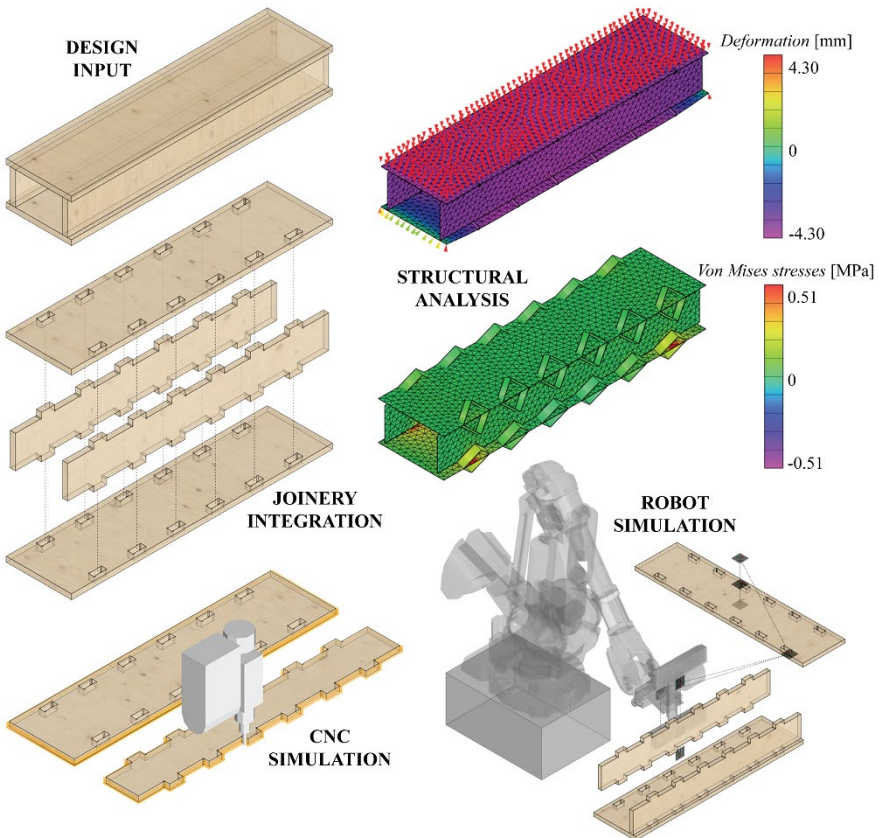


Figure 6. The developed plugin enables the integration of fabrication, assembly and structural constraints into the design process of an orthogonal slab made of 4 timber panels.

3.2. SECOND CASE STUDY: DOUBLY-CURVED TIMBER VAULT

A piece of the doubly-curved timber structure of Annen head office in Manternach (Rezaei Rad et al., 2020) has been chosen as the second case study. The prototype is a modular structure composed of 9 boxes with 4 panels each (Figure 7). Sunrise dovetails and through tenon joints connect the pieces to each other. The choice of the joint is automatically determined according to the relative position of the plates (Rogeanu et al., 2021). As for the previous case study, the algorithm allows us to test different joinery configurations while visualising their influence on structural performance. A uniform load is applied on the top layer of the vault and subsequent deformations and stresses are automatically retrieved. The Finite Element Analysis of all 36 plates is performed with a computational time of approximately 1 minute which maintains the possibility of evaluating several design iterations. The full design workflow has also been recorded and is available on Vimeo (IBOIS EPFL, 2021).

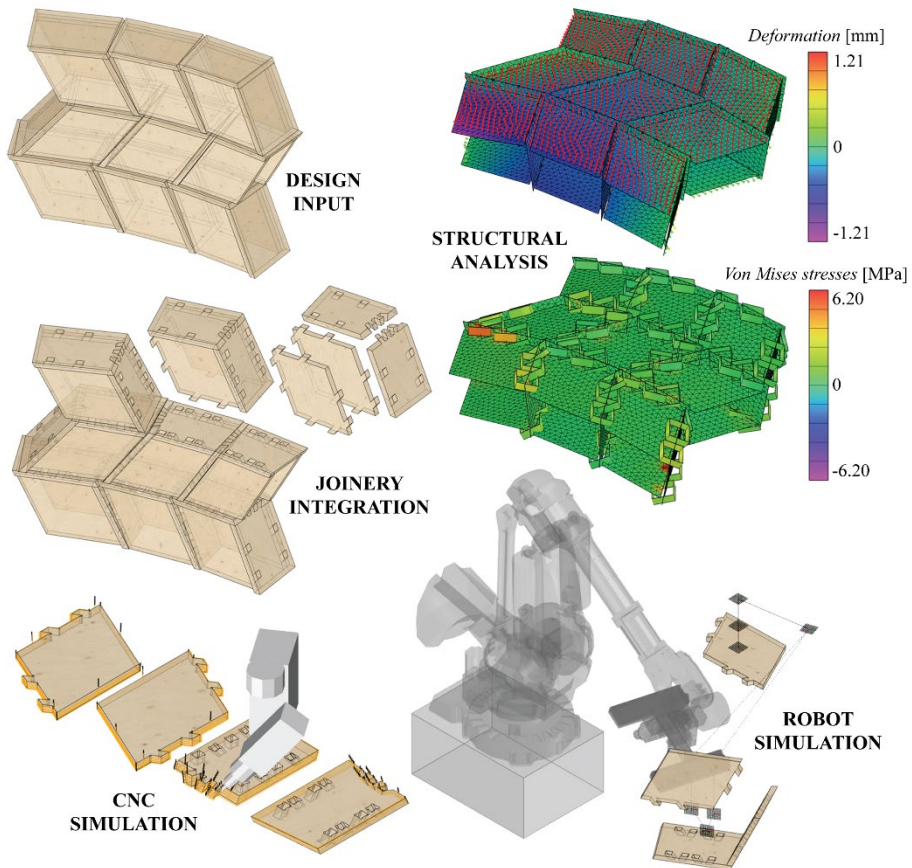


Figure 7. The tool design space ranges from standard to bespoke timber plate structures as demonstrated with this doubly-curved timber vault made of 9 boxes of 4 plates each.

To assess all steps of the design-to-fabrication pipeline, one box of the doubly-curved vault prototype was fabricated (Figure 8). The four panels of the box were cut with a 5-axis CNC after simulating the toolpath in the design interface. Next, robot trajectories, computed by the algorithm, made it possible to perform the assembly by seamlessly transferring the data to a 6-axis robotic arm (ABB 6400). The position of the first plate of the box was manually referenced. Then, the three remaining plates were lifted from a square base with a vacuum gripper attached on the robot end effector. To ease the insertion with the robot, the joints were manually sanded beforehand. This proved to be particularly necessary when inserting the last two plates of the module as 4 tenons had to be assembled simultaneously in two adjacent plates (Figure 8.7). This made it possible to compensate for the slight differences between the virtual model and the prototype.

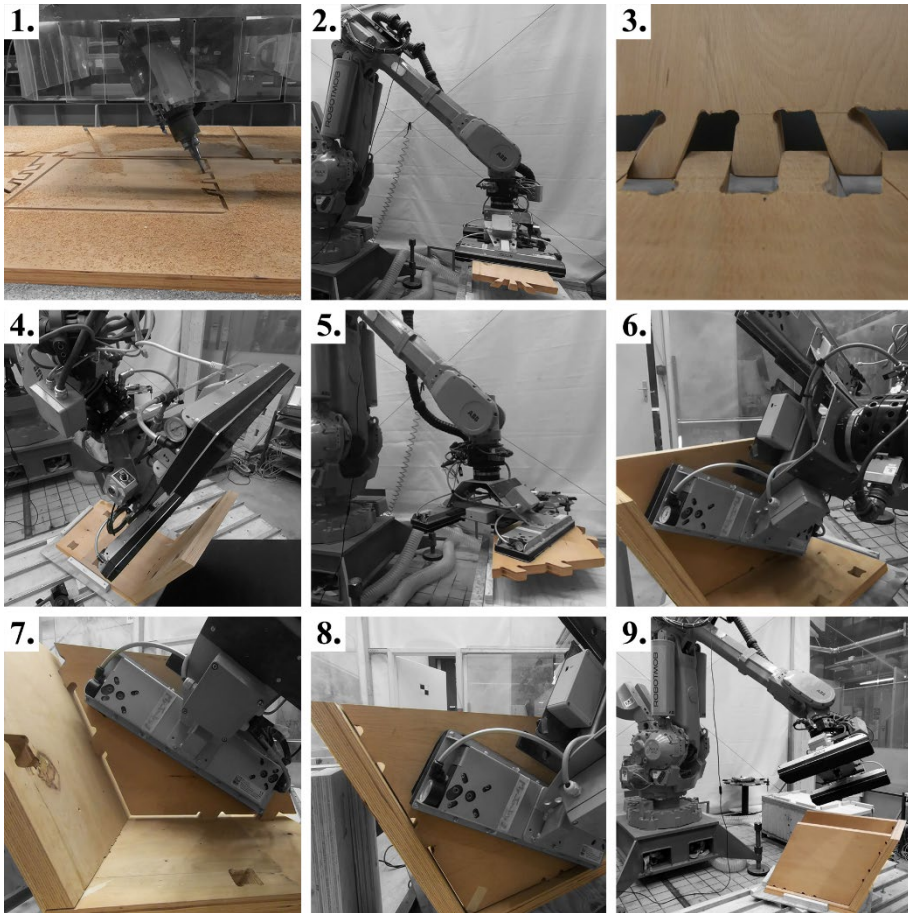


Figure 8. CNC cutting and robotic assembly of one module of the doubly-curved vault prototype.

4. Conclusion

An open-source collaborative design workflow for Integrally-Attached Timber Plate Structures (IATPS) has been developed and tested through two case studies. Using COMPAS and COMPAS_FEA frameworks allows to remain independent of the structural analysis backend. A major achievement consisted in unifying architectural design, structural analysis, digital fabrication, and robotic assembly in one single interface. Consequently, barriers among construction stakeholders are removed and the integration of physical constraints in the project can happen at a very early stage of the design process. Furthermore, both standard and bespoke geometries have been handled by the algorithm, demonstrating that a wide range of architectural applications can be explored.

While the present research facilitated the design of IATPS by enabling a collaborative design workflow, future research should focus on the construction phase and its automation. Indeed, to foster the use of timber in standard and bespoke architecture, streamlined prefabrication processes need to be developed and implemented. More specifically, upcoming investigations on IATPS should tackle challenges linked to the insertion of the joints with a robotic arm. Parameters such as the tolerance and the shape of the connections have a significant impact on the success of the robotic assembly as well as on the rigidity of the connections. Further experimental studies are therefore required to better understand the influence of those design parameters. From a broader perspective, the development of future robotic set-ups should aim for more flexibility by allowing the assembly of different types of joints in various configurations.

As far as structural engineering and associated simulation are concerned, the computational cost could be reduced by employing reduced-order Finite Element models for timber plates, i.e., macroscopic elements. The interdisciplinary aspect of this collaborative design workflow could also be expanded further by integrating other design considerations such as economic factors and environmental impact measures. Quantitative data about material savings and avoided CO₂ emissions would typically be a great addition to better inform the design team. Assembling the knowledge of different fields of expertise in a single platform will contribute to making better design decisions and lead to a more sustainable building environment. In this regard, the particular focus should be to develop design tools that accommodate for a holistic approach of specific building systems instead of generic tools dedicated to one professional discipline.

Acknowledgements

This research was supported by the NCCR Digital Fabrication, funded by the Swiss National Science Foundation (NCCR Digital Fabrication Agreement #51NF40-141853). In addition, the authors would like to acknowledge Imax Pro S.A. and Maka GmbH for their assistance with the robotic assembly and CNC machining respectively. The authors are also grateful to the COMPAS development team and especially to Dr Tom Van Mele for his support with COMPAS FEA.

References

- Carpo, M. (2017). *The second digital turn: design beyond intelligence*. Writing architecture. The MIT Press. <https://doi.org/10.7551/mitpress/9976.001.0001>
- Dalla Valle, A. (2021) Challenge of Managing the Design Team Multidisciplinarity in View of Environmental Goals. In: *Change Management Towards Life Cycle AE(C) Practice, SpringerBriefs in Applied Sciences and Technology*. Springer, Cham. https://doi.org/10.1007/978-3-030-69981-9_8.
- Dambrosio, N., Zechmeister, C., Bodea, S., Koslowski, V., Gil Pérez, M., Rongen, B., Knippers, J., Menges, A. (2019). BUGA Fibre Pavilion: Towards an architectural application of novel fiber composite building systems. In *39th Annual Conference of the Association for Computer Aided Design in Architecture: Ubiquity and Autonomy* (pp. 140-149). *The Association for Computer Aided Design in Architecture (ACADIA)*.
- Gammero, J., Bocquet, J.F., Weinand, Y. (2020). A calculation method for interconnected timber elements using wood-wood connections. *Buildings*, 10(3). <https://doi.org/10.3390/buildings10030061>.
- IBOIS EPFL. (2021, October 17). Manis - Annen case study (Part 1: General workflow) [Video]. Vimeo. <https://vimeo.com/635127909>
- IBOIS EPFL. (2021, October 17). Manis - Annen case study (Part 2: Focus on integrated structural design) [Video]. Vimeo. <https://vimeo.com/635128815>
- Knippers, J., Kropp, C., Menges, A., Sawodny, O., Weiskopf, D. (2021). Integrative computational design and construction: Rethinking architecture digitally. *Civil Engineering Design*, 3, 123–135. <https://doi.org/10.1002/cend.202100027>.
- Oti, A. H. & Tizani, W. (2010). Developing incentives for collaboration in the AEC Industry. In *13th International Conference of Computing in Civil and Building Engineering* (pp. 319-325). Nottingham University Press. ISBN 978-1-907284-60-1.
- Rezaei Rad, A., Burton, H., Rogeau, N., Vestartas, P., Weinand, Y. (2021). A framework to automate the design of digitally-fabricated timber plate structures. *Computers & Structures*, 244(2021), 106456. <https://doi.org/10.1016/j.compstruc.2020.106456>.
- Röck, M., Saade, M. R. M., Balouktsi, M., Rasmussen, F. N., Birgisdottir, H., Frischknecht, R., Habert, G., Lützkendorf, T., & Passer, A. (2020). Embodied GHG emissions of buildings – The hidden challenge for effective climate change mitigation. *Applied Energy*, 258, 114107. <https://doi.org/10.1016/j.apenergy.2019.114107>.
- Rogeau, N., Latteur, P., Weinand, Y. (2021). An integrated design tool for timber plate structures to generate joints geometry, fabrication toolpath, and robot trajectories. *Automation in Construction*, 130(2021), 103875. <https://doi.org/10.1016/j.autcon.2021.103875>.
- United Nations Environment Programme (2021). *2021 Global Status Report for Buildings and Construction: Towards a Zero-emission, Efficient and Resilient Buildings and Construction Sector*. Nairobi.
- Van Mele, T., Liew, A., Méndez Echenagucia, T., Rippmann, M., and others (2017). *COMPAS: A framework for computational research in architecture and structures*.
- Wagner, H.J., Alvarez, M., Groenewolt, A., Menges, A. (2020). Towards digital automation flexibility in large-scale timber construction: integrative robotic prefabrication and co-design of the BUGA Wood Pavilion. *Construction Robotics*, 4, 187–204. <https://doi.org/10.1007/s41693-020-00038-5>.
- Zimmermann, R. K., Andersen, C. M. E., Kanafani, K., & Birgisdottir, H. (2021). *Whole Life Carbon Assessment of 60 buildings: Possibilities to develop benchmark values for LCA of buildings*. Polyteknisk Boghandel og Forlag. BUILD Report No. 2021:12. <https://sbi.dk/Pages/Whole-Life-Carbon-Assessment-of-60-buildings.aspx>.

ADAPTIVE ROBOTIC FIBER WINDING SYSTEM FOR MULTIPLE TYPES OF OPTIMIZED STRUCTURAL COMPONENTS

ZHUOYANG XIN¹, GUANQI ZHU², ERYU NI³, CHONGYI TANG⁴
and DAN LUO⁵

^{1,2,3,5}*School of Architecture, University of Queensland.*

⁴*School of Civil Engineering, University of Queensland.*

lz.xin@uq.net.au, 0000-0002-7695-0745

2uqgzhu3@uq.edu.au, 0000-0003-3228-7053

3erunina@outlook.com, 0000-0002-7667-2896

⁴*chongyi.tang@uqconnect.edu.au*

⁵*d.luo@uq.edu.au, 0000-0003-1760-0451*

Abstract. Coreless fiber winding (CFW) as a digital and automated fabrication technology presents high customization and productivity in fabricated components and has been utilized in some large-scale pavilion constructions. However, the existing CFW technology broadly utilized one-off prefab support frames, that limits the flexibility of the fabricated unit design and wastes the frame material. This study proposes an adaptive robotic fiber winding system by introducing a temporary support frame in CFW and validates the feasibility and reliability of the system in a unitized table base prototype. The table base showcase has resolved the digital workflow of the method and presents a consequential improvement in reusability and design flexibility for existing CFW technology. The proposed method in this study collaborates sustainable fabrication with computer-aided design, robotic automation and fibrous composite construction material. It is expected to gain more attraction in house building market and reduce the construction carbon impact to the environment.

Keywords. Digitization and Automation; Sustainable Fabrication; Robotic Technology; FRP Filament Winding; Lightweight and Customizable Structure; Stress-optimized Structure; SDG 9; SDG 12.

1. Introduction

The increasing prevalence of digital and automation technologies in the fabrication process has significantly improved the productivity of customized nonstandard building components (Hack et al., 2017; Wu et al., 2016). Owing to their performative material characteristics, fiber composite materials have shown significant potential in the fabrication of architectural parts, such as the coreless fiber winding (CFW) (Christie et al., 2021; Estrada et al., 2020; Prado et al., 2014) developed for large-scale monocoque structures (La Magna et al., 2014) and adapted modularized components (Knippers et al., 2016). CFW has exhibited exceptional performance for large-scale

customized structures, with highly flexible and structurally efficient FRP composite materials, and extraordinary sustainability, by significantly minimizing waste in the formwork construction and demolding process (Felbrich et al., 2017). However, the current CFW technology is implemented with one-off prefab support frames during the winding process, which limits the design flexibility for aggregate components, and is a trade-off for the lightweight fabricated performative fiber structure.

This article proposes a robotic fiber weaving technology based on adaptive temporary supports, which expands the existing CFW technology by integrating robotic assembly and robotic weaving in the fabrication of customized components. Rather than employing a prefab framework, the new technology utilizes robotic positioning of temporary support points to accommodate a large variation in component geometries. With high customizability and reusability, the new support system allows flexibility in component design and minimizes the fabrication cost for a fixed frame.

2. Adaptive Winding System Methodology

The proposed adaptive fiber winding system aims to build customized components in a cost-efficient and productive manner. To achieve successful fabrication for components with highly variable geometries, the system was developed using the following approaches.

One outstanding scheme is the customized robotic positioning of temporary supports in place of a prefab fixed frame. The temporary support system is designed to allow arbitrary reference points to be positioned within the working space for the subsequent weaving process, instead of being constrained to the prefab frame. The reference points of the temporary supports are accurately positioned in physical space with absolute coordinates. Compared with the fixed framework method, this method eliminates the need for the prefabrication of unique fixed frames for each geometric variation of a component, as well as framework positioning deviation during coordinate conversion from the physical world to the design model. The new method is rooted in the interwinding relationship between robotic assembly and robotic winding. Overall, it is an innovative research technique that combines sustainable development strategies with robotic construction.

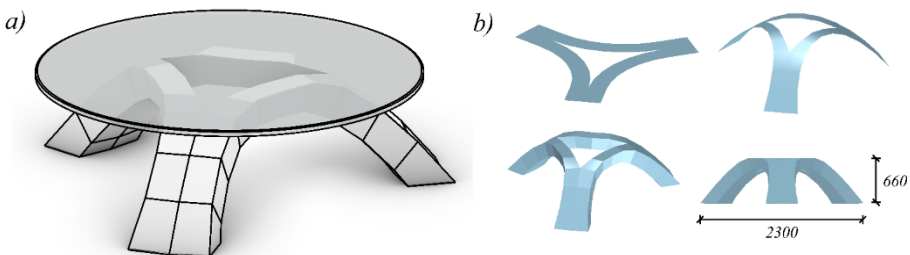


Figure 1. Table base geometry and generation

A systematic weaving design is essential for implementing this fabrication technique. In this regard, two aspects should be carefully considered. First, the weaving

sequence, which is a crucial part of the process, affects the generation of the objective geometry and structural performance of the fabricated components. Second, the robot movement, which is an equally essential part, significantly influences successful fiber winding at the reference anchor points. A systematic design and planning for both segments is required to achieve fluent progress of the fiber winding process that avoids collisions between the fibers and robot setup, avoiding damage to the prototype during fabrication.

3. Prototype Fabrication Workflow

To validate the feasibility of the proposed winding system, a customized table base prototype was developed, as shown in Figure 1a. The designed base model was a unitized structure comprising 30 components. To achieve a customized shape, a free-form relaxation technique was adopted on a 2D shape to generate the base shape, as shown in Figure 1b, and the obtained shell was extruded to a certain thickness based on the shell stress distribution obtained from a uniform loading structural analysis. Post-processing of the table base was conducted to flatten the top surface and trim the bottom unit to make it self-standing. The final dimensions of the table were 660 mm (height) by 2300 mm (width).

3.1. WINDING PATTERN GENERATION AND OPTIMIZATION

The prototype was designed to be built in a truss pattern and fabricated with a carbon fiber filament, as shown in Figure 2a. To understand the structural performance of the truss base under a typical table surface load, a numerical model was analyzed, and the stress distribution is shown in Figure 2b, with red and blue indicating compression and tension, respectively.

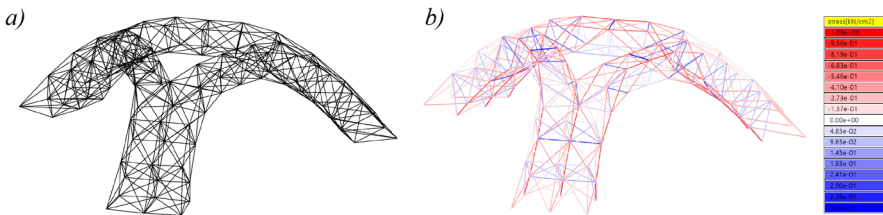


Figure 2. a) Table base truss pattern b) Estimated stress distribution of the table base

As a material designed to be utilized under tension, carbon fiber filaments can only serve as compressive truss elements if they have sufficient stiffness from the resin matrix. In this prototype, laminating epoxy resin was used to reinforce the filament strength. Regarding the fiber material, a polyester line was utilized in the prototype rather than directly applying carbon fiber to showcase the technique owing to its wide availability and low cost. Based on the numerical analysis, high compressive stress occurred in numerous elements, and the governing failure mode was hypothesized to be buckling owing to the slender geometry. To increase the buckling capacity, the number of polyester lines must be increased in the elements under high compressive stress to enlarge the cross-sectional area.

The number of lines for each element was determined based on Figure 2b and a simple structural test. As shown in Figure 3a, a manual weaving polyester line truss unit was fabricated, with 10 lines for each element. The laminating epoxy resin was then applied and cured to obtain sufficient stiffness and compressive capacity. The finished unit was loaded with weights on the top and ultimately held 30 kg. The results were used to estimate the compressive capacity of a single cured polyester line of unit length, which was input into the numerical results to obtain the number of lines. Based on the analysis, the number of lines varied from 9 to 27 for all the elements. Nine was the minimum number of lines required to stabilize the unit and was applied on tensile elements and low compressive elements; 27 was the maximum number of lines, which was used for the truss elements under the highest compressive stress. All the units and number of lines were then correlated, as shown in Figure 3b.

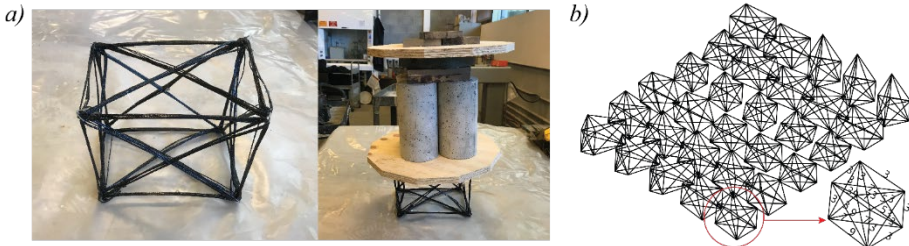


Figure 3. a) Structural test of a manual weaving truss unit b) Units with correlated line information

3.2. EQUIPMENT SET-UP

The prototype unit was fabricated using a UR10 robot system. The robot was installed on an aluminum profile table, and the temporary support, as proposed, was directly connected to the table. Prior to anchor point positioning by the robotic assembly, four vertical supports were installed directly on the table, as shown in Figure 4a. The bar holders were bolt-connected to the table, and the vertical steel bars were tightened inside the holders. The four-support system was input into the Grasshopper Plug-in for robotic path planning as previewed in Figure 4b and calibrated with robot to ascertain its position accuracy.

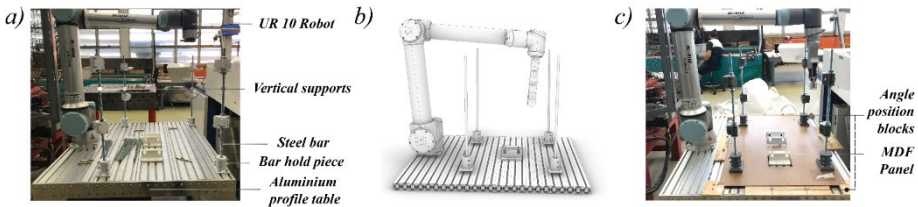


Figure 4. Equipment set-up

In the above assembly approach, the equipment setup must remain on the table until each unit is completely finished, which wastes considerable time considering the resin application and curing process. A second version of the equipment setup was developed by installing the four supports on an MDF panel to allow relocation of the

fabricated unit before resin application, as shown in Figure 4c. A new unit could then be fabricated with the robot while resin was applied to the previous one and cured without occupying the robot. The support locations on the panel were all positioned by a CNC cut, and the panel was constrained by four angle positioning blocks on the table, which ensured consistent equipment setup locations for every unit. This new approach increases the fabrication productivity by reducing unnecessary time on the robot table and allowing simultaneous work on multiple units.

3.3. ROBOTIC ASSEMBLY AND WEAVING

The core part of this table base manufacturing process is the integration of robotic assembly and robotic weaving. With the implementation of these two steps, customized units can be accurately fabricated. Prior to assembly and weaving, the units shown in Figure 3b must be oriented in the robotic working space to define the eight anchor point locations for subsequent work.

3.3.1. Robotic Assembly

Robotic assembly provides customized assembly of adaptive temporary anchor points. The anchor points were pre-installed on the horizontal bars and placed on a fixed station (Figure 5a). The robot arm located the anchor points in the design position by the pick-and-place process, as shown in Figure 5a-c. Subsequently, the horizontal bar was manually fixed to the vertical support frame to secure the anchor points, as shown in Figure 5d. During this process, the movement of the robot requires strict control to avoid collision with the surrounding environment and sufficient tolerance to install the fixing pieces.

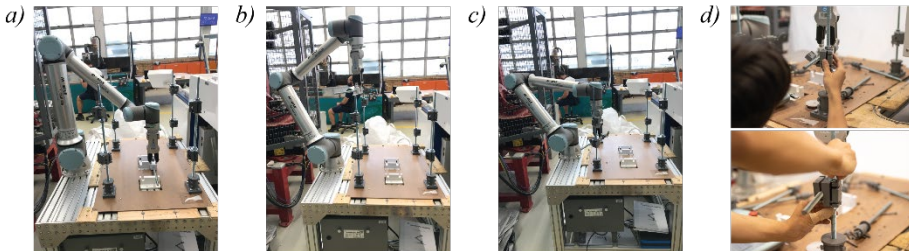


Figure 5. Robotic assembly

3.3.2. Polyester Line Winding

Following adaptive support assembly, a systematic robotic weaving process was explored. First, the anchor points must be specifically designed to assist in the weaving process. As shown in Figure 6a, the initial design was a circular hook made of steel wire, which failed owing to easy deformation of the soft material and polyester line spreading on the hook due to the circular geometry. The second design was a waterjet-cut steel hook with a long guiding rail for polyester line weaving and a small accumulation area to concentrate the polyester line to increase weaving accuracy. The second attempt increased the feasibility of the robotic winding process, but it was difficult to demold from the unit in the subsequent resin application and curing stage.

Then, a third design was proposed which maintained the main features of the first and second designs. The accumulation area was inherited from the first design with a circular geometry, which facilitated the demolding of the fabricated unit after curing. The separated guiding rail inherited from the second design can be attached to the hook during robotic weaving and removed when the weaving process is complete.

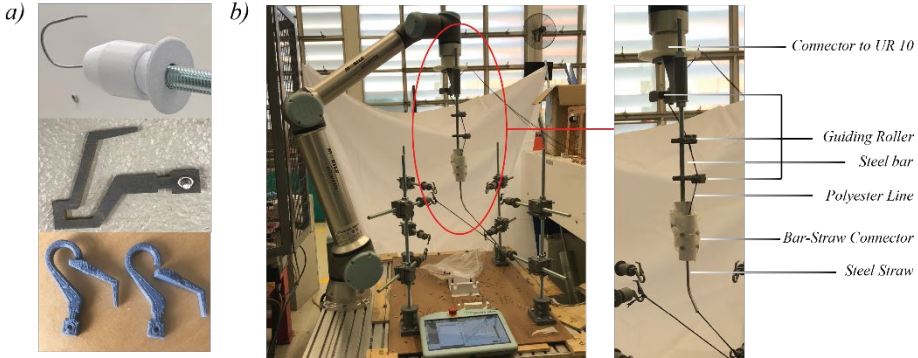


Figure 6. a) Hook geometry evolution b) Winding head design

The robotic winding process was implemented within the fabricated unit, which required a slender winding head to allow more movement for successful fiber winding on the anchor points without collapse with the existing setup. As shown in Figure 6b, the winding head was designed as a combination of a long steel bar and steel straw to guide the polyester line. Additional smaller guiding rollers were attached to the steel bar to avoid fiber entanglement with the winding head during the weaving process.

Through multiple attempts, the systematic design of the robotic path evolved from a simple winding movement to adaptive motions.

- The first attempt involved a simple movement around the anchor point. To sufficiently weave the fiber in the hook gap and tighten it during the entire process, the hooks all faced outward, with the top hooks opening upward and the bottom hooks opening downward. This path design categorized the anchor points into top and bottom points and applied the same path pattern on all of them, moving the winding head around the hook opening to weave the fiber into the hook gap, as shown in Figure 7a.

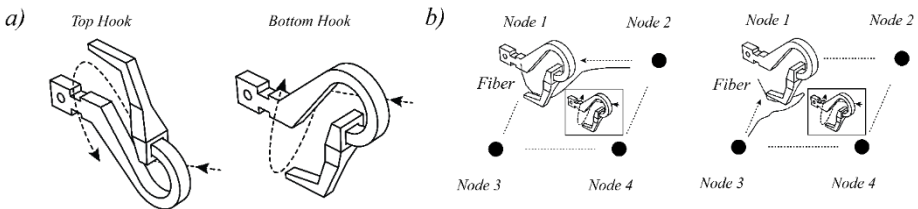


Figure 7. a) Movement path in the first attempt b) Weaving failure for the first attempt

- Building on the first attempt, the second attempt considered the direction from

which the fiber approached the hook. As observed from the first attempt, a simple movement path can successfully weave the fiber on the top hooks but not on some particular bottom hooks owing to the sagging geometry of the fiber. For example, as shown in Figure 7b, the fiber coming from node 2 to node 1 can be successfully captured by the anchor hook but will fail when coming from node 3 to node 1. The capture of the fiber on the hook obviously relies on the direction of approach, and the movement path must be mirrored for the bottom hooks that receive the fiber from different directions.

- In the third attempt, the bottom anchor hook orientation was nearly parallel to the unit edge, as shown in Figure 8a. Edge I in the sketch is more likely to collapse with the original path design in the first two attempts, and the area between the hook and edge I is not sufficient to fit the winding head. The weaving quality is affected when the previously woven fiber at edge I is disrupted and becomes loose, as shown in Figure 8b. In this attempt, the bottom anchor points were further categorized into near edge I or near edge II based on a comparison between their skew angles and adjacent edges. The winding head entered from the large-angle side (skew angle II in this example), and the tip of the winding head was tilted upward to perform winding on the near-edge side, as shown in Figure 8c.

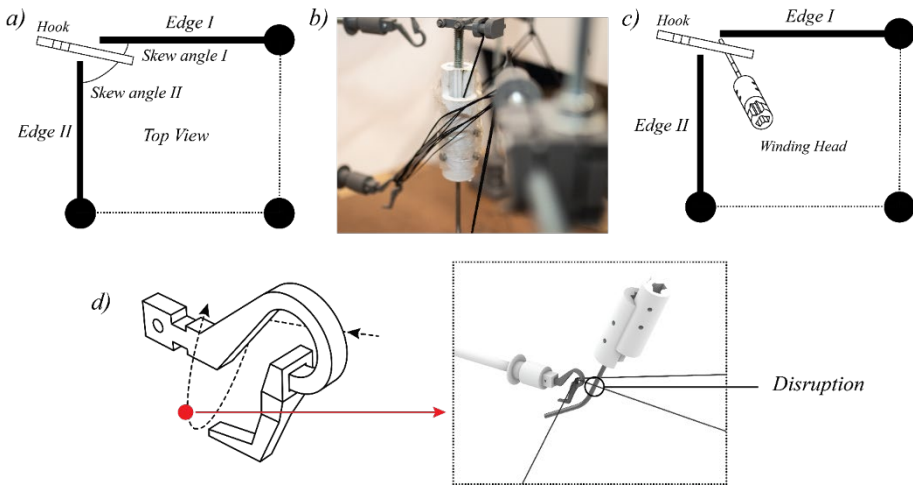


Figure 8. a) Sketch of hook orientation b) Disrupted fiber c) Tilted winding head d) Fiber interruption

- The final attempt considered the influence of the previously woven fiber frame on the new winding fiber geometry. As shown in Figure 8d, the fiber coming from the winding head is expected to be wound on the anchor point, but it can be disrupted by the existing fiber frame and fail to wind. With this consideration, the fiber weaving order must be strictly controlled to reduce winding interruption.

The final robotic winding path design was categorized into five main types, but all must be mirrored based on the fiber entry side at the anchor points. The robotic movements are shown in Figure 9a. Following the basic path pattern design, further

calibration or improvement of the path details must be implemented for the following two main reasons. The first reason is the material imperfection of the equipment setup, including the bending curvature of the connected steel bars and the rough surface of the 3D-printed pieces. This induces an error of approximately 3 to 5 mm at the anchor point locations, which has a negligible influence on the unit geometry (200-400 mm in size) but increases the difficulty of the fiber winding process. The second reason is the nature of the fiber, which sags when no tensile stress is applied. This can generate unexpected patterns, causing the winding process to fail, but it can also be exploited to help the anchor hook catch the fiber. A photograph of the fiber winding process is shown in Figure 9b.

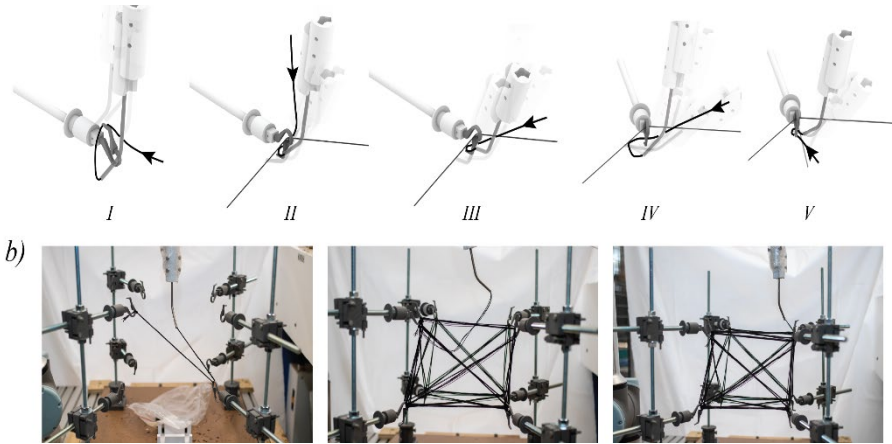


Figure 9. a) Five main types of winding path b) Fiber winding process

3.4. PROTOTYPE RESINING AND CURING

The combination of robotic assembly and fiber winding generated customized units for the table base. The subsequent step was resin application and curing to obtain sufficient strength. As shown in Figure 10a, the finished unit was relocated together with the anchoring setup, and the epoxy resin was manually applied. The unit was left to cure for several hours while the next unit was fabricated. After curing, the unit was demoulded by disassembling the hooks from the support (Figure 10b) and sliding them out of the unit (Figure 10c). The space left by the hooks was used to connect the units.

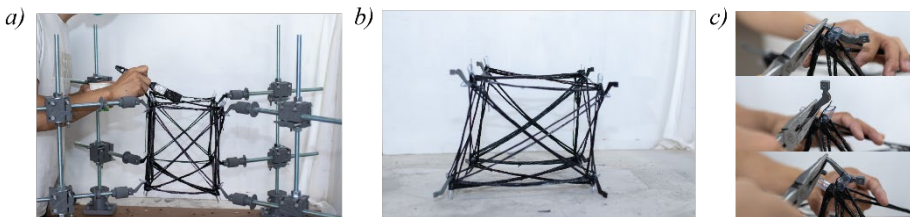


Figure 10. a) The manual resin applying b) Cured unit. c) Demoulding process

An automatic resining system was explored, as shown in Figure 11a. Rather than using epoxy resin, which has a working time of only 15 min, UV resin was utilized. The advantage of applying UV resin is that it can be quickly cured under UV light in 1-2 min, which considerably reduces the time required to cure the fabricated unit before demolding from the anchor points. However, the units with UV resin did not have sufficient strength to maintain the geometry and sustain any load, as shown in Figure 11b. Therefore, the plan was suspended. Further improvement of the automatic resining system should be conducted to increase the efficiency of the adaptive fiber winding system.

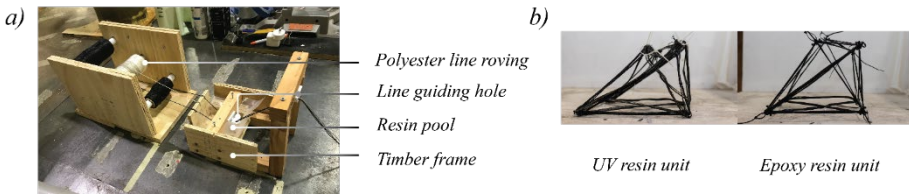


Figure 11. a) Auto-resin apply system set-up b) Comparison of unit geometry with different resins

3.5. UNIT ASSEMBLY

To assemble all the components into the final table base prototype, cable ties were used to link all the fabricated units through the anchoring holes, as shown in Figure 12a. A cable line connection was utilized between the prototype legs to stabilize the structure and avoid collapse failure owing to leg sliding. The final prototype, as shown in Figure 12b, validates the feasibility of the proposed method for the fabrication of customized structures, providing an abundance of geometrical freedom with effective structural support for general applications.

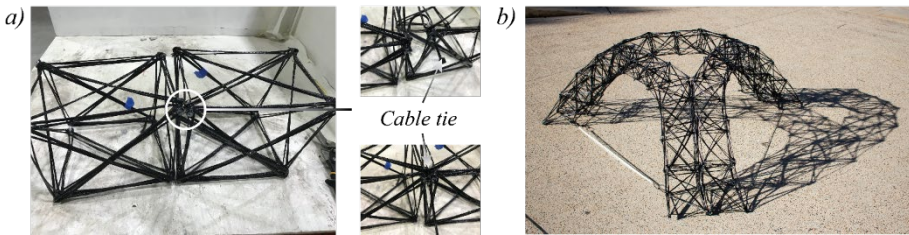


Figure 12. a) Connection details between units b) Completed table base prototype

4. System Evaluation

The fabricated prototype was evaluated from two perspectives, geometric accuracy and structural performance, to prove the reliability of the proposed adaptive winding technique.

The final dimensions of the prototype were measured to be 2280 mm (width) and 655 mm (height), which is only a 1% error compared to the designed dimensions. The tectonics of the fabricated table base also match the design model. A loading test was conducted on the table base to assess the final structural performance. It held approximately one adult male on top without failure. Therefore, the ultimate capacity

was estimated to be 75 kg.

5. Conclusion and Discussion

In this study, a new fabrication system for large-scale spatial structures was developed based on a combined workflow of robotic assembly and robotic winding. This study validates the feasibility of the proposed system via the design, fabrication, and testing of a one-truss table base prototype. The reusability of the robotically assembled temporary support system in the fabrication process further increases its competitiveness among CFW methods. The proposed adaptive robotic winding system also presents significant potential for fabricating different unitized structural systems, for example shell structure whereas the shell surface is composed by multiple layers of organized fiber filaments. This fabrication system provides a novel method to build adaptive, lightweight, sustainable, low-cost, and reliable structures.

Furthermore, the fabrication system proposed in this study could be upscaled for larger units, such as transportable house components. This paves the way for highly customized housing construction with affordable prices, accessible materials, and sustainable construction. The development of this technology can enhance productivity in the housing market, expand aesthetic possibilities in housing design, and attract more attention from communities and cities because of its low cost and low environmental impact.

References

- Christie, J., Bodea, S., Solly, J., Menges, A., & Knippers, J. (2021). Filigree Shell Slabs.
- Duque Estrada, R., Kannenberg, F., Wagner, H. J., Yablonina, M., & Menges, A. (2020). Spatial winding: cooperative heterogeneous multi-robot system for fibrous structures. *Construction Robotics*, 4(3), 205-215.
- Felbrich, B., Prado, M., Saffarian, S., Solly, J., Vasey, L., Knippers, J., & Menges, A. (2017). Multi-Machine fabrication: An integrative design process utilising an autonomous UAV and industrial robots for the fabrication of long-span composite structures.
- Hack, N., Wangler, T., Mata-Falcón, J., Dörfler, K., Kumar, N., Walzer, A. N., & Buchli, J. (2017). Mesh mould: an on site, robotically fabricated, functional formwork. Paper presented at the *Second Concrete Innovation Conference (2nd CIC)*.
- Knippers, J., Koslowski, V., Solly, J., & Fildhuth, T. (2016). Modular coreless filament winding for lightweight systems in architecture. Paper presented at the *Proceedings of the 8th international conference on FRP composites in civil engineering, CICE*.
- La Magna, R., Waimer, F., & Knippers, J. (2014). Coreless Winding-A Novel Fabrication Approach for FRP Based Components In Building Construction. Paper presented at the *Proceedings of the international conference on FRP composites in civil engineering, Vancouver, Canada*.
- Prado, M., Dörstelmann, M., Schwinn, T., Menges, A., & Knippers, J. (2014). *Core-less filament winding*. In *Robotic fabrication in architecture, art and design 2014* (pp. 275-289), Springer.
- Wu, P., Wang, J., & Wang, X. (2016). A critical review of the use of 3-D printing in the construction industry. *Automation in Construction*, 68, 21-31.

FORMING STRATEGIES FOR ROBOTIC INCREMENTAL SHEET FORMING

QIANG CUI¹, SIDDHARTH SUHAS PAWAR²,
MENGXI HE³ and CHUAN YU⁴

¹*Tsinghua University.* ^{2,4}*PIX Moving Inc.* ³*University of Stuttgart.*

¹*cui-q18@mails.tsinghua.edu.cn, 0000-0002-0876-5054*

²*smsusi@pixmoving.com, 0000-0002-6917-9489*

³*st175143@stud.uni-stuttgart.de, 0000-0002-8766-1711*

⁴*angelo@pixmoving.com, 0000-0001-6269-064X*

Abstract. Incremental Sheet Forming (ISF) is a flexible forming technology that can process parts without special mould, where-in an indenter moves over the surface of a sheet metal forming a 3D shell through localized deformation. Despite being fundamentally advantageous than stamping for low-volume production, there are many drawbacks to this technique, a major being the low geometrical accuracy of the achieved products, thereby limiting its widespread industrial application. In this paper, flexible support strategies and precise forming compensation have been considered as promising approaches in terms of improving the geometric accuracy in ISF. Four support strategies and a compensation forming method based on FEA and three-dimensional scanning are discussed in detail. Finally, we deploy the technique for the manufacturing of automotive products. The technique is applied to several automotive products of varying topologies and thus form the basis for successful verification of our technique.

Keywords. Incremental Sheet Forming; Robotic Fabrication; Forming Path; Error Compensation; SDG 12.

1. Introduction

Incremental Sheet Forming (ISF) is a flexible sheet forming technology that can process complex sheet components without a special mould, where in a simple tool moves over the surface of a sheet metal forming a 3D shell through localized plastic deformation. Typically, the tool is formed using a hemispherical toolhead attached to a robotic arm or a CNC machine. The tool moves along a pre-programmed tool-path creating localized plastic deformation on the sheet metal thereby giving it the desired shell shape. The technology is especially suitable for the research and development of new products and the production of small-batch customized products giving greater degrees of freedom to architecture and designers, thanks to the fact that no mould or die is needed as in the case of stamping process. Thus, for building the initial prototypes

and for small batch production, ISF is at least two orders of magnitude cheaper, and less energy-intensive process compared to stamping.

However, there are many drawbacks to this technique, the major being the low geometrical accuracy of the achieved products, thereby limiting its widespread industrial application. One of the most fundamental research questions in ISF research is how to accurately and efficiently program the robot's toolpath in ISF to achieve the desired geometric accuracy of parts. The other important question is on how to use the data obtained from visual or other sensors attached to the robot to make improvements to the geometric accuracy of the part.



Figure 1. The ISF Setup

This paper attempts to answer these two questions. We first discuss the current state of research in the field of ISF. We propose to use corresponding support strategies in different feature regions to minimize the forming error. Next, we discuss a new methodology for compensating accuracy errors in the achieved geometric shape through the use of a new compensation-based tool-path algorithm and prove its use through FEA simulation and application on real-world products.

2. State of the art

Bulk of the ISF research has mainly been driven in the field of manufacturing for engineered shell products. In the recent years, however, research has also been driven by the needs of architects and the industrial design community, as surface textures are commonly used design elements. Because accuracy plays a vital role in engineered shell products, most of the research has been done to predict final shapes through simulation, predict springback action and required compensation. Gatea et al. (2016) provides a detailed review of the current state-of-the-art of ISF processes in terms of its technological capabilities and specific limitations with discussions on effects process parameters on the ISF process. The forming quality is affected by many factors such as material property, forming tool and geometric shape. In addition, springback prediction and compensation are also effective methods to improve the forming accuracy. Stoerkle et al. (2016) proposed the application of machine learning techniques to increase the geometric accuracy of ISF process. Ren et al. (2019)

developed a generic methodology, suitable for arbitrary part geometries and various ISF processes. These methods all require large data sets. Numerical simulation of ISF (Cai et al., 2020) can simulate the machining process and save the time and cost of data collection. However, the simulation calculation of ISF is difficult, and realizing feedback in real time still remains a challenge.

In the architectural field, Kalo et al. (2014) developed an indirect method for achieving part accuracy through design modification, by overlaying of rib – like design patterns on to the main design, thereby achieving part accuracy and aesthetics simultaneously. Zwierzycki et al. (2018) attempted to improve forming tolerance by using machine learning to predict springback and thus generate corrected fabrication models. Chadha et al. (2020) presented a methodology to optimize long-drawn-out ISF operation by using geometrical intervention informed by supervised machine learning algorithms.

3. Methodology

In this paper, flexible support strategies and precise forming compensation have been considered as promising approaches in terms of improving the geometric accuracy in ISF. This section details how to achieve flexible support strategy and compensation path generation. Grasshopper is used to generate robot tool path from 3D model and convert tool path into machine code using KukaPrc. Communication and collaboration between the two robots are achieved through KUKA.RoboTeam, which enables up to four robots to cooperate in a team.

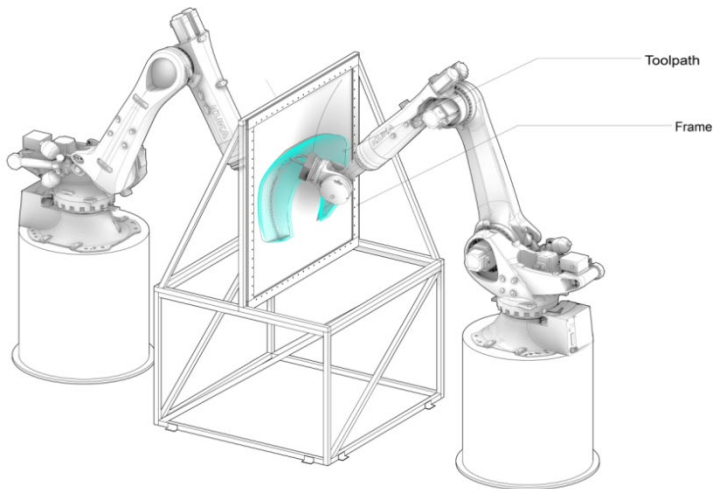


Figure 2. Robotic fabrication setup with two KUKA KR-210

3.1. SYSTEM SETUP

In the aspect of hardware two KUKA KR-210 robots were used that collaborate with each other as well as a metal frame holding the metal sheet (Figure 1). The master robot

pushes incrementally on the sheet, forming the sheet in the direction of the tool-path. There are four supporting strategies for the slave robot, including global support, local peripheral support, local alignment support and local following support. Each supporting strategy has different shaping effects. For example, global support is to provide support at the edge of the forming contour to minimize the elastic deformation at the edge of the metal plate. Local peripheral support can reduce the elastic deformation of forming details. By using local alignment support and local following support, concave and convex can be made within the same part. We use different support strategies for different feature areas to reduce the overall deformation.

3.2. PATH PLANNING

The tool path planning has a great influence on forming accuracy and forming time. The most commonly used method is the parallel contour strategy wherein the design geometry is sliced into horizontal segments and the tool moves along these contours.

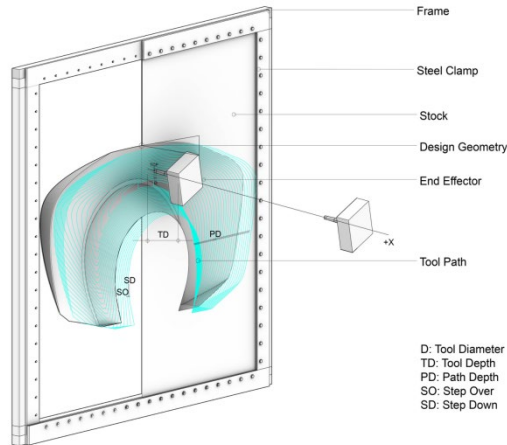


Figure 3. Robotic fabrication setup with a forming tool

The forming path and the corresponding support path are generated using Rhino Grasshopper. We use the Offset-on-surface function to form layers in a specific (X -axis) direction with a certain thickness, and build 2D curve paths. These 2D curve paths are then divided into a specific number of discrete points according to the curvature. Finally, we generate the forming path of the master robot through these sequential discrete points and planes. There are four support strategies, each of which has a different support path. To achieve stable cooperation between the two robots, we generate support paths at each forming step which contains a single contour.

1) The first policy is global support, in which the slave robot moves the support tool along the boundary of the part, acting like a back-plate, providing support on the opposite side of the sheet for the master robot to push against (Figure 4a). The global support path was generated by a distance offset (tool head radius) of the outer contour of the forming region, and each forming path points were mapped to the corresponding global support path.

2) The second is local alignment support, in which the slave robot's tool follows directly opposite the forming tool (Figure 4b). The forming path was offset to obtain the local alignment support path with a distance of the sheet thickness.

3) The third is local peripheral support, in which the slave robot's tool follows outer side of the forming tool, creating a forming gap between the tools (Figure 4c). The local peripheral support path is obtained by offsetting the local alignment support path outward by the distance of the tool head diameter.

4) The last policy is the local following support, which follows behind the forming tool (Figure 4d).

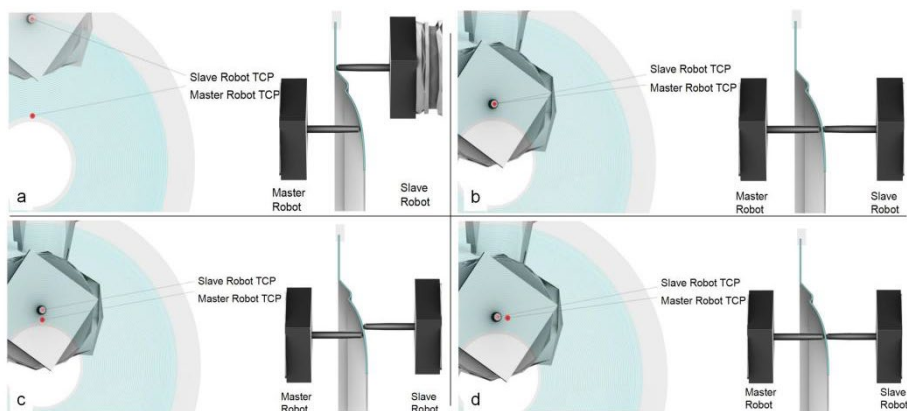


Figure 4. Support strategies. (a)Global support. (b)Local alignment support. (c)Local peripheral support. (d)Local following support.

3.3. 3-D SCANNING

To evaluate the geometric accuracy, the forming result is digitized with scanner sensor. We first tried Kinect Azure, which can get point clouds and depth maps in real time. However, due to the reflection of the metal sheet and low accuracy of scanner, the quality of the scanning results did not meet our requirements. We then use a hybrid blue laser 3D scanner (EinScan HX) to scan the forming result, which is less sensitive to ambient light, gives better performance to reflective surface, as shown in Figure. The scanning accuracy is with 0.1mm and only takes about 30s for each shape, which is accurate and fast enough for the shape measurement.

3.4. DEVIATION ANALYSIS AND COMPENSATION

The deviation can be calculated by analysing the difference between the target shape (Figure 6a down) and the scan shape (Figure 6a up). To calculate the difference from all regions on the sheet metal part accurately, an algorithm was proposed based on minimum distance from point to surface. First, the scan surface is aligned with the target surface in the same coordinate system (Figure 6b). Second, according to the specified 2000 vertices of the target surface, we find the corresponding 2000 closest points on the scan surface. In the figure 6c, red points are the nodes on the target surface, and the green points on the scan surface are the corresponding closest points

red points. Then, the distance between each red point and the corresponding green point is calculated, which is the deviation value. In the figure 6d, the deviation value between the scan surface and the target surface is visualized where the red area represents high deviation value, while the green area represents low deviation value. Because there is no global support strategy, the most inaccurate regions are at the outline of the formed part as expected. We now use then deviation values to adjust the forming path for a second re-run.

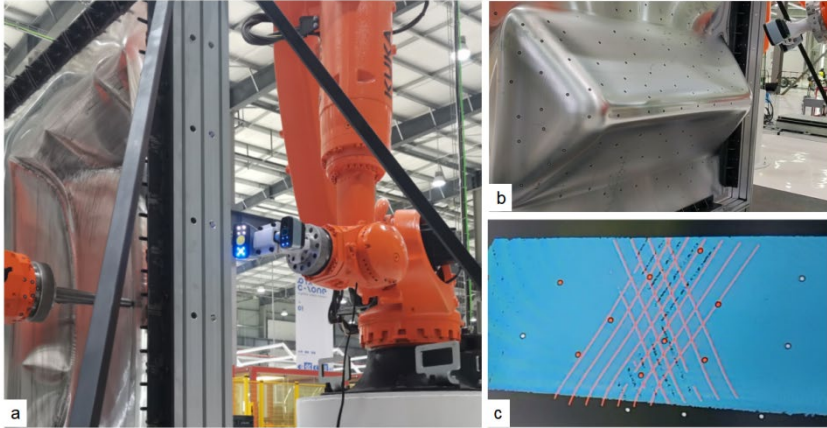


Figure 5. 3D scanning. (a) Robot with a laser 3D scanner. (b-c) Scanning process.

The forming deviation is inevitable owing to springback and complex plastic deformation dynamics, but it can be reduced by some methods. The most straightforward and common approach is to run the same forming path multiple times, but this approach has limited effectiveness and is time-consuming. We tried a new method to reduce the deviation. Instead of using target surface to generate forming path directly, we generate a new forming path based on a computed compensation error between the achieved surface and the desired surface. Experiments show that this compensation model can greatly improve the forming accuracy, because this region was drawn past the target depth. We take the red point on the target surface as the vertex before the offset, and the vector from the green point to the red point is the compensation vector (Figure 7b). Then, the vertex of the compensation surface can be obtained by offsetting the red point according to the compensation vector, and the compensation surface can be generated from the vertices of the compensation surface (Figure 7c). Finally, the compensation surface is used to generate forming path and support path. When the results of the first compensation re-run do not meet the requirements, a second compensation can be carried out and meets the requirements of accuracy.

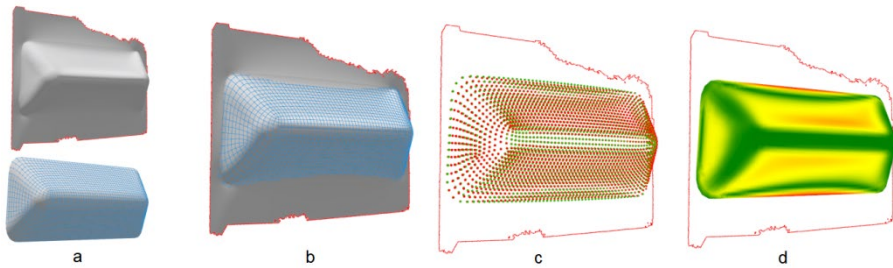


Figure 6. Deviation analysis. (a) Scan and target surface. (b) Two surfaces aligned. (c) Points on two surfaces. (d) Accuracy colour plot.

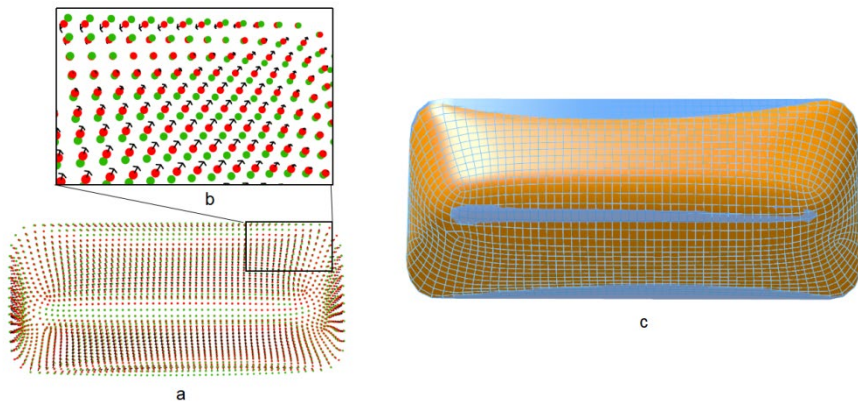


Figure 7. Compensation method. (a-b) Compensation vector. (c) Compensation surface.

3.5. FEA SIMULATION

An explicit integration scheme, with the choice of Belytschko-Tsay shell element type is employed in the finite element analysis of the ISF process, in order to gain insight into the deformation mechanics of the process, and more importantly, to predict the results of the technique with reasonable accuracy. The FEA simulations are performed through Abaqus. The simulation is performed using a 1.5mm thick rectangular Aluminium sheet of the size 1740mm x 1250mm. The diameter of the toolhead is 19mm. A non-linear explicit integration scheme is chosen with semi-automatic mass-scaling. Two surface-to-surface interactions are defined, one between the tool and the sheet, and the other between the sheet and the boundary support. The material properties of aluminium are taken as 70 GPa Elastic Modulus, 0.3 Poisson's ratio, and a mass density of 2700kg/m³. A tangential behaviour contact is set with a coefficient of friction of 0.1 and penalty contact method is deployed for formulation of the mechanical constraint. A four node S4R shell element is selected for this process. The results obtained are shown for a particular model above. FEA is able to obtain the shape with reasonable accuracy and forms a cheaper way to check for failure in the sheet material before performing the actual experiment.

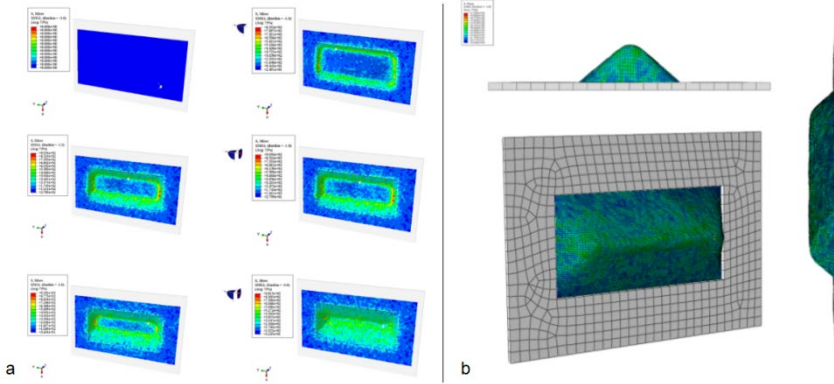


Figure 8. FEA Simulation. (a)Simulation Process. (b)Simulation surface.

In order to meet the forming requirements at one time, we use FEA to predict the deviation and generate the compensation surface. When the accuracy reaches the specific accuracy requirement of the part, the actual forming begins. Computational experiments show that the range of geometric error of uncompensated surface is between -16mm to 12 mm. When our technique is employed, this range is effectively brought down to -7mm to 5mm, significantly improving accuracy.

4. Applications

In order to verify that our method can meet the requirements of high-precision manufacturing, we apply it in the automotive industry. The application aims to develop a continuous sheet metal typology that fulfils the special requirement of the ISF process and enables rapid customization of automotive parts. We first apply it to a vehicle wheel hub that aims to explore the rules and boundaries of design for customizable ISP manufacturing processes.

The ISP process for producing the wheel hub geometry was tested through proof-of-concept full-scale prototypes, one of which was successfully implemented into a new energy vehicle (NEV). In general, the wheel hub was designed through its section. The vehicle wheel hub's symmetrical circular geometry allows for a "Revolving section" method. One-half of the wheel hub's section was designed and the final geometry was formed by revolving it along the centre axis. When considering the design of the section line, designers have to design with continuous curvatures that do not contain sharp turns. Each edge of the section has to be a soft "fillet" instead of a sharp "chamfer"; the radius of the fillet edge cannot be smaller than the tool radius.

The design prototype is inspired by the water drop wave. It is worth noting that the curvature of each "wave" has to be tuned so that it will not exceed the "scratch limit" of the end effector. Several other design prototypes that follow the "revolving section" method were also tested during the development (Figure 9). Further research could look into asymmetrical designs. Asymmetrical designs are, in principle, possible as long as the robot travel path of the ISP process follows a continuous forming line, and

the slope of the geometry does not exceed end effector limits. Tire hubs and shell cover for the door opening mechanism of the NEV were built using the current method and deployed on the vehicle.

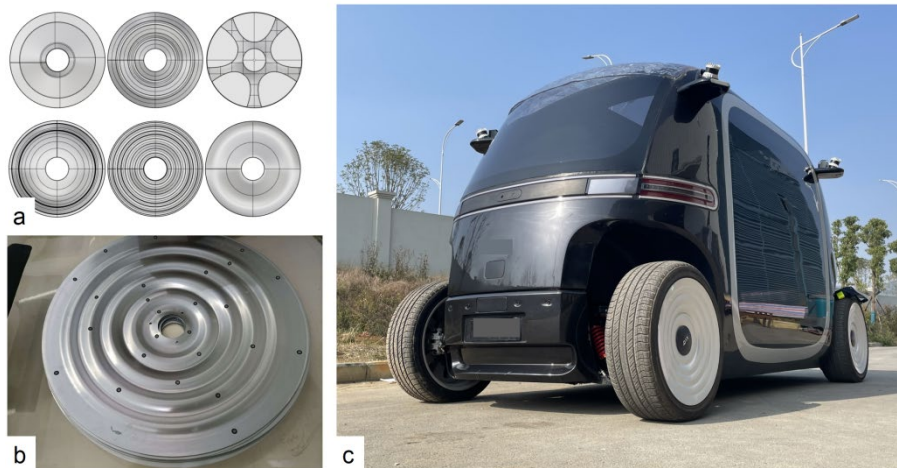


Figure 9. Application in the automotive industry. (a)The design process of the wheel hub. (b)The prototype. (c)The New energy vehicle with the wheel hub.

5. Process Comparison

If we were to manufacture this metallic wheel hub using the traditional manufacturing technique, we would need to turn to stamping, or casting + CNC machining. The cost of making a mould and renting a stamping machine unit from a supplier company would far exceed the current cost by at least a factor of 1000. In the case of casting + final CNC machining, the costs would exceed our manufacturing costs at least by a factor of 100. Our method only uses standard metal sheets, an industrial robot and thus our operating costs are limited to the cost of the raw sheet metal and electricity. Since each robot can produce a wheel hub every three hours, a group of ten robots could produce about 25,000 pieces a year, running continuously, with only running costs of sheet metal and electricity.

In terms of accuracy of the part, the parts are still not as accurate as a CNC machined part, and this paper attempted to find ways to improve part accuracy. An important question to consider is how much geometric accuracy is really needed for a given design. For a wheel hub, for instance, a geometric accuracy of 2mm is acceptable.

6. Conclusion and future work

This paper discusses the development of an ISF technique that solves the problem of low geometric accuracy through the use of flexible support strategies, novel robot path-planning technique and the use of real-time sensor feedback to make minor changes to the tool-path in order to minimize geometric errors. We first introduce our path-planning algorithm to create the first shape and use a feedback loop from the data obtained through a 3D scanner to compute adjustments needed in the tool-path to

drastically reduce the errors and bring them within an acceptable limit. The tool-path is re-run again on the deformed sheet metal piece and the final obtained results show satisfactory improvements in geometric accuracies to be applied to product manufacturing. The technique is tested using finite element analysis code Abaqus and is then used to manufacture several automotive products that forms the basis for successful evaluation of our compensation-based path planning algorithm for incrementally formed shell structures.

The design freedom offered suggests their use as cladding elements in a building envelope. For instance, in the architectural field, façade systems form an important part of a building. Design freedom, relative speed and associated efficiencies of our process all strongly endorse the feasibility of production of high-performance façade systems directly from digital models with this method.

Future research from this investigation could rely on a Reinforcement Learning based agent that could train on the geometric error data and compute tool-paths needed to achieve satisfactory geometric accuracy, with training data being obtained from finite element calculations.

References

- Cai, S., Wu, R., Wang, Z., Li, M., & Chen, J. (2020). Numerical simulation of friction stir-assisted incremental forming with synchronous bonding of heterogeneous sheet metals. *The International Journal of Advanced Manufacturing Technology*, 106(7), 2747-2763.
- Chadha, K., Dubor, A., Puigpinos, L., & Rafols, I. (2020). Space Filling Curves for Optimising Single Point Incremental Sheet Forming using Supervised Learning Algorithms. *Proceedings of the 38th eCAADe Conference* Volume 1, pp. 555-562
- Gatea, S., Ou, H., & McCartney, G. (2016). Review on the influence of process parameters in incremental sheet forming. *The International Journal of Advanced Manufacturing Technology*, 87(1), 479-499.
- Kalo, A. and Newsum, M.J. (2014). An Investigation of Robotic Incremental Sheet Metal Forming as a Method for Prototyping Parametric Architectural Skins. *Robotic Fabrication in Architecture, Art and Design*, 33-49.
- Lublasser, E., Braumann, J., Goldbach, D., & Brell-Cokcan, S. (2016). Robotic forming: rapidly generating 3d forms and structures through incremental forming. *Living Systems and Micro-Utopias: Towards Continuous Designing, Proceedings of the 21st International Conference of the Association for Computer-Aided Architectural Design Research in Asia CAADRIA 2016*, 539-548.
- Ren, H., Xie, J., Liao, S., Leem, D., Ehmann, K., & Cao, J. (2019). In-situ springback compensation in incremental sheet forming. *CIRP Annals*, 68(1), 317-320.
- Stoerkle, D. D., Seim, P., Thyssen, L., & Kuhlenkoetter, B. (2016). Machine learning in incremental sheet forming. In *Proceedings of ISR 2016: 47st International Symposium on Robotics* (pp. 1-7). VDE.
- Zwierzycski, M., Nicholas, P., & Thomsen, M. R. (2018). Localised and learnt applications of machine learning for robotic incremental sheet forming. In *Humanizing digital reality* (pp. 373-382). Springer, Singapore.

AUGMENTED ACTIVE-BENDING FORMWORK FOR CONCRETE

A Manufacturing Technique for Accessible Local Construction of Structural Systems

ALVARO LOPEZ RODRIGUEZ¹, PABLO ISAAC JARAMILLO
PAZMINO² and IGOR PANTIC³

^{1,2,3}*The Bartlett School of Architecture*

¹*alvaro.rodriquez.14@ucl.ac.uk, 0000-0002-5561-1365*

²*pablojaramillo@gmail.com*

³*i.pantic@ucl.ac.uk, 0000-0001-8802-5592*

Abstract. This research introduces Augmented Reality (AR) for manufacturing concrete structures through an open platform for autonomous construction. The study was developed under the following scopes: computational algorithms for bending simulations, materiality tests, system implementation, and a set of Augmented Reality (AR) tools. AR devices offer a technological tool that allows for a self-built environment through holographic guidance, allowing the untrained workforce to participate in the process. This technology can help users select the system to construct through an Open-Source platform, reducing the gap between complex computational geometries and construction processes. The research aims to investigate a building system that could benefit the UN Objectives SDG 10 by increasing the access to technology in undeveloped communities, SDG 11 and SDG 12 by promoting a self-sustainable method of construction based on local resources and material efficiency. In conjunction with the development of the AR Platform and augmented manufacturing, a 1:1 prototype was built in Quito, Ecuador, with the help of seven people with no previous knowledge of digital tools or construction. Presenting a novel, fast, and affordable concrete formwork connected with AR assisted assembly methods that facilitate access to more efficient and advanced building technology.

Keywords. Mixed Reality; Distributed Manufacturing; Online Platforms; Affordability; Local Communities; SDG 10; SDG 11; SDG 12.

1. Introduction

Augmented Reality is a group of technologies that belongs to a spectrum called Mixed Realities. This set of technologies allows for different interactions between humans and machines. A variety of media can be used to achieve this, as long as they fulfil the requirement of altering the typical understanding and perception of the real world by

humans. (Milgram, 1994). Augmentation devices will soon become mainstream media for future workers (King, 2016), and with the use of these devices, users can have easy access to skills-enhancing technology.

1.1. ARCHITECTURAL CONTEXT

The development of assisted manufacturing is not new. Several projects have been testing the capabilities for AR to help with the building process. From an assembly perspective, "Real Virtuality" project (Retsin, 2019) presents the design of modular timber blocks that can be assembled in a discrete manner using AR through HoloLens. The model itself could be changed in real-time due to its non-fixed design. Similarly, in regards to AR assisted manufacturing, the Steampunk pavilion, designed by Jahn, Newnham, Hahm, and Pantic, proposes an alternative to automation and robotic production. This project explores the production and assembly of steam-bent timber elements coupled with steel sections for joints. Both of which are formed into place following holographic guides projected through Microsoft HoloLens (Pantic, 2019). As a result, unskilled workers were able to build the pavilion, demonstrating the skill-enhancing capabilities of AR technology.

1.2. OPEN PLATFORM FOR AUTONOMOUS CONSTRUCTION.

Technological devices such as smartphones or tablets have exceeded many predictions. The implementation of such devices is now mainstream and is evident even in the most undeveloped areas (King, 2016). Countries like India have doubled their user base within six years. There are more smartphone users in India than in the US (Newzoo.com). This trend generates a significant opportunity to open and modernise the building industry in rural or isolated areas. With the smartphone as a mainstream tool, local communities have access to various platforms to increase participation in the building environment. Projects like WIKI House (2012) or the work developed by AUAR in London (2018) could exemplify how the implementation of the platform performs a more participatory workflow allowing for community involvement.

1.3. AUGMENTATION FOR IMPROVED REMOTE SKILL ACCESS.

Access to some technologies or construction techniques is an extended issue in remote or underdeveloped areas. The difficulty of finding qualified technicians is an important matter. Usually, this is why design and construction techniques are limited among these contexts (Auwalu et al., 2018). Augmentation could be one of the most accessible options to improve skills access (Coppens, 2017). Using computational design and platforms, simple systems can be computerised and managed by a non-expert user through a simplified interface where the user selects and defines the building needs, after which the algorithm proposes the best solution. This shift on the typical workflow increases the user's autonomy, facilitating advanced design for areas traditionally isolated from the latest technology. Here, the use of AR during the construction process and access to such platforms instantly skills up the builders to the needs of the applied construction system (Goepel, 2019). Using AR manufacturing, workers can access a more varied range of building techniques and technologies, facilitating more efficient or versatile design ideas in inaccessible or remote areas (Hahm et al., 2019).

1.4. ACTIVE-BENDING STRUCTURES.

The main structural principle is bending deformation and force transmission to neighbour elements (Lienhard et al., 2013). Most of its use has been recorded worldwide in various vernacular architectures, demonstrating that this structural principle is familiar to most cultures (Suzuki and Knippers, 2018). The primary process of bending active structures is generating a 3D curve geometry from planar 2D compositions (Nicholas and Tamke, 2013). As an illustration, the AA Hybrid project presents a plywood structure, incorporating analogue and digital parameters to rearrange local behaviours (Laccone et al., 2020).

1.5. COMPUTATION AND CONSTRUCTION IMPLEMENTATION

Most bending-active structures present unpredictable bending events within their compositions. As Lienhard explained, it is due to the high resilience of the material used because of the elastica law presented when actively bending (Lienhard et al., 2013). To reduce this gap, Suzuki and Knippers's research presents a recalculation of unpredictable fabrication irregularities by incorporating the Iguana software, reducing the gap of computational geometries and physical models (Suzuki and Knippers, 2018). Something that could be connected with AR to promote a higher precision when fabricating. AR introduces a novel method for better accuracy in fabrication and construction by translating 3D geometries to the real environment, avoiding 2D drawings that might be inaccurately reproduced due to computational geometrical complexity (Goepel, 2019).

2. Design Methodology

This project explores Augmented Reality's boundaries to reduce the complexity of fabricating active-bending structures, promoting an autonomous execution aided by holographic visualisations. The novelty relies on using these structures to create inhabitable spaces and test its capacity to generate long-term compositions by using them as concrete formwork. The design incorporates an experimental formwork system to build complex concrete small-scale structures that can be constructed without expensive machinery and can prove the versatility to adopt any design solution.

The polygon system implements a generative solution for straight curve positioning, where each curve is attached with its neighbouring vertex as a single closed bending iteration, as shown in Figure 1. The design strategy is based on polygons based on 3D polyhedrons inside a single voxel. The straight lines of each polygon are constrained by length and attached using vector points and curve self-attraction. To avoid inaccuracies in the translation of the computational active bending simulations to the physical models, the bending behaviour is controlled by tangents, not allowing the curve to have closed angles that could not be replicated in physical models.

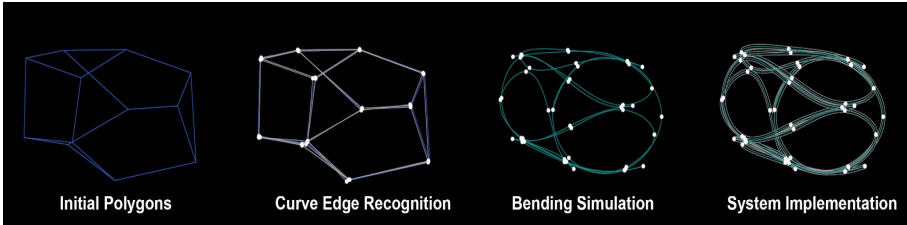


Figure 1. Curve bending from control points within polygons

The extension of this system acknowledges the difficulty of producing a large-scale proposal, considering the workforce and the number of people building a single compound space. Therefore, it incorporates chunks of concrete from several components that function as formwork. These chunks represent a part of a whole, which means that the different sections can be constructed separately and built-in situ, creating small-scale structures with a minimum length of 1.85 m.

2.1. MATERIALITY

This project aims to use locally sourced materials that are globally found for easy experimentation to follow the SDG12. Although the PVC's sustainability is not optimal, in this case, it was selected as an accessible material to test the concept, and further research will explore more sustainable materials like bamboo or other natural fibre-based pipes. PVC Pipes were also selected due to the ease of purchase worldwide and thickness needed for concrete spraying. The properties of these elements vary depending on their use and Size; therefore, 20 mm hollow PVC pipes were selected due to their physical bending performance and malleability, following Georgiou's 'God's eye' pavilion structural implementation with these types of pipes (Georgiou et al., 2014).

2.2. DIGITAL DESIGN AND CONSTRUCTION SYSTEM

The physical performance for active-bending and the structural behaviour is also tested and analysed to ensure a correct transition from the virtual model to the actual prototype using Grasshopper and Kangaroo Plug-ins. The explorations showed that each time a composition reaches a high displacement, more elements need to be added, forming a packing system of pipes. The structural simulations also predicted the displacement within large-scale compositions, allowing the re-adaptation of the components for structural optimisation.

The need for a more resistant and stable structure was solved by integrating a reinforcement strategy based on bundling several pipes on the weakest areas and reinforcing the future concrete by installing steel rods along the curves attached with 3D printed TPU brackets as described in Figure 2. This system increased the rigidity of the formwork and allowed for easier spraying of the concrete.



Figure 2. Construction System - PVC Pipes/Rebars/Joins

2.2. CONCRETE SPRAYING

The first small series of explorations were tested with different types of concrete mixture to assess its addition capability onto the PVC pipes. We determined that Glass Fibre Reinforced Concrete (GFRC) was optimal due to its high malleability due to the fibreglass elements within its mixture. The first layer of concrete did not attach continuously onto the surface; therefore, it was decided to spray glue on the pipes, which solved this issue. It was established that the number of layers directly relates to the amount of bending stress of the geometry, determining a minimum of three layers for simple shapes and a minimum of 5 layers of GFRC for demanding areas, the results of the system are shown in Figure 3.



Figure 3. System Implementation with Concrete

3. The Augmented Reality Platform

With the idea of promoting the SDG 11 goal for a more accessible quality housing with the inclusion of local communities, a bespoke software application was developed in Unity© for the Augmented Manufacturing to be used with Hololens and supported by Windows Mixed Reality Toolkit (W-MRTK). The Microsoft Hololens application processes the model from the design development logic and transforms it into building data to generate the construction sequence that any individual can easily access and use.

Starting with a home screen to choose between a new project or a work in progress, the AR platform is then reduced to a single menu for project interaction. As shown in Figure 4, this menu can be found the primary information about the project's construction, the quantity of elements specification, fabrication steps, and component assembly. Through this display, the user can easily prepare and program every section

of the assembly process, knowing in advance the number of elements and the types needed.

The holographic visualisations facilitate a tutorial-like interaction on a step-by-step process. The user interacts with the holograms to replicate their shape with the different pipes, introducing an efficient self-assessment process. Each component is represented by different colours, where the final input shows the coloured components altogether. To reduce time in constructing or reviewing a work in progress, the app allows the user to go back, visualise the final composition, or skip steps if the user decides to build a different iteration. The AR Platform adapts to different scenarios where the user is the one who manages the operation and construction of the pre-designed systems. It promotes the autonomous and efficient construction of complex concrete structures, eliminating the need for printed plans or constant laptop screen checking.

3.1. AR APP IMPLEMENTATION AND TESTING

The test of the platform and the construction of a prototype were both tested in Quito, Ecuador. The pavilion design comprises a stable core structure with wings extending to both sides. The geometry was designed to test complex cases and test-proof its versatility. The composition was divided into three sections for assembly, one roof and two walls. With the help of 5 people, the 7m long by 2m high prototype was built within two days, working 5 hours each day. The people involved had no prior knowledge of the technology used or previous construction experience. All of the components were assembled using AR visualisations. The initial architecture was divided into three large sections, as mentioned above, fabricated on the ground. Then, AR visualisations were used to guide the assembly order, direction, and casting to enhance the stability of the structure portrayed in Figure 5.

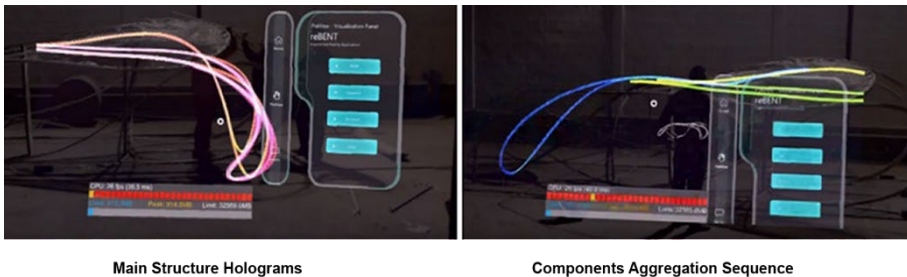


Figure 5. Platform Mock-up and Real Implementation

3.2. IN-SITU BUILDING TEST

The bending of the PVC Pipes for component construction was easily replicated thanks to the holographic visualisation. Only one Hololens device was available; therefore, Fologram©, a Grasshopper© plug-in for AR visualisation, was used in two mobile devices, one iPhone X and one iPad Pro as shown in Figure 6. The team was formed by people from the local area that participated voluntarily and whose professional background was not related to the architecture or building industry.

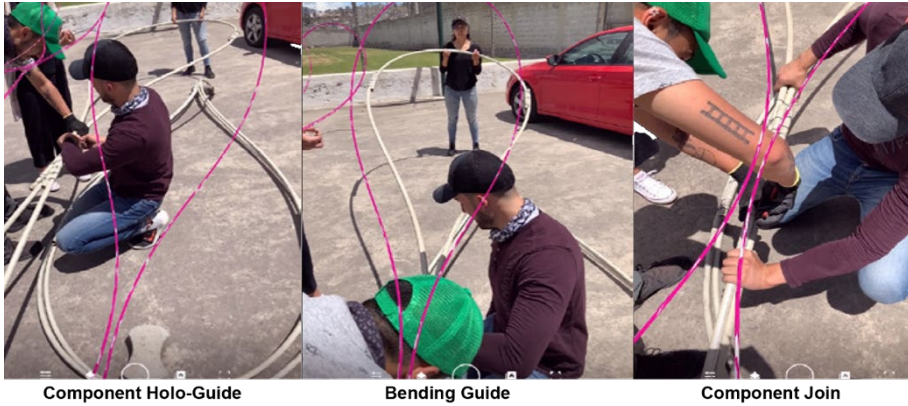


Figure 6. Fologram Implementation

The people in charge of the AR guidance marked specific points in the ground to follow the bending sections of the pipes. Then after bending them, the rest could see the visualisations inside the iPad to check its intended shape. The components then were constructed easily, efficiently, and with precision.

The inaccuracies mainly occurred in the connection of the components. Even with the pre-established bundling system, the expected flimsiness was higher than projected. The rebar diameter was not enough to add stiffness to the structure, re-designing the packing system to the following elements: 1 PVC Pipe of 20mm requires 4 x 6mm rebar, 4 PVC Pipes 20mm – 8 x 4mm rebar, and 10+ PVC 20mm – 12 x 4mm rebar, where most compositions should have at least four pipes as packing system. An additional 4 mm rebar was placed inside the main pipe for a stable bending moment, avoiding the pipe's rupture in stressed sections. Once implemented, the flimsiness reduced significantly, although still presenting some stagger level. After the assembly, the PVC + Rebar skeleton was sprayed from bottom to top in several layers with GFRC to complete the structure. The result was satisfactory as the model was fully achieved as well as fully functional and stable, portrayed in Figure 7. The fact that all the people involved had no prior experience in construction was also a remarkable fact.



Figure 7. Pavilion test results.

3.3. AUGMENTATION AND ACCURACY

The use of Fologram© was necessary for fast changes within the pre-designed components. Some of them did not work correctly for the structural stability of the pavilion. Therefore, changing them in real-time for physical reproduction was highly efficient. The pavilion presented a deviation of around 0.21m in length from its right side compared to the left side and 0.08m in height from the original model. The use of the Hololens App was essential but limited. If a pre-designed object did not work correctly, changing this takes more time than pre-loaded inside the app. A small but noticeable difference in accuracy was shown in the process between Hololens sections and other devices sections. That was due to the fact that Hololenses have a more accurate set of cameras and sensors than an average iPhone or iPad. Still, the precision was sufficient to achieve a correct construction process.

The holographic visualisations were easy to follow for construction processes, but the mentioned difference between devices also slightly slowed the assembly. It is significantly more practical to work with a HUD while assembling than a handheld device. Also, the assembly process was done at night because of the sun's glare, which impeded the correct visualisation of the holograms.

4. Conclusions

The extent of opportunities and social applications of an Augmented Reality (AR) platform allows effective communication of pre-designed components. It provides an opportunity for users to self-build pre-designed objects, transforming simple archetypes into systems that generate other systems. This research tests the boundaries of AR fabrication for construction without using expensive machinery such as robotic arms for 3D printing, and the use of prefab architectural elements, promoting an autonomous work interface.

The research presented here was conceived as an early approach to how the XR can influence the future of manufacturing and construction in architecture. The prototype experiment shows that Skills Augmentation and deployment into undeveloped communities is possible. The volunteers could achieve a prototype of a new system for flexible formwork for concrete without any previous experience. Also relevant is that only a single AR Head Mounted Device (HDM) was necessary for the construction, which shows the excellent synergy between the experimental system and the guided assembly from the AR HDM. Regarding the concrete formwork technique, it is clear that further improvements must be made to make it viable for a more mainstream application. In the same direction, additional research will be needed in the material aspect. Although GFRC and PVC were selected for their ubiquity and easy access, more sustainable and locally sourced materials have to be explored in the future to guarantee that the project improves its alignment with the SDG goals. Materials like bamboo or the use of natural fibres and concrete replacements will be analysed in future iterations. However, the prototype was stable and can be considered a success. Finally, we can also conclude that Augmented Reality creates new opportunities for the building industry, in alignment with the SDG 10 and SDG 11, therefore, having the potential to bring digital technologies to remote areas facilitating access to technical skills for unskilled workers broadening access to a more efficient, collaborative and

technological architecture.

5. Acknowledgements

This paper is part of a wider research agenda conducted by RC9 at the B.Pro AD program in the Bartlett School of Architecture. The research project on which this paper is based was developed during 12 months by the Master's students Pablo Isaac Jaramillo Pazmino, Xi He and Ziqi Song with Alvaro Lopez Rodriguez and Igor Pantic's supervision as the RC9 Unit Directors. We would also like to acknowledge and thank the Quito team for their essential collaboration in the prototype construction.

References

- Carpó, M. (2017). *The Second Digital Turn, Design by intelligence*. London. The MIT Press.
- Claypool, M. Jimenez, M. Retsin, & G. Soler, V. (2019). *Robotic Building: Architecture in the Age of Automation*. Munich, Edition Detail.
- Coppens, A. (2017). Merging real and virtual worlds: An analysis of state of the art and practical evaluation of Microsoft HoloLens, *Master's Thesis*, University of Mons.
- De la Fuente Prieto, J., Castaño Perea, E., & Labrador Arroyo, F. (2017). Augmented Reality in architecture: Rebuilding the archaeological Site. *Remote Sensing and Spatial Information Sciences*, 2(3).
- Georgiou, M., Georgiou, O., & Kwok, T. (2014). Form Complexity - Rewind | God's Eye Sukkahville. *ACADIA 2014 design agency: Proceedings of the 34th annual conference of the Association for Computer-Aided Design in Architecture*.
- Goepel, G. (2019). Augmented Construction - Impact and opportunity of Mixed Reality integration in Architectural Design Implementation. *Proceedings of the 39th Annual Conference of the Association for Computer Aided Design in Architecture (ACADIA)*, 430-437.
- Hahn, S., Maciel, A., Sumitomo, E., & Lopez Rodriguez, A. (2019). FlowMorph: Exploring the Human-Material Interaction in Digitally Augmented Craftsmanship. In *Intelligent & Informed, Proceedings of the 24th International Conference of the Association for Computer-Aided Architectural Design Research in Asia (CAADRIA)*, Volume 1, 553-562.
- Kaku, M. (2014). *The Future of the Mind: The Scientific Quest to Understand, Enhance and Empower the Mind*. New York, Doubleday.
- King, B. (2016). *Augmented: Life in the Smart Lane*. Singapore: Marshall Cavendish International.
- Laccone, F., Malomo, L., Perez, J., Pietroni, N., Ponchio, F., Bickel, B. & Cignoni, P. (2020), A bending-active twisted-arch plywood structure: computational design and fabrication of the FlexMaps Pavilion, *SN Applied Sciences*, 2(9), 1505.
- Lienhard, J. (2014). Bending-active structures: form-finding strategies using elastic deformation in static and kinetic systems and the structural potentials therein, *PhD thesis*, Universität Stuttgart.
- Lienhard, J., Alpermann, H., Gengnagel, C., & Knippers, J. (2013). Active Bending, A Review on Structures where Bending is used as a Self-Formation Process 1. *International Journal of Space Structures*, 187 – 196.
- Maierhofer, M., V. Soana, M. Yablonina, S. Suzuki, A. Körner, J. Knippers, and A. Menges (2019). Self-Choreographing Network: Towards Cyber-Physical Design and Operation Processes of Adaptive and Interactive Bending-Active Systems, *Proceedings of the 39th Annual Conference of the Association for Computer Aided Design in Architecture (ACADIA)*, 654–663.

- Microsoft. (2021). *MRTK-Unity Developer Documentation -Mixed Reality Toolkit*. Retrieved July 10, 2021 from <https://docs.microsoft.com/en-us/windows/mixed-reality/mrtk-unity/?view=mrtkunity-2021-05>
- Milgram, P., Kishino, F. (1994). A taxonomy of mixed Reality visual displays. *IEICE Transactions on Information Systems*, 77 (12).
- Pantic, Igor. (2019). *TAB 2019 Steampunk Pavilion*. Retrieved July 10, 2021 from <https://www.igorpantic.net/work/steampunk-pavilion>
- Retsin, Gilles. (2019). *Real Virtuality, Royal Academy of Arts*. Retrieved July 10, 2021 from <https://www.retsin.org/Royal-Academy-of-Arts>
- Rosenberg, L. B. (1992). The Use of Virtual Fixtures as Perceptual Overlays to Enhance Operator Performance in Remote Environments. *Technical Report AL-TR-0089*, USAF Armstrong Laboratory, Wright-Patterson AFB OH.
- Sani S., Auwalu. I. Y., & Ibrahim I. I. (2018). Building projects delivery challenges on remote sites in northern Nigeria. *IOP Conf Series: Materials Science and Engineering*, 513.

AUGMENTED REALITY FOR CONSTRUCTION FROM STEAM-BENT TIMBER

GWYLLIM JAHN¹, CAMERON NEWNHAM² and NICK VAN DEN
BERG³

^{1,2,3}*Fologram.*

¹*gwyll@fologram.com, 0000-0003-2072-5423* ²*cam@fologram.com*

³*nick@fologram.com*

Abstract. Digital models viewed in augmented reality can serve as guides to form and assemble parts during construction and reduce the need to build temporary formwork or sub structures. However, static digital models are often inadequate for describing the behaviour of material that is dynamically formed over time, leading to breakages and difficulty following augmented reality guides during assembly. To address this issue, we propose a method for fast and approximate simulation of material behaviour using a goal-based physics solver, enabling the design and fabrication of steam bent timber parts using an adaptable system of sparse formwork. Through the design and construction of a pavilion from steam bent timber we demonstrate that approximate simulation of material behaviour is adequate for wide tolerance construction by hand and eye in augmented reality, avoiding part breakages and accumulative error.

Keywords. Augmented Reality; Digital Fabrication; Generative Design; Material Simulation; SDG 9.

1. Introduction

Although popularly associated with viral mobile games and face tracking filters in social media apps, the etymology of “augmented reality” has origins in manufacturing and fabrication. Augmented reality can refer to any display technology that blends digital content with a physical environment (Milgram & Kishino, 1994), and the term was first used to describe a heads-up display of complex manufacturing and assembly diagrams for construction of aircraft (Caudell & Mizell, 1992). Similar applications were developed by researchers at Columbia University to assist with assembly and inspection of space frame structures (Webster et al., 1996). By displaying construction information directly within a wearer’s field of view, augmented reality can improve spatial understanding and reduce the need for switching between cognitive tasks. However, until recently the limited precision and fidelity of available augmented reality displays has inhibited the development of practical large scale construction applications (Shin & Dunston, 2008).

To overcome these limitations researchers have utilized projection-based methods to assist with subtractive sculpture (Rivers, 2013) or guide in the deposition of chopsticks to form double curved structures (Yoshida et al., 2015). Computer vision systems have also been shown to facilitate complex masonry construction in augmented reality by providing visual feedback on brick placement using tracked markers (Fazel and Izadi, 2018) or the bricks themselves (Mitterberger et al., 2020). Commercially available devices such as the Microsoft HoloLens now provide researchers with a general-purpose hardware platform for delivering augmented reality applications. The HoloLens is a standalone Windows device capable of rendering digital models on a transparent, stereoscopic display. Digital models appear fixed in physical space by inferring the position of the device from the motion of feature points in the surrounding environment that are visible to the onboard cameras (Kress & Cummings, 2017). Fologram provides a general-purpose software toolkit for developing augmented reality applications for the HoloLens and mobile devices using Rhino and Grasshopper. The simplicity of developing augmented reality applications with Fologram has facilitated a proliferation of research (Song et al., 2020) into the use of augmented reality for assembly from unique parts, human-robot collaboration, operation of analogue tools and conventional masonry construction (Jahn et al., 2019a).

In most of these projects, structures are assembled by aligning rigid parts with corresponding digital models viewed in augmented reality. Viewing construction information in augmented reality where it is needed tends to reduce mistakes and construction time, thereby enabling designs with more detailed and intricate collections of parts to be built than what would ordinarily be possible with 2D documentation. Beyond improving productivity of conventional construction, augmented reality may also enable new approaches to design and construction by adding digital precision to traditional hand crafts. Woven structures are one example where augmented reality allows the innate flexibility and elasticity of bamboo to form curves described by digital models (Goepel & Crolla, 2020).

Building from flexible materials ordinarily requires fabricating a temporary structure to use as formwork with significant time, cost and design implications. Although working from digital models in augmented reality removes the necessity of sub structures to define the location and shape of parts, it is still challenging to control and manipulate flexible materials during assembly. Furthermore, common CAD model formats tend to be static representations of form without embedded material properties, constraints or motion and offer limited utility for describing dynamic processes of formation. As a result, the examples to be found in literature of free-forming surfaces in augmented reality are limited to sculptures made from model-making plastics that can be “bent to any curvature” in the same unconstrained fashion as NURBS surfaces (Song, 2020, p.349).

Steam bending long timber boards over sparse formwork benefits from both the malleability of plastic forming and the speed and adaptability of elastic bending. Curving timber elements can be an efficient method for producing lightweight, stiff, double curved shell structures capable of spanning large distances with minimal materials and no sub structure. Furthermore, steam bending boards into three dimensional splines produces no offcut waste and is a faster, simpler, and cleaner method of fabrication than glue lamination of lamellas or subtractive milling from

blocks. Historically, steam bending was used to reduce the number of fasteners required to form-fit boards to boat hulls, or as a cost-effective way of mass-producing timber furniture by companies such as Thonet around the turn of the 19th century. Standardisation or form fitting was required to overcome the spring of steam bent parts when removed from moulds, the prediction of which required extensive trial and error and prohibited exploration of all the formal possibilities of the technique. Variability in timber grain inevitably resulted in breakages, and the practice of steam bending was largely discontinued when plywood and steel became cheaper and more consistent alternatives.

In the last decade there has been a renewed interest in steam bending to materialize 3D splines produced with parametric design software. These include furniture by Mathias Pleisnig, experimental structures by Harvard GSD students (Menges, 2011), small pavilions at the University of Michigan (Mankouche et al., 2012), and permanent shelters at the Architectural Associations Hooke Park campus (Self, 2014). In each of these projects, the design space of parametric models is deliberately constrained to geometry that is deemed within the bending limits of the timber, and steam bent parts are confined to underlying surface geometry or small jigs.

There are however still relatively few examples of building-scale steam bent timber structures. This is due to the limited design and engineering tools available for imagining dynamic forms (Menges, 2011), and the necessity of first-hand knowledge of timber properties and behaviours during fabrication. Steam bending unique parts is notoriously costly and difficult, typically requiring the preparation of one-off moulds to hold the bent part in a desired shape. Avoiding breakages during bending requires an intimate knowledge of timber grains, lignans, moisture content and malleability. Attempts have been made to replace moulds with 6 axis robotic manipulators, and to automate responses to spring back and other bending parameters using real time sensory feedback (Schwartz et al., 2014). However, these fully automated systems constrain part geometries to forms that can be bent by the motion of a single robotic arm and prevent working with large parts with multiple bends.

2. Aims

We demonstrate an augmented reality method for construction from double curved, steam-bent timber boards that builds on earlier work with steam bent structures. By constraining design geometry to standard lengths of dimensional timber and steel, double curved structures can be fabricated at low cost, with no offcut waste or machine time. Our system enables fabricators to work on a spectrum from fully digitally documented formwork positions displayed in augmented reality, to intuitive formwork positioning from only design models. We demonstrate our method in the design and construction of the Steampunk Pavilion; the winning proposal for the 2019 TAB Installation Competition.

To ensure that digital models displayed in augmented reality can be formed from available physical materials, design tools are needed that can simulate properties of materials and tools to within the tolerances of manual assembly processes. We aim to demonstrate that these design tools can be developed by describing material and tool constraints (bending limitations, twists, clash detection, material distribution by curvature etc) as goals in the Kangaroo physics solver running in Grasshopper. We aim

to show that approximate modelling of material behaviour is sufficient to avoid unbendable geometry, enabling the physics solver to run in real-time and be used as an interactive design tool. Our method has been developed for working with steam bent timber but is equally applicable to any process of forming material by hand.

3. Method

The design of the pavilion consists of 133 timber boards and 336 steel brackets modelled as developable surfaces that unroll to straight sections bendable from linear stock. Digital models of boards and brackets were initially modelled explicitly as strips of four-sided mesh faces to suit design intent, with no consideration of fabrication constraints. The vertices and topology of these meshes then defined particles and inter-particle relationships in the Kangaroo physics solver. The physics solver modified the position of particles to create new strip shapes that adhered as closely as possible to design models while remaining within the tolerances of the steam bending process.

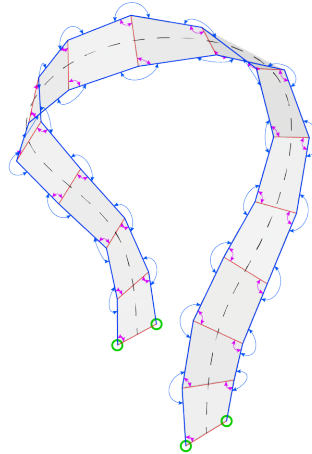


Figure 1. A strip showing the centreline (dashed line), axial springs (blue lines), lateral springs (red lines), lateral bends (magenta arrows), axial bends (blue arrows) and anchors (green circles)

3.1. GOAL BASED PHYSICS SOLVERS

Particle positions were modified in Kangaroo by executing a list of explicit functions called goals. The relative effect of each goal on the position of a particle is determined by a weight value. Simulated strips followed the shape of their designed centreline by adhering to goals that moved particles towards the nearest point on the centreline during simulation. The length and width of the strip was preserved by lateral and axial ‘spring’ goals that maintained the length of edges in the input mesh. Attachments to footings were modelled with anchor goals that prevented any motion of particles located at the strip corners. The bending stiffness of the timber was approximated with a goal that set the angles between axial edges of the strip to 180 degrees. Constraining the strip geometry to a linear length of material was achieved with a goal that maintained interior face angles of the input mesh to 90 degrees (Figure 1). The same

method was implemented to constrain bracket geometry to the mechanical limits of an analogue bar bender.

3.2. EMBEDDING FABRICATION CONSTRAINTS

The intended output of the simulation were strips that formed the same curves and twists that a timber board would naturally form during and after bending and reduce the need to elastically bend parts into shape during assembly. The resting form of each strip was difficult to model explicitly or parametrically due to the complex interactions between many competing constraints, in particular the requirement for strips to unroll to straight sections for fabrication from linear stock material. Constraining simulated strip geometry in this way eliminated offcut waste and the need for custom cut profiles, and increased adaptability in the workshop as any part could be changed or re-made from the same stock. We observed that while simulations rarely converged on solutions that produced unrolled parts that were perfectly straight, approximately straight boards were well within the tolerances of our board to bracket joints and typically could be derived within 100 simulation steps (Figure 2).

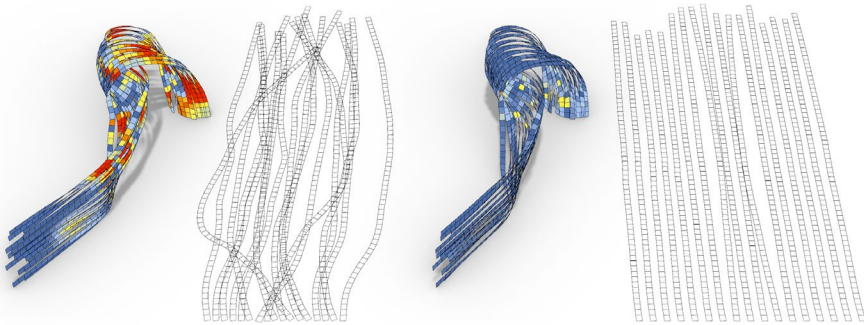


Figure 2. Before (left) and after simulation, colour indicates deviation from straight profile

3.3. INTERACTIVE DESIGN TOOLS

A set of goal weights was found such that strips would typically unroll to close to straight sections with minimum deviation from the designed centreline. However, even small deviations tended to introduce intersections with neighbouring strips, and the design language of the pavilion required strips to be as close as possible to suggest a continuous surface. Intersection algorithms are computationally expensive and adding goals to the simulation to avoid collisions would prevent real-time experimentation or design changes. Furthermore, we wanted a high degree of control over the expression (twists, curves and overlaps) of the strips and these subjective design criteria are difficult to describe as goal functions. To overcome these limitations, strip simulations were batched in small groups with intersection algorithms run once after completing the simulation. Because there was no significant perceptual delay between changing the control points and seeing the simulated result and collisions, designers could effectively use control points to model surfaces with embedded material constraints. Small adjustments could be made to control points to remove intersections, create tightly nested strips at the footings and introduce subtle changes in curvature to

minimize dramatic changes in board orientation and twists across the suggested surface.

3.4. ADAPTABLE FORMWORK

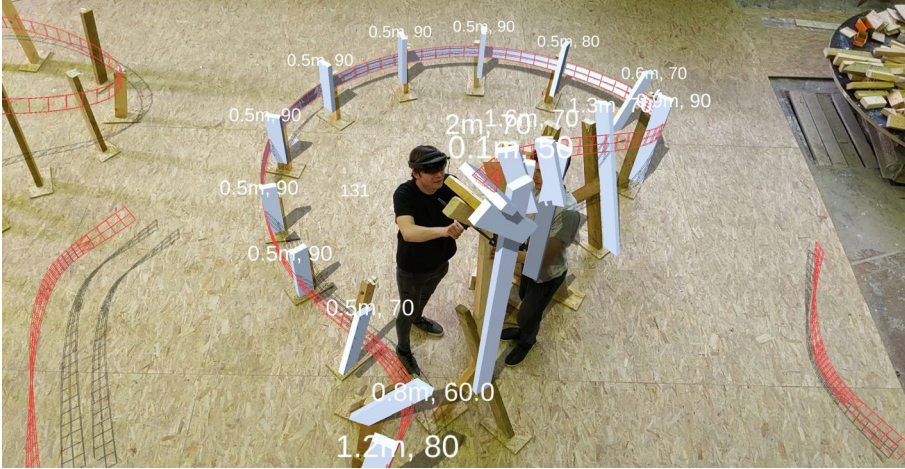


Figure 3. Setting out formwork from parametric models

A simple formwork system was developed as a temporary scaffold that could be clamped to during steam bending. The formwork system consisted of framing timber cut to lengths of 100mm increments and with one edge docked to angles of 10-degree increments. The docked face of the timber was then fixed to a sheet of particle board that could be screw fixed to a false floor in the workspace to locate the formwork. Because bent boards could be clamped anywhere along the length of framing timber, we found there was no need for unique lengths of formwork. Similarly, because the geometry of each board was simulated to behave elastically, boards only needed to be loosely clamped to formwork and exact formwork angles were convenient but not essential. Formwork could also act as a stand to attach a second piece of framing timber at any location along the length and at any angle, enabling working at height or forming up exact angles where required.

Several methods were used to locate formwork for each strip, beginning with working from parametric models that explicitly described the location and type of all formwork (Figure 3) and eventually favouring an ad-hoc approach with only the digital model of the strip as a guide. Parametrically generating formwork at uniform spacing along strips or inflection points was often either not structurally optimal (requiring very long pieces of framing timber), not optimal for bending (creating obstacles for the strip or requiring weaving between formwork during bending) or simply not available due to use as scaffolding for drying parts. When volunteers were inexperienced and required guidance, formwork locations were digitally modelled and followed explicitly. However, the fastest and most accurate solution to ad-hoc formwork placement was to work from only the strip geometry as a guide in augmented reality. This enabled volunteers to improvise formwork from available materials and locate formwork with more flexibility than was possible with the parametric model.

3.5. LAYUP AND STEAM BENDING

The local curvature of each strip in the design was used to guide fabricators during layup of 3000x120x12 millimetre Ash boards into required lengths up to 12 meters long. The angles between the normals of adjacent faces in the strip were mapped to a colour gradient and assigned to vertex colours to create a clear visual guide to where each board would be under maximum stress during bending. The coloured strip was then unrolled to create a 2D holographic model that was used to measure the lengths of timber required and locate bolted lap joints, knots and grain runouts in areas of minimal curvature and bending stress. This enabled the use of low grade, flat sawn timber to form long and complex parts without frequent breakage during bending.

Assembled boards were then steamed using polyethylene bags as a steaming chamber. The lightweight flexible bags allowed parts to be bent without removing them from the heat of the steam, allowing the work time necessary to make multiple bends. Parts were formed by first aligning and clamping the start of the board with the start of the strip as shown in augmented reality. A volunteer wearing the HoloLens would then direct a team as to how to proceed with bending the strip around the formwork. This required working from the augmented reality model to identify the polarity of twists, the location of inflection points and the location of the strip on each piece of formwork. Direction from augmented reality models required considerable skill and understanding of the bending process to maintain an exact adherence to the digital model.

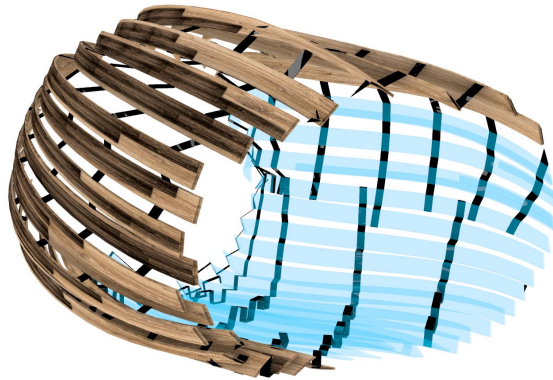


Figure 4. A sectional perspective of a typical assembly of boards and brackets

Knots and grain alignment introduced variable spring back and tensile strength along the length of timber stock and volunteer fabricators needed to be trained to spot these and adjust application of bending force accordingly. Steam bending tight bends by hand required leverage that had to be provided by the unbent part, and linking several tight bends required planning and skill to avoid clamping over- or under-bends and introducing accumulative error. Formwork and clamps could easily introduce kinks and local stresses that caused fractures, and lap joints between boards would often under-bend or fracture at points of sudden changes in stiffness. Correctly bending a board to match a digital model therefore required carefully and rapidly balancing

observed material behaviour with forcing material into the desired shape.

3.6. ASSEMBLY

The digital design model of the pavilion was used as the sole documentation for assembly of completed parts on site. Viewed in augmented reality, the model was used to set out the location of concrete pad foundations and steel angle footings. Once fixed in place, the footings then became reliable reference points for locating the ends of boards, thereby eliminating the possibility of accumulative error in board placement. This was an essential design constraint as the length of boards relative to their thickness meant that they deformed under self-weight and would not follow the shape of the hologram without the induced curvature from bracket attachments (Figure 4).

4. Discussion

Attaching boards to brackets therefore became an exercise not only in assembly but also in re-forming boards into the geometry described by the design model. By strategically installing a sparse distribution of brackets along the length of the board as described by the design model in augmented reality, the board could be pulled into the correct shape after bolting to footings and existing boards in the structure. Deciding where and when to add brackets or boards to the structure became a complex planning exercise as existing structure would limit accessibility and occasionally introduce the need to 'weave' boards or brackets through the structure in such a fashion that was beyond the elastic bending capacity of the timber or steel. However, frequently checking the holographic model to plan bracket placement also provided constant quality assurance and made it obvious when boards had been attached to the incorrect side or joint on a bracket - mistakes that were frequently and easily made.

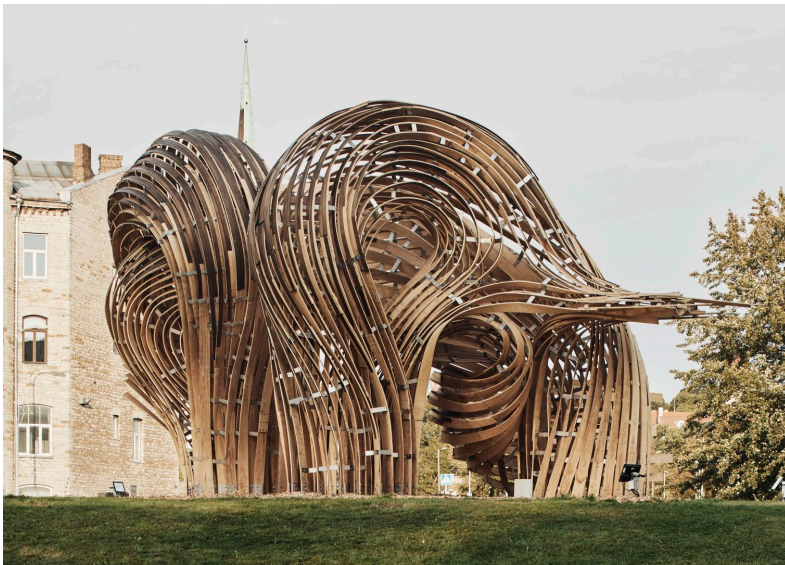


Figure 5. Steampunk Pavilion (Photo: Peter Bennetts)

Assembling parts that move after placement or forming parts that take different shapes to those described by digital models results in the augmented reality guide no longer serving as a reliable, single source of truth to design intent. In this case, incorrect placement of a single part would increase the difficulty of correctly placing subsequent parts or cause existing parts to move out of alignment. In some cases, incorrect alignment was due to drift in the position of the digital model relative to the physical environment. More often alignment was unavoidable due to the static digital model lacking the ability to describe changing forms over time resulting in the incorrect inference of 3D position of parts. Developing models that are capable of matching as built conditions of flexible structures during construction was beyond the scope of this project but presents opportunities for future research and development.

5. Conclusion

Our approach to the design and fabrication of the Steampunk Pavilion illustrates that fast and approximate simulations of material behaviour are well suited to the equally fast and approximate method of forming timber and steel by hand and eye in augmented reality. Augmented reality models eliminate the need for building the pavilion twice as sub-structure or formwork composed most likely of CNC cut waffle structures; a convenient cost saving and expediency. Furthermore, the lack of sub structure forces a departure from typical examples of steam-bending in which bent planks ‘form up’ existing hulls or surface models. By allowing parts to deform freely in space following augmented reality guides, the pavilion can introduce twisting elements that weave in and out of any explicit surface, playing with notions of inside and outside, surface and poche (Figure 5). Likewise, the capacity to easily position formwork in augmented reality during fabrication of individual parts eliminates the marginal cost of producing parts of different shapes. Constant variation negates the legibility of individual parts in favour of a woven continuity of form, and the dissolution of part-to-whole relationships critiques the necessity of explicitly defined and discrete parts in favour of elements that are formed during assembly from physical forces and constraints.

The design of the Steampunk Pavilion prioritizes nuance, craft, resilience and flexibility over precision, repeatability, and efficiency. The design language arising from a system of forming and assembling flexible parts from linear stock material is intimately tied to the capacities and constraints of hand fabrication in augmented reality. For this reason, it is not reasonable to make comparisons between traditional approaches to constructing the design and the augmented reality approach, as the former would be impossible and thus the design would be significantly different. We therefore argue that the act of construction in augmented reality enables new design languages to emerge that occupy territory somewhere between the precision of digital models and the imprecision of analogue craft. By introducing imperfection and wide tolerance into both digital design tools and fabrication practices we suggest an alternative set of heuristics, norms and gestures to the prevailing approaches to computer-aided design and manufacturing.

Acknowledgements

This research has been made possible by the support of the Tallinn Architecture Biennale and the generous contributions of countless volunteers. Please see tab.ee for all project credits.

References

- Caudell, T. P., & Mizell, D. W. (1992). Augmented reality: An application of heads-up display technology to manual manufacturing processes. *Proceedings of the Twenty-Fifth Hawaii International Conference on System Sciences*, 2, 659–669.
- Fazel, A., & Izadi, A. (2018). An interactive augmented reality tool for constructing free-form modular surfaces. *Automation in Construction*, 85, 135–145.
- Goepel, G., & Crolla, K. (2020). AUGMENTED REALITY-BASED COLLABORATION - ARgan, a bamboo art installation case study. *RE: Anthropocene, Design in the Age of Humans - Proceedings of the 25th CAADRIA Conference*, 313–322.
- Jahn, G., Newnham, C., Berg, N., Iraheta, M., & Wells, J. (2019). Holographic Construction. *Impact: Design With All The Senses*, 314–324.
- Kress, B. C., & Cummings, W. J. (2017). 11-1: Invited Paper: Towards the Ultimate Mixed Reality Experience: HoloLens Display Architecture Choices. *SID Symposium Digest of Technical Papers*, 48(1), 127–131. <https://doi.org/10.1002/sdtp.11586>
- Mankouche, S., Bard, J., & Schulte, M. (2012). Digital Steam Bending: Re-Casting Thonet Through Digital Techniques. *Proceedings of the 32nd Annual Conference of the Association for Computer Aided Design in Architecture (ACADIA)* San Francisco 18-21 October, 2012, pp. 117–126.
- Menges, A. (2011). Integrative Design Computation: Integrating Material Behaviour and Robotic Manufacturing Processes in Computational Design for Performative Wood Constructions. In *Proceedings of the 31th Conference of the Association For Computer Aided Design In Architecture (ACADIA)*, Banff (Canada) 13-16 October 2011, 72-81
- Milgram, P., & Kishino, F. (1994). A Taxonomy of Mixed Reality Visual Displays. In *IEICE Transactions on Information and Systems*, E77(12), 1321-1329.
- Mitterberger, D., Dörfler, K., Sandy, T., Salveridou, F., Hutter, M., Gramazio, F., & Kohler, M. (2020). Augmented bricklaying: Human-machine interaction for in situ assembly of complex brickwork using object-aware augmented reality. *Construction Robotics*, 4.
- Rivers, A. (2013). *Augmented manual fabrication methods for 2D tool positioning and 3D sculpting*, Thesis, Massachusetts Institute of Technology.
- Schwartz, T., Bard, J., Ganon, M., Jacobson-Weaver, Z., Jeffers, M., & Tursky, R. (2014). All Bent Out.... In W. McGee & M. Ponce de Leon (Eds.), *Robotic Fabrication in Architecture, Art and Design 2014* (pp. 305–317). Springer International Publishing.
- Self, M. (2014). *Timber Seasoning Shelter / AA Design + Make*. Retrieved from <https://designandmake.aaschool.ac.uk/project/timber-seasoning-shelter/>
- Shin, D. H., & Dunston, P. S. (2008). Identification of application areas for Augmented Reality in industrial construction based on technology suitability. *Automation in Construction*, 17(7), 882–894. <https://doi.org/10.1016/j.autcon.2008.02.012>
- Song, Y., Koeck, R., & Luo, S. (2021). Review and analysis of augmented reality (AR) literature for digital fabrication in architecture. *Automation in Construction*, 128, 103762.
- Webster, A., Feiner, S., Macintyre, B., Massie, W., & Krueger, T. (1996). Augmented Reality in Architectural Construction, Inspection, and Renovation. *Proceedings of 1996 ASCE Congress on Computing in Civil Engineering*.
- Yoshida, H., Igarashi, T., Obuchi, Y., Takami, Y., Sato, J., Araki, M., Miki, M., Nagata, K., Sakai, K., & Igarashi, S. (2015). Architecture-scale human-assisted additive manufacturing. *ACM Transactions on Graphics*, 34(4), 88:1-88:8.

TRAINING A VISION-BASED AUTONOMOUS ROBOT FROM MATERIAL BENDING ANALYSIS TO DEFORMATION VARIABLES PREDICTIONS WITH AN XR APPROACH

CHI-FU HSIAO¹, CHING-HAN LEE², CHUN-YEN CHEN³ and TENG-WEN CHANG⁴

¹*Tamkang University.*

^{2,3,4}*National Yunlin University of Science and Technology.*

¹*chifu.research@email.com, 0000-0002-9018-635X*

²*chinghanglee@gmail.com, 0000-0002-9001-5972*

³*chunyan056@gmail.com, 0000-0001-9503-2766*

⁴*tengwen@gmail.yuntech.edu.tw, 0000-0003-4798-4580*

Abstract. This paper proposes a "Human Aided Hand-Eye System (HAHES)" to aid the autonomous robot for "Digital Twin Model (DTM)" sampling and correction. HAHES combining the eye-to hand and eye-in hand relationship to build an online DTM datasets. Users can download data and inspect DTM by "Human Wearable XR Device (HWD)", then continuous updating DTM by back testing the probing depth, and the overlap between physics and virtual. This paper focus on flexible linear material as experiment subject, then compares several data augmentation approaches: from 2D OpenCV homogeneous transformation, autonomous robot arm nodes depth probes, to overlap judgement by HWD. Then we train an additive regression model with back-testing DTM datasets and use the gradient boosting algorithm to inference an approximate 3D coordinate datasets with 2D OpenCV datasets to shorten the elapsed time. After all, this paper proposes a flexible mechanism to train a vision-based autonomous robot by combing different hand-eye relationship, HWD posture, and DTM in a recursive workflow for further researchers.

Keywords. Digital Twin Model; Hand-Eye Relationship; Human Wearable XR Device; Homogeneous Transformation; Gradient Boosting; SDG 4; SDG 9.

1. Introduction

The integration of artificial intelligence, autonomous robot aided fabrication, and "Human-Computer Interaction (HCI)" workflow present a rising tendency in nowadays "Architecture, Engineering and Construction (AEC)" workflow.

Traditional HCI robot arm operation needs operators to take a lot of time in configuring the tedious, point-to-point processing, and path teaching planning before the work starts. Moreover, when the AEC workflow getting much more complex, there

had to divide work stream into several stages, not only each period of robot operation must be recalibrated for different configured environment, but also the entire production will be interrupted for a lot of time-losing. Besides, real construction environments are usually much more chaotic and unpredictable, how to measure the deformation features of operating materials need to be processed before they are going to be operated within CAD-CAM system. In other words, autonomous robot construction is chasing for a kind of more flexible, sensible inference mechanism, which can apply to more complicated, unpredictable in-site environment.

Thus, this paper proposes a "Human Aided Hand-Eye System (HAHES)" to aid autonomous robot before AEC environment by establishing a digital model experiment to sample and update material features. HAHES mixes eye-to hand, and eye-in hand relationship of robot arm, then use "Human Wearable XR Device (HWD)" to observe the linear material for examining the difference between optical results and reality.

In addition, HAHES keeps updating the "Digital Twin Model (DTM)" from different perspective views from camera, HWD, and back-testing values by executing the autonomous robot to probe the deformation variables of material, and then make sure DTM is as precisely as the real scene configurations. With the recorded sampling datasets from above recursive examining tasks, HAHES then train an additive regression model to inference the approximate 3D coordinates of nodes distribution on bending materials for reducing the time losing of the latter examining works.

2. Precedents

2.1. HAND-EYE RELATIONSHIPS

There are two kinds of observing and executing system in autonomous robot construction relationships, known as "eye-in hand" and "eye-to hand" (Flandin et al., 2000). Eye-to hand means that the camera and the arm are fixed in two positions separately, camera pictures overall environments in a pre-settled configuration, but inevitable occlusions by moving arms or involving team members.

In comparison, eye-in hand hangs the camera on the end-effector of robot arm, camera takes picture when the arm is driven to achieve the executing command, so that users can control the arm dynamically by locating the relative relationship with homogeneous coordinates calculations in real time. Batliner had showed several projects to combine eye-in hand and projection with real-time robotic motion operations (Batliner et al., 2015).

Different from eye-in hand, eye-to hand system is fixed in a static transformation matrix, when camera capturing and recognizing, the arm is moving and executing commands at the same time. Therefore, there is better cycle time, but the end-effector and the camera view field must be ensured in a certain and clear moving path.

Otherwise, eye-in hand maintains a relative relationship with homogeneous coordinates though, the flexibility of free moving end-effector also causes several optical deviation issues of picture taken, such as focal length, chromatic aberration, contrast sensibility or overexposed... etc. which will raise the difficulty of the artificial intelligence sampling pre-processing model built.

2.2. OBJECT-RECOGNITION

Cheng presents an autonomous robot mechanism practice with eye-in hand object-recognition. They use pre-trained 2D depth computer vision to recognize the targets on a plan surface, then use Computer in the Human Interaction Loop (CHIL) to choose desired object. CHIL insert an initialize eye-to hand stage in to the eye-in hand setting. They configure the robot arm and camera posture into a specific perpendicular state to plan plate each time human selection occurs. Thus, they can build a stable digital twin model, and segmented monitor the task process (Cheng et al.).

2.3. ACTIVE BENDING SIMULATION

Chang propose a XR relative digital twin model: Cofab, to simulate a mixed-reality weaving structure, record physical nodes states disturbs, and adjust the morphing shapes via gesture at the same time. They use a variable parameter (Pa) to modulate the degree of active-bending states globally, then adjust this Pa value to simulate the morphing between the virtual and physical changes and observe the displacement of the connective nodes cloud with XR.

Because the structure was relative connected and shifted overall structure displacement. Afterall, they also build a practical weaving structure then using robot arm to measurement the precision in virtual and the physical expression (Chang et al., 2020).

2.4. AI PREDICTION IN 2D LINEAR GEOMETRY

Yang proposed a tool to choose predictable linear natural material. In amount of 4,000 mm length, 50 mm width, 10mm thickness unprocessed bamboo strips. This tool predicts both the number and locations of nodes on nature material in 2D distribute pattern and apply to desired geometry deformation simulation. He setups a bending experiment environment workflow with 5 stages:

- Pre-marked nodes on material, holding clamps,
- Setup a static eye to hand position, and initialize the computer vision background with black fabric and black PVC boards,
- Corresponding pressure the active bending material with 2 stabilize robot end effectors,
- Processing the computer vision output into curve and nodes into automatic "Neural Architecture Search (NAS)" datasets to approach the reality curvature,
- Training and predict material node distribution patterns, then post-test for promising accuracy for further deformation design task (Yang & Xu, 2021).

Yang utilising the NAS machine learning techniques to predict natural material behaviours by 2D camera setting. However, a bending curvature material may actually twist or offset by 3D direction forces, which is hard to apply in NAS vision algorithm.

2.5. 3D LINEAR GEOMETRY KEY FACTOR SEARCHING

We propose another approach to describe the linear material nodes in 3D distortion point datasets. By combining eye-to hand and eye-in hand camera projection datasets, we can complement the depth losing of 2D camera by homogenous equation transformation, theoretically. But we then figure out that DTM still need to adjust several key factors to approximate the robot back-testing results by probe depth after several time retests.

From 2D coordinates retrieving, homogeneous equation calculation, to recorrecting DTM, the sequences of the processes have closely related each other from previous to after task results.

We introduce additive regression models by sequentially fitting 2D eye-to hand and eye-in hand sample coordinates into the back-testing 3D coordinates at each iteration. Friedman proposed that randomly selected subsample from coordinates data type is then effective in place of the full sample to fit the base learner and compute the model update for iteration. Randomized approach also increases the robustness against overcapacity of the base learner (Friedman, 2002).

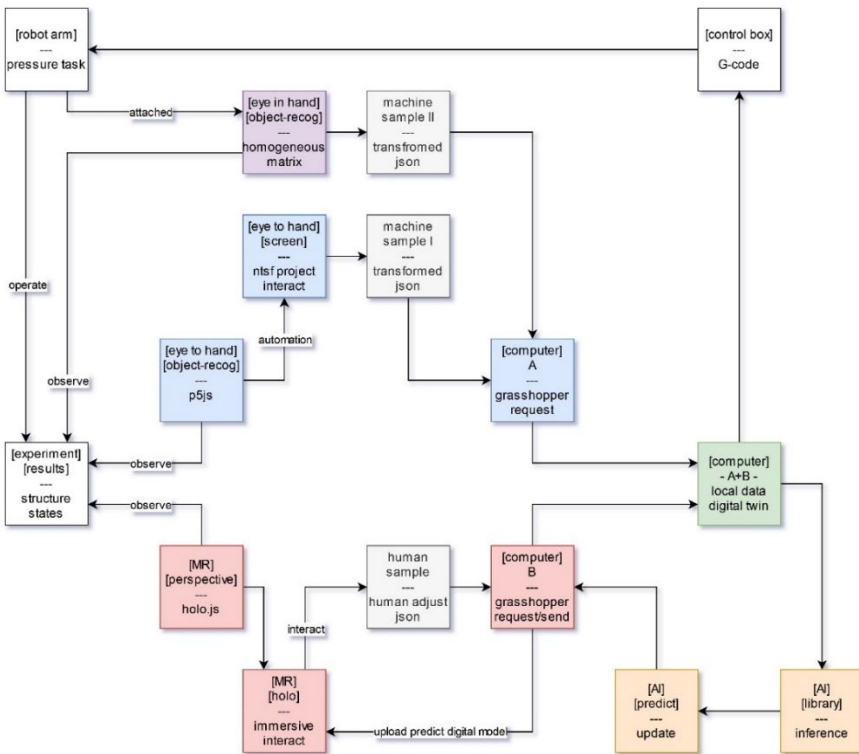


Figure 1. framework of HAHES.

3. Autonomous Robotic Sampling and Training Workflow

The process of HAHES workflow can be divided into 4 stages (shown as Figure 1):

- Eye-to hand sampling: Homogenous matrix transform from 2D to 3D calculation.
- Eye-in hand complement: Upload robot arm probe plumbs depth and camera inputs, then complement the Z-axis correction of previous 3D calculated oriental plane in DTM.
- HCI correction: Relocated the overlap of marked nodes with HoloLens multi-view scopes.
- AI prediction: Train additive regression model with gradient boosting algorithm from the datasets of previous 4 stages.

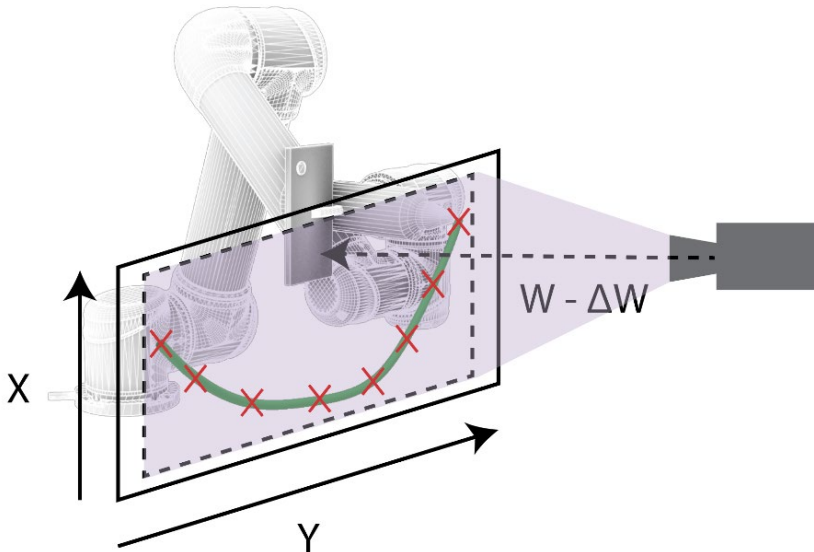


Figure 2. Fixed eye-to hand camera with potential rotation correction matrix.

3.1. SAMPLING

The consideration of each stages provides different datasets in a sequences of matrix transformation. Eye-to hand camera (as shown in Figure 2) fix the camera on the tripod in front of the workspace and use OpenCV to find out the relative coordinates of bending material nodes in camera 2D projection.

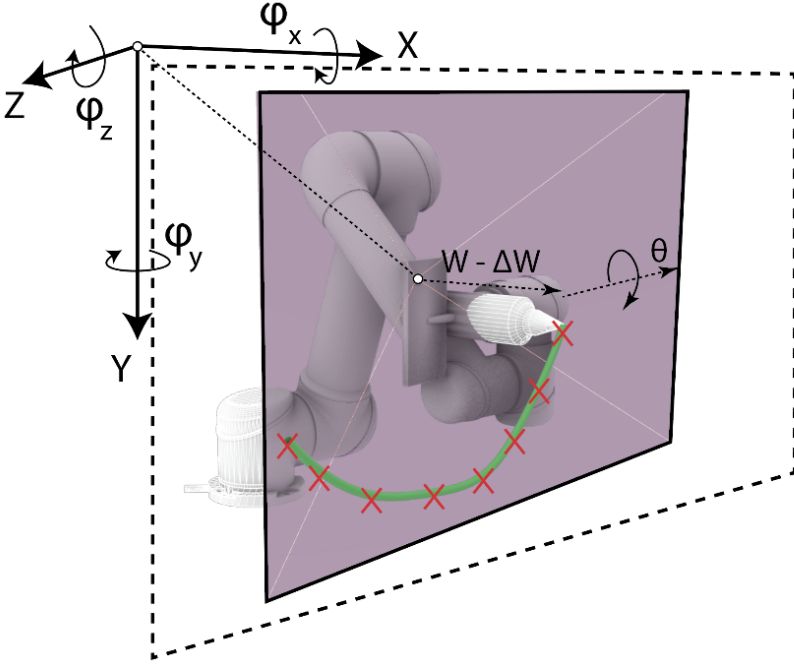


Figure 3. Eye-in hand camera generates 3D modify coordinates with translation, rotation, scale, and shear matrices.

3.2. COMPLEMENT OF HOMOGENEOUS MATRIX

After upload these 2D projection coordinates into cloud datasets, we then use the eye-in hand camera projection to process the 3D coordinates from projective coordinates (shown as Figure 3). The equation of homogeneous coordinates transformation matrix will be inferred from below equations:

$$D = H \cdot M \cdot H \cdot C \quad (1)$$

$$\begin{bmatrix} x' \\ y' \\ z' \end{bmatrix} = \begin{bmatrix} 1 & 0 & -w/2 \\ 0 & 1 & -h/2 \\ 0 & 0 & 1 \end{bmatrix} \cdot \begin{bmatrix} m_{00} & m_{01} & m_{02} & m_{03} \\ m_{10} & m_{11} & m_{12} & m_{13} \\ m_{20} & m_{21} & m_{22} & m_{23} \\ m_{30} & m_{31} & m_{32} & m_{33} \end{bmatrix} \cdot \begin{bmatrix} f & 0 & w/2 & 0 \\ 0 & f & h/2 & 0 \\ 0 & 0 & 1 & 0 \end{bmatrix} \cdot \begin{bmatrix} x \\ y \\ 0 \end{bmatrix} \quad (2)$$

$$f = \sqrt{x^2 + y^2} \cdot \sin(\theta)^{-1} \quad (3)$$

Among equation (1) and (2), M is the homogeneous coordinates transformation matrix we are looking forward, D is the recognized 3D Cartesian coordinate in digital twin space, C is the camera input coordinates nodes values, H is the appearance of the variable f which corresponds to the focal length of our camera. Equation (3) presents the forward or backward states from the operation scene with a distance ΔW .

$$M = T \cdot R \cdot S_c \cdot S_h \quad (4)$$

Equation (4) abbreviated our approaching transforming matrix M with translation, rotation, scale, and shear transformation. For the situation in eye-to hand relationship, each of above matrixes will be static, because the camera is fixed in front of the workspace. But for the camera on the robot arm end effector, the matrixes are constantly changing through the process of robot arm moving.

$$T = \begin{bmatrix} 1 & 0 & 0 & 0 \\ 0 & 1 & 0 & 0 \\ 0 & 0 & 1 & 0 \\ 0 & 0 & 0 & 0 \end{bmatrix} \cdot t_z := \begin{bmatrix} t_x \\ t_y \\ (f - t_z) \cdot s_z^{-2} \\ 1 \end{bmatrix} \quad (5)$$

$$R = R_x \cdot R_y \cdot R_z \quad (6)$$

$$R = \begin{bmatrix} 1 & 0 & 0 & 0 \\ 0 & \cos(\theta_x) & -\sin(\theta_x) & 0 \\ 0 & \sin(\theta_x) & \cos(\theta_x) & 0 \\ 0 & 0 & 0 & 0 \end{bmatrix} \cdot \begin{bmatrix} \cos(\theta_y) & 0 & -\sin(\theta_y) & 0 \\ 0 & 1 & 0 & 0 \\ \sin(\theta_y) & 0 & \cos(\theta_y) & 0 \\ 0 & 0 & 0 & 0 \end{bmatrix} \cdot \begin{bmatrix} \cos(\theta_z) & -\sin(\theta_z) & 0 & 0 \\ \sin(\theta_z) & \cos(\theta_z) & 0 & 0 \\ 0 & 0 & 0 & 1 \\ 0 & 0 & 0 & 0 \end{bmatrix} \quad (7)$$

Translation matrix expresses as equation (5), and the rotation matrix would be calculated by equation (6) and (7). The θ is the changing value from the direction of 6-axes robot TCP and will relate to the camera plane orientations.

$$S_c = \begin{bmatrix} S_{c_x} & 0 & 0 & 0 \\ 0 & S_{c_y} & 0 & 0 \\ 0 & 0 & S_{c_z} & 0 \\ 0 & 0 & 0 & 1 \end{bmatrix} \quad (8)$$

The S_c in equation (8) represents the scale transformation from operation scene to DTM, in this case we equally scaling up the object recognition pixel values into same parameter after measuring the physical scene in millimetres unit.

$$S_h = S_{h_x} \cdot S_{h_y} \cdot S_{h_z} \quad (9)$$

$$S_h = \begin{bmatrix} 1 & 0 & 0 & 0 \\ \tan(\varphi_y) & 1 & 0 & 0 \\ \tan(\varphi_z) & 0 & 1 & 0 \\ 0 & 0 & 0 & 1 \end{bmatrix} \cdot \begin{bmatrix} 1 & \tan(\varphi_x) & 0 & 0 \\ 0 & 1 & 0 & 0 \\ 0 & \tan(\varphi_z) & 1 & 0 \\ 0 & 0 & 0 & 1 \end{bmatrix} \cdot \begin{bmatrix} 1 & 0 & \tan(\varphi_x) & 0 \\ 0 & 1 & \tan(\varphi_y) & 0 \\ 0 & 0 & 1 & 0 \\ 0 & 0 & 0 & 1 \end{bmatrix} \quad (10)$$

For the perspective configuration of eye-in hand camera, we also need to add a shearing modification, the abbreviated matrix is shown as equation (9) and expended 3 direction axes as equation (10). We introduce S_h matrix to modify the losing depth of eye-to hand 2D camera projectivity sample when the robot arm is moving, then complement 3D coordinates with this reverse inference process.

3.3. COORECTION

After above period of workflow, we map both 2 camera results on an external spreadsheet table synchronously online to monitor the material bending status, then build a primitive DTM to describe the experiment scene.

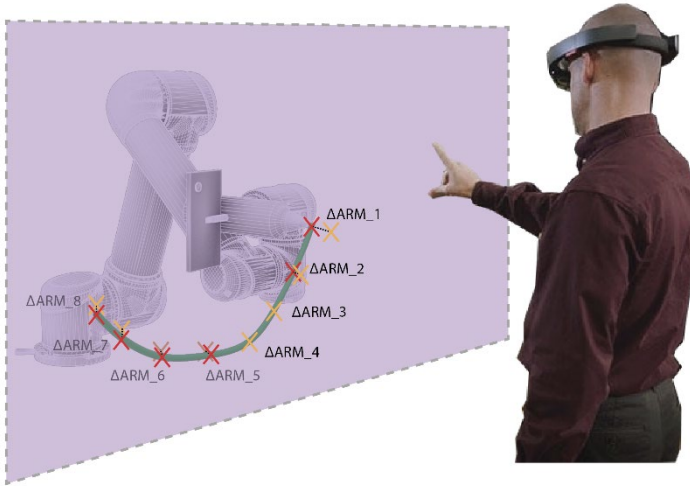


Figure 4. Use HWD to observe the difference between reality scene and DTM, then control the probe on the robot arm to update confirm the depth of delta vectors.

After settling the DTM environment, we use HWD to examine the difference between nodes marked on physical material, and generated model (shown as Figure 4). Observers need to fit the bending model upon the reality structure in every perspective by gesture, then HAHES will upload modified values of each node into the spreadsheet sample library online as Table 1.

Table 1. Online DTM spreadsheet table of bending material nodes, each cell will be updated asynchronously with the experiment processing for one time correction.

[mark]	[opencv recognition]		[marix transform]			[robot check]	[human check]	[predict / correction]		
ID	X	Y	cal. X	cal. Y	cal. Z	ARMdelta	HOLOdelta	cor. X	cor. Y	cor. Z
ID0	47	150	-168	-891	339	-1	1	?	?	?
ID1	96	116	-67	-891	289	-2	0	?	?	?
ID2	138	107	19	-891	250	-2	1	?	?	?
ID3	187	108	120	-891	252	-3.5	0	?	?	?
ID4	220	132	188	-891	302	-1	0	?	?	?
ID5	254	175	258	-891	390	0	-1	?	?	?

3.4. PREDICTIONS

From camera capturing pictures, uploading 2D datasets, generates 3D coordinates, HCI confirming to robot arm probes back-testing, the elapsed time will be 3-5 minutes for a complete detection task.

We then use "GradientBoostingRegressor" package from scikit-learn library to

build an additive model in a forward stage-wise, which allows the optimization of arbitrary differentiable loss functions. In our case, we need to rearrange previous sampling, complement, and correction stages of all nodes in each repeating operation results into a list of row data (shown as Table 2).

Table 2. Executing previous Table 1 multiple times to train an additive model, then predict the relationship between datasets X (2D calculation) and datasets Y (3D correction results).

REPEATING	DATASETS X [2D CALCULATION]										DATASETS Y [3D CORRECTION]				
	cam_0	cam_1	cam_2	cam_3	cam_4	cam_5	DTM_0	DTM_1	DTM_2	DTM_3	DTM_4	DTM_5			
0	47.32	96.42	137.50	138.56	167.92	220.43	-168.45	-67.43	19.15	120.17	188.20	258.29			
1	48.18	96.95	138.19	139.49	188.38	220.91	-168.58	-67.48	19.72	119.60	187.42	259.26			
2	48.00	97.13	137.89	140.01	188.25	220.73	-169.54	-66.96	20.33	119.26	188.03	258.96			
3	49.15	96.39	138.05	140.11	188.90	219.74	-169.21	-67.65	19.77	118.44	188.75	258.65			
4	49.98	96.43	138.58	139.22	188.60	219.92	-168.58	-67.13	19.60	117.75	189.69	258.50			
5	50.45	96.92	139.18	138.40	189.53	218.97	-168.02	-67.57	20.11	117.84	189.76	257.70			
6	49.56	97.11	138.57	138.65	189.19	218.89	-168.77	-67.88	20.45	117.96	189.51	258.36			
7	49.68	97.62	138.10	138.98	188.24	219.57	-169.28	-67.53	19.84	118.86	190.39	257.58			
8	49.97	97.36	137.94	139.03	188.73	219.03	-169.79	-66.96	19.62	119.86	189.60	258.41			
9	50.30	96.93	138.34	139.67	189.43	219.69	-170.14	-67.39	19.45	119.66	189.92	258.51			
10	51.00	96.16	137.59	140.67	190.28	219.25	-169.15	-67.36	19.65	119.19	189.84	259.17			
11	50.14	96.60	138.03	140.43	189.88	219.21	-169.32	-66.58	18.93	118.38	189.98	259.79			
12	49.17	95.75	137.52	140.74	190.37	218.48	-169.98	-66.20	18.44	119.05	190.21	259.62			
13	50.16	95.18	136.75	141.19	190.86	218.53	-169.51	-65.20	19.68	119.98	190.89	259.35			
14	50.95	94.22	137.65	141.51	190.10	218.09	-168.90	-65.89	19.92	120.44	189.97	258.45			
15	50.92	94.30	137.85	142.07	190.31	218.29	-168.51	-66.01	19.40	121.03	189.14	258.79			
16	50.84	93.70	137.90	141.77	190.28	217.88	-168.32	-66.73	18.66	120.88	189.02	259.05			
17	49.96	93.80	137.95	140.87	189.71	218.77	-168.04	-66.70	19.18	120.62	188.82	258.54			
18	50.18	93.31	138.82	141.61	189.25	219.43	-168.35	-66.96	19.44	120.13	189.60	259.47			
19	49.99	94.17	138.72	141.12	188.58	220.13	-167.87	-66.72	19.34	120.87	188.76	259.78			

Furthermore, because of the predict datasets Y are sequence of coordinates, we also import the "MultiOutputRegressor" package for the multivariate output target of parallelize regressors. Afterall, HAHES is able to inference approximate coordinates for a shorter time duration. In our tasks, we repeated HCI approaches for 37 times, and the time elapsed from 3-5 minutes into 3-5 seconds; the accuracy of AI prediction coordinates in X is 93.64%, in Y is 90.84%, and is 98.65% in Z (shown as Figure 5).

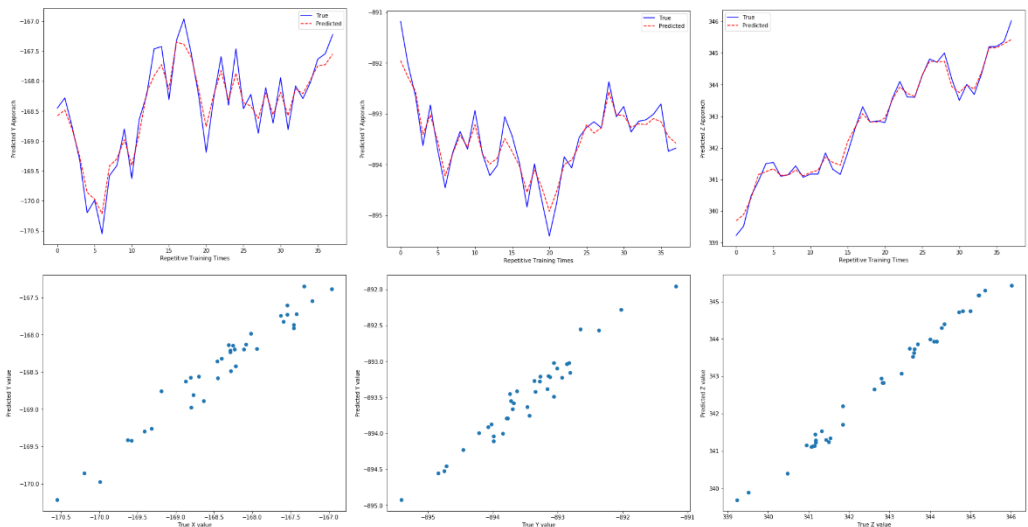


Figure 5. The prediction value from 2D camera inputs to 3D DTM coordinates with the gradient boosting regression inference of additive model.

4. Conclusion

This paper proposes another co-existing approach of "Multi-View Scopes (MVS)". The sequence proceeds from marking the nodes distribution on material, use 2D vision based DTM with different hand-eye relation configured camera, to physical back-testing probes. Then we confirm the nodes position in 3D immersive perspective by HWD. To reduce the time elapsed of bending material inputs, we also use previous back-testing datasets to train an additive regression model and predict parameterized nodes distribution by gradient boosting algorithms. However, further adjustments must be examined in detail. The integration of HWD adjustment is of focus as the authors intend the observer to be the intervene aid to recheck the effectiveness of DTM during the detecting process. An advantage of using interactive stage instead of fully automated is that fewer iterations are needed to conclude, but more importantly there would be a dialogue between the algorithm and the user is introduced. Currently the determination of the coordinates is hypothesis the pre-given nodes is able to describe the bending materials, we can use add more possible nodes on HWD, and recheck the nodes by pasting another physical mark on the bending material.

With the integration of the additive regression model, HAHES proposes a more flexible occasion to decide when to teach system with HWD reflecting behaviours via human gesture sampling, or general use the hand-eye relationship AI prediction results. We expect the consequences of this paper can provide future researchers another kind of human aided approaching in training a vision-based autonomous robot from material bending analysis to deformation variables predictions.

References

- Batliner, C., Newsum, Jake, M., & Rehm, M.C. (2015). Live: Real-Time Platform for Robot Design Interfaces. In *33rd Education and Research in Computer Aided Architectural Design in Europe, eCAADe 2015* (pp.277-286). Education and Research in Computer Aided Architectural Design in Europe (*eCAADe*).
- Chang, T., Hsiao, C., Chen, C., Huang, H., Datta, S., & Mao, W. (2020). Fabricating Behavior Sensor Computing Approach for Coexisting Design Environment. *Sensors and Materials*, 32(7), 2409-2417. <https://doi.org/https://doi.org/10.18494/SAM.2020.2809>
- Cheng, F., Yen, C., & Jeng, T. (2021). Object recognition and user interface design for vision-based autonomous robotic grasping point determination. In *26th International Conference of the Association for Computer-Aided Architectural Design Research in Asia, CAADRIA 2021* (pp. 633-642). The Association for Computer-Aided Architectural Design Research in Asia (CAADRIA).
- Flandin, G., Chaumette, F., & Marchand, E. (2000). Eye-in-hand / Eye-to-hand Cooperation for Visual Servoing. In *IEEE International Conference on Robotics and Automation, ICRA 2000*, (pp. 2741-2746). Institute of Electrical and Electronics Engineers (IEEE).
- Friedman, J. H. (2002). Stochastic gradient boosting. *Computational Statistics & Data Analysis*, 38(4), 367-378. [https://doi.org/https://doi.org/10.1016/S0167-9473\(01\)00065-2](https://doi.org/https://doi.org/10.1016/S0167-9473(01)00065-2)
- Yang, X., & Xu, W. (2021). A Tool for Searching Active Bending Bamboo Strips in Construction via Deep Learning. In *26th International Conference of the Association for Computer-Aided Architectural Design Research in Asia, CAADRIA 2021* (pp.2409-2417). The Association for Computer-Aided Architectural Design Research in Asia (CAADRIA).

Innovative Material Systems and 3D Printing

ROBOTIC FABRICATION PROCESS OF GLUED LAMINATED BAMBOO FOR MATERIAL EFFICIENT CONSTRUCTION

CHUNG-CHIEH CHENG¹, YU-TING SHENG² and SHIH-YUAN WANG³

^{1,2} *School of Architecture, Feng-Chia University*

³ *Graduate Institute of Architecture, National Yang Ming Chiao Tung University*

¹*m0822931@mail.fcu.edu.tw, 0000-0002-4625-6146*

²*ytsheng@fcu.edu.tw, 0000-0002-0525-7572*

³*yuan@arch.nctu.edu.tw, 0000-0002-4675-7290*

Abstract. This paper aims to introduce the development of a new-style glue-laminated bamboo (GLB) board structure and evaluating computational technologies aiming to enhance the performance of fibre materials and a set of digital manufacturing processes. Specifically, this paper develops a method to introduce the concept of topology optimisation into the properties of fibre materials. At the same time, it explains the unique structure optimisation design and manufacturing process (including the design process, digital tools and auxiliary equipment system). To test the design, this paper compares the data obtained via the gravity suspension test of the physical model and the simulation. Through digital manufacturing methods, the project aims to establish structural elements that could improve material efficiency. Furthermore, it may establish a GLB floor structure system in line with the material economy.

Keywords. Digital fabrication; Robotic Assembly; Glued Laminate Bamboo; SDG 11; SDG 12; SDG 15.

1. Introduction

This research introduces the concept of topology optimisation. Via the combination of calculation and manufacturing technology, the mechanical properties of bamboo fibre materials are converted into controllable parametric variables, which are brought into consideration in the design of architectural elements. This research also investigates the interrelationships among computing, materials and manufacturing systems. At the same time, it proposes a form-finding mode based on material optimisation calculations to produce particular structural patterns, which evolve a new design method that emphasises material performance and laminated material mechanical behaviour, analysis technology and digital manufacturing capabilities.

By virtue of computational tools, such as topology optimisation and finite element analysis, this paper further develops the form explorations of this study via design

thinking that influences the overall structure layout by the purpose of force. It focuses on processing the arrangement of the bamboo sheet direction and then on the complex geometric arrangements and gluing procedures performed with the help of digital arithmetic tools. In addition, it proposes a process for automatically arranging the direction of bamboo sheets and spraying glue in the application of a six-axis industrial robotic arm. Then, a set of manufacturing processes is demonstrated with the formation of an experimental glue-laminated bamboo (GLB) board using a vacuum lamination system. Compared with the typical laminated bamboo manufacturing process, in which each layer keeps the same orientation of bamboo fibre (Mahdavi et al., 2011), this experiment develops a bamboo sheet by laminating small, thin units with locally controllable fibre orientation. Finally, a set of lightweight GLB board systems conforming to the mechanical structure is developed using digital computing tools and robotic arms. Apart from saving weight under the same strength, it also provides a possible lightweight expansion compared with the typical structural system, allowing large-scale applications of GLB board in the construction industry. The three main contributions of this research are as follows:

1. Verifying that with assisted digital tools, such as robotic arms and vacuum lamination, it is possible to develop a customised discrete structural bamboo laminated board to meet various structural requirements.
2. Establishing a structural numerical visualisation and verification system to discuss the difference between expected results and finished products while also clarifying the influence of essential parameters, which can serve as a reference for future research.
3. Opening up a new possibility for the manufacture of laminated bamboo, which offers opportunities for GLB in the field of architecture.

2. Context and Previous Experiment

Bamboo laminate is a new engineering material in a few decades; it is processed into rectangular bamboo slices of a particular specification, then treated with anti-corrosion, anti-mildew and moth-proof agents, dried and glued together. Its specifications are often restricted by the size of the original bamboo material. Although there is a continuous manufacturing method involving stacking interlacing, problems still exist in structural considerations and frequent increases in the complexity of the manufacturing process. At the same time, if there are design requirements for different stacking angles, manufacturing difficulty is further enhanced. Therefore, there has not been a complete, practical and flexible manufacturing method developed as of yet.

In recent years, theoretical models and experiments have been established in many studies to explore the effect of fibre orientation on the mechanical properties of laminate material (Figure 1). For instance, Dong Ying Lee, Feng-Cheng Chang and Ming-Jer Tsai (2019) simulated the theoretical elastic properties of laminated bamboo that configured different fibre directions based on the lamination theory model. Chow, Ramage and Shah (2019) optimised ply orientation in structural laminated bamboo. Takeuchi, Estrada and Linero (2016) determined the elastic modulus in the load direction and the Poisson's ratio to show that the material's physical anisotropy leads to an anisotropic mechanical behaviour. Moreover, Rindo, Manik, Jokosisworo, Putri

and Wilhelmina (2020) investigated the effect of the direction arrangement of bamboo blades on the interface of the laminated bamboo fibre matrix. However, bamboo laminate is currently used primarily in furniture scales (Mahdavi et al., 2011) whereas it is rarely used in architecture structure. This may be mainly attributable to the difficulty in processing the raw materials of the existing bamboo glulam (i.e. drying raw bamboo, cutting and scraping the bamboo green and making square strips). In addition, if the original material is too small in size, this situation can lead to extremely low efficiency in making significant components.

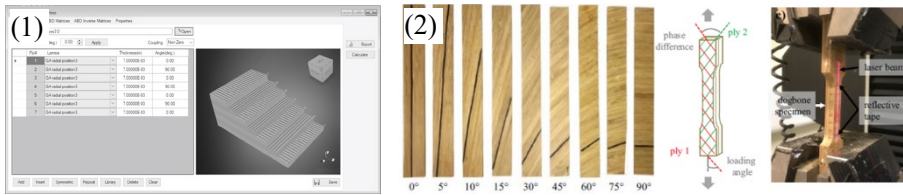


Figure 1. (1) Related studies that established the theoretical model of glue-laminated bamboo (Dong Ying Lee et al., 2019) and (2) Optimising ply orientation in structural laminated bamboo (Chow et al., 2019)

3. Robotic Aided Glued Laminate Bamboo Fabrication System

This system mainly consists of three parts, which are as follows: a KUKA six-axis industrial robotic arm (KUKA Agilus KR 10 R1100, 110-cm working range and 10 kg load) equipped with an automated glue spray gun (GPPT WS-03); a vacuum grabber used as the end effector (Figure 2); a vacuum pump that serves as a stressor for pressing with a working platform connected to it. The fabrication process uses TACO based on the Rhino and Grasshopper platforms to operate the robotic arm, controlled by program editing to arrange the bamboo sheets accurately in the specified position. Following this, the pre-mixed epoxy resin is coated with an automatic glue spray gun so that the bamboo sheets can be cold-pressed and combined in the subsequent steps, and the two steps of arrangement and gluing are repeated until reaching the required number of sheets. Finally, the uncured bamboo board and the working platform are sealed with a Thermoplastic Polyurethane (TPU) membrane, and then the vacuum pump is started to generate a vacuum until the resin curing time.

Through the manufacturing system, the manufacturing of the 1.2 m x 1.2 m complex structure GLB board can be resolved into the eight following steps:

- Cut the bamboo veneer material into 10 cm x 10 cm (0°, 30°, 45° three-fibre direction unit modulus). Cut the 1.3 m x 1.3 m plywood as the base of the working platform, pre-lay the vacuum system's consumables, prepare the resin to be sprayed, and mix it evenly.
- Install an automated glue spray gun on the arm to pre-coat the working platform with resin so that the first layer of the bamboo unit can be temporarily fixed on the working platform.
- Install the vacuum grabber, adjust the position above the first bamboo unit in the vertical material area of the arm and start it.

- Keep the vacuum grabber activated and move the bamboo unit to the designated position according to the programming design. This process may include the necessary rotation of the robot arm.
- Repeat the first two steps until the first layer of the bamboo unit is arranged.
- Repeat this mode until the design is completed, considering the working time limit of resin curing.
- Finally, cover the working platform with a TPU membrane for sealing, start the vacuum pump to generate pressure and wait for curing.

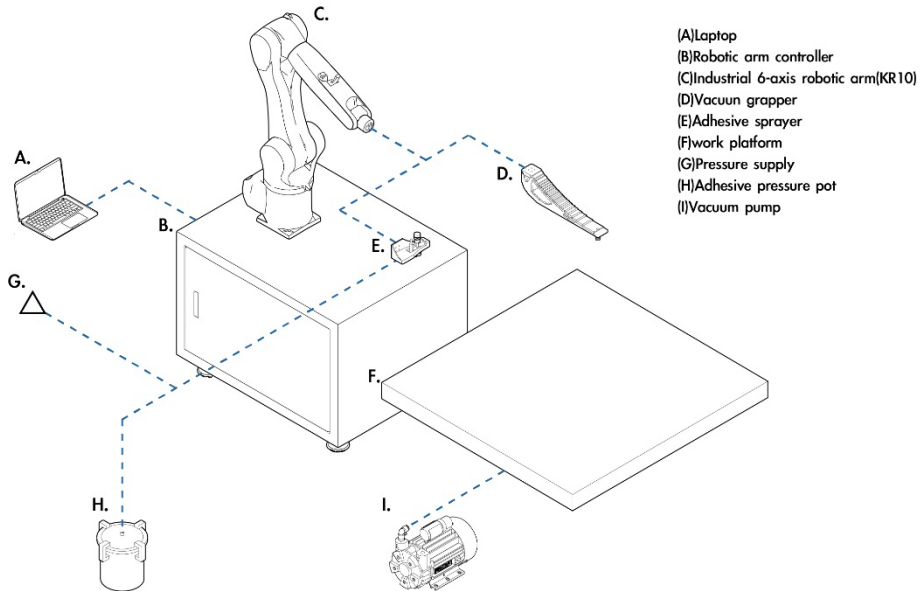
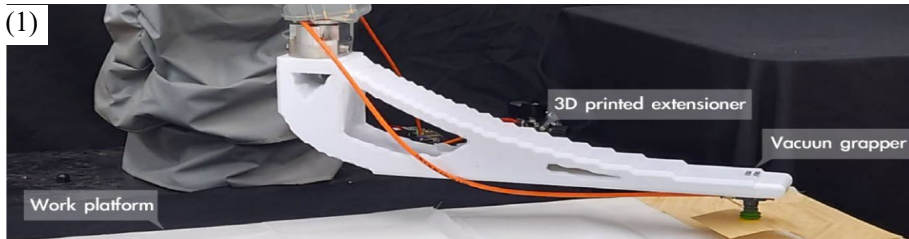


Figure 2. Related devices in the system.

3.1. END EFFECTORS

To achieve the quick arrangement of bamboo sheets with different fibre directions, a vacuum grabber (Piab BX25P) can be installed on the flange of the robot arm as an end effector. Driven by an air compressor, a solenoid valve is used to control its on-off state. The end effector is equipped with a plastic suction cup that can perform the functions of grasping, moving and accurately arranging the position and rotation direction of the bamboo sheets.



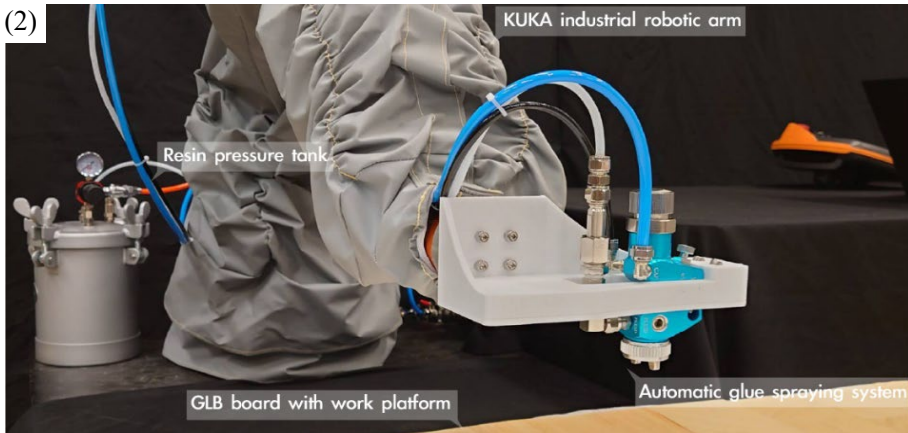
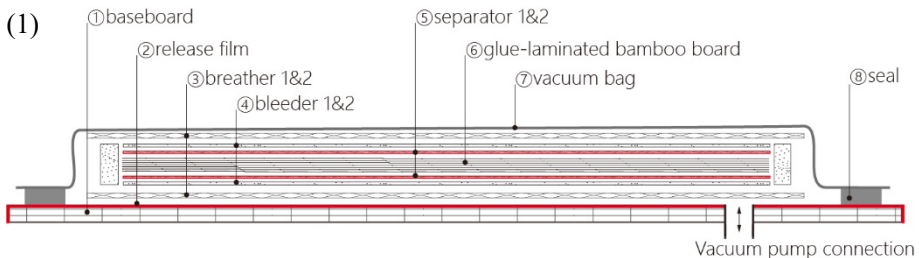


Figure 3. End effectors in the system: (1) vacuum grabber, (2) automatic glue sprayer

3.2. VACUUM LAMINATION SYSTEM

The vacuum lamination system includes the vacuum pump (Value VE-160) and the setting of the working platform. The vacuum pump provides a source of operating power for the system, and the purpose of the working platform is to make the pressing fully successful, allowing the finished GLB board to be smoothly de-moulded and the excess glue absorbed. For this purpose, it is necessary to have a mirror structure on the upper and lower sides of the GLB board. Vacuum pump operation will generate high temperatures quickly, and long-term operation may cause the motor to overheat. The curing time of different adhesives is different; thus, the working platform needs to be sealed when it reaches the vacuum state so that the vacuum lamination system can still provide continuous pressure for the curing of the GLB board even when the vacuum pump is off. So far, the complete assembly materials of the working platform and their related uses from bottom to top are as follows: (1) baseboard (plywood, provides a rigid substrate to help shape the GLB board); (2) release film (prevents the adhesive from sticking to the substrate); (3) breather 1 (porous material, provides vacuum pump airflow channel); (4) bleeder 1 (absorbs excess adhesive); (5) separator 1 (helps glulam de-moulding); (6) GLB board (the central part of the system); (7) separator 2; (8) bleeder 2; (9) breather 2; and (10) TPU membrane (Figure 4).



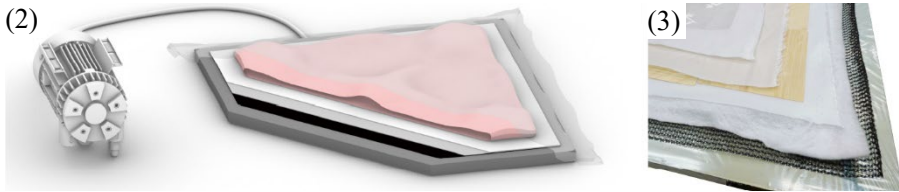


Figure 4. Vacuum lamination system: (1) profile description of system, (2) schematic diagram, (3) installation photo of working platform

4. Material Study

This study emphasised the discussion on the mechanical behaviour of bamboo fibre orientation and demonstrated a digital manufacturing process of GLB board to explain. The bamboo lamina in this experiment was a processed bamboo made of native bamboo. To verify the relationship between its fibre direction and mechanical behaviour, this study created samples of laminated bamboo lumber that were interlaced and glued at different angles for three-point bending tests (Figure 6-1, 6-2). The test results are as follows:

- The relationship between fibre direction and mechanical performance: This test uses 0° (parallel), 30° , 60° and 90° (vertical) samples (Figure 5) for testing. The resulting damage loads are 2559.536, 2294.756, 1353.318, and 1627.904 (unit: Newton) in order (Figure 6-3). It was found that the parallel glued sample has the largest failure load, followed by the 30° sample, verifying that the parallel direction can withstand larger forces.

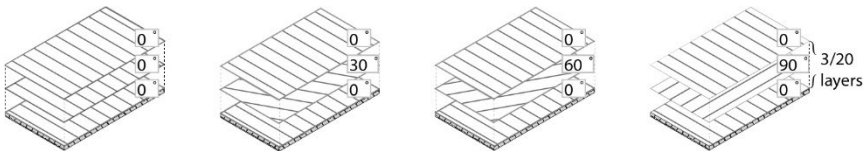


Figure 5. Schematic diagram of three points bending test sample (0° 、 30° 、 60° 、 90°)

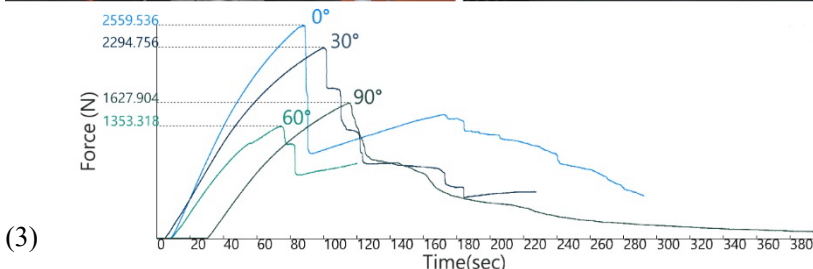
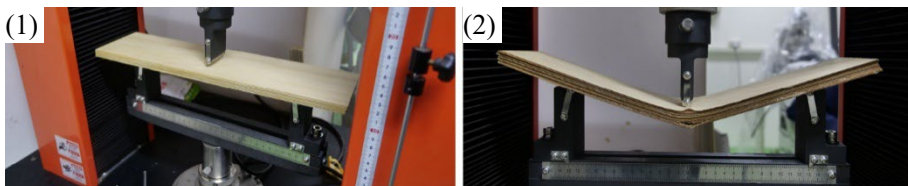


Figure 6. Three-points bending test: (1) test environment (2) test record (3) test result

5. Design Experiment

We designed a new GLB board structure to illustrate the concept described throughout the paper. This kind of structure helps show the material’s mechanical properties to maximise the structural benefit, thereby achieving the purpose of saving material. Under the guidance of the finite element method, the single-layer rectangular bamboo board (1.2 m x 1.2 m) was cut into bamboo units (10 cm x 10 cm), and each point was marked according to the horizontal axis A–M and the vertical axis 1–13 (Figure 8). Then, customised force conditions were pre-set by Karamba3D built on Rhino and Grasshopper (Figure 7-1). Among these, while the four corner points are used as supports, the points D-6, G-4 and K-6 are used as single-point loads, generating the force streamline distribution of the board (Figure 7-2). Finally, the divided bamboo fibre units are arranged in an approximated direction by the output streamline’s differential concept (Figure 7-3) to conform to the force situation. In this way, the bamboo fibre characteristics could be visual, with the structure optimised.

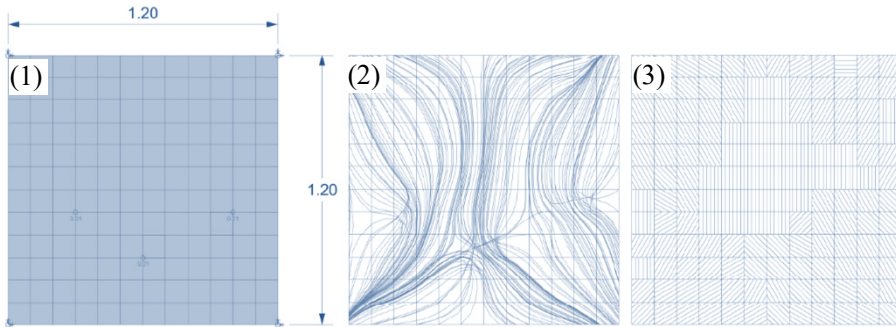


Figure 7. Form-finding process: (1) load environment and board size, (2) force stream line distribution, (3) fibre direction morphology result of the bamboo unit

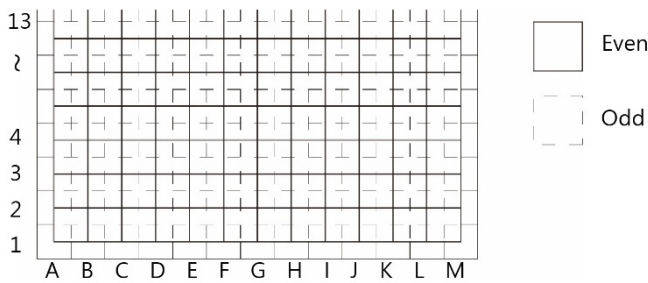


Figure 8. Coordinate system

To avoid the concentration of fracture points in the laminated layer after splitting, the odd- and even-numbered layers are designed to dislocate the bamboo unit. The breaking point that is prone to stress concentration is reduced by the continuous upper and lower layers, forming a special force transmission relationship (Figure 9-2). At the same time, after the board is developed, the material is cut to remove the excess part of the misalignment to retain the solid board of central 1.2 m x 1.2 m. A board with a crossed orientation layer has been manufactured using the same method.

For the hanging experiment part, fixed points is established to ensure that the GLB board is not stressed as initial that is no pre-existing tension or contraction is carried out except for its weight and single-point loads during the testing period. Meanwhile, several plywood moulds are made as additional tools, which can help fix the four corners of the GLB board to the mould in a flat state and remove the supporting material (Figure 10). Finally, the GLB board is installed on the metal frame. Next, an infrared distance meter is used to measure the distance between D-6, G-4, and K-6 points and the ground as the background parameters bearing its weight. Then, 4 kg iron balls are hung with high-tension wires at the three points in sequence to measure the distances to the ground again and record them. Figure 11 shows the final result of the hanging test. According to Table 1, the optimised board has better bending resistance; therefore, the effect of the bamboo fibre on the bending behaviour can be verified.

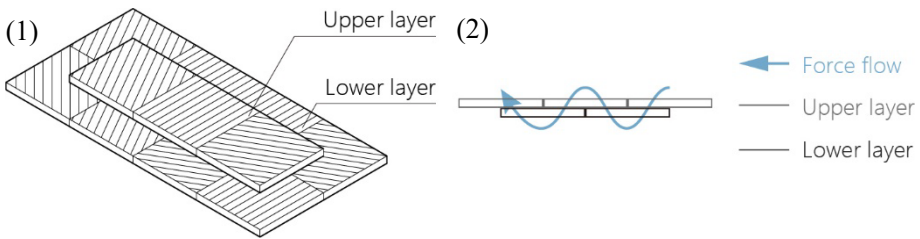


Figure 9. Description of dislocation layer: (1) schematic diagram of parity layer, (2) force transmission path

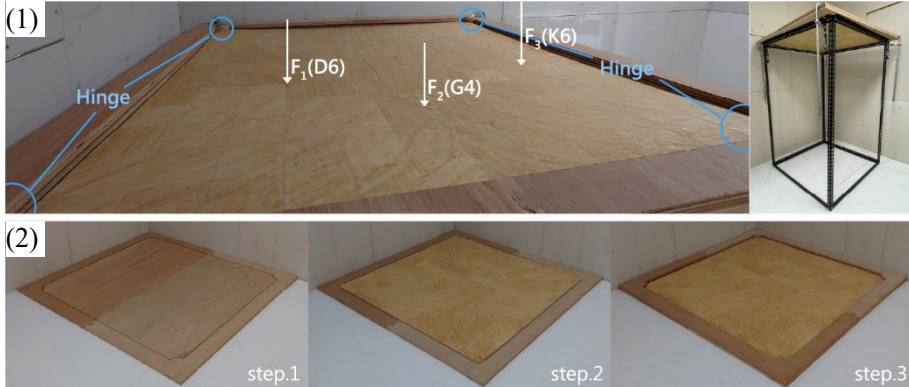


Figure 10. Result photo: (1) glue laminate bamboo board suspension method, (2) mould installation process

Unit: m	Crossed orientation sample		Fibre orientation optimised sample	
	Initial	Suspended	Initial	Suspended
D6	1.841	1.822	1.842	1.833
G4	1.840	1.819	1.837	1.829
K6	1.842	1.817	1.844	1.834

Table 1. Record of glue-laminated bamboo board with suspension



Figure 11. glue-laminated bamboo board structure on a 1:1 scale

6. Visualization Verification System

Taking advantage of the system, which relies on Abaqus software, the paper attempts to simulate an actual GLB board with heavy objects hanging from it and compare the similarities and differences in terms of the board model's construction and the force environment's setting. We are trying to achieve the following: (1) feeding the actual suspension situation back to the simulation end to modify the material parameters; and (2) using the simulation as a preview of the two-way visual verification system results. Its setup needs to build a four-story structure model divided into unit of bamboo sheets. According to the aforementioned physical test model, the mechanical parameters of the material and the fibre direction of the designated bamboo element are set, with the four corner points fixed as boundary conditions and the force point loaded with a force of 4 kg. Next, this simulation mimics the adhesive effect through the application of surface polymerisation interaction force between the layers; the numerical simulation strain results are shown in Figure 13. According to the numerical legend, the deformation of the corresponding colour block is obtained, demonstrating that the deformation of the simulated load range is about 12 mm; this shows some discrepancies with the actual test data. The errors may come from incomplete material parameters and the production process of the sample. However, the two have the same deformation area and mechanical behaviour. (From the magnified inspection of the simulation results, it can be found that there is a unique material deformation path, and it is an asymmetric model) (Figure 12).

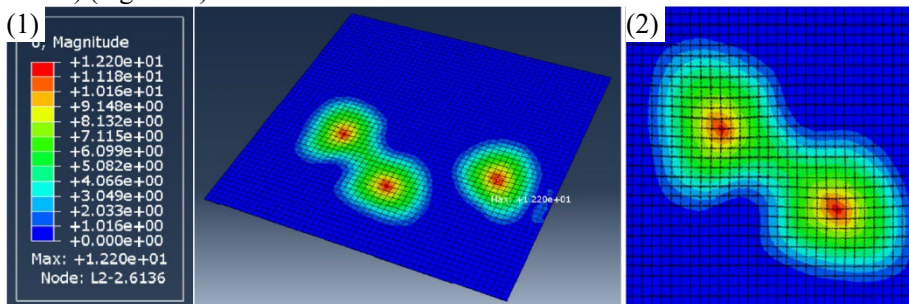


Figure 12. Visualisation verification system: (1) glue-laminated bamboo board simulation, (2) detail of simulation

7. Conclusion and Further Steps

In this study, a GLB board form that combines computational thinking based on actual testing and simulation was introduced. At the same time, the concept of introducing

analysis technology to show the characteristics of fibre materials was demonstrated using a digital manufacturing process. Because of the complexity of fibre direction optimisation, the workflow mainly included the arrangement of fibre direction and continuous circulation of automatic adhesive coating and auxiliary curing forming of the vacuum system. In addition, this paper proposed a customised fibre arrangement production method to optimise the GLB board to generate a more efficient material structure.

This paper explored a verification method that included physical suspension testing and computer simulation. Although the final research results are different between the simulated and actual results, they have the same mechanical behaviour and deformation. It can be inferred that the possible influencing parameters are as follows: 1) different material mechanical parameters; 2) an imprecise defined failure criterion parameter (traction-separation law) of the adhesive. At this stage, a scale of 1.2 m x 1.2 m can initially become a structural component of the building. As the possibility of an automated manufacturing process increases, it is likely to be used as a floor structure system that saves material resources. The next step of this project will be to continue developing a simulation system to provide maximum load and destructive assessment.

Acknowledgements

This project would not have been possible without the valuable support of ROSO (the school of Architecture, Feng-Chia University), and the Ministry of Science and Technology (MOST) (Taipei, TW) (GRANT_NUMBER: MOST 110-2222-E-035 - 003 -MY2).

References

- Chow, A., Ramage, M. H., & Shah, D. U. (2019). Optimising ply orientation in structural laminated bamboo. *Construction and Building Materials*, 212, 541–548.
<https://doi.org/10.1016/j.conbuildmat.2019.04.025>
- Lee, D. Y., Chang, F. C., & Tsai, M. J. (2019). Applying the Lamination Theory to Analyze of the Influence of Different Configuration Conditions on the Elastic Properties of Laminated Bamboo. *Journal of the Experimental Forest of National Taiwan University*, 33(4), 247-258.
[http://dx.doi.org/10.6542%2fEFNTU.201912_33\(4\).0002](http://dx.doi.org/10.6542%2fEFNTU.201912_33(4).0002)
- Mahdavi, M., Clouston, P. L., & Arwade, S. R. (2011). Development of Laminated Bamboo Lumber: Review of Processing, Performance, and Economical Considerations. *Journal of Materials in Civil Engineering*, 23(7), 1036-1042.
[https://doi.org/10.1061/\(ASCE\)MT.1943-5533.0000253](https://doi.org/10.1061/(ASCE)MT.1943-5533.0000253)
- Rindo, G., Manik, P., Jokosisworo, S., Putri, C., & Wilhelmina, P. (2020). Effect analysis of the direction of fiber arrangement on interfaces of laminated bamboo fiber as a construction material for wood vessel hulls. *AIP Conference Proceedings*, 2262(1), 030002.
<https://doi.org/10.1063/5.0016147>
- Takeuchi, C. P., Estrada, M., & Linero, D. L. (2016). The Elastic Modulus and Poisson's Ratio of Laminated Bamboo *Guadua angustifolia*. *Key Engineering Materials*, 668, 126-133.
<https://doi.org/10.4028/www.scientific.net/KEM.668.126>

DIGITAL CONSTRUCTION OF BAMBOO ARCHITECTURE BASED ON MULTI-TECHNOLOGY COOPERATION

Constructing a new parameterized digital construction workflow of bamboo architecture from traditional bamboo construction technology

KENAN SUN¹, TIAN TIAN LO², XIANGMIN GUO³ and JINXUAN WU⁴

^{1,2}*Harbin Institute of Technology (Shenzhen).*

¹1322742583@qq.com, ²skyduo@gmail.com, 0000-0002-1992-0777

³24904404@qq.com, ⁴741906932@gmail.com

Abstract. Limited by the non-standard nature of bamboo, bamboo has always been regarded as a traditional, restrictive, and time-consuming building material. Therefore, there is an urgent need for an enhanced parametric design system and digital construction workflow to upgrade the traditional bamboo construction process. In this paper, through the analysis of the bamboo pavilion "Diecui Gallery" under the traditional construction method, five main factors restricting the development of bamboo architecture are obtained: difficult positioning of supporting structure, low efficiency of material selection and matching, the manual processing of materials, non-standard node and low utilization rate of non-standard waste materials. Then, through literature review, we proposed the technical means to improve these factors and put forward a multi-technology collaborative digital construction workflow. The workflow will comprise augmented reality, 3D scanning, robot-aided construction, 3D printing, and design rules. Moreover, by building parametric benches, we used augmented reality technology and new design rules to verify multi-technology collaborative fabrication workflow possibilities and effectiveness. This paper wants to explore a parametric design method based on bamboo material characteristics and multi-technology collaborative workflow, to improve the utilization rate of non-standard bamboo components in parametric design.

Keywords. Bamboo Material; Multi-technology Collaboration; Parametric Design System; Augmented Reality; Digital Construction Method; SDG 11.

1. Introduction

Compared with wood, bamboo has the advantages of a short growth cycle, easy to obtain, and low economic cost, so it is a better eco-sustainable building material.

Nowadays, designers have been widely studying bamboo as an eco-friendly building material. In ancient China, people used the excellent bending properties of bamboo to weave it and made many nonlinear living utensils. With the improvement of science and technology, modern architects explore nonlinear bamboo architecture or bamboo construction design. However, the specific growth and non-standard bamboo pose many parametric bamboo architectural design challenges. This paper will compare and analyze the traditional construction and multi-technology cooperative mode of Diecui Gallery bamboo pavilion and bamboo chair and discuss a new parameterized bamboo architecture design workflow. The design form of the bamboo gallery is nonlinear and parameterized (Fig. 1).



Figure. 1. The bamboo pavilion "Diecui Gallery"

2. Background

Chaozhou-Xidong Cooperative, which is located on the bank of Han River, has an ideal ecological environment. Bamboo is rich in local resources, with green, low-carbon, beautiful, fast growth, and excellent characteristics. Furthermore, a group of experienced and skilled bamboo craftsmen, the local traditional bamboo craft industry is developed.

There are flowerbeds, farmland, and riverside culture here, which attracts many tourists to sightseeing. However, the purely natural environment lacks rest space with humanistic flavor, and tourists lack a structure to protect themselves from the sun and rain and enjoy tea in the process of playing here. In order to be in harmony with the natural environment, we designed a bamboo pavilion called Diecui Gallery for the small town of Xidong in Chaozhou based on local materials.

Through parametric construction, a modern-style bamboo promenade was designed. Through careful material selection, cutting, forging, splicing, and joint efforts by local bamboo masters, we have worked together to solve many problems to successfully build a bamboo promenade and quickly put it into use. We explored the reasons for the decline of local bamboo architecture. Firstly, the local design works are too traditional and unattractive; the automation level of the construction process is low, and the production efficiency is low. Secondly, the material selection takes too long and wastes a lot of staffing and material resources; the utilization rate of non-standardized bamboo materials is low, resulting in much material waste. In order to

help the local bamboo industry revitalize and promote bamboo culture, we will discuss a new multi-technology fusion processing flow.

3. Traditional construction methods and limiting factors

To understand the traditional construction process (Fig. 2), designers used video recording equipment to record the whole process and count the time needed for each stage. The analysis found that it took the longest time in the material selection and design communication stage (Fig. 3). The reason is that the utilization rate of bamboo is low, always looking for suitable bamboo but wasting bamboo at hand.



Figure. 2&3. Construction process and schedule

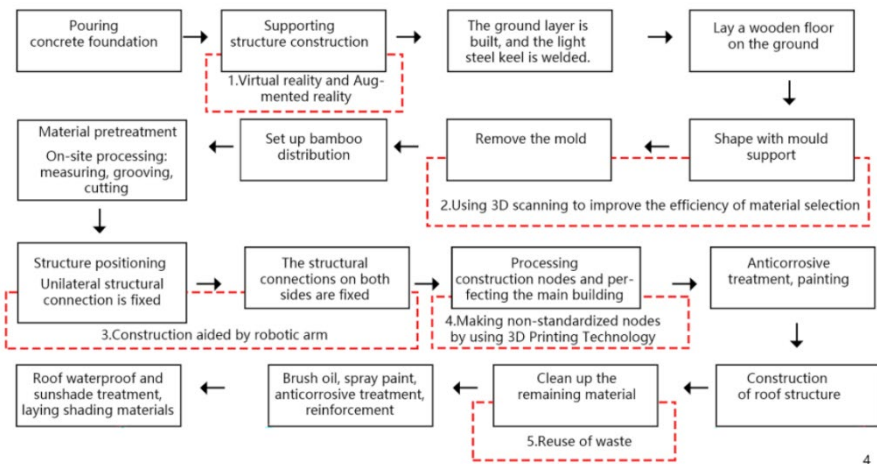


Figure. 4. Five restrictive factors in the process of construction and the digital technologies to solve them

Five factors restrict the construction speed of parametric bamboo buildings in the whole construction process. We have found five digital technologies to optimize these problems (Fig. 4).

3.1. DIFFICULT POSITIONING OF SUPPORTING STRUCTURE

When building a more complex building shape, it is usually necessary to determine the location of the main structure or the main force-bearing structure. Significantly, there is broad variation in the material properties of bamboo, and reducing errors when using unskilled labor is difficult (Imanishi. N. et al., 2017). Once the main load-bearing structure is mislocated, it may lead to the failure of the whole construction. However, due to the irregular and non-standardized form of parametric design, the location of the main stress structure is a complex problem to solve. When the curve's shape is found in space, the positioning will be much more difficult. In this regard, some scholars try to use augmented reality technology and mixed reality technology to locate the parameterized shape in space. ARgan is a geometrically complex bamboo sculpture that relied on Mixed Reality (MR) for its joint creation by multiple sculptors and used the latest Augmented Reality (AR) technology to guide manual fabrication actions (Goepel & Crolla, 2020).

3.2. LOW EFFICIENCY OF MATERIAL SELECTION AND MATCHING

The second problem lies in the selection of materials. In the process of building parametric buildings with bamboo as the primary material, because the length, coarseness, and curvature of each bamboo are different, operators often spend several times to find a large number of bamboo and select the right size of bamboo. As the selection of materials takes much time, it takes a long time to wait for the next step of construction after the foundation construction, which seriously reduces the speed of construction. In order to improve the selection efficiency and model matching degree of non-standard bamboo materials, Katie MacDonald uses sensing, scanning, and other feedback techniques to explore new opportunities that may arise in the field of non-standard materials. To better understand the natural changes in diameter, straightness, and cross-sectional area, they created a catalogue of pole attributes, which were then calibrated using a 3D scanning system (Katie. M. 2019).

3.3. SLOW PROCESSING SPEED OF MATERIALS

The third factor that restricts the speed of construction is material processing. The parameterized design contains mathematical rules and has strong logic. Therefore, the material processing process has a lot of repetitive work, such as slotting, drilling, bending, grinding, etc. However, the local bamboo master still uses the traditional manual operation without any mechanical automation means, which will bring some problems: firstly, the pure manual operation often depends on the work experience of the constructors, and different builders have different experiences, which leads to errors in the processing of materials. The building must be overturned and redone when the error is too large to be resolved. It will waste builders' time and energy. Secondly, designers will make a series of parameter adjustments when carrying out parametric design, which leads to different sizes of each groove or curvature of each bamboo, and the builders are unable to accurately measure the curvature or the size of the notch,

which makes it difficult to build buildings. Based on these problems, studies are done towards the auxiliary construction of the manipulator, through the algorithm to control the manipulator can accurately cut or bend and other operations. These methods will significantly increase the possibility of parametric design landing. Pradeep Devadass elaborated a method of robot positioning and machining non-standard wood components in the Wood Chip Barn project by the students of design + Make at the Architectural Association's Hooke Park campus (Pradeep. D. 2016).

3.4. NON-STANDARDIZED JOINT CONNECTION

The fourth problem belongs to the problem of joint connection. At present, the main joints used in bamboo construction are binding connection + mortise connection, bolt connection, sleeve connection, groove connection, metal belt or U-shaped iron plate connection, prefabricated metal connection, and cast-in-place cement connection. The joints of parametric design are usually not uniform and non-standardized. The binding connection will lead to poor structural stability, and the joints need to be regularly overhauled and replaced. The use of bolt connection is easy to cause the bamboo to crack along the grain direction, and it is easy to cause construction error when opening holes. Sleeve connection requires high unity and standardization of bamboo diameter, which is contrary to parametric design and material properties. Connecting with metal belts will reduce the structural stability. The use of prefabricated metal parts can effectively reduce the difficulty of construction. However, the loosening of metal components can quickly reduce structural strength, and non-standard metal components will increase the construction cost. The method of pouring cement connection is not easy to control the amount of cement, and the joint can not be adjusted after fixed. It is not suitable for flexible parametric design. We can understand the limitations of applying these joint processing methods to parametric design through the above analysis. Therefore, ETH's design team developed a new bamboo connection system based on 3D printing technology (Kladefira, M. et al., 2021). The generation of the connections was automated thanks to a digital process and developed to fulfil mechanical requirements.

3.5. LOW UTILIZATION RATE OF NON-STANDARD WASTE MATERIALS

The fifth problem is the reduction of waste materials and waste utilization. Parameterized bamboo buildings consume much bamboo of different sizes. Due to the unique properties of parametric design and the material characteristics of bamboo itself, there will be a surplus of bamboo of different sizes in the processing process. On the one hand, to reduce the waste of materials, we need to rethink the logic of parametric design. At the beginning of construction, we should consider a series of waste problems and seek effective design methods to improve material utilization.

On the other hand, it is necessary to balance design innovation and material characteristics. The characteristics of parametric design should not be sacrificed to pursue the efficient use of materials. This requires us to consider the reuse of non-standardized components in the construction stage, redefine the allowable range of errors in the material processing stage and try to eliminate and balance the errors in the processing and construction stages by design means. The TOROO project effectively

absorbs accidental errors in the construction process and challenges the construction environment under highly unpredictable conditions (Crolla & Goepel, 2020).

3.6. MULTI-TECHNOLOGY FUSION WORKFLOW

We have summarised five related digital construction technologies through a critical analysis of traditional construction workflows and literature review. The multi-technology convergence construction workflow is a free combination and optimization of these five digital technologies. The multi-technology fusion workflow has many irreplaceable advantages: firstly, we can freely combine different digital technologies according to the constraints of a specific project, increasing the flexibility and diversity of the workflow; secondly, the combination of two or more different digital technologies can significantly improve construction efficiency and reduce construction costs; thirdly, the synergy of multiple digital technologies opens up the possibility of industrial production of parametric bamboo buildings. Thirdly, the synergy of multiple digital technologies opens up tremendous possibilities for the industrial production of parametric bamboo buildings (Fig. 5).

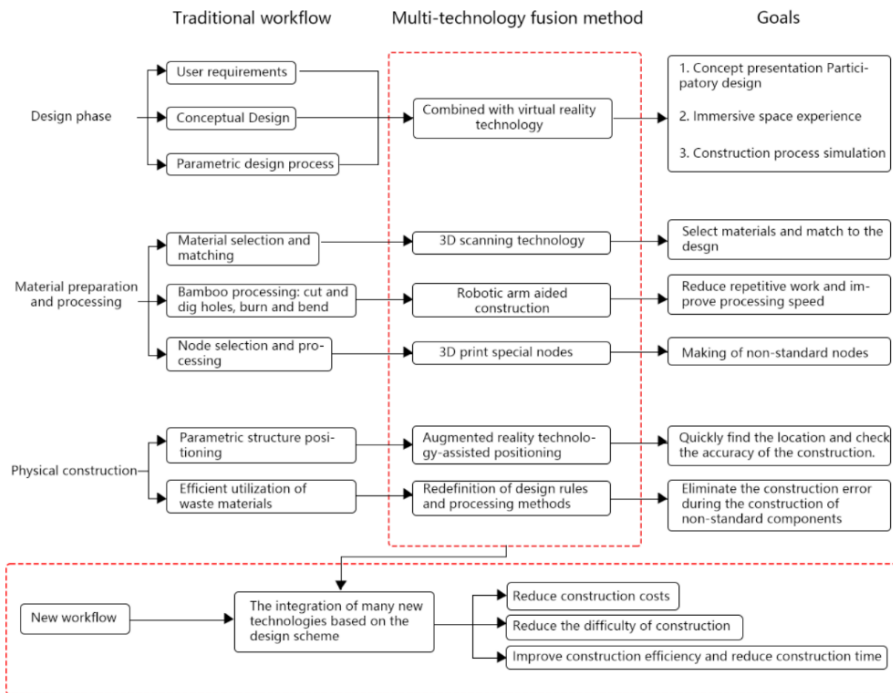


Figure 5. Traditional construction methods and multi-technology fusion workflow.

4. Exploration of Multi-Technology Fusion Workflow

For the Diecui gallery, to provide people with rest facilities. We designed a parameterized bamboo chair throughout the experience of building the Diecui gallery.

We designed a bamboo chair unit under each bamboo pavilion, the length of each bamboo chair unit is 5m, and the whole chair is composed of seven bamboo chair units. For designers, the logic of form generation can be clearly expressed in grasshopper. However, it is not easy to convey the whole form generation logic and construction model accurately to the bamboo master.

At first, we showed the expected construction effect to the workers in drawings and 3D models. Nevertheless, the chairs built are far from satisfactory (Fig. 10 stage1). Because of the limited cultural level of the builders, they can not accurately understand the generative logic of the designers. They can not consider the parametric design with multiple variables when machining chairs. Therefore, we have to rethink how to convey the designer's intention accurately and clearly express the construction logic to the builders. Finally, we use augmented reality technology to assist the construction and eliminate the size error through the new design method.

4.1. DESIGNER'S INTENTION: UNIT-HANDOVER-POSITIONING-CONSTRUCTION

4.1.1. Unit and handover combination

On the one hand, there is a size limitation for the bamboo material used as structural support, and each bamboo can be used as a load-bearing member for a portion of about five meters. On the other hand, for the sake of easy construction and transportation, we divide the chair nearly 40 meters long into seven units for construction; each unit is 5.6 m (Fig. 6). The back part of each unit is natural bamboo, which is tied and inserted between the backs of the chairs by twine (Fig. 7). The back part of the chair can use the leftover material after processing.

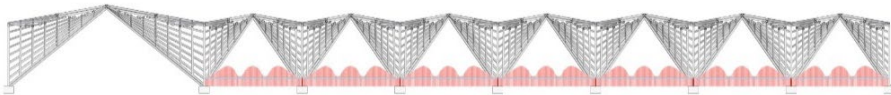


Figure 6. Unit

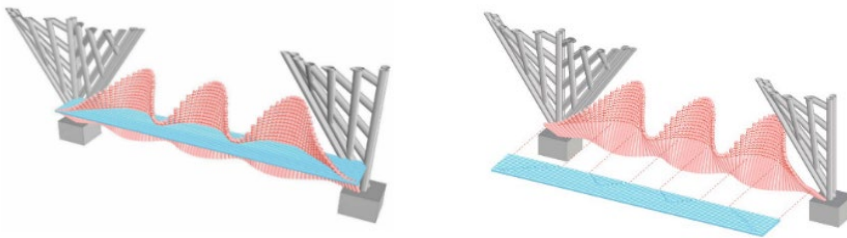


Figure 7. Handover combination

4.1.2. Eliminate dimensional error

In addition, the back of each unit is made of 92 bamboos, each with a diameter of about 6 cm. Since bamboo is a non-standard material, we had to consider the possible dimensional errors of non-standard materials in the design phase. Therefore, we chose to leave a redundant space between two units to dissipate dimensional and construction errors (Fig. 8).

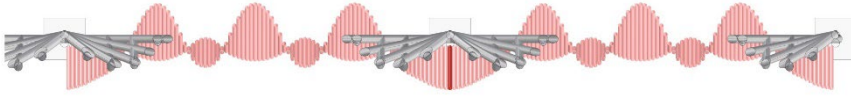


Figure 8. Eliminate dimensional error

4.1.3. Positioning and construction in the traditional way

In order to locate the bamboos, we numbered each unit's bamboos from left to right sequentially as 1-92 (Fig. 9). In addition, the bottom center of the first bamboo on the left (near the inner measurement of the pavilion) was used as the origin to determine the relative position of the bottom centers of the remaining bamboos. As shown in Figure 12, (0.060, 0.006) represents: the position of the bottom center of this bamboo is shifted 0.060 m to the right and 0.006 m upward (near the inner side of the pavilion) relative to the first one. The logic of the cell morphology generation is the same for each. In addition to the variable of relative position, the length of the bamboo and the angle of inclination are the other two variables of the chair. Again, we numbered each bamboo in order from left to right as 1-92. As shown on the right side of Figure 12, within the chart (0.838; 76.1°) stands for: this bamboo has an angle of 76.1° with the ground and a length of 0.838m.

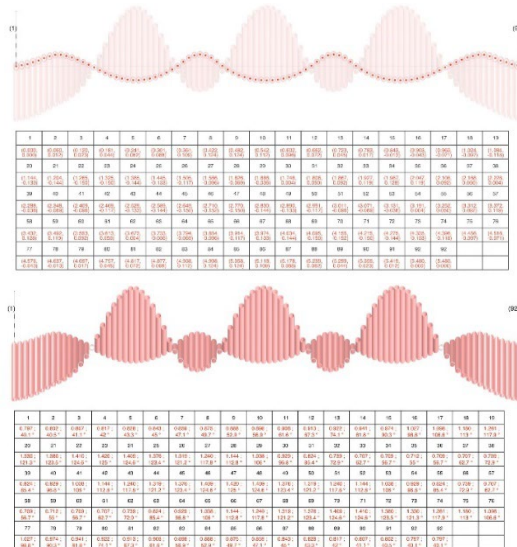


Figure 9. Positioning and construction in the traditional way

4.2. MULTI-TECHNOLOGY FUSION CONSTRUCTION METHOD

Building builders based on traditional experience is a standard form, and even if they have drawings and text descriptions to help them understand, they will still build the wrong form (Fig. 10 stage 1). Using HoloLens can help people understand the shape or position of the target intuitively and interactively (Fig. 10 stage 2 & 3). It helps achieve the visual effect of parametric design without drawings or is challenging to understand. AR provides an intuitive visual display for the builders accustomed to the traditional technology, such as the bamboo master in Chaoshan.

In a parameterized bamboo structure, the builders use the AR model to assist the positioning and installation of the bamboo structure, which avoids the missing and wrong installation of the bamboo structure members and ensures the integrity of the bamboo structure installation. For bamboo buildings with a high degree of parameterization and special-shaped bamboo structures, AR-aided construction is precise at a glance, which dramatically improves construction efficiency from a visual point of view. There is no need to flip through the drawings. By integrating improved design methods and augmented reality technology, the accuracy and speed of construction are effectively improved (Fig. 10 stage 4).

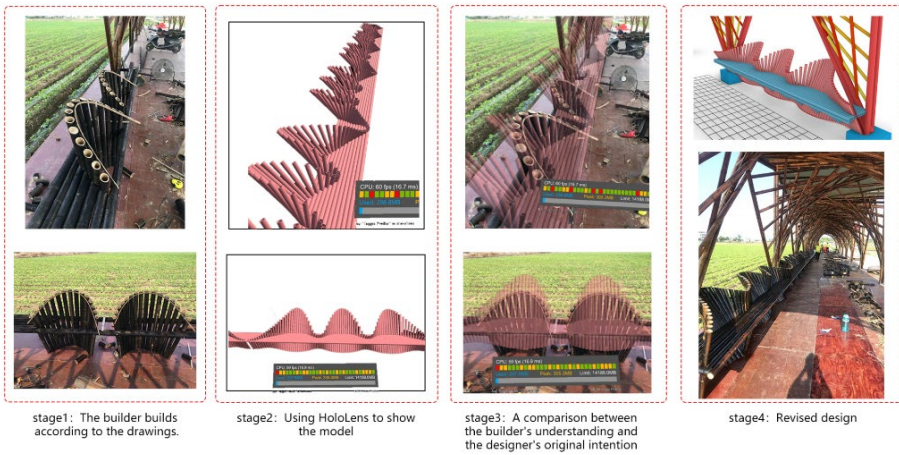


Figure 10. Exploration of Auxiliary Construction of augmented reality

5. Conclusion

The geometric shape of the parameterized bamboo building is complex, and each bamboo pole's shape, size, and structural properties are unique. The traditional construction methods use professional intuition and construction experience for material selection and processing. It is not easy to ensure the applicability and coordination of materials in this process. There are many contradictions between nonlinear parametric design and irregular non-standardized bamboo from design to material selection and processing and construction. For example, in material selection, the master has to spend much time selecting the appropriate scale and similar structural properties of bamboo for processing, which wastes a lot of time and energy. In the construction process, bamboo components of different scales dazzle the bamboo

master, and it takes a long time to find matching components.

After analysis and summary, five limiting factors limit the industrial construction of bamboo buildings, but each limiting factor should have relevant solutions. The workflow of multi-technology collaboration is to be combined by adaptive technical means according to different projects. These technologies include augmented reality technology, 3D scanning, 3D printing of non-standard components, robot-aided construction, and non-standard material design systems. Because these technologies have their limitations, it is necessary to integrate them and work together to improve the production efficiency of bamboo buildings and reduce their processing costs. Last but not least, we will build a series of bamboo buildings for Chaozhou. We will constantly improve the collaboration of multi-technology integration workflows to build different parameterized bamboo buildings. We will also contribute to the industrial production of bamboo buildings.

Acknowledgements

This research was supported by the following funds: Later Funded Projects of National Philosophy and Social Science Foundation of China (No. 19FXWB026); Youth Project of National Natural Science Foundation of China (No. 51908158); Higher Education Research and Reform Project of Guangdong Province (No. HITSZERP19001); General Project of Stabilization Support Program of Shenzhen Universities (No. GXWD20201230155427003-20200822174038001); Shenzhen Excellent Science and Technology Innovation Talent Training Project (No. ZX20210096).

References

- Crolla, K., & Goepel, G. (2020). Designing with uncertainty – *Objective vibrancy in the TOROO bamboo pavilion*. *25th International Conference on Computer-Aided Architectural Design Research in Asia: CAADRIA 2020* (pp. 507-516). The Association for Computer-Aided Architectural Design Research in Asia (CAADRIA)
- Devadass, P., Dailami, F., Mollica, Z. & Self, M.(2016). Robotic Fabrication Techniques for Material of Unknown Geometry. In (pp. 206-213).
- Goepel, G. & Crolla, K., (2020). Augmented reality-based collaboration: ARgan, a bamboo art installation case study. *25th International Conference on Computer-Aided Architectural Design Research in Asia: CAADRIA 2020* (pp. 313-322). The Association for Computer-Aided Architectural Design Research in Asia (CAADRIA).
- Imanishi, N., Hinoki, S., Muraoka, M., Tateyama, R., Abe, U., Kensuke, H., & Ikeda, Y. (2017). BAMBOO CONCRETE SHELLS: An Adaptable Construction Method Using Onsite Materials in a Remote Location. *Protocols, Flows and Glitches, Proceedings of the 22nd International Conference of the Association for Computer-Aided Architectural Design Research in Asia (CAADRIA) 2017*, 445-456. The Association for Computer-Aided Architectural Design Research in Asia (CAADRIA), Hong Kong.
- Kladeftira, M. (2021, September 29). *Digital bamboo*. ETH Zurich. Retrieved December, 2021, from <https://dbt.arch.ethz.ch/project/digital-bamboo/>.
- MacDonald, K., Schumann, K., & Hauptman, J. (2019). *Digital Fabrication of Standardless Materials*.

SOFTNESS AND HARDNESS: WHAT DOES CONCRETE WANT?

Concrete physical form finding based on computational combined formwork

CE LI¹, ZHE GUO², CHENGZHI CAI³, JUNYI MIAO⁴, XIAOYU CAO⁵, CONG LI⁶, YEFEI GUO⁷, QINGNING CAO⁸, ZIFEI ZHENG⁹, YUCHEN GUO¹⁰, WANLING WU¹¹, ZHIYAN XU¹² and XINYAN ZHOU¹³

¹Wuhan University, ²Hefei University of Technology.

³⁻¹³Studio Alpha Math Lab.

¹26650299@qq.com, 0000-0002-6290-4297

²guogal@hotmail.com, 0000-0002-7660-0622

³394658940@qq.com, 0000-0002-7230-2695

⁴miaomiao789@ucla.edu, 0000-0003-1500-9350

⁵bb52121591@ms.nagasaki-u.ac.jp, 0000-0002-5741-4787

⁶cli07@risd.edu, 0000-0002-2168-3547

⁷yefei.guo@columbia.edu, 0000-0001-5000-3099

⁸qc2290@columbia.edu, 0000-0002-6238-130X

⁹zifei.zheng@cooper.edu, 0000-0003-3052-4422

¹⁰gyuchen@umich.edu, 0000-0002-9323-9170

¹¹wu.wanling@aaschool.ac.uk, 0000-0003-1324-9879

¹²xxxxzy_1224@berkeley.edu, 0000-0003-1738-0284

¹³503081729@qq.com, 0000-0002-1038-6205

Abstract. This project proposes a physical form finding design method by generating concrete flexible formwork through digital algorithm, which aims to explore the potential formal correlation between real material as the medium of transmitting information in physical space and virtual data, so as to discuss the autonomy and intelligence of material under the support of digital design technology. The first part of this paper first discusses the current situation of the application and development of concrete materials in the field of digital construction in recent years, and then studies the adaptability of flexible formwork to the flowable characteristics of concrete materials; Then, the second part puts forward the moulding method of concrete physical shape finding through flexible and rigid composite formwork, and tries to explore the influence of formwork shape under the control of digital algorithm on this process; The third part of the paper records the process of concrete moulding experiment under this method to discuss the internal relationship between the physical form of concrete and combined formwork.

Keywords. Physical Form Finding; Textile Concrete Formwork; Material Attributes; Concrete Fabrication; SDG 9.

1. Background

1.1. CONCRETE APPLICATION IN DIGITAL FABRICATION

As an ancient building material, concrete has been used for thousands of years in human civilization. In the field of digital design, concrete material is used by many research teams for innovative application research of digital construction because of its unique material properties and cheap raw material sources.

The application of concrete in digital construction mostly focuses on additive manufacturing technology. In these studies, the layered 3D printing manufacturing process is carried out by loading the concrete extruder with a robotic arm (see Figure 1. a) (Breseghello et al., 2021) (Ahmed et al., 2016). The ETH BRG research team led by Philippe block proposed a textile fabric template as the basic flexible material for curved plastic shape, and then sprayed the concrete evenly on the fabric surface to form a curved weighing structure (see Figure 1.b) (Popescu et al., 2018). Early to 2001, compared with those innovation manipulation with concrete, in the research history about the application of textile concrete formwork, Mark West has applied a new construction method replacing rigid formwork panels with a flexible textile membrane that deflects under the dead weight of wet concrete in both advanced and basic building economies, which provides numerous advantages and opportunities for architecture, engineering, and construction technology (see Figure 2.c) (West, 2001). Years later, Andrew Kudless proved the point focused on flexible formwork castings are resonant with material energy which borne from the complex negotiation between liquid mass and tensile constraint, by fabrication series of precast architectural assemblies. (see Figure 2.d) (Kudless, 2011). Besides, in the 2019 digitalFUTURES workshop held in Tongji University, the group “computational design and engineering of tensioned formworks for concrete shells” using waterproof fiber cloth as double curved structural formwork and moulding concrete into the cavity between two layer (see Figure 1. e).

1.2. CONCRETE MATERIAL ATTRIBUTE

Up to now, the dialogue between Louis Kahn and brick is a very classic discussion in the architectural field on exploring the construction form and following the material properties. When he asked “*what be brick want*”, he not only focused on how to maximize the effect of the physical properties of brick materials in the structural stress, but also put forward a way to reorganize the traditional architectural elements, which can tap the aesthetic value in the formal rationality of materials. Such as the hypothetical conversation between Kahn and brick, our project also focuses on how to innovate the structural form by using the material properties of concrete.

Concrete material is mainly divided into two stages and states: the fluid state before setting and hardening, that is, fresh concrete or concrete mixture; The hard state after hardening, this special state change gives concrete unparalleled application expansibility (Akçay et al., 2020). By virtue of the fluid properties of concrete, the flexible formwork is applied in this project as the boundary of wrapping concrete. In this way the concrete will form a natural solid form after it's drying under influence by gravity. The flexible formwork discussed here refers fabric formwork which is a construction technique that involves the use of structural membranes as the primary finishing material for concrete molds (Veenendaal et al., 2011). Unlike traditional rigid formwork, this material is highly flexible and can deflect under the pressure of fresh concrete. Early in 2008, Remo Pedreschi discussed the relationship on a conceptual and methodological level between form, force and mass (Pedreschi, 2008). Along these methodology, whose research group has explored series of flexible formwork technologies that embrace the fluidity of concrete to facilitate the practical construction of concrete structures with complex and efficient geometries (Hawkins et al., 2016). The resulting form exhibits curvature as well as good surface treatment, which is usually independent of concrete structures. The use of fluid responsive formwork is a technique of constructing which allows the behaviour of material to engage with and influence the building process itself.

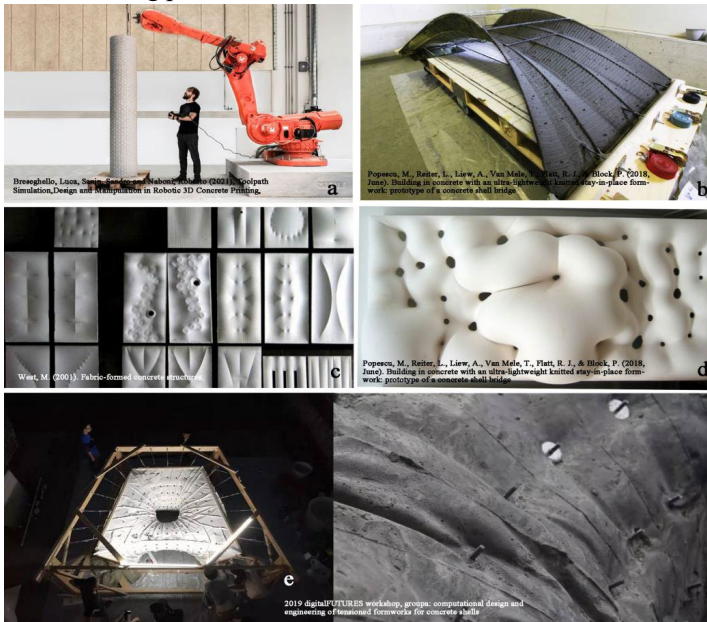


Figure 1. a-Bresghehlo, Luca, Sanin, Sandro and Naboni, Roberto (2021), Toolpath Simulation, Design and Manipulation in Robotic 3D Concrete Printing; b-Popescu, M., Reiter, L., Liew, A., Van Mele, T., Flatt, R. J., & Block, P. (2018, June). Building in concrete with an ultra-lightweight knitted stay-in-place formwork: prototype of a concrete shell bridge; c-West, M. (2001). Fabric-formed concrete structures; d-Popescu, M., Reiter, L., Liew, A., Van Mele, T., Flatt, R. J., & Block, P. (2018, June). Building in concrete with an ultra-lightweight knitted stay-in-place formwork: prototype of a concrete shell bridge; e-2019 digitalFUTURES workshop, groups: computational design and engineering of tensioned formworks for concrete shells

2. Method

2.1. WORKFLOW

Physical form finding requires simulation experiments under the condition of controlling some constraints, which means a experiment-based study process. Exploration of three key parts are carried out in turn, namely testing flexible forms and characteristics of concrete under formwork restriction, conducting combination relationship between rigid and flexible formwork and the bard boundary shape design of rigid formwork itself, next in the process arrangement of the moulding process, especially the flexible formwork set, which needs to give full space for concrete.

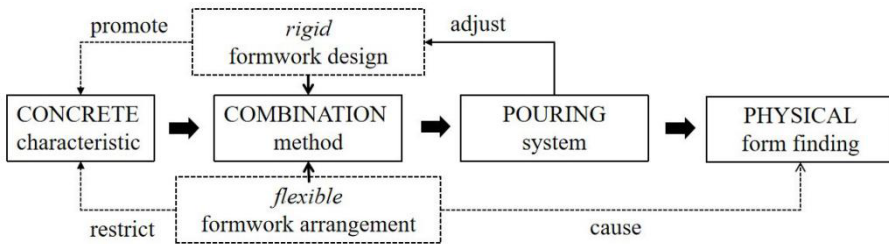


Figure 2. Workflow

In the workflow shown in the Figure 2, the combination of formwork is the key content of this research, which is determined by rigid and flexible formwork respectively. Flexible formwork will comply with the flow force of concrete and limit the movement of that according to its elasticity. On the contrary, rigid formwork will restrict the movement of concrete, limit it to a certain flow range and form a clear boundary on the edge of soft and hard boundary. The results of physical finding are all influence by fabrication process, which should be designed according to the expectation.

2.2. PHYSICAL FORM FINDING METHOD

In the preliminary study of concrete physical form finding, a simple square cylindrical is built for moulding concrete with rigid formwork surrounding outside (using wood board as the hard boundary of) and flexible formwork (using nylon stockings as the soft boundary) placing in inside. In the middle of these two frames, another hard shape of PVC circular pipe was also inserted. By adjusting the diameter and insertion height of the circular pipe and the geometric relationship between pipes (as shown in the diagram on the left of Figure 3). Together integrating into a complete concrete moulding mold, two materials with different physical properties constitute a complete composite formwork. According to its modeling characteristics, one wire is buried inside the concrete to create the support of the lamp.

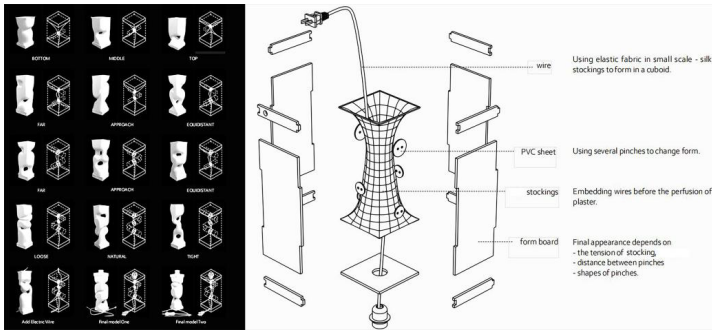


Figure 3. Simple square cylindrical poring formwork

Through the combined formwork, the fluid concrete flows slowly and uniformly under the influence of its own gravity and rigid formwork pressure under the wrapping of flexible materials. This physical system finally achieves a force balance so that concrete can be given full play to its advantages of material characteristics and presents a seemingly soft form. Using this method, several combination method of flexible and rigid formwork are explored in further experiments (shows in Figure 4). Since the same Lycra fabric was used in the subsequent experiments, there was a certain formal similarity in the form finding results formed by different formwork templates.

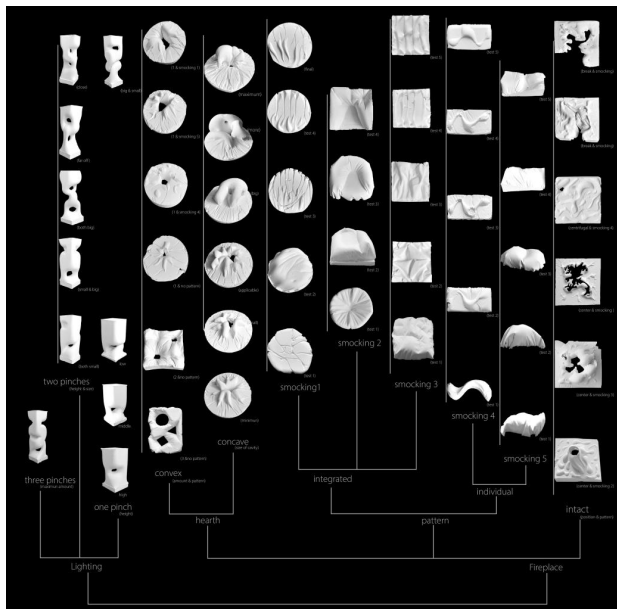


Figure 4. Physical form finding by combined moulding formwork

2.3. PARAMETRIC DESIGN FOR RIGID FORMWORK PATTERN

In the boundary pattern design inside the rigid formwork, a parametric generation method of Differential Growth rules is used to create the edge between flexible and rigid formwork. Shows in the Figure 5, through the form finding research on the design of several boundary forms, by using the hard formwork cut by several different boundary shape shows in Figure 5 right side to carry out the concrete shape finding experiment, the boundary shape shown on the left side of Figure 5 is finally obtained, and its size and geometry characteristics are more suitable for flexible physical finding.

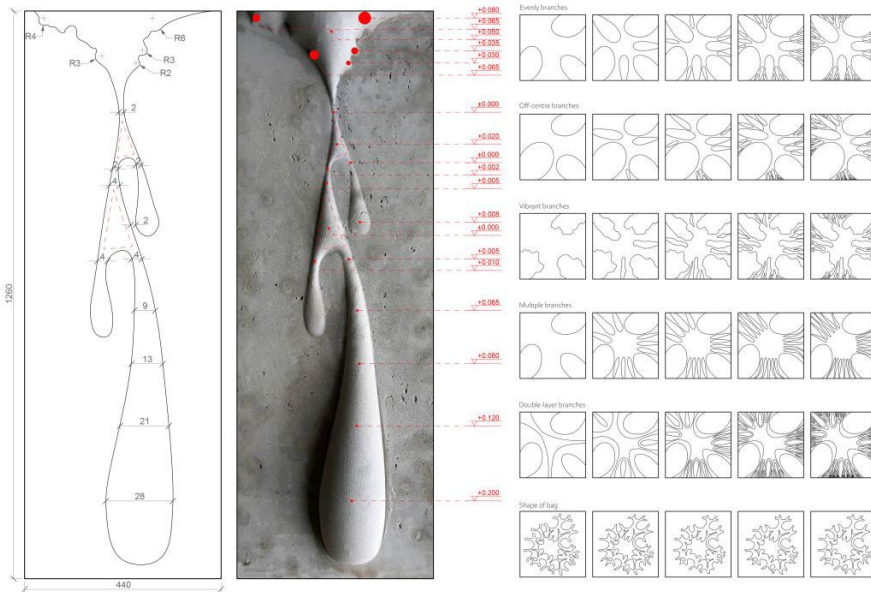


Figure 5. Logic of pattern design and experiment test result

3. Fabrication

3.1. FABRICATION SYSTEM

The fabrication process includes pattern design of form finding rigid template and construction of supporting frame. Due to the functional requirements of this design is to make a table that can support multiple barbecue pots, a central hole is required which means the rigid pattern formwork that will applied in the centre of the whole frame should be considered in the process of design (see figure 6, in this part one rigid wooden plank is applied between two elastic fabrics in order to limit the natural flow of concrete).

The diagram in Figure 6 shows the horizontal relationship between the formwork structure. From the top to bottom, the hanger is used to tie with the elastic fabric. A pinch is created in the centre part of the formwork in the order of wood plank, elastic fabric, second wooden plank, the second layer of elastic fabric, third wood plank. The concrete is moulding in between two layers of elastic Lycra fabric. The supports in the bottom of the formwork is used to protect the pinch and the main pattern from broken.

The main structure of the formwork consists of one layer of 9-mm-thick wood plank and a layer of elastic fabric. Other parts of it is built by 9-mm-thick plank which are cut in the factory then transported to the site. The bearing structure is the vertical wood planks around sides, which are strengthened by central symmetrical structure forming beams along sides. The elastic fabric is hung on the beam upon it by nylon cable ties. The plate pinch in the middle is hang on the beam by steel strand. The concrete is poured from those four sides and the final total weight of concrete is over 300 kg.

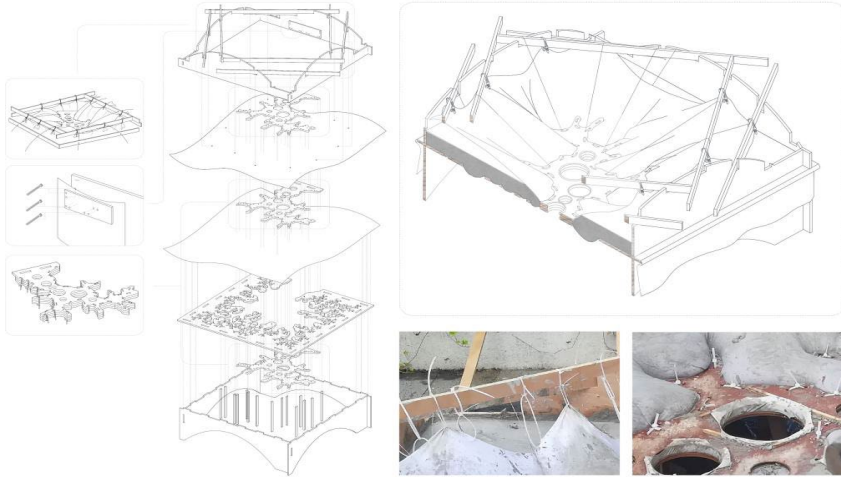


Figure 6. Supporting frame design

3.2. FABRICATION PROCESS

The complete fabrication process is divided into four steps (shows in Figure 8). Under the restraint of the upper and lower layers of fabric and the extrusion of the middle rigid formwork, the concrete presents the physical phenomenon of natural flow, and the final hardening is shown in the Figure 9.

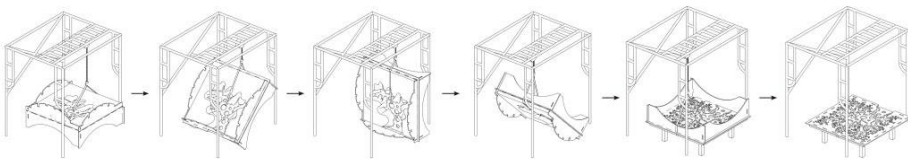


Figure 7. Exploded diagram of scaffold flipping

- Formwork installation in order
- Moulding concrete between two layer of Lycra fabric (see Figure 6)
- Flipping after concrete hardening (see Figure 7)
- Dissemble the whole supporting frame



Figure 8. The fabrication process



Figure 9. Form finding result with parametric generated pattern

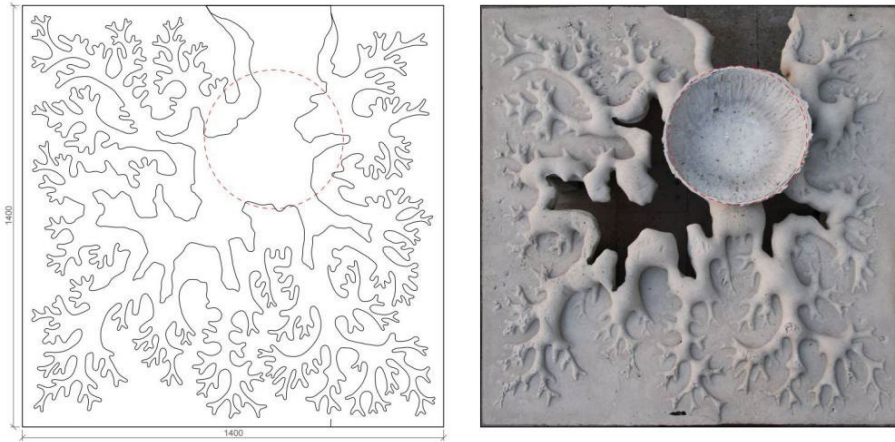


Figure 10. Form detail

4. Conclusion

The use of fluid responsive formwork is a technique of constructing which allows the behaviour of material to engage with and influence the building process itself. In this project, the construction practicability of this method is discussed by applying a combined formwork with flexible and rigid. Under the restriction of rigid formwork generated and processed by digital tools, the state of concrete combines the free flow characteristics of its own material attribute and the control of the physical attributes under the restriction of combined formwork. It is obvious from the experimental fabrication results that this form finding system has great expansion potential by change rigid pattern edge shape and the relation between two type of formwork. Interestingly, before the concrete moulding experiment based on the form finding method proposed in this study, there is no clear use of functional significance to endow this structure, from that a new concept of "form follows fabrication" could be draw.

Acknowledgements

Thanks to all those who provide help during the research of this project. First the thanks would go to Junyi Miao, Qingning Cao, Wanling Wu, Zhiyan Xu, Xiaoyu Cao, Cong Li, Zifei Zheng, Yuchen Guo, Yefei Guo, Xinyan Zhou. They are the main student members of the workshop, besides construction of the final project, they also draw most beautiful diagrams in this paper. Secondly, the deepest gratitude goes to Chengzhi Cai, who manage the whole process of the workshop and provide the site and the opportunity of making the design real. Finally, we really appreciate writing help from Zhe Guo, the corresponding author of the paper.

References

Ahmed, Zeeshan Y.; Freck P. Bos, Rob J.M. Wolfs and Theo A.M. Salet (2016). Design Considerations Due to Scale Effects in 3D Concrete Printing. *Parametricism Vs.*

- Materialism: Evolution of Digital Technologies for Development [8th ASCAAD Conference Proceedings* (pp. 115-124).
- Akçay Kavakoglu, Aytegin, Beyond Material - Digital Tectonics of Fabric and Concrete. Werner, L and Koering, D (eds.), *Anthropologic: Architecture and Fabrication in the cognitive age - Proceedings of the 38th eCAADe Conference* (pp. 89-96), TU Berlin, Berlin, Germany, 16-18 September 2020,
- Brescghello, Luca, Sanin, Sandro and Naboni, Roberto (2021), Toolpath Simulation, Design and Manipulation in Robotic 3D Concrete Printing, A. Globa, J. van Ameijde, A. Fingrut, N. Kim, T.T.S. Lo (eds.), *PROJECTIONS - Proceedings of the 26th CAADRIA Conference - Volume 1, The Chinese University of Hong Kong and Online* (pp. 623-632), Hong Kong.
- Hawkins, W. J., Herrmann, M., Ibell, T. J., Kromoser, B., Michaelski, A., Orr, J. J., ... & West, M. (2016). Flexible formwork technologies—a state of the art review. *Structural Concrete*, 17(6), 911-935.
- Kudless, A. (2011). Bodies in formation: The material evolution of flexible formworks. *ACADIA 11: Integration through Computation Proceedings of the 31st Annual Conference of the Association for Computer Aided Design in Architecture (ACADIA)* (pp. 98-105).
- Veenendaal, D, West, M and Block, P (2011) History and overview of fabric formwork: Using fabrics for concrete casting , *Structural Concrete*, 12, 164-177.
- Popescu, M., Reiter, L., Liew, A., Van Mele, T., Flatt, R. J., & Block, P. (2018). Building in concrete with an ultra-lightweight knitted stay-in-place formwork: prototype of a concrete shell bridge, *Concrete In Structures*, 14, 322-332. Elsevier.
- Pedreschi, R. (2008). Form, force and structure: a brief history. *Architectural Design*, 78(2), 12-19.
- West, M. (2001). Fabric-formed concrete structures. *In Proceedings First International Conference on Concrete and Development* (pp. 133-142), Tehran, Iran, April.

S.N.O.W_SINTERING TPU VIA NICHROME WIRE

TSUNG-HAN TSAI¹, TING-CHIA CHEN², CHING-WEN HAUNG³,
YEN-CHEN LU⁴ and SHIH-YUAN WANG⁵

^{1,2,3,4,5}*Graduate Institute of Architecture, National Yang Ming Chiao
Tung University*

^{1,2,3,5}{*tsunghan.tsai|tingchia|chinghuang|yuan*}@arch.nctu.edu.tw
¹0000-0002-0995-5845 ²0000-0003-1357-0275 ³0000-0002-1048-
872X ⁵0000-0002-0995-5845

⁴*yclu.roso@gmail.com, 0000-0002-3143-9150*

Abstract. This paper introduces and investigates NiChrome wire sintering, a novel fabrication technique in the field of additive manufacturing. With a combination of differentiated material states and material properties, this research generates forms with different sintering strategies through computation and fabrication systems. Rather than creating objects through selectively depositing melted material in a predetermined path, layer-by-layer, this rapid prototyping methodology generates 2D or 3D spatial wireframes by weaving NiChrome wire and sintering thermoplastic polyurethane (TPU) onto it by utilizing the instantaneous high temperature of NiChrome wire after electrification. A series of experiments is presented utilizing a proportional integral derivative (PID) temperature control system in cooperation with thermal camera equipment to ensure consistent results under the same conditions. In addition, the project focuses not only on developing NiChrome wire sintering systems but also on the applicabilities of this technique by fabricating wireframe surfaces under different situations.

Keywords. NiChrome Wire Sintering; Rapid Prototyping; Elastic Material; Digital Fabrication; SDG 12.

1. Introduction

This research explores the concept of Selective Laser Sintering (SLS) to propose a novel digital fabrication method of sintering TPU powder via NiChrome wire (S.N.O.W) through investigating reciprocal processes between computational design, material experiments, and sintering systems. Compared to the prototyping process of FDM 3D printing, which creates objects through selectively depositing melted material in a predetermined path, layer-by-layer, S.N.O.W generates 2D or 3D spatial

wireframes by weaving NiChrome wire and sintering TPU onto it to demonstrate the possibility of freely generating surfaces. The intent of this paper is to explore the phenomenon of the instantaneous high temperature of NiChrome wire after electrifying and exemplify a unique idea in digital fabrication. To further this study, a series of experimental projects (sintering TPU via NiChrome wire) is presented, which utilized a PID heating system and related fabrication system that rapidly wound and sintered three-dimensional surfaces. In contrast to the general weaving method, which strengthens the structure by layering filaments on top of each other, this experiment focuses on intensifying the overall structure by combining the nodes produced by sintering TPU powder on the weaving NiChrome wire. The sintering temperature is controlled at a fixed range for each sintering result through a PID heating system, and the data from the material study is used to adjust the sintering parameters such as temperature and time to ensure consistent thickness and structural strength of each sintered node under different situations. This paper presents a novel digital fabrication workflow for winding and sintering surfaces through integrating material research, sintering system, and computational design. First, this paper begins by examining existing works and papers that inspired this research. Second, it explains in terms of material research and sintering system including PID temperature control and parallel circuit prevention method. Third, the results of the current experiments. The following are the contributions of this paper. (1) A research of the instantaneous high temperature of NiChrome wire after electrifying, which may create new possibilities in digital fabrication. (2) The results from TPU and NiChrome wire material experiments, the development of PID heating system, 3D sintering method, and pre-3D sintering method. (3) A summary of current progress for further development.

2. Content and Previous Experiment

In recent years, the development of 3D printing has become relatively mature and advanced. However, due to the prototyping method, most 3D printers today are still limited to small printing range and long printing time. Researchers at MIT presented a rapid manufacturing method that could freely print and produce almost any shape by depositing liquid material into a granular gel, in response to the limitations of conventional 3D printers (Hajash et al., 2017). In addition, researchers at TU Wien, KAUST and NJIT proposed a new type of planar-to-spatial portable structure with movable nodes on a flexible bamboo mesh (Pillwein et al., 2020). By changing the position and angle of the nodes, curved surfaces can be quickly generated from the plane, enabling designers to explore forms and structures in a manageable way. These two cases demonstrate different fabrication methods to generate the goal geometric forms in space with effective fabrication process and material utility. Since the 1950s, filament materials have been a promising technology with great potential in constructions. In recent years, many studies have been conducted to find new values for the use of filament materials in digital fabrication. For example, the Research Pavilion 2012 (Knippers et al., 2015) successfully demonstrated the freedom and possibilities of using filament materials in large temporary buildings by using an industrial six-axis robotic arm with a programmed path. On the other hand, Mobile Robotic Fabrication System for Filament Structures (Yablonina et al., 2017) addressed space limitations and insufficient mobility of six-axis robotic arms with the assistance

of mobile robots and demonstrated the possibility of multiple mobile robots cooperating in single fabricating task. In both cases, attempts were made using woven filament materials to develop extremely lightweight structures at a low material waste rate and explore new architectural possibilities. Inspired by these projects, this paper proposes a unique way of sintering powder to form wireframe structures and shows the advantages of this fabrication system, which entails no physical restriction on the build volume. This paper is aimed not only towards the development of weaving and sintering systems, but also the exploration of the elasticity of materials, demonstrating a method to rapidly materialise forms using elastic materials—NiChrome wire and TPU—and exploring the possibilities of this fabricating system.

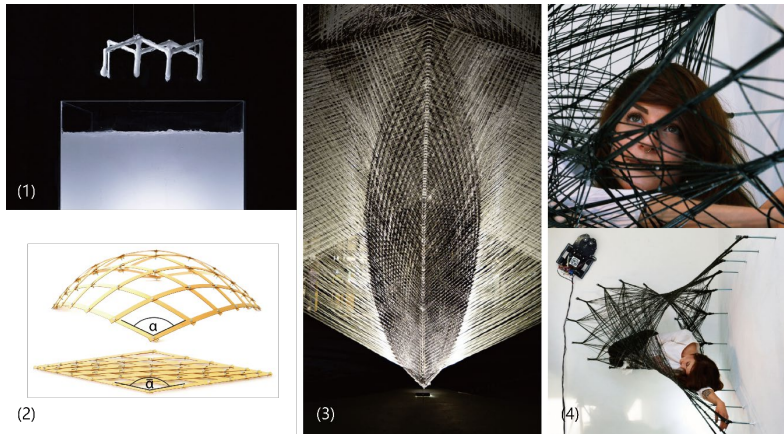


Figure 1. Related works mentioned above.

(1) Large-scale rapid liquid printing (Hajash et al., 2017). (2) On elastic geodesic grids and their planar to spatial deployment (Pillwein et al., 2020). (3) ICD/ITKE research pavilion 2012 (Knippers et al., 2015). (4) Mobile robotic fabrication system for filament structures (Yablonina et al., 2017).

3. Sintering System

The entire system consists of three main parts: the powder tank and mold with anchor points connected to a temperature control system and a thermal camera (Figure 2). Due to the different fabricating methods and purposes, there are two main types of molds: 2D and 3D. The temperature control system mainly includes the power supply, PID, SSR, and a thermal probe to maintain the sintering temperature at a fixed range. The thermal camera is used to visualize the heat distribution and to detect the parallel circuit of NiChrome wire after electrifying. During the fabricating process, the overall form and structure are initially mocked up by weaving NiChrome wire on a mold covered with anchor points. After the winding process is completed, the wire mesh on the mold is electrified and heated. Then, a thermal camera is used to detect whether the intersected wires are in parallel circuit condition, which would cause incomplete or inhomogeneous grid surfaces after the sintering process. Finally, the mold is placed in a powder tank filled with TPU, and the NiChrome wire is heated up to a preset temperature by the sintering system (PID) to sinter TPU on the wire mesh.

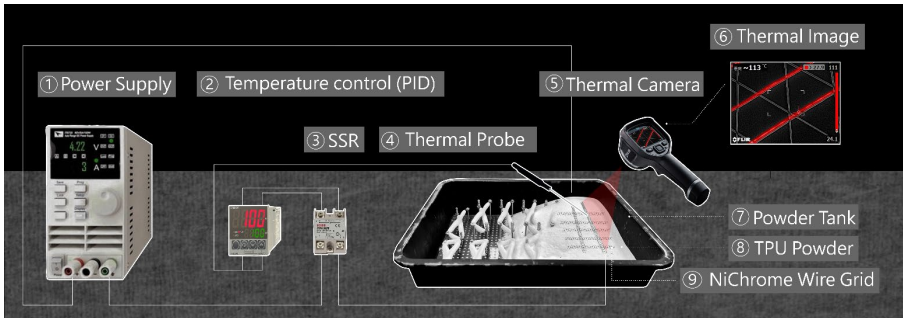


Figure 2. Sintering System.

3.1. TEMPERATURE CONTROL SYSTEM

The method of temperature control system involves three main factors: (1) the length of NiChrome wire, (2) the power supply, and (3) the control and measurement of temperature. NiChrome wire's rapid heating after electrification is widely used in manufacturing processes and commercial products. Under ideal conditions, the relationship between power and temperature of the wire is proportional. To maintain the same temperature, the power supply must be adjusted using different lengths of NiChrome wire. For the power supply, an adjustable DC power supply was used as the output power source for the initial material experiments, and the parameters were adjusted to observe the relationship between temperature and the given power. In the later stage, 110V and 220V AC power were used to heat longer NiChrome wire (>10m) to fabricate larger scale sintering experiments. For temperature measurement and control, a small contact thermal probe with a high-temperature response is used as the temperature measurement tool to accurately measure the temperature change of the NiChrome wire during the sintering process. A PID is then used to maintain the temperature within a precise range to ensure the same results under the same conditions.

3.2. MATERIAL STUDY

In this experiment, Nichrome wire was tested to certify its sintering performance. A power supply was connected to Nichrome wires with different diameters and placed in a tank full of TPU powder. Sintering time and temperature were controlled to establish the basic experimental data for TPU sintering applications. After a suitable sintering diameter of NiChrome wire was chosen, the experiment would proceed to the testing of nodes that were produced by sintering TPU powder on the intersection points of NiChrome wire. The experiments would be divided into two parts as follows.

3.2.1. Selecting proper parameter for sintering

In this part of the material experiment, NiChrome wires with different diameters (0.1mm、0.3mm、0.5mm、0.8mm) were set at a fixed length (15cm) and heated by different power (60W、80W、100W) to certify the relationship between the power supply、sintering time (1 min-10 mins) and sintering temperature (135°C、201°C、270°C) of NiChrome wire and TPU. After a comprehensive evaluation, we concluded

that the NiChrome wire with a 0.5mm diameter heated to 135°C has the most proper TPU sintering capability (Figure 3.1). Although an upward adjustment of the sintering temperature could increase the TPU forming diameter per unit time, a higher sintering temperature would cause a lot more deformation due to the expansion of NiChrome wire caused by the large temperature difference, which also increased uncertainty factors to maintain constant diameter under the same conditions (Figure 3.2, 3.3).

3.2.2. Node Sintering Experiment

In this stage of the experiment, it was found that adjacent NiChrome wires which were intersected generated higher temperatures due to heat concentration (Figure 4.2). This phenomenon generated nodes by sintering the two wires together. To test the correlation between the intersection distance and the sintering temperature, NiChrome wires were cross-winded on four anchor points of the mold at different distances (2mm-20mm) to test how different distances would affect the sintering results (Figure 4.1). In the previous stage of material experiments, a higher temperature difference would cause a lot more deformation due to the expansion of NiChrome wire. If the distance between the intersected wires was too small, the wires would be connected and become a parallel circuit causing incomplete or inhomogeneous sintering results. However, if the distance between the intersected wires was too large, the strength of the sintered node would be insufficient. Therefore, a series of experiments were proposed to solve the inconsistent sintering results caused by parallel circuits.

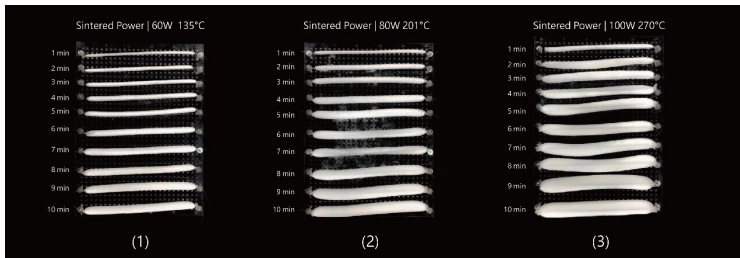


Figure 3. Different temperature's linear sintering results.

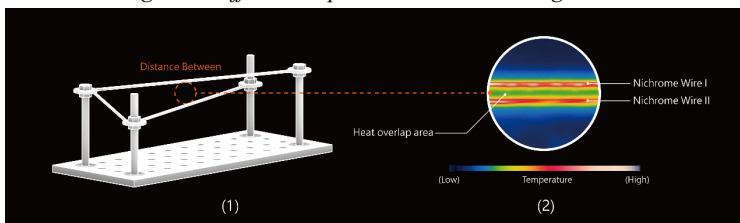


Figure 4. Heat concentration between two NiChrome wires.

3.3. PARALLEL CIRCUIT PREVENTION METHOD

A parallel circuit comprises multiple branches so that the current divides and only part of it flows through any branch. The voltage, or potential difference, across each branch of a parallel circuit is the same, but the currents may vary. Therefore, once the NiChrome wire is connected during the sintering process, the current may vary on each

branch of the circuit resulting in different diameters of sintered TPU. To avoid NiChrome wires connecting and becoming a parallel circuit, the solutions are as follows: (1) Insulating material between NiChrome wire (2) Glass fiber tube wrap NiChrome wire (3) Enameled NiChrome wire. Under ideal conditions, inserting insulating material (PTFE Heat Resistant Tape) between intersected NiChrome wire can prevent parallel circuits. However, the wire will shift and connect easily due to the expansion when it is heated up, which would still cause a parallel circuit. In addition, inserting insulating material into each intersection is an inefficient process. Instead of inserting it between the intersections, another solution is to wrap the whole NiChrome wire with another insulating material (Glass Fiber Tube). Therefore, even if the NiChrome wire is heated up, the glass fiber tube can prevent the whole network from becoming a parallel circuit. Although the glass fiber tube is an effective insulating material, once the scale of the form increases, the length of the wire would make the wrapping process inefficient. Therefore, when the length of NiChrome wire is longer than 10 meters, we use enameled NiChrome wire in substitution for glass fiber tube. With the special insulating coating and high-temperature resistance up to 180°C, the enameled NiChrome wire not only solves the wire being connected but also avoids complicated steps in the fabricating process.

4. Design Experiments

This research explores two sintering strategies to rapidly materialize forms without supports through presenting a series of complex surfaces. These strategies may assist in overcoming the inefficient process and material waste in traditional additive fabricating when facing complex surfaces. The following experiment is divided into two parts to explain the process and differences between the two strategies. (1) 3D sintering method (2) Pre-3D sintering method

4.1. 3D SINTERING METHOD

This study is aimed to represent a complex surface to examine the freedom of the method in generating different forms of geometries. 3D sintering focuses on the formation of 3D objects using custom molds inside a tank of TPU powder. NiChrome wire is then woven along anchor points located on the mold, and TPU is sintered onto it, which creates a surface without using support material, reducing material waste during the process. The overall geometry was a (160cm W by 140cm D by 45cm H) three-sided Hyperbolic Paraboloid surface. In this case, the surface was split into four parts two types (1) Core-Shell (2) Long Span Shell (Figure 5). The fabrication process was as follows (Figure 6). The three edges of the Core-Shell and the four edges of the Long Span Shell were divided into 14 anchor points individually. Using Rhino Grasshopper to simulate various winding patterns to optimize the final winding surface. NiChrome wire with 0.5mm diameter was used to wind the 14 anchors points on each edge to create the initial mesh surface. Before the sintering process, the winded NiChrome wire was heated up and checked by a thermal camera for uneven heating. The sintering temperature was set at 135°C for five minutes. After sintering, the NiChrome wires, which are crisscrossed and interlaced up and down, produce nodes, which enhance the structural strength. Finally, the sintered units were assembled to

form a three-sided Hyperbolic Paraboloid surface (Figure 7).

Figure 5. Anchors points of Hyperbolic Paraboloid surface.

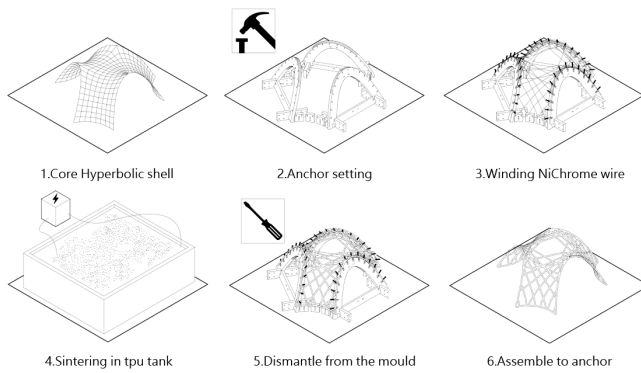
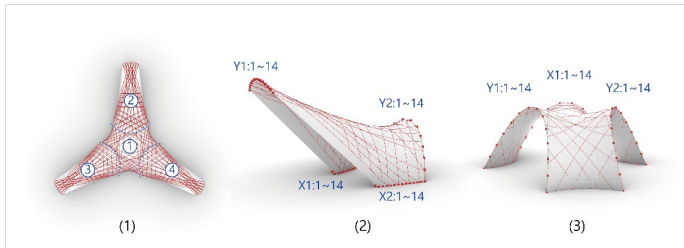


Figure 6. Process of 3D sintering method.

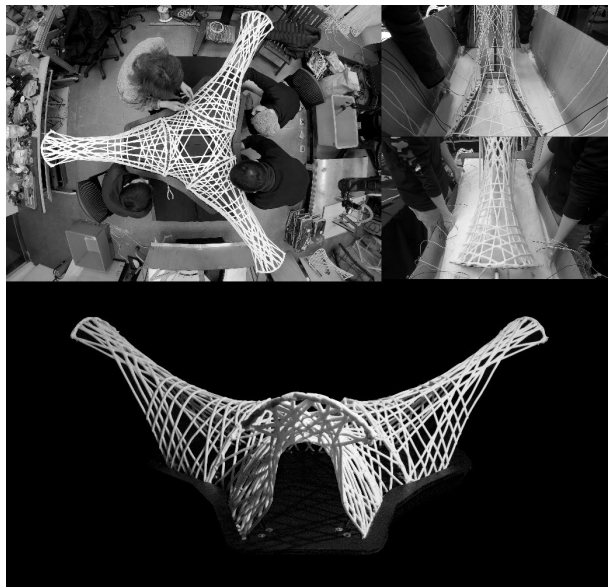


Figure 7. Final result of 3D sintering.

4.2. PRE-3D SINTERING METHOD

This study presents three surfaces to demonstrate a rapid forming method by adjusting the pattern of the sintered surfaces. The deformable wireframe structures take advantage of the elasticity of TPU to reinforce the structure. After sintering TPU with the grid-shaped NiChrome wire, a freeform surface can be generated by applying force along the edge of the wire mesh, and 2D grids can thus be manipulated and deployed easily into a specific 3D position. The six edges of the hexagon were divided into eight anchor points individually with different dividing distances (1) equidistant (2) tight in the middle (3) loose in the middle. The fabrication process was as follows (Figure 8): Controlling the spacing distribution between the eight anchor points on each edge, a 2D mesh with three different patterns was wound using 0.5mm diameter NiChrome wire under the same sequence (Figure 9). Before the sintering process, the wound NiChrome wire was heated up and checked by a thermal camera for uneven heating. The sintering temperature was set at 135°C for three minutes. The three edges were pushed inward to determined positions forming three different surfaces due to different 2D sintered grid patterns. The final results show that different patterns wound with different dividing anchor points on the same hexagon edges create a different degree of curvature in the center of the sintered mesh surface (Figure 10).

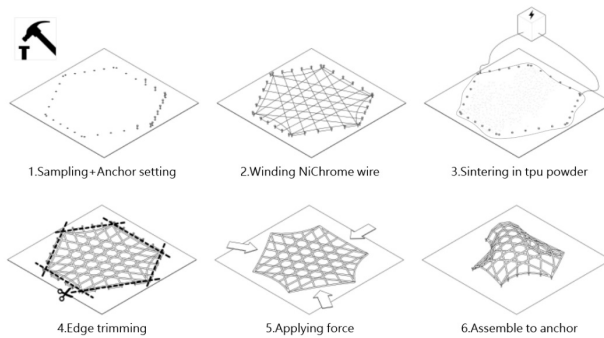


Figure 8. Process of Pre-3D sintering method.

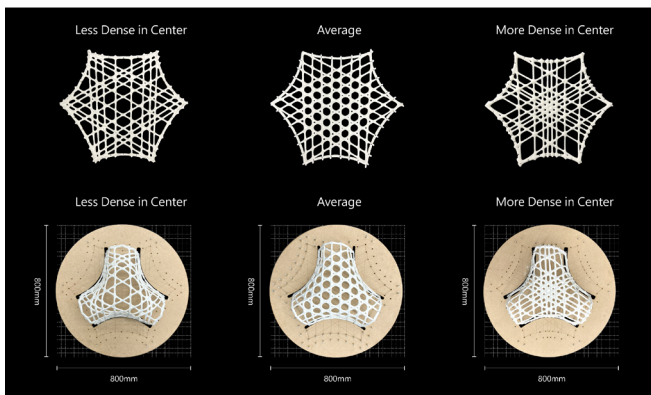


Figure 9. Three types of patterns and space distribution of anchor points.

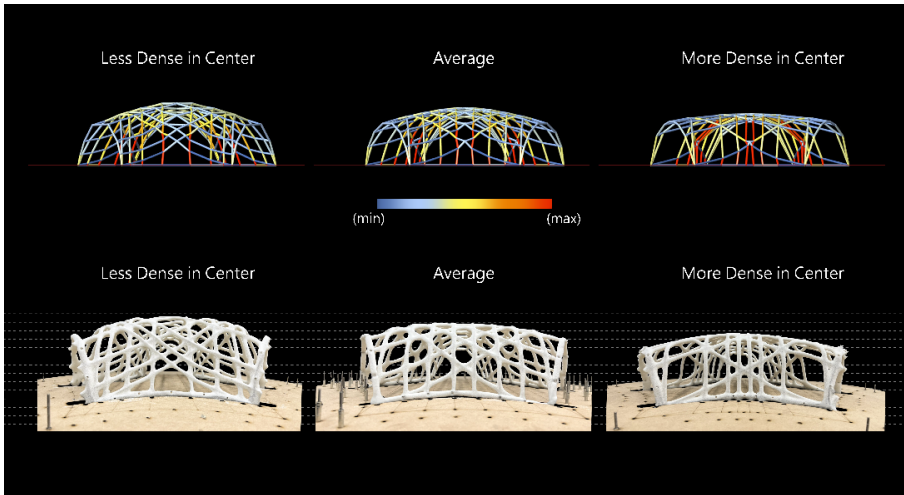


Figure 10. Bending level of the three sintering results.

5. Conclusion and Future Work

In conclusion, this research exploits the differential material states of NiChrome wire and TPU, digital tools, and computational design to create a novel digital fabrication workflow for sintering winded surfaces. Based on a series of experiments, two sintering fabrication strategies are proposed to demonstrate their applicabilities and possibilities under different conditions. (1) 3D sintering method: This method focuses on the formation of various complex surfaces without support by using custom molds inside a tank of TPU powder, which also reduces material waste in the fabricating process. (2) Pre-3D sintering method: After sintering TPU with the grid-shaped NiChrome wire, a freeform surface can be quickly generated from the plane by applying force along the edge of the wire mesh. This method shows the possibility of creating temporary structures (e.g., decorative facades, emergency bunkers, etc.) and enables designers to explore forms and structures in a manageable way by adjusting the pattern of the sintered surfaces. Compared to the conventional 3D printing method, S.N.O.W proposed a rapid, free-form geometric surface generating method demonstrating a unique way of sintering powder to form wireframe structures without using supporting materials and entails no physical restriction on the build volume. However, in order to sinter NiChrome wire to form desired surface without support material, the molds should be customized for different surface, which makes the whole fabricating process inefficient. Considering future aspects, this method has great potential to fabricate temporary buildings or temporary structures rapidly. Therefore, the system should be optimized before moving on to larger-scale fabrication. Due to the limitation of the current sintering system, the length of the wire must be less than 30m to achieve a stable sintering temperature at 135°C. In addition, although the sintering temperature is precisely controlled during the entire sintering process, the winding process is executed manually, which causes many errors and imprecisions results. Last, the manufacturing method of the mold should be optimized to reduce material waste and improve fabricating efficiency. Further research in this area will require: (1)

Improvement to the current sintering system to extend the length limitation of NiChrome wire. (2) Development of robotic winding system (e.g., winding tools or mobile robots) to improve efficiency and precision of fabricating process and results. (3) Design adjustable anchor points on the mold to adapt different forms of surfaces.

Acknowledgements

S.N.O.W would not have been possible without the valuable support of ROLA (Graduate Institute of Architecture, National Yang Ming Chiao Tung University), and the Ministry of Science and Technology (MOST) (Taipei, TW) (GRANT_NUMBER: MOST 108-2218-E-009 -054 -MY2). Some parts presented in this paper result from an initial exploratory research study by Chun-Yu Lo, Shi-Ci Yueh, and Yian Yang. Therefore, an extra thanks goes for their valuable support on this research.

References

- Hajash, K., Sparman, B., Guberan, C., Laucks, J., & Tibbits, S. (2017). Large-scale rapid liquid printing. *3D Printing and Additive Manufacturing*, 4(3), 123-132.
- Pillwein, S., Leimer, K., Birsak, M., & Musialski, P. (2020). On elastic geodesic grids and their planar to spatial deployment. *arXiv preprint arXiv:2007.00201*.
- Knippers, J., La Magna, R., Menges, A., Reichert, S., Schwinn, T., & Waimer, F. (2015). ICD/ITKE research pavilion 2012: coreless filament winding based on the morphological principles of an arthropod exoskeleton. *Architectural Design*, 85(5), 48-53.
- Yablonina, M., Prado, M., Baharlou, E., Schwinn, T., & Menges, A. C. H. I. M. (2017). Mobile robotic fabrication system for filament structures. *Fabricate: Rethinking Design and Construction*, 3.

AUTONOMOUS TRANSHUMANCE

TUSHAR MONDAL¹

¹*tushar.mondal.19@ucl.ac.uk, 0000-0001-8108-176X*

Abstract. The Arctic is a zone of confluent resources where climate change has begun disrupting the once stable ecological and transhumant lifestyles. Encroachment on pastureland by oil, gas and mining facilities limit reindeer herding activity, and the presence of such infrastructure continues to alter their sensory perceptions and consequently their capacity to read and navigate their environment. Parallel to this, thawing permafrost results in the release of gaseous methane, causing landforms called pingos to explode without detectable warning. This paper proposes a strategy for adapting to these rapid changes by implementing an autonomous system to balance the Arctic ecology through two mutual dependent interventions- (1) Regenerating the pingos to prevent explosion and create new pastoral lands. (2) Seasonally herding the reindeer to these new pastures. The project uses primary data, physical tests, and current technological tools to inform the discourse and suggest a derivative solution. Advanced computational tools like machine learning, robotics, and simulations are used to speculate upon the post-carbon Arctic ecology. The project performs through a strategy of local interventions, networking the living and non-living agents in a tight rope act that balances the Arctic ecology.

Keywords. Arctic; Pingo; Regenerated Landscape; Reindeer; Autonomous Herding; SDG 13; SDG 15.

1. Introduction

Imagine if we were to switch off the electricity supply for the entire world right now, the whole world would standstill, which would, in turn, invoke chaos. But the native people of the Arctic region, for instance, the Nenets, would be continuing with their lives. They have their vernacular ways independent of the technological advances of the rest of the world. Nenets are facing increasing difficulties in continuing their way of life. The thawing Arctic leads to a plethora of consequences, forcing Nenets to abandon their way of life and move to cities (Raygorodetsky, 2017). As the human populace moves away, the reindeer are left to fend for themselves in an increasingly uncertain landscape (Kumpula et al., 2020). As a keystone species of the Arctic, any

changes in the reindeer behavioural patterns have far-reaching implications on the whole ecosystem (Bernes et al., 2015). This project attempts at adapting to these rapid changes by networking the living and non-living Arctic, as summarised in Figure 1. It aims at preserving the endangered by integrating existing behaviour with endemic knowledge and automation. The project derives its aims from the Sustainability Goals, particularly SDG 13 and SDG 15. It aims to mitigate the impacts of climate change, prevent land degradation, and preserve Arctic biodiversity.

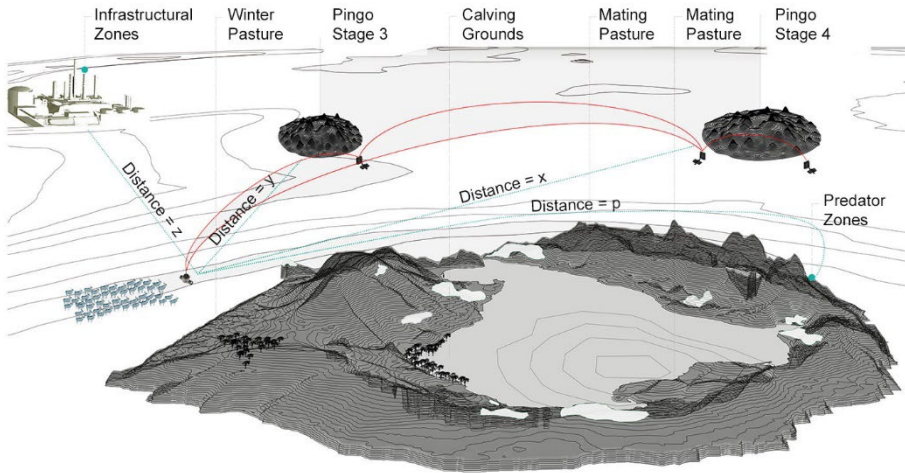


Figure 1. Network of the living and non-living Arctic

2. Site and Stakeholders

2.1. SITE - YAMAL PENINSULA

Located on the northern edge of Siberia, the Yamal Peninsula is a part of the Arctic tundra, a permafrost zone with low lying flatlands which turn green during summers and completely freeze during winters. It is home to the Nenets, a Samoyedic tribe of nomadic reindeer herders. The landscape has been analysed through four layers, each

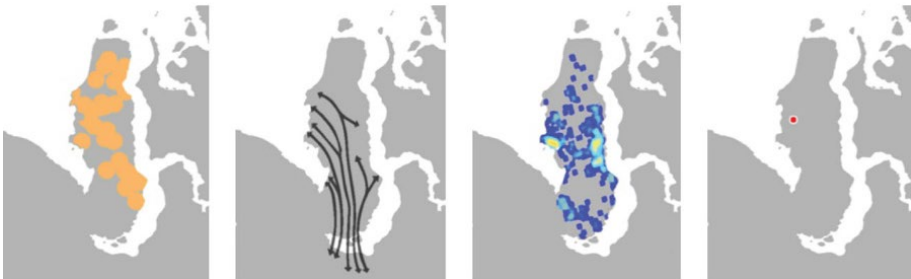


Figure 2. Layers of Yamal

layer providing a specific dataset. Figure 2 depicts the four layers (from L to R): The gas deposits, attractors of infrastructure development (Bambulyak et al., 2015). The Nenets migration routes (National Geographic Society & Tierney, 2019). The pingo location and concentration, which are potential danger zones (Grosse & Jones, 2011). The first recorded pingo explosion (Buldovicz et al., 2018). When overlapped, the resultant map provided an insight into the consequential nature of changes occurring in the landscape.

2.2. PINGOS

One of the prominent landforms is known as pingo. Pingos are periglacial mounds that dot most of the Arctic region. They form through the process of repeated freezing and thawing. Pingos can range from 3m to 50m in height and 5m to 100m in diameter. Figure 3 shows a pingo documented in Longyearbyen, Svalbard.

Pingos are spread across the Arctic landscape. Two independent documentations of the pingos in Siberia and Alaska estimate upwards of 6000 pingos in each location (Grosse & Jones, 2011; Jones et al., 2012). Besides existing pingos, recent surveys by NASA documented the presence of millions of methane leak spots across the Arctic (Smith, 2020), a good proportion of which might form new pingos, at an accelerated rate compared to a normal pingo life cycle. Methane build-up inside the pingos cause them to explode, releasing large quantities of gaseous methane into the atmosphere, adding to the positive feedback loop for global warming. The explosions also expose deeper layers of permafrost, propagating thaw (Buldovicz et al., 2018).



Figure 3. Pingo

2.3. REINDEER

As stated, reindeer are one of the keystone species of the Arctic. Also known as Caribou, reindeer species occupy both Alaskan and Siberian tundra, often as semi-domesticated herds. Observation of reindeer herds highlights a few interesting behavioural patterns. The herd does not have a designated leader. The leader is decided based on movement. When any reindeer starts moving if multiple individuals start following it, it becomes the leader for that movement. Reindeers show a tendency to turn anti-clockwise as an instinct when suddenly spurred to start moving, such as by a predator (Weisberger, 2019). Reindeer have a heightened olfactory sense. They can sniff out vegetation under ~60cm thick snow cover (Heggberget et al., 2002). Since the reindeer diet is particularly deficient in salt, they are overly sensitive to seaweed, and human urine and sweat, a fact used by early Samoyedic tribes to domesticate them

(Staaland et al., 1980).

To ensure sufficient pasture for the reindeer, the Nenets of Yamal Peninsula undertake an annual migration spanning ~1300 km, from the north of the Yamal Peninsula (summer pastures) to the south (winter pastures). This transhumance is one of the longest such annual migrations. It begins in September, as summer shifts into autumn. The return journey is in March, at the peak of the spring season (Raygorodetsky, 2017). Nenets are facing increasing difficulties in continuing their way of life. As gas companies seek to tap the natural resources, they impinge upon and create barriers on the land, resulting in the loss of pastureland as well as Nenet homes. The development of new pipelines and roads creates a network of barriers in their lands (Degteva & Nellemann, 2013).

3. Autonomous Transhumance

This project proposes a new way of seasonal transhumance, where we herd the reindeer to food resources by triggering their sense of smell. As shown in Figure 4, it responds to a warming arctic by non-invasively re-taming the region with a family of two autonomous robots: AuRoRaH and AuRega. AuRoRaH is a robotic shepherd that guides reindeer to various seasonal pastures by triggering their sense of smell. While AuRega is a robotic landscape acupuncturist that regenerates the landscape by relieving methane build up.

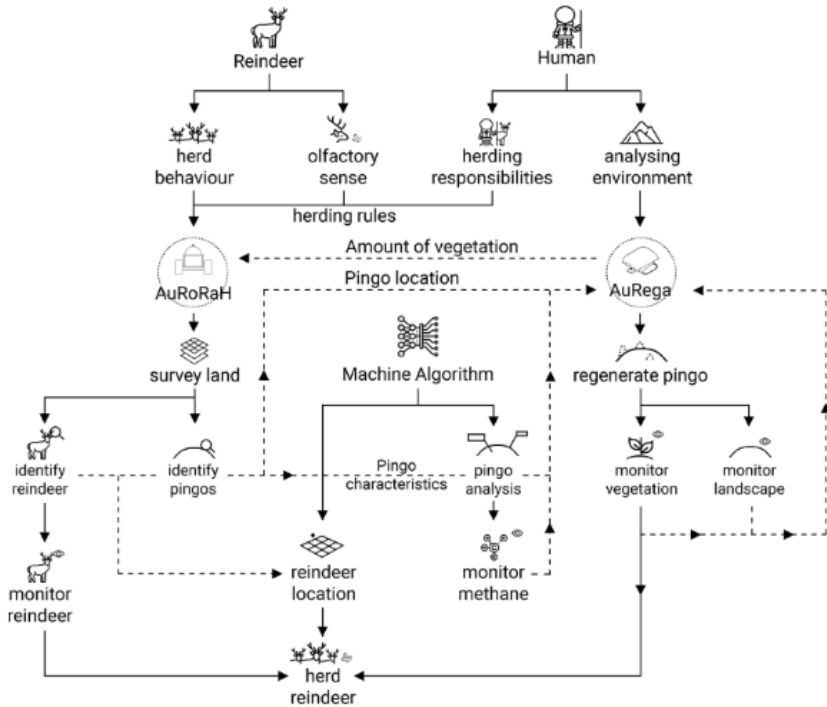


Figure 4. Autonomous Transhumance process flowchart

3.1. AURORAH

AuRoRaH, or the Autonomous Robotic Reindeer Herder, is a robotic shepherd for the reindeer. It aims to non-invasively guide the reindeer to food sources, ensuring that reindeer can survive in the absence of human care in the constantly changing Arctic. It does so by triggering their sense of smell to guide them towards food or away from danger. It actively monitors the Arctic for changes and takes herding decisions based on them. Figure 5 shows the final design for the AuRoRaH bot. The bot collects scents using the extendable headspace bell at the bottom, which are stored in individual chambers. AuRoRaH can store six scents at a time, which can be mixed in the mixing chamber at the top. The extendable spray allows flexible dispersal of the scent.

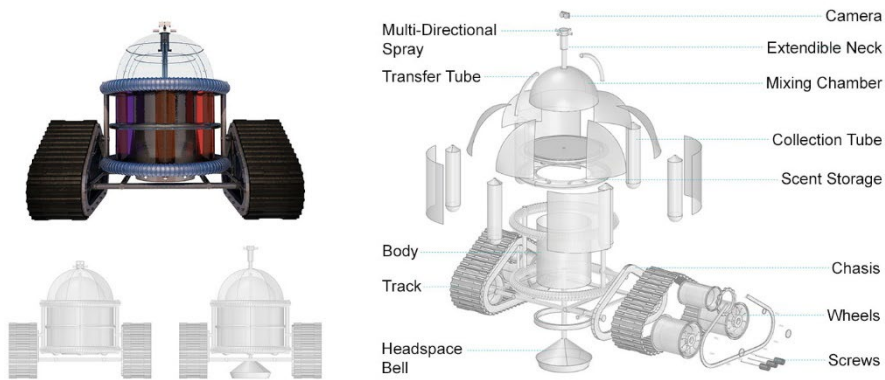


Figure 5. AuRoRaH final prototype

Smells are capable of triggering emotions and can store specific memories (Wainwright, 2013). Armed with this knowledge, the scents of Arctic are identified and analysed based on their chemical compositions, potency, and their effect on reindeer. Based on these factors, a selection of smells and odours are catalogued to form a 'smell library' used for herding the reindeer. As depicted in Figure 6, after assigning a potency value to each scent and odour a series of Grasshopper simulations pit two mixes against each other to see the effect and reindeer behaviour. Reindeer behaviour has been emulated using the Quelea plugin for Grasshopper. Based on the simulation results, a list of mixes and rules were offloaded into AuRoRaH. It will use these rules to herd the reindeer.

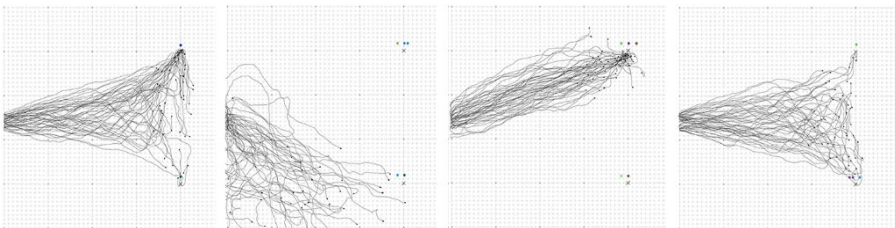


Figure 6. Simulation testing reindeer behaviour to scents and odours

AuRoRaH changes the current reindeer transhumance, which is an annual cycle, to a three-season cycle. As shown in Figure 7, migration times and routes are planned according to set herding rules. Once an AuRoRaH unit locates a reindeer herd, it releases a scent to attract (or repel) the reindeer. Based on the reindeer behaviour the bot may spray again, spray at a higher potency, or relocate and repeat the steps. By repeating the process over, AuRoRaH guides the reindeer to the desired location.

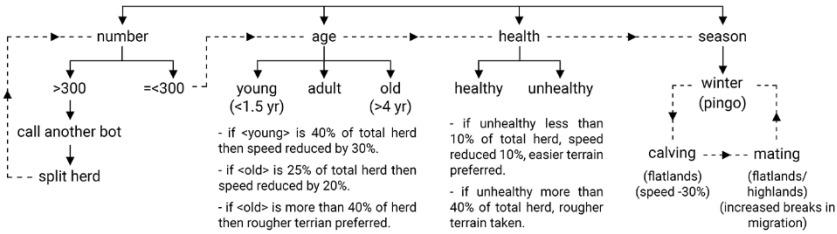


Figure 7. Reindeer herding rules

3.2. AUREGA

AuRega, or the Autonomous Regenerator, is a robotic landscape acupuncturist. It aims to non-invasively re-tame the landscape for both humans and non-humans. It does so by detecting methane leak spots on pingos, acupuncturing the points to relieve pressure, and regenerating them. It actively monitors the pingo and prevents explosions due to methane build-up, transforming the pingo into a methane storage unit and new pastoral land for the reindeer. It also helps visualise methane emissions in the Arctic to the layman. Figure 8 shows the final design for the AuRega bot. The main component is the mouldable formwork, which allows for several simultaneous functions. It can bend at multiple angles allowing for several AuRega units to work together. It also serves as the cover for the unit. The formwork can also generate multiple patterns by using a network of anchor points and inflating the impermeable reindeer skin layer.

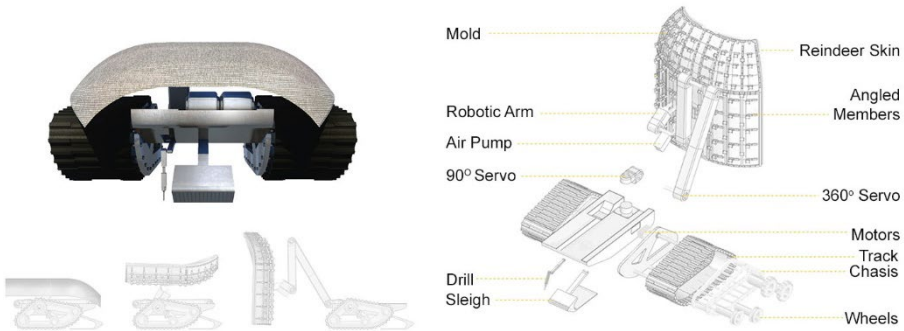


Figure 8. AuRega final prototype

AuRega regenerates the pingo by repeating a set of actions multiple times, depicted in Figure 9. As the mound builds up, it also gets pushed up by the methane trapped inside. The pingo thus grows over multiple cycles of regeneration. While generating the mound, AuRega generates various patterns on it, creating preferable conditions for vegetation growth. AuRega also monitors the pingo for vegetation growth, relaying it to AuRoRaH for herding decisions. As AuRega regenerates the pingo, it creates a distinct new landscape. It will act as a new vocabulary for reading methane emission rates, one legible to machines and humans alike, read by the changes in height and number of mounds on a pingo. This would serve as a marker for tracking climate change in the Arctic, while also significantly reducing landscape methane emissions.

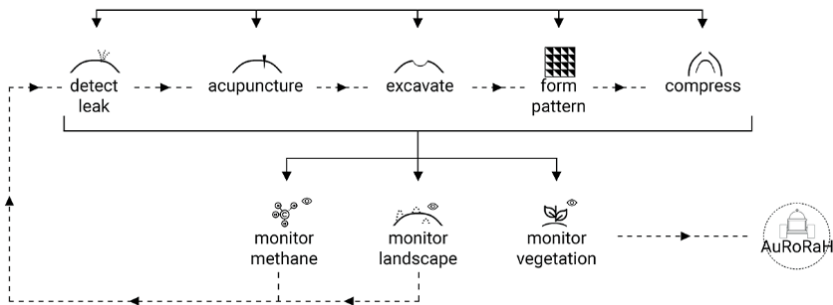


Figure 9. Process of pingo generation

3.3. TECHNICAL SYSTEM OVERVIEW

AuRoRaH and AuRega form a sentient family of robots, managing the Arctic landscape. The system can decode elements of the Arctic landscape like pingos, highlands, lowlands, forests, water bodies, and infrastructure to optimize routes for transhumance. As depicted in Figure 10, two machine learning algorithms, a Convolutional Neural Network followed by a Linear Regression model, allow the bots to identify reindeer and classify pingos.

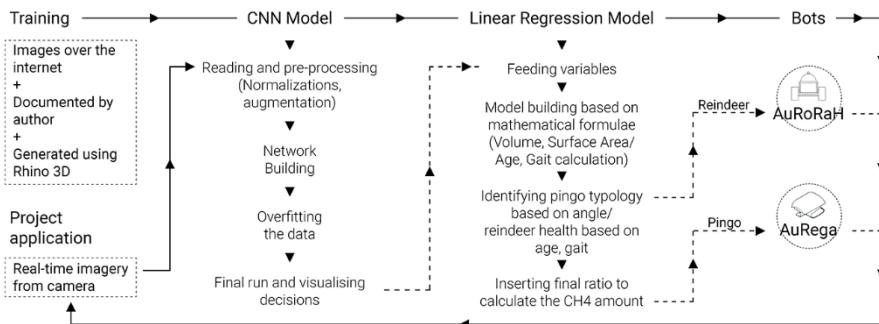


Figure 10. Machine learning models implemented

To train the model for the herding rules, distance, stage, and estimated methane amount of the pingo are considered. The robots are trained following the smell attractor logic to attract a given number of reindeer, depending on the destination pingo capacity. The goal for the agents is that they need to attract reindeer in the environment to follow them until they reach their maximum capacity. The reindeer were scripted with a random walker and would follow the bots as soon as they enter their sphere of influence. Next, a reinforcement learning model is created in Unity where the herding rules are simulated by assigning a different number of reindeer to each robot and then training it in various stages of pingo growth vs several reindeer. Distance is the first criteria of assessment followed by the stage of the pingo, the methane to ice ratio, and reindeer capacity. In a scenario where there are sufficient pingos in the vicinity, the pingo at the most matured stage, with higher methane-to-ice ratio content, takes priority. AuRoRAH also follows one herd, one pingo rule, where an average batch consists of 250-300 reindeer.

4. Supplementary Tests

4.1. MATERIAL TESTS

Tests were done to determine the physical properties of the earth as a material. The initial tests checked the mould-ability of soil with different earth-water ratios. Next, the ability for only water to act as a binder for the earth, in sub-zero conditions, was tested, again with different earth-water ratios. Based on the results and findings from these two tests, the last set of tests focused on a few different parameters, namely- mould-ability on a larger scale, the effect of organic matter in the soil as a binder with water, stability of different patterns when moulded, thermal heat retention capability of these patterns. As shown in the left set of images in Figure 11, each specimen was shaped and left for a week at room temperature and then inspected through thermal imaging. Patterns retaining more heat were selected since heat retention is preferable for vegetation in the Arctic. Selected patterns were then tested for varying depths using the Ladybug plugin for Grasshopper, depicted in the right set of images in Figure 11.

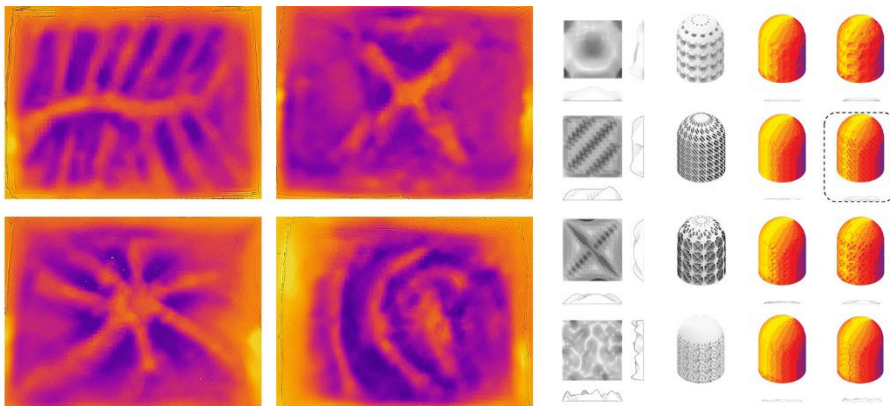


Figure 11. Soil heat retention tests

4.2. OLFACTION TESTS

Tests were conducted to understand the olfactory sense, and smells and odours, using the human olfaction as a replacement for a reindeer. The first set of tests determined the maximum distance a smell can travel in favourable and unfavourable wind conditions. The scent was the same. The duration of the spray was as similar as possible each time, subject to human error. Then same tests were repeated, but this time the diffusion was at half-human height to mimic the bot releasing at half-reindeer height. The results are listed in Table 1.

Table 1 Spray test results

Spray Height	Distance (m)	Wind Direction	Wind Speed (kph)	Detected?
Spray at human height	1	Favourable	17	Yes
Spray at human height	3	Favourable	17	Yes
Spray at human height	5	Favourable	17	Yes
Spray at human height	7	Favourable	17	No
Spray at human height	1	Unfavourable	17	Yes
Spray at human height	2	Unfavourable	17	No

5. Conclusion

This paper proposes a non-invasive approach to re-taming an increasingly uncertain Arctic. It uses native herding and landscape knowledge and encodes it into machine language, which not only ensures that the knowledge is not lost, but also puts it to practice. At the same time, the proposal can be seen as a prototype which can be applied across any ecology threatened by climate change, not being limited to the Arctic. The family of sentient robots can be of any make and form. They would be vernacularly made to be best suited the task at hand and undergo multiple stages of evolution.

At its core, the proposal works with currently available technology such a machine learning and robotics, thus it can be replicated if the need arises. At the same time, the proposal will benefit from further development in design of artificial intelligence and swarm robotics. To progress this project, one assumption taken is regarding the analysis and classification of smell using machine learning algorithms. It is assumed that the technology to autonomously detect, capture, analyse and classify smells will be available soon. Research is already underway on testing and teaching machine learning algorithms about olfaction and smells (see Harrison, 2019; Wainwright, 2013).

Acknowledgements

This research was carried out as a part of the Research Cluster 1, March AD at the Bartlett School of Architecture, University College London, UK. The work was undertaken with Sitanan Bhengbhun and Tashi Zaidi. Gratitude is extended to Deborah Lopez Lobato and Hadin Charbel for their continuous support and guidance throughout

the process of this research.

References

- Bambulyak, A., Frantzen, B., & Rautio, R. (2015, October). *Oil transport from the Russian part of the Barents Region. 2015 status report*. Retrieved January 16, 2020, from https://www.researchgate.net/publication/292966364_Oil_transport_from_the_Russian_part_of_the_Barents_Region_2015_status_report
- Bernes, C., Bråthen, K. A., Forbes, B. C., Speed, J. D., & Moen, J. (2015). What are the impacts of reindeer/caribou (*Rangifer tarandus* L.) on arctic and alpine vegetation? A systematic review. *Environmental Evidence*, 4(1). <https://doi.org/10.1186/s13750-014-0030-3>
- Buldovicz, S. N., Khilimonyuk, V. Z., Bychkov, A. Y., Ospennikov, E. N., Vorobyev, S. A., Gunar, A. Y., . . . Amanzhurov, R. M. (2018). Cryovolcanism on the Earth: Origin of a Spectacular Crater in the Yamal Peninsula (Russia). *Scientific Reports*, 8(1). <https://doi.org/10.1038/s41598-018-31858-9>
- Degteva, A., & Nellemann, C. (2013). Nenets migration in the landscape: impacts of industrial development in Yamal peninsula, Russia. *Pastoralism: Research, Policy and Practice*, 3(1), 15. <https://doi.org/10.1186/2041-7136-3-15>
- Grosse, G., & Jones, B. M. (2011). Spatial distribution of pingos in northern Asia. *The Cryosphere*, 5(1), 13–33. <https://doi.org/10.5194/tc-5-13-2011>
- Harrison, S. (2019, October 24). *Now the Machines Are Learning How to Smell*. Retrieved December 8, 2020, from <https://www.wired.com/story/now-machines-learning-smell/>
- Heggberget, T. M., Gaare, E., & Ball, J. P. (2002). Reindeer (*Rangifer tarandus*) and climate change: Importance of winter forage. *Rangifer*, 22(1), 13. <https://doi.org/10.7557/2.22.1.388>
- Jones, B. M., Grosse, G., Hinkel, K. M., Arp, C. D., Walker, S., Beck, R. A., & Galloway, J. P. (2012). Assessment of pingo distribution and morphometry using an IFSAR derived digital surface model, western Arctic Coastal Plain, Northern Alaska. *Geomorphology*, 138(1), 1–14. <https://doi.org/10.1016/j.geomorph.2011.08.007>
- Kumpula, T., Laptander, R., & Forbes, B. C. (2020, March). Impacts of infrastructure and climate changes on reindeer herding in the Yamal, west Siberia. *Göttingen, Germany: Copernicus GmbH*. <https://doi.org/10.5194/egusphere-egu2020-13995>
- National Geographic Society, & Tierney, L. C. (2019, June 28). *The Paths of Resilience*. Retrieved December 17, 2020, from <https://www.nationalgeographic.org/photo/paths-resilience/#the-paths-of-resilience>
- Raygorodetsky, G. (2017, October). They Migrate 800 Miles a Year. Now It's Getting Tougher. *National Geographic Magazine*. Retrieved December 17, 2020, from <https://www.nationalgeographic.com>
- Smith, E. (2020, February 19). *NASA Flights Detect Millions of Arctic Methane Hotspots*. Retrieved January 10, 2020, from <https://climate.nasa.gov/news/2954/nasa-flights-detect-millions-of-arctic-methane-hotspots/>
- Staaland, H., White, R. G., Luick, J. R., & Holleman, D. F. (1980). Dietary influences on sodium and potassium metabolism of reindeer. *Canadian Journal of Zoology*, 58(10), 1728–1734. <https://doi.org/10.1139/z80-238>
- Wainwright, O. (2013, June 28). *Scentography: the camera that records your favourite smells*. Retrieved December 8, 2020, from <https://www.theguardian.com/artanddesign/architecture-design-blog/2013/jun/28/scentography-camera-records-smells-memory>
- Weisberger, M. (2019, February 15). *Reindeer Cyclones Are Real, and You Definitely Don't Want to Get Caught in One*. Retrieved December 17, 2020, from <https://www.livescience.com/64778-vikings-reindeer-cyclone.html>

SUSTAINABLE RAPID PROTOTYPING WITH FUNGUS-LIKE ADHESIVE MATERIALS

STYLIANOS DRITSAS¹, JIAN LI HOO² and JAVIER G. FERNANDEZ³

^{1,2,3}*Singapore University of Technology and Design.*

¹*stylianosdritsas@sutd.edu.sg, 0000-0002-9609-2784*

²*javier.fernandez@sutd.edu.sg, 0000-0003-2961-6506*

³*jianli_hoo@sutd.edu.sg, 0000-0002-9548-5404*

Abstract. The purpose of the research work presented in this paper is to develop a sustainable rapid prototyping technology. Fused filament fabrication using synthetic polymers is today the most popular method of rapid prototyping. This has environmental repercussions because the short-lived artifacts produced using rapid prototyping contribute to the problem of plastic waste. Natural biological materials, namely Fungus-Like Adhesive Materials (FLAM) investigated here, offer a sustainable alternative. FLAM are cellulose and chitin composites with renewable sourcing and naturally biodegradable characteristics. The 3D printing process developed for FLAM in the past, targeted large-scale additive manufacturing applications. Here we assess the feasibility of increasing its resolution such that it can be used for rapid prototyping. Challenges and solutions related to material, mechanical and environmental control parameters are presented as well as experimental prototypes aimed at evaluating the proposed process characteristics.

Keywords. Rapid Prototyping; Sustainable Manufacturing; Digital Fabrication; Robotic Fabrication; SDG 12.

1. Introduction

Ensuring responsible consumption and production is a grand challenge part of the Sustainable Development Goals (SDG #12) by the United Nations (UN, 2015). It calls for considering the utilization of natural resources from the extraction of raw materials to the design of products, the energy intensive manufacturing processes involved and their end-of-life disposal. The example used by UN to illustrate the idea of the “global material footprint” is that of plastic waste; a problem its magnitude we recently begun to appreciate (Geyer et al, 2017).

Additive manufacturing (Chua and Leong, 2014) is a technology for the design and fabrication of products using material resources in a highly efficient manner (Thomson et al. 2016), unlike conventional techniques which often produce substantial amounts

of waste (Tofail et al, 2018). Rapid prototyping (Chua and Leong, 1997) is the earliest and still most popular use of additive manufacturing. With long history in architecture (Kvan et al, 2001, 2002; Burry, 2003; Sass and Oxman, 2006); most prototyping in both academia and practice is performed today using 3D printing (Agirbas, 2015).

Despite its popularity, there is a growing concern regarding the negative effects of rapid prototyping on health (Short et al, 2015) and the environment (Drizo and Pegna, 2006; Ford and Despeisse, 2016). The dominant use of plastics for creating short-lived artifacts is at the heart of the problem (Wang et al, 2018). While certain plastics can be recycled, in practice it is highly uneconomic and energy intensive to perform (Baechler et al, 2013). Advances in polymers gave rise to renewable and biodegradable plastics such as polylactic acid. While bioplastics are more sustainable compared to petroleum polymers, they are often produced from food sources, such as corn starch and sugar cane, and require industrial composting for recovery (Tokiwa and Calbia, 2006).

The objective of this work is to overcome the over-use of plastics by developing a new sustainable rapid prototyping technology. Our approach employs renewable, abundant, locally available, and naturally biodegradable materials, deposited, and cured using a low energy additive manufacturing process.

2. Background Work

In the past, we presented the design of Fungus-Like Adhesive Materials (FLAM); a family of natural biological composites comprised exclusively of environmentally benign ingredients, namely cellulose and chitin (Sanandya et al, 2018). Those are two of the most abundant and ubiquitous natural components, available in nearly every ecosystem on earth. FLAM resemble high-density synthetic foams and low-density natural timbers (Figure 1). Synthesis of FLAM is performed without modifying their raw natural form, avoiding both health and safety as well as environmentally harmful chemicals. Exactly because they are not modified to behave like conventional plastics, FLAM they retain their property of natural recovery.

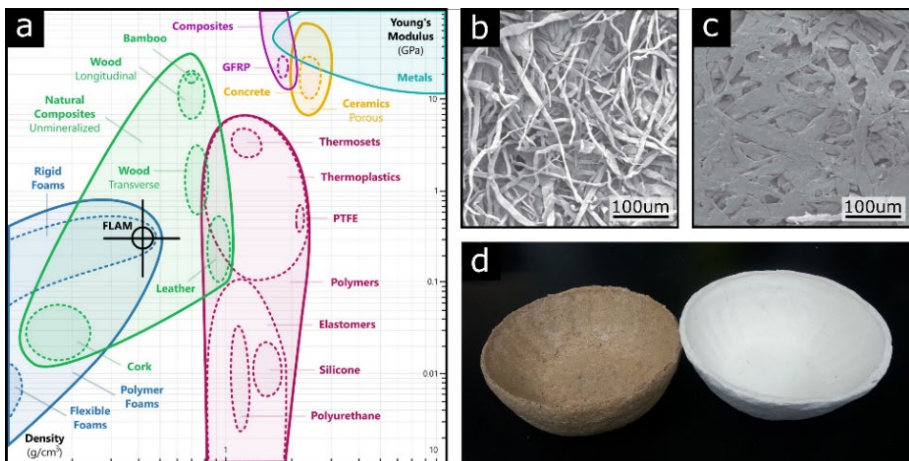


Figure 1. (a) Ashby plot of FLAM properties, (b) Scanning electron microscopy of pure cellulose fibre and (c) FLAM, (d) Objects produced with FLAM using wood waste and pure cellulose

Cellulose and chitin used in FLAM are sourced from by-products of the timber and fishing industries, namely saw dust and shrimp shells. Use of waste streams aims at keeping cost low and competitive with commodity synthetic polymers. In addition, FLAM do not require use of agricultural land or food sources for their production. To assess the potential for regionalized manufacturing, we performed a study using urban waste to synthesize FLAM (Sanandya et al, 2020). Production thus does not need to rely on forestry or coastal regions, because the material can be synthesised at the place of its consumption, which may be even highly urbanized environments (Fernandez and Dritsas, 2020). This does not merely eliminate a substantial amount of energy for transportation (Ng, Song and Fernandez, 2021), but it also provides a new paradigm for circular manufacturing and urban ecology.

The 3D printing process created for FLAM (Dritsas et al, 2018a; 2018b) is based on material extrusion (ISO/ASTM 52900, 2015). The system is comprised of a robotic positioner and a volumetric dispensing system (Figure 2). The material is deposited in the form of a viscous paste which hardens by evaporation of its water content overtime. Unlike fused filament fabrication (FFF), which relies on energy input for melting and fusing thermoplastics, FLAM are deposited and cured at ambient temperature. Thus, apart from requiring lower energy, cold extrusion enables increased speed of printing using large nozzle diameters, exactly because the material does not need to transition phase at the point and time of its extrusion. The system developed for 3D printing initially targeted large-scale artefacts to demonstrate those unique process features (Dritsas et al, 2019). In this study we modified the system to assess the potential for using FLAM in smaller scale rapid prototyping applications.

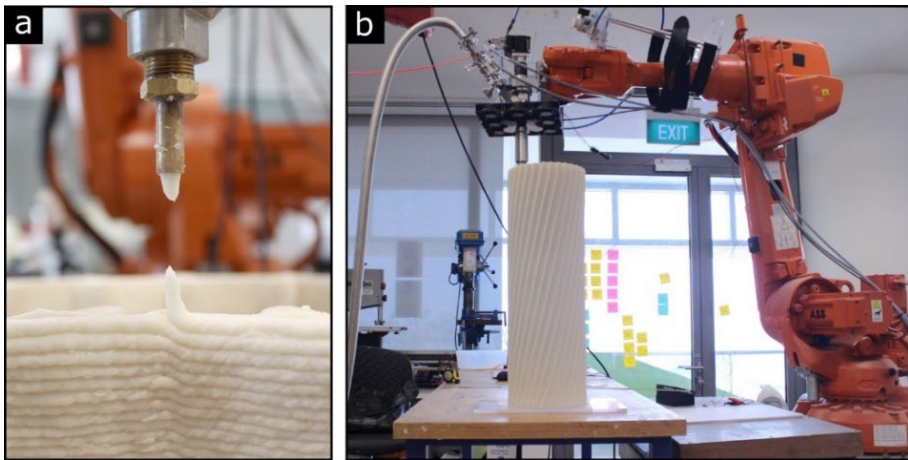


Figure 2. (a) Large-scale FLAM 3D printing using 7mm diameter nozzle. (b) Industrial robot positioner and extrusion dispensing system printing prototype using 1.5mm nozzle

3. Challenges and Solutions

There are different types of challenges when 3D printing large-scale artifacts, using nozzle diameters of a few millimetres, versus 3D printing at rapid prototyping scales, situated at a few hundred microns. Process parameters previously calibrated for large-

scale artifacts (Vijay et al, 2018), turned out to be scale dependent. The challenges, result of the change of scale, may be categorized as being related to: (a) the material properties, (b) the mechanical system, and (c) the environment conditions.

Material challenges are in ensuring that the FLAM paste is fine enough to flow through a small diameter nozzle such that 3D printing is uninterrupted. Cellulose and chitosan are sourced in the form of powders. Pure cellulose has nominal fibre length of 200 μm , but over 500 μm if raw wood waste is used. Chitosan crystals are dissolved into an adhesive paste with no discernible particles, in theory. However, there are often traces of unground shells, as we are using low-cost fertilizer-grade chitosan. Without additional material processing, compared to large-scale printing, we managed to reduce the nozzle used down to 1.0-1.5mm. Smaller nozzles, such as the typical 200-400 μm used for fused filament fabrication, were unsuitable.

The mechanical system developed for large-scale 3D printing was unideal for rapid prototyping, with challenges including: (a) the robot's positional accuracy, (b) the controller's inability to process machine code files containing hundreds of thousands of instructions, and (c) the dispensing system, designed for high flow rates, whereas precise micro-dosing is required. To address those problems, we updated our slicing software forcing for interpolated motions, such that the robot could synchronize with the dispenser, and developed a new binary file format for progressively downloading machine code for very large 3D prints.

The amount of material extruded in the large-scale 3D printing setup, is large enough that environmental parameters, such as temperature and humidity, have no discernible effects during the extrusion process. At ambient conditions, objects dry overtime, with the most rapid phase of water mass loss taking place within the first 24 hours. Hardening is mainly related with the surface and cross-sectional area of the objects printed. Therefore, with finer nozzle sizes, aiming at rapid prototyping, curing takes place much faster and most importantly during 3D printing. Change of mass however is accompanied with change of volume; shrinkage of FLAM is anisotropic (Vijay et al, 2019). Geometric change during 3D printing is a problem that requires control, because otherwise consecutive runs and layers of material may not be spatially located where they should be. The solution was to integrate a fan array to control drying (Figure 2b). Not only this solved the problem but also allowed for printing and curing concurrently.

4. Calibration and Experiments

Key process parameters for extrusion-based 3D printing are: (a) the motion speed of the positioner, (b) the flow rate of material deposited, (c) the vertical offset between consecutive layers, and (d) the nozzle diameter. Those require calibration such that the material deposited is consistent. Problems are encountered, such as over-extrusion, if motion speed is too low in relation to the flow rate, or under-extrusion, where material continuity is interrupted, in the extreme opposite scenario.

We approached this task experimentally by varying the motion speed and flow rate, while retaining the layer offset and nozzle size constant (Figure 3). We then measured the width of the runs and identified settings with the lowest variation. While there are multiple feasible feed-and-flow rate combinations, we used 1.5mm nozzle diameter,

0.75mm layer offset, 3.8cc/min flow and 36mm/sec feed rates.

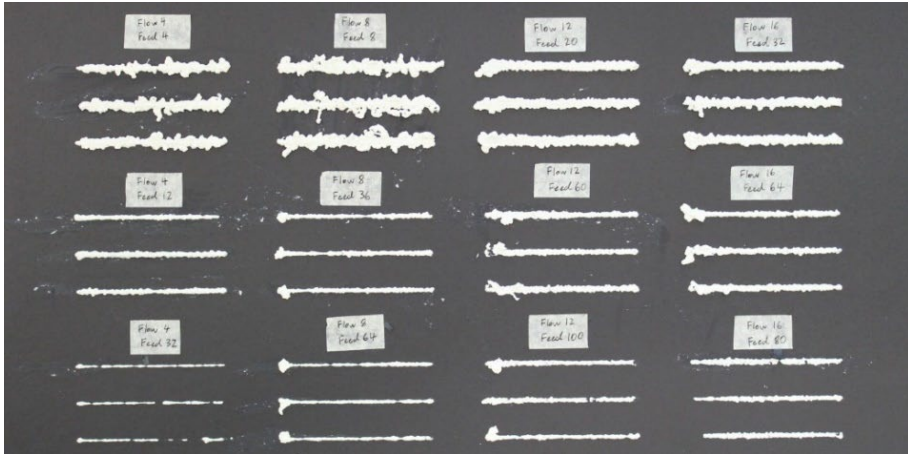


Figure 3. Experiments using various feed and flow rate combinations. The top right cases demonstrate over-extrusion, while the bottom right under-extrusion problems

Several prototypes were produced to evaluate the process including variations of both material composition, namely FLAM from pure cellulose and wood waste, and geometry, such as vertical, twisting, and cantilevered forms. Early results of successful prints (Figure 4) illustrate overall satisfactory layer consistency with minute diametral fluctuation. An important result from early prototypes is in that even though the layer height was 0.75mm at print time, after the material was cured completely, its apparent resolution increased. This is because the vertical shrinkage of 3D printed FLAM is circa 67%. Cured layer height therefore reduced to about 0.5mm. This layer height is thus comparable to conventional rapid prototyping systems.

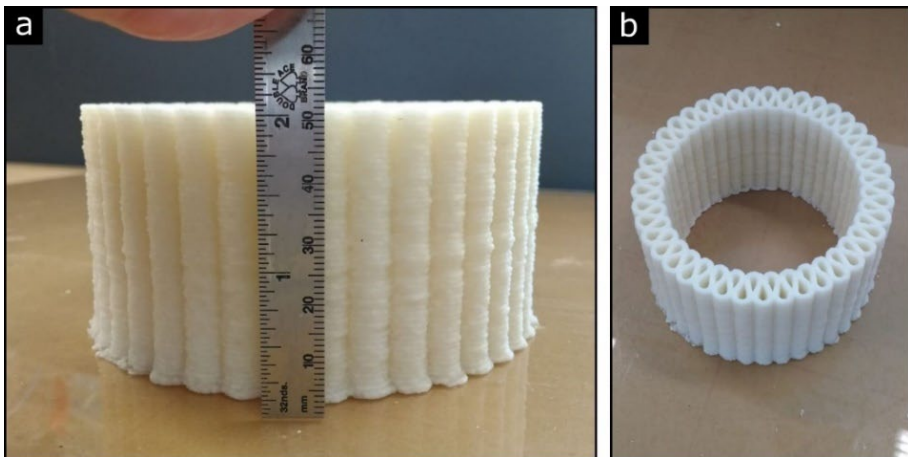


Figure 4. (a) Extruded cylindrical prototype using 1.5mm nozzle and 0.75mm layer height. (b) View of the same prototype where the corrugated wall pattern can be seen

Concurrent curing, using convective airflow, enabled 3D printing prototypes with significant taper angles, approximately 45deg. This was also an important achievement because the FLAM paste has poor mechanical properties before curing, even though it is highly viscous. This allowed for 3D printing prototypes without temporary support structures. To demonstrate this capability, we designed and 3D printed several complex geometry prototypes. The entangled element pillar prototype (Figure 5a) for instance, cantilevered for several layers before being supported by a cross-bracing member.

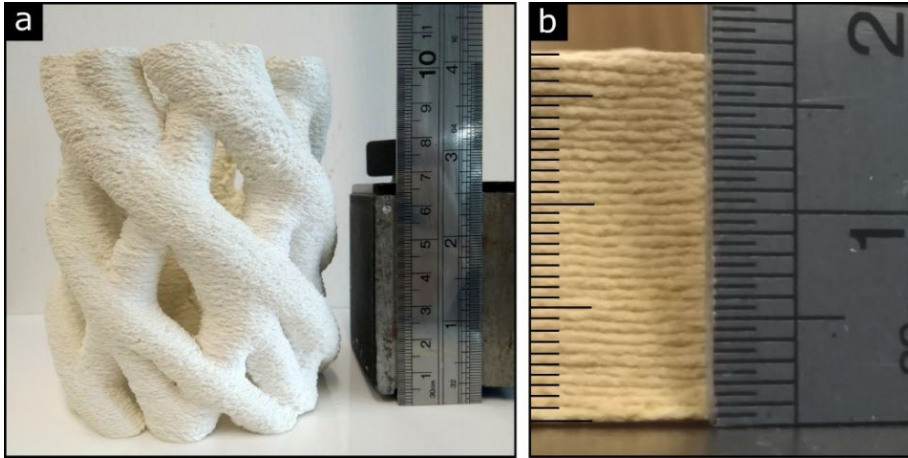


Figure 5. (a) Composite pillar prototype demonstrating the ability of layer tapering and cantilevering. (b) Detail of dry prototype with 20 layers per centimetre or 0.5mm per layer

The last experiment aimed at answering how tall we could possibly 3D print before the prototype collapsed under its own weight. It was a test of the material's mechanical properties and the reliability of the system, as those prototypes required 12 hours of printing each. We printed two fluted columns featuring a corrugated wall profile for structural stability. The first column (Figure 6) was vertically extruded while in the second prototype each layer was rotated minutely creating a spiral form (Figure 7). Both reached approximately 500mm at which point the material supply hose became a limiting factor. From the surface texture of the prototypes, namely several punctuated points of over-extrusion, we infer that the dispenser's nozzle clogged multiple times during the long printing process, but the pumping pressure was sufficient to recover and continue the print without loss of tracking between layers.

While we do not know what the limit is for how tall we can 3D print FLAM, due to technical difficulties, the experiments demonstrated that: (a) tracking between the previous and current layer is retained even after several hundred layers, (b) the material hardens sufficiently to support itself without discernible deflection such as bulging as due to buckling effects, (c) the process is both robust and resilient after performing several hours of continuous printing, and (d) it is compatible with rapid prototyping equipment which feature work envelopes of typically 300mm in vertical range.

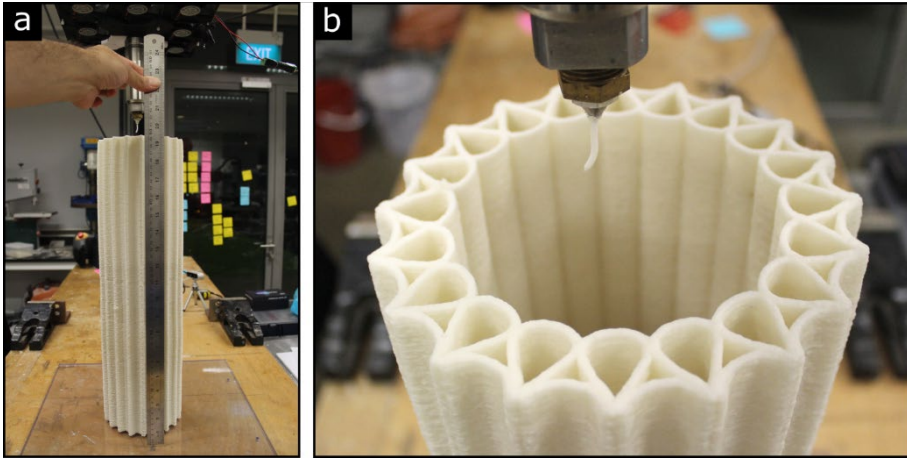


Figure 6. (a) Straight extruded fluted column prototype measuring vertically approximately 500mm. (b) Detail of 3D printing using a 1.5mm diameter nozzle

5. Conclusions

We presented research progress, including the challenges, solutions, and results, in adapting a large-scale additive manufacturing technology to resolutions relevant for rapid-prototyping applications. The objective of the project is to develop a sustainable general-purpose alternative to the currently available commercial rapid prototyping systems that 3D print synthetic plastics. Rapid prototyping became an essential part of the design process from architecture to consumer products in the last decades. Today desktop 3D printing is both highly popular and widely available, not only to design professionals and students but general audiences for educational as well as recreational purposes. With such rapid adoption, the predominant use of plastics for making objects which are rarely recycled and most often disposed is a problem with environmental implications we need to consider.

Natural biological materials offer a profoundly sustainable alternative as far as they are renewably sourced and can be recovered without human intervention. However, because they do not behave like synthetic polymers, where control of temperature and pressure is of main interest, they require new methods for spatial assembly effected by water content and pH levels. In this study we aimed to demonstrate that Fungus-Like Adhesive Materials can be used for rapid prototyping reaching similar resolutions. We discovered and presented several new insights, namely (a) the vertical shrinkage can be exploited to create a form of super-resolution, (b) finer nozzle sizes and environment control enable concurrent 3D printing and curing, and (c) the material's mechanical properties can support large cantilevers and quite substantially tall prototypes.

The hiatus between 0.1 to 0.4mm layer height of a typical fused filament fabrication plastic 3D printer versus 0.5mm achieved here, can be closed with improvements in material preparation regimes and optimization of the mechanical system. This requires re-formulation of the material in terms of reducing the fibre length of the cellulose used to allow for finer nozzle sizes and higher resolutions. Change of fibre size however

affects critical rheological material properties such as viscosity which are relevant to extrudability and requires further investigation. In addition, the robotic system while it offered motion flexibility and an extended work envelope, it also introduced positional errors due to its cantilevered structure supporting a heavy dispensing system. Moving forward, a conventional Cartesian positioning system may be thus more relevant for rapid prototyping in terms of positional accuracy and overall stiffness. Development of a miniaturized high-precision volumetric metering system for high-viscosity materials is also a design and development challenge we are looking forward to investigating.

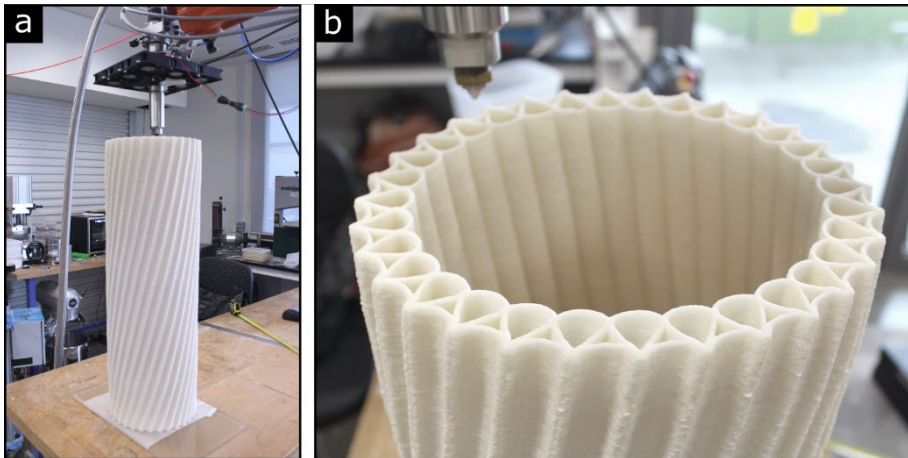


Figure 7. (a) Twisting fluted column prototype showing fan array mounter on dispenser and material supply hose. (b) Detail of 3D printing and corrugated wall pattern for structural stability

In conclusion, we consider the results of this study successful as they support the possibility for rapid prototyping using natural biological materials. We hope our work will assist in addressing the problem of plastic waste as per of the UN's sustainable development goals and motivate further research in environmentally considerate digital design and fabrication.

Acknowledgements

The research has been supported by the Singaporean Ministry of Education MOE2018-T2-2-176 grant.

References

- Agirbas, A. (2015). The Use of Digital Fabrication as a Sketching Tool in the Architectural Design Process - A Case Study. In *Proceedings of the 33rd eCAADe Conference* (pp. 319-324), Vienna University of Technology, Vienna, Austria, 16-18 September 2015. Education and research in Computer Aided Architectural Design in Europe (eCAADe).
- Baechler, C., DeVuono, M. & Pearce, J. (2013). Distributed recycling of waste polymer into RepRap feedstock, *Rapid Prototyping*, 19(2), 118–125, <https://doi.org/10.1108/13552541311302978>

- Burry, M. (2003). *Between Intuition and Process: Parametric Design and Rapid Prototyping, Architecture in the Digital Age*, Taylor and Francis.
- Chua, CK. and Leong KF. (1997). *Rapid Prototyping: Principles and Applications in Manufacturing*, John Wiley.
- Chua CK. and Leong KF. (2014). *3D Printing and Additive Manufacturing: Principles and Applications*, 4th edition, World Scientific.
- Dritsas, S., Vijay, Y., Dimopoulou, M., Sanandiya, N. and Fernandez, J. (2018). An Additive and Subtractive Process for Manufacturing with Natural Composites, *Proceedings of Robotic Fabrication in Architecture, Art and Design*, https://doi.org/10.1007/978-3-319-92294-2_14
- Dritsas, S., Halim, E.P.S., Vijay, Y., Sanandya, G.N. and Fernandez, G. J. (2018) Digital Fabrication with Natural Composites, *Journal of Construction Robotics*, 2, 41-51, <https://doi.org/10.1007/s41693-018-0011-0>
- Dritsas, S., Vijay, Y., Halim, E.P.S., Teo, R., Sanandya, N. and Fernandez, J. (2019) Additive Manufacturing with Natural Composites, *Proceedings of the Association for Computer Aided Architectural Design Research in Asia, Intelligent and Informed, Wellington, New Zealand*.
- Drizo, A. & Pegna, J. (2006). Environmental impacts of rapid prototyping: An overview of research to date, *Rapid Prototyping*, 12(2), 64–71, <https://doi.org/10.1108/13552540610652393>
- Fernandez, G. J., Dritsas, S. (2020). The Biomaterial Age: The transition toward a more sustainable society will be determined by advances in controlling biological processes, *Matter*, 2(6), 1352-1355, <https://doi.org/10.1016/j.matt.2020.04.009>
- Ford, S. & Despeisse, M. (2016). Additive manufacturing and sustainability: an exploratory study of the advantages and challenges, *Journal of Cleaner Production*, 137, 1573-1587, <https://doi.org/10.1016/j.jclepro.2016.04.150>
- ISO/ASTM 52900 (2015), Additive manufacturing – General principles – Terminology, *International Standardization Organization / American Society for Testing and Materials*.
- Geyer, R., Jambbeck, R. J. & Law, K. L. (2017). Production, use, and fate of all plastics ever made, *Science Advances*, 3(7), <https://doi.org/10.1126/sciadv.1700782>
- Kvan, T., Gibson, I. & Ling, W. M. (2001). Rapid prototyping for architectural models, *Euro RP 10th European Conference on Rapid Prototyping and Manufacturing, Paris, France*.
- Kvan, T., & Kolarevic, B. (2002). Rapid prototyping and its application in architectural design, *Automation in Construction*, 11(3), 277–278. [https://doi.org/10.1016/S0926-5805\(00\)00110-2](https://doi.org/10.1016/S0926-5805(00)00110-2)
- Ng, S., Song, B., & Fernandez, G.J. (2021). Environmental attributes of fungal-like adhesive materials and future directions for bioinspired manufacturing, *Journal of Cleaner Production*, 282, 125335, <https://doi.org/10.1016/j.jclepro.2020.125335>.
- Sanandiya, N., Dimopoulou, M., Vijay, Y., Dritsas, S. and Fernandez, J. (2018) Large-Scale Additive Manufacturing with Bioinspired Cellulosic Materials, *Scientific Reports*, 8, 8642, <https://doi.org/10.1038/s41598-018-26985-2>
- Sanandiya, N.D., Ottenheim, C., Phua, J.W. Caligiani, A., Dritsas, S. and Fernandez, J. (2020) Circular manufacturing of chitinous bio-composites via bioconversion of urban refuse, *Scientific Reports*, 10, 4632. <https://doi.org/10.1038/s41598-020-61664-1>
- Sass, L. & Oxman, R. (2006). Materializing design: the implications of rapid prototyping in digital design, *Design Studies*, 23(3), 325–355. <https://doi.org/10.1016/j.destud.2005.11.009>
- Short, D.B., Sirinterlikci, A., Badger, P. & Artieri, B. (2015). Environmental, health, and safety issues in rapid prototyping, *Rapid Prototyping*, 21(1), 105–110. <https://doi.org/10.1108/RPJ-11-2012-0111>
- Thompson, M.K., Moroni, G., Vaneker, T., Fadel, G., Campbell, I., Gibson, I., Bernard, A., Schulz, J., Graf, P., Ahuja, B. & Martina, F. (2016). Design for Additive Manufacturing:

- Trends, opportunities, considerations, and constraints, *CIRP Annals*, 65(2), 737-760. <https://doi.org/10.1016/j.cirp.2016.05.004>
- Tofail, S. A. M., Koumoulos, E., Bandyopadhyay, A., Bose, S., O'Donoghue, L. & Charitidis, C. (2018). Additive manufacturing: scientific and technological challenges, market uptake and opportunities, *Materials Today*, 21(1), 22-37. <https://doi.org/10.1016/j.mattod.2017.07.001>
- Tokiwa, Y., & Calabia, B. P. (2006). Biodegradability and biodegradation of poly (lactide). *Applied microbiology and biotechnology*, 72(2), 244-251. <https://doi.org/10.1007/s00253-006-0488-1>
- UN (2015). *Transforming our world: The 2030 agenda for sustainable development*, A/RES/70/1, United Nations.
- Vijay, Y., Sanadiya, G.N., Dritsas, S. and Fernandez, J. (2018) Control of Process Settings for Large-Scale Additive Manufacturing with Sustainable Natural Composites, *International Design Engineering Technical Conferences and Computers and Information in Engineering Conference, Design for Manufacturing and the Life Cycle, American Society of Mechanical Engineers*, Quebec, Canada. <https://doi.org/10.1115/DETC2018-85994>
- Vijay, Y., Sanadiya, G.N., Dritsas, S. and Fernandez, J. (2019) Control of Process Settings for Large-Scale Additive Manufacturing with Sustainable Natural Composites, *Journal of Mechanical Design*, 141(8): 081701. <https://doi.org/10.1115/1.4042624>
- Wang, Q., Sun, J., Yao, Q., Ji, C., Liu, J., & Zhu, Q. (2018). 3D printing with cellulose materials. *Cellulose*, 25, 4275-4301. <https://doi.org/10.1007/s10570-018-1888-y>

EXTRUSION-BASED 3D PRINTING FOR RECYCLABLE GYPSUM

LEI GONG¹, YIFAN ZHOU², LANG ZHENG³ and PHILIP F. YUAN⁴

^{1,4}*Tongji University*

²*Fab-Union*

³*University College London*

¹*gonglei0318@tongji.edu.cn, 0000-00003-2685-9668*

²*zhou@fab-union.com, 0000-0002-0774-6871*

³*lang.zheng.20@alumni.ucl.ac.uk, 0000-0003-2748-7077*

⁴*philipyuan007@tongji.edu.cn, 0000-0002-2871-377X*

Abstract. Gypsum is one of the most commonly used construction materials in cladding and non-load-bearing decoration. Recently, 3D printing technology has been involved in creating complex geometry. The particle-based method is the principal approach in 3D gypsum printing. However, the complex device and limited printable range limit the massive production of large-scale building components. This paper proposed a novel extrusion-based gypsum printing method and corresponding robotic fabrication workflow. First, several experiments are conducted to analyze the effect of different admixtures (retarder, activation agent, and accelerator) on the material setting properties. Second, a set-on-demand gypsum-based material is proposed by actively controlling multiple admixtures. Then, a process parameter-based robotic fabrication workflow is proposed, and a set of extrusion-based 3D gypsum printing equipment is built. A curved gypsum panel sample is printed as experimental verification. By comparing to the particle-based method, The test sample shows that the extrusion-based method can effectively improve the production efficiency and reduce the production cost. Therefore, the proposed method gives a relatively efficient and cost-effective way to produce recyclable gypsum material massively.

Keywords. 3D Gypsum Printing; Extrusion-based; Set-on-Demand Material; Material Modification; Robotic Fabrication Workflow; SDG 9.

1. Introduction

Gypsum-based composites have been widely used in interior linings such as walls and ceilings due to their unique advantages: low cost, good habitability, and good fire resistance (Jia et al., 2021). With the rapid development of industry in China, gypsum as a by-product is stacked as waste, not being effectively treated. It is imperative to develop efficient and feasible treating methods to reduce the harm of this solid waste to humans and the environment and create economic benefits by turning the waste into

a resource (Huang et al., 2021). According to the research, in the past period of time, conventional gypsum products are generally produced by casting (Zhou et al., 2015).

3D printing technology is an emerging rapid prototyping technology and develops rapidly in the manufacturing sector, which is the core element of digital fabrication (Huang et al., 2021). Powder-bed binder jetting (PBBJ) and extrusion-based 3D printing are two commonly used 3D printing methods for gypsum-based material (Huang et al., 2021). In comparison with the machining of slip cast structures, there are many advantages of PBBJ. One of the most important is the form freedom, once many details impossible or very hard to be machined can be produced by 3D printing (Dantas et al., 2016).

However, The PBBJ printing product has low strength due to the low level of hydration caused by poor mixing of powder and water and porous structure within the product caused during powder spreading. Compared with PBBJ, extrusion-based 3D printing, also known as a direct ink writing technique, has advantages over PBBJ (Huang et al., 2021). Since the hydration-hardening process of gypsum materials is difficult to control, there is a need to modify the gypsum treatment and propose material control parameters related to the process.

The main contribution of this paper is to propose a set-on-demand materials by the active control of multiple material modification components and Parameter-based fabrication workflow.

Currently, extrusion-based methods have become the underlying methodology for many 3D printing digital fabrication technologies, such as spatial printing, modified plastic printing, and concrete printing. Compared with other printing technologies, gypsum 3D printing technology is also a derivative of extrusion-based method; however, unlike other printing technologies, gypsum 3D printing requires a two-step modification operation of gypsum hardening in a rather short period of time, and both interventions result in chemical rather than physical changes; therefore, the research based on the material modification aspect is also a major contribution.

2. Method

To realize the objective of this research, we conducted material modification studies, explored the parameter-based workflow, selected proper printing equipment, and successfully obtained a 600mm×75mm×130mm curved gypsum panel using a KUKA six-axis robot (KR90r2900).

During the hydration of calcium sulfate hemihydrate, calcium sulfate dihydrate (gypsum plaster) is formed. Three steps can be distinguished in the hydration reaction of calcium sulfate hemihydrate: the dissolution of hemihydrate yielding a partially saturated gypsum solution, the nucleation and growth of gypsum crystals, and the final formation of solid material through the entanglement of gypsum needle-like crystals (Mucha et al., 2020).

Therefore, the modification treatment of gypsum is mainly carried out in these following three directions :

2.1. MATERIAL

Commercially available α -hemihydrate (α -HH) gypsum that meets the requirement of Chinese standard GB/T 9776–2008 was used in this research. This kind of α -HH was made from natural gypsum with high purity, reducing the influence of inherent impurities. The chemical composition analyzed by XRF is shown in Table 1.

Table 1. Chemical composition of gypsum (Qi et al., 2021).

	CaO	SO ₃	Fe ₂ O ₃	MgO	SiO ₂	Al ₂ O ₃	K ₂ O	LOI.
Gypsum wt.%	39.96	51.65	0.076	0.393	0.335	0.116	0.026	10.29

2.1.1. Retarder

After environment scanning electron microscope (ESEM) observation, it was learned that small hemihydrate particles rapidly dissolved and hydrated, forming dihydrate crystals network around large hemihydrate particles, which makes an increasingly dense microstructure and promotes the setting of gypsum slurry (Liu et al., 2019).

In this study, Protein Salt (PS) was used as the main retarding additive. PS is made of protein macromolecule, surfactants, and inorganic ions. Functional groups in surfactants can hinder the dissolution of gypsum, and the gypsum crystal nucleus is wrapped in the protein macromolecule (Zhi et al., 2017).

Commonly, polycarboxylate superplasticizer (PCE), which is the most effective water-reducing agent, is used to achieve high fluidity and low porosity; hydroxypropylmethylcellulose (HPMC), one of the most widely used thickeners, is also used to ensure that the proper viscosity can be achieved to avoid bleeding and segregation (Zhi et al., 2018).

So, PCE and HPMC were used as secondary additives to ensure good rheological properties and to set rates (Zhi et al., 2018).

2.1.2. Activation Agent

To ensure the retarded slurry solidifies rapidly after extrusion, sodium oxalate (Peng et al., 2009) and dihydrate gypsum powder were used as an activation agent in this research.

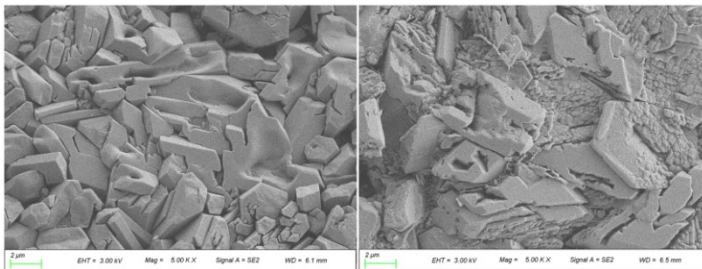


Figure 1. Left: Micro-structure of gypsum crystal without active excitation component (Group A)

Figure 2. Right: Micro-structure of gypsum crystal with active excitation component (Group B)

The micro-structure of gypsum crystal can explain the action mechanism of active excitation components to a certain extent. Through scanning electron microscope (SEM), we can observe that the crystal structure of gypsum crystal with active excitation component (Group B) (Figure 2) is more compact than that of gypsum crystal without active excitation component (Group A) (Figure 1). $\text{Na}_2\text{C}_2\text{O}_4$ promotes the dissolution of gypsum, increases the supersaturation of gypsum dihydrate, decreases its critical nucleation radius, accelerates the nucleation and growth rate of crystals, and the formation of SO_4^{2-} rich liquid phase by $\text{Na}_2\text{C}_2\text{O}_4$ facilitates the formation of gypsum dihydrate crystal matrix and increases the nucleation centre of gypsum dihydrate crystals (Peng et al.,2009).

2.1.3. Water demand of retarded slurry

By process arrangement, when the material was extruded by the printer, the materials were built layer by layer (building stage) and allowed to be cured (curing stage) to develop strength. In the latter two stages, the material would solidify. Compared to the former and latter two stages, the material needs to transform rapidly from fluid to solid (Huang et al., 2021).

For the slurry treated with retarding components, due to the addition of PCE, the water demand of gypsum under standard consistency will be reduced. At the same time, to ensure sufficient hydration, kaolin is introduced to ensure the integrity and workability of the slurry. Therefore, before the formal printing, the water demand gradient experiment is adopted to determine the water demand in the mixing process (Figure 3).



Figure 3. water demand of retarded slurry research

Experiments have learned that the standard consistency of gypsum slurry after retarder has changed, so in the actual printing, to ensure that the slurry extrusion can be quickly formed, to strictly control the amount of water required for mixing, not only to ensure that the gypsum gets fully hydrated, but also can avoid too much water hindering the formation of early strength.

2.1.4. Accelerator

The setting time of the gypsum slurry was measured by using a Vicat apparatus

according to Chinese national standard GB/T 17669.4 (Liu et al., 2018).

It is generally accepted that the mechanism of hydration hardening of gypsum accepts the theory of precipitation-dissolution equilibrium. The action mechanism of the accelerator is to significantly increase the concentration of sulfate ions in the slurry in a short time to form a supersaturated solution of dihydrate gypsum; therefore, the dihydrate gypsum crystal will be precipitated at a reasonably rapid rate. At the same time, the existing gypsum continues to dissolve and is replenished with new calcium and sulfate ions. Under the action of the original active excitation component, the crystallization power of dihydrate gypsum continues to increase. The rate of crystal nucleation and growth increased rapidly and finally achieved the effect of rapid solidification.

Sulfates such as sodium sulfate (NS) and potassium sulfate (KS) were effective accelerators for gypsum (Huang et al., 2021).

2.2. WORKFLOW

2.2.1. Modified gypsum recyclable life cycle

The hardening process of gypsum is the process of a chemical reaction between hemihydrate gypsum and water to form dihydrate gypsum. After a high temperature of 170°C-190°C, dihydrate gypsum can lose crystalline water to form α -hemihydrate gypsum or β -hemihydrate gypsum, and we can make use of this recycling process to realize the recycling of gypsum (Figure 4).

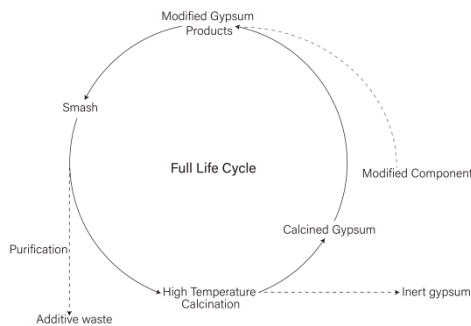


Figure 4. The life cycle of modified gypsum

2.2.2. Parameter-based gypsum 3D printing workflow

The core of the workflow (Figure 5) proposed in this paper lies in the synergy of the material modification study, the conveying-extrusion unit, the robot system, and the control system. The control system (SIEMENS S7-1200PLC) allows real-time adjustment of the operating rate of each motor on the robot, while the intervention of the material directional modification means creates the possibility of long-term stable operation of the large-scale process.

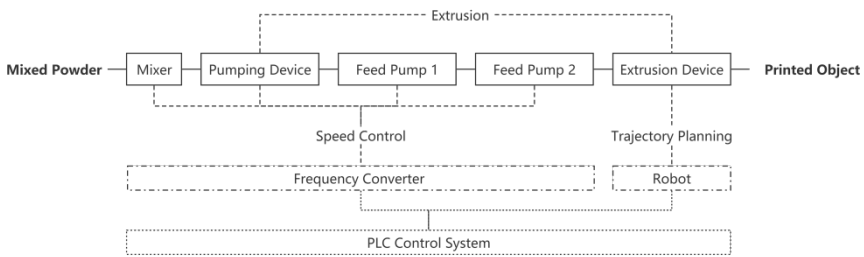


Figure 5. Robot-based gypsum 3D printing workflow diagram

3. Experiment

3.1. DIGITAL FABRICATION EQUIPMENT

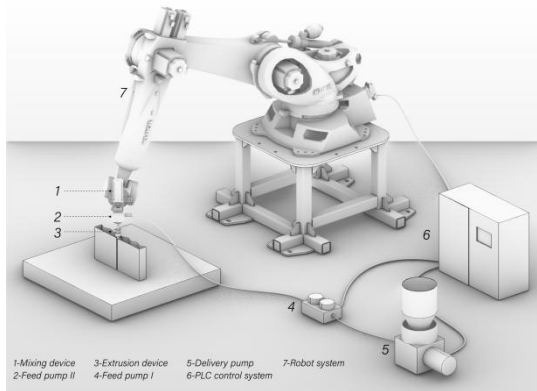


Figure 6. Coupling of model printing speed with process characteristics

The 3D printing device is also designed in a targeted manner based on the characteristic data presented in different stages of the preliminary material modification experiments (Figure 6). Firstly, the slow-setting gypsum slurry can not harden within the effective time while maintaining good fluidity and integrity. Therefore, a dosing screw pump (86 stepper motor) can be used to convey the slow-setting gypsum slurry without worrying that the gypsum will harden in the conveying tube, and the process will not unfold continuously. Secondly, the transported slurry is excited to the active state after passing through the active excitation component dosing pump (dosing pump 1), and the hardening process of the gypsum slurry begins. Therefore, in the actual production, the distance between the charging pump 1 and the fast-setting component (charging pump 2) should not be too long so that the residence time of the active slurry in the delivery pipe is less than the stable holding time of the active slurry to prevent the active gypsum slurry from hardening in the tube. Finally, the charging pump 2 and the stirring device will mix the active slurry with the fast-setting component

sufficiently, and the extruded gypsum slurry will achieve initial setting and initial strength formation in a short time.

3.2. PARAMETER-BASED CONTROL EXPERIMENT

The rate control technology of the printing equipment is also an essential factor in determining the outcome of the process route. The robot's movement rate, pumping rate, the pumping rate of the active excitation component, and the pumping rate of the fast-setting component are all used as dependent variables for preset printing requirements, and different printing requirements require different rate control techniques. Moreover, the radius size of the extrusion end is directly related to the width of the print trajectory, so the size and specification of the printed components should be determined before each printing process, and the rates should be determined by the correlation coefficients of the equations, and the process details should be regulated in the signal control system. In the printing experiment, we selected the extrusion end with a radius of 4mm.

The following is a summary of the equations related to rate control based on the test printing process.

V is the pumping volume flowrate.

S₁ is slurry pumping rate.

r is the radius of the extrusion end.

S₂ is the pumping rate of the excitation component.

S₃ is the pumping rate of the quick setting component.

Both α and β are processing coupling parameters.

$$V = \pi r^2 \cdot S_1, V = \alpha \cdot S_2, V = \beta \cdot S_3$$

Therefore:

$$S_2 = (\pi r^2 / \alpha) \cdot S_1 \quad (1)$$

Similarly:

$$S_3 = (\pi r^2 / \beta) \cdot S_1 \quad (2)$$

According to the above equation, we can see that the slurry pumping rate, active excitation component pumping rate, and rapid solidification component pumping rate show a linear relationship under the premise of constant extrusion head radius, but in actual production, this linear correlation coefficient will also fluctuate within a specific error interval due to the difference of ambient temperature and humidity.

The following figure (Figure 7) represents two scenarios of the rate control experiment. The left figure reflects the ratio of S₂ to S₃ is greater than the error range of the specified interval, resulting in the gypsum slurry not being able to achieve rapid curing after extrusion, unable to form structural strength, and the lower trajectory being crushed by the weight of the upper trajectory and structural damage occurring; the right

figure reflects the printing effect where the ratio of the two is within the standard error range.



Figure 7. Rate control experiment

3.3. EXPERIMENT PROCESS

Scale is an unavoidable topic for any laboratory process to develop into a mature industrial process. To develop the existing desktop-scale printing process into a building-scale printing process, it is necessary to ensure a continuous and stable large-scale production workflow.

The workflow of 3D modified gypsum printing is explored by coupling material properties with process characteristics after separate studies of material modification components and 3D printing equipment, which should firstly introduce different material modification components into the gypsum hydration and hardening process in stages according to the different characteristics of different stages of the expected process. The illustration (Figure 8) process is mainly realized through the printing device, while the modified components adjust the setting time, molding strength, and micro-structure of the gypsum slurry.

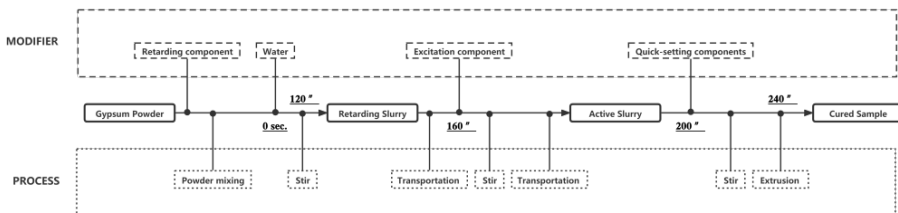


Figure 8. Coupling of process characteristics and material properties

4. Result

In the end, a 600mm×75mm×130mm curved gypsum panel is successfully printed in 30 minutes as experiment verification. By contrast, the PBBJ technique takes far more time to achieve a object of the same size than this technique.

Different printing targets are suitable for different precision printing processes. PBBJ technology has advantages in achieving desktop-level decorations but is not suitable for the manufacture of architectural components, and extrusion-based gypsum printing has made exploration in this direction.



Figure 9. Print process and micro-structure of gypsum treated with modified components

The SEM result shows that, after the gypsum slurry treated with modified components is cured, the intervention of two induced hydration hardening behaviors can be seen. The active excitation component makes the remaining tiny crystals continue to grow on the existing crystal core, quickly form the crystal cluster structure, and realize the rapid hardening of the gypsum slurry (Figure 9).

5. Conclusion and Prospect

The modification status retention time at each stage is the most critical element of the envisioned printing process. After the experiment of curing time of materials, we got the stable holding time of each stage, and the holding time of the retarded state could be maintained over and under 40 minutes, which created conditions for the stable delivery in the process flow; Prompt intervention of rapid curing component within 5 min after the action of active excitation components can allow the gypsum to achieve incipient solidification 2-4 minutes after extrusion from the tool head, achieving the intended conception goals (Table 2).

Table 2. Effect of modified components

Component	Phase	Stabilization Time
PS PCE HPMC	Retarding State	40±5 min
Dihydrate Gypsum Sodium Oxalate	Active Excited State	7±2 min
KS NS	Rapid solidification State	3±1 min

This paper takes materials research as the starting point. It proposes three material modification components (slow-setting component, fast-excitation component, and fast-setting component) for the reaction characteristics of natural gypsum materials in the two stages of hydration and hardening, which are used to modulate the original properties of gypsum and adapt them to the robotic construction process. Among them, the introduction of the active excitation component and the rapid hardening component can make the gypsum paste develop strength rapidly after extrusion at the tool end, which can prevent the structural damage caused by the upper print path crushing the lower print path and keep the printed components with good molding stability.

In addition, this paper also designs a set of extrusion-based gypsum 3D printing equipment with the phase characteristics presented by the modified gypsum slurry. It

proposes a gypsum 3D printing workflow that couples the process steps with the material properties after continuous experiments. For the recyclable characteristics of gypsum dihydrate, this paper composes a practical flow of the recyclable life cycle of modified gypsum based on industrial production.

Moreover, this research has many subsequent development directions. Issues like how to induce the hydration process of gypsum by temperature control, and how to print lightweight gypsum sheets, etc, are worth further investigation in the future.

References

- Dantas, A. C. S., Scalabrin, D. H., De Farias, R., Barbosa, A. A., Ferraz, A. V., & Wirth, C. (2016). Design of Highly Porous Hydroxyapatite Scaffolds by Conversion of 3D Printed Gypsum Structures – A Comparison Study. *Procedia CIRP*, 49, 55–60. <https://doi.org/10.1016/j.procir.2015.07.030>
- Doleželová, M., Scheinherrová, L., Krejsová, J., Keppert, M., Černý, R., & Vimmrová, A. (2021). Investigation of gypsum composites with different lightweight fillers. *Construction and Building Materials*, 297, 123791. <https://doi.org/10.1016/j.conbuildmat.2021.123791>
- Huang, J., Duan, B., Cai, P., Manuka, M., Hu, H., Hong, Z., Cao, R., Jian, S., & Ma, B. (2021). On-demand setting of extrusion-based 3D printing gypsum using a heat-induced accelerator. *Construction and Building Materials*, 304, 124624. <https://doi.org/10.1016/j.conbuildmat.2021.124624>
- Jia, R., Wang, Q., & Feng, P. (2021). A comprehensive overview of fibre-reinforced gypsum-based composites (FRGCs) in the construction field. *Composites Part B: Engineering*, 205, 108540. <https://doi.org/10.1016/j.compositesb.2020.108540>
- Liu, C., Gao, J., Tang, Y., & Chen, X. (2018). Preparation and characterization of gypsum-based materials used for 3D robocasting. *Journal of Materials Science*, 53(24), 16415–16422. <https://doi.org/10.1007/s10853-018-2800-8>
- Liu, C., Gao, J., Tang, Y., & Zhao, Y. (2019). Early hydration and microstructure of gypsum plaster revealed by environment scanning electron microscope. *Materials Letters*, 234, 49–52. <https://doi.org/10.1016/j.matlet.2018.09.071>
- Mucha, M., Mróz, P., Wrona, D., Konca, P., & Marszałek, J. (2020). Microstructural formation of gypsum by setting in the presence of hydroxypropyl methylcellulose (HPMC). *Journal of Thermal Analysis and Calorimetry*. <https://doi.org/10.1007/s10973-020-10398-3>
- Qi, H., Ma, B., Tan, H., Su, Y., Lu, W., & Jin, Z. (2021). Influence of fluoride ion on the performance of PCE in hemihydrate gypsum pastes. *Journal of Building Engineering*, 103582. <https://doi.org/10.1016/j.jobbe.2021.103582>
- Zhi, Z., Huang, J., Guo, Y., Lu, S., & Ma, B. (2017). Effect of chemical admixtures on setting time, fluidity and mechanical properties of phosphorus gypsum based self-leveling mortar. *KSCE Journal of Civil Engineering*, 21(5), 1836–1843. <https://doi.org/10.1007/s12205-016-0849-y>
- Zhi, Z., Ma, B., Tan, H., Guo, Y., Jin, Z., Yu, H., & Jian, S. (2018). Effect of Competitive Adsorption between Polycarboxylate Superplasticizer and Hydroxypropylmethyl Cellulose on Rheology of Gypsum Paste. *Journal of Materials in Civil Engineering*, 30(7), 04018141. [https://doi.org/10.1061/\(ASCE\)MT.1943-5533.0002346](https://doi.org/10.1061/(ASCE)MT.1943-5533.0002346)
- Zhou, J., Liu, C., Shu, Z., Yu, D., Zhang, Q., Li, T., & Xue, Q. (2015). Preparation of specific gypsum with advanced hardness and bending strength by a novel In-situ Loading-Hydration Process. *Cement and Concrete Research*, 67, 179–183. <https://doi.org/10.1016/j.cemconres.2014.09.004>

DROOP – AN ITERATIVE DESIGN TOOL FOR MATERIAL DRAPING

GABRIELLA PERRY¹ and JOSE LUIS GARCÍA DEL CASTILLO Y LÓPEZ²

^{1,2}*Harvard Graduate School of Design.*

¹*gperry@gsd.harvard.edu, 0000-0001-7246-5745*

²*jgarciaadelcasti@gsd.harvard.edu, 0000-0001-6117-1602*

Abstract. Advances in large-scale 3D printing technology have opened up explorations on novel non-solid, non-layered 3D printing techniques such as spatial lattices and material draping. These new printing techniques have potential to reduce the wasted material from printing support structures and optimize overall material use. However, due to the inherent material unpredictability of many of these systems, they are often difficult to approximate with digital tools, often requiring simple trial and error to achieve a specific result, with the consequent waste of time and resources. Droop is a work in progress material-informed simulation environment that serves as an iterative design tool for material draping fabrication processes. Droop explores the material potential of thermoplastics through the fabrication process of robotic draping to achieve complex linked catenary forms. This bespoke simulation environment approximates the spatial form of a material draping process and serves as a useful iterative design tool that allows designers to better understand and predict how a 2D pattern translates into a 3D droop form. The simulation also reduces the amount of wasted material produced by trial-and-error material draping processes. In this paper, we present the digital simulation framework, discuss methods for material-informed calibration, and show a set of experiments produced with this tool.

Keywords. Material Draping; Physics Simulation; Additive Manufacturing; Robotic Fabrication; Catenary Geometry; SDG 12.

1. Introduction

Before the advent of 3D printing and digital fabrication technologies, architects experimented with complex 3D spatial modelling using physical materials and tools. The primary example of this is Antonio Gaudí's modelling work on the Colònia Güell chapel and the Sagrada Família (Burry 2016). Gaudí designed the structure for the Güell chapel using catenary curves and paraboloids and modelled the vaulted spaces of his work using hanging weighted chain models. (Figure 1.1) Because of gravity, the chains hung in a compressive form, and by changing the model's parameters, Gaudí could iteratively generate other spatial configurations. (Makert and Alves 2016). The principles from Gaudí's models are still relevant in new digital fabrication processes,

more specifically in non-layered additive processes involving material deposition.



Figure 1.1 Antonio Gaudi's chain model hanging in the Sagrada Família

Non-layered additive processes are a subsection of additive manufacturing techniques that create objects without building up planar layers (Rosenwasser 2017). These processes include the printed layering of truss-like spatial lattices (Chen 2019; Im et al. 2018), the weaving of material so that layers become interlaced (Friedman et al. 2014), and other additive processes (Bilotti et al. 2018). Companies like Branch Technology are utilizing printed spatial lattices in architectural elements like facades and pavilions (BranchMatrix 2021). However, none of these have explored draping malleable material over a supporting contour with unsupported voids as a method for achieving 3D form. Form draping has been done in the Robosense 2.0 project (Bilotti et al. 2018), but the form is only inches from the print nozzle. Droop explores the formal potential of draping malleable material over a supporting contour to generate 3D spatial geometry with minimal material.

2. Methods

2.1. INTRODUCTION

This paper presents Droop, a work in progress material-informed simulation environment that serves as an iterative design tool for material draping fabrication

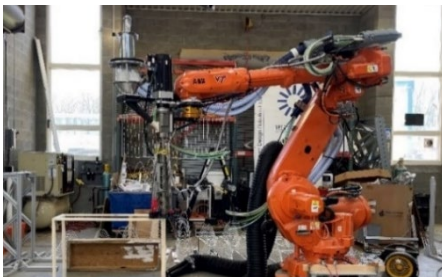


Figure 2.1 Material draping set up using an industrial robot arm, a large thermoplastic pellet extruder, and a wooden profile template.



Figure 2.2 Completed material draping test over wooden profile template.

processes. In particular, Droop is specifically optimized for the draping of molten plastic over a "profile template" to produce parabolic, 3-dimensional catenary shapes— noted in this paper as "droops". A profile template is a form made of solid material, typically a laser cut plywood sheet, supported by a frame, such as 2x4" wood studs, where the topmost surface serves as the anchoring support for the droops.

Droop is a particle simulation system written in the C# language and executable in Grasshopper (Davidson 2007), a visual programming interface for the 3D modelling software Rhino (McNeal et. al 2010). Droop simulates the material draping by treating tool paths as node and spring models, discretizing them dynamically and iteratively as the simulation evolves, and deforming them elastically over time. The goal of Droop was to simulate this particular fabrication process--draping molten plastic with a moving extruder--as close as possible. The process is difficult to approximate without a digital tool because of the dynamic extrusion of material, unpredictability of the material with consistent settings, and the collisions between fresh molten droops and older, hardened droops. The particularities of this process were the main motivation for the development of a bespoke solution, as opposed to using readily available particle simulation tools, such as Kangaroo (Piker 2012). The hope is that Droop as a design tool will be able to simulate the outcome of the physical robotic draping process with a reasonable degree of accuracy, and allow designers to perform digital form-finding previous to the fabrication process.

2.2. PRELIMINARY STUDY

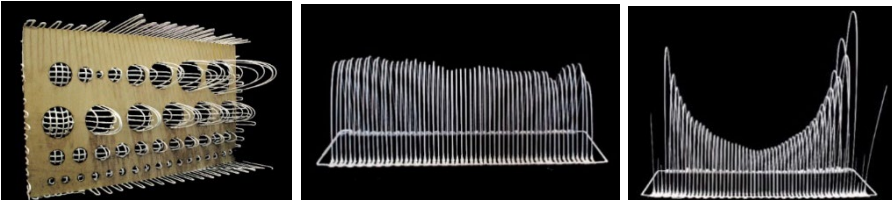


Figure 2.3 A preliminary test with the profile template still attached. Figure 2.4 The speed control test. Figure 2.5 The speed variation test.

A preliminary study was conducted to assess the feasibility of digitally simulating the fabrication process. The testing was conducted using a large Strangpresse thermoplastic pellet extruder mounted to an ABB 6640 industrial robotic arm (Figure 2.1). Our bespoke robotic draping process involves the extrusion of fiber-reinforced PETG plastic over a profile template (Figure 2.2). Preliminary profile templates were designed to experiment with the material, and had cut-outs of varying sizes to produce droops with longer or shorter "depth". Depth is defined as the linear distance between the midpoint between droop supports, and the vertex of the parabola it forms.

An initial round of tests was designed to determine what families of forms could be created using material draping, and to explore the affordances of this process (Figure 2.3). These tests were conducted without any prediction simulation. The most

significant of these preliminary tests were designed to quantify the unpredictability of the process and the relationship between the robot speed and droop depth. These two tests were ran using the same profile template: a simple rectangular void shape, 12 in. wide by 36 in. long, with droops being draped in the transversal direction.

The first test was a control test, with the extruder moving at a constant speed and draping droops with identical spans (Figure 2.4). Upon physical measuring, it was found that there was significant variation from droop to droop, even with consistent settings. The largest droop depth in the control test was 13 in, while the shortest was 9.5 in. The standard deviation from the average was 1.5 in, a 13.5% margin of error. These results showed early evidence of the inconsistent behaviour of the material, even under constant parameters, possibly due to internal variations in the melting process of the pellets, or unaccounted variations in material temperature.

The second test was designed to quantify the relationship between robot speed and droop depth. It was speculated that by draping droops at linearly increasing robot speeds, the result would be droop depths increasing quadratically. In this test, all droops were draped using the same extrusion speed, and a starting robot linear speed of 44 mm/s. Successively, each additional droop was draped with a robot speed 2 mm/s larger, until the speed reached 100mm/s in the last droop. This pattern was then inversely replicated, draping the same number of droops at robot speeds 2 mm/s smaller. The result of the test validated the hypothesis, producing a set of droops collectively approximating the form of a downward-facing parabola (Figure 2.5). However, this test further showcased the inconsistency in depth variability found between droops draped at the same speed.

2.3. DROOP SIMULATION

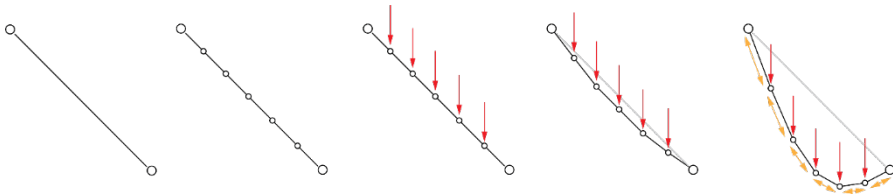


Figure 2.6 Diagram of Droop Simulation. From left to right, the line is input, the line is divided into nodes and springs, gravity is applied to the nodes, gravity is applied continuously until the force of the springs is equivalent to that of gravity.

Droop is a physics particle system that simulates material draping by treating tool paths as node and spring models, discretizing them dynamically and iteratively as the simulation evolves, and deforming them elastically over time. Node mass is computed by estimating the linear weight of the actual material deposited by the extruder, divided by the number of nodes per unit of length in the simulation.

The simulation is dynamic, continuously updating and applying gravity to each node until the spring forces reach an equilibrium with the gravitational forces (Figure 2.6). Since the robot performing the material draping pro-

cess currently follows linear paths, the lines are progressively fed to the simulation in the order that the robot would complete each line, and draped sequentially to help detect collisions between droops. Nodes are merged upon collision detection, based on proximity. The simulation also incorporates time-dependent node fixing, to emulate the hardening of the plastic over time.

2.4. PHYSICAL TESTING

A preliminary round of testing was conducted, using a profile template with 24 rectangular openings of increasing span distances, from 1 in. to 12.5 in. in increments of 0.5 in. (Figure 2.7 & 2.8). With extrusion speed set to a fixed value, six robot linear speeds were tested: 100, 85, 70, 55, 45 & 35 mm/s. During this testing, it was found that the linear length of material deposited along the supports of a droop played a large role in determining the depth of said droop. This distance was fixed to a constant in subsequent tests. A second profile template was designed with the same rectangular gaps but with a consistent edge condition (Figure 2.9), and rounds of physical drooping were conducted at the same set of robot speeds (Figure 2.10).



Figure 2.7 Profile template #1 with inconsistent edge conditions on the right side.

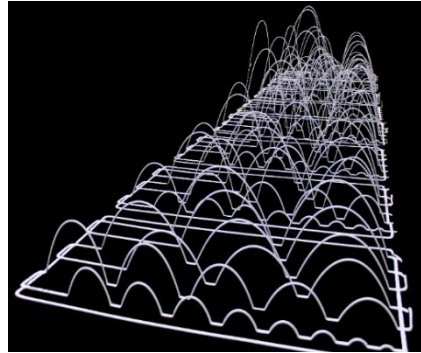


Figure 2.8 All eight tests in the first round lined up from robot speed 100 – 55 mm/s and then extruder speeds 700 – 400 RPMs



Figure 2.9 Profile template #2 with a one-inch edge condition.

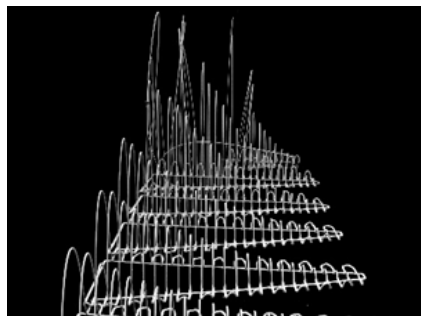


Figure 2.10 Second round of testing with robot speeds 100 to 35mm/s, showing the increase in droop depth based on speed and gap size.

The tests confirmed that the relationship between droop span and droop depth for a set speed value approximates a parabolic shape (Figure 2.12). Every droop from this round was manually measured, recorded, and plotted, and polynomial regression was used to fit second-degree curves for each robot speed, to model the material behaviour (Figure 2.11). It was observed that the slower robot speeds and the larger spans resulted in depths diverging from the model, meaning the more material deposited over a longer distance, the more unpredictable a droop becomes.

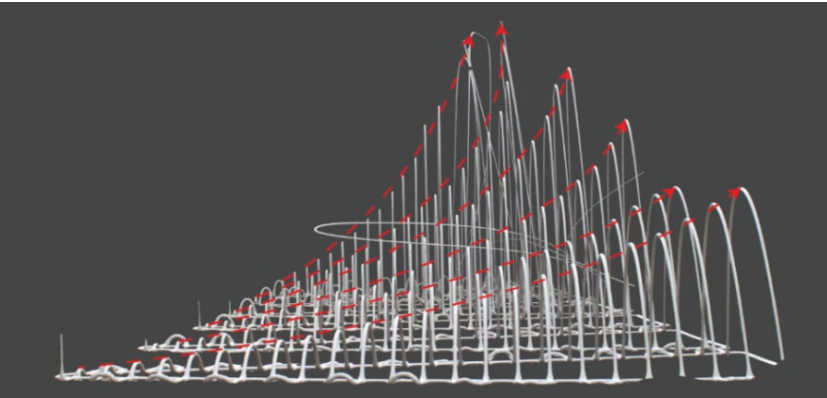


Figure 2.11 The combined physical tests with an approximated droop depth trendline.

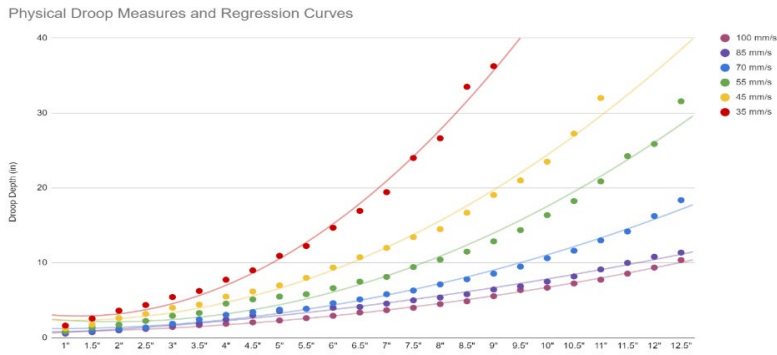


Figure 2.12 A plot of all measured droop depths from the physical prototypes for each robot speed and gap size, and fitted regression curves.

2.5. MODIFYING SIMULATION FOR PHYSICAL TESTING

According to Hooke's Law, spring forces are linearly dependent on the stretch length, factored by a spring constant that defines their strength. The value of this constant is characterized by the physical configuration of the spring and, as an abstract model representing molten plastic, could not be explicitly measured

from physical prototypes. To calibrate the digital simulation to the physical process, the spring constant in the simulation was chosen as the open parameter. In this research, we applied heuristic testing methods to determine appropriate empirical values for the simulated spring constant.

A digital simulation was created using Droop, mimicking the parameters of the physical tests: unsupported droop widths and robot speeds. A random value of the spring constant was selected for this initial test. The droop depths of these digital tests were measured and recorded, and plotted against the droop depths of the physical tests for comparison (Figure 2.13).

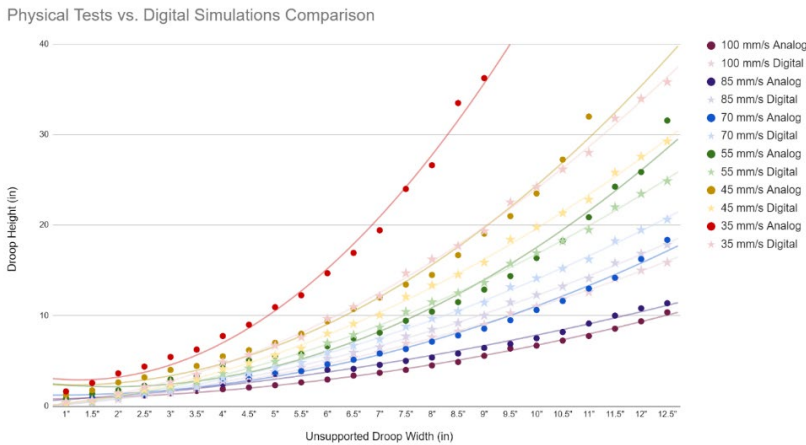


Figure 2.13 Comparison between physical tests (circles) and digital simulations (stars). The only initially correlated results are for the 55 mm/s tests.

Upon comparison of the digital and physical tests results, it was found that only the measures for the 55 mm/s robot speed were correlated. Additionally, it was observed that different speeds had different degrees of droop depth variations in the digital and physical tests. It was speculated that the spring constant should be considered variable depending on robot speed, potentially due to differential flow and accumulation of material along the drooping bead during the molten state.

To improve the simulation, a model for a spring constant linearly dependent on robot speed was tested. Two spring constants k_{35} and k_{100} were heuristically determined to obtain simulation results that correlated with the physical tests at the bounds of speed ranges 35 and 100 mm/s respectively (Figure 2.14). The hypothesis behind this method was that, for a given robot speed S , a matching spring constant k_S could be calculated linearly interpolating between these two extremes, based the robot speed:

$$k_S = k_{35} + (S - 35) \frac{k_{100} - k_{35}}{100 - 35}$$

To verify this hypothesis, a series of digital simulations were conducted with interpolated spring constants based on their simulated robot speed. The results of these tests showed that there was a large discrepancy between the simulation results and the physical tests, except for the heuristic k35 and k100 values, rendering this hypothesis invalid (Figure 2.15). A possible reason for this lack of correlation might be that the relation between robot speed and spring constant is nonlinear, and small differences in robot speeds at lower ends produce much larger variations in spring constants. Further research will be done in this direction to explore higher-degree regression methods for the generation of speed-based virtual simulation parameters.

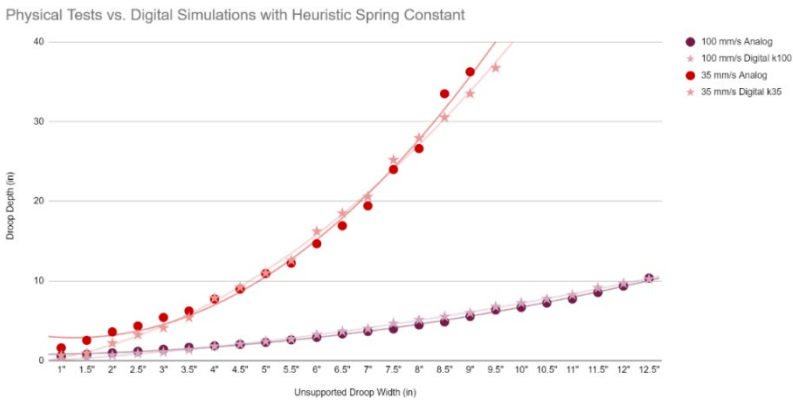


Figure 2.14 Comparison between physical tests and digital tests 35 mm/s and 100 mm/s with modified spring constants.

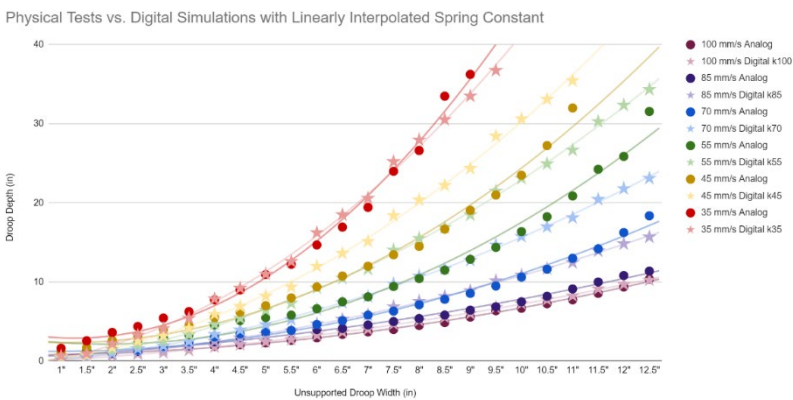


Figure 2.15 Comparison between physical tests and digital tests with linearly interpolated spring constants.

3. Results

A final round of testing was conducted to determine the viability of the Droop simulation as an iterative design tool. Six tool paths were designed to be ran through the Droop simulation to predict the outcome droop geometry. The robot speed used for all six tool paths was 100 mm/s, with a constant extruder speed of 500 RPM. The physical parameters for robot and extruder speed were consistent between the simulation and the physical testing, and all tests used the same wood profile template, a rectangular void shape 10 in. wide and 36 in. long.

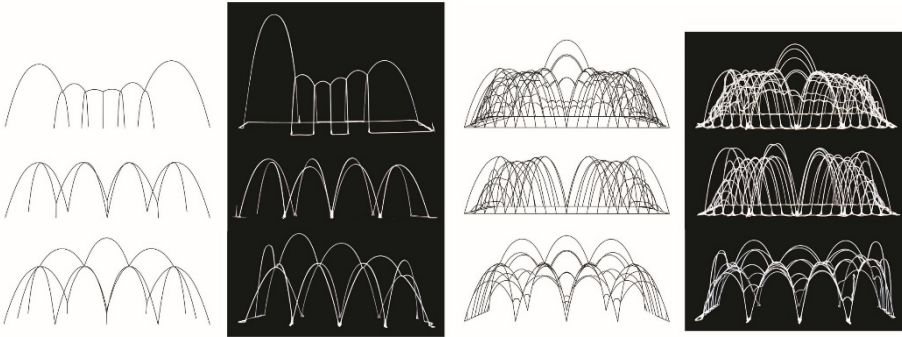


Figure 3.1 Left: Views of the simulated deformation of the test tool paths. Right: photos.

The outcomes of these physical tests were formally like those of their Droop simulation (Figure 3.1). The most significant errors between the simulation and the physical test are due to the fact that the robot extrudes continuously, and the droops start sagging while the robot is completing a tool path segment, whereas the current simulation also sags droops in sequential order, but starts sagging only from complete toolpath segments. This difference produces simulations that do not account for the inherent bias in the fabrication process towards the direction the robot is traveling.

4. Conclusion

In this paper we presented Droop, a bespoke simulation environment able to approximate the spatial form of a material draping process. Droop was designed for a specific combination of fabrication components and material. However, the same method could be applied to different setups, to determine the parameters that correctly characterize the computational simulation. Droop is a useful iterative design tool that allows designers to understand better how a 2D pattern translates into a 3D droop form. Additionally, we presented a heuristic testing process for digital/physical calibration, which could be applied to other additive and malleable material processes, such as clay.

Currently, the accuracy of this simulation is limited to the robot speeds of 35 – 100 mm/s and unsupported distances up to 12.5 in. Further testing must be performed to widen the working range of the simulation. Further improvements will include the

simulation of material hardening over time, and exploration into non-linear scaling the spring constant in order to accurately predict a wider range of robot speeds. The viability of this process for other materials such as different plastics, clay bodies, and other phase-changing materials could be addressed. Finally, increasing the scale could potentially lead to the development of human-scale structures that are lightweight and easily fabricated on-site. These human scale structures could be used as exterior pavilions or shading devices, or potentially be integrated with other materials in the construction of a full-scale building.

Acknowledgements

This research was supported by Virginia Tech's Center for Design Research and the Harvard Graduate School of Design. Thank you to Dr. Nathan King and Robert Dunay for your assistance with this project.

References

- Bilotti, J., Norman, B., Rosenwasser, D., Leo Liu, J., & Sabin, J. (2018). Robosense 2.0. Robotic sensing and architectural ceramic fabrication. *ACADIA Recalibration. On imprecision and infidelity 2018* (pp. 276-285).
- BranchMatrix (2021). *oneCITY Pavilion*. Retrieved January 25, 2022, from <https://branchtechnology.com/design-miami-pavilions-2/>.
- Burry, M. (2016). Antoni Gaudi and Frei Otto: Essential precursors to the parametricism manifesto. *Architectural Design*, 86(2), 30-35.
- Chen, Z., Zhang, L., & Yuan, P. F. (2019). Innovative design approach to optimized performance on large-scale robotic 3D-printed spatial structure. *Proceedings of the 24th CAADRIA Conference 2019* (pp. 451-460).
- Claire Im, H., AlOthman, S., & Garcia del Castillo y Lopez, J. L. (2018). Responsive Spatial Print. Clay 3D printing of spatial lattices using real-time model recalibration. *ACADIA Recalibration. On imprecision and infidelity 2018* (pp. 286-293).
- Davidson, S. (2007). *Grasshopper, Algorithmic Modeling for Rhino*. Retrieved from <https://www.grasshopper3d.com/>
- Friedman, J., Kim, H., & Mesa, O. (2014). Experiments in additive clay depositions. In *Robotic Fabrication in Architecture, Art and Design* (pp. 261-272). Springer.
- Makert, R., & Alves, G. (2016). Between designer and design: Parametric design and prototyping considerations on Gaudi's Sagrada Familia. *Periodica Polytechnica Architecture*, 47(2), 89-93.
- McNeel, R., & Others. (2010). *Rhinoceros 3D, Version 6.0*. Robert McNeel & Associates, Seattle, WA.
- Piker, D. (2012). *Kangaroo Physics*. Retrieved from <http://kangaroo3d.com/>.
- Rosenwasser, D., Mantell, S., & Sabin, J. (2017). Clay non-wovens: robotic fabrication and digital ceramics. *ACADIA: Disciplines & Disruption 2017* (pp. 502- 511).

BIO-SYNTHETIC ASSEMBLAGES

Computational Assembly of Synthetic Bio-sand Units Made from Dune Sand

MARCUS FARR¹

¹*Tongji University / American University of Sharjah*

¹*mfarr@aus.edu*

Abstract. Biomineralization is the process by which living organisms produce minerals to harden or stiffen exoskeletons and existing tissues. Mineralization is a widespread phenomenon among all taxonomic animal kingdoms. The material used in this project attempts to replicate the process of hardening and mineralizing dune sand found in the Sahara and Arabian deserts. This material is found in vast quantities but thought to be of little use in modern construction. The new bio-synthetic material used in this study is paired with the process of augmented construction and computational placement of tectonic units. The paper overlays a broad question of how organizational systems might integrate architecturally with regionally appropriate bio-material composed of dune sand and, more specifically, how this material process creates a consistent, viable architectural outcome with dune sand as a primary ingredient for architectural material. As the material agenda reaches maturity, we ask how the production of this bio-material can be combined with computation to articulate consistent architectural outcomes within a desert-specific environment. The role of this computational and material process adds to the current dialogue of designing in extreme environments and aligns with the UN Sustainable Development Goals for sustainable communities, responsible consumption and production, climate action, and life living on land.

Keywords. Performance-based design; Bio-material; Computational design; Innovative material use; Augmented Construction; SDG 11; SDG 12; SDG 13; SDG 15.

1. Introduction

Dune sand is known to be an unstable material compared to river sand and as a result it is not normally used for construction. Because of this, desert regions have grown a reliance upon imported materials. This research indicates there is a viable opportunity to leverage dune sand as an ongoing line of material inquiry, establishing that there is very little being done in architectural research that responds to the populations living

in harsh desert environments partnered with bio-sand material and computational design. The methodology begins with experiments in bio-material with sand as a compound, and then, through empirical testing, establishes an ongoing construction sequence selected from a manifold of recreations based on successful experiments. This process uses the Scientific Testing Method and Hypothesis in Action, allowing the results to inform "design by research", followed by application.

Computational parameters are used to determine a series of performative results for regionally appropriate construction based upon the characteristics of the material strength and dimension. The material demonstrates it can be used in a variety of capable configurations that make unit based, porous constructions such as those used for thick stereotomic wall types, and ventilated mashrabiya walls. These are computationally designed to be culturally appropriate to the region. Grasshopper is used to arrange the units into compositions that are also environmentally responsive and controllable. The computational patterns can be opened or closed in varying degrees to adjust for orientation and site conditions. The work illuminates possible solutions for the regional problem of building in the Arabian and Sahara Desert utilizing a surplus of dune sand to construct locally appropriate wall types that build upon vernacular traditions but offer a more performative result. Compared with other methods such as concrete or masonry, which use high degrees of imported material, this solution can be more sustainable. To meet the UN sustainability goals, we must research and discover more applications for available resources in extreme environments. This paper documents a method, a material, and an outcome with a variety of potential possibilities.

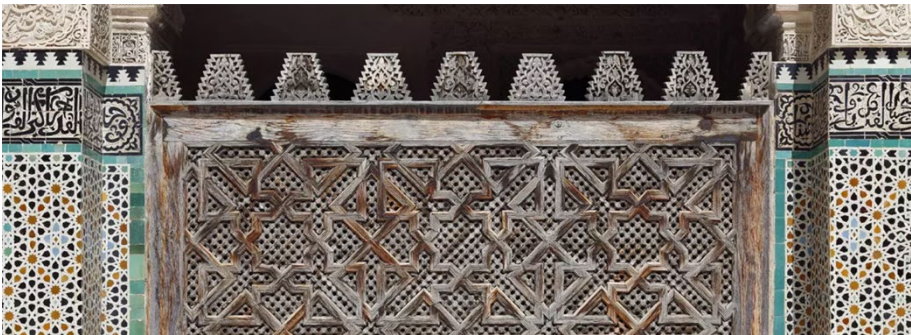


Figure 1. Bou Inania, Mashrabiya barrier, Fez, Fez-meknes, Morocco, 1350, photo, B. Hemer

2. Context

The context for this research begins in the deserts of Arabia and North Africa by looking for answers relative to how we might design in this context in current day. The vernacular traditions in these regions are limited by their material resources. Mud, arish, coral stone and rock were used traditionally when available, especially along the coasts. Fabric was used for nomadic tribes who circulated through the deserts seeking favourable weather patterns as it was light weight and offered architectural flexibility and could be transported on camel back. The question arises as to what local materials are widely available and what can be leveraged for research as a further line of inquiry relative to architecture. These regions have a massive surplus of sand, and yet very

little of it is utilized for construction. Modern cities such as Dubai, Sharjah, Abu Dhabi, and Jeddah are literally surrounded by sand yet it is mostly unused. Instead, other types of sand are imported from other countries for construction because river sand is deemed to be of higher quality for architecture and manufacturing. In these regions, imported sand is brought in from Southeast Asia and Australia by boat to manufacture concrete, glass, mortar and block which increases the carbon footprint and overall sustainability factor for every architectural project in the region. So, what is the role of the desert in modern construction? What opportunities arise from this situation?

Sand is a resource heavily in demand. It is the most widely used resource in the world besides air and water. It is in everything we use in modern society, cell phones, glass, concrete, roads, computers. Yet the largest concentration of sand is not used. The importance of understanding how desert sand can be used is a critical environmental concern especially for the regions living closest to it.

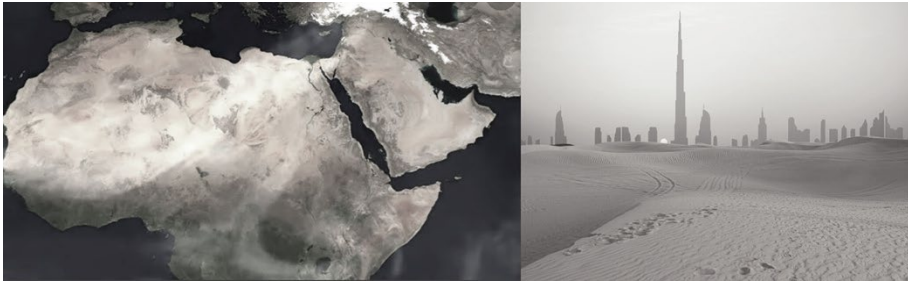


Figure 2. Satellite image of Sahara & Arabian Deserts and Dubai.

3. Properties and Necessity

“Natural sands are eroded or weathered particles of rocks. Sand is made by simply grinding up rocks into increasingly smaller pieces. Sand can also be made out of living creatures, from shells and other organisms of the living world, and many beaches are composed of pulverized animal shells. Sand grains can originate from catastrophic geologic phenomena, as when molten lava erupts from volcanoes and shatters in the air, scattering particles across the oceans to land as tiny grains.” (Rael and San Fratello, 2018). Sand is different depending on its origin and the potential uses are different as well compared to origin. Desert sand has a different set of physical characteristics compared to river sand. River sand is sharp and angular as the grains were conditioned by water rather than air, it contains higher concentrations of quartz, and as a result it compacts successfully as a mixture for concrete. Desert dune sand is round and does not self-organize in the same way river sand does. Because it was conditioned by air, the grains are round in shape, so it organizes like a bag of marbles. The grains have a smooth surface finish and the particle size of desert sand is very fine, it is slightly alkaline in nature, and it is very dense, similar to dirt, all of which make it less useful for modern construction. Sand is a self-organizing material, as are all aggregates, and adheres to a consistent behavior when poured. As the architect Frei Otto noted with extensive studies of spoil piles and sand, these materials have "a funnel that is formed within the granule mass with a natural angle of repose" (Otto, 1992). Measuring a material angle of repose produces slightly different results. (Nichols and

Franklin,1898), however in sand it is normally a 34 degree angle, which limits it (Glover, 1995), and asks for additional binders to be involved in this material research.

Sand is a global necessity and UN reports suggest this will continue, for example the UN 2060 projections indicate that sand is most widely consumed construction resource, and past UN studies in both 2011 and 2017 have accurately predicted the future of sand and aggregate to advance beyond other materials, (Torres and Simoni, 2021) and even though research through sustainability is allowing some material mining to slow down, sand and aggregates will remain massively mined and used well into the future. It is estimated to be a widely used material even in 2060 projections which also illuminate the further environmental problems that will follow with mining, habitat loss and global importation.

Because this is a problem that has both regional and global implications, it was deemed appropriate to study as a further line of inquiry. In the UAE, almost all materials are imported or made from imported resources so the importance of employing regional resources and finding new ways of building and designing with local sand as an option for regional materiality can lead to productive solutions for architecture and the UN Sustainable Development Goal for life on land. In order to move forward with this research, the project re-considered what regional architecture is in this location, how computational approaches can intervene with new material options, and how an advent of bio-technology/bio-engineering can alter our current understanding.

4. Methodologies

For this project, the methodology manifests in two parts. The first being a material study for the creation of a bio-sand unit that can be used architecturally. The second being an overlay of computational technology to begin understanding what can be constructed from this bio-material performatively. Experiments using bio-material with sand are very complicated and often unsuccessful due to the nature of the material. Previous precedents have been successful in making structurally stable units using resins and binders that are unsustainable and toxic. This study called for an approach that was not using resins or toxic binders. We began with recreations of experiments using scientific testing method (STM) that implemented a workflow for a hypothesis in action, design by research and application. The project followed this method using desert dune sand sourced from the wild in the desert of the UAE paired with three biological substances that could act as a sustainable binder, *Sporosarcina Pasteurii*, sodium thiosulphate, and urea.



Figure 3. Material tests using sand and sodium to create bio-synthetic sandstone

Sodium thiosulphate was the material that worked most consistently with the project trials and subsequently became the dominant material additive with the sand for the project. This material was used to create a series of additive molding trials based on thick casts and thin casts. Sodium thiosulfate is a colorless crystal of sodium, sulfur, hydrogen, and oxygen. Both the Environmental Protection Agency (EPA) and Federal Food and Drug Administration (FDA) in the United States consider it a safe substance and permit its inclusion in human foods such as table salt. (World Health Organization, 2019). It is often present at therapeutic bath spas or thermal spas in contact with the human body, and other uses include waste water treatment plants where it is used to clean water before releasing it back to a river. In principal it is more un-toxic than table salt. It is on the World Health Organization's List of Essential Medicines as one of the safest and most effective medicines needed in a health system.

This additive is affective because it changes states with temperature variation allowing the sand and salt to bind in a superheated mixture and upon cooling this process forms a composite unit. The strength varies based upon the amount of sodium and sand added together. It works by creating a monolayer of sodium around the sand, binding it at the same time, and resulting in the production of multiple layers of hardened sand material solidified by the sodium as it dries into a hardened state.

This material combination ultimately was used to create a series of bio-synthetic units made from sand that simulated standard masonry sizes. Rhino and Grasshopper were then used to demonstrate the material in a series of compositional arrangements, essentially by creating a surface in the X-Z directions, adding an ability to move freely and create twisted openings while stacking the units, and orienting the bricks in various positions so as to become performative in a variety of different positions. This in turn is being used in a second set of tests which involve Fologram and augmented construction processes, to be discussed in a separate paper.

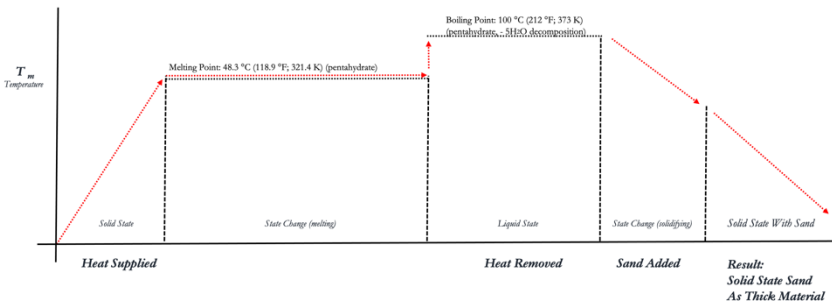


Figure 4. Phase change material process featuring superheated mixture of sodium and sand.

5. Results

During the course of research for this project, four distinct and separate processes were tested all using varying concentrations of dune sand and sodium as a mixture. The natural self-organizing behaviours of sand were observed and also researched. One can observe the behaviour of sand as a self-organizing material especially with pourings

and pilings. Although pourings and pilings were studied initially, molds and casting became the primary vehicle for making the architectural units in this study. Different thicknesses were tested with these processes to understand the material behavior in a solid state ranging from thin (6.35 mm) to thick (76.2 mm).

Out of the tests conducted, Experiment 3 entitled "Solid State Sand as Thick Material" performed with the most consistency and the most strength. This material was generated by combining one part dune sand to one part Sodium Thiosulphate (sand & sodium equal by percentage), which created a unit of 76 mm in thickness. This was achieved by heating solid state sodium to a melting point, superheating to reach boiling temperature, removing from burner, creating a "Solid State" to "Liquid State". The super-heated bath of liquid state sodium thiosulphate was poured into a sand-filled mold 3" / 76 mm deep. Solidification was achieved through stirring the mixture as the sand particles were allowed to bind with sodium and the mixture cooled. The solid-state Sodium Thiosulphate is now effectively combined with sand as a hardened material, proving the hypothesis that when melted Sodium Thiosulphate comes into contact with sand, they form a bond (a biological cementation), creating a sandstone-like biomaterial.

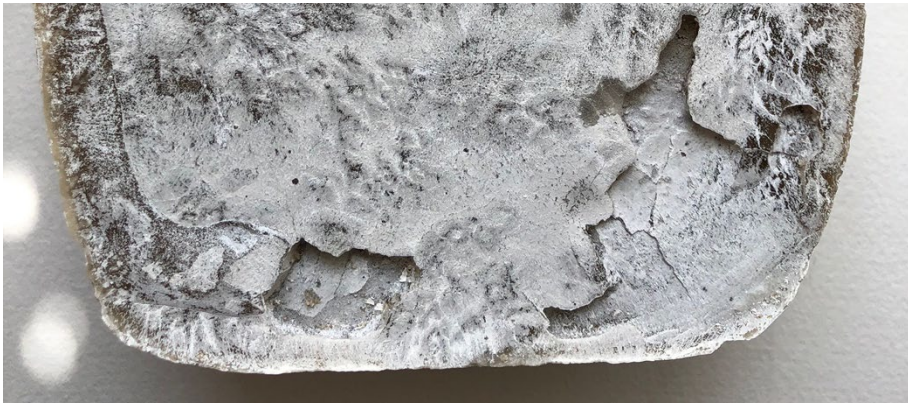


Figure 5. Detail, Bio-synthetic sandstone from superheated mixture of desert dune sand and sodium.

The creation of the bio material was a significant component to this research project, however the second phase was to test how this material can be used in an architectural scenario. In the Middle East, mashrabiya are commonly used architectural features. Their existence dates back hundreds of years and were originally used as water storage areas in houses so that the ventilated openings could cool the water (Ashour, 2018). The continued use of the mashrabiya allowed for its evolution from water storage to devices that protruded or cantilevered over irregular plots in dense urban areas to correct the language of the architecture and increase the sizes of spaces on the upper floors of stacked housing without changing the size of the ground floor or moving past the plot limit. They were also used for privacy which is an important concern in Middle Eastern architecture. They are found in both historical and contemporary architecture as a commonly used feature for regional architecture. For this reason, it was used as an initial typological reference. In grasshopper, a definition was made that arranges stacks of sandstone units. These stacks were given

inputs the same size as the units made from the final sandstone test mold. With grasshopper, the units were then allowed to rotate from one unit to the next so as to create a ventilated façade. The control of the openings can be calibrated to be fully open or fully closed.

The strength of the sand brick was tested for compression using a calibrated Form+Test M1 3000 kN machine. The material proved to be very durable and held up well under continuous compression with 1750 kg/m³ being used for Bulk Density, and 1511.6 kN being applied for Normalized Compression, and 51.4 MPa for Strength, where one MPa is equal to one million pascals (Pa); a pascal is one newton of force per square meter, a megapascal is one million newtons per square meter. As a rule, the higher the MPa of a material, the stronger the material will be, and the less likely it is to fail. For example a 32 MPa (at 4,600 psi) for concrete is often used in the region (Giancoli, 2000). However, important to note that Load was not calculated as it was not an ASTM test.



Figure 6. Strength of material testing, result of sand brick after normalized compression test.

To design with this unit in mind, the step by step Grasshopper definition starts by defining the Output Parameters for P (Plane) and World XZ (Plane) to reference a planar surface. It then moves to Input Parameters for the P (Plane) component and Surface base plane in the X (Domain) for dimensions in the X direction, and Y (Domain) for the dimensions in the Y direction. The Output parameters of the surface connect to a panel for custom values which was plugged into the parameters for the surface. The next part of the definition works to explode the referenced curves into smaller segments. The Output parameters: S (Curve) was connected to Item L (Generic Data) to retrieve specific item data from a list. This was connected to a Cull Index along with a Divide component. This effectively allows for an offset to be created in the direction of the Z. The Cull was connected to Sub List which extracts a subset from the list. Elements in the list are identified by their index. The subset allows for a continuous range of elements to be copied as a new list.

The next part of the definition divides the referenced curves into equal points and a Domain Box was defined by XYZ in order to orient the units. This transformation is critical as it allows for the remapping of geometry from one axis-system to another, and allows the units to be transformed more systematically. With this process, the

Grasshopper definition allows for a flexible mashrabiya to be modeled along with the synthetic bio-material. This acts as the primary design tool that facilitates a workflow for a bio-synthetic mashrabiya. The mashrabiya can move from a closed wall surface to a system with various openings and closing in a very systematic way. This design workflow can benefit regional architecture and can be custom controlled to allow for different lighting situations, privacy requirements, ventilation needs and can accommodate the breeze patterns for a particular area in a city.

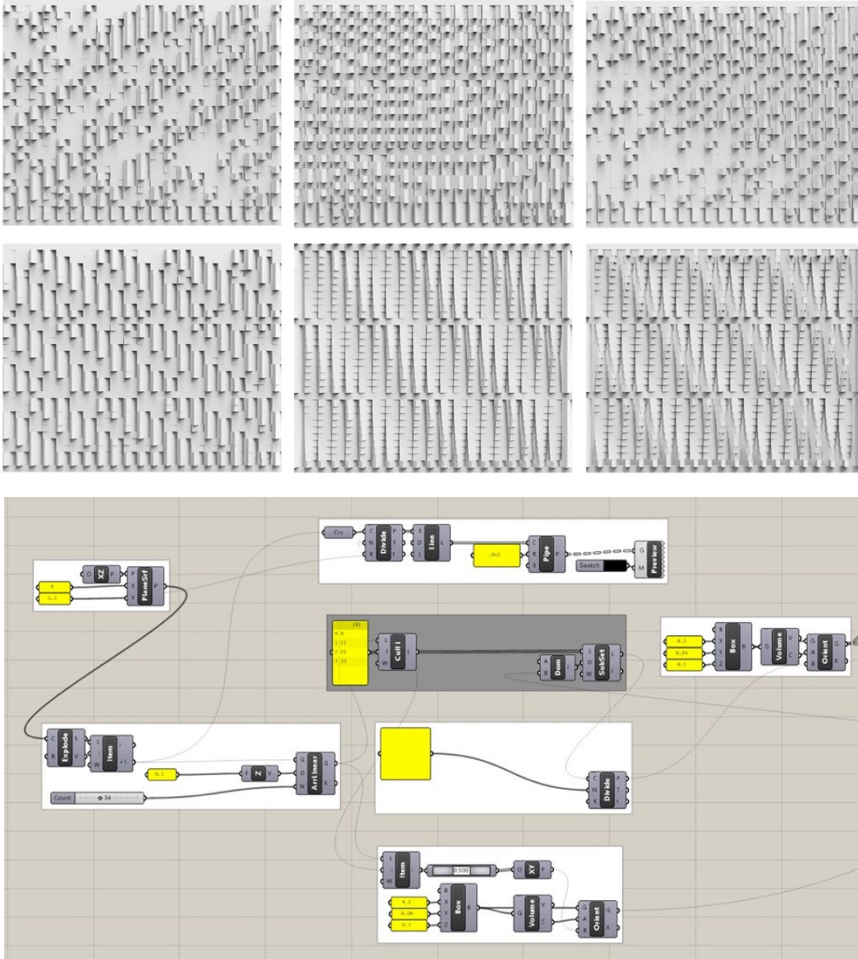


Figure 7. Grasshopper definition for Bio-synthetic mashrabiya compositions

6. Conclusion

The research project asks how a regionally appropriate architectural system might integrate with a computational process to allow for the use of a new material agenda using dune sand from local deserts. To facilitate this line of inquiry, the research

followed a hypothesis using salt and salt mixtures such as Sodium Thiosulphate to create bio-synthetic material from local dune sand. This was important due to the fact that desert dune sand is rarely used in modern construction. Cities in the Middle East and North Africa import massive quantities of river sand from Southeast Asia and Australia to fuel the need for concrete and masonry products. Based upon previous scientific evidence, the project research found that Sodium Thiosulphate and bacteria using Microbial Induced Calcite Precipitation could successfully help to create sand based material systems. This thesis tested Sodium Thiosulphate and concluded that in certain situations it is a viable material outcome that can have the strength needed for material assemblages. It is relatively safe and easy to mold. Concerns however are the amount of Sodium required to create the material and the durability of the material if exposed to weather and water. The referenced test in this paper (Experiment Three) concludes that with a dimension of 76 mm or more, it is a stable unit capable of being stacked and arranged in compositions similar to masonry construction, lending additional viability due to the skillsets of local craftsmen and their familiarity with brick.

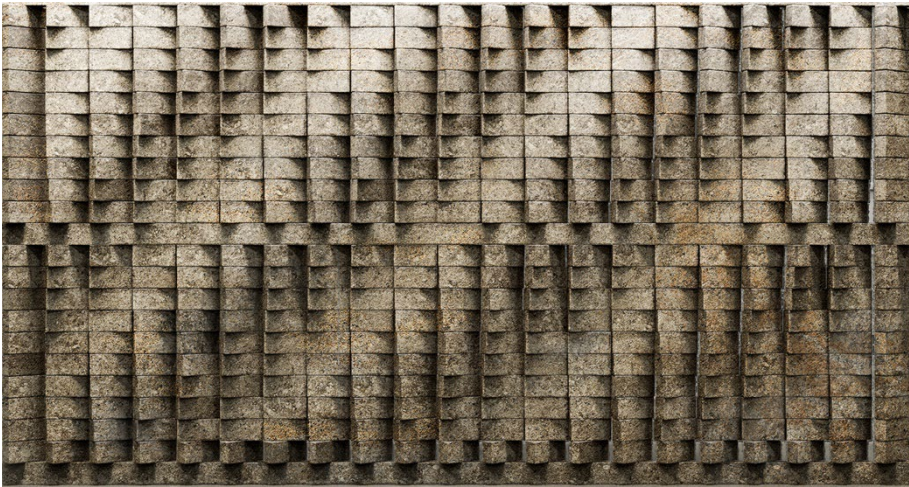


Figure 8. Bio-synthetic masonry material composition

A design workflow incorporating this bio-material can be combined with computation to articulate specific architectural outcomes that have regional relevance. The research points to the fact that local sand material can create typological prototypes such as mashrabiya and façade units requiring breezes, offering a method for viable human scale architectural prototypes to be further explored and designed. Further research can be done on the material responses to weather and the structure limitations of the material. This is needed to continue conversations regarding how designers can replace current proprietary media such as mass-produced masonry and concrete created from unsustainable methods using imported sand. The project responds to pressing global issues as identified by the following UN Sustainable Development Goals: SDG11, "Sustainable Cities and Communities" by helping to design resilient, and sustainable cities and human settlements, and designing material that aids in

the reduction of environmental impacts of cities and city building by fostering resource efficiency in sustainable and resilient building processes. SDG12 by fostering responsible consumption and production in order to ensure sustainable consumption and production patterns, and to ensure good use of resources. SDG13, "Climate Action" by reducing greenhouse gases due to transportation and importation on a global scale. (Fagan, 2020).



Figure 9. Bio-masonry mashribiya prototype

References

- Ashour, A. (2018). *Islamic Architectural Heritage: Mashrabiya, Islamic Heritage*, Architecture and Art II. WIT Press.
- Fagan, J. (2020, November 1). UN *United Nations Environment Programme*. UNEP Commons. Retrieved December 12, 2021, from <https://www.unep.org/>
- Giancoli, D. (2000) *Physics for Scientists & Engineers*, Third Edition. Prentice Hall.
- Glover, T. J. (1995). *Pocket Reference (for Mechanics)*. Sequoia Publishing.
- Nichols, E. L.; Franklin, W. S. (1898). *The Elements of Physics. Vol. 1*. Macmillan.
- Otto, F., Rasch, B. (1992). *Finding Form*. Deutscher Werkbund.
- Rael, R., San Fratello, V. (2018). *Printing Architecture*. Princeton Architectural Press.
- Torres, A., Simoni, M. (2021). *Sustainability of the Global Sand System in the Anthropocene, One Earth*, Volume 4, Issue 5. ScienceDirect.
- WHO (2019, October 12). World Health Organization. *Model List of Essential Medicines*. Retrieved December 10, 2021, from <https://apps.who.int/iris/bitstream/handle/10665/325771/WHO-MVP-EMP-IAU-2019.06-eng.pdf>

ROBOTICALLY PRINTED SEAWEED AS A BIOMATERIAL WITHIN ARCHITECTURE AND DESIGN

ILAENA NAPIER¹

¹*Institute for Advanced Architecture of Catalonia (IAAC)*

¹*ilaena.napier@gmail.com, 0000-0001-6768-1750*

Abstract. This research aims to develop and understand the impact of seaweed as a bio-based material within architecture and design. The research is influenced by current global challenges, outlined by the Sustainable Development Goals (SDG), such as carbon drawdown, the problem of material waste, and the need to create more sustainable manufacturing processes. Seaweed is an organic biomass that does not require land, fresh water or fertilisers to grow, and growing it can reduce the effects of global warming as it sequesters large amounts of carbon dioxide. In turn, it can be harvested and used for a range of products including food, biofuel, fertiliser and bioplastic. The research focuses on the development of an organic, water-based biocomposite material made from sodium alginate, a derivative of brown seaweed, combined with cellulose powder, vegetable glycerine, and kelp powder. A set of methodical experiments were conducted and studied, with the aim of creating a novel material which can adapt to its surrounding environment and can degrade naturally. By creating and fabricating using renewable resources, one can create novel materials that are carbon neutral and contribute to a natural resource cycle. Ultimately, the material decays and returns to the earth, for the purpose of remediating soils and replenishing growth.

Keywords. Seaweed Biocomposite Material; Paste Extrusion Method; Water-based Robotic Fabrication; Circular Design; SDG 12; SDG 13; SDG 14.

1. Introduction

The global challenges we are facing due to climate change and the depletion of natural resources is forcing us to radically change the way we design and construct our built environment by taking a new critical stance on the materials we use and the resource cycles that we create. The construction industry plays an important role in all industrial sectors, as it currently is responsible for a substantial share of resource consumption, energy use, carbon dioxide emissions and waste generation (Bekkering et al., 2021). This is having a catastrophic effect on our surrounding environment which can be seen within our natural ecosystems. With growing concerns about the effects of global warming on the environment, there needs to be a shift in the way we interact with our natural environment by integrating nature-based solutions into all sectors of our daily

lives, especially in architecture and design.

The research is framed within the same aspects as the UN's Sustainable Development Goals (SDG) or Global Goals which are a collection of interlinked goals designed to be the starting point in achieving a more sustainable world for future generations. The SDGs were set up in 2015 by the United Nations General Assembly and are aimed to be achieved by 2030. This research focuses on three interrelated goals of the SDGs, namely goals: (12) Responsible Consumption and Production: to ensure sustainable consumption and production patterns, (13) Climate Action: to take urgent action to combat climate change and its impacts, and (14) Life Below Water: to conserve and sustainably use the oceans, seas and marine resources (United Nations, 2015). The challenge is to reduce non-renewable resource consumption by turning to renewable resources that alleviate the effects of climate change in their production instead of contributing to it. The research focuses on tackling these goals by looking to the ocean and its resources for alternative solutions. Coastal ecosystems are some of the most productive ecosystems on Earth and are made up of biomass such as seagrass meadows, mangrove forests, salt marshes and kelp forests. These ecosystems are collectively known as Blue Carbon ecosystems as they account for large amounts of carbon sequestration from the ocean and atmosphere, acting as carbon sinks.

2. Blue Carbon Strategies

The oceans itself accumulates vast amounts of carbon within coastal ecosystems, known as Blue Carbon. These ecosystems occur in shallow waters and account for 50% of long-term carbon sequestration, while only making up 2% of the ocean (IUCN, 2021). These coastal systems, though smaller in size compared to terrestrial forests, sequester carbon at a much faster rate. They provide numerous other benefits such as shoreline protection from storms, rising sea levels and erosion, regulation of coastal water quality, provision of habitat for marine life, as well as food security for many coastal communities (The Blue Carbon Initiative, 2021). Despite their importance, Blue Carbon ecosystems are largely under threat from climate change, fishing, pollution, marine pests, and coastal urban development (Duarte, 2021). Therefore, coastal habitat conservation is a good strategy to implement in order to reduce the effects of climate change on these important coastal ecosystems.

2.1. KELP FORESTS

The research considers the production, harvesting, and use of seaweed as a Blue Carbon strategy, and how this material can be harvested sustainably as a building material. Seaweed is a term that can be used to describe many different species of macroscopic, multicellular marine-based plants and algae. Seaweed grows in a variety of forms and colours in the ocean as well as in freshwater environments. There are thousands of species of seaweed, with kelp being the largest subgroup of seaweed. Seaweed can be broken down into three main categories based on pigmentation: Rhodophyta (red), Chlorophyta (green) and Phaeophyta (brown). Kelp is placed in the Phaeophyta (brown) category and includes the largest and fastest growing seaweeds, such as *Macrocystis pyrifera*, more commonly known as giant kelp. On average, giant kelp grows at a rate of 28cm a day but can grow up to 60cm a day in ideal conditions,

making it one of the fastest growing plants on the planet (NOAA, 2021). Kelp grows in dense groupings that form ocean forests that harbour a greater variety and higher diversity of marine plants and animals than almost any other ocean community, making it one of the most productive and dynamic ecosystems on Earth.

2.2. REGENERATIVE OCEAN FARMING

Aquaculture or regenerative ocean farming is a farming practice that is found in the ocean and incorporates the growing of seaweed and other marine life such as oysters, mussels and scallops. These farms are cultivating and harvesting seaweed, which is becoming a competitive biomass production candidate for food and related uses. There are several organisations such as AtSeaNova and GreenWave that are developing systems that focus on regenerative seaweed farming. GreenWave has come up with a 3D vertical ocean farming system which consists of underwater vertical gardens that grow kelp and shellfish on suspended floating ropes. This vision aims to combat the effects of climate change as well as create jobs in local communities and rebuild marine ecosystems. The National Oceanic and Atmospheric Administration (NOAA) is investigating this industry's benefits, as it is still in a developmental stage, which will lead to more efficient permitting and allow seaweed farming to expand while being economically and environmentally sustainable (NOAA, 2021).

3. Seaweed Material Research

As a natural biomass, seaweed is not only beneficial to the environment as it grows but is also rich in various nutrients that are beneficial to other organisms such as plants and animals. Seaweed is made up of organic compounds such as proteins, amino acids, lipids, cellulose and vitamins, and is also rich in alginate and polysaccharides that are not always present in terrestrial plants. This is one of the many reasons that this versatile macroalgae is harvested and used in both its raw and extracted form for a range of products including food, biofuel, pharmaceuticals, cosmetics, bioplastics, fertilisers and livestock feed. Seaweed extractions such as agar, alginate and carrageenan are widely used in the food industry for their gelling, water-retention, emulsifying and thickening properties (Martău et al., 2019).

3.1. SEAWEED EXTRACTION: SODIUM ALGINATE

Above is Hydrocolloids are defined as a long chain of hydrophilic polymers that are characterised by their capability to form viscous dispersions and/or gels when dissolved in water (Khalil, et al., 2018). Sodium alginate is a naturally occurring biopolymer, extracted from the cell walls of brown seaweeds, which has been extensively investigated and used for many biomedical applications such as tissue engineering and drug delivery, due to its biocompatibility, low-toxicity, relatively low cost and mild gelation by addition of ions such as calcium. The use of alginates is based on two main properties. The first is their ability to thicken in the presence of water and the second is their ability to form gels due to cross-linking of ions in the presence of calcium (Lee and Mooney, 2012). Gels formed from alginates can withstand heat and temperature of up to 150 degrees Celsius without melting, giving it water-resistant and durable properties that can be used within design and architecture.

The aim of the research was to develop a novel, bio-based material using an extraction of brown seaweed as the core biopolymer, which would be combined with additional materials to create a stable and extrudable composite. Bioplastic composites are created by combining biopolymers for strength, plasticisers for flexibility, additives for additional properties such as texture, colour, strength and durability, and a solvent such as water. This is made by cooking the materials using a heat source to create a homogeneous solution that can be cast into a die and dried using a heat source (to speed up the curing time and to prevent the material from molding). The materials chosen to start the experiments were water as the solvent, sodium alginate powder as the biopolymer, vegetable glycerine as the plasticiser and kelp powder as an additive. Based on bioplastic material research, other natural materials such as sunflower oil (which shows promising results in reducing the shrinkage), cornstarch combined with vinegar, chitosan, hemp fibre and calcium chloride solution (used to create a gel layer by cross-linking of sodium and calcium ions) were added methodically to gain an understanding of each material's characteristics and qualities.

3.2. INITIAL MATERIAL STUDIES

A set of methodical experiments were conducted with different combinations of materials, based on the starting composition of 100ml of water, 2ml of vegetable glycerine, 2g of kelp powder and 5g of sodium alginate powder. A cooking process was used to make the material where water was measured and heated while the sodium alginate powder and kelp powder was slowly added and whisked until a homogenous solution was formed. The vegetable glycerine was mixed in and the mixture was heated while continuously being mixed until it reached a temperature of 90 degrees Celsius before being cast into acrylic frames of 100x100mm and oven dried at 60 degrees Celsius for 2 hours. Because this material is water-based, the time in which they take to cure is an important factor that affects the quality of the outcome. The way in which the material dried and shrunk through evaporation was a key aspect that was considered and was able to be measured against the original acrylic frame dimensions.

After a catalogue of material experiments were tested by adding more of a certain material at a time and measured, it was noted that: the more vegetable glycerine, the more flexible the material became and the less it shrunk (Figure 1A); the addition of spraying a mixture of 10% calcium chloride (10ml calcium chloride in 100ml of water) onto the wet mixture created a gel layer that caused the material to shrink instantly away from the edges of the frame (Figure 1B); and the more sodium alginate added, created a brittle material, which causes the material to tear in multiple places as it dries (Figure 1C). The material experiments were recorded and analysed based on their strength (resistance to tearing), translucency and flexibility during the curing process.

Based on the material experiments carried out, one base recipe was then chosen consisting of a ratio of 100ml water, 6ml vegetable glycerine, 2g kelp powder, 10g sodium alginate and 6g cellulose powder. The addition of another biopolymer (cellulose powder) was added in order to improve the characteristics of the material in which sodium alginate is lacking, such as poor water vapour barrier and mechanical strength. Casting of bioplastics is a common way of exploring base properties of different ingredients and is largely done in bioplastic research, however it is limited in size and control of the material. The viscosity of the wet material was also taken into

consideration as alginate can be robotically extruded. Because of this material quality, additive manufacturing strategies were explored to challenge scalability problems that are often seen within bio-based materials.

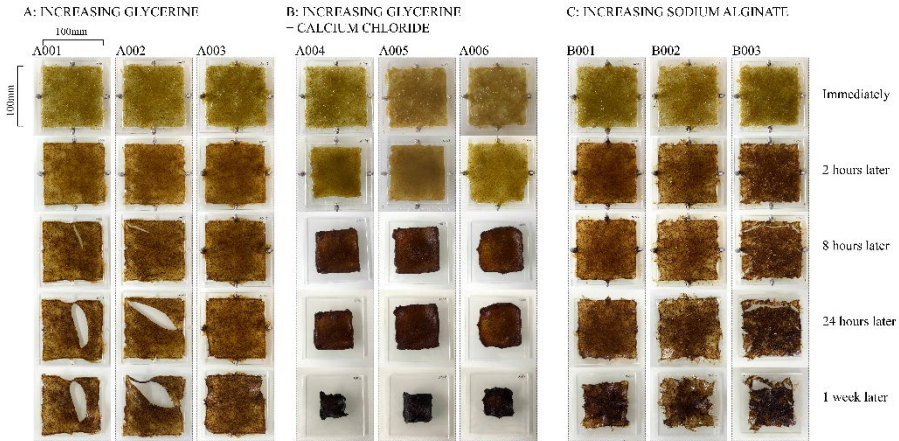


Figure 1. Initial Seaweed Biocomposite Casting Experiments

4. Additive Manufacturing Strategies

The methodology chosen for fabricating this novel material was to start on a small scale to determine the possibilities and limitations of the material and to then gradually progress to a larger scale. Extrusion printing was chosen to ensure no possibility for material wastage during the additive manufacturing process. A Creality Ender-3 Pro 3D printer with printing dimensions of 220x220x250mm was bought and manually changed to be able to extrude a paste-based solution. This included attaching a 3D printed piece which allows for the attachment of a cartridge containing the material which is then extruded using air pressure. In addition, there is a metal screw attached to a stepper motor placed at the top of the 3D printed piece to assist with the extrusion of the material. It was seen that because the seaweed biocomposite material has a gel-like consistency, it can be extruded using less than 1 pascal of air pressure.

The first experiments looked at extrusion printing three-dimensionally. The alginate biocomposite paste was able to extrude and stick together horizontally and vertically, however the outcome of the material due to shrinkage was not desirable. The printed prototypes shrunk by more than 50%, resulting in brittle elements. An alternative solution was to print two-dimensionally, in order to get results that are characterised by the material properties (Figure 2). Flat sheet printing was chosen and explored, bringing resemblance to the previously explored casting method, but instead of the material being deposited into a die, the material was extruded evenly without scaffolding, giving rise to possibilities within the printing process, including scalability of the material.

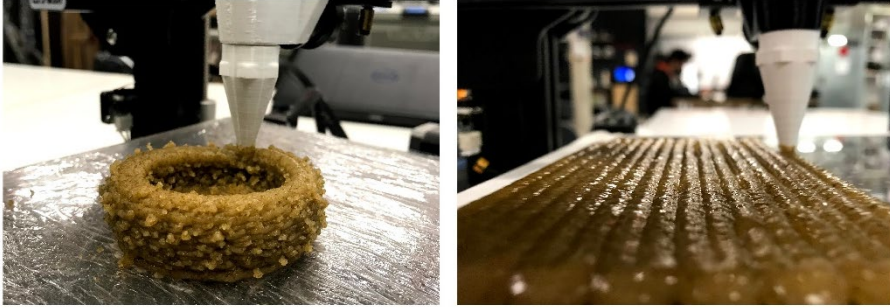


Figure 2. Initial Seaweed Biocomposite 3D Printing Outcomes

The extrusion printing method naturally progressed onto a larger scale by using an ABB140 (IRC5) 6 axis robotic arm where sheets of up to 1000mm could be printed. The novel seaweed material easily adapted to the fabrication process and resulted in one-layered, large, flexible membranes (Figure 3A). During the drying process, the material loses water content due to evaporation. If this happens too quickly, the material has the potential to split in vulnerable areas, however, if the drying process is done within a controlled environment, at room temperature, the material dries evenly across the surface area.

Once there was an understanding that the material was extrudable and dried to form functional membranes, a complexity to the process was added. Multiple layers in the form of vertical and horizontal lines, which were strategically designed to act as structural supports or ribs were added on top of the initial (one-layered) membrane. This gave way for interesting shrinkage patterns and deformations as there was an equal distribution of shrinkage which occurred across the sheet, always towards the centre point of the sheet area. Due to this shrinkage and pulling of the material, the edges of the sheet curl up and away from the surface bed and form evenly distributed sine waves along the length (Figure 3B). In this regard, the material showed resemblance to its original seaweed form found naturally. These unique material behaviours were chosen to be understood and implemented into the design of the material. Instead of working on a way to eliminate them and control the material entirely, the design process emerged from these unforeseen material behaviours.

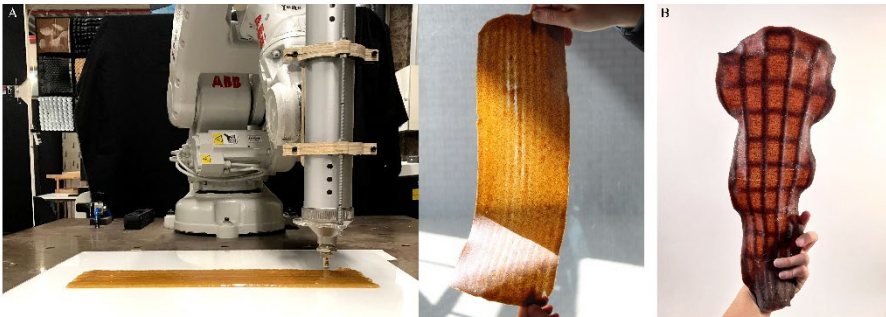


Figure 3. Robotically Extruded Seaweed Biocomposite Outcomes

A catalogue of shapes and strategies were tested all with two to four layers and using a combination of 4-, 6- and 8-millimetre diameter round nozzles. All sheets were recorded and analysed on their size, percentage of shrinkage, as well as effects of translucency, strength and flexibility (Figure 4). It can be seen on average that the sheets shrink 10 to 20 percent in length and 5 to 10 percent in width. Top layer 'ribs' that were designed for structure, and during the drying process started emerging on the underside of the sheets, giving more rigidity. Uniform sine waves appeared along the edges, due to shrinkage and pulling of material between the strategically placed ribs. Uniform gaps and openings started to emerge during the shrinking process where there was not enough overlapping material or weak points in the print.



Figure 4. Catalogue of Robotically Extruded Multi-layered Sheets

This additive manufacturing process and design was then applied on an even larger scale using a Kuka KR 150 L110-2 Robot. This enabled the membrane to reach a printing length of up to 2000mm, showing that this seaweed biocomposite material can be manufactured on a large scale. There were many factors that affected this large print. Firstly, the 1.4 litre Luthum end effector (used during the printing on the ABB140 robot) was attached to the Kuka, therefore limiting the amount of material that could be deposited at one time. This delayed the completion time, and the top layers and bottom layers were printed separately, which resulted in the layers being disconnected when drying. This affected the overall shrinkage and deformation outcome and produced unexpected results (Figure 5). This research opens possibilities of a novel seaweed biocomposite material that can be additively manufactured on a large scale to produce elements that are natural and biodegradable and can be designed for uses

within the built environment such as building skins as facade panels.



Figure 5. Large-scale Printing using the Kuka Robot (left) and Dried Results (right)

5. Material Informed Design

In general, water-based bioplastics shrink due to evaporation of water content as they dry and cure. In this case, the loss of water causes the prototypes to shrink evenly towards the geometric centre point, causing spatial deformations. The inverse of shrinkage happens when you expose bioplastic to water. The presence of water or humidity can alter the overall shape of the element because of swelling due to sodium alginate related properties of water-retention. The fact that this research focuses on the recyclability of the elements, being able to dissolve within water is a key aspect that water-based materials have. The elements will need to be studied over time as they adapt to their surrounding environment. In a humid environment they tend to swell and become flexible, however, in a dry environment they stiffen. This research can be further developed to be designed into architectural elements that are durable and degradable and respond symbiotically to its environment so that over time the contents can return to the earth, and as seaweed is a natural fertiliser, it will encourage future growth.

6. Conclusions

The research is driven by current issues of global warming, the problem of material waste, as well as the need to create more sustainable manufacturing processes. The use of seaweed brings attention to underutilised resources that are found naturally in abundance and can be used and produced in a sustainable manner to create alternative renewable materials. Seaweed does not require land, fresh water or any additive fertilisers to grow naturally or farm, therefore, it does not compete with conventional agriculture practises for land space. As a natural polymer, sodium alginate is shown to have many environmental uses and benefits due to its high nutrient and salt content and remarkable mechanical and hydrophilic properties making it biocompatible and biodegradable. Due to its ability to thicken in the presence of water and form gels in the presence of calcium, it can easily be robotically extruded, dried and cured to create a water-resistant membrane which can biodegrade or be broken down and reprinted.

The research is a starting point for further research in this field. The general problem seen today is trying to find a solution to manufacturing these natural materials at a large scale. The use of additive manufacturing of water-based materials, specifically in

engineering, design and architecture, is still in its early stages and needs to be explored further. Potential future research can be done to improve the extrusion process of multi-material extrusions, material distribution, or other geometric shapes and patterns to suit specific applications. In terms of further material exploration, the addition of chopped fibres or sand particles could be added to the bioplastic recipe and tested to provide enhanced mechanical properties of the printed sheets. Additionally, combining seaweed biocomposite membranes with a substructure of alternate materials such as timber or bamboo can also be investigated in future research.

By approaching the SDGs and tackling topics as large as climate change, the ocean and consumption and production patterns, one needs to find solutions on a small scale that can have a large impact. Seaweed farming has the potential to sequester large amounts of carbon and act as a carbon sink. It can then be harvested and used to create new material systems that encourage the protection and nourishment of the ecosystems from which they come. Replacing non-renewable resources with their bio-polymer alternatives will enable the ability to customise materials to be created, used, recycled and replenished to reduce the effects of climate change while fuelling future growth.

Acknowledgements

This research was developed at the Institute of Advanced Architecture of Catalonia (IAAC) as part of the Master in Advanced Architecture II (MAA02) Program as a Master Thesis Project. The thesis was developed in the C-Biom.A thesis studio, under the supervision of Marcos Cruz and Kunaljit Chadha.

References

- Bekkering, J. D., Nan, C., & Schröder, T. W. A. (2021). *Circularity of Biobased Materials in Architecture and Design*.
https://downloads.ctfassets.net/h0msiyds6poj/4cUyquZDX8Zx6WlmxEgw94/b32f801bbb24050527d10a00108617b9/CIRCULAR_Report.pdf
- Duarte, C. (2021). *Kelp Help: Seeking Options for Blue Carbon* | KAUST Discovery. [online] Discovery.kaust.edu.sa. Retrieved December 11, 2021 from
<https://discovery.kaust.edu.sa/en/article/1017/kelp-help:-seeking-options-for-blue-carbon>
- Fernandez, J.G., & Ingber, D.E. (2014). Manufacturing of Large-Scale Functional Objects Using Biodegradable Chitosan Bioplastic. *Macromolecular Materials and Engineering*, 299, 932-938.
- IUCN - International Union for Conservation of Nature (2021). *IUCN: Blue Carbon* [online] Retrieved December 11, 2021 from <https://www.iucn.org/theme/marine-and-polar/our-work/climate-change-and-ocean/blue-carbon>
- Khalil, A., Tye, Y., Saurabh, C., Peng, L.C., Lai, T.K., Chong, E., Fazita, M., Jaafar, M.H., Banerjee, A., Syakir, M.I., (2017). Biodegradable polymer films from seaweed polysaccharides: A review on cellulose as a reinforcement material. *Express Polymer Letters* 11, 244–265
- Kretzer, M., Mostafavi, S., Anhalt, H., City, B., Anhalt, H., n.d. (2020). *Robotic Fabrication with Bioplastic Materials*. p. 604-612.
- Lee, K. Y., & Mooney, D. J. (2012). Alginate: Properties and Biomedical Applications. *Progress in polymer science*, 37(1), 106–126.
<https://doi.org/10.1016/j.progpolymsci.2011.06.003>
- Lesna, J. and Nicholas, P. (2020). *DE GRADUS, RE: Anthropocene*, 2, p. 383–392.

- Martău, G., Mihai, M. and Vodnar, D.(2019). The Use of Chitosan, Alginate and Pectin in the Biomedical and Food Sector - Biocompatibility, Bioadhesiveness and Biodegradability. *Polymers*, 11(11), p.1837
- NOAA - National Oceanic and Atmospheric Administration. (2021). *Seaweed Aquaculture* [online] Retrieved November 15, 2021 from <https://www.fisheries.noaa.gov/national/aquaculture/seaweed-aquaculture>
- The Blue Carbon Initiative (2021). *What is Blue Carbon?* US Department of Commerce, N.O. and A.A.[online] Retrieved September 20, 2021 from <https://oceanservice.noaa.gov/facts/bluecarbon.html>
- United Nations (2015). *Transforming our World: The 2030 Agenda for Sustainable Development*. [online] Retrieved December 11, 2021 from <https://sustainabledevelopment.un.org/content/documents/21252030%20Agenda%20for%20Sustainable%20Development%20web.pdf>

Computational Design Education, Theory and Methodology

EXPLORING THE EFFECT OF IMMERSIVE VR ON STUDENT-TUTOR COMMUNICATION IN ARCHITECTURE DESIGN CRITS

HADAS SOPHER¹, JULIE MILOVANOVIC² and JOHN S. GERO³

¹CRENAU/AAU – UMR_CNRS 1563, School of Architecture Nantes.

¹Design Research Laboratory Hybridlab, University of Montreal.

^{2,3}Computer Science and Architecture, University of North Carolina at Charlotte, USA

¹hadas.sopher@crenau.archi.fr; 0000-0001-6565-6949

²jmilovan@uncc.edu, 0000-0001-8643-9812

³john@johngero.com, 0000-0001-9026-535X

Abstract. Using digital tools like immersive Virtual Reality (iVR) reduce the carbon footprint by providing collocated and remote communication through virtual design studios. By providing a sense of presence in a digital display, iVR systems impact student-tutor communication during design critiques or crits. Research lacks studies articulating how iVRs change crits' communication to increase the ability to integrate iVRs as educational media and promote a quality education in inter-university studios. To this end, this study explores the cognitive structure of student-tutor communication during collocated architecture crits using iVR and non-immersive media. We employed protocol analysis to analyze divergent thinking by tracking the distribution of First Occurrences of design issues. Combining protocol analysis with Natural Language Processing, we explored the size of the design space generated during the crits. Results from a case study that includes twelve crits from three students show an increase in students' exploration of the design space and divergent thinking in the iVR crits, providing evidence that iVR enhances learners' communication. iVRs can be integrated to support remote design studios without the generation of carbon due to physical travel.

Keywords. Immersive VR; Design Cognition; Architecture Studio; NLP; First Occurrence; Design Networks; SDG 4.

1. Introduction

Immersive Virtual Reality (iVR) systems provide a uniform setting for collocated and remote communication through virtual design studios that enables tutors and learners to be immersed in life-scale virtual design representations, and reduce the need to physically travel. Design representations are key to support design communication in situated pedagogic settings known as "crits" (Schön, 1985) and design progress (Goldschmidt and Smolkov, 2006; Goldschmidt, 2014). Following the situated learning approach (Lave and Wenger, 1991), the studio encourages a learner-centered

learning through enhanced learner engagement during crit sessions (Oh, et al., 2013). In the case of architectural design studios, iVR offers the possibility of experiencing designs at a real scale, demonstrating relevance to architecture learning that mostly relies on scaled representations. Shifting between 2D and 3D types of representations has the potential to alter learners' experiences (Milovanovic and Gero, 2020) and design development (Sopher et al., 2019). If the use of iVR systems in design crits is to become a pedagogical tool, we need a better understanding of its impact on students' learning. We should examine how these representation systems impact communication during the learning process in design crits. More studies are necessary to understand how communication in iVR crits differs from non-immersive ones to move toward integrating iVR systems in studio pedagogy. Integrating immersive systems into design courses can accomplish a sustainable design goal (SDG) quality education that foresees updated education facilities that provide inclusive and effective learning environments for all. This exploratory case study examines how iVRs impact student-tutor communication in iVR crits, compared to commonly used non-immersive media. It provides insights on the benefit of using iVR to support communication between students and tutors during design crits.

1.1. IMMERSIVE VIRTUAL REALITY SYSTEMS AS CARBON FREE COMMUNICATION MEDIA

iVRs are not restricted to collocated activity and can be used remotely without any change in functionality. This provides the opportunity to reduce the carbon footprint of users as they do not need to travel to be physically in a single location. Further, it creates novel opportunities to engage tutors from geographically dispersed locations. iVRs are characterized by immersion and presence, principal components that lead the interaction between the system and the users. Immersion refers to the system's hardware, and software components that provide for a surrounding and continuous display synchronized with the user's movement (Sanchez-vives and Slater, 2005). Presence refers to the user's experience of being in a situation as conveyed by the system (Slater, 2009). Despite the awareness of the situation to be less than real, presence experience leads to behaviours similar to ones that would occur in a similar real situation (Ibid).

These characteristics enable iVRs to support situated learning that relies on gaining desired skills through handling simulated real-life situations (Slater, 2017). Prior studies highlighted the advantages of iVRs as carbon-free educational media through supporting spatial comprehension of 3D models (Gómez-Tone et al., 2021; Zhao et al., 2020), increased design performance (Sopher et al., 2017) and design convergence (Sopher et al., 2019). Using iVRs in crits tends to increase the number of newly generated design issues introduced by students (Sopher and Gero, 2021), providing evidence for the medium's capacity to support a learner-centred education desired in situated pedagogy (Slater, 2017). iVRs support collocated and remote communication through using conversational elements considered to support collaborative ideation from abstract to concrete ideas (Boudhraa et al., 2019; Dorta et al., 2016) and in achieving creative design solutions (Hong et al., 2019). This demonstrates iVRs' role in shaping communication in a carbon-free educational setting. Surveys report a lack of rigorous methods able to track progress in situated learning (Mikropoulos and

Natsis, 2011), and few studies focusing on design education (Milovanovic et al., 2017; Ummihusna and Zairul, 2021) and related objectives such as interaction during exploration (Beck et al., 2020). More research is needed to determine how iVRs change student-tutor communication to take advantage of iVR systems as educational media and provide a carbon-free SDG4 quality education.

1.2. COMMUNICATION DURING STUDIO CRITS

Studio crits form the core setting for learning how to design. Learning requires the development of a solution to a design problem. During crits, students present their work and discuss it with tutors and peers to accomplish progress (Schön, 1985). Following the situated learning approach, the studio fosters a quality education by encouraging a learner-centred activity framed in tutor-student discussions (Oh, et al., 2013). Crit-communication comprises divergent thinking that expands the design space by generating new design issues and convergent thinking in which existing issues are refined (Goel, 2014). Divergent thinking is a cognitive behaviour indicating design progress (Dorst and Cross, 2001). Crits' activities are recurring as the course progresses until a more converged solution is achieved towards the course's final phase. Links between issues, or connectivity, testify to designers' capacity to account for multiple issues during the design process (Goldschmidt, 2016). Divergent thinking and connection between concepts, particularly the ones generated by students, serve as important indicators in supporting high-quality learning aimed at enhanced learner engagement (Oh, et al., 2013). Considered wicked (Rittel and Webber, 1973), design problems have no determined solution, creating difficulties in assessing whether further development in the form of new design issues is required. This activity tends to be particularly challenging for inexperienced designers such as students.

Representational media are embedded in design activity (including crits), as these support communicating information about design artifacts or their components (Kalay, 2004). Prior works show the role of representations in stimulating ideas and design progress (Goldschmidt and Smolkov, 2006; Goldschmidt, 2014). Interaction over representational media poses a challenge for learners. Considering that the medium plays a significant role in delivering the information (McLuhan, 2006), as it differs from the object in mind (E.g., scale), communication may be affected. Consequently, altered communication can enhance or hinder design activity. Early design phases may confront more challenges as the representations carry little or unclear information. Most representational media used in architectural design provide static and scaled representations, which lack the life-scale and surrounding context of the built environment, making iVRs particularly relevant for architecture students.

These challenges make crit communication an essential educational means in supporting SDG quality education. Crits tend to be tutor-dominated (Goldschmidt, et al., 2010; Milovanovic and Gero, 2018) and in generating new design issues (Gero and Jiang, 2016). Tutor-lead crits are criticized as they can hinder students' generation of alternative ideas and learners' engagement (Wang, 2010). In such crits, students can find tutors' feedback ambiguous (Salama, 2015), raising a need to find educational means that support crit communication to better achieve a learner-centered education. iVR systems appear as an interesting tool to support such an approach.

1.3. RESEARCH QUESTIONS

Explicating how iVRs impact the design activity during crits provides a basis for integrating these systems in design pedagogy as means to support learning. Demonstrating whether and how iVRs positively change student-tutor communication can promote integration of iVR systems as educational tools and promote inter-university design studios. This exploratory study articulates how iVR affects communication in design crits. The research questions are:

- Does iVR better support divergent thinking during design crits?
- Does using iVR impact students and tutors' exploration of the design space during design crits?

2. Method

2.1. CASE STUDY

We examined communication patterns in studio crits in a case study involving both iVR and non-immersive crits. Tutor and student natural verbalizations are compared between the two types of crit. The case study involves a studio course, taught by Associate Professor Fisher-Gewirtzman at the Faculty of Architecture and Town Planning, Technion, that alternately used immersive and non-immersive media on a weekly basis. Two weekly crits were given during a sixteen-week semester. The brief required the adaptive reuse of an existing electricity station, that was inaccessible to visitors. Data collected for this study includes twelve crits from three students (aged 22-25) in their third year of studies. Six crits were given in the early course phase, and the other six occurred towards the end of the course (Figure 1), allowing for tracking differences as the course progressed. The iVR system (Figure 2, left) is a 35sqm room, equipped with a 7 x 2.5 meter screen and synchronized sensors that allow single user navigation in a 3D display of digital design models, done in Sketchup, Revit, and Rhino types of digital modeling software. The system enables a shared presence for twenty attendees. The desk-crits sessions took place at the collocated studio workshop using various non-immersive media (Figure 2, right). The tutor had prior teaching experience in the iVR, whereas the students had no such experience prior to the course.

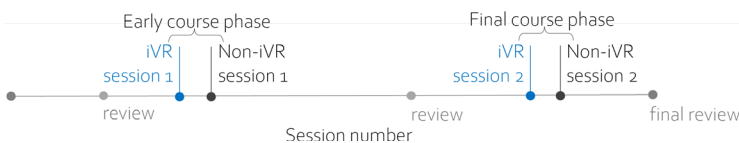


Figure 1. Sessions recorded during the course



Figure 2. A crit using the iVR system (left) and a non-immersive desk-crit (right).

2.2. MEASURING DIVERGENT THINKING IN DESIGN CRITS

We employed protocol analysis techniques to produce evidence of divergent thinking and used results to measure the size of the design space generated. 4.6 hours of crit discussions were recorded, transcribed, and segmented based on conversational turns. The transcripts, originally in Hebrew, were translated into English using Google Translate. Divergent thinking is analyzed by tracking the distribution of First Occurrence (FOs) of design issues generated during design activity (Gero and Kan, 2016). FO is the introduction of an idea for the first time in the design session. The number of FOs in a session is a measure of the size of the design space. FOs generated when using a given medium provides evidence for that medium's capacity in supporting this activity. Using Natural language processing (NLP) on design protocols, we automatically identified FOs generated by each participant. We used statistical testing to compare the number of FOs for each participant and each medium. We also analyzed the cumulative occurrence of FOs over time (Gero and Kan, 2016). The slopes of the cumulative FOs are a measure of the rate of divergent thinking. We normalized the time and the number of FOs to overcome different crits' durations.

2.3. ANALYZING THE DESIGN SPACE EXPLORED IN DESIGN CRITS

To assess how iVR is used for the exploration of the design space, we used a network to represent unique ideas generated by each participant. We used the FOs as concepts and generated connections between FOs based on a syntactic approach. To represent the network of FOs, we used the Networkx and Holoview Python libraries. The network of concepts generated by all the participants in a session represents the design space explored, allowing assessment of the medium's capacity to support this activity.

3. Results

3.1. DIVERGENT THINKING IN DESIGN CRITS

The analysis resulted in 2,398 FOs. For most crits, the occurrence of FOs over time is uniform as the curve of the cumulative occurrences is linear. The average value of the slope of the students' cumulative FOs in the iVR is higher compared to the non-immersive media (Table 1). A paired t-test determined that there was a significant difference between the two media types ($t(5) = -3.54, p = 0.016$). The tutor's average slope of cumulative FOs is higher in the non-immersive environment compared to the iVR (Table 1), with no significant difference ($p > .05$).

Table 1. Average slope of the cumulative FOs generated in immersive and non-immersive crits

FOs per segment	Communication media	Mean (SD)	Significant difference (P values)
Student FOs	Immersive VR	0.69 (0.32)	0.016
	Non-immersive	0.24 (0.06)	
Tutor FOs	Immersive VR	0.58 (0.19)	0.280
	Non-immersive	0.66 (0.06)	

The average cumulative occurrence of FOs generated by students is shown in Figure 3 (left) and by tutors in Figure 3 (right) in iVR and non-immersive media. iVR crits result in an increase in students' divergent thinking over time (Figure 3 (left)), indicating the medium's capacity to foster an increased activity. The opposite behaviour is seen as the tutor's cumulative FOs shows a higher slope when using the non-immersive media. This suggests that these media supported enhanced teaching activity. The graphs in Figure 3 also represent the variance between cases (shaded areas). The variance of the cumulative FOs over time using non-immersive media is smaller than in the one using the iVR. It accounts for more individual differences in the iVR that could imply differences in individual abilities to use the iVR, which were seen in a former study (Sopher and Fisher-Gewirtzman, 2020). Such feedback can support tutors in integrating different media to support individual competences and promote custom-tailored teaching. Examining the early and final phases of the course reveals a decrease in the slope of the cumulative occurrence of FOs generated in both media types during the final phase (Table 2). This is an expected behaviour, considering that the design solution converges as the course progresses. In this sense, the decrease in the slope value in iVR crits, compared to non-immersive ones, may be interpreted as the system's capacity to better support convergence.

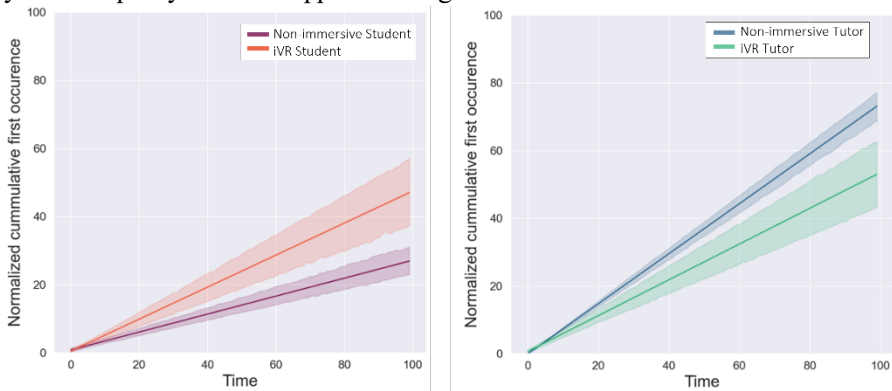


Figure 3. Cumulative occurrence of the FOs generated with immersive and non-immersive media by students (left) and tutors (right).

Table 2. Average slope of the cumulative occurrence of FOs generated during early (session 1) and final (session 2) phases for immersive and non-immersive media.

	Session 1-Early phase	Session 2-Final phase
iVR	0.94	0.43
Non-immersive	0.25	0.23

3.2. EXPLORATION OF THE DESIGN SPACE

The effect of different media on tutor-student exploration of the design space is illustrated in the network of FOs' concepts. Figure 4 presents the network of FOs for crits given to student S1. The networks show concepts generated during each session.

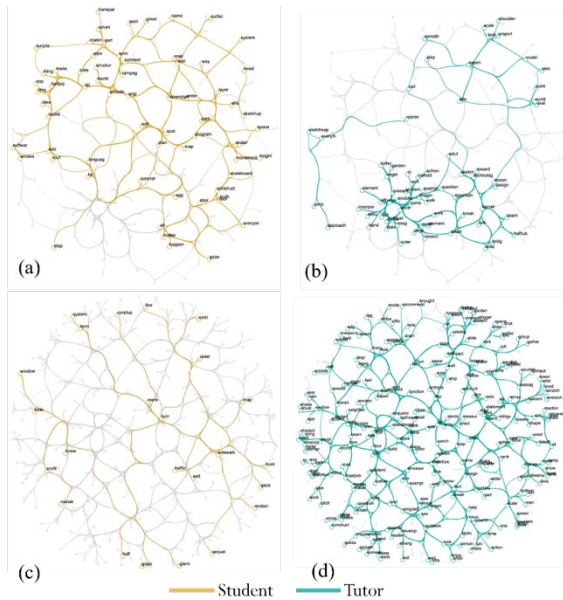


Figure 4. The design space explored by Student S1 in the early course phase: (a) Student's network in the iVR, (b) Tutor's network in the iVR, (c) Student's network in a non-immersive crit, and (d) Tutor's network in a non-immersive crit. The networks are presented against the backdrop of the full design space.

In the early phase iVR crit (Figure 4(b)) we observed a hub of highly connected ideas in the tutor's design space. This could indicate a topic that invoked feedback during this crit. In the iVR crit, the student's exploration of the design space is higher (see Figures 4(a) and (c)). The networks generated in the non-immersive early phase (Figure 4(d)) show a tutor dominance in the exploration of the design space. Using networks of FOs reveals differences regarding how participants explored the design space with the medium used. Non-immersive crits are observed with more tutor FOs (Figures 4(b) and 4(d)). The iVR had more student FOs and a greater connectivity during the iVR, indicating the medium's capacity to benefit the activity.

4. Discussion

This case study demonstrates how iVR systems, flagged as supportive of SDG, affect communication during architecture studio crits through measurements of the design space and learner activity, considered important in achieving a quality education. The results show that iVR crits have a significantly higher frequency of FOs generated by students, indicating the medium's capacity in supporting a learner-centred activity, considered a challenge as the studio is commonly tutor-dominated (Gero & Jiang, 2016; Goldschmidt et al., 2010; Milovanovic & Gero, 2018).

The increase in student FOs in iVR compared to non-immersive media, demonstrates the iVR's capacity in supporting divergent thinking, defined as a quality educational objective. These results provide quantitative support for results of former studies (Dorta et al., 2016; Sopher et al., 2017; Sopher et al., 2019; Sopher & Gero,

2021) and expand them to account for the syntactical and temporal characteristics of the conversations exhibited in the media, information that can support the integration of iVRs in studio pedagogy.

The tutor generated more FOs with non-immersive media, while achieving a smaller variance between the two media, which may imply a greater competence regardless of the medium used. The non-immersive crits had more tutor-student imbalance in the generation of FOs, indicating a stronger tutor dominance, found in other studies investigating design activity in non-immersive crits (Goldschmidt et al., 2010; Milovanovic & Gero, 2018).

Evidence showing differences in activity in iVR during early and final course phases provides ground for further research to increase the ability to integrate iVR in future courses. No significant differences were found in the tutor's FOs over the media, indicating that the tutor was less affected by the medium involved. More research is needed to study how iVRs affect teaching behaviours.

Exploring the connections generated by students shows that the iVR supports greater connectivity between design issues, particularly during the early course phase, which is considered more challenging. Using NLP to track FOs and networks to represent the design space enabled conducting automated quantitative and qualitative analyses. This may be useful in providing detailed feedback to support individually tailored teaching approach, known to lack in the studio (Salama 2015).

This study has several limitations. As a case study, the small number of subjects limits the ability to generalize conclusions. Since the study has a single tutor, further investigation is needed to determine how iVRs affect teaching behaviours.

5. Conclusions

Aiming to increase the possibilities of SDG quality education through carbon free inclusive educational means, this explorative study examined how an iVR system affects communication during design crits by comparing it with non-immersive crits. The results show evidence that iVR increases student engagement in design crits as they generate more FOs and connections between concepts, while potentially reducing carbon emissions. The iVR medium enhanced students' engagement in the crits during the early course phase that is more challenging. No significant differences were found in the tutor's FOs over the media, implying that the tutor is less affected by the medium used. Since only one tutor participated, more research is needed to determine how iVRs affect teaching activities. In addition, since this was a case study, further research is needed to determine whether these results are generally applicable.

The study results provide insights for integrating iVRs in design studios to support remote and collocated communication in inaccessible situations, without generating carbon due to physical travel. This could be extended to inter-university iVR design studios that can enrich learning by engaging with tutors and peers from diverse backgrounds and accomplish an SDG4 quality education with updated education facilities that provide inclusive and effective learning environments for all.

Acknowledgements

This study is supported by the West Creative Industries grant and the National Science

Foundation (NSF). The authors wish to thank Associate Professor Dafna Fisher-Gewirtzman and the participating students.

References

- Beck, D., Morgado, L., & O'Shea, P. (2020). Finding the gaps about uses of immersive learning environments: a survey of surveys. *J.U.C.S.*, 26, 1043–1073.
- Boudhraa, S., Dorta, T., Milovanovic, J., & Pierini, D. (2019). Co-ideation critique unfolded: an exploratory study of a co-design studio 'crit' based on the students' experience. *CoDesign*, 1–20. <https://doi.org/10.1080/15710882.2019.1572765>
- Dorst, K., & Cross, N. (2001). Creativity in the design process: co-evolution of problem–solution. *Des. Stud.*, 22(5), 425–437. [https://doi.org/10.1016/S0142-694X\(01\)00009-6](https://doi.org/10.1016/S0142-694X(01)00009-6)
- Dorta, T., Kinayoglu, G., & Boudhraâ, S. (2016). A new representational ecosystem for design teaching in the studio. *Design Studies*, 47, 164–186. <https://doi.org/10.1016/j.destud.2016.09.003>
- Gero, J. S., & Jiang, H. (2016). Exploring the Design Cognition of Concept Design Reviews Using the FBS-based Protocol Analysis. In R. S. Adams & J. A. Siddiqui (Eds.), *Analyzing Design Review Conversations* (pp. 177–198). Purdue University Press. <https://doi.org/10.5703/1288284315931>
- Gero, J.S., & Kan, J.W.T. (2016). Empirical results from measuring design creativity: Use of an augmented coding scheme in protocol analysis, *Fourth International Conference on Design Creativity* (pp. 1-8), Atlanta, GA, USA.
- Goel, V. (2014). Creative brains: designing in the real world. *Frontiers in Human Neuroscience*, 8(241), 1–14. <https://doi.org/10.3389/fnhum.2014.00241>
- Goldschmidt, G. (2014). Modeling the role of sketching in design idea generation. In A. Chakrabarti & L. T. M. Blessing (Eds.), *An Anthology of Theories and Models of Design* (pp. 433–450). London: Springer London. https://doi.org/10.1007/978-1-4471-6338-1_21
- Goldschmidt, G. (2016). Linkographic Evidence for Concurrent Divergent and Convergent Thinking in Creative Design. *Creativity Research Journal*, 28(2), 115–122. <https://doi.org/10.1080/10400419.2016.1162497>
- Goldschmidt, G., Hochman, H., & Dafni, I. (2010). The design studio “crit”: Teacher–student communication. *Artificial Intelligence for Engineering Design, Analysis and Manufacturing*, 24(03), 285–302. <https://doi.org/10.1017/S089006041000020X>
- Goldschmidt, G., & Smolkov, M. (2006). Variances in the impact of visual stimuli on design problem solving performance. *Design Studies*, 27(5), 549–569. <https://doi.org/10.1016/j.destud.2006.01.002>
- Gómez-Tone, H. C., Martin-Gutierrez, J., Bustamante-Escapa, J., & Bustamante-Escapa, P. (2021). Spatial skills and perceptions of space: Representing 2D drawings as 3D drawings inside immersive virtual reality. *Applied Sciences (Switzerland)*, 11(4), 1–23. <https://doi.org/10.3390/app11041475>
- Hong, S. W., El Antably, A., & Kalay, Y. E. (2019). Architectural design creativity in Multi-User Virtual Environment: A comparative analysis between remote collaboration media. Environment and Planning B: *Urban Analytics and City Science*, 46(5), 826–844. <https://doi.org/10.1177/2399808317733267>
- Kalay, Y. E. (2004). *Architecture's new media: principles, theories, and methods of computer-aided design*. Cambridge, Massachusetts: MIT Press.
- Lave, J., & Wenger, E. (1991). *Situated learning: Legitimate peripheral participation* (24th ed.). Cambridge: Cambridge University Press.
- McLuhan, M. (2006). The medium is the message. In M. G. Durham, & D. M. Kellner (Eds.), *Media and Cultural Studies: Keywords* (second, pp. 107–116). Blackwell Publishing Ltd.

- Mikropoulos, T. A., & Natsis, A. (2011). Educational virtual environments: A ten-year review of empirical research (1999–2009). *Computers & Education*, 56(3), 769–780. <https://doi.org/10.1016/j.compedu.2010.10.020>
- Milovanovic, J., & Gero, J. S. (2018). Exploration of cognitive design behaviour during design critiques. In *Proceedings of International Design Conference, DESIGN* (Vol. 5, pp. 2099–2110). <https://doi.org/10.21278/idc.2018.0547>
- Milovanovic, J., & Gero, J.S. (2020). Exploring the use of digital tools to support design studio pedagogy through studying collaboration and cognition, *DCC'20 Ninth International Conference on Design Computing and Cognition*, Virtual Conference.
- Milovanovic, J., Moreau, G., Siret, D., & Miguet, F. (2017). Virtual and Augmented Reality in Architectural Design and Education. An Immersive Multimodal Platform to Support Architectural Pedagogy. In *CAADFutures 17* (pp. 513–532).
- Oh, Y., Ishizaki, S., Gross, M. D., & Do, E. Y.-L. (2013). A theoretical framework of design critiquing in architecture studios. *Design Studies*, 34(3), 302–325. <https://doi.org/10.1016/j.destud.2012.08.004>
- Rittel, H. W. J., & Webber, M. M. (1973). Dilemmas in a general theory of planning. *Policy Sciences*, 4(2), 155–169. <https://doi.org/https://doi.org/10.1007/BF01405730>
- Salama, A. M. (2015). *Spatial Design Education: New Directions for Pedagogy in Architecture and Beyond*. New York: Routledge. <https://doi.org/10.4324/9781315610276>
- Sanchez-vives, M. V., & Slater, M. (2005). From presence towards consciousness. *Nature Reviews Neuroscience*, 6(10), 332–339. <https://doi.org/10.1038/nrn1651>
- Schön, D. A. (1985). *The design studio : an exploration of its traditions and potentials*. London: RIBA Publications.
- Sopher, H., & Fisher-Gewirtzman, D. (2020). Immersive behaviour setting in architectural education. In R. Almendra & J. Ferreira (Eds.), *Research & Education in Design: People & Processes & Products & Philosophy* (pp. 77–86). London: Taylor & Francis Group. <https://doi.org/10.1201/9781003046103-9>
- Sopher, H., Fisher-Gewirtzman, D., & Kalay, Y. E. (2019). Going immersive in a community of learners? Assessment of design processes in a multi-setting architecture studio. *Br. J. Educ. Technol.*, 50(5), 2109–2128. <https://doi.org/10.1111/bjjet.12857>
- Sopher, H., & Gero, J. S. (2021). Effect of Immersive VR on Communication Patterns in Architectural Design Critiques. In Stojakovic, V., and Tepavcevic, B. (Eds.), *The 39th eCAADe 2021* (pp. 123–130). Novisad: CumInCAD.
- Sopher, H., Kalay, Y. E., & Fisher-Gewirtzman, D. (2017). Why Immersive? - Using an Immersive Virtual Environment in Architectural Education. In A. Fioravanti, S. Cursi, S. Elahmar, S. Gargaro, G. Loffreda, G. Novembri, & A. Trento (Eds.), *The 35th eCAADe Conference* (pp. 313–322). Rome: CumInCAD.
- Slater, M. (2009). Place illusion and plausibility can lead to realistic behaviour in immersive virtual environments. *Philosophical Transactions of the Royal Society B: Biological Sciences*, 364, 3549–3557. <https://doi.org/10.1098/rstb.2009.0138>
- Slater, M. (2017). Implicit learning through embodiment in immersive virtual reality. In D. Liu, C. Dede, R. Huang, & J. Richards (Eds.), *Virtual, augmented, and mixed realities in education* (pp. 19–33). Springer, Singapore. https://doi.org/10.1007/978-981-10-5490-7_2
- Ummihusna, A., & Zairul, M. (2021). Investigating immersive learning technology intervention in architecture education: a systematic literature review. *J. Appl. Res. High. Educ.* <https://doi.org/10.1108/jarhe-08-2020-0279>
- Wang, T. (2010). A new paradigm for design studio education. *Int. J. Art Des. Educ.*, 29(2), 173–183. <https://doi.org/10.1111/j.1476-8070.2010.01647.x>
- Zhao, J., Sensibaugh, T., Bodenheimer, B., McNamara, T. P., Nazareth, A., Newcombe, N., Minear, M., and Klippel, A. (2020). Desktop versus immersive virtual environments: effects on spatial learning. *Spatial Cognition and Computation*, 20(4), 328–363. <https://doi.org/10.1080/13875868.2020.1817925>

COCKROACH: AN OPEN-SOURCE TOOL FOR POINT CLOUD PROCESSING IN CAD

ANDREA SETTIMI¹, PETRAS VESTARTAS² and JULIEN GAM-ERRO³ and YVES WEINAND⁴

^{1,2,3,4}*École Polytechnique Fédérale de Lausanne (EPFL).*

¹*andrea.settimi@epfl.ch, 0000-0001-5020-7331*

²*petras.vestartas@epfl.ch, 0000-0002-4428-1110*

³*julien.gamero@epfl.ch, 0000-0001-7802-5345*

⁴*yves.weinand@epfl.ch, 0000-0002-8088-6504*

^{1,2}*These authors have equally contributed to the research.*

Abstract. In the architecture, engineering and construction (AEC) sector, the use of point cloud data is not a novelty. Usually employed to retrieve data for inspecting construction sites or retrofitting pre-existing buildings, sensors like LiDAR cameras have been known to practitioners such as architects and engineers for a while now. In recent years, the growing interest in 3D data acquisition for autonomous vehicles, robotic and extended reality (XR) applications has brought to the market new compact, performant, and more accessible hardware leveraging different technologies able to provide low-cost sensing systems. Nevertheless, point clouds obtained from such sensors must be processed to extract valuable data for any design or fabrication application. Unfortunately, most advanced point cloud processing tools are written in low-level languages and are hardly accessible to the average designer or maker. Therefore, we present Cockroach: a link between computer-aided design (CAD) modeling software and low-level point cloud processing libraries. The main objective is an adaptation to C# .NET via Grasshopper visual scripting interface and C++ single-line commands in native Rhinoceros workspaces. Cockroach has proved to be a handy design tool in integrating building components with unpredictable geometries such as raw wood or mineral scraps into new design and industrial fabrication processes.

Keywords. Computer-vision; Point-clouds; Data-processing; 3D modeling; CAD interface; Open-source tools; Quality education; Industry innovation and infrastructure; SDG 9.

1. Introduction

In recent years, computer vision hardware has become increasingly accessible (stereo cameras, LiDAR, and AI-based sensors), allowing rapid data acquisition to model the world around us from small-scale objects to large-scale buildings. Given the sparse character of available point cloud processing libraries, which contain a different set of

specific functions with other data structures or method calls, development can frequently become cumbersome when adding, compiling, referencing, and converting code among these repositories. In addition, when processing point clouds, the programming language C++ often results as an indispensable language for performance issues. Unfortunately, average designers lack knowledge and time to post-process point clouds. To address these challenges, we propose Cockroach: a point cloud post-processing open-source tool based on C++ (Vestartas and Settimi, 2020). Cockroach acts like an umbrella library able to regroup, compile and make communication possible among the many libraries for point cloud processing, currently Open3D, Cilantro, CGAL, and PCL (Figure 1). The majority of the code is wrapped around C#.NET, specifically tailored to be integrated into the Rhinoceros 3D and Grasshopper environment. The proposed processing tools have proven to be useful in research applications dealing with irregular geometries such as architectural modeling and structural analysis. The current document aims to provide an overview of Cockroach’s most recent point cloud processing applications applied to digital fabrication and design.

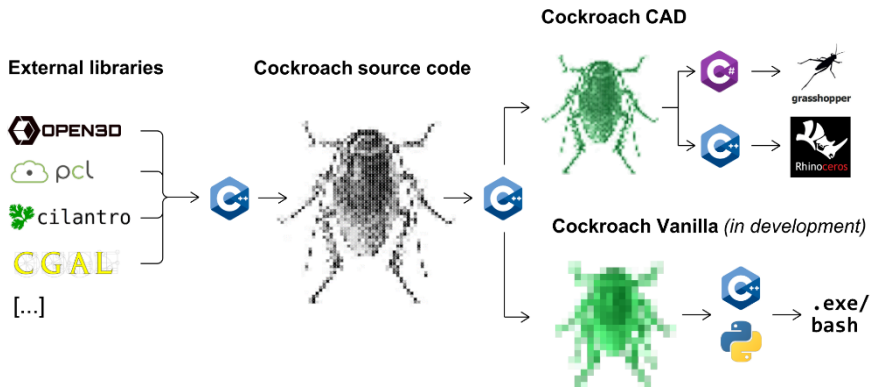


Figure 1: Cockroach architecture, dependencies, and current development branches.

2. State-of-the-art

2.1. OPEN-SOURCE INSIDE CAD ENVIRONMENT

The following point cloud processing software review is based on open-source applications targeting either standalone or hybrid CAD and visual programming interfaces such as Rhinoceros 3D. Volvox (Zwierzycki et al., 2016) was one of the first tools available to post-process heavy point cloud data to link the scanning methods with architectural and engineering design. Beforehand, this data was not accessible to designers due to the overly complicated workflows of closed commercial applications required to import and export geometry. The DURAARK project (Tamke et al., 2016) revealed five critical steps of point-cloud processing: 1) retrieve data, 2) allocation, 3) analysis and verification, 4) focus and abstraction and 5) design. The third and fourth points pose a technical problem when higher-level computer languages, e.g. C#, VB,

IronPython, are insufficient to post-process point clouds. The lower-level languages result in a faster execution time, memory management and, more importantly, are used in many research fields associated with open-source point cloud processing tools. Therefore, it is more accessible for integration and access to existing development teams. Point Cloud Components (Ervine and Girot, 2014) also addresses the problem of point cloud manipulation using a Rhino and Grasshopper interface. One possible reason why these tools are not commonly used and developed is that point cloud processing remains a daunting task, as the available tools are more akin to quantitative engineering analysis than to interactive design. The developed methods are limited to cropping, merging, subsampling, file transfer, and Delaunay meshing. Lastly, small-scale open-source projects, such as Tarsier (Newnham and Gwyllim, 2016), can mainly be used for visualization, while most users apply these methods for analysis, reverse-engineering 3D modeling, and visualization. The remaining question is how these tools can be used for fabrication or assembly, especially for relatively small and medium scale scans. Methods like registration, point-set alignment, abstraction to geometric primitives, and clustering techniques are missing features in the reviewed plug-ins.

2.2. OPEN-SOURCE OUTSIDE CAD ENVIRONMENT

Aside from CAD environments, there is a vast literature of free-to-use point cloud processing software written and used in less accessible languages and less interacting interfaces than a modeling environment, with few exceptions given.

Point Cloud Library (PCL) (Rusu and Cousins, 2011) is the most widely known open-source software for point cloud processing. The library has been employed in numerous research works, especially in autonomous robotic vehicles. It integrates several state-of-the-art algorithms, including filtering, feature estimation, surface reconstruction, registration, model fitting, and segmentation. PCL is implemented in C++, and it is organized in separately compilable modules which can run on Linux, macOS, Windows, and Android. Although extremely powerful, PCL presents many challenges (e.g., compiling issues, C++ intrinsic code complexity), making it hardly accessible for the broader public of developers, not to mention average designers. Although hard to maintain and fragmented in various projects, multiple wrappers written in high-level languages like Python exist (Caron et al., 2020). Open3D (Zhou et al., 2018) is the most recent point cloud processing library. Natively written in C++, it offers a lean, well-documented, and modern Python application programming interface (API). To this day, this represents the most maintained library for point cloud processing. In its recent release (0.13.0), the library features advanced GPU acceleration, real-time 3D reconstruction pipelines, and a web visualizer. Cilantro (Zampogiannis et al., 2018) is another lean and fast C++ library dealing with point cloud data. Besides more ordinary functionalities (I/O utilities, resembling algorithms, normal estimation, convex hulling, etc.), it implements multiple clustering techniques such as connected-component, mean-shift, general dimension k-means, and spectral clustering techniques. There are several open-source point cloud processing software that tends to be mainly used with desktop graphical user interface (GUI). Cloud Compare (Girardeau-Montat, 2020) is an open-source library particularly famous thanks to its well-designed GUI and robust functions to manipulate and register clouds. It also features a valuable plug-in system for contributors to deploy their work on self-

contained modules. In this GUI category, MeshLab (Cignoni et al. 2008) offers a more limited set of point cloud tools but a very user-friendly interface. Despite the high level of user accessibility for GUIs, such interfaces often lack tools to automate processing tasks. Nonetheless, Geometry-central (Sharp et al., 2019a), a mesh library with several point-set processing possibilities visualized by Polyscope GUI (Sharp et al., 2019b), provides parametrization of point-cloud. Point Data Abstraction Library (PDAL) (Bell et al. 2020) also proposes a proper level of automation with a slightly lower-end interface. Thanks to its JSON layout, this library offers the possibility to stage multiple processing operations and automatically execute them on different point clouds. Although its very core is written in C++, PDAL provides various interfaces to meet with the different skill levels of its user base: JSON, command line from the terminal, Python, and native C++ API. A more extensive geometric library like CGAL (The CGAL Project v. 5.3, 2021) also provides packages with point cloud data structure for essential processing functions such as normal estimation, up/down-sampling, smoothing, but also more advanced ones, such as point cloud re-structuring, multiple registration techniques, polygonal surface reconstruction from a point cloud, classification methods from unordered point clouds, and a shape detection algorithm for point clouds. In particular for registration functions, CGAL implements them from two open-source libraries: OpenGR (Mellado, 2018) for global alignment and Libpointmatcher (Pomerlau et al., 2013) for the Iterative Closest Point (ICP) algorithm. Registration methods for aligning point cloud fragments are illustrated and further discussed in the following sections.

3. Application of the Point-cloud Processing Library Cockroach

Two applications from the Cockroach library are detailed focusing on two key methods that were previously missing in point-cloud processing applications for CAD users: registration and clustering. The registration method takes an example of a tree fork truss fabrication and clustering is explained using an experiment of a stone wall assembly. Nonetheless, all functions can be retrieved in the library repository (Vestartas and Settimi, 2020): 1) crop and cut by box, polyline, mesh or plane, 2) normal estimation, uniform orientation and visualization; 3) cleaning and downsampling techniques like random point removal and voxelization, 4) meshing methods such as Poisson and ball-pivoting surface reconstruction, mesh repairing functions, skeletonization and mesh boolean operations, and 5) several utility functions like point cloud serialization, merging, coloring, properties and normal display.

3.1. REGISTRATION METHODS

Point cloud registration consists in finding a spatial transformation such as scaling, rotation, and translation that aligns two point cloud data sets. Cockroach implements two typical alignment algorithms into one method called Recursive Registration (RR), including 1) global Random Sample Consensus (RANSAC) registration and 2) local-global ICP. First, point clouds (Figure 2A) are downsampled to reduce computation time (Figure 2B). Second, point-cloud normal and geometric features are estimated. Third, distance, edge length, and angle correspondence are computed. Fourth, the previous inputs are given to the RANSAC algorithm to align point clouds globally

(Figure 2C). Fifth, registration is refined using local ICP point-to-plane registration (Figure 2, D). The two transformations are applied to the original high-resolution point clouds (Figure 2E). The five steps are repeated several times until the desired fitting is achieved according to the user's tolerance. The combined methods are illustrated in the tree fork example in Figure 2, showing the registration of two point cloud fragments belonging to the same object.

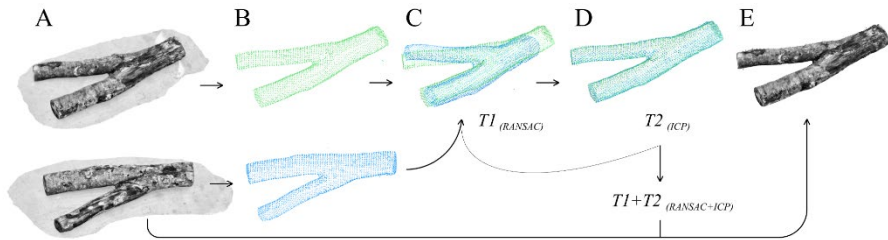


Figure 2: Basic application of the combined registration method to obtain a complete 3D model from two different scans. Without this function, it would be hard to acquire the entirety of the object's geometry without missing parts in the point cloud.

The proposed RR is also employed in alignment problems when the position and orientation of the workpiece, irregular in shape, is not known regarding the fabrication setup (Vestartas, 2021). In our case study developed for timber construction, manufactured elements are scanned twice: 1) before fabrication to obtain a tree stock and create a design model, and 2) after the design is made with a second scan made during fabrication to align tool-paths for cutting (see Figure 3). The previous publication describes that it is enough to use three reference points when mounting on a rig (Mollica, 2016) without pre-scanning. However, our experiment shows that scanning is needed to acquire a precise position of a tree fork because three pre-drilled mounting holes are not precise enough (see Figure 4E). The darker scan shown in Figure 3B is taken without the fabrication rig and was used for a design of a truss (see Figure 4F). When the design was fixed, a second scan is taken for fabrication and the two point clouds were aligned as shown in Figure 3 C-D.

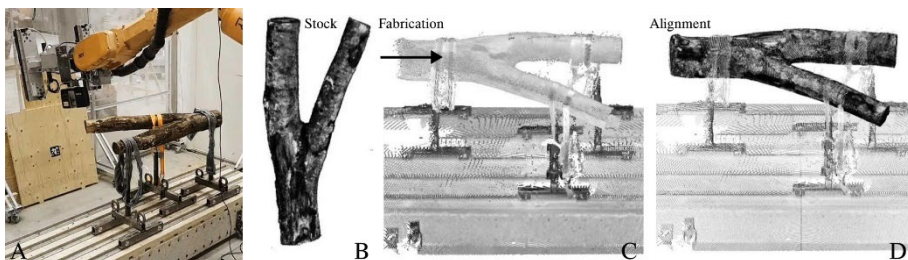


Figure 3: Registration process: a) robot scan, b) point-cloud taken months before for a design phase, c) scan with a mounted object and d) alignment of the two point-clouds.

Afterward, the fabrication can be started because pre-scanned tree-forks are combined with timber joinery tool-paths as illustrated in Figure 4F. The sequence of

fabrication steps are as follows: a) mounting, b) scanning and alignment of the two point clouds, c) cutting, d) de-mounting, and e) repeating the process. Lastly, the raw timbers are assembled, as shown in Figure 5.



Figure 4: Workflow: a) mounting, b) scan, c) cut, d) demounting, and e) machined forked, and f) individual element with joinery geometry.

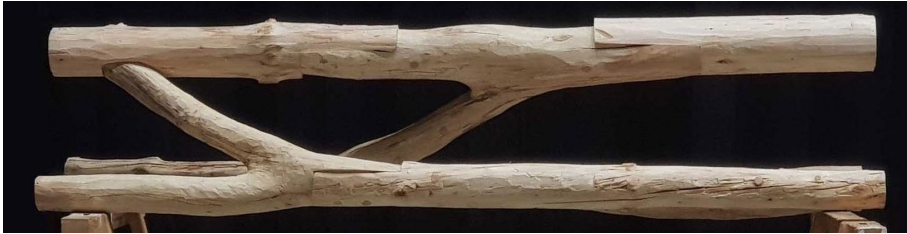


Figure 5: Assembly of the prototype using three tree forks and four straight segments.

3.2. CLUSTERING

Point cloud clustering subdivides a point cloud model into smaller elements. Cockroach implements multiple clustering methods such as color-, normal-, and distance-based clustering. The last method, Euclidean clustering, can segment detached elements belonging to the same scene. This function is particularly useful to identify multiple objects, as shown in Figure 6. The objects in the scene are first isolated by removing the plane via the RANSAC fitting plane. Second, the elements are filtered from noise with statistical outlier removal and the remaining point cloud is segmented. The same procedure is repeated twice per rock once it is turned. Finally, the stones are recomposed (see Figure 6B) and meshed (see Figure 6C). Point cloud normal-based clustering and key points detection allow digital reconstruction of larger objects composed of several complex irregular geometries, as illustrated in the preliminary study for digitizing dry-stone walls (see Figure 7). Automatic point cloud segmentation in a CAD environment can become a performant tool for architects and designers to describe and rapidly obtain 3D models out of any significant quantities of irregular elements or re-used components in construction. By building new digital catalogs from

stocks of re-used elements, designers can be informed from the early project stage with reliable CAD models of unpredictable geometries or non-standard building components. We designed and made available an online catalog with numerous scanned and reconstructed models of mineral construction waste that designers can inspect and download (Broyet et al., 2021). The website has been developed and made publicly available as a proof-of-concept for a novel approach to design with re-used elements and construction cataloging thanks to accessible point cloud processing tools.

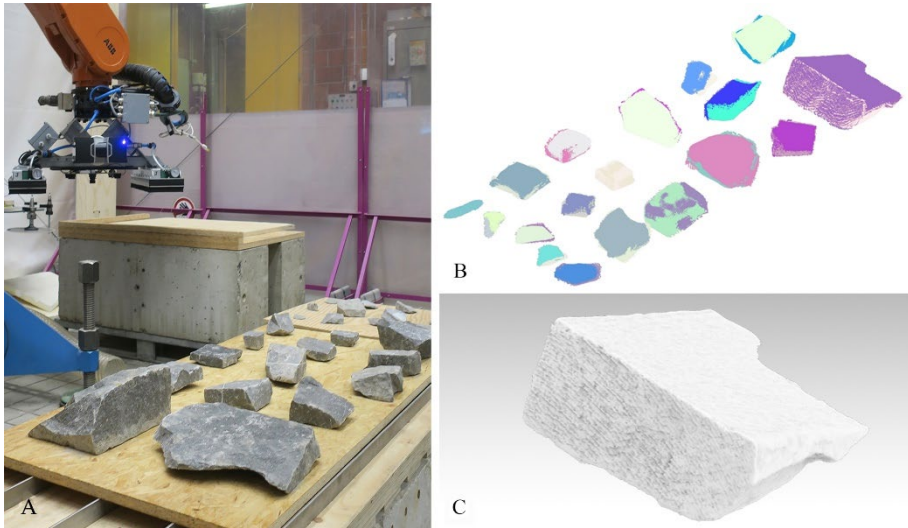


Figure 6: Automated point cloud scanning and post-processing for CAD models of irregular mineral scraps. The process can be applied to any other batch of irregular objects.

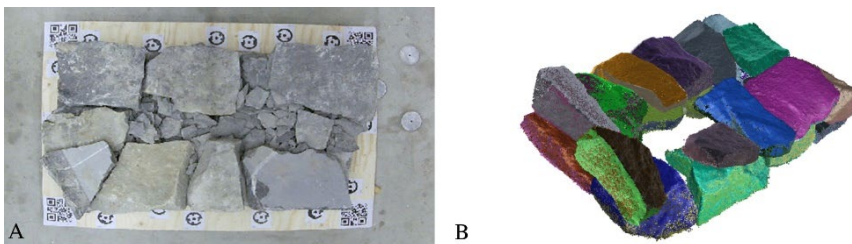


Figure 7: Segmentation of the dry-stone wall for 3D reconstruction and position identification.

4. Conclusions and Future Work

Cockroach showed how it is possible for designers to efficiently model even the most irregular objects from LiDAR scans. Given the rising need for using recycled, non-standard elements, we believe that high-level point cloud processing will be proved to be a valuable asset for sustainable computational design. Accessible advanced point cloud manipulation tools allow every designer to extrapolate meaningful information from the most intricate scan of any building, component, or raw resource. Considering the rise of embedded systems in the AEC practice and the growing presence of spatial sensors in renovation applications, point clouds may well be geometric data with which

architects will need to become increasingly familiar. The drafting process itself can be done using scan data instead of 2D or 3D drawing, whether for architectural heritage projects or real-time manufacturing and assembly processes. From the review of existing point cloud processing tools, it is evident that these tools are still not user-friendly and the only available solutions are stand-alone software applications making them difficult to implement into existing CAD software. While Cockroach was started from concrete research goals for robotic fabrication of irregular timbers and mineral scraps, the developed .NET interface allows this library to be used in several software packages such as Rhinoceros3d, Unity, Revit-Dynamo. In addition, the lack of documentation and maintenance of the open-source repositories makes state-of-the-art methods hardly accessible. The proposed tool attempts to reduce this step through research projects and applications, although they are not the main goal. The focus is given to a structured, well-documented, and maintained open-source repository Cockroach.

Regarding Cockroach's future developments, the main objective is to migrate the current library towards a self-contained, shippable, standalone, and cross-platform version of the software. The software will be composed of a basic visualizer (e.g., OpenGL or Vulkan), a GUI system (e.g., DearImgui), an integrated shell input as the main UI, a macro reader, and a file importer. The goal of developing the standalone Cockroach version is to extend the usability of the software to a broader public of users from different disciplines. This format may allow other high-level users than AEC designers to profit from intuitive but effective point cloud processing tools like Cockroach.

Acknowledgements

The authors would like to acknowledge the financial support of the Ecole Polytechnique Fédérale de Lausanne (EPFL), and in particular the ENAC Faculty with the Cluster Grant which partially contributed to fund the development of Cockroach.

References

- Bell, A., Chambers, B., Butler, H & others (2021). *Point Data Abstraction Library* (version 2.3.0). <https://doi.org/10.5281/zenodo.4031609>.
- Broyet, A., Settimi, A., Gamberro, J. & Weinand, Y. (2021). *Eesd-Ibois Scanned Stones Dataset*. Retrieved November 19, 2021 from <https://ibois-epfl.github.io/eesd-ibois-scanned-stones-dataset/>.
- Caron, D., Vulgar, M. & Allen, A. (2020, April 21). *Pclpy: PCL for Python*. Retrieved November 19, 2021 from <https://github.com/davidcaron/pclpy/releases/tag/0.12.0>.
- Cignoni, P., Corsini, M. & Ranzuglia, G. (2008). *ERCIM Newy. MeshLab: an Open-Source 3D Mesh Processing System*. Retrieved November 19, 2021 from <http://vcg.isti.cnr.it/Publications/2008/CCR08>.
- Ervine, L. & Girot C. (2014). *Point Cloud Components: Tools for the Representation of Large Scale Landscape Architectural Projects*. Retrieved November 30, 2021 from https://archive.arch.ethz.ch/dla2014/talk_pdfs/DLA_2014_4_Lin.pdf.
- Girardeau-Montat D., (2020). *CloudCompare*. Retrieved November 19, 2021 from <http://www.danielgm.net/cc/release/>.
- Mellado, N. (2018). *OpenGR: a 3D Global Registration Library*. Retrieved November 19, 2021 from <https://github.com/STORM-IRIT/OpenGR>.

- Mollica Z. (2016). *Tree Fork Truss: An Architecture of Inherent Forms*. Retrieved November 30, 2021 from <https://zacharymolli.ca/assets/download/Mollica-DMThesis-Tree-Fork-Truss-an-Architecture-of-Inherent-Forms.pdf>.
- Newnham, C. & Gwyllim, J. (2016). *Tarsier* (version 1.0.1.0). Retrieved November 30, 2021 from <https://bitbucket.org/camnewnham/tarsier/src/master/>.
- Pomerleau, F., Colas, F., Siegwart, R. & Magnenat, S. (2013). Autonomous Robots. *Comparing ICP Variants on Real-World Data Sets*, 34(3) (pp. 133-148). <https://doi.org/10.1007/s10514-013-9327-2>.
- Rusu, R. B. & Cousins, S. (2011, May 13). 3D is here: Point Cloud Library (PCL). In *IEEE International Conference on Robotics and Automation*, (pp. 1-4). <https://doi.org/10.1109/ICRA.2011.5980567>.
- Sharp, N. & others (2019b). *Polyscope*. Retrieved from November 29, 2021 from www.polyscope.run.
- Sharp, N., Keenan, C. & others (2019a). *Geometry-central*. Retrieved November 30, 2021 from www.geometry-central.net.
- Tamke, M., Edvardsen, D.F., Beetz, J., Evers, H.L., Krijnen, T., Hecher, M., Zwierzycki, M., Panitz, M., Wessel, R., Vock, R., Ochmann, S. & Gadiraju, U (2016). *DURAARK Evaluation Report D7.4, FP7 – ICT – Digital Preservation*, Grant agreement No.: 600908. Retrieved November 30, 2021 from https://www.researchgate.net/publication/340267140_Parametric_architectural_design_with_point-clouds_Volvox.
- The CGAL Project (2021). *CGAL*. In CGAL User and Reference Manual (version 5.3). Retrieved November 19, 2021 from <https://doc.cgal.org/5.3/Manual/packages.html>.
- Vestartas P. (2021). *Design-to-Fabrication Workflow for Raw-Sawn-Timber using Joinery Solver*. Thesis. EPFL. <http://dx.doi.org/10.5075/epfl-thesis-8928>
- Vestartas, P., Settimi, A. (2020). *Cockroach: A Plug-in for Point Cloud Post-Processing and Meshing in Rhino Environment*, EPFL ENAC ICC IBOIS. Retrieved November 19, 2021 from <https://github.com/ibois-epfl/Cockroach>.
- Zampogiannis, K., Fermuller, C. & Aloimonos, Y. (2018). Cilantro: A Lean, Versatile, and Efficient Library for Point Cloud Data Processing. *Proceedings of the 26th ACM international conference on Multimedia* (pp. 1364-1367). <https://doi.org/10.1145/3240508.3243655>.
- Zhou, Q., Parl, J. & Koltun, V. (2018). Open3D: A Modern Library for 3D Data Processing. *ArXiv, abs/1801.09847*. <https://arxiv.org/abs/1801.09847>.
- Zwierzycki, M., Evers, H. L. & Tamke, M. (2016). Parametric Architectural Design with Point-clouds: Volvox. In *Complexity & Simplicity: Proceedings of the 34th eCAADe Conference* (Vol. 2, pp. 673-682).

TOWARDS AI-ASSISTED DESIGN WORKFLOWS FOR AN EXPANDED DESIGN SPACE

SHERMEEN YOUSIF¹ and EMMANOUIL VERMISSO²

^{1,2}*Florida Atlantic University.*

¹*syousif@fau.edu, 0000-0003-4214-1023*

²*evermiss@fau.edu, 0000-0001-9116-8877*

Abstract. The scope of this paper is to formulate and evaluate the structure of a viable design workflow that combines a variety of computational tools and uses artificial intelligence (AI) to enhance the designer's capacity to explore design options within an expanded design space. In light of the autonomous and progressively post-anthropocentric generative capability of recent AI strategies for architectural design, we are interested in investigating some of the challenges involved in the insertion of such AI strategies into a new generative design system, involving data curation and the placement of any AI-assisted model in the overall workflow, as well as its (AI's) reciprocity with other computational methods such as discrete assembly and agent-based modeling. The paper presents our interrogation of the proposed AI-assisted framework, demonstrated in experiments of formulating multiple design workflows following different strategies. The workflow strategies show that integrating AI networks into a framework with other computational tools affords a different kind of design exploration than other methods; the prospect of novel solutions is heavily dependent on the interconnectedness of such methods and the dataset curation process. Collectively, the work contributes to innovation in architectural education and practice through enhancing scientific research (in line with UN Sustainable Development Goal 9).

Keywords. Artificial Intelligence; Deep Learning; AI-assisted Design Workflows; Design Space Exploration; Generative Systems; SDG 9.

1. Introduction

Generative design systems (GDSs) have been implemented as powerful supportive schemes for designers' exploration. The first generation of GDSs involved rule-based and/or performance-driven algorithms that evolve design as a product of a parametric exploration, with specific parameters and constraints, often to satisfy a set of objective functions (Stocking, 2009). Such deterministic algorithms require designers to input a set of parameters and examine a feasible search space. Such an approach addresses design activity as a generalized reductive process, and the design space to be confined and limited to pre-programmed feasible solutions (Chen & Stouffs, 2021). Recent AI methods, (i.e. deep learning) are "learning systems" that do not require input-rules and

learn directly from raw data to offer “unexpected” solutions (Hassabis, 2018). Benefitting from the widespread applications of AI, a recent second generation of GDSs is emerging, marking a shift in design, towards an unlimited exploration of the design space, which sometimes becomes a “hyper-dimensional” space, such as the latent space of StyleGAN models (Gui et al., 2020). AI models are now capable of autonomously defining their own parameters from information present in their input datasets (Chaillou, 2019a). Generative adversarial networks (GANs), which are subclasses of DL models, can be incorporated to extend the lateral thinking constraints in current generative systems. Inserting AI into a generative approach expands the opportunities for exploring the complexity of a design problem within a larger, more representative search space where design decision-making based on a local examination, can determine how it contracts or expands (Bolojan, 2022).

This work addresses two research problems: (1) investigating new AI-assisted design workflows, and (2) researching methods of dataset acquisition-curation. Addressing Problem (1), we aim to interrogate methods and workflows for leveraging AI to coordinate other computational methods in the overall process. We examine how the “idea” of employing deep learning disrupts the “conventional” generative workflow and identifies possible combinations of methods and corresponding workflows to arrive at novel AI-assisted design systems. Such hybrid workflows require pre-design and intermediate tasks to be considered beforehand. Problem (2) addresses dataset acquisition-curation, a significant and time-consuming activity within AI approaches (Hasey et al., 2021). AI’s performance is evidently contingent on the quality of data from which AI learns and extracts “knowledge”. This investigation offers insight into the relevance of specific computational methods to produce custom datasets for AI processes. Proper dataset generation requires a prior clarification of the design intent so that the data reflects and supports the desired search direction. AI models seem to “learn” better from datasets that are explicitly designed for the training task relative to a specific design problem, compared to pre-existing data (i.e. available online). The “innovation” of AI-generated designs depends on the originality of the training datasets. Using AI to cross-pollinate architecture-specific domains with other types of references is analogous to architectural ideas’ evolution through breeding different fields. The importance of this work lies in its research-driven pedagogy within an undergraduate architecture curriculum. Such work can act as a catalyst to attract funding towards advanced undergraduate research, a strategic goal in our institution, and create ties with the AI technology industry, (aligned with SDG 9) ensuring resiliency in the curriculum vis-à-vis future adoption of data-driven processes.

2. Theoretical Framework & State-of-the-Art

Reviewing state-of-the-art literature, Makoto Watanabe pioneered the use of AI within architectural design through an “inductive design approach”. His method generated unpredicted “magic-like” aesthetics without a preconceived notion of “what good is”. The process entailed an inter-exchange between the designer and the machine, where the computer inferred the design purpose based on designer’s sketches, offering further ideas, followed by review until the design is satisfied (Watanabe, 2004). In interactive media art, Refik Anadol’s process represents an excellent example for controlling the data curation to produce a creative artistic expression (Forbes, 2020). Chaillou’s

(2019b) work represents early research of AI and architecture. His method, ArchiGAN, is a Pix2Pix-based GAN model that employs deep learning models at multiple scales to generate floor plans automatically. The model is trained with a database of annotated plans, starting with building footprints and moving to interior spatial distributions. Another research project employed CycleGAN to perform a heuristic search, cross-pollinating domains of Sagrada Familia with forests, hinting at ways that the network can learn structures and morphology (Bolojan & Vermisso, 2020). Daniel Bolojan and the work of Deep-Himmelb(l)au offer new possibilities for 3D-based GAN models (2022). In a different approach to 3D, Immanuel Koh (2021) uses discrete sampling to produce 3-dimensional representations for AI learning, in a hybrid workflow of computational and AI tools. Speculating on AI's role in architecture, Leach (2021) speaks of a future dominant "architectural intelligence". AI-assisted design is still experimental without yet leveraging AI's full capabilities in system-driven approaches. This work examines AI's potential for multiple design tasks across different phases.

We adopt here Christopher Alexander's systems thinking and his theory of "systems generating systems" (1968). In this sense, "a generating system is not a view of a single thing, it is a kit of parts, with rules about the way these parts may be combined" (Menges & Ahlquist 2011, p. 64). We consider the complex design problem as a process that involves multiple tasks (activities), and that AI models and computational methods can be connected in a sequential logic to achieve an "augmented" generative system. The significance of this work lies in demonstrating how DL models can be integrated into architectural design pedagogy, and their explicit support towards various aspects of design like concept, design development, etc. Emphasis is placed on the benefits and limitations of these hybrid workflows instead of the design outcomes because we believe the strategies are not project-specific and can be extrapolated to design studios in general. In order to expand the design space to include reference datasets (architectural, inspirational), computationally generated and behavior simulation-driven approaches can be incorporated, operating as dataset generation tools for the AI models. We herewith propose a hybrid prototype, that involves interlacing deep learning models and computational methods to control (guide) a generative system. To achieve that, the prototype involves developing multiple design workflow strategies (Section 4) to address: (i) identification of possible structures for integrating AI within different phases of the design cycle, (ii) identification of methods for dataset generation-curation, and (iii) evaluation of the AI-assisted generative workflows. The objective is to experiment with developing possible AI-assisted design workflows and offer insight into the potential and disadvantages of specific combinations of AI and computational methods for creative exploration.

3. Methodology

Our discussion addresses the importance of crafting custom design workflows that synthesize a variety of computational tools, as we place gravity on the impact of "process" for creativity. Indeed, neuroscience accepts several approaches for assessing creativity, focusing on "product" and "process" (Abraham, 2018). We believe that examining the advantages of the overall workflow and calibration of computational tools involved can provide a better intuition on their potential for novelty, than an independent evaluation of the design results. It is important to note that the creative

potential of this hybrid process is contingent on its degree of flexibility; predetermined parameters and objectives do not necessarily support creative exploration. In fact, in computational design processes, design objectives and evaluation criteria often co-evolve with the development of the project. Researching how designers can intervene within GDSs becomes important to achieve an adaptable, mediated, and guided design process (Harding & Brandt-Olsen, 2018). Moving beyond rule-based systems and allowing machines' self-learning and creative exploration to occur necessitates a thorough investigation of the design steps and their continuity within the overall cycle. This way, designers engage in non-deterministic methods through ideas and reflections that resemble their creative thinking within an open-ended search space, without being constrained to a predetermined end. The research methods used in this study comprised literature study, experimentation, prototyping, testing, and evaluation. To represent and test the proposed design process, a system's framework (a prototype) has been developed. Three essential components were pursued in developing the computational system: generating mechanisms, testing mechanisms, and a control approach (Mitchell, 1990). Within generating mechanisms, methods of discrete assembly, in particular the wave function collapse (WFC) method, agent-based modeling (ABM), and GANs were connected to evaluate possible scenarios of those methods; AI was used as a control mechanism for guiding the general framework (Fig.1).

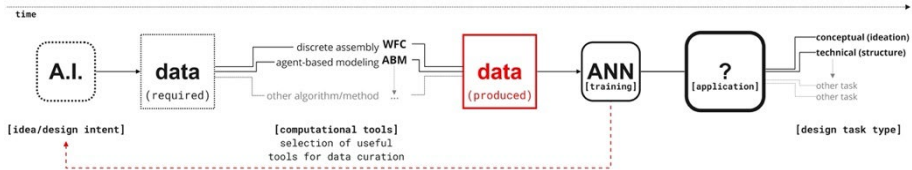


Figure 1. Proposed AI-assisted design framework: AI guides the initial activities, informing the subsequent processes. Multiple methods are used to generate datasets for AI training and several ANNs are applied to tackle different design scales at variant phases.

4. Testing and Implementation

The proposed prototype was a pilot study within a graduate design studio setting. The design brief addressed the concept of a post-pandemic, high-density, mixed-use residential township. One of the project objectives was to generate speculative, resilient futuristic design propositions, additionally inspired by natural systems. Different groups addressed the same design problem through different combinations of computational approaches (WFC, ABM, GANs), for the three targeted phases (Fig.2), resulting in three workflow strategies (4.1., 4.2., 4.3.). Experiments of the WFC method were performed using a C# program embedded into a Rhino/Grasshopper[®] algorithmic definition. Studies of agent-based modeling were conducted using the Culebra tool (developed by Complicit-Matter group). PyTorch[®] and Tensorflow[®] deep learning packages were used within the PyCharm environment for training the neural networks. A number of Python algorithms were written specifically for management of datasets.

4.1. WORKFLOW STRATEGY 1: DL-WFC-ABM

This workflow strategy applied an AI model first, followed by the WFC algorithm and ABM simulations, for the aforementioned design stages, respectively (Fig.2). (1)

Explore-Conceptualize: AI (CycleGAN) was used as an inspirational and suggestive approach to establish a new design concept by cross-pollinating different domains: natural structural patterns (Domain A) and architectural sections (Domain B). Thereby new spatial configurations and relationships were retrieved. The CycleGAN model trained for 200 epochs (# of iterations to process the whole dataset), using a dataset of 2000 images for each domain and 500 images for testing at 512x512 resolution. The new AI-generated sections informed massing strategies. (2) *Generate-Revise:* The WFC generated design iterations of discrete assemblages to occur within the massing generated in the previous step that served as an input for the spatial distribution and design generation (floor plans). (3) *Develop-Qualify:* Behavior simulation was used to "qualify" successful design iterations and progress to design development. ABM simulations (tracking behavior) informed building circulation, revising the discrete aggregations. Although this strategy yielded inspirational and suggestive designs from the AI model, there were certain shortcomings. Starting with AI excluded the possibility of using our own computationally generated datasets and relied exclusively on existing online data. Furthermore, the AI-synthesized images were manually post-processed as projection templates to acquire volumetric sculpting, leading to abstraction and loss of certain features of the original AI designs. Consequently the AI step was diluted overall, relinquishing control to the other methods (WFC, ABM).

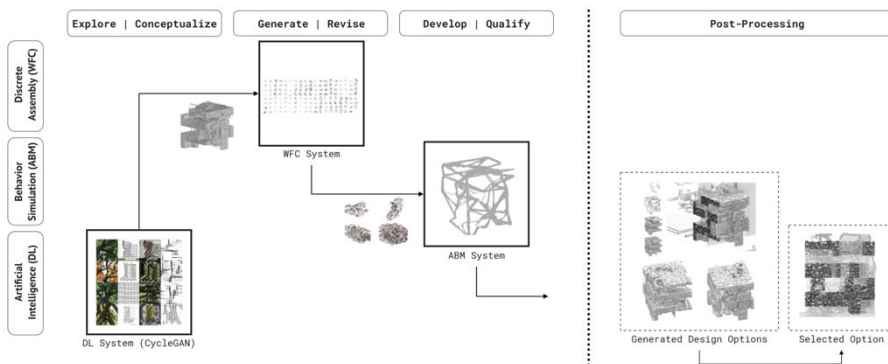


Figure 2. Workflow strategy 1 curates combined methods (DL, WFC, ABM) for three design phases.

4.2. WORKFLOW STRATEGY 2: ABM-WFC-DL

This experiment was conducted in a different order of methods. To begin with, the ABM system was used as a starting point for exploration, followed by the discrete assembly, and then AI, as explained next (Fig.3). (1) *Explore-Conceptualize:* Starting with the context variables, a behavior simulation method was employed, establishing a generative system that informed initial conceptualization. The trails of the ABM simulation (stigmergy) were converted into a topological mesh, serving as an initial volumetric exploration. (2) *Generate-Revise:* For this phase, the WFC method was utilized to produce design options contained within the massing suggested in the previous step, leading to variations and iterations of spatial distributions. Intentionally, the system produces a large dataset of "computationally-generated" design options, to be used for the later AI process. (3) *Develop-Qualify:* In the third phase, this

exploration examined the possibilities of disrupting the orthogonal rule-based logic of the WCF-generated floorplans and their spatial qualities by breeding that dataset with a more organic system (termite nest structure). The CycleGAN model was used to train two domains (Domain A: WFC-based floorplans; Domain B: Natural system of termite-nest pattern). The model was trained for 200 epochs, using 2500 images (512x512 pixels) for each domain, and 500 images for testing.

This experiment has led to new, algorithmically-generated, architectural datasets, bred with natural patterns in the AI training as a further exploration task to modify the architectural language (Fig.4). Overall, the pseudo-random qualities of the termite nest pattern redefined the spatial relationships in the floorplans.

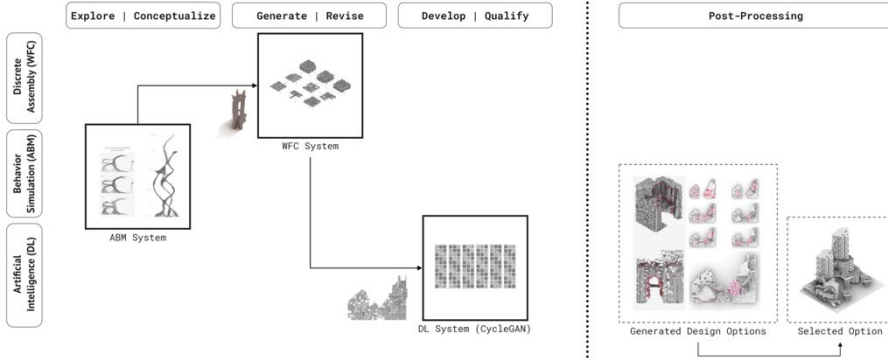


Figure 3. Workflow strategy 2 curates combined methods (ABM,WFC,DL) for three design phases.

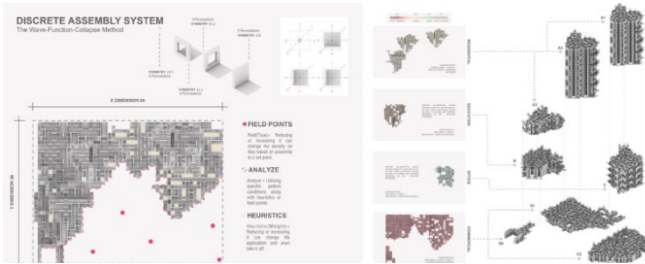


Figure 4. The Wave-function-collapse method to generate datasets.

4.3. WORKFLOW STRATEGY 3: WFC-DL-DL

This strategy included the WFC method for conceptualization and two DL models for subsequent phases (Fig.5). (1) *Explore-Conceptualize*: The WFC system was customized to generate initial design configurations involving massing or "global variables" and unit assembly options of "local" qualities. This rule-based generative system yielded a specific language of stacking and orthogonal spatial configurations due to the use of orthogonal tiles. It is important to note that the WFC can produce curved and rounded geometry, yet the aggregation was constrained by the 3D voxel-based field, leading to a specific DA language. (2) *Generate-Revise*: Here, a DL model (CycleGAN) was used to modify and revise the WFC-generated system, by cross-

pollinating two domains: WFC-produced section designs (Domain A) and forests and tree structures (Domain B) in an elevation view. The model trained for 200 epochs with 2000 images (training) and 500 images (testing) at a 512 resolution. The results suggested altered section designs (Fig.8). (3) *Develop -Qualify*: Synthetic sections from the CycleGAN training were combined with architectural building designs of green roofs and terraces using a StyleGAN (50% for each domain). The StyleGAN trained for 18 hours (stopped at Network snapshot 131). The image size was 1024x1024 pixels. Synthetic images generated by the StyleGAN model re-designed the WFC-based designs, incorporating greenery into the building. Multiple interpolation walks through the StyleGAN's latent space were examined, offering design ideas to transition from "brutalist" to "green" design options. This strategy demonstrated reciprocity between AI-assisted steps, where AI-generated images from the second phase (CycleGAN) informed an AI model (StyleGAN) in the final phase.

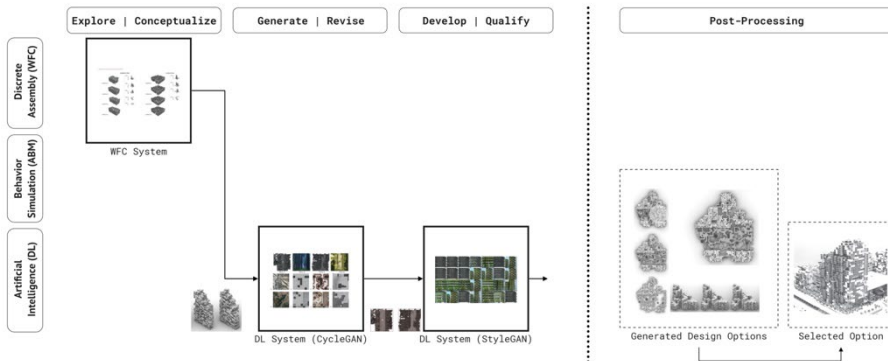


Figure 5. Workflow strategy 3 curates combined methods (WFC, DL, DL) for three design phases.

5. Results and Discussion

Strategy 1 Results: The AI-synthesized images (Fig.6) offered possibilities for new approaches to design spaces with unexpected sections that suggested initial design concepts and defined new spatial relationships. The process did not fully benefit from AI stage, since starting with CycleGANs remained vaguely suggestive for design initiation, i.e., later phases and tasks did not involve other AI models. Such an approach has also been found in existing research where AI is primarily used for representation and applied to one design aspect (floor plans, sections, facades). *Strategy 2 Results:* The AI exploration, with breeding computational and natural systems has led to the definition of a new language, a modified discrete assembly with higher complexity, which offers inspirational concepts of unpredicted spatial configurations and relationships (Fig.7). This workflow offered a new application of AI, to be integrated as an intermediate process for design revision of the computationally produced designs. AI intervened in the rule-based generated design process and allowed for parallel exploration, expanding the design search space. In this case, AI has allowed a translation from a strictly modular vocabulary to a more geometrically fluid system, using a CycleGAN network. *Strategy 3 Results:* The CycleGAN synthetic designs offered design revision concepts, suggesting an update in the section design, moving

away from the stacking effect resulting from the WFC algorithm to non-Euclidean possibilities that allow reciprocal visual connectivities in space (Fig.8). The StyleGAN model’s hyper-dimensional latent space allowed review and exploration of other design alternatives, behaving like an additional parametric environment where unlimited design alternatives can be examined. This experimental outcome offered insight into the necessity of considering connecting multiple AI models so that one model’s output can intentionally encode design intent into another model.

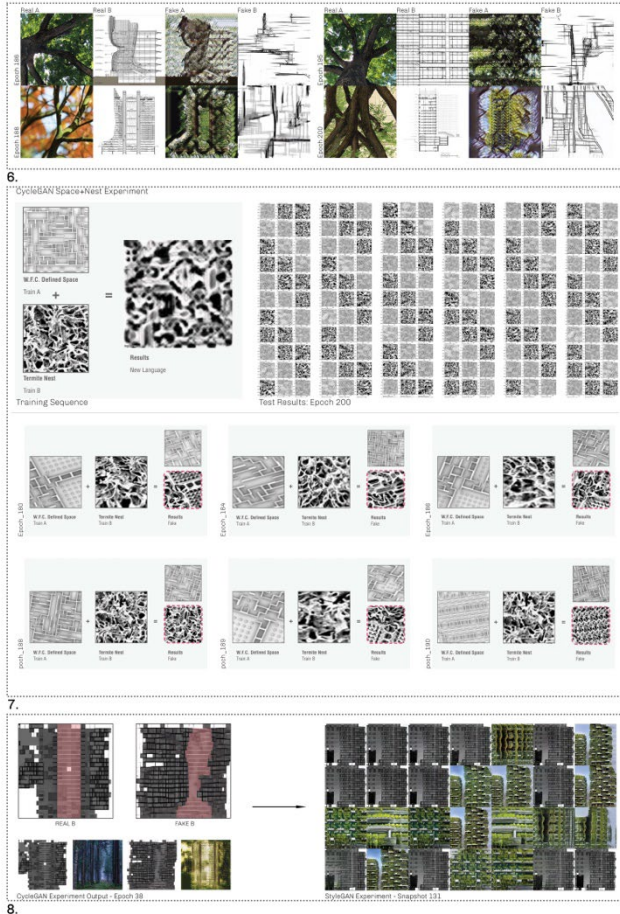


Figure 6. Strategy 1 CycleGAN model outputs. Design: K. Schilling, Y. Etielins

Figure 7. Strategy 2 CycleGAN output, breeding the WFC patterns (Domain A) and natural patterns (Domain B). Design: T. Taylor, C. Candelier

Figure 8. Left: output of the CycleGAN model of Strategy 3 breeding the WFC patterns (Domain A) and natural patterns (Domain B); Real and synthetic images of the trained StyleGAN model, in the latent space (Network Snapshot 131). Design: A. Milani, E. Alawadi

The students used a variety of tools and methods to investigate AI-assisted design workflows that support explorative search and design space expansion. Although different groups addressed the same design problem, they employed various

computational approaches, using the same tools for different reasons (i.e., geometry module distribution/propagation; pattern application) and in a different order. Some used AI before the WFC algorithm, and others began with ABM simulations. Overall, three distinct strategies were identified (S1: DL-WFC-ABM, S2: ABM-WFC-DL, S3: WFC-DL-DL, Fig.9). The relevance of the order of a given method depends on the reciprocity between these specific approaches and their usefulness for each other (input-output connection). It is especially important to outline the efficiency of certain methods only in relation to this order of execution. The exploration of all strategies tried to overcome the constraints imposed by generative design systems and their own rules and algorithms and expand the search space of possible solutions. Sometimes, if an exploration occurs in a local area of the design space, we may misinterpret neighbouring solutions as optimal (the most successful design candidate, aesthetically or performatively). Finding different ways to explore design space is important, to avoid getting stuck with locally optimal solutions and missing the global maxima/minima that may be located elsewhere in the design space.

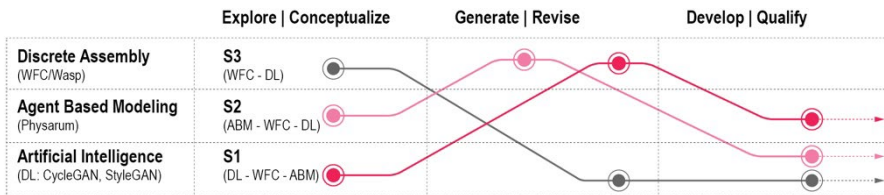


Figure 9. Workflow Strategies: Three main strategies were used by the students, each one combining computational tools in various order during the early, middle, and final stages of the design project. All strategies used at least one deep learning model for some part of the design.

6. Conclusions and Future Work

The incorporation of artificial intelligence into design in recent years foreshadows substantial impact on the overall design process, yet it is usually assessed as a singular tool/method. This paper examined the opportunities of innovative AI-assisted design workflows and their promise for refining current research-based pedagogy (SDG 9). This is an initial phase in a larger project about the efficient combination of AI with other computational tools based on their input requirements and degree of automation. Hybrid frameworks using generative adversarial networks (GANs) can augment design thinking, reaching into an expanded search space. The strategies discussed herewith allow reciprocal exchange between parametric models and AI models. Moving between rule-based generative algorithms and unsupervised deep learning models (CycleGAN, StyleGAN), designers can connect multiple computational models to search for "unexpected" design propositions. Our comparison of three strategies (Fig.9), has identified shortcomings and opportunities in specific combinations of neural networks before or after other tools, like ABM or WFC, depending on user experience and design intentionality. The evaluation of the resulting latent space (solution space) in StyleGAN using more than one domain, depends on understanding how the percentage of different domain samples in the dataset affects the domain "breeding" process, unlike CycleGAN, where equal domain input is used. CycleGAN is considered a good strategy for pursuing extrapolative creativity -finding

new ways beyond how human designers think, but still within the same general context/field (Hassabis, 2018). CycleGAN best serves scenarios where design intentions are already defined; in Strategy 1, CycleGAN was used early on-before certain parameters had been set, bringing forward limitations in dataset preparation (also due to students' inexperience with such tools). On the other hand, the StyleGAN network can be used as a heuristic tool at any stage, perfect for exploration that is a priori undetermined. Its architecture is suitable for interpolation (average or merging) between existing datasets (Hassabis, 2018), so this could serve as a starting point for inspiration within a design studio.

References

- Abraham, A. (2018). *The neuroscience of creativity*: Cambridge University Press.
- Alexander, C. (1968). Systems generating systems. *Architectural Design*, 38 (Dec.), 605-610.
- Bolojan, D. (2022). From Artificial to Architectural Intelligence. In N. Leach & M. del Campo (Eds.), *Machine Hallucinations: Architecture and Artificial Intelligence*: Wiley.
- Bolojan, D., & Vermisso, E. (2020). Deep Learning as heuristic approach for architectural concept generation. Paper presented at the *ICCC*.
- Chaillou, S. (2019a). *The advent of architectural AI*. Retrieved from towards data science <https://towardsdatascience.com/the-advent-of-architectural-ai-706046960140>.
- Chaillou, S. (2019b). *AI+ Architecture: Towards a New Approach*. Harvard University.
- Chen, J., & Stouffs, R. (2021). From Exploration to Interpretation-Adopting Deep Representation Learning Models to Latent Space Interpretation of Architectural Design Alternatives.
- Forbes, A. (2020). *Creative AI: From Expressive Mimicry to Critical Inquiry*. *Artnodes*, 26, 1-10.
- Gui, J., Sun, Z., Wen, Y., Tao, D., & Ye, J. (2020). A review on generative adversarial networks: Algorithms, theory, and applications. *arXiv preprint arXiv:2001.06937*.
- Harding, J., & Brandt-Olsen, C. (2018). Biomorpher: Interactive evolution for parametric design. *International Journal of Architectural Computing*, 16(2), 144-163.
- Hasey, M., Elliott, S., & Rhee, J. (2021). Archi_Base: Automated Dataset Construction of Architectural Imagery for Deep Neural Networks. Paper presented at the *CAAD Futures 2021*. https://github.com/michaelhasey/Archi_Base
- Hassabis, D. (Producer). (2018). Creativity and AI. *The Rothschild Foundation Lecture*.
- Koh, I. (2021). *AI Sampling*. Retrieved from <https://www.digitalfutures.world/workshops/91.html>
- Leach, N. (2021). *Architecture in the Age of Artificial Intelligence: An Introduction to AI for Architects*: Bloomsbury Visual Arts.
- Menges, A., & Ahlquist, S. (2011). *Computational design thinking: computation design thinking*: John Wiley & Sons.
- Mintrone, A., & Erioli, A. (2020). Cognizant Architecture - What If Buildings Could Think? Paper presented at the *eCAADe 2020, Anthropologic - Architecture and Fabrication in the cognitive age*.
- Mitchell, W. J. (1990). *The logic of architecture: Design, computation & cognition*: MIT press.
- Stocking, A. W. (2009). *Generative design is Changing the face of architecture*. Building Design. Retrieved from <https://www.cadalyst.com/cad/building-design/generative-design-is-changing-face-architecture-12948>
- Watanabe, M. (2004). *ALGORITHMIC DESIGN / INDUCTION DESIGN, Three Kinds of Flow / Three Stations. AI / AD / ID*. Retrieved from <https://www.makoto-architect.com/kashiwanohaCSt.htmlreferences>.

LEARNING TIMBER TECTONICS THROUGH DIGITAL COLLABORATION

NANCY CHENG¹ and MARIAPAOLA RIGGIO²

¹University of Oregon, ²Oregon State University.

¹nywc@uoregon.edu, 0000-0002-8112-4587

²mariapaola.riggio@oregonstate.edu, 0000-0002-9013-7304

Abstract. A dual university collaboration challenges students in architecture, wood science and engineering to partner on a timber design and detailing project. Five years of student projects reveal how the mix of backgrounds, design media abilities and design development process impact the learning experience. Team design submissions, individual reflections and observed collaboration activities were analysed along with patterns of design ideation, transformation, and conflict resolution. Learning experiences vary according to the mix of student backgrounds and roles within the team. Teams mixing students of different levels and backgrounds on average performed better than more homogenous teams. While beginners do not have the skills to play a central role in the team, they have the most to learn from more advanced students. Keeping all team members engaged may require giving up some efficiency of a streamlined digital workflow.

Keywords. Digital Collaboration; Architectural Education; Integrated Design; SDG 12; SDG17.

1. Introduction - training for 21st century collaborations

Timber design and construction has been evolving rapidly with technology affecting forest management, engineered materials, prefabrication, and construction automation. New digital workflows are being pioneered that extend from forest to factory, with 4D planning for construction and building management. This process requires agile technical skills to nimbly bridge between disciplinary and global boundaries, as in the United Nations Sustainable Development Goal (SDG) 17 Partnerships to achieve the goal (2021).

Digital collaboration skills are particularly crucial as the timber industry adopts prefabrication, integrated design and optimized construction processes that rely on robust Building Information Models (BIM). The European leanWOOD project identified factors including scarce IT-literacy and limited interoperability as hindering full technological adoption (le Roux et. al, 2016). Staub-French et. al. (2018) explains that for the growing mass timber industry, BIM needs to be consolidated with Design for Manufacturing and Assembly (DfMA) with data sharing across the supply chain. Digital component descriptions are crucial for efficient production and assembly of

standardized and customized components.

1.1. COURSE DESCRIPTION

To prepare a new generation for this quickly evolving environment, the Timber Tectonics in the Digital Age course immerses students into interdisciplinary partnerships to learn parametric design, structural analysis, and construction prototyping. The course is predicated on the belief that parametric design is best learned with simulation for design assessment and learning occurs most effectively through applied team design scenarios. The Timber Tectonics in the Digital Age course is jointly and concurrently taught to Architecture students at University of Oregon and Wood Science and Engineering students at Oregon State University. This paper describes how the course has evolved and lessons learned from five iterations of teaching digital workflows for AEC collaborations. The students work in cross-disciplinary small groups to design, detail and prototype a small structure.

The course introduces archetypal structural systems and how digital methods are facilitating innovation in structural efficiency. Historic and contemporary examples illustrate how timber forms and connections maximize the capabilities of the material. Students use Rhino Grasshopper and Karamba to generate geometric variations of structural systems and the effects of form transformation on structural behaviour. They are asked to apply the structural principles, material understanding and software skills in the context of a collaborative design challenge. In small groups, students brainstorm and find a design direction, and after then, identifying appropriate timber materials, they develop, detail and prototype assemblies of increasing scale, as allowed by wood shop access.

Our pedagogical approach is based on Bloom's Taxonomy (1956) that shows student learning retention is improved via active application of concepts in project-based learning, the heart of most design studios. The learning pyramid's hierarchy endorses that interacting with concepts, as occurs in team peer-teaching and negotiation, helps student retain skills and knowledge. We have been operating on these additional assumptions:

Experiential hands-on applied learning can help students understand structural principles, material properties, and digital/physical tool capabilities and limitations.

Students educated together about common content can apply this knowledge more smoothly in interdisciplinary teams due to shared vocabulary and greater interoperability.

Practice with collaboration tools will prepare students for future remote digital partnerships.

The design project's scale is small and program simple to keep the focus on tectonic design and construction. In the first three years, students designed a small pavilion for a campus location. For the fourth iteration, the Architecture course was changed from a seminar to a design studio to provide more time for project development and the design program was enlarged to a full community design. Students were asked to design housing for refugees from wildfires, houselessness, or political strife, with small self-build cabins and a long-span community centre. This allowed students to learn about trauma-informed design, site design and envelope detailing appropriate to SDG

11 Sustainable Cities and Communities (2021). Since the expanded scope also divided student energy across many issues, for the fifth iteration in 2021, the focus returned to a relatively small pavilion - a nomadic modular performance stage. The requirement for portability, ease of construction and deconstruction focused student energy into pre-fabrication and on-site assembly. The re-usability of a seasonal or event-based structure reinforces the SDG 12 Responsible Consumption and Production.

All versions of the course began with an introduction to the context and accelerated getting-to-know-you activities for quick team formation. Students interview each other with prompting questions and write simple profiles for a marketplace of partners. Students self-organize teams around the guideline to find complementary abilities.

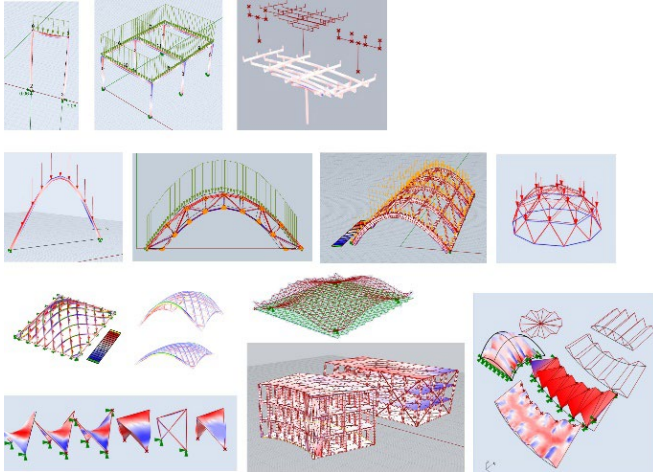


Figure 1. Students first learn about linear structural systems (top) and gradually work with funicular form-finding and more complex structures (bottom).

Students are introduced to structural systems that progress in complexity to correspond with the gradual development of parametric design skills as in Figure 1. This begins with structural systems made of linear elements: first section-active systems (columns, beams, and frames) and then vector-active systems (trusses and dendriform structures). Hands-on workshops teach Rhino navigation, vector drawing, Grasshopper parametric basics along with Karamba structural analysis. Beginners stay in 2D while the more advanced proceed quickly to 3D forms. Students can import geometry from other programs for analysis, albeit without fluid parametric adjustability.

After linear elements, planar elements are introduced, beginning with grids, plates, and folded plates. Once the students understand the operations of defining elements, supports, loads, cross-sections, joints, and material characteristics, they learn about Form-active systems (cables, arches, vaults, and domes) or Surface-active systems (shells and gridshells). At this point, students also learn how to use the parametric design tool for form-finding with buoyant forces. The students choose from these systems to develop their design project. External experts contribute guest lectures and review the projects three times during the term.

Course delivery began with two parallel Canvas sites and WebEx video conferencing in 2017. For Fall 2020, the fourth version of the course, lectures and tutorials were recorded to enable a flipped classroom format (Bishop et. al. 2013) that maximizes large and small group interaction over live Zoom connection. Microsoft Teams and Miro whiteboard were added to provide more immediate interaction and tracking of communication for both small groups and the entire blended class. Students from the two universities meet in person at the start of the course, for a first introduction and team building activity, and at the end for the final review,

Project quality is assessed on the following criteria:

Architectural design: Integrates the construction into a graceful, coherent form that meets all functional & site requirements. Explains the user experience.

Structural thinking: Optimal use of material and structural elements/systems, proven by structural models.

Digital methods: Shows the relationship between geometry and structural forces through design variants

Material understanding: Wood products are well-chosen according to properties such as mechanical properties, durability, and workability

Fabrication / Construction: Explains how components would be created, sourced and assembled. Describes the construction and deconstruction process. (Figure 2)

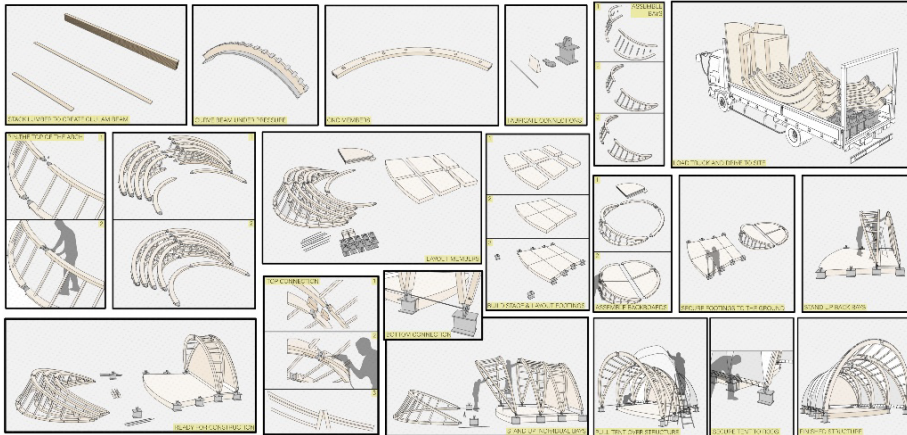


Figure 2. Storyboard shows processes of pre-fabrication and on-site construction

2. Methodology and prior analysis on interoperability and collaboration.

To identify ways to improve the course, we began this study by focusing on how interoperability, the ability to share data, correlates with a team's collaboration success attributes (Riggio and Cheng, 2021). Our qualitative methodology characterized each project according to collaboration indicators and interoperability achieved while also considering the major project drivers and types of design media used. For each project, we examined three successive rounds of student self-assessment reports and design presentations in order to assess and tabulate the qualitative attributes. We checked for

collaboration indicators (explained by Tran 2013, such as task coordination, effective assistance, constructive feedback and exploring different points of view) and student engagement via the written and graphic documents. Final project grades reveal the team's success in addressing course criteria. Main findings from this analysis:

Teams with strong interoperability were able to coordinate concurrent work and showed high coordination with equal sharing of work. Conversely, cases of poor interoperability were more frequently characterized by a sequential division of tasks and poorer coordination among team members. Individuals needed initial time for free exploration before finding a common design direction that allowed them to better coordinate tasks. While teams could try to assign roles at the beginning of a project, it took some time for them to develop a deeper understanding of each other's abilities and work styles (through both synchronous meetings and seeing team members' work). Once the design direction was established, teams found ways to work in a more coordinated, concurrent fashion, with or without data interoperability. Teams that were unable to seamlessly share 3D project data typically would export or reconstruct information with a loss of efficiency and/or consistency.

The initial design driver influenced whether the team's project development path was direct or convoluted. Those teams that started with a structural or construction concept could more efficiently and deliberately develop their project through material choices, component and connection choices and construction assembly sequencing. In contrast, those who generated their design project using a visual inspiration or design metaphor often would need several design revisions to find a constructable form.

3. Factors shaping the student learning experience

This paper builds on the methodological approach used in our prior study to focus on the range of student learning experiences. We examine the mix of student backgrounds and the number of designs schemes considered and expand the analysis from the first three iterations of the course to include the fourth and fifth versions which have the same learning objectives, albeit with amended course delivery mechanisms. We are interested in how a student learning experience is affected by 1) an individual's position in a team's mix of disciplines and seniority, 2) an individual's ability to share 3D project information and 3) incremental or radical design shifts.

3.1. TEAM MIX, COLLABORATION & INDIVIDUAL LEARNING

Teams have had three to five members, with students ranging from third year undergraduates to third year graduate students, from majors including Architecture, Civil Engineering, Wood Science and Engineering, Construction Management and Architectural Engineering. We rated the groups from 0 for completely homogenous to 3 for extremely varied. Figure 3 shows that on average, higher project quality correlates with students from more diverse academic levels and disciplines, but individual projects reveal that the student mix is neither necessary nor sufficient to guarantee success. Motivated students produced strong work in both homogenous and diverse groups.

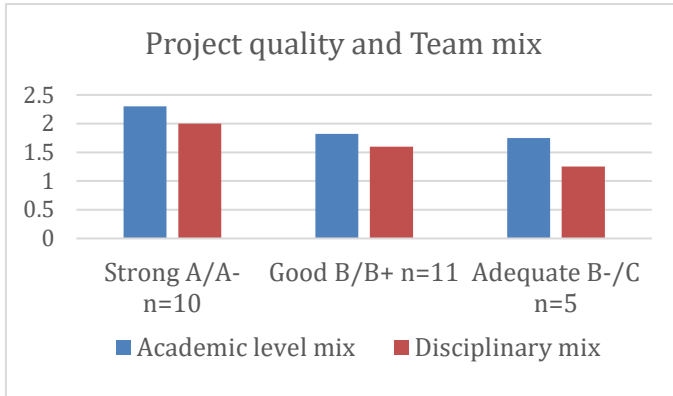


Figure 3. The projects earning higher grades generally had a wider range of student experience - both years in school and different majors.

In groups with a wide range of academic or professional experience, a natural leader often emerged, which helped in delegating tasks and negotiating design decisions. Consistent with Tucker and Reynolds 2014, groups without a senior member could become frustrated with the lack of hierarchy. A student said having equal status made it hard, that it was easier to make decisions when there is a boss. For this reason, in 2021, five Architecture post-professional graduate students who originally wanted to work together were grouped with less experienced students to spread their experience and reduce competition. Each one became a successful team leader.

Groups with students from different disciplines could more easily assign specialized complementary roles. Team members were more likely to stay engaged in non-overlapping tasks that required responsibility, provided autonomy, and gave a chance to shine. The digital whiteboard helped track task completion.

Within these groups, the students had varied learning outcomes. Given the robust course agenda, students specialized according to interests and prior knowledge. So often they learned one aspect deeply and gained awareness of aspects completed by others. While some of the strong projects came out of well-balanced collaborations, others came to a strong result due to one or two dominant members. In the first few years, those with the strongest Grasshopper-Karamba skills became the team leaders and others played more supporting roles. When team members were asked to rate the contributions of their small group members, there was often agreement about who contributed the most and who contributed the least, though they portrayed varying magnitudes of unequal contributions. While some team members resented having to shoulder more work than others, the asymmetry did not necessarily yield a weaker project outcome or poor learning for the less active member, consistent with Tucker and Rollo's observation of team design studios (2006).

In many cases, the students with less experience, who played supporting rather than leading roles, enjoyed working with agile, more experienced students. Even if it wasn't their own hands working on the computer or driving the CNC machine, they were able to observe the incremental development process up close and appreciated the substantial contributions of others. In contrast, two more experienced students reported

less satisfying learning experiences. When one of the more agile designers surprised team partners by presenting an individually developed design idea as the team design, the person reflected that "it felt like the fault fell on me for producing work 'too fast', but the other student was moving at a pace too slow for a studio course." While most of the students expressed gratitude for the opportunity to work in interdisciplinary groups, one grad student expressed that the teamwork was redundant with a prior professional office experience, echoing Tucker and Abassi's finding (2014) that mature students were less satisfied with the teamwork process than younger peers.

3.2. ABILITY TO SHARE 3D INFORMATION AND LEARNING

In a sense, the non-architecture students operated in foreign territory because the course is dominated by architectural software and by architectural education conventions such as graphic presentations, qualitative feedback, and integrated design. Some of the most effective groups found ways to shift the project to more familiar ground for the Wood Science and Engineering students, who commonly are responsible for identifying appropriate connection techniques or hardware. They have captured the imagination of classmates when they have additionally performed structural testing on wood samples, such as measuring the bending ability of wood laths or taken the lead on prototyping.

Similarly, structural engineering students have flourished when they could perform either SAP2000 or hand calculations that inform the process. While taking the model out of Grasshopper breaks the parametric interoperability, the activity boosts the collaboration and has not impeded much of the workflow (Figure 4). Students see the value of the parametric adjustability in conceptual design; exporting to other platforms can efficiently support a more detailed analysis once the design is set.

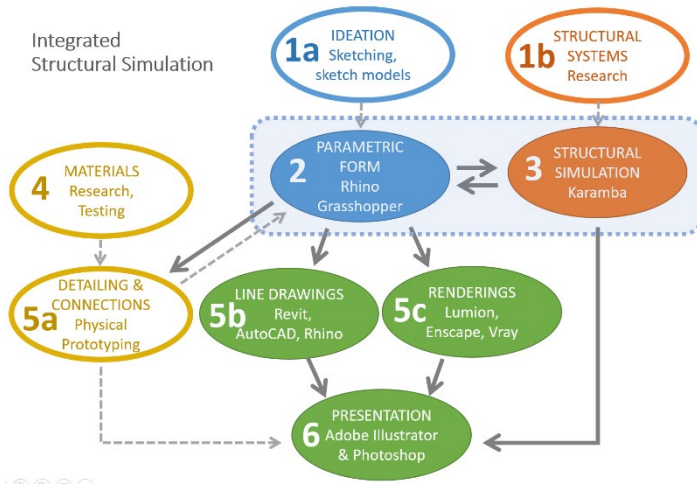


Figure 4. Exporting the model for analysis breaks the quick feedback cycle but could enable engineers to flourish. Filled shapes represent the digital workflow, outlined can be independent.

The ability to describe and share information is key to being an active design participant. In the first ideation phase, students who can show their ideas through sketching, cardboard or digital models can engage peers and invite further

development. Those without visualization abilities must use words and visual examples. As the team considers parametric variations and structural stability, students who are most adept with the software often assume a leadership role. To have a voice, students must be able to interact with 3D information. Those who lack data sharing skills can only act as consultants or helpers, as they must work with a static snapshot rather than driving the active model. Well-organized teams can separate tasks, such as creating an abstract line model for structural analysis vs. a robust model for physical prototyping and visualisation. Less experienced students have provided valuable support through researching structural, material and construction options. With peer guidance, they can develop subassemblies and contribute graphics.

3.3. INCREMENTAL OR RADICAL DESIGN SHIFTS AND LEARNING

Groups that take a more circuitous route to the final design project have to consider a wider range of structural and construction issues, while those who initially have a viable scheme instead focus on subtle refinements. Students with experienced team members often started with a strong idea based on a structural system that they could efficiently develop and detail. In their incremental process, they do not experience as full a range of parametric exploration as those who have more false starts. Those students taking a more indirect path have to consider, discuss, and evaluate alternative design options as in Figure 5. This aligns with Emam et. al. (2019, p. 164) view that collaborative design is effective for learning because students need to find a direction through team discussion and active negotiation.

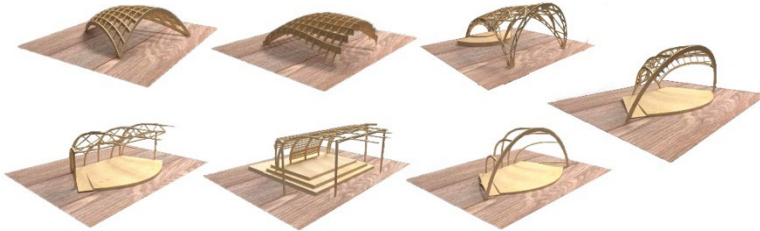


Figure 5. This team generated a sequence of options for the modular stage and had to deliberate about each one's structural stability and aesthetic expressiveness. Final is on the right.

4. Challenges and Attempted Remedies

Unequal playing field: A major challenge is how to have parity between students of different backgrounds as less experienced students can feel overwhelmed or disenfranchised. For example, our architectural engineering, civil engineering, and construction management students enter the course without experience in Rhino Grasshopper, while architecture students have earlier initial exposure. Architecture students generally take the lead as the engineers want a definite form before starting structural analysis, even though we encourage bottom-up thinking about materials, structural systems, and modular constructions. One student offered a possible remedy to how the course caters to architecture students, "Maybe engineering students should be introduced later in the term.... I feel like that is more realistic in the process of a real project.... Maybe during the time period [architecture] students are designing, other

students [could be] properly taught how to use Rhino and Grasshopper."

Differential class meeting times means imbalanced participation: As in any collaboration, differences in disciplinary conventions must be bridged. An unforeseen consequence of moving to the design studio class for the Architecture students has been to greatly imbalance the amount of participation for the two universities: While the Architecture students spend 12-hours per week in class for six-credits, the Wood Science and Engineering students only spend 5-hours per week for four credits. The synchronous videoconference was typically split between large group activities and small group collaboration time with roving instructor conferences. While this schedule provided a predictable rhythm to the class, it precluded extended discussions or workshop sessions. As a remedy in future years, it may be possible to offer a studio course for more credits to the Architectural Engineering students to give them more parity and provide more intensive software training.

Challenges with remote communication tools: Students eagerly engaged multiple digital communication platforms during Fall 2020, the first year of the pandemic. An MS Teams forum called "Ask an Expert" fostered lively discussion between students, reflecting their interests and importantly provided a chance for Wood Science and Engineering students to shine. On returning to campus in Fall 2021, complaints about the proliferation of platforms arose as students expressed confusion over where to look for course information or feedback. It arose because students seeing each other face-to-face did not use MS Teams' mobile chat function and they preferred to set up private team chats without tutors. For the next round, expanded communication capabilities in Miro whiteboard could allow elimination of MS Teams.

The live Zoom video conference in class proved to be effective for instructor-to-class interactions, and it created audio problems when multiple groups in one room connected with different remote teammates. We improved these small group meetings, by splitting teams into multiple rooms, with some individuals joining remotely.

To foster better partnerships, we have increased teaching about the collaboration process with help from business school specialists. Students generally begin eager to meet from other majors. Then teams needed to work through different expectations, conceptual frameworks, work styles and vocabulary. To support agile team interaction, we added a workshop on project management and another on negotiation styles and strategies. The utility of the workshops depends on their timing within the team development process. For example, the teams were receptive to developing plans and roles according to the project management workshop guidelines. By the time the second negotiation workshop was held, students were less engaged. A student explained that they had already figured out approaches to conflict resolution. Students receive teamwork training information differently, according to their prior experiences.

5. Lessons learned

Five iterations of this course teaching integrated timber design have indicated that it has fostered awareness and appreciation of disciplinary perspectives and collaboration, and challenges to interdisciplinary learning still exist. Notably, the pervasive use of digital tools as part of the learning objectives and for the content delivery and collaboration has introduced some difficulties, such as unequal skill preparation for the

digital design process, redundancy of communication platforms and “digital burnout” i.e. Zoom fatigue. Furthermore, pedagogical, programmatic, and logistic constraints pose challenges in the development of interdisciplinary, inter-institutional courses (e.g., access to remote resources and spaces, class schedules, administrative obstacles).

Nonetheless, this course demonstrates the impact of experiential learning in the development of soft skills highly desired by employers. Our study shows that vertically integrated teams provide leadership opportunities for the more experienced and give beginners a crash course in design processes. Even those who lacked software agility or had a circuitous project development experienced a valuable immersion into digital collaboration and peer-to-peer learning. The majority were able to find a useful role, create productive working relationships and ended the term proud of the team output. The microcosms of the student interdisciplinary groups show that teamwork must be carefully planned to fully engage all capabilities into interdisciplinary collaborations.

References

- Bishop, J., & Verleger, M. A. (2013). *The Flipped Classroom: A Survey of the Research in 2013 ASEE Annual Conference & Exposition*, Atlanta, Georgia. 10.18260/1-2--22585
- Bloom, B. S. et.al. (1956). *Taxonomy of Educational Objectives, Book 1: Cognitive Domain*, David McKay Company.
- Emam, M., Taha, D., & ElSayad, Z. (2019). *Collaborative pedagogy in architectural design studio: A case study in applying collaborative design*. *Alexandria Engineering Journal*, 58(1), 163-170. <https://doi.org/10.1016/j.aej.2018.03.005>.
- Le Roux, S., Bannier, F., Bossanne, E., & Stieglmeier, M. (2016). Investigating the interaction of building information modelling and lean construction in the timber industry. In *Proceedings of the World Conference on Timber Engineering*, Vienna, Austria (pp. 22–25), 2016.
- Staub-French, S., Poirier, E.A., Calderon, F., Chikhi, I., Zadeh, P.D., & Huang, S. (2018). *Building Information Modeling (BIM) and Design for Manufacturing and Assembly (DfMA) for Mass Timber Construction*; BIM TOPiCS Research Lab University of British Columbia.
- Riggio, M., & Cheng, N. (2021). Computation and Learning Partnerships: Lessons from Wood Architecture, Engineering, and Construction Integration. *Education Sciences*, 11(3), 124.
- Tran, V.D. (2013). Theoretical Perspectives Underlying the Application of Cooperative Learning in Classrooms. *International Journal of Higher Education*. 2(3), 102-115. doi:10.5430/ijhe.v2n4p101
- Tucker, R., Abbasi, N. (2014): The architecture of teamwork: examining relationships between teaching, assessment, student learning and satisfaction with creative design outcomes, *Architectural Engineering and Design Management*, DOI: 10.1080/17452007.2014.927750
- Tucker, R., Rollo, J. (2006). Teaching and Learning in Collaborative Group Design Projects. *Architectural Engineering and Design Management*, 2 (1-2),19-30.
- Tucker, R., Reynolds, C. (2006) The Impact of Teaching Models, Group Structures and Assessment Modes on Cooperative Learning in the Student Design Studio. *Journal for Education in the Built Environment*. 1(2). 39-56

LEARNING FROM LOGS

Introductory Analog and Digital Pedagogy Addressing Material Irregularity

KYLE SCHUMANN¹

¹*University of Virginia / After Architecture.*

¹*schumann@virginia.edu, 0000-0002-0619-0541*

Abstract. Advanced computational visioning, modeling and fabrication technologies are becoming increasingly accessible to non-expert users, allowing designers to engage complex forms and materials with increasing control and precision. Nonetheless, beginning designers often struggle to maintain authorship when mastering new software, resulting in designs shaped by the biases of the digital tools at hand. The act of translation between physical and digital poses particular difficulty. This paper presents a sequential pedagogy in which students are introduced to both manual and digital analytical and fabrication processes with the goal of understanding, analyzing, and addressing material irregularity. Techniques and tools employed include digital modeling in Rhinoceros, 3D scanning, computational analysis in Grasshopper, traditional woodshop tools, 3D printing, laser cutting, and CNC routing. The outcomes and criteria for evaluating student projects are discussed: in particular, the learning opportunities afforded by using irregularly sized and shaped material that allowed students to develop creative ways of working with standard woodworking and digital fabrication tools. Additional challenges due to virtual teaching and financial considerations are addressed through salvaged materials and democratized technologies.

Keywords. Digital Pedagogy; Democratized Technology; Digital Fabrication; Computation; Material Irregularity; SDG 4; SDG 13; SDG 12.

1. Introduction

This paper presents a sequence of introductory pedagogical exercises prescribed to undergraduate architecture students aimed at rapid skill development in analog and digital workflows. With a focus on analysis and translation, the methods preference accessibility and democratization by using industry standard tools and consumer-grade software and minimizing material cost. Irregular material, harvested from fallen trees on campus, functions as a complex generator containing information on form, age, structure, texture, and more (Carpo 2017).



Figure 1. Completed student projects

The students are enrolled in the third year of a non-professional, undergraduate, four-year architecture program. The students were previously introduced to woodshop tools in their first year, but due to the COVID-19 pandemic and a shift to virtual learning, time had elapsed since these means of production were engaged. This sequence of assignments served to reintroduce students to these tools and forge a link between analog and digital fabrication through the introduction of advanced computational tools. In particular, the relationship between digital and physical is investigated within a rapidly developing scholarly area in which digital design processes optimize natural form in varying capacities. Many of the processes introduced and skills developed in this set of exercises were applied to longer-term fabrication projects later in the semester.

2. Methods

The pedagogy consists of four exercises that sequentially introduce manual and computational skills through four phases: manual analysis, manual fabrication, digital analysis, and digital fabrication. Emphasis is placed on translating knowledge and understanding between analog and digital workflows and developing strategies for utilizing irregular natural materials that are both scalable and translatable to other geometries and assemblies.

Each student is provided an approximately rectilinear fragment of wood prepared for them prior to the semester in the following manner: wood is rough sawn with a chainsaw to measure six inches deep by a variable width and height, containing a partial void and exposed live edges that retain and display natural irregularities. The wood is salvaged from campus landscaping waste and provided at no charge to students. As such, each wood fragment is of a different age, state of decay, and moisture content. Wood is not dried prior to use, providing opportunities and challenges to engage with a material that will move, warp, and crack — a challenge that some students took on as an opportunity to respond to material behavior.

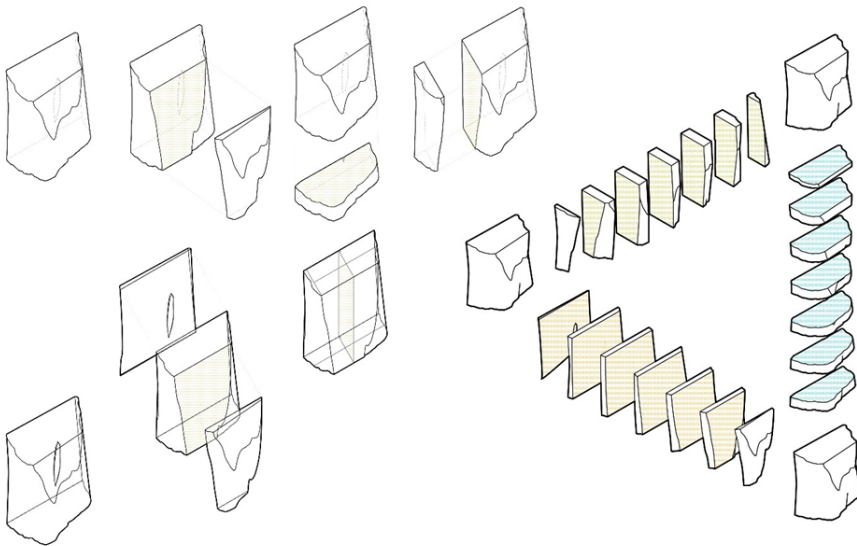


Figure 2. Analytical drawings from manually constructed digital model. Work by Audrey Lewis

2.1. MANUAL ANALYSIS

Each student develops a comprehensive understanding of the wood piece by manually measuring and digitally reconstructing the object as a model in Rhinoceros and a set of axonometric drawings (Figure 2). This process serves to equip students with a baseline set of skills, as many began the project without experience taking precise measurements or in digitally modeling complex surfaces. Commands such as loft, sweep, and boolean operations become a part of the students' modeling vocabulary.

Building on their digital models, students produce a series of axonometric drawings describing physical qualities of the material – geometry, form, texture, etc. These drawings prime students to interpolate characteristics of the organism from which the material was harvested through the production of a subsequent drawing which projects the form of the tree and location from which the material was harvested. A model-to-drawing workflow is implemented across the class in which base drawings extracted from Rhinoceros are completed and assigned lineweights in AutoCAD.

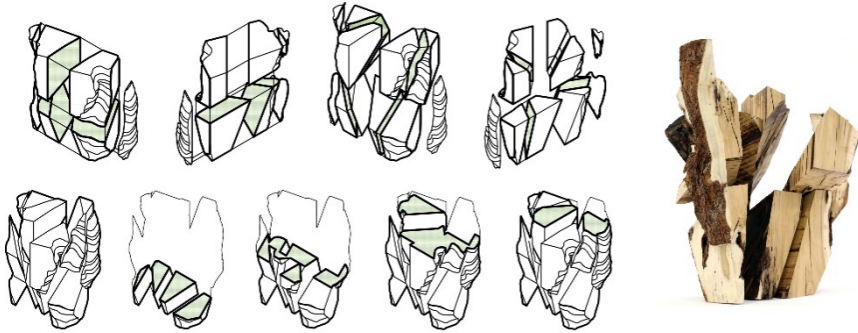


Figure 3. Operations are planned digitally and then executed manually. Work by Turner DeShon

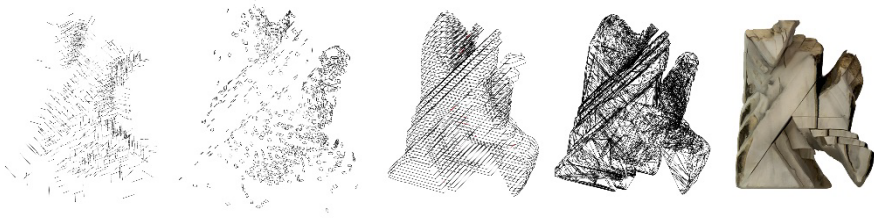


Figure 4. Digital analysis (left) generated from 3D scan mesh data (right). Work by Mak Johansen

2.2. MANUAL FABRICATION

Students are provided a set of operational rules aimed at eliciting a clear formal organizational system: (1) cuts must (a) be straight or angular but not curved, (b) be visible on at least three faces, and (c) result in a single object; (2) glue is allowed but hardware is not; (3) a maximum of one-quarter of the material can be removed. Beginning from their digital models and drawings, students digitally develop operations and then enact them physically in the fabrication lab using analog woodworking tools (Figure 3).

Students receive training on a series of woodworking tools including a planer, jointer, table saw, band saw, miter saw, drill press, and disc and belt sanders. The first step is to square several faces of their material, after which various designed operations can be executed accurately. When employing these tools with their material, students must overcome several challenges stemming from the size and irregular form of the wood. Creative solutions must be developed, including building custom jigs to accurately position and cut material that has several non-planar sides.

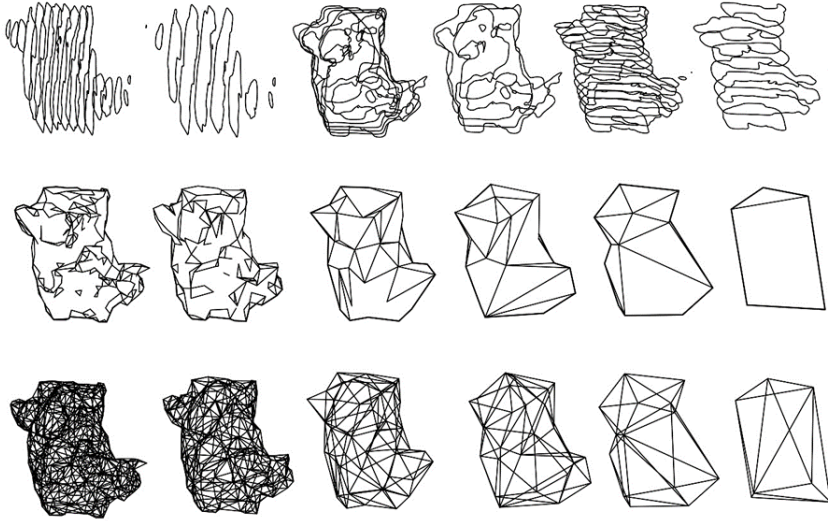


Figure 5. Distillation methods to extract specific qualities or geometries. Work by Abbie Weissman

2.3. DIGITAL ANALYSIS

The transformed material is 3D scanned using a consumer-grade smartphone app (www.qclone.pro) to produce a digital doppelganger which can be compared to the manually constructed digital model. This new model is analyzed computationally in Grasshopper and translated into a series of axonometric diagrams (Figure 4). Focus is placed on understanding and responding to the natural irregularities of the material and how these irregularities relate to the prior operations (Figure 5).

Students are provided with a series of example Grasshopper scripts that each distill data from the 3D scan to extract a certain quality from the object: sorting mesh faces by size and orientation, tracing sharp edges by measuring angles between faces, generating contours and measuring curvature, identifying light and dark zones using mesh vertex colors, etc. (MacDonald and Schumann 2021). The scripts are further developed and customized by the students based on their design intent and material irregularity. This step proved to be the most challenging overall, with students often needing to be individually led through how to develop their script to achieve the desired analysis.

2.4. DIGITAL FABRICATION

Students are introduced to three digital fabrication processes: CNC milling, laser cutting, and 3D printing, through comprehensive recorded videos followed by in-person tutorials. Students develop a second set of operations to perform on their material that deploys one or more of these techniques in response to a material irregularity that was identified computationally in the previous step. A secondary material is incorporated to engage with the pre-existing material (Oyler Wu Collaborative 2021).

A system diagram is constructed to articulate the relationships between design intent, material qualities, computational analysis, and fabrication processes (Figure 6). The system diagram is a critical step in the final part of the sequence, as it creates a platform for the students to synthesize ideas developed throughout and articulate a model of shared authorship between designer and material, mediated by computationally driven analysis.

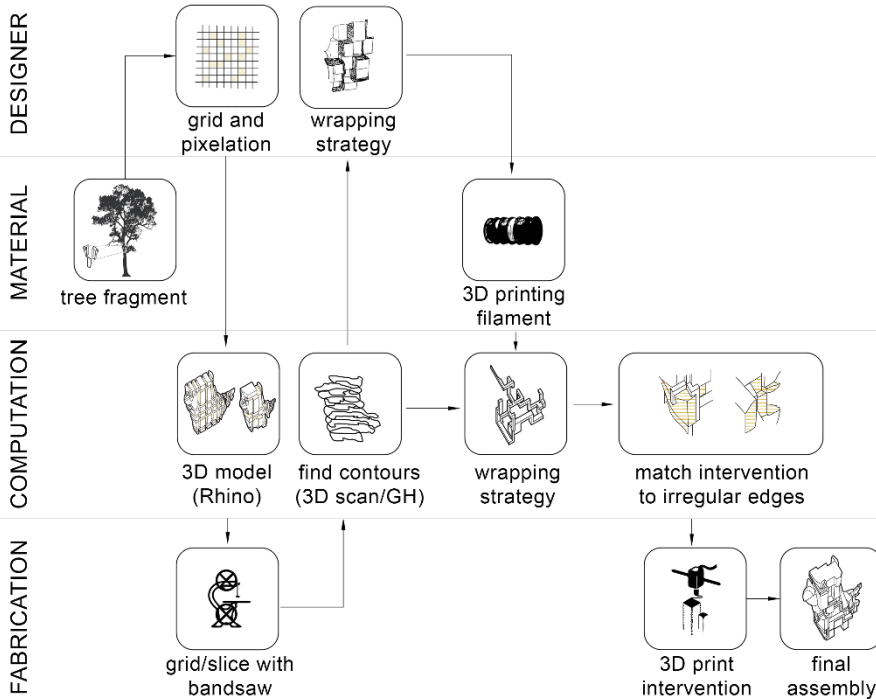


Figure 6. System diagram choreographing design intent, material qualities, computational analysis, and fabrication processes. Work by Abbie Weissman

3. Results

Following the sequence, students gained foundational skills in digital modeling, woodworking, 3D scanning, Grasshopper scripting, and at least one digital fabrication process, as well as an advanced understanding of tools and processes allowing for close engagement with material irregularity.

Providing free salvaged material to students removed financial barriers, allowing all students to begin the project with the same assets, creating an equitable learning environment. Providing students with pre-recorded training videos on equipment and example Grasshopper scripts served to expedite skill building but following up with hands-on training with tools and individual aid in developing scripts proved necessary. This was due in part to the nature of the operations needed, which often required Grasshopper plugins with which the students were unfamiliar. These included Firefly

to analyze and trace 2D images, Weaverbird to process and extract data from 3D meshes, and LunchBox to reduce mesh complexity in terms of face count.



Figure 7. Comparing 3D scans (above) and physical material (below). Work by Abbie Weissman

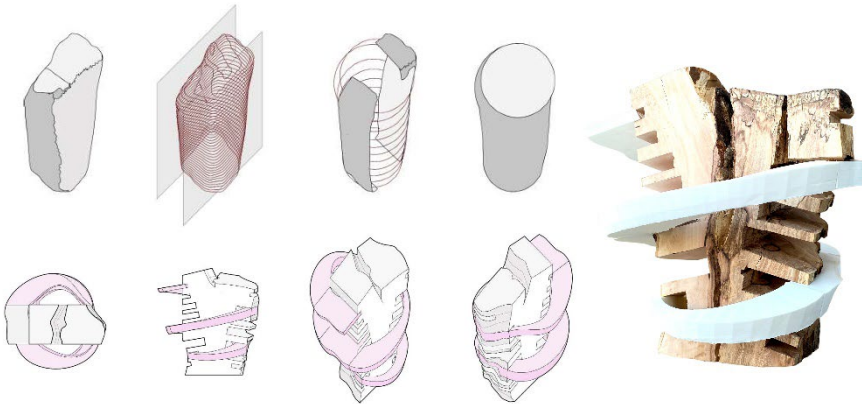


Figure 8. Reconstructing trunk volume by interpolating 3D scanned bark. Work by Daisy Wegener

Projects were evaluated based on ability of the work to convey, emphasize, or respond to material irregularity, its general formal and aesthetic interest, and the level of skill or craft in the physical execution of the work. The most novel projects precisely responded to specific material irregularities in a way that is clearly legible to the viewer. Various methods were implemented, including 3D scanning and distilling to extract critical data, and analyzing 2D images with edge detection. Students are equipped with

conceptual and technical understandings of how material irregularities can be understood and processed computationally, preparing them to participate in contemporary advances using computation to advance sustainable fabrication (Self and Vercruyse 2017; Larsen and Aagaard 2019; Johns and Foley 2014; Bechert et al. 2021; Saslawsky et al. 2021).

The success of the project was also evaluated on how well it prepared students for their work over the rest of the semester. Following this sequence, students worked in groups to develop and construct full-scale site-specific installations on campus, using novel wood fabrication strategies. Many students were able to take skills and approaches applied in the described sequence and translate and scale them to larger applications and complex assemblies. This included translating woodworking and digital modeling skills to other fabrication tools, including a CNC waterjet and a mobile sawmill.



Figure 9. Using edge detection to locate cracks and mill wedges. Work by Stuart Ingram

4. Conclusion

One of the largest challenges in implementing this pedagogy was that of working mostly remotely during the COVID-19 pandemic. Students had access to fabrication shop resources throughout the semester, but course meetings were conducted online, and students were often developing work digitally at home while their physical materials were located at school. In future iterations of the course, it is anticipated that the ability to conduct digital work while in the presence of the physical material will allow for an even closer relationship between design intent and material irregularity from direct and constant observation of the physical material.

The challenge of virtual teaching and the need for students to isolate due to the pandemic meant the project timeline was extended past the originally planned dates. Without these issues in the future, it is anticipated that the sequence can be completed over four to five weeks from start to finish. This will allow one week each for manual analysis, manual fabrication, and digital analysis, and one to two weeks for digital fabrication, due to the extended learning curve and machine times necessary on these tools. Each step is introduced independently, but some steps can be introduced on a Friday while the prior is due the following Monday. This slight overlap will allow students some flexibility with their own schedules and allow an extra weekend during which fabrication tools can be accessed to complete any particular phase of the project.

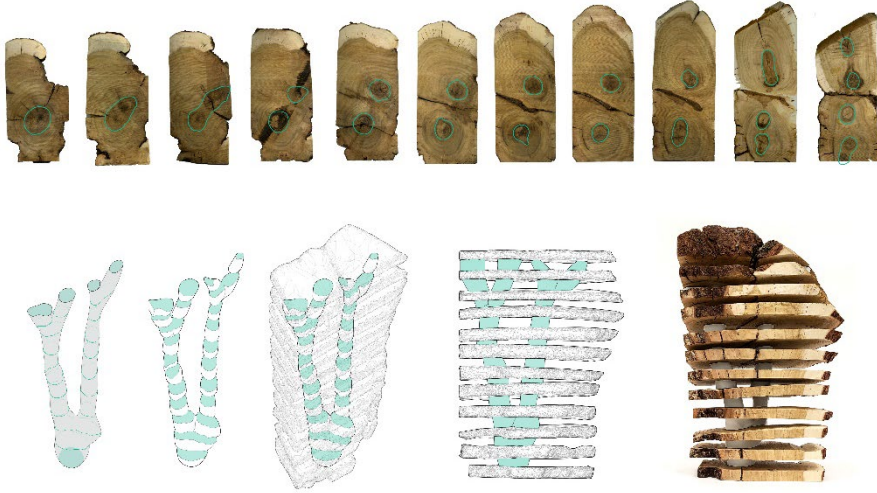


Figure 10. Analyzing 2D images of wood slabs to identify and interpolate heartwood form. Work by Jacob McLaughlin

Another challenge came from the material itself. Since the wood was not dried prior to use, several pieces warped or split throughout the project. Some students viewed this as an opportunity, developing projects that identified these regions with edge detection and operated upon them through digital fabrication methods. This strategy was aimed at materially programming certain behaviors into the wood such that natural distortions were enhanced, exaggerated, or otherwise shaped as the material aged or dried. This built an understanding that while the digital model is fixed, the physical artifact is not static and is subject to transformation as it ages and reacts to various environmental conditions.

The irregular size and shape of the material served to provide some of the most productive learning opportunities for students. The need to develop custom jigs for cutting the material precisely with various saws, a drill press, and a CNC mill demonstrated a contrast between the ease of digital modeling and the realities of physical fabrication. Students were encouraged to develop ways of inventively using the tools at their disposal while still doing so safely, which led to more creative freedom in the fabrication projects that followed. This approach reasserts the authorship of the designer relative to digital tools and analog craft, encouraging students to use tools creatively to realize their designs, rather than altering their designs to fit the available tools. Teaching such approaches through this pedagogical sequence has the potential to build knowledge in advanced fabrication and computation studios and courses prior to embarking on larger and more complex projects, but also to embed an adaptive and fluid understanding of the relationship between analog and digital tools and workflows into introductory design courses.

Acknowledgements

The work presented was conducted as part of the 'Material Cybernetics' studio taught

by the author at the University of Virginia. The author would like to thank the students for their dedicated efforts in advancing the work: Andrea Alfaro, Carolena Bastiaan Beatley, Jude Carver-Kay, Katie Debbas, Turner DeShon, Brandon Eley, Abby Hassell, Stuart Ingram, Aryana Jimenez, Mak Johansen, Audrey Lewis, Jacob McLaughlin, Logan Parham, Ana Cristina Pino Cucalon, Rohan Singh, Cate Southwell, Audrey Watson, Daisy Wegener, Abbie Weissman, and Annabelle Woodcock, as well as student instructor assistants Adam Johnson and Evan Sparkman. Thank you to Ila Berman, Dean of the School of Architecture, for supporting the course with material funding, and to UVA Sawmilling for providing raw materials.

References

- Bechert, S., Aldinger, L., Wood, D., Knippers, J., & Menges, A. (2021). Urbach Tower: Integrative structural design of a lightweight structure made of self-shaped curved cross-laminated timber. Gardner, L. et al. (Eds.), *Structures*, 33, 3667-3681.
- Carpó, M. (2013). Twenty Years of Digital Design. In *The Digital Turn in Architecture 1992-2012* (pp. 8-14). John Wiley & Sons Ltd.
- Carpó, M. (2017). The New Science of Form-Searching. In *The Second Digital Turn: Design Beyond Intelligence* (pp. 40-55). MIT Press.
- Johns, R.L. & Foley, N. (2014). Bandsawn Bands: Feature-Based Design and Fabrication of Nested Freeform Surfaces in Wood. In McGee, W. & Ponce de Leon, M. (Eds.), *Robotic Fabrication in Architecture, Art and Design* (pp. 17-32). Springer.
- Larsen, N.M. & Aagaard, A.K. (2019). Exploring Natural Wood: A workflow for using non-uniform sawlogs in digital design and fabrication. In Bieg, K., Briscoe, D., & Odum, C. (Eds.), *Ubiquity and Autonomy: Proceedings of the 39th Annual Conference of the Association for Computer Aided Design in Architecture* (pp. 500-509) The Association for Computer Aided Design in Architecture (ACADIA).
- MacDonald, K. & Schumann, K. (2021). Twinned Assemblage: Curating and Distilling Digital Doppelgangers. In *Projections: Proceedings of the 26th International Conference of the Association for Computer-Aided Architectural Design Research in Asia* (pp. 693-702) The Association for Computer-Aided Architectural Design Research in Asia (CAADRIA).
- Martin, S., & Vercruyse, E. (2017). Infinite Variations, Radical Strategies. In Menges, A., Sheil, B., Glynn, R., & Skavara, M. (Eds.), *Fabricate: Rethinking Design and Construction* (pp. 30-35). UCL Press.
- Oyler Wu Collaborative. (2021). *Active Inlay Studies*. Retrieved November 23, 2021, from <https://www.oylerwu.com/info-active-inlay-studies>.
- Saslowsky, K., Sanford, T., MacDonald, K. & Schumann, K. (2021). Branching Inventory: Democratized Fabrication of Available Stock. In *Projections: Proceedings of the 26th International Conference of the Association for Computer-Aided Architectural Design Research in Asia* (pp. 513-522) The Association for Computer-Aided Architectural Design Research in Asia (CAADRIA).

OPTIMIZATION OF PARTITION WALL INFILLED PATTERN FOR MINIMIZING CARBON FOOTPRINT

A method that integrates parametric design interface with FEM analysis engine

HANMO WANG¹, ABHIMANYU GOEL² and ALEXANDER LIN³

^{1,2,3}*National University of Singapore, Singapore.*

¹*hanmo@u.nus.edu, 0000-0001-6856-3705*

²*ar.abhimanyugoel@gmail.com, 0000-0001-8908-9715*

³*bdgal@nus.edu.sg, 0000-0002-3773-7503*

Abstract. The term “biomimicry” has been discussed and studied for a long time in the research field. A triply minimal surface geometry called gyroid was found to have the potential to present lightweight but solid structures and possess good thermal insulation properties, thus possibly minimizing the carbon footprints during both building construction and operation stages. Therefore, this paper will deliver research on the physical properties of the gyroid structure at different scales and explore the feasibility of scaling microstructure onto a partition wall system, which seeks opportunities to set up an efficient connection between parametric modelling and finite element engine. The integration work allows evaluating the performance of the gyroid structure with various variables as the wall infillings, which supplies the critical information and assist the engineers in figuring out the ideal design candidates at a given condition. This workflow requires a parametric approach including Rhino and Grasshopper, a finite element analysis tool ANSYS APDL (ANSYS Parametric Design Language), and Excel to save the essential data for further use. This project studies the suitable scales of the selected gyroid structure and the technical details on the interoperability between the parametrical system and the structure analysis engine for performance-based optimization. The expected outcome is to provide a tool that assists designers in optimizing the building components at the early stage and finally enrich the methods of computer-aided design.

Keywords. Low-carbon Solution; Bio-inspired Solution; Design Simulation; FEA Method; Design Optimization; SDG 12; SDG 13.

1. Introduction

The term "biomimicry" has been used as a model in architectural design to guide and induce sustainability (Gamage and Hyde, 2012), which has been widely used to learn

the various abilities of biology, study their mechanism of action, as a way to carry out technical design, to improve existing or create new mechanical systems, instruments, and equipment, building structures and technological processes. Inspired by graphene materials, researchers at MIT developed a new triply minimal surface structure called “Gyroid.” In their findings, this new structure has exceptionally high strength at a relatively high density based on the 3D graphene assembly, for which it has a density of 4.6% that of mild steel and is ten times as strong as mild steel (Zhao et al., 2017). Gyroid concrete is not only ultra-strong and lightweight but also has been experimentally proven to be insulated against heat (Piccioni et al., 2020), which makes it huge potential in building material and construction to minimize the emissions of both building construction and operation stages. As the construction technique evolves, the additive manufacturing technique has become an efficient tool for generating geometry-complex structures such as gyroid. Although advanced manufacturing technology has laid a solid foundation for transferring the bio-inspired pattern onto the building components, the lack of proper knowledge of the material’s properties and the absence of appropriate simulation engines and building codes is still hindering the successful implementation of bio-inspired texture in building components.

One of the critical issues is the lack of an efficient linkage between the parametric modeling interface and corresponsive software for simulation, which separates the design and simulation work rather than integrates them. Some plugins based on finite element methods are available in parametric software like Rhino and Grasshopper. Still, the existing tools are designed explicitly for large-scale structures like beams, shells, etc. Besides, for evaluating the 3D heat transfer performance of the customized 3D model, there are no available plugins inside the parametric software. Therefore, to design and select the preferred infill pattern for further manufacturing, it is significant to set up a direct connection between the parametric software and the finite element analysis simulation engine. In this paper, we will explore the carbon emission capability of the partition wall system with the customized infill gyroid pattern by establishing and testing a linkage between parametric modelling and the finite element engine. Lastly, this research is a proof of concept for a multi-phase optimization scheme to design bio-inspired building components. The next stage will discuss a mature fabrication and construction for deploying this structure.

2. Main Workflow

This part will give a detailed illustration in constructing the basic gyroid model, writing the prepared text file of boundary conditions, interlinking the modelling interface with the simulation platform, and ultimately conducting the optimization and selection work based on the simulation results. A brief workflow is shown as a diagram below in Figure 1. The simulation engine in this project is ANSYS APDL based on finite element analysis (Thompson et al., 2017), which is well recognized in the academic filed and widely used in various industrial domains. The programming language Gh Python that is inbuilt within the parametric interface is as stable as the other languages such as Java, C++, and etc, which is able to pass and transport the essential information between ANSYS APDL and Rhino/Grasshopper.

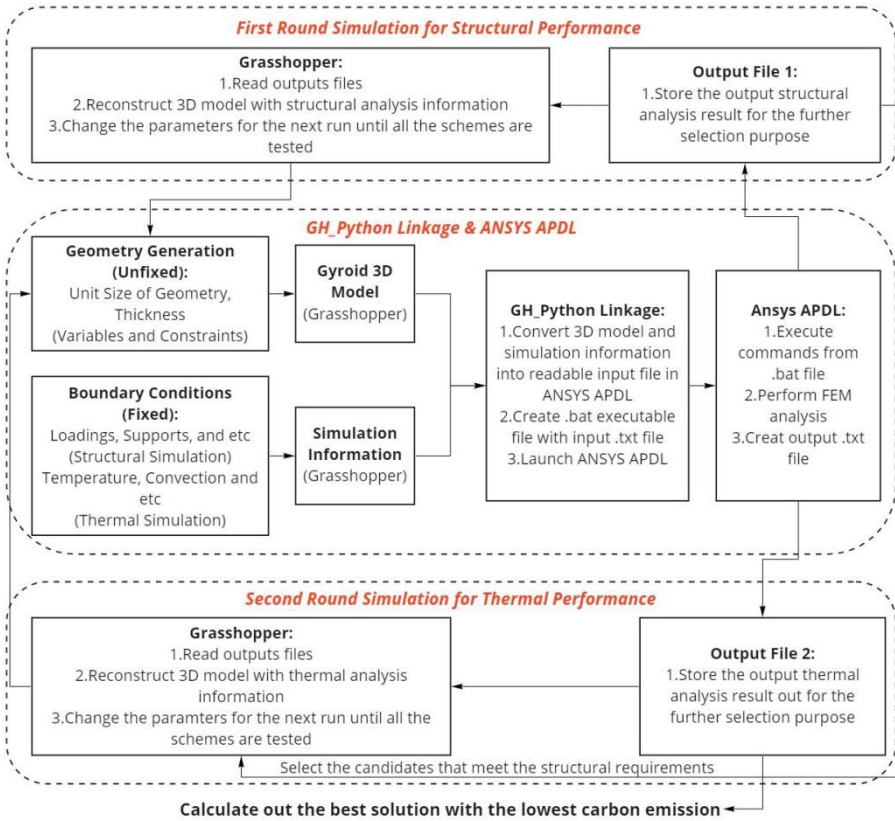


Figure 1. An image with a caption (Resource: author)

At the beginning, the 3D gyroid model is defined by several design variables, which are decided by the constraints in real applications. The prepared 3D model and the coded boundary condition files are sent to ANSYS APDL for analysis using Grasshopper Python as the linkage. When the simulation is finished in ANSYS APDL, the results are saved as text files and read in Rhino and Grasshopper for visualization and further optimization. In the process of the optimization procedures, the design candidates are arranged to go through two rounds of selection to obtain the best low carbon emission design. At the first round, the structural simulation starts to run under the given model and condition script, and the exported results from ANSYS APDL along with the input parameters are saved accordingly, after which the candidates meet the structural requirements are kept for the following stage selection. In the next round, the selected design schemes are sent to ANSYS APDL for the heat transfer simulation, and the results are retrieved and read from the saved file in Rhino and Grasshopper. Ultimately, the decision-making for the selection of a low carbon emission scheme is based on the material consumption that is stored in round 1 during the construction as well as the heat transfer that is stored in round 2 during the operation.

2.1. PARAMETRIC MODELING FOR GYROID STRUCTURE

To construct the gyroid structure in the parametric model, several ways can be used with the help of Grasshopper plugins. The standard method uses Millipede plugin coupled with a mathematical equation to construct the gyroid form where the gyroid structure is made of smaller meshes rather than the NURBS curves that use control points to build the geometry. Since the meshed geometry generated by Millipede is hard to be converted into a surface which takes less time to be imported into ANSYS, this paper is to use another optional way to construct the gyroid surface through NURBS rather than using a mathematical equation. Referring to Figure 2, the boundary of the surface patch is based on the six faces of a cube, and eight of the surface patch forms the cubic unit cell of a gyroid. Based on this, this paper proposes to construct the six surface patches first to create the $\frac{1}{8}$ gyroid element, after which the $\frac{1}{8}$ gyroid element is rotated and transformed to form the extra seven gyroid elements. This method is comparatively complex when constructing the needed gyroid structure, but the generated geometry can be utilized for efficiently exporting the IGES file.

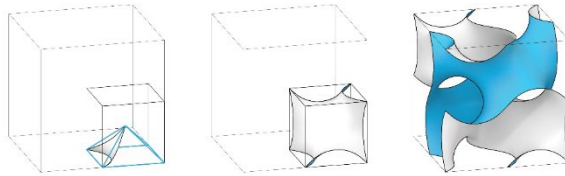


Figure 2. Formation of Gyroid Structure (Resource: (Whitehead, 2019))

Apart from understanding the mechanism of forming the gyroid structure in Rhino/Grasshopper, the size parameters also need to be decided. For the convenience of comparison of structural simulation results and reference experiment index, the project uses a 15 cm^3 bounding box to contain the infill gyroid pattern that is to be analysed in ANSYS APDL in the next stage because the compressive strength of a specific concrete under the international standard is usually measured by using a 15 cm^3 cube. Therefore, the size variables are defined for constructing the gyroid structure within this domain. Since the design is aimed at being applied in real construction in the future, both the print machine profile and the material property decide the value domain of the gyroid module. In this project, there are two variables: thickness and the gyroid structure's unit size. Considering printability by 3D printer, this project uses a bigger unit size domain containing 3.75cm, 5cm, 7.5cm, 15cm, which means that each side has 1 to 4 unit gyroid structures. For the thickness, it also uses a bigger unit size domain with consideration on the structural performance, in which it has five numbers containing 0.30cm, 0.35cm, 0.40cm, 0.45cm, 0.50cm. Therefore, the total test number is 20. The project didn't test as many design candidates as possible since the main target is to test the feasibility of this interoperability method and its efficiency to find better solutions to optimize the cellular structure size for the construction application.

2.2. DEFINING ESSENTIAL SIMULATION INFORMATION OF GYROID STRUCTURE

To complete the preparation work for the further simulation in ANSYS APDL, the necessary information needs to be input, including the material properties and the boundary conditions. Consequently, these values become the user inputs of the tool to accommodate the analysis under different requirements.

2.2.1. Material properties

According to EN 1992-1-1 (European Committee for Standardization, 2004), the C30 concrete (compressive strength class of 30 MPa) is used as the simulation material in this research since the standard material is easily used to judge if the designed gyroid structure meets the structural requirements in the simulation result analysis. The essential material properties for ANSYS APDL cover young's modulus, poisson's ratio, material density, and gravity, for which the proper property parameters are indicated in Table 1 below.

2.2.2. Structural simulation setup

The gyroid structure is modeled as one shell and is further meshed for the finite element analysis. There are many element types available in ANSYS APDL. Based on the field of application and the formulation of the element, shell 281 element is chosen. Since the simulation of a complete partition wall infilled with the gyroid pattern needs more computer power, the project uses a 15 cm³ cube as the test sample to replace a whole partition wall. Usually, the wall bottom bears the largest pressure, and this cube is proposed to be placed at the position of the wall bottom to undertake the loading from its top. In this project, the height of a partition wall is deemed as 3.0m high, which means that the 15 cm³ cube will bear the weight of 2.85m high volume above. The surface pressure is calculated by using the weight of the upper volume to divide the cube surface area. The volume of the loadings above is calculated using the Grasshopper volume function to obtain the weight loadings. Besides the loading from the external objects, self-weight is also considered. The horizontal shear force is ignored to simplify the analysis. The bottom surface of this cube will be constrained as support. Finally, the gyroid infill cube only undertakes vertical compressive stress and self-weight, for which the 1st principal stress is used to evaluate the simulation results. As long as the maximum stress from all the meshed elements is below 30MPa, the design scheme is viable for the construction and kept for the following selection. The detailed parameter information for the structural simulation is described in Table 1.

2.2.3. Thermal simulation setup

For the heat transfer analysis in ANSYS APDL, shell 131 is selected as the element type. In order to define the boundary conditions, two convective heat fluxes through non-solid materials are given on the front and back sides of the cube, and the heat transfer coefficients are specified according to the standard calculation methods: 20 W/m²·K for internal heat flux and 30 W/m²·K for external heat flux. The four sides of the cube are assigned an insulation boundary to represent the insulation condition, and the front and back of the cube are given a fixed temperature of 30 °C and 25 °C respectively. The simulation model directly considers heat conduction and uses the simplified method of an effective thermal conductivity of air proposed in NEN-EN-

ISO 6946 (NSAI, 2017) to replace convection and radiation. Since the internal wall has complex thermal transfer behaviour, including conduction, convection, and radiation, we use a simplified approach to convert these three heat transfer modes into one equivalent conduction for a convenient calculation. Under this method, there are two ways to set up the 3D thermal model. One option is to deem the air as a solid object attached to the shell structure, in which the solid “air” object is assigned a thermal mass element and uses the equivalent thermal resistance. Another method is to equate this geometry-complex form into a cube box according to NEN-EN-ISO 6946. The new conductivity of the equivalent cube box is calculated by combining the concrete thermal resistance and air thermal resistance. In this research, we used the second method for accelerating the simulation speed. Finally, to evaluate the insulation ability of the gyroid cube, a reference simulation is made where a solid 15 cm³ cube with the same material properties and external boundary conditions is given for the comparison test. The detailed boundary conditions for the thermal simulation are described in Table 1.

Name	Value	Unit
Youngs' modulus	3.2837e11	dyne/cm ²
Poisson's ratio	0.2	N/A
Density	2.5	g/cm ³
Gravity	9.806e2	cm/s ²
Surface pressure	Loading weight/surface area	dyne/cm ²
Internal/external temperature	20/30	°C
Internal/external heat flux	25/30	w/m ² ·k
Conductivity(concrete)	3e5	erg·s-1/cm·k
Conductivity(air)	Varies based on the shell thickness	erg·s-1/cm·k

Table 1: Parameters for simulation

2.3. INTEROPERABILITY BETWEEN PARAMETRIC DESIGN AND FEM ANALYSIS SYSTEM

There are two available ANSYS simulation engines, including Mechanical APDL and Workbench, for the analysis. In this paper, ANSYS APDL is used as the simulation engine behind the parametric interface. A grasshopper python plugin (Figure 3) helps to build up the connection between the parametric model and the simulation engine.

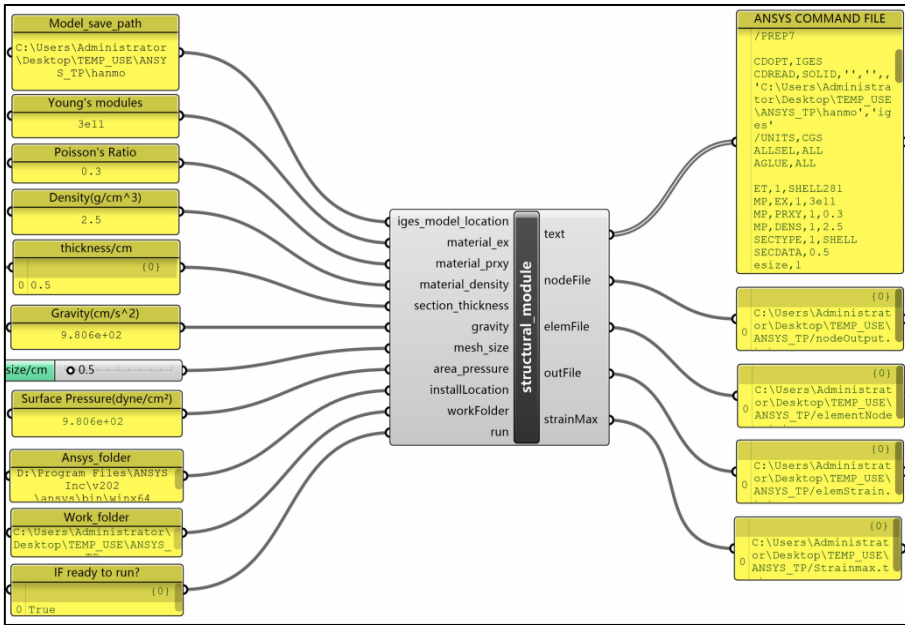


Figure 3. Grasshopper Python Linkage for Structural Simulation (Resource: author)

For a successful linkage between the parametric modeling and the ANSYS engine, the first step is reconstructing the 3D model in ANSYS APDL. For representing the geometry in ANSYS APDL, two ways are tested based on the precedent study. One solution is to mesh the gyroid structure in Rhino/Grasshopper and then use the mesh vertices and faces to represent the key points and areas in ANSYS APDL (Schoina, 2016). Another method is to export the whole model in IGES format and import the exported 3D model in ANSYS APDL (Magna, 2013). The plugin “Pancake” realizes the export work that converts the Grasshopper geometry into the IGES file directly in the work folder. After the preparation of the 3D model, the next step is to write the APDL command text file for the successful simulation in ANSYS APDL, which includes the necessary scripts like importing the geometry exported from Rhino and Grasshopper, setting up the material properties, meshing the volumes, constructing the boundary conditions, running the simulation (static analysis) and exporting the results as text in the work folder. The Grasshopper python plugin helps convert the command words above into the text file under the format of APDL. When the boolean toggle of this plugin is activated, the ANSYS APDL batch mode runs automatically to execute the tasks written inside the command file. For each time simulation, when the new result is calculated out and read in Rhino and Grasshopper, the plugin helps to tune the parameters, and the new simulation starts.

2.4. VISUALIZATION OF SIMULATION RESULTS

For the structural displacement visualization, the exported text files from ANSYS APDL include the deformed node coordinates, the nodes’ number of each element, and

the maximum 1st principal stress of each element. To reconstruct the deformed geometry, the nodes' numbers of each element are used to rebuild the 8 - node polysurface with the exact coordinate of each node. According to the range of stress, one colour value domain is established, and each reconstructed polysurface is given a colour based on its stress value. Similarly, for heat transfer visualization, the nodes' numbers of each element are used to rebuild the meshed surface. But since the only concern is the heat flow through the cube, the visualized surface is the back surface of the cube. With each element's heat flux and area, we calculate each node's heat flow assigned to each reconstructed polysurface so that the heat flow performance is visualized through this 2D surface. Figure 4 shows the visualization interface for both structural and thermal results.

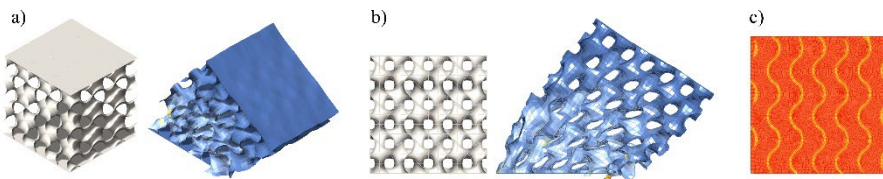


Figure 4. Visualization of Structure and Thermal Simulation (Resource: author) - (a) isometric view of deformation; (b) elevation view of deformation; (c) top view of thermal transfer

2.5. DATA COLLECTION AND PROCESSING

The structural analysis results are saved in the work folder through the Grasshopper plugin TT Toolbox in the first round. Apart from the simulation results, the geometry parameters, including the gyroid structure's unit size and thickness, are also saved. The simulation results are compared with the reference compressive strength 30MPa and filtered based on its structural performance when all the schemes are tested. All the schemes that meet the structural requirements in the first round simulation is saved. For the thermal analysis of the next round, the left-over schemes are sent to ANSYS APDL for the simulation, and the results are retrieved, after which the comparison work is made between the heat flow of the proposed schemes and that of the reference cube. Since this research aims to minimize carbon emissions during the construction and operation stages, an evaluation function is constructed to rank all the schemes. In the construction stage, the reduction in carbon emissions depends on how much material is used. The first evaluation index equals the weight of the saved material multiplied by the amount of carbon dioxide per unit weight. In the operation stage, a higher heat flow rate means more air conditioners are used to control the indoor temperature, increasing the total electricity consumption and indirectly inducing carbon emission. Therefore, we use the heat flow difference between the proposed schemes and the reference cube as the variable and convert it to the reduced carbon emission volume. We propose this elemental partition cube will be used in the next ten years. Then the second evaluation index equals the reduced carbon emission per unit time multiplied by ten years. Ultimately, the evaluation function equation is written as (1) below.

$$\text{Reduction} = W_{\text{concrete}} \times W_{\text{contocO2}} + HF \times \text{Time} \times W_{\text{HFtoCO2}} \quad (1)$$

Where:

$W_{concrete}$ = Weight of reduced concrete

$W_{contoCO2}$ = Weight of CO2 per concrete unit weight

HF = Amount of reduced heat flow per unit time

$W_{HFtoCO2}$ = Conversion ration from heat flow to weight of CO2

After the calculation, we select the top 5 schemes and present them in the below table 2 with their parameters.

Parameters/Number	Unit size (cm)	Thickness (cm)	Reduced weight (kg)	Reduced heat flow (J/s)	Carbon reduction by weight (kg)	Carbon reduction by heat flow (kg)	Total carbon reduction (kg)
1	3.75	0.75	3.41	0.78	0.28	15.85	16.10
2	3.75	0.7	3.61	0.76	0.25	15.51	15.77
3	5	0.85	3.68	0.72	0.27	14.71	14.97
4	5	0.9	3.48	0.72	0.25	14.66	14.91
5	5	0.8	3.88	0.70	0.28	14.26	14.54

Table 2: Calculated results for carbon reduction

3. Conclusion and Limitations

In this research, based on the simulation and the objective value calculations, it is found that the size of the infill pattern for an elemental cube of the partition wall has an effect on insulating the heat from the outdoor environment. The optimized scheme with the suitable shape parameters has the potential to be further developed into the real manufactured product to minimize carbon emission. Besides, the research’s initial idea was to develop an approach that could help optimize and evaluate the structure design schemes by integrating the parametric interface with finite element software such as ANSYS APDL. However, validation work has not been conducted in this research. The hand calculation work and the physical test work need to be carried out to test the accuracy of this approach, which will be further discussed in the next stage of research. Besides, the structural and thermal simulation evaluation principles also ignore the potential factors affecting the results. In the structural analysis, the shear force was removed, and in the thermal analysis, the convection and radiation inside the wall were equated to the thermal resistance or conductivity. Therefore, a more standard and accurate evaluation method needs to be explored to regularize this process. Secondly, the efficiency of such a method is low since each simulation takes more than five minutes to finish to calculate the results and send back the data, which is time-consuming and makes the visualization effect unsmooth. Besides, this method is not applicable when it comes to a larger number of candidates for evaluation. Lastly, using the plugin requires knowledge including parametric modeling, python language, and ANSYS parametric design language, making it not friendly to designers who are weak

in one or more of them.

4. Recommendations and Future Works

A more systematic and accurate validation method needs to be conducted in the next stage of work, and the approach in this paper can be further improved and developed based on the information after validation. The current development of this design tool has a limitation in simulation speed. And consequently, only when the total test number is less, this method is applicable. Therefore, a surrogate or machine learning model needs to be developed for simulation acceleration rather than using the software engine as the simulation tool. Although the visualization is viable in this research, the speed of reconstruction work is based on the mesh density. When the mesh density is very heavy, the visualization process is unsuitable. A more efficient visualization method needs to be tested. Also, the plugin itself should be revised and more user-friendly to designers with less knowledge in the finite element field and python language field. It is essential to convert these parts into readable input modules. Lastly, as mentioned, this research is more of a proof of concept for a multi-phase optimization scheme to design bio-inspired building components, and therefore, further researches on fabrication and cost consideration of deploying this structure need to be discussed at the next stage.

References

- European Committee for Standardization. (2004). *Eurocode 2: Design of concrete structures—Part 1-1: General rules and rules for buildings* (EN 1992-1-1). <https://www.phd.eng.br/wp-content/uploads/2015/12/en.1992.1.1.2004.pdf>
- Gamage, A., & Hyde, R. (2012). A model based on Biomimicry to enhance ecologically sustainable design. *Architectural Science Review*, 55(3), 224–235. <https://doi.org/10.1080/00038628.2012.709406>
- Magna, R., Reichert, S., & Knippers, J. (2013). Integrated design methods for the simulation of fibre-based structures. *Design Modelling Symposium Berlin*. https://www.researchgate.net/publication/292745702_Integrated_design_methods_for_the_simulation_of_fibre-based_structures
- NSAI. (2017). *Building components and building elements—Thermal resistance and thermal transmittance—Calculation method* (ISO 6946: 2017). The National Standards Authority of Ireland. <https://infostore.saiglobal.com/preview/is/en/2017/i.s.eniso6946-2017.pdf?sku=1961927>
- Piccioni, V., Turrin, M., & Tenpierik, M. J. (2020). A Performance-Driven Approach for the Design of Cellular Geometries with Low Thermal Conductivity for Application in 3D-Printed Façade Components. *Symposium on Simulation in Architecture and Urban Design, SimAUD2020*.
- Qin, Z., Jung, G. S., Kang, M. J., & Buehler, M. J. (2017). The mechanics and design of a lightweight three-dimensional graphene assembly. *Science Advances*, 3(1), e1601536. <https://doi.org/10.1126/sciadv.1601536>
- Schoina, S. (2016). *Performance-based form-finding and material distribution of free form roof structures* [Master Thesis, Delft University of Technology]. <https://repository.tudelft.nl/>
- Thompson, M. K., & Thompson, J. M. (2017). *ANSYS mechanical APDL for finite element analysis*. Butterworth-Heinemann.

COMPLEX SHAPE MODELLING BY TESSELLATION

Advanced Geometry Control for Variably Curved Surfaces

ALESSANDRO ZOMPARELLI¹ and ROBERTO NABONI²
^{1,2}*CREATE Group - University of Southern Denmark (SDU), Section
for Civil and Architectural Engineering.*
¹*alzo@iti.sdu.dk, 0000-0001-7446-3700*
²*ron@iti.sdu.dk, 0000-0001-9647-0426*

Abstract. Tessellation is a flexible modelling method for computational designers that allows to articulate and detail complex topological surfaces by repeating components along target surfaces. This technique provides a discretization strategy compatible with many digital-fabrication processes. Well-known geometrical issues limit such an approach on surfaces characterized by highly variable curvature, which can output errors such as self-intersections and undesired deformations. This research shows geometrical methods to manage such problems and implement them in an open-source tool. In particular, automatic and manual procedures for manipulating normal vector fields are utilized and applied to the modelling of complex shape case studies.

Keywords. Industry; Innovation; Infrastructure; Architectural Geometry; Computational Design; Topology-based Design; Tessellation Mesh Subdivision Modelling; SDG 9.

1. Introduction

Since the early 2000s, complex modelling has been a major area of development for the CAAD-related research fields, paving the way to systematic studies on the topics of form-finding, digital manufacturing, and data-driven design. The use of computational tools in the last decade rendered accessible the design and construction of complex architectural shapes through tessellation, by combining non-destructive implicit and explicit modelling logics (Chang, 2018). In existing modelling software, different methods are employed to represent complex geometry. A first approach relies on the use of implicit surfaces as defined by (Opalach and Maddock, 1995). Marching Cubes (MC) are often employed as a technique to conveniently visualize arbitrary shapes (Lorensen and Cline, 1987). With an appropriate resolution, MC provides dimensionally accurate unstructured mesh models, i.e. characterized by irregular edge connectivity (Bern and Plassmann, 2000). A second approach uses computationally less expensive explicit surface representation, which relies on the use of NURBS or polygonal mesh surfaces. The latter, when combined with mesh subdivision

techniques, allows for smooth modelling that outputs structured meshes surfaces. These enable a high-degree of flexibility that is fundamental in complex multi-steps modelling applications (Ovar et al., 2021). Free-form architectural shapes can be beneficially modeled and manufactured from the use of paneling methods that rely on tessellated explicit surfaces (Eigensatz et al., 2010), which are populated with parametrically morphed planar/three-dimensional components. The emergence of such a modelling approach into architectural design has been streamlined in the last decade by the development of tools such as Paneling Tools (Issa, 2012) and Pufferfish (Pryor, 2021) for Rhino and Grasshopper; and Tissue for Blender (Zomparelli, 2019). These tools simplify the tessellation operation into a few steps: defining a *component* of any complexity (Figure 1a); obtaining polygonal *sub-domains* from the quadrilateral tessellation of a target mesh or NURBS surface (Figure 1b); utilizing the UVW coordinates to generate box-like volumes (Figure 1c); using these to generate *seamless geometry* by the array of parametrically deformed components (Figure 1d). Modelling complex shapes through tessellate operations is extremely intuitive. However, geometrical issues can arise when engaging with forms characterized by highly variable curvature. In this study, we aim at extending the capability of such modelling workflows by implementing open-source methods to some of the known geometrical limitations that are easily encountered by designers without a technical specialization in architectural geometry.

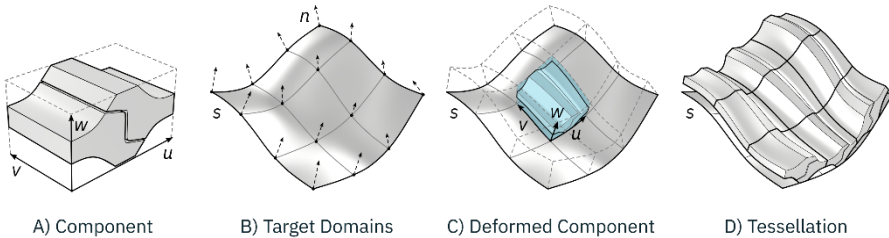


Figure 1. The fundamental steps involved in tessellation

2. Research Problem and Methodology Overview

Figure 2 shows monoclastic, synclastic and anticlastic surfaces and geometrical issues emerging when their respective components are thickened along their normals in presence of concave narrow curvature, such as (1) the self-intersection of thick element on surfaces with narrow concave curvature; and (2) the distortion of thick elements due to convergent or divergent normal vectors in the target surface (Figure 3). Wallner et al. (2001) described a method to determine the maximum offset distance for a given input surface, and thus, minimize such modeling issues. Issues with self-intersections were previously addressed alterations of the original topology through trimming operations (Elber, 2003). However, none of the existing approaches are systematically overcoming the intersection and deformation issues generated during mesh tessellation operations with target geometries of largely variable curvature (Shi-Yu, 2011). In this work, we present a set of geometrical methods to tackle such problems and their software implementation into an existing modelling tool which systematizes the

advanced control of tessellate operations.

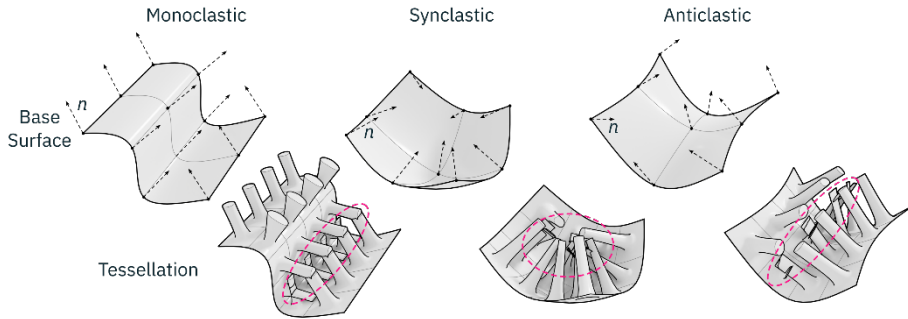


Figure 2. Examples of tessellation of thick elements on monoclastic, synclastic and anticlastic sub surfaces. The thickness of the components produces self-intersections

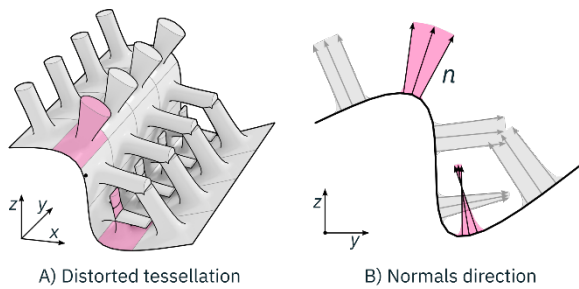


Figure 3. Distortion of the components according to normals convergence or divergence

3. Methods

The overall research methodology involves the definition of the geometrical problem on a number of modelling case studies, the development of a modelling method and its implementation as a tool. The presented techniques have general architectural geometry validity, but were here implemented within the open-source environment of Blender, which also facilitate a complete access to mesh data information. Two approaches that solve the self-intersection of components are presented, which define displace directions different to the normal vectors. Both approaches face a common issue, related to the correct estimation of the displacement factor to achieve the desired thickness. The components deformation of convex and concave surfaces once they are remapped along non-parallel displacement vectors is also addressed. We implemented an approach to differentiate and customize the normal directions for the different parts of a component and reduce the deformations in critical areas.

3.1. SELF-INTERSECTIONS PREVENTION METHODS

Smooth Normals Method - The first presented method offers an automated procedure to correct the normals vector field of a mesh surface, to avoid intersections. A

smoothing iterative algorithm is therefore employed to reduce and diffuse singularities in the normals vector field. This operation distributes the individual coordinates (x,y,z) of the normal vectors, based on a diffusion value $diff$ and a number of iterations to control (Figure 4).

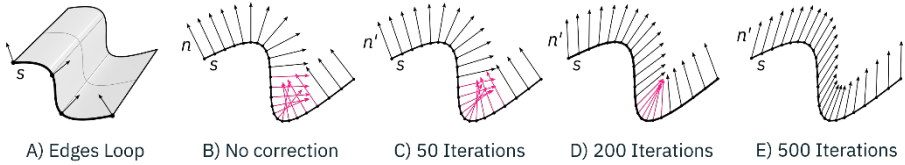


Figure 4. Iterative smoothing of Normal Vectors

The amount of smoothing iterations varies according to the mesh density and the specific surface features, the number of smoothing iterations (Figure 5).

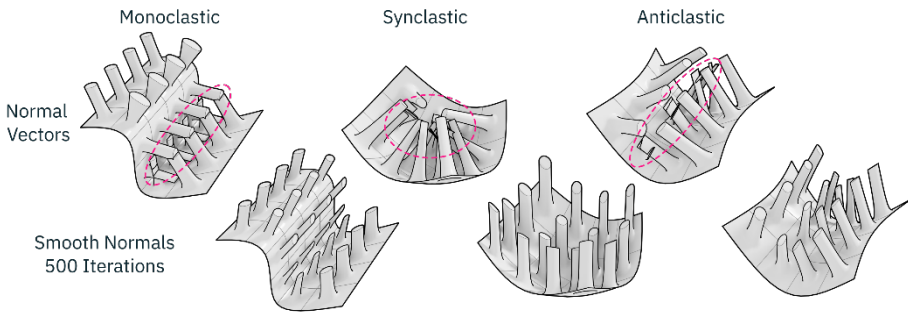


Figure 5. Comparison of the normal smoothing correction on different surfaces. The picture shows different levels of corrections according to the number of smoothing iterations

Target Surface Method - Figure 6 shows the second method based on the use of a target surface, topologically identical to the base surface, in order to define a new vectors' direction, from the vertices of the *base*, to the vertices of the *target*. It is therefore important that the indexing order of the vertices for both meshes is the same.

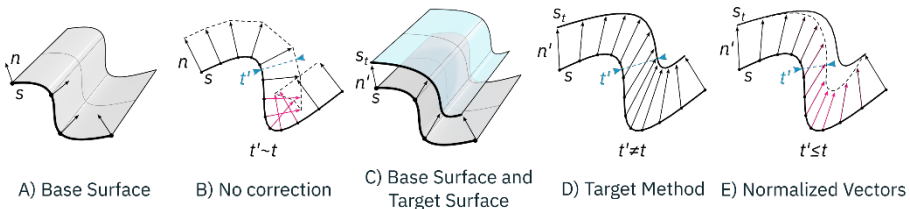


Figure 6. Visualization of custom normals according to the Target Method

This method, while being more complex, allows for a complete control of the displacement direction and the component's shape (Figure 7).

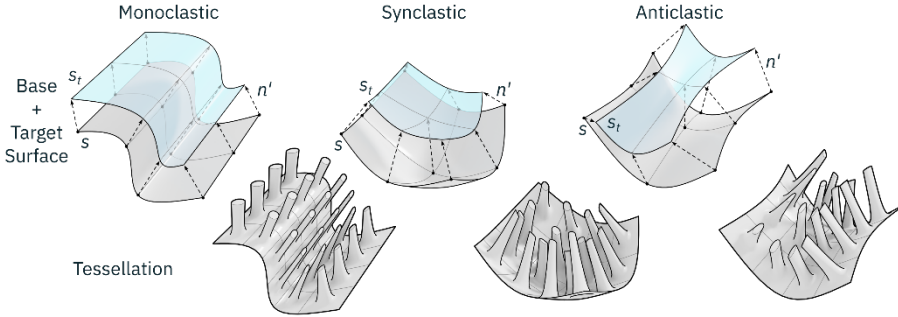


Figure 7. Comparison of the target surface correction on different types of surfaces

3.2. THICKNESS COMPENSATION METHODS

Local Thickness Compensation - Working on Custom Normal directions allows to avoid self intersections in the geometry. In certain cases, this causes an alteration of the generated thickness, especially using the *target surface method* where alterations of the vector length connecting the two surfaces may happen. A simple normalization of the vectors is insufficient to ensure a uniform thickness because the altered vectors are not perpendicular to the surface. A solution is offered by a subsequent adjustment of the vector length based on the angle between the original normal vectors and the new *custom normals*. The accuracy of the result will depend on the proportion between the size of the faces and the adopted thickness. Figure 8A shows how moving a vertex P along its custom normal with the desired offset d , its displacement P' is obtained. P'' is defined as the perpendicular projection of this point onto the starting mesh surface. When P'' falls within one of the neighboring faces of P (f_1 or f_2), the local adjustment produces correct results. Otherwise, the resulting thickness will depend on faces that have not been taken into consideration in the first place. In those cases a more global method is required, involving a larger portion of a surface beyond the neighbor faces.

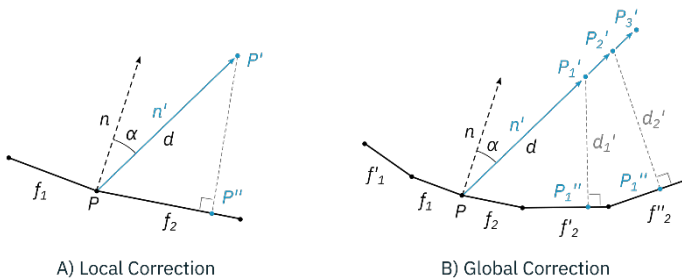


Figure 8. Thickness compensation methods

Global Thickness Compensation - Figure 8B describes a global compensation approach based on a series of iterations that progressively refine the length of the vector according to a desired thickness t . The iterative procedure begins with a tentative vector length d defined according to the previously described local method. The distance d' between P' and P'' is then checked. Further adjustment iterations multiply the previously used distance d by a factor equal to t/d' , until the gap between d' and t is irrelevant for the design purpose. As visible in Figure 9, the thickness quality improves with dense meshes and with a high number of iterations, while in Figure 10 is possible to see the effect of such a correction using the target surface method, in comparison with the default method that generates intersections.

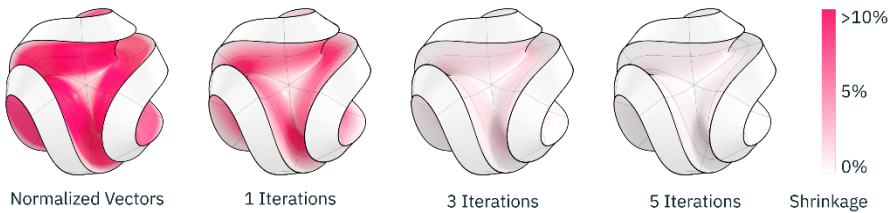


Figure 9. Comparison between a simple thick mesh and thickness operation based on the Target Surface method using an iterative Global Thickness Compensation

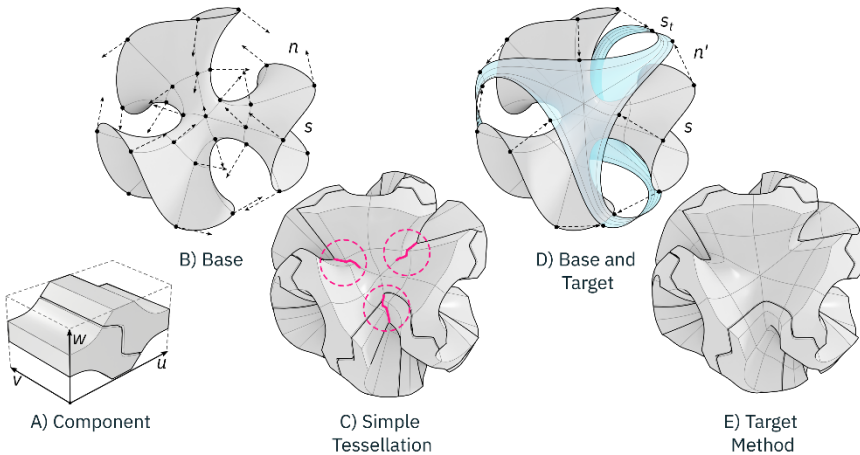


Figure 10. Tessellation of the Component (A) on a Base Surface (B). The Default method (C) produces self-intersections. Target Surface method (D) produces a correct geometry (E)

3.3. NORMALS DISTORTION CONTROL

The position of each vertex of a component along a surface (or subd patch) is defined by the remapped coordinates from XY (absolute coordinates) to UV (parametric coordinates). According to the UV coordinates, a specific normal vector $N(uv)$ is used to displace the vertex defining the third coordinate from Z to W. The method in Figure 11 operates a distinction between the UV coordinates (A) representing the position of

each vertex on the surface according to its XY coordinates, and the $U'V'$ coordinates (B) used to evaluate the normal directions $N'(u'v')$, to determine the W axis used for the Z component. With this approach, it is possible to assign to a portion of the component object the same direction N' , scaling down the vertices of such a portion to a single point in $U'V'$, while the UV coordinates remain proportional to XY. This is a series of parallel translations of the vertices of the interested part (D). Mesh modelling software typically employs UV coordinates for texture mapping, and the same information is here used to manipulate $U'V'$ and the normal directions.

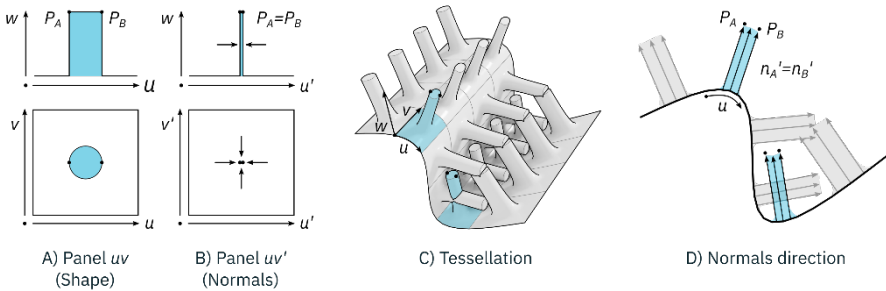


Figure 11. Distinction between UV and $U'V'$ spaces and result of the distortion control

4. Software Implementation

The presented methods were implemented within Tissue for Blender, in the tessellation settings. In the current implementation, the Smooth Normal method can be activated when the default Normals direction is used. A specific number of iterations can be set, together with a *Vertex Group*, a technique that allows the differentiation of the smoothness according to a scalar field along the surface. When a specific Target Object is used for the Thickness Direction, an *Even Thickness* option allows the use of the Thickness Compensation with the possibility to specify the number of iterations. The distortion control is implemented in the add-on as *Evaluate Normals* and is taking advantage of the UV Mapping tools inside Blender. It is indeed possible to define the coordinates $U'V'$ of the component object as a dedicated UV layer that can be easily manipulated according to the specific design needs.

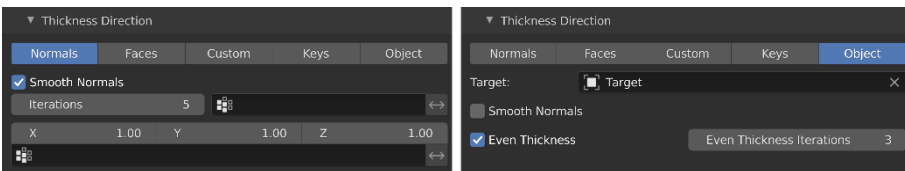


Figure 12. a) *Smooth Normals* option with a specific number of iterations b) *Even Thickness* option with a parameter controlling the number of iterations when using a Target Object

5. Results and Discussion

The Normals Smoothing method is an automatic procedure. It is compatible with both anisotropic and non-uniform diffusion of the normals along the surface, allowing selective operations. Despite this level of control, on more complex surfaces it may produce an inversion of the thickness direction when some of the normals intersect the surface itself. With a high number of iterations, the vectors tend to become parallel, losing coherence with the shape of the surface. The Target Surface method offers a highly customizable tool able to solve complex cases that cannot be addressed by the Normal Smoothing method (Figure 13).

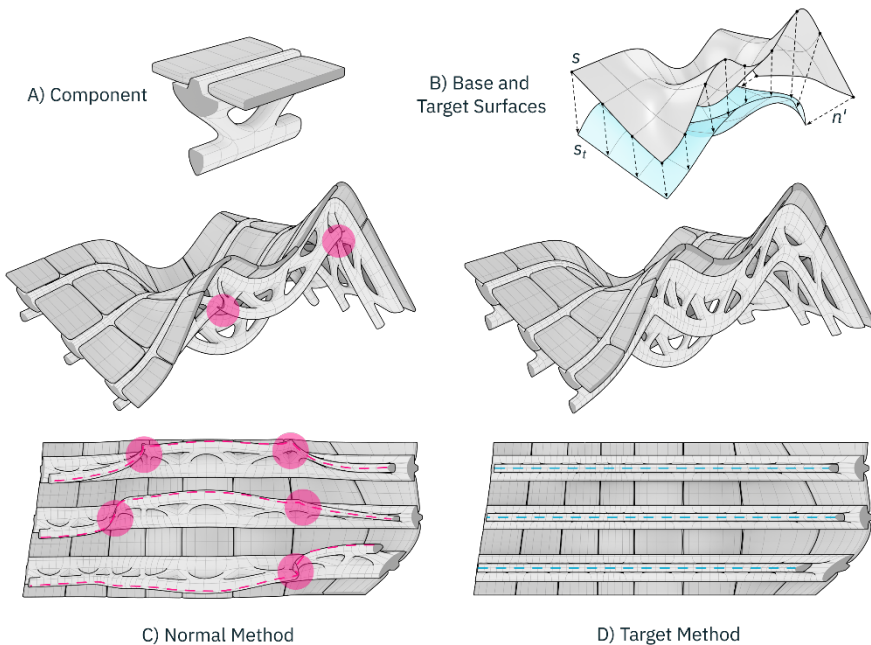


Figure 13. Comparison of a Tessellation of the Component (A) on a Base Surface. The Default method (C) produces self-intersections, while the Target Surface method produces a more controllable geometry (D)

The use of this method is recommended when i) both the original mesh and target mesh can be automatically generated from the same algorithm that ensures a coherent indexing and parametric shape control; ii) when the operation is performed from a flexible mesh modelling tool, that easily allows for manual editing of the target mesh. The implementation of the global thickness compensation is defining two different corrective factors for the custom normals: positive and negative, on the two opposite sides of the base surface. As an approximation, those corrective factors are applied to the bounding box of the component object, while for higher accuracy, it is instead necessary to use different values for every vertex of the component. This approximation is the result of a compromise between the accuracy and efficiency of the algorithm. There are some specific aspects that should be taken into consideration

when using this method: i) the problem should have a possible solution, meaning that for a given vector direction it should be possible to find a displacement factor resulting in a point at the desired distance t from the surface; ii) the initial tentative displacement d has an important role for the convergence of the solution, and ideally, for each vertex P of the component it should be a function of the coordinate W_p , since they should eventually be displaced with a different value; iii) some open meshes may produce incorrect values along the borders, if the desired solution is outside the surface itself, since in every iteration the points are projected back on the surface. This may produce a divergence in the solution.

The developed techniques successfully tackle some limitations of tessellation strategies on extremely complex surfaces. The developed tool uses both automatic and manual procedures to control the described geometrical issues. This extends the range of possible applications of topology-based modelling by offering both design flexibility and dimensional control.

The methods can be generalized and easily replicated inside other modelling pieces of software operating with Mesh and NURBS geometries. Future research will include options for the advanced control of both the position and shape of specific geometrical features in UV, and specific conditions such as the planarity of certain portions within a specific component.

References

- Agustí-Juan, I., Habert, G. (2017) Environmental design guidelines for digital fabrication. *Journal of Cleaner Production*, 2017 (142), 2780–91. <https://doi.org/10.1016/j.jclepro.2016.10.190>.
- Bern, M., Plassmann, P. (2000). Mesh Generation. In J.R. Sack, J. Urrutia (Eds.), *Handbook of Computational Geometry* (1st ed., pp. 2991–332). North-Holland.
- Burley, B., Lacewell, D. (2008) Ptex: Per-face texture mapping for production rendering. *Computer Graphics Forum*, 2008(27), 1155–64, <https://doi.org/10.1111/j.1467-8659.2008.01253.x>.
- Chang, W. (2018) Application of Tessellation in Architectural Geometry Design. *E3S Web Conf 2018*(38), 1–8. <https://doi.org/10.1051/e3sconf/20183803015>.
- Eigensatz, M., Kilian, M., Schiffner, A., Mitra, N.J., Pottmann, H., Pauly, M. (2010) Paneling architectural freeform surfaces. *ACM Transactions on Graphics*, 29(4), 1-10. <https://doi.org/10.1145/1778765.1778782>.
- Elber, G. (2003). Trimming Local and Global Self-intersections in Offset Curves Using Distance Maps. In *Mathematics of Surfaces. Lecture Notes in Computer Science*, 2768, 213-222. https://doi.org/10.1007/978-3-540-39422-8_15
- Horvath, A. (2004) Construction materials and the environment. *Annu Rev Environ Resour* 2004(29),181–204. <https://doi.org/10.1146/annurev.energy.29.062403.102215>.
- Issa, R. (2012). *Paneling Tools for Rhinoceros 5*. Robert McNeel & Associates. Retrieved December 8, 2021, from https://wiki.mcneel.com/_media/labs/panelingtools.pdf.
- Lorensen, W. E., Cline, H. E. (1987). Marching cubes: A high resolution 3D surface construction algorithm. *ACM SIGGRAPH Computer Graphics*, 21(4), 163–169. <https://doi.org/10.1145/37401.37422>.
- Oval, R., Mesnil, R., Van Mele, T., Block, P., Baverel, O. (2021). Two-Colour Topology Finding of Quad-Mesh Patterns. *CAD Comput Aided Des*, 2021(137). <https://doi.org/10.1016/j.cad.2021.103030>.
- Opalach, A., Maddock, SC. (1995). An overview of implicit surfaces. *Introduction to Modelling and Animation Using Implicit Surfaces* (1.1–1.13).

- Pryor, M. (2021). *Pufferfish*. Food4Rhino. Retrieved December 8, 2021, from <https://www.food4rhino.com/en/app/pufferfish>.
- Sacht, L., Jacobson, A., Panozzo, D., Schüller, C., Sorkine-Hornung, O. (2013). Consistent Volumetric Discretizations Inside Self-Intersecting Surfaces. In *European Symposium on Geometry Processing 2013*. The Eurographics Association and Blackwell Publishing Ltd.
- Shi-Yu, Xing, Q., Akleman, E., Chen, J., Gross, J. (2011). Pattern mapping with quad-pattern-coverable quad-meshes. In *ACM SIGGRAPH 2011 Talks (SIGGRAPH '11)*. Association for Computing Machinery.
- Wallner, J., Sakkalis, T., Maekawa, T., Pottmann, H., Yu, G. (2001). Self-Intersections of Offset Curves and Surfaces. *International Journal of Shape Modelling*, 7(1), 1–21. <https://doi.org/10.1142/S0218654301000023>.
- Zomparelli, A. (2019). *Tessellate Documentation*. Tissue page on Github. Retrieved December 8, 2021, from <https://github.com/alessandro-zomparelli/tissue/wiki/Tessellate>.

ROBUST ATTRIBUTED ADJACENCY GRAPH EXTRACTION USING FLOOR PLAN IMAGES

JIELIN CHEN¹ and RUDI STOUFFS²

^{1,2}*Department of Architecture, National University of Singapore.*

¹*chen.jielin@u.nus.edu, 0000-0003-0666-8725*

²*stouffs@nus.edu.sg, 0000-0002-4200-5833*

Abstract. Architectural design solutions are intrinsically structured information with a broad range of interdependent scopes. Compared to conventional 2D Euclidean data such as orthographic drawings and perspectives, non-Euclidean data (e.g., attributed adjacency graphs) can be more effective and accurate for representing 3D architectural design information, which can be useful for numerous design tasks such as spatial analysis and reasoning, and practical applications such as floor plan parsing and generation. Thus, getting access to a matching attributed adjacency graph dataset of architectural design becomes a necessity. However, the task of conveniently acquiring attributed adjacency graphs from existing architectural design solutions still remains an open challenge. To this end, this project leverages state-of-the-art image segmentation techniques using an ensemble learning scheme and proposes an end-to-end framework to efficiently extract attributed adjacency graphs from floor plan images with diverse styles and varied levels of complexity, aiming at addressing generalization issues of existing approaches. The proposed graph extraction framework can be used as an innovative tool for advancing design research infrastructure, with which we construct a large-scale attributed adjacency graph dataset of architectural design using floor plan images retrieved in bulk. We have open sourced our code and dataset.

Keywords. Attributed Adjacency Graph; Floor Plan Segmentation; Ensemble Learning; Architectural Dataset; SDG 9.

1. Introduction

Architectural design is a representation saturated problem domain as the design process intimately relates to the adopted representation format (Stouffs, 2008). Orthographic drawings such as floor plans and sections have conventionally played a crucial role in embedding architectural design information in a 2D Euclidean data space, which are somehow inherently limited by the diminution of 3D information. Architectural design solutions are intrinsically structured information with a broad range of interdependent scopes. Compared to 2D Euclidean data space, non-Euclidean data space can be more efficient and accurate for embedding structured data, especially in a 3D domain with complex geometric and semantic information (Bronstein et al., 2017). The paragon of

a sophisticated non-Euclidean data structure is a graph, which is an abstract data structure that can encode both individual features and relational information. In fact, architectural design solutions can be naturally converted to a graph-based representation, which is part of the conventional architectural design activities such as spatial analysis and reasoning (Hillier et al., 1987).

Attributed adjacency graphs (also referred to as layout graphs/bubble diagrams/semantic building fingerprints in literature) can embed architectural information with multiple attributes, with nodes denoting different features of spaces and edges denoting various types of connections between spaces, which can be useful for numerous design tasks such as spatial analysis and reasoning (Al-Jokhadar & Jabi, 2020). Meanwhile, recent years have witnessed the surge of machine learning-based architectural design research (As et al., 2018). By analysing large amounts of architectural design data with a graph-based representation, it is possible to capture latent design patterns and high-level structural information using graph representation learning techniques, which can then be leveraged to facilitate applications such as floor plan parsing and generation (Lu et al., 2021).

Thus, getting access to matching graph-based architectural design datasets becomes a necessity. Nevertheless, approaches to conveniently construct such datasets are still scarce in literature. Although graph extraction can be more straightforward using 3D building information models or CAD drawings, the accessibility of these kinds of design data in bulk can be difficult. Given the comparatively easy access to floor plan images of existing architectural design projects from architectural repository websites, it can be beneficial to extract attributed adjacency graphs using floor plan images. However, although the task of extracting architectural information from floor plan images has been broadly investigated in literature (Gimenez et al., 2015; Kim et al., 2021; Zeng et al., 2019), existing approaches all come with specific weaknesses, such as incompleteness of detected room regions, and limitations of generalization for diverse floor plan styles and complexities, making the task of extracting attributed adjacency graphs from floor plan image still an open challenge. To this end, this project leverages state-of-the-art segmentation techniques using an ensemble learning scheme and proposes an end-to-end framework to efficiently extract attributed adjacency graphs from floor plan images with diverse styles and varied levels of complexity, aiming at addressing the generalization issue of existing approaches. Using the proposed framework, we also construct a large-scale attributed adjacency graph dataset of architectural design using floor plan images retrieved in bulk.

2. Related Work

A popular subtask of extracting architectural information from floor plans is to parse architectural elements, such as walls, openings and rooms, and to vectorize a raster floor plan. Conventional algorithms for detecting junctions and edges from raster floor plans rely on low-level pattern recognition heuristics (Gimenez et al., 2015), which have limitations concerning high-level geometric and semantic requirements of floor plan configuration and various floor plan styles with different complexity level. In recent years, deep learning-based approaches have been introduced to address the high-level semantic feature extraction task, and have achieved promising breakthroughs with improved accuracy and generalization level (Kim et al., 2021; Wu et al., 2021).

To the best of our knowledge, the task of extracting attributed adjacency graphs from a given floor plan image still remains an open challenge, as readily available approaches in literature all come with different aspects of weaknesses. Ferrando (2018) adopts a heuristic approach to identify room connections as edges and room regions as nodes with the assumption that all doors are axis-aligned, making it difficult to be generalized to complex floor plans. Renton et al. (2019) apply a graph neural network to detect and classify indoor elements from a floor plan image and transform them into adjacency graphs, excluding other important architectural elements such as walls and rooms. Song and Yu (2021) convert floor plan images into polygon graph data using graph neural networks. Yet their work has similar limitations regarding generalization to complex floor plans.

Although there are a bunch of available floor plan image datasets of real architectural design projects in current literature, they have varying degrees of defects concerning architectural design research, including annotation granularity, size of the dataset and data sample diversity. Seldom, accessible datasets offer relatively complete contents of segmented architectural elements. Only datasets provided by Song and Yu (2021) (with 400 floor plans) and Wu et al. (2021) (with 122 floor plans) have the stair element, yet the sizes of the datasets are somehow limited. Meanwhile, the floor plans' diversity is mostly homogeneous concerning both image style and design category. The CubiCasa5K dataset (Kalervo et al., 2019) (with 5K floor plans), the largest open-sourced floor plan dataset of real design projects, contains images with various styles, yet only residential design is covered in the dataset. Moreover, graph-based architectural design datasets are still scarce. The recent CubiGraph5K dataset (Lu et al., 2021) has derived graphs from vectorized floor plans of CubiCasa5K, yet inheriting the limitation of homogeneity regarding the design category.

3. Research Methodology

The proposed end-to-end attributed adjacency graph extraction framework is composed of three major steps: Floor plan image segmentation, region adjacency graph extraction and attributed adjacency graph distillation. As there is no jack of all trades available, this project has managed to fuse the merits of state-of-the-art floor plan segmentation models, and has used existing labelled floor plan datasets to train supplementary models. By integrating multiple floor plan parsing models and leveraging their capacities in a supplementary manner, architectural information, including both spatial and element-wise information, can then be identified and extracted from floor plan images.

There are two different approaches for floor plan segmentation in current literature, semantic segmentation and instance segmentation: Semantic segmentation treats multiple objects of the same class as a single entity (Song and Yu, 2021), while instance segmentation treats detached objects of the same class as distinct individual instances (Wu et al., 2021). Aiming at style-agnostic floor plan image segmentation, we first tested multiple state-of-the-art floor plan segmentation models, including models proposed by Zeng et al. (2019), Kalervo et al. (2019), Wu et al. (2021) and Song and Yu (2021). The testing results (Figure 1) have revealed the limitations of existing floor plan image parsing models regarding the level of robustness and generalization. Compared with models proposed by Zeng et al. (2019), Wu et al. (2021) and Song and

Yu (2021), the model provided by Kalervo et al. (2019) has demonstrated better performance. Meanwhile, the only datasets that have included the annotation of stairs, namely datasets provided by Wu et al. (2021) and Song and Yu (2021), could not provide satisfactory performance for the segmentation task. Thus, it is necessary to train supplementary models to parse stair elements. Another essential issue with existing models is that the detected room regions are incomplete and fragmented. Hence, it is also necessary to consider alternative strategies for detecting room regions.

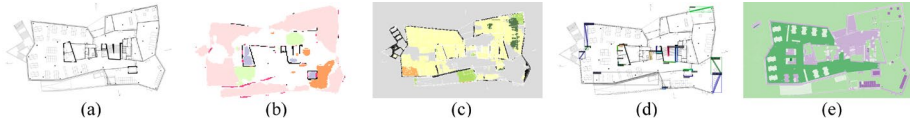


Figure 1. Testing results: (a) Original floor plan image; (b) Semantic segmentation (Zeng et al., 2019); (c) Semantic segmentation (Kalervo et al., 2019); (d) Instance segmentation (Wu et al., 2020); (e) Graph neural network-based segmentation (Song and Yu, 2021)

The proposed framework (Figure 2) can be decomposed into 8 steps: 1) the floor plan image is first pre-processed to improve performance of the segmentation models; 2) the mask of the floor plan is extracted using region adjacency graph extraction algorithm (Song and Yu, 2021) for later usage; 3) semantic segmentation is conducted to obtain initial segmentation of walls, doors and windows; 4) instance segmentation is conducted to obtain wall, door, window and stair instances; 5) the segmentation outputs from step 3 and 4 are used to smooth the wall boundaries and close up wall gaps; 6) pixel-level arithmetic operation is conducted based on the floor plan mask and other architectural elements to extract the room regions; all segmentation results are then fused and vectorized; 7) the region adjacency graph is extracted from the vectorized segmentations; 8) the region adjacency graph is distilled to acquire simple- and multi-attributed adjacency graphs.

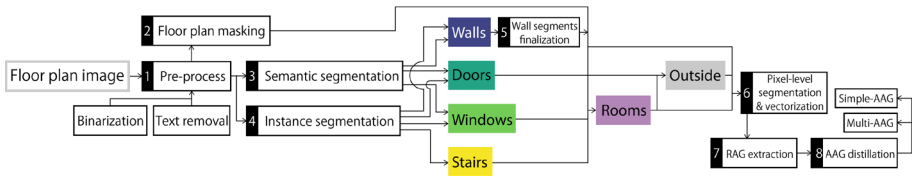


Figure 2. Implementation details of the attributed adjacency graph extraction framework (RAG: Region adjacency graph, AAG: Attributed adjacency graph)

Using the proposed framework, a customized large-scale attributed adjacency graph dataset is constructed using floor plan images retrieved in bulk. As existing floor plan image datasets are seldom constructed for general architectural design research, this project acquires a large collection of floor plan images retrieved from ArchDaily®. The resulting dataset has 159 architectural categories and 17K floor plans in total.

4. Experiment

The adopted algorithms and implementation mechanisms of each step of the proposed framework are further elaborated in this section. An implementation example is

illustrated in Figure 3.

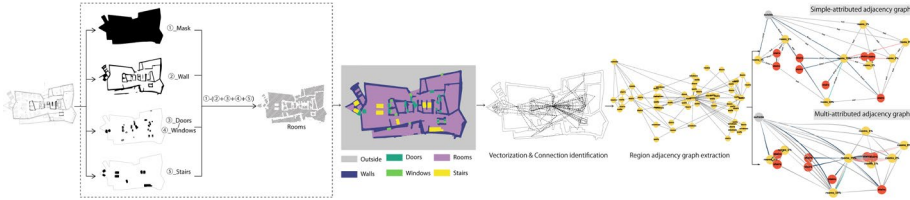


Figure 3. An implementation example of the attributed adjacency graph extraction framework.

4.1. IMAGE PRE-PROCESS

The floor plan image is first converted to grayscale and binarized. As some floor plan images have text annotations, which can potentially beset the performance of segmentation, we adopt a text filtering tool (yu45020, 2018) to automatically detect and remove texts from the floor plan image.

4.2. FLOOR PLAN MASKING

The pre-processed image is then vectorized into a set of polygons; an area enclosed by black pixels is identified as one polygon object, and a set of polygons are generated from all enclosed white areas. The floor plan mask is then identified as the polygon with the largest area from the obtained polygon set.

4.3. SEMANTIC & INSTANCE SEGMENTATION

We adopt the semantic segmentation model provided by Kalervo et al. (2019) and the instance segmentation model proposed by Wu et al. (2021) for detection of wall, door, window and stair elements. Compared with semantic segmentation that outlines walls into complex shapes, instance segmentation can simplify wall elements into rectangles with varied direction and thickness. The geometrical simplification also makes further topological refinement easier to implement, which is essential for accurately subdividing indoor spaces into room regions. As aforementioned, the only existing datasets that have stair annotations are provided by Wu et al. (2021) and Song and Yu (2021), and while the former offers multiple floor plan styles, the latter has only one simple style. Thus, we derive an individual floor plan dataset with mere stair annotations based on the dataset provided by Wu et al. (2021), and train complementary Mask R-CNN models for detecting stair elements with the help of the Detectron2 API. We adopt rotation augmentation and an ensemble learning scheme for the detection of wall and stair elements, and experiments have shown that both strategies can effectively improve the detection performance for complex floor plans (Figure 4).

4.4. WALL SEGMENTS FINALIZATION

Next, we refine the wall elements obtained in the previous steps. The wall instances detected using instance segmentation are vectorized and fed into an algorithm (Figure 5) to repair latent topological inconsistency. As the originally detected wall instances

are not in rectangular shapes, the minimum rotated bounding rectangle of each wall instance is first obtained, then the long and short axes of bounding rectangles are retrieved. Adjacent rectangle pairs are then identified by calculating the distances between the end points of the long axes. If the distance is shorter than a certain threshold, the corresponding endpoints of the long axes are connected. The rectangles are then recreated using the new long axes together with the original short axes. As a result, potential gaps between wall instances are removed, which provides the premise to subdivide indoor space into room regions directly.

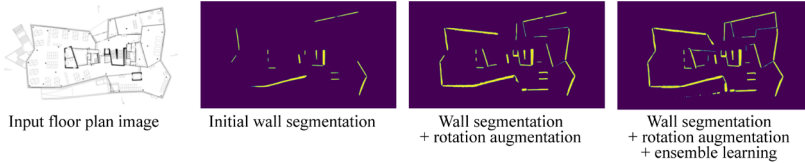


Figure 4. Comparison of wall segmentation results with or without the rotation augmentation and the ensemble learning strategy

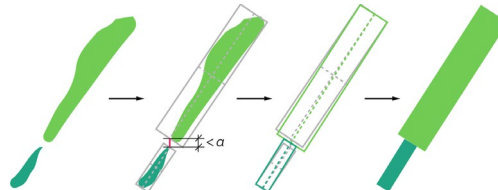


Figure 5. Wall instances refinement

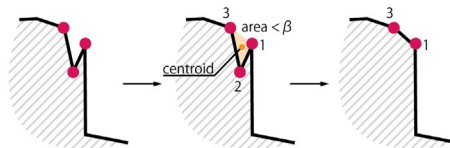


Figure 6. Wall segmentation boundary smoothing

After getting the refined set of wall instances, all previously obtained wall segments are merged. As semantic segmentation produces wall elements with rugged boundaries, a boundary smoothing algorithm is conducted to finalize the wall segments (Figure 6). All wall segments are first vectorized. For any three adjacent vertices of one wall segment, the area of the triangle formed by the three vertices is calculated. If the calculated area is smaller than a certain threshold and the centroid of the triangle is outside the wall polygon, the vertex in the middle is then removed and the wall polygon is updated.

4.5. PIXEL-LEVEL SEGMENTATION & VECTORIZATION

After finalizing wall segments, room regions are extracted from the refined building elements, including walls, doors, windows and stairs, to produce the final pixel-level floor plan segmentation. Our proposed segmentation pipeline can considerably improve the room region detection completeness and accuracy for complex floor plans compared with state-of-the-art segmentation models (Figure 7). All detected architectural elements are then vectorized into polygon instances with labels, using the

Rasterio package of Python.

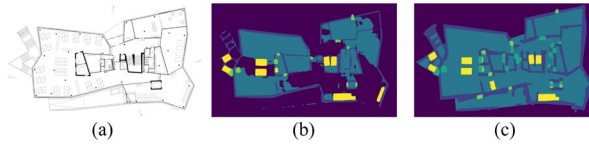


Figure 7. Comparison between room region segmentation: (a) original floor plan image; (b) original segmentation (Kalervo et al., 2019); (c) improved segmentation using proposed pipeline

4.6. REGION ADJACENCY GRAPH EXTRACTION

We adopt the RAG extraction algorithm proposed by Song and Yu (2021) to extract the region adjacency graph from the vectorized floor plan segmentation (Figure 8). To construct the node set of the region adjacency graph G , for each polygon element p in the polygon set P , if the area of p is larger than the minimum area parameter r , p is added as a node of the region adjacency graph, together with its centroid, area value and label as attributes. To construct the edge set of G , the STRtree algorithm (Pfoser et al., 2000), a spatial indexing algorithm based on R-tree, is adopted to assist the query for polygon intersection. The key idea of an R-tree data structure is to group nearby objects and represent them with their minimum bounding rectangle in the next higher level of the tree; the "R" in R-tree is for rectangles; A query that does not intersect the bounding rectangle also cannot intersect any of the objects inside the bounding rectangle. A polygon set Q is then acquired when p in the polygon set P queries the intersection function. If a polygon element q in Q has larger area than the minimum area parameter r , an edge between p and q is added to the edge set E .

Algorithm 1: RAG extraction

Input: The polygon set P of architectural elements with labels, a minimum area parameter r
Output: The floor plan RAG graph G

1. $G \leftarrow \text{Graph}()$ # Create an empty graph
2. **for** p in P **do**
3. $a = p.\text{area}$
4. **if** $a > r$ **then**
5. $c = p.\text{centroid}$
6. $l = p.\text{label}$
7. $G.\text{addNode}(p, \text{center} = c, \text{area} = a, \text{class} = l)$
8. # Build STRtree with the polygon set
9. $\text{tree} \leftarrow \text{STRtree}(P)$
10. **for** p in P **do**
11. # Query intersections
12. $Q \leftarrow \text{tree}.\text{INTERSECTS}(p)$
13. **for** q in Q **do**
14. **if** $q \neq p$ **and** $q.\text{area} > r$ **then**
15. $G.\text{addEdge}(p, q)$
15. **return** G

Figure 8. The implementation pseudo code for RAG extraction

4.7. ATTRIBUTED ADJACENCY GRAPH DISTILLATION

After obtaining the region adjacency graph of the floor plan image, a region adjacency graph distillation algorithm is implemented to extract the final attributed adjacency graphs using the NetworkX package of Python. Two types of attributed adjacency graphs are obtained: simple- and multi-attributed adjacency graphs. The distillation is implemented by replacing a node with ‘door’, ‘window’ or ‘wall’ label with an edge with the same label if the original node is adjacent to two ‘room’ nodes (Figure 9).

Meanwhile, the original edge directly connecting two ‘room’ nodes is updated to a ‘direct’ edge.

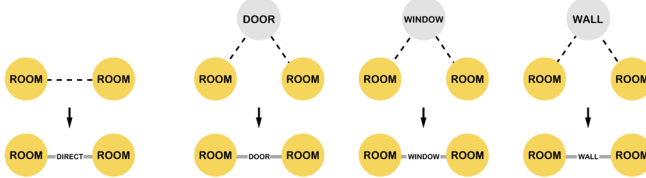


Figure 9. Distillation of RAG by replacing nodes with ‘door’, ‘window’ and ‘wall’ labels to edges with the same corresponding label if the node is adjacent to two ‘room’ nodes; Edge connecting two ‘room’ nodes is updated to a ‘direct’ edge

For extracting simple-attributed adjacency graphs, we assign an arbitrary hierarchy of edge types as follows: ‘direct’, ‘door’, ‘window’, and ‘wall’. Figure 10 visualizes the distillation process based on this predefined edge hierarchy. If two ‘room’ nodes are directly adjacent, the edge connecting the two ‘room’ nodes is updated to a ‘direct’ edge, and all in-between nodes with other labels are removed. Similarly, if two ‘room’ nodes are not directly adjacent and are connected with a ‘door’ node, the edge connecting the two ‘room’ nodes is updated to a ‘door’ edge, and so forth. The same edge updating mechanism also applies to the pairs of an ‘outside’ node and a ‘room’ node, or a ‘stair’ node and a ‘room’ node. The edge updating mechanism for multi-attributed adjacency graphs is also similar, except that there is no edge hierarchy. All nodes with ‘door’, ‘window’ and ‘wall’ labels which are adjacent to two ‘room’ nodes (or an ‘outside’ node and a ‘room’ node, or a ‘stair’ node and a ‘room’ node) are replaced with edges of the same labels while the original ‘door’, ‘window’ or ‘wall’ nodes are removed. Also, if two ‘room’ nodes are directly adjacent to each other, a ‘direct’ edge is added to connect the two ‘room’ nodes.

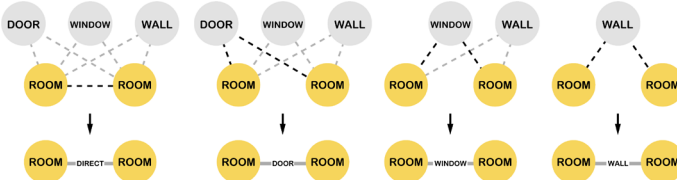


Figure 10. The edge update process based on a predefined edge hierarchy

The ‘room’ nodes of the distilled attributed adjacency graph keep the original attributes of the region adjacency graph, namely the centroid coordinates, the area values and the labels. However, the ‘outside’ nodes keep only the label attribute, and the ‘stairs’ nodes keep the centroid coordinates and labels, as the area value has no significant reference value for both node types and the centroid coordinates of the ‘outside’ nodes are meaningless. Meanwhile, to cope with the divergence of the total floor plan areas of different architecture projects, an area ratio attribute is added to the ‘room’ nodes with value $v_{\text{room_ratio}} = v_{\text{room_area}} / \sum v_{\text{room_area}}$. The polygon information of a ‘room’ node, namely the vector of coordinate values of the polygon vertices, is also attached as an attribute. The property information of a typical ‘room’ node is demonstrated in Figure 11, together with extracted samples of a simple-

attributed graph and a multi-attributed graph.



Figure 11. Left: The key value pairs of all property information of a room node in JSON format; Middle: A simple-attributed graph sample; Right: A multi-attributed graph sample

5. Discussions and Future Works

The proposed attributed adjacency graph extraction framework is implemented by leveraging existing floor plan image datasets and image segmentation models, together with rule-based graph manipulation methods. The performance of the graph extraction tool can be somehow limited by the diversity and scale of the floor plan image datasets and the performance of the image segmentation models. To further improve the accuracy for extracting attributed adjacency graphs, we outline a potential pathway to be explored in future works. The task of attributed adjacency graph extraction from floor plan image can be further decomposed into two subtasks: A) architectural elements segmentation from the floor plan image, and B) attributed adjacency graph estimation based on architectural elements segmentation. On one hand, it can be promising to leverage a scribble-based weakly-supervised segmentation approach (Lin et al., 2016) for subtask A, especially for complicated floor plans that are tedious to annotate using mask-level methods and have difficulties adopting box-level approaches for instance annotation. On the other hand, it would be beneficial to consider adopting scene graph generation techniques (Faез et al., 2021) for subtask B. The two subtasks can then be integrated and trained in an iterative manner. Meanwhile, the outputs of the two subtasks can form a self-supervision loop and enhance the performance of each other.

6. Summary

In this project, we have proposed an end-to-end framework for the task of attributed adjacency graphs extraction from floor plan images, an open challenge in literature, by leveraging state-of-the-art floor plan segmentation techniques and a series of graph data processing tools. We have also outlined some practically-likely pathways which can be further explored to improve the accuracy of attributed adjacency graph extraction from floor plan images in future works.

7. Data Availability Statement

The code and data are available from <https://github.com/JanineCHEN/AAG-FP>.

References

- Al-Jokhadar, A., & Jabi, W. (2020). Spatial reasoning as a syntactic method for programming socio-spatial parametric grammar for vertical residential buildings. *Architectural Science Review*, 63(2), 135–153. <https://doi.org/10.1080/00038628.2019.1646631>

- As, I., Pal, S., & Basu, P. (2018). Artificial intelligence in architecture: Generating conceptual design via deep learning. *International Journal of Architectural Computing*, 16(4), 306–327. <https://doi.org/10.1177/1478077118800982>
- Bronstein, M. M., Bruna, J., LeCun, Y., Szlam, A., & Vandergheynst, P. (2017). Geometric deep learning: Going beyond Euclidean data. *IEEE Signal Processing Magazine*, 34(4), 18–42. <https://doi.org/10.1109/MSP.2017.2693418>
- Faez, F., Ommi, Y., Baghshah, M. S., & Rabiee, H. R. (2021). Deep Graph Generators: A Survey. *IEEE Access*, 9, 106675–106702. <https://doi.org/10.1109/ACCESS.2021.3098417>
- Ferrando, C. (2018). *Towards a Machine Learning Framework in Space Syntax*. PhD Thesis. Carnegie Mellon University.
- Gimenez, L., Hippolyte, J.-L., Robert, S., Suard, F., & Zreik, K. (2015). Reconstruction of 3D building information models from 2D scanned plans. *Journal of Building Engineering*, 2, 24–35. <https://doi.org/10.1016/j.jobe.2015.04.002>
- He, K., Gkioxari, G., Dollár, P., & Girshick, R. (2017). Mask r-cnn. In *Proceedings of the IEEE international conference on computer vision* (pp. 2961-2969).
- Hillier, B., Hanson, J., & Graham, H. (1987). Ideas are in things: An application of the space syntax method to discovering house genotypes. *Environment and Planning B: Planning and Design*, 14(4), 363–385. <https://doi-org.libproxy1.nus.edu.sg/10.1068/b140363>
- Kalervo, A., Ylioinas, J., Häikiö, M., Karhu, A., & Kannala, J. (2019). CubiCasa5K: A Dataset and an Improved Multi-Task Model for Floorplan Image Analysis. In *Image Analysis: 21st Scandinavian Conference, SCIA 2019* (Vol. 11482, pp. 28-40). Springer.
- Kim, S., Park, S., Kim, H., & Yu, K. (2021). Deep Floor Plan Analysis for Complicated Drawings Based on Style Transfer. *Journal of Computing in Civil Engineering*, 35(2), 04020066.
- Lin, D., Dai, J., Jia, J., He, K., & Sun, J. (2016). ScribbleSup: Scribble-Supervised Convolutional Networks for Semantic Segmentation. In *Proceedings of the IEEE conference on computer vision and pattern recognition* (pp. 3159-3167).
- Lu, Y., Tian, R., Li, A., Wang, X., & Jose Luis, G. del C. L. (2021). CubiGraph5K-Organizational Graph Generation for Structured Architectural Floor Plan Dataset. In *26th International Conference on Computer-Aided Architectural Design Research in Asia: Intelligent and Informed, CAADRIA 2021* (Vol. 1, pp. 81-90). The Association for Computer-Aided Architectural Design Research in Asia (CAADRIA).
- Pfoser, D., Jensen, C. S., & Theodoridis, Y. (2000). Novel Approaches to the Indexing of Moving Object Trajectories. In *Proceedings of the 26th International Conference on Very Large Databases* (pp. 395-406).
- Renton, G., Héroux, P., Adam, S., & Gaüzère, B. (2019). Graph Neural Network for Symbol Detection on Document Images. In *2019 International Conference on Document Analysis and Recognition Workshops* (Vol. 1, pp. 62-67). IEEE.
- Song, J., & Yu, K. (2021). Framework for Indoor Elements Classification via Inductive Learning on Floor Plan Graphs. *ISPRS International Journal of Geo-Information*, 10(2), 97. <https://doi.org/10.3390/ijgi10020097>
- Stouffs, R. (2008). Constructing design representations using a sortal approach. *Advanced Engineering Informatics*, 22(1), 71–89. <https://doi.org/10.1016/j.aei.2007.08.007>
- Wu, Y., Shang, J., Chen, P., Zlatanova, S., Hu, X., & Zhou, Z. (2021). Indoor mapping and modeling by parsing floor plan images. *International Journal of Geographical Information Science*, 35(6), 1205–1231. <https://doi.org/10.1080/13658816.2020.1781130>
- yu45020. (2018). *Text Segmentation and Image Inpainting*. Retrieved February 19, 2021, from https://github.com/yu45020/Text_Segmentation_Image_Inpainting.
- Zeng, Z., Li, X., Yu, Y. K., & Fu, C.-W. (2019). Deep floor plan recognition using a multi-task network with room-boundary-guided attention. In *Proceedings of the IEEE/CVF International Conference on Computer Vision* (pp. 9096-9104).

A REMOTE SHARING METHOD OF 3D PHYSICAL OBJECTS WITH INSTANCE-SEGMENTED 3D POINT CLOUD ACQUIRED IN REAL TIME

RYO ONISHI¹, TOMOHIRO FUKUDA² and NOBUYOSHI YABUKI³

^{1,2,3}*Osaka University.*

¹*onishi@it.see.eng.osaka-u.ac.jp, 0000-0003-10130-7308*

²*fukuda.tomohiro.see.eng@osaka-u.ac.jp, 0000-0002-4271-4445*

³*yabuki@see.eng.osaka-u.ac.jp, 0000-0002-2944-4540*

Abstract. In the field of architecture and urban design, physical models are used in design meetings. Furthermore, teleconferencing via the internet has begun to be widely used in society due to COVID-19 and in preparation for disasters. Although conventional web conferencing can share only 2D information through screens, it is expected that interactive screen sharing of physical objects will enable smoother remote conferencing. A system that can manipulate point clouds in clusters by dividing real-time point clouds captured from 3D real objects by distance has been reported as a way to share physical objects. However, because the point clouds are divided by distance between the two clusters when the point clouds get closer than some threshold, they become treated as a single object. In this study, we aim to develop a system that uses instance segmentation to divide point clouds by region rather than by distance between objects. This system is expected to contribute to the realisation of better architectural and urban design processes without any misunderstandings among the parties involved and to the reduction of unnecessary energy consumption due to travel for face-to-face meetings.

Keywords. Remote Meeting; Fast Point Cloud; Instance Segmentation; Three-dimensional Remote Sharing; Mixed Reality; SDG 11; SDG 13.

1. Introduction

In the fields of architecture and urban design, physical models such as design study models and building material samples are used in design meetings to help stakeholders, including experts and non-experts, understand the content of a project. Furthermore, remote meetings via the internet and hybrid meetings that combine these two methods are beginning to be widely used in society in addition to traditional face-to-face meetings as a result of COVID-19 and in preparation for disasters. Although conventional web conferencing can share only 2D information such as images and video via a screen, there is a demand for interactively sharing physical objects on the screen to enable smoother remote conferencing.

3D virtual models can be created using computer-aided design and building information modelling and shared over a network from remote locations. However, creating a 3D virtual model from scratch is time-consuming and sharing a physical object that moves and deforms is difficult. A point cloud is a set of points with coordinates and colour information that can be acquired using a 3D scanner or RGB-D camera. As a system for sharing point clouds, a client-server system has been developed that captures a static 3D physical scene in real time and allows a large number of users to explore it (Stotko et al., 2019).

However, although this system can build 3D virtual models in mixed reality (MR) scene, it cannot manipulate them. Therefore, a system that can manipulate point clouds in clusters by using fast point cloud segmentation has been reported (Ishikawa et al., 2020). However, the Euclidean cluster method used in this study divides the point cloud by the distance between two clusters, so if the distance between point clouds is below a certain threshold, they are treated as the same.

The purpose of this research was to develop a system that uses instance segmentation to divide a real-time point cloud captured from a real 3D object by the area of the object rather than the distance between objects. This system displays the sender object and its physical object in MR as a segmented point cloud, even if the sender touches a shared physical object, and the receiver can manipulate the point cloud remotely and individually. We experimentally analysed the relationship between the number of points in the transmitted point clouds and the frames per second (fps) at which the point clouds are displayed in MR, and examined the number of point clouds that can be transmitted in real time, as well as down-sampling point clouds to make it possible to remotely share more objects in real time. This system allows the receiver to freely move and rearrange the shared objects on the sender's side, thus facilitating a teleconference for design review while communicating with the sender. This system will enable a better architectural and urban design process while resolving misunderstandings between the parties involved, contributing to SDG 11. In addition, Greenhouse Gas (GHG) emissions generated by the transportation sector are increasing rapidly, especially in emerging countries (Yan and Crookes, 2009). Smooth video conferencing can contribute to SDG 13 by facilitating remote work and reducing GHG emissions associated with commuting.

2. Previous Research

2.1. TELEPRESENCE

Telepresence (Minsky, 1980) is a technology that allows people to experience a sense of presence as if they were sharing the same space face-to-face while in a remote location. Currently, many immersive telepresence systems are being developed using augmented reality and MR, such as head-mounted displays (HMDs), to share virtual 3D information. One such system has been developed that can capture a person in a space surrounded by cameras and display an elaborate 3D avatar in a virtual space (Petit et al., 2010). However, this system is difficult to use for teleconferencing because it requires large-scale equipment. Later, the widespread availability of inexpensive RGB-D cameras such as Microsoft Kinect has led to the development of room-scale virtual space sharing. Client-server systems have been developed to capture static 3D

scenes in real time and allow a large number of users to explore them (Stotko et al., 2019). However, although such systems can build 3D models in MR, they cannot manipulate them. A system that can manipulate the created point clouds by using fast point cloud segmentation has also been developed (Ishikawa et al., 2020). However, the Euclidean cluster method used in this research divides a point cloud based on the distance between two points, so if the distance is less than a certain threshold, the points are processed as the same point cloud.

2.2. INSTANCE SEGMENTATION

Instance segmentation can classify objects of the same class and solve the problem of overlapping objects of the same class by detecting object candidate regions and creating mask images for each candidate region. It also solves the problem of overlapping classes. Because of its importance, a lot of research has been performed to improve the accuracy of instance segmentation. Mask R-CNN (He et al., 2017) is a typical two-stage instance segmentation method in which candidate regions of interest are first generated and then classified and segmented. However, this two-stage method requires reporting of features for each region of interest and processing in subsequent computations, which does not allow for real-time performance even when the image size is small. Although fast processing semantic segmentation also exists, there is still little research that focuses on fast processing instance segmentation. However, systems able to perform fast instance segmentation by performing detection and identification in parallel have been proposed, including YOLACT (Bolya et al., 2019a) and YOLACT++ (Bolya et al., 2019b).

2.3. POINT CLOUD SEGMENTATION

The conditions for inputting point cloud data into a convolutional neural network are that changing the order of the point cloud does not change the result, the relationship between close points must be preserved, and rotation and translation do not change the result. However, PointNet (Qi et al., 2017) was developed to improve the problem by segmenting the point cloud as-is. In addition, PointNet++ (Qi et al., 2019), which can recognise point clouds regardless of their density scales, was also developed. However, this method has problems, such as not being able to handle large-scale point clouds. Highly accurate point cloud segmentation methods such as 3D-BoNet (Yang et al., 2019) have also been reported, but these do not offer sufficient processing speed for real-time capability. For fast 3D segmentation, there is RangeNet++ (Milioto et al., 2019), SalsaNext (Cortinhal et al., 2020) and others. However, these are semantic segmentation, not instance segmentation, and cannot be used in this research.

In this study, we use YOLACT++, which is a fast image instance segmentation method that can operate on multiple real objects of the same class, to segment the RGB image before creating the point cloud and then classify the point cloud after combining it with the depth image by category for point cloud segmentation.

3. Proposed Method

An overview of the system is shown in Figure 1. We propose a remote-sharing system that allows a receiver wearing an MR-HMD to manipulate the point cloud of a 3D

object from real-time point clouds captured at a remote location. This method can be used at two separate locations (Sites A and B) connected by a local area network (LAN). At Site A, an RGB-D camera continuously generates a real-time point cloud of the shared real object, classifies the points into individual clusters, and stores the location, colour, and cluster labels of the point cloud data. At Site B, the MR-HMD acquires and renders the transferred point cloud data, allowing the recipient to manipulate objects individually.

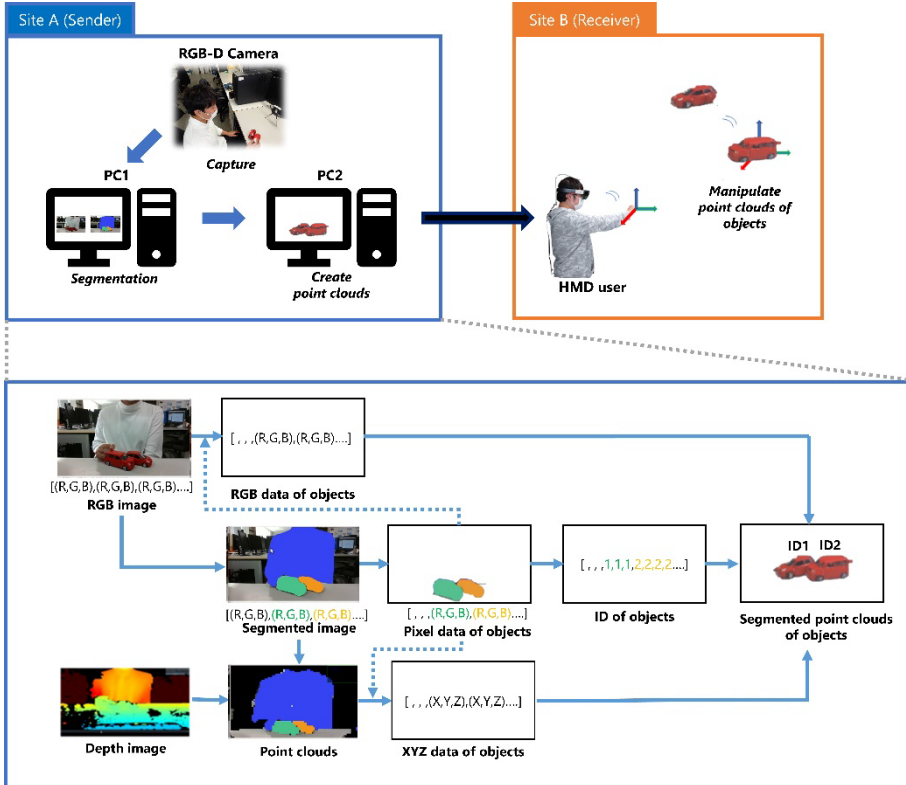


Figure 1. System overview

3.1. POINT CLOUD SEGMENTATION PROCESS

Point cloud processing first performs instance segmentation on the RGB images acquired by the RGB-D camera to obtain an array of 2D images of the object regions of the shared real object or person. Next, the RGB values of the object regions are obtained from the array of RGB images against the array information of each object region obtained, and the xyz values of the object regions are obtained from the array of point cloud images. Cluster labels are then assigned to each object region, and the data are sent to PC2 to be combined to create a point cloud segmented by instance. The real-time point cloud is then transferred to the MR-HMD at Site B via wireless LAN as point cloud data which includes coordinates, colours, and cluster labels. The number

of points in the point clouds to be created afterwards can be reduced by thinning out the 2D image array of the object region extracted by segmentation, thereby decreasing the rendering fps of the point cloud.

3.2. PROCESS OF DISPLAY AND OPERATION IN MR

For MR display and manipulation, the MR-HMD receives the point cloud data and draws the virtual object as a point cloud in the real world. The point cloud has cluster labels so that each virtual object can be identified individually, and the HMD user can use hand gestures to move each segmented point cloud up, down, left, right, forward, and backward, individually, using a pinch motion that requires the thumb and forefinger of one hand to close. In order for the viewpoint cursor to appear on the object, collision detection is used, which requires a mesh for the object. However, since it is difficult to accurately mesh the surface of a 3D point cloud, we use a convex hull to create an invisible mesh that allows pinch operations to be used.

4. Verification

In this section, we describe the verification experiments conducted to evaluate the proposed method. Section 4.2 verifies whether the proposed method can segment and manipulate objects even if they are close together. In section 4.3, we analyse the relationship between the number of point clouds to be sent and the fps at which the point clouds are displayed in MR, and verify the number of point clouds that can be sent in real time.

4.1. BUILDING A PROTOTYPE SYSTEM

We used an Intel RealSense D435 as the RGB-D camera. On PC1 running Ubuntu OS, an Intel RealSense D435i was used for RGB image, depth image acquisition, point cloud creation using the Intel RealSense software development kit (SDK), and segmentation using YOLACT ++. On PC2 running Windows OS, Visual Studio was used for MR rendering, Unity was used for output to MR-HMD, and HoloToolkit was used for frame rate measurement of the MR rendering process and point cloud manipulation. Microsoft HoloLens was used as the HMD for experiencing MR.

4.2. VERIFICATION OF OPERATION OF THE PROPOSED METHOD

The system was tested in two rooms connected by a wireless LAN. Figure 2 shows the positions of the sender, who captures the shared object using the RGB-D camera, and the receiver, who wears the HMD. In order to check whether segmentation is possible even when the sender touches the shared object, segmentation is performed while the sender touches a toy car. The results of the sender and receiver are shown in Figure 3. On the sender's side, the sender and the two vehicles are split exactly. In MR, the red car toy is extracted from the sender's hand, and only the two shared objects are transmitted. When the sender pinches the red car in the MR, only the red car in MR approaches the sender. This suggests that the point cloud of objects of the same class

at a short distance can also be divided and manipulated.

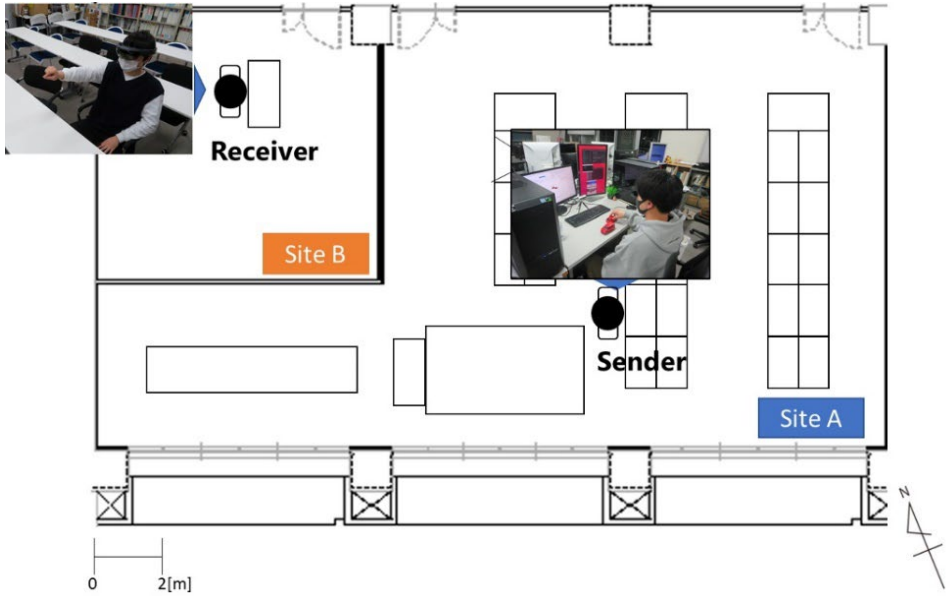


Figure 2. Verification environment

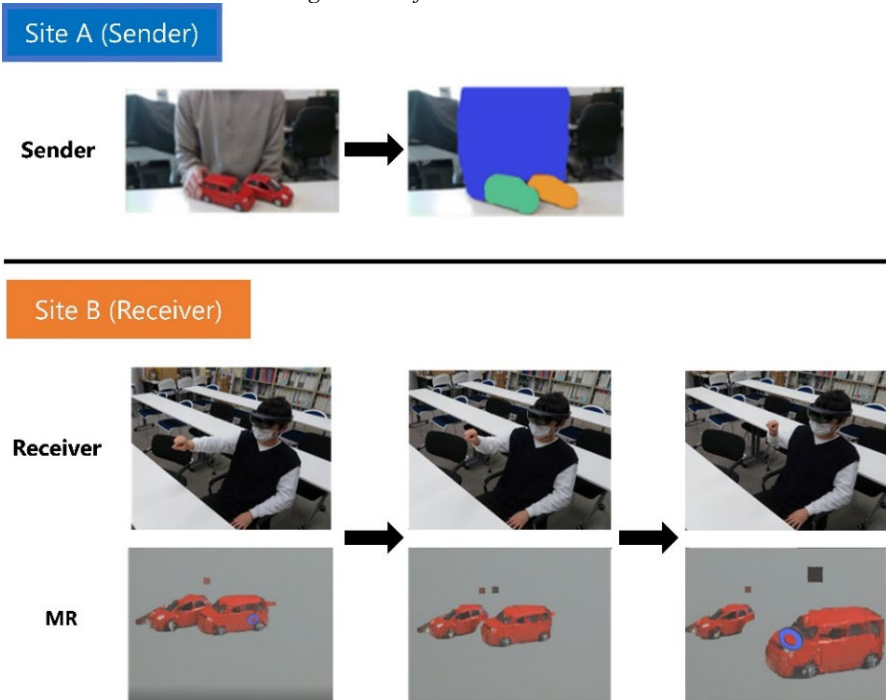


Figure 3. Verification result

4.3. EVALUATION OF POINT CLOUD DATA COMMUNICATION

In order to verify the relationship between the number of points in the point clouds and the fps rendered on the HMD, we increased the number of transmitted point clouds by 1000 units and examined the fps of rendering the point clouds in MR corresponding to each number of points 50 times. The relationship between these point clouds and the fps is shown in Figure 4. As shown in the figure, the coefficient of determination R exceeds 0.7 when expressed using the power approximation, so these values may be used for verification. From this figure, we confirmed that the number of points in the point clouds at 15 fps, which ensures real-time performance, is less than 4000 points, and after 5000 points, the rendering rate decreases to less than 15 fps, which cannot be said to have real-time performance (Chen and Thropp, 2007).

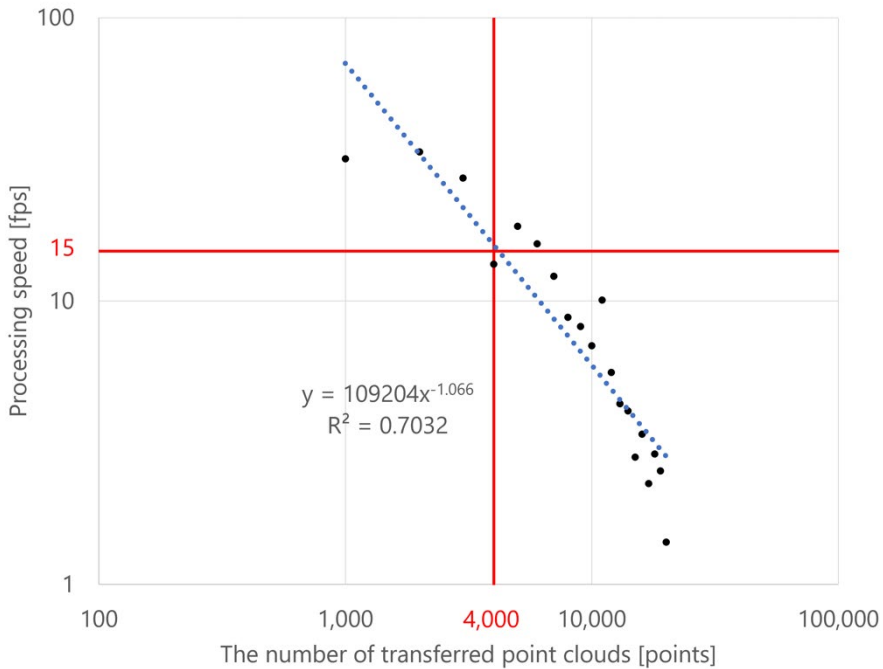


Figure 4. Relationship between rendering fps and number of points in point clouds

Next, the number of points in point clouds with about 12,000 points for the two shared objects was reduced to 1/2, 1/3, 1/4, and 1/5 by down-sampling the point clouds by thinning the 2D array. The measured average of the number of points in the point clouds and rendering fps is shown in Figures 5 and 6. The measurement results show that when the number of points in point clouds was reduced to 1/4 and 1/5, the FPS exceeded 15 fps and real-time performance was achieved. In addition, since the down-sampling process reduced the rendering fps, the difference in the number of points in point clouds that can ensure real-time performance was confirmed.

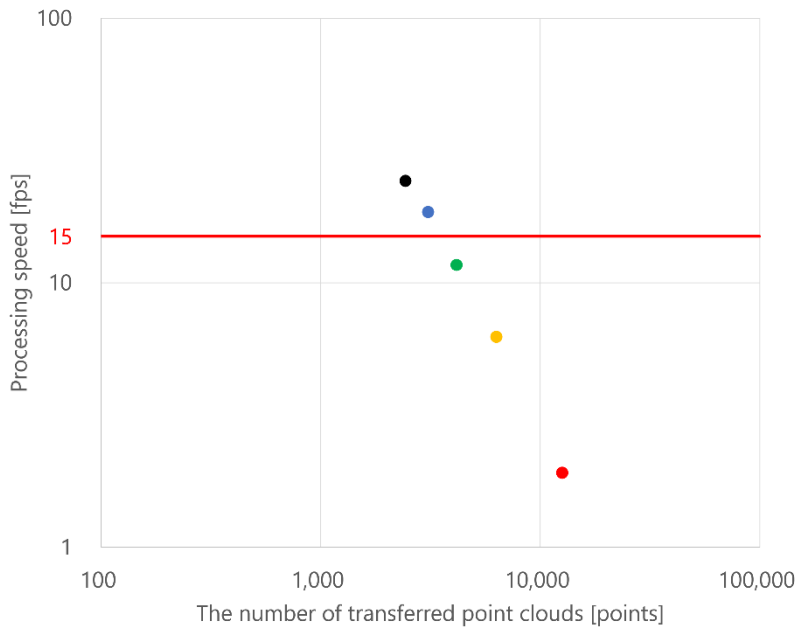


Figure 5. Relationship between rendering fps and number of points in point clouds (down sampling)

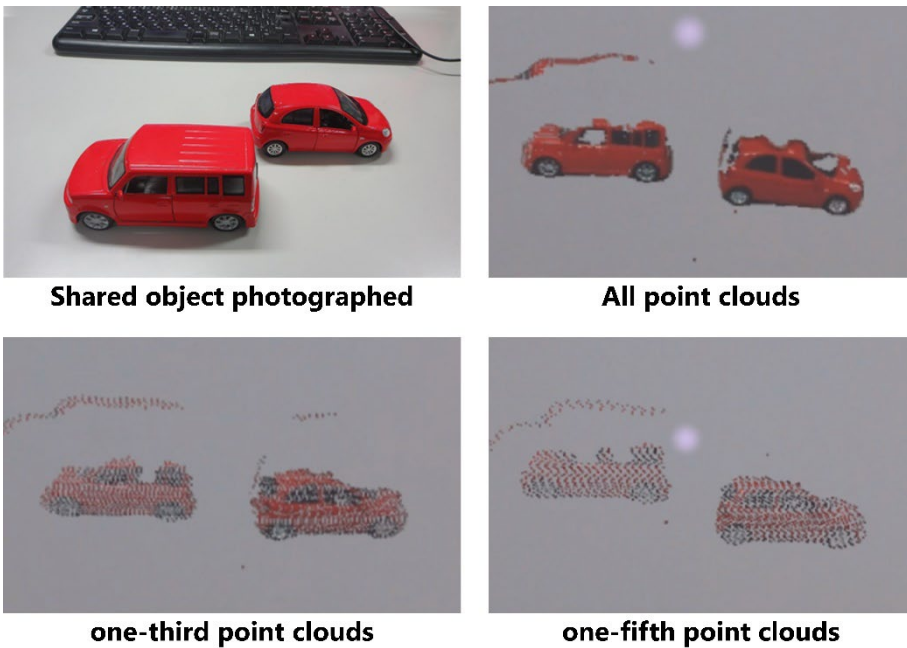


Figure 6. Down sampling result

5. Discussion

Verification of the operation of the proposed method found that the sender can extract only shared objects by dividing 3D real objects into object regions in real time by instance segmentation. On the receiver side, it was confirmed that the real-time point cloud could be segmented and manipulated individually even for objects of the same class separated by a short distance. By measuring the relationship between the number of points in the point clouds and the drawing fps, we found that the number of points in the point clouds that can ensure real-time performance is less than 4,000, and multiple objects are difficult to share. To solve this problem, we down-sampled the point clouds created by thinning out the 2D image array, and were able to render and manipulate multiple objects in MR in real time. As a result, we were able to realise a system for sharing and manipulating 3D real objects in a remote location in real time, regardless of the distance between the objects.

One issue is that if the number of points in point clouds is greatly reduced, the visibility of the point clouds of the shared object is reduced. This issue is expected to be improved in the future when the amount of data that can be transmitted is greatly increased as emerging technologies such as 5G become more widespread. Another issue was that point clouds of overlapping objects and areas not visible to the camera were missing. This problem can be solved by using multiple cameras to capture images from different angles and then combining the point clouds to create a complete point cloud of the 3D real object without any missing points.

6. Conclusion

In this study, we proposed a system for remotely sharing 3D real objects such as models that can be easily understood by stakeholders in architecture and urban design projects. Previous studies (Ishikawa et al., 2020) have raised the issue that segmentation cannot be performed when objects are closer than some threshold value. To solve this problem, we designed a system that creates a point cloud segmented by each object using instance segmentation of the point cloud and allows the object to be manipulated individually in MR even if it is touched or moved by a person, independent of distance. Objects of the same class can also be classified by instance segmentation and can be manipulated individually in MR. Even when multiple objects are shared, instance segmentation removes non-object point clouds, and down-sampling further reduces the number of point clouds, enabling real-time rendering. Issues related to when the sender's shared object is hidden and when the point cloud in the area that cannot be captured by the RGB-D camera is missing will be addressed in future work.

Acknowledgements

This research has been partly supported by the research grant of Nohmura Foundation for Membrane Structure's Technology.

References

- Bolya, D., Zhou, C., Xiao, F., & Lee, Y. J. (2019a). YOLACT: Real-time instance segmentation. *Proceedings of the IEEE/CVF International Conference on Computer Vision&ICCV* (pp. 9157-9166).
- Bolya, D., Zhou, C., Xiao, F., & Lee, Y. J. (2019b). YOLACT++: Better Real-time Instance Segmentation. *IEEE Transactions on Pattern Analysis and Machine Intelligence*, 44(2), 1108-1121. <https://doi.org/10.1109/TPAMI.2020.3014297>.
- Chen, J. Y. C., & Thropp, J. E. (2007). Review of Low Frame Rate Effects on Human Performance; *IEEE Transactions on Systems Man and Cybernetics - Part A Systems and Humans*, 37(6), 1063-1076.
- Cortinhal, T., Tzelepis, G., & Aksoy, E. E. (2020). SalsaNext: Fast, Uncertainty-Aware Semantic Segmentation of LiDAR Point Clouds, *Lecture Notes in Computer Science*, 12510, 207-222.
- He, K., Gkioxari, G., & Dollar, P. (2017). Mask R-CNN. *IEEE International Conference on Computer Vision (ICCV) 2017* (pp. 2980–2988). <https://doi.org/10.1109/ICCV.2017.322>.
- Ishikawa, D., Fukuda, T., & Yabuki, N. (2020). A Mixed Reality Coordinate System for Multiple HMD Users Manipulating Real-time Point Cloud Objects - Towards virtual and interactive 3D synchronous sharing of physical objects in teleconference during design study. *Proceedings of the 38th eCAADe Conference* (pp. 197-206).
- Live Telepresence. *IEEE Transactions on Visualization and Computer Graphics*, 25(5), 2102-2112. <https://doi.org/10.1109/TVCG.2019.2899231>.
- Milioto, A., Vizzo, I., Behley, J., & Stachniss, C. (2019) RangeNet ++: Fast and Accurate LiDAR Semantic Segmentation. *IEEE International Conference on Intelligent Robots and Systems* (pp. 4213-4220). <https://doi.org/10.1109/IROS40897.2019.8967762>.
- Minsky, M. (1980, June). Telepresence. *OMNI Magazine*, 44-52.
- Petit, B., Lesage, J.-D., Menier, C., Allard, J., Franco, J.-S., Raffin, B., Boyer, E. & Faure, F. (2010), Multicamera Real-Time 3D Modeling for Telepresence and Remote Collaboration. International, *Journal of Digital Multimedia Broadcasting* 2010, 247108. <https://doi.org/10.1155/2010/247108>
- Qi, C. R., Su, H., Mo, K., & Guibas, L. J. (2017). PointNet: Deep learning on point sets for 3d classification and segmentation. *Proceedings of the IEEE Conference on Computer Vision and Pattern Recognition* (pp. 652-660).
- Qi, C. R., Su, H., Mo, K., & Guibas, L. J. (2017). PointNet++: Deep hierarchical feature learning on point sets in a metric space. In *31st Advances in Neural Information Processing Systems (NIPS 2017)* (pp. 5099-5108).
- Stotko, P., Krumpfen, S., Hullin, M. B., Weinmann, M., & Klein, R. (2019). SLAMCast: Large-scale, real-time 3D reconstruction and streaming for immersive multi-client live telepresence. *IEEE transactions on visualization and computer graphics*, 25(5), 2102-2112.
- Yan, X., & Crookes, R. J. (2009). Reduction potentials of energy demand and GHG emissions in China's road transport sector. *Energy Policy*, 37(2), 658-668. <https://doi.org/10.1016/j.enpol.2008.10.008>
- Yang, B., Wang, J., Clark, R., Hu, Q., Wang, S., Markham, A., & Trigoni, N. (20). Learning Object Bounding Boxes for 3D Instance Segmentation on Point Clouds. In *33rd International Conference on Neural Information Processing Systems* (pp. 2940-2949).

ON-SITE HOLOGRAPHIC BUILDING CONSTRUCTION

A Case Study of Aurora

SIJI LIU¹, ZIRU WEI² and SINING WANG³

^{1,2,3}*School of Architecture, Soochow University.*

¹*1912865039@qq.com, 0000-0003-2443-7760*

²*1064901102@qq.com, 0000-0001-8312-9421*

³*snwang@suda.edu.cn, 0000-0002-3466-6201*

Abstract. Geometrically complex building components' reliance on high-touch implementation often results in tedious information reprocessing. Recent use of Mixed Reality (MR) in architectural practices, however, can reduce data translation and potentially increase design-to-build efficiency. This paper uses Aurora, a single-story residential building for 2021 China's Solar Decathlon Competition, as a demonstrator to evaluate the performance of on-site holographic building construction. This paper firstly reviews recent studies of MR in architectural design and practice. It then describes an MR-aided construction process of Aurora's non-standard building envelope and rooftop mounting structure, where in-situ holographic registration, human-machine cooperation, and as-built analysis are discussed. This paper concludes by stating that MR technologies provide unskilled implementers with a handy approach to materialise complex designs. The research was guided by the UN Sustainable Development Goals, especially aligning with the GOAL 9 which seeks innovations in industry and infrastructure.

Keywords. Mixed Reality; Non-standard Architecture; Low-tech Construction; Solar Decathlon Competition; SDG 9.

1. Introduction

Architects' use of computation-driven design techniques has widely expanded their design solution space, leading to a proactive exploration of complex architectural forms. Conventional design annotation methods may appear inefficient, especially in construction environments lack of advanced fabrication means and skilled labourers, the 3D-to-2D translation of non-standard design intent can be tedious and repetitive. The recent use of Mixed Reality (MR) among experimental architectural projects, however, suggests a new path for virtual-actual interactions. By projecting computationally generated geometries onto the field of vision with wearable devices or smartphones, it creates an immersive environment for implementers. The interactive holography allows architects to translate design intentions to intelligent instructions instead of static plans and sections, offers a significant opportunity to

reduce construction complexity, and potentially increases precision (Jahn et al., 2018). MR-based architectural design practices are situated within a post-digital context, where the humanisation of digital is addressed via the interplay between digital and analogue culture, between high-tech and high-touch experiences, between global and local matters (Crolla, 2018). It presents a refined human-machine interaction that extends human intuition and tactile sense, and encourages collaborative knowledge that emerged from on-site serendipity. By constructing an information feedback loop between the as-built condition and the digital model, MR-based architectural practice improves designers' capacity to respond and adapt to local idiosyncrasies.



Figure 1. Aurora in snow (Zhang Jiakou, China, 2021)

This research aligns with the GOAL 9 of UN Sustainable Development Goals which seeks innovations in industry and infrastructure. It uses Aurora, a single-story passive residential building designed for 2021 China's Solar Decahedron Competition (SDC), as a demonstrator project to discuss the process and performance of on-site holographic construction (Figure 1). Aurora was built in Zhang Jiakou, China, in August 2021 with its main steel structure and partial components had been prefabricated in a Suzhou factory. In order to increase resource-use efficiency and reduce construction waste, the building was transported and assembled in modules. The challenge left to the construction team, consisting of mostly college students with no on-site experience, is the realisation of a non-standard building envelope made of flipped panels and a laminated bamboo mounting structure for the solar system. With the help of holographic instructions provided by Microsoft HoloLens and smart devices, unskilled students were able to assemble these parts in a short time with precision.

This research aims to illustrate human's extended implementation capacity enhanced by MR technology and whose feasibility for real-world architectural practices. It argues that such human-machine interaction breaks away from a conventional paradigm of design annotation, allows on-site implementers to directly communicate with digital design models, therefore stimulating a successful delivery of non-standard design.

2. MR in Building Practice

Paul Milgram and Fumio Kishino (1994) defined MR as a continuum of virtual reality technologies that overlays virtual objects with in-situ conditions. Today, MR is ubiquitously available to the general public with SDK such as ARCore and ARKit for smart devices. MR-based applications, therefore, have been adopted across various research fields including design, education, and entertainment. Within building industries, most fabrication and construction processes still heavily rely on human operations despite the dramatic rise of robotic automation. MR technologies, comparatively speaking, aim to augment manual operations instead of removing human factors off the equation. By providing holographic visual guidance like operating checklist and instructions, architectural designers can maximize the use of building information model.

Recent studies mainly focus on MR-aided architectural design innovations, human-centric manual fabrication and assembly tasks. Meža et al. (2015) applied holographic instruction to track and monitor the process of construction projects; Fazela and Izadi (2018) introduced an interactive tool for constructing complex modular surfaces in Mix Reality environment; Goepel (2019) tested MR with HoloLens in the assembly of non-standard prefabricated elements based on an optimized parametric structure. Mitterberger et al. (2020) referred to the major deficiency derived from the previous MR-aided manual constructions is the insufficient alignment of the digital model with the physical environment. In response, they presented a customized MR system based on an object-based visual-inertial tracking method in the construction of a brick envelope. This system, however, requires future development of app-based applications for HMD or smart devices otherwise cannot be pervasively feasible to building constructions across different contexts.

Marker-based 3D registration technique is currently widely used in Virtual Reality (VR) and MR applications. Developed by Gwyllim Jahn, Cameron Newnham, and Nicholas van den Berg, Fologram is among the popular MR applications adopted by architectural researchers, designers, and builders. Its capacity to connect with the parametric procedural modelling allows users to make ad-hoc design modifications according to site-specific conditions and restrictions. The dynamic holographic projection that Fologram creates can potentially establish a real-time feedback loop between the virtual objects and the actual builds. Research projects worked with Fologram, such as Timber De-Standardized (Lok et al., 2021), Augmented Grounds (Hahm et al., 2020), and Steampunk Pavilion (Jahn et al., 2019), revealed a strong bond between design intention, visual instructions, and tangible operations.

However, outdoor building-scale experiments still require further investigation because the accuracy of a marker-based registration can easily be influenced by matters such as lighting condition, project size, and user's field of vision. This paper discusses an MR-aided construction process of Aurora's non-standard envelope and mounting structure. It examines the potential use of Fologram and HoloLens in real-world building projects within an outdoor environment. The major research goals include the increase of marker-tracking accuracy by working with associative modelling, the test of system stability within volatile environment, and the exploration of in-situ human-machine collaboration.

2. The Aurora Case

As a joint research project carried out by Technical University of Denmark and Soochow University, Aurora's design and construction aimed to demonstrate the integration of energy-efficient systems, the use of environmental-friendly building materials, and the adoption of BIM for paperless project delivery. The entire realisation process lasted a month including off-site prefabrication and on-site assembly.

2.1. DESIGN OF BUILDING ENVELOPE

Aurora's envelope was designed to study how computation can offer design opportunities while maintaining construction rationality for the sake of a high-touch implementation. The design of the continuously varying façades not only intended to address an image of Aurora but also to respond to façade performance. With McNeel Rhinoceros and its procedural modeller plug-in Grasshopper, the pattern was visualized through differentiated flipping of bamboo panels which have been designed with the same height of 100mm but in different lengths due to openings of doors and windows. There are in total 2303 panels of 42 types used in Aurora's envelope and they are staggered in a vertical direction and overlaid by 20mm for the sake of water penetration (Figure 2).



Figure 2. The use of laminated bamboo material in Aurora's façade

The shape of the pattern was influenced by a NURBS control curve and the solar radiation of the site. Two major variables were determining the flipping angle of a bamboo panel: the relative distance between the geometric centre of the panel unit and its closest point on the control curve; also, the solar radiation intensity it gets during a summer day. The closer a panel to the curve and the more energy it receives; the larger angle it flips (Figure 3). These flipped panels help to reduce exterior wall temperature and humidity in summer by stimulating passive ventilation in between façade layers.

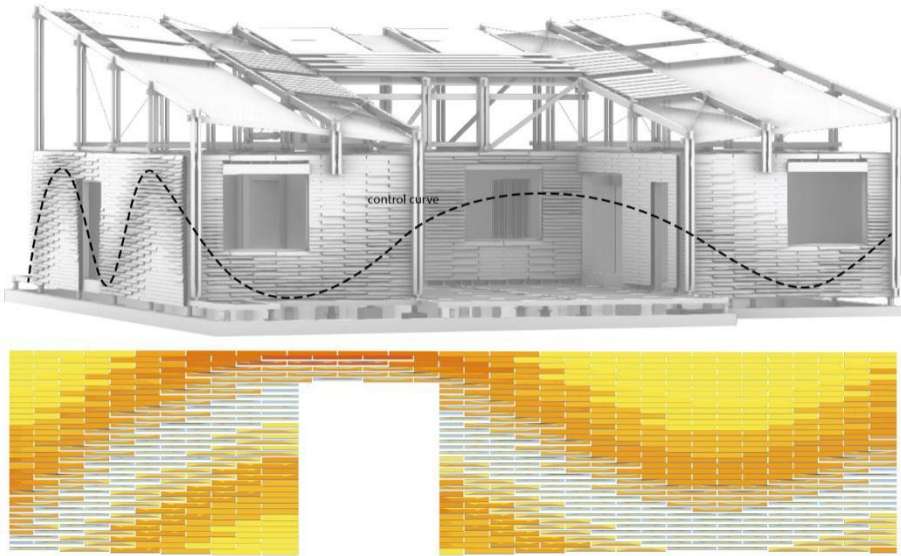


Figure 3. Design variables defining panels' flipping angles: a control curve (up) and the intensity of solar radiation (bottom)

2.2. DESIGN OPTIMIZATION AND PREFABRICATION

A visually smooth pattern is made of continuous differentiated flipping panels which, however, was impossible to realize in this case. Since the students decided to take over façade materialisation, the initial design intention must be optimized to accommodate a high-touch implementation process by unskilled labourers. Figure 4 shows an assembly diagram of the non-standard building envelope, where the bamboo panels were cut into needed lengths and mounted on vertical wood keels using self-tapping screws. The flipping mechanism is the angle blocks connecting the panels and the keels, and these wood blocks had to be manually fabricated by students and later installed in position. Hence, in order to seek a feasible design solution not only meets the aesthetic demand and the ventilation performance, but also accommodates low-tech operations, the design team eventually adopted four types of flipping angles in 25, 40, 55, and 70 degrees.

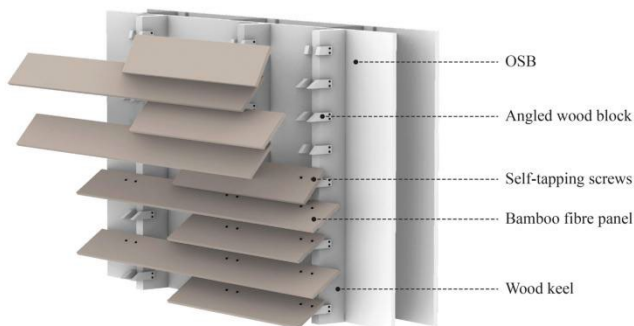


Figure 4. Assembly diagram of the non-standard building envelope

All of Aurora's components were pre-fabricated within a factory in Suzhou. The building was divided into 5 modules for the sake of road transportation. Before arriving on site in Zhang Jiakou, most of the building exterior parts have been installed except the bamboo panels and the mounting structure for solar system. It only took four hours to position and assemble the modules on-site (Figure 5).



Figure 5. From left to right: students cut bamboo panels; position a module to the foundation; and the on-site assembly of five modules

2.3. MR-AIDED CONSTRUCTION

To reduce on-site construction complexity, the implementation team adopted Fologram with HoloLens and handheld smart devices to assist the assembly of bamboo panels and mounting structures for the solar system. A portable hotspot device was brought to the site to ensure a live link between the holographic instructions and the parametric model. By setting parameters to control model movement, rotation, and display colours, implementers were able to fine-tune the alignment between virtual and actual objects, and to adjust projection clarity according to the lighting condition at the time. The MR implementation team relied on ArUco marker to map the design model to the as-built environment. Because both HoloLens and smart devices track 2D markers through a front camera, the team placed three 600*600mm ArUco markers to the designated positions. This allowed the implementers to register from a relatively further distance and to amend alignment at need.

In the construction of Aurora's non-standard envelope, the implementation team applied five different colours to identify flipping and non-flipping panels (Figure 6). Through HoloLens and iPad, this colourized model was holographically presented to the field of vision of the implementers. Also, to make it convenient for camera tracking, the implementers placed the ArUco markers both vertically on the wall and horizontally on the ground. A parametrically flexible projection helped to reduce the misalignment that has been caused by the deviation from previous module assembly and the issue of model drifting. In the beginning, a student implementer wearing HoloLens had labelled all the flipping types on each wood keel so that others without holographic instructions were able to install angled wood blocks simultaneously.

Since all the installation work was carried out manually by inexperienced students, construction deviation was inevitable. The augmented implementers, fortunately, could make ad-hoc adjustments based on the projection of an initial design idea, and make up construction errors to the greatest extent (Figure 7). To illustrate this point, Aurora's non-standard facade was finished within 3 days by 12 people.



Figure 6. Holographic projection of Aurora's facade on actual building

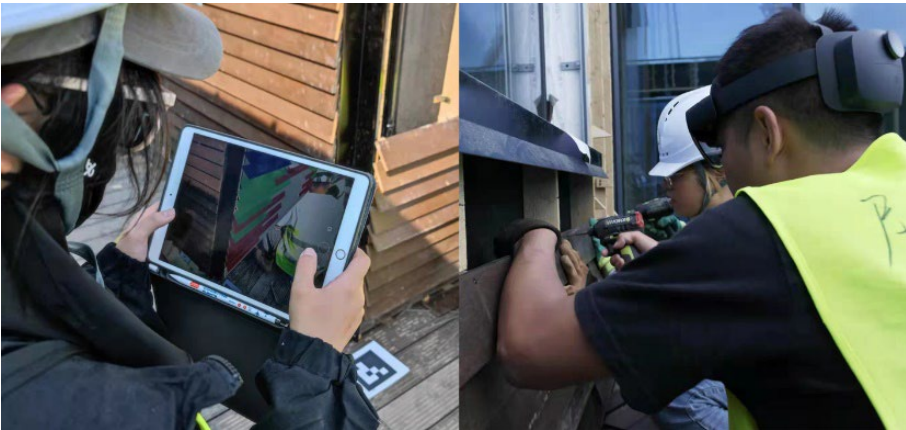


Figure 7. 3D registration with iPad (left); augmented panel installation with HoloLens (right)

The implementation team also adopted MR technology to assist the positioning and the assembly of rooftop mounting structure. Made of laminated bamboo strips, the mounting structure of solar system consists of 112 components that were pre-fabricated in Fujian Province. The plan to preassemble the structure on the ground and lift in one piece turned out to be impractical due to site restrictions and a potential irreversible deformation. The implementation team, instead, had decided to install these components one at a time directly on the roof, which extensively increased the construction difficulty. The holographic projection of the design model provided the

implementers a general sense of the structure in place (Figure 8) and enabled them to coordinate with the crane operator more effectively.

Since an accumulation of construction deviation is inevitable in this case, MR technology offered the implementer an approach to increase construction tolerance. By accordingly modifying the design model based on the structural components which have been installed on the roof, the implementers were able to continuously assess constructability and reshaped the uninstalled ones. For example, some of the structural components had to be trimmed in length and their pre-drilled holes were also re-made so that they could fit in place.



Figure 8. Holographic projection of the overall structure model

2.4. AS-BUILT ANALYSIS

Virtual-actual feedback is crucial to ensure implementation accuracy in a high-touch construction process. The above-mentioned materialisation processes can potentially lead to the actual building deviates greatly from the design model. Therefore, the project team had retrieved the as-built information and compared it with the initial design data, so that they were able to identify areas demand adjustment or reassembly.

Aurora's exterior as-built information was collected using a FARO laser scanner (Figure 9). The point cloud data was generated from in total seven scanning stations, then being integrated and converted to mesh objects. By overlaying the initial design model on top of the recreated one, the project team was able to calculate virtual-actual differences. Taking part of the south facade as an example, the project team appointed the cuboid geometry of the sunshade system as the overlaying reference, then analysed the differences between the scanned mesh model to the designed model. The green area in the figure10 means the deviation value is within 10mm. However, the red and blue dots represent the built panels are in front of or behind the designed ones. Deviations range from 10mm to 50mm and darker colours indicate larger distances. Based on the result, the implementation team adjusted some of the installed bamboo panels. Again, through Fologram and HoloLens, revising instructions were holographically presented to on-site implementers so that they were able to locate and fix the problem in short time.

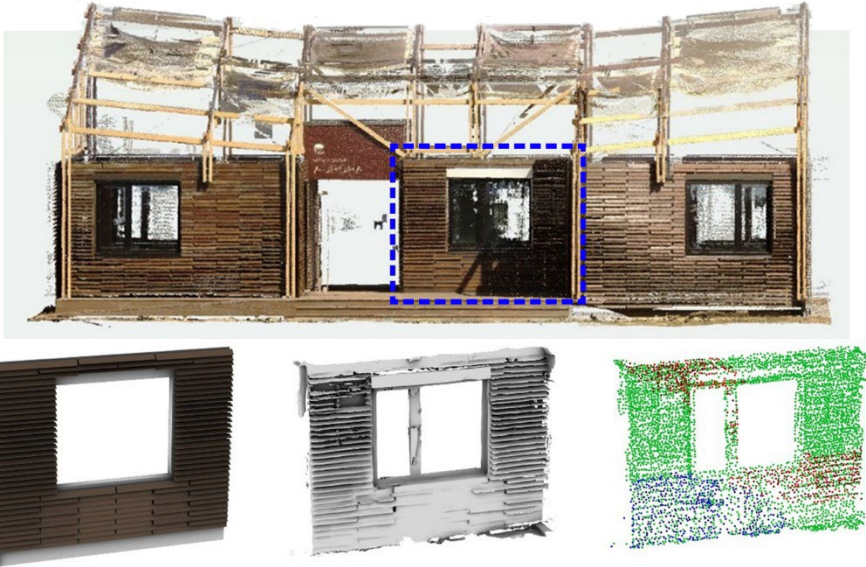


Figure 9. Aurora's exterior as-built information by laser scanner (up) and error analysis of a façade from the South elevation (down)

3. In conclusion

The use of MR technology in the construction of Aurora's non-standard envelop and the mounting structure for the solar system demonstrates how the participation of MR leads to the reform of the construction process, and reveals the potentially wide application of the highly effective low-tech implement. By removing the redundant annotation work from a design-to-build workflow, MR technology increases architects' agency in design exploration and materialisation. This study presents a real-time interaction between virtual and actual matters. Opposing to pre-programmed 'high-tech' robotic fabrications and assemblies, the MR-based human-machine collaboration promises architects an increasing role in today's post-digital discourses. Instead of chasing zero-tolerance implementation and avoiding any potential deviations, MR-aided design practices aim to increase construction allowance by injecting computation into human operations. This sheds light on the construction activities that still heavily rely on manual labour. Especially for non-standard building practices that are carried out within developing regions, the involvement of holographic instructions makes the entire implementation process more systemic and resilient to meet design expectations. Also, the easy access to hardware devices like HoloLens and smartphones, together with their MR applications such as Fologram and TwinBuild, lowers the threshold for adopting this technology in action.

Compared to small-scale architectural experiments or full-scale research projects that have taken place in controlled lab environments, the holographic construction of Aurora investigated the influence of outdoor matters, like sunlight and temperature, to a precise overlay of the digital information. The study discusses a marker-based

approach for on-site alignment. The use of parametric associative modelling allows the implementers to procedurally control data outputs. In return, this allows them to absorb process uncertainties and to accommodate project-specific idiosyncrasies. Demanding feedback from an as-built condition and followed by corresponding adjustments also indicate a potential workflow change in project delivery. This leads to a more productive dialogue between designers and implementers. With MR's accessibility and quick response, architects might delay decision-making and further expand the design solution space.

Acknowledgements

This research was funded by Natural Science Foundation of Jiangsu Higher Education Institutions (grant No. 20KJB560022) and by College Students' Innovative Entrepreneurial Training Plan Program (project No. 202110285017Z).

References

- Crolla, K. (2018). Building Simplicity: The “more or less” of post-digital architecture practice [PhD Thesis]. RMIT University.
- Fazel, A., & Izadi, A. (2018). An interactive augmented reality tool for constructing free-form modular surfaces. *Automation in Construction*, 85, 135-145. <https://doi.org/10.1016/j.autcon.2017.10.015>
- Goepel, G. (2019). Augmented Construction - Impact and opportunity of Mixed Reality integration in Architectural Design Implementation. In *39th Annual Conference of the Association for Computer Aided Design in Architecture: Ubiquity and Autonomy, ACADIA 2019* (pp. 430-437). The Association for Computer Aided Design in Architecture (ACADIA).
- Hahm, S., Lee, Y., & Jung, J. H. (2020, October 21). *Augmented Grounds Landscape Design Installation*. Archdaily. Retrieved February 13, 2022, from <https://www.archdaily.com/949961/augmented-grounds-landscape-design-installation-soomeen-hahm-design-plus-yumi-lee-plus-jaecheon-jung>
- Jahn, G., Newnham, C., & Beanland, M. (2018). Making in Mixed Reality. Holographic design, fabrication, assembly and analysis of woven steel structures. In *38th Annual Conference of the Association for Computer Aided Design in Architecture (ACADIA)* (pp. 88-97). The Association for Computer Aided Design in Architecture (ACADIA).
- Jahn, G., Newnham, C., Hahm, S., & Pantic, I. (2019, October 11). *Steampunk pavilion*. Archdaily. Retrieved February 13, 2022, from <https://www.archdaily.com/926191/steampunk-pavilion-gwyllm-jahn-and-cameron-newnham-plus-soomeen-hahm-design-plus-igor-pantic>
- Lok, L., Samaniego, A., & Spencer, L. (2021, August 25). *Timber de-standardized*. Cornell Architecture Art Planning (AAP). Retrieved February 13, 2022, from <https://labs.aap.cornell.edu/rubi-lab/research/de-standardized-timber>
- Meža, S., Turk, Ž., & Dolenc, M. (2015). Measuring the potential of augmented reality in civil engineering. *Advances in Engineering Software*, 90, 1-10. <https://doi.org/10.1016/j.advengsoft.2015.06.005>
- Milgram, P., & Kishino, F. (1994). A taxonomy of mixed reality visual displays. *IEICE TRANSACTIONS on Information and Systems*, 77(12), 1321-1329.
- Mitterberger, D., Dörfler, K., Sandy, T., Salveridou, F., Hutter, M., Gramazio, F., & Kohler, M. (2020). Augmented bricklaying. *Construction Robotics*, 4(3), 151-161. <https://doi.org/10.1007/s41693-020-00035-8>

ARCHITECTURE VALUE CHANGE IN RESPONSE TO THE ANTHROPOCENE: THE CONTRIBUTION OF DIGITAL INNOVATION

DERMOTT MCMEEL¹ and EMINA K. PETROVIĆ²

¹ *AUT University, Auckland, New Zealand*

² *Victoria University of Wellington, New Zealand*

¹ *dermott.mcmeel@aut.ac.nz, 0000-0002-3790-3444*

² *emina.petrovic@vuw.ac.nz, 0000-0003-3446-093X*

Abstract. The confluence of different interests—the Anthropocene, productivity, sustainability, economics—calls for a need to re-think how the professions evaluate the built environment. There is a myriad of different strands of work under this umbrella which—broadly—point to a shift in the value framework for those people and professions who have agency in, and are responsible for, the creation of the built environment. This paper has two objectives. First, by drawing from the writing of architectural theorist Juhani Pallasmaa it teases out themes useful to conceptualise the value change. The goal is to delineate particular views around the creation of and our relation to the built environment. Second, it presents three projects: (1) tracking chemical composition of construction materials, (2) an app that encourages e-commerce in building multi-species environments, and (3) a concept for an economy in construction waste leveraging possibilities presented by blockchain technology. The aim is to shed light on how the emerging blockchain technology might alter values and organisational systems of the built environment in response to the Anthropocene and climate crisis.

Keywords. Design; Anthropocene; Value Change; Blockchain; System Design; SDG 9; SDG 11; SDG 12.

1. Introduction

In 1992 at a symposium in Trondheim the architectural theorist Juhani Pallasmaa was arguing that architecture was becoming a highly self-referential and over-intellectualised pursuit. Architects were losing sight of the inhabitant, those that 'dwell' in their creations (Pallasmaa, 1992). He cites the court case of Mies van der Rohe versus Farnsworth, who was claiming the famous Farnsworth House was unsuitable as a home. Conversely, the house—architecturally speaking—is recognised as one of the most important buildings of the century. The court, incidentally, agreed that the contribution the house made to architecture trumped its deficiencies as a home.

This example brings into sharp relief the tension between different value frameworks for valuing architect and the built environment. Viewed one way, the

Farnsworth House has questionable value to the client and the dweller. Viewed another, it is valued highly to the professional disciple of architecture. This tension is central to the challenges of the discipline of architecture for much of the 20th century and into the 21st century. Since Pallasmaa's presentation in 1992, we have been through the age of the Starchitects (Fajardo, 2010; Klimek, 2013), where, possibly, both the architect and the architecture were celebrated over and above the environments they create. Arguably more recently this has progressed further with a current shift to architecture being valued for its 'instagrammability' and a presence on the video focused social media platform TikTok (Wainwright, 2018, 2021).

However, this tension between the architect and the client/dwellers is further complicated when faced with the Anthropocene, climate change, and the need to consider the planet as a third interested party. While the client/dwellers, as people, have always been able to express their interests, the planet needs the others to speak on its behalf. Yet, sustainable and passive buildings seem to continue as specific categorical sub-sets of architecture rather than core of the mainstream. Further to that, much of the existing work in this space is limited to carbon considerations and the well-recognised need to optimise existing practices; which are important, but that is not all that is needed. The built environment contributes to the devastation of the planet through significant material extraction, landfill disposal, and toxicity of construction materials.

This is the tension—the value shift—being explored in this paper. It asks: How do we support better inclusion—and valuing—of complex considerations of planetary needs in architecture? How can digital technologies accelerate these needed changes? But most importantly, what sort of value framing is needed for a shift away from self-referential Starchitects criticised by Pallasmaa to architects proactively re-shaping human engagement with the planet for the betterment of all.

The paper links with a range of United Nations Sustainable Development Goals (SDGs): most directly with SDG11: sustainable cities and communities; SDG9: industry, innovation and infrastructure; and SDG12: responsible consumption and production, because it is proposing a different way of thinking about sustainable architecture through innovative reshaping of industry and consumption. The examples presented in Section 4 aspire to contribute to improved health of people, and life on land and below water (SDG3; SDG14; SDG15).

1.1. PAPER OUTLINE

Section 2 looks at the material extraction and other planetary costs associated with designing and constructing built environment. Section 3 delineates and unpacks two conceptual themes, which serve as a way to organise particular changes in this shift away from Pallasmaa's concern for the 'self-referential.' These themes point to a shift from an *assertoric* gaze to an *alethic* gaze; also drawn from Pallasmaa's writings they provide a language to explore the implications for architecture. Finally, Section 4 discusses three projects that shed light on social and organisational systems that are reorienting around these values.

2. On Material Extraction

In the developed world it is estimated that construction contributes to almost half of all

planetary material extraction and one to two thirds of all municipal landfill waste (Behrens et al., 2007; Bossink & Brouwers, 1996; Purushothaman & Seadon, 2020; Schandl et al., 2018; Schandl & Eisenmenger, 2006). For example, despite currently not being recognised as an issue, aggregate extraction of sand and gravel, primarily for use in construction, is by volume the largest extraction of any solid material on the planet, with extraction rate exceeding natural replenishment rates and already causing coastal erosion and ecosystem destruction (UNEP, 2019). On the other side, in recent years some real progress with recycling rates of construction waste has been noted in the European Union due to regulations requiring a high level of recycling (EEA, 2021). The issue remains that much of such recycling is downcycling of masonry waste into backfill, and possibly excessive backfill (EEA, 2021). Further issue is that such practices are not an international norm, with other countries, like the United States reporting that as much as 90% of construction and demolition waste is actually demolition waste (EPA, 2021), due to buildings not being built to easily dismantle.

There are several reasons for this high level of extraction and subsequent waste from construction. First, in many parts of the world overconsumption and waste are built into the business of construction. It is a percentage that is presumed lost and thus tendered against the total cost of a project. Suppliers may provide extra material to a contractor at no additional cost. Typically, this is an informal social contract intended to increase the likelihood of the contractor returning to the supplier for future orders. Second, there are cultural factors. Anecdotal evidence points to contractors in the small to medium enterprise category (SME) using surplus to increase resilience. For example, moving it between projects, offsetting a deficit on one site by moving surplus from another. Third, building materials in many cases are complex composites not designed for decomposition and recycling. Finally, the built environment is still not designed for deconstruction, when a building is no longer fit for purpose, most of it will end up in landfill.

Further to that, there is insufficient information on how many—up to 95%—of the chemicals used in construction products impact health (Pacheco-Torgal, 2012). Inadequate recognition of health risks associated with construction materials is a complex problem (Petrovic et al., 2017), amplified by the limitations of the existing scientific knowledge (Binetti et al., 2008). This limits accuracy of the reports such as Environmental Product Declarations which are based on the available knowledge (EPD Australasia, 2021). Chemicals harmful for humans tend to also present issues for natural ecosystems, and improvements in this area are much needed for less adverse impacts of built environment on the planet.

In order to develop more sustainable solutions, a shift out of these patterns is needed, which is why it is important to question the values and agency that underpins the creation of the built environment. If we bring into the consideration the voice of the planet, it is clear that such patterns cannot continue because architecture has to find the way for effective inclusion of planetary interests. That means developing systems to help articulate this relationship, which needs to include carbon reductions, material extraction, toxicity, waste and carefully evaluating other impacts on the ecosystem.

3. Themes for the Anthropocene

In order to develop a better understanding of the dynamics which might be at play

behind the values discussed here, this section unpacks the two themes as defined by Pallasmaa: the assertoric gaze and the alethic gaze. They present two possibilities for different ways to see and value the built environment, either as designer or as inhabitant.

3.1. THE ASSERTORIC GAZE

Assertoric is an Aristotelian proposition, Pallasmaa's appropriation puts forward the 'assertoric gaze' as one of two modes of vision.

"The assertoric gaze is narrow, dogmatic, intolerant, rigid, fixed, inflexible, exclusionary and unmoved." (Pallasmaa, 2012, p. 34)

It could be argued that the celebrated architecture of the 20th century is based on this type of 'gaze'. Projects and people that have been elevated in importance often have the characteristics of dogmatic in personality; or a process or vision that—under pressures—remained focused, fixed and unmoved.

Our opening example of Mies van der Rohe's Farnsworth House illustrates the limitation of this view; a thing highly valued from one perspective be profoundly flawed from others. So, while this gaze has been useful for inspiring and communicating by simplifying architecture and its ideologies, this paper suggests it is increasingly inadequate for engaging with the complexity of the needs to frame, value and articulate 'architecture' within the context of the Anthropocene. Concerns over material toxicity, waste and carbon footprints are continuing to increase. The discourse finds itself wanting a more pluralistic multi-standpoint lens through which to view express the built environment - what Pallasmaa refers to as an 'alethic' gaze.

3.2. THE ALETHIC GAZE

Pallasmaa discusses his appropriation of the 'alethic' gaze.

"The alethic gaze, associated with the hermeneutic theory of truth, tends to see from a multiplicity of standpoints and perspectives, and is multiple, pluralistic, democratic, contextual, inclusionary, horizontal and caring." (Pallasmaa, 2012, p. 34)

An alethic gaze shifts away from narrow dogma, whether that is aesthetics or ideology or geometry. It moves instead towards a multiplicity of values (material toxicity, energy efficiency, waste), this is an important fundamental shift in the way society sees and values the built environment, from assertoric to alethic. The value of a building or collection of buildings is fundamentally changed. While their aesthetic value or architectural ideology is not necessarily overlooked, the alethic gaze is asking for more context and data to evaluate the architecture. A useful analogy may be the difference between data (information) and metadata (data about the information) (Duval et al., 2002). To evaluate a piece of data or information, its metadata is interrogated. We use: author; date of publication; publisher; who is citing—or dismissing—the information and where. To extend this analogy to our current topic, the alethic gaze suggests a shift away from looking at a single piece of architecture and instead is searching for what we might term 'meta-architecture,' richer datasets to help

evaluate the architecture.

3.3. THE IMPLICATIONS FOR ARCHITECTURE

Metadata's emergence is closely linked to the increase in volume of information available on digital systems (Duval et al., 2002). This increased volume required a step change in the sophistication of techniques needed to evaluate data. The Anthropocene causes us to reconsider the built environment; to consider not just the built object, but its material supply chain, its waste and carbon/greenhouse gas emission, lifecycle energy use and multi-generation material recovery and reuse. Existing data structures IFC (Industry Foundation Class), BIM (Building Information Models) and COBie (Construction Operations Building Information Exchange) are inadequate to articulate this information in relation to the environment. The current value shift appears to need additional data, tools and systems to express this new meta-architecture.

This section has contextualised a value shift in terms of two different frameworks, that of the assertoric and alethic gaze. We suggest these are two fundamentally different ways for viewing our relationship with the built environment and its relationship to wider planetary systems. We suggest moving forward into the Anthropocene that it is the alethic view of the environment that can accommodate shifting pluralistic value systems because it offers the possibility of engaging with the multiplicity of factors—the meta-architecture—of the built environment that is increasingly being demanded.

4. Organisational and Value shifts

This section discusses three approaches or projects which embody the change, and reorient the organisational systems through new opportunities presented by emerging digital technologies. We start first with an expansion upon the more traditional database approaches through the application of the blockchain technology. Second, an app that encourages e-commerce in building multi-species environments. Third, a concept for an economy in construction waste leveraging possibilities presented by blockchain technology.

4.1. TRACKING CHEMICAL COMPOSITION OF THE CONSTRUCTION MATERIALS

We open with a collaborative project within the Victoria University of Wellington, New Zealand which explores application of the blockchain technology for tracking of toxic and other components in building materials. Many composite construction materials are comprised of a number of components. These are manufactured in various facilities by different companies, which presents challenges when trying to obtain full value chain information. Blockchain technology offers opportunities for applications in law, especially in tracking of contractual succession of relevant information, for example for ownership of a property. The ability to lock-in specific providence information into the blockchain as impossible to change, gives certainty needed for such tracking. Applying the same logic, if all components of building materials were tracked using blockchain, the final purchaser of the material would be able to have easy access to the total composition of the material. This can be tracked in the blockchain by lodging the contractual transactions between different manufacturers

when the material components change hands.

The advantages of this approach are that it improves upon the existing systems where documents such as Environmental Product Declarations are used based on periodical reviews, and often present average or estimated summaries of the particular material (EPD Australasia, 2021). It also provides the full accuracy required by the more progressive labelling systems such as the Living Building Challenge (Int. Living Futur. Inst., 2021). The disadvantages are that for this approach to work, all companies in the particular manufacturing chain would have to agree to participate, and at the current level of development of blockchain platforms.

Returning to the value shift, this approach enables easier access to the information required for alethic gaze at construction materials, and shows that we have technologies capable of providing far more complex information needed for alethic gaze. However, this approach is not especially agile or easy to implement because: it requires agreements from a range of companies, and data storage for each batch of manufactured materials. Tracking of the composition is easier than interpretation of impacts those present, which would be more useful.

4.2. CO DE|GT: AN APP FOR MULTI-SPECIES CO-LIVING

A more agile approach which can stimulate change is the Co DE|GT mobile application is being developed at the Welsh School of Architecture's Synergetic Landscape Unit (Davidová, 2020). The unit has collaborated with Computer Science at Cardiff University as well as the School of Architecture and Planning Bhopal, India and the School of Future Environments at Auckland University of Technology, New Zealand.

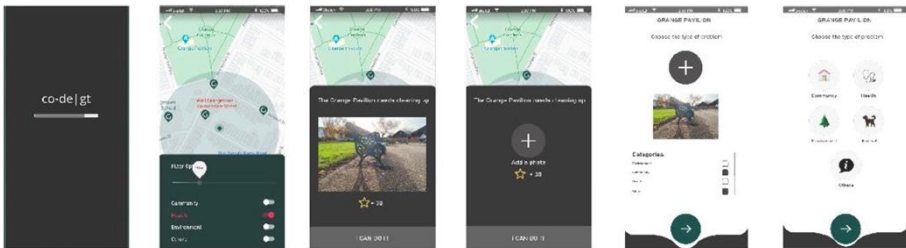


Figure 1. Co DE|GT Application.

The application illustrated in Figure 1, builds on the burgeoning research into, and potential for, crypto-currency and smart contracts for social good (WEF, 2018). It seeks to challenge the dominant 20th century view that the natural world and its flora and fauna are to be colonized for capitalisation. The app aims to grow commerce that supports diverse flora and fauna. For example, one user provides a design for a 'bug hotel' and another user who builds the hotel earns tokens. In this the app tries to redress the economic imbalance where non-human species rarely have agency within financial markets. While in this prototype the community is trading on behalf insects, future versions may speculate on future scenarios where 'things' have wallets and buying power (Pschetz et al., 2017).

By way of reflection this project embodies three shifts in relation to the shift from an assertoric to an alethic perspective. First, it challenges the dogma of economic supply and demand and the material extraction from the natural world that drives it. Second, it expands beyond the narrow view economics and into a concept of multi-species economics. Finally, whereas economic growth is generally seen as problematic in regards to climate change and emissions. The app speculates on an economy that attempts to sustain rather than deplete the natural environment.

4.3. WASTING TIME: A CRYPTO-ECONOMY FOR WASTE

In section 1.1 we outlined in some depth the problem of waste in the construction sector as a combination of economics and culture; and the provision of surplus is part of the system. 'Wasting Time' is a research collaboration between several New Zealand Universities: Auckland University of Technology, Victoria University, The University of Auckland and Unitec. It is tasked with investigating ways to reduce waste from the construction process. One of the strands of research within this programme is exploring opportunities that emerging technology might offer to address the economic problem of waste and surplus in construction.

Trash to Things Coin (TTTCoin) is a crypto-trading concept being developed by the group in collaboration with industry stakeholders. It is a concept complementary currency which can only be traded on a limited network for products and services that are verified as reusing and reusing construction surplus. In this scenario—explained in a short presentation (McMeel, 2020)—specific products can be verified as reducing or reusing construction surplus materials, and can only be purchased with TTTCoin. The manufactures of these products can pool TTTCoin to purchase waste from contractors in that currency. Contractors can use that currency to buy verified products for their projects or they can be approved to 'cash-out' converting TTTCoin to government currency and increasing cash profits. Thus, incentivising greater care of surplus material for resale to this network.

Unique currency ecosystems are not new, they have existed in the gaming world for some time, where a specific 'currency' can be purchased within a game. In the last decade unique crypto-currencies have emerged to circulate in the real world (Nakamoto, 2008). Bitcoin is the most famous but there are others such as Ethereum and Dogecoin. Complementary currencies that function in parallel to national currency are not a new phenomenon, although they are usually local in nature and only circulated within a specific geographic area (Amato & Fantacci, 2020). With both bitcoin and traditional complementary currencies goods or services can be bought and sold, but only within a specific limited network.

Returning to our point, the shift from assertoric to alethic gaze. This project offers two shifts. First, it is speculating on organisational systems that are focused not on the material that goes into building but the material that is left out. Second, such a scenario prompts us to ask if the systems and processes—the meta-architecture—is in place to adequately quantify what and where surplus materials are available in the supply chain and on sites and to trade efficiently with them.

5. Conclusion

To conclude, the paper has introduced two perspectives from which to evaluate the built environment, the assertoric and the alethic. Specifically, it foregrounds how history has privileged the assertoric, whereas the future requires the alethic. The alethic being particularly suited to embracing a multitude of standpoints; a necessary future requirement for society to evaluate if the built environment is fit for purpose during the Anthropocene. The introduction of the term 'meta-architecture' helps to ground this emerging departure from historic consideration of the building as 'object,' instead favouring a multiplicity of factors that need to be wholistically considered for evaluation of the built environment within the context of the Anthropocene.

Presented works show that there is scope for much innovation, and we should consider is how much particular approaches are endorsing or facilitating the improvements of the existing, or offer potential to be a dramatic 'game changer' innovation. Within this context, the first project can be seen as facilitating needed improvements within the existing: although helpful, it would not lead to a dramatic change. The other two examples show greater potential to make systemic change, and they ground how this complexity is beginning to emerge. CoDE|GT in trying to embrace a multi-species economy and TTTCoin unpacking the granular information, systems and process that might be required for evaluating and reducing waste in the construction process.

Finally, the paper, and the research projects bring to centre stage the inadequacy of existing information exchange (BIM, IFC, COBie etc.) to respond to the informational needs of the Anthropocene. Where there is a need to track material toxicity; more explicitly quantify the relationship between the built and natural environment; as well as track materials for reuse and redirection from demolition and landfill. It is an exhortation for developing new tools, systems and schema to enable an entirely different type of quantification and evaluation of the built environment.

Acknowledgements

The authors would like to thank Alex Sims, Yusef Patel, Maria Davidova and Alan Brent and Catherine Iorns Magallanes, long-time collaborators and investigators in the research projects discussed in Section 4. Some of the work in Section 4 was also supported with funding from the BRANZ Building Research Levy.

References

- Alofsin, A., Reed, P., & Riley, T. (1994). *Frank Lloyd Wright Architect*. Museum of modern art.
- Amato, M., & Fantacci, L. (2020). Complementary Currencies. In S. Battilossi, Y. Cassis, & K. Yago (Eds.), *Handbook of the History of Money and Currency* (pp. 501–522). Springer Singapore. https://doi.org/10.1007/978-981-13-0596-2_50
- Behrens, A., Giljum, S., Kovanda, J., & Niza, S. (2007). The material basis of the global economy. Worldwide patterns of natural resource extraction and their implications for sustainable resource use policies. *Ecological Economics*, 64(2), 444–453. <https://doi.org/10.1016/j.ecolecon.2007.02.034>

- Binetti, R., Costamagna, F. M., & Marcello, I. (2008). Exponential growth of new chemicals and evolution of information relevant to risk control. *Annali-Istituto Superiore Di Sanità*, 44(1), 13.
- Bossink, B. A. G., & Brouwers, H. J. H. (1996). Construction waste: quantification and source evaluation. *Journal of Construction Engineering and Management*, 122(1), 55–60. [https://doi.org/https://doi.org/10.1061/\(ASCE\)0733-9364\(1996\)122:1\(55\)](https://doi.org/https://doi.org/10.1061/(ASCE)0733-9364(1996)122:1(55))
- Davidová, M. (2020). *Synergetic Landscapes Unit: The MultiSpecies BioDigital Community CoDesign*. In P. Jones (Ed.), *Relating Systems Thinking and Design (RSD9) 2020 Symposium* (pp. 1–14). Systemic Design Association.
- Duval, E., Hodgins, W., Sutton, S., & Weibel, S. L. (2002). Metadata principles and practicalities. *D-Lib Magazine*, 8(4), 1–10.
- EEA. (2021). *Construction and demolition waste: challenges and opportunities in a circular economy*. European Environmental Agency.
- EPA. (2021). *Sustainable management of construction and demolition materials*. Environmental Protection Agency, US (EPA).
- EPD Australasia. (2021). *Environmental Product Declaration*. EPD Australasia.
- Fajardo, J. (2010). *Starchitects: Visionary architects of the twenty-first century*. Harper Collins.
- Klimek, A. (2013). The Emergence of the ‘Starchitect’ Category. In *The Performance of Celebrity: Creating, Maintaining and Controlling Fame* (pp. 59–66). Brill. https://doi.org/https://doi.org/10.1163/9781848882546_007
- McMeel, D. J. J. (2020). *TripleT Coin*. YouTube.
- Minton, A. (2015). *Byker Wall: Newcastle’s noble failure of an estate – a history of cities in 50 buildings, day 41*. The Guardian.
- Nakamoto, S. (2008). Bitcoin: A peer-to-peer electronic cash system.
- Pacheco-Torgal, F. (2012). Introduction: types of potentially toxic building materials. Elsevier.
- Pallasmaa, J. (1992). Identity, intimacy and domicile Notes on the phenomenology of home. *The Concept of Home: An Interdisciplinary View - Symposium*. the University of Trondheim.
- Pallasmaa, J. (2012). *The eyes of the skin: architecture and the senses*. John Wiley & Sons.
- Petrovic, E. K., Vale, B., & Zari, M. P. (2017). *Materials for a Healthy, Ecological and Sustainable Built Environment: Principles for Evaluation*. Woodhead Publishing.
- Pschetz, L., Tallyn, E., Gianni, R., & Speed, C. (2017). Bitbarista: exploring perceptions of data transactions in the Internet of Things. *Proceedings of the 2017 CHI Conference on Human Factors in Computing Systems* (pp. 2964–2975).
- Purushothaman, M. B., & Seadon, J. (2020). A critical review of the system-wide waste in the construction industry. *Proceedings of the International Conference of Architectural Science Association, 2020-Novem* (pp.51–60).
- Schandl, H., & Eisenmenger, N. (2006). Regional patterns in global resource extraction. *Journal of Industrial Ecology*, 10(4), 133–147. <https://doi.org/10.1162/jiec.2006.10.4.133>
- Schandl, H., Fischer-Kowalski, M., West, J., Giljum, S., Dittrich, M., Eisenmenger, N., Geschke, A., Lieber, M., Wieland, H., Schaffartzik, A., Krausmann, F., Gierlinger, S., Hosking, K., Lenzen, M., Tanikawa, H., Miatto, A., & Fishman, T. (2018). Global material flows and resource productivity forty years of evidence. *Journal of Industrial Ecology*, 22(4), 827–838. <https://doi.org/10.1111/jiec.12626>
- UNEP. (2019). *Sand and sustainability: finding new solutions for enviromnetal governance of global sand resources*.
- Wainwright, O. (2018). *Snapping point: how the world’s leading architects fell under the Instagram spell*. The Guardian. Retrieved from <https://www.theguardian.com/artanddesign/2018/nov/23/snapping-point-how-the-worlds-leading-architects-fell-under-the-instagram-spell>

- Wainwright, O. (2021). *No Title A strangely alluring cocktail of dad dancing and traffic chat: architecture on TikTok*. The Guardian.
- WEF. (2018). *Fourth Industrial Revolution for the Earth Series Building block(chain)s for a better planet*. In Weforum.Org (Issue September). Retrieved from http://www3.weforum.org/docs/WEF_Building-Blockchains.pdf
<https://es.weforum.org/reports/building-block-chain-for-a-better-planet>

THE SPATIAL ENVIRONMENT AFFECTS HUMAN EMOTION PERCEPTION-USING PHYSIOLOGICAL SIGNAL MODES

XINYUE DING¹, XIANGMIN GUO², TIAN TIAN LO³ and KE WANG⁴

^{1,2,3} Harbin Institute of Technology (Shenzhen), ⁴Tongji University.

¹ xinyueding00@gmail.com

² 24904404@qq.com

³ skyduo@gmail.com, 0000-0002-1992-0777

⁴ kew@tongji.edu.cn

Abstract. In the past, spatial design was mainly from the perspective of designers. With the increasing demand for quality spaces, contemporary architecture has gradually shifted from focusing on form creation to human well-being, once again advocating the concept of "human-centered" spatial design. Exploring how the spatial environment affects human emotions and health is conducive to quantifying the emotional perception characteristics of space and promoting the improvement of human quality of life and sustainable survival. At the same time, the development of contemporary technology and neuroscience has promoted the study of the impact of spatial environment on human emotion perception. This paper summarizes the research on the impact of the spatial environment on human emotion perception in recent years. First, 28 relevant studies were screened using the PRISMA framework. Then a set of research processes applicable to this study is proposed. Next, the physiological signals currently used to study the effects of the spatial environment on human emotions are summarized and analyzed, including electroencephalography (EEG), skin response (GSR), pulse (PR), and four other signals. The architectural features studied in the related literature are mainly building structural features, building spatial geometric features, and building spatial functional attributes. The study of urban space is divided into different parts, such as urban environment characteristics and urban wayfinding behavior. Finally, we point out the shortcomings and perspectives of studies related to the influence of spatial environment on human emotion perception.

Keywords. Architectural Space Environment; Urban Space; Human Emotional Feelings; Physiological Signals; SDG 11.

1. Introduction

With the continuous improvement of human material living standards, the concepts of liveable environment, sustainable development, and humanized design are gradually

advocated by people. People's demand for architectural space is limited to functional requirements and puts forward new needs for the comfort and spirituality of the spatial environment. In order to meet the high quality requirements put forward by people for the spatial environment, the design thinking perspective of designers has changed from "usable" to "comfortable". Focusing on people's emotional perception of spatial environment characteristics has become an emerging research direction in spatial design at present, while promoting the enhancement of human life quality and the development of society in the direction of human-centeredness.

Traditionally, people's experiential feelings about space have been expressed mainly through language, such as oral narratives in the form of interviews, questionnaires to record feelings. However, these methods are highly subjective. People have been searching for ways to quantify the changes in people's emotions objectively.

In 1997, Rosalind W. Picard proposed that machines learn human emotions through scientific means: affective computing. Affective computing hopes that computers can recognize, understand and express human feelings (Picard, 1999), focusing mainly on the direction of human language, facial expressions, body gestures, and physiological signals. At the same time, the maturity and development of sensor device technology have facilitated the collection and analysis of human body modality data, making it possible to quantify people's feelings and emotions.

In recent years, with the development of artificial intelligence, affective computing has gradually become a hot topic in the development of science and technology. Numerous studies on psychology, behavior, architecture and other fields have attempted to redefine and explain the impact of the spatial environment on human emotional feelings by using affective computing technology. Effective computing techniques can quantify human emotions while observing the effects on the body that humans do not subjectively perceive. Among the many effective computing modalities, physiological signals are considered ideal for objectively quantifying human emotions because they most directly reflect the physiological changes when human emotions change. However, it is still challenging to explain the influence and relationship of the spatial environment on human emotional feelings. One establishes the correlation between human physiological data and human emotions; the second is how different spatial environments induce human emotions, i.e., the spatial environmental factors that influence human emotions.

This paper contributes to the conference SDG11 of sustainable cities and communities through discussing the current state of research on the effects of spatial environment on human emotion perception and summarizing the current state, limitations, and future trends in the use of physiological signalling technologies. The future development of cities and communities still follows the principle of "people-centered" development, and it is necessary to use human emotions as the entry point for research and design.

2. Methodology

2.1. DATA COLLECTION

This article searches the literature from 2010 to the present and focuses on using human physiological sensors to study the effects of the spatial environment on human emotional perception. Human physiological sensors can detect human physiological indicators such as heart rate, blood pressure, skin electrical activity, EEG. The spatial environment includes urban space and architectural space. The spatial form consists of the physical spatial environment, and the study of the virtual spatial environment is included in the search and analysis.

We followed the Preferred Reporting Items for Systematic Reviews and Meta-Analyses (PRISMA) study to select the research literature. This included the following steps: literature search, primary literature screening, inclusion, and literature synthesis. In the literature search phase, first, we conducted a database literature search in web of science using pre-defined keywords, such as "architecture space," "physical space," "virtual space," and "emotion recognition," "sensors." After the initial literature screening, we screened a total of 197 articles. Other sources were 31 articles (Figure 1).

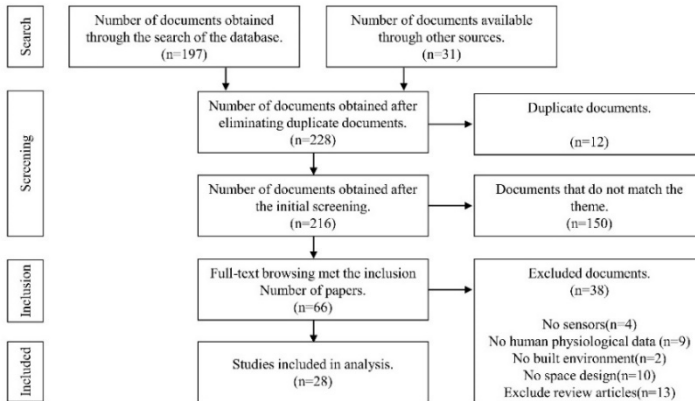


Figure 1. The review process using the PRISMA analysis framework

Next, we screened the retrieved literature, and the screening steps were.

(1) first, investigating and analyzing the titles to de-duplicate the 12 groups of duplicate literature.

(2) Then, by investigating the titles and abstracts, the literature that did not match the study of spatial characteristics of buildings as the object of study while using physiological signal sensors as the study approach was investigated for exclusion. A total of 150 records were excluded because they did not correspond to the study topic.

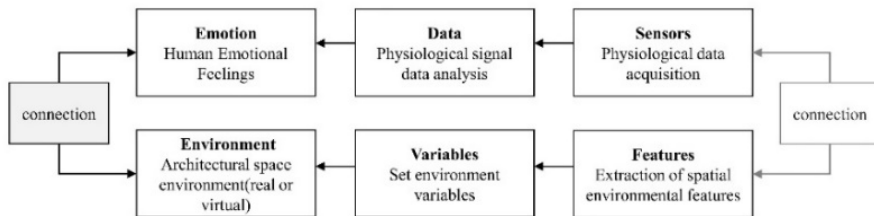
(3) Next, we conducted further in-depth research on these 66 records to filter out those that fit the research topic. We filtered our final range of research literature by the following filtering sequence: ① literature that used sensor technology as a research method was selected. Four studies were excluded because they did not use physiological sensors; ② the studies were conducted on human physiological data changes, with human physiological data as the primary influencing variable for the overall research. Nine studies were excluded because they did not use human

physiological sensor data as the data source; ③ the study environments were architectural or urban spatial environments. Both real and virtual environments were used as the scope of this review. Two of the studies were excluded because the environments were non-building or urban-related; ④ the literature should focus on the changing relationship between people's physiological data and the spatial environment, rather than on other unrelated areas such as mental illness treatment and product design. Ten studies were excluded because they were not related to spatial environment design; ⑤ relevant research literature was excluded from this study, and 13 articles were reviewed.

Twenty-eight studies were eventually included in the research analysis, and they used sensors to collect data on human physiological signals and, at the same time, to study the relationship between 3D spatial environments and human emotional feelings, from which they analyzed how architectural or urban spatial environments affect human emotions, thoughts, and behaviors. Figure 1 illustrates the process of deriving our final study database using the PRISMA framework.

3. Research Framework and Research questions

After conducting a literature search and screening, we will propose the following process applies to this study by analyzing and studying these screened 28 papers based on the research topic. Firstly, we will clarify the research content, and the research topic is the influence of spatial environment on human emotional feelings. Next, it should be defined which spatial environment features change human emotional feelings. The built spatial environment features are extracted as spatial environment variables for the analysis of the study. Then, regarding the quantification process of human experience feelings, physiological characteristics are converted into measurable physiological signal data by physiological signal sensors, and physiological data are converted into human emotions using relevant models. Finally, an attempt is made to obtain two associations through the above process, one between human emotion and spatial environmental features and the other between spatial environmental features and



human physiological signals. The whole research process is shown in Figure 2.

Figure 2. Research Framework

We ask the following questions based on the above research framework and analyze the association between the built spatial environment and human emotional feelings.

Question 1: What physiological signals have been used to study the relationship between spatial environments and human emotional feelings?

Question 2: Which built spatial environment features have been studied in the literature?

Question 3: Is it possible to obtain associations between built environment features and human physiological signals?

The above questions guide our findings. Question 1 is about the relationship between sensor devices and human physiological signals, and we list the relationship between human body modalities, physiological signals, and sensors. Question 2 is about architectural spatial environment characteristics, and we establish the relationship between architectural spatial elements and research methods and human emotions. Regarding question 3, we analyze the physiological signals against the architectural spatial features.

4. Results and discussion

4.1. HUMAN PHYSIOLOGICAL CHARACTERISTICS AND PHYSIOLOGICAL SIGNALS (QUESTION 1)

A total of 8 physiological characteristics were extracted from these 28 papers: EEG, skin electrical response, heart rate, blood pressure, pulse, eye movements, and facial expressions (Table 1).

Table 1. Human physiological characteristics and physiological signals in the literature

Category	Features	Sensors	Products	Number of References
Nerve Activity	Brain Waves	Electroencephalography(EEG)	Emotiv EPOC; NeuroSky	N=16
	Skin Electrical Value	Galvanic Skin Response (GSR); Electrodermal Activity(EDA)	Shimmer 3 GSR	N=8
Physiological Activities	Pulse Rate	Pulse Rate(PR)	near-infrared spectroscopy(NIRS)	N=1
	Blood Pressure	Blood Pressure(BP)	near-infrared spectroscopy(NIRS)	N=1
	Heart Rate	Heart Rate (HR)	Photoplethysmogram (PPG); Electrocardiogram (ECG)	N=6
Physical Activity	Gazing Point	Eye-tracking (ET)	Eye tracking cameras	N=4
	Facial Action Data	Facial Action Data	The iMotions software	N=1

EEG is the collection of brain nerve cell activity signals at the human cerebral cortex through EEG detection equipment, and then after extraction and processing, the EEG signal is divided into different human emotional states using the frequency domain of EEG frequency (Nunez et al., 1997; Shemesh et al., 2021). Skin electrical response is when human beings are subject to external stimuli or internal emotional fluctuations. It will cause changes in skin electrical conductivity by detecting human

skin resistance. You can have a preliminary judgment of people's emotions (Shemesh et al., 2021). Heart rate changes can reflect people's emotional state in different spatial environments. In contrast, signals such as blood pressure and pulse rate can collect the moments when people feel "excited" or "calm." (Tsunetsugu et al., 2005). Eye movements visually show people's attention in different spatial environments, and at the same time, according to people's eye movement signals also reflect human emotional changes (Sussman & Ward, 2019).

In Table 1, different physiological features and sensors affect human emotions in the spatial environment. Human physiological characteristics are classified as neural, physiological, and physical features, and various human physiological features have a strong connection with human emotions. The commonly used human physiological signals are EEG signals, skin electricity, heart rate, and eye movement data compared to other physiological features. The most frequently used physiological feature was EEG, with 16 studies using EEG as the primary human physiological feature, accounting for 57.14% of the total studies. This was followed by skin electrical, heart rate, and eye movements, accounting for 28.57%, 21.42%, and 14.28%, respectively.

Human emotional, perceptual responses to the spatial environment are potential and unconscious. The potential human reactions to different spatial environments can be observed concretely by detecting human physiological signals. Among many physiological features, EEG can directly observe the neural activity of the human cerebral cortex using sensors, which is the most direct indicator of human emotional changes among physiological signals and has a significant role in identifying human emotions.

4.2. SPATIAL ENVIRONMENT FEATURES (QUESTION 2)

In recent years, related scholars have studied the relationship between spatial environmental features and human emotions. Table 2 shows the analytical studies of using physiological signals for spatial features in different spatial scenes.

Among the spatial forms in related studies, realspace is mainly used in urban space research, and both real space and virtual space are used in architectural space experiments. The possible reasons for the less adoption of virtual space form in the research about the urban spatial environment are: 1) the 3D virtual model of urban space is not easy to obtain; 2) it is difficult to ensure that the virtual urban environment is entirely consistent with the real urban environment. At the same time, compared with the controllability of architectural space features, urban street space has stronger uncertainties.

Second, about relevant research characteristics. Research on urban space can be roughly divided into the following categories: 1) the influence of environmental features on human emotions in urban space, 2) emotional changes in human wayfinding behavior in urban environments, 3) the influence of building facades on human points of interest in cities, and 4) human spatial preferences in virtual urban environments. Research on architectural space can be broadly divided into the following categories: 1) functional properties of architectural space, which refers to the focus on office space, living space or others in the experiment; 2) physical environmental characteristics of architectural space, which refers to the focus on the

physical environment such as temperature and humidity in the space; 3) structural characteristics of architectural space, which refers to the focus on the structural elements of the space such as wooden elements; 4) geometric characteristics of architectural space, which refers to the focus on the geometric shape of the space such as rectangular or curved; 5) wayfinding behavior of architectural space, focusing on the change of people's emotional perception in the process of space wayfinding.

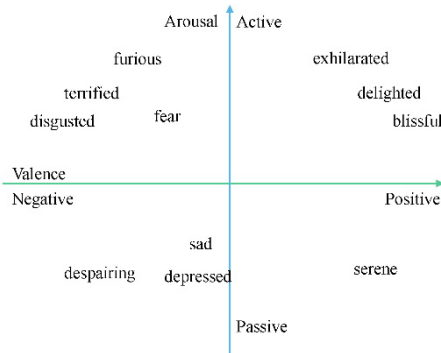
Research in urban space focuses on the influence of environmental features on human emotions. Research on architectural space includes structural characteristics, physical environmental characteristics of space, geometric characteristics of architectural space. Most studies focus on architectural interior spaces and are more diverse regarding research within architectural spaces.

Table 2. Different spatial scenarios are studied using physiological signals for the analysis of spatial features

Category	Form	Research Subjects	Emotion	Sensors	Reference
Urban Space (Outdoor Space)	Real Environment	Urban built environments	Valence	HR EEG ET GSR PPG	N=8
		Urban trails pathfinding behavior	Arousal	EEG	N=1
		Building elevation points of interest	Arousal	ET	N=1
	Virtual Environment	Environmental preference	Arousal	EDA HR	N=1
Architectural Space (Interior Space)	Real Environment	Nature of architectural space	Valence	EEG	N=2
		Features of the physical environment of the building space	Valence	GSR Facial Action Data	N=1
		Architectural space structure characteristics	Valence or Arousal	EEG PR BP ECG EDA rCBF	N=5
	Virtual Environment	Geometric features of space	Valence	EEG GSR ET	N=3
		Architectural space structure characteristics	Valence or Arousal	EDA EEG GSR PPG	N=3
		Spatial pathfinding behaviour	Valence	EEG	N=1

Third, about human emotions in research. The influence of spatial environment on human emotions is subtle, and humans may not realize the influence of space on their own emotions when they are in the environment. The use of physiological signal sensors can detect emotional changes that humans do not detect. Human emotion classification is mainly based on the VA emotion model proposed by Russell. Emotional dimensions are not independent but interconnected. He describes emotions through two dimensions: valence and arousal (Table 2). Valence indicates the degree

of perceived positivity or negativity to distinguish between positive or negative emotions; arousal indicates the degree of emotional calmness or arousal (Russell, 1980). The categorization of human emotions in most studies is based on valence, i.e., most studies have analyzed the positive and negative emotional effects of humans on the spatial environment. Studies of wayfinding behavior in urban spaces and points of



interest on building facades have mainly analyzed the arousal aspect of emotion.

Figure 3. Valence-Arousal model

Human emotion perception of the spatial environment is complex. An urban environment, many elements of the spatial environment affect human emotion perception, not only urban spatial components (such as road width, whether there are street lights and seats, building scale, and facade) will have an impact on human emotion, but also the light, temperature and social factors (whether there are people around, the influence of traffic vehicles in the environment) will have a The light, temperature, and social factors (presence of people and traffic in the environment) also have a significant impact on human emotions. In urban space, it is impossible to ignore the influence of disturbing environment on the study, and how to control the environmental disturbance should be the next issue to be considered in the study. Since the architectural space is mainly located indoors, the factors affecting mood change are conducive to controlling environmental variables compared to outdoors, which is more helpful for the experiments to exclude the effects. On the other hand, the measurement and classification of human emotions in the study are relatively single, and more studies can only analyze the influence of spatial environment on human emotions positively or negatively. However, the deeper emotions cannot be analyzed and expressed.

4.3. SPATIAL FEATURES AND PHYSIOLOGICAL SIGNALS (QUESTION 3)

We tried to obtain the relationship between spatial features and physiological signals in related studies by categorical analysis (Table 3). The main spatial environmental features used in the study about the influence of spatial environment features were EEG, ET, GSR, HR, EDA, and PPG. the EEG was used to study the influence of spatial types on humans. The GSR was used to study the influence of spatial, physical environment on humans with human facial expression features. Building surface

concerns EEG is used in the study of wayfinding behavior.

The physiological signals used are related to the characteristics of the spatial environment under study, and also, the content of the study impacts the physiological signals used. Focusing on human emotional changes mainly uses EEG and physiological signals such as EDA and GSR, where EEG is the primary way to detect human emotions. Focusing on physical characteristics in the spatial environment, such as temperature comfort research, in addition to focusing on human's emotional responses, about human body physiological function responses are also among the practical concerns.

Table 3. Spatial features and physiological signals

Research Subjects	Sensors	Reference
Structural characteristics of the spatial environment	EEG ET GSR HR EDA PPG	N=19
Building space type	EEG	N=3
physical environment of the building space	Facial Action GSR	N=1
Points of interest on building surfaces	ET	N=1
Spatial environment pathfinding behavior	EEG	N=2

5. Conclusion

Human beings are now living in an increasingly wide variety of scenes that stimulate neural perception and emotional changes all the time. It is essential to understand the impact of different life scenes on human emotion perception, and it also helps quantify the spatial characteristics corresponding to human emotion objectively. With the support of modern technology, it is possible to quantify human emotions objectively: 1) using physiological data as the evaluation index of spatial design, quantifying human emotions evaluates this initially subjective behavior objective; 2) from the perspective of people themselves, using the user's emotional data as a direct source of design reference, making the evaluation of design features more data-supported.

However, studies on human emotions to assess spatial design features are still in the minority. First, the associated technical difficulties may pose a threshold for research scholars. Second, non-research influences in the objective environment become the primary source of interference in experiments. At the same time, the current research still has more lacking aspects, 1) in the use of physiological signal sensors, it is ideal to use EEG technology to analyze human mood changes. However, the device itself has limitations in the way it is worn and the scenario in which it is used, the way to reduce the impact of the device itself is to conduct experiments in the laboratory; 2) In terms of using the spatial environment to influence people's emotions, the spatial environment has a milder effect on human emotions, and people's emotional responses to changes in the spatial environment are more subdued, requiring the use of

more sophisticated physiological sensory equipment for detection, such as the use of EEG technology.

As an intersection of architecture, neuroscience, and psychology, it has a broad research prospect to analyze the influence of spatial environment on human emotion perception. With the continuous enrichment of human life scenes, human's mental needs for space are increasing, and quantifying spatial emotional characteristics can help advance human understanding of the spatial environment affecting human mental health and emotional perception.

In today's rapidly developing human technology, people's lives are changing rapidly, and new products and devices are constantly flooding the spatial environment where people live. However, the research on the emotional perception of features in the spatial environment has been in a vacant state. By analyzing the research on human physiological perception of spatial environment in recent years, we continue to promote the research on the emotional characteristics of human spatial environment by summarizing the application of physiological signal technology, architectural spatial characteristics and emotional classification.

Acknowledgements

This research was supported by the following funds: Later Funded Projects of National Philosophy and Social Science Foundation of China (No. 19FXWB026); Youth Project of National Natural Science Foundation of China (No. 51908158); Higher Education Research and Reform Project of Guangdong Province (No. HITSZERP19001); General Project of Stabilization Support Program of Shenzhen Universities (No. GXWD20201230155427003-20200822174038001); Shenzhen Excellent Science and Technology Innovation Talent Training Project (No. ZX20210096).

References

- Nunez, P. L., Srinivasan, R., Westdorp, A. F., Wijesinghe, R. S., Tucker, D. M., Silberstein, R. B., & Cadusch, P. J. (1997). EEG coherency: I: statistics, reference electrode, volume conduction, Laplacians, cortical imaging, and interpretation at multiple scales. *Electroencephalography and Clinical Neurophysiology*, 103(5), 499–515. [https://doi.org/10.1016/S0013-4694\(97\)00066-7](https://doi.org/10.1016/S0013-4694(97)00066-7)
- Picard, R. W. (1999). Affective Computing for HCI. In *8th International Conference on Human-Computer Interaction on Human-Computer Interaction: Ergonomics and User Interfaces-Volume I-Volume I*, HCI International '99 (pp. 829-833). International Conference on Human-Computer Interaction (HCI International).
- Russell, J. A. (1980). A circumplex model of affect. *Journal of Personality and Social Psychology*, 39(6), 1161–1178. <https://doi.org/10.1037/h0077714>
- Shemesh, A., Leisman, G., Bar, M., & Grobman, Y. J. (2021). A neurocognitive study of the emotional impact of geometrical criteria of architectural space. *Architectural Science Review*, 64(4), 394–407. <https://doi.org/10.1080/00038628.2021.1940827>
- Sussman, A., & Ward, J. (2019). Eye-tracking Boston City Hall to better understand human perception and the architectural experience. *New design ideas*, 3(1), 53-9.
- Tsunetsugu, Y., Miyazaki, Y., & Sato, H. (2005). Visual effects of interior design in actual-size living rooms on physiological responses. *Building and Environment*, 40(10), 1341–1346. <https://doi.org/10.1016/j.buildenv.2004.11.026>

THE WHAT, WHY, WHAT-IF AND HOW-TO FOR DESIGNING ARCHITECTURE

Explainability for auto-completion of computer-aided architectural design of floor plan layouting during the early design stages

JESSICA BIELSKI¹, CHRISTOPH LANGENHAN², CHRISTOPH ZIEGLER³, VIKTOR EISENSTADT⁴, FRANK PETZOLD⁵, ANDREAS DENGEL⁶ and KLAUS-DIETER ALTHOFF⁷

^{1,2,3,5}*Technical University Munich.*

^{4,6,7}*DFKI/ University of Hildesheim.*

¹*jessica.bielski@tum.de, 0000-0003-4936-1993*

²*langenhan@tum.de, 0000-0002-6922-2707*

³*c.ziegler@tum.de, 0000-0001-8095-416X*

⁴*viktor.eisenstadt@dfki.de, 0000-0001-6567-0943*

⁵*petzold@tum.de, 0000-0001-8974-0926*

⁶*andreas.dengel@dfki.de, 0000-0002-6100-8255*

⁷*klaus-dieter.althoff@dfki.de, 0000-0002-7330-6540*

Abstract. In the next thirty years, the world's population is expected to increase to ten billion people, posing major challenges for the construction industry. To meet the growing demands for residential housing in the future, architects need to work faster, more efficiently, and more sustainably, while increasing architectural quality. The hypothetical intelligent design assistant WHITE BRIDGE, based on the methods of the 'metis' projects, suggests further design steps to support the architectural design decision-making processes of the early design phases. This facilitates faster and better decisions early in the process for a more responsible resource consumption, better mental well-being, and ultimately economic growth. Through a case study we investigate if additional information supports the understanding of these suggestions to reduce the cognitive workload of architectural design decisions on the backdrop of their respective representation. The paper contributes an approach for visualising explanations of an intelligent design assistant, their integration into paper prototypes for case studies, and a workflow for data collection and analysis. The results suggest that the cognitive horizon of the architects is broadened by the explanations, while the visualisation methods significantly influence the usefulness and use of the conveyed information within the explanations.

Keywords. Explainability; Artificial Intelligence; XAI; SDG 3; SDG 8; SDG 12.

1. Introduction

The world population is expected to reach ten billion by 2050 (Statista Research Department, 2020), with about two thirds of the population living in an urban area (United Nations, 2019, p. 19). In order to meet the growing demands for residential housing, architects need to be able to work faster, and more sustainably and efficiently, while simultaneously increasing architectural quality. In order to satisfy these requirements, the decisions of the early design stages are of significant importance for the architectural quality of the constructed building (Harputlugil et al., 2014). Derived from the Vitruvian Principles the authors (Ibid.) define architectural quality as the weighted sum of ‘functionality’ (i.e. use and usefulness for intended purpose), ‘built quality’ (i.e. quality of built substance), and ‘impact’ (i.e. aesthetics, relation to context). The design process is built on controlled convergence, meaning that constantly new ideas and problem solutions are generated and only a selected few are further pursued to run through this process again. Thus, the sooner well-informed design decisions are made, and issues are identified and addressed, the better the final building. Vice versa, the later fatal flaws are recognised within the design process, the more difficult correcting them and changing the design becomes (Buxton, 2007, pp. 146-149). This has impacts on the duration, the quality of architecture, and the sustainability of the entire building of both the design and construction process. Thus, efficient design, designing, and data management of the early design phases can result in an estimated waste reduction of 33 percent (Haeusler et al., 2021, p. 347).

Intelligent systems have been applied in other fields to support the user in completing tasks faster and more efficiently, such as digital keyboards on everyday digital devices, predicting and auto-completing words and sentences. Through adaptation and specific extensions within the workflow of Computer-Aided Architectural Design (CAAD), the methods of intelligent systems have also been applied to support the architect in fulfilling the complex tasks of architecture. Derived from these principles, the ‘metis’ projects pursue an intelligent design assistant suggesting further design steps for spatial layouting during the early design phases. In the following we propose methods of explainability for such an intelligent system, utilising a hypothetical application called WHITE BRIDGE. With our system, we aim to support architects within the decision-making of the early phases through future interaction methods of intelligent systems and architects. Thus, we facilitate more intuitive work and high quality architecture, while speeding up the process and reducing the work-related stress on architects.

2. Related Work

The field of explainable artificial intelligence (XAI) is a quickly expanding area of research. While Palacio et al. (2021) focus on establishing a consensus and framework for XAI strategies for implementation, Wang et al. (2019) propose a conceptual framework for designing explainability for a specific target group and building blocks for a theory-driven adaptation for any user group.

The framework of Figure 1 is divided into human reasoning process to the left and explainable intelligent system methods to the right. Human reasoning is differentiated into ideal reasoning (‘should reason’) and true human reasoning (‘actually reason with

errors’) of heuristic ‘System 1’ and analytical ‘System 2’ (see Figure 1, left). On the right-hand side is the intelligent system which generates explanations through different XAI strategies to support the human reasoning methods (see Figure 1, right). The system answers to both the ideal and true human reasoning with different strategies through either the support of human reasoning or the mitigation of biases of heuristic ‘System 1’ and analytical ‘System 2’. Wang et al. summarise the following four steps to adapt the framework for a specific target group (Wang et al., 2019, p. 9):

- Clarify the user's reasoning goals through a literature review, ethnography, and/or participatory design
- Identify possible biases for the respective applications through a literature review, ethnography, and/or participatory design.
- Deduce appropriate explanation ways for reaching the reasoning goals and/or mitigating cognitive biases using the pathways of the framework
- Integrate the explainable intelligent system facilities to create an explainable user interface

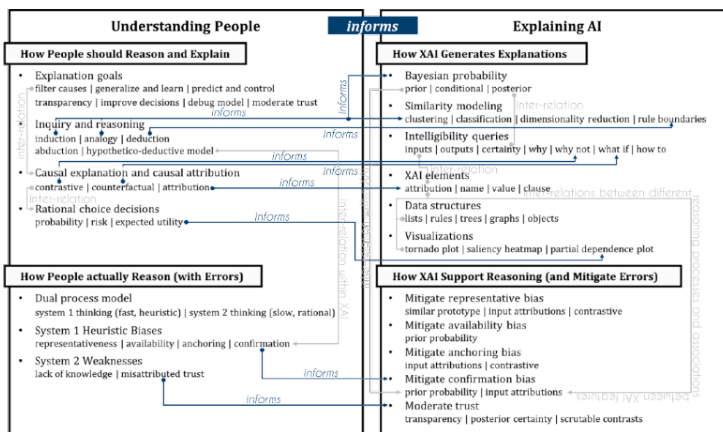


Figure 1. Conceptual framework for reasoned explanations (Adapted from Wang et al., 2019, p. 4)

The common practice of architects of using reference buildings (e.g. floor plans and other visualisations), is a well-recognised approach in architectural design for using exemplary designs with originality and for creating innovation (Richter, 2011, pp. 139-154). Architects use these examples as a basis for their process - as a source of inspiration, design conditions and explicit information, as a tool for evaluation of their own design, and as a medium for communication (Ibid.) - combined with their knowledge from other sources and previous experiences to synthesise new original architectural designs. Considering the similarities between the architectural design process and Case-Based Reasoning (CBR), an intelligent design assistant using reference buildings for suggesting further design steps (i.e. solutions or solution aspects) builds on the same principles, including its design requirements and workflow.

By assuming the position of Harputlugil et al. (2014), the architectural design decision-making process can be described as an orderless analytical hierarchy process

(AHP) with multi-criteria decision-making (MCDM) to design a solution for the unique problem to achieve the best possible quality of architecture (Laseau, 2000, p. 13; Lawson, 2004, p. 90). Thus, the design decisions of the early design phases have significant influence on architectural quality of the final building (Buxton, 2007, pp. 146-149; Harputlugil et al., 2014, p. 140). Derived from the Vitruvian Principles 'utilitas', 'firmitas', and 'venustas', Harputlugil et al. (2014) formulate 'functionality', 'built quality', and 'impact', whereat 'functionality', with its sub-criteria 'use', 'access' and 'space', is ranked highest on average and architects within their (Ibid.) case study during early design stages. Furthermore, architects aim to create and increase the quality of their design solutions through life-long learning to eventually outline their own design philosophy. These 'Guiding Principles' (Lawson, 2004, p. 112) are 'sets of ideas, beliefs and values that operate for the designer' (Ibid.), created from a mental collection of reference buildings and personal experiences throughout their career.

In order to provide the best possible human-computer-interaction (HCI) or human-system-interaction (HSI) for architects designing during the early design phases, the interface of the architect and the system should assimilate to the best practises of the respective design stage (Negroponte, 1973). Nevertheless, the design of graphic user interfaces (GUIs) of contemporary CAAD tools and software largely focuses on computer systems as the interaction device, while neglecting sketching as an essential practice of the early design for conceptualisation, visualisation of abstract ideas and communication (Lertsithichai, 2005, pp. 357-358). However, the adoption of users' mannerisms to increase the acceptance and productivity of interactive systems is deeply rooted in the common design principles for user interfaces (Lee, Chuang & Wu, 2011, p. 4), including the ISO standard 9241-210 for user experience (UX) based on User-Centred Design (UCD). This design practice facilitates a short learning process and the mitigation of errors by considering the users' needs and goals, and improves efficiency and effectiveness of an interactive system. Further, Lee, Chuang and Wu (2011, p. 3) state that the more intuitive and aesthetically pleasing the GUI is for architects, the higher the satisfaction with the application. Consequently, the GUI is the focal point of interaction between architects and an intelligent design assistant.

3. Problem Statement

Contemporary research for intelligent design assistants mostly revolves around CBR and Deep Learning (DL). CBR approaches have been adapted as Case-Based Design (CBD) as early as the 1990s, while the application of DL in the field of architecture is fairly recent, focusing mostly on the mechanisms and the possibilities of the system, e.g. retrieval or design style manipulation. Further, explainability for intelligent systems against the backdrop of a specific target group, such as physicians (Wang et al., 2019), has been researched. However, there is no concept of the nature and communication methods of the necessary information for architects to understand suggested further design steps of an intelligent design assistant aiming to relieve the cognitive workload of the early design phases.

4. Approach

The described vision of an intelligent design assistant aims to mimic the architectural

design process of the early design phases by suggesting further design steps of spatial configurations when designing a building's 'functionality'. The requirements and goals for such a system are assumed to be equivalent to those of the common architectural design decision making process. During this process architects apply inductive and analogical reasoning, e.g. explorative creation of alternatives to select the most promising solutions or solution aspects (Laseau, 2000). This kind of reasoning is supported by contrastive ('Why?', 'Why not?'), counterfactual ('What if?'), and transfactual ('How to?') explanations to iterate the priority ranking of selected criteria and sub-criteria, e.g. through pairwise comparison (e.g. tangible/intangible, subjective/objective).

By using the pathways of the framework (see Figure 1) by Wang et al. (2019), explanation methods to support the reasoning process and mitigate errors can be deduced. The latter will be specifically described for the use of reference buildings by architects in a paper of the eCAADe 2022. The findings of the architectural workflow, design requirements, design decision making process and quality assessment on the backdrop of the framework are synthesised into explanation visualisations for the visually driven target group, using common, established and domain knowledge. The strategies of the system itself, e.g. Bayesian probability and XAI facilities, for generating these explanations and their visualisations, will be discussed in detail in a paper planned to submit to an AI conference. The proposed paper prototype of the hypothetical intelligent design assistant WHITE BRIDGE integrates the explanation visualisations without any operational functionality. With the best practices for designing GUIs in mind, the proposed digital paper prototype, integrating suggestions for further design steps by an intelligent design assistant and corresponding explanations for architects, has two main views: the drawing view and the suggestion view, both containing visualisations for facilitating better understanding of the suggestions of the hypothetical intelligent design assistant WHITE BRIDGE. The latter view is pictured with dropped down windows of textual information in Figure 2, followed by a detailed description of the individual explanation visualisations and their purposes.

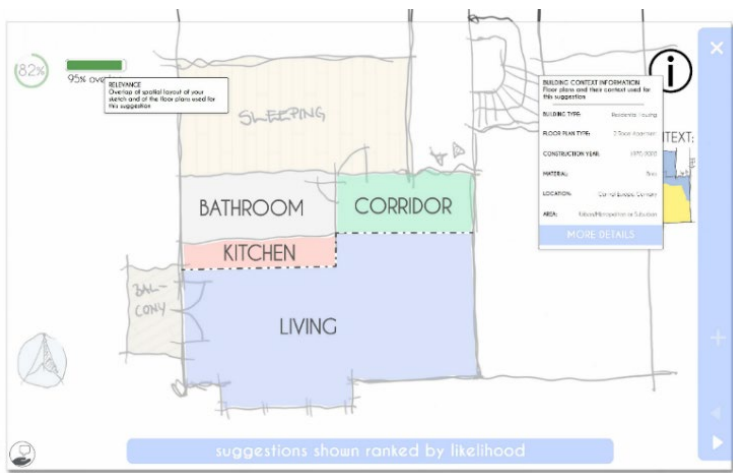


Figure 2. Graphic User Interface of Paper Prototype of suggestion view and opened windows.

For supporting the architect's design process, the intelligent design assistant WHITE BRIDGE presents suggestions on a top layer mimicking sketch paper for facilitating contrastive comparison with colour coded indicators (see Figure 3, left), while highlighting its suggestiveness. Simulations, e.g. daylight simulations, are suitable for creating 'What if?' and 'How to?' scenarios for counterfactual and transfactual design decision making, placed on the respective suggestion (see Figure 3, right). Further, by supporting a well-informed criteria ranking within the AHP, possible anchoring bias (Wang et al., 2019) can be mitigated.

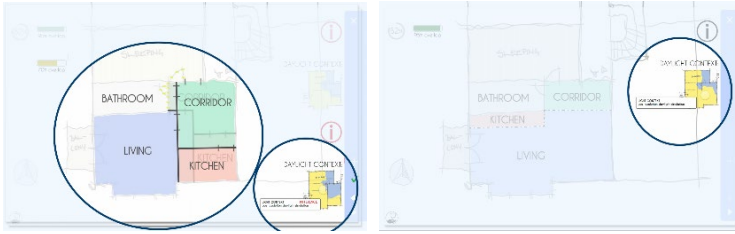


Figure 3. Highlighted explanation visualisations for reasoning support.

The mitigation of the representative bias (Ibid.) is enabled by offering the design conditions (i.e. classification and clustering) called 'Building context information' of both the floor plans for generating the suggestion (see Figure 2, upper right) and the for the drawn sketch (see Figure 4, upper left) with categories derived from the Cultural Objects Name Authority (CONA) (Harpring, 2019, pp. 65-69). The toast notification 'suggestions shown ranked by likelihood' (see Figure 4, upper right) indicates that the suggestions are presented in the order of prior probability to mitigate possible availability bias (Wang et al., 2019). For mitigating the heuristic bias of confirmation (Ibid.), the architect is offered a health bar with colour coding (see Figure 4, lower middle) representing the matching (i.e. similarity) of the sketched floor plan (e.g. room adjacencies) and the floor plans for generating the suggestion.



Figure 4. Highlighted explanation visualisations for mitigating heuristic biases.

Transparency, scrutability and debugging options moderate trust between the architect and WHITE BRIDGE to mitigate analytical and logical weaknesses (Wang et al., 2019). The 'Confidence of the system' (see Figure 4, upper left) in the own classification of the drawn sketch is displayed as a colour-coded loading circle, which can be further investigated through a drop down window. The system communicates the recognition of rooms in the sketch through colour and hatches as an indicator of the room type (e.g. 'wood flooring' for a 'bedroom') (see Figure 5, left). Finally, the original floor plans (see Figure 5, right) for generating the displayed suggestion, can be accessed in a second step (see Figure 2: 'More Details' of 'Building context information').

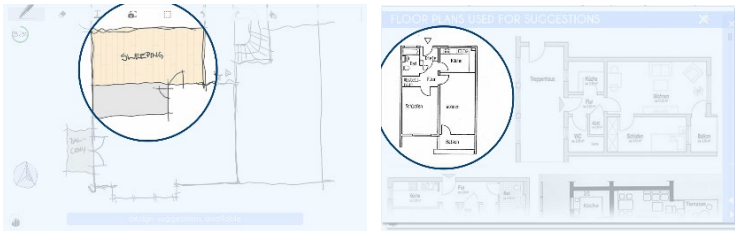


Figure 5. Highlighted explanation visualisation for moderating trust.

5. Case Study

The described interactive high-fidelity prototype was created for a case study with domain experts. Due to the current Covid-19 pandemic it was decided to conduct the study remotely ensuring the health of researcher and participants. In order to overcome possible hindrances of the remote study, such as bad internet connectivity, bugs within the prototype, or focus on the unfamiliar hypothetical application (instead of the explanation visualisations), the architects received preparatory material beforehand, i.e. instructions, a narrated and choreographed video presentation of the digital prototype, and an introduction to WHITE BRIDGE. The latter text was devised as narrated storytelling for near-future concepts to speak to the reader's emotions and personal memories, while leaving room for ambiguity (Spaulding and Faste, 2013). An imaginary persona describes the own experiences with the hypothetical application WHITE BRIDGE, while addressing possible fears and suspicions, and its modus operandi, illustrated with a photo collage of the application in an everyday setting.

After two test sessions with volunteers, eleven participants of diverse background (e.g. Europe, North Africa, South-East Asia, Middle East), aged between 25 and 35 years and working in Central Europe (i.e. Germany, Switzerland, France and Italy), were recruited for the study with individually scheduled sessions held in German or English. After autonomously reading the introductory text to WHITE BRIDGE, the joint sessions consisted of the narrated video presentation of the paper prototype and a semi-structured interview with three question sections: explanations, explanation visualisations and user perception.

The data analysis consists of three stages (see Figure 6): primary data, secondary data and processed data. The primary data of the video recordings was asynchronously transcribed, revised, and divided by speaker and further by question section. The textual results of each questions section were fed into an algorithm to create word clouds for visualising the participants' words and their frequency in an attempt to adjust

the interpretation of the researcher with prior domain knowledge. Simultaneously, the answers of the participants were extracted, and revised on the backdrop of the participants' expressions if and how users were supported, trust between system and user was moderated and/or biases were successfully mitigated. A conformed terminology was used to re-sort all resulting tables by answer for each question. These tables were further processed through interpretation in one mind map per question section. Both the mind maps and the word clouds are further interpreted by the researcher for formulating and formalising the findings of the study.

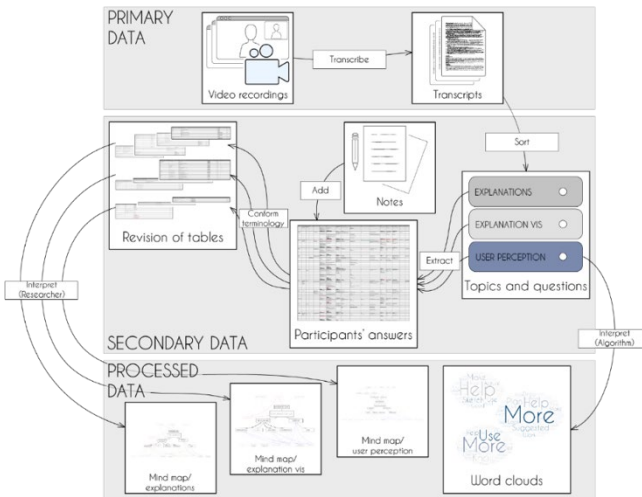


Figure 6. Workflow of the data analysis.

6. Discussion

The findings of the study indicate a broadening of the cognitive horizon of the participants through the explanations and their respective visualisations. During the sessions explanation methods were applied by the architects as intended, as well as for other purposes depending on the application method. For example, the multitude of suggestions for supporting the AHP through comparison was used instead for mitigating the confirmation bias through self-validation. Thus, greater design decision support than expected could be achieved. Especially information of the 'next step' (Participants 3, 6), e.g. the daylight simulation, was deemed highly useful, while the visibility of information for decisions beyond the current phase was rather irritating for most users (Lawson, 2004, p. 53), e.g. 'Material' of 'Building context information'.

The whole concept, explanation visualisations and the experience concerning the explanations, their own design decision and the hypothetical application of WHITE BRIDGE were widely positively received by the participants. One architect, even though recognising possible opportunities, expressed increasing mistrust and insecurity due to deprived ownership over their own design process. Most participants wished only for minor adjustments for working even faster and some even expressed the desire to use the hypothetical application in real life (Participant 4, 11). Summarising, the explanations used within WHITE BRIDGE expanded the cognitive limits of all

participants within the study, even in unanticipated ways. However, if the information did not seem useful (see above) it may irritate the architect. To conclude, the usability of explanations is significantly influenced by their visualisations for the visually driven target group. Consequently, the perception of the explanation visualisations, positive or negative, can affect the perception of the entire application correspondingly.

Nevertheless, these findings of the conducted study need to be viewed on the backdrop of its limited number and diversity among the participants, who are of roughly the same age, work experience (i.e. duration and digital tools) and education, and personally affiliated with the study supervisor. Thus, this study can only be considered a pilot study without true scientific significance. Further, the study was conducted remotely suggesting that the entirety of the body language of the participants (i.e. gestures, mimic) could not be observed.

7. Conclusion

The results suggest that the cognitive horizon of the architects is broadened by the explanations, while the visualisation methods significantly influence the usefulness and use of the conveyed information within the explanations. Architects are supported and themselves identify opportunities in working with an intelligent design assistant, while a sense of control and ownership over design decisions is given. Individual design decisions can be made more quickly and confidently, speeding up the entire architectural design process. Expressed relief by the study participants suggests that the intelligent design assistant also contributes to reducing the architect's stress and mental strain caused by the increasing challenges and workload of the future.

By adapting the framework of Wang et al. (2019) through following their provided steps, the created explainability methods are suitable for an intelligent design assistant to support architects in their design-decision making processes. This paper contributes an established workflow adapted for the domain of architecture for the integration of explanation visualisations in paper prototypes for case studies, the preparation of the study participants, and the data collection and analysis process. Thus, it offers an approach for designing and visualising explainability of an intelligent design assistant for architects, suggesting further design steps during the early design stages. Further, it is transferable to different domains of the construction industry as well as other fields.

In order to determine the right time for the explanation visualisations, we aim to integrate the findings of our sketch study analysing the design process on the backdrop of the design phases (Lawson, 2004; Laseau, 2000), described within our papers of CAADRIA 2022 and ICCO 2022. By utilising these findings, we are enabled to determine the timing for the suggestions and their respective explanation visualisations to avoid answering to future questions or implying "that more is known about the solution than is really the case" (Lawson, 2004, p. 53).

As mentioned in the beginning, quick, efficient and sustainable work is essential for meeting the future demands on the construction industry, while shaping both space on a micro-scale in apartments and on a macro-scale of the urban space. The hypothetical intelligent design assistant WHITE BRIDGE aims to support architects in their design decision making process of the early design stages through suggestions, enriched with explanations. The intelligent design assistant intends to help architects to

meet the increasing demand of high-quality architecture, while enabling architects to focus on the creative aspects of the design process. Finally, we hope that our work may inspire and guide future research for supporting architects in designing with confidence and in more informed ways early on to create high quality architecture more efficiently and more sustainably.

Acknowledgements

We want to thank the participants of the study for their time and valuable feedback, as well as the DFG for funding the 'metis' projects.

References

- Buxton, W. (2007). *Sketching user experience: Getting the design right and the right design*. Morgan Kaufmann.
- Haeusler, M.H., Butler, A., Gardner, N., Sepasgozar, S., & Pan, S. (2021). Wasted... again: Or how to understand waste as a data problem and aiming to address the reduction of waste as a computational challenge. In *Proceedings of CAADRIA 2021, 26th International Conference of the Association for Computer-Aided Architectural Design Research in Asia*, (pp. 371-380).
- Harpring, P. (2010). *Graphic Thinking for Architects and Designers Introduction to controlled vocabularies: Terminology for art, architecture and other cultural works*. Getty Research Institute.
- Harputlugil, T., Gultekin, A., Prins, M., & Topcu, Y.I. (2014). Architectural Design Quality Assessment Based On Analytic Hierarchy Process: A Case Study. *METU Journal of the Faculty of Architecture*, 31, 139-161.
- Laseau, P. (2000). *Graphic Thinking for Architects and Designers*. Wiley.
- Lawson, B. (2004). *What Designers know*, 1st edition. Elsevier, Oxford.
- Lertsithichai, S. (2005). A tangible modelling interface for computer-aided architectural design systems. In *Proceedings of CAADRIA 2005, 10th International Conference on Computer Aided Architectural Design Research in Asia* (Vol. 2, pp. 357-363).
- Negroponte, N. (1973). *The architecture machine: Toward a more human environment*. The MIT Press.
- Palacio, S., Lucieri, A., Munir, M., Hees, J., Ahmed, S., & Dengel, A. (2021). XAI Handbook: Towards a Unified Framework for Explainable AI. In *Proceedings of 2021 IEEE/CVF International Conference on Computer Vision Workshops*, (pp. 3766-3775).
- Richter, K. (2019). *Augmenting Designers' Memory: Case Based Reasoning in der Architektur*. (Doctoral Dissertation, Bauhaus-Universität Weimar).
- Spaulding, E., & Faste, H. (2013). Design-driven narrative: Using stories to prototype and build immersive design worlds. In *Proceedings of CHI 2013, Conference on Human Factors in Computing Systems* (pp. 2843-2852).
- Statista Research Department. (2020, April 10). *Prognose zur Entwicklung der Weltbevölkerung von 2010 bis 2100 (in Milliarden)*. Retrieved April 22, 2021, from <https://de.statista.com/statistik/daten/studie/1717/umfrage/prognose-zur-entwicklung-der-weltbevoelkerung/>
- United Nations (2019). *World Urbanization Prospects: The 2018 Revision (ST/ESA/SER.A/420)*. United Nations.
- Wang, D., Yang, Q., Abdul, A., & Lim, B. (2019). Designing Theory-Driven User-Centric Explainable AI. In *Proceedings of CHI 2019, Conference on Human Factors in Computing Systems* (pp. 1-15).

DESIGNING A FRAMEWORK FOR METAVERSE ARCHITECTURE

A preliminary framework for mixing holographic and physical architectural elements

SHENG KAI TANG¹ and JUNE-HAO HOU²

^{1,2}*Graduate Institute of Architecture, National Yang Ming Chiao Tung University.*

¹*shengkait@gmail.com, 0000-0001-8394-7838*

²*jhou@arch.nycu.edu.tw@email.com, 0000-0002-8362-7719*

Abstract. Metaverse, which was first interpreted as an isolated virtual universe, is now evolving into a multiverse, where virtual worlds superimpose on the real one. Spaces, people, and activities in both physical and virtual formats are going to be seamlessly integrated. Architecture is seen as a container of spaces, people, and activities. Architectural elements are arranged to define spaces guiding people to conduct required activities. The emerging duality of the metaverse will change not only the architectural requirements but also the nature of architecture in terms of form and function. While holograms are becoming a new kind of architectural material, envisioning a potential framework to guide future exploration of metaverse architecture is the goal. In this paper, we conduct a qualitative user study to collect users' needs, identify architectural requirements, and build a preliminary framework for metaverse architecture. This framework provides strategies for mixing holographic and physical architectural elements to fulfill the users' needs of the metaverse. It could further lead to a potential way of reducing the production and consumption of carbon to contribute to the post-carbon framework.

Keywords. Metaverse; Mixed Reality; Hologram; Metaverse Architectural Framework; SDG 11.

1. Introduction and Goal

Metaverse, first coined in Neal Stephenson's 1992 science fiction book "Snow Crash," is interpreted as a virtual universe separate from the real one (Stephenson, 1992). It is a simulated world where people go to escape from their daily lives (Cline, 2011). In the metaverse, people can interact with each other to create, socialize, play, and trade via custom avatars (Ball, 2020). With the advancement of wearable optical see-through display technology (Bimber and Raskar, 2005), the metaverse is no longer an isolated virtual world but a digital multiverse where virtual worlds superimpose on the physical one. Spaces, people, and activities in physical and virtual formats will be seamlessly integrated (Microsoft, 2019; Microsoft, 2021).

Architecture is a container of spaces, people, and activities. Architectural elements, such as horizontal and vertical elements, closures, and openings, are arranged to define spaces and guide people to conduct required activities (Alexander et al., 1977). However, the metaverse, where virtual and physical worlds coexist and collocate, creates a dual representation of spaces, people, and activities. The emerging duality of metaverse will change not only architectural requirements but also the very nature of architecture in terms of form and function.

Computational technologies currently serve as architectural design tools that assist with design thinking (Menges and Ahlquist, 2011), design communication, and construction management (Eastman et al., 2008). However, mixed reality technology, which was mostly adopted to enhance design visualization and simulation (Bertol, 1997), means they can no longer be viewed solely as design tools but must now be seen as architectural materials. Holograms can be used in the same way as wood, glass, concrete, and steel to create brand new architectural elements, reshaping the way people interact with architecture in the metaverse.

Hence, the goal of this research is to envision a potential architectural framework for guiding future exploration of metaverse architecture by answering two key questions:

- What are the new architectural requirements that would serve the emerging needs of metaverse?
- What are the design strategies guiding designers to explore ways of mixing physical and virtual architectural elements to fulfill those requirements?

2. Methodology and Steps

A four-step research and design plan is developed and executed in this study to answer the proposed research questions. First, six potential metaverse early adopters are interviewed to collect qualitative data on user needs. Second, architectural requirements are identified based on the users' needs. Third, a preliminary framework of metaverse architecture is generated consisting of strategies and goals for mixing physical and virtual architectural elements. Lastly, the framework is explained with a design example.

3. Qualitative Interviews

This qualitative research study conducted a series of interviews with six early adopters of the metaverse. As the metaverse is still a developing concept, there are currently no actual products providing metaverse experiences. Hence, early adopters are defined as subjects who with experience using Mixed Reality (MR) devices, including Microsoft HoloLens 2 (Microsoft, 2019) and Oculus Quest 2 (Meta, 2020), with at least two of the chosen 3D remote collaboration and social applications, including Microsoft Mesh (Microsoft, 2021), Spatial (Spatial, 2021), AltspaceVR (Microsoft, 2017), Rec Room (Rec Room, 2016), and Horizon Workrooms (Meta, 2021). These devices and applications are recognized as products offering pioneer experiences in the metaverse. The minimum experience of participants using the above-mentioned MR products should be more than one hour.

Five key questions are used to guide subjects' think-aloud processes. Subjects are asked to answer the questions based on their personal experiences with using MR products, materials related to MR, and metaverse concepts they have seen and heard, as well as their own expectations of MR and the metaverse. The five key questions are:

- What is MR/metaverse based on your understanding?
- What kinds of experiences with MR/metaverse have you tried?
- What benefits of MR/metaverse have you noticed?
- What pain points of MR/metaverse have you encountered?
- Are there any missing features/functions you would like to include in future MR/metaverse products?







						
Subject	Subject 1	Subject 2	Subject 3	Subject 4	Subject 5	Subject 6
Age	26	36	30	22	40	25
Occupation	Grad Student	Professor	SW Engineer	College Student	3D Content Creator	Project Manager
Metaverse HWs	HoloLens 2 Oculus Quest 2	HoloLens 2 Oculus Quest 2	Oculus Quest 2	Oculus Quest 2	HoloLens 2 Oculus Quest 2	HoloLens 2
Metaverse SWs	Mesh Spatial	Mesh Rec Room	Spatial Horizon Workroom	Altspace VR	Mesh Spatial	Mesh Spatial
SW Experiences	~ 1 hour	4 ~ 8 hours	2 ~ 4 hours	1 ~ 2 hours	> 8 hour	1 ~ 2 hours

Figure 1. Subject recruitment criteria

4. User Needs

After interviewing the six subjects, the results were grouped and summarized into four categories: spaces, activities, people, and objects. Within each category, the benefits and pain points that subjects articulated are listed off and discussed. To make the findings more concise and focused, opinions were only considered if they came from more than two subjects.

4.1. SPACES

- **[Benefit] Metaverse offers a three-dimensional (3D) spatial experience.** Virtual world experience is no longer bounded by screen real estate. For example, a user can participate in a 3D virtual remote meeting via a headset, providing full-body interaction instead of a computer monitor constrained by finger and touch screen.
- **[Benefit] Metaverse shows virtual and real spaces at the same time.** Users can perceive, interact with, and be guided by virtual and physical spaces overlaid on top of each other. For example, a user can have a 3D virtual meeting room placed in his real living room.

- **[Benefit] Metaverse makes virtual spaces persistent.** Users can revisit or retrieve the virtual spaces according to physical context. For example, a 3D virtual meeting room previously placed in a living room can be set to auto-launch when a user visits the living room again at the planned meeting time.
- **[Pain Point] Forms of virtual and physical spaces are conflicted.** Physical and virtual spaces overlaid on physical spaces should be further integrated by embedding simulated physics or correlation rules to avoid conflicts. For example, when placing a virtual meeting room in a real living room, the metaverse system should avoid placing a virtual wall and a physical chair in the same location.
- **[Pain Point] Functions of virtual and physical spaces are mismatched.** Physical and virtual spaces that are overlaid should be further merged into a new space that can host two different functions simultaneously. For example, a living room could be divided into two subspaces to host TV watching in the physical space and a virtual meeting in the metaverse simultaneously.

4.2. ACTIVITY

- **[Benefits] Activities in metaverse are not bounded by geolocation.** Activities happening at the same time in different locations are overlaid for users to join in simultaneously. For example, a user can participate in a 3D remote meeting in New York while at home in Taipei.
- **[Benefit] Activities in the metaverse are not affected by time zones.** Activities happening asynchronously are 3D recorded for users to review later. For example, a user can replay a recorded 3D virtual meeting that happened in New York from his home in Taipei.
- **[Pain Point] Virtual activities are constrained by physical boundaries.** Virtual and physical activities should be integrated to adapt to physical contexts. For example, activities in a medium-sized 3D virtual meeting room should be reconfigured to fit into a small-sized physical living room so that remote users are not being obstructed by physical walls.
- **[Pain Point] Physical and virtual activities interfere with each other.** Virtual and physical activities should be considered to prevent interference. For example, a 3D virtual meeting room is placed away from a TV in the living room to avoid interference.

4.3. PEOPLE

- **[Benefit] Users can select avatars to represent themselves.** Avatars and real people can be overlaid in the same viewport. For example, a user can see collocated colleagues and avatars of their remote coworkers in a 3D mixed meeting room.
- **[Benefit] Users can use real-time, 3D-captured representations as their presences.** 3D-captured human representation enables high fidelity and photorealistic communications. For example, a user's appearance, body and hand gestures, and facial expressions can be captured to better communicate with remote

coworkers.

- **[Pain Point] Remote users cannot substantially interact with onsite users.** Both physical and virtual human representations should be integrated to provide interactive feedback, such as hand touch and body touch. For example, a user can use a physical hand to touch the avatar hand of a remote coworker to give them a high-five.
- **[Pain Point] Physical and virtual appearances are separated.** Merging physical and virtual body representations to create a partially real and partially virtual one. For example, a user can wear a physical jacket with virtual decorations augmented on it.

4.4. OBJECT

- **[Benefit] Users can manipulate physical and virtual objects at the same time.** Physical and virtual objects are overlaid to enable users to continue their physical tasks while remaining in the metaverse. For example, a user can drink water from a physical glass and sketch on a virtual whiteboard of a 3D virtual meeting room simultaneously.
- **[Benefit] Digital properties can be augmented on physical objects.** Physical and virtual objects are merged to gain new object-leveraging advantages from both physical and virtual properties. For example, a physical cup can have virtually augmented textures, colors, and even parts.
- **[Pain Point] Physical objects have no correlation with virtual ones.** Physical and virtual objects should be integrated into a physical simulation to make interaction perceptually seamless. For example, using a physical cup to hit a virtual one moves the virtual cup and generates sound feedback.
- **[Pain Point] Physical objects cannot be seen by remote participants.** Physical objects could be scanned to share with remote users. For example, a user could scan a physical cup to make the cup visible and interactable with remote coworkers.

5. Architectural Requirements

Based on the feedback collected on user needs, four requirements of metaverse architecture emerged.

- Metaverse architecture consists of virtual and physical elements, which are persistent, shareable, and integrated, providing continuous 3D spatial experiences.
- Metaverse architecture integrates distant and present elements to conduct both synchronous and asynchronous remote collaborative activities.
- Metaverse architecture hosts real and avatar participants, who can interact with each other via intuitive and natural communication channels.
- Metaverse architecture provides hybrid artifacts which leverage the advantages of physical and digital properties for users to manipulate.

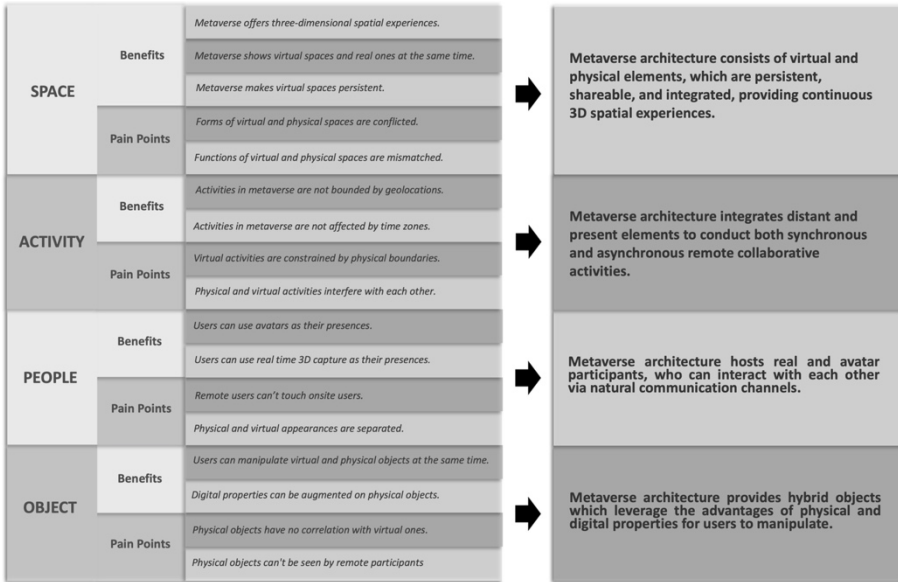


Figure 2. User needs and architectural requirements

6. Strategies and Framework

Based on the requirements of the metaverse architecture we identify, we figure out that mixing virtual and physical entities, including architectural elements, human presences, and artifact properties, to host hybrid and dynamic activities is the core of designing metaverse architecture. In order to create a framework to guide future design explorations, we come up with four strategies tackling different levels of the mixture, including transform, collocate, correlate and stitch. These strategies further form a framework for designing metaverse architecture.

- Transform forms to duplicate functions. Physical forms are transformed into virtual ones via 3D scanning. The goals of this transformation are to capture shapes of architectural elements, store contextual information, and duplicate the functions of the elements.
- Collocate forms to overlay functions. Physical and virtual forms are collocated without any connection or relationship. Users can perceive and interact with physical and virtual forms without causing any functional chain reactions.
- Correlate forms to integrate functions. Physical and virtual forms are correlated by embedding connections and relationships among them. Interacting with one form would cause functional chain reactions of another.
- Stitch forms to merge functions. Physical and virtual forms are stitched together to create a new function. A merged form leverages the advantages of the physical and virtual to provide advanced functions.

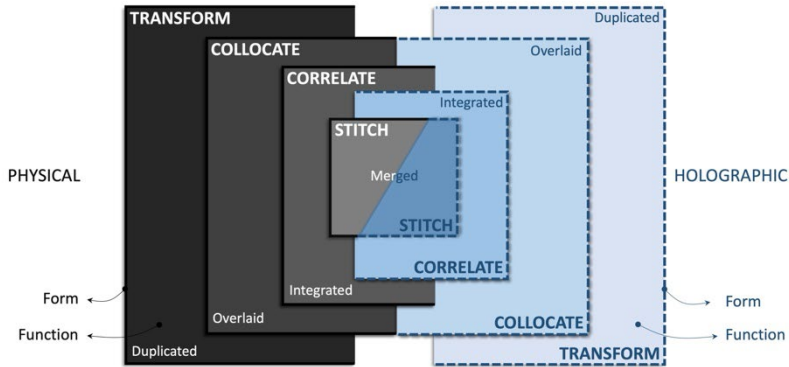


Figure 3. A preliminary metaverse architecture framework

7. Design Example

To make the preliminary framework more understandable, an example is used to demonstrate the applications of the proposed strategies. The scenario has two locations with both architectural and non-architectural elements within them. In location A, elements include a space shaped by two walls and a ground, a regular chair, and a male. In location B, the elements include a space shaped by five columns and a ground, a long chair, and a woman.

- Transform: All elements are duplicated (in blue wireframe). Spaces are mapped, people are 3D captured, chairs are scanned.
- Collocate: All elements from one location are duplicated and teleported to the other location with their original orientations. As shown in the diagram, all teleported elements of one location are overlaid on elements in the other location. The positions of the elements from one location are overlapped with the second location, which may cause conflicts.
- Correlate: All elements of one location are teleported to the other location with rotations and displacements to prevent conflict. For the man, his space is reshaped by five holographic columns, making the east and north sides semi-open. For the woman, her space is also reshaped by two solid walls, making the east and north sides visually blocked. For both the man and the woman, they can see how their own space is seamlessly integrated with the other.
- Stitch: All elements of one location are teleported to the other location with rotations and displacements. The man's north wall is overlapped with the woman's west columns. With the overlapped architectural elements, the two spaces seem to be stitched together to merge into a new space with a different sense of openness.

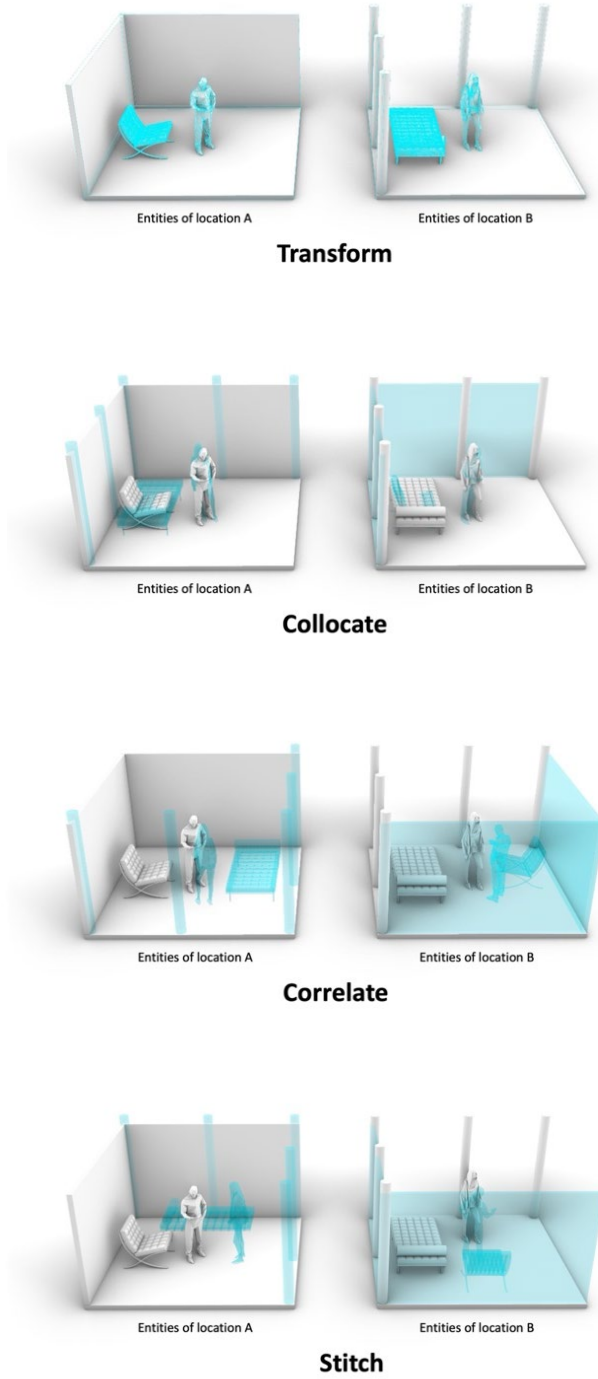


Figure 4. Design examples

8. Conclusion and Future Work

In this research study, a preliminary framework for metaverse architecture was generated based on findings from qualitative user interviews. The framework represents strategies for mixing physical and virtual architectural forms and functions. This framework could be further used to explore potential metaverse architectural patterns. The authors plan to conduct further research to validate the usefulness of this framework.

This study only focused on evolving the framework for architectural elements. However, the gathered data reflected similar findings from other categories of user needs, such as people, activities, and objects. The authors believe this framework could be extended to other design fields, such as avatar design, service design, and industrial design for the metaverse in future work.

Although the findings of this study offer a clearer understanding of potential user needs, a six-subject user study is still not representative enough. Future research could employ a larger sample size to determine if the framework developed here should be expanded or modified.

This preliminary framework also reveals that architectural elements no longer need to be physical, solid, and static. They can be virtual, holographic, and dynamic. It would be even more powerful to merge physical and digital properties to create hybrid architectural elements. We believe such a Holo-physical architectural material could lead to a potential way of reducing the production and consumption of carbon and further contribute to the post-carbon framework.

References

- Alexander, C., Ishikawa, S., & Silverstein, M. (1977). *A Pattern Language: towns, buildings, construction*. New York: Oxford University Press.
- Ball, M. (2020). *The Metaverse: What It Is, Where to Find it, Who Will Build it, and Fortnite*. Retrieved December 15, 2021, from <https://www.matthewball.vc/all/themetaverse>.
- Bertol, D. (1997). *Designing Digital Space: An Architect's Guide to Virtual Reality*. New York: John Wiley & Sons, Inc.
- Bimber, O. and Raskar, R. (2005). *Spatial Augmented Reality: Merging Real and Virtual Worlds* (pp. 149). CRC Press, ISBN 978-1568812304.
- Cline, E. (2011). *Ready Player One*. Crown Publishing Group, ISBN 978-1524763282.
- Eastman, C., Tiecholz, P., Sacks, R., and Liston, K. (2008). *BIM Handbook: a Guide to Building Information Modeling for owners, managers, designers, engineers, and contractors (1st ed.)*. Hoboken, New Jersey: John Wiley. ISBN 9780470185285.
- Grimshaw, M. (2014). *The Oxford Handbook of Virtuality* (pp. 702). New York: Oxford University Press, ISBN 9780199826162.
- Menges, A. and Ahlquist, S. (2011). *Computational Design Thinking*. John Wiley & Sons. ISBN 978-0470665657.
- Microsoft (2015). *AltspaceVR*. Retrieved December 15, 2021, from <https://altvr.com/>.
- Microsoft (2019). *HoloLens 2*. Retrieved December 15, 2021, from <https://www.microsoft.com/en-us/hololens>.
- Microsoft (2021). *Microsoft Mesh*. Retrieved December 15, 2021, from <https://www.microsoft.com/en-us/mesh?activetab=pivot%3aprimary7>.
- Meta (2020). *Meta Quest 2*. Retrieved December 15, 2021, from <https://www.oculus.com/quest-2/>.

Meta (2021). *Horizon Workrooms*. Retrieved December 15, 2021, from <https://www.oculus.com/workrooms/>.

Rec Room (2016). *Rec Room*. Retrieved December 15, 2021, from <https://recroom.com/>.

Spatial (2021). *Spatial*. Retrieved December 15, 2021, from <https://spatial.io/>.

Stephenson, N. (1992). *Snow Crash*. Bantam Books. ISBN 0-553-08853-X.

NET ZERO GAME: A PILOT STUDY OF GAME DEVELOPMENT FOR GREEN BUILDING EDUCATION

A mini game development with parametric BIM-based simulations

JONG BUM KIM¹, DANIELLE OPEREAN², LAURA COLE³ and
LAURA ZANGORI⁴

^{1,2,3,4}*University of Missouri Columbia.*

¹*kimjongb@umsystem.edu, 0000-0001-8762-9554*

²*opreand@missouri.edu, 0000-0001-8052-0791*

³*colelb@missouri.edu, 0000-0001-5730-1881*

⁴*zangoril@missouri.edu, 0000-0002-7512-5559*

Abstract. The research investigates the design and development of a serious game to teach green building design and energy literacy in rural middle schools in the United States. The paper presents a pilot study, education mini-game development integrated with parametric BIM and energy simulations. The game scenario was built on the developed science curriculum modules in our funded research, teaching building energy technologies such as daylighting, artificial lighting, window configurations, building materials, solar panels, etc. The mini game presents a baseline science lab and a media library of typical public schools in the United States. The players have the opportunity to improve energy literacy in several ways: manipulating the building configurations and the energy options, reviewing energy cost and the emission level changes, and monitoring the performance from the dashboards. This paper presents background theory, curriculum design, the mini-game development framework, methods and tools for energy simulation and BIM visualization, and the findings and challenges.

Keywords. Serious Game; Energy Literacy; Green Building Education; Parametric BIM; Energy Simulation; SDG 4; SDG 11.

1. Context of Game-based Learning for Green Building Education

Energy literacy becomes essential in the energy workforce education to achieve zero energy and gas emission reduction. However, the teaching apparatus and curriculums of formal education in the United States still do not reflect these global demands (Kandpal & Broman 2014). Although these concepts of Green Building are simple, achieving these goals is still challenging because of complex energy mechanisms and behavior. Understanding energy flow through the built environment requires systems thinking abilities (Lacy et al. 2014). Still, it is challenging to master without high-order thinking skills and intentional learning experiences (Hmelo-Silver & Azevedo 2006).

Serious games take the concept of video game technologies and repurpose the Game for training, education, advertising, national defense, and more (Dib, H., 2014). Serious games provide an innovative approach to computer-based modeling to support the development of systems thinking (Liarakou et al., 2012). In addition, serious games show promise for learning through informal means of creativity (Kalinauskas 2014), play (Ampatzidou et al. 2018), collaboration (Hummel et al. 2011), and role-playing (Jenkins et al. 2009). Studies described the benefit of serious games in comparison with the conventional education media, including intrinsic motivations, greater attention, enhancing the sense of engagement, lowering the threat of failure and mistakes, application of learned skills, greater intellectual intensity, and more (Klopfer et al. 2010; Coller et al. 2009; Papastergiou 2009).

During the past decades, various serious games were developed as a medium to improve energy literacy in the built environment, such as Efficient City (2001), ElectroCity (2007), Climway (2010), CityOne (2011), EnerCities (2011), EnergyVille (2011), etc. ElectroCity challenged gamers to balance energy consumption, the development revenue, and renewable energy generation in town planning and design. Climway asked users to monitor and reduce the energy consumption of the community plan during a 50-year life cycle. More recently, serious game research addressed behavior change of the specific end-user, widely accepted as the most impactful factor for energy savings. For example, Serena Supergreen (2018) was designed to motivate and educate female students between 12 and 16. Powersaver Game (2019) challenged virtual family members to save 15% on energy, electricity, and gas consumption in three weeks. Rossano (2017) claimed that these serious game developments show the advantages, including better visualization of energy consumption, increased end-user engagement, their energy behavior change, and collectible end-user feedback.

However, educational technologies are still poorly interweaved with science curriculum units despite rapid research and development. Energy data in the game does not interact with various energy options and game scenarios. Since Woodbury et al. (2001) claimed the potential of CAAD and serious game integration in architectural design education, a growing number of studies have explored BIM and game integration for visualization, design decision making, design education, professional training, etc. Our multi-disciplinary research team envisioned that the advancement of BIM, increasing graphics capabilities, accessible game developments, and multi-criteria energy simulations would boost the efforts in this field.

2. Mini game development

The section presents a pilot study, education mini-game development integrated with parametric BIM and energy simulations. The goal is to create a theoretical and empirical framework for Net Zero Game, a serious game to teach green building design and energy literacy in rural middle schools. This section describes background theory, developed curriculum, the mini-game development framework, and methods and tools for energy simulation and visualization. The target application is the rural school districts in Missouri, underserved populations for science, technology, engineering, mathematics (STEM) interventions with limited access to STEM learning opportunities.

2.1. MODEL-BASED REASONING AND EYE CURRICULUM

Prior work has focused on the numerous energy misunderstandings students have about energy systems (Duit et al., 2014). Research outcomes suggest that teaching energy systems should make energy transfer and transformation visible, observable, and manipulable (Lee et al., 2013). We content this occurs through model-based reasoning ([MBR] Duschl et al. 2016; Verhoeff et al. 2008). Within MBR, students first develop an energy system responding to a question. When students develop, they can deconstruct a complex system to focus on critical systems elements (Gouvea et al., 2017). Next, students use their models to make sense of system behavior (Zangori & Cole, 2019, Jordan et al., 2009). Finally, students evaluate and revise their models as their knowledge increases in sophistication (Ben-Zvi Assaraf & Orion 2010).

The Game was designed to be embedded within a six-lesson curriculum unit called Energy and Your Environment (EYE), funded by NSF. EYE fosters place-based education by using local school buildings to enhance systems thinking about energy consumption and flow between buildings and Earth systems. Systems thinking is taught through the MBR framework in which students have ample opportunities to break large systems into smaller components to look closely at key components, causal interactions, and inputs/outputs within systems. The research team aligned with the EYE curriculum and the mini-game scenario for better game-based learning.

2.2. PROCESS

Before creating a full-scale 3D serious game, the research explored and examined a small-scale 2.5D game. A 2.5 game uses fixed isometric views to enable 2D game play in 3D environment. Players can move throughout the game environment, but the camera view does not change until a new game scene is accessed, such as changing locations. The game scenario was built on EYE curriculum modules, teaching energy technologies such as daylighting, artificial lighting, window configurations, building materials, solar panels, etc. The Game presents a baseline science lab and a media library of the typical public schools in the United States. The players can have the opportunity to improve energy literacy in several ways: manipulating the building configurations and the energy options, reviewing energy cost and the emission level changes, receiving interactive feedback from a dashboard and virtual consultants, and iterating the changes to achieve net-zero.

The game prototype was developed from the three phases, including (i) EYE curriculum development (C1, C2), (ii) Game design and development (G1, G2, G3), and (iii) Energy modeling and simulation (S1, S2, S3) shown in Figure 1.

First, parametric BIM was used to create manipulatable virtual models, such as a ceiling height change, exterior wall configuration, a window ratio, shading device, and artificial lighting configurations. Then, the real-time visualization platform converted the parametric BIM into a series of game scenes. The research explored Unreal Engine's Twinmotion and Enscape 3D. For energy simulations, the research used BIM-based cloud simulation. The simulation results and the benchmark results were compiled to produce an energy performance matrix based on the energy options in the game interface, including Energy Use Intensity (EUI), energy cost, and CO₂ emission levels. For the game development, Unity3D and the game assets were used. In addition,

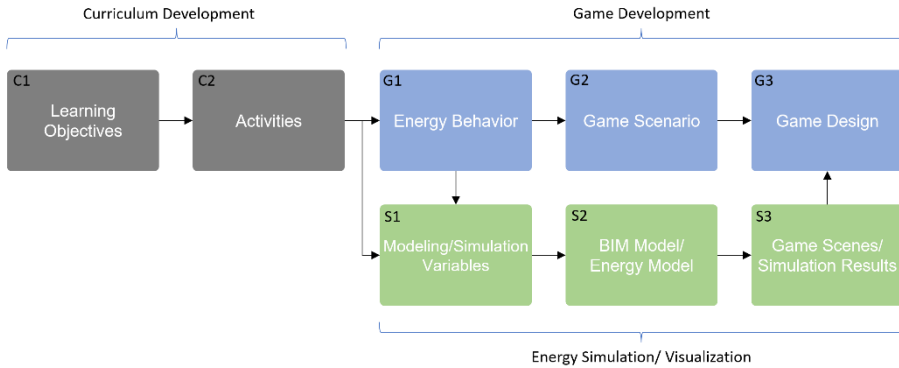


Figure 1. Research phases of mini-game development

the research created custom creature characters for better student engagement, breeding at the science lab to show the varying health conditions according to the energy performances. Although the linear process is presented sequentially, the research was built on bidirectional data exchange, frequent feedback loops, and iterative synchronizations across three domains of curriculum design, game design, and BIM-based modeling/ simulations.

2.3. BUILDING MODELING AND VISUALIZATION METHODS

The mini-game development attempted to take advantage of parametric BIM for rapid model changes and expeditious synchronization between the building model, energy simulation, and game scenes. In the context of the net-zero Game, the number of building/energy models could incrementally increase when the Game allows players to manipulate building configurations and energy choices. It makes manual creation of the game scenes manually a less viable approach.

Architecture design and construction domains rigorously investigate BIM and visualization integration. The relevant technique to this research includes real-time AR/VR creation from BIM, passing BIM data to visualization interfaces, and bi-directional model synchronization between BIM and visualizations. Ideally, these features would give students various learning experiences: students can vary a wide range of energy options in BIM; they can monitor how their choices change the indoor environment; and students can access building information such as materials, dimensions, and other energy-related building parameters within BIM. In that regard, the research has investigated and benchmarked the feasibility and applicability of BIM-based real-time visualization and BIM-game integration.

2.4. ENERGY SIMULATION METHODS

Towards serious game development, the research investigated three methods for game and energy simulation integration, including (i) cloud-based pre-simulation, (ii) iterative parametric pre-simulation, (iii) and algorithm-based prediction. Three approaches vary in view of process time, feedback latency, maintainability, and dissemination capability.

Pre-simulation: Complete simulations first and pass the simulation results to the game development phase. Legacy-simulation engines provide rich validity in results, but time and effort-intensive input processing is needed. The research explored BIM-based cloud simulations to eliminate redundancies and errors in energy modeling in the legacy simulation engines. Benchmark data from Autodesk Insight 360 enabled the prediction of various energy scenarios.

Iterative parametric simulation: Automate the energy model update and simulation execution using parameter iteration. Parameters need to be fully identified before the simulation run. Also, software prototypes could automate the conversion from building models to energy models, parameter updates, simulation runs, and result aggregation. Our prior works examined the iterative parametric simulation using BIM, multi-criteria simulation interfaces, and legacy simulation engines (Kim et al., 2021). The research used Revit for energy modeling, Grasshopper simulation plus-ins such as Ladybug and Honeybee tools, TT Toolbox for the iterator, and Rhino.Inside for the crossover data communication.

Algorithm-based prediction: Identify the energy performance pattern from the iterative parametric simulation using BIM, parametric simulation iteration, legacy simulation engines, and prediction algorithm. Our current investigation examines cross-platform integrations using BIM for energy modeling, parametric training and validation data generation iterations, and machine learning algorithms to produce the prediction rules.

The mini game presents our first implementation of pre-simulation using selected curriculum modules, BIM-based cloud simulations, and BIM-based visualizations.

3. Mini game development

The mini game is developed based on Lessons 4 and 5 in the EYE curriculum, teaching energy knowledge of building materials, daylighting, artificial lighting. Sub lecture modules in EYE challenge students to conduct specific activities to test energy knowledge gain. The following sections explain the research phases illustrated in Figure 1.

3.1. EYE ACTIVITIES AND LEARNING OBJECTIVES

The first phase was critical to align the curriculum contents, game scenarios, and building/energy modeling. Table 1 shows examples of essential activities of EYE that provided a foundational framework for game scenarios and energy simulation variables (C1, C2 in Figure1). The curriculum was initially designed to use analog teaching tools for rural schools without technology access. The mini-game is an attempt to substitute these analog tools with interactive digital learning platforms. The research identified a series of energy behavior from these curriculum contents and relevant activities such as building material change, window configuration change, and lighting fixture change.

Table 1. Main module's activities and learning objectives

<i>[Module] "Activity"</i>	<i>Learning Objectives</i>
<i>[Sun and Building] "Light Where You Live"</i> Use climate simulations to examine how sunlight interacts with your school building in your unique location.	Apply knowledge of the sun path and solar accessibility, considering building siting and façade configurations
<i>[Building Operation] "How you use your building."</i> Change building operation of HVAC, lighting, and other electric equipment. Then observe changes in overall energy use level	Recognize the impact of building occupancy and operation on energy use
<i>[Daylighting] "Light & Your School Building"</i> Apply what you have learned about the characteristics of light energy and light energy transfer to your school building. As you tour the building, make observations about how light travels inside.	Apply understanding of climate data to analyze how light interacts with the school building
<i>[Artificial Lighting] "Which Lightbulb?"</i> Students measure the heat output and illumination of different lightbulbs, making and testing their hypotheses about lighting, heat, energy use, and cost over time.	Develop an artificial lighting plan that balances the lighting quality and energy cost.

3.2. ENERGY BEHAVIOR AND SIMULATION VARIABLES

Next, we identified energy behavior and simulation variables required for scenario development and energy modeling criteria (G1 and S1 in Figure1). Table 2 shows energy behavior and simulation variables implemented in the mini game.

Table 2. Energy Behavior and Simulation Variables

<i>Curriculum Modules</i>	<i>Energy behavior in Game</i>	<i>Simulation variables</i>
<i>[Sun and Building]</i>	Reposition the buildings	Orientation
	Resize the rooms	Energy model dimension
<i>[Building Materials]</i>	Select roof materials	R-value, U-value
	Select wall materials	
<i>[Building Operation]</i>	Select occupancy schedule	Occupant heat gain
	Select equipment efficiencies	Equipment heat gain
<i>[Daylighting]</i>	Select window size/ numbers	Window to Wall ratio
	Select glass materials	R-value, U-value
	Select shading devices	Window transmission
	Select window opening frequency	Infiltration rate
<i>[Artificial Lighting]</i>	Select lighting types	Lighting efficiency

3.3. PARAMETRIC MODELING AND ENERGY SIMULATION

The energy behavior and simulation variables provided criteria of parametric modeling in BIM for game visualization, energy modeling variables, and energy simulation scenarios. In this phase, the research coincided with game design and game scenario

development and had frequent feedback loops to align Game, simulation, and visualization. The mini game tested the following simulation variables in Table 3.

Table 3. Simulation category and variables

Category	Variable Types		
Wall/ Roof Materials	High performance (R38)	Moderate performance (R20 to 25)	Low performance (Uninsulated)
Window-to-wall ratio	Large window (80%)	Medium window (40%)	No window (0%)
Window shades	Large shading (1/2 window height)	Medium shading (1/4 window height)	No shading devices
Glass materials	High performance (Triple Low-E glass)	Moderate performance (Double clear glass)	Low performance (Single clear glass)
Lighting efficiency	High performance (LED)	Moderate performance (Fluorescent bulb)	Low performance (Incandescent bulb)

The research performed 243 pre-simulations in the mini game, calculated EUI, energy cost, and CO2 emission levels, and fed the simulation results into the game interface. To match the simulation set and the game scenario, we assigned simulation ids to simulation results. The simulations used Autodesk Revit and Insight 360. The visualization was based on BIM-based real-time visualization plug-ins, including Enscape and Unreal engine's Twin motion.

3.4. GAME DESIGN AND SCENARIO

The game scenario and interface design aimed to enrich engagement and motivation in learning. The Game takes place in a research facility located on an isolated island in the Galapagos, where the player can interact with other characters working at the facility. The Game places learners in the role of a scientist tasked with caring for evolving new species of creatures that are sensitive to climate change in Figure 2. The game design was informed by entertainment games popular with middle school-aged students. Games, such as Pokémon with the involvement of evolving a creature through various actions, played a role in the larger story development. The social mechanic used for decision-making to design the lab space was influenced by the popular gaming space such as Roblox.

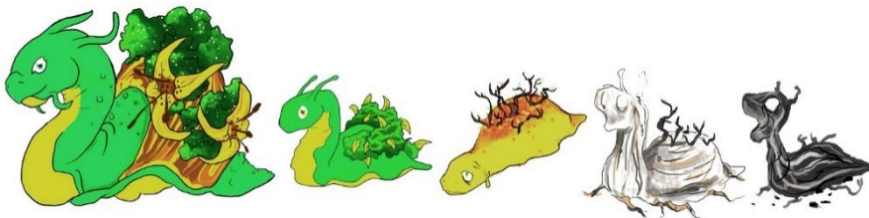


Figure 2. Creature design with five health levels

Other characters include a director of the research station, responsible for the overall energy facility and cost. A lab assistant assists the player with making decisions and finalizing results at the end of each game day. A librarian provides additional information about related energy subjects. An engineer helps the player make critical decisions about energy technology and options. The game world consists of a multi-building research facility that generates its power. The facility consists of five different spaces: main lab, library, staff lounge, research center, and observation deck.

The pilot game was developed using Unity3d with purchased assets to enable us to focus on how to connect the simulation data into the Game that would be meaningful. We created a 2.5d game that uses a 2.5d Toolkit to facilitate player movement around isometric environments. Combined with the 2.5d Toolkit, we utilized a dialogue tool to form the core gameplay and dialogue selection to make choices (Figure 3)

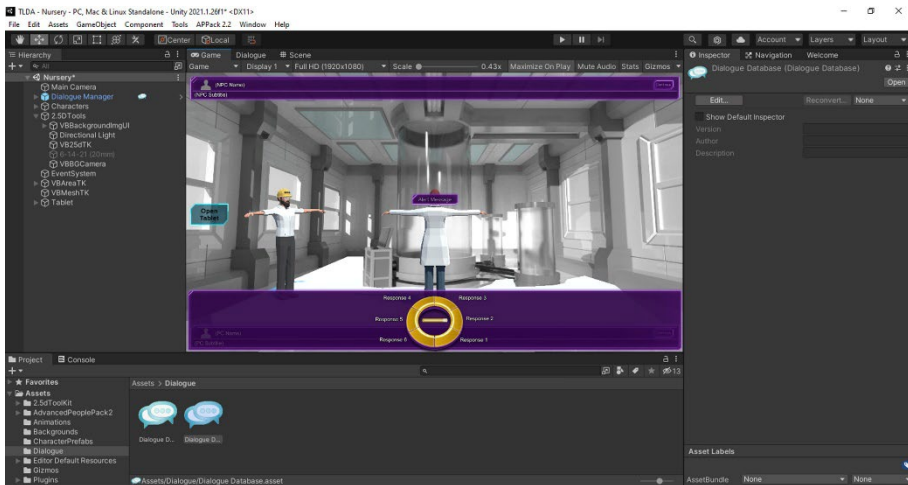


Figure 3. The lab scene development in Unity3D

4. Results

The research investigated game development based on our energy curriculum, including game scenarios, characters, dialogues, and game interfaces. The research also explored BIM-based parametric modeling and interactive visualizations to expedite game scene creation, energy modeling, and simulation result creation. To feed performance data into Game, the research examined BIM-based cloud-based simulation.

Figure 4 shows the resulting Game, a mini version of the larger NetZero game. To evolve the creature, the player must first power the lab to be energy efficient based on energy simulation variables listed in Table 3. The Game starts off in the main lab where the player is introduced to the creature and the lab assistants. The main goal is to evolve and release the creature found on the island. Within 30 game days, the player will be prompted to engage with the other characters in the research facility. The player



Figure 4 The game interface (left) and the dashboard (right)

observes the evolved creatures to determine the best decision to improve the creature's health. Players would also maintain information on the dashboard that would track decisions made as the game progressed. Based on the pre-simulation results and unique ids, the dashboard displays updated energy performances of EUI, energy cost, and CO₂ emissions. The game interface swaps the background scenes created from the Revit models and visualization tools. Players monitor how their energy choices affect the environmental conditions from the creatures' status.

5. Conclusion

The mini-game development produced a theoretical and empirical foundation for the full net-zero Game. The research attempted to facilitate seamless communication and data flow across three domains of curriculum development, energy modeling/simulation, and game development. We observed that the linear and top-down process could deteriorate flexibility in revisions, content alignment, and data exchange across three domains. However, the game designed here fits within the curriculum structure as it was specifically designed to work within the EYE unit. This is a novel educational intervention that is new to the field of science education.

Within the U.S., rural school districts are underserved populations for STEM education. They do not have ready access to green buildings in their communities. This challenge presents crucial equity issues as rural student expectations towards energy workforces increase, such as the gas, oil, wind, water, and solar energy industries. The described game is expected to bring knowledge about energy flow, human energy use, and green buildings to the rural students.

BIM adoption in serious games still faces several challenges. For instance, real-time communication between BIM and games is available when the classroom has access to full software licenses. Data exchange between BIM and games is still limited. The game development platforms have limited access to BIM data, and BIM tools have insufficient features for game developments vice versa. In addition, mini game relied on prerendered images and the image swapping function to update game scenes.

When considering the broad curriculum scopes, various energy options in the Game can exponentially increase the cost of energy simulations. Pre-simulations based

on the predefined game scenario can prevent flexible game scenario and curriculum revisions. Reversely, it can cause complex changes in game design after the energy simulation runs. We anticipate that algorithm-based prediction may mediate the limitation of top-down and pre-simulation. We envision that it can eliminate the potential software license issues when distributing the serious Game to the classrooms. The full net-zero Game will further investigate this simulation method. The game development is still in early stage and needs feedback from the teachers and students. The under-developing research phase is the usability test of the mini game, planned to be performed at rural middle school districts in Southern Missouri.

Acknowledgments

This research was supported by NSF Project, Enhancing Energy Literacy through Place-Based Learning: The EYE Project (DRL- 2009127), and College of Human Environmental Sciences (HES) program for Proposal Enhancement Support. DTI: The Net Zero Game: Integrating Role-Playing and Model-Based Reasoning in a Serious Game for a Green Building Unit. Thanks to research assistants Steve Gallo, Aysegül Aktürk, and Hanbin Kim.

References

- Ampatzidou, C., Constantinescu, T., Berger, M., Jauschneq, M., Gugerell, K., & Devisch, O. (2018). All work and no play? Facilitating serious games and gamified applications in participatory urban planning and governance. *Urban Planning*, 3(1), 34-46.
- Dib, H., & Adamo-Villani, N. (2014). Serious Sustainability Challenge Game to Promote Teaching and Learning of Building Sustainability. *Journal of Computing in Civil Engineering*, 28(5).
[https://doi.org/10.1061/\(ASCE\)CP.1943-5487.0000357](https://doi.org/10.1061/(ASCE)CP.1943-5487.0000357)
- Hummel, H. G., Van Houcke, J., Nadolski, R. J., Van der Hiele, T., Kurvers, H., & Löhr, A. (2011). Scripted collaboration in serious gaming for complex learning: Effects of multiple perspectives when acquiring water management skills. *British Journal of Educational Technology*, 42(6), 1029-1041.
- Jenkins, H., Camper, B., Chisholm, A., Grigsby, N., Klopfer, E., Osterweil, S., ... & Guan, T. C. (2009). From serious games to serious gaming. *Serious games: Mechanisms and effects*, 448-468.
- Kandpal, T. C. & Broman, L. (2014). Renewable energy education: A global status review. *Renewable and Sustainable Energy Reviews*, 34, 300-324.
- Kim, J. B., Aman, J., and Balakrishnan, B. (2021). Forecasting performance of Smart Growth development with parametric BIM-based microclimate simulation. Projection, *Proceedings of the 26th International Conference of the Association for Computer-Aided Architectural Design Research in Asia (CAADRIA) 2021*, March 29-April 1, Hong Kong.
- Liarakou, G., Sakka, E., Gavrilakis, C., & Tsolakidis, C. (2012). Evaluation of serious games, as a tool for education for sustainable development. *European Journal of Open, Distance and E-learning*, 15(2).
- Rossano, V., Roselli, T., & Calvano, G. (2017). A serious game to promote environmental attitude. In V. L. Uskov, R. J. Howlett, & L. C. Jain (Eds.) *International Conference on Smart Education and Smart E-Learning* (pp. 48-55). Switzerland: Springer International.
- Zangori, L., & Cole, L. (2019). Assessing the contributions of green building practices to ecological literacy in the elementary classroom: an exploratory study. *Environmental Education Research*, 25(11), 1674-1696.

CO-PRESENCE IN REMOTE VR CO-DESIGN

Using Remote Virtual Collaborative Tool Arkio in Campus Design

SHUVA CHOWDHURY¹ and JOHAN HANEGRAAF²

¹*Southern Institute of Technology, ²Arkio.*

¹*shuva.chowdhury@sit.ac.nz, 0000-0001-8261-4468*

²*johan@arkio.is, 0000-0002-7886-383X*

Abstract. A participatory co-design approach is most often counted as a time-consuming method and ends without any concrete solution. Since the new evolution of virtual reality-based communication tools, researchers are trying to integrate citizens in the spatial design making process in-situ situation. However, there has been little research on how remotely co-presence in VR can integrate end-users in a co-design environment in re-envisioning their own using spaces. This study adopts a remote VR collaborative platform Arkio to involve novice designers remotely to design their known urban places. Participants are in three different virtual communication systems. Groups can actively engage in co-creating 3D artefacts relevant to a virtual urban environment and communicate through audio together in a remote setting. The platform was tested with a group of graduate students. The given design task was to re-envision the urban places of their academic institute campus. The sessions have been recorded and transcribed for analysis. The analysis of remote conversations shows that co-presence existed while they were engaged in co-design.

Keywords. Affordable Tools; Remote Collaboration; Smart City; Participatory Design; SDG 11.

1. Introduction

UN-Habitat's people-centred smart city agendas focus on leveraging technological services for the common good by delivering inclusive and equitable participation of local communities in the design decision-making process (Royall, 2022). As a result, many cities have become testbeds for new, untested and sometimes unregulated technologies, forcing local authorities to respond to these disruptive technologies. The trend became urgent as soon as COVID-19 hit the universe. A fast reformation of urban regeneration has been needed to re-envision our urban neighbourhood. Innovation in the integration of disrupted visual communicative tools and design processes leverage the local to re-envision their own neighbourhood by themselves. Such inclusion of the end-users in the design process brings users perspectives which are essential to finding relevant, meaningful and sustainable design solutions. Any participatory design

solution develops through a meaningful conversation of participants. The process gets influenced by the engagement tools, which traditionally are physical artefacts, drawings and rendering images produced via any digital method. In participatory urban design, people (Chowdhury, 2020) use tools like Virtual Reality (VR) to visualise and construct the design contents in the virtual world, which is more like reality. The three-dimensional (3D) environment offered in the VR conveys and contains information in ways that are not possible using analogue techniques. The tool allows the participants to construct instant 3D artefacts as design inputs relevant to the virtual urban environment (Chowdhury & Schnabel, 2020). However, there is hardly any research where all participants share the sense of co-presence in the virtual environment and actively generate 3D artefacts and collaborate inside the virtual urban space. Traditionally, most urban design community engagement uses VR applications as tools for consultations. They allow the public to walk through the virtual environments and experience the proposed design scenarios but do not collaboratively co-create content in the virtual environment. As opposed to that, UN-Habitat runs a game based participatory design intervention for the marginalised community using 'Minecraft'. The virtual artefacts offered in the participation process is abstract, non-immersive and missing the aspect of participating as individual designers to produce design instantly together at the same time and in the same virtual space. Due to the lack of enough perceptual relevant information of the virtual spaces, the tool struggles to construct relevant imagination in the immersive environment. Compared to that, this research looks at how both remote VR and urban co-design can be done together in the virtual space. The participants can act as a design unit and contribute to conclusive design outcomes. The study employed a VR tool, "Arkio", involving remote participants more effectively via audio chat and experiencing instantaneous generation of 3D artefacts. Together, the representation of the virtual contents in the tool, its capability to produce instant 3D artefacts with design actions and audio conversations engage the users in constructing meaningful urban design ideas.

2. Virtual Co-Presence

In general, the term presence (also known as physical presence) mainly refers to individuals' sense of being' in a virtual environment (Sheridan, 1992). According to Slater (1999), there are three aspects of presence: the sense of 'being there', an individual's response to what is 'there' as real, and an individual's memory of the environment as a 'place' similar to real situation. In the immersive virtual environment, the sense of presence is affected by the vivid, matching and inclusive surroundings in the computer display (Slater, Usoh, & Chrysanthou, 1995). Witmer and Singer (1998) define presence as a subjective experience that depends on the ability to focus on certain stimuli in a virtual environment and exclude the unrelated stimuli of real life. The focused and attentive attributes of the environment involve an individual psychologically and attaches to the stimuli and experiences and allow them to interact with the virtual content. The degree of involvement and immersion in the virtual environment depends on the degree of sense of presence.

The sense of being together is developed through a focused "psychological connection of minds" (Nowak, 2001), which researchers conceptualised as co-presence. The definition of co-presence is the sense of being in the same virtual place

with some sensory properties of place presence and having a mutual awareness of the individuals in the virtual environment (Bulu, 2012). It consists of a sense of feeling that others are actively perceiving us and being part of the group. It mainly addresses the psychological interaction of the individuals.

Designing a place in virtual environments should be rich enough to activate all the human perception, cognition, and emotion components. The effective engagement with the virtual content depends on the physical properties of the display, objects, actors and the flow of events as design actions. They are responsible for keeping the user interested and involved in the design process. All of them together impact the sense of presence in the virtual environment. In shared virtual environments, the participants are involved in co-presence situations to collaborate actively in design activities. This study reflects on the concept and characteristics of co-presence between immersive and non-immersive virtual environments. The employed system provides distributed designers with a more effective design environment with the sense of “being there” and “being together”.

3. Immersive Design Collaboration and Arkio

Co-design or collaborative design is a term to define a process of designing where different parties like designers, architects, engineers and sometimes clients work together to achieve a shared design goal (Gül, 2020). They work together on a design artefact or parts of it. Co-design process is similar to an individual’s mental process, which establishes shared goals and develops a shared understanding of design brief, design constraints, framing and examining design problems, and the materialisation of a design solution. In a virtual co-design situation, designers are co-located in the same virtual environment allow verbal and visual communication between parties. The effectiveness of visual communication depends on shared representations of the virtual contents and the types of experiential media, either immersive or non-immersive. In the process, external representation of the virtual environment plays a significant role to interact with the 3D artefacts. The external representation brings the relevancy of the virtual artefacts to the real world. When design thoughts are externalised through artefacts, each artefact contains properties for future interpretations that designers can negotiate during further design development. The representation of artefacts develops conversation both with oneself and with others. These external representations also become the ground for conflicts and collaboration.

Intuitive design collaboration depends on the scope of the artefacts offered by the virtual tools. In participatory design, the role of the tools plays a major part in engaging with the cognitive level of the design decision-making system. Participants decide through verbal communication and responses on the artefacts with design actions. The participants construct the virtual artefacts’ representational meaning in the process by relating the visualised information with the actual context. The continuity of design conversation depends on the instantaneous creative responses to the 3D artefacts. Every design action builds a new organisational representation of the artefacts, creating new thoughts for design conversation. The quality of tools’ response against design actions is mainly responsible for the quality of the design conversation. This instrumental quality depends on the perceptual affordance of the tool, which Gaver (1991) coined for computer-aided interfaces.

An immersive co-design environment supports an active and real-time experience with the design, therefore presenting a sense of being in the environment. The immersive environment carries a less cognitive load to the participant. In one of the earlier research on remote design collaboration with architectural students, Schnabel (2011), employed communication happened via text and 3D models. In that research, creating 3D artefacts required additional steps, which broke the continuity of design conversations between remote participants and due to that the communication wouldn't happen in a co-present environment. In contrast, in Arkio's virtual environment, users usually experience the higher level of immersion by its extension to the Head Mounted Display (HMD) option. A remote participant can immerse in the virtual environment and locate where the other fellow participants are standing (Arkio, 2021). The interface allows the participants to navigate in the virtual space themselves freely. They can have some self-directed and interactive experiences. Participants can see each other's design actions in the VE and continue conversations. The users feel a sense of co-presence. The tool also offers several default 3D artefacts to place and create new content in the environment. The instantaneous quality of generating 3D artefacts allow the immersive participants to engage in virtual collaboration with the design contents. In this study, the student participants utilise Arkio in a multimodal communication system, where the sense of co-presence is a bit compromised from immersive to non-immersive. One participant was in an immersive environment, and the other two participants were in a non-immersive environment.

4. Research Methodology

The research methodology starts with developing the low-mesh 3D model of the investigation and uploading them in the Arkio (figure 1). The remote collaborators invite the other participants in the Virtual Environment (VE). From the first-person point of view, the remote participants are shown as avatars who talk and take operational design decisions by placing and adding design artefacts in the VE. The

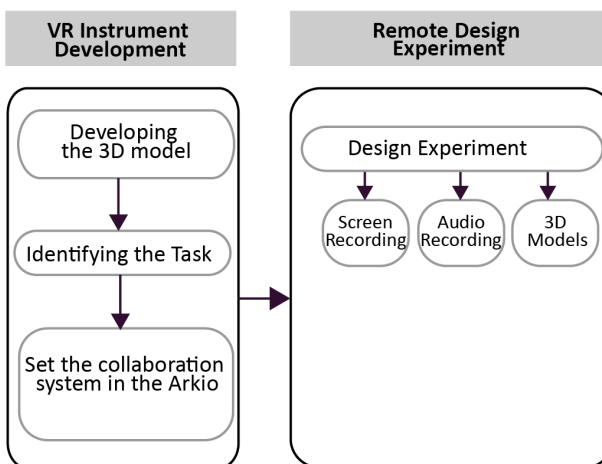


Figure 1. Research framework

design task is given to re-design the landscape of the campus area. The participants can comment on other participants actions and take active efforts in the VE by repositioning the placed artefacts or adding new artefacts. The engagement sessions are recorded, and back-ended data has been saved to report the types of design conversations in the VE.

5. Design Unit

An experimental setup has been developed to leverage designers to participate together in VR urban design. Designer A sees the VE immersed through a Head-Mounted Display (HMD), and as a first-person point of view, he interacts with the 3D artefacts via a controlling device to generate, delete and alter the design. Designers B and C see the 3D artefacts through 15-inch laptop display screens. They together act as a design unit. They interact with the artefacts by instructing others through verbal chat and executing their design ideas by themselves. Figure 2 shows a diagram of a design unit. The diagram is triadic as they are closely related entities and depend on each other actions. Designers generate design action and seek verbal feedback from other co-designers. The process follows a sequence of actions among Designers through the representation of 3D artefacts in the display screen. Designer A is immersed in VE, and Designers B and C are partially immersed through the laptop screens, as screen-based immersed. They together discuss and locate representational 3D artefacts like trees, humans, seatings, vehicles and building forms in the VE. An individual designer generates 3D artefacts as a representation of landscape elements as input in VE, and the output from VE goes to other designers. The communication process let the designers design together as a team rather than acting as individual actors. The collected data from the design experiments reflect on design collaboration.

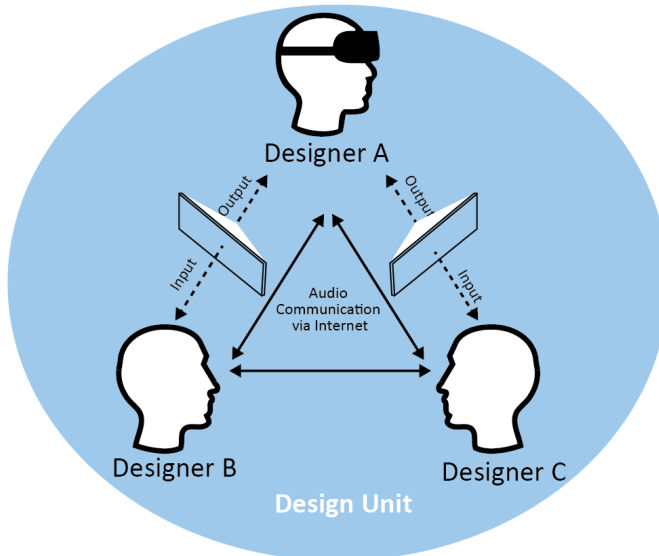


Figure 2. Design unit.

6. Design Task and Participation

The design task is to re-envision the urban settings of the Southern Institute of Technology's campus area. A three-dimensional model of the campus has been provided in the online environment. In the beginning, the designers had been introduced with Arkio for 15 minutes on the basic commands of creating and navigating objects. Then they were allowed to take part in the design collaboration session for 20 mins (figure 3). The design sessions have been recorded to do transcription analysis.



Figure 3. Participants in remote design collaboration.

7. Transcription Analysis

The research gets the influence from the protocol analysis technique developed by (Chowdhury, 2020; Chowdhury & Schnabel, 2019). The video recorded during the design session has been analysed using “descript”, an online tool to transcribe any recorded video (Descript, 2021). A general observation on the trans-coded data, it seems the design discussion went quite well among the participants. Though, in the beginning, the immersive Designer A struggled to orient with the immersive interface. However, Designer B and Designer C were actively engaged in conversation between themselves and progressed with the design. The designers mostly used the 3D artefacts provided by the Arkio interfaces. They placed trees, humans, cars and chairs. They

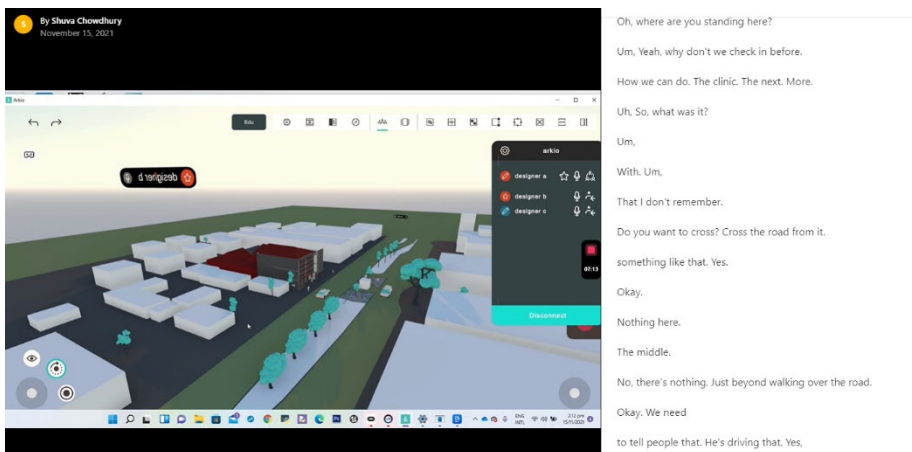


Figure 4. Design negotiation.

planted new trees in the road divider of their campus. In the stage of the design, the students started to propose a pedestrian bridge to connect the building blocks of the both sides of the road. Like one of the conversations regarding that design initiation, *“Do you want to cross? Cross the road from it”* (figure 4). Due to the nature of being co-presence in the virtual environment, students can locate any specific place of the virtual city.

At some stage, the conversation went to the level of negotiation. Like in one conversation, one of the participants said, *“You said it’s a bad idea. And I think it’s a good idea to have like a. Something that people can walk over...”* (figure 5). Such conversation indicates the quality of the engagement. They consulted between them before producing any content in the virtual place. They sought fellow co-designers choices and, in cases, also instructed each other’s to place any specific 3D artefact (figure 6). The quality of the perceptual environment allowed the designers to perceive the scale relevant to their design environment. Like in one conversation, a participant stated, *“Because at the moment. Bridge. Obviously, like it would be quite steep, kind of straight. It down to try and get into G-Block”* (figure 6). There were quite a lot of affirmative and exclamatory word exchanges between the designers, like *“yeah”* and *“Oh”* (figure 5, 6 and 7). The affirmative conversation indicates that the designers are experiencing the same design contents in the VE and the exclamatory words indicate the conversation’s natural flow. The designers felt the experience of *“sense of being there”* and interacted on the same design issue as they were co-present at the same virtual location. The continuation of the design conversation went well. In the end, they started to build a pedestrian cross-over bridge in their virtual campus site. The video transcription revealed that the Designers got the chance to jump on the bridge and visualise the surroundings in different locations in the virtual city.

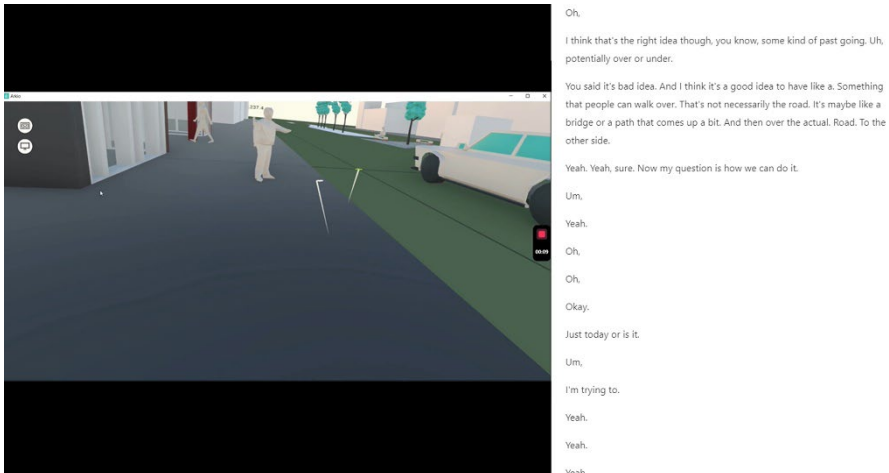


Figure 5. Design conversation in Arkio.

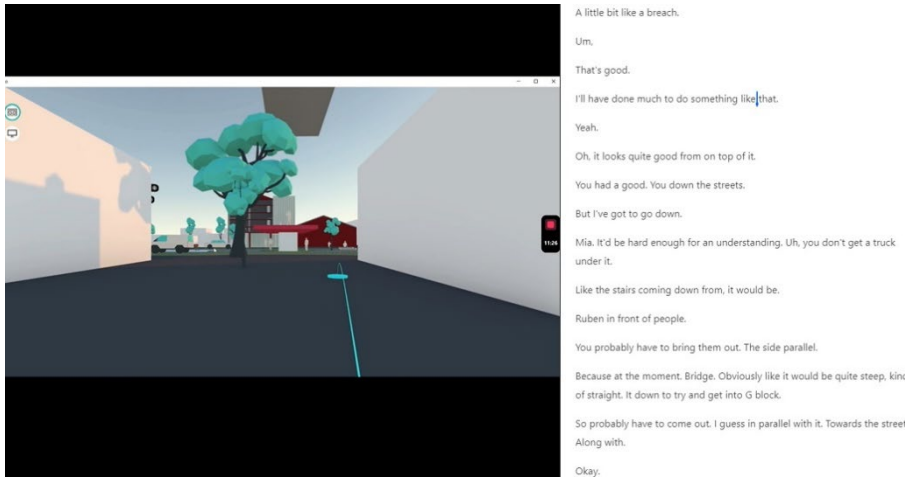


Figure 6. Design instruction.

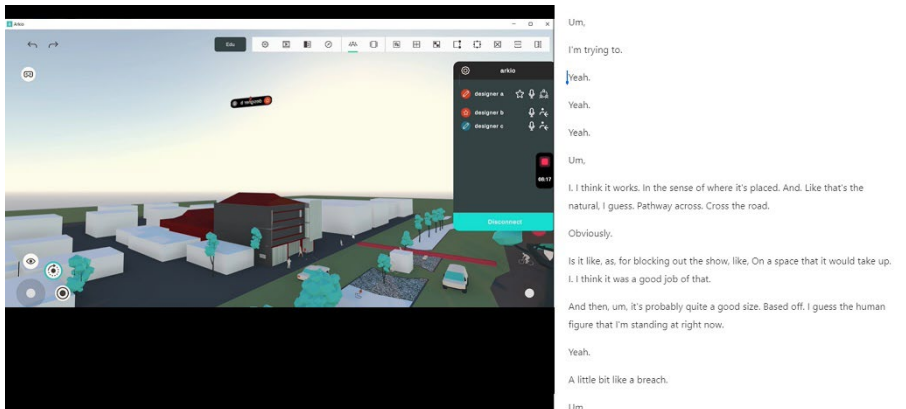


Figure 7. Affirmative and exclamatory conversation.

8. Discussion and Conclusion

In the study, the seamless interaction with the participants reflects the level of presence in the virtual environment. The success of design communication lies in the tool's ability to facilitate the sense of the co-presence of all the remote participants. The participants had enough freedom to input their design aspirations and negotiated with the remote participants to form a collective decision. The VR stimuli involve participants senses and are produced in real-time by their actions. The full immersive Designer A communicates successfully with the non-immersive Designers B and C. The compromise on the immersion does not affect the conversation. Through the video transcription, it has been identified that the immersive Designer A struggled to orient himself in the VE. It is due to the new orientation of the HMD and the perceptual quality of the surrounding environment. Besides, the user interface was also new to

him. However, Designers B and C interacted in the virtual space without technical barriers.

The study shows that the visualisation process carries genuine and powerful potential to act as innovative and creative communication tools and that communication can go in all directions. The novice designers have undertaken the development and rolling out of methods of 3D modelling and visualisation. The outputs seamlessly incorporate with a formal planning and design process.

Under the framework of participatory urban design, this employed engagement setup can potentially engage the non-expert participants in remote VR collaborative settings. Research on VR-assisted participatory urban design (Chowdhury, 2020) developed a setup where the co-designers experience the immersive designer's design input in screen-based media. The co-designers were not allowed to generate virtual artefacts during the design participation sessions actively. In this study, the proposed design unit configuration allows all participants to contribute to design decisions by actively producing virtual artefacts in the VE. They act as a design team though they are located remotely.

In future, the research intends to explore with the local non-experts community by ensuring equal opportunity and reducing inequalities between policymakers and general citizens. Such wider community participation provides transparency in the decision-making process. Besides, such remote collaboration also shows the scope of exchange knowledge from stakeholders based on different continents. The framework can be a part of the UN's city resilience profiling tool. UN habitat's holistic approach to increasing resilience requires engagement with local government stakeholders and identifying the risk factors that could be prioritised to mitigate. The bottom-up design solution can be found through collaboration and participation in decision-making. In that sense, this kind of remote co-presence virtual co-design tool can facilitate them to identify the priority on spatial planning by visualising possible optimised and sustainable design solutions.

References

- Arkio. (2021). *Arkio Software*. Retrieved 18th Nov, 2021, from <https://www.arkio.is/>
- Bulu, S. T. (2012). Place presence, social presence, co-presence, and satisfaction in virtual worlds. *Computers & Education*, 58(1), 154-161.
- Chowdhury, S. (2020). Virtual Environments as Medium for Laypeople's Communication and Collaboration in Urban Design. *Architectural Science Review*, 63(97), 1-14.
- Chowdhury, S., & Schnabel, M. (2020). Virtual environments as medium for laypeople to communicate and collaborate in urban design. *Architectural Science Review*, 1-14.
- Chowdhury, S., & Schnabel, M. A. (2019). Laypeople's Collaborative Immersive Virtual Reality Design Discourse in Neighborhood Design. *Frontiers in Robotics and AI*, 6(97).
- Descript. (2021). *All-in-one audio/video editing, as easy as a DOC*. Retrieved 18th Nov, 2021, from <https://www.descript.com/>
- Gaver, W. W. (1991). Technology affordances. *Proceedings of the SIGCHI conference on Human factors in computing systems*.
- Gül, L. F. (2020). *Co-design*. Retrieved 6 May, 2020, from <https://www.materiart.org/glossaryofmateriart-co-design>
- Nowak, K. (2001). Defining and differentiating copresence, social presence and presence as transportation. *Presence 2001 Conference, Philadelphia, PA*.

- Royall, E. (2022). *UN-Habitat - People-Centered Smart Cities: A playbook for local and regional governments*. Retrieved from <https://unhabitat.org/programme/people-centered-smart-cities/centering-people-in-smart-cities>
- Schnabel, M. A. (2011). The immersive virtual environment design studio. *Collaborative Design in Virtual Environments*, 177-191.
- Sheridan, T. B. (1992). Musings on telepresence and virtual presence. *Teleoperators & Virtual Environments*, 1(1), 120-126.
- Slater, M. (1999). Measuring presence: A response to the Witmer and Singer presence questionnaire. *Presence*, 8(5), 560-565.
- Slater, M., Usoh, M., & Chrysanthou, Y. (1995). The influence of dynamic shadows on presence in immersive virtual environments. *Virtual environments*, 95, 8-21. Springer.
- Witmer, B. G., & Singer, M. J. (1998). Measuring presence in virtual environments: A presence questionnaire. *Presence*, 7(3), 225-240.

EXPLORING USERS' VISUAL IMPRESSION OF A JAPANESE STREETScape BY CORRELATING ATTENTION WITH SPEECH

Utilizing eye-tracking technology for computer-aided architectural planning

KHANG NGUYEN-TRAN¹, YUVAL KAHLON², TAKUYA OKI³,
NAYA MARSATYASTI⁴, RYO MURATA⁵ and HARUYUKI FUJII⁶
^{1,2,3,4,5,6}*Tokyo Institute of Technology.*

¹*khang.ntr@gmail.com 0000-0002-0535-0179*

²*kahlon.y.aa@m.titech.ac.jp 0000-0002-3914-7945*

³*oki.t.ab@m.titech.ac.jp 000-0002-4848-0707*

⁴*naya.marsatyasti@gmail.com 0000-0001-9654-9222*

⁵*murata.r.ac@m.titech.ac.jp 0000-0003-4010-2178*

⁶*fujii.h.aa@m.titech.ac.jp 0000-0002-8984-8512*

Abstract. Considering users' subjective impressions is a challenging question in architectural design. Answering this question is a human-centred approach which is critical for designing spaces that afford true well-being for their users relating to Sustainable Development Goal 3, or SDG 3: "Good Health and Well-being"). While various methods for evaluating users' subjective impressions exist, their focus is mainly on classifying spaces into pre-determined categories representing the users' impressions. Such classification fails to capture the richness of users' actual interpretation, as reflected in descriptions provided by users when they express freely their impression about architectural space. Aiming to capture this richness, we extend the current state-of-the-art methods and propose an integrated approach to extract and analyse the users' interpretations while interviewing them observing a Tokyo streetscape. In addition, by comparing their comments and gaze, we expose correlations between abstract descriptions and the architectural space, which are difficult to obtain using existing methods. Our insights are a stepping-stone for enhancing computer-aided architecture by integrating visual impressions into the design processes.

Keywords. Visual Impression; Gaze Analysis; Japanese Architecture; Oku; Well-being; SDG 3.

1. Introduction

In the rapidly evolving research into visual impressions of architectural space (VIAS), an important question is how to consider people's subjective impressions when designing architectural space. Since people can effectively express their subjective interpretation in natural language, it is essential to understand how to relate linguistic

expressions with architectural spaces. Currently, the field is led by quantitative approaches that often use methods to match visual stimuli with linguistic descriptions, with or without numerical scales. While these approaches have shed light on how we experience architectural spaces, they are limited in their ability to extract and precisely describe users' VIAS. One reason for this is their reliance on pre-determined categories, which subjects are requested to choose from in reporting VIAS. Such pre-determined categorization is bound to miss some of the subtleties and richness which characterize VIAS. Recently, the research on VIAS has taken a new approach using state-of-the-art technologies for eye tracking (Oki and Kizawa, 2021). This approach yields valuable information regarding the subject's attention, which is necessary for developing a comprehensive understanding of individual reports of VIAS. Our work aims to further the efforts beyond the previous findings by integrating them with a qualitative analysis of verbal reports. The findings are expected to contribute to a new approach for studying VIAS and could be integrated into computer-aided architecture design. Furthermore, considering how complexly the visual representation of architectural space can influence human perception, the architectural design process must involve a hidden but crucial sense concerning people. This study's findings can offer a unique method to provide insights that decrypt the user's interpretation of architectural space and allow designers to configure spaces that ensure and promote human well-being in urban spaces and cities. This contribution to the well-being of inhabitants via a human-centred design approach accords with the Sustainable Development Goal 3 (SDG 3) to "Ensure healthy lives and promote well-being for all at all ages."

2. Background

2.1. EXTRACTING VISUAL IMPRESSION OF STREETSCAPES

Concerning current work on extracting VIAS, various methods have been developed. The Semantic Differential method is commonly used in research to correlate the subject's opinion with the stimuli in photographs or the actual space as in the studies of the impression of streetscapes based on indications such as the sky factor (Nishio and Ito, 2015), the green ratio (Nakamura et al., 2010), or the perceived attractiveness of urban spaces via the relation between the distance from skyscrapers and VIAS (Wada and Kishimoto, 2011). Moreover, impression evaluation using Affinity Diagrams also provided insights into differences in perception of different age groups, genders, and cultural backgrounds (Kacha et al., 2015).

In recent years, eye-tracking devices have become available at a lower price, which allows designers and researchers to use this technology more frequently in studies attempting to evaluate VIAS. For instance, a study analysed the relationship between landscape order, gaze tendency and impression factors (Ohno, 2018). Concerning urban streetscapes, a study analysed how urban street edges affected pedestrians' field of vision and how spatial factors impacted this relation (Simpson et al., 2019). Developing an objective way to evaluate VIAS, our previous experiment examined the relationship between the subjects' gazing tendency and their evaluation of streetscape attractiveness (Oki and Kizawa, 2021) by comparing the gaze tendencies and visual saliency estimated by a deep learning model. However, how to get insight from such data is still in its infancy, and the interpretability of eye measurement results also

remains an issue. Building upon these efforts, this study aims to obtain better comprehensive descriptions of VIAS through speech and attention and retrace them in the visual representation of the streetscape. Also, to reflect the subjects' impression with a high degree of reliability, we combined the benefits offered by gaze analysis with the diligence given by the long-standing method of protocol analysis (Jiang and Yen, 2010) into a framework correlating subjective understanding and interpretation of VIAS.

2.2. THE CONCEPT OF OKU FOR JAPANESE STREETSCAPE

The Japanese concept of 'Oku', literally translated as 'innermost space' (Maki, 2018, p.156), often used to describe spatial formation in Japan. This concept signifies relative distance obtained from a visual permeability through a sequence of screens, planes, or filters toward the core of space. Although understood as 'spatial depth' (Monnai, 2009, p.183) or 'multilayers space' (Jonas, 2011, p.99), Oku is not limited in the narrow sense of physical distance but is often associated with a subjective sense of feeling 'moving into unknown places' (Kohte, 2017, p.25) or evoking a 'sense of curiosity' (Totten, 2016, p.258). This abstract concept cannot be understood using a single, all-encompassing definition but is also manifested in different architectural approaches seeking to express the sense of Oku via the manipulation of spatial boundaries and sequences. For example, in his book *Exterior Design in Architecture*, Ashihara mentioned it in the discussion about the hidden order of how to break the spatial monotony and create a sense of profundity by the 'ingenious use of the inside and outside corners' (Ashihara, 1970, p. 94-95). Also, Ando incorporates this concept in his masterpiece *The Church of the Light* to an articulation of 'sentiment-fundamental space' (Ando, 1995, p.74) that incites the visitor to seek symbolism in horizontal depth. While this notion of Oku is an essential characteristic of dwellings or spiritual spaces somehow related to the idea of 'hidden', 'inner', or 'secret' (Maki, 2018, p.157), when applied to streetscapes, it represents a particular character of Japanese cities. Discussions regarding the overlapping external layers of building facades, the gap in topography, and the volume of objects (Maki, 2018, p.135-148) are essential to understand this spatial formation. Outside of Japan, similar concepts existed in western literature using definitions such as 'here and there' (Cullen, 1961, p.182), 'phenomenal transparency' (Rowe, 1963, p.46), 'soft edges' (Gehl, 2011, p.183-184), etc. It is clear that the richness of Oku presents a potentially wide range of interpretations from the designer and users and is, therefore, a suitable topic for this study.

3. Method

3.1. DATA COLLECTION

The case studies were collected from the Daikanyama streetscape with Hillside Terrace, a masterpiece of Maki and an exceptional representation of the concept Oku. This is where buildings, streets, public spaces are composed of elements that allow multiple visual penetrations. To understand the visual impression mechanism, we introduced a combined method of data collection using photo segmentation, eye tracking, and interviews in three steps according to the framework in Figure 1.

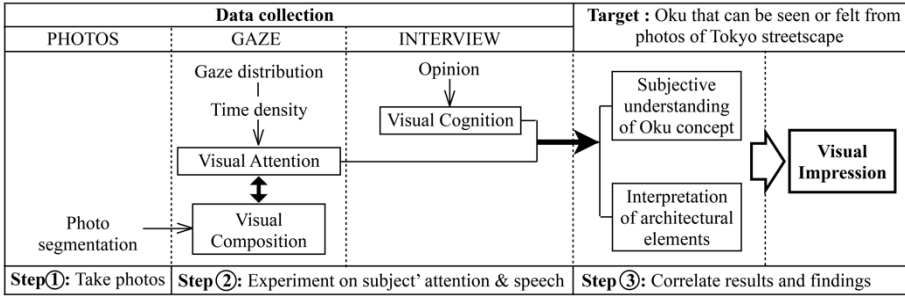


Figure 1. Framework and process of study

First, in the process, 13 photos of the streetscape in the Daikanyama area were collected using a Fujifilm XT-10 digital camera with a setting closest to a human viewpoint. Following the classification of elements based on their 'environmental meaning' (Rapoport, 1982, p.87), photos were segmented into five types of elements such as vertical (building parts), horizontal (pavement), artificial shape (street furniture), natural shape (vegetation), and others (people, sky, background scenery, etc.). Second, we ran an experiment in a laboratory environment by projecting the original photos on a screen while interviewing nine subjects. The subjects from various countries are trained in the architectural design field and represent a variety of nationalities. We observed them as they shared their impressions about Oku from the photos and collected data regarding their comments and gazes. During the experiment, a screen-based eye tracker (Tobii Pro nano) is used to collect data on the subject's gazes. The data collection settings are described in Figure 2.

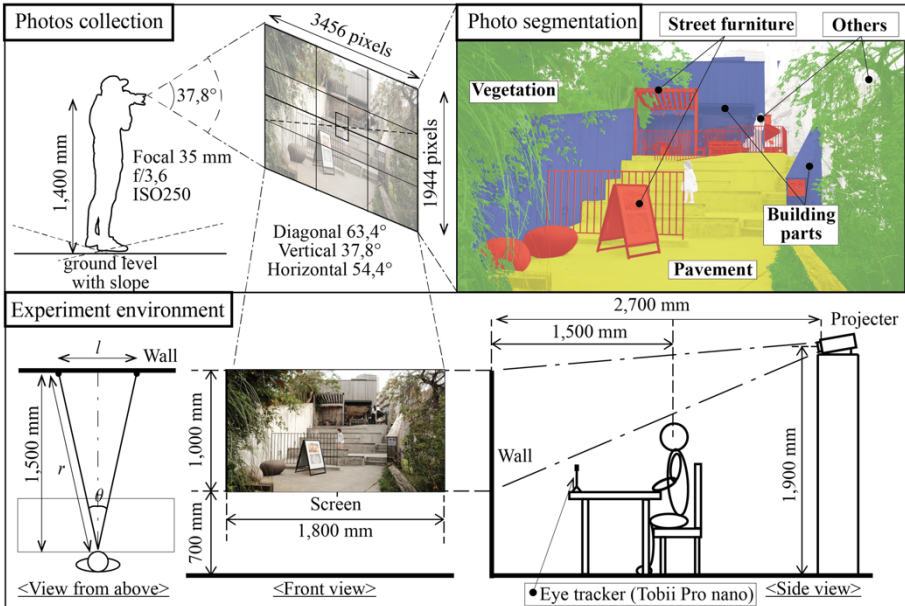


Figure 2. Data collection

3.2. DATA PROCESSING AND ANALYSIS

We extracted subjects' interpretations from the protocols, as well as their gaze data at the corresponding times in the experiment, then integrated them into diagrams. A deep examination by comparing verbal descriptions with the subjects' attention enables us to identify the connections and the deviations between the different types of data, thus yielding important insights about VIAS. It should be noted that during the data collection and processing, invalid data were removed due to calibration issues.

3.2.1. Protocol Analysis

Transcriptions were used to identify all moments when the concept of Oku is discussed by each subject, which we defined as 'an event'. In each event, we first marked the time when the subject began speaking about Oku, then extracted the subject's interpretation of the concept of Oku, which is expressed in their utterances regarding VIAS. Finally, if applicable, the degree of Oku was included with the interpretation (e.g., 'strong feeling' of Oku). These interpretations were then classified into those in which the subject associated Oku with a physical architectural element, such as a 'longwall', and others in which the concept was associated with abstract qualities of the space, such as 'mysterious atmosphere'. These classifications served as the basis for understanding how the subject related the concept of Oku with the actual or visual space in each photo.

3.2.2. Gaze Analysis

By using a small screen-based eye tracker, the subjects' gaze coordinates and pupil diameter were recorded with a 1/60-second cycle. Although saccades, in which the gaze moves quickly, are included in the gaze behaviour data, in this study, we analysed gazing behaviour in which the subjects were looking at objects. Specifically, we defined attention 'as a state in which the eye movement speed is less than 10 degrees/second for more than 100 milliseconds' (Fukuda et al., 1996, p. 203) based on the distribution of the measured eyes movement speed to extract the attention points. Then, we created a kernel density distribution of attention points for each conversation by subject and photo. From this distribution, we visualized the subjects' attention as heat maps reflecting their visual behaviour during the event. Besides, attention heat maps were generated to capture the gaze behaviour in the minute before and after an event. This step resulted in an image set showing their visual focus, which accompanied their speech during the event. Finally, by extracting the visual attention in the heat maps during the moment that Oku was mentioned or discussed, we listed the physical parts of the streetscape, which were focused on in each event.

4. Results and Discussions

4.1. GAZE TENDENCIES DURING INTERPRETATION OF OKU

We have extracted six photos that were indicated among all subjects as possessing the quality of Oku. For each of these, we display a heat map reflecting the subject's gaze during discussion of Oku, thus forming the 5x6 matrix in Figure 3. This matrix can be used to search for gaze tendencies among the subjects. For instance, by examining

photo number 9 in terms of similarities, five out of six subjects were attracted to the vanishing point. This observation seems reasonable, as this point represents the deepest visible area. Notwithstanding, S6 gazed at an elongated element on the ground belonging to the foreground. This observation poses a challenge for the previous explanation of Oku relating to a relative distance concerning depth. Considering that the element points to the vanishing point, it seems reasonable to assume that Oku is experienced since the vanishing point is implied. In other words, the directionality of an element can lead our eyes into the depths of the space and result in an experience of Oku. Contrary to the above, the subject's explanation revealed another aspect of interpretation. He mentioned that the element frames a 'small space' for sitting, which he associated with 'the Japanese tea house', thus rendering an impression of Oku. This episode demonstrates the value in the analysis of VIAS by integrating gaze data with qualitative analysis of speech, which can reveal deep insights about one's views.

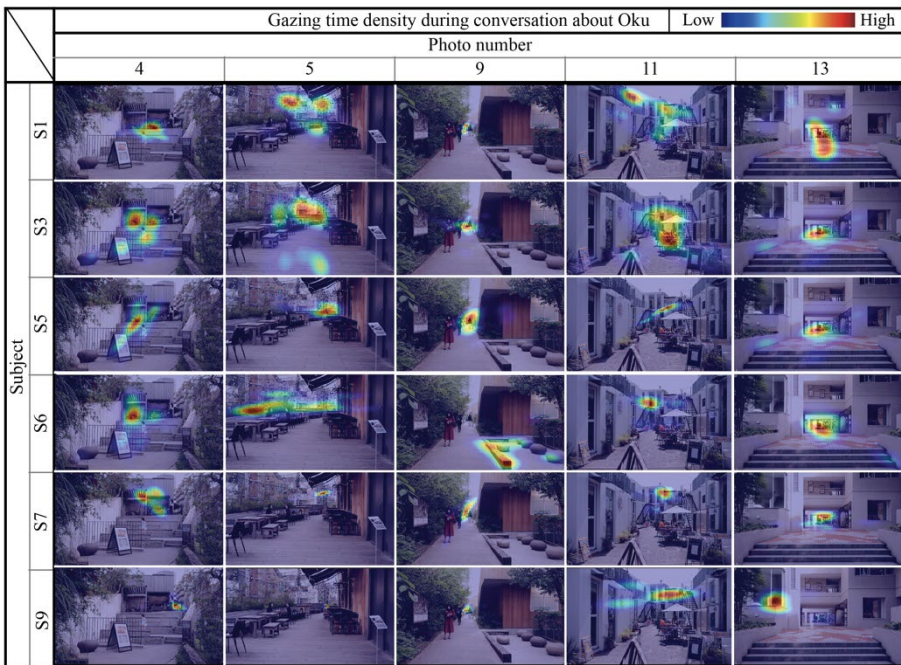


Figure 3. Gazing tendency in subject's response during conversations about Oku

4.2. ESTIMATING FREQUENCY AND VARIETY OF INTERPRETATION VIA SPEECH AND ATTENTION

By collecting the words subjects used to talk about Oku and presenting them along with gaze time density in heat maps, we can see the variety of VIAS across several subjects, as shown in Figure 4. These contain various interpretations of Oku, not only as an abstract concept but also as related to physical elements and their perception (for example, for S1, Oku is described by 'building's part' linked to 'barrier', while S9 linked it to a sense or a feeling that can or cannot be seen).

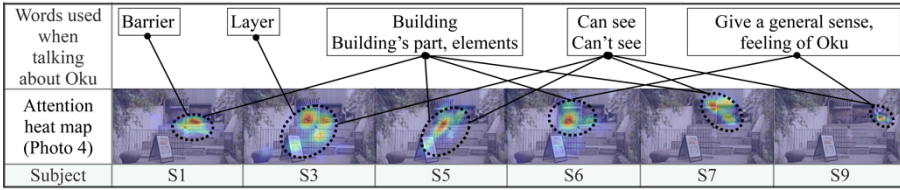


Figure 4. Variety in speech related to Oku

Furthermore, by superimposing the probability distribution obtained from kernel density estimation and segmentation images as shown in Figure 5, we can estimate which elements were being gazed at. This estimation enables us to raise hypotheses regarding the variety of elements in the formation of VIAS, both individually and collectively. For instance, vegetation showing in green colour seems to catch a very small portion of S4's and S7's attention. Meanwhile, the prevalence of tall blue columns indicates a collective tendency to gaze at building façades more than other elements.

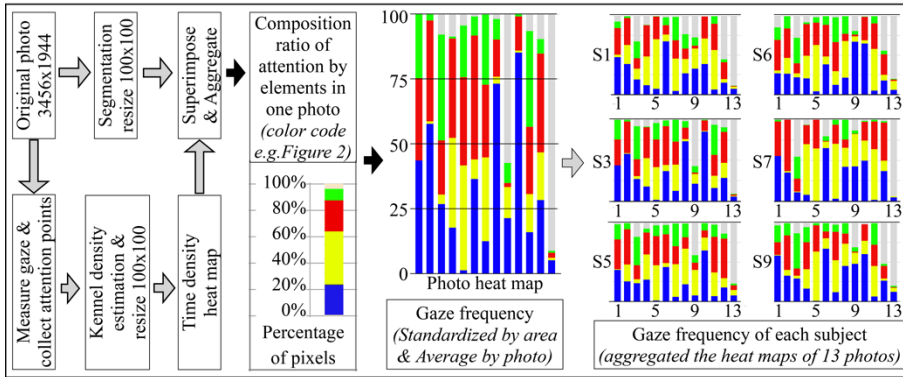


Figure 5. Frequency in attention related to photo segmentation

4.3. TRACING SOURCES OF VIAS

After extracting the heat maps and utterances reflecting subjects' attention and thoughts when discussing the concept of Oku, we combined them into concise yet informative episodes in Figure 6. For each subject, three attention heat maps are presented: before discussing Oku, during the initial report on their impression, and immediately after that moment. The initial instance refers to the moment in time which follows the interviewer's question regarding Oku, which naturally draws their attention to this concept (note that, in some cases, a subject began speaking of Oku without being prompted to discuss it). Relevant time durations appear at the bottom of each heat map. Each heat map is accompanied by speech data, where important phrases are marked in a bold font. The interviewer is represented by the letter 'I' and subjects are represented by the letter 'S'. Finally, the subject's VIAS regarding Oku and its potential source are summarized at the bottom left of each episode. For example, consider S1, who reported that the space has a '...type of Oku'. The subject tied this to the existence of a staircase, which then creates a 'barrier'. Thus, Oku is interpreted here as related to the existence of barriers, which finds its source in the architectural elements of the staircase.

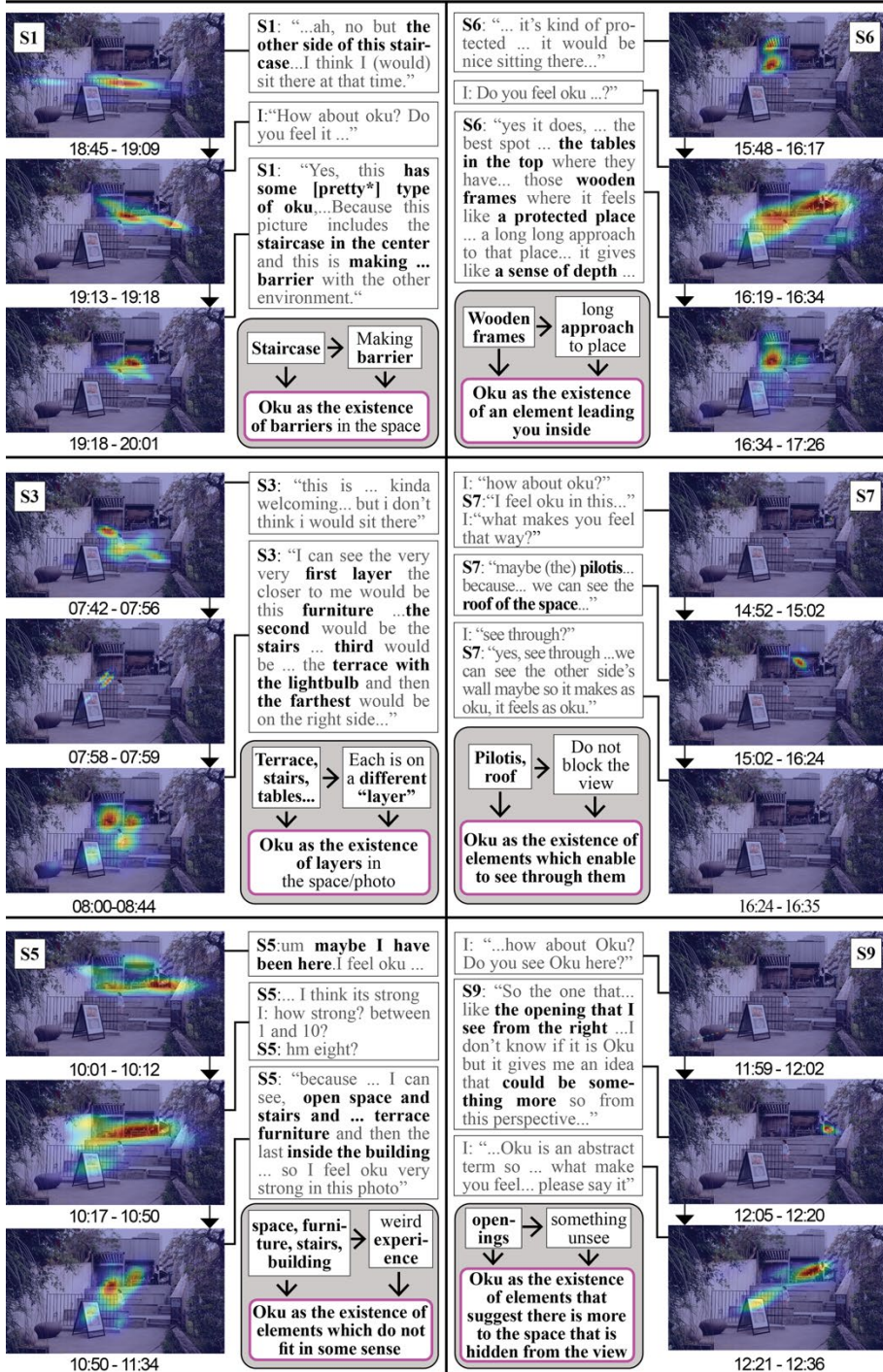


Figure 6. Interpretation of Oku in speech with the gaze of each subject

Besides, by setting heat maps side-by-side with the relevant explanations provided by the subjects, we can have a better understanding of subjective interpretation. For example, how S1 above has traced the impression of Oku to the existence of a 'barrier', and that element is caused by the fact of the 'staircase in the centre'. A question that could be raised is how does the staircase create a sense of 'barrier'? To answer it, we examine what S1 was referring to when talking about a 'staircase'. Consulting the accompanying heat maps reveals that the subject was focused on a small area at the end of the central staircase while ignoring most of the staircase's mass. Also, the focused area coincides with the staircase end, which is the visual boundary limit between it and what lies beyond it. Furthermore, notice that before the question regarding Oku, S1 was focusing on the child playing at the centre of the staircase. This observation strengthens the assumption that his focus on the edge was prompted by the question and thus is tied with his subjective interpretation of Oku. Other similar in-depth examinations are possible by checking the other episodes. For example, in the case of S7, we can relate the subject's interpretation of Oku as the ability to see through elements. In the attention heat map, the focus is on a specific area of the pergola (i.e., the wooden planks hung on the outdoor terrace) and do not obstruct the view.

5. Conclusion and Future Work

This work explored VIAS on the topic of Oku. Based on aspects related to the streetscape, we have qualitatively assessed users' impressions containing speech and attention. The findings provided insights into an approach that decrypts the complexity of the user's interpretation. First, it allows us to access the tendency and variety of interpretations of tangible aspects in spatial design via the combination of gaze and photo segmentation. Second, it enhances the ability to decrypt the subjective understanding of spatial formation via the proposed method of tracing the source of VIAS. Applying this method has proved useful in offering insights into subjective impressions observed when discussing Oku based on the tendency of attention. Consequently, the existing theories of VIAS can be enriched via this human-centred approach. For example, Okabe's related concept of 'subjective depth' (Okabe, 2017, p.158) can now be related with empirical findings concerning VIAS and thus be enriched or even reassessed. From a broader perspective, similar experiments can be reconstructed, moving beyond streetscapes and the concept of Oku in studying VIAS.

As for the scope and limitations of this study, the number of samples is limited. While the proposed method showed a certain degree of reliability when correlating the interpretation with the spatial design abstract concept, further investigation is necessary to understand how subjects construct impressions based on interpretation. Also, using more samples could further provide enough data to build a deep learning model describing the people's gaze movement or attention. Such a model will enable us to evaluate the attractiveness of places as a computer-aided design simulation tool that integrates into the design process. Finally, the insights collected from this research represent a unique direction for exploring the hidden mechanism of the user's perception. The findings will help designers enhance the design processes for urban assessment that involve users' evaluations. Access to this intangible dimension of architectural space is essential for urban dwellers' well-being, which corresponds to the aim of indication SDG 3 and is a step forward to designing sustainable cities.

References

- Ando, T. (1977). *A Wedge in Circumstances. The Japan Architect*, 52(6), 73-76.
- Ashihara, Y. (1970). *Exterior design in architecture*. Van Nostrand Reinhold.
- Cullen, G. (1961). *The concise townscape*. The Architecture Press.
- Fukuda, R., Sakuma, M., Nakamura, E. & Fukuda, T. (1996). An experimental study on the definition of gazing point. *Ergonomics*, 32(4), 197-204. <https://doi.org/10.5100/jje.32.197>
- Gehl, J. (2011). *Life Between Buildings: Using Public Space*. Island Press.
- Jiang, H., & Yen, C.-C. (2010). Protocol Analysis in Design Research: A review. *International Association of Societies of Design Research Conference*, 78(24), 1-10.
- Jonas, M. (2011). Oku: the notion of the interior in Tokyo's urban landscape. In R. U. Hinkel, & S. Attiwill (Eds), *Urban interior: informal explorations, interventions and occupations* (1st ed., pp. 99-110). Baunach.
- Kacha, L., Matsumoto, N., & Mansouri, A. (2015). Study on the Evaluation of Impression in Streetscapes in Algeria and Japan using Kansei Engineering. *Journal of Architecture and Planning (Transactions of AIJ)*, 80(712), 1357-1363. <https://doi.org/10.3130/aija.80.1357>.
- Kohte, S., Adam, H. & Hubert, D. (2017). *Encounters and Positions: Architecture in Japan*. Basel: Birkhäuser.
- Lynch, K. (1960). *The image of the city*. The MIT Press.
- Maki, F. (2018). *City with a hidden past*. Kajima Institute Publishing.
- Manyoky, M., Wissen Hayek, U., Pieren, R., Heutschi K., & Gret-Rêgamey, A. (2016). Evaluating a visual-acoustic simulation for wind park assessment. *Landscape and Urban Planning*, 153, 180-197. <https://doi.org/10.1016/j.landurbplan.2016.03.013>.
- Monnai, T. (2009). *Fumihiko Maki (Search for an Architectural Language of Group Form)*. Phaidon Press.
- Nakamura, K., Kita, M. & Matsumoto, K. (2010). Evaluating Impression of Vertical Greenery using SD Method. *Journal of Architecture and Planning (Transactions of AIJ)*, 75(654), 1943-1951. <https://doi.org/10.3130/aija.75.1943>.
- Nishio, S., & Ito, F. (2015). The Effect of Sky Factor and the Change on Impression of Townscape. *Journal of Architecture and Planning (Transactions of AIJ)*, 80(710), 907-914. <https://doi.org/10.3130/aija.80.907>.
- Ohno, R. (2018). Studies on environmental perception during locomotion - A review of empirical studies by the Ohno laboratory. *Japan Architectural Review*, 1(2), 194-206.
- Okabe, A. (2017). Dynamic spaces with subjective depth. The public space in monsoon Asia. *Kult-ur*, 4(7), 151-164. <https://doi.org/10.6035/Kult-ur.2017.4.7.6>
- Oki, T., & Kizawa, S. (2021). Evaluating Visual Impressions based on Gaze Analysis and Deep Learning. A Case Study of Attractiveness Evaluation of Streets in Densely Built-up Wooden Residential Area. In *The International Archives of the Photogrammetry, Remote Sensing and Spatial Information Sciences* (pp. 887-894), *ISPRS Congress*. <https://doi.org/10.5194/isprs-archives-XLIII-B3-2021-887-2021>.
- Rapoport, A. (1982). *The Meaning of the Built Environment. A Nonverbal communication approaches*. SAGE Publications.
- Rowe, C. & Slutzky, R. (1963). Transparency: Literal and Phenomenal. *Perspecta*, 3, 45-54. The MIT Press. Retrieved October 21, 2021, from <https://www.jstor.org/stable/1566901>.
- Simpson, J., Freeth, M., Simpson, K. J. & Thwaites, K. (2019). Visual engagement with urban street edges: insights using mobile eye-tracking. *Journal of Urbanism: International Research on Placemaking and Urban Sustainability*, 12(3), 259-278. <https://doi.org/10.1080/17549175.2018.1552884>
- Totten, C-W. (2016). *An architectural approach to level design*. CRC Press.
- Wada, S., Kishimoto, T. (2011). Impressions and Oppressed Feelings according to the Distance from a Skyscraper. *Journal of Architecture and Planning (Transactions of AIJ)*, 76(667), 1651-1657. <https://doi.org/10.3130/aija.76.1651>.

PLACEMAKINGAI: PARTICIPATORY URBAN DESIGN WITH GENERATIVE ADVERSARIAL NETWORKS

DONGYUN KIM¹, GEORGE GUIDA² and JOSE LUIS GARCÍA
DEL CASTILLO Y LÓPEZ³

^{1,2,3}*Harvard University Graduate School of Design.*

¹*dongyun_kim@gsd.harvard.edu, 0000-0003-1193-3845*

²*gguida@gsd.harvard.edu, 0000-0002-2477-0064*

³*jgarciaadelcasti@gsd.harvard.edu, 0000-0001-6117-1602*

Abstract. Machine Learning (ML) is increasingly present within the architectural discipline, expanding the current possibilities of procedural computer-aided design processes. Practical 2D design applications used within concept design stages are however limited by the thresholds of entry, output image fidelity, and designer agency. This research proposes to challenge these limitations within the context of urban planning and make the design processes accessible and collaborative for all urban stakeholders. We present PlacemakingAI, a design tool made to envision sustainable urban spaces. By converging supervised and unsupervised Generative Adversarial Networks (GANs) with a real-time user interface, the decision-making process of planning future urban spaces can be facilitated. Several metrics of walkability can be extracted from curated Google Street View (GSV) datasets when overlaid on existing street images. The contribution of this framework is a shift away from traditional design and visualization processes, towards a model where multiple design solutions can be rapidly visualized as synthetic images and iteratively manipulated by users. In this paper, we discuss the convergence of both a generative image methodology and this real-time urban prototyping and visualization tool, ultimately fostering engagement within the urban design process for citizens, designers, and stakeholders alike.

Keywords. Machine Learning; Generative Adversarial Networks; User Interface; Real-time; Walkability; SDG 11.

1. Introduction

The process of urban planning is an iterative and collaborative process, often limited to designers and city stakeholders. There is an inherent challenge in communicating and inclusively producing design solutions. If capitalizing on GANs (Goodfellow et al., 2014) can aggregate hundreds of images and characteristics of spaces, an intuitive design tool can help bridge this missing communication. With the intention to imagine and conceive improved future cities, this project speculates on ways in which

computational statistical models can facilitate this dialogue from citizens and architects to urban planners and policymakers.

In this paper, we present PlacemakingAI, a tool that allows users to envision improved streetscapes and alternative versions of existing cities. We introduce methods of collecting datasets based on metrics of walkability, designed to train on two known GAN models – CycleGAN (Zhu et al., 2017) and Pix2Pix (Isola et al., 2016), to generate synthetic images in real-time. By encoding the concepts of genius loci of space (Norber-Schulz, 1980) – in particular, the character, life, and the everyday, and imageability of space (Lynch, 1960) – in this case, the node or street as a connector and way-finder, the resultant images can provide insights of novel and improved urban spaces. By explaining this framework, we will show a feasibility study and describe a real-time participatory user interface (UI) that could be used by all urban stakeholders and conclude with limitations and future outlooks.



Figure 1. Generated street scene with embedded metrics of urban walkability.

2. Background: Machine Learning and the Perception of the City

The concept of imageability by Kevin Lynch finds relevance to this day in urban design and city planning practices. First introduced in his ‘Image of the City’, it presents a novel way of reading and observing the city based on the classification of paths, edges, districts, nodes, and landmarks. The aggregation of these elements forms the memory or mental images of place, which informs this paper’s methodology in the participatory creation of images of improved green and public spaces. Encompassing this within a real-time UI gives agency to citizens and designers to improve collaborative urban planning.

Of Lynch’s 5 major elements in cities, the path can be considered a space of most active human experience, including streets, sidewalks, trails, and canals (Lynch, 1960). Functioning as the binding component that connects all other elements, this will be the main element considered when visualizing future sustainable cities. Norber-Schultz’s reading of the city instead provides a granular understanding of place. This environment is composed firstly of concrete things, having material substance, shape,

texture, color, and most importantly character. Defined by the phenomenology of everyday life, the character is then defined by how things are, providing insight into the genius loci or “spirit of a place” (Norber-Schulz, 1980) as first identified by Kyle Steinfield in Gan Loci (Steinfield, 2019).

The phenomenological reading of the city and its potential in visualizing the potential future genius loci of place through machine learning encounters additional practical applications this paper seeks to address. With the recent shortcomings of many cities during the COVID-19 pandemic, it has become increasingly meaningful to maintain a high quality of the environment in urban areas. Home to around 40% of the EU population, the average satisfaction of green and public spaces is at 77%, however, in cities such as Athens the overall satisfaction of public and green spaces remains critically low (Dijkstra et al., 2020). Interactive tools such as Treepedia (Li et al., 2015) provide awareness on the urban vegetation present in cities through a Green View Index, which indicates how several large cities have contrasting levels of green spaces indices ranging from Paris (8.8%) to Singapore (29.3%).

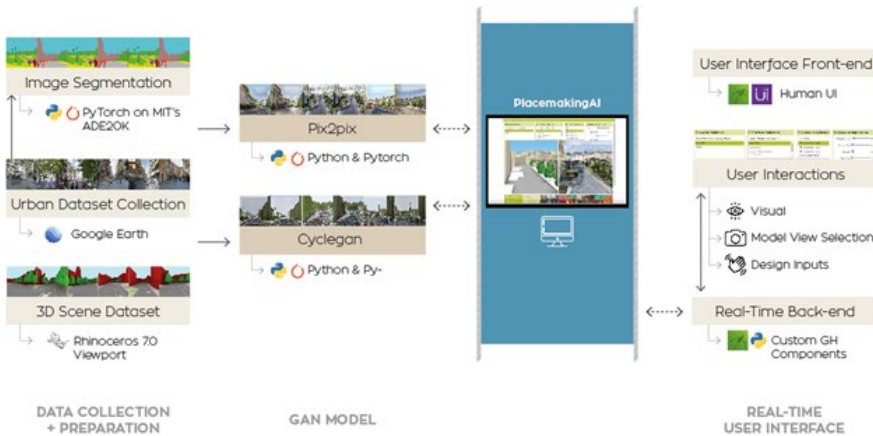


Figure 2. PlacemakingAI architecture.

From the perspective of the seventeen UN Sustainable Development Goals, this project seeks to “enhance inclusive and sustainable urbanization and capacity for participatory, integrated and sustainable human settlement planning and management in all countries” in the creation of “safe, inclusive, and accessible green and public spaces” for all citizens; GOAL 11: Sustainable Cities and Communities (United Nations, 2015). With this, the work seeks to expand on current research on the quantitative assessment of qualitative urban data (Zhang, et al., 2018) into an accessible generative space planning tool. This is made possible by identifying a set of spatial characteristics based on metrics of walkability - a term that can be viewed from both qualitative and quantitative perspectives. Lynch’s concept of imageability can be used to identify physical features and urban design qualities such as enclosure, human scale, transparency, linkage, complexity, and coherence (Ewing and Handy, 2009). The genius loci can be used to add a subjective reading of an urban environment and its atmosphere. This can include measures of individuals' senses of safety, comfort, and

levels of interest, further establishing a relationship between the physical features of a street and walking user behavior (Ewing and Handy, 2009). Jan Gehl describes this as “life in the space, the climate, and the architectural quality support and complement each other to create an unforgettable total impression” (Gehl, 2011). The subjectivity associated with walkability presents wide opportunities to reimagine the city while confirming an implicit bias during the design ideation and evaluation process.

Previous architectural and urban design applications of ML have ranged from stylistically designing 2D plans (Del Campo et al., 2019), and building facades (Özel & Ennemoser 2020), to form-based optimization with SpacemakerAI (Spacemaker, n.d.). Each of these embraces human-machine collaboration to different degrees while acknowledging the limitations of human agency within the design process. Due to the inherently iterative and collaborative process of urban planning, extending the feedback loop of the user beyond that of the collection of the dataset into a comprehensive UI becomes critical. The combination of tangible UI’s and web-based platforms such as CityScope from the MIT Media Lab (Noyman et al., 2018) has improved this lacking dialogue. The project ambition is therefore to speculate the use of this real-time prototyping GAN tool to be used as a platform for citizens, designers, and city stakeholders to have meaningful conversations on improving the environment in urban streets.

3. Methodology

PlacemakingAI is a design tool intended to provide ease in creating iterative design solutions and supporting user feedback. This UI prototype facilitates the use of machine learning models to stylize images or 3D models of city streets, based on neural networks trained on walkable street datasets. In this section, we describe the main steps in the development of this prototype including Data preparation, Model Training, and the real-time UI.

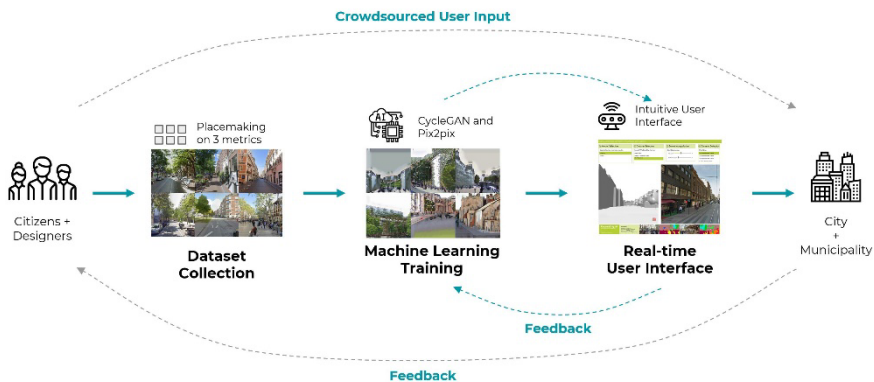














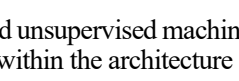
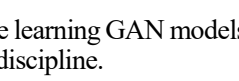
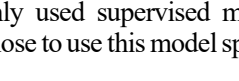
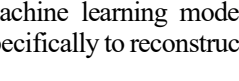






Figure 3. PlacemakingAI concept workflow and feedback loop.

3.1. DATA PREPARATION

The first step in the process of training each GAN model is the selection and curation of the image datasets. While the term walkability adopts a broad spectrum of metrics, we first established the general criteria and then divided these into two proof of concept datasets for users to choose from. The first step was to select cities and streetscape images that satisfy a variety of urban design qualities relating to walkability. These include qualitative qualities such as enclosure, human scale, transparency, linkage, complexity, coherence (Ewing & Handy, 2009), and that ideally contain a lively atmosphere. The second step was to manually separate these into Dataset A: Green Spaces, which contains active green street scenes with trees, plants, and low-level greenery, and Dataset B: Pedestrian Commercial, which contains lively pedestrian-only streets, with commercial frontages, kiosks, restaurants, or cafes. Both datasets comprised of 620 images, which were captured from Google Street View within Google Earth at resolutions above 1024x1024 pixels. Images were selected from model streets and cities across North, West, and Southern European cities familiar to the authors (Table 1). The data was then augmented, a common practice in machine learning to improve output resolution, to 3720 images by extracting the left, center, and right quadrant of each image and additionally mirroring these.

Table 1. Sample images from walkable street datasets.

Street	City	No	Dataset A		Dataset B	
			Green Spaces	Pedestrian	Commercial	Commercial
Carrer de Tàrrag	Barcelona	9	✓	✓		
La Rambla	Barcelona	22	✓	✓		
Passeig del Born	Barcelona	13	✓	✓		
Boulevard Born	Palma de Mallorca	30	✓	✓		
Calle de Preciados	Madrid	12	✓	✓		
Kongens Englavue	Copenhagen	22	✓	✓		
Strøget	Copenhagen	18	✓	✓		
Västra hamnen	Malmo	11	✓	✓		
Sivoriengatan 9	Malmo	12	✓	✓		
Ruokolaisten Street	Helsinki	11	✓	✓		
Karl Johans Gate	Oslo	30	✓	✓		
Thorbeckeplein	Amsterdam	25	✓	✓		
Loosdrecht	Amsterdam	8	✓	✓		
Cafe 't Smalle	Amsterdam	19	✓	✓		
Eijndaan	Rotterdam	32	✓	✓		
Avenida da Torre de Belem	Lisbon	10	✓	✓		
Avenida Dom Carlos I	Lisbon	14	✓	✓		
Amstelsquare Square	Theocharisli	20	✓	✓		
Via Corso Massimo d'Azeglio	Turin	16	✓	✓		
ViaE Settembrini	Bergamo	12	✓	✓		
Via de Torralbours	Bonence	10	✓	✓		
Via del Corso	Rome	26	✓	✓		
Longotevise Bradevise	Rome	4	✓	✓		
Giardini	Venezia	10	✓	✓		
Via Toledo	Naples	26	✓	✓		
Münsterbergstraße	Hamburg	10	✓	✓		
Königsallee	Düsseldorf	10	✓	✓		
Unter den Linden	Berlin	17	✓	✓		
Oxford Street	London	15	✓	✓		
Carnaby Street	London	21	✓	✓		
Buchanan Street	Glasgow	29	✓	✓		
Griffin Street	Dublin	20	✓	✓		
Champs Elysee	Paris	30	✓	✓		
Rue Mouffetard	Paris	18	✓	✓		
Graben	Vienna	12	✓	✓		
Kärntner Strabe	Vienna	16	✓	✓		
Total		620				

3.2. MODEL TRAINING

In this research, we chose supervised and unsupervised machine learning GAN models to explore their respective applications within the architecture discipline.

The first was Pix2Pix, a commonly used supervised machine learning model composed of a conditional GAN. We chose to use this model specifically to reconstruct

synthetic images of street scenes based on labeled or segmented images, for the most effective results. By labeling street images, we can extract several key features that define each street and allow us to implant these characteristics onto the targeted street, ranging from roads, building frontages, people, benches, trees, etc. This process requires two inputs to train the Pix2Pix model: the original street image (Image A) and the equivalent segmented image (Image B). Therefore, Dataset A was trained with segmented Dataset A, and Dataset B was trained with segmented Dataset B (Figure 4). The image segmentation was implemented in PyTorch on MIT’s ADE20K (Zhou et al., 2018), one of the largest open-source datasets for semantic segmentation and scene parsing. 1024x1024 pixel segmented images were created of both datasets. The second model, CycleGAN is in contrast based on an unsupervised GAN architecture, allowing the use of an unpaired dataset. Therefore, each dataset did not require the additional segmented dataset. Both models were equally run for 200 epochs of training cycles over the course of 2 days, on Google Colab Pro environment (P100 GPU was used).

For the training of both models, a new Dataset C was introduced, based on 3D viewport images of streets from a selected test city. Both Datasets A and B were trained separately (in each model) with Dataset C (Figure 4) to provide users with multiple trained models to select from. A 3D digital model of a test city with streetscapes, in this case, Cambridge, USA, was used to provide greater user control over the generated output within the user interface. This same methodology could be used with an image overlay, for example of a derelict, misused, or car-centric street. However, this would limit the user control and output image fidelity as explained in the following section.

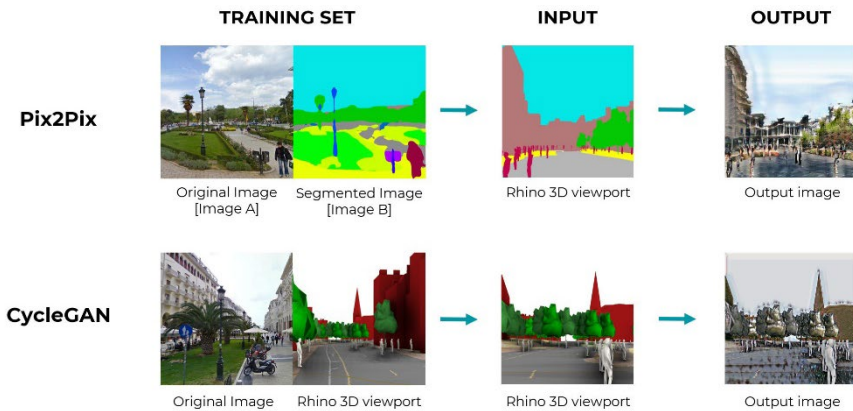


Figure 4. Dataset training workflow of each GAN model.

4. Results & Discussions

4.1. TRAINING RESULTS

Both models present diverse outcomes, reflecting on their supervised and unsupervised architecture. In the Pix2Pix model, the results trained from the green Dataset A revealed a variety of trees and greenery, while the pedestrian model indicates a lively urban character, containing amenities and people. This spatial identity could be used to

determine and visually evaluate the quality of space.

The outcomes of both training models produced varied results, representing a diverse synthesis of the different European streets. Both formal qualities and atmosphere or character (genius loci) emerge to different degrees and are intended to be taken as a starting point within the current exponential developments in machine learning. Several iterations demonstrated how increases in the dataset size and quality generated greener, livelier, and more varied streetscapes.



Figure 5. Sample output images.

Original Image	Pix2Pix		CycleGAN	
UI Interface Scene	Green Spaces	Pedestrian Commercial Spaces	Green Spaces	Pedestrian Commercial Spaces

Table 2. Training result comparison.

The results demonstrated by the Pix2Pix model show notably better results than CycleGAN, capturing specific spatial features to a greater extent. Figure 5 shows that certain synthetic output images begin resembling the abstracted white facades of Oxford Street, street activity of La Rambla, or bright green trees in the streets of Amsterdam.

This visual difference in part emerges from the difference between supervised and unsupervised learning. For this reason, Pix2Pix can be used to generate more detailed results per segmented object, while CycleGAN can be utilized to get unexpected results, at times mapping building surfaces with green textures.

4.2. REAL-TIME USER INTERFACE

The UI is intended for both citizens and stakeholders alike to visualize and interact in real-time with selected street views. Prototyped on HumanUI (Human UI, 2016), a plugin to Rhinoceros Grasshopper, several user inputs and sliders were used to provide high levels of design control (Figure 6). The inputs are divided into two parts. The first includes the selection of one of the two trained models, Datasets A and B, and the selection of a camera location based on the chosen city. The second is related to the urban inputs within the 3D scene. These include the manipulation of sample urban elements including pedestrian, tree, and bench count or pavement width, which visually improve the streetscape quality of the generated images.

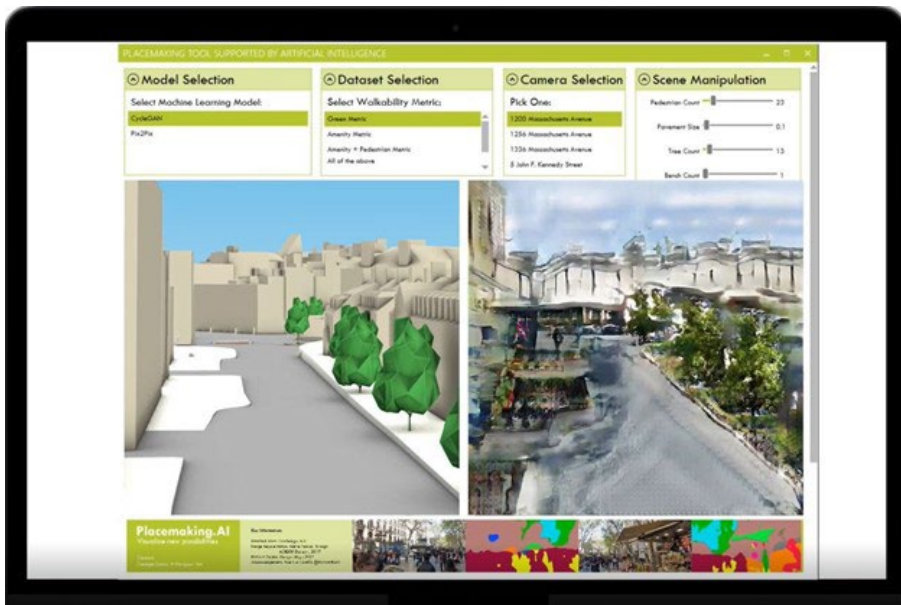


Figure 6. PlacemakingAI user interface.

This novel method of using GANs reflects a similar way designers originate ideas. In the same way, one sketches or uses architectural software, a feedback loop and level of the agency are provided, revealing future potentials of AI. On the left display, users

can interact seamlessly with their chosen street in 3D and design intent, and on the right screen, the chosen machine learning model presents the generated output in real-time. Users can zoom in, pan, and orbit around the scene to the preferred camera location on a chosen street.

In the back end, the current Rhino viewport was refreshed every 20 frames per second and this image was directly fed through custom python components into the Pix2Pix model to generate the resulting image. Each time a new model, dataset, camera or scene manipulation was made, both images would update. This however revealed the limitations in computing power to process high-resolution images, for example of 1024x1024 pixels. While this methodology was successful, only 256x256 pixel images provided sufficient real-time updates to respond to the user inputs on Human UI.

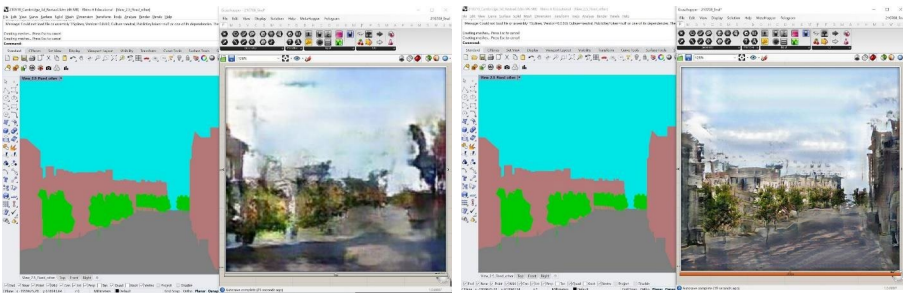


Figure 7. Back-end realtime (256x256) and Back-end realtime (1024x1024).

5. Conclusion

PlacemakingAI explores the possibilities of GANs in the generation and visualization of walkable urban streets. Building on the concept of imageability and genius loci, physical features, urban design qualities, and atmospheric characteristics of space can become embedded within the trained machine learning models. The variety of images produced and visualized provides an insight into early developments of real-time ML applications within the architecture engineering and construction industry and how generating and communicating design within the urban design could be overcome. This tool provides a framework in response to the UN Sustainability Goal 11: Sustainable Cities and Communities in enhancing this participatory process of urbanization into improved public spaces. Future work seeks to expand on the notion of feedback and accessibility, providing users with further intuitive design and dataset creation tools for increased agency and user testing through web-based applications or tangible user interfaces. PlacemakingAI seeks to advance current uses of machine learning into participatory processes and human-centric design solutions.

References

- Del Campo, M., Manninger, S., & Carlson, A. (2019). Imaginary Plans. *Acadia 19: Ubiquity and Autonomy*, (pp. 412–418). The Association for Computer Aided Design in Architecture (ACADIA).
- Dijkstra, L., D’Hombres, B., Montalto, V., Montalto, N., Bolsi, P., Castelli, C., de Dominicis, L., & Poelman, H. (2020). *Report on the Quality of Life in European Cities, 2020*.

- Publications Office of the European Union.
<https://doi.org/10.2776/600407>
- Ewing, R., & Handy, S. (2009). Measuring the Unmeasurable: Urban Design Qualities Related to Walkability. *Journal of Urban Design*, 14(1), 65–84.
- Gehl, J. (2011). *Life between buildings: using public space*. Island Press.
- Goodfellow, I. J., Pouget-Abadie, J., Mirza, M., Xu, B., Warde-Farley, D., Ozair, S., Courville, A., & Bengio, Y. (2014). Generative Adversarial Networks. *ArXiv.org*.
<https://arxiv.org/abs/1406.2661>
- Heumann, A. (2016, January 31). *Human UI*. Food4Rhino.
<https://www.food4rhino.com/en/app/human-ui>
- Isola, P., Zhu, J.-Y., Zhou, T., & Efros, Alexei A. (2016). Image-to-Image Translation with Conditional Adversarial Networks. *ArXiv.org*.
<https://arxiv.org/abs/1611.07004>
- Li, X., Zhang, C., Li, W., Ricard, R., Meng, Q., & Zhang, W. (2015). Assessing street-level urban greenery using Google Street View and a modified green view index. *Urban Forestry & Urban Greening*, 14(3), 675–685.
<https://doi.org/10.1016/j.ufug.2015.06.006>
- Lynch, K. (1960). *Image of the City* (20th ed.). The MIT Press.
- Norberg-Schulz, C. (1980). *Genius loci: towards a phenomenology of architecture*. Rizzoli.
- Noyman, A., Sakai, Y., & Larson, K. (2019). CityScopeAR: Urban Design and Crowdsourced Engagement Platform. *ArXiv.org*.
<https://arxiv.org/ftp/arxiv/papers/1907/1907.08586.pdf>
- Özel, G., & Ennemoser, B. (2020). Interdisciplinary AI: A Machine Learning System for Streamlining External Aesthetic and Cultural Influences in Architecture. *Architectural Intelligence*, 103–116.
https://doi.org/10.1007/978-981-15-6568-7_7
- Spacemaker - AI Architecture Design | Building Information Modelling. (n.d.).
<https://www.spacemakerai.com>
- Steinfeld, K. (2019). GAN Loci Imaging Place using Generative Adversarial Networks. *Acadia 19: Ubiquity and Autonomy*, 392–403. The Association for Computer Aided Design in Architecture (ACADIA).
- United Nations. (2015). #Envision2030 Goal 11: Sustainable Cities and Communities | *United Nations Enable*. Un.org.
<https://www.un.org/development/desa/disabilities/envision2030-goal11.html>
- Zhang, F., Zhang, D., Liu, Y., & Lin, H. (2018). Representing place locales using scene elements. *Computers, Environment and Urban Systems*, 71, 153–164.
<https://doi.org/10.1016/j.compenvurbsys.2018.05.005>
- Zhang, F., Zhou, B., Liu, L., Liu, Y., Ratti, C., & H Fung, H. (2018). Measuring human perceptions from street view imagery. *Landscape and Urban Planning*, 180, 148–160.
- Zhou, B., Zhao, H., Puig, X., Xiao, T., Fidler, S., Barriuso, A., & Torralba, A. (2018). Semantic Understanding of Scenes Through the ADE20K Dataset. *International Journal of Computer Vision*, 127(3), 302–321. <https://doi.org/10.1007/s11263-018-1140-0>
- Zhu, J.-Y., Park, T., Isola, P., Efros, A., & Research, B. (2017). Unpaired Image-to-Image Translation using Cycle-Consistent Adversarial Networks. *ArXiv.org*.
<https://arxiv.org/pdf/1703.10593.pdf>

CONTINUOUS ADAPTABILITY: WEB-BASED RESIDENTIAL PARTICIPATORY DESIGN USING MODULAR PREFABRICATED CONSTRUCTION

HUIYAO HU¹, BUI DO PHUONG TUNG² and PATRICK
JANSSEN³

^{1,2,3}*National University of Singapore*

¹*huiyaohu@gmail.com, 0000-0001-8427-2676*

²*phuongtung1231992@yahoo.com, 0000-0003-3951-8192*

³*patrick@janssen.name, 0000-0002-2013-7122*

Abstract. High-rise residences are typically very homogeneous and only allow for very limited variability in apartment configurations. Since the 1960s, practitioners and researchers have been exploring alternative visions of adaptable housing solutions that involve residents in the design process. Recent research has proposed digital platforms for residential participatory design. However, methods of modifying apartment configurations after building construction have not yet been developed in detail. This paper suggests a high-rise housing system that supports continuous adaptation and a web application that facilitates participatory design. The proposed construction system leverages on the prefabricated building modules and the open building concept to allow constant renewal of its non-structural building parts. This is complimented by a preliminary prototype of an online platform developed to streamline the design, negotiation and transaction of apartments by the homebuyers. The research conceptually investigates the potential of modern technology in redefining the role of architects and the relationship between residents and their buildings.

Keywords. Participatory Design; Mass Participation; Modularity; Prefabrication; Open Building; User-driven Design; Web Application; Self-renewal; SDG 11.

1. Introduction

Contemporary residential high-rises in Asia are often characterised by their homogeneity and repetition. They are designed through a top-down approach for inhabitants who are alienated in the process (Lee, 2003). Despite significant shifts in values and family compositions of the new generations in some now developed Asian nations, most dwellings still share the same legacy layouts, designed for ideal nuclear families with regular work life patterns, with the goal of tackling demographic challenges and housing shortage in the past (Nagore, 2014). The buildings are rebuilt around every 40 years, wasting embodied energy and producing large amounts of waste in the process (Heckmann, 2016).

Social and cultural changes have increased demand for new lifestyles such as co-living and working from home. As argued by Henri Lefebvre, space should not be a pre-existing and unchanging container which people fill up and move around it, but a product of human activities (Lefebvre, 1991). The old system of Fordism and static spaces have become incompatible with emerging understandings of a Post-Fordist world that is heterogeneous, pluralist, and ever-changing (Ma & van Ameijde, 2021). It is time for architects to start thinking about how to catalyse mass participation in the customisation of residential designs.

This research proposes a novel high-rise housing system, based on two core ideas developed in the 1960s: the open building concept and participatory design (Habraken 1962). It serves as a response to the United Nations' (UN) Sustainable Development Goals of making cities and human settlements inclusive, resilient and sustainable (United Nations, n.d.). The main novelty of the proposed system is the possibility for residents to continually change the spatial configuration of their apartments during the lifetime of the building, referred to in this research as 'continuous adaptation'. In the proposed concept, such adaptations are made possible by new technical advancements in the domain of prefabricated modular design.

The open building concept suggests that there should be multiple layers of control in a collective housing building. Two key layers are the support layer and an infill layer. The support layer consists of the immovable, structural parts of the building, such as columns and beams, while the infill layer consists of the non-structural, replaceable parts of the building such as partition walls. The two layers can be treated as separate entities, with different life cycles (Brand, 1995). Together, they allow for a building design that is highly adaptable and optimised for participatory design whereby the professionals configure the support layer, and the residents can design the infill layer with some guidance.

Historically, several built residential projects have used participatory design approaches, where future residents are able to influence the design of their apartments. Three key projects were La MéMé, Ökohaus and Next 21. La MéMé, a medical faculty housing project by Lucien Kroll, was designed with inputs from the workshops conducted for students and school staff (Williams, 1979). Ökohaus, a project by Frei Otto, used the open building concept separating structure from infill, and allowed each family to plan their own infill apartment (Callahan, 2013). Next 21, a project by Yositika Utida, also used the open building concept and allowed 13 different architects to design the infill apartments. In this case, all designs followed a set of common rules and materials, resulting in a more unified appearance (Kim, Brouwer & Kearney, 1993). In all three cases, participatory design approaches resulted in residents having significant influences over the design process. However, a key limitation of these examples is that most designs are defined pre-construction. During the lifetime of the buildings, it would be difficult for later residents to change the spatial configuration of their apartments, due to various constructional limitations and constraints.

The idea of continuous adaptation has been a core concept of various post-war movements, including both Archigram and the Metabolist Movement. An iconic example of a built project that incorporated the concept of continuous adaptation was The Nakagin Capsule Tower. The design was based on a series of capsules that could be plugged into (and out of) the vertical core of the building. However, in practice, the

capsules were never replaced because removing any one capsule requires all the capsules above to also be temporarily removed (Maeda & Yoshida 2021).

More recently, researchers have proposed various digital platforms for mass-participatory design that will allow apartment designs to be adapted to the specific requirements of the residents. Chien & Shih (2000) describe an application developed to help the designers manage buyers' selection of finishes and interior layouts. Lee & Li (2007) explored a 3D Layout generator that creates interior designs based on questionnaires answered by the buyers. Lo, Schnabel & Moleta (2017) suggested the need to gamify the design platform and provide opportunities for negotiations between users in a participatory design project. Ma and van Ameijde (2021) proposed a Hybrid Structural System that generates customised housing floor plan layouts based on inputs collected from the house buyers.

While the proposed platforms highlight the potential of digital platforms to streamline participatory residential design, two key issues are identified. First, the platforms do not allow residents to directly create their own designs. Instead, they process residents' opinions in the form of questionnaires. Second, the platforms all focus on design adaptability before construction starts. The idea of continuous adaptability during the lifetime of the building is not developed in detail.

In this research, a novel high-rise housing system is proposed that supports both continuous adaptation and participatory design. To enable continuous adaptation, an innovative modular prefabrication system is proposed that allows infill structures to be modified while the building is in operation. The participatory design process takes place on a prototype web application that allows residents to design the spatial configuration of their apartments.

Section 2 gives an overview of the proposed construction system. Section 3 describes a prototype of the web application for residents to create apartment configurations. Finally, Section 4 draws conclusions and discusses future research directions.

2. Modular Construction System

The proposed construction system implements the open building concept using two key material systems: reinforced concrete for the support and prefabricated modules for the infill. The concrete structure will have a long lifespan while the prefabricated modules have a short lifespan. The prefabricated modules are Structurally Insulated Panels (SIPs), which are light-weight, energy efficient and environmentally friendly. The construction system is defined within an orthogonal 3D grid to facilitate effective and efficient production and assembly of building modules.

The support consists of the load-bearing reinforced concrete structure, which includes the basement retaining walls, shear wall around vertical cores, horizontal corridor slabs on each level, and a 3D frame of columns and beams, as illustrated in Figure 1. The building cores include the staircases, passenger lifts as well as freight elevators that are large enough for transporting SIP panels.

Apartments are the infill, created by inserting prefabricated modules within the columns and beams of the 3D frame. The modules are used to create the complete enclosure of the apartment, including floors, walls, and roofs. They are mechanically connected to the frame, to facilitate the physical installation or removal of the panels. Throughout the life span of the building, residents can reconfigure their apartments by replacing the prefabricated modules.

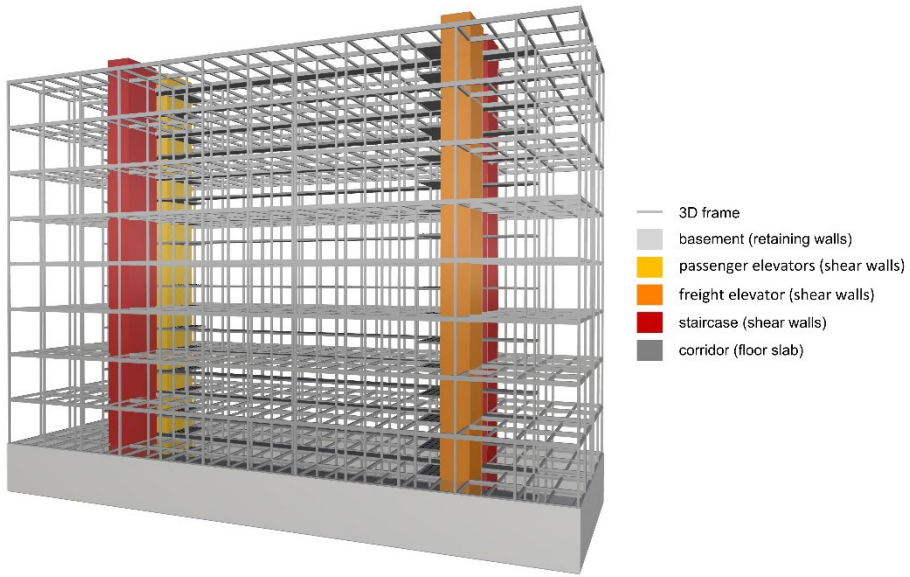


Figure 1. 3D visualisation of the building support

2.1. SUPPORT

A typical building typology is envisaged, as shown in Figure 2. On all floors, a central corridor runs down the length of the building, acting as a street in the sky. On either side of the corridor, the concrete frame extends two bays deep. Each bay is 7m deep, 3.5m wide and 3.5m high. The 3.5m width means that SIP floor modules can easily span the distance without requiring any additional structural support.

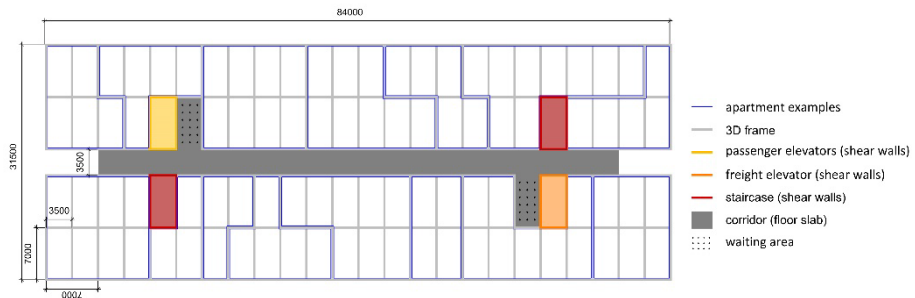


Figure 2. Plan of a storey in the building indicating the support layer components

The vertical cores connect the floors and create lateral structural stability. Apartments can then be created on either side of the corridors, with their entrance always directly accessible from the corridors. The corridors are laid with integrated services containing the mechanical, electrical and firefighting systems for the apartments. Heating and air-conditioning are centralised, resulting in improved efficiency and minimising noise disturbances.

The building cores includes the fire-escape staircases, passenger lifts as well as freight elevators. The basement serves as the temporary storage space for the prefabricated modules, which are delivered from the factory to the building in trucks before they are carried up the building in the freight elevator with minimal disruption to the other residents. The central corridors and freight elevator are sized to allow the delivery of modules to and from each apartment.

The overall form of the buildings can be computationally generated or manually tweaked to take various shapes, depending on the site constraints, as shown in Figure 3. The porosity of the building would be maintained by limiting apartments to filling up to a maximum of 70% of the frame. The void spaces can then be used as terraces and outdoor spaces and can also improve ventilation and daylight penetration.

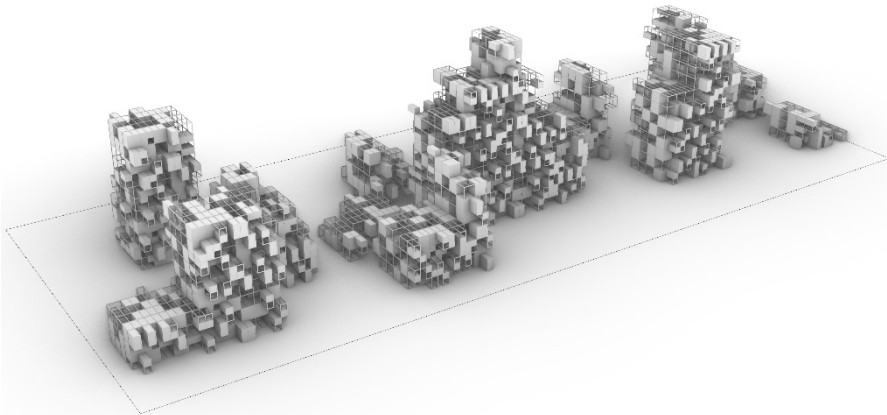


Figure 3. Example of a building cluster

2.2. INFILL

SIPs are chosen as the predominant infill material of walls, floors and ceilings for their environmental-friendliness, ease of installation and affordability. They are prefabricated construction elements that can be mass-produced in a factory and subsequently jointed on site using mechanical connections. They can be made from scrap wood, hence making them even more eco-friendly than timber.

The SIPs and other infill components such as windows and doors make up the prefabricated infill modules for the apartments, as illustrated in Figure 4. Residents will be provided with a catalogue of prefabricated modules to choose from when creating their apartments. The mass production of these modules allows the ease of configuration and replacement.

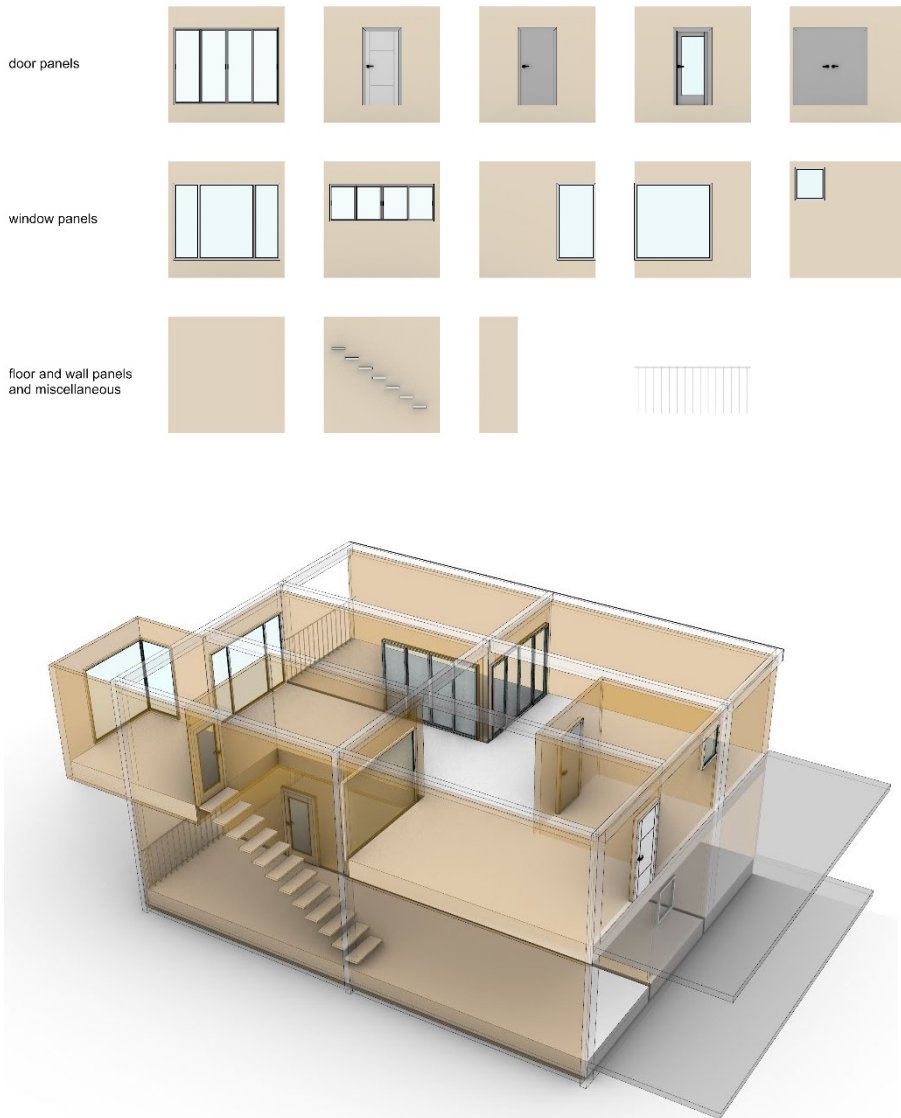


Figure 4. Apartment prototypes designed using infill modules from the catalogue

The prefabricated modules are secured in position by mechanical connections to the concrete columns or beams in a frame. The installation of the modules is done by professional renovation teams. No exterior scaffolding is required. The process starts at the corridor, laying floor SIPs that then form a working surface. The mechanical, electrical, and plumbing systems run under raised floors in each apartment and connect to the corridor, as shown in Figure 5.

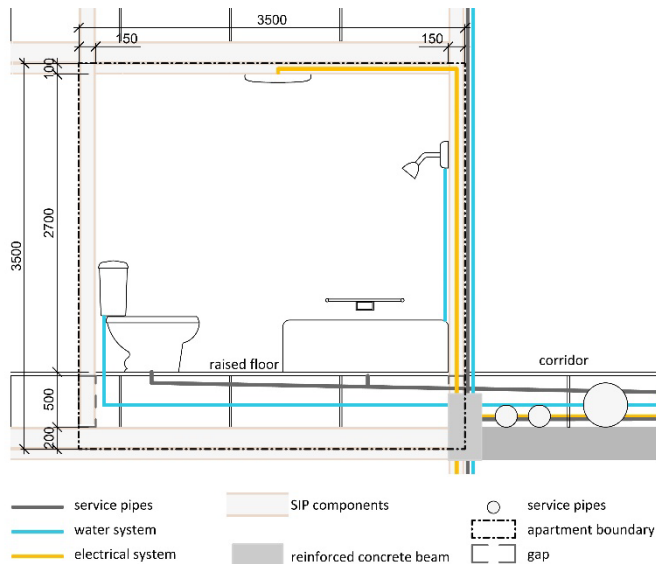


Figure 5. Section of an apartment bathroom

3. Prototype Web Application

The proposed housing system is supported by a web application for residents to purchase or sell infill space, as well as to configure apartments.

The web application allows residents to perform four main functions:

- **Space Transaction:** Buy and sell space in the grid, based on the financial market value of the space. Spaces can be put up for sale, and people can bid for the space.
- **Infill Configuration:** Design an apartment within the space that they own, by configuring infill modules from the catalogue.
- **Negotiations:** If a proposed design breaks any environmental rules, the resident can use the platform to negotiate with neighbours to try and reach a financial settlement.
- **Approval:** When the apartment configuration has been completed, the design can be submitted to the building committee for final approval.

The most challenging part is the second step, in which residents create spatial designs of the infill space on the web application. The residents are assumed to have no 3D design experiences. As such, the web application must be highly user-friendly.

For this reason, a gamified approach is proposed to make it easier for people to create a complex 3D model of their apartment. Game design elements, such as operation and interface commonly found in popular home design games, are implemented in the design of the platform. The aim of gamification is to allow the users to navigate and engage with the platform more intuitively (Deterding et al. 2011).

In order to test the feasibility of this approach, a prototype web application has been created. The web application facilitates the Space Transaction and Infill Configuration functions as described above.

3.1. USER INTERFACE

In the web application, users are first asked to select a set of eligible infill space units for which they want to configure an apartment. These units may either be owned by them or are for sale. The volume, costs and number of floors of the selected units are presented to the users to assist them in their decision making, as shown in Figure 6.

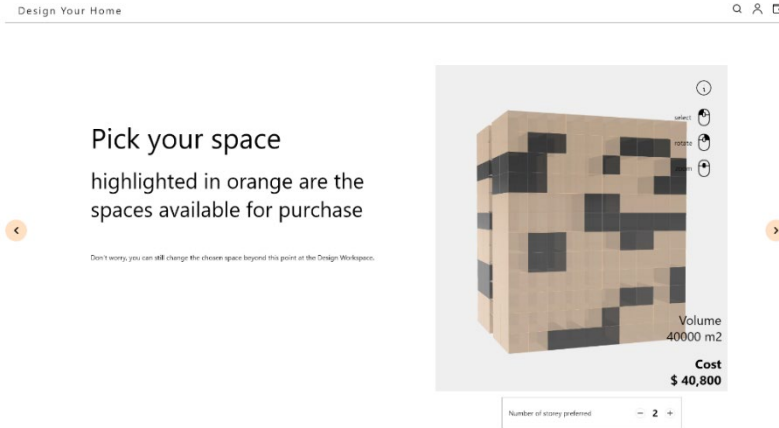


Figure 6. 3D viewport for users to select infill spaces to design or perform transactions upon

After completing their infill space selections, the users can access the 3D Workspace of the selected spaces to configure their apartment. As presented in Figure 7, users can customise the layout and appearance of the apartment spaces using a range of infill modules provided in the catalogue to the left of the webpage. The costs of the spaces and modules are tabulated on the right of the webpage to help the users keep track of their expenses. For users who find it challenging to design an apartment from scratch, they can kickstart the process using a template provided in the system before modifying it to their preferences.

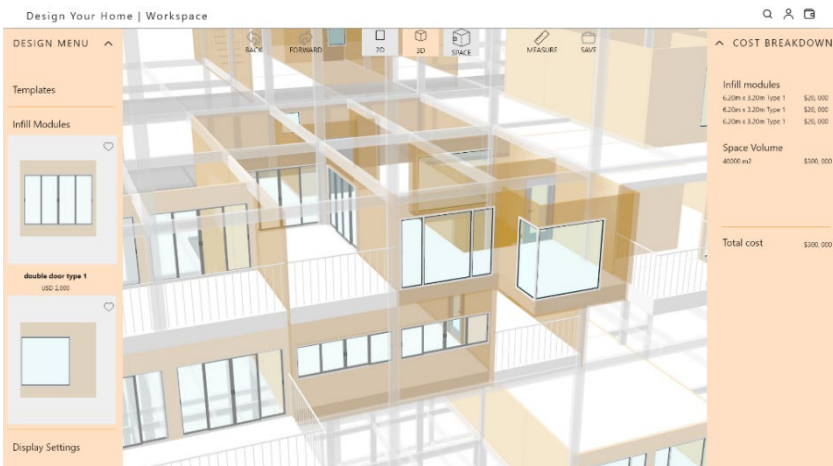


Figure 7. 3D Workspace for residents to design their apartment using a catalogue of modules

In the 3D Workspace, users can turn on the display of the neighbouring apartments in the settings. The ability to see the designs of neighbouring apartments is to allow users to review and negotiate any conflicts of interest that may arise.

3.2. USABILITY TESTING

In order to test the prototype web application, two user-studies have been conducted. The first group consisted of architecture students, while the second group consisted of citizens with no architectural training. In both cases, the users were asked to create apartment configurations that fulfilled specific requirements. The results show that in both cases, users were able to create apartment configurations with ease. However, certain configurations negatively impacted neighbouring apartments, such as infringing on privacy or blocking daylight access. Future prototypes and trials are needed to work out more robust rules that can prevent design flaws while maximising the users' liberty in customising apartments.

4. Discussion

Modern-day residents are diverse and are often very far from the idealised nuclear family. Given the shifts in values and family compositions, existing generic residential apartment layouts are outdated. The proposed approach aims to overcome this issue by imagining a novel type residential building that allows both continuous adaptation and participatory design. It is enabled by the open building concept: the support being a concrete frame into which apartments are inserted as infills. Modifications of the infill panels are facilitated by a modular system of prefabricated panels. The web application is designed using a gamified approach, making it easy for non-designers to create 3D models of their apartments. It facilitated the ongoing participatory design that allows residents to buy and sell space, design apartment configurations, negotiate with neighbours, and finally get approval for their apartment.

The prototype web application demonstrates that the proposal is feasible although further development is required. Its usability tests confirmed that users, who may not have a design background, can successfully configure their apartments on the platform.

Under the proposed approach, the role of an architect focuses more on being a designer of spatial rules rather than the designer of a final spatial form. Future research will investigate how architects can more effectively use spatial rules and guidelines to coordinate the participatory design by residents.

The proposal challenges the concept of a building: it is no longer a static entity, but instead a dynamic process that will undergo continuous adaptation through participatory design. In many existing projects, the concept of adaptability ends up becoming purely symbolic due to various practical limitations. Learning from past built projects, this research proposes both a user-friendly web application and a modular prefabricated construction system that aims to make continuous adaptation through participatory design a viable reality. It is a work in progress towards achieving the UN Sustainable Development Goal 11 of participatory, integrated and sustainable housing.

Acknowledgements

We thank Dr Hossein Rezai-Jorabi (National University of Singapore) for reviewing and giving feedback on the structural design of the proposal.

References

- Brand, S. (1995). *How buildings learn: What happens after they're built*. Penguin.
- Callahan, A. (2013). *Eco-Houses*. *Architectuul*. Retrieved November 7, 2021, from <http://architectuul.com/architecture/eco-houses>
- Chien, S. F., & Shih, S. G. (2000). *A Web Environment to Support User Participation in the Development of Apartment Buildings*.
- Habraken, N. J. (1962). *Supports: an alternative to mass housing*. Routledge.
- Heckmann, O. (2016). Operative Design Strategies for High-Dense Living in Asian Cities. In *European Network for Housing Research Conference 2016*.
- Kim, J., Ryan B., & Jennifer K. *NEXT 21: A Prototype Multi-Family Housing Complex*. University of Michigan, College of Architecture and Urban Planning (1993).
- Lee J. (2003) Is There an East Asian Housing Culture? Contrasting Housing Systems of Hong Kong, Singapore, Taiwan and South Korea, *Journal of Comparative Asian Development*, 2:1, 3-19.
- Lee, J, & Li, T. *Fuzzy-based Direct Manipulation: focused on user participation in apartment plan design process*. (2007).
- Lefebvre, H., Nicholson-Smith, D., & Harvey, D. (1991). *The production of space*.
- Lin, Z. Nakagin capsule tower: revisiting the future of the recent past. *Journal of architectural education* 65.1 (2011): 13-32.
- Lo, T. T., Schnabel, M. A., & Moleta, T. J. (2017). Gamification for user-oriented housing design. In *CAADRIA 2017-22nd International Conference on Computer-Aided Architectural Design Research in Asia: Protocols, Flows and Glitches* (pp. 63-72).
- Loss, C., Piazza, M., & Zandonini, R. (2016). Connections for concrete–timber hybrid prefabricated buildings. Part II: Innovative modular structures. *Construction and Building Materials*, 122, 796-808.
- Ma, C. Y., & van Ameijde, J. (2021). Participatory Housing: Discrete Design and Construction Systems for High-Rise Housing in Hong Kong. In *26th CAADRIA Conference - Volume 1* (pp. 271-280)
- Maeda, T., & Yoshida, Y. (2021) *Heritage in danger the real reason why Nakagin Capsule Tower was never metabolized*. https://www.docomomo.com/wp-content/uploads/2021/09/DocomomoJournal65_2021_TMaedaYYoshida.pdf
- Nagore, S. I. (2014). Towards an open and user driven housing architecture: Layers principle, infrastructure types and technical devices. In *I Congreso Internacional de Vivienda Colectiva Sostenible, Barcelona 2014* (pp. 96-101). Máster Laboratorio de la Vivienda Sostenible del Siglo XXI.
- Schuler, D., & Namioka, A. (Eds.). (1993). *Participatory design: Principles and practices*. CRC Press.
- Teo, A. (n.d.). *List of HDB BTO brochures*. The World of Tealida. Retrieved November 7, 2021, from <https://www.tealida.com/singapore/btobrochures/>
- United Nations. (n.d.) *UN Sustainable Development Goal 11*. UN Sustainable Development Goals. Retrieved December 7, 2021, from <https://sdgs.un.org/goals/goal11>.
- Williams, S. (1979). Ecological Architecture of Lucien Kroll. *Architectural Review (U.K.)*, 984(165), 94-101.

PARTICIPATORY PLANNING:

Heritage Conservation through Co-design and Co-decision

SIEW LENG LEONG¹ and PATRICK JANSSEN²

^{1,2}*National University of Singapore*

¹*leong.siewleng@u.nus.edu, 0000-0002-7907-0110*

²*patrick@janssen.name, 0000-0002-2013-7122*

Abstract. Citizen participation in urban planning and architectural design has been long discussed and experimented with since the 1960s. With existing participatory design approaches, two key challenges can be identified. First, the power of citizens to directly affect the decision-making processes is typically quite limited. Second, the use of traditional face-to-face design workshop results in low levels of participation. This paper proposes an innovative participatory design approach with a focus on co-design and co-decision. The co-design stage provides citizens with a tool that empowers them to think critically of their built environment and to initiate design development in their own city. The co-decision stage gives citizens real power in determining the future changes to their city by embedding the participatory design approach into the planning permission system. This participatory design approach is implemented through a web application that allows participants to view design proposals within the existing site context from a birds-eye views and from multiple immersive views, leading to a better understanding of the design proposal's scale and impact. The design proposal viewer has been demonstrated on a heritage site in Singapore, showing its potential to be used as evidence for supporting or rejecting design proposals.

Keywords. Participatory Planning; Co-design and Co-decision; Citizen Power; Visualisation Method; Bird's-eye View; Immersive View; Web Application; SDG 11.

1. Introduction

Heritage conservation is a complex domain that involves multiple stakeholders with varying perspectives and value systems. In Singapore, the three key groups of stakeholders for conservation projects are the government planning departments, the developers, and the citizens. Of these three groups, the planning departments and the developers have disproportionate influence, while the citizens have almost no influence. This has led to many ineffective heritage conservation projects where profit reigns while the historical value and cultural sustainability are neglected. This research

explores Participatory Design (PD) as a way of empowering citizens to have a stronger influence over the future developments of heritage sites in their city.

Citizen participation in urban planning and architectural design has been a topic that is long discussed and experimented with by various scholars (Davidoff, 1965; Arnstein 1969; Sanoff, 2000; Falco, 2019; Tomarchio et. al, 2019). PD typically involves holding various types of workshops that bring together citizens, designers, and other key stakeholders (Sanoff, 2000). Such workshops are complex to organise and labour-intensive. Furthermore, when reviewing design proposals, there is often a high communication barrier between citizens and other design experts, so multiple workshops are usually required. Due to the time commitment that is required, only a small segment of the population can participate, which can lead to biased results. The key problem with workshop-based PD is therefore the lack of scalability.

To overcome the challenge of scalability, practitioners have explored various web-based digital tools to support the PD process. In many cases, these tools focus on the process of collecting feedback from citizens. One example is ArgooMap, a map-based discussion forum that supports place-based comments (Rinner, 2008). The discussion forum allows users to visualize their discussion in relation to the surrounding context. Another example is ChangeExplorer, an application that prompts citizens to provide short feedback on proposed development change as they walk through the city (Wilson et. al, 2019). The application provides a low barrier for participation and only requires a short interaction time.

Another approach is to set up design competitions and to gather feedback from citizens on shortlisted proposals. Some well-known architectural design competitions using this approach include the World Trade Centre Site Memorial Competition and the Sendai Mediatheque Municipal Library Competition. In the context of Singapore, an example is the Singapore Founders' Memorial Design Competition held in 2019. The competition resulted in five designs being developed, which were presented to the citizens of Singapore through an online website and offline through a two-month roving exhibition. Both online and in the exhibition, citizens were given the opportunity to leave feedback and to vote for their preferred design. At the end of the competition, the jury panel evaluated the submissions and selected the winning design.

A key issue with many existing PD approaches is that the level of citizen participation falls under what Arnstein (1969) has described as "tokenism". Under this category of participation, citizens' inputs have little impact on the actual outcomes. The perception by citizens that this might be the case, in turn, results in a low motivation for participation.

This research sets out to explore PD approaches that are both scalable and that allow citizens to have a real impact on outcomes, focusing specifically on heritage sites. A key strategy is to develop more advanced types of web-based tools to allow citizens to be involved in both the design process and the decision-making process.

The research proposes a PD method that includes two stages: a 'co-design' stage and a 'co-decision' stage. In the co-design stage, various groups can make design proposals and citizens can comment and give feedback on those proposals. In the co-decision stage, the planning permission process includes a citizen approval step, in which citizens get to vote for or against finalised design proposals. The proposed approach thereby devolves some of the power currently held by the planning authority

to the citizens. This ensures that citizens have a direct and tangible impact on the evolution of the cities they live in.

Section 2 will describe the proposed PD process for heritage projects. Section 3 presents a prototype web platform for viewing design proposals, for supporting both the co-design and co-decision stages. Section 4 gives summarises the results of a set of demonstrations. Finally, section 5 draws conclusions and discusses future research directions.

2. PD Method

This research proposes a novel and scalable participatory co-design and co-decision method applicable to key heritage sites, specifically focusing on heritage conservation practice in terms of adaptive reuse and new-build around heritage sites. The method will focus on design aspects that have an impact on the public, including the proposed building programme, proposed massing of new buildings, proposed demolitions, and architecture detail including materials, colours, patterns, and so forth.

The co-design and co-decision processes focus on citizens with differing levels of involvement in the PD process. The co-design process will require a high level of participation. This is envisaged as being driven by both developer organisations and by committed citizen groups, often in conflict with one another. We refer to these collectively as ‘proposal makers’. They participate directly in a combative process by creating design proposals and counter-proposals.

The co-decision process will require a low level of participation. This is envisaged as involving a much larger group of citizens who participate purely by exercising their right to vote for or against a design proposal. The level of involvement is not to be confused with the level of power. The co-decision citizens may not be participating so intensively as the co-design citizens, but their act of voting holds significant power.

In the building design process, the typical stages are conceptual design, schematic design, detailed design, and finally tender documentation. Application for planning permission will typically start during or at the end of the schematic design stage.

In the proposed process, the new co-design and co-decision stages will occur during the conceptual design phase, prior to application for planning permission. Citizen approval needs to be obtained before any application for planning permission can be made. The process, therefore, reverses the power structure. In the proposed method, the citizens are in charge of making the primary planning decisions. The government-planning department can then come in later to ensure that other secondary requirements are met. Once a design proposal has received citizen approval, the planning authority has no right to overrule the decision unless compelling technical reasoning is provided.

Section 2 will describe the proposed PD process for heritage projects. Section 3 presents a prototype web platform for viewing design proposals, for supporting both the co-design and co-decision stages. Section 4 gives summarises the results of a set of demonstrations. Finally, section 5 draws conclusions and discusses future research directions.

2.1. CO-DESIGN AND CO-DECISION

In the proposed process, the new co-design and co-decision stages will replace the conceptual design phase, prior to application for planning permission. Citizen approval needs to be obtained before any application for planning permission can be made. The process, therefore, reverses the power structure. In the proposed method, the citizens are in charge of making the primary planning decisions. The government-planning department can then come in later to ensure that other secondary requirements are met. Once a design proposal has received citizen approval, the planning authority has no right to overrule the decision unless compelling technical reasoning is provided.

The co-design process is initiated whenever a proposal for a heritage site is submitted by proposal makers. A process with a fixed time window is then initiated, during which various proposal makers can submit counter-proposals and or create new proposals by modifying or merging some other proposals. During this process, citizens can give feedback on proposals. However, no voting can occur. The key steps in the co-design process are shown in Figure 1.

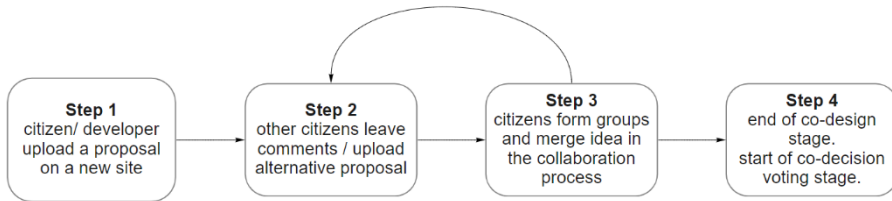


Figure 1. Co-design process.

Once the co-design time window has run its course, a new time window will then start for co-decision, during which citizens can vote on proposals. The co-design process may result in multiple proposals being put forward for voting. Proposal makers are likely to seek support for their proposals from the broader public through various social media platforms. Citizens can vote for multiple proposals, and for each proposal, they can vote either in for or against. The total number of votes for each proposal are then added up, with votes against being counted negatively. Proposals that reach a certain minimum total number of votes are then automatically approved. The key steps of the co-decision process are shown in Figure 2.

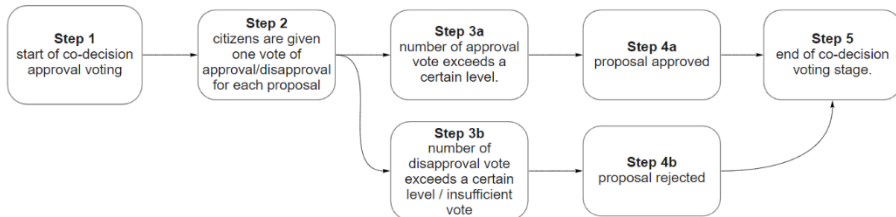


Figure 2. Co-decision process.

3. PD Web Platform

To support both the co-design and co-decision processes, a web platform is proposed.

This web platform aims to achieve greater citizen involvement in the PD process. The platform will support all aspects of the PD method, including uploading design proposals, giving design feedback, and voting on design proposals.

Two key issues are the process of generating design proposals, and the process of visualizing design proposals. For citizens with little design experience or training, these are both challenging aspects of the PD method.

3.1. GENERATING DESIGN PROPOSAL

For the co-design process, proposal makers need to be able to create their own design proposals. Proposal makers are assumed to be more committed and have more time than most citizens. Nevertheless, the process should still be made as easy as possible.

For creating designs, various web-based tools were studied that allow citizens to model their own designs. Two examples are the “Ideas for Tanjung Pagar” study (Tomarchio et. al, 2019) using the Qua-Kit tool and the “NIMBY” web game (Yenardi et.al, 2021). These examples are interesting since they allow citizens to create their own design proposals as a way of gathering feedback. However, to make the 3D modelling process simple and easy to use, these tools are constrained to produce only simplified geometric models. The approach would not work well for this use case, since design proposals for heritage sites cannot be easily constrained in this way.

For this reason, the decision was made to allow proposal makers to use existing 3D modelling tools to create 3D models of their proposals. To keep the modelling process as simple as possible, BIM modelling formats and tools would not be required. Instead, since the design proposals focus mainly on the exterior, geometric modelling tools such as Sketchup can be used. Models can then be uploaded in geometric forms such as Obj or GLTF.

3.2. VISUALISING DESIGN PROPOSAL

For both the co-design and co-decision processes, citizens need to be able to easily view and understand the impact of proposed designs from a variety of different vantage points in the city. For proposal makers, the level of expertise may be assumed to be a little higher. But for citizens that are giving feedback or participating only in co-decision, the assumption must be that they have little time and little experience in evaluating design proposals. The process of viewing design proposals, therefore, has to be fast and easy.

Relying on traditional representations such as architectural drawings will be too complex. To properly understand the impact of design proposals, it is critical to view proposed designs in 3D, within the urban context. The 3D models that are uploaded therefore need to be geo-located and viewable in ways that show the surrounding streets and buildings. Through tools such as Google Maps, citizens are mostly already familiar with two modes of viewing 3D models: birds-eye view and immersive view. We proposed to integrate these two modes into the proposed web app.

3.3. PROTOTYPE DESIGN PROPOSAL VIEWER

To test the feasibility of the proposed PD method, a prototype web application has been

developed for citizens to evaluate design proposals (Figure 3). This prototype focuses on the contextual viewing of 3D models within the urban context, as this is a critical requirement to make the whole approach viable.

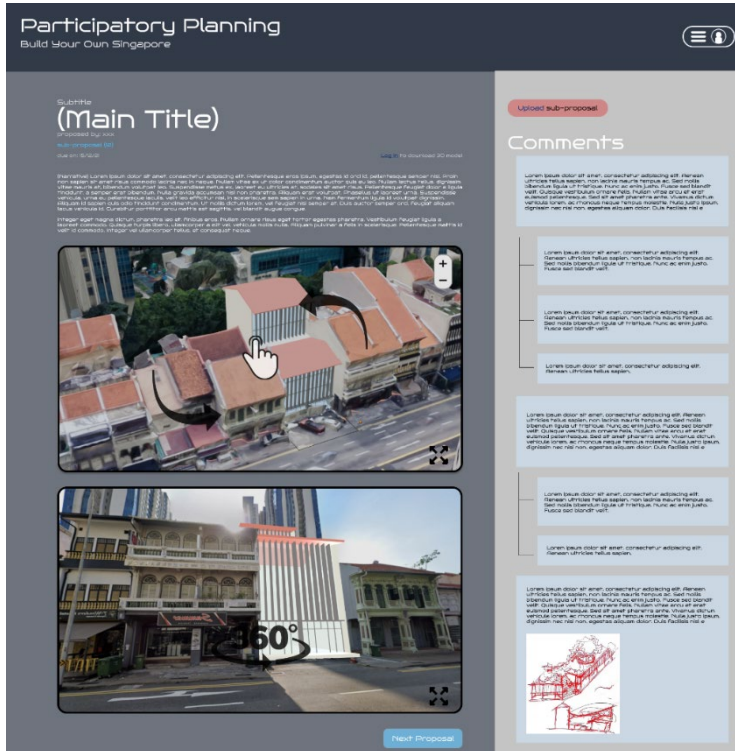


Figure 3. User-interface for reviewing individual proposal during the co-design stage.

The prototype allows users to view the uploaded 3D models in both bird's eye view and the immersive view, as shown in Figure 3. Both views include the surrounding context, allowing for a better understanding of the design proposal's scale and impact.

3.4. BIRD'S EYE VIEW

The bird's eye view mode allows citizens to understand the scale of the design in relation to the rest of the cityscape. Citizens can zoom in and rotate around the viewport to have a better understanding of the spatial relation between the design proposal and its neighbouring buildings.

One limitation of the Google Maps model is that it does not support modification and removal of existing geometry. For design proposals that include demolition of existing buildings, it is therefore not possible to remove these parts of the model. The research, therefore, envisages that, for the final implementation, a locally developed 3D city model would need to be used, with APIs that allow removal as well as the addition of geometry. In Singapore, the government has already developed such a

model, referred to as the Virtual Singapore model. Unfortunately, at the current time, the model is not yet made publicly available. As a result, the prototype will use static models extracted from Google Maps through RenderDoc as an interim solution for testing purposes. The existing Google Map base allows for easy navigation.

The prototype uses the JavaScript library three.js to display the uploaded .glTF 3D model file in the web application. This 3D model is overlaid onto the extracted 3D Google Map model and integrated with the different viewers.

3.5. IMMERSIVE VIEW

The 360° immersive view mode allows citizens to have immersive views of the proposed design from specific vantage points. In this viewing mode, the camera can be rotated, but the camera position cannot be moved. Similar to Google Street View, citizens can still navigate from one immersive view to another, which can still give a semblance of walking around.

The immersive view embeds the 3D model within a 360° equirectangular image of the urban context. This image wraps around the model, giving the impression that the model is placed inside a 3D context of surrounding buildings. In cases where the image includes objects that are both in-front of the design proposals as well as behind it, two equirectangular images can be created. In the example in Figure 3, we can see that various objects such as trees, signs, and lampposts appear in front of the design proposal, while everything else appears behind.

The key advantage of the immersive view mode is that is a highly efficient way of obtaining a realistic representation of the surrounding context. Citizens can easily create their own equirectangular images using a simple smart-phone app and upload the images to the web application, thereby creating new street-view locations. We can imagine that proposal makers will initially create a set of immersive-view locations that show their design proposal from the best point of view. Citizens can then create their own immersive-views, possibly highlighting some negative aspects of the proposed design. The immersive views can include images at different times of the day, images from surrounding buildings, or images from distant vantage points.

All design proposals can be viewed using the same set of immersive views. The prototype web app allows design proposals to be switched while in an immersive view, without changing the camera angle. This allows design proposals to be easily compared and contrasted.

4. PD Web Platform

To test the proposed method, a demonstration has been created for one of the heritages sites in Singapore, the Jalan Besar Secondary Settlement Conservation Area. The heritage site consists of a series of pre-war and post-war shophouses that were preserved mainly along the main streets. Certain plots of land along the strip were not under conservation status due to the original buildings being demolished prior to the site being gazetted as a conservation area (Figure 4 - left). Even though the allowable gross plot ratio on-site is 3.0 and the construction of rear extensions is permissible by law, plenty of buildings on-site have not maximized their development rights (Figure 4 - right). In the demonstration, the participatory design web platform is used to

simulate potential development changes on-site with two main purposes: i) to ensure careful insertion and modification of conserved buildings; ii) to monitor new developments on sites next to existing conserved buildings.



Figure 4. Jalan Besar Conservation Area analysis.

For the demonstration, two different design proposals have been created and a set of immersive views have been added. Both design proposals showcase how a new building can be built next to existing heritage buildings.

In the first set of views (figure 5 - left), the proposal shows a design intervention that responds to the gable roof form of neighbouring historical buildings by continuing the design language. However, looking at the 360-degree view on street level, we notice that the louvers façade design is too overwhelming compared to the bay-window design of the neighbouring architecture. In the second set of views (figure 5 - right), the design proposal shows a flat roof building with a roof garden on the building block in front. Even though the second proposal does not use the same gable-roof language, it still blends in well with the surrounding building due it having similar height and levels with neighbouring buildings. The 360-degree view on street level also shows that the second design proposal with three-bay windows blends in well with other historical buildings on site which also utilises the same three-bay windows language.

A user-test was carried out with laypersons with no architectural training, to test the efficacy of the web platform for obtaining feedback on potential future developments. Interviews were carried out in which participants were asked to evaluate and discuss the two designs created for the demonstration. The result indicated that the birds-eye and immersive views were easy to understand and were able to support design proposals discussion among laypersons.

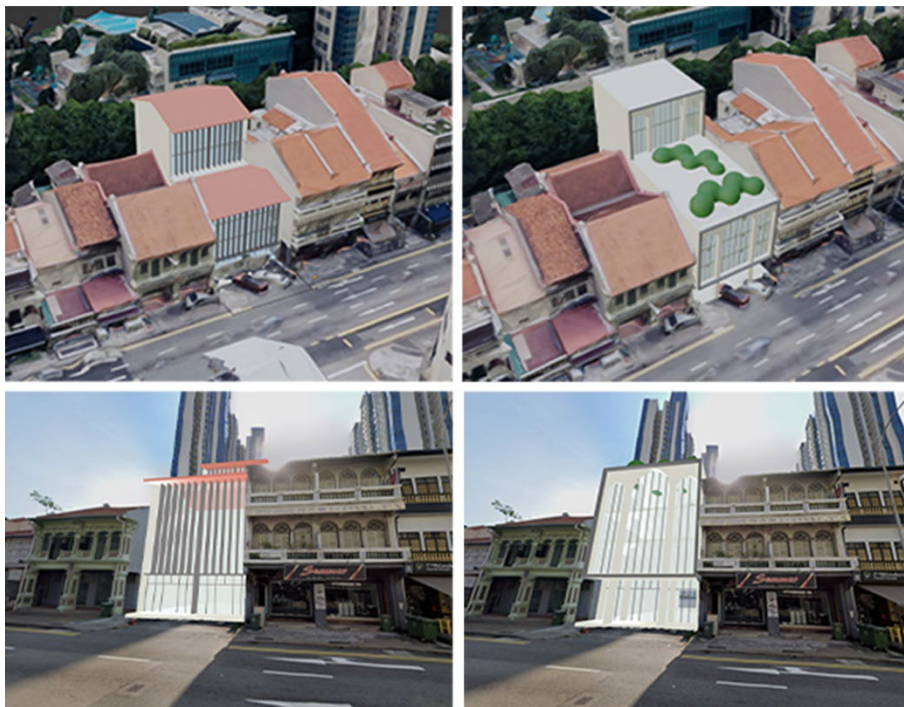


Figure 5. Demonstration showing different design proposals

5. Discussion

A proposed PD method devolves significant power to citizens. The method gives citizens direct control over the evolution of urban neighbourhoods in and around heritage sites in their cities. In the proposed method, citizens are able to participate in both a co-design process and a co-decision process. In the co-design process, they can gather to form committed citizen groups that make proposals and counter-proposals. Through this process, they have complete freedom to develop their own designs or to adapt other existing designs. In the co-decision process, the citizens get to vote on proposed designs. Design proposals are then approved or rejected solely based on the results from this voting process, without interference from external parties. The co-decision process gives citizens real power in determining the future changes to their city.

To support the proposed PD method, a web platform is proposed that supports all aspects of the PD method, including uploading design proposals, giving design feedback, and voting on design proposals. One of the key parts of this web platform is the process of viewing design proposals within the urban context.

To test the feasibility of the proposed PD method, a prototype of the web application has been developed for citizens to evaluate design proposals. The prototype allows design proposals to be viewed within the urban context from a birds-eye view and from multiple immersive views, submitted by citizens themselves.

The design proposal viewer has been demonstrated on a heritage site in Singapore, highlighting how different views can be used as evidence for supporting or rejecting design proposals. The web application contributed towards SDG Goal 11, 'sustainable cities and communities', by proposing a heritage conservation approach that values the contribution of the communities in both the design and decision-making processes.

In future research, the prototype web application will be further developed to include additional features. In particular, a more intuitive 3D modelling method is being explored that allows citizens to make changes to design proposals submitted by others. This will allow a more fluid conversation to emerge between citizens, all modifying each other's designs, with gradual convergence on a number or preferred options. Further research can also be conducted on the communication between the citizens and the architects to ensure that the citizens' choice of design in the conceptual stage can be accurately represented during the final detailed design stage.

References

- Arnstein, Sherry (1969). A Ladder of Citizen Participation. *Journal of the American Planning Association*, 35(4), 216–224. <https://doi.org/10.1080/01944366908977225>
- Davidoff, Paul. (1965). Advocacy and Pluralism in Planning. *Journal of the American Planning Association*, 31(4), 331–338. <https://doi.org/10.1080/01944366508978187>
- Falco, Enzo. (2019). *Digital Community Planning: The Open Source Way to the Top of Arnstein's Ladder*. <https://doi.org/10.4018/978-1-5225-7030-1.ch067>
- Rinner, Claus & Carsten Keßler and Stephen Andrusis. (2008). The Use of Web 2.0 Concepts to Support Deliberation in Spatial Decision-Making. *Computers, Environment and Urban Systems*. 32. 386-395. <https://doi.org/10.1016/j.compenvurbsys.2008.08.004>
- Sanoff, Henry. (2000) *Community Participation Methods in Design and Planning*, New York: John Wiley & Sons, Inc.
- Tomarchio, Ludovica, Stéphanie Hasler, Pieter Herthogs, Johannes Müller, Bige Tuncer and Peijun He. (2019). Using an online participation tool to collect relevant data for urban design: the construction of two participation exercises. *Intelligent & Informed, Proceedings of the 24th International Conference of the Association for Computer-Aided Architectural Design Research in Asia (CAADRIA) 2019*, Hong Kong, Volume 2, pp. 747-756.
- Wilson, Alexander, Mark Tewdwr-Jones, and Rob Comber. (2019). Urban Planning, Public Participation and Digital Technology: App Development as a Method of Generating Citizen Involvement in Local Planning Processes. *Environment and Planning B: Urban Analytics and City Science* 46(2), 286–302. <https://doi.org/10.1177/2399808317712515>
- Yenardi, Anna Claudia and Patrick Janssen. (2021). Mass Participatory Design on the Web: A Voxel-Based 3D Modelling Approach. *PROJECTIONS, Proceedings of the 26th International Conference of the Association for Computer-Aided Architectural Design Research in Asia (CAADRIA) 2021*, Hong Kong, Volume 2, pp. 31-40.

Building Information Modelling

DFD-BASED DESIGN, ASSEMBLY, HIGH-ACCURACY REAL-TIME MONITORING AND LEVELLING CALIBRATION FOR LARGE-SCALE PREFABRICATE STRUCTURE WITH MULTIPLE MEASURING SYSTEMS

XIANG WANG¹, ZIQI ZHOU², XUEYUAN LV³, PHILIP F. YUAN⁴ and LEI CHEN⁵

^{1,4}*College of Architecture and Urban Planning, Tongji University.*

^{2,3,5}*China Construction First Group Corporation Limited.*

¹*178975753@qq.com*

⁵*18310021@tongji.edu.cn*

Abstract. This article introduces a novel monitoring method for the construction of high-precision prefabricated structures based on multiple sensors and measurement technologies. The proposed method introduces the optical motion capture system and combines it with traditional construction measurement technology to achieve real-time dynamic monitoring of more than hundreds of points within a large construction area more than 18*10m. Tolerance fitting algorithms and the correction methods are developed and testified to provide a global tolerance with $\pm 1\text{mm}$. Meanwhile a real-time visualization interface is developed to provide the feedback and analysis of the tolerance for each structure components. As demonstrator, such monitoring system is applied in the real construction of a DfD (Design for Disassembly)-based prefabricated steel structure in the “Water Cube” (Chinese National Aquatics Centre) in Beijing. With the demand to control the flatness tolerance within 6mm (within a 25*50m area), a large area monitoring system was applied in the project and finally reduced the construction time within 20 days.

Keywords. Design for Disassembly; Real-time Monitoring; Precise Levelling Calibration; Motion-capture System; Error Fitting Algorithm; SDG 9.

1. Introduction

At present, prefabricated buildings characterized by industrialized construction are being vigorously promoted in China and around the world, and the rapid emergence of new technologies also provides new methods for efficient and recyclable constructions. For example, in the field of industrialization, worldwide researchers have already carried out a lot of practice in many , and DfD is one of such theories. The purpose of DfD (design for disassembly) is to give full play to the performance of the material and to enhance the potential sustainability of a building. In this sense, the disassembly of

the whole life cycle is considered in the design stage, so that the components are easy to disassemble and can be recycled to the maximum extent, effectively improving its green performance (Guy and Ciarimboli, 2008).

In fact, since the birth of modernist architecture, prefabricated buildings, especially variable houses with good adaptability, have attracted a large number of architects to try, and there are also leaders of all ages. Today, as human environmental problems become increasingly prominent, low-carbon measures such as extending the life of buildings and reducing material waste are becoming more and more necessary. How to replace demolition with disassembly in a way of sustainability is a problem worth studying (Figure 1). It is also noticed in the UN's sustainable development goals that decent work/ economic growth as well as the industrial innovation for infrastructure would be some important goals for the future of human beings. Therefore, DfD is a promising concept for such development in the building industry.

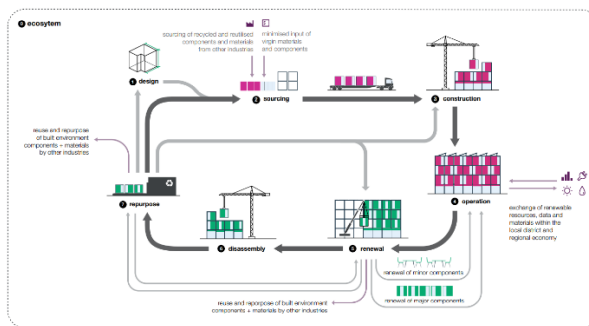


Figure 1. Application of Circular Economy Principles in Construction Industry (Arup, 2021)

Design for disassembly requires both the design process to split building into components system and the construction techniques to assemble the structure. Splitting is the reverse operation of the connection. Tracing the root, the adaptability structure still depends on the component connection method, which belongs to the controllable design content of the architect, and is also the focus of DfD. In the modern prefabricated building structure system, compared to the integrated joints produced by wet work, the DFD system responds to fast installation and damage-free detachment, and clearly puts forward the demand for dry joints. And the object includes structural components and is not limited to enclosure components. The DfD system responds to fast installation and damage-free detachment, and clearly puts forward the demand for dry joints, and the object includes structural members and not only enclosure members.

At the same time, due to the highly discretized characteristics of prefabricated building components, the integrity and assembly tolerance have also become an important issue for repetitively disassembled prefabricated buildings. Therefore, many issues, such as the structural design of the assembly system, the application of the building information model of the component system, the installation process planning, and the on-site installation monitoring, have also become important issues in the research of prefabricated structure construction technology based on DfD theory.

This paper discusses mostly the application of the building information models as

well as the IOT (Internet of Things) system to trace the components' information during the assembly and disassembly process of a prefabricated steel structure. At the meantime, a novel highly-precise levelling monitoring system with multiple sensors is also presented as a main characterized technique innovation.

The main case of this article is a DfD-based quick assembly and disassembly steel structure system, which is mainly used for the construction of the competition platform of the Beijing 2022 Winter Olympics curling venues. For the first time in the history of the Olympic Games, the curling venue of the Beijing Winter Olympics has applied a DfD construction system that can be repeatedly disassembled and assembled (figure 2). The main swimming pool of the original 2008 Summer Olympics Swimming Centre- "the Water Cube"- is used for reconstruction, trying to achieve a repeatable "winter and summer" scene change for the different uses. Since the construction time of the structural conversion has greatly affected the daily operations of the venues, the efficiency of the structural conversion has become the core issue of this project. At the same time, because curling has extremely high requirements for the flatness of the venue platform (the vertical height difference of any two points of the venue platform within the entire 50*25m range must be guaranteed within 6mm), the overall stability of the prefabricated structure and the accuracy of the installation also determines the success of the entire project.



Figure 2. Application of a DfD-based fast-built steel structure system in the ice-to-water conversion system for the Olympic curling Hall in the Chinese National Aquatics Centre("Water-Cube")

2. Methodology

Since there is no related project case similar to this project at present, which has realized the full life cycle digital and systematic management of the production-installation-disassembly process as well as the high-precision on-site construction monitoring, therefore, in this study, a process system diagram from design to disassembly to on-site construction monitoring was first built (Figure 3), the key procedure development and key techniques were extracted, and then the technical feasibility analysis and technology research and development were carried out.

The structural design and the component design consider both the possibilities to maintain the integrity of the structure and to make the component small enough for transportation. Based on that, a definition system and its related building information model is built in REVIT. For each component, a customized family is created with several special defined fields to trace its condition, such as the transportation stages, assembly stages as well as the levelling information. To provide a real-time information

for all these fields, several main techniques, such as the IoT-based information gathering and feedback system, the real-time multiple points height monitoring system, and the intelligent auto-leveling system is developed.

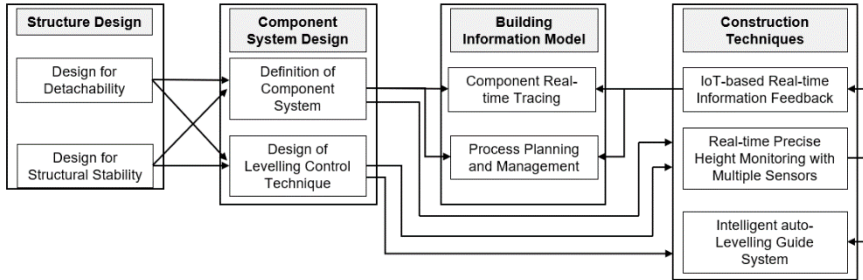


Figure 3. System Framework of the Methodology and Main Processes

As the many aspects of construction information make the system very complex, a simple and hierarchical software system is selected for this project. For the general visualization and data processing of the building information modelling, Autodesk REVIT is selected as the main software platform. With the use of the “Rhino-inside-REVIT” technique, a computational design approach could be achieved by using Grasshopper Platform inside REVIT, and interacting with the same data system. For the sensors and tracing system, extra special plugins are developed inside Grasshopper, including the RFID-based transportation tracing system, the QR-Code-based assembly information tracing system, the signal synchronization of the total station, electronic levelling instruments, as well as the motion-capture system (Figure 4).

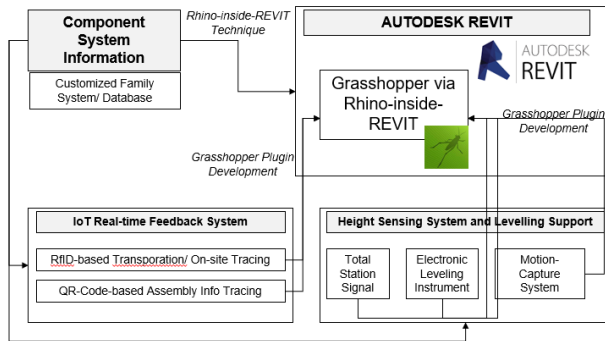


Figure 4. Tool chain and workflow in this research

The construction site has an area of 60*25m, which is far beyond the sensing range of some sensors (such as the resolution range of the infrared cameras of the motion capture system). At the same time, due to the existence of the original swimming pool, the site has a height difference of 3m. Therefore, in the configuration of the hardware system, the relevant sensors are set up by the principle of unilateral arrangement (Figure 5). The RFID chips and QR codes with component information are arranged

on the building components, and the components are stacked in the yard on the opposite side of the site. The construction phase of all components is tracked in real time by means of divisional construction on site.



Figure 5. Construction site and the arrangement of the sensors

3. 3. Design of the prefabricated system

The final construction structure is 56.7m long and 26.7m wide. The supporting frame body is made of prefabricated steel columns and beams, covered with light-weight precast concrete slab to meet the ice-making conditions. The structural beams and column members are all high-frequency welded thin-walled H-section steel. The steel used for the members is Q235B grade steel, and the connection is bolted. The connections used are M16 high-strength structural bolts. The surface layer adopts lightweight concrete prefabricated slabs, the main specification is 1m*1m*1m, the strength grade is L40. Finally, a total of 1,568 prefabricated slabs and a steel structure of 140t are used.

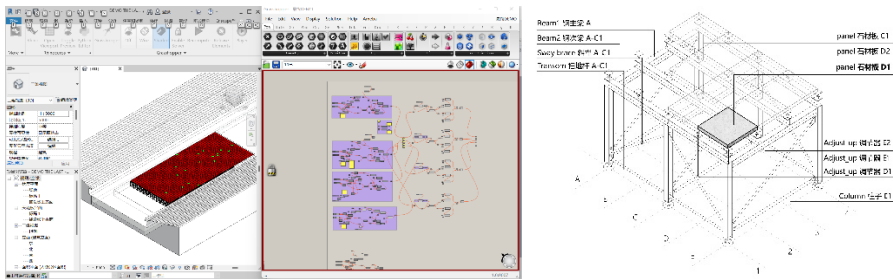


Figure 6. Construction site and the arrangement of the sensors

After the structural design meets the stiffness and stability requirements, its detailed design is completed in REVIT by means of customize family components. All components are defined parametrically through the use of computational design methods in the Grasshopper platform, so the establishment of the component system database and custom modifications can be quickly realized. In terms of the hierarchy of the structural components, in addition to the steel columns, steel main beams, steel secondary beams, and concrete slabs which are necessary for the original structure, steel diagonal braces and steel sweeping poles used for tie-down stabilization structures have been added according to the structural requirements. At the same time, according

to the levelling requirements, a knob-type adjusting device at the bottom of each column and a fine-tuneable knob-type adjusting device for the corner position of each concrete slab are added (Figure 6).

In order to realize real-time positioning and tracking and information visualization of the component system, all components in the database are named using unique coding rules. At the same time, in order to realize the collection and processing of information based on IoT theory, a plug-in suitable for reading RFID beacon information has been developed in the relevant Grasshopper platform. Meanwhile, a WECHAT-based Application which is suitable for QR code scanning and information filling has been created. Data crawling and real-time analysis of QR code database information is realized in Grasshopper (Figure 7). Therefore, the repetitively disassembled steel structure system realizes the real-time perception and analysis of the construction information of the whole process at each component level, and is integrated accordingly through the BIM software platform.

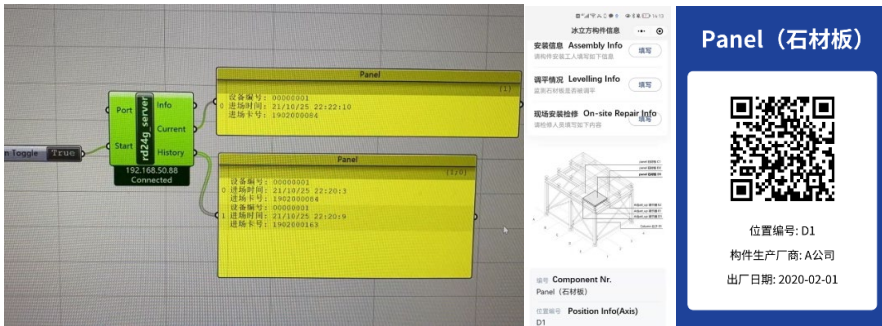


Figure 7. IoT-based Data Collection technique via RFID and QR code techniques

4. Levelling Calibration with multiple sensor systems

The construction of a large-scale DfD system usually have to solve the problem of tolerance that would be caused by the frequent and repeatedly use of the prefabricated components. Therefore, it is also the vital technique problems to ensure the assembly accuracy of the prefabricated structure systems. In the case of this paper, due to the use of the final structure (its top surface would be used as competition curling venues of the Beijing 2022 Winter Olympics), it is of great importance that the flatness of the platform should achieve a very high standard. For the construction, the measuring methods of the top surface of the structure becomes the most challenging task of the whole project.

In traditional construction monitoring, the measurement of surface flatness often relies on traditional measuring instruments, such as the levels, total stations and other equipment. However, due to their operational characteristics, it is often difficult to guarantee the measurement accuracy, measurement speed, and number of measurement target points at the same time. Meanwhile, such traditional construction measurement methods are highly dependent on the operation of the construction personnel on site, so it is difficult to realize real-time construction adjustment of multiple construction sites based on measurement feedback.

It is innovated in this project that a variety of elevation monitoring equipment based on multi-source data was used in collaboration, and for the first time in the construction industry, motion capture system was used as the main height information collection system for the requirements of multi-point (simultaneous monitoring of more than 100 points), real-time (monitoring frequency greater than 100hz), high-precision (repetitive positioning accuracy below 1mm). Due to the problem of unilateral placement of relevant sensors on site, the absolute positioning accuracy of the motion capture system shows a nonlinear error in the depth direction. At the same time, due to the imaging principle of the infrared vision camera, the overall positioning accuracy presents irregular distortions (Eichelberger et al., 2016).

In order to solve this problem, a set of coordinate system compensation and correction algorithm based on ICP (Iterative Closest Points) algorithm was developed in this research, and was finally developed as plugins inside the Grasshopper platform. The basic principle is: after the main beam of the structure is installed, use the midpoint of the structural column top to arrange the positioning beacons applicable to the motion capture (mocap) system, collect the relevant column top coordinate information in the mocap software, and establish a coordinate grid composed of the column points. At the same time, the electronic level and the total station were used as reference data, and the total station was used to collect the horizontal XY coordinates, and the electronic level was used to collect the vertical Z coordinates to generate a second set of real coordinate grids for correcting errors. Finally, the corresponding regions of the two sets of grids were fitted, the error correction translation matrix and the rotation matrix of the different regions were calculated, and they were applied to the error correction prediction process of the points to be measured in the different regions, so as to make the possible global distortion error which would be caused by the motion capture system finally corrected.

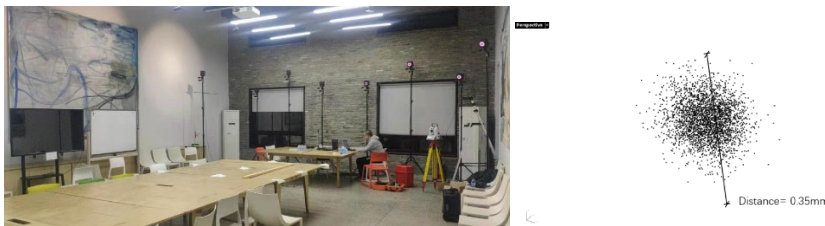


Figure 8. Off-site experiments to test the feasibility of the ICP algorithm

To test this algorithm, a full-scale off-site test was done in a 18m*7m room with the similar configuration (Figure 8). Experiments showed that the repeat positioning accuracy of the motion capture system was high, reaching below 0.4mm (Figure 8), while the global distortion effect was more obvious. The plane error at the farthest point and the total station was more than 3cm, and the level error was more than 1cm. The ICP algorithm test experiment selected a 3m*3m square grid (unified with the steel structure column span) for testing. Two sets of coordinate systems were collected using the grid vertices, and the ICP algorithm was used to estimate the coordinate transformation matrices of different grid areas. 20 arbitrary test points was collected to correct and predict the related errors, and finally are compared with the target results

measured by the electronic level and the total station. Finally, it was shown that among the 20 tested points, the difference between the coordinate results after error correction and the real elevation is small (within -1.67mm - 1mm), which could meet the global and local elevation error control of the concrete slab layer (Figure 9).

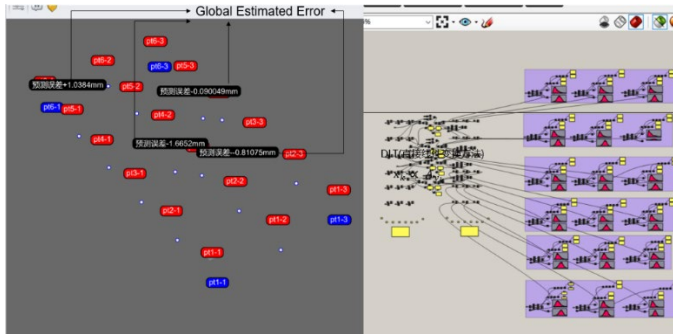


Figure 9. Control grids and the outcome of the levelling calibration tests

5. Feedback System and its on-site Application

Based on related sensor placement principles and error correction algorithms, similar error test experiments were also firstly completed at the construction site. Due to the limitation of the number of lenses of the motion capture system, the overall area of the site construction was divided into four sub-areas. Through the positioning of the total station and the elevation measurement of the electronic level, the four peripheral reference points were first located as the main reference for the determination of the overall elevation. During the construction process, the related algorithm of elevation adjustment was applied twice to the levelling process. Firstly, after the installation of the steel column at the bottom of the structure, the main beam and the secondary beam, the coordinates of the relevant reference points are collected. For this reason, this research has developed a set of height adjustment guide system for this project in the grasshopper platform. By inputting the motion capture measurement elevation of the column apex of the target area to be monitored and the actual elevation measured by the levelling instrument, the relevant error correction and the expected true elevation can be automatically calculated. Then, a large number of beacons of the motion capture system were used to calculate the expected true elevation of their location, and were compared with the theoretical elevation of the point in the BIM system, to give an error alarm when the error was greater than $\pm 3\text{mm}$. Secondly, after the column and beam system were levelled in the first stage, the concrete slabs would be secondly carefully tuned to meet the final global and local height requirements. At the same time, the system has also developed different display modes for the corner area and central area of the concrete slab. Due to the high degree of discretization of the concrete roof, the four corners where the grid intersects needed to be levelled separately. Therefore, if the system monitored that the measurement points were located at the corners of the slab, the coordinates and prediction errors will be displayed in dots; If it was detected that the measurement point was located in the centre of the slab, its elevation would be displayed as the overall elevation of the entire slab (Figure 10).



Figure 10. On-site application of the tuneable structures with the mocap beacon and the levelling support system

At the construction site of this project, the BIM control system and related levelling support system were connected to the central control screen, and the construction personnel were assisted to fine-tune the relevant structure through real-time playback. This construction method greatly saved the time required for on-site installation, especially the levelling process, and provided a large amount of data support for the construction planning. Compared with the previous structural conversion construction using traditional level measurement, it is in the first construction that only a final concrete slab elevation measurement was once applied, and that the measurement point only included the centre point of each concrete slab. The overall construction time was more than 40 days. In the second construction test that combined all new technologies, the structure realized two elevation adjustments in different stages, and realized real-time elevation adjustment and feedback of multiple points in the construction area. For the elevation control of the final concrete slab, the second construction experiment realized the coordinate feedback and adjustment of the four corner points and both the centre point of each concrete slab. At the same time, because of the existence of digital technology and real-time feedback technology, the entire construction process has been improved and optimized, and the entire process of installation and levelling of the entire steel structure has been completed within 20 days.

In the second construction, a part of the construction area that did not use levelling monitoring was reserved as a comparison verification area in all areas. It was tested via scanning with the laser tracing instrument to test all the slab centre coordinates. The results showed that the area with levelling monitoring basically meet the requirements of the project for global and local elevation errors, and the overall accuracy was controlled between -1.5mm - 1.5mm (Figure 11). Compared with the levelling monitoring area, the unmonitored area had a larger elevation error, and it was related to the experience of the construction personnel. A large number of measurement points in the area were lower than the global elevation, and the error was in the range of -2 to -10 mm. (Normally, the construction personnel would firstly control the concrete slab at a lower height, and then fine-tune its height upwards by adjusting bolts).

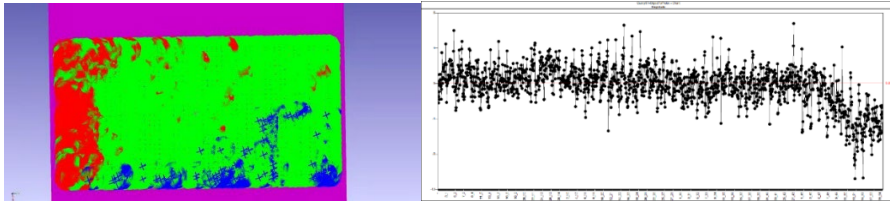


Figure 11. Final levelling check with laser tracing instrument of centre point of each concrete slab

6. Conclusion

This research demonstrates a systematic and integrated design-build-monitoring workflow for rapid disassembly and assembly of steel structures based on DfD theory, integrating related BIM technology and construction monitoring technology, and developed on the REVIT and Grasshopper platforms related software systems. The research successfully helped the China National Aquatics Centre in the rapid and repeatable scene transition from the 2008 summer swimming venue to the 2022 winter curling venue, effectively reducing the required structural construction time and ensuring the structure itself the high standard of elevation control requirements. In the current era of pursuing digitalization and sustainability of the construction industry, it is expected that the relevant design and construction methods proposed in this study can contribute to the intelligent reform of the construction technology in the future. At the same time, the related research on related sensor applications and algorithms in this study is still experimental in nature, and the related equipment is relatively expensive and the installation cost is relatively high. In future research, it is also expected that more advanced and cost-effective sensors can be added, and more environments in the construction process can be assisted and optimized.

Acknowledgements

This paper is supported by the National Key R&D Program of China (2020YFF0304303).

References

- Arup. (2021, December 20). *The Circular Economy in The Built Environment*. Retrieved December 20, from <https://www.arup.com/perspectives/publications/research/section/circular-economy-in-the-built-environment>.
- Eichelberger, Patric, et al. Analysis of accuracy in optical motion capture—A protocol for laboratory setup evaluation. *Journal of biomechanics*. 49.(10), 2085-2088.
- Guy B, Ciarimboli N.(2008). *DfD: Design for Disassembly in the Built Environment: A Guide to Closed-Loop Design and Building*. Hamer Centre.

UNITYREV - BRIDGING THE GAP BETWEEN BIM AUTHORIZING PLATFORMS AND GAME ENGINES BY CREATING A REAL-TIME BI-DIRECTIONAL EXCHANGE OF BIM DATA

KIERAN W. MAY¹, JAMES WALSH², ROSS T. SMITH³, NING GU⁴ and BRUCE H. THOMAS⁵

^{1,2,3,4,5}*University of South Australia, Australian Research Centre for Interactive and Virtual Environment*

¹ *kieran.may@mymail.unisa.edu.au*, 0000-0002-5461-4927

^{2,3,4,5} *{james.walsh|ross.smith|ning.gu|bruce.thomas}@unisa.edu.au*,

²0000-0002-4822-990X, ³0000-0002-9044-9199, ⁴0000-0002-5555-9165, ⁵0000-0002-9148-085X

Abstract. We present UnityRev: An open-source software package that enables a workflow designed to facilitate a real-time bi-directional and synchronous exchange of Building Information Modelling (BIM) data, by creating a direct link between a BIM authoring platform (i.e. Autodesk Revit) and a game engine (i.e. Unity 3D). Although previous works have explored the integration of BIM with game engines, the currently available tools are limited to a non-synchronous or uni-directional exchange of BIM data, and they do not address specific design issues required to make a BIM authoring platform and game engine compatible (i.e. parametric modelling). This paper describes our software which consists of a compact overview of the system, including design decisions, implementation details, and system capabilities. Two example applications are presented as concept demonstrators to showcase practical collaborative use-case scenarios between BIM authoring platforms and game engines which were not previously achievable without a real-time bi-directional workflow. This work will expand future Computer Aided Architectural Design (CAAD) research, and more specifically, Virtual Reality (VR)/Augmented Reality (AR) based BIM development and integration, by providing new possibilities and bridging the gap between BIM authoring platforms and game engines. The application of the system as demonstrated in the paper for real-time lighting performance simulation contributes to achieving the UN Sustainable Development Goal 11: Sustainable Cities and Communities.

Keywords. Building Information Modelling; Game Engines; Revit; Unity; Virtual Reality; Augmented Reality; Lighting Performance Simulation; SDG 11.

1. Introduction

This paper presents UnityRev, an open-source and freely available software package that enables a workflow designed to facilitate a real-time bi-directional and synchronous exchange of Building Information Modelling (BIM) data between a BIM authoring platform (i.e. Autodesk Revit) and a game engine (i.e. Unity 3D). Game engines play a pivotal role in recent research, as they act as a stepping-stone for researchers to virtually prototype and build software applications by providing them with a set of software development tools. Previous works comparing game engines and BIM authoring platforms have highlighted three primary motivations for using game engines for architectural representation. Specifically, the interaction, visualisation, and real-time capabilities associated with game engines provide a layer of functionality that BIM authoring platforms are unable to provide (Pelosi, 2010, Boeykens, 2011). Over the last decade, the usage of game engines within Computer Aided Architectural Design (CAAD) research has risen significantly with a large focus on incorporating BIM models with advanced visualisation tools such as Virtual Reality (VR) and Augmented Reality (AR) displays. However, despite the importance of game engines in current VR/AR BIM research, the ability to communicate BIM data between BIM authoring platforms has remained a consistent issue for researchers working within this particular field.

To bridge the gap between BIM authoring platforms and game engines, various tools have been released to support the integration of BIM within game engines; however, these tools lack the capability to support a natural real-time, and synchronous exchange without loss of BIM data. Due to the uni-directional flow of data from these tools, manipulations that occur to the BIM model within game engines are not synchronised back to the BIM authoring platform that contains the original BIM model. Due to the limited tools available, and lack of BIM support provided by game engines, many researchers utilising game engines to prototype BIM-based applications export BIM models from BIM authoring platforms into a file format that is natively supported by the game engine. This process generally involves exporting a BIM model from Revit as a Filmbox (FBX), Object (OBJ) file or other similar data formats supported by game engines that only provide geometric or partial metadata (Bille et al., 2014). As a result, a large portion of the metadata (e.g. cost, schedule, manufacturer, etc.) associated with the geometric model is lost, subsequently transforming the information-rich BIM model into a generic three-dimensional Computer-Aided Design (CAD) model. We believe this limitation to be one of the major gaps in the adoption of immersive BIM-based research within the Architectural, Engineering, and Construction (AEC) industrial sectors. Recent works from the authors have a validated this claim where a workshop was held by the researchers with four AEC industry representatives. The AEC industry representatives stated that the loss of BIM data caused by cross-platform BIM communication was one of the major barriers associated with BIMs, and the integration of VR, and AR applications with BIM models (May et al., 2022).

To address the aforementioned issues, an open-source workflow capable of facilitating a real-time bi-directional and synchronous exchange of BIM data between BIM authoring platforms and game engines could be particularly useful to addressing one of the major research gaps associated with the process of integrating BIM with

immersive VR/AR displays and game engines.

The specific contributions of this paper are:

1. An open-source software package that enables a workflow for linking Unity and Revit through a bi-directional synchronous exchange of BIM data.
2. An approach for enabling parametric CAAD modelling within a physics-driven game engine.
3. Two example applications highlighting the potential advantages of the proposed workflow and demonstrating two scenarios that were not previously possible without the use of a synchronous bi-directional BIM workflow.

In the remainder of this paper, we explore previous works in the field, and identify the common gaps and limitations of currently available tools and literature. We then present the system capabilities of the 'UnityRev' software package that enables the workflow to achieve a bi-directional synchronisation of BIM data. Two example applications are presented as concept demonstrators to showcase practical collaborative use-case scenarios linking BIM authoring platforms and game engines using UnityRev. The application of the system as demonstrated in the following sections for a VR-based Lighting Performance Simulator addresses the UN Sustainable Development Goal 11: Sustainable Cities and Communities. We released UnityRev as an open-source GitHub repository under the MIT license (<https://github.com/kieran196/UnityRev-ProjectExchange>).

2. Related Works

To identify common tools and previous research exploring the process of linking BIM authoring platforms and game engines, we conducted a literature review focusing specifically on asynchronous and synchronous workflows designed for CAD/BIM authoring platforms to game engine integration.

2.1. ASYNCHRONOUS WORKFLOWS

The most widely adopted approach for the transferal of BIM data across BIM authoring platforms is using the Industry Foundation Class (IFC). IFC is a standardised BIM file-format supported by several BIM-driven CAD platforms. The IFC data format supports the transferal of BIM data by storing the metadata, and geometric properties associated with a BIM into a single file format. Although IFC can maintain partial metadata properties associated with a BIM model, modern game engines such as Unreal and Unity do not provide native support for IFC. As a result, third-party libraries have been released to support parsing IFC files into game engines. Additionally, researchers have developed their own systems capable of parsing IFC files into game engines to provide partial uni-directional integration of BIM data. Previous researchers who utilised a Revit to Unity workflow reported limitations associated with using an IFC-based workflow due to IFC standard only providing partial metadata (Motamedi et al., 2017). Due to the complex structure of the IFC data model, difficulties emerge when attempting to write BIM changes directly back to the original IFC file, making it significantly challenging to achieve a two-way transferal of BIM data when strictly using IFC. However, (Nandavar et al., 2018) were successful in achieving this by proposing an XML-based approach to store manipulations that occurred to the BIM

model within VR (i.e. Unity). The XML file could then be parsed back to the original IFC file using an open-source IFC management software: xBIM toolkit (Lockley et al., 2017). Similar investigations have also been conducted by (Khalili, 2021); however, using the FBX data model which is natively supported by game engines as opposed to IFC. Our review shows that, the primary advantage of an IFC-based approach is the interoperability and adaptability of the workflow, as it can be integrated with any BIM authoring platform which provides support for IFC. This is a considerable step towards achieving an intuitive integration of BIM data across all BIM authoring platforms and game engines.

2.2. SYNCHRONOUS WORKFLOWS

Fewer works have demonstrated the ability to achieve a real-time exchange of BIM data between BIM authoring platforms and game engines. (Du et al., 2018) created a system called 'BIM-VR Real-time Synchronization' (BVRs), which can perform a real-time synchronous uni-directional exchange of BIM data by autonomously synchronising changes made to the BIM model in Revit back to Unity in real-time. This was achieved by creating a Revit plugin that constantly sends manipulations made to the BIM model within Revit to a cloud-based server that stores and transfers data based on IFC.

In 2018, (Nandavar et al., 2018) identified Fuzor and BIMXplorer as the only two publicly available software packages capable of achieving a complete exchange of BIM data between BIM and VR. Earlier works by (Chotrov and Maleshkov, 2013) also presented an approach using a TCP/IP network communication that achieved a bi-directional synchronisation of CAD geometry between a CAD platform (Solid-works) and VR application. However, all three described systems utilised a customised VR rendering pipeline to achieve this communication as opposed to game engines.

The Unity development team recently released Unity Reflect (Reflect, 2021), which we believe to date is the most advanced publicly available software package capable of achieving a linkage between a BIM authoring platform (Revit) and game engine (Unity). Unity Reflect provides a uni-directional exchange of BIM data by instantaneously sending data from Revit to Unity across a server. The primary limitation we have identified with Unity Reflect is that the transferal of data flows in one direction, and as a result, manipulations that occur to the BIM model within Unity are not sent back to the original BIM model. Furthermore, modifications made to the BIM model in Revit are not updated within Unity in real-time, and users are required to reload the model to synchronise changes from Revit. Both limitations are specifically addressed in UnityRev.

(Edwards et al., 2015) demonstrated the ability to incorporate a network to bi-directionally exchange BIM data between a BIM authoring (Revit) and game engine (Unity). A custom OBJ data-model was used to facilitate the initial geometry associated with the BIM model into Unity. The authors, however, reported they encountered various issues such as manipulations made to the position of elements within VR not updating correctly within Revit.

Recently, (Harlan et al., 2020) presented a three-module system to integrate a CAD platform (Simens NX) and game engine (Unreal). The system presented a unique

approach capable of loading and reloading meshes at run-time by accessing CAD functionality through the NXOpen C++ API. The authors are actively using their proposed software to research hand-tracking based natural user-interfaces for design sketch creation in VR.

2.3. SUMMARY OF PREVIOUS WORKS

In summary, UnityRev addresses the following issues and limitations associated with the prior works discussed above and the currently available tools that produce a link between a BIM authoring platform and game engine:

Of the available CAD to game engine workflows: No tools provide a bi-directional exchange of BIM data and only supports a CAD to game engine directional flow of data. No tools support a real-time synchronous transfer of BIM data. Only one tool (Unity Reflect) can achieve a complete integration of BIM metadata into a game engine with constraints as discussed above.

Of the available CAD/BIM authoring platform to game engine workflows from our review: No prior works produced a workflow capable of supporting a game engine to adhere to the parametric CAAD modelling platforms. No prior works produced a workflow capable of supporting a real-time two-way transfer of BIM data with geometric orientation and geometric mesh manipulation.

3. UnityRev: System Overview

To enable the real-time integration between BIM and game engines, we developed a customised network based on a Transmission Control Protocol and Internet Protocol (TCP/IP) network architecture to facilitate the exchange of BIM data between Revit, a BIM authoring platform and Unity, a game engine. A local server is set up, which is hosted from the Unity software, with Revit connecting to the server as a client. To achieve this connection from the BIM authoring platform, a plugin was developed based on the Revit API, which is run as an add-in directly from Revit. The process of transmitting data between the server and client consists of retrieving the element IDs, position, rotation, scale, metadata, and mesh data via the Revit API and converting it into a bytes array, which is then sent through a socket. This data is then decoded and parsed by the receiver to synchronise modifications within the corresponding software. A custom network protocol was developed to exchange commands between the server and client to represent the transmission of specific data. Similarly, BIM elements are identified when being transferred across platforms based on their unique IDs, which are automatically generated within Revit. An error-checking system was integrated into the system, ensuring that only valid actions adhering to Revit's parametric modelling can be supported within the Unity engine. The software was written entirely in the C# programming language.

3.1. ADHERING TO PARAMETRIC CAAD MODELLING

Typical BIM authoring platforms such as Autodesk Revit provide parametric modelling to assist users in correctly designing architectural structures. However, physics-based game engines such as Unity and Unreal were not designed to support BIM or CAAD and therefore do not follow parametric modelling rules and

conventions. For example, if a user manipulated the position of a door, causing it to become unattached or floating in a scene within a game engine, this would be perfectly valid manipulation. However, within a parametric based BIM authoring platform, the same manipulation would violate the built-in parametric constraints, and result in an exception to occur. As a result, ensuring that Unity adheres to the specific parametric rules of Revit is a fundamental step in ensuring the compatibility of the BIM authoring platform and game engine when linking the two. However, due to the complex nature of parametric modelling, it was not realistic to re-write the parametric constraints within Unity from scratch. Therefore, our solution to solve this problem is to leverage the parametric functionality in Revit by querying the Revit API whenever a manipulation occurs to an element's geometry within a game engine. For example, if the position of an element is modified in Unity, the new coordinate values are sent to the Revit client, where an error-check is performed to determine whether the new coordinates of an element are valid based on the parametric constraints of Revit. If the new position is invalid, an exception is thrown, and the Revit client sends a query back to the Unity server, and the element within the Unity scene is automatically reverted to its previous position.

3.2. REAL-TIME RETRIEVAL AND MANIPULATION OF BIM DATA

The ability to seamlessly transfer BIM metadata between a BIM authoring platform and game engine in real-time with no loss of data is one of the significant features provided by UnityRev. Upon running the Revit plugin, the Revit client will connect to the server and instantaneously send all parametric metadata associated with each element to the Unity server. The metadata is then retrieved in Unity and stored in a 'RevAttributes' class, which is attached as a component to each BIM element within the Unity scene. Within this class, the parametric metadata associated with each element is stored in a dictionary data structure where the Key is the unique name of each parameter, and the value is the value of each parameter. Real-time manipulation of BIM metadata is handled by having the Revit and Unity software continuously checking whether the value of element parameters have been modified. Once a modification occurs to an element's parameter value, the new parameter value is sent back to the corresponding software and updated. Whilst the metadata is present within the Unity inspector, it is not directly utilised within the scene. However, users can easily extract and use the necessary metadata within their Unity applications. This is demonstrated in Section 4.2 where lighting metadata is extracted from a Revit lighting fixture and used directly within the scene by a Unity-based lighting performance simulator.

3.3. GEOMETRIC DATA MANIPULATION AND SCALING

Initially, we encountered several issues associated with sending the direct coordinates of elements from Unity to Revit. Therefore, we employed an approach that sends an offset Vector representing the coordinate change between the previous and current position of elements over a one-second interval. The purpose of this one-second delay is to ensure the server is not overloaded by requests due to the Unity engine running at multiple frames per second. This delay is not required in Revit due to the non-real-time

structure of Revit when modifying the position, rotation, or scale of an element.

Current game engines typically utilised a three-axis vector-based scaling system a scale of one is equal to the original scale of the geometric model. In contrast, Revit splits the scaling of elements into two separate three-axis vectors: `BoundingBoxMin`, and `BoundingBoxMax`. The scale is represented based on the constraints of an element using an imperial-based measurement system. To convert this into a scaling-based system supported by Unity, we rewrote a customised scaling system in Revit to adhere to the scaling requirements of Unity. Additionally, this approach allowed us to bypass the need to account for different measurement systems when sending scaling data between the two platforms.

4. Demonstration of UnityRev's Capabilities

The real-time and synchronous capabilities of UnityRev present new opportunities for collaboration between a BIM authoring platform and game engine, which were not previously possible. In this section, we present two example applications that use UnityRev as a workflow to demonstrate how it could be incorporated within practical use-case scenarios. The first example application uses UnityRev to create a collaborative design platform between a Revit (CAAD) user and a Unity (VR) user. The second example application connects the Revit software with a real-time lighting performance simulator developed in the Unity game engine.

4.1. COLLABORATIVE ARCHITECTURAL DESIGN BETWEEN BIM AUTHORIZING PLATFORMS AND GAME ENGINES

The first application demonstrates the ability to create a collaborative architectural design scenario between a Revit and Unity user. Using the Unity game engine, an immersive VR application was developed, allowing users to manipulate the geometry (e.g. position, rotation, and scale) of elements within a virtual environment (VE). The following two three-dimensional interaction techniques supporting six degrees of freedom (DOF) were implemented using the 3D User Interaction Toolkit (May et al., 2019): 3D Bubble Cursor (Vanacken et al., 2007) and Flashlight (Liang and Green, 1994).

The motivation behind the presented example application is to explore and encourage the development of alternative CAD tools in architectural design and collaboration. In this case, we demonstrate a scenario where a VR user using alternative 6DOF 3D interaction techniques can manipulate elements whilst simultaneously collaborating with a desktop-based user using a standard 2DOF mouse input. Although we believe a cursor is overall more intuitive, and suited for the complex user interface, and fine movements required in a CAD environment, limited research has been conducted exploring the potential benefits of using immersive 6DOF interaction in CAD. We believe one aspect linked to the limited research in this field could be due to the difficulties associated with integrating sophisticated parametric CAAD modelling within a game engine making it difficult to realistically compare a CAD platform with a game engine-based VR application. However, using UnityRev enables this link to be achieved by connecting the two platforms and providing a layer of support for parametric modelling within a game engine.

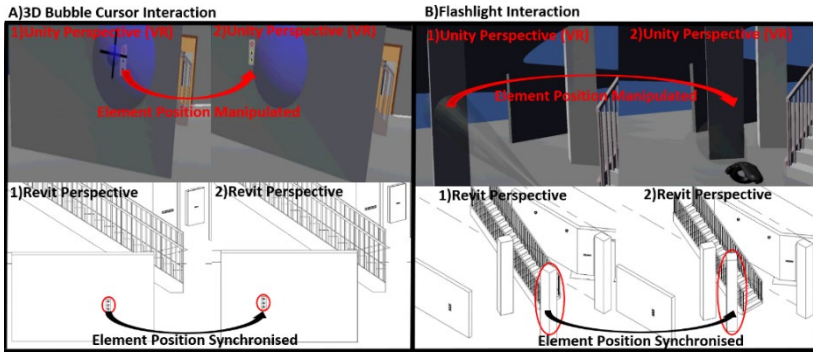


Figure 1. Two demonstrations of using immersive VR interaction techniques (left: 3D Bubble Cursor, right: Flashlight) to manipulate building elements' positions within the game engine and update their counterparts synchronously within Revit using UnityRev.

4.2. LINKING A REAL-TIME LIGHTING PERFORMANCE SIMULATOR WITH A BIM AUTHORIZING PLATFORM FOR COLLABORATIVE DESIGN

The second application integrates a VR-based Lighting Performance Simulator developed by the authors (May et al., 2020) using Unity to simulate the lighting performance of the environment through BIM. The lighting metadata (lumens, wattage, and range) is retrieved from the BIM model's lighting fixture elements to initialise the simulated artificial lighting within the game engine. The lux and unified glare rating (UGR) values outputted from the simulator are sent and linked back to the Revit model in real-time using UnityRev.

The presented example application not only provides an approach for integrating a game-engine based simulator directly with Revit, but also autonomously synchronising lighting performance data back to the Revit model, thus maintaining and updating the original BIM model. Additionally, typically architects would have to complete a draft of their architectural design prior to using a cross-platform simulator. However, using UnityRev provides the ability for users to run simulations much earlier and more

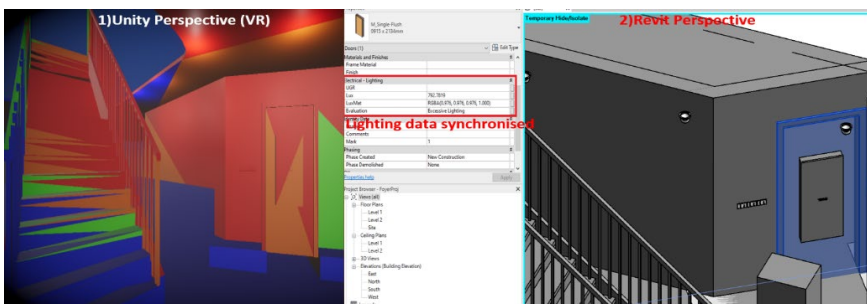


Figure 2. Two demonstrations of a VR-based Lighting Performance Simulator using a heatmap visualisation to simulate the lighting in the building (left), and the calculated lux, and lighting evaluation for each element sent directly back to the Revit model (right).

readily within the design phase. This could potentially allow an architect to identify design issues and discrepancies much earlier in the design and mitigate the need for major re(iterations) later, resulting in time and cost saving.

5. Limitations

The initial development of UnityRev could be potentially improved in various aspects. Firstly, the initial implementation of the network is not well optimised and is designed to focus primarily on the functionality goals we set out to achieve as opposed to performance. Additionally, limited user-testing has been carried out on the initial software, and comprehensive user-testing to identify issues could significantly improve the usability of the software. We also encountered limitations associated with using the Revit API; for example, creating new elements is only capable of flowing from a Revit to Unity direction. Lastly, the dependency of the Revit API to achieve this real-time two-way communication between a BIM authoring platform and game engine prevents us from providing future support for UnityRev on alternative BIM authoring platforms. These limitations are being addressed in the current enhancement of the research.

6. Conclusion

This paper presented UnityRev: An open-sourced software package that enables a network-based workflow designed to bridge the gap between a BIM authoring platform (Revit) and game engine (Unity) by creating a real-time bi-directional exchange of BIM data. In summary, we conducted a literature review in the field and an analysis of previous CAD/BIM authoring platforms to game engine workflows and their implementations. We then presented a system overview of UnityRev which describes the system capabilities and how UnityRev addresses specific gaps identified in the review and analysis. Next, we presented two example applications as concept demonstrators that aimed to showcase two practical collaborative use-case scenarios between a BIM authoring platform and game engine that were not previously achievable without the use of the synchronous bi-directional workflow being proposed. The general future directions of this work can be improving upon the software by addressing the limitations described in Section 5. We are also motivated by the recent announcements from Facebook and Microsoft that are working towards creating a metaverse - a network of 3D virtual worlds. We envisage the tools presented in this paper can provide a bridge between BIM allowing bi-directional communications to extend the future capabilities of the metaverse. This work was specifically designed to pilot for a larger project by the authors, which focuses on integrating immersive displays with building performance simulators for real-time visualisation and simulation of architectural design. Our broader motivation of this research is to advance BIM research by encouraging new possibilities and use-cases that can be achieved through VR/AR-based approaches adopting UnityRev. As described above, we demonstrated in Section 4.2 that a game-engine based VR building performance simulator could be efficiently integrated with BIM models to support the architectural design process. This highlights a scenario where UnityRev could be used in green building research, potentially leading to designing more energy-efficient and sustainable buildings and cities.

References

- Bille, R., Smith, S. P., Maund, K., & Brewer, G. (2014, December). Extending building information models into game engines. *Proceedings of the 2014 conference on interactive entertainment* (pp. 1-8).
- Boeykens, S. (2011). Using 3D Design software, BIM and game engines for architectural historical reconstruction. *Designing Together-CAADfutures* (pp. 493-509).
- Chotrov, D., & Maleshkov, S. (2013, July). Simultaneous bidirectional geometric model synchronization between CAD and VR applications. *In International Symposium on Visual Computing* (pp. 288-297).
- Du, J., Zou, Z., Shi, Y., & Zhao, D. (2018). Zero latency: Real-time synchronization of BIM data in virtual reality for collaborative decision-making. *Automation in Construction*, 85, ((pp. 51-64).
- Edwards, G., Li, H., & Wang, B. (2015). BIM based collaborative and interactive design process using computer game engine for general end-users. *Visualization in Engineering*, 3(1), 1-17.
- Harlan, J., Schleich, B., & Wartzack, S. (2020). Linking a game-engine with CAD-software to create a flexible platform for researching extended reality interfaces for the industrial design process. *Proceedings of the 31st Symposium Design for X (DFX2020)* (pp. 169-178).
- Khalili, A. (2021). An XML-based approach for geo-semantic data exchange from BIM to VR applications. *Automation in Construction*, 121, 103425.
- Liang, J., & Green, M. (1994). JDCAD: A highly interactive 3D modeling system. *Computers & graphics*, 18(4), 499-506.
- Lockley, S., Benghi, C., & Cerny, M. (2017). Xbim. Essentials: a library for interoperable building information applications. *The Journal of Open Source Software*, 2(20), 473.
- May, K. W., KC, C., Ochoa, J. J., Gu, N., Walsh, J., Smith, R. T., & Thomas, B. H. (2022). The Identification, Development, and Evaluation of BIM-ARDM: A BIM-Based AR Defect Management System for Construction Inspections. *Buildings*, 12(2), 140.
- May, K. W., Walsh, J., Smith, R. T., Gu, N., & Thomas, B. H. (2020). VRGlare: A Virtual Reality Lighting Performance Simulator for real-time Three-Dimensional Glare Simulation and Analysis. In ISARC. *Proceedings of the International Symposium on Automation and Robotics in Construction* (Vol. 37, pp. 32-39). IAARC Publications.
- May, K., Hanan, I., Cunningham, A., & Thomas, B. (2019, October). 3duitk: An opensource toolkit for thirty years of three-dimensional interaction research. *In 2019 IEEE International Symposium on Mixed and Augmented Reality Adjunct (ISMAR-Adjunct)* (pp. 175-180).
- Motamedi, A., Wang, Z., Yabuki, N., Fukuda, T., & Michikawa, T. (2017). Signage visibility analysis and optimization system using BIM-enabled virtual reality (VR) environments. *Advanced Engineering Informatics*, 32, 248-262.
- Nandavar, A., Petzold, F., Nassif, J., & Schubert, G. (2018). Interactive Virtual Reality Tool for BIM Based on IFC-Development of OpenBIM and Game Engine Based Layout Planning Tool-A Novel Concept to Integrate BIM and VR with Bi-Directional Data Exchange. *Proceedings of the 13th International Conference on Computer Aided Architectural Design Research in Asia (CAADRIA)*.
- Pelosi, A. W. (2010). Obstacles of utilising real-time 3D visualisation in architectural representations and documentation. *Proceedings of the 15th International Conference on Computer Aided Architectural Design Research in Asia / Hong Kong* (pp. 391-400).
- Vanacken, L., Grossman, T., & Coninx, K. (2007, March). Exploring the effects of environment density and target visibility on object selection in 3D virtual environments. *In 2007 IEEE symposium on 3D user interfaces*. IEEE.

BUILDING INFORMATION MODELLING BASED TRANSPARENT ENVELOPE OPTIMIZATION CONSIDERING ENVIRONMENTAL QUALITY, ENERGY AND COST

DIAN ZHUANG¹ and XING SHI²

¹*School of Architecture, Southeast University, China.*

²*College of Architecture and Urban Planning, Tongji University, China.*

¹*zhuangdian@seu.edu.cn, 0000-0003-0747-2775*

Abstract. The balance of energy consumption, indoor environmental satisfaction and cost is a continuing challenge in the field of building energy efficiency research. Building transparent envelope play a key role in building energy-saving design. While in existing BIM system, the separation of component family and local supply chain hinders the integrated performance evaluation and design. This paper proposes a general sustainable performance optimization model for transparent envelope design from the product perspective. A performance data integrated BIM technique framework, linking BIM with multi-dimension performance data stored in external database, is introduced as the foundation of local supply chain based optimization process. A multi-objective optimization model for window components is constructed for the early design stage. Three comprehensive design targets in the engineering practice, energy consumption, life cycle cost and IEQ are evaluated and optimized, representing the concern from government, developer and occupant, respectively. Autodesk Revit as the technique platform, its internal material library and adaptive component system are directly integrated for model control and feedback. An optimization tool is developed as an individual plug-in for user interaction and performance visualization. As a case study, the multi-objective optimization process is applied to design a school building in China.

Keywords. BIM; Multi-objective Optimization; Transparent Envelope; Sustainable Performance; SDG 3; SDG 7; SDG 11; SDG 12.

1. Introduction

Energy shortages and the climate problem caused by it have been the focus of global attention in recent years. In 2018, building construction and operations accounted for the largest share of global final energy use (36%) and energy-related carbon emissions (39%) (UN Environment and the International Energy Agency, 2019). In response to these problems in the Architecture, Engineering and Construction (AEC) industry, various concepts of sustainable building have been proposed. The optimization of

sustainable performance in the building design stage is also playing a key role in practice. Figure 1 is the modified MacLeamy Curve (Piroozfar et al., 2019) representing the influence of building design decisions on life-cycle environmental impacts. It shows the importance of performance optimization in the early stage. The impacts of performance optimization will gradually decrease with the development of the engineering stage, and the required cost will gradually increase. On the other hand, building transparent envelopes have a huge impact on the sustainable performance of the building, and its use is maintained high popularity in public buildings (Zhao and Du, 2020). Compared with the site construction of nontransparent envelopes, transparent envelopes such as windows are usually procured directly from local suppliers and installed in reserved window openings during the project. However, the performance optimization in the early design stage always deviates from the local supply chain, resulting in the gap between the actual performance and the expected performance. This paper proposes a performance integrated BIM (P-BIM) framework oriented by sustainable performance-driven design. A real-time updated external component product library with essential performance information is integrated in Building Information Modelling (BIM) for data management and further usages. A multi-objective optimization model considering three comprehensive performance indicators for transparent envelope design is constructed based on P-BIM.

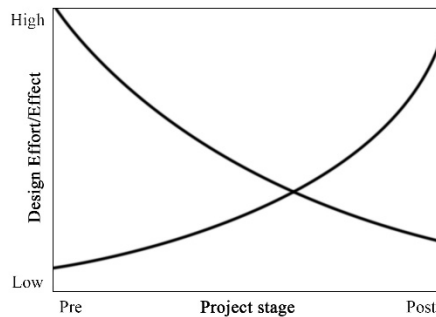


Figure 1. Modified MacLeamy Curve

1.1. BUILDING SUSTAINABLE PERFORMANCE

At present, there are many types of sustainable building evaluation systems with different classifications of sustainable performance. From the perspective of AEC industry, the stakeholders of a construction project can be divided into three categories: the occupant, the government, and the developer. Occupants needs include comfort, functional convenience, etc.; government needs include energy consumption, carbon emissions, etc.; developer needs include cost control, land use, etc. These stakeholders also represent three basic types of performance that are always contradictory and need to be balanced regardless of the stage in the sustainable design of buildings: applicability, environmental protection and economy. The ISO: 14040-14044 standard also divides the generalized life cycle performance evaluation into three categories: Environmental, Social, Economic (ISO, 2006), and the international organization Calcas also emphasized this classification method in the D20 full life cycle analysis

blue book (Action et al., 2009). Hashempour divided the performance of green building design into three basic types: environment, economy and society in the review article (Hashempour et al., 2020). Thus, this study attempts to realize the evaluation and optimization of these three comprehensive performance in the early design stage. They are further specified as energy consumption, Indoor Environmental Quality (IEQ) and Life Cycle Cost (LCC).

1.2. SUSTAINABLE PERFORMANCE IN BIM

Recently, the research on the integration of BIM and sustainable performance mainly focus on two performance types. The first is the overall performance of BIM-based building projects, including building energy consumption, carbon emissions, costs and environmental comfort indicators. This research has made great progress in the past ten years, mainly concentrating on the performance evaluation based on the standard BIM interactive format (Ying and Lee, 2019; Kim et al., 2016) and the integration of the external simulation engine with BIM platform (Jin et al., 2019; Cemesova et al., 2015). However, existing studies indicate shortages of the ability to evaluate multi-dimensions performances and interact with BIM data. The second is the performance defined by basic elements like building components or materials, including the heat transfer performance, sound insulation performance and light transmission performance. This research are still in the exploratory stage. The integrated data is mostly building monitoring data and IoT data (Tang et al., 2019; Riaz et al., 2014), lacking of the basic performance data in the design stage. The P-BIM framework established in this paper aims to realize the interaction and management of building basic performance data, and construct a series of comprehensive performance evaluation technologies to support the performance-driven design process in the early design stage.

1.3. TRANSPARENT ENVELOPE

Transparent envelope plays a decisive role in the sustainable performance. For energy consumption, its heat transfer coefficient is much greater than that of the nontransparent envelope, which leads to great heat loss (Sun et al., 2018). The heat loss caused by the air tightness of doors and windows accounts for a large amount of energy consumption (Grynning et al., 2014). The natural light from the windows has a complex effect on energy consumption. Studies have shown that transparent envelopes are associated with 60% of building energy consumption (Lee et al., 2013). From the perspective of occupant comfort, transparent envelope brings natural light into the room, which increases the illuminance and brings glare at the same time (Alam and Islam, 2017). Solar radiation also causes thermal comfort changes such as overheating (Lai et al., 2017). Transparent envelope has the lowest surface density thus has a great impact on acoustic comfort. In our previous study, it has been confirmed that the transparent envelope has too much influence on the IEQ so as to hinder the simultaneous decision-making of the nontransparent envelope (Dian et al., 2021). The optimization model in this paper is carried out for the transparent envelope independently.

2. Methods

P-BIM framework is proposed as the basis of the optimization model. Based on the

framework, a multi-objective optimization model of window size and configuration considering energy consumption, IEQ and LCC is established.

2.1. P-BIM FRAMEWORK

Performance integrated BIM (P-BIM) technical framework is proposed to support the digital energy efficient design of building under the BIM system. The technology introduces external databases to store various external related data information, establishing a dynamic relationship between external data and BIM model data. The specific technology platform and data interaction logic in P-BIM are shown in Figure 2. Autodesk Revit platform is used as the basic model data back-end, and the MySQL database is introduced as the external data back-end; Rhino.Inside digital design platform is selected as the data center to realize the interaction and management of data stored in the data back-end. Visual programming is the basic method to develop the performance evaluation and optimization procedures using Rhino.Inside. Finally, GHPlayer platform are selected to complete user interaction and model feedback for specified functions. The multi-objective optimization model constructed in the following article is a specific performance-driven design application under the framework of P-BIM.

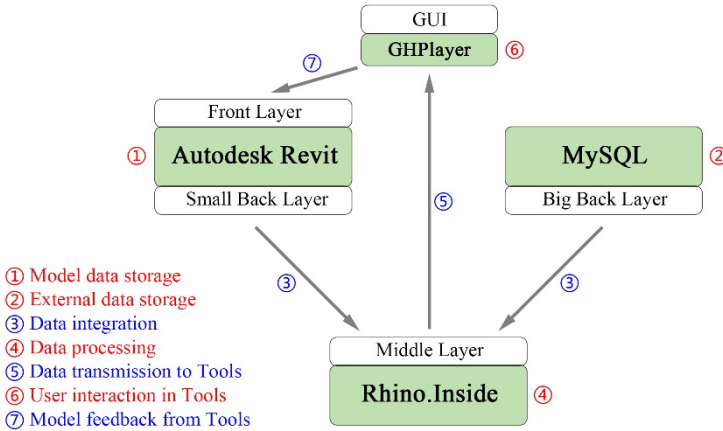


Figure 2. P-BIM components and workflow

2.2. INTEGRATION OF LOCAL SUPPLY CHAIN

Building transparent envelope size and configuration are selected as the optimization variable. The variables emphasize the design characteristics of the P-BIM of the local building product industry, referring to the product lists of various Chinese window manufacturers (SHANGHAI LEAD GLASS CO.,LTD, 2021; Jin Jing Group, 2021). The performance data of the transparent envelope is stored in multiple independent table in MySQL platform. The basic construction logic of the form is shown in Figure 3. The top-level table is a specific window product family, which includes three main contents: size, window frame type and glass configuration. These items are stored in three bottom-level independent tables. The data query from bottom to the top is realized

by unique codes as a primary key.

Figure 3. Window performance data tables

Family	Size	Type	Configuration
P Code	P Code	P Code	P Code
Name	Width	Frame Material	Physical Property
Type Code	Length	Air-tightness	...
Size Code		Cost Coefficient	Appearance Property
Configuration Code			...
			Thermal Property
			...
			Cost Coefficient

2.3. OPTIMIZATION MODEL

The parametric control of design variables, the multi-dimensional performance evaluation and the optimization algorithm are three main parts of the optimization model. Model control and performance evaluation are based on the parametric building energy model translated from BIM model. Building form, envelope construction and operating parameters are translated from Revit to Rhino.Inside platform. On this basis, a dynamic link between the MySQL and the Rhino.Inside based on SQL scripts is built to complete the real-time update of optimized design variables and related performance data.

In terms of performance evaluation, LadybugTools is selected as the simulation platform for energy consumption and IEQ. For the IEQ index, this paper introduces the evaluation method of the indoor environment from Tiberiu et al. in 2012 (Catalina and Iordache, 2012). The energy consumption and thermal comfort are simulated by the EnergyPlus engine; the visual comfort is simulated by Radiance and DAYSIM engines; the acoustic comfort is directly calculated by the indoor sound pressure level calculation formula; and the indoor air quality is calculated by the indoor ventilation volume per person. The whole building envelope LCC evaluation is implemented using the Global Cost calculation formula in the EN 15459 standard (GB-BSI, 2007). The energy cost in the operation stage is further added to the formula to increase accuracy.

Genetic algorithm (GA) is selected as the core optimization algorithm in this study. GAs' performance has been tested in a myriad of reviews and comparative studies, and the literature overwhelmingly suggests that GAs have been the most popular and robust heuristic approach to Multi-objective Optimization problems in the field of building optimisation (Ines et al., 2020; Ciadiello et al., 2007). This study uses the Octopus tool in Rhino.Inside as a genetic optimization engine. Focusing on the Strength Pareto Evolutionary Algorithm (SPEA-2) and the Hypervolume Estimation algorithm (HypE), Octopus yields the best trade-offs to choose among different searched objectives, and is widely used in architectural multi-objective optimization (Li et al., 2020).

2.4. PROJECT INFORMATION

A school building located in the city of Nanjing, Jiangsu Province, China, is selected to validate the proposed optimization model. The school building has three floors with a total construction area of 2311.6 m², including 15 standard classrooms shown in Figure 4. The windows in these classrooms are optimized of their size and configuration.

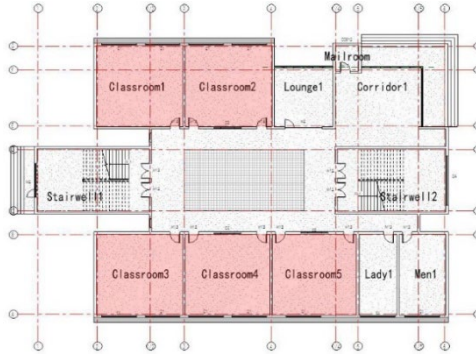


Figure 4. Target rooms in the case building

3. Results

The optimization process tends to be stable in the 15th iteration. In the 31th iteration, 73 Pareto front solutions are generated. The Pareto front is defined as the set of non-dominated solutions, where each objective is considered as equally good (Ranajeet et al., 2020). The performance distribution of Pareto front solutions in the steady state tends to be separated into two groups as shown in Figure 5 and Figure 6. Solutions in group 1 have better performance in cost (30.08-30.80*105¥), with relatively poor IEQ points (64.82-72.89 points) and energy consumption (227.54-229.60 kwh/m²); solutions in group 2 have better performance in energy (225.86-227.37 kwh/m²) and environment quality (67.07-73.88 points), with relatively higher price (31.37-32.28*105¥).

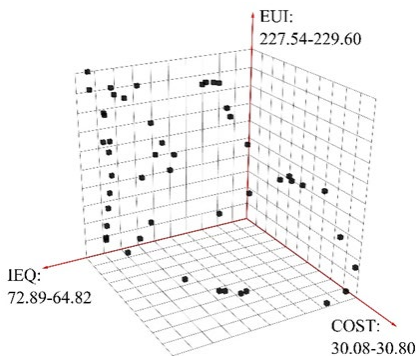


Figure 5. Pareto front solutions group 1

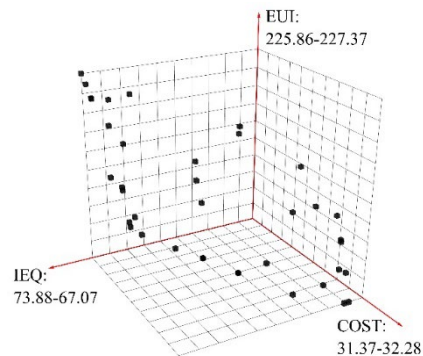


Figure 6. Pareto front solutions group 2

The formation of the two Pareto front solution groups is caused by the difference of window configurations. Group 1 represents various types of single-layer glass, including ordinary glass of different thicknesses and coated glass configurations while group 2 represents multi-layer low-e glass configurations. The distributions of the two groups are basically the same, forming a fusiform shape in the 3D solution space, which represents the mutual restraint relationship between the three performances. Among them, the cost and the other two performances show an obvious non-linear negative correlation, while the relationship between energy and IEQ is relatively fuzzy but still showing a negative correlation. The distribution is consistent with the actual situation, which indicates the reliability and necessity of the optimization process.

For final decision, two Pareto front solutions in the two groups are selected after calculating the Euclidean distance between Pareto front points and origin. We selected the point with the smallest distance to the origin point as the optimized solution. The optimized window configurations and window size information in the two Pareto front solution groups are shown in Table 1. Solution 1 represents the choice of achieving better energy saving and occupant comfort with little cost. Solution 2 represents the choice of achieving the best performance with sufficient funds.

Table 1. Decision-making solutions.

	Solution 1	Solution 2
Frame type	Aluminium alloy	Aluminium alloy
Glass configuration	Single glass 6	Double low-e 6 + Air 12 + Glass 6
Width	South: 2.3 North: 2.2	South: 2.2 North: 2.4
Length	South: 0.8 North: 1.2	South: 0.9 North: 0.9
Sill height	South: 1.5 North: 1.5	South: 1.5 North: 1.3
EUI	228.47	226.40
LCC	30.48	31.97
IEQ	70.07	72.54

4. Discussion

In this study, the optimization process of window components in the local supply chain is conducted by introducing P-BIM framework. Compared with the traditional optimization process in window construction and size, the proposed optimization process indicates the following advantages.

The proposed optimization process enables the industrialized products to play a part in advance in the preliminary design stage. The current construction engineering industry has gradually completed the industrialization transformation, and various building components have gradually completed marketization reforms. On the other hand, the architect responsibility system is being implemented rapidly, and architects' attention should shift from the design stage to the complete project life cycle. Based on the above requirements, the traditional operation mode of separating the design phase from the procurement phase is no longer adequate for the current industry status. The technology proposed in this paper can take industrialized products to the initial stage

and integrate them into the design process, which responds to the above needs.

The proposed optimization process adapts to the needs of regional differences. The supply chain of building component products will change following the project location and project undertaker. The proposed optimization model is automatically linked with the structured database by the index query. The constructed database provides a standardized data storage method, ensuring the stability with the change of component data, which guarantee the adaptability and flexibility of the optimization process.

The proposed optimization process bridges the gap between expected performance and actual performance. In the traditional building sustainable performance optimization design, the window size and layer thickness are optimized directly in the form of continuous variables. The design results obtained often cannot correspond to specific component products, so the component products with similar parameters to the optimal solution are selected for further use. However, the performances and parameters often do not follow a simple linear relationship, and neither do parameters amongst themselves. Huge performance gap may be caused from the seemingly similar building components. The optimization model constructed in this study directly screens the building component products as variables, and directly evaluates the performance changes caused by the actual components to guide decision-making. This eliminates an important factor leading to the performance gap from the root.

5. Conclusions

In response to the emergency needs of digital energy efficiency design based on BIM, a performance integrated BIM framework and a multi-objective optimization model constructed on it are introduced. The study integrates external supply chain products and multiple performance driven design functions in BIM system. The optimization model is constructed to optimize the size and configuration of the windows, which plays a key role in building sustainability. With the aid of P-BIM technique, three comprehensive performance are evaluated and optimized dynamically in a digital building energy model in BIM. The optimization results demonstrate that there is a contradictory relationship between the three comprehensive objectives, and the window glass configurations lead to the separation of solution groups obviously. Best solutions in each group are finally picked up with different performance preference trends.

Energy consumption, life cycle cost, and occupant comfort represent the core demands of construction projects from the perspective of the government, developers, and users respectively. Among them, energy consumption responds to the needs of energy efficiency in SDG 7. The optimization of indoor environmental quality responds to the concerns for mental health, well-being and communicable diseases in SDG 3. For the purpose of economizing on raw materials and reducing consumption, LCC optimization responds to the needs of sustainable consumption and production in SDG 12. The three performance are highly comprehensive and always contradict with each other. The holistic optimization of the economic, social and environmental performance enhance sustainable built environment in SDG 11. This study establishes the evaluation and optimization tools of the three performance under BIM system through the introduction of the P-BIM framework. The tools can be widely applied to

different types of projects and industrial supply chains, and has strong practical significance.

On the other hand, the optimization model established in this paper puts forward the perspective of building products in the initial stage of design. The integration of local supply chain has the following three aspects of significance for construction engineering. First, it conforms to the current trend of industrialization and marketization of building components. Second, it conforms to the local characteristics of the project and the industry. Third, it reduces the gap between expected performance and actual performance.

In summary, the local supply chain based comprehensive sustainable performance optimization is taken into the early design stage with the help of P-BIM framework. The gap between the expected performance and the actual performance is reduced, and the architect's control of the project life cycle is promoted.

References

- Action, C. C., & Analysis, L. (2009). *D20 Blue Paper on Life Cycle Sustainability Analysis*. Institute of Environmental Sciences, Leiden University (CML).
https://www.leidenuniv.nl/cml/ssp/publications/calcas_report_d20.pdf.
- Alam, M. J., & Islam, M. A. (2016). Effect of external shading and window glazing on energy consumption of buildings in Bangladesh. *Advances in Building Energy Research*, 1-13.
<http://dx.doi.org/10.1080/17512549.2016.1190788>.
- British Standards Institution. (2007). *Energy performance of buildings - Economic evaluation procedure for energy systems in buildings* (BS EN 15459-2007).
<https://www.thenbs.com/PublicationIndex/documents/details?Pub=BSI&DocID=284777>
- Catalina, T., & Iordache, V. (2012). Ieq assessment on schools in the design stage. *Building & Environment*, 49(Mar.), 129-140. <http://dx.doi.org/10.1016/j.buildenv.2011.09.014>.
- Cemesova, A., Hopfe, C. J., & Mcleod, R. S. (2015). Passivbim: enhancing interoperability between bim and low energy design software. *Automation in Construction*, 57(SEP.), 17-32. <https://doi.org/10.1016/j.autcon.2015.04.014>.
- Cardiello, A., Rosso, F., Dell'Olmo, J., Ciancio, V., Ferrero, M., & Salata, F. (2020). Multi-objective approach to the optimization of shape and envelope in building energy design. *Applied Energy*, 280. <https://doi.org/10.1016/j.apenergy.2020.115984>.
- Dian, Z., Xinkai Z., Yongdong, L., Chao, W., Xing, J., Xin, Z., & Xing, S. (2017). A performance data integrated BIM framework for building life-cycle energy efficiency and environmental optimization design. *Automation in Construction*, 127, 103712.
<https://doi.org/10.1016/j.autcon.2021.103712>.
- Grynning, S., Time, B., & Matusiak, B. (2014). Solar shading control strategies in cold climates - heating, cooling demand and daylight availability in office spaces. *Solar Energy*, 107(Sep.), 182-194. <http://dx.doi.org/10.1016/j.solener.2014.06.007>.
- Hashempour, N., Taherkhani, R., & Mahdikhani, M. (2020). Energy performance optimization of existing buildings: a literature review. *Sustainable Cities and Society*, 54, 101967. <https://doi.org/10.1016/j.scs.2019.101967>.
- Ines, C., Rokia, R., & Javier, N. G. (2020). A systematic review of genetic algorithm-based multi-objective optimisation for building retrofitting strategies towards energy efficiency. *Energy and Buildings*, 210, 109690. <https://doi.org/10.1016/j.enbuild.2019.109690>.
- International Organization for Standardization. (2006). *Environmental management – Life cycle assessment – Principles and framework* (ISO Standard No. 14040:2006).
<https://www.iso.org/standard/37456.html>.

- International Organization for Standardization. (2006). *Environmental management – Life cycle assessment – Requirements and guidelines* (ISO Standard No. 14044:2006). <https://www.iso.org/standard/38498.html>.
- J. W. Lee., H. J. Jung., J. Y. Park., J. B. Lee., & Y. Yoon. (2013). Optimization of building window system in Asian regions by analyzing solar heat gain and daylighting elements. *Renewable Energy*, 50(3), 522-531. <https://doi.org/10.1016/j.renene.2012.07.029>.
- Jin Jing Group. (2021). *Product center*. Retrieved November 7, 2021, from <http://www.cnggg.cn/product/>.
- Kim, H., Shen, Z., Kim, I., Kim, K., & Yu, J. (2016). Bim ifc information mapping to building energy analysis (bea) model with manually extended material information. *Automation in Construction*, 68, 183-193. <https://doi.org/10.1016/j.autcon.2016.04.002>.
- Kun, L., Wen, W., & Harry, G. (2017). Solar shading performance of window with constant and dynamic shading function in different climate zones. *Solar Energy*, 147, 113-125. <https://doi.org/10.1016/j.solener.2016.10.015>.
- Li, Z., Binghua, W., & Yong, S. (2020). Multi-objective optimization for energy consumption, daylighting and thermal comfort performance of rural tourism buildings in north China. *Building and Environment*, 176, 106841. <https://doi.org/10.1016/j.buildenv.2020.106841>.
- Poroozfar, P., Farr, E., Zadeh, A. (2019). *Facilitating Building Information Modelling (BIM) using Integrated Project Delivery (IPD): A UK perspective*. Journal of Building Engineering, 26, 100907. <https://doi.org/10.1016/j.job.2019.100907>.
- R. Jin, Zhong, B., Ma, L., Hashemi, A., & Ding, L. (2019). Integrating bim with building performance analysis in project life-cycle. *Automation in Construction*, 106, 102861. <https://doi.org/10.1016/j.autcon.2019.102861>.
- Ranajeet, M., Shakti, S., & Sarat, K. D. (2017). Chapter 16 - Modeling the Axial Capacity of Bored Piles Using Multi-Objective Feature Selection, Functional Network and Multivariate Adaptive Regression Spline. *Handbook of Neural Computation*, 295-309. <https://doi.org/10.1016/B978-0-12-811318-9.00016-8>.
- Riaz, Z., Arslan, M., Kiani, A. K., & Azhar, S. (2014). Cosmos: a bim and wireless sensor based integrated solution for worker safety in confined spaces. *Automation in Construction*, 45(sep.), 96-106. <https://doi.org/10.1016/j.autcon.2014.05.010>.
- SHANGHAI LEAD GLASS CO., LTD. (2021). *Product center*. Retrieved November 7, 2021, from <http://www.leadglass.cn/p/6.html>.
- Sun, Y., Robin, W., & Wu, Y. (2018). A review of transparent insulation material (tim) for building energy saving and daylight comfort. *Applied Energy*, 226, 713-729. <https://doi.org/10.1016/j.apenergy.2018.05.094>.
- Tang, S., Shelden, D. R., Eastman, C. M., Pishdad-Bozorgi, P., & Gao, X. (2019). A review of building information modeling (bim) and the internet of things (iot) devices integration: present status and future trends. *Automation in Construction*, 101(MAY), 127-139. <https://doi.org/10.1016/j.autcon.2019.01.020>.
- UN Environment and the International Energy Agency. (2019). *2019 Global Status Report for Buildings and Construction*. World Green Building Council. <https://www.worldgbc.org/sites/default/files/2019%20Global%20Status%20Report%20for%20Buildings%20and%20Construction.pdf>.
- Ying, H., & Lee, S. (2019). An algorithm to facet curved walls in IFC BIM for building energy analysis. *Automation in Construction*, 103(JUL.), 80-103. <https://doi.org/10.1016/j.autcon.2019.03.004>.

INTERACTIVE VIRTUAL CONSTRUCTION

A Case Study of Building Component Assembly Towards the Adoption of BIM and VR in Business and Training

HASSAN ANIFOWOSE¹, WEI YAN² and MANISH DIXIT³

^{1,2,3}*Texas A&M University, U.S.A.*

¹*hassancortex@tamu.edu*

²*wyan@tamu.edu*

³*mdixit@arch.tamu.edu*

Abstract. Present day building product manufacturers face difficulties in scaling businesses. Key decisions surrounding technology adoption are typically measured against feasibility of use and long-term profit. Building Information Modelling (BIM) and Virtual Reality (VR) provide the potential for teaching building product assembly to employees and construction contractors. This eliminates the need for deploying training personnel to job sites, reduces manufacturing carbon footprint and wastes in product samples required for training. VR content development is difficult and performance within VR applications must be near reality in order to improve adoption of such technology through training. This exploratory study investigates important factors that enhance adoption in business cases through training. We developed an innovative BIM+VR prototype for SwiftWall; a temporary wall manufacturing company, highlighting rigorous processes for in-house BIM anatomy and VR development. This paper provides a step-by-step approach to replicate the prototype. The prototype was tested in several demonstration sessions. The approximate time to install 40 linear feet of SwiftWall is 30-minutes at the simplest level. This timing is equivalent to 28 linear feet installation in 21-minutes achieved with the BIM+VR prototype demonstration. The matching timing results show a significant potential for adoption in business, improved sustainability and employee training from a time and cost-efficient standpoint. Concerns and key issues from development to deployment are discussed in detail. The BIM+VR virtual construction prototype provides adoption potential for training remote partners thereby increasing possibilities of SwiftWall scaling to distributors and product carriers across a larger geographic region.

Keywords. BIM; Virtual Reality; Unity; Training; Game Design; Construction Assemblage; Construction Material; Virtual Construction; SDG 9.

1. Introduction

New technologies such as E-commerce, Big Data, internet of things (IOT), Artificial Intelligence (AI) all provide disruption potentials for business landscapes. However, design and construction firms are still struggling on how best to harness them (Syamimi et al., 2020). Virtual Reality (VR), which is fast gaining ground, has become an essential tool for the transfer of knowledge in educational settings (Alizadehsalehi et al., 2021; Bashabsheh et al., 2019; Caesaron, 2017). On the other hand, in most industries, there are identifiable adoption barriers that stifle the successful implementation of such technologies. Such barriers span from corporate strategic alignment, talent retention, market fragmentation to sales or growth projections (Cacho-Elizondo et al., 2018). Brands in the design and construction industry are racing to catch on the Virtual Design and Construction (VDC) trends to gain competitive advantage. Frustration and abandonment of adoption strategies may occur at various levels of an organization if proper understanding of diverse platforms and phases required for adoption is not achieved. It has been established that the visualization power of VR affords clients the abilities for rapid decision making (Tariq et al., 2019). VR apps, demonstrations and games are currently created by professional designers, thereby making the skillset required a very niche one (De Regt et al., 2020) hence the adoption dilemma. For big firms, a large opportunity is identified in communication between workforce and also in improving manufacturing processes, (Bosché et al., 2016; Fernandes et al., 2006).

This research provides a step-by-step approach to the development and adoption of Building Information Modeling (BIM) and Virtual Reality (VR) in a case study for building product manufacturing business; SwiftWall, located in Michigan, USA. We seek to understand BIM and VR adoption techniques highlighting use cases that contribute to success rates for small and medium size companies. A BIM+VR prototype was developed for this purpose, highlighting best practices for content development and usability.

2. Background Study

There is a need for more extensive research work regarding the adoption of VR in teaching architecture with a potential to providing better design understanding for students beyond the traditional methods (Bashabsheh et al., 2019). There are also limitations in adopting BIM and VR in construction safety trainings with drawbacks in large-scale adoption although mobile VR provides improved portability for job sites compared to PC-based VR. A paradigm shift is required to transform the construction industry from a craft-based one to a knowledge and value-driven industry (Goulding et al., 2012). Innovative and flexible training options are essential to drive the transformation. Beyond the technology, on a larger scale, several factors that limit rates of adoption have been identified by a study (Fernandes et al., 2006). Such factors include, for instance, top management support, internal needs, degree of competition and champion within a company. This study however, was limited to the UK construction industry and its results may vary widely across other geographic regions like the United States where business practices, market size, access to technology, resources and funding are largely different. Results from other sectors may provide

variables to these factors if compared. Conventional methods of operation at SwiftWall include issuing quotations and basic 2-Dimensional drawings alongside image annotations to customers. There has been a need to cut down on manufacturing wastes, improve productivity and sales for upwards business scaling for training distributors and installers across various regions.

2.1. REQUIREMENTS FOR VR ADOPTION

There are technical and financial decisions important for the adoption of VR in business cases. There is limited evidence to support claims regarding skill levels of project teams being a major determinant for adoption, however, cost is a major factor for decision as financial experts have more decision making power than technical experts within a company (Fernandes et al., 2006). End users also provide clarity regarding needs thereby increasing the possibilities of adoption. This factor alone, is a big component in the overall scheme of this BIM+VR research. For the purpose of adoption for training, real construction projects are peculiar in nature and require different tasks which may have varying results in terms of cost and time implications. As a result of cost overruns, delays and errors associated with training on real projects, real project environments have been simulated in the past to address this. These training simulations allow for safety with little or no impact on project performance (Bosché et al., 2016).

For the development of BIM and VR, there must be a balance between data required for use in a VR model and the level of performance required for an optimal experience. This often requires culling objects, simplifying geometry, and improving object face. Unity provides entry level game development for novices who can use its pre-loaded asset store for content development (Foxman, 2019).

2.2. GAPS IN RESEARCH

Although VR research has been extensive in theoretical spectrum, there is limited research addressing problems encountered in development for adoption using a business case study. Previous research has focused on cost, installation time and high risk as major factors of non-adoption (Fernandes et al., 2006). Current BIM and VR workflows are limited. There is an increasing need for researchers in academia, industry, hardware and software developers to collaborate for improved and established workflows (Alizadehsalehi et al., 2019).

Four major problems were identified in this study for the business and training case. They surround upward business scaling with products, processes and people viz -

- Cost of building prototypes – physical product prototypes are costly. This research proposes a simplified virtual product prototype development process.
- High risk of safety & high cost of staff deployment – Our research proposes a safer training use case in a shared remote environment.
- Cost of adoption – BIM and VR content development is difficult and costly if poorly executed. Our research highlights optimized business use cases for SwiftWall.

As shown, cost is a major determinant in business operations and sustainability, and

therefore, proposed solutions must be cost-effective. This research does not address directly the costs of the adoption of BIM+VR technology as it has been explored in previous research (Fernandes et al., 2006). In VR training applications, purposes are specific and are typically equipment, machine or process operation based. It is established however, that the development of such training content is challenging (Motejlek & Alpay, 2019). We highlight the development process for content development for improved usability thereby providing a manufacturer-specific business use case for adoption in SwiftWall.

3. Methods

This exploratory case study proposes a two-phase approach to adopting BIM and VR in the SwiftWall business environment. The first stage covers prototype development while the second phase demonstrations and findings.

The inclusion of detailed virtual models is an essential part of the VR experience to mimic real-life situations and assembly sequence. To achieve improved realism, various components like tracks, channels, panels and accessories were modelled in real scale and matching product texture. As indicated in previous research, it is important to work closely with industry to accurately model situations that are peculiar to processes, controls and responses in the field in order to improve interactive learning (Anifowose et al., 2022; Xiao et al., 2004). Six different departments were contacted for development direction input. Experts totalling thirteen from all departments; Architecture & Engineering, Production, Installation, Sales, Training, Safety discussed essential milestones for successful product development in VR. Management input was sought for business integration after demonstration.

3.1. BIM+VR PROTOTYPE DEVELOPMENT

Digital BIM models of various SwiftWall components were developed to high level of detail 400 i.e. fabrication-ready geometry which was important for visual and dimensional realism of the assembly process.

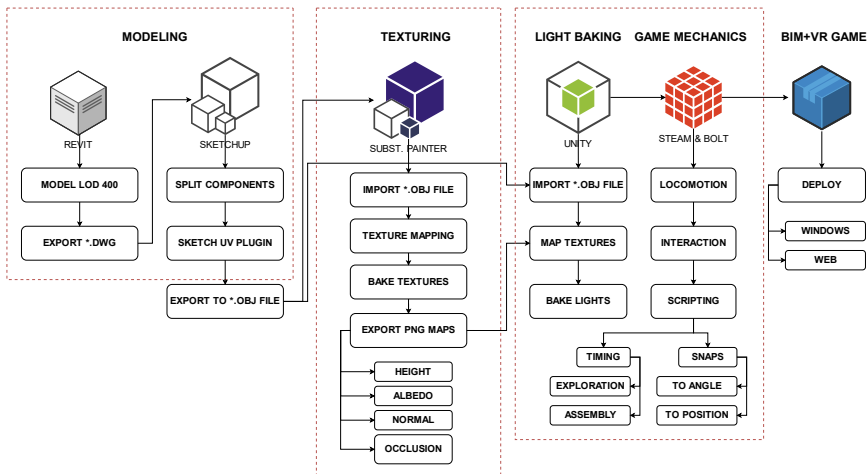


Figure 1. Prototype Development & Software Workflow

Revit 2020, Sketchup 2019, Substance Painter 2019.3.3 and Unity 2020.1 are readily available licensed software tools used for the prototype development shown in Figure 1. SwiftWall components were modelled in Revit, exported and optimized for geometry in SketchUp and converted to *.obj files. This allowed the retention of geometry details and UV (axes) mapping based on the material files. These digital models with their corresponding spatial properties and scale were imported into Substance painter. Unity game engine was used to develop the components in VR. These tools provided the most optimized methods for visual details and performance. A mock-up of an airport lobby; the most common product usage scenario was developed to mimic real life application. As shown in Figure 2, a staging area allows users to setup various wall configurations after inspecting a ready-made wall configuration. Stacked components are made readily available within the environment for use and the player/user has an in-game time to monitor how long they have been completing the assemblage task in VR.

To prepare the prototype for modelling and lighting, SwiftWall components were carefully modelled from real photographs and dimensioned CAD files. The file exchange process between software is extremely important for successful execution. Optimized geometry and file export format for precise geometry and faces was *.obj file format, among all file format types tested. In an installation environment for a factory with lower levels of lighting, a similar level of lighting must be achieved to increase realism. Installation of SwiftWall products in an overly bright scene can lead to visual discomfort also as the panels are bright in colour. Downlighting at higher levels and reflection probes at mid-level were located to replicate realistic lighting especially for the task assemblage area.



Figure 2. SwiftWallVR Prototype: Virtual Construction Scene Setup

The model's texturing process was completed in Substance Painter software to achieve near-realism product representation. However, for optimum texturing results, object faces were unwrapped to receive scanned texture projections on each face using SketchUp and SketchUV plugin. Previous related work in our research lab (Anifowose

et al., 2022) has explored various impacts of good texturing towards improved realism. Various texture channels are combined to improve baking results. The ambient occlusion and roughness texture channels increased visual clarity in the scenes.

3.2. PROTOTYPE DEMONSTRATION

Several demonstration sessions were carried out by three (3) users who are experienced installers and thirteen (13) department representatives in attendance. Recordings of the demonstration sessions in Figure 3 are stored in a safe storage and can be retrieved for future analysis. We considered specific content integration techniques and developing VR interaction features aimed at improving the overall VR experience. In order to make the prototype usable for first-time VR users which is suspected to be most of the population in future user studies, features such as an in-game timer, snap-to-position and snap-to-angle are incorporated. These features are overall intended to improve user engagement for better learning outcomes in a training use case. As highlighted in previous works on VR, integrating text into virtual environments is important for users to read (Xiao et al., 2004).



Figure 3. Demonstration setup for BIM+VR Prototype at SwiftWall Innovation Center

To measure effectiveness in training, a timer was developed in-game to allow time tracking of tasks for various stages. The first stage, which features a new user exploring an already-built SwiftWall assemblage counts down onboarding time. Thereafter, timing commences for the assemblage execution where the user builds walls of different configurations. On a corporate level, this can be compared with average install times. A timed assemblage match was achieved between the BIM+VR optimized prototype and physical SwiftWall assemblage. Video demonstration can be found here - <https://youtu.be/Qt4Om4MMt4E>.

4. Experimental Results & Discussion

This section will explain opportunities and limitations based on the BIM+VR prototype. Stemming from the real scale objects to human body ratio in the VR scene, near reality discomforts are reproduced as physical body adjustment must be made to complete VR actions. Installers typically carry the long-sized panels on their sides with directional vision obscured by the sheer size of the panels. This requires users to carefully manipulate objects while also being conscious of virtual movements and directions for successful installation. There is a safety risk in on-site training that decreases in VR. A BIM+VR training prototype, however, is not just less risky but it also prepares the user for a real on-site scenario, providing a much smoother transition from a safe training environment to a riskier and chaotic construction site.

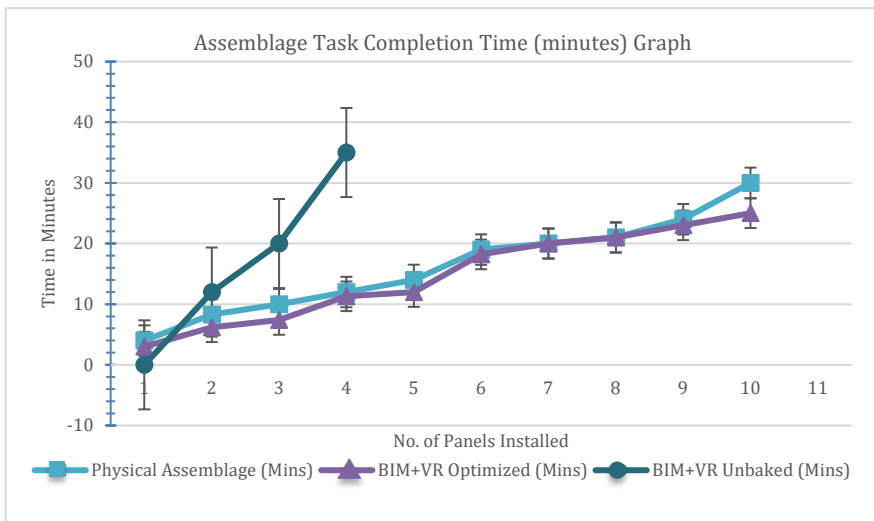


Figure 4. Graph showing matched completion time between physical and BIM+VR assemblage

In this section, results from the development process are first discussed. The BIM+VR prototype was rigorously developed to simulate realism in geometry, materials and product features for example, the proprietary tongue and groove system in SwiftWall Assemblage. The texturing for Acrylonitrile butadiene styrene (ABS) skin material was scanned before applied to the geometry thereby increasing realism. Visual comfort was further attained by texture baking with Ambient Occlusion. During the preliminary tests and early stages of development, without the baking, visual comfort was not achieved in unbaked scenes. This led to higher task completion times as users struggle with visual precision; in one case, 35 minutes was spent on 12 linear feet installation in VR which could negatively impact its adoption as indicated in Figure 4.

The approximate time to physically install 40 linear feet of SwiftWall is 30-minutes at the simplest level. Using a Distance/Time calculation, this provides a Constant K of 1.33 (linear foot of SwiftWall installed per minute). A similar installation time match for 28 linear feet (7 panels) was achieved in 21-minutes (average timing result from the three installers) in the optimized BIM+VR prototype. On the contrary, the unbaked

scene produced higher installation times and higher levels of visual discomfort. With an increased level of realism, the assemblage task can be completed as the user makes more precise judgements of object placement based on interactions. We acknowledge that the installation time results can vary if the difficulty level of assembly is higher or lower. Since this is possible, the next phase will feature flexibility in game level difficulty in order to train participants from easier to more difficult assemblage scenarios.

4.1. LIMITATIONS

One of the key concerns is the current availability of development hardware. A large percentage of hardware are consumer grade which create a challenge for rigorous development endeavours (De Regt et al., 2020). There are also performance limitations that slowed down development due to model complexity of the game scene and the available hardware . Deploying a BIM and VR solution is known to require high performance hardware beyond model optimization (Sampaio, 2019). Product innovation and BIM+VR development rate must match in order to be successful. If product innovation outpaces updates and development of the BIM+VR system, there are high possibilities that such systems might become obsolete very quickly. This may necessitate redevelopment thereby increasing adoption business cost and hindering long term sustainability.

4.2. ADOPTION MATRIX

Time and cost benefit analyses were derived from the BIM+VR prototype development thereby providing a case for management and financial decisions to be taken regarding the route for adoption in the business workflow and future scaling. Two classes of use cases were highlighted below:

- Internal Use Case – Internal design team and internal employee training.
- External Use Case – External architect use case, single partner training (no support), remote partner training (with multiplayer support) and consumer use cases.

After several demonstrations to in-company representatives, discussions surrounding adoption was undertaken in a 13-person vote style consensus from department representatives. Using development/deployment cost and business scaling benefit analysis, the most viable option for adoption was a single partner training. We believe that the BIM+VR prototype provides SwiftWall the best opportunity to train their partners and grow business rapidly. Internal employee training was the next most preferred adoption method based on costs and perceived benefits. Consumer use case was the least desired as the cost of deployment and benefits will not serve the business' scaling purpose.

5. Conclusions and Future Work

From a technical standpoint, the highlighted processes for developing the prototype in this research provides an easy entry for any organization or research group intending to develop VR prototypes for construction assembly. We have successfully designed

and tested VR precision features such as snap-to-position, snap-to-angle, texturing, baked lighting and time tracking to improve training. These features have not been previously studied towards BIM & VR adoption within the research community. This research has also identified the most preferred business and training use cases towards adoption using SwiftWall as a case study business.

This type of research and development help manufacturing companies achieve sustainability goals by reducing manufacturing wastes and production carbon footprint. The development processes highlighted in this research and adoptable by future researchers include -

- Accurate product modelling, best file exchange formats and software workflow.
- Unwrapping geometry face for accurate UV texturing to improve realism by texture baking.
- Improving user visual comfort & task performance with optimized baked lighting.

A first barrier to BIM and VR adoption is the lack of education and training. A lack of BIM expertise within an organization limits in-house development capabilities of BIM+VR. Management must make decent strides in employing new hands or educating existing employees about their products and BIM systems. BIM trainings could be made prerequisite requirements for product design teams and employee onboarding process. To further improve performance & adoption, the next prototype release scheduled for the user study has been designed to include text instructions for easier sequential installation.

Building a prototype of this nature outweighs verbal conversations surrounding adoption. Developing details and increased realism can lead to improved usability based on near-reality experiences. The process presented in this paper showcases a novel approach to establishing grounds for adopting BIM and VR prototype (product) as part of the business scaling strategy (process) while transforming how employees (people) and prospective partners are trained. By developing a prototype, a business use case is identified, and the people are emotionally subscribed to adopt the technology as the value added to the chain becomes obvious. In a future study, users will be invited to test the prototype upon approved Institutional Review Board (IRB) number IRB2022-0057. Assemblage completion times will be measured and compared with a physical task assemblage.

References

- Alizadehsalehi, S., Hadavi, A., & Huang, J. (2021). Assessment of AEC Students' Performance Using BIM-into-VR. *Journal of Applied Sciences*, 11, 23. doi:10.3390/app11073225
- Alizadehsalehi, S., Hadavi, A., & Huang, J. C. (2019). Virtual Reality for Design and Construction Education Environment.
- Anifowose, H., Yan, W., & Dixit, M. (2022). BIM LOD+ Virtual Reality--Using Game Engine for Visualization in Architectural & Construction Education. *arXiv preprint arXiv:2201.09954*.
- Bashabsheh, A. K., Alzoubi, H. H., & Ali, M. Z. (2019). The application of virtual reality technology in architectural pedagogy for building constructions. *Alexandria Engineering Journal*, 58(2), 713-723. doi:https://doi.org/10.1016/j.aej.2019.06.002

- Bosché, F., Abdel-Wahab, M., & Carozza, L. (2016). Towards a Mixed Reality System for Construction Trade Training. *Journal of Computing in Civil Engineering*, 30(2), 04015016. doi:10.1061/(ASCE)CP.1943-5487.0000479
- Cacho-Elizondo, S., Álvarez, J.-D. L., & Garcia, V.-E. (2018). Exploring the Adoption of Augmented and Virtual Reality in the Design of Customer Experiences: Proposal of a Conceptual Framework. *Journal of Marketing Trends* (1961-7798), 5(2).
- Caesaron, D. (2017). Reviews of Virtual Reality and Virtual Environment and It's Applications Particularly in Education. *Journal of Industrial Engineering Management Systems*, 6(1).
- De Regt, A., Barnes, S. J., & Plangger, K. (2020). The virtual reality value chain. *Business Horizons*, 63(6), 737-748. doi:https://doi.org/10.1016/j.bushor.2020.08.002
- Dibbern, C., Uhr, M., Krupke, D., & Steinicke, F. (2018). Can WebVR further the adoption of Virtual Reality? *Mensch und computer 2018-usability professionals*.
- Fernandes, K. J., Raja, V., White, A., & Tsinopoulos, C.-D. (2006). Adoption of virtual reality within construction processes: a factor analysis approach. *Technovation*, 26(1), 111-120. doi:https://doi.org/10.1016/j.technovation.2004.07.013
- Foxman, M. (2019). United We Stand: Platforms, Tools and Innovation With the Unity Game Engine. *Social Media + Society*, 5(4), 2056305119880177. doi:10.1177/2056305119880177
- Getuli, V., Capone, P., & Bruttini, A. (2021). Planning, management and administration of HS contents with BIM and VR in construction: an implementation protocol. *Engineering, Construction and Architectural Management*, 28(2), 603-623. doi:10.1108/ECAM-11-2019-0647
- Goulding, J., Nadim, W., Petridis, P., & Alshawi, M. (2012). Construction industry offsite production: A virtual reality interactive training environment prototype. *Advanced Engineering Informatics*, 26(1), 103-116. doi:https://doi.org/10.1016/j.aei.2011.09.004
- Motejlek, J., & Alpay, E. (2019). A Taxonomy for Virtual and Augmented Reality in Education. *arXiv preprint arXiv:12051*.
- Shaghaghian, Z., Burte, H., Song, D., & Yan, W. (2021). Learning Geometric Transformations for Parametric Design: An Augmented Reality (AR)-Powered Approach. *arXiv preprint arXiv:2109.10899*.
- Syamimi, A., Gong, Y., & Liew, R. (2020). VR industrial applications—A singapore perspective. *Virtual Reality & Intelligent Hardware*, 2(5), 409-420. doi:https://doi.org/10.1016/j.vrih.2020.06.001
- Tariq, M. A., Farooq, U., Aamir, E., & Shafaqat, R. (2019). Exploring adoption of integrated building information modelling and virtual reality. Paper presented at the *2019 International Conference on Electrical, Communication, and Computer Engineering (ICECCE)*.
- Xiao, A., Bryden, K., & Brigham, D. (2004). Virtual Reality Tools For Enhancing Interactive Learning.

REVIT ADD-IN FOR DOCUMENTING DESIGN DECISIONS AND RATIONALE

A BIM-based tool to capture tacit design knowledge and support its reuse

ATA ZAHEDI¹ and FRANK PETZOLD²

^{1,2} *Chair of Architectural Informatics, TUM School of Engineering and Design, Technical University of Munich.*

¹*ata.zahedi@tum.de, 0000-0003-0296-9205*

²*petzold@tum.de, 0000-0001-8974-0926*

Abstract. The building design is a problem-solving process in which the demands of the customer are turned into a design job. Throughout the design process, several specialists from various fields cooperate to develop the final design. The key deliverables that are exchanged and passed over are the generated designs. However, no explanation of design intentions or evidence of argumentations behind the design decisions is included in the design deliverables. Design documentation helps with communication and coordination between designers and other domain experts and stakeholders. Proper design documentation also preserves and protects corporate design knowledge and makes it available for future design problems and projects. This paper presents the implementation of an add-in for Revit that features the concepts of so-called Explanation Tags and Design Episodes to digitally explain and document design rationale and decisions, and ultimately capture the tacit design knowledge. As an extra feature, the add-in also enables the export of design episodes to a Graph-Database (Neo4j) as well as CSV files for future reference and use. Subsequently, the goal is to search and query inside the graph database for similar designs that can solve and answer the new design tasks in the future. This paper contributes to the UN Sustainable Development Goals, namely SDG 9 & SDG 11 among others.

Keywords. Design Documentation; Explanation Tags; Design Episodes; Building Information Modelling (BIM); Design Rationale; SDG 9; SDG 11.

1. Introduction

Designing a building is a problem-solving activity in which the clients' wishes and needs are translated into a design task taking into account the various regulations and building codes. The design task and its solutions co-evolve throughout the design process while all parties are trying to fulfill numerous requirements and guidelines

(Zeiler et al., 2007). Furthermore, during the project's life-cycle, multiple experts from multiple domains collaborate in developing the different partial models, including architectural, structural, and HVAC, among others (Cao & Protzen, 1999). Accordingly, explicitly communicating the rationale behind design decisions is crucial for developing regulatory compliant designs that also fit the owner's needs. In everyday practice, documentation of the architectural design process is not mandatory. Sometimes design variants are documented textually and graphically as an intermediate step, but usually, only the final result is documented graphically, e.g. in digital models or drawings and elevations, as well as textually. However, developing designs that meet the various requirements and regulations is a complex task, especially since building designs are composed of various elements that are connected by topological relationships and functional interdependencies. Therefore, documenting the design rationale and intent, while incorporating the individual building elements, facilitates the investigation and evaluation of the design that meets these regulations. Recording and sharing explanations of decisions made during the design process will enhance mutual understanding and collaboration among all parties and professionals involved in the design process and promote the cross-organizational distribution and reuse of shared tacit knowledge and designs for other future projects and tasks.

This paper addresses the problem of capturing tacit design knowledge and documenting design decisions and rationale. To this end, a novel approach is introduced by Zahedi et. al. (Zahedi et. al., 2021) based on BIM methodology to link customer requirements and building codes to design concepts and ideas, and to record and document design decisions, argumentation, and rationale in a way that is transparent to all stakeholders. Consequently, this paper contributes to the UN Sustainable Development Goals, in particular 'Industry, Innovation and Infrastructure' and 'Sustainable Cities and Communities'.

2. Literature Review

Storytelling is one of the methods for imparting architectural knowledge that has been studied in the literature (Heylighen, Martin, & Cavallin, 2007; Martin et al., 2003, 2005). It is recognized as a means of accelerating comprehension. Storytelling, at the same time, allows for numerous important challenges to be addressed in terms of architectural complexity. In addition to being straightforward, easy to read, and amusing, stories that recognize the deep relationships of things are unforgettable. As a result, narrative allows for a rich and compact means of conveying complexity in a short amount of time. The "Building Stories" project (Heylighen, Martin, & Cavallin, 2007; Martin et al., 2003, 2005), has demonstrated the effectiveness of storytelling in collecting and storing tacit design knowledge. Thus, the concept of design episodes introduced by Zahedi et. al. (Zahedi et. al., 2021) utilizes storytelling techniques to encapsulate and capture different bits and pieces of design in various episodes.

In architectural building design, the usage of references is regarded as a recognized strategy (Gänshirt, 2012) for assisting design, testing ideas, defining design parameters, and demonstrating new suggestions and possibilities. The built and planned models act as an architectural knowledge repository, containing both spatial forms and solutions for specific architectural expressions. At the same time, graph structures are widely used in various disciplines for analyzing and extracting information and knowledge, as

well as in the BIM context, because of their capacity to describe complicated relationships (Isaac et al., 2013). In the AEC sector, graph structures have been employed for a variety of applications, such as path planning (Hamieh et al., 2020), retrieval of comparable designs (Ayzenshtadt et al., 2018; Langenhan et al., 2013), modeling and management of BIM-based design variants (Mattern & König, 2018). That is why the Revit add-in discussed in this work, also enables the export of the design episodes to a graph structure. Abualdenien & Borrmann categorized the graph representations in the AEC industry into four groups (Abualdenien & Borrmann, 2021); space connectivity graphs (He et al., 2018; Langenhan et al., 2013), navigation graphs (Al Hattab & Hamzeh, 2018; Dubey et al., 2020), IFC model graphs (Exner et al., 2019; Ismail et al., 2018), Knowledge representation graphs (Hor et al., 2018). The graph typology presented in this paper for the export of design episodes is broadly based on the Parametric Building Graph that was introduced by Abualdenien & Borrmann (Abualdenien & Borrmann, 2021) for capturing and storing the detailing patterns.

In Case-Based Reasoning (CBR), qualitative evaluations have been proposed as a mapping mechanism for recording design scenarios. Episodic case-based design is a type of design that represents individual design circumstances using design episodes that match certain design elements' configurations (Maher et al., 1995). Accordingly, the concept of design episodes (Zahedi et al., 2021) follows the same principle in breaking down the whole final design into various episodes that can be traced and used in the future to address similar recurring problems and tasks. Zahedi et al. (Zahedi et al., 2021) proposed a way for digitally recording tacit design knowledge and decisions while also taking into account their aim and subjective evaluations. Explanation tags and spatial and semantic restrictions are assigned to specific model elements and/or their attributes to express architectural concepts and subjective assessments and explanations. By applying Design Episodes and storytelling techniques, various sections and parts of a design are digitally documented and Natural Language Processing (NLP) is used to facilitate querying owner requirements and regulatory documents (Zahedi et al., 2021). Neuckermans et al. (Neuckermans et al., 2002) and Heylighen et al. (Heylighen, Neuckermans, et al., 2007) took a graphical approach, designing and prototyping "visual keys" for visually indexing complete design cases. They also used this approach as an access mechanism in the context of their case-based design (CBD) tool called DYNAMO (Dynamic Architectural Memory Online).

3. Concept and Methodology

There are numerous implicit design considerations and domain-specific experiences hidden in every building design. Figure 1 shows the design process and its abstraction levels projected by our concept and methodology. As shown in this figure, every building project must adhere to a variety of owner specifications, rules, and boundary constraints. Next are the architectural principles and concepts, which are selected and used on the concept level to meet the clients' needs and represent them in the design. The chosen concepts are subsequently implemented by modeling and describing the individual pieces, including geometric and semantic information, topological connections, and functional dependencies (on the design level). This paper utilizes the notions of design episodes and explanation tags that play a role in documenting design

decisions on the concept level. These concepts will be discussed based on another manuscript submitted for publication by Zahedi et. al. (Zahedi et. al., 2021).

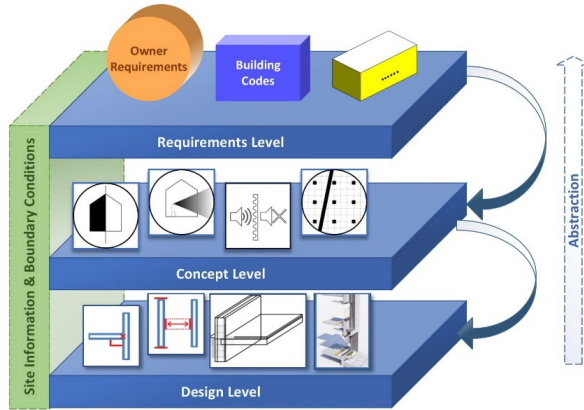


Figure 1. The design process is depicted using abstraction layers (Abualdenien & Borrmann, 2021; Zahedi et. al., 2021)

3.1. EXPLANATION TAGS

Rejecting, selecting, and further detailing architectural design decisions and variants depends not only on objective (quantitative) criteria but also on subjective (qualitative) criteria. In addition to recording the building model and quantitative criteria, qualitative and descriptive explanations and evaluations are also necessary to be captured, for the documentation of variant selection to make the decisions made and their justifications, e.g. design quality or aesthetics, comprehensible and to support the correct interpretation of the designers' choices (Zahedi et. al., 2021).

The goal is to store and document design decisions and variant selections without significantly interrupting the design process. For this purpose, a collection of identified keywords and visual icons (from the vocabulary of architectural design and other domain experts) with descriptions and examples of usage, are offered to the architect as so-called Explanation Tags, in the interest of clarifying and documenting his design decisions (Zahedi et. al., 2021). In designing the explanation tags, specific attention is paid to sustainability requirements introduced by the Federal Ministry of Transport and Digital Infrastructure in Germany (Fuchs et. al., 2013). However, this is just an open-ended collection of explanation tags, and the add-in provides the possibility to add custom-designed tags to this collection. Furthermore, the users can export or import their individual collections of tags as an archive via the add-in. During design in a BIM authoring tool, (Autodesk Revit in the case of this paper) the architect is given a collection of structured pictogram explanatory tags that cover most design criteria and concepts in the architects' vocabulary so that one can argue and justify the design decisions by adding and tagging these explanatory tags to building components or spaces and their respective attributes (Zahedi et. al., 2021).

3.2. DESIGN EPISODES

One of the solutions discussed in the literature for conveying tacit architectural knowledge is storytelling (Martin et al., 2003). Although this does not transfer large amounts of information, it is a means of promoting a better understanding (Heylighen et al. 2007). The outcome is more about the ideas, processes, decisions, and implications of the interactions presented in the story (Zahedi et. al., 2021). To this end, the design episode method, developed by Zahedi et. al. is used to divide the final design into smaller chapters and sections where each of these episodes relates to a design situation and offers a solution for it using storytelling techniques (Zahedi et. al., 2021). Design Episode is a method for summarizing and documenting a certain part of the design, using textual descriptions, coupled with the selection of the associated building elements and spaces (Zahedi et. al., 2021). Both concepts of explanation tags and design episodes and their utilization via our Revit add-in will be further explained using an example in the implementation section. Another associated goal is to export the recorded tacit design knowledge to a graph database and prepare this captured knowledge for future inquiries by other architects in search of inspirations and answers to similar design tasks and problems. Subsequently, the add-in that is developed for Autodesk Revit will be further explained in the next chapter.

4. Implementation

In summary, the implemented add-in in Revit, allows the architects to accomplish the following:

- They can use design episodes to explain their motivations and intentions for different sections and aspects of the design via storytelling and in the form of textual descriptions together with the inclusion of corresponding model elements.
- They can use explanation tags to highlight and clarify the reasons and goals for different design decisions in a more graphical and explanatory way.
- They can export the documented tacit design knowledge in the form of various design episodes to a graph database (Neo4j) for later use and retrieval.

In general, the add-in simply adds a tool to Revit's toolkit, which collectively implies adding a tool to the Revit-ribbon. The add-in was written in C# (Microsoft programming language) for the code-behind and backend, whereas XAML (Extensible Application Markup Language) was used for the User Interface (UI). The add-in interacts with the Revit API, allowing users to communicate with the Revit environment and, as a result, read and write to any open Revit models. After being installed, the add-in is accessible under the Design Documentation tab in the Revit toolbar.

The add-in serves two main purposes, each of which is featured via its main tab in the tool. The first is to provide users with capabilities related to explanation tags. Namely, to allow the users to set and search explanation tags in the BIM model. To do so, the users can stage their desired tags and elements, and then assign various tags to either elements or their attributes. In other words, the user can associate a set of explanation tags to an element as a whole (*element-global explanation tag*), or assign them to a specific parameter or attribute of an element (*parameter-local explanation*

tag) within the Revit context. An element in the Revit context is understood as a Revit element with an ID which could be different building components or spaces. Figure 2 shows the staging of several building elements and explanation tags for assigning. Moreover, an info log explains and reports on different actions that are taken in the add-in. In addition to setting explanation tags to elements, the user can also explore and search for certain elements that have specific explanation tags assigned to them, together with various sorting and filtering capabilities. Furthermore, the users can edit and explore the list of the already available explanation tags. At the same time, they can also create their own new tags and add them to the collection of existing explanation tags. Within the scope of this add-in, an explanation tag is an object that has a name, an image, a description, and zero or more synonyms. Synonyms are different explanation tags that have overlapping meanings or are synonymous with each other. The add-in is developed in a way so that the explanation tags are model-independent, which means they are kept globally and under the user's application data. This implies that explanation tags may be imported and exported to archives and used across various models.

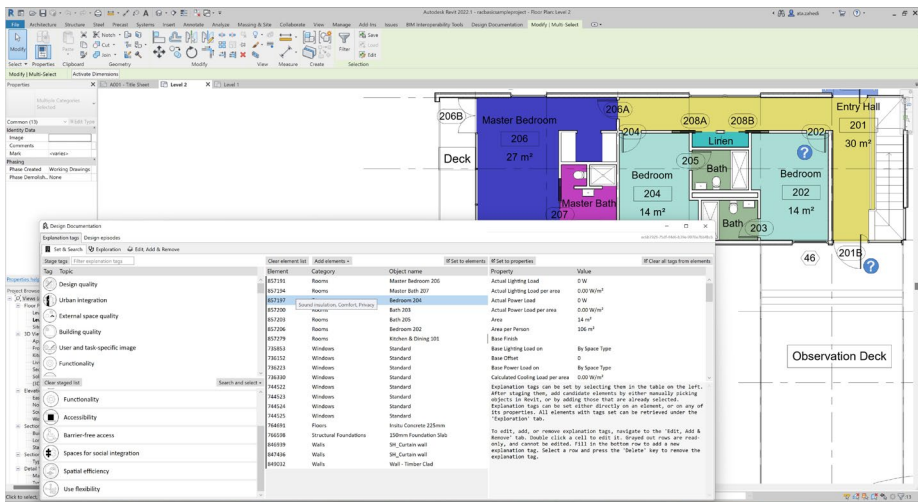


Figure 2. Revit Add-in Tab for manipulating Explanation Tags showcasing the staging of some building elements and tags for assigning.

The second purpose of the add-in is to create and retrieve design episodes. Within the scope of the plugin, a design episode is an object with a name and description that contains a set of elements from the Revit model. In other words, upon creating a design episode, the user selects the set of elements (together with their attributes and possible explanation tags) that express this episode or chapter of design and then provides a name and description, using storytelling manner, for this design situation while explaining in more details the design motives, rationale, and argumentation. Figure 3 illustrates an example for creating design episodes. Unlike the explanation tags, the design episodes are model-bound rather than model-agnostic. This means that the design episodes are stored within a Revit document and can be passed on together with

the BIM model. Just like explanation tags, design episodes can be also explored and retrieved, while different search and filtering possibilities are available to facilitate this feature. Additionally, design episodes can be modified or deleted, and if need be, collectively imported or exported to an archive.

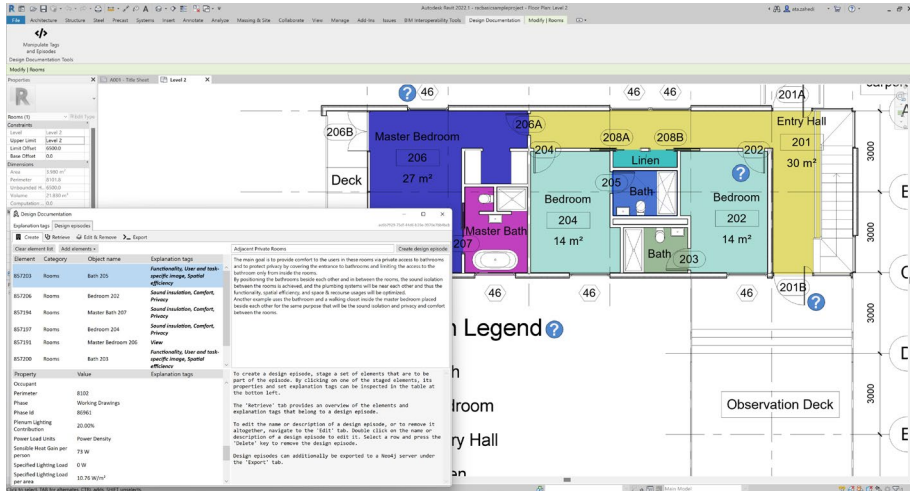


Figure 3. Revit Add-in Tab for manipulating Design Episodes showcasing the "Adjacent private rooms" as an example for creating a design episode.

Individual design episodes can also be exported as a CSV file or a Labeled Property Graph (LPG) in Neo4j. In order to start with the exported graph typology, we need to have a better understanding of what this Neo4j export implies. Neo4j enables us to model objects and relationships between them as a labeled property graph. As mentioned before, the graph typology provided in this research for the export of design episodes is loosely based on Abualdenien & Borrmann's Parametric Building Graph for capturing and storing detailed patterns (Abualdenien & Borrmann, 2021). Figure 4 demonstrates an example graph visualization of a design episode in the Neo4j database. Two sorts of nodes will be present in our network. The *Design Episode* node, which, as the name suggests, is an exported design episode, and the *Element* node, which is an exported episode element, also depicted via an *EpisodeElement* flag that is set to true on these nodes. There are several relationships among the elements and design episodes. The first relationship is the *EpisodeElement* relationship, which indicates that an element belongs to a design episode. Some other relationships between the elements are, *ContainedIn*, *IsAdjacent*, *IsConnected*, and *Has* relationships. *ContainedIn* relationship specifies that an element is contained in another element. An *isAdjacent* relationship between two nodes implies that the corresponding elements in the Revit model are adjacent to each other, whereas, *IsConnected* suggests that the originating elements are directly connected to each other in the Revit model. The *Has* relationship indicates that one element belongs to another element. In addition, each node has several attributes associated with it. *Model Identifier* and *Export DateTime* as strings are assigned to design episode nodes in order to link them to their originating Revit

model and make it easier to trace them. The GUID attribute helps us in distinguishing between different design episodes with similar names. Finally, there's the design episode's Name and Description, which respectively represent and describe the corresponding design situation and the motives behind this episode of design, using storytelling techniques. Furthermore, as the basis for the element nodes, we have the EpisodeElement boolean flag, and some properties that are directly taken from Revit, such as ID, Unique ID, and Object Name, which are in that order; element's Revit-provided id and unique id, and name. The *ExplanationTags* property holds the element's *element-global explanation tags*. Moreover, when exporting a design episode to Neo4j, the user can select and choose the desired parameters of each element in the design episode to be exported or not. For each of these parameters that get exported, there is also a property (assigned to the element node) that contains the corresponding parameter along with its value from Revit. Similarly, there is an *ET[Property Name]* attribute that maps the set of *parameter-local explanation tags* to the element node for each of the exported parameters that has parameter-local explanation tags assigned to them.

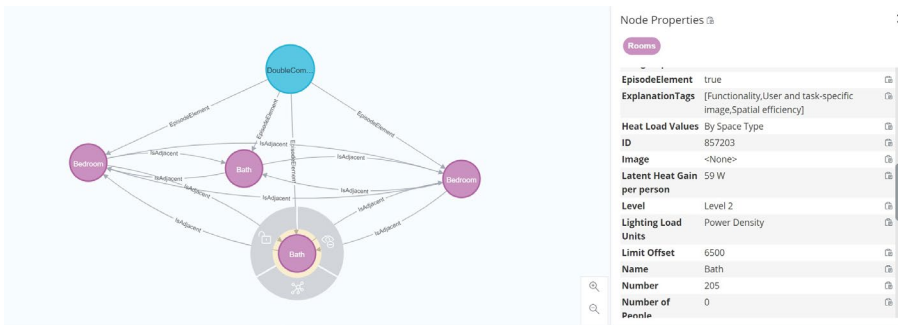


Figure 4. An Screenshot of the Neo4j database showcasing the graph Typology of the same "Adjusent private rooms" design episode when exported into Neo4j database.

5. Conclusion

A crucial step in communicating with owners and domain experts is to document design knowledge, objectives, and conclusions. This also makes future assessment and reuse of finished projects easier. Building industry and especially the architectural design process lack proper documentation and preservation of tacit design knowledge, which could be enormously useful to address and solve similar design tasks and problems in the future. This precious knowledge often gets lost and forgotten due to the absence of appropriate explanation and documentation. Proper design documentation, we believe, may lead to improved reuse of design knowledge and expertise.

Existing BIM models contain only plain geometry and semantics, with no reasoning or explanation for design choices. The development and demonstration of an add-in for Revit that utilizes the ideas of so-called Explanation Tags and Design Episodes introduced in another manuscript submitted for publication by the authors

(Zahedi et. al., 2021) to digitally explain and document design reasoning and choices is described in this work. Furthermore, the add-in also allows the user to export design episodes as LPG to a Graph-Database (Neo4j) or CSV file for future reference. Following that, the next step is to explore and query the graph database for similar designs that can address and resolve future design challenges. By explicitly documenting the design decisions and rationale, resulting in capturing the tacit architectural design knowledge, this work adds to the United Nations Sustainable Development Goals, particularly those related to 'Industry, Innovation, and Infrastructure' and 'Sustainable Cities and Communities'. Special attention is made to 'Sustainability Requirements in Planning Competitions' (SNAP-Systematik für Nachhaltigkeitsanforderungen in Planungswettbewerben) upon identifying appropriate explanation tags for design decisions' documentation in the developed Revit add-in.

Acknowledgements

We gratefully acknowledge the support of the German Research Foundation (DFG) (DFG, last updated: 2021) for funding the project under the grant FOR-2363. We also thank Max van Deuzen for helping us to implement this add-in as part of his interdisciplinary student project.

References

- Abualdenien, J., & Borrmann, A. (2021). PBG: A parametric building graph capturing and transferring detailing patterns of building models. In *Proc. of the Conference CIB W78*.
- Al Hattab, M., & Hamzeh, F. (2018). Simulating the dynamics of social agents and information flows in BIM-based design. *Automation in Construction*, 92, 1–22.
- Zahedi, A., Abualdenien, J., Petzold, F. & Borrmann, A. (2021). Documenting Design Decisions using Design Episodes, Explanation Tags and Constraints: Manuscript submitted for publication.
- Ayzenshtadt, V., Espinoza-Stapelfeld, C., Langenhan, C., & Althoff, K.-D. (2018). Multi-Agent-Based Generation of Explanations for Retrieval Results Within a Case-Based Support Framework for Architectural Design. In *ICAART* (1).
- Cao, Q., & Protzen, J.-P. (1999). Managing design information: Issue-based information systems and fuzzy reasoning system. *Design Studies*, 20(4), 343–362.
- DFG. (last updated: 2021). *Deutsche Forschungsgemeinschaft e.V.* <https://www.dfg.de/>
- Dubey, R. K., Khoo, W. P., Morad, M. G., Hölscher, C., & Kapadia, M. (2020). AUTOSIGN: A multi-criteria optimization approach to computer aided design of signage layouts in complex buildings. *Computers & Graphics*, 88, 13–23.
- Exner, H., Abualdenien, J., König, M., & Borrmann, A. (2019). Managing Building Design Variants at Multiple Development Levels. In *Proc. of the 36th International Council for Research and Innovation in Building and Construction (CIB W78)*.
- Gänshirt, C. (2012). *Werkzeuge für Ideen: Einführung ins architektonische Entwerfen*. Walter de Gruyter.
- Hamieh, A., Makhlof, A. B., Louhichi, B., & Deneux, D. (2020). A BIM-based method to plan indoor paths. *Automation in Construction*, 113, 103120.
- He, T., Zhang, J., Lin, J., & Li, Y. (2018). Multiaspect similarity evaluation of BIM-based standard dwelling units for residential design. *Journal of Computing in Civil Engineering*, 32(5), 4018032.

- Heylighen, A., Martin, W. M., & Cavallin, H. (2007). Building stories revisited: unlocking the knowledge capital of architectural practice. *Architectural Engineering and Design Management*, 3(1), 65–74.
- Heylighen, A., Neuckermans, H., Casaer, M., & Dewulf, G. P. M. (2007). Building memories. *Building Research & Information*, 35(1), 90–100.
- Hor, A. E., Gunho, S., Claudio, P., Jadidi, M., & Afnan, A. (2018). A semantic graph database for BIM- GIS intergated information model for an intelligent urban mobility web application. *Annals of Photogrammetry, Remote Sensing & Spatial Information Sciences*, 4(4).
- Isaac, S., Sadeghpour, F., & Navon, R. (2013). Analyzing building information using graph theory. In *ISARC. Proceedings of the International Symposium on Automation and Robotics in Construction*. Symposium conducted at the meeting of IAARC Publications.
- Ismail, A., Strug, B., & Ślusarczyk, G. (2018). Building knowledge extraction from BIM/IFC data for analysis in graph databases. In *International Conference on Artificial Intelligence and Soft Computing*. Symposium conducted at the meeting of Springer.
- Kolltveit, B. J., & Grønhaug, K. (2004). The importance of the early phase: the case of construction and building projects. *International Journal of Project Management*, 22(7), 545–551.
- Langenhan, C., Weber, M., Liwicki, M., Petzold, F., & Dengel, A. (2013). Graph-based retrieval of building information models for supporting the early design stages. *Advanced Engineering Informatics*, 27(4), 413–426.
- Maher, M. L., Balachandran, M., & Zhang, D. M. (1995). *Case-based reasoning in design*. Psychology Press.
- Martin, W. M., Heylighen, A., & Cavallin, H. (2003). Building² Stories. A hermeneutic approach to studying design practice. In *Proceedings of the 5th European Academy of Design Conference*.
- Martin, W. M., Heylighen, A., & Cavallin, H. (2005). The right story at the right time. *AI & SOCIETY*, 19(1), 34–47.
- Mattern, H., & König, M. (2018). BIM-based modeling and management of design options at early planning phases. *Advanced Engineering Informatics*, 38, 316–329.
- Meng, Z., Zahedi, A., & Petzold, F. (2020). Web-Based Communication Platform for Decision Making in Early Design Phases. In *Proceedings of the 37th International Symposium on Automation and Robotics in Construction (ISARC)*.
- Neuckermans, H., Heylighen, A., & Morisse, P. (2002). Visual Keys to Architectural Design. Fuchs, M., Hartmann, F., Henrich, J., Wagner, C., & Zeumer, M. (2013). SNAP Systematik für Nachhaltigkeitsanforderungen in Planungswettbewerben-Endbericht. Bonn, Berlin.
- Steinmann, F. (1997). *Modellbildung und computergestütztes Modellieren in frühen Phasen des architektonischen Entwurfs*. [Bauhaus University, Weimar, Germany].
- Zahedi, A., Abualdenien, J., Petzold, F., & Borrmann, A. (2019) Minimized Communication Protocol Based on a Multi-LOD Meta-Model for Adaptive Detailing of BIM Models. In *EG-ICE 2019*.
- Zahedi, A., & Petzold, F. (2019). Adaptive Minimized Communication Protocol based on BIM. In *2019 European Conference on Computing in Construction*.
- Zeiler, W., Savanovic, P., & Qanjel, E. (2007). Design decision support for the conceptual phase of the design process.

IMPLEMENTATION OF POINT CLOUD AND BIM TECHNOLOGIES IN A CONSTRUCTION WORKFLOW

A case study of a building project in Yuecheng District, China

ANDRE LI¹, HONG ZHANG², WEIWEN CUI³ and JIE HUANG⁴

^{1,2,3,4}*School of Architecture, Tsinghua University.*

¹ *lad20@mails.tsinghua.edu.cn, 0000-0002-6723-0033*

² *zhanghong@tsinghua.edu.cn, 0000-0002-1793-0429*

³ *cuiww19@mails.tsinghua.edu.cn, 0000-0001-9486-7681*

⁴ *jie-huan18@mails.tsinghua.edu.cn, 0000-0001-6720-7530*

Abstract. In recent years, there has been a surge of retrofitting and building projects in rural China, to elevate the living standards in local areas. However, with the conventional use of surveying and inspection instruments, the amount of construction errors account to substantial waste of materials, time and labour. The issue is magnified in the current context that emphasises on efficient utilisation of resources. The emergence of laser scanning and BIM technologies is evident with scanning equipment and software being more accessible. This paper explores the use of the two technologies, to be integrated into the a construction workflow. The research includes a self-conducted site survey, data collection, data processing and analyses. The processed point cloud data is extracted and compared to the as-designed BIM model, to analyse and assess the construction errors in various scales. The result displays a significant portion of the building being out of tolerance and its causes. A theoretical framework is proposed to integrate point cloud and BIM technologies, not only to document and assess the overall building dimensional accuracy, but also to minimise construction errors and waste, ensuring a responsible consumption and production of building materials.

Keywords. BIM; Laser Scanning; Point Cloud; Construction Workflow; Cast-in-situ Concrete Structure; Tolerance Compliance; SDG 12.

1. Introduction

Architectural design in rural China has played a significant role in recent years, as part of the rural revitalisation strategy, leading to a significant increase of construction projects. Concurrently, digital technologies such as BIM have been utilised more widely in the context of information revolution. Their role to improve the sustainability of architecture and its construction process has been continually explored. It is noted

by the International Energy Agency (IEA, 2019, p. 9) that the building and construction sector is responsible for '39% of energy and process-related carbon dioxide (CO₂) emissions in 2018, 11% of which resulted from manufacturing building materials and products such as steel, cement and glass'. Furthermore, construction quality control remains a problem that additional costs of removal and replacement of defective concrete elements could account to 12% of a project's contractual value (Puri et al., 2018). This issue is magnified with construction in rural China (Ru et al., 2020): 1) Safety; 2) Quality; 3) Lack of technical drawings; 4) Lack of geological survey; 5) Lack of training and basic building knowledge for rural construction workers.

Conventionally, the role of dimensional accuracy in construction is ensured by the contractors, surveyors or inspectors, with the use of tape measures, theodolite, total stations, etc. In the context of reconsidering the global carbon impact, for Sustainable Development Goal 12 in particular, it is vital to minimise waste generation through reducing additional building materials and preventing construction errors. With the emergence of laser scanning technologies that captures the complete point cloud scan of the entire surrounding, its potential to be integrated into the construction workflow and assist with the current issue is questioned.

2. Literature Review

Point cloud technologies not only are able to conduct more accurate surveys, architectural elements unreachable can now also be scanned, modelled and analysed. The current application of point cloud and building information modelling (BIM) technologies is explored across the AEC industry. Methods have been implemented for the generation of 3D elements from point cloud data to BIM models, as Tamke et al. (2014) investigated the approach to automatically extract semantic spatial information of point cloud from interior building scans and Rodríguez-Moreno et al. (2018) proposed a method of modelling heritage architecture from point cloud. Laefer and Truong-Hong (2016) proposed a method to identify automatically steel structural members from laser point cloud scans and generate the geometry compatible for BIM models. Advantages and effectiveness have been shown by incorporating point cloud and BIM for tracking construction progress (Kim et al., 2020), despite the labour intensity of converting point cloud to BIM (Qu & Sun 2015). Methods have also been proposed for assessment of structural elements for compliance in a surface level (Puri et al., 2018).

3. Research Objective

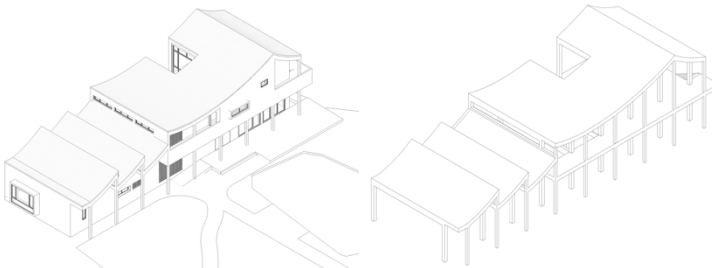
This paper seeks to further extend the use of the two technologies, to be integrated into the workflow of a construction. It questions the limitations of current surveying and construction methods, especially for building projects in rural China. This paper aims to provide a framework for incorporating BIM and point cloud scanning technologies into future projects in similar context, scale and type, addressing the Sustainable Development Goal 12 of responsible consumption and production.

4. Methodology

A case study is conducted to explore the use of BIM and point cloud technologies in a building project. The investigated building is located in Anqiaotou village in Yuecheng District, Zhejiang Province, China. The building is a two-storey concrete structure with masonry walls (Figure 1&2). Its floor area is approximately 380sqm. A BIM model is built in Autodesk Revit, including the disciplines of architecture (Figure 3) and structural engineering (Figure 4) according to the final design intentions.



*Figure 1. Image of the investigated building during construction (left);
Figure 2. Image of the investigated building after construction (right)*



*Figure 3. Architectural model of the investigated building in BIM (left);
Figure 4. Structural model of the investigated building in BIM (right)*

A set of point cloud data is collected with a 3D laser scanner, Leica BLK360, during its construction, after the concrete structure and part of the masonry walls were built. The accuracy of the scanner is specified to be 4mm at 7m and 7mm at 20m. The point cloud scans are automatically registered using point cloud processing software, Trimble Realworks, forming the complete point cloud models of the surveyed building (Figure 5). The overall cloud-to-cloud error from the registration is 5.95mm. The two numbers of error would be considered for the surface analysis. As the analysis is focused on the concrete structure of the building, the components of the cast-in-situ concrete, including columns, floor slab, beams and roofs are extracted from the point cloud model (Figure 6).



*Figure 5. Registered point cloud of the building (left);
Figure 6. Extracted structural point cloud model (right)*

Geomagic Control X, a quality control and inspection software, mainly used in the manufacturing industry, is implemented to align the point cloud and its respective structural part in the BIM model. As the entire building is a new construction, there is no reference point, therefore an effective way to compare the overall building geometry is to apply the software's automatic alignment with the least-squares method.

Surface analyses are carried in both 3D and 2D. Comparisons are made with the national standards for construction tolerance in China, GB50204-2015 'Code for quality acceptance of concrete structure construction' (Ministry of Housing and Urban-Rural Development of the People's Republic of China, 2015). The dimensional tolerance for various components is summarised in Table 1.

Table 1. Summary of tolerance for relevant components

Component	Tolerance (mm)
Axis location of columns, walls and beams	8
Floor level	± 10
Cross sectional dimensions of columns, slabs, walls and beams	+10, -5

Using the method of worst-case analysis, the errors from the laser scanner and point cloud registration are accounted with summation. After the overall building is compared and analysed, the process is repeated for smaller components to draw further observations and conclusions.

5. Result and Analysis

5.1. OVERALL BUILDING

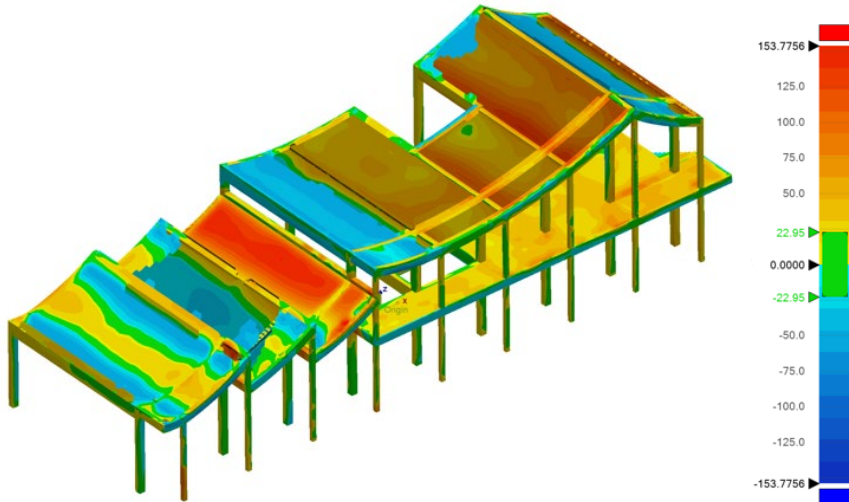


Figure 7. 3D comparison result

Taking the largest tolerance from Table 1, an overall tolerance of 10mm is used for analysing the entire building. Combining with the errors of the scanning equipment and point cloud registration, the sum equals 22.95mm for the assessment of the overall building. As shown in Figure 7, a range of deviation is detected, from -145mm to 208mm. Only 29.77% of the building is within tolerance. As the surfaces within tolerance is shown in green, it can be seen visually that columns generally stay within the tolerance. Most major deviations are observed from the floor and roof slabs.

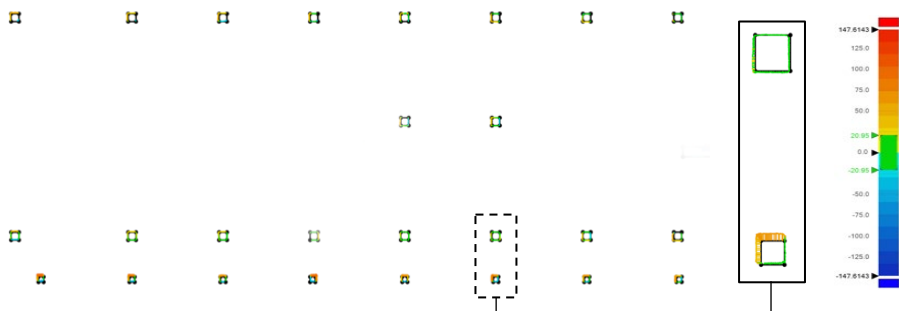


Figure 8. 2D comparison in plan (left); Figure 9. Close-up view on two of the columns (right)

An analysis in plan is made at the centre level between the ground and first floor levels as shown in Figure 8. Referring to Table 1, the location of the columns is taken as 8mm, therefore tolerance is added with other errors to 20.95mm. As observed from the 3D comparison, the columns have a larger portion being within tolerance, 46.86%. Furthermore, Figure 9 displays a close-up of two of the columns. The top one is shown to be in the correct cross-sectional size. The bottom column has two sides deviated outwards by 40-60mm, while the other two sides shown to be correct, indicating the structural member size difference between the as-built and as-designed dimensions.

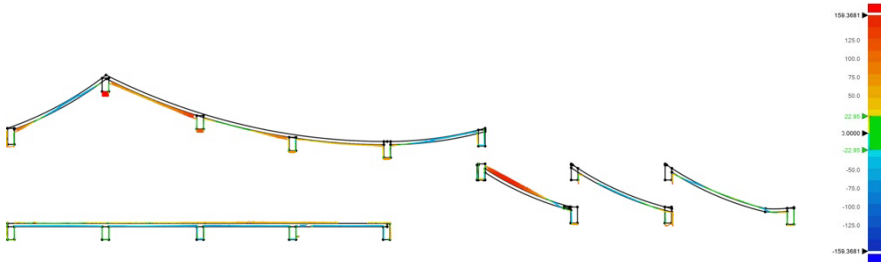


Figure 10. 2D comparison in long section

The deviation of roof slabs is more clearly shown in section (Figure 10). As the tolerance is set to be the same as for the overall building, 22.95mm, the portion of the section being within tolerance is 24.51%. It is evident that there is a significant deviation of the built roof slabs, with the maximum being 180mm away. Comparing the top and bottom surfaces, the entire floor slab is also observed to be elevated by approximately 50mm. Both the roof and floor slabs are explored individually. It can also be seen that the sides of floor and roof beams mostly stay within tolerance.

5.2. FLOOR SLAB

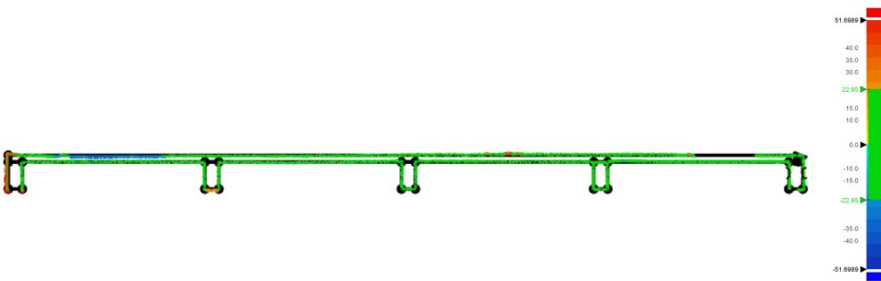


Figure 11. 2D comparison in long section of the slab in the first floor

The first-floor slab is further extracted to be individually compared to its respective point cloud model. The comparison displays a much higher alignment between the two, having 87.11% being within the tolerance of 22.95mm. There are spots showing unevenness of the slab. The reason is possibly due to pieces of occlusion during construction.

5.3. ROOF SLAB

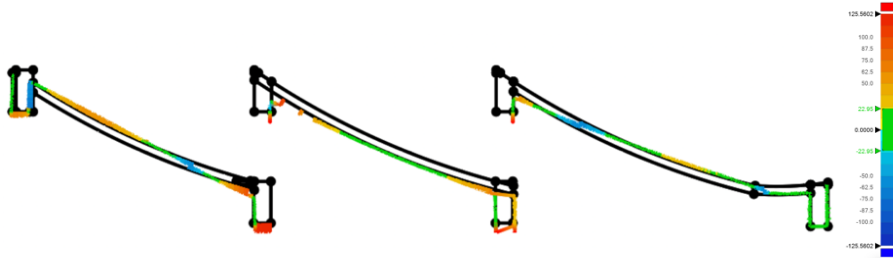


Figure 12. 2D comparison in long section for the first-floor slab

As observed from the overall building analysis, the roof slabs have a significant difference from its as-designed form, despite being aligned independently. The deviation ranges between -67mm to 166mm. Furthermore, the deviation is too high that the wrong surface of the roof is compared for some parts, therefore the true deviation would be larger. From Figure 12, it can be observed that the built roof form has been straightened, hence creating such deviation from the curved roof as designed.

6. Discussion

Table 2. Summary of analysis results

Component	Within Tolerance	Deviation Range
Entire building	29.77%	-145mm to 208mm
Columns - plan	46.86%	-147mm to 134mm
Entire building - section	24.51%	-124mm to 180mm
Floor slab - section	87.11%	-37mm to 68mm
Roof slab - section	46.82%	-67mm to 166mm

From the overall analysis, it is observed that even as a worst-case analysis, only 29.77% is within the allowable tolerance. If tolerance compliance is strictly enforced, a significant amount work would be required to be demolished and rebuilt, leading to a great amount of construction waste.

From the separate analyses, further general observations are drawn visually. For example, a structural member size difference can be indicated with two adjacent sides deviating outwards while the other two sides stay correct in position. The dimensions in the construction are relatively more accurate in the horizontal plane, as observed from the horizontal locations of the beams and columns. In comparison, the elements in the vertical plane such as roof slabs are more difficult to control. It is also noted that elements with curved surfaces require additional attention.

The analyses reveal several limitations of conventional surveying and modelling techniques used in the project. The analyses in various scales display that with the use of instruments such as tape measures and theodolites, the local dimensions of each component can generally be maintained within construction tolerance. However, as

human errors accumulate, it creates a big portion being out of tolerance. It displays the significance of overall building dimensions that can be captured accurately by a laser scanner.

Before the construction continues, it is important to identify the crucial dimensions, forms and levels. In this case, the masonry walls are enclosed by the concrete structural frame. Without the awareness, errors would be carried on and magnified to the later stages of the construction process, such as prefabricated elements and fixed cabinets.

7. Conclusion

The case study displays a method to comprehensively assess the construction quality of a building in terms of dimensional tolerance compliance. Apart from analysing the overall building, the components of a building can also be extracted to be analysed separately to investigate the cause for each unexpected result. As the number of studies accumulate, the common spots of possible errors would become more apparent. The architect or the site inspector would be able to pay more attention to the common points before construction. In this case, it would be the curved roof form and the height of vertical elements. The case study reveals the importance of maintaining dimensional accuracy to minimise additional materials and works.

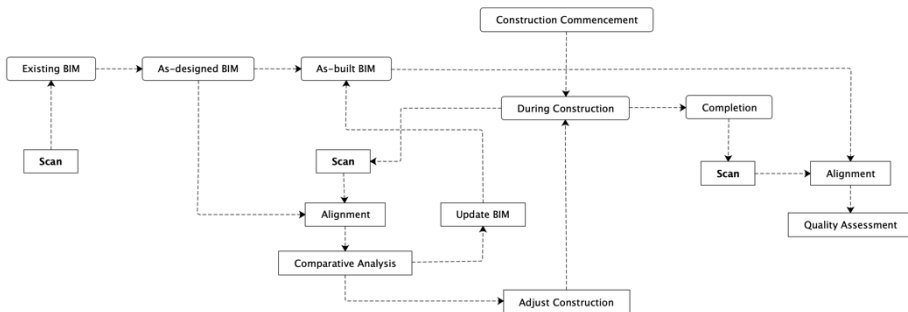


Figure 13. Construction workflow integrated with point cloud and BIM technologies

A theoretical framework (Figure 13) is proposed for implementing point cloud and BIM technologies into projects in similar scale and contexts. The framework is advised to be utilised in three stages (before, during and after construction), to have a more informed design decision-making, to prevent inaccuracy and to improve construction quality. Before construction, especially for projects with existing building parts, a scan is advised to record and reconstruct the existing building model. The scan during construction is vital to determine the as-built condition, to determine if there should be a redesign or reconstruction if there is any part with significant error. There can be multiple scans during construction, such as main structure, external walls, fixed furniture, etc. The scan after construction assists to document and provides a way of assessment of the construction quality of the project.

The proposed workflow allows architects to extend their roles, as the designer of the building, to discover and communicate the construction issues. In addition, it extends the responsibility of the construction team to maintain their accuracy as the

constructed buildings are now able to be documented objectively. As the critical components can be identified, the additional costs of construction waste and labour can be reduced, ultimately leading to a more efficient and sustainable construction workflow.

8. Future Works

For cast in-situ concrete structure, as opposed to structure such as steel frames, there is an issue of using formwork that the final form of the concrete structure is unknown until the concrete is poured, cured and its formwork is taken off. When an intolerable error or deviation is discovered, it would require a significant amount of costs, material and labour to demolish and rebuild the parts. With a known consistent thickness of the formwork material, it presents the potential of predicting and modelling the external surfaces of the formwork, then be compared to the point cloud scan of the formworks before pouring the concrete.

As the technologies of point cloud scanning become more advanced and affordable, it is anticipated that the tool-set will be able to be implemented into the construction process in realtime. In addition, due to the lower accuracy level of aerial-based scanning with drones, the study was focused on terrestrial point cloud scans. As the accuracy of drone-based scanning improves over time, it would also be beneficial to be integrated into the process.

Acknowledgements

This work is supported by the General Program of National Natural Science Foundation of China (52078265), "Research on the Building Information Theory and BIM-based Integrated Mechanism for Existing Building Retrofitting".

References

- IEA. (2019). *Global Status Report for Buildings and Construction 2019*. IEA. Retrieved February 6, 2022, from <https://www.iea.org/reports/global-status-report-for-buildings-and-construction-2019>
- Kim, S., Kim, S., Lee, D-E. (2020). Sustainable Application of Hybrid Point Cloud and BIM Method for Tracking Construction Progress. *Sustainability*. 2020; 12(10):4106. <https://doi.org/10.3390/su12104106>
- Laefer, D. & Truong-Hong, L. (2017). Toward automatic generation of 3D steel structures for building information modelling. *Automation in Construction*. 74. 66-77. <https://doi.org/10.1016/j.autcon.2016.11.011>.
- Ministry of Housing and Urban-Rural Development of the People's Republic of China. (2015). *Code for Quality Acceptance of Concrete Structure Construction: GB50204-2015*. China Architecture & Building Press. <https://www.chinesestandard.net/PDF.aspx/GB50204-2015>
- Puri, N., Valero, E., Turkan, Y. & Bosché, F. (2018). Assessment of Compliance of Dimensional Tolerances in Concrete Slabs using TLS data and the 2D Continuous Wavelet Transform. *Automation in Construction*, 94(2018), 62-72. <https://doi.org/10.1016/j.autcon.2018.06.004>
- Qu, T., & Sun, W. (2015). Usage of 3D point cloud data in BIM (building information modelling): Current applications and challenges. *Journal of Civil Engineering and Architecture*, 9(11), 1269-1278.

- <https://doi.org/10.17265/1934-7359/2015.11.001>.
- Rodríguez-Moreno, C., Reinoso, J. , Rivas-López, E., Gómez-Blanco, A., Ariza-López, F., Ariza-López, I. (2016). From point cloud to BIM: an integrated workflow for documentation, research and modelling of architectural heritage. *Survey Review*. 50. 1-20. <https://doi.org/10.1080/00396265.2016.1259719>.
- Ru, Q., Fen, J. & Lu, Q. (2020). Application and Prospects of Prefabricated Buildings in Rural Areas of China. *Journal of Physics: Conference Series*. Volume 1637. 012078. <https://doi.org/10.1088/1742-6596/1637/1/012078>
- Tamke, M., Blümel, I., Ochmann, S., Vock, R., & Wessel, R. (2014). From Point Clouds to Definitions of Architectural Space: Potentials of Automated Extraction of Semantic Information from Point Clouds for the Building Profession. In E. M. Thompson (Ed.), *Fusion: Proceedings of the 32nd International Conference on Education and research in Computer Aided Architectural Design in Europe* (Vol. 2, pp. 557-566). eCAADe (Education and Research in Computer Aided Architectural Design in Europe) and ITU / YTU.

ENABLING COMPONENT REUSE FROM EXISTING BUILDINGS THROUGH MACHINE LEARNING

Using Google Street View to Enhance Building Databases

DEEPIKA RAGHU¹, ARETI MARKOPOULOU², MATHILDE MARENGO³, IACOPO NERI⁴, ANGELOS CHRONIS⁵ and CATHERINE DE WOLF⁶

^{1,6}*ETH Zurich, Dept. of Civil, Environmental and Geomatic Engineering (D-BAUG), Stefano-Franscini-Platz, 8093 Zurich, Switzerland.*

^{2,3,4,5}*Institute for Advanced Architecture of Catalonia, Carrer de Pujades, 102, 08005, Barcelona, Spain*

¹*draghu@ethz.ch, 0000-0003-0725-6415*

²*areti@iaac.net, 0000-0002-5400-0837*

³*mathilde.marengo@iaac.net, 0000-0002-6249-0960*

⁴*iacopo.neri@iaac.net, 0000-0002-9246-6494*

⁵*angelos.chronis@iaac.net, 0000-0002-6961-2975*

⁶*cdewolf@ethz.ch, 0000-0003-2130-0590*

Abstract. Intense urbanization has led us to rethink construction and demolition practices on a global scale. There is an opportunity to respond to the climate crisis by moving towards a circular built environment. Such a paradigm shift can be achieved by critically examining the possibility of reusing components from existing buildings. This study investigates approaches and tools needed to analyse the existing building stock and methods to enable component reuse. Ocular observations were conducted in Google Street View to analyse two building-specific characteristics: (1) façade material and (2) reusable components (window, doors, and shutters) found on building facades in two cities: Barcelona and Zurich. Not all products are equally suitable for reuse and require an evaluation metric to understand which components can be reused effectively. Consequently, tailored reuse strategies that are defined by a priority order of waste prevention are put forth. Machine learning shows promising potential to visually collect building-specific characteristics that are relevant for component reuse. The data collected is used to create classification maps that can help define protocols and for urban planning. This research can upscale limited information in countries where available data about the existing building stock is insufficient.

Keywords. Machine Learning; Component Reuse; Google Street View; Material Banks; Building Databases; SDG 11; SDG 12.

1. Introduction

Billions of tonnes of construction and demolition waste (CDW) is annually disposed of in landfills, causing severe environmental damage (Duan et al., 2019). Mismanagement of CDW significantly contributes to climate change as it causes water, ground, and air pollution which consequently damages ecosystems and affects human health. Studies show that up to 95% of non-hazardous CDW is either reusable or recyclable (Ma et al., 2020). Yet, insufficient access to information on the CDW stream hinder reuse opportunities, resulting in a linear “take-make-waste” economy. The concept of a “circular economy” (CE) is quickly gaining momentum in the construction industry. In a CE, the value resources are maintained for as long as possible to minimise the generation of waste. Recent studies for a CE in the construction industry view ‘buildings as material banks’ (BAMB; Debacker et al., 2016). The focus is on new buildings which are being developed with building information modelling (BIM) to retain high value components for future use. However, these studies do little to address the fundamental barriers of reusing materials and components in already existing buildings which lack digital records. This has led to the reframing of BAMB to ‘existing buildings as material banks’ (E-BAMB; Rose and Stegemann, 2018). In order to successfully reuse components from existing buildings, detailed information about the building stock is required.

The contribution of this research is to investigate the prospect of estimating component reuse from residential buildings that are currently facing renovation or demolition needs in two European cities: (i) Barcelona and (ii) Zurich. The buildings chosen to be studied were built in the 20th century and are deficient of necessary data to enable reuse. Image processing techniques such as deep learning are employed for extracting information on the building components. The methods are applied on street view images of both Barcelona and Zurich to show its applicability despite regional differences. To the authors’ knowledge, this is the first study to identify materials on existing building facades using Google Street View. Prospective reuse measures are then tailored to each building component based on their as-built characteristics. This can enable long-term strategic planning for effective reuse of the residential building stock built in the 20th century.

2. 'As-built' documentation of existing buildings

Public building registers generally collect information on general building statistics (built up area, height, number of floors, etc.) but still lack key indicators on the components of the building. In recent years, laser scanning (LS) technology that can be used to produce BIM models is being increasingly explored to identify component attributes in existing buildings. Although the technology is quite promising, some of the barriers to LS include high costs for the sophisticated equipment, the time consuming and laborious processing of the complex data and the inconvenient and large file types (Uotila et al., 2021). Due to the high expenses associated with the technology, it is only viable in large projects when scheduled for immediate demolition. Another source of information on reusable building components are reused material marketplaces (RMMs). RMMs are supply-led interfaces where building components or products are sold online. Usually, contractors lack incentive to use

RMMs and don't put up their unwanted items for sale. For this reason, RMMs have still not gained enough traction for effective sales. Furthermore, the items are put up on the platform at the very moment they arise as waste, making it difficult to incorporate them into the design of new buildings.

Architects require detailed information about the reusable elements early in the design process. The Pareto principle outlines the importance of time in its ability to influence a project (Figure 1a). The earlier in time decisions are taken in a project lifecycle, the greater the potential to affect the outcome of the project, when compared to decisions taken at a later stage (Chini and Balachandran, 2012). Hence, generating data for an inventory of reusable building components at an urban scale requires quick, economically feasible and simple methods that can complement existing computer vision methods of data collection. Such a 'material database' of reusable materials can allow designers to check the forthcoming availability of components and assess their suitability for reuse in new building projects ahead of time (Figure 1b).

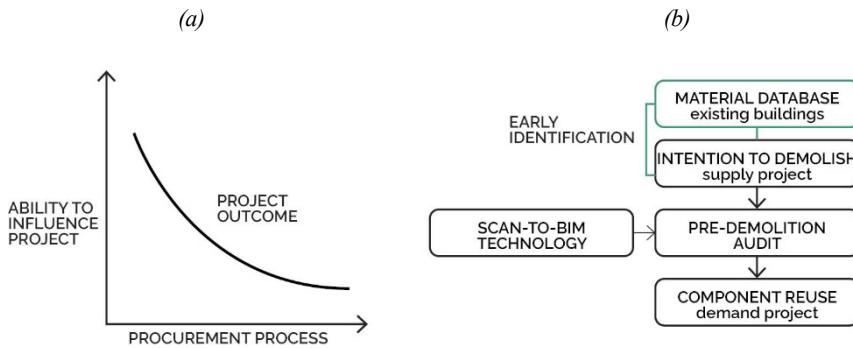


Figure 1a. The Pareto principle as described by Chini and Balachandran et al.; Figure 1b. Material database for cataloguing information on existing buildings using early identification techniques.

Untapped data sources that could help enable E-BAMB through early identification are open, unstructured image datasets of buildings. In this paper, Google Street View, which provides 360-degree panoramic imagery of streets and their surroundings in urban and rural areas across the globe is studied. Many applications in urban planning have been implemented using Google Street view such as estimating the demographic makeup of the cities (Gebru et al., 2017), estimating the building age (Li et al., 2018) and studying the relationships between city appearance and the health of its residents (Dubey et al., 2016). However, utilizing Google Street View for predictions of building-specific suitability for reuse remains an unexplored area of research.

3. Methods

In this section, the methods of collecting data, developing ML models, and applying the algorithms to the residential building stock built between 1925 and 1975 that are facing renovation or demolition needs in Barcelona and Zurich are described. First, public registers in both cities are examined to identify gaps in information required for component reuse. Second, ocular observations are conducted in Google Street View to obtain a comprehensive image dataset. For processing this data, ML models are trained

to predict building-specific characteristics that are hitherto unknown. Third, tailored strategies that help assess the feasibility of reusing the building components are presented. Finally, the potential of using the generated data in building classification maps for urban planning is depicted.

To investigate the data availability in public registers that could be relevant for building component reuse, open government databases in Barcelona and Zurich were queried (Table 1). Registrations of construction year, built-up area or building use, provide insights on the distribution of building types in cities (Figure 2). Furthermore, notifications on ongoing construction, renovation and demolition projects in the cities support studies for estimating the supply and demand of reusable components. Yet, these databases are still limited by the lack of information on reusable components from existing buildings. Based on the gap between the available data in the public registers and the data needed to assess the feasibility of reusing building components, two building-specific characteristics: (i) façade materials and (ii) reusable components (window, doors, and shutters) were chosen to be studied.

Table 1. An overview of the relevant data available to enable reuse in Barcelona and Zurich.

Data source	Building characteristics	Measurement type
Ajuntament de Barcelona	Year of construction	Scale variable (year)
	Number of floors	Ordinal
	Construction condition	Ordinal (ruins, bad, okay, good)
	Building permit	Nominal (construction, renovation, demolition)
Stadt Zurich	Year of construction	Scale variable (year)
	Number of floors	Ordinal
	Building volume	Scale variable (m ²)
	Building permit	Nominal (construction, renovation, demolition)

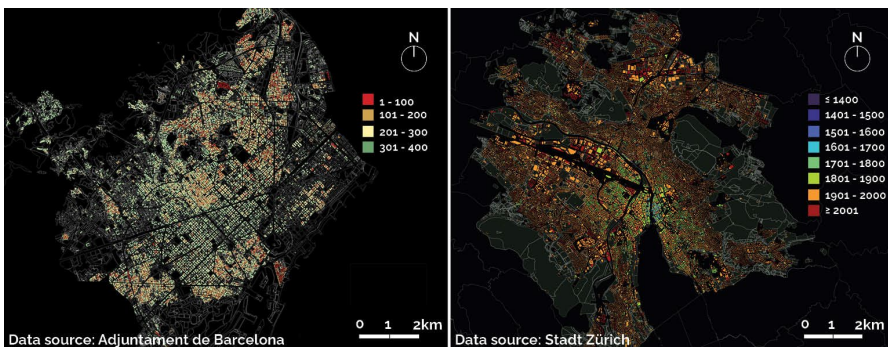


Figure 2a. Map of Barcelona building stock distributed by built-up area (m²).; Figure 2b. Map of Zurich building stock distributed by date of construction (year).

4. Scheme 1: Façade material

Historically, the construction industry has made use of structured data (3D models, databases, spreadsheets) but tended to ignore all other sources of data (text documents, site images, project schedules) as it was too overwhelming to draw conclusions from due to the challenges of data preparation, representation and analysis (Soibelman et al., 2008). Today, emerging technologies like ML allow the processing and management of vast sources of unstructured data. Material classifications via ML are popular among the research community in almost every domain. In the construction industry, most existing literature on material recognition focuses on construction activities in site images for monitoring purposes (Akinosho et al., 2020). This section explores the use of a ML algorithm to detect three building facade materials, namely brick, stone, and mixed material facades. To generate a dataset, 2160 images of the residential stock in Barcelona and 1780 images of the residential stock in Zurich that were constructed between 1945 and 1975, facing renovation or demolition needs were observed in Google Street View. The geo-tagged images are downloaded through the Google Street View API, with the associated metadata, i.e., the image size and pitch value which were set to be 610×610 pixels and 0 degrees, respectively. In some cases, observations were not possible due to lack of coverage in Google Street View. However, the dataset was still sufficient for iterative testing. Samples of the captured images are illustrated in Figure 3a. Images of each facade material type were manually classified by placing them in folders with corresponding IDs. The data was divided into three sections: 70% was used for training, 10% for validation and 20% for testing. Since the training data set was limited in size, data augmentation was employed to extend the dataset for training by manipulating images in the dataset artificially. The data was augmented by changing the contrast, gamma, and saturation of the image to prevent overfitting. This helped validate the robustness of the model to recognize not just different colours and appearances but also the texture of the material (Figure 3b).

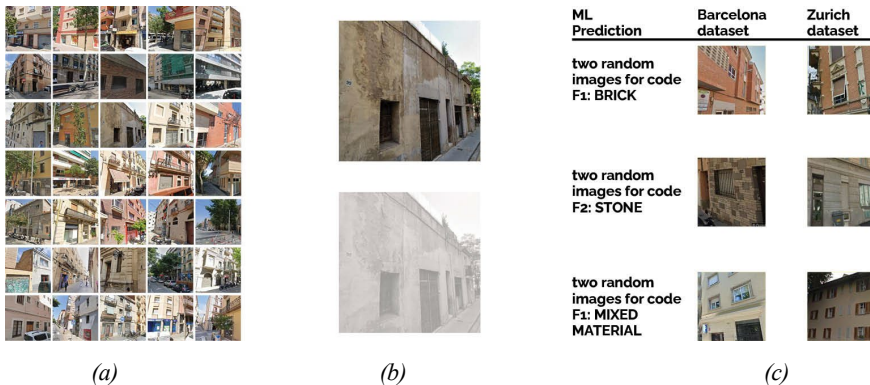


Figure 3a. Samples of the ocular observations conducted in Google Street View; Figure 3b. Data augmentation by changing illumination of image.; Figure 3c. Results of the façade material prediction.

A convolutional neural network (CNN) is a deep learning approach that has been widely used for analysing visual images. CNNs can learn highly abstract features and

can identify objects efficiently. To optimize computing power, the lightweight neural network MobileNetV2 (Sandler et al., 2019) with transfer learning was employed. Transfer learning is the process of training and predicting on a new dataset using a pre-trained model that has been learned on a previous dataset. This has been proven to be an efficient way for adaptation of the CNN to a new training task for datasets that are not large enough to train a CNN with many parameters from scratch. The model was created from the MobileNetV2 model pre-trained by Google on the ImageNet dataset utilizing dropout and batch normalization. An accuracy of 67% was achieved with 150 epochs per run. With an increase of epochs per run to 300, 74% accuracy was attained. Thus, with further data augmentation and training, more accurate and reliable results can be achieved. The system yields sufficient results on facade images of both Barcelona and Zurich, despite regional and architectural variation in the facades', showing general applicability of the technique (Figure 3c).

The predicted characteristics can then help estimate the reuse potential of the building facades (Figure 4). It is advantageous to know whether a building has a brick façade or not, as brick facades must often be preserved due to their cultural and historical value (Šekularac et al., 2020). Tailored reuse strategies for the facades are put forth based on a priority order of waste prevention.

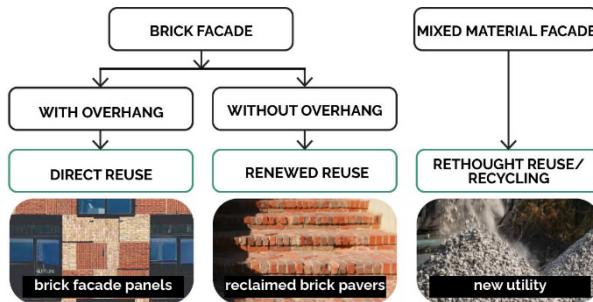


Figure 4. Tailored reuse strategies for facades from buildings marked for demolition

The deep learning model used to identify facade materials can be replicated to predict other characteristics such as if a building has an eave overhang. Buildings marked for demolition with a brick façade and an eave overhang may be directly reused as the elements are close to their original status and for their original purpose, needing almost no further processing. Lendager Group's Resource Rows project in Copenhagen demonstrates such brick façade reuse as seen on the left in Figure 4. Brick modules from historical breweries are cut out, installed in steel frames, and stacked on a new building (Lendager Group, The Resource Rows in 2021). Brick façades with no eave overhang may require operations of cleaning, renovating, or repairing. This method of reuse alters the brick to serve a new function. The reclaimable materials from mixed material façades are more complex. In this case, rethinking the function of the material is necessary. In combination with other substances, the waste material can be utilized to produce secondary goods with a new utility.

The dataset of buildings due for renovation or demolition were identified from building permits in the year 2020. Due to the relatively short time span of the building permit, some permits may not have been issued at the time of study or the work on the

building may already have been completed. Given the time-sensitivity of building permits, accounting for their temporality is critical. Methods to augment existing databases dynamically by building owners or contractors are essential. Supplementarily, anomaly detection techniques on facades as investigated by Barahona et al., 2021, can help automate the identification of buildings requiring retrofits.

5. Scheme 2: Reusable components (windows/doors/shutters) on building facades

Public datasets such as the Ecole Centrale Paris (ECP) have been used as a benchmark for facade parsing previously (Teboul et al., 2010). The ECP dataset only contains facades that are manually rectified and viewed in a front-parallel direction. Hence, the same dataset generated in Scheme 1 was used with the intention of encompassing a large variety of window types from different camera positions. This scheme explores the use of the state-of-art neural network Mask R-CNN (Girshick et al., 2014) for window detection. The VGG Image Annotator (VIA) was used to manually annotate the images. VIA is a single HTML file that can be opened in a browser. The tool saves the annotations in a JSON file with each mask as a set of polygon points. A collection of 150 images with 1478 annotated windows was generated. These images were then split into a training (120 images) and validation dataset (30 images). Transfer learning was applied with weights pre-trained from the COCO dataset. The implementation was hosted on Google Colaboratory, for free GPU usage. Some predicted results were imprecise, and the window boundary was incorrectly annotated due to the presence of open shutters (Figure 5). Overall, experimental detection results showed that with only transfer learning, the suggested approach can produce instance segmentation of windows on façade images of different countries despite variation in the façade and window appearance.

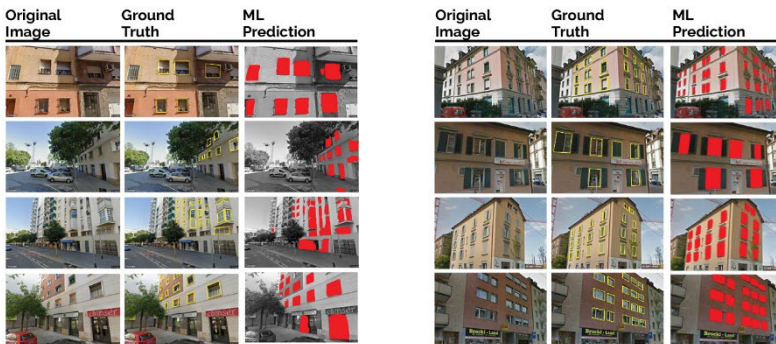


Figure 5. Detection of windows for reuse on the Barcelona (left) and Zurich (right) image datasets

These results obtained can be combined with public register data to identify tailored reuse strategies (Figure 6). For example, windows in new buildings or buildings which have undergone recent renovation and have an energy performance certificate (EPC) rating of 'A' to 'C' may be directly reused in new construction. This is because of the high thermal quality of the windows. For older buildings with an EPC rating of 'D', improving the insulation of the window glazing or changing the window frames may be necessary. For very old buildings with an EPC rating of 'E' to 'G', alternate design strategies for using the glazing material will need to be considered because of the poor thermal quality of the windows.

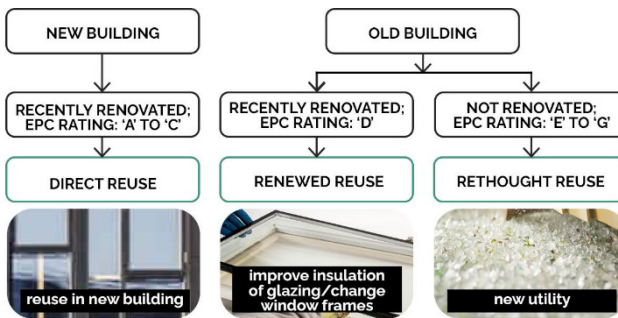


Figure 6. Tailored reuse strategies for windows from buildings marked for demolition

This section is limited to identifying the quantity of reusable components from street view images. Additional information on the surface area of each identified component can be retrieved with a reference of the height of the building. This calculation can be performed with traditional computer vision techniques as shown by Kolenbrander et al., 2017.

6. Data navigation and impact

Enhanced E-BAMB databases with component information could generate more long-term reuse strategies that can be used for decision-making. Most components that are picked out for reuse are most often just about to be consigned as waste. This makes it difficult to incorporate reuse in new design workflows. In this regard, building classification maps, wherein a building address is provided to visually collect building specific information can be useful (Figure 7a). The time buffer generated with this approach increases the likelihood of components being reused when they are available for sale (Figure 7b). The process also expands the prospect of finding a substitute for common components in advance. This methodology will not eliminate the need for intermediate storage altogether, but it may help in partial reduction of storage time, thereby also reducing warehouse costs. The introduction of a material database that can be accessed during the planning stage of projects allows identified reusable components to be incorporated into new design development schemes. Detailed specifications can be updated after the procurement of the components is complete.

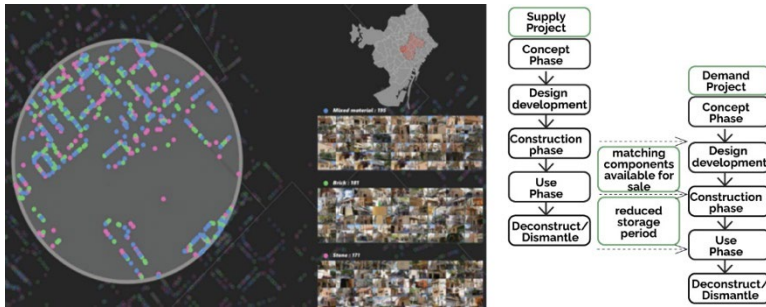


Figure 7a. Urban-scale E_BAMB classification map showing the location of brick, stone, and mixed material facades in the city of Barcelona; Figure 7b. Project-scale understanding of E-BAMB data

7. Conclusion and future work

This paper explores the opportunity to make better estimations about component reuse from existing buildings. To do so, machine learning methods are used to enhance building databases with information relevant for reuse. This is especially important as the review of public registers showed no data on materials or components. Data can be expensive to obtain, hence, it is essential to clarify for what purpose the register is established so that the data collection methods are feasible. ML methods can be used to find time-dependent patterns which makes them quite suitable for obtaining building-specific information. The methodology proposed in this paper can be used for data collection on materials and components available for reuse in existing buildings at national or regional levels. The contribution of this paper is the addition of façade material and window count as building-specific characteristics. Furthermore, the purpose of this study is to showcase how existing buildings stock data can be easily accessed to make decisions during early planning stages for matching supply and demand of reusable components in a quick and inexpensive way that can enable a wide range of analysis.

The scope of this paper is limited to the building specific predictions from street-view images. However, the automated methods described in this study can be used on other non-centralized, geo-located data, such as social media images to collect data on the building interior. Clarity on how much uncertainty can be allowed concerning the data quality needs to be established. For greater data accuracy or for filling critical data gaps that cannot be met with the automated methods described in this paper, pre-demolition audits with physical inspections can be carried out. Future work could explore other techniques to enrich building databases with more building characteristics relevant for energy retrofitting (von Platten et al., 2020).

References

- Akinosho, T. D., Oyedele, L. O., Bilal, M., Ajayi, A. O., Delgado, M. D., Akinade, O. O., & Ahmed, A. A. (2020). Deep learning in the construction industry: A review of present status and future innovations. *Journal of Building Engineering*, 32, 101827. <https://doi.org/10.1016/j.jobee.2020.101827>
- Barahona, B., Buck, R., Okaya, O., & Schuetz, P. (2021). Detection of thermal anomalies on building façades using infrared thermography and supervised learning. *Journal of*

- Physics: Conference Series*, 2042(1), 012013. <https://doi.org/10.1088/1742-6596/2042/1/012013>
- Debacker, W., Manshoven, S., & Denis, F. (2016). *DI Synthesis of the state-of-the-art: Key barriers and opportunities for Materials Passports and Reversible Building Design in the current system*. BAMB Horizon 2020.
- Duan, H., Miller, T. R., Liu, G., & Tam, V. W. Y. (2019). Construction debris becomes growing concern of growing cities. *Waste Management*, 83, 1–5. <https://doi.org/10.1016/j.wasman.2018.10.044>
- Dubey, A., Naik, N., Parikh, D., Raskar, R., & Hidalgo, C. A. (2016). Deep Learning the City: Quantifying Urban Perception at a Global Scale. In B. Leibe, J. Matas, N. Sebe, & M. Welling (Eds.), *Computer Vision – ECCV 2016* (pp. 196–212). Springer International Publishing. https://doi.org/10.1007/978-3-319-46448-0_12
- Gebru, T., Krause, J., Wang, Y., Chen, D., Deng, J., Aiden, E. L., & Fei-Fei, L. (2017). Using deep learning and Google Street View to estimate the demographic makeup of neighborhoods across the United States. *Proceedings of the National Academy of Sciences*, 114(50), 13108–13113. <https://doi.org/10.1073/pnas.1700035114>
- Girshick, R., Donahue, J., Darrell, T., & Malik, J. (2014). *Rich Feature Hierarchies for Accurate Object Detection and Semantic Segmentation*. 580–587. https://openaccess.thecvf.com/content_cvpr_2014/html/Girshick_Rich_Feature_Hierarchies_2014_CVPR_paper.html
- Kolenbrander, T., van Oort, B., de Ruiter, F., & Yue, T. (2017). *Facade labelling using neural networks*. <https://repository.tudelft.nl/islandora/object/uuid%3A8b7a82e1-9188-4b68-b582-2b5632e14501>
- Li, Y., Chen, Y., Rajabifard, A., & Khoshelham, K. (2018, September 1). Estimating building age from Google street view images using deep learning.
- Ma, M., Tam, V. W. Y., Le, K. N., & Li, W. (2020). Challenges in current construction and demolition waste recycling: A China study. *Waste Management*, 118, 610–625. <https://doi.org/10.1016/j.wasman.2020.09.030>
- Rose, C., & Stegemann, J. (2018). Characterising Existing Buildings as Material Banks (E-BAMB) to Enable Component Reuse. *Proceedings of the Institution of Civil Engineers - Engineering Sustainability*, 172, 1–42. <https://doi.org/10.1680/jensu.17.00074>
- Sandler, M., Howard, A., Zhu, M., Zhmoginov, A., & Chen, L.-C. (2019). MobileNetV2: Inverted Residuals and Linear Bottlenecks. *ArXiv:1801.04381 [CS]*. <http://arxiv.org/abs/1801.04381>
- Šekularac, N., Ivanovic-Sekularac, J., Petrovski, A., Macut, N., & Radojević, M. (2020). Restoration of a Historic Building in Order to Improve Energy Efficiency and Energy Saving—Case Study—The Dining Room within the Žiča Monastery Property. *Sustainability*, 12, 6271. <https://doi.org/10.3390/su12156271>
- Soibelman, L., Wu, J., Caldas, C., Brilakis, I., & Lin, K.-Y. (2008). Management and analysis of unstructured construction data types. *Advanced Engineering Informatics*, 22, 15–27. <https://doi.org/10.1016/j.aei.2007.08.011>
- Teboul, O., Simon, L., Koutsourakis, P., & Paragios, N. (2010). Segmentation of building facades using procedural shape priors. *2010 IEEE Computer Society Conference on Computer Vision and Pattern Recognition*. <https://doi.org/10.1109/CVPR.2010.5540068>
- Uotila, U., Saari, A., & Junnonen, J. M. (2021). Investigating the barriers to laser scanning implementation in building refurbishment. *Journal of Information Technology in Construction*, 26, 249–262. <https://doi.org/10.36680/j.itcon.2021.014>
- von Platten, J., Sandels, C., Jörgensson, K., Karlsson, V., Mangold, M., & Mjörnell, K. (2020). Using Machine Learning to Enrich Building Databases—Methods for Tailored Energy Retrofits. *Energies*, 13, 2574. <https://doi.org/10.3390/en13102574>

DATA, STAKEHOLDERS, AND ENVIRONMENTAL ASSESSMENT: A BIM-ENABLED APPROACH TO DESIGNING-OUT CONSTRUCTION AND DEMOLITION WASTE

GABRIELA DIAS GUIMARAES¹, NING GU², VANESSA GOMES³,
JORGE OCHOA PANIAGUA⁴, RAMEEZ RAMEEZDEEN⁵,
WOLFGANG MAYER⁶ and KI KIM⁷

^{1,2,4,5,6,7}*University of South Australia.*

³*University of Campinas.*

¹*gabriela.dias_guimaraes@mymail.unisa.edu.au, 0000-0002-7198-6028*

²*ning.gu@unisa.edu.au, 0000-0002-5555-9165*

³*vangomes@unicamp.br, 0000-0003-3246-7150*

⁴*jorge.ochoapaniagua@unisa.edu.au, 0000-0001-9282-7168*

⁵*rameez.rameezdeen@unisa.edu.au, 0000-0001-9639-2624*

⁶*wolfgang.mayer@unisa.edu.au, 0000-0002-2154-2269*

⁷*ki.kim@unisa.edu.au, 0000-0003-3018-5504*

Abstract. Construction and Demolition waste has started to become a target in the path for a more sustainable industry mainly due to massive resource consumption, land depletion and emissions. As a substantial amount of waste originates due to inadequate decision-making during design, strategies to design-out waste are required. Accurate environmental impact of, not only the whole building, but construction materials and elements are crucial to the development of these strategies, but dependent on data availability, expert knowledge and proper sharing and storage of information. Hence, this study aims to investigate the relation between data, stakeholders and environmental assessment to properly build a design-out waste framework. An in-depth data collection from literature review and stakeholders' interviews guided the development of a conceptual framework to assist designers with information related to waste production and its reduction. After that, the necessary technical specifications for its adoption through a BIM environment were analysed. Its contribution is firstly on a shift of thinking during the design phase, as the goal is to provide environmental information so designers can take into consideration the long-term consequences of waste from different strategies and solutions; and secondly in the development of a computational tool that facilitates the design-out process.

Keywords. Construction and Demolition Waste; Design; BIM; Environmental Data; Stakeholders; SDG 11.

1. Introduction

With the accentuated increase of the built environment over the last decades, C&D waste started to gain global attention. Without any consideration, this type of waste can have a significant impact on both the economy and environment. Current efforts in construction management mainly focus on addressing waste after it has occurred, such as reuse, recycle and landfill. However economically appealing or sustainable they might sound, these practices require transportation, energy, water, labour hours and site space, as well as a probable non-existing acceptance from clients and stakeholders. Beyond that, those strategies can even generate more waste by liberating consumers' consciences and being conservative enough not to change capitalist conventions (Baker-Brown, 2017).

The concept of minimization at source is preferable since it offers preventive measures, that is, decreases waste production instead of dealing with it once it is originated. It can contribute to reduction of environmental impacts related to waste management options such as landfill and incineration facilities, promote resource efficiency by reducing material and energy use, cut down on harmful processes such as extraction, manufacturing and distribution and improve conditions for public health by minimizing hazardous waste (European Commission Directorate - General Environment, 2012).

To avoid or minimize C&D waste it is imperative to create strategies for the design phase, when materials and construction technologies are being chosen and decisions can generate waste as a consequence, directly or indirectly. However, clear and comprehensive information is needed during the decision-making process to assist the development of waste reduction mechanisms.

From the premise that designers are unaware of how their decisions influence C&D waste generation in terms of quantity and criticality, this study aims to investigate the relation between stakeholders, construction information and holistic assessment to properly feed a computational tool that targets waste minimisation. Accurate environmental impact value of, not only the whole building, but construction materials and elements are crucial to the development of waste minimisation strategies, but dependent on data availability, expert knowledge and proper sharing and storage of information.

The objectives then are to, with data collected from theory and practice, develop a framework to produce, assess and present waste impact information during the design phase, reducing the environmental impact of cities by focusing on waste management. To enable the collection, share and use of this information throughout the supply chain, as well as its future demonstration and validation, the framework is focused for an implementation in a BIM environment. Hence, this study will also specify its technical specifications and discuss possible methods for its adoption.

2. Background and Motivation

The process of waste production during a building's lifespan generates considerable amount of carbon emissions, mainly CO₂, CH₄ and N₂O (Xu, Shi, Xie, & Zhao, 2019), primarily related to transportation, centre handling processes, equipment operations (Wang et al., 2016) and, depending on the disposal treatment and material

composition, chemical reaction. In addition, while the majority are considered inert, building materials may have absorbed harmful elements that can leach toxic heavy metals to the soil (Zheng et al., 2017). Furthermore, due to inappropriate treatment and dumping, it causes excessive land use, natural resource consumption and human health depletion, apart from imposing extra cost for management, regardless of its disposal path (Jalaei, Zoghi, & Khoshand, 2019).

In the build environment sphere, there is a consensus among professionals that a considerable amount of waste originates as a result of inadequate design planning and decision-making during this phase; thus, a design that fully considers the overall construction can prevent unnecessary waste (Enshassi, 1996; Llatas & Osmani, 2016; Osmani, Glass, & Price, 2008; Osmani, Price, & Glass, 2005; Wang, Li, & Tam, 2015). Although the causes of waste generation can vary – last minute changes, detailing errors, materials specification, high complexity, ineffective communication, lack of standard dimensions, poor documentation, clarification on materials quantity and quality (Olanrewaju & Ogunmakinde, 2020) – it is clear that a proper design-out waste approach demands the delivery of accurate and comprehensive data during a projects development to assist environment conscious decision-making.

However, the overall process of C&D waste production through design is complex, as buildings embody a range of materials, diverse stakeholders, unique clients/users, all contributing, directly or indirectly, to waste (Keys & Baldwin, 2000); hence, one of the main barriers to achieving this goal is on the practical implementation of designing out waste, that is, what are the necessary parameters required during the design phase to help waste reduction, how to collect and analyse them and how to inform the designer.

Although some existing waste management tools target the design stage, they are not entirely appropriate as they are detached from the design process and required the bill of quantities to function (Akinade et al., 2018). To bridge the gap between minimizing waste and design strategies, more comprehensive environmental information is required, which means sets of data based on accurate and holistic assessment throughout the building's life cycle.

3. Methodology

This paper is divided in (1) comprehensive systematic literature review to identify gaps and analyse existing approaches, to understand the requirements for proper waste minimisation strategies during the design stage; (2) an in-depth case study with different professionals involved in the same construction project to analyse materials and waste streams throughout the supply-chain and understand how to accurately propagate necessary data and calculate environmental impact; (3) development of a conceptual framework to demonstrate the process flow and specify parametric design capabilities to indicate to designers how to acquire information related to waste production and manage their decisions focused on its reduction; and (4) description of technical specifications required by the framework for a BIM-enabled prototype.

3.1. SYSTEMATIC LITERATURE REVIEW

An extensive systematic literature review was employed as a first qualitative approach

to unveil and analyse previous studies focused on C&D waste management during the design phase. The review was performed in the databases Web of Science and Scopus, with the following keywords: TITLE-ABS-KEY (("C&D" OR "construction and demolition waste" OR "construction waste" OR "demolition waste") AND ("design* phase" OR "design* stage" OR "designing out")). The search targeted journal papers and no particular period of time was fixated. The main aim was to understand existing design-out approaches, identify current challenges surrounding waste prevention techniques in the building industry, and identify que factors that influence design strategies/solutions targeting waste reduction. After analysis following a title and abstract screening, as well as inclusion per snowballing method, 35 articles were assessed.

3.2. INTERVIEWS

To understand the practice scenario with data regarding current building project's supply chain and its stakeholder's perspective, this study used interviews with experts to obtain in-depth information. To assess both individual perspectives and communication streams, a building project was chosen, and the stakeholders involved in a full material stream, from design to end-of-life, were interviewed - architect, builder, supplier and waste/recovery manager. The choice of project, although bounded by data availability, was guided by average characteristics and building typology. For this research, semi-structured interviews were preferable because it facilitates open-ended discussions, exploring building waste and each stakeholder's responsibility of its impact (Babbie, 2016).

The questions were firstly piloted with two experts and, after revised, a short description and overview of the research was provided to each participant prior to the meeting. The interviews were individual, typically lasted between 40min to 1 hour and began with a series of semi-structured questions, followed by an informal discussion regarding waste streams and their position in the building's life cycle. Each interview was recorded, transcribed, and analysed to inform the development of the C&D waste design-out conceptual framework.

4. Conceptual Framework for Designing-out C&D waste

With data collected from theory and practice, a framework was developed to produce and present waste environmental information during the design phase. Firstly, a theoretical framework was built based on existing approaches and the current gaps of information. After that, to comprehensively assess the current scenario it was necessary to "take a picture" of an existing supply chain of a building project in order to understand technical aspects, such as BIM adoption levels, data availability and communication paths, and contextual aspects, like their opinions regarding waste minimization and perspectives on building management. Hence, the interviews have been conducted to improve knowledge found in the literature and guide the development of the proposed framework from the theoretical one.

4.1. LITERATURE FINDINGS

Despite the general knowledge of minimizing C&D waste through appropriate

decisions during the design stage, there is still a lack of approaches focused on improving the information and the required process to aid designers during the project development. Beyond technical integration issues, environmental impact data needs to be accurate to properly influence decision-making.

Figure 1 displays different topics, based on the literature, that should be considered. The knowledge necessary to analyse waste is spread out through different stakeholders in a project’s life cycle and all this information needs to be collected, assessed, and provided back to the designer. The assessment should consider all material streams, from product stage to its end-of-life stage, so that every waste sources and causes are accounted for. Finally, a technology to help storage, manage and share the information is required, to help quantify environmental impacts and evaluate design options, while being attached to the design process.

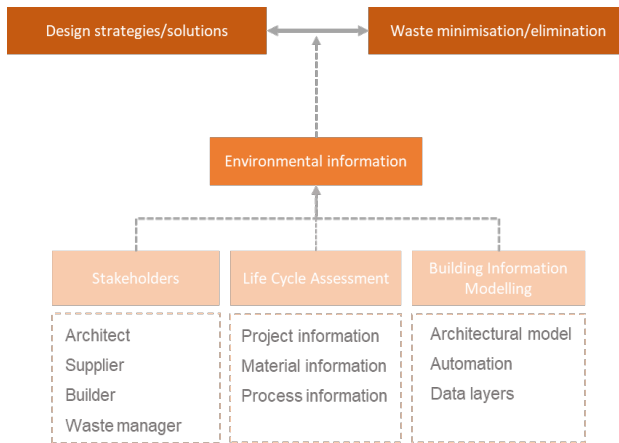


Figure 1 - Theoretical framework on design-out waste information

4.2. INTERVIEW FINDINGS

After an in-depth qualitative analysis, some themes started to appear from the interviews. The questions were related to their view on responsibility for the waste generation, consideration taken to reduce C&D waste and how feedback is shared with the designer. Figure 2 summarises the key findings from the interviews, divided by topics.

Environmental layers	BIM adoption	Stakeholder's responsibility	Accessible outcome	External driver
<ul style="list-style-type: none"> Life cycle impact categories Design for Disassembly score Material Circularity Indicator 	<ul style="list-style-type: none"> Focus on 3D modelling Individual and static use Lack of LOD flow enhancement 	<ul style="list-style-type: none"> Designers' perspective Timeframe 	<ul style="list-style-type: none"> Comparability of material/element Visual data 	<ul style="list-style-type: none"> Client choices Cost variable Impact balancing

Figure 2 - Summary of findings from stakeholder's interviews

Taking into consideration the required information necessary to assess C&D waste, three main points arise: the source of materials, the amount you can recover from each

material/system and the impact that this recovery to the supply chain will generate. Hence, although a holistic environmental impact is needed, other environmental layers should also be analysed: Design for Disassembly score, that focus on functional dependence, time for disassembly, lifespan, disposal path, and Circularity Indicator, that is based on the amount of virgin materials and unrecoverable waste.

Although BIM is commonly used between stakeholders, it is interesting to note that its adoption is focus on 3D modelling and highly separated into disciplines, that is, professionals use its object-oriented characteristics to develop part of the project specific to its stage. There is a lack of collaborative use, proper enhancement of Level of Detail (LOD) as the project advances and exchange of information among stages.

From the designer's perspective, on a realistic scenario, there is not enough time to research, collect and compare environmental information of different materials or construction choices. In addition to that, decisions are highly dependent on budget. Nonetheless, their responsibility to the C&D waste production is very clear and strategies to minimise it should be expected to come from themselves.

Also related to the timeframe is the accessibility of environmental outcomes. Besides being accurate and comprehensive, waste impact measures should be clear to non-experts as well as supportive of a collaborative workflow among stakeholders. Visual representation of the environmental outcome and comparable options with benchmarks or other standard options can help designers make fast informative choices during the decision-making process.

Since external drivers will dictate specific choices, whether is a tight budget or a client driven decision, it is important to allow the designer to balance its impact. Changes on one material or element might influence others and this can be used by the designer to absorb a "non-negotiable" waste impact.

4.3. CONCEPTUAL FRAMEWORK

Based on the findings from theory and practice, a framework was developed to generate and present waste environmental impact data during the design phase of a building, as displayed in Figure 3.

From the Theoretical Framework is clear that comprehensive environmental data is imperative for the development of design strategies focused on waste minimisation, and for that the information needs to encompass three important topics: people, process, and technology. Since information is scared around the supply chain, different stakeholders need to be involved and actively share their knowledge; a life cycle assessment is imperative to properly grasp the impact waste has on the environment; and building information modelling is the technology proposed for the collection, sharing and analysis of the required data. From the interview findings important practical aspects were identified and need to be included in the framework for it to become a feasible approach for the current construction project reality, such as a more comprehensive outcome that has different environmental layers to cover more C&D waste aspects, the use of visual data for more clear results and easy comparability, and an overall feature that allows the user to choose on their own, so they have the power to balance the impact throughout the project design.

As a framework built with an object-oriented approach, the assessment is

conducted whenever the user chooses an object and requests its waste information. The inputs necessary are related to the chosen object and how it is inserted in the design in place, hence primary information from the project being developed needs to be added, such as location, gross floor area, net floor area and building typology. Beyond that, the type and amount of material, as well as the building layer being assessed need to be described. This information, together with secondary datasets from environmental databases, available EPD's and national benchmarks, will feed the Waste Analytics step. To generate a more comprehensive output, as per the findings, three environmental layers are calculated: Life Cycle Assessment (LCA) impacts (Global Warming Potential, Embodied Energy and Embodied Water), Design for Disassembly Score and Circularity Indicator.

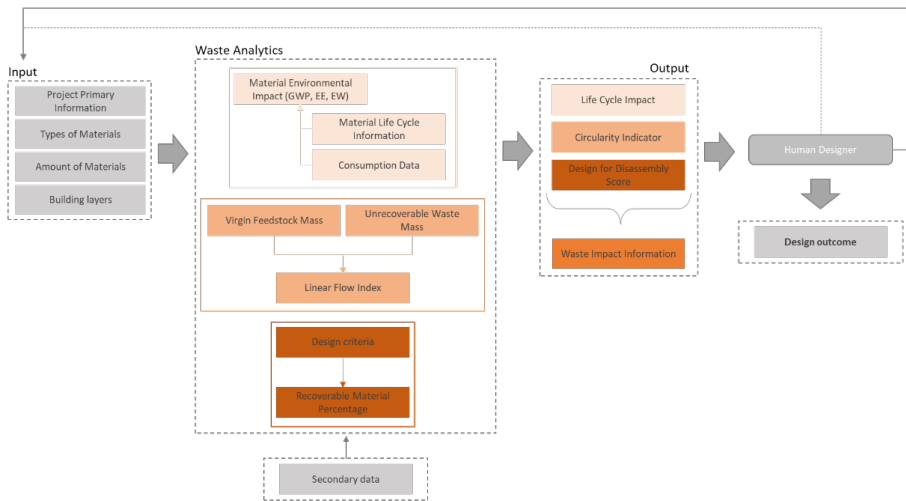


Figure 3 - Conceptual framework for design-out C&D waste

The framework does not generate a new design or chooses a new object, but rather inform the user about its choice and shows the results in a scale with other alternative/benchmarks. The user can then decide on a different approach, and insert new information as input, or keep this object, based on the project's requirement and personal preferences, and resume the modelling. The whole process keeps ongoing with each request for new object waste information, and the environmental impacts will change according to the choices that influence that building's life cycle. Once the design is finished, the whole-building waste environmental impact can be calculated, based on the three environmental layers being considered for each object.

5. Technical Specifications for a BIM-enabled development

To demonstrate the capability of the framework and how it can assist professionals on estimating and minimizing waste environmental impact, a computational prototype is proposed. As a first step towards the development of its system architecture and validation with a practical tool, the technical specifications required by the framework

for a BIM-enabled approach tool were listed. In that scenario, BIM was chosen as it is an object-oriented modelling method that allows users to create digital 3D models, while also helping to storage, manage and share information regarding construction materials that are imperative to quantify environmental impacts related to waste.

The basic requirements for a successful platform focused on design use include having a user-friendly environment, support for collaboration and integrate different types of data into the design process to aid design decisions (Calixto et al., 2021). In addition, there are current requisites for improving waste effectiveness of the construction industry, such as benchmarking of waste generation rates, waste management from a life cycle perspective and integration of newly emerging technologies such as BIM, GIS and Big Data (Jin, Yuan, & Chen, 2019).

The framework also requires a collaborative workflow amongst stakeholders, as the outcomes are based on parameters and knowledge divided throughout the project's life cycle and there is a need for work in real-time, with sharing of data, feedback, and inputs. As per the literature and interviews, it is expected that BIM-enabled tools have a high adoption rate, with broad use in different stages of the project and supply-chain of materials/products. Exporting projects in different formats to use in other parametric tools is a valid option, however, although there are several existing options that are technically capable of data-driven flow and have a high potential for collaborative work, the preferable choice, for a seamless exchange of information, is the use of one tool for all project stages. The following technical requirements are presented based on the framework steps:

Input: The object being assessed needs to be identified, both physically and practically; hence, a few features must be entered by the user within the BIM environment. The first qualitative one is related to the materials that constitute the object and the second is the building layer that the object is a part of. The next feature is related to quantity, and it must be a numerical parameter related to the object. Beyond that, some project primary information is requested as well, to be included in the Waste Analytics as primary data.

Secondary data: The use of different secondary databases and primary datasets to generate environmental layers from a range of parameters is imperative to comprehensively assess waste, which requires an exchange of information between separate data formats, such as EPI's, material environmental impact datasets, national waste reports, etc.

Waste Analytics: Both primary and secondary data will be used to quantitatively calculate the proposed environmental layers. This will be happening outside the BIM-environment and, once the outcome is defined, it will be sent as a set of additional information for that object's library inside BIM.

Waste Impact Information: For a more accessible outcome, the result is required to be presented in a visual way. The results are generated separately, but displayed both together and individually, as well as correlated to benchmarks or BAU (business as usual) options. A proper visualization approach will assist in the comparability of materials/elements, which is imperative for a realistic designer timeframe, and the usability of the tool, since users are not necessarily experts in environmental strategies.

Finally, within the BIM environment, the user will decide the next course of action

based on the information they were given.

6. Conclusion and Future Work

This paper discusses the relation between data, stakeholders and environmental assessment to properly build a design-out waste framework. Despite the attention C&D waste is obtaining nowadays, a comprehensive approach for its reduction from source is still missing. In the present work, a conceptual framework was proposed based on findings from both theory and practice, i.e. systematic literature review and interviews with stakeholders.

From the findings, it was concluded that the development of design strategies focused on waste minimisation require comprehensive environmental information that encompass people, process, and technology, that is, knowledge and collaboration from different stakeholders, a life cycle assessment of impacts caused by waste, and a BIM methodological approach to support the assessment. Beyond that, after "taking a picture" of an existing stakeholder chain from a real-life project, important practical aspects were identified and included in the framework for it to become a feasible approach for the current construction industry: different layers of output and the best way of visualizing it, BIM software adoption consideration, the existing timeframe and automation necessary for it and flexibility of balancing the project's impact by receiving the information and deciding their preference.

The limitation of the interview findings must be acknowledged as, although part of a qualitative method, the number of participants is not high enough due to data security and availability. However, because the intent was to understand the relation between stakeholders and how data is shared within the same project, the outcome is still valid and representative of a medium size construction project.

The proposed approach is part of an on-going PhD research focused on designing-out C&D waste by supporting designers during their decision-making process. The next steps will be focused on the technical features, with the development of a BIM-enabled prototype and the demonstration will be conducted with a case study, the building project from the stakeholder's interview. Possible options for technical development are plug-ins on popular BIM software, such as Revit, or an Algorithm Design approach, with a programming on Grasshopper. Both options fit the technical specifications required by the framework, and the difference lies on the coding development process. Finally, a validation will be conducted by going back to the architect responsible for the case study, to analyse how well the prototype addresses this type of stakeholder's needs and expectations.

References

- Akinade, O. O., Oyedele, L. O., Ajayi, S. O., Bilal, M., Alaka, H. A., Owolabi, H. A., & Arawomo, O. O. (2018). Designing out construction waste using BIM technology: Stakeholders' expectations for industry deployment. *Journal of Cleaner Production*, 180, 375–385. <https://doi.org/10.1016/j.jclepro.2018.01.022>
- Babbie, E. (2016). *The Practice of Social Research* (14th ed.). Boston, MA: Cengage Learning.
- Baker-Brown, D. (2017). *The Re-Use Atlas* (1st ed.). RIBA Publishing.

- Calixto, V., Canuto, R., Noronha, M., Afrooz, A. A., Gu, N., & Celani, G. (2021). A layered approach for the data-driven design of smart cities. *Projections - Proceedings of the 26th International Conference of the Association for Computer-Aided Architectural Design Research in Asia, CAADRIA 2021*, 2, 739–748.
- Enshassi, A. (1996). Materials control and waste on building sites: Data in the study was obtained from 86 housing projects on several locations in the Gaza Strip. *Building Research and Information*, 24(1), 31–34. <https://doi.org/10.1080/09613219608727495>
- European Commission Directorate - General Environment. (2012). *Preparing a waste prevention programme - Guidance document*. European Commission Directorate-General Environment, 1–62. Retrieved from <http://ec.europa.eu/environment/waste/prevention/guidelines.htm>
- Jalaei, F., Zoghi, M., & Khoshand, A. (2019). Life cycle environmental impact assessment to manage and optimize construction waste using Building Information Modeling (BIM). *International Journal of Construction Management*. <https://doi.org/10.1080/15623599.2019.1583850>
- Jin, R., Yuan, H., & Chen, Q. (2019). Science mapping approach to assisting the review of construction and demolition waste management research published between 2009 and 2018. *Resources, Conservation and Recycling*, 140(October 2018), 175–188. <https://doi.org/10.1016/j.resconrec.2018.09.029>
- Keys, A., & Baldwin, an. (2000). Designing to encourage waste minimisation in the construction industry. *Proceedings of CIBSE National Conference, Dublin*. Retrieved from <https://dspace.lboro.ac.uk/dspace/handle/2134/4945>
- Llatas, C., & Osmani, M. (2016). Development and validation of a building design waste reduction model. *Waste Management*, 56, 318–336. <https://doi.org/10.1016/j.wasman.2016.05.026>
- Olanrewaju, S. D., & Ogunmakinde, O. E. (2020). Waste minimisation strategies at the design phase: Architects' response. *Waste Management*, 118, 323–330. <https://doi.org/10.1016/j.wasman.2020.08.045>
- Osmani, M., Glass, J., & Price, A. D. F. (2008). Architects' perspectives on construction waste reduction by design. *Waste Management*, 28(7), 1147–1158. <https://doi.org/10.1016/j.wasman.2007.05.011>
- Osmani, M., Price, A. D. F., & Glass, J. (2005). Potential for construction waste minimisation through design. In Kungolos, A and Brebbia, CA and Beriatos, E (Ed.), *Sustainable Development and Planning II*, Vols 1 and 2 (pp. 575–584).
- Wang, J., Li, Z., & Tam, V. W. Y. (2015). Identifying best design strategies for construction waste minimization. *Journal of Cleaner Production*, 92, 237–247. <https://doi.org/10.1016/j.jclepro.2014.12.076>
- Wang, J., Wu, H., Duan, H., Zillante, G., Zuo, J., & Yuan, H. (2016). Combining life cycle assessment and Building Information Modelling to account for carbon emission of building demolition waste: A case study. *Journal of Cleaner Production*, 172, 3154–3166. <https://doi.org/10.1016/j.jclepro.2017.11.087>
- Xu, J., Shi, Y., Xie, Y., & Zhao, S. (2019). A BIM-Based construction and demolition waste information management system for greenhouse gas quantification and reduction. *Journal of Cleaner Production*, 229, 308–324. <https://doi.org/10.1016/j.jclepro.2019.04.158>
- Zheng, L., Wu, H., Zhang, H., Duan, H., Wang, J., Jiang, W., & Song, Q. (2017). Characterizing the generation and flows of construction and demolition waste in China. *Construction and Building Materials*, 136, 405–413. <https://doi.org/10.1016/j.conbuildmat.2017.01.055>

DEVELOPMENT OF TECHNOLOGY FOR AUTOMATIC EXTRACTION OF ARCHITECTURAL PLAN WALL LINES FOR CONCRETE WASTE PREDICTION USING POINT CLOUD

TAEHOON KIM¹ SOONMIN HONG² DAVID STEPHEN PANYA³
HYEONGMO GU⁴ HYEJIN PARK⁵ and JUNGHYE WON⁶
SEUNGYEON CHOO⁷

^{1,2,3,4,5,6,7}*Kyungpook National University*

¹*thlouiskim@gmail.com*

²*soonmin.hong@knu.ac.kr*

³*david.panya@gmail.com*

⁴*ghm3186@knu.ac.kr*

⁵*gpwls3143@gmail.com*

⁶*wonjeonghye97@gmail.com*

⁷*Choo@knu.ac.kr*

Abstract. Recently, as more and more projects on residential environment improvement in cities are actively carried out, the cases of demolishing or remodelling buildings has been increasing. Most of the target buildings for such projects are made of concrete. In order to reduce energy use as well as carbon emissions, the amount of concrete used as a building material should be reduced. This is because the concrete is the largest amount of construction waste, which the exact amount of concrete needs to be predicted. The architectural drawings are essential for the estimation and demolition of building waste, but the problem is that most of the old buildings' drawings do not exist. The 3D scanning process was performed to create the plans for such old buildings instead of the conventional method that is long time-consuming and labour-intensive actual measurement. In this study, we scanned 40 old houses that were scheduled to be demolished. The result showed that the 3D scanned drawings' accuracy - 99.2% - was higher than the ones measured by the conventional way. Through the algorithm developed in this study, the various processes of demolition, drawing measurement, and discarding quantity prediction can be solved in one process, thereby reducing work efficiently. And, considering the reliability of the research results, it is possible to reduce the economic loss by predicting the exact amount of waste in advance. After that, if the algorithm, developed in this study, can be further subdivided and supplemented to identify the materials for each part of the old buildings, it will be able to propose an efficient series of processes that distinguish between recyclable materials and wastes and thereby efficiently dispose of them.

Keywords. Point Cloud; Construction Waste; Parametric Design; Algorithm; Automatic Extraction; SDG 8.

1. Introduction

1.1. RESEARCH BACKGROUND AND PURPOSE

Recently, as more and more projects on residential environment improvement in cities are actively carried out, the cases of demolishing or remodelling buildings has been increasing. Most of the target buildings for such projects are made of concrete. In order to reduce energy use as well as carbon emissions, the amount of concrete used as a building material should be reduced. This is because the concrete is the largest amount of construction waste, which the exact amount of concrete needs to be predicted. The architectural drawings are essential for the estimation and demolition of building waste, but the problem is that most of the old buildings' drawings do not exist. The 3D scanning process was performed to create the plans for such old buildings instead of the conventional method that is long time-consuming and labour-intensive actual measurement. In this study, we scanned 40 old houses that were scheduled to be demolished. The result showed that the 3D scanned drawings' accuracy - 99.2% - was higher than the ones measured by the conventional way. After that, if the algorithm, developed in this study, can be further subdivided and supplemented to identify the materials for each part of the old buildings, it will be able to propose an efficient series of processes that distinguish between recyclable materials and wastes and thereby efficiently dispose of them.

1.2. SCOPE AND METHOD OF RESEARCH

The research method is as follows. Firstly, we present the current methods and problems of the manual measurement to draw the decrepit building's plans, and address the limitations of current technology and methods, in accordance with the analysis of the current status of reverse engineering technology. Secondly, the preceding Authors

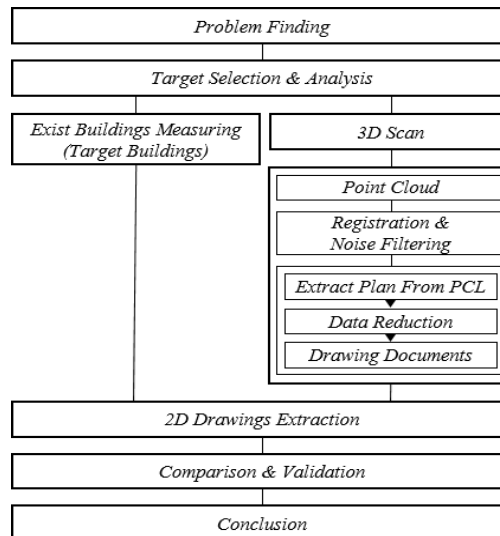


Figure 1. Research Flow

on point cloud-based reverse engineering and parametric technology research are examined. The point cloud of the target building is acquired by using a 3D scanner for the selected buildings. After going through the 3D point cloud registration process, the drawings are produced by an algorithm which is created by Grasshopper - a graphical algorithm editor integrated with Rhino 3D modelling tool. Finally, the information of the drawings extracted through the algorithm and the drawings produced by actual measurement are compared and verified. In addition, the expected amount of concrete waste is derived by calculating the concrete volume of the building using the matched point cloud data.

2. Background

Reverse engineering technology is actively applied in various fields such as shipbuilding, architecture, and MEP(Mechanical, Electrical, and Plumbing). Collecting point cloud data for reverse engineering requires a point cloud for each scanned location by employing equipment such as a depth camera and 3D scanner and a separate software that matches the various point cloud data matched to complete the building. Many reasearch on the development of point cloud-based reverse engineering technology have been conducted. Particularly, it is focused on modelling for building maintenance and restoration or recording of cultural properties.

In the field of building maintenance, there have been many studies on checking the building information, such as its location, concrete damage, and cracks in the exterior wall, on the basis of the point cloud data (Kim, 2019).

A study for point cloud-based building inspection required the process of extracting the drawing information of the building from the 3D model, and the 3D modelling had a limitation in having to align the location with the point cloud (Park, 2016). In a study to manage facilities in a BIM environment without going through manual modelling work, the point cloud was automatically mapped to objects in the BIM environment (Kang, 2019). BIM objects were created by searching for objects with a high degree of similarity in the BIM library by extracting the shape features of flat objects such as floors, walls, and doors (Yoon, 2020). As described above, studies on modelling objects derived from point clouds are in progress, but such studies are still challenging. The studies conducted so far have extracted point clouds for the 3D model, but modelling work was carried out according to the point cloud or modelling was performed based on existing drawings. Therefore, this study compares the proposed algorithm and the coherence of extracting objects as elements of geometry type by determining the reference point from the point cloud and generating drawings based on this.

Parametric design is a technology specialized in atypical design. It is actively used not only in the fields of architecture, shipbuilding, medical care, and mechanical equipment, but also mainly as a method to visualize or model objects (Koo, 2009). However, there are few studies related to extracting drawings from point clouds or parametric design.

Among them, there are several parametric studies using point clouds of buildings. One of studies implemented a method of acquiring a point cloud using lidar and projecting a 3D object observed from multiple locations onto a 2D plan. It was

conducted for the purpose of visualization to inquire the point cloud as an image using CUDA-based 'Octree' and parametric algorithms, but the shape and scale of the building can be checked from the produced image. In spite of it, cross-sectional information such as the floor plan of the building cannot be known (Kim, 2016). In addition, another study developed a parametric algorithm to build a BIM library for each member for a 15th century dome building (Capone, 2019). In the other study, 3D mesh was extracted from a point cloud using 'Voronoi equations' to create a BIM model improved the model efficiency (Mesrop, 2020). As such, in the parametric field for point cloud-based modelling, algorithms are created for model creation. However, the created modelling algorithm has a structure that is difficult to fully operate when applied to other buildings.

In addition, the extracted 3D model has a problem in that it is possible to obtain information about the 2D drawing of the building only through the process of BIM modelling and drawing extraction. As such, most of the research in the parametric field using the existing point cloud is used in the medical field by creating a 3D model, or dealing with the intermediate stage process for BIM in the architectural field. Therefore, this study proposes a parametric algorithm that can be applied to various buildings as a differentiated study for extracting 2D drawings from the point cloud of a building.

3. Point cloud data pre-processing and experimental design

3.1. SELECTION AND ANALYSIS OF TARGET BUILDINGS

For the experiment to extract architectural drawings using point clouds, the buildings in the scope of this paper are located in Buk-gu, Daegu, South Korea. Although this target site is determined to conduct the residential environment improvement project, and existing buildings will be demolished or remodelled. There are many old and decrepit buildings that was built without permission and proper documentation, so that it is unlikely to find drawing materials, such as building drawings and land use plans, necessary for demolition and remodelling. Therefore, it is essential to secure digital data of buildings such as 2D drawings.

There are 51 buildings in the site, selected for this paper, they were classified into 4 based on the type of residence, structure, and number of floors. For the experiment, one building per type was selected and the point cloud of the building was acquired.

3.2. POINT CLOUD DATA REGISTRATION AND PRE-PROCESSING

First of all, consent was obtained in advance to scan the housing environment in which residents live, and the work before 3D scanning. For the point cloud acquisition, 3D scanning equipment 'BLK360' was used, which can acquire 360,000 points per second at a distance of up to 60m, and a manual measurement was conducted to obtain a comparison building measurements for this paper. In addition, 3D scanning was performed only when the roof or roof scanning environment was judged to be safe

The 3D scan was carried out for each room, interior and exterior of the building, and the higher the overlap of the scanned area, to make the pre-processing process more convenient. In the process of matching, unnecessary scans of people, vehicles, and

moving objects, that are difficult to recognize, are excluded and considered noise. When the matching process is finished, the data can be reduced primarily by removing the point cloud not related to the target building, and the point cloud of the target building can be checked.

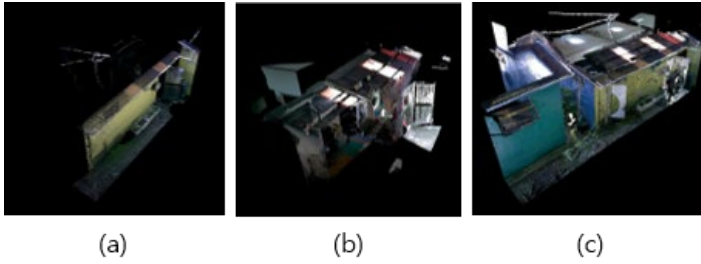


Figure 2. Original PCL (a, b) and Registered PCL (c)

3.3. DEVELOPMENT OF DRAWING EXTRACTION PROCESS USING POINT CLOUD

Rhino6 was used for point cloud-based building drawing extraction. In this study, we used the '.pts' extension because we needed the point cloud data of the point cloud. And the parametric algorithm was written using Grasshopper.

First, through the process of section extraction of the point cloud (Figure 3), the area to create the drawing of the building is extracted. A horizontal cross section extracts the length, location and thickness of the wall, through this process the shape of the entire building plane can be realized. In this process, the point cloud of the section to be extracted is selected by adjusting the height and thickness based on the boundary circumscribed to the point cloud of the building. And by adjusting the height and thickness of the section, you can work while visually checking the height of the wall where objects do not cover it. Wall openings can be realized at the points extracted from different x, y, z axis coordinate values.

Second, the data is lightened to enable smooth operation of the extracted point cloud

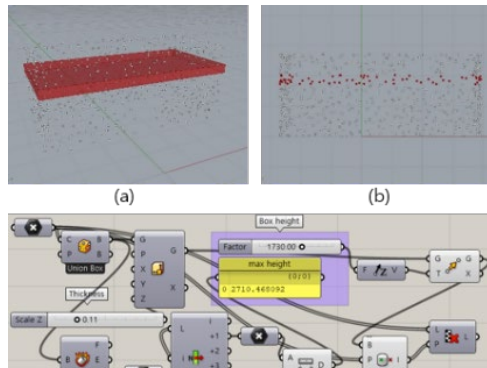


Figure 3. Section Bounding Box(a), Front View of Extracted Section(b), Section Extraction Algorithm(c)

in Grasshopper and the z-coordinate is deleted (Figure 4). If the x, y, z coordinate values of the point cloud are replaced with x, y, 0 values, the point cloud is changed to points on the x and y planes, making it easier to create drawings. And the z coordinate value becomes 0, and overlapping points are generated, and the plane point cloud is reduced in weight by erasing them. Through this process, the weight of the point cloud has been reduced to about 30%, but the shape is maintained, so it is possible to extract drawings.

Third, the drawing process is carried out by creating the centre line of the wall based on the lightweight planar point (Figure 5). By selecting points forming a straight wall, the centre line can be extracted by calculating the average distance of the points. At this time, if there is an opening in the wall, the process of erasing the centre line by selecting the point of the opening portion is performed, and the centre line of the wall is extracted. After that, the floor plan of the building can be extracted by inputting an interval so that the generated centre line matches the thickness of the wall. In the extracted drawing, the centre line and the wall line with the openings can be confirmed.

Through this algorithm, it is possible to extract the cross-section, light weight, and

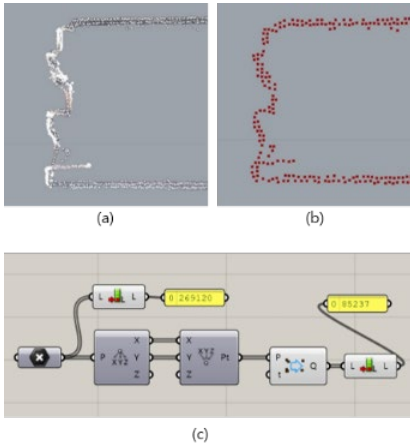


Figure 4. Original PCL(a) and Data Reduced PCL(b), Data Reduction Algorithm(c)

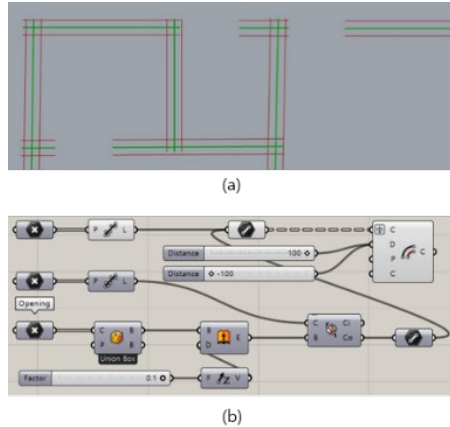


Figure 5. Generated Centre-line, Wall line, Opening(a), 2D Drawing Extraction Algorithm(b)

drawing of a building from the point cloud regardless of the size or number of floors of the building. However, since Rhino is not a software that handles point clouds, but a 3D modelling was conducted in 'Nurbs' format, there is a problem that the calculation time is extensive in Rhino and Grasshopper due to a high amount of point cloud consisting of about 20 million points or more. Therefore, it is necessary to reduce the weight as much as possible in the pre-treatment process. To reduce amount of the points, the values of the z-axis are adjusted using parameters for plane extraction. At this time, the corresponding height value must be adjusted manually, since the height including all the flat walls must be adjusted. Points included in this range are possible even as 0.1% of the total points, so pointer data can be lightened.

4. Extraction of architectural plan wall lines using point cloud for concrete waste prediction

4.1. EXTRACTION OF ARCHITECTURAL WALL LINES USING POINT CLOUD AND VERIFICATION

In the process of extracting a drawing from a point cloud through an algorithm, task such as drawing and length input was omitted, unlike the method of creating a drawing by actually measuring it. In addition, although the number of 3D scans varies depending on the size of the building or the number of rooms, the time and task of drawing up drawings have been simplified. The results extracted from the point cloud of the target building (Figure 6) are as follows.


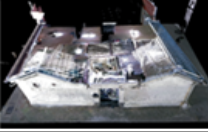

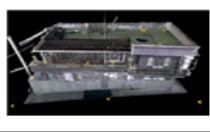

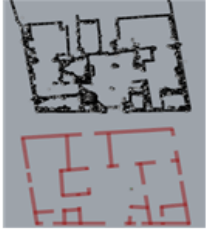

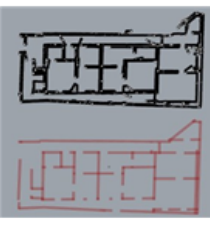
Type	A	B	C	D
3D Scan Count	50	18	11	43
Point Cloud				
Extracted Cross Section & Results				

Figure 6. Cross Sections and 2D Drawings Extracted from Point Cloud

Building A is an unused, abandoned house with one side of the building adjacent to another building. It could be seen that some spaces were flat, not at right angles, and drawings could be extracted without the process of drawing. Due to the missing point cloud, it was possible to extract the intermediate planes of some walls by calculating from adjacent points.

Building B is a house in use, and it was not possible to acquire a point cloud for one side of the exterior wall. In addition, since the structure of the interior room is mostly at right angles, it was not possible to recognize the inclined square-shaped plane at the site, but it was possible to create an accurate drawing by grasping the shape of the building plane from the acquired point cloud.

Building C is a house inhabited by residents, and it was impossible to acquire a point cloud of the exterior wall because the two sides of the building were in contact with the neighbouring buildings. In addition, hidden spaces such as the plumbing room inside the wall of the bathroom could be found from the point cloud, and could be confirmed through the drawing process.

Building D is a two-story villa building that is scheduled to be demolished on a

sloped site. Among the two floors, the drawings of the first floor with 3 out of 5 villas were extracted through an algorithm. Because the exterior of the building was partially used as the yard of an adjacent house, it was impossible to measure it, but it was possible to acquire a point cloud through 3D scanning from the outside of the second floor. Inside, only minimal furniture such as built-in cabinets remained, making it possible to extract a flat point cloud during the cross-section extraction process of the algorithm. Since the wall of the building was refracted in the process of extracting the drawing, the centre line of the wall was extracted by dividing it twice. Also, the space between the building and the retaining wall could be found in the inner room in the direction of the elevation of the site.

The difference was derived by comparing the drawing extracted from the point cloud through the parametric algorithm with the drawing prepared by actual measurement (Figure 7). The difference in area was compared to compare the difference in the overall size of the building.

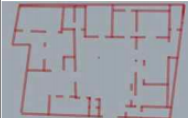

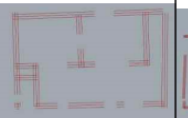



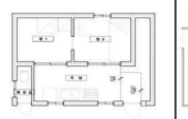

Type	A			B			C			D		
Extracted Drawing												
Measured Drawing												
	M	E	D(%)	M	E	D(%)	M	E	D(%)	M	E	D(%)
Wall Length(m)	13.3	13.1	1.5	7.61	7.54	0.9	6.05	6.07	0.3	7.24	7.33	1.2
Depth of Space(m)	2.85	2.80	1.7	2.62	2.59	1.1	2.6	2.58	0.7	3.20	3.16	1.5
Square Measure(m ²)	226.8	220.6	2.8	74.3	75.0	0.9	24.2	24.1	0.04	127.9	140.1	8.5
● M : Measured, E : Extracted, D : Difference												

Figure 7. Comparison of Measurement 2D Drawings and 2D Drawings Extracted through Algorithms

4.2. BUILDING WASTE PREDICTION

The area of the wall can be calculated from the extracted drawings. The currently developed algorithm is at a stage where the expression of openings included in buildings is not performed. When the z-axis is 0, the area of the x and y planes can be calculated. At this time, since there is a possibility that all the wall lines are not straight, the area can be automatically calculated using the 'area' command from the extracted file.

$$\text{Concrete Waste Volumn (m}^3\text{)} = \text{wall area (m}^2\text{)} * \text{height (m)}$$

And to obtain the volume, the height degree can be obtained from the point cloud registration data, and the volume of the wall can be obtained by multiplying the area obtained through the drawing by the height. Through this height information, the volume of the wall at the location of the opening can be obtained. Creating a BIM model is convenient because it is possible to automatically calculate the quantity for each material.



Figure 8. Height extract form 3D point cloud registration

5. Conclusion

Due to the residential environment improvement project, drawings of buildings are needed to proceed with the demolition and remodelling of old buildings. Recognizing the limitations of drawing extraction from point cloud through 3D modelling process through reverse engineering and parametric design related technical research to create drawings from buildings that have been carried out so far, and in the modelling process, 3D object modelling and reference drawings for placement This necessary problem was identified. In this study, we created a parametric algorithm that performs the process of section extraction, weight reduction, and drawing from the point cloud for buildings that require drawing. Through this, we tried to extract 2D drawings and construction waste, especially the amount of concrete, and the results of the derived study are as follows.

First, the method of extracting drawings from the point cloud did not require any work on the drawing unlike conventional method such as drawing plans through actual measurement. Moreover, it was possible to accurately create the refraction of the wall according to the shape of the road or site. Furthermore, by accurately creating a plan in which two different walls do not form a right angle, this algorithm was possible to extract the plan shape of the entire building within the legal tolerance range.

Second, it was easy to find the plumbing room that is difficult to see with human eyes when making drawings by measuring the actual measurements. Also, this method can find easily the hidden space between the building and the wall. As can be seen from the actual experiment in this study, a space that human eyes could not find was found, and the wall that was slightly curved could be reflected in the drawing.

Finally, it was possible to predict the amount of concrete on the wall of the selected target building by using the derived architectural drawings and 3D point cloud data,

due to the fact that the volume is easily found by multiplying the area by the height. This is because the area can be easily derived by extracting the drawing, and height information can also be easily obtained from point cloud.

The architectural drawing extraction algorithm using the point cloud presented in this study can increase the drawing accuracy for buildings that require drawing, and can reduce errors that occur when drawing drawings. Additionally, by predicting the amount of building waste in advance, it is possible to plan in advance for building waste during demolition and remodelling of buildings. However, algorithm developed in this study, is limited in its application to buildings containing various materials, such as insulation materials included in walls in general. Therefore, it is expected that it will be able to develop highly effective algorithms and methodologies by reducing errors depending on the size of the building and minimizing the post-processing process to extract drawings that can be applied in practice.

Acknowledgements

This work is supported by the Korea Agency for Infrastructure Technology Advancement (KAIA) grant funded by the Ministry of Land, Infrastructure and Transport (Grant 22AATD-C163269-02).

References

- Capone, M. & Lanazara, E. (2019). Scan-to-BIM vs 3D Ideal model HBIM: parametric tools to study domes geometry. The International Archives of the Photogrammetry, *Remote Sensing and Spatial Information Sciences* (Volume XLII-2/W9, 2019).
- Jung, R., Koo, B., & Yu, Y. (2019). Using Drone and Laser Scanners for As-built Building Information Model Creation of a Cultural Heritage Building. *Journal of KIBIM*. 9(2), 11–20.
- Kang, T. (2016). Study on 3D Image Scan-based MEP Facility Management Technology *Journal of KIBIM*. 6(4), 18–26.
- Kim, H., & Lee, Y. (2018). Implementation of CUDA-based Octree Algorithm for Efficient Search for LiDAR Point Cloud. *The Korean Society of Remote Sensing*. 34(6), 1009-1024.
- Kim, T., & Kwon, J. (2019). The Maintenance and Management Method of Deteriorated Facilities Using 4D map Based on UAV and 3D Point Cloud. *Journal of the Korea Institute of Building Construction*. 19(3), 239 – 246.
- Koo, B., & Kim, J. (2009). The parametric model generation of human skeleton using Computerized Tomography images. *The Korean Society of Mechanical Engineers*. 1337-1342.
- Mesrop, A., Juan, M., Juan, E., & Daniel, A. (2020). From Point Cloud Data to Building Information Modelling: An Automatic Parametric Workflow for Heritage., *Remote Sens*. 12(7), 1094.
- Park, H., Ryu, J., Woo, S., & Choo, S. (2016). An Improvement of the Building Safety Inspection Survey Method using Laser Scanner and BIM-based Reverse Engineering. *Journal of the Korea Institute of Building Construction Planning & Design*. 32(12), 79-90.
- Yoon, J., & Ryu, S. (2020), A Study on the Advancement of Wooden Cultural Heritage Documentation through 3D Scanning, *Architectural Institute of Korea* (97 – 10).

HOW A FLOODED CITY CAN BE VISUALIZED FROM BOTH THE AIR AND THE GROUND WITH THE CITY DIGITAL TWIN APPROACH

System Integration of Flood Simulation and Augmented Reality with Drones

NAOKI KIKUCHI¹, TOMOHIRO FUKUDA² and NOBUYOSHI YABUKI³

^{1,2,3}*Osaka University.*

¹*kikuchi@it.see.eng.osaka-u.ac.jp, 0000-0002-9403-5671*

²*fukuda.tomohiro.see.eng@osaka-u.ac.jp, 0000-0002-4271-4445*

³*yabuki@see.eng.osaka-u.ac.jp, 0000-0002-2944-4540*

Abstract. City digital twins are becoming increasingly important for the sustainable development of cities, and augmented reality (AR) has been attracting attention as a tool for visualizing city digital twins. In addition, from the perspective of SDG 11, it is essential to manage flood risk in urban spaces. However, there are no case studies that present a bird's-eye view of a simulated city. Visualizing the state of a flooded city during a disaster is one potential use case. From the perspective of information graphics, people want to understand urban data at the micro and macro levels. This study proposes a city-digital-twin approach for visualizing a simulated city using a large-scale AR and drone integration method that does not require a specific software development kit (SDK). This system can visualize the state of a city flooded by a disaster from both a bird's-eye view of the city at several tens of metres above it and from a first-person perspective of the user's area of activity. The applicability of the system is demonstrated through verification and case studies.

Keywords. Virtual and Augmented Realities; City Digital Twin; Occlusion Handling; Flood Visualization; Web-based Augmented Reality (Web AR); SDG 11.

1. Introduction

Augmented reality (AR) is used in the fields of architecture, engineering, and construction to visualize urban information and promote consensus building among stakeholders. In addition, from the perspective of SDG 11, 'holistic disaster risk management at all levels' (United Nations, 2015, "Goal Targets" section), it is essential to manage flood risk in urban spaces. AR-based flood simulation has been used to promote consensus building through citizen participation and reduce flood risks in urban spaces. An overhead-view method (Tomkins and Lange, 2019) using a digital terrain model (DTM) has been proposed in conventional AR-based flood simulation.

A first-person-perspective method (Haynes et al., 2018) has also been proposed to display real-scale 3D data outdoors. Although traditional overhead-view AR can provide a real-time view of the exact extent of flooding, the virtual representation of the terrain in DTM-based methods may cause differences in understanding of the presented information between experts and non-experts. Also, in conventional AR (Haynes et al., 2018; Tomkins and Lange, 2019), which displays real-scale 3D data outdoors, stakeholders, including non-experts, can easily imagine the flooding situation in the physical environment, but residents may not be able to understand the information at the macro level.

Currently, the use of city digital twins, which are detailed 3D models of cities, is becoming increasingly important for sustainable urban development (Shahat et al., 2021). Visualizing city digital twins by using AR and virtual reality can facilitate the participation of non-expert citizens in the decision-making process (Mohammadi and Taylor, 2019). However, the number of reported studies using AR to visualize city digital twins is limited. From an information graphics perspective, residents should understand urban information from both the micro and macro perspectives (Offenhuber and Seitingner, 2014). An integrated method using AR and drones has been proposed for achieving an aerial view of AR that contains a bird's-eye view of the city (Unal et al., 2020; Wen and Kang, 2014). However, the issue of occlusion has persisted in the conventional methods for integrating AR and drones. The challenge of occlusion is that the 3D virtual model hides the physical object that should be displayed. Occlusion handling is one solution to this problem (Roxas et al., 2018).

Furthermore, the integration of AR and drones was based on software development kits (SDKs) specific to both technologies, and the system integration required the use of devices that were compatible with the specific SDKs. A study was reported (Kikuchi et al., 2021) that visualized the future landscape with occlusion handling using 3D models of cities. This study uses versatile techniques, such as virtual cameras and mirroring, to integrate AR and drones without using any specific SDK. In addition, there have not been any cases in which a flooded virtual city can be viewed from a bird's-eye view in AR at an accurate outdoor scale.

In this study, we propose a city-digital-twin approach for visualizing a large-scale city with simulated flood conditions by integrating the system of the previous study with a flood simulation system in a hydrograph. Using occlusion-handled AR, the user can visualize the simulated flood conditions of the city from a bird's-eye view at several tens of metres above the ground or from a first-person view of the user's area of activity. The applicability of the system is shown through verification and case studies.

2. Methodology

The method's conceptual diagram and flow diagram are shown in Fig. 1 and Fig. 2, respectively.

2.1. FLOOD SIMULATION USING HYDROGRAPHS

The flowchart for reproducing an urban flood situation is shown in Fig. 3. To reproduce urban flooding conditions simply, a water surface (3D virtual model) is output based

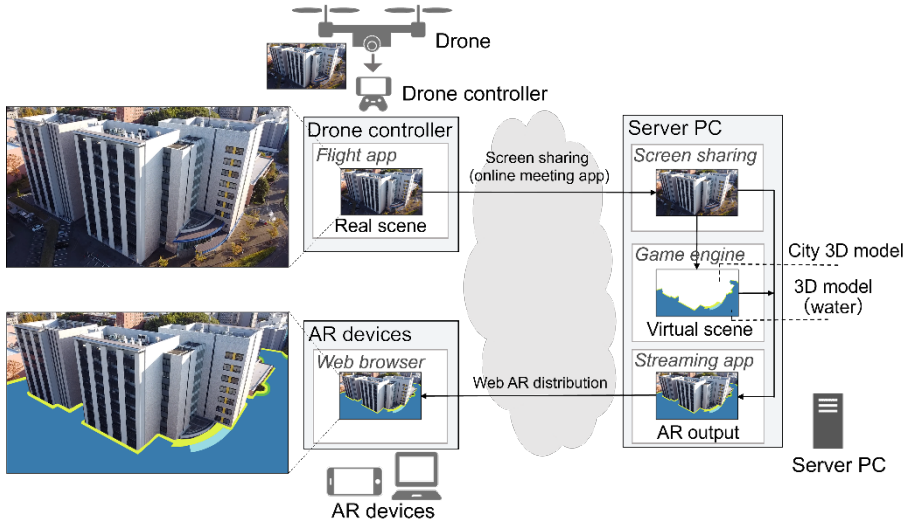


Figure 1. Conceptual diagram of the proposed method

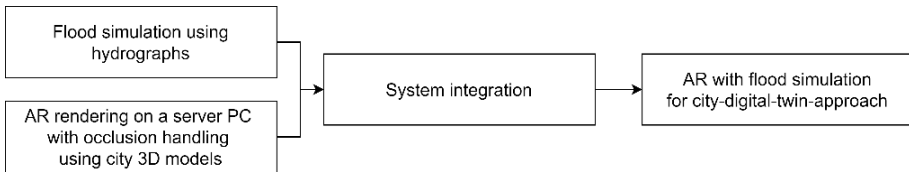


Figure 2. System integration flow for the proposed method

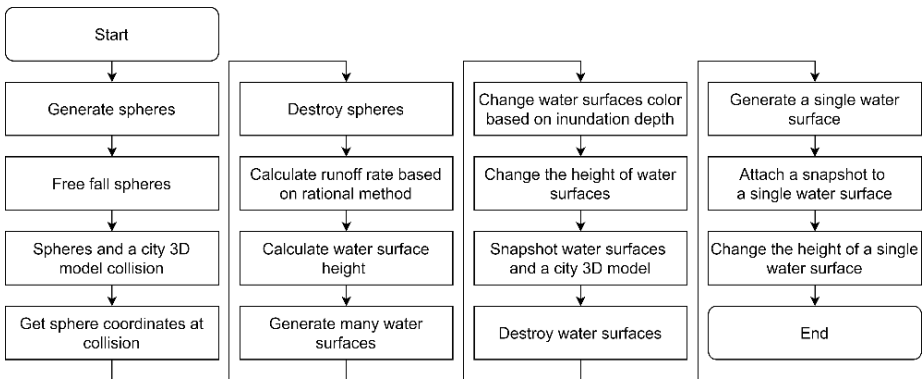


Figure 3. Flow for reproducing urban flood conditions

on the rational method (Kuichling, 1889; Tallapragada et al., 2020) (Equation 1). Using this method, we calculate the water runoff corresponding to the input rainfall time and rainfall amount. The hietograph and hydrograph are shown in Fig. 4 for the rational method (Crobbedu et al., 2007). In Fig. 4, the time of concentration indicates the time required for water at the farthest point in the basin to flow out of it. The hietograph shows the change in rainfall (inflow) over time, and the hydrograph shows the change

in rainfall runoff. The amount of flood water is determined by the difference between the inflow and outflow during the rainfall duration.

$$Q = \frac{1}{3.6} CIA \quad (1)$$

In Eq. 1, Q is the runoff rate (m^3/s), C is the runoff coefficient, I is the rainfall (mm/h), and A is the watershed area (km^2).

The 3D city model shape is estimated by allowing many generated spheres to fall freely on it and obtaining the coordinates at the time of collision with the model. The inundation depth and water height are calculated from the 3D city model shape and the flooding amount, which output a virtual 3D model of the water surface to the game engine. The water surface reflects the water height and the colour changes according to the inundation depth. In this study, to reproduce urban flood conditions simply, the flood extent was limited to the area of the created 3D city model and did not consider the inflow and outflow of water from other areas. A 3D model of a city with a floor area of several hundred thousand square metres was used to reproduce urban flood conditions from a bird's-eye view.

2.2. AR RENDERING ON A SERVER PC WITH OCCLUSION HANDLING USING A 3D CITY MODEL

This section is based on content reported in our previous study (Kikuchi et al., 2021). However, it is a necessary module for our system and will be briefly explained. To represent the simulated flood conditions of a city in AR, it is necessary to handle occlusion (Haynes et al., 2018). Based on the system from our previous study, the AR is rendered with occlusion handling on a server PC using a 3D model of a city (Fig. 5). The 3D city model and background are changed to an emissive colour with RGB values that do not exist in the real world. The range of the changed emissive colour is chroma keyed to enable occlusion handling. In addition, the start time, flight route, and the orientations of both the drone's camera in the real world and the camera in the virtual world are synchronized by pre-settings to align them. To encourage the participation of a wide range of stakeholders, the AR information is uploaded to the web by using a video distribution service.

3. Experiments and Results

A prototype system was built to evaluate the proposed method. The system comprised the following hardware. We used a DJI Mavic mini (199g) drone to achieve the aerial perspective. An iPhone 11 (iOS v14.8) was used to operate the drone. The server was a home-made PC with an Intel® Core™ i7-8700K CPU (3.70 GHz, 32 GB of RAM) and an Nvidia GeForce GTX 1080 Ti GPU running Windows 10 Education 64 bit OS, and was used to output web AR with occlusion handling for the 3D city models. An iPad (iOS v15.1) was used as the AR device.

The software used in the prototype system was Litchi for DJI Drones (iOS v2.10.1), which can control a drone by setting waypoints for the drone autopilot. Microsoft Teams (Server PC: v1.4.00.31569 64 bit, Controller: iOS v3.19.0), an online meeting

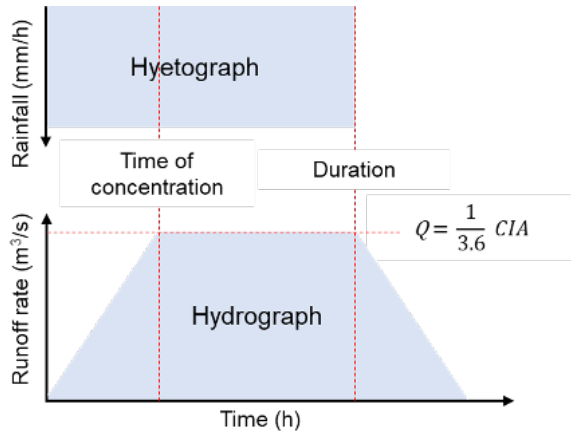


Figure 4. Hyetograph and hydrograph of the rational method under constant precipitation

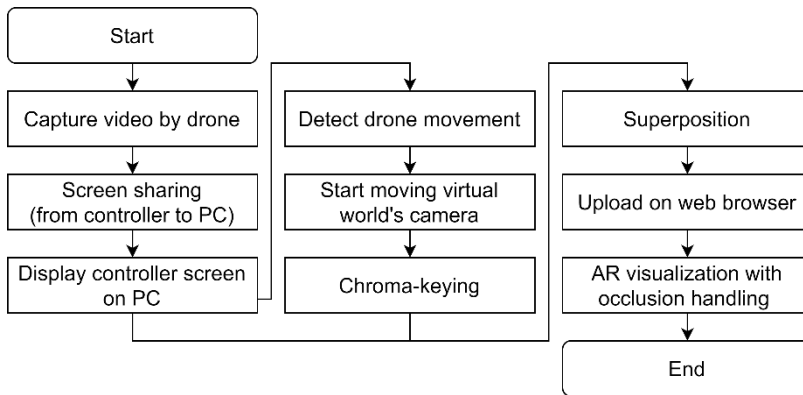


Figure 5. Flow of AR rendering with occlusion handling

application, was used for screen sharing. OBS Studio (v27.1.3) was the video distribution application used for web AR distribution. Unity (2020.1.7f1 64bit), a game engine, was used to construct the virtual world. Metashape Professional (v1.6.0 build 9925 64 bit, Agisoft), a 3D spatial data generation tool using structure from motion (Westoby et al., 2012), was used to create a 3D city model with roof geometry. Structure from motion was used as an automatic method for creating 3D point cloud data from multiple 2D images. YouTube was used to distribute AR in a web browser and Firefox Daylight (v38.0) was used as the web browser for viewing YouTube.

3.1. PRE-SETTING FOR EXPERIMENTS

Using Agisoft Metashape Professional, a 3D city model was created from 508 photos shot by the drone's camera and then placed in Unity (Fig. 6). The specifications of the created 3D city model are shown in Table 1. In addition, to clarify the relation between the angles of the drone camera and the virtual world camera with the flight altitude, the pre-set camera angles of both worlds are shown in Fig. 7.

3.2. FLOOD VISUALIZATION

An outdoor AR experiment was conducted to verify whether the proposed system can simulate flooded urban conditions during a disaster. An outdoor area of private property with flight permission was chosen as the experiment site to safely fly the drone. To hypothetically flood the city, the runoff coefficient was set to 0.8, the rainfall rate to 100 mm/h, the runoff duration to 10 m, and the rainfall duration to 10 h. Figure 8 (a) shows the situation for the experiment. In Fig. 8 (a), the drone is flown for 18 s, going from 20 ± 1 m to 60 ± 1 m. Figure 8 (b) shows the city during the outdoor AR experiment. Figure 8 (c) shows the city in the virtual world for flood simulation. In Fig. 8 (c), the 3D city model and the background of the camera on the virtual world are changed to a white emissive colour $[(R, G, B) = (255, 255, 255)]$. This colour change is enacted to perform chroma-keying and to apply occlusion handling (Kikuchi et al., 2021). Figure 8 (d) shows the specification of the change in water surface colour based on the inundation depth. Figure 9 shows the results. An example of the results is shown in Fig. 10. In Fig. 11, the accuracy of the occlusion handling is visualized by superimposing parts of the virtual world's buildings onto the drone video. Figure 11 was created by extracting parts of the virtual world and the real-world buildings using Adobe Photoshop CS4 (v11.0). This experiment confirmed that it is possible to simulate the urban flooding conditions during a disaster in an expansive outdoor space with overhead view AR.

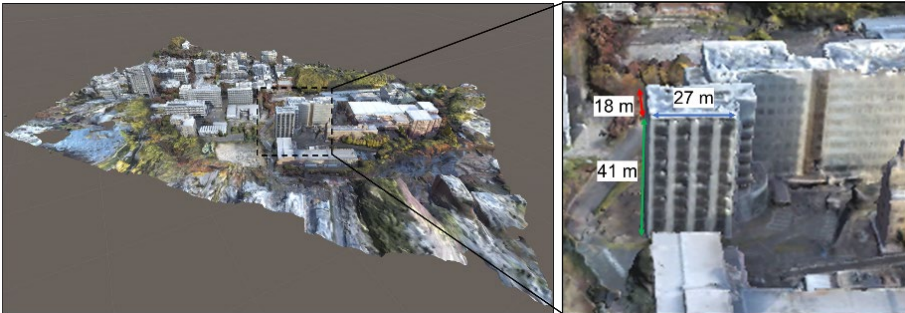


Figure 6. 3D city model

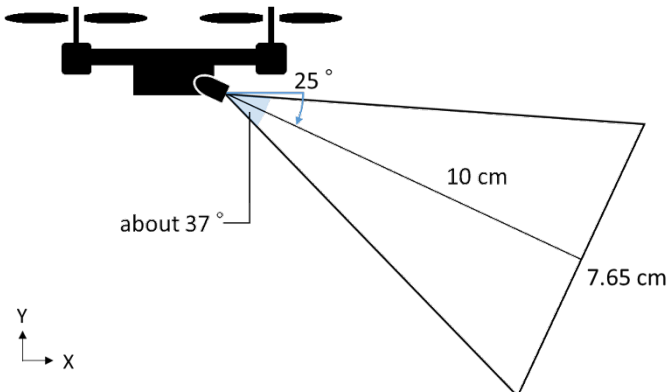


Figure 7. Camera angles in the real and virtual worlds

3D model	Number of polygons	12.5×10^6
	Number of vertices	7.4×10^6
	Data amount [MB]	2.62×10^2
Texture	Number of textures	1
	Number of texture pixels	16777216

Table 1. Specifications of the 3D city model

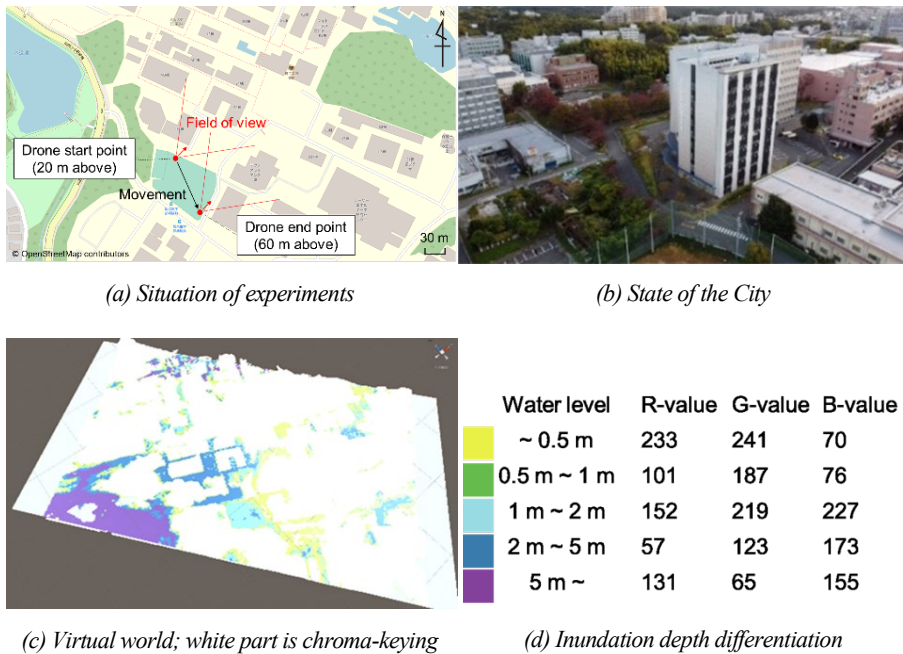


Figure 8. Real world and virtual world for flood visualization

3.3. PROTOTYPE SYSTEM PERFORMANCE

We measured the overall processing speed, delay, and intersection over union (IoU) for the proposed system. IoU was used to evaluate the matching accuracy between the real world and the virtual world buildings (Liu et al., 2021). The frame rate of the drone video was about 30 fps, the frame rate of the video acquired from the camera in the virtual world was about 105 fps, and the frame rate on the web was about 30 fps. The delay between the controller and the AR device display was about 4 s. The IoU was about 0.77.

4. Discussion

In the outdoor AR experiment, the AR system was confirmed to simulate urban flood conditions. In Fig. 10, the water surface is displayed lower than the expected height,

which is presumably due to the low occlusion handling. In addition, our system was able to reproduce a large-scale flooded city by integrating the system in our previous study (Kikuchi et al., 2021) with the flood simulation system in the hydrograph. Also, the system reproduced urban flood conditions from an overhead perspective by using a 3D city model of several hundred thousand square metres. The entire system's frame rate was about 30 fps. This value is higher than the threshold of around 15 fps, which is a good frame rate for video (Chen et al., 2007). The IoU was about 0.77, which is higher than 0.5, the value of IoU at which buildings were adequately detected (Jabbar et al., 2017).

5. Conclusions

A digital-twin-city approach was developed to visualize a simulated large-scale city from both user-level and aerial-overhead viewpoints. Using a 3D model of a city of several hundred thousand square metres makes it possible to reproduce the urban flood situation from a bird's-eye view. It was confirmed that the frame rate of the entire prototype system was about 30 fps, the delay was about 4 s, and the IoU was about 0.77.

In this study, we used motion structure to create a 3D city model for occlusion handling. We plan to use pre-created 3D models of various cities, such as PLATEAU (Ministry of Land, Infrastructure, Transport and Tourism, 2020), with the aim of reducing the cost of creating such models.

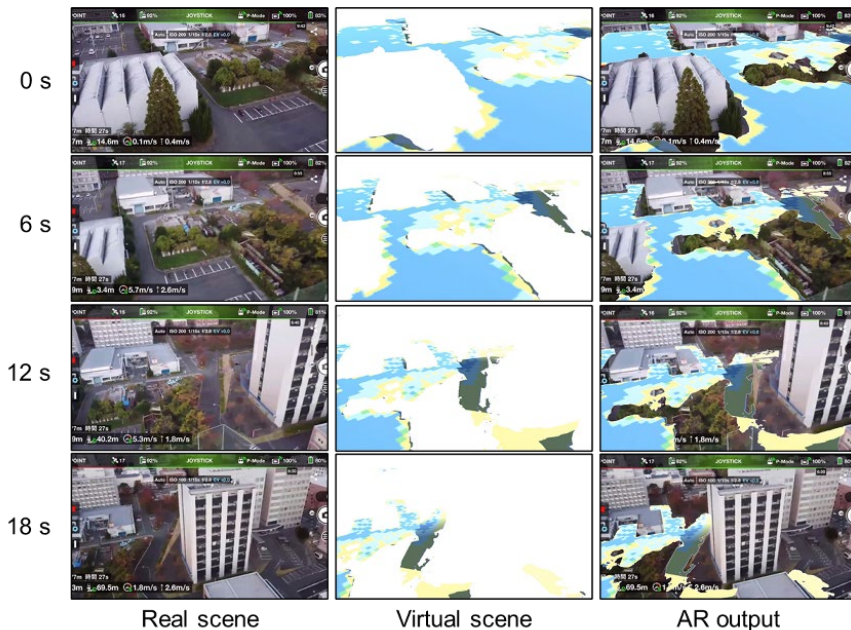


Figure 9. AR snapshots from the field test



Figure 10. Example of the results

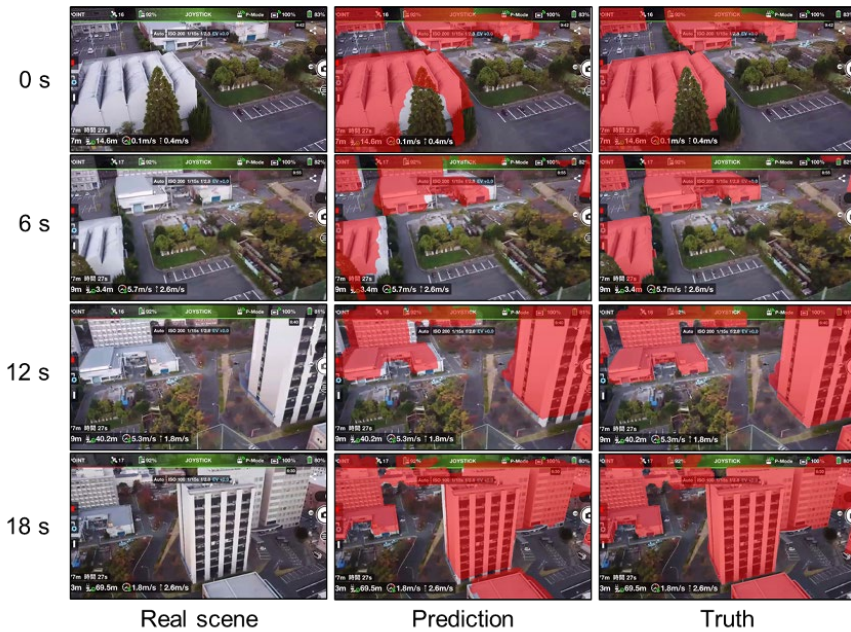


Figure 11. Occlusion handling accuracy

Acknowledgements

This research was partly supported by JSPS KAKENHI Grant Number JP19K12681.

References

Chen, J. Y. C., & Thropp, J. E. (2007). Review of low frame rate effects on human performance. *IEEE Transactions on Systems, Man, and Cybernetics - Part A: Systems and Humans*, 37(6), 1063-1076. <https://doi.org/10.1109/TSMCA.2007.904779>.

- Crobeddu, E., Bennis, S., & Rhouzlane, S. (2007). Improved rational hydrograph method. *Journal of Hydrology*, 338 (1–2), 63–72. <https://doi.org/10.1016/j.jhydrol.2007.02.020>.
- Haynes, P., Hehl-Lange, S., & Lange, E. (2018). Mobile Augmented Reality for Flood Visualization. *Environmental Modelling and Software*, 109, 380–389. <https://doi.org/10.1016/j.envsoft.2018.05.012>.
- Jabbar, A., Farrawell, L., Fountain, J., & Chalup, S. K. (2017). Training deep neural networks for detecting drinking glasses using synthetic images. In *International Conference on Neural Information Processing* (pp. 354–363). Springer, Cham. https://doi.org/10.1007/978-3-319-70096-0_37.
- Kikuchi, N., Fukuda, T., & Yabuki, N. (2021). Landscape visualization by integrating augmented reality and drones with occlusion handling to link real and virtual worlds - towards city digital twin realization. *Proceedings of the 39th eCAADe Conference* (pp. 521–528), University of Novi Sad, Novi Sad, Serbia.
- Kuichling, E. (1889). The relation between the rainfall and the discharge of sewers in populous places. *Transactions of the American Society of Civil Engineers*, 20, 1–60.
- Liu, D., Xia, X., Chen, J., & Li, S. (2021). Integrating building information model and augmented reality for drone-based building inspection. *Journal of Computing in Civil Engineering*, 35, 1–40. [https://doi.org/10.1061/\(ASCE\)CP.1943-5487.0000958](https://doi.org/10.1061/(ASCE)CP.1943-5487.0000958).
- Ministry of Land, Infrastructure, Transport and Tourism. (2020). *PLATEAU*. Retrieved December 20, 2021, from <https://www.mlit.go.jp/plateau/>.
- Mohammadi, N., & Taylor, J. (2019). Devising a game theoretic approach to enable smart city digital twin analytics. *Proceedings of the 52nd Hawaii International Conference on System Sciences* (pp. 1995–2002), <https://doi.org/10.24251/HICSS.2019.241>.
- Offenhuber, D., & Seitingner, S. (2014). Over the rainbow: information design for low-resolution urban displays. *Proceedings of the 2nd Media Architecture Biennale Conference: World Cities* (pp. 40–47). Association for Computing Machinery. <https://doi.org/10.1145/2682884.2682886>.
- Roxas, M., Hori, T., Fukiage, T., Okamoto, Y., & Oishi, T. (2018). Occlusion handling using semantic segmentation and visibility-based rendering for mixed reality. *Proceedings of the 24th ACM Symposium on Virtual Reality Software and Technology* (pp. 1–8). <https://doi.org/10.1145/3281505.3281546>.
- Shahat, E., Hyun, C. T., & Yeom, C. (2021). City digital twin potentials: A review and research agenda. *Sustainability*, 13, 3386. <https://doi.org/10.3390/su13063386>.
- Tallapragada, K. R., Bhawe, H. D., & Tiwari, M. S. (2020). Application of geoinformatics in ground water augmentation of aam water shed. *Helix*, 10(1), 109–115.
- Tomkins, A., & Lange, E. (2019). Interactive landscape design and flood visualisation in augmented reality. *Multimodal Technologies and Interaction*, 3(2), 43. <https://doi.org/10.3390/mti3020043>.
- Unal, M., Bostanci, E., & Sertalp, E. (2020). Distant augmented reality: bringing a new dimension to user experience using drones. *Digital Applications in Archaeology and Cultural Heritage*, 17, 1–12. <https://doi.org/10.1016/j.daach.2020.e00140>. 47.
- United Nations Development Programme. (2015). Goal 11 SUSTAINABLE CITIES AND COMMUNITIES. Retrieved January 22, 2022, from <https://www.undp.org/sustainable-development-goals#sustainable-cities-and-communities>.
- Wen, M., & Kang, C. (2014). Augmented reality and unmanned aerial vehicle assist in construction management. *Computing in Civil and Building Engineering*, 1570–1577. <https://doi.org/10.1061/9780784413616.195>.
- Westoby, M. J., Brasington, J., Glasser, N. F., Hambrey, M.J., & Reynolds, J.M. (2012). Structure-from-motion' photogrammetry: A low-cost, effective tool for geoscience applications. *Geomorphology*, 179, 300–314. <https://doi.org/10.1016/j.geomorph.2012.08.021>.

Environmental Performance Based Design and Sustainability

CONSIDERING ENERGY, MATERIALS AND HEALTH FACTORS IN ARCHITECTURAL DESIGN

Two renovation strategies for the Portuguese building stock

ADRIAN KREZLIK¹

¹*Faculty of Architecture, University of Porto.*

¹*adrian.krezlik@gmail.com, 0000-0003-3200-8851*

Abstract. According to the Intergovernmental Panel on Climate Change, the built environment has a significant share in global final energy use, greenhouse gases emission, land-system change, and biodiversity loss to list some indicators. In Europe, the biggest challenge is to regenerate existing building stock to create a positive impact on Nature. The Portuguese housing stock is old: 56% is more than 30 years old, and it has a low level of thermal comfort and energy efficiency. The first thermal regulations appeared in 1990 and therefore most of the houses need urgent renovation to meet EU decarbonization goals, and to improve energy efficiency, as well as well-being and comfort of residents. This paper presents a method that aims to verify existing solutions known from vernacular architecture as complementary to existing strategies. It employs digital simulation to verify whether they could be used for renovation, measuring their impact on human and planetary health. The paper shows that there is a wide spectrum of parameters that influence the renovation process and that it is possible to enhance building performance using vernacular knowledge.

Keywords. Building Energy Modelling; Life Cycle Assessment; Occupant Health; Energy Renovation; Vernacular Mimicry; SDG 3; SDG 11; SDG 13.

1. Introduction

According to the Renovation Wave directive, 75% of the existing building stock in Europe needs to be renovated (European Commission, 2020). Particularly in Portugal, the 2011 National Census (Instituto Nacional Estatística, 2011) shows that 65% of the housing was built before the introduction of energy-efficient regulations in 1990.

Energy inefficient buildings are negatively impacting the residents and the environment. In Europe, buildings are responsible for about 40% of total energy consumption, and for 36% of greenhouse gas emissions (GHG) (European Commission & Joint Research Centre., 2019). A study shows that operational energy

consumption in buildings can be reduced by 50% with the adoption of energy-efficiency methods (Magalhães et al., 2016). New buildings must meet the Energy Performance of Building Directive, therefore new buildings' negative impact on the environment in the operational phase must be significantly lower. This essentially means that to cut the GHG emission by 55%, renovation actions must be prioritised.

Today, in Portugal, research on renovation focuses mostly on engineering solutions (Almeida et al., 2014), (Sousa et al., 2013) and (Bragança et al., 2007), typically adding an HVAC system, placing insulation or changing windows. The same approach is taken by the National Agency for Energy in its recommendations (ADENE, 2016). Similarly, 'part 13' of the Recovery and Resilience Plan covers energy efficiency and focuses on engineering and material solutions. Simultaneously, there is a wide range of bioclimatic solutions present in vernacular architecture in Portugal (Fernandes, 2020), that in the last decades have been neglected.

Europeans spend almost 90% of their time in interior spaces (European Commission, 2002), therefore it is important to evaluate the impact of architecture on health. Comfort is an immediate expression of the human body condition and is related to health (Ortiz et al., 2017). In the study, thermal and visual comfort will be used as metrics of health.

In this context, the current paper wants to evaluate renovation strategies from the context of energy, materials and health for Portuguese housing. With that goal, it presents a study exploring the concept of patterns, first presented in the book 'A pattern language: towns, buildings, construction' (Alexander, 1977) that connected geometrical features of architectural components with human cognition, behaviour, and relationships

The paper also looks to contribute to the local discussion on the opportunities connected to regional solutions to enhance energy efficiency and resident comfort. The study simulates the impact of a vernacular pattern following the notions of the Age of

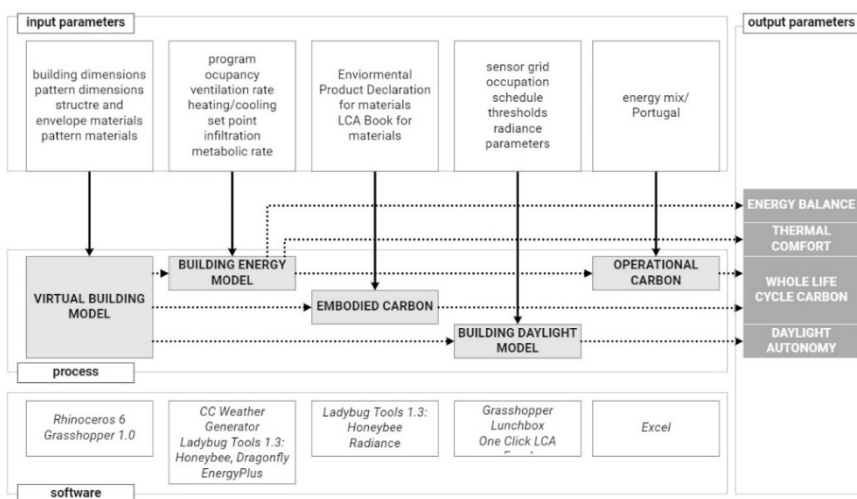


Figure 1 Workflow

Data, not the rule of thumb which has been done multiple times before (Moholy-Nagy, 1957). This article is an answer to Susane Roaf's studies (Roaf, 2020) on traditional architecture in Yazd and her suggestion to review solutions because they might not be accurate.

2. Methodology

2.1. WORKFLOW

The study is organised in two parts: (1) research and selection of patterns, and (2) analysis of the impact of the selected pattern on the environment and resident comfort, as per 'Figure 1'. The research of patterns is conducted through a literature review and on-site observation of vernacular patterns in Portugal and northern Spain.



Figure 2 Balcony in Távira (Portugal)



Figure 3 Balcony in Vitoria (Spain)

2.2. SELECTING THE PATTERN

Among multiple vernacular solutions that could be listed in traditional architecture in the selected region is a balcony. A survey of popular architecture in Portugal run in the 1950s has already observed balconies across the north as a pattern to protect from the summer heat (open) or cold (glazed) in the winter (SNA, 1961). So far there has been no comprehensive study measuring the impact of a balcony on the environment and resident comfort (Huang & Liu, 2020) In the scope of this study, two types of balconies (Figure 2, 3) are examined:

- Open, protected with a balustrade, of three different depths (1.0m, 2.0m, 3.0m)
- Closed/Operable, of three different depths (1.0m, 2.0m, 3.0m)

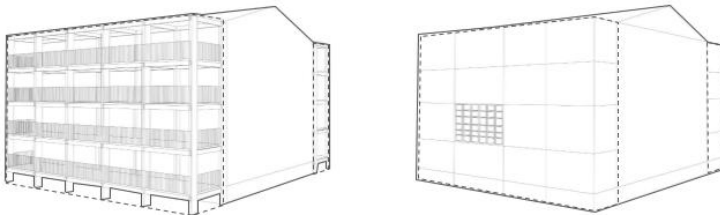


Figure 4 Renovation options: open balcony (left), closed balcony (right)

2.3. SELECTING AND MODELLING THE VIRTUAL BUILDING

Each balcony will be an addition to the Virtual Building (VB). A Virtual Building is a digital 3D model of a building based on a typical housing building in Porto from the fifties and sixties (Ramos et al., 2009).

The Virtual Building is a 4 storey collective housing, with four apartments on each floor (Figure 4). Each apartment is divided into 4 or 5 rooms, two of which were selected: South facing Room [SR] and North facing Room [NR], with Window-to-Wall Ratios of 0.2 (south) and 0.3 (north).

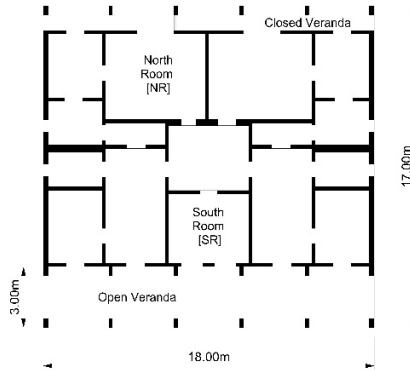


Figure 5 Typical floor plan

In the modelling phase of the Virtual Building, the author used typical materials of the 1950s and 1960s which can be listed as:

- columns and slabs: reinforced concrete,
- envelope an (uninsulated) cavity brick wall ($U\text{-value}=2.08 \text{ W/m}^2\text{K}$) of 27.5 cm,
- single glazed windows ($3.50 \text{ W/m}^2\text{K}$),
- concrete roof (uninsulated) with bituminous waterproofing ($1.10 \text{ W/m}^2\text{K}$).

To renovate, two types of balconies are used with two renovation strategies, as per Table 1: conventional (following typical constructive solutions available in the market) and regenerative (using materials aiming to reduce the environmental impact).

While the open balcony is an addition to the building without requiring demolition works or significant changes to the existing structure, the closed balcony needs the removal of the exterior wall to connect with the additional space.

The material's properties (including embodied carbon) come from One Click LCA database. Table 1 shows the materials used in the simulations and calculations: The data on the embodied carbon used in the study is heterogeneous (e.g. different sources of certificates, different countries) and reflect only the cradle-to-gate part of the life cycle. Also, the difference between the estimated size of structure causes differences lower than 0.005%. Therefore, for a more in-depth, detailed structural study is needed, which includes sizing.

	open balcony		closed balcony	
	Conventional (C)	Regenerative (R)	Conventional	Regenerative
Columns, Purlins,	Reinforced		Reinforced	
Beams, Slabs	Concrete	CLT	Concrete	CLT
Balustrade	Galvanised Steel	CLT	no balustrade	no balustrade
Windows	no windows	no windows	Aluminium	Wooden

Figure 6 Materials used for building components

2.4. SETTING UP THE ENERGY MODEL

To simulate the operation of the VB, a Building Energy Model is created and parametrized in Ladybug and Honeybee plugins (connected to EnergyPlus) for Grasshopper for Rhinoceros 6 (Figure 01). To simulate the observed climate, data from the closest weather station (PORTO 85450) are used. To generate future climate scenarios, based on the Intergovernmental Panel on Climate Change Third Assessment Report model, the CCWorldWeatherGen (Jentsch et al., 2013) tool is used. It is a climate data morpher developed by the University of Southampton. For the existing building, further parameters were defined to reflect the local conditions, namely:

- energy zones are considered as conditioned,
- typical occupancy schedule for Portugal (Barbosa et al., 2016),
- no central heating or cooling system, mechanical ventilation (Vilhena et al., 2013),
- a typical gas unit heater, with the setpoint at 15°C,
- high infiltration rate: 0.004m³/s/m² (due to the age of the VB),
- a series of metabolic rates and clothing level for different kind of activities in domestic space (American Society of Heating, 1992),

For the closed balcony, all parameters are kept and a lower infiltration rate is used (0.002m³/s/m²) due to the placement of a new exterior, sealed facade system.

2.5. SETTING UP THE DAYLIGHT MODEL

To simulate visual comfort, a Daylight Model is created and parametrized in Ladybug and Honeybee plugins (connected to Radiance) for Grasshopper for Rhinoceros 6 (Figure 01). The test plane was generated at a height of 0.7m, with sensors distributed on a grid with unit squares of 0.5m by 0.5m. There are no interior elements (partition walls, furniture, etc.). The Radiance parameters are set up to obtain a mid-quality simulation. The glass' visible transmittance is set to 0.6, and the solar heat gains coefficient to 0.25.

2.6. SIMULATING

To compare the different solutions, 10 simulations for the SR and 10 for the NR were performed for the observed and future climate (2050) for Porto, in total 40 simulations. This article will focus on the future climate results only. The simulation started with 15°C and the open balcony options. 15°C is selected as a benchmark

temperature, lower than the recommendation of the World Health Organisation (World Health Organization et al., 2018) or Portuguese building code (Presidência da República, 2013), but the prevalent indoor temperature in the north of Portugal (Magalhães et al., 2016).

Simulation name	Group	Subtype	Comfort
baseline		baseline	setpt=15°C
option 01	open balcony	1.00	setpt=15°C
option 02		2.00	setpt=15°C
option 03		3.00	setpt=15°C
option 04	closed balcony	1.00	setpt=15°C
option 05		2.00	setpt=15°C
option 06		3.00	setpt=15°C
option 07	closed balcony	1.00	setpt=18°C
option 08		2.00	setpt=18°C
option 09		3.00	setpt=18°C

Table 1. Options legend

2.7. MEASURING THE IMPACT

This study compares a conventional with a regenerative strategy, measuring Global Warming Potential (GWP), an indicator of GHG emissions, in the life cycle of the VB following the standard ISO 14040:2006 in the perspective of 30 years considering climate change according to the IPCC scenario A2 (IPCC, 2021: Climate Change 2021). The carbon life cycle assessment includes material embodied carbon. In this study, residents' comfort is based on two elements: thermal comfort and daylight availability. Other aspects of daylight, such as glare or view out, were omitted to simplify the model. The following indicators are used to evaluate each solution:

- Embodied Carbon, EC [kg CO₂ equiv/m²];
- Operational Energy, OE (heating) [kWh/year/m²], to calculate GHG emissions and to understand the impact of Solar Energy Gains on thermal comfort;
- Operational Energy, OEI (lighting) [kWh/year/m²], to calculate GHG emissions and to understand the impact of daylight on visual comfort;
- Solar Gains, SG [kWh/year/m²], heat gained through the solar radiation;
- Operational Carbon, OC [kg CO₂ equiv/m²], total GHG emissions related to building operation, calculated as a product of total Operational Energy and carbon intensity of the energy sources;
- Carbon LCA [kg CO₂ equiv/m²], total carbon, a sum of EC and OC;
- Thermal Comfort [%], hours that residents are comfortable;

- Spatial Daylight Autonomy, sDA [%], time of the year that for a sensor, distributed on a grid 0.5 by 0.5m on the height of 0.7 m, a threshold of 100 is achieved.

3. Results

To summarise the results of renovation of the VB with an open balcony for both the SR and the NR it is observed that:

- it decreases residents' (thermal and visual) indoor comfort and therefore is likely to have negative impact on their health,
- it brings extra Outdoor Domestic Space that could be comfortably occupied for 69% of the year (according to the simulation of the Universal Climate Thermal Index) with a good quality of visual comfort,
- the sDA is reduced significantly, meaning that there is not enough daylight to perform everyday activities, lack of daylight influences human health too [41],
- indoor temperature is below the level proposed by the WHO (18°C) ,
- the environmental cost of this solution is quite large, the Carbon LCA increases by at least 30% compared with no intervention,
- the negative impact on the thermal comfort is noticeable especially while comparing the SR and the NR, the open balcony blocks longwave radiation and does not allow to capture heat,

	Total Operational Energy (heating)	Annual Solar Gain	Spatial Daylight Autonomy	Thermal Comfort	Total Carbon
South Room	15% to 26%	-11% to -49%	-21% to -70%	-18% to -22%	47% to 65%
North Room	0% to +4%	-60% to -79%	-30% to -60%	-1% to -4%	31% to 100%

Table 2. Open balcony: rooms performance in different categories in comparison to the baseline (current state).

The closed balcony brings significantly better results. First of all it reduces energy consumption, brings more daylight, and increases thermal comfort. However, the interventions in the building come with a significant carbon cost (Table 4). The Total Carbon of the NR is significantly higher than the SR. After analysing data of simulation one can observe that:

- to achieve 15°C in the wintertime (like in Table 4), which is not considered comfortable, but common in north Portugal, at least 1.61E+02 kg CO2 equiv/m2 is needed,
- additionally to achieve 18°C in the wintertime, carbon expenses are almost tripled. Minimising both embodied carbon and operational carbon is crucial, and thus comfort should be achieved for most of the year without using an HVAC system,

Total Operational Energy (heating)	Annual Solar Gain	Spatial Daylight Autonomy	Thermal Comfort	Total Carbon
---------------------------------------	----------------------	---------------------------------	--------------------	-----------------

				Comfort	Carbon
South Room	-42% to -11%	40%	4%	6% to 9%	31% to 60%
North Room	-41% to -27%	-23%	4%	11% to 16%	50% to 138%

Table 3. Closed balcony: rooms performance in different categories in comparison to the baseline (current state).

While examining the building from the point of the life cycle (Table 5) one can clearly observe that the operational carbon prevails, which aligns with other studies in Portugal (Rossi et al., 2012). It is important to mention that since the space is equipped with a gas heater, and the purpose of this study is to introduce passive solutions, the replacement of a heating system was not considered. Therefore, no energy decarbonization actions were taken into consideration. It opens a door for another research on the renovation expenses in the light of energy decarbonization. It is inevitable to question what type of renovation is actually benefiting users and the environment in the perspective of 30 and 50 years.

To ensure the thermal comfort of the residents, an additional study was run to verify how much more carbon would be released as per Table 5. In comparison with the same renovation solution, it is almost 2.5 times more. According to this simulation, Human Comfort (100%) would cost an additional 521 kg CO₂ equiv/m² in the perspective of 30 years. As mentioned before, the renovation calculation includes only cradle-to-gate material impact, which means that the real embodied carbon values are higher. The Operational Carbon is likely to reduce if a better performing heating system is used.

	Total Operational Carbon [kWh/m ²]	Total Operational Carbon [%]	Embodied Carbon [kWh/m ²]	Embodied Carbon [%]
baseline	3.47E+02	100.00%	0.00E+00	0.00%
option 02	4.22E+02	76.02%	1.33E+02	23.98%
option 05	2.75E+02	69.76%	1.19E+02	30.24%
option 08	7.96E+02	86.99%	1.19E+02	13.01%

Table 4. Embodied and operation carbon for selected options.

4. Discussion

The paper does not conclude in one best solution, as per every multiobjective problem such does not exist. Looking from the human comfort point of view, renovating with a Closed Balcony and the set point of 18°C on the SR is the best but it brings the highest environmental costs, while the 15°C set point might represent a compromise of lowering human comfort to create less negative environmental impact. Additionally changing the heating system from the gas unit to another will bring significant savings in carbon emission. Considering creation of an extra Outdoor Domestic Space for the North Façade, the Open Balcony might be considered the best option. But, again this renovation favors human comfort over the planetary safety.

The paper does not focus on questioning modern, conventional engineering solutions, it rather looks to complement them with architectural ones and looks for alternatives known from history of architecture. This study opens the author's research to find a robust workflow to verify other vernacular patterns. Future studies would benefit from collaboration with a structural engineer who can propose detailed structural solutions. The workflow is thought to be universal and possible to test, in different locations, elements such as climate (past, current and future), material availability and modus vivendi, as they are input parameters that need to be reviewed every time.

From the planetary crisis point of view, the article follows the carbon tunnel. It is focused only on one of the aspects of the earth systems; other dimensions, like Acidification Potential, that could be found in the Environment Product Declaration were not considered. It follows European policies for renovation, decarbonisation and energy. There is a research gap to clearly connect other dimensions with the built environment. The database of materials is still limited, as many vernacular materials like straw, woodfibers, and eucalyptus timber do not have EPDs or another type of assessment. This is likely to change with the European Green Deal expressed in the New European Bauhaus initiative.

Acknowledgements

This research of Adrian Krezlik was supported by the doctoral Grant I Scholarship SFRH/BD/151418 financed by the Portuguese Foundation for Science and Technology under MIT Portugal Program.

References

- ADENE. (2016). *10 Soluções de Eficiência Energética*. ADENE.
- Alexander, C., et al. (1977). *A pattern language: Towns, buildings, construction*.
- Almeida, M. et al. (2014). Cost optimality and nZEB target in building renovation of Portuguese residential buildings. *IiSBE Net Zero Built Environment 2014 Symposium*, 231–241.
- American Society of Heating, (1992). *ASHRAE standard thermal environmental conditions for human occupancy*. Atlanta, Ga.: The Society, 1992.
- Barbosa, J. A., Mateus, R., & Bragança, L. (2016). Occupancy Patterns and Building Performance – Developing occupancy patterns for Portuguese residential buildings. *SBE16 Brazil & Portugal*. <https://doi.org/10.13140/RG.2.2.27296.58881>
- Braganca, L., Almeida, M., & Mateus, R. (2007). Technical improvement of the housing envelopes in Portugal. *COST C16 Improving the Quality of Existing Urban Building Envelopes*. Amsterdam. IOS Press.
- European Commission. (2002). *Indoor air pollution: New EU research reveals higher risks than previously thought* European Commission.
- European Commission. (2020). *Renovation Wave: Fact Sheet*. doi:10.2833/535670
- European Commission, (2019). *Achieving the cost-effective energy transformation of Europe's buildings: Combinations of insulation and heating & cooling technologies renovations: methods and data*. Publications Office. Retrieved from <https://data.europa.eu/doi/10.2760/278207>
- Fernandes, J. (2020). *Modelling the life cycle performance of Portuguese vernacular buildings: Assessment and contribution for sustainable construction*. University of Minho.

- Huang, Y., & Liu, W. (2020). Measurement and Analysis of the Thermal Insulation Effect of the Transition Space of a Building Veranda in the Hot Summer and Cold Winter Zone. *Future Cities and Environment*, 6(1), doi.org/10.5334/fce.86
- Instituto Nacional Estatística. (2011). *Inquérito ao Consumo de Energia no Sector Doméstico*. IPCC. (2021). *Climate Change 2021: The Physical Science Basis*. Contribution of Working Group I to the Sixth, Assessment Report of the Intergovernmental Panel on Climate Change. Cambridge University Press. In, & Press. (2021).
- Jentsch, M. F., et al. (2013). Transforming existing weather data for worldwide locations to enable energy and building performance simulation under future climates. *Renewable Energy*, 55, 514–524, doi.org/10.1016/j.renene.2012.12.049
- Magalhães, S. M. C. et al (2016). Predicting and characterizing indoor temperatures in residential buildings: Results from a monitoring campaign in Northern Portugal. *Energy and Buildings*, 119, 293–308. <https://doi.org/10.1016/j.enbuild.2016.03.064>
- Moholy-Nagy, S. (1957). *Native Genius in Anonymous Architecture*. Horizon Press.
- Ortiz, M. A., et al (2017). A review of comfort, health, and energy use: Understanding daily energy use and wellbeing for the development of a new approach to study comfort. *Energy and Buildings*, 152, 323–335. <https://doi.org/10.1016/j.enbuild.2017.07.060>
- Presidência da República. (2013). *Decreto -Lei n.o 118/2013*.
- Ramos, R. J. G., et al (2009). *Mapping Public Housing Research Project Database*. Retrieve from https://db.up.pt/mapa_habitacao_db
- Roaf, S. (2020). *739: The Traditional Technology Trap (2): More lessons from the Windcatchers of Yazd*.
- Rossi, B., Marique, A.-F., & Reiter, S. (2012). Life-cycle assessment of residential buildings in three different European locations, case study. *Building and Environment*, 51, 402–407. <https://doi.org/10.1016/j.buildenv.2011.11.002>
- SNA. (1961). *Arquitetura Popular em Portugal*.
- Sousa, J., et al (2013). Research on the Portuguese Building Stock and Its Impacts on Energy Consumption – An Average U-Value Approach. *Archives of Civil Engineering*, 59(4), 523–546. <https://doi.org/10.2478/ace-2013-0029>
- Vilhena, A., Pedro, J., & Delta, S. (2013). *O parque habitacional e a sua reabilitação. Análise e evolução 2001-2011*. INE.
- World Health Organization, (2018). *WHO housing and health guidelines*. <http://www.ncbi.nlm.nih.gov/books/NBK535293/>

SENSITIVITY AND UNCERTAINTY ANALYSIS OF COMBINED BUILDING ENERGY SIMULATION AND LIFE CYCLE ASSESSMENT

Implications for the Early Urban Design Process

ROLAND REITBERGER¹, FARZAN BANIHASHEMI² and WERNER LANG³

^{1,2,3}*Institute of Energy Efficient and Sustainable Design and Building, Technical University of Munich (TUM)*

¹*roland.reitberger@tum.de, 0000-0002-1823-6367*

²*farzan.banihashemi@tum.de, 0000-0001-5661-275X*

³*w.lang@tum.de, 0000-0002-6593-8388*

Abstract. Life Cycle Assessment (LCA) is a suitable approach for evaluating environmental impact (e.g. Global Warming Potential (GWP)) related to construction elements and building operation. Since both contribute significantly to the lifecycle based GWP of buildings, combined consideration is necessary. This applies especially for the early design stages when measures for climate change mitigation can be implemented in a cost-efficient manner. In this paper, we describe a sensitivity and uncertainty analysis (SA/UA) for energy simulation and LCA with a total of 8,000 parameter combinations. Thereby, we investigated valuable input for the setup of a collaborative design process with limited information. Standardised Regression Coefficients (SRCs) were used to obtain sensitivity and resulting uncertainties were investigated. The results indicate Primary Energy Source (PES), compactness and energy standard to be the most important information for the robustness of the combined LCA approach. Uncertainty can be reduced by e.g. defining the energy system in an early stage or by designing compact buildings. Related to the early design stages, the application of combined approaches for SA and UA is recommended, as the results differ for embodied and operational emissions.

Keywords. Early Design Stages; Sensitivity Analysis (SA); Uncertainty Analysis (UA); Life Cycle Assessment (LCA); Urban Scale; Synergy Potential; SDG 13.

1. Introduction and Use Case

For achieving a climate-neutral building sector, building energy simulations (BES) give valuable information on how to reduce buildings Global Warming Potential (GWP). While energy standards improve, it is also necessary to consider CO₂-eq. emissions related to the materials used for construction, as their share over the lifecycle

of buildings increases (Roeck et al., 2021), (Longo et al., 2019). LCA is an established method to calculate these so-called embodied emissions which result from production, use (replacement and exchange) and end-of-life stages. While operational and embodied emissions have been extensively investigated separately, research on combined approaches is still limited. Determination of sensitive inputs is necessary to improve the robustness of results. This knowledge is required to show which properties of buildings allow for high synergetic potential and point out possible deteriorations caused by their insufficient consideration. Especially in the early design stages, there is a high optimisation potential due to uncertainties in the design process. We investigate the main parameters for reducing building-related CO₂-eq. emissions from a lifecycle perspective by combining energy and LCA simulation. We show to which extend input parameters affect these emissions separately, but also to which extent there is an interaction between construction and operation, leading to differing results. The findings shall be used to develop an LCA plugin for the Collaborative Design Platform (CDP) (Schubert, 2021), enforcing the consideration of the most important information in an early stage of urban design. Inside the framework, buildings are represented by simplified models, providing a minimum level of information. Within our research project 'Densification in the Context of Climate Change' we enrich the urban model with metadata for basic calculations concerning densification. Nevertheless, there is a vast amount of possible information that could be added by user interaction (energy standard, construction type, ...). As the project is developed for an urban scale, users cannot define all buildings in detail, as this would decrease the intuitive handling. Instead of specifying exact values with numerous assumptions, we aim to provide a range of results for LCA, to show users the optimisation potential for the selected set of general inputs. To ensure focussing on the most important aspects of urban planning while not overloading the necessary inputs, we want to clarify which parameters should be examined in depth to obtain robust results for the CO₂-eq. footprint of buildings.

2. Literature Review

LCA allows considering emissions resulting from operation as well as embodied emissions related to the materials used in buildings. Both parts have overlapping inputs, thereby causing interaction in the overall results (Heeren et al., 2015). SA has been applied for operational (Hemsath and Bandhosseini, 2015), (Singh and Geyer, 2019) or embodied CO₂-eq. emissions (Schneider-Marin et al., 2020), (Basbagill et al., 2013). It is proven that SA can be utilised to show which parameters are most influential for the results of BES models and in which order their further consideration should be proceeded. The investigation of early design stages will thus improve results, as they offer great optimisation potential (Meex et al., 2018). While Harter et al. focus on reducing the uncertainty of results by adding information to building models, they consider operational and embodied primary energy usage (Harter et al., 2019). Other combined approaches, e.g. (Mukkavaara and Shadram, 2021) show how solutions can be selected and optimised on a multi-objective (embodied and operational) scale. They suggest an approach for post-optimisation SA to achieve the maximum outcome for the design progress. Nevertheless, SA is limited to the investigated context, as design parameters and observed outputs vary. We want to investigate the case of collaborative urban design in the early stages with the available information at that point.

3. Concept and Methodology

Our approach is based on a parametrised BES model which was integrated into an LCA calculation for a broad range of combinations. From the results, sensitivity and uncertainty were calculated to show which parameters influence the variance of operational and embodied CO₂-eq. emissions. The methodology is summarised in Figure 1 and further explained in the following sections.

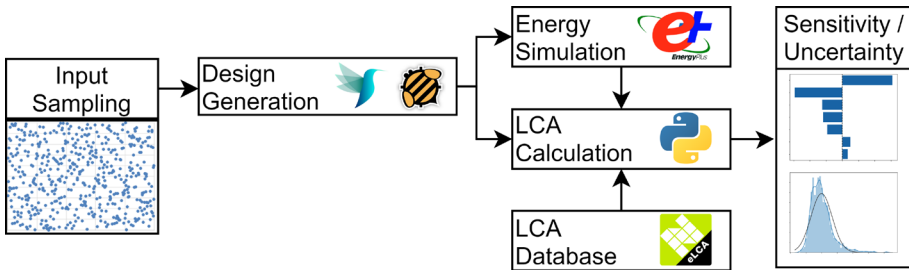


Figure 1: Summary of the proposed methodology

3.1. SAMPLING AND PARAMETRISATION

For creating a sufficiently large dataset of buildings, we used a parametrised, rectangular shape. The parametrisation was done in Rhino - Grasshopper with the Honeybee plugin (Roudsari and Pak, 2013) and Energy Plus simulation engine (Version 8.9.0). Latin Hypercube Sampling (LHS) is a common sampling method for building simulation inputs (Nguyen and Reiter, 2015) and was therefore utilised to create samples for the varied parameters (McKey et al., 1979). In addition to the continuous parameters shown in Table 1, we added a variation in energy standard and construction materials by assigning them based on ranges obtained from LHS as discontinuous variables (Table 2), which has been done before by e.g. (Mukkavaara and Shadram, 2021). Building geometry was limited to 28 meters, as the results should be used in the context of urban densification, which set our focus on geometries that can be added to the existing urban landscape. The parameters were selected based on shown influence on sensitivity and uncertainty in separated energy and LCA research (see section 3) as well as information available from CDP users. A number of 500 sets for the energy calculation was chosen, according to research where this was shown to be a sufficiently large number (Singh and Geyer, 2020), (Macdonald et al., 2009).

Parameter continuous	Unit	Min	Max
Building Width	Metre	10	28
Building Length	Metre	10	28
Building Height	Metre	10	28
Orientation	Degrees	0	90
Window-to-Wall Ratio (WWR)	%	0	90

Table 1: Parameters for the creation of the model

Parameter set	Subsets	Range LHS	U-value [W/m ² K] [base, wall, roof, window]
Energy Standard	GEG (legal standard)	[0, 0.33),	[0.30, 0.24, 0.20, 1.1]
	KfW 55 (improved standard)	[0.33, 0.66),	[0.25, 0.20, 0.14, 0.90]
	KfW 40 (high standard)	[0.66, 1.0]	[0.19, 0.15, 0.11, 0.70]
Constr. Material	Timber	[0, 0.5),	-
	Mineral	[0.5, 1.0]	-

Table 2: Assignment of subsets for energy standard and construction material by sampling

3.2. ENERGY AND LCA CALCULATION

A multi-zone model was used for the energy simulation, as we also obtained construction masses from the honeybee model (e.g. ceiling area). Weather data was used for the city of Kempten (South Germany). After sampling the described inputs, the other necessary boundary conditions for energy simulation were set according to the German standard for the calculation of heating and cooling energy demand DIN V 18599-10:2018-09. The creation of simulation files and mass recording was done using the Colibri plugin for Grasshopper. The generated simulation files were run through Energy Plus group simulation afterwards and the results for heating and cooling energy demand were collected with the Eppy library for Python.

To assess a broad range of material combinations, we used the open-source tool eLCA (Federal Institute for Research on Building, U. A. and S. D., 2021) with the freely available LCA-Database Oekobaudat in version 2020-II (Federal Ministry of the Interior, B. and C., 2020). Typical components for timber and mineral structures (timber frame, solid timber, masonry, reinforced concrete) with two roof types (flat, pitched) were modelled and the results exported related to one square metre of a construction. We considered the building envelope as well as interior ceilings and walls. The system boundaries were set according to DIN EN 15978:2012-10 with LCA phases production (A1-A3), exchange (B4), operation (B6), end-of-life (C3-C4) and benefits beyond the system boundaries (D) under consideration. The buildings reference service life was set to 50 years and the functional unit was one square metre net floor area. Although the methodology could observe a broad range of impact categories, we focused on the GWP, as it is highly relevant in terms of climate change mitigation. Accordingly, it is contributing to Sustainable Development Goal (SDG) 13 - Climate Action.

To calculate the results for each of the 500 samples, we used Python programming language and Pandas library. First, each of the 500 samples was expanded using the LCA values generated in eLCA for construction. Second, we used heating and cooling demand in combination with Oekobaudat datasets for PES (gas, district heating, heat pump with 2020 electricity mix for Germany, pellet) to obtain the operational impact (LCA phase B6). Finally, the results of operational LCA and construction LCA were merged. The approach resulted in a total number of 8,000 combinations.

3.3. SENSITIVITY AND UNCERTAINTY ANALYSIS

Sensitivity analysis is commonly used to identify input parameters whose uncertainty contributes highly to uncertainty in the outputs (Saltelli et al., 2008). In the field of building simulations, the Standardised Regression Coefficient (SRC) has been applied before and was shown to give an indication of parameter importance (Loeffler et al., 2021), (Sing and Geyer, 2020). Higher absolute SRCs mean more impact on the model outputs, where positive SRCs cause an increase and negative SRCs a decrease of the model outputs. For a second proof of the parameter order, Standardised Rank Regression Coefficients (SRRC) were also calculated. The use of these coefficients brings up the need to check inputs for significance. A calculation of probability-values (p-values) was therefore utilised and inputs above the significance level of 0.05 were excluded. For the following calculation of SRC, Scipy and Statsmodel libraries were used, plotting was done with Seaborn. We conducted the analysis first for operational and embodied emissions in isolation. These results were then compared to the ranking of input sensitivity after the combination.

UA allows observing the possible variation in model outputs, caused by the uncertainty present in the inputs (Saltelli et al., 2004). It has been applied to energy simulations (Kotek et al., 2007) and is gaining importance in LCA (Röck et al., 2021). From our results, we investigated uncertainty in the outputs by analysing their distribution via boxplots.

4. Results

4.1. SENSITIVITY ANALYSIS

The regression model was built with significant inputs resulting in R² values of 0.771, 0.932 and 0.922 for embodied, operational and combined assessment. These values are above the usability threshold of 0.7 given by (Saltelli et al., 2008). Residual differences for combined results came close to a normal distribution (see Figure 2 (d)), thus the information is sufficiently represented by the models. From the regression models, SRC was calculated for the remaining inputs, resulting in the order shown in Figure 2 for embodied (a), operational (b) and combined (c) GWP. Calculation of SRRC resulted in values close to the SRC, where only construction material (CM) and energy standard (ES, represented by the global U-value calculated for the thermal envelope) changed position in the ranking but with a little deviation (SRC CM = 0.1348, SRC ES = 0.1447, SRRC CM = 0.1283, SRRC ES = 0.1221).

For embodied GWP, results showed the highest sensitivities to geometric values (surface area to volume ratio, A/V), WWR and construction types. Operational GWP was highly influenced by the chosen energy system, WWR, geometrical parameters and the energy standard. When operation and embodied emissions were regarded in combination, energy system, compactness, WWR and energy standard were the most sensitive inputs. Negative SRCs as e.g. in Figure 2 (a) for global U-value can be interpreted in such a way that an increase in the global U-value (which means lower energy standard and thus less material use for insulation) results in a decrease of

embodied emissions.

To confirm our approach for energy simulation gives reliable results, we also calculated SRC for heating demand ($R^2 = 0.858$), resulting in the order geometry, quality of thermal envelope and WWR. The energy system resulted in an SRC of zero, as final heating demand and not primary energy demand for heating was observed. For the regarded parameters of our research, this agrees with current research (Singh and Geyer, 2020), (Loeffler et al., 2021).

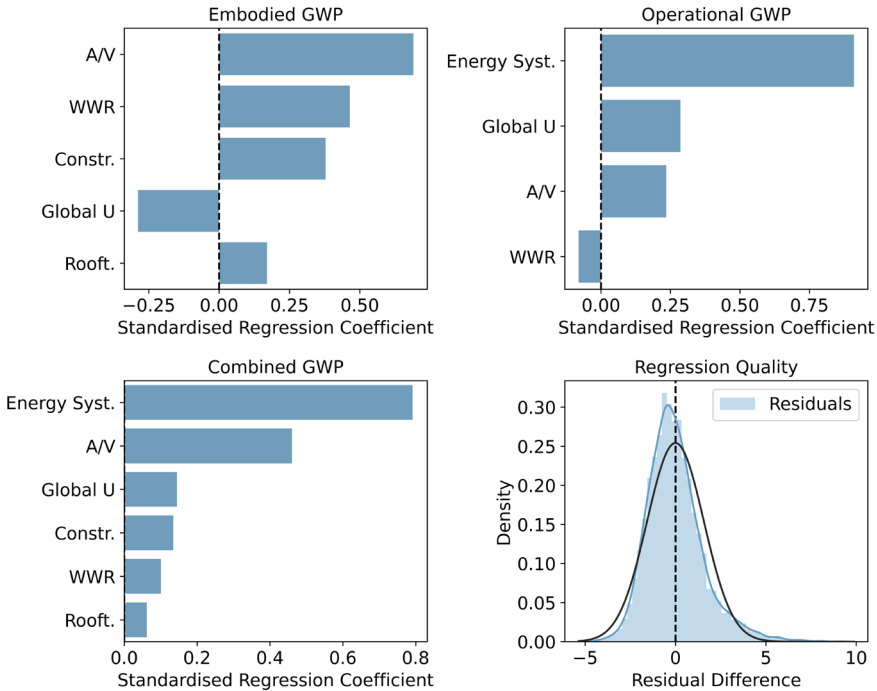


Figure 2: (a - top left) SRC Embodied GWP, (b - top right) SRC Operational GWP, (c - bottom left) SRC Combined GWP, (d - bottom right) Residual Error of Combined Regression

4.2. UNCERTAINTY ANALYSIS

To gain a deeper understanding of the optimisation potential for the identified variables, UA was conducted. For uncertainty especially the categorical variables were used for differentiating (energy standard, primary energy source, construction type). Regarding the PES, we observed a high contribution to uncertainty in the combined results, see Figure 2 (c). Figure 3 (a) shows the results for energy systems, where (I) a high difference between the energy systems is observable and (II) the comparison with the uncertainty induced by energy standards (Figure 3 (b)) confirms the calculated order of sensitivity ranking. Improved energy standards contributed to a reduction in uncertainties (Figure 3 (b)). An improved thermal envelope resulted in slightly reduced emissions over the building's lifecycle. In general, timber constructions performed better than mineral ones in terms of combined GWP, due to the lower embodied emissions associated with wooden materials.

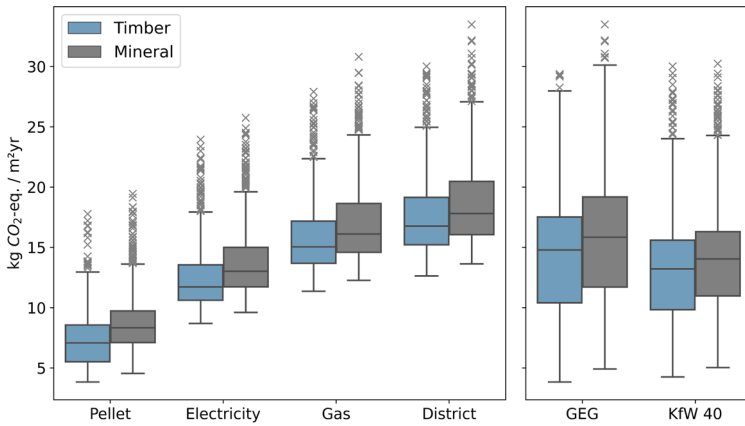


Figure 3: Boxplots for combined results (a - left) split for construction type and energy standard (b - right) split for energy source and construction type

As WWR showed high sensitivity in terms of embodied emissions and is also relevant for combined consideration, we categorised it into groups of 0.1 ranges to print boxplots for it. The results are shown in Figure 4 (a), indicating a slight rise in combined GWP with higher WWRs. Categorisation was also done for A/V ratios (fig. 4 (b)), showing a rise in GWP for increased values, meaning more compact geometries have a lower environmental impact than less compact forms. Furthermore, a reduction of uncertainty for more compact shapes is observable, as 1.5 quartile ranges get closer to the interquartile, resulting in a 33% decrease of standard deviation from 0.55 to 0.25 A/V-ratio.

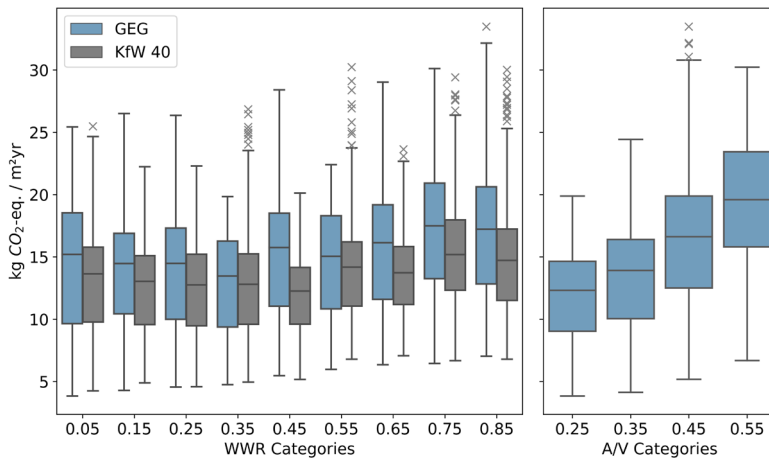


Figure 4: Observation of uncertainty contribution to combined GWP through (a - left) categorised WWRs and (b - right) categorised A/V ratios

5. Discussion

Due to the rising importance of climate change mitigation, lifecycle-based approaches gain attention, as they allow a holistic consideration of buildings CO₂-eq. emissions. To assist planners in early stages of design, we set up a SA and UA on a combined approach of embodied and operational emissions. Due to the overlapping inputs for the two parts, an interaction was expectable. From the results we observe, that a combined consideration shows a change in the order of sensitivity. PES remains the most sensitive parameter for operation and combined consideration, thus its fixing will contribute most to narrowing the range of results. For operational GWP this is to be expected, as research has shown that despite the rising share of embodied CO₂-eq. emissions, building operation is still the main source of energy and resource consumption (UBA, 2019). The impact of PES has also been shown and discussed in the context of building refurbishment, where e.g. (Panagiotidou, 2021) concluded that net zero energy buildings cannot be achieved without decarbonisation of the electricity grid. While the construction type is of importance for the embodied impact, its sensitivity decreases for the combined assessment. By conducting a further UA, we observe reduced optimisation potential for higher energy efficiency standards in terms of GWP, due to the increase in embodied emissions caused by adding insulation. This is in line with the conclusions drawn by (Mukkavaara and Shadram, 2021), who investigated primary energy use over a building's lifecycle. Also this trade-off in energy standards contradicts efforts to achieve CO₂-eq. neutral buildings, an improvement of energy standard decreases uncertainty of results. This study was conducted for a specific use case, thus it is limited to that context. To provide conclusions for other locations, the methodology should be expanded to different climatic zones with a more extensive consideration of inputs. Further validation against case study buildings is also valuable, as this research was limited to synthetic data from the parametric model.

6. Conclusion

Emissions from building production, operation and end-of-life stages are highly interdependent. In order to set up a collaborative urban design plugin, we determined the most sensitive inputs which users need to give. We conducted parametric energy simulations and combined the results with typical building constructions and primary energy sources. Regression analysis was used to calculate sensitivity for embodied, operational and combined GWP.

In general, the need for a combined consideration of lifecycle emissions can be derived. Our analysis shows a change in the sensitivity ranking compared to considering embodied and operational emissions in isolation. As PES is of high sensitivity, it should be fixed in an early stage of design. By that, the possible range of results can be reduced most and further optimisation is most effective. This study was conducted with the German electricity mix 2020. As energy systems showed high sensitivity it can be concluded, that future changes in emission factors of energy carriers will affect the outcome of LCA noticeably. Thus, an improvement in e.g. electricity or district heat generation will also improve GWP from a combined perspective and is recommended. From the results, we also derive the need for high compactness of buildings, as this reduces uncertainty while synergistically optimising

the overall outcome. By applying the described methodology to other climates or building shapes, influential parameters for lifecycle based GWP in early design stages can be identified and planners are enabled to focus on their optimisation first.

The findings described in this paper serve as a basis for the development of a CDP simulation plugin in the next step. Regarding our initial intention to provide robust ranges of LCA results during collaboration it is concluded, that beyond the geometrical information, especially information regarding the PES and energy standard should be basic input parameters. By that, users are enabled to observe the high variability of results due to their interactions with the CDP. Finally, providing the identified parameters during the urban design process will entail a reduction of uncertainty, setting the stage for further optimisation.

Acknowledgements

This work was carried out within the research project 'Densification in the Context of Climate Change', funded by Bavarian State Ministry of the Environment and Consumer Protection (StMUV) and the TUM Centre for Urban Ecology and Climate Adaptation (ZSK).

References

- Basbagill, J., Flager, F., Lepech, M., Fischer, M. (2013): Application of life-cycle assessment to early stage building design for reduced embodied environmental impacts. *Building and Environment*, 60, 81–92. <https://doi.org/10.1016/j.buildenv.2012.11.009>.
- DIN EN 15978:2012-10 (2012). *Sustainability of construction works – Assessment of environmental performance of buildings – Calculation method*, German version EN 15978:2011. <https://dx.doi.org/10.31030/1917049>.
- DIN V 18599-10:2016-10 (2016). *Calculation of the net, final and primary energy demand for heating, cooling, ventilation, domestic hot water and lighting –Part 10: Boundary conditions of use, climatic data*. <https://dx.doi.org/10.31030/2874317>.
- Federal Institute for Research on Building, Urban Affairs (U.A.) and Spatial Development (S.D.). (2021). Bauteileditor eLCA. Available at <https://www.bauteileditor.de/>.
- Federal Ministry of the Interior, Building (B.) and Community (C.). (2020). *Oekobaudat Database*. Retrieved September 1, 2021, from <https://www.oekobaudat.de/>.
- Harter, H., Singh, M., Schneider-Marin, P., Lang, W., Geyer, P. (2019): Uncertainty Analysis of Life Cycle Energy Assessment in Early Stages of Design. *Energy and Buildings*, 208, 109635. <https://doi.org/10.1016/j.enbuild.2019.109635>.
- Heeren, N., Mutel, C., Steubing, B., Ostermeyer, Y., Wallbaum, H., Hellweg, S. (2015): Environmental Impact of Buildings - What Matters? *Environmental Science & Technology*, 49 (16), 9832–9841. <https://doi.org/10.1021/acs.est.5b01735>.
- Hemsath, T. L., Bandhosseini K. A. (2015): Sensitivity analysis evaluating basic building geometry's effect on energy use. *Renewable Energy*, 76, 526–538. <https://doi.org/10.1016/j.renene.2014.11.044>.
- Kotek, P., Jordán, F., Kabele, K., Hensen, J. (2007): Technique of Uncertainty and Sensitivity Analysis for Sustainable Building Energy Systems Performance Calculations. *10th International Building Simulation Conference 2007* (pp. 629-636). The International Building Performance Simulation Association (IBPSA).
- Loeffler, R., Österreicher, D., Stoeglehner, G. (2021): The energy implications of urban morphology from an urban planning perspective – A case study for a new urban

- development area in the city of Vienna. *Energy and Buildings*, 252, 111453. <https://doi.org/10.1016/j.enbuild.2021.111453>.
- Longo, S., Montana, F., Riva S., Eleonora (2019): A review on optimization and cost-optimal methodologies in low-energy buildings design and environmental considerations. *Sustainable Cities and Society*, 45, 87–104. <https://doi.org/10.1016/j.scs.2018.11.027>.
- Macdonald, I. A. (2009): Comparison of Sampling Techniques on the Performance of Monte Carlo base Sensitivity Analysis. *11th International Building Simulation Conference* (pp. 992-999). The International Building Performance Simulation Association (IBPSA).
- McKay, M. D., Beckman, R. J., Conover, W. J. (1979): A Comparison of Three Methods for Selecting Values of Input Variables in the Analysis of Output from a Computer Code. *Technometrics*, 21 (2), 239-245. <https://doi.org/10.2307/1268522>.
- Meex, E., Hollberg, A., Knapen, E., Hildebrand, L., Verbeeck, G. (2018): Requirements for applying LCA-based environmental impact assessment tools in the early stages of building design. *Building and Environment*, 133, 228–236. <https://doi.org/10.1016/j.buildenv.2018.02.016>.
- Mukkavaara, J., Shadram, F. (2021): An integrated optimization and sensitivity analysis approach to support the life cycle energy trade-off in building design. *Energy and Buildings*, 253, 111529. DOI: <https://doi.org/10.1016/j.enbuild.2021.111529>.
- Nguyen, AT., Reiter, S. (2015): A performance comparison of sensitivity analysis methods for building energy models. *Building Simulation*, 8 (6), 651–664. <https://doi.org/10.1007/s12273-015-0245-4>.
- Panagiotidou, M., Aye, L.; Rismanchi, B. (2021): Optimisation of multi-residential building retrofit, cost-optimal and net-zero emission targets. *Energy and Buildings*, (252), 111385. <https://doi.org/10.1016/j.enbuild.2021.111385>.
- Röck, M., Baldereschi, E., Verellen, E., Passer, A., Sala, S., Allacker, K. (2021): Environmental modelling of building stocks – An integrated review of life cycle-based assessment models to support EU policy making. *Renewable and Sustainable Energy Reviews*, 151, 111550. <https://doi.org/10.1016/j.rser.2021.111550>.
- Roudsari, M., Pak, M. (2013): Ladybug: a parametric environmental plugin for grasshopper to help designers create an environmentally-conscious design. *13th International Building Simulation Conference* (pp. 3128–3135). The International Building Performance Simulation Association (IBPSA).
- Saltelli, A., Ratto, M., Andres, T., Camplongo, F., Cariboni, J., Gatelli, D. et al. (2008): *Global sensitivity analysis. The primer*. Chichester, England, Hoboken, NJ: John Wiley.
- Saltelli, A., Tarantola, S., Camplongo, F., Ratto, M. (2004): *Sensitivity analysis in practice. A guide to assessing scientific models*. Hoboken NJ: Wiley.
- Schneider-Marín, P., Harter, H., Tkachuk, K., Lang, W. (2020): Uncertainty Analysis of Embedded Energy and Greenhouse Gas Emissions Using BIM in Early Design Stages. *Sustainability*, 12 (7), 2633. <https://doi.org/10.3390/su12072633>.
- Schubert, G. (2021). *Interaction forms for digital design: a concept and prototype for a computer-aided design platform for urban architectural design scenarios*. Dissertation. Technical University of Munich, Munich. <https://dx.doi.org/10.14459/2021md1610329>
- Singh, M., Geyer, P. (2020): Information requirements for multi-level-of-development BIM using sensitivity analysis for energy performance. *Advanced Engineering Informatics*, 43, 101026. <https://doi.org/10.1016/j.aei.2019.101026>.
- UBA, German Environment Agency. (2019). *Energieaufwand für Gebäudekonzepte im gesamten Lebenszyklus*, Final Report. Nr. 132/2019, Dessau. <https://www.umweltbundesamt.de/publikationen/energieaufwand-fuer-gebäudekonzepte>

HOW TO PREVENT A PASSIVE HOUSE FROM OVERHEATING

An industry case study using parametric design to propose compliance strategies

MAX MARSCHALL¹ and PABLO SEPULVEDA²

^{1,2}*Aurecon, 850 Collins St, Melbourne VIC 3008, AUSTRALIA*

¹*max.marschall@aurecongroup.com*

²*pablo.sepulveda@aurecongroup.com*

Abstract. The airtight, well-insulated building fabric of a Passive House can reduce operational energy consumption but can also present a risk of overheating during summer. PHPP, the Excel tool used to model Passive Houses, considers the whole building as a single thermal zone; a simplification that might be partly responsible for the tool's limited ability to predict overheating risk. The current study on a real-world project provides insights on two topics. First, we compare PHPP's overheating assessment with that of CIBSE's TM59 standard that requires dynamic energy modelling at a room level. Our results support the claim that PHPP underestimates overheating; in our case, glazing SHGC and air change rate were some of the most important parameters affecting compliance, as were some other, rarely analysed factors like ratio of external wall to room volume. Second, we report on the effectiveness of using parametric design for compliance modelling of this kind, and found that parameter studies, coupled with appropriate data visualisation, are an effective way to build intuition on a design problem of this kind.

Keywords. Passive House; Social Housing; EnergyPlus Modelling; PHPP Modelling; Overheating Risk; Parametric Data Visualisation; SDG3; SDG13.

1. Introduction

A warming climate, heightened expectations for indoor air quality, embodied and operational carbon reductions, housing affordability; these are some of the new global challenges that face the building sector. To solve them requires new approaches; one such approach is the Passive House standard. This standard was developed in Germany and focuses on the following principles to reduce operational energy consumption while increasing occupant thermal comfort: increased thermal insulation; construction practices that result in a continuous, airtight thermal envelope; mechanical heat recovery ventilation; high-performance windows; and thermal bridge-free construction.

This paper addresses the United Nations Sustainable Development Goal 3 "Good

Health and Well-Being", by highlighting a thermal comfort risk inherent in Passive House buildings, and by documenting an approach to mitigate it. The well-insulated airtight building envelope of a Passive House keeps the building warm in winter and can reduce external heat gain in summer (Truong and Garvie, 2017). However, the design of the building requires careful consideration to prevent overheating during warm periods, when heat loss through the envelope would in fact be beneficial, but where an airtight, highly insulated façade may prevent this. Several studies have shown a tendency of Passive House buildings to overheat during warm periods (e.g. Kang et al., 2021; Sameni et al., 2015).

A requirement for Passive House compliance is to use the Passive House Institute's Excel tool "Passive House Planning Package" (PHPP) to predict whether a building design will meet the standard's requirement of not exceeding heating and cooling demands of 15kWh/m²/a each. Part of the reason for why PHPP may sometimes underestimate overheating risk, is that it considers the heat balance of the building as a whole; the building is simplified to a single space, without considering internal partitions of walls and floors. This resolution may not always account for individual rooms overheating due to their specific conditions.

While there are many examples in literature where researchers have conducted parametric modelling for sustainable building design in general, there are very few such studies related to Passive Houses specifically. Commonly, Passive House Designers will exclusively use PHPP from within Excel to run analyses, making iterative changes manually based on their expert knowledge until they find a feasible solution that meets the performance requirements. There appears to be a missed opportunity to leverage parametric modelling to provide more holistic advice for achieving compliance.

While PHPP allows comparing options, this feature is currently limited in a way that restricts more largescale parameter studies. The few researchers who have run this type of analysis do so using other software like MATLAB (e.g. Mengyuan et al., 2020), IES-VE (e.g. McLeod et al., 2016) or Python and EnergyPlus (e.g. Chiesa et al., 2019) to automate the simulation of many design options, and sometimes use algorithms to optimise parameter settings (e.g. Chen et al., 2020; Li et al., 2021) or conduct sensitivity analyses (e.g. McLeod et al., 2016). The outcomes of these studies are generally used to form insights on how to achieve Passive House compliance most efficiently within a certain context, e.g. related to a specific building type or climate zone. While many of the existing studies are very thorough, their methods lack evidence of being helpful in communicating simulation outcomes to clients in real-world consulting scenarios.

The studies that specifically analyse overheating risk in Passive House buildings tend to conclude that glazing fractions and shading are the most important factors (e.g. Lavafpour and Sharples, 2015; McLeod et al., 2016). However, this is based on a very small number of studies; more research is required to shed light on this complex issue.

1.1. PROJECT BACKGROUND

Above Kāinga Ora, a government agency that provides rental housing for New Zealanders in need, is aiming to achieve high levels of comfort and sustainability for their social housing project 'Ngā Kāinga Anamata' (Māori for 'homes of the future'). The project is therefore designed for Passive House certification. It involves five almost

identical three-level walk-up buildings in Auckland, New Zealand.

Each building will be constructed using a different structural system (precast concrete, light timber frame, cross-laminated timber (CLT), light gauge steel frame, hybrid light timber and CLT). The purpose of this is to compare the ease of planning and construction, cost, and other challenges, as a case study for future reference. Aurecon was engaged as a Passive House design consultant and services engineer for the project.

1.2. AIM

The aim of this study was to complement the PHPP modelling for the 'Ngā Kāinga Anamata' project through high-resolution dynamic building performance modelling, to test the current building design for the risk of overheating, and to recommend design and operational strategies to reduce this risk.

2. Methodology

2.1. APPROACH

In order to provide holistic design advice with several potential pathways towards compliance, we decided to employ a parametric modelling approach. We used the Ladybug Tools Grasshopper plug-in to conduct energy dynamic energy simulations through EnergyPlus. To visually analyse the results from the parametric modelling, we used the interactive web dashboard Design Explorer.

In order to provide holistic design advice with several potential pathways towards compliance, we decided to employ a parametric modelling approach. We used the Ladybug Tools Grasshopper plug-in to conduct energy dynamic energy simulations through EnergyPlus. To visually analyse the results from the parametric modelling, we used the interactive web dashboard Design Explorer.

2.2. SITE AND BUILDING GEOMETRY

All five buildings on site have the same orientation; their longitudinal axis is rotated about 11° clockwise away from a true east-west orientation. Since overshadowing from neighbouring buildings was determined a rare occurrence, and the study followed a worst-case scenario approach, we decided to not include the neighbouring buildings in the simulations at all. TM59 recommends using CIBSE design summer year (DSY) weather files, however no such file exists for Auckland; instead, we used the NIWA EPW file for current conditions, and the C875 weather file to account for increased risks due to future climate change.

Since all five buildings have identical geometries, we only modelled one of them, namely the one with the light-gauge steel (LGS) construction since this was the one deemed most likely at risk of thermal performance issues. The buildings each have two apartments per floor with a north-facing balcony and separated by a core zone with a communal staircase (see Figure 1). The assumed number of occupants per apartment is five; two adults occupying the northern bedroom and three children occupying the southern bedroom.

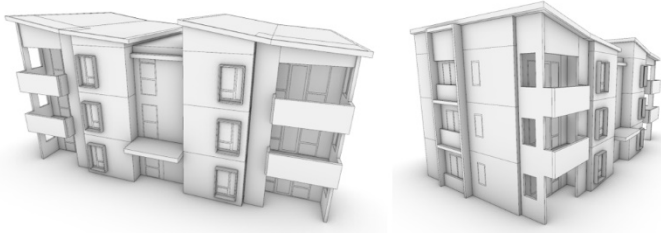


Figure 1. 3D model generated for the analysis

2.3. CONSTRUCTIONS

Where available, constructions were extracted from the project's PHPP model; unspecified constructions (e.g. interior floors and walls) were obtained from the architectural plans available at the time of planning. EnergyPlus requires entering materials on a layer-by-layer basis per construction. In cases where several materials occupy a single layer (e.g. studs and insulation), we applied a cross-section area-weighted average to all properties of the materials found in the layer.

From the PHPP model, we extracted all building-wide thermal bridges that were not related to window constructions and accounted for them in EnergyPlus by converting them to an exterior wall construction U-value degradation. The EnergyPlus U-value was matched with the PHPP U-values that consider the linear (e.g. slab-wall junction) and punctual (e.g. cladding fixation points) thermal bridges. We determined that the external U-value had to be increased from 0.191 to 0.296 in order to account for thermal bridging; this was achieved by reducing the wall insulation layer thickness from 100mm to 78mm.

We calibrated the individual glazing layer properties, such that the resulting U-values and SHGCs of the constructions matched the glazing systems found in a glazing specification document that had been shared with the project team.

Window frames were modelled as separate wall sections with simplified 'no mass' materials. This allowed us to incorporate the window-related thermal bridges into the frame definitions. Corresponding values were calculated using the thermal bridge modelling software FLIXO PRO 7.1. We extracted average thermal bridges from the PHPP model, which we converted to equivalent U-value degradations that we added to the frame U-value specifications.

2.4. LOADS AND SCHEDULES

We used the load and schedule assumption recommendations from TM59, but specified additional, continuous loads from the domestic hot water (DHW) piping to the affected rooms (cores, stairwell, lobbies, hallways, bathrooms) from the pipe lengths and level of insulation specified in the PHPP model.

We specified an outdoor air supply with 80% sensible heat recovery, operable at all times in all rooms. As per TM59, we assumed that operable windows were open whenever the indoor temperature exceeded 22 °C. However, since the staircase windows will be operated mechanically based on indoor and outdoor temperature sensors, we set these windows to be open when the indoor ambient temperature

exceeded 21 °C, but only if the outdoor ambient temperature was at least 1 °C cooler than the indoor temperature. All doors, including balcony sliding doors, were modelled as closed at all times.

2.5. METRICS FOR THERMAL COMFORT

TM59 defines the following compliance criteria:

- HE ('Hours of Exceedance') for living rooms, kitchens, and bedrooms: the number of hours during which ΔT is greater than or equal to 1K during the warmer months may not be more than 3% of occupied hours. ΔT is the difference between the indoor operative temperature and the upper adaptive thermal comfort temperature threshold, rounded to the nearest integer. The warmer months are defined in TM59 as May to September inclusive which applies to the northern hemisphere; we therefore changed this to November to March inclusive.
- NT ("Nigh-time Threshold") for bedrooms only: to guarantee comfort during the sleeping hours, the operative temperature in the bedroom from 10pm to 7am may not exceed 26 °C for more than 1% of annual hours.

While not mandatory, we included the additional metric recommended in TM59:

- HE ("Hours of Exceedance") for communal corridors (in this case, the staircase): if an operative temperature of 28 °C is exceeded for more than 3% of the total annual hours, then this should be identified as a significant risk within the project.

Furthermore, in order to gain an understanding of the extent to which different rooms fail or comply with the above criteria, we also logged the average number of yearly hours during which rooms exceeded an operative temperature of 26 °C:

- Ke: Kids' bedrooms
- Pe: Parents' bedrooms
- Se: Staircase

2.6. DESIGN PARAMETERS

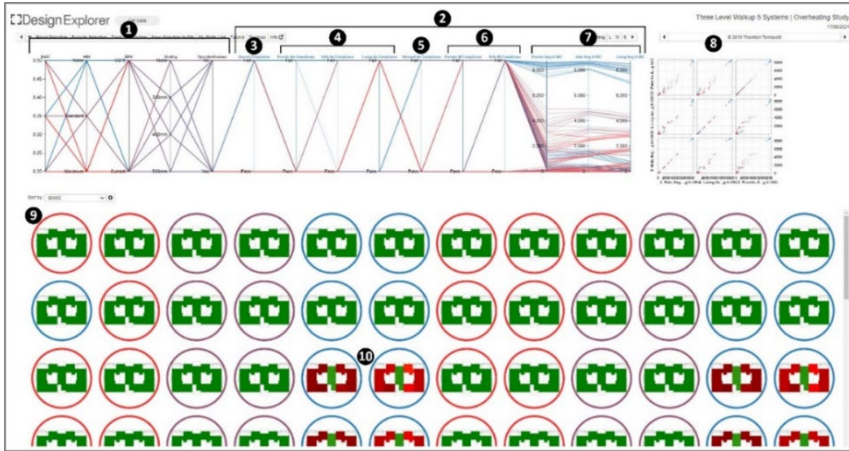
The parametric study consisted of energy simulations for all 144 combinations of the following parameter settings:

- Weather file: current (NIWA) and future (C875)
- Glazing solar heat gain coefficient (SHGC): 0.50, 0.35, and 0.20
- Heat recovery ventilation air changes per hour (ACH): none (0 ACH), standard (0.64 ACH), and maximum (0.83 ACH)
- Depth of 'shading aprons' for the parents' bedroom windows: none, 300mm, 400mm, 500mm. A shading apron is an exterior shading device; geometrically, it is an outward extrusion of the outline of a window.
- Operable windows: with and without

3. Results

3.1. DASHBOARD

The elements of the dashboard created in Design Explorer are shown in Figure 2.



1. Inputs (design parameters)
2. Outputs (compliance & performance metrics)
3. Overall compliance to TM59
4. Compliance to TM59 criterion "hours of exceedance" (separately for parents' bedrooms, children's bedrooms, and living rooms)
5. Non-mandatory TM59 criterion "hours of exceedance" for staircase
6. Compliance to TM59 criterion "night-time threshold" (separately for parents' bedrooms and children's bedrooms)
7. Additional performance metric "hours over 26 °C operative temperature" (separately for parents' bedrooms, children's bedrooms, and living rooms)
8. Correlation matrix between parents' bedrooms, children's bedrooms, and living rooms in terms of the additional performance metric "hours over 26 °C operative temperature"
9. Thumbnails for each design variation showing the "hours of exceedance" compliance for the top floor rooms
10. Non-compliant design variations have rooms coloured in yellow or red

Figure 2. Parametric data visualisation dashboard created using Design Explorer

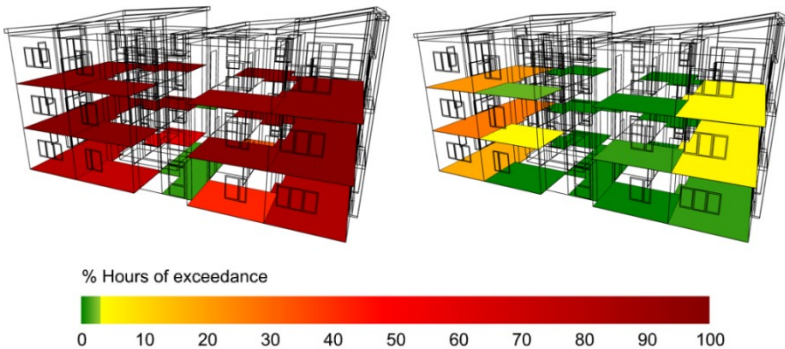


Figure 3. Examples of the 3D visualisation of the 'Hours of exceedance' metric

3.2. SENSITIVITY OF METRICS

Several patterns emerged when exploring the 3D visualisations (see Figure 3) of the Hours of Exceedance metric in the dashboard. Different parts of the building tend to have different levels of risk in terms of meeting this criterion:

- The top floor is at higher risk than the other floors. This was to be expected since heat rises, and because the top floor is adjacent to the roof space which has a high solar exposure.
- The western rooms are at higher risk than the eastern rooms. This was also to be expected since temperatures after midday tend to be higher than those before midday, and the western spaces receive more direct solar radiation during this time.
- The kids' rooms are at higher risk than parents' rooms. This was somewhat unexpected since in the southern hemisphere north-facing rooms are commonly at higher risk of overheating than south-facing rooms. However, it is explained on the one hand by the increased internal gains due to the fact that the southern bedroom is occupied by three people instead of two, and on the other hand due to the fact that shading elements were included to the northern bedroom windows for most of the analysed design variations.
- The living rooms are at higher risk than the kids' rooms. This is explained through the TM59 assumptions on schedules and loads, as well as the rooms' boundary conditions and geometry. TM59 assumes living rooms to be fully occupied (in this case by 5 occupants) for most of the day. Their assumed peak equipment load is almost 6 times higher than that of the bedrooms. Furthermore, the living rooms have a higher glazing fraction (25% compared to 11%) as well as a higher ratio of exposed façade area to room volume (0.46 compared to 0.37).

The abovementioned indicator "ratio of exposed façade area to room volume" appears to be a factor that is rarely explicitly analysed in other research. This may be because dynamic energy simulation programs consider interior room partitions; the effect of the indicator is therefore accounted for in the simulation and reflected in the results. The importance of this indicator in our study exposes a shortcoming of the PHPP methodology, which is to model the building volume as a whole and discount interior room partitions.

Which of the individual criteria outlined in Section 2.5 are most difficult to fulfil? To gain insight on this question, we counted how many of the 144 analysed design variations failed on each of the individual criteria (see Figure 4). Assuming that the number of failed design variations is an indicator of the how difficult the different TM59 criteria are to fulfil, we made the following observations:

- The Night-time Threshold (NT) criterion is more critical than the Hours of Exceedance (HE) criterion. There is a natural tendency to assume that overheating is more of a risk during daytime than night-time. However, 95 design variations failed the NT criterion for the kids' bedrooms while only 32 design variations failed the HE criterion for the kids' bedrooms. This is because the HE criterion is more forgiving of high temperatures since it follows the adaptive comfort model, thereby allowing indoor operative temperature of up to 29 °C during hot periods, while the

NT criterion has a hard cut-off at 26 °C.

- The living rooms and staircase are more critical than bedrooms in terms of HE. The reasons for why the living rooms performed worse than the bedrooms are explained in the section above. The fact that the staircase runs a higher risk of failing its criterion may have several reasons. One reason is the fact that the threshold temperature defined for overheating is constant at 28 °C, whereas the threshold for the other rooms is dynamic. Other reasons for the poor performance of the staircase is its high glazing fraction of 35%, as well as the continuous DHW loads.
- The kids’ rooms are more critical than the parents’ rooms. The reasons for this are explained in the section above.

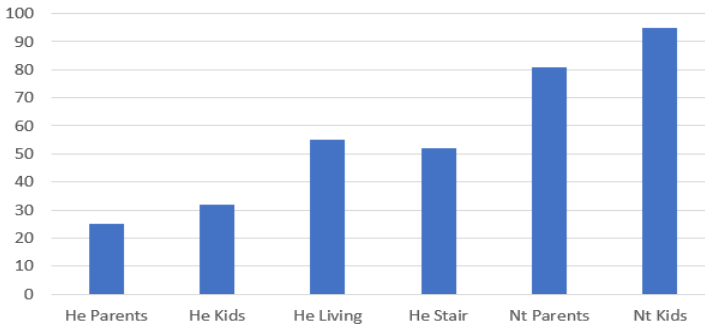


Figure 4. Number of failed design variations by criterion. “HE” stands for Hours of Exceedance, “NT” for Night-time Threshold, see Section 2.5

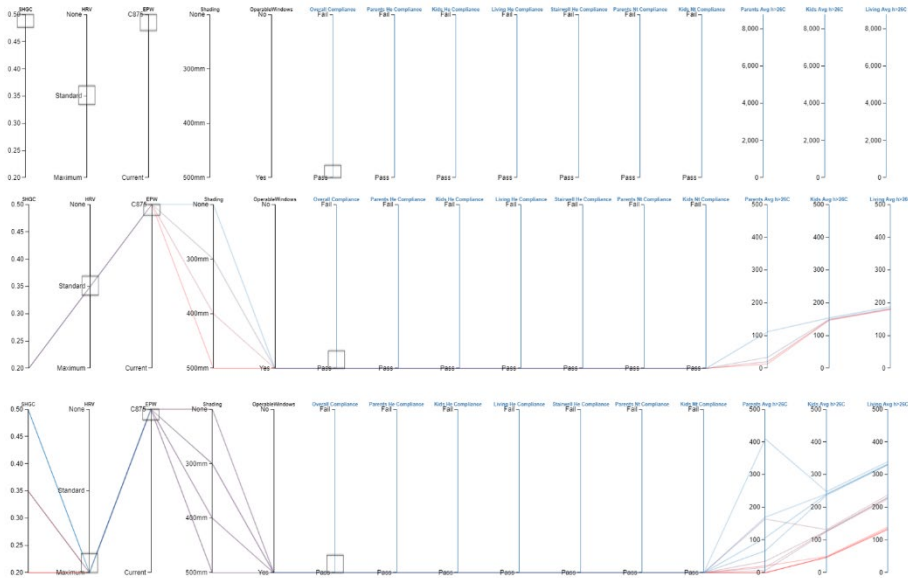


Figure 5. Top: For the baseline design parameters, the modelling could not produce a design that passes TM59. Middle: TM59 compliance could be achieved by decreasing the glazing SHGC. Bottom: TM59 compliance could also be achieved by increasing the air change rate of the HRV

3.3. COMPLIANCE

Figure 5 shows that, based on our modelling, we found that the current design did not comply with TM59, despite PHPP indicating no overheating risk. To meet compliance, we found two options. The first was to lower the SHGC. Specifically, we tested SHGCs of 0.20 and 0.35; 0.20 complied while 0.35 did not. This means that the required maximum SHGC is somewhere between 0.20 and 0.35. While the choice of shading for the parents' bedrooms did not affect the compliance, it did substantially reduce the predicted number of hours where these bedrooms had high temperatures, from 122 hours to between 14 and 34 hours, depending on shading depth.

The second option to meet compliance was to increase the HRV air changes to "Maximum". While this technically allows SHGCs of up to 0.50, it performs worse than the previous solution on the latter metrics. Without shading, the predicted number of hours where the parents' bedrooms have high temperatures is 402, and between 67 and 170 with shading, depending on shading depth.

4. Conclusions

Similar to other studies (e.g. Li et al, 2021), we found that glazing SHGC had the largest impact on overheating risk; this was followed by HRV air changes. Shading had a lesser impact in our study than in other studies (e.g. Lavafpour and Sharples, 2015), however in our case the project constraints limited the use of shading which limited its potential to combat overheating; furthermore the dense occupancy assumed for the current project increases the importance of internal loads over external ones. While the window dimensions were fixed, we noticed that rooms with higher glazing fractions had a higher overheating risk. A similarly impactful factor, and one that we have yet to find mentioned in the literature, was the ratio of exposed façade to room volume.

Both latter parameters are of particular interest for Passive House design, since they relate to room-level characteristics that PHPP does not consider. While we understand that PHPP has been carefully developed with the intention of striking a reasonable balance between accuracy and simplicity, our study points out its risk of underestimating overheating as an argument for increasing the PHPP modelling complexity to include room partitions in future. Our study supports the claim that PHPP underestimates overheating, since the predicted overheating was much higher when following the more detailed modelling procedure laid out in TM59, a standard specifically focused on assessing this risk. Following TM59, we were still able to advise the client on omitting active cooling for the project - a win in terms of operational energy and emission reduction. For future research, the TM59 standard should be further validated regarding its assumptions on occupant behaviour, which has a significant impact on energy consumption and overheating (Sameni et al., 2015), especially occupancy (Chiesa et al., 2019) and window operation (Robinson and Haldi, 2011; Truong and Garvie, 2017).

We found that a parameter study, combined with interactive dashboarding, is an efficient way to assess to what extent different design factors impact compliance, and to be able to propose multiple compliance pathways. Our method of counting how many of the analysed design variations pass along each compliance criteria helped assess which of the individual criteria are most critical. Including additional continuous

metrics instead of just binary compliance metrics furthermore helped determine the extent to which individual designs complied. However, a parameter study is limited by the 'curse of dimensionality'; since all parameter combinations are assessed, the simulation runtime limits the number of parameters that can be included, as well as the number of options along each parameter. Such studies are useful for gaining intuition on a design problem and determining parameter ranges that meet performance criteria, but assessing a specific parameter combination usually requires additional simulation runs.

References

- Chen, M., Gao, C., Yu, Z., & Wang, J. (2020). Optimization Design Method Based on Energy Balance Calculations for Passive House. *IOP Conference Series: Earth And Environmental Science*, 555(1), 012081. doi: 10.1088/1755-1315/555/1/012081
- Chiesa, G., Acquaviva, A., Grosso, M., Bottaccioli, L., Florida, M., Pristeri, E., & Sanna, E. (2019). Parametric Optimization of Window-to-Wall Ratio for Passive Buildings Adopting A Scripting Methodology to Dynamic-Energy. *Simulation*. *Sustainability*, 11(11), 3078. doi: 10.3390/su11113078
- Kang, Y., Chang, V., Chen, D., Graham, V., & Zhou, J. (2021). Performance gap in a multi-storey student accommodation complex built to Passivhaus standard. *Building And Environment*, 194, 107704. doi: 10.1016/j.buildenv.2021.107704
- Lavafpour, Y., & Sharples, S. (2015). Summer Thermal Comfort and Self-Shading Geometries in Passivhaus Dwellings: A Pilot Study Using Future UK Climates. *Buildings*, 5(3), 964-984. doi: 10.3390/buildings5030964
- McLeod, R., Hopfe, C., & Kwan, A. (2013). An investigation into future performance and overheating risks in Passivhaus dwellings. *Building And Environment*, 70, 189-209. doi: 10.1016/j.buildenv.2013.08.024
- Li, X., Deng, Q., Ren, Z., Shan, X., & Yang, G. (2021). Parametric Study on Residential Passive House Building in Different Chinese Climate Zones. *Sustainability*, 13(8), 4416. doi: 10.3390/su13084416
- Robinson, D., & Haldi, F. (2011). Modelling Occupants' Presence and Behaviour – Part I. *Journal Of Building Performance Simulation*, 4(4), 301-302. doi: 10.1080/19401493.2011.599157
- Truong, H., & Garvie, A. (2017). Chifley Passive House: A Case Study in Energy Efficiency and Comfort. *Energy Procedia*, 121, 214-221. doi: 10.1016/j.egypro.2017.08.020

MATERIAL COMPUTATION WITH MYCO-MATERIALS

PHILLIP GOUGH¹, ANASTASIA GLOBALA² and DAGMAR REINHARDT³

^{1, 2, 3} *The University of Sydney School of Architecture, Design and Planning*

¹*phillip.gough@sydney.edu.au, 0000-0003-3687-6365*

²*anastasia.globa@sydney.edu.au, 0000-0002-4749-5675*

³*dagmar.reinhardt@sydney.edu.au, 0000-0003-0477-492X*

Abstract. A sustainable, circular, post-carbon economy of the future will take waste material from one part of the economy and give it new value. This will reduce energy and material leakage from the economy and create new opportunities for innovation in materials. Myco-materials provide an opportunity to transform ligno-cellulosic matter, such as waste cardboard and sawdust, into useful materials. This is achieved by using a fungus to bind together these substrates into useful forms. This paper explores how computational design parameters can be informed from the mycelia growth process. We created several prototype forms that show behaviour of myco-materials through the growing and drying process. These show how inclusion of cardboard substructures may improve the performance of the resulting material by increasing its stability during the drying process. We also demonstrate limits to the size of myco-materials through computational design. Myco-materials will likely be part of a sustainable post-carbon economy, by bringing new value to waste material, and this paper shows how computational design can be informed by mycelial growth.

Keywords. Mycelia; Biodesign; Growing Designs; Computational Design; SDG 12.

1. Introduction

A circular economy is needed, in addition to addressing atmospheric CO₂, for humans to live sustainably with Earth's ecosystems. A sustainable economy will mean that economic activities could continue forever. However, many current patterns of consumption and production in our current linear economy are unsustainable. Through sustainable and circular economic models, value can be added to wood or paper-based waste to create new markets and opportunities (Schandl et al., 2021), such as by using this unwanted material as a substrate to grow myco-materials: composites based on fungi.

Myco-materials are formed by mycelia; the roots of fungi that colonise and degrade lignocellulosic material, such as a fallen tree in the wild, or a compost pile, but also

industrial materials including paper, cardboard and timber waste. This research uses a locally endemic, edible species of mushroom, *Ganoderma Steyaertanum* (known as Australian reishi mushroom), to bind together a substrate as the fungus grows, so that it can form a strong but lightweight myco-material. We extend a biodesign approach to design, applying the natural abilities and behaviours of a living organism to the design problem (Gough, 2021), through computational methods, generating forms that demonstrate the capabilities of the material at the growth stage, to identify applications of the material.

Rather than adopting a design-to-production approach, where computation is performed during the form-making design stage, followed by fabrication and assembly, our intent is to flip this process. We observe the growth and material changes to provide knowledge for simulation and computational design. The research explores the potential of mushrooms growing into designed forms and how the resulting myco-material deforms during the finishing process.

2. Background and Context

2.1. SUSTAINABLE CONSUMPTION AND PRODUCTION - SDG 12

The UN's Sustainable Development Goal 12 (Sustainable Consumption and Production) focuses on increasing resource efficiency and reducing waste for sustaining natural resources and environments. As cardboard is commonly abandoned to landfill, despite being one of the simplest products to recycle, there is ample opportunity to maximise the reuse of this material (Schandl et al., 2021).

In this context, mycelium is of interest as a change agent with a capacity to transform cellulose waste products into designed shapes; to develop surfaces that are durable and applicable for the fashion industry; to substitute packaging; and to deliver structural components for the built environment. By adopting mycelium for engineered natural processes, new resources can be generated out of waste products and so environmental degradation can be decreased. Natural biodegradable myco-composites can be returned to lifecycles and thus contribute to circular economies.

2.2. CIRCULAR ECONOMY

The circular economy is one strategy for humanity to live sustainably within the finite resources of earth's ecosystems. A circular economy that can grow efficiently will need to minimise energy and resource leakage (Jørgensen and Pendersen, 2018). Importantly, a single design cannot be circular as it is a property of a system (Konietzko, et al., 2020), and hence collaboration and multidisciplinary approaches are important. Considering key environmental criteria during the design of digitally fabricated building elements is crucial. Consequently, design adaptability of systems as enabled through computational methods should include material efficiency beyond a production context, evaluating and compensating for potential negative impacts caused by end-of-life processing (Agustí-Juan et al. 2008). A model of the myco-material lifecycle starts with the preparation of bio-materials (Figure 1). These may include agricultural waste, wood chips and dust, coffee grounds, used cardboard and paper, clay and beached kelp. Source materials are pasteurised and blended to ensure

successful inoculation with and colonisation by mushroom spores. Various moulding approaches, substrate extrusion or 3D-printing and other techniques can be adopted to give shape to myco-materials during a form-making stage.

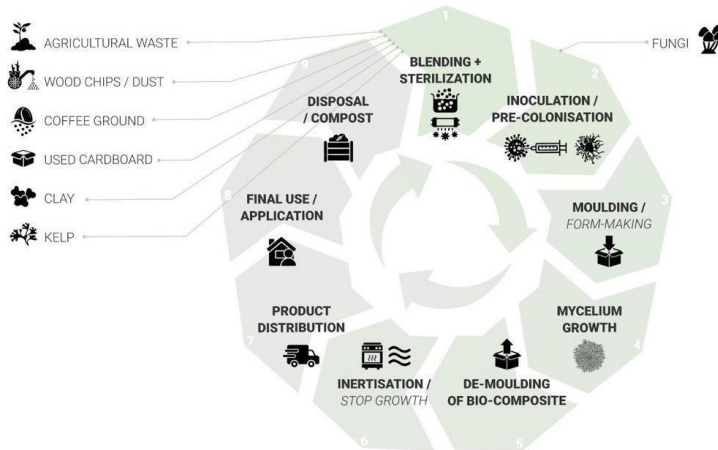


Figure 1. Life Cycle: Mycelium-based composites

The case study discussed in this paper used Poly-lactic Acid (PLA) 3D prints for the form-making stage using a pre-colonised substrate. After mycelium has grown inside the moulds and is structurally solid, it can be demoulded and hold its shape. Further growth can be stopped by drying colonised substrates in a low oven ($\sim 50^{\circ}\text{C}$ - 80°C). Deactivated myco-material products can be distributed, used, and finally composted, forming part of the biological cycle of materials for a circular economy (Jørgensen and Pendersen, 2018). Importantly, this biological material hybrid of 3D print and mycelium can be designed for disassembly and composting. To this end, this research explores how computational design and 3D print variations can be used to test detailed temporary myco-structures.

2.3. MYCELIUM APPLICATION SCENARIOS

Research has increased for myco-materials across a range of applications from product design, textile design, engineering to architecture. Product oriented uses of mycelium growth to date have included aesthetically intriguing shapes and functions, including chair composites and lamps (Fearson, 2017a), a water resistant and fully functioning canoe (Davidson, 2020), brick components with mycelium grown in moulds and arranged in a three-segment tower formation (Frank, 2014), a funicular roof structure (Ross 2020), a hanging structural system with bespoke mycelium modules grown in PVC customised moulds, intersections and tensile inset (Fearson, 2017b), or lattice structures (Morby, 2017).

Mycelium-based composites have been successfully tested for combinations with cellulose-based waste products, such as paper and cardboard (Jones, 2021) but also combinations with mineral substrates including clay (Jauk et al. 2021).

Adopting robotic fabrication and manufacturing for fluid deposition material composites is increasingly tested, including 3D printing and process-oriented investigations for mycelium with a focus on node structures (Cheng et al., 2021). Robotic extrusion with discrete non-repetitive patterns for a tower structure variable material appearance (Goidea et al. 2021) and the robotic pneumatic extrusion of complex modules at CITA (Lim et al. 2021) indicate new approaches to structural specification. 3D printing of soil-based myco composites combined with hay substrates have been investigated for myco-remediation (Como et al. 2020). Continued growth as a key attribute has prompted novel non-finite fabrication processes whereby prefabricated myco-based building components continue to grow together (Elsacker et al. 2021).

3. A Case Study on Growing Designs with Mycelia

The research investigates how well mycelium-based objects can hold their intended shape, and what level of detail, size and complexity of form-making elements could be feasibly achieved. Group samples are rigorously measured in terms of weight and volume throughout the fabrication, growth, drying process. Volume calculation is performed using measured inputs and corresponding algorithms in Grasshopper GH.

The process for growing myco-materials is relatively simple and develops over a few weeks. This research used Australian Reishi (*G. Steyaertanum*) provided from a commercial supplier. The substrate was stored at 5°C prior to its use in the moulds, to temporarily pause mycelium growth. Test samples were allowed up to 21 days of growth inside their moulds and 2-3 days of further growth after demoulding in sealed plastic bags, with openings covered with porous tape to allow air transfer and while preventing contamination from wild mould spores. The temperature range was 18-26°C and humidity varied from 35% to 65%. Samples placed in moulds and stored in the dark during the substrate colonisation process to avoid growth of mushroom bodies.

Three case study series are discussed in the following with specific focus: on increasing the percentage of waste material (cardboard) to myco-material prototype; on shape retainment; and on form-making and form-retaining properties. The Mycelium-Cardboard Composite tests (Figure 2) investigate the effect of incorporating cardboard inserts into myco-material prototypes. Eight samples were developed for this test, each having the same shape and volume (Figure 2). Sample 0 had no cardboard insert, serving as a benchmark prototype containing 100% working culture inoculated with Australian *G. steyaertanum*. Sample S1 had 3 grams (equivalent of 3 inserts) of shredded cardboard introduced into the mix homogeneously distributed throughout the substrate. Samples 1 to 6 had a progressively increasing number of cardboard walls (inserts) introduced into the mycelium composite, where each insert weighed approximately 1g. Each insert dimensions being maximum width and height of the base container (55mm and 35mm respectively). The limit of 6 max inserts was used because it became progressively more challenging to distribute the base substrate throughout the sample, to the point where this manual process was impractical.

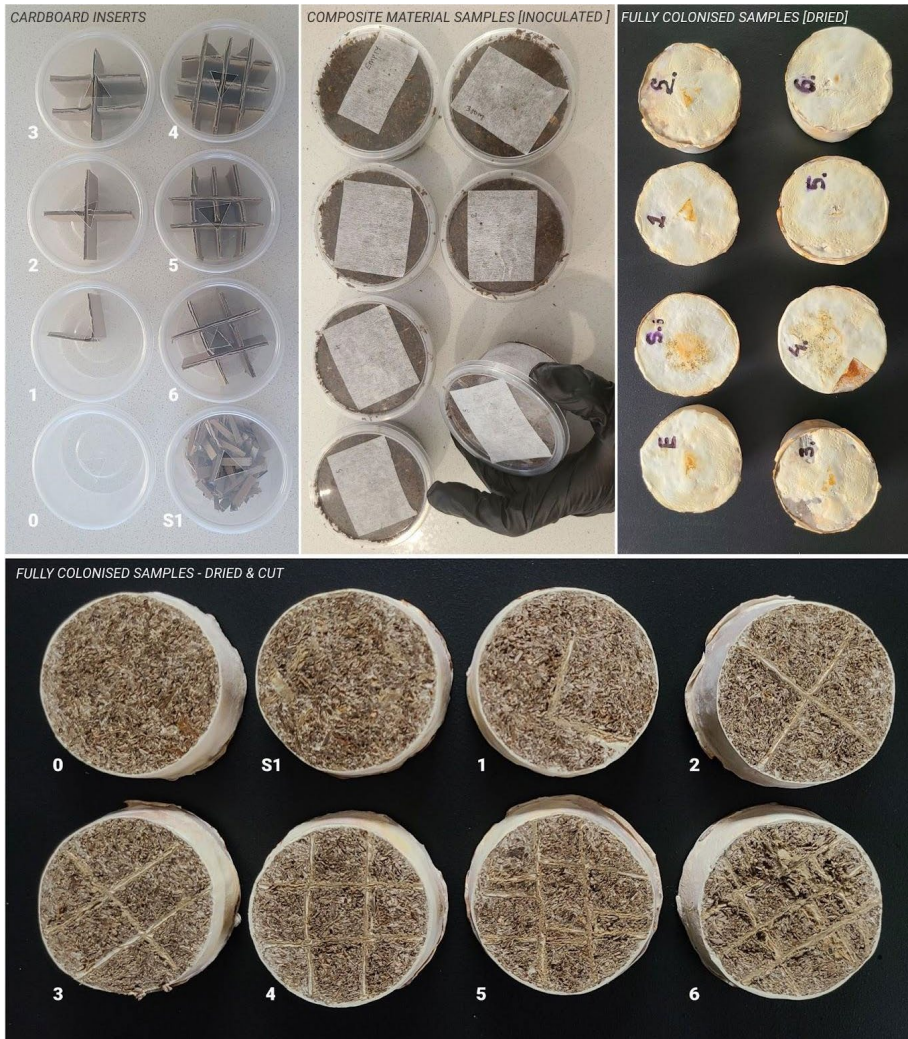


Figure 2. 'Mycelium-Cardboard Composites' case study, test samples.

Test samples were successfully colonised during mycelium growth stages and able to hold their form and obtained similar mycelium white smooth leathery 'skin' layers on the outer surface of composites, which is typical for *G. Steyaertanum*. Figure 2 shows cardboard interventions that successfully integrated into mycelium culture as an integral part of the bio-composite material. It should be noted that it was much harder to pack sample 6 with the base mix, because the spaces between the cardboard inserts were so small. Arguably the waffle structure of cardboard inserts did have a capacity to provide an extra internal structural support for this sample. However, this internal scaffold was not strictly necessary for the chosen form-making approach, as it had fully enclosed moulds. Blending or shredding the cardboard prior to its introduction into the

mix might be a more effective and feasible strategy, for cases when the solid moulds are being used for the prototype fabrication.



Figure 3. Weight (left) and volume (right) change overtime: 'Cardboard Composites' study

Samples had similar progression of weight loss throughout the process (Figure 3). Average weight was 10-20% during mycelium growth period, lasting 21 days inside the mould and 3 days outside the mould. The drying stage was performed using a fan-forced electric oven set at 50°C for 3.5 hours, resulting in a loss of 35-40% of the remaining weight. Over the period of the next 7 days the prototypes continued to get lighter, losing 5% compared to their weight after inertisation. The samples with more cardboard content resulted in a lighter final composite material. The samples retained between 93-96% of their initial volume compared to the calculated internal mould volume (Figure 3 right). Although the difference in volumes across all samples was not statistically significant, we have observed that sample 0 (with no cardboard) lost more volume compared to other samples (93%), while sample 6 (with max number of cardboard inserts) retained 96% of its original volume.

The 'Pyramid Panels' case study looked at the mid-scale applications and form granularity for interior insulation or soundproofing. The modular pyramid shapes and triangular footprint of the panels allow for easy assembly in different configurations for various wall surfaces. The target dimensions of the panels were 160mm side length and 50mm height, in three forms: solid, perforated and wireframe (Figure 4). The two-part moulding used corner clips to reach the target forms for these panels. 30mm openings on one side of the form provide air exchange. The corner clips were designed to hold the two parts of the mould together; connected through the 6mm opening slots with two 300mm zip ties (Figure 4). The solid panel lost 92% of its original volume and 62% of its original weight during the process, compared to the perforated panel (94% volume/63% weight) and the wireframe (96% volume/64% weight).

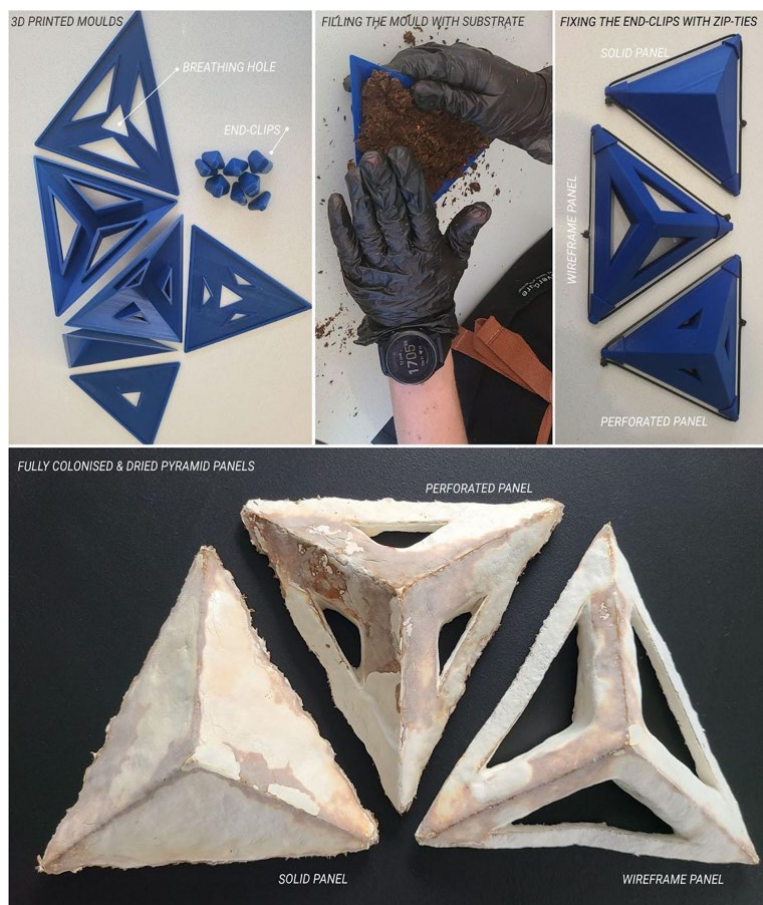


Figure 4. 'Pyramid Panels' case study. 3D printed moulding system and resulting panels

The 'Segment Iterations' test group was developed to further investigate form-making and form-retaining properties of mycelium-based materials, particularly focusing on the small-scale forms and subdivisions. Nine test samples were produced to compare the effect of level of detail and element size. The 3D printed form-making moulds were designed using Grasshopper 3D with 6-21 segments (walls), subdivisions ranging from 3mm to 30mm segment height and 1mm to 5mm wall thicknesses. The results in Figure 5 compares the 3D printed negative moulds and resulting mycelium products seven days after the interisation (oven-drying) stage.

The substrate size meant that the mixture was not able to fill all the cavities inside the moulds (see samples I, E and F in Figure 5). Although mycelium roots (hyphae) did attempt to grow into these vacant spaces, not all gaps were filled during the growth process. In these cases, the mycelium roots, without substrate, showed greatest deformation after drying. Elements smaller than 3mm appear more likely to be deformed. This shows limitations of the form-retaining properties of the myco-materials and could be studied further.



Figure 5. 'Segment Iterations' case study

As some of the samples (iterations) contained fine elements and detailing, they were more affected by the deformation and loss of overall volume. Samples shrunk to various degrees varying from 85% to 96% of their original volume. These samples also lost most of their weight during inertisation (oven drying for 3.5 hours at 50°C). Although all samples did continue to lose more moisture and weight afterwards during the air-drying stage. In total, the samples lost between 61% and 71% of their original weight.

4. Discussion

The case studies show consistent results from the combination of computation and materials from biological growth process, and 3D printed mould making. The dried objects reduced in volume with a mean dry volume being 92.85% ($\sigma = 3.2$) across all samples. The cardboard composite samples had slightly lower and more consistent mean reduction in volume ($M = 94.86\%$, $\sigma = 0.69$), while the samples without cardboard reinforcement varied more ($M = 91.77\%$, $\sigma = 3.59$), possibly due to added

structural integrity and reduced shrinkage. It is worth noting that the shredded cardboard did not appear to perform differently to one with waffle structure. The final mass of the samples also varied substantially, with the average final mass for cardboard composite structures being 54.68% ($\sigma = 1.39$) of the initial weight, and the average final mass of the non-reinforced samples being 34.36% ($\sigma = 3.00$).

The process shows that there was a consistent change in volume during drying. The density of the scaffold structure appears to have limited importance, but it increased the consistency of the volume change. However, any overall volume change may also be dependent on the fineness or granularity of the substrate. The substrate we used had pieces measuring up to 5mm in length, but only up to 1mm in diameter. Further research could explore the impact of substrate coarseness, and if finer inclusions (such as spent ground coffee) may have an impact on the deformation of the final design.

In contrast to robotic extrusion of hybrid myco-composites with varying aggregates, which focus on building components, nodal connections and structural differentiation of customised design variations, this research reverts to 3D printing and thus provides a large palette of options for material adoption by fine-tuning 3D printed formworks. Significantly, in a context of ubiquitous 3D printers, a maker space culture can therefore connect with and contribute to conversion of waste products into desirable products or artefacts. With affordable and simple processes and materials as has been demonstrated here. Combinatory degrees of myco-material with different waste products offer a rich domain for user participation in design. Thus, complexities of forms, geometry and shape can stimulate community initiatives for reconsidering waste as new resource material, exchanges by sharing source files and production codes across maker spaces. In the context of architecture potential application of myco-materials can be extended to both interior and exterior finishes as well as self-supporting structural elements. Future work on this project will be carried out using full-scale triangular grid wall-panels drawing upon the 'Pyramid panel' prototypes as the initial experimental iteration.

5. Conclusion and Future Work

This paper has described an investigation into how the growth of mycelia can impact computational design of myco-material composites. Our study showed that with a single substrate, and consumer-level fabrication equipment, consistent results can be achieved. An initial benchmarking of specific substrates will be necessary, but future research into sustainable computational design has the potential to improve the performance of myco-materials. For a circular, post-carbon future, myco-materials demonstrate a clear potential to give new value to cardboard, as a showcase for domestic waste material that is ultimately suitable for composting rather than disposal at its end of life. More research is required in the domain of growth behaviour and simulations, to which these case studies have contributed through a tracking of weight, volume, density, and moisture. Computational simulation coupled with robotic 3D printing can further advance the fabrication of customised modules onsite or in a specific local context, including post fabrication tracking of behaviour, including maintenance.

References

- Agustí-Juan, I., Jipa, A., & Habert, G. (2019). Environmental assessment of multi-functional building elements constructed with digital fabrication techniques. *The International Journal of Life Cycle Assessment*, 24(6), 1027-1039.
- Davidson, J. (2020). *Could Mushrooms Help Us Fight the Climate Crisis?* Ecowatch. Retrieved January 28, 2022, from <https://www.ecowatch.com/mushrooms-climate-crisis-2645762381.html>
- Elsacker, E., Søndergaard, A., Van Wylick, A., Peeters, E., & De Laet, L. (2021). Growing living and multifunctional mycelium composites for large-scale formwork applications using robotic abrasive wire-cutting. *Construction and Building Materials*, 283, 122732.
- Fearson, A. (2017b). *Tree-shaped structure shows how mushroom roots could be used to create buildings*. Dezeen. Retrieved January 28, 2022, from <https://www.dezeen.com/2017/09/04/mycotree-dirk-hebel-philippe-block-mushroom-mycelium-building-structure-seoul-biennale/>
- Frank, P. (2014). *This Living, Sustainable Mushroom Building Could Be The Future Of Green Architecture*. Huffington Post. Retrieved January 28, 2022, from https://www.huffpost.com/entry/moma-hy-fi-_n_5549107
- Frearson, A. (2017a). *Mushroom mycelium used to create suede-like furniture by Sebastian Cox and Ninela Ivanova*. Dezeen. Retrieved January 28, 2022, from <https://www.dezeen.com/2017/09/20/mushroom-mycelium-timber-suede-like-furniture-sebastian-cox-ninela-ivanova-london-design-festival>
- Goidea, A., Floudas, D., & Andréen, D. Transcalar (2021). Design: An Approach to Biodesign in the Built Environment. *Proceedings of Conference: International Conference on Construction, Energy, Environment and Sustainability* (pp. 1-9). Portugal.
- Gough, P., Yoo, S., Tomitsch, M., & Ahmadvpour, N. (2021). Applying Bioaffordances through an Inquiry-Based Model: A Literature Review of Interactive Biodesign. *International Journal of Human-Computer Interaction*, 37(17), 1–15.
- Jauk, J., Vašatko, H., Gosch, L., Christian, I., Klaus, A., & Stavric, M. (2021) Digital Fabrication Of Growth, Combining Digital Manufacturing Of Clay With Natural Growth Of Mycelium. *Caadria 2021* (pp. 753-762).
- Jones, M., Gandia, A., John, S., & Bismarck, A. (2021). Leather-like material biofabrication using fungi. *Nature Sustainability*, 4(1), 9–16.
- Jørgensen S., Pedersen L.J.T. (2018) The Circular Rather than the Linear Economy. In: *RESTART Sustainable Business Model Innovation*. Palgrave Macmillan.
- Konietzko, J., Bocken, N., & Hultink, E. J. (2020). Circular ecosystem innovation: An initial set of principles. *Journal of Cleaner Production*, 253, 119942.
- Lim, Ariel Cheng Sin and Thomsen, Mette Ramsgaard (2021) Multi-Material Fabrication for Biodegradable Structures - Enabling the printing of porous mycelium composite structures, in: Stojakovic, V and Tepavcevic, B (eds.), *Towards a new, configurable architecture - Proceedings of the 39th eCAADe Conference*, (pp. 85-94)
- Lim, A. & Thomsen, M. (2021) Multi-Material Fabrication for Biodegradable Structures - Enabling the printing of porous mycelium composite structures, in: Stojakovic, V & Tepavcevic, B (eds.), *Towards a new, configurable architecture - Proceedings of the 39th eCAADe Conference - Volume 1*, pp. 85-94.
- Morby, A. (2017). *Structure grown from “mushroom sausages” shows potential for zero-waste architecture*. Dezeen. Retrieved January 28, 2022, from <https://www.dezeen.com/2017/06/20/aleksi-vesaluoma-mushroom-mycelium-structure-shows-potential-zero-waste-architecture/>
- Ross, P. (2014). *Mycotecture: architecture grown out of mushrooms* | Parsons The New School for Design. The New School. Retrieved from <https://youtu.be/7q5i9poYc3w>
- Schandl, H., King, S., Walton, A., Kaksonen, A., Tapsuwan, S., & Baynes, T. (2021). *Circular economy roadmap for plastics, glass, paper and tyres*. CSIRO.

MODULAR FORMWORK TECHNIQUES FOR FUNICULAR SLABS

MAYANK SINGH¹

¹*RV College of Architecture.*

¹*mayanksingh.rvca@rvei.edu.in, 0000-0002-2945-3690*

Abstract. The research dealt with developing low-cost formwork techniques for funicular slabs by trying to achieve similar-sized triangular modules to help achieve a near-perfect funicular shape. Instead of applying meshing patterns on already developed funicular shapes, the approach taken in this research was to mesh the planar topology and then analyse the similarity of triangles achieved on the relaxed geometry. 3 types of meshing patterns were applied to 5 types of planar shapes for a span of around 4 to 7 meters and the similarity of the triangles was measured through standard deviation. The meshes were structurally analysed and results like deflection and bending stresses helped in assessing which meshing pattern performed better under gravity and imposed loads. Prototypes in different scales were created to suggest a low-cost buildable solution.

Keywords. Funicular; Form-Finding; Meshes; Shells; SDG 9; SDG 11.

1. Introduction

Conventional RCC floor slabs in framed structures contribute to around 60-70% of the total structural weight of a building. Employing shallow vaulted, funicular slabs can result in significant savings in the amount of concrete and elimination of steel reinforcement, reducing cost and the embodied energy of the slab. While conventional flat beam-slab systems are cast using timber, plywood and steel formwork and placed in position through wooden or steel props, doubly curved or vaulted shells require custom single-use formwork that produces significant waste. The cost of formwork required for such slabs can go up to 70% of the cost of the material itself as compared to less than 10% for standard slabs. The existing innovations in custom formwork systems still face difficulty in acceptance, especially in third-world countries, where the scope of built work and developable infrastructure is immense. There is a need to develop systems for funicular slabs that maximise reusability and minimise waste, are easily adaptable without a massive amount of skill introduction and are competitively placed in the market.

Recent developments in construction techniques of doubly-curved structures demonstrate ribbed funicular slabs with custom 3D printed formwork (Block et al, 2017) and complex shells constructed using custom-fabricated, stretchable fabric (Knitcrete, Popescu et al, 2014). Geometrically, as verified by *Theorema Egregium* (Gauss, 1827), it is not possible to tile a doubly-curved surface with a polygon mesh of

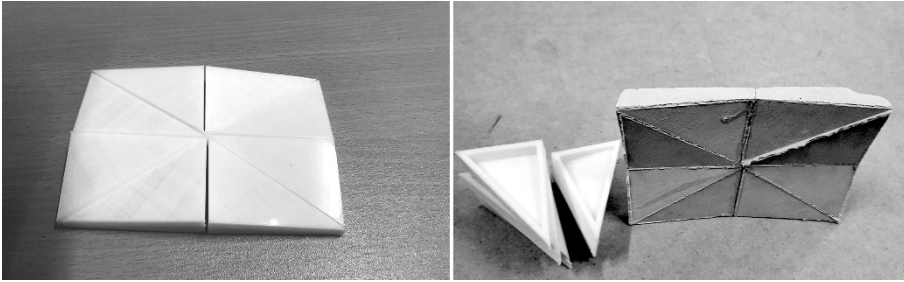


Figure 1. A small funicular shell in POP made of 8 identical pieces

equivalent faces (with the geodesic dome being an exception). However research by Bagrianski and Halpern (2014) has demonstrated that prescriptive dynamic relaxation applied on a triangulated mesh allows member similarity to a sufficient degree using forcing equations and corner supports as boundary conditions.

2. Meshing

For the study, a variety of planar geometrical shapes were chosen and different meshing algorithms were applied. Figure 2 shows the planar geometries - (1) a rectangle, (2) a right-angle trapezoid, (3) a regular hexagon, (4) an L-shaped hexagon and (5) an irregular pentagon. The edge lengths ranged from 3 m to 7 m. Meshing pattern 'a' was auto-generated by the program's in-built meshing algorithm. In meshing pattern 'b', the planar geometry was divided into segments by lines emerging radially outward from the centroid. This would lead to isosceles triangles in each segment. Meshing pattern 'c' involved superimposing an equilateral triangle grid trimmed at the boundary edges. For the L-shaped hexagon (geometry 4), a fourth meshing process was adopted which involved divided the plan into 2 rectangles and meshing them separately. Each triangle mesh face had an edge length varying from 300 mm to 600 mm, however the desired module size was kept at 450 mm. In Figure 2, the faces are colour-coded to indicate similarity. The faces in white were all unique and would have to be custom fabricated.

It was observed that the pattern 'c' – the one with the equilateral triangle grid – achieved the maximum number of similarly sized modules or conversely, the least number of unique faces, making it seem like the obvious choice for form-finding and fabrication. However, since theoretically it is impossible to have all edges equal in a doubly-curved surface, it was necessary to look into other meshing patterns demonstrated here.

3. Form-Finding

The meshes were form-found by dynamic relaxation method using the plugin Kangaroo within Grasshopper3d. The target edge lengths of mesh faces were desired to be of 450 mm. The support conditions were kept as hinged and the mesh corners were assigned as anchor supports. The maximum rise of the geometry was kept at 1/10th of the span i.e. around 500 mm to 600 mm depending upon the span of the geometry.

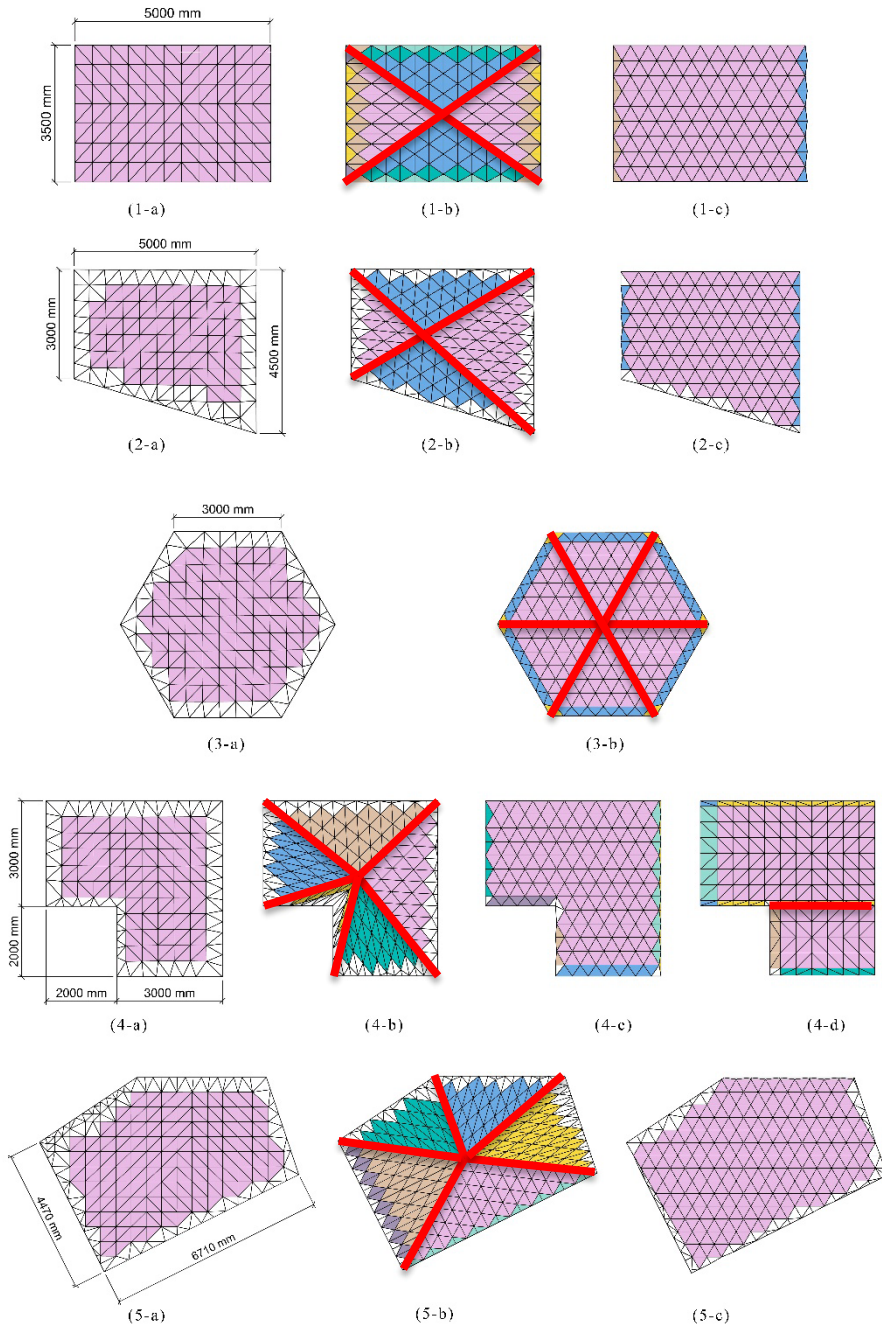


Figure 2. Meshing processes applied on different planar geometries

3.1. ITERATIVE LOADING

Since a prime necessity of a usable funicular slab is a flat, levelled top, it was necessary to include loads of the filler material in addition to dead and live loads of and on the slab itself to obtain an accurate funicular form. Obtaining the magnitude of the forces due to the filler material across the slab involved an iterative process of funicular form-finding.

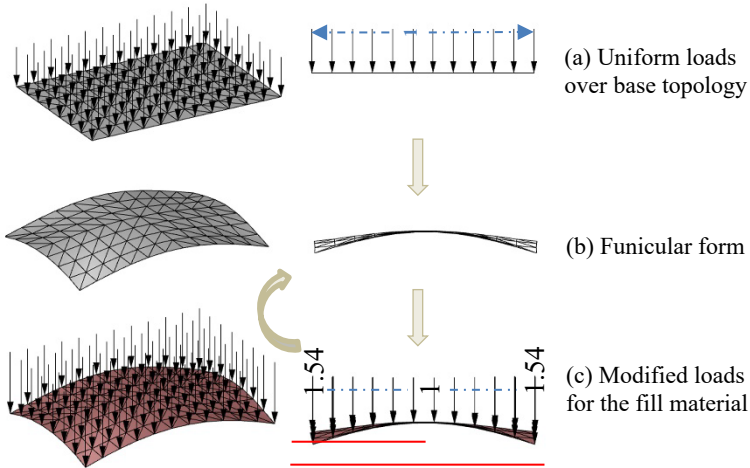


Figure 3. Funicular form-finding incorporating additional load of the fill material

For the first iteration, point loads of unit value were assigned at every mesh vertex (Figure 3 (a)). Once the first iteration of the funicular form-finding was completed (Figure 3 (b)), the corresponding height differences between the highest vertex of the funicular geometry (i.e. the rise) and funicular mesh vertices were found. These new values were remapped between 1 and a Maximum (1 being the value at the highest point in the geometry, implying no fill, and Maximum being the vertices near the supports implying maximum fill) as shown in Figure 3 (c). If the new list of height differences were different from the previous one, the loads were remapped and the process repeated; otherwise, if the list matched, convergence was achieved and the funicular geometry finalised.

A simple calculation of remapping of loads over a 6-meter span funicular slab is as follows:

Unit weight of concrete = 25 KN/m³

Area load of a 60 mm thick slab = 25 KN/m³ x 0.06 m = 1.5 KN/m²

Area live load considered = 5 KN/m²

Total Load without fill = 1.5 + 5 = 6.5 KN/m²

Unit Weight of Cinder filling = 6.5 KN/m²

Maximum depth of filling = Max Rise – Slab Thickness = 0.6 – 0.06 = 0.54 m

Maximum area load of filling = 6.5 KN/m³ x 0.54 m = 3.51 KN/m²

Total Load with fill = 6.5 + 3.51 = 10.01 KN/m²

Interpolating, 6.5 : 10.01 :: 1 : Maximum \Rightarrow Maximum = 1.54

Point loads at the highest mesh vertex in the geometry corresponded to '1' (an area load of 6.5 KN/m², concrete dead load and live load) whereas near the supports, the point loads corresponded to '1.54' (an area load of 10.01 KN/m²).

Additionally, since these had to be vertex-based point loads, the values obtained above were tweaked based on the proximity of vertices in plan. Hence, a Voronoi dual was created out of the planar projection of these mesh vertices, and remapped values were (Area loads in KN/m² as indicated above) multiplied with their respective Voronoi cell areas to convert the area loads into true point loads. (Figure 4)

3.2. DEGREE OF SIMILARITY OF FACES

Once the process of funicular form-finding was complete, the edge lengths of the individual mesh faces for all forms were analysed for similarity. Figure 5 shows the 5 kinds of forms generated under various meshing processes. Similar faces have been colour coded in the same way as shown in Figure 2, although some edge faces that were deemed identical before the relaxation process underwent some stretching and were eliminated afterwards. In the case of meshing processes 'a' (auto-meshing algorithm based) and 'b' (centroid based), as well as the meshing process in L-shaped hexagon in '4-d', the similar faces were isosceles triangles. The degree of similarity of the isosceles triangles was assessed by computing the standard deviation of the 2 shortest edges of every isosceles triangle face (the equal edges). In the case of meshing process 'c' which employed an equilateral triangle mesh, standard deviation was computed for all 3 edges of every face. As shown in Figure 5, for each set of similar mesh faces, the centroid-based meshing process 'b' yielded the lowest standard deviation, although it may require more sets of identical triangles than say, process 'a' or 'b'.

4. Structural Analysis

The dual-purpose of triangulated meshes in this study was not only to generate triangular modules for the formwork but to use the same mesh for structural analysis. It was observed that different planar meshes resulted in different shapes after dynamic relaxation, even with the same rise. Hence it was imperative to structurally analyse the 15 funicular meshes for dead and imposed loads. The support conditions were kept as pinned at the mesh corners. The analysis models were checked for deflection, in-plane, out-of-plane, and Von Mises stresses. Unlike the point loads used in the form-finding step, the following area loads were used:

- Dead Load: Self-weight of Concrete @ 25 KN/m³, 60 mm thickness
- Imposed Live Load: 5 KN/m² of planar area
- Imposed Fill Load: 6.5 KN/m³ of Cinder filling, varying thickness, based on the distance between corresponding face centroids of the relaxed mesh and a projected flat mesh.

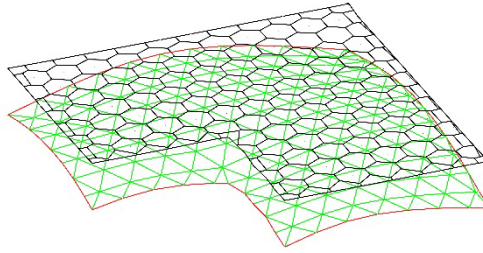


Figure 4. Generating Voronoi cells to convert area loads to point loads for form-finding

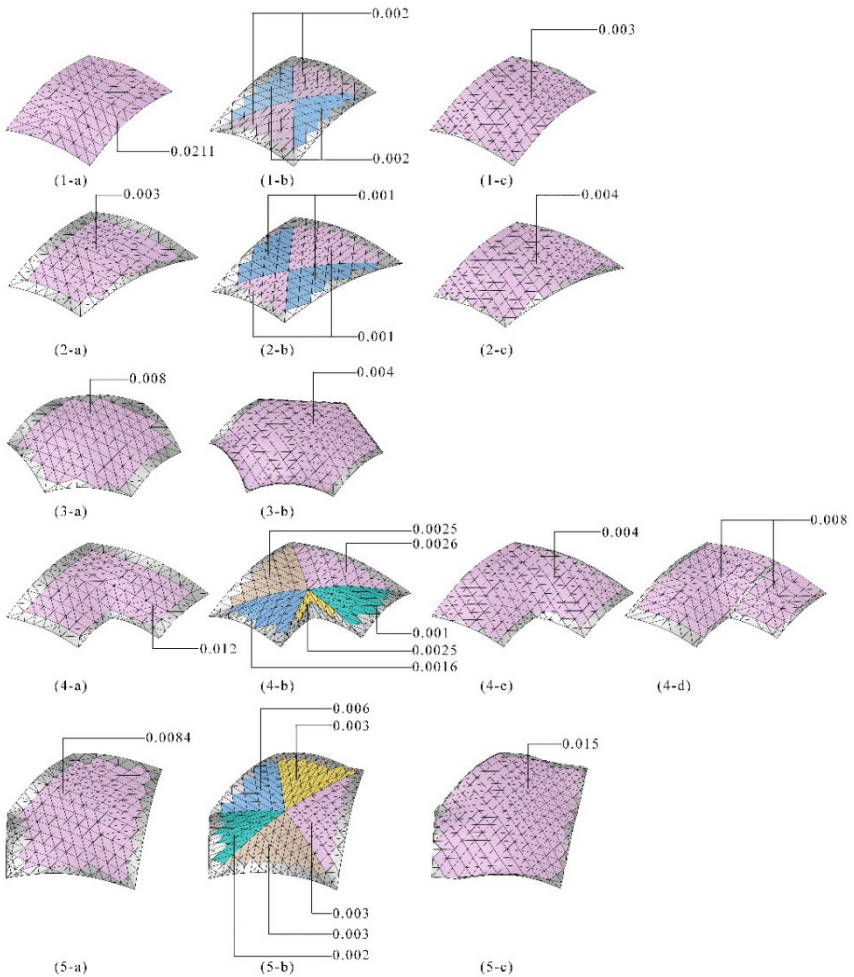


Figure 5. Funicular forms with mesh faces colour-coded for similarity along with the standard deviation of the edge lengths (in meters)



Figure 6. MDF prototype in 1:10 scale of the auto-meshed trapezoid geometry '2a'

5. Prototyping

MDF prototypes in different scales were created to (1) understand the working of conjoined triangles to form the desired geometry especially at scale 1:10; and (2) replicate an idealised work-flow of placing props and formwork, pouring concrete, curing and de-shuttering, at scale 1:5.

5.1. PROTOTYPE 1

The geometry '2a' (right-angle trapezoid, auto-meshed) was selected for the smaller 1:10 scale prototype, using 3 mm MDF board. The mesh faces were exploded and arranged for fabrication (Figure 6). Slots were modelled perpendicular to the individual edges of the mesh faces to be keyed-in with tiny 14 x 14 mm pieces, facilitating rotational movement in the plane of the slot.

The purpose of developing a prototype with slots was not to indicate exact replication in 1:1 scale but to bring together the identical central pieces and unique peripheral pieces (Figure 5, geometry '2a') and try and achieve a doubly-curved geometry (Figure 6, image on the right).

5.2. PROTOTYPE 2

The geometry '2b' (right-angle trapezoid', centroid-base meshing) was chosen to be prototyped in a larger 1:5 scale. A steel frame was fabricated for the entire assembly with 4 mm planks on the side and 3 mm triangular modules for the slab, both in MDF, joined at places using masking tape. MDF props laser-cut to their required height were placed at their designated location to support the formwork modules. A fines-only 1:3 cement-sand mix was used with a curing period of 10 days (Figure 7). Since achieving a uniform thickness at this scale was difficult, a varying thickness ranging from 10 mm to 30 mm was achieved.

It is important to note that the pieces in this prototype would translate in 1:1 scale as isosceles triangles of plywood of size 450 mm and a standard thickness of 20 mm. This size of modules was considered manually handle-able and replicable (75% from Table 1) for a slab of size 5 x 4.5 m. Also, the laser cut props employed here in varying heights would be translated in 1:1 by steel telescopic props or nailed bamboo poles, which is widespread practice for RCC formwork.

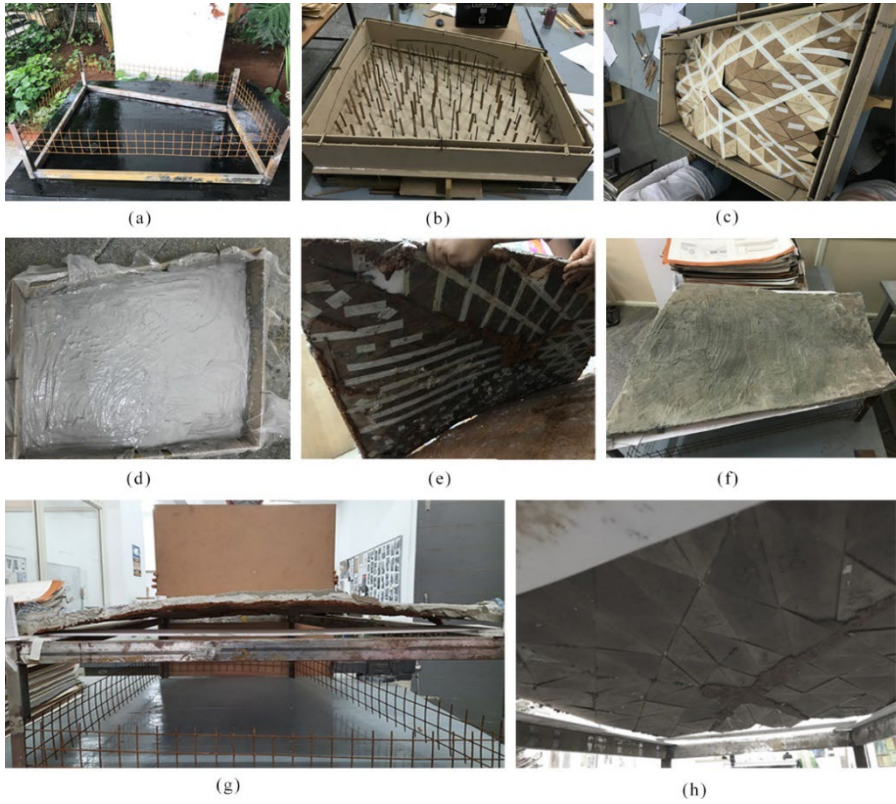


Figure 7. Step-by-step photos of prototype in 1:5 - (a) Steel frame, (b)MDF sides and props, (c) MDF triangular modules taped, (d) Fine-only concrete mix poured, (e) Slab lifted up with the pieces unremoved, (f) View of the slab, (g) Front elevation of the slab with the evident curvature, (h) Triangulated soffit of the slab.

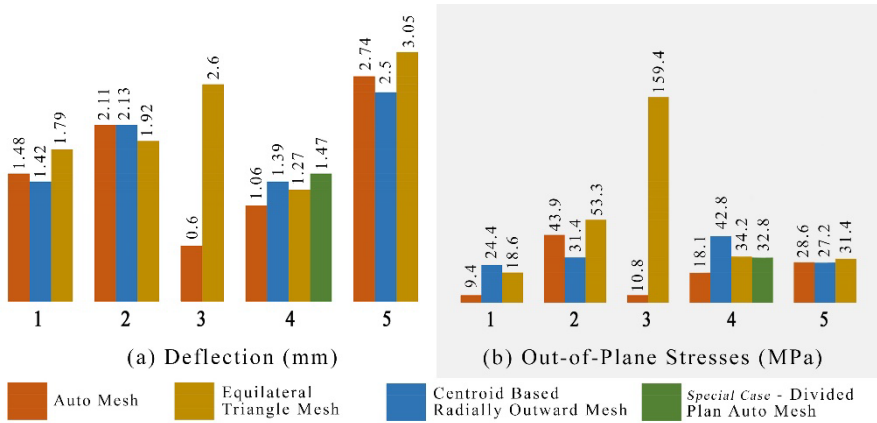


Figure 8. Structural Analysis results of the 15 funicular shells showing Deflection and Out-of-Plane Stresses

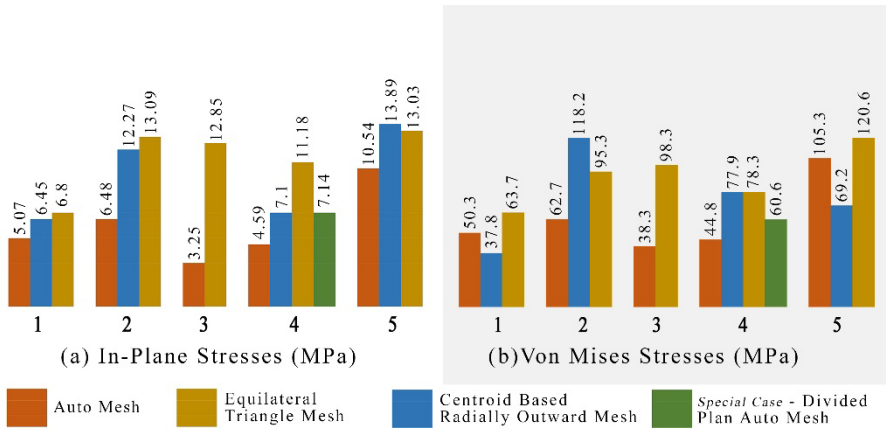


Figure 9. Structural Analysis results of the 15 funicular shells showing In-Plane Stresses and Von Mises Stresses

6. Results and Discussion

This research was a probe in the simplification of construction of shallow funicular shells. As per Figure 5 and Table 1 given at the end, the centroid-based meshing in all shells resulted in the lowest standard deviation. The 1:5 prototype of the geometry ‘2b’ demonstrated that a successful erection of a funicular floor system is possible where the modules had edge lengths with an extremely low standard deviation of 1 mm. In the structural analysis results of the shells across all meshing techniques, the lowest deflection generally was achieved where the shells had centroid-based meshing (Figure 8). Although the stresses told a different story with auto-meshing techniques resulting in the lowest stresses, none of the stress results indicated requirement of additional thickness or reinforcement. The column % Planar area of the slabs considered 'similar' (Table 1) signifies the range of standardization possible in obtaining planks of similar sizes that could be reused. Conversely, it could be deduced that the percentage of custom pieces can come down to 10-20 %.

Through the various meshing exercises and prototypes, a plausible solution to construct funicular slabs using computational design was successfully demonstrated. The research tries to align the idea of construction of a low-curvature slab to that of a regular RCC flat slab with planks and props. Additionally, a simple rotatable clamp to attach the plank to the prop (as suggested in Figure 10) could be used in 1:1.

Employing funicular geometry with its several advantages through computational design, the research was an exploration of basing theory over an existing low skill-transfer, practical construction technique, already widespread in third-world countries. Strongly addressing floor slabs as the crux of the problem of massive carbon footprint in RCC construction, the paper aligns itself to the Sustainability Goals 9 and 11 of building sustainable cities through sustainable industrialization and innovation.

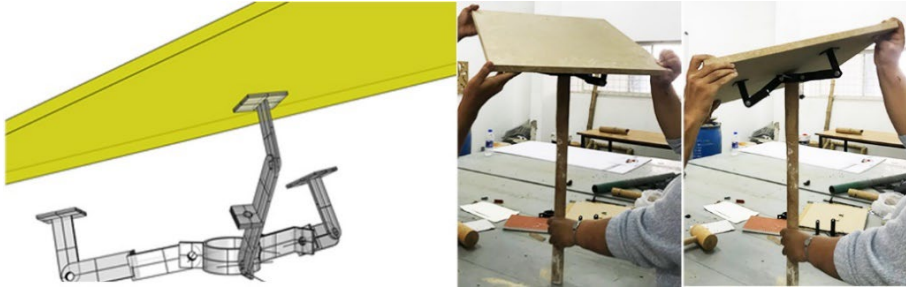


Figure 10. 360° Rotatable Clamp

Mark	Shape	Meshing	Max Std Deviation of edge lengths of triangle faces considered similar (mm)	% Planar area of slab of faces considered 'similar'
1a	Rectangle	Auto-Mesh	21.1	100
1b	Rectangle	Centroid-based	2	70
1c	Rectangle	Equilateral Triangle	3	95
2a	Trapezoid	Auto-Mesh	3	87
2b	Trapezoid	Centroid-based	1	75
2c	Trapezoid	Equilateral Triangle	4	92
3a	Regular Hexagon	Auto-Mesh	8	83
3b	Regular Hexagon	Equilateral Triangle	4	90
4a	L-Hexagon	Auto-Mesh	12	81
4b	L-Hexagon	Centroid-based	2.6	73
4c	L-Hexagon	Equilateral Triangle	4	88
4d	L-Hexagon	Divided Plan	8	80
5a	Irregular Pentagon	Auto-Mesh	8.4	89
5b	Irregular Pentagon	Centroid-based	6	85
5c	Irregular Pentagon	Equilateral Triangle	15	90

Table 1 Max Standard Deviation of Edge Lengths and % Planar Area considered 'similar'

References

- Bagrianski, S., & Halpern, A. B. (2014). Form-finding of compressive structures using Prescriptive Dynamic Relaxation. *Computers & Structures*, 132, 65-74.
- Block Research Group (2017, September 21). *NEST HiLo Roof Prototype Zurich*. Retrieved December 2020 from <https://vimeo.com/234883130>
- Block, P., Kilian, A., & Pottmann, H. (2015). Steering of form—New integrative approaches to architectural design and modeling. *Computer-Aided Design*, 61, 1.
- Jiang, C., Tang, C., Tomići M., Wallner, J., & Pottmann, H. (2014). Interactive Modeling of Architectural Freeform Structures: Combining Geometry with Fabrication and Statics. *Advances in Architectural Geometry 2014*, 95-108.
- Liew, A., López, D. L., Van Mele, T., & Block, P. (2017). Design, fabrication and testing of a prototype, thin-vaulted, unreinforced concrete floor. *Engineering Structures*, 137, 323-355.
- Popescu, M., Reiter, L., Liew, A., Van Mele, T., Flatt, R. J., & Block, P. (2018). Building in Concrete with an Ultra Lightweight Knitted Stay-in-place Formwork: Prototype of a Concrete Shell Bridge. *Structures*, 14, 322-332.
- Singh, M., & Schaefer, S. (2010). Triangle surfaces with discrete equivalence classes. *ACM SIGGRAPH 2010 Papers on - SIGGRAPH*.

COMPILING OPEN DATASETS TO IMPROVE URBAN BUILDING ENERGY MODELS WITH OCCUPANCY AND LAYOUT DATA

AYCA DURAN¹, ORCUN KORAL ISERI², CAGLA MERAL AKGUL³, SINAN KALKAN⁴ and IPEK GURSEL DINO⁵

^{1,2,5} *Department of Architecture, Middle East Technical University*

³ *Department of Civil Eng., Middle East Technical University*

⁴ *Department of Computer Eng., Middle East Technical University*

¹ *aycad@metu.edu.tr, 0000-0001-6027-2962*

² *koral.iseri@metu.edu.tr, 0000-0001-7735-3363*

³ *cmeral@metu.edu.tr, 0000-0001-8720-1216*

⁴ *skalkan@metu.edu.tr, 0000-0003-0915-5917*

⁵ *ipekg@metu.edu.tr, 0000-0003-2216-9192*

Abstract. Urban building energy modelling (UBEM) has great potential for assessing the energy performance of the existing building stock and exploring various actions targeting energy efficiency. However, the precision and completeness of UBEM models can be challenged due to the lack of available and reliable datasets related to building occupant and layout information. This study presents an approach that aims to augment UBEM with open-data sources. Data collected from open data sources are integrated into UBEM in three steps. Step (1) involves the generation of occupant profiles from census data collected from governmental institutions. Step (2) relates to the automated generation of building plan layouts by extracting data on building area and number of rooms from an online real-estate website. Results of Steps (1) and (2) are incorporated into Step (3) to generate residential units with layouts and corresponding occupant profiles. Finally, we make a comparative analysis between data-augmented and standard UBEM based on building energy use and occupant thermal comfort. The initial results point to the importance of detailed, precise energy models for reliable performance analysis of buildings at the urban scale.

Keywords. Urban Building Energy Modelling; Occupancy; Residential Building Stock; Unit Layout Information; Open-source datasets; Energy Demand; Indoor Thermal Comfort; SDG 11.

1. Introduction

Buildings alone account for 40% of energy consumption and 36% of greenhouse gas

emissions (European Commission, 2020). The global population might reach 11 billion by 2050, with the majority of the additional population residing in cities, bringing the total urban population to 6.5 billion (United Nations, 2019). Cities must be able to assess their energy use and investigate methods for reducing energy consumption and environmental effect to contribute to achieving one of the Sustainable Development Goals (SDGs) of the United Nations, SDG11, focusing on "Sustainable cities and communities" (United Nations, 2015). In order to estimate, compare, rank, and contrast the energy used in cities by building stock, Urban Building Energy Modelling (UBEM) has gained an increasing research interest in past decades. Varying between scales of a city block to an entire city, UBEM has been extensively used to guide energy-efficient design, ensure code compliance, obtain performance rating credits, evaluate retrofit options, and optimise building operations (Hong et al., 2020).

UBEM requires several parameters for building characteristics as inputs, such as building geometry, location, climate, use type, energy systems and occupancy data. Modelling occupancy, which is a complex problem even for a single building since occupants interact with buildings in many different ways and cause uncertainty in building energy use estimations, has been a challenge for UBEM. Studies have shown that up to 30% of the variation in building energy performance can be attributed to occupants (Tian et al., 2018). Therefore, modelling occupancy has been one of the critical factors for UBEM to estimate building performance indicators accurately.

Accurate estimations in urban scale modelling are significantly affected by the availability and adaptability of large datasets to UBEM. The availability and cost of the occupancy data, along with privacy concerns, obstructed the process to obtain data for energy models (Putra et al., 2021). In most UBEM attempts, building occupancy information is rather simplified due to the lack of necessary data in district or urban scales (Mosteiro-Romero et al., 2020). When data directly linked to occupancy presence or activity is unavailable, synthetic population generation based on various data resources become one of the key solutions.

Researchers adopted several methods to model occupancy from outside resources, such as surveys, data-mining techniques, and sensors to generate synthetic occupancy data in recent decades. For instance, a recent study examined occupant presence and characteristics based on 12 years of survey data representing occupant presence in buildings and household characteristics to generate annual occupancy schedules (Mitra et al., 2020). Generated occupancy schedules relied on age, day of the week, number of household members and the age distribution of occupants in households. Researchers have found a 41% difference between commonly accepted default occupancy schedules and the schedules they generated for residential buildings, although both schedules share similar patterns. Similarly, another study relied on a time use survey and census data to assess occupancy and behavioural information (Jeong et al., 2021). Researchers obtained information for household composition and occupant activities during different periods of the year. Although similar studies have demonstrated that the generation of synthetic occupancy data is not new, implementation of the approach in the UBEM framework is yet to be explored (Happle et al., 2018).

Estimating the occupant density within a thermal zone is critical. However, estimating the exact occupant presence for a large number of thermal zones is hard to specify when data is not available. Collecting data for each residential unit of a

neighbourhood is not practical and, in most cases, data is not available due to privacy concerns. Generally, standardised measures for occupancy, a fixed value for people per floor area, is supplied to energy models which do not represent the actual occupant presence and systematically lower heating energy loads (Tahmasebi & Mahdavi, 2017). In this respect, previous studies relied on the relationship between tenant units and the number of occupants (Sun & Erath, 2015). Unit layout information has the potential to reflect the probable household size. For residential buildings, the number of bedrooms can imply the number of people that could occupy the unit. Although exact modelling of interior unit division is not possible, occupant presence in units can be inferred from the number of rooms and floor areas available in real-estate service databases. Therefore, this study contributes to previous methods for synthetic occupancy generation based on census data by integrating the data obtained from real-estate advertisements to associate generated occupant profiles with building units.

This study aims to support UBEM with occupancy and layout data by compiling publicly available datasets. The proposed occupancy modelling approach contributes to the knowledge in synthetic occupancy generation for UBEM when data directly linked to occupancy is not present. The proposed approach is applied to UBEM of a neighbourhood in Ankara, Turkey, with 599 residential buildings. To contrast the results of the proposed occupancy generation approach with the default midrise apartment occupancy, two sets of simulations are compared based on performance indicators of heating energy demand (QH) and indoor overheating degrees (IOD).

2. Methodology

This paper presents a methodology for occupancy generation and residential unit division planning to increase the resolution of the UBEM framework based on real-world data sets. Generated occupant profiles were associated with residential unit layouts in terms of total area and room number (e.g., 1+1, 2+1). The building stock performance of the generated occupancy and default occupancy schedules were compared (Figure 1).

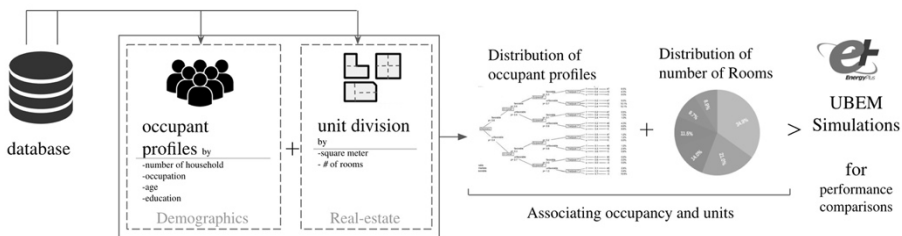


Figure 1. The proposed methodology.

2.1. CASE STUDY

The proposed methodology is applied to the Bahçelievler neighbourhood, Turkey (Figure 2). The analysis region is home to a dense mass of buildings since it is located in Turkey's second largest city, Ankara. Three to four-story buildings occupy 574,353 square meters (sqm) floor areas in the city. The residential buildings represent 93% of the building stock (599 residential buildings out of 642). The building typology of the region consists of primarily residential buildings with retail and office units on the ground floors (approximately 10% of the total units per building). Ankara is in ASHRAE 4B climate region; thus, heating energy demand is dominated, and cooling demand was not calculated in the scope of this study.

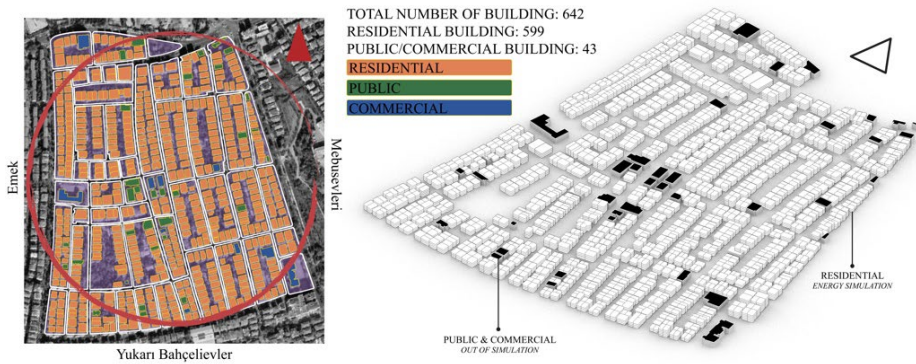


Figure 2. Bahçelievler neighbourhood.

2.2. OCCUPANT PROFILE GENERATION

Detailed household information for residential building stock is not available for the studied region. Therefore, the proposed occupancy modelling was produced based on the analysis of publicly available census data obtained from the Turkish Statistical Institute (TUIK). The proposed occupancy modelling consists of two phases: the formation of occupant profiles and the modelling of the household combination according to the conditional probability methodology. Several assumptions were made during the various steps of this exploratory modelling study. In the first step, occupant profiles were formed according to the age ranges of the occupants (TUIK, 2021b), and divided into three subgroups: 0to24, 25to64, and 65+. As a next step, age groups were separated into three classes: work, school, and home (Table 1) according to their education, employment status and the information of whether residents were present at home or not (TUIK, 2021c). Occupant profiles were created by modelling their presence at home at different rates within 24 hours on weekdays. For instance (Table 1), children aged 0-5 who are at home, children aged 6-24 who goes to school and children between the ages of 15-24 who do not study or work were gathered under the same group of kids aged 0to24. Independent of the profiles, all occupants are assumed to be at home on weekends.

Occupant profile	Kids, 0to24 (38.23% of the population)	Adult, 25to64 (52.26% in all population)	Senior, 65+ (9.51% in all population)
Subgroups	Home (e.g., infant) School (e.g., elementary, kindergarten) Work	Work Home (e.g., unemployed, retired)	Home (i.e., retired)
Weekdays	Home: 8.96% School: 51.94% Work: 39.1%	Home: 39.6% Work: 60.4% (65+ employment status excluded)	Home (in): 100%
Weekend	Home: 100%		

Table 1. Occupant profiles and subgroups for weekdays and weekends.

In the second step, occupant profiles were divided into seven groups according to the size of the household, e.g., one-person household, two-person household (TUIK, 2021a). Densities of different household combinations were defined based on conditional probability in terms of the number of households and the characteristics of the members of the family. Three different family types were defined: family with children, family with children and elderly, and no family. Children, adults, and elderly groups were assigned to these groups according to their proportion in the total population. These characteristics were determined according to census data obtained from the TUIK, e.g., two-person family with kids, four-person family kids and elderly (Figure 3).



Figure 3. Occupant profile generation

For instance, the proportion of a family with five children in the total population was 7.6%. This ratio is supported by the conditional distribution of child, elderly and adult groups. Specifically, a combination of 3 adults, one child, and one elderly person is 2.327%, according to census data. The ratio found was also multiplied by the total

housing unit of the neighbourhood to determine how many times this household occupant combination is repeated in the model. On the other hand, it is noticed that while some combinations are theoretically possible, they are probabilistic unlikely. For example, the proportion of households consisting of five members of non-family in the total population is 0.10%. The probability of a five-person household combination consisting of five elderlies in this combination set is minimal so that it can be ignored.

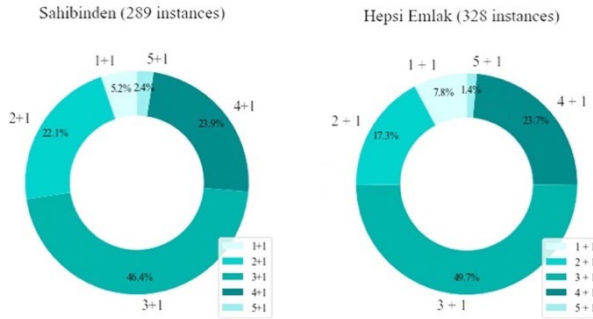


Figure 4. Frequencies of unity types based on number of rooms.

2.3. UNIT LAYOUT GENERATION

The level of detail of the building energy modelling process affects the accuracy of the results (Biljecki et al., 2014). Initially, a total number of units in the buildings was obtained through the address inquiry system (Nüfus ve Vatandaşlık İşleri Genel Müdürlüğü, n.d.). However, the total number of units for each building obtained from the address inquiry system does not relate to household information. Therefore, the number of occupants and their likelihood of being present at home for each unit is unknown. At this stage, real-estate advertisements belonging to the studied district is interpreted. Initially, floor area and the number of rooms belonging to building units in Bahcelievler were obtained from two of the most accessed online real-estate web services in Turkey, namely, *Hepsi Emlak* (*Hepsiemlak*, 2006) and *Sahibinden* (*Sahibinden*, 2000). Advertisements available on October 8, 2021, for the Bahcelievler neighbourhood were recorded for each resource. After data preprocessing of two datasets and removal of outliers, a total number of 671 data points, 382 from *Hepsi Emlak* and 289 from *Sahibinden*, are analysed individually due to the possibility of the same advertisement taking place in both resources.

According to both the data sets, slightly less than half of the buildings in Bahcelievler have three rooms and a living room (3+1) with 46% and 49% in the examined resources (Figure 4). 2+1 and 4+1 houses occupy around 22% of the datasets, following the most common 3+1 houses. The relationship between the number of rooms and the unit floor areas (Figure 5) is also investigated to identify the number of rooms in the units in the digital model. The floor area of modelled units' is used to find the number of rooms. The probability of a unit with a specific floor area having a particular number of rooms is calculated based on the floor area and reflected in the number of rooms in units.

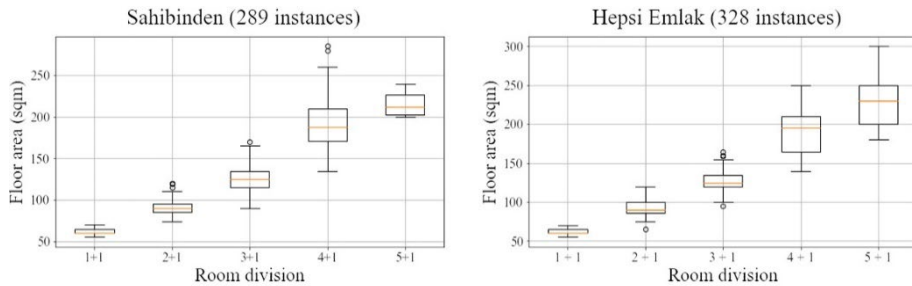


Figure 5. The relationship between number of rooms and unit floor areas.

2.4. ASSOCIATING OCCUPANCY AND UNIT LAYOUT INFORMATION

Detailed occupancy modelling for residential units is critical since internal space conditioning and electrical equipment power usage is affected by occupants. First, residential units were grouped according to floor areas and the number of rooms obtained from open-source real-estate advertisements. The number of rooms can vary according to architectural layout design; even the floor areas are the same. For instance, units between 100 and 110 sqm can contain 2+1, 3+1, 4+1. During the calculations, overlaps in the floor area and the number of rooms was also considered. Secondly, generated occupancy is mapped into the units based on the number of rooms based on the assumption that the number of people is strongly correlated with the number of bedrooms of a residential unit. With this assumption, unlikely assignments, such as, a family of 7 people living in 1+1 units, were eliminated.

2.5. UBEM PROPERTIES AND SIMULATION PROCESS

Each residential building in the case study was modelled in detail down to the size of a unit (Figure 6). For the non-residential buildings, neither floor nor unit partitioning was made, and these buildings were only included as context buildings in the building energy simulations. The original drawings of the layout of buildings were converted to simple four-corner rectangles to reduce the computational cost of the simulations. 10% of the total area of a parcel was given to the vertical circulation area. Each building and its neighbours in close proximity is parametrically modelled and simulated. Since the large number of inputs and outputs of UBEM increase computation time and modelling difficulty, each building was simulated with the residential and office units it contains together with the buildings nearby, impacting insolation as context geometries.

Building energy simulations are conducted using the EnergyPlus (Crawley et al., 2000) engine through the Ladybug Tools (Sadeghipour Roudsari & Pak, 2013). Materials were selected following TS-825-2013 (i.e., heat insulation rules in buildings) (T.C. Çevre Bakanlığı, 2013) and ASHRAE (ASHRAE, 2013) standards. A representative climate data for the typical meteorological year was used for simulations. Energy model parameters other than selected occupancy-dependent parameters, such as u-values, infiltration rate, window to wall ratio so on, are kept constant for simulations with the default and generated occupant profiles.

Two sets of simulations are conducted. The total number of floors of the buildings and the number of units per floor were determined with the data collected from the address inquiry system and real-estate agencies. Only the occupancy schedules, the number of people per sqm and the equipment density are determined as occupant profile dependent variables (Heydarian et al., 2020). The equipment use has been determined based on the age ranges of the occupants (Table 1). 65+ is assumed to have an equipment density of 2W/sqm, while the other profiles have 3W/sqm.

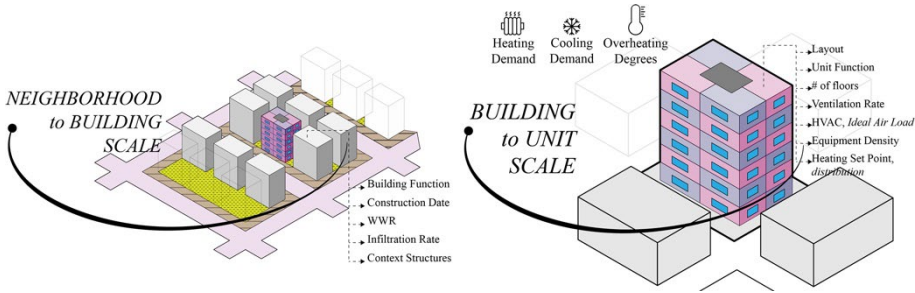


Figure 6. Properties of building energy model

Simulations with the default and generated occupancy schedules are compared based on QH (kWh/sqm) and IOD (°C). IOD estimation reflects the impact of design parameters in summers when the cooling system is not actively used. The calculation of IOD is the annual summation of the indoor operative temperature above 28°C for the whole residential units (CIBSE, 2006).

3. Results

599 residential buildings of the studied neighbourhood were simulated to observe the difference between generated and default occupancy profiles. While the QH is significantly greater, with the mean difference of 17.77 kWh/sqm, in simulations with generated occupant profiles, IOD values are similar in both cases.

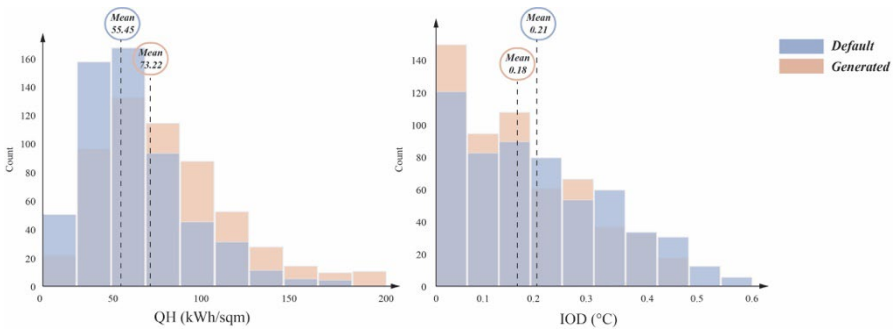


Figure 7. Default vs. generated occupancy schedule for energy demand (kWh/sqm)

Simulation outputs for QH imply that generated occupancy profiles increase

instances located towards the upper ends of the data set, shifting the distribution mean to the right (Figure 7). More instances close to the median value are observed with the standardised schedules. On the other hand, IOD for generated occupancy schedules does not differ considerably from the default schedules.

4. Discussion and Conclusion

We have proposed a methodology to infer occupant profiles by compiling census and real-estate data when a direct source of occupancy information is not available. In addition to widely used census data for occupancy profile generation, we analysed real-estate advertisements to obtain data for building layouts and the possible combination of their inhabitants. Performance simulations with the proposed occupancy profile generation approach have increased the number of observations above the mean value of the QH. In contrast, the use of default occupancy profiles resulted in the accumulation of data points around the mean value of the complete dataset. QH with the generated occupancy profiles was around 32% greater than the simulation with default profiles. Unsurprisingly, default occupancy produced standardized results, while the proposed approach increased the observation of less common data points. On the other hand, the observed difference in IOD was much smaller. This result could stem from the use of mechanical ventilation during the summer period.

Results of this study rely on several assumptions and generalizations that were made and explained in the methodology chapter of this paper. The findings of this exploratory study aligns with the previous research reporting that the default occupancy underestimates the heating energy demand (Tahmasebi & Mahdavi, 2017; Tian et al., 2018). To increase the reliability of the results, multiple simulations with different yet random household profile allocation will be tested in the following study. Future studies should also consider validating the results of the proposed methodology with data directly relating to occupancy.

Acknowledgements

The study was conducted within the scope of a project titled "Tool development for urban building energy modelling (UBEM) against climate change supported by machine learning and building simulations." (No. 120M997). The project is granted by the Scientific and Technological Research Council of Turkey (TUBITAK).

References

- ASHRAE. (2013). *ASHRAE Standard 90.1-2013 -- Energy Standard For Buildings Except Low-rise Residential Buildings*.
- Biljecki, F., Ledoux, H., Stoter, J., & Zhao, J. (2014). Formalisation of the level of detail in 3D city modelling. *Computers, Environment and Urban Systems*, 48, 1–15. <https://doi.org/10.1016/j.compenvurbsys.2014.05.004>
- CIBSE. (2006). *Guide A, Environmental Design*.
- Crawley, D. B., Lawrie, L. K., Pedersen, C. O., & Winkelmann, F. C. (2000). EnergyPlus: Energy Simulation Program. *ASHRAE Journal*, 42.
- European Commission. (2020). *Energy efficiency in buildings*.

- Happle, G., Fonseca, J. A., & Schlueter, A. (2018). A review on occupant behavior in urban building energy models. *Energy and Buildings*, 174, 276–292. Elsevier Ltd. <https://doi.org/10.1016/j.enbuild.2018.06.030>
- Hepsiemlak. (2006). Retrieved October 8, 2021, <https://www.hepsiemlak.com/>
- Heydarian, A., McIlvennie, C., Arpan, L., Yousefi, S., Syndicus, M., Schweiker, M., Jazizadeh, F., Rissetto, R., Pisello, A. L., Piselli, C., Berger, C., Yan, Z., & Mahdavi, A. (2020). What drives our behaviors in buildings? A review on occupant interactions with building systems from the lens of behavioral theories. *Building and Environment*, 179. <https://doi.org/10.1016/j.buildenv.2020.106928>
- Hong, T., Chen, Y., Luo, X., Luo, N., & Lee, S. H. (2020). Ten questions on urban building energy modeling. *Building and Environment*, 168. <https://doi.org/10.1016/j.buildenv.2019.106508>
- Jeong, B., Kim, J., & de Dear, R. (2021). Creating household occupancy and energy behavioural profiles using national time use survey data. *Energy and Buildings*, 252. <https://doi.org/10.1016/j.enbuild.2021.111440>
- Mitra, D., Steinmetz, N., Chu, Y., & Cetin, K. S. (2020). Typical occupancy profiles and behaviors in residential buildings in the United States. *Energy and Buildings*, 210. <https://doi.org/10.1016/j.enbuild.2019.109713>
- Mosteiro-Romero, M., Hischer, I., Fonseca, J. A., & Schlueter, A. (2020). A novel population-based occupancy modeling approach for district-scale simulations compared to standard-based methods. *Building and Environment*, 181. <https://doi.org/10.1016/j.buildenv.2020.107084>
- Nüfus ve Vatandaşlık İşleri Genel Müdürlüğü. (n.d.). *Adres Kayıt Sistemi (Address inquiry system)*. Retrieved December 20, 2021, from <https://adres.nvi.gov.tr/Home>
- Putra, H. C., Andrews, C., & Hong, T. (2021). Generating synthetic occupants for use in building performance simulation. *Journal of Building Performance Simulation*, 14(6), 712–729. <https://doi.org/10.1080/19401493.2021.2000029>
- Sadeghipour Roudsari, M., & Pak, M. (2013). Ladybug: A parametric environmental plugin for grasshopper to help designers create an environmentally-conscious design. *Proceedings of BS 2013: 13th Conference of the International Building Performance Simulation Association* (pp. 3128–3135).
- Sahibinden. (2000). Retrieved October 8, 2021, <https://www.sahibinden.com/>
- Sun, L., & Erath, A. (2015). A Bayesian network approach for population synthesis. *Transportation Research Part C: Emerging Technologies*, 61, 49–62. <https://doi.org/10.1016/j.trc.2015.10.010>
- Tahmasebi, F., & Mahdavi, A. (2017). The sensitivity of building performance simulation results to the choice of occupants' presence models: a case study. *Journal of Building Performance Simulation*, 10(5–6), 625–635. <https://doi.org/10.1080/19401493.2015.1117528>
- T.C. Çevre Bakanlığı. (2013). TS-825-2013, *Binalarda ısı Yalıtım Kuralları*.
- Tian, W., Heo, Y., de Wilde, P., Li, Z., Yan, D., Park, C. S., Feng, X., & Augenbroe, G. (2018). A review of uncertainty analysis in building energy assessment. *Renewable and Sustainable Energy Reviews*, 93, 285–301. Elsevier Ltd. <https://doi.org/10.1016/j.rser.2018.05.029>
- TUIK. (2021a). *Number of households by size and type, 2015-2020*. Retrieved October 20, 2021, from <https://data.tuik.gov.tr>
- TUIK. (2021b). *Population by sex and age group, 1950-2020*. Retrieved October 20, 2021, <https://data.tuik.gov.tr>
- TUIK. (2021c). *Population by sex and age group, 1950-2020*. Retrieved October 20, 2021, <https://data.tuik.gov.tr>
- United Nations. (2015). *#Envision2030 Goal 11: Sustainable Cities and Communities*.
- United Nations. (2019). *World Population Prospects 2019*.

INVESTIGATING URBAN HEAT ISLAND AND VEGETATION EFFECTS UNDER THE INFLUENCE OF CLIMATE CHANGE IN EARLY DESIGN STAGES

For Performance-Based Early Urban Design Decisions

FARZAN BANIHASHEMI¹, ROLAND REITBERGER² and WERNER LANG³

^{1,2,3}*Institute of Energy Efficient and Sustainable Design and Building Technical University of Munich.*

¹*farzan.banihashemi@tum.de, 0000-0001-5661-275X*

²*roland.reitberger@tum.de, 0000-0002-1823-6367*

³*w.lang@tum.de, 0000-0002-6593-8388*

Abstract. Different criteria need to be considered for optimal strategies in the early design stages of urban developments. Under the influence of climate change, the urban heat island effect (UHI) is a phenomenon that gains importance in the early design stages. Here, different parameters, for instance, vegetation ratio in the city district and building density, play a significant role in the UHI effect. These parameters need to be quantified through different simulation tools for optimal climate adaptation and mitigation measures on the urban district scale. However, not all parameters and their influence are clear to the decision-makers and actors in the early design stages. Hence, we propose a Monte Carlo based sensitivity analysis (SA) and uncertainty analysis (UA) to show the significance of different parameters and quantify them. The SA aims to identify the major influencing parameters, whereas the UA quantifies the effect on the energy performance and indoor thermal comfort of occupants. The workflow is integrated into a collaborative design platform and applied in a case study to support decision-makers in the early design stages for new developments, densification, or refurbishment scenarios.

Keywords. Monte Carlo Simulation; Sensitivity Analysis; Uncertainty Analysis; Building Energy Simulation; SDG 13; SDG 11.

1. Introduction

Climate change and urbanization and the resulting transformations are challenges that need to be considered in the early design stages of buildings and urban districts. The density of the built environment, the resulting lower natural ventilation in the urban canyons, and the utilized materials in buildings instead of natural resources lead to warmer nighttime and temperature peaks in cities compared to a rural site,

acknowledged as the urban heat island effect (UHI) (Nakano et al., 2015).

Designing new urban districts, retrofitting, and densifying the current stock requires a holistic approach that assesses the environmental impacts over the whole life cycle of buildings. In the life cycle assessment (LCA) of buildings, the usage stage of buildings is usually considered over a time span of 50 years. During this period, the morphology of urban districts might change. Hence, climate change and UHI need to be considered to optimize not only the outdoor spaces of the buildings but also the energy demand and thermal comfort of the occupants. In the usage stage, a double-side effect between buildings and the surrounding environment is present. Therefore, optimization of the buildings is dependent on the decisions made on the whole district or neighbourhood. Consequently, a performance-based approach in early design stages should be considered to enable a holistic method. The holistic method would allow climate adaptation and mitigation (SDG 13) measures on a district scale and help in developing sustainable cities and communities (SDG 11).

The influence of urban heat island (UHI) effect and climate change on the performance of buildings have been addressed by previous research in this field (Nakano et al., 2015). Adaptation measures from building to district level can reduce the impact of the changing climate and UHI on the occupants and the energy performance of buildings. This impact can be quantified through coupling building energy simulation (BES) and climate model tools.

Different climate model tools exist, which differ in their temporal and spatial resolution, and computational complexity. These climate models can be grouped into microscale and mesoscale tools. An obstruction in the early design stages is that detailed information is not available. For instance, the microclimate model tool Envi-met (Bruse et al., 1998) requires detailed information about the green infrastructure and the buildings. Furthermore, the tool is computationally time demanding. The output of the simulation results is limited to a small grid in a neighbourhood and the temporal resolution is not sufficient for an annual BES. Hence, the temporal resolution and computational costs limit its usability in BES.

Urban Weather Generator (UWG) is a physics-based climate simulation tool with low computational expense (Bueno et al., 2013) that requires limited input from the user. The performance of UWG is comparable to more computationally expensive mesoscale models (Nakano et al., 2015), and the tool can capture seasonal effects of the UHI phenomena (Bande et al., 2019). A workflow of integrating UWG in the urban modelling interface (umi) (Reinhart et al., 2013) was introduced in (Nakano et al., 2015). A sensitivity analysis was performed to identify the key parameters influencing UHI, energy performance, and thermal comfort under the influence of climate change. It was shown that the sensitivity of the parameters is case-specific and dependent on the investigated climate locations (Nakano et al., 2015). In another research paper, the authors performed a global sensitivity analysis based on Monte Carlo techniques on different input parameters to identify the significant ones for the case of Abu Dhabi (Mao et al., 2017). Hence, a general approach for different case studies and climate zones is required in the early design stages.

In this paper, we build upon previous research and introduce an iterative approach to support decision-makers in the early design stages. The approach and method are integrated into the Collaborative Design Platform (CDP) (Schubert, 2021) as a plugin,

which is described in section 2. As proof of concept, we deployed our method in a case study in Kempten, Germany. Section 3 demonstrates the case study and its boundary conditions for an urban densification project in the early design stages. One iteration of the workflow is demonstrated in the case study with the results shown in section 4. Finally, the discussion and conclusions drawn are summarized in sections 5 and 6, respectively.

2. Method

The method in this paper is an iterative approach that assists the decision-makers in the early design stages. It is based on a global uncertainty and sensitivity analysis to aid urban planners, energy analysts, architects, and other decision-makers. The approach enables the identification of significant input parameters influencing the energy performance and indoor thermal comfort through sensitivity analysis (SA). Furthermore, the uncertainty analysis (UA) helps to recognise the potential of optimizing/defining the mentioned input parameters. The SA and UA in this work are performed by a Monte Carlo based technique and aims to aid the decision-makers to focus on specific parameters to improve the design decision and to retrieve more robust results. Through the combined SA and UA the decision-makers get feedback on the CDP in each design iteration, which enables them to define relevant parameters, and enhance the urban design. The readers are referred to (Schubert, 2021) for detailed information on the CDP.

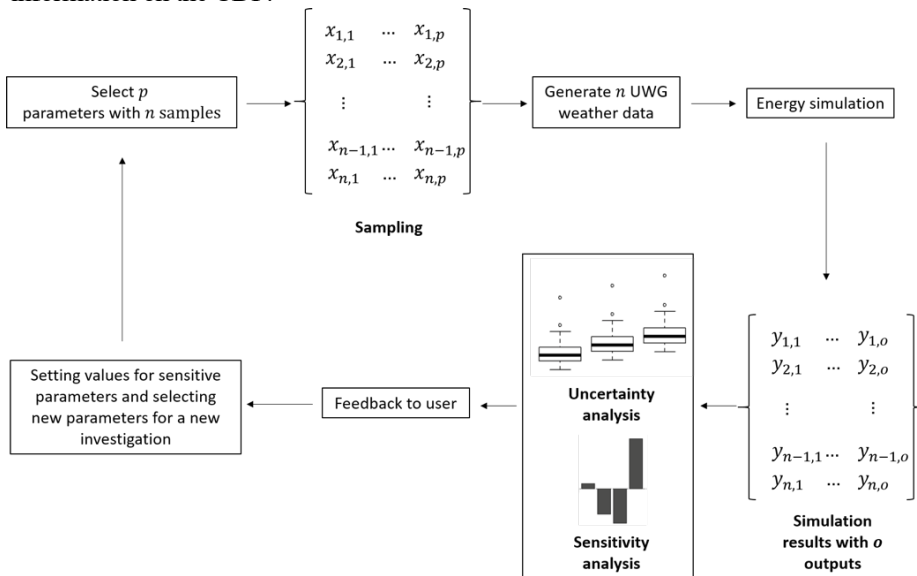


Figure 1: The Monte Carlo based sensitivity and uncertainty analysis

The different steps of the iterative method are summarized in Figure 1. In the first step, UWG parameters (p) that need to be investigated can be either set manually by the CDP user or general parameters are selected. In the next step, a sample matrix is generated through random sampling of the parameters in a pre-defined range. The

sampling in this paper is performed through quasi-random samples generated through Sobol's algorithm (Sobol and Levitan, 1999). The matrix size is the multiplication of the number of samples (n) and the number of parameters (p). Through the sampled parameters n weather data is morphed for the investigated urban district. The simulations and generation of the morphed weather data are performed through UWG Python Application Programming Interface (API) which is part of Ladybug tools (Ladybug Tools, 2021). The UWG tool is also implemented in practical component based tools (e.g. Dragonfly (Ladybug Tools, 2021)) but for the results of this paper the original code was utilized to enable multiprocessing through the Python API. The simulated weather data are used in a building energy model (BEM) in Honeybee (Sadeghipour and Pak, 2013). The outputs from the BEM simulation build the basis for the UA and SA. In the proposed method, different output parameters (o) can be investigated. Furthermore, the UHI calculated by the morphed weather data can also be utilized for the SA and UA, which is out of the scope of this study. Through the results, the decision-makers can define values for the sensitive parameters and iterate the process with more detailed parameters.

3. Case study

The approach is investigated in a current urban district in Kempten, Germany. The district is planned to undergo densification and refurbishment of the current stock. The proposed approach aims to aid decision-makers in integrating microclimate performance into their design process. For the BEM simulations, Ladybug with Energy Plus backend was utilized. One of the current buildings was modelled for the investigation. Surrounding buildings and shadowing effects were excluded, as the procedure aims to only investigate the influence of the morphed weather data on the energy performance and quantify the uncertainties. The BEM is a multi-zone model and its geometry is illustrated in Figure 2. Three different constructions were analysed in our investigation, which are based on German standards GEG, KfW 55, and KfW 40. The U-values of the standards are summarized in Table 1. The output of the simulations is the net cooling and heating demand and overheating degree hours. As the investigated building is a multi-zone model, the zone with the highest overheating degree hours was selected for the results. The simulation boundaries were set based on the (DIN V 18599-10:2018-09, 2018) standard.

General urban parameters were selected for the UWG simulation. The selected parameters and the corresponding mean and standard deviation (std) are summarized in Table 2, the more detailed description of the variables is available in (Ladybug Tools, 2021). The broad range of the parameters aims to give the decision-makers feedback in the first design iteration. The sample size (n) for the input parameters was set to 100 based on previous research on Monte Carlo techniques in building simulations (Macdonald, 2009).

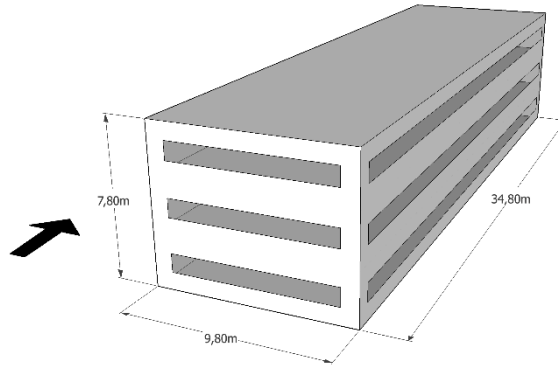


Figure 2: Investigated BEM located in Kempen, Germany

Energy standard	Base [W/m ² k]	Wall [W/m ² k]	Roof [W/m ² k]	Window [W/m ² k]
GEG	0.3	0.24	0.20	1.10
KfW 55	0.25	0.20	0.14	0.90
KfW 40	0.19	0.15	0.11	0.70

Table 1: Investigated energy standards and the corresponding surface U-values. The solar heat gain coefficient (SHGC) is set to 0.85 for all the investigated standards

Property	Description	Mean	Std
blddensity	Building footprint to urban area ratio	0.30	0.23
treecover	Tree coverage to urban area ratio	0.30	0.23
grasscover	Grass coverage to urban area ratio	0.30	0.23
albwall	Building albedo	0.50	0.23
glzr	Glazing ratio	0.50	0.23
vegroof	Roof vegetation coverage	0.50	0.23
albroof	Roof albedo	0.50	0.23
lattree	Fraction of latent heat absorbed by urban trees	0.50	0.23
latgrss	Fraction of latent heat absorbed by urban grass	0.50	0.23
albveg	Vegetation albedo	0.50	0.23
vertohor	Façade to urban site ratio	0.50	0.23
bldheight	Average building height [m]	17.50	7.20

Table 2: Investigated UWG input parameters (Ladybug Tools, 2021) and their mean, standard deviation after Sobol's sampling

The rural climate data were generated through the Meteonorm software (Remund et al., 2020). The moderate scenario Representative Concentration Pathway (RCP) 4.5 was selected for the two climate years 2020 and 2070. The selection of the climate years is based on the building's Reference Service Life (RSL) of the usage stage. The rural climate for Kempten builds the basis for generating the morphed weather data through UWG.

4. Results

4.1. UNCERTAINTY ANALYSIS

The simulation results for net heating and cooling demand, and overheating degree hours of the three construction standards are summarized in Figure 3 for the two years of 2020, and 2070. The uncertainty of the results is due to the 100 generated weather data through UWG. The simulation results demonstrate that the heating demand, and overheating degree hours as an index for thermal comfort are more robust to the generated weather data compared to cooling demand in our investigation. Furthermore, through only adapting higher energy standards the results do not get more robust. This shows the high impact of the microclimate situation on the investigated building.

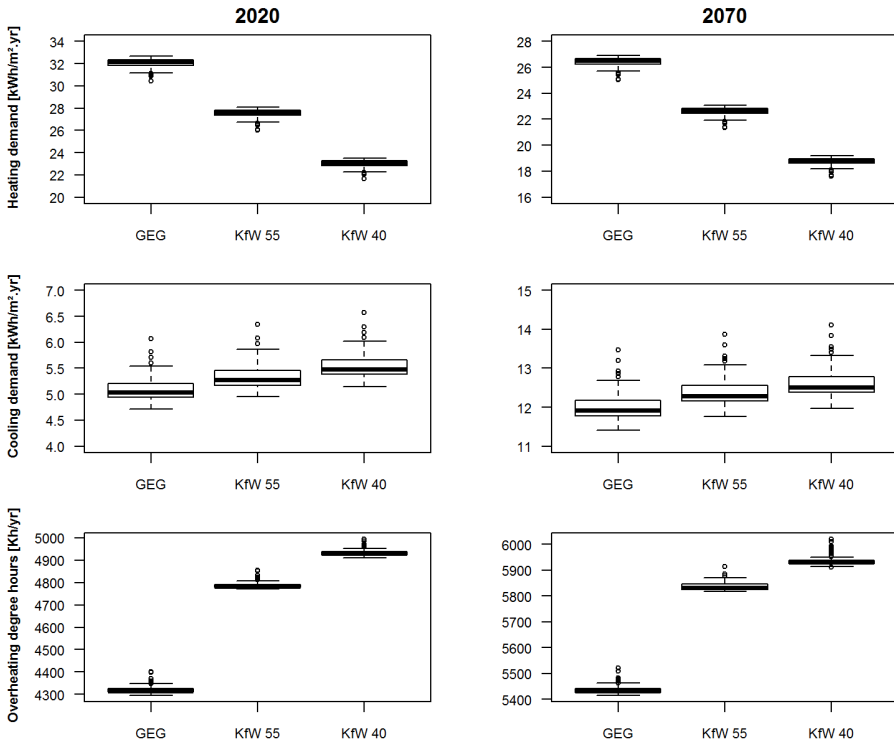


Figure 3. Net heating and cooling demand, and overheating degree hours of the three energy standards in the year 2020 and 2070

Comparing the simulations of the year 2020 and 2070 shows that the heating demand of the building will decrease due to climate change. However, the increase of the potential cooling demand especially in higher energy standards shows the requirement for climate adaptation measures.

4.2. SENSITIVITY ANALYSIS

Based on the results of the uncertainty analysis we investigated the sensitivity of the UWG input parameters on the cooling demand of the building. The selection of the SA technique is crucial, and the method should be selected carefully. Our investigation analysed correlation-based SA through Spearman's rank correlation coefficient (Spearman's rho) utilizing the Sensitivity package in R (Iooss et al., 2021). The sensitivity analysis was performed for both investigated years and the results are demonstrated in Figure 4. The SA shows that the building density in the urban district has the highest positive correlation to cooling demand in both years. This means that higher densities lead to an increase in the potential cooling demand due to the UHI effect. Tree and grass coverage decrease this negative impact on the cooling demand. The findings that these parameters have a significant influence on the cooling demand are consistent with previous research (Nakano et al., 2015).

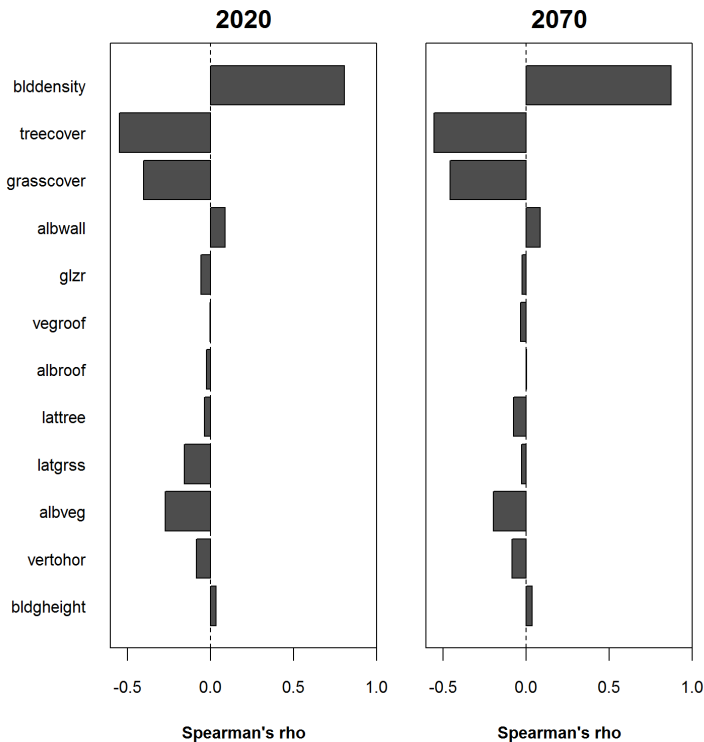


Figure 4. Sensitivity of different input parameters of UWG on the net cooling demand in the year 2020 and 2070 based on Spearman's rank correlation coefficient (Spearman's rho)

Comparing the SA for the climate years 2020 and 2070 demonstrates that the major sensitive parameters were consistent. The other input parameters investigated through the SA need to be reconsidered after defining the significant ones. As the SA coefficients are smaller compared to the three major ones. In this step, the decision-makers get feedback on these parameters on the CDP. After defining concrete values for the significant parameters, the process of UA/SA with other more detailed parameters should be iterated.

5. Discussion

The application of the method in the case study showed the significant influence of the microclimate on the energy performance of the building, especially the potential net cooling demand. The majority of residential buildings in Germany are not equipped with active cooling systems. Hence, climate adaptation measures both on the building itself and its surrounding should be considered to avoid the requirement for a mechanical cooling system. This requires a holistic approach considering both the building and its surroundings. Consequently, an optimization based on the energy performance of the building, indoor and outdoor comfort should be carried out to find the best fitting solution.

The results demonstrated that in a first iteration of the method building density, tree and grass coverage of the urban district had the highest sensitivity regarding the cooling demand. However, the effects are just based on the morphed UWG weather data. The limitation of our work is that the shadowing effect of higher building density or tree coverage on the energy performance of the BEM was not investigated. Furthermore, a more detailed investigation is required that allows parameter changes both in UWG and BEM. For instance, changing the albedo value of the buildings requires modification in both the BEM and UWG models. Another limitation of our approach is that the consideration of evapotranspiration effects in UWG is limited to the outside temperature. This could be addressed by using the recently developed Vertical City Weather Generator (VCWG) (Moradi et al., 2022). The same approach can be utilized by the VCWG tool to get more robust results considering the evapotranspiration effects.

6. Conclusion and future work

In this paper, we introduced a workflow for investigating the influence of different building and outdoor parameters on the energy performance and indoor comfort of buildings in the early design stages of urban districts through a Monte Carlo based SA and UA. The methodology was tested on a case study in Kempten, Germany. The results showed the importance of building density and green infrastructure in the first iteration of the design.

This study aimed to implement the insights and the approach in CDP. The microclimate simulations through UWG are not computationally expensive. However, the interdependence on building energy simulation and the UWG computation hinders real-time feedback to the decision-makers on the CDP. For future work, we aim to train a surrogate or meta-model of the BEM based on the microclimatic insights to deliver real-time simulation results. The meta-model will be based on different building

parameters and variables from the surrounding environment. With this approach, a coupled simulation of building and the microclimate should be feasible.

Acknowledgements

This work was carried out within the research project 'Densification in the Context of Climate Change', funded by Bavarian State Ministry of the Environment and Consumer Protection (StMUV) and the TUM Centre for Urban Ecology and Climate Adaptation (ZSK).

References

- Bande, L., Afshari, A., Al Masri, D., Jha, M., Norford, L., Tsoupos, A., Marpu, P., Pasha, Y., Armstrong, P. (2019). Validation of UWG and ENVI-met models in an Abu Dhabi District, based on site measurements. *Sustainability*, 11(16), 4378. <https://doi.org/10.3390/su11164378>.
- Bueno, B., Norford, L., Hidalgo, J., Pigeon, G. (2013). The urban weather generator. *Journal of Building Performance Simulation*, 6(4), 269-281. <https://doi.org/10.1080/19401493.2012.718797>.
- Bruse, M., & Fleer, H. (1998). Simulating surface-plant-air interactions inside urban environments with a three dimensional numerical model. *Environmental Modelling & Software*, 13(3/4), 373–384. [https://doi.org/10.1016/S1364-8152\(98\)00042-5](https://doi.org/10.1016/S1364-8152(98)00042-5).
- DIN V 18599-10:2018-09 (2018). *Calculation of the net, final and primary energy demand for heating, cooling, ventilation, domestic hot water and lighting –Part 10: Boundary conditions of use, climatic data*. <https://dx.doi.org/10.31030/2874317>.
- Iooss, B. et al. (2021, December 20). *sensitivity: Global Sensitivity Analysis of Model Outputs*. Retrieved December 20, 2021, <https://CRAN.R-project.org/package=sensitivity>.
- Ladybug Tools (2021, December 20). *uwg's documentation*. Retrieved December 20, 2021, from <https://www.ladybug.tools/uwg/docs/>.
- Macdonald, I.A. (2009). Comparison of sampling techniques on the performance of Monte Carlo based sensitivity analysis. In *11th Conference of International Building Performance Simulation Association, BS2009* (pp. 992-999).
- Mao, J., Yang, J.H., Afshari, A., Norford, L.K. (2017). Global sensitivity analysis of an urban microclimate system under uncertainty: Design and case study. *Building and Environment*, 124, 153-170. <https://doi.org/10.1016/j.buildenv.2017.08.011>.
- Moradi, M., Krayenhoff, E.S., Aliabadi, A.A. (2022). A comprehensive indoor–outdoor urban climate model with hydrology: The Vertical City Weather Generator (VCWG v2.0.0). *Building and Environment*, 207 Part B, 108406. <https://doi.org/10.1016/j.buildenv.2021.108406>.
- Nakano, A., Bueno, B., Norford, L., Reinhart, C. F. (2015). Urban weather generator – a novel workflow for integrating urban heat island effect within urban design process. In *14th Conference of International Building Performance Simulation Association, BS2015* (pp. 1901-1908).
- Reinhart, C., Dogan, T., Jakubiec, J., Rakha, T., & Sang, A. (2013). UMI - An urban simulation environment for building energy use, daylighting and walkability. In *13th Conference of International Building Performance Simulation Association, BS2013* (pp. 476-483).
- Remund, J., Müller, S., Schmutz, M., Graf, P. (2020). Meteororm Version 8. In *37th European Photovoltaic Solar Energy Conference and Exhibition, EU PVSEC 2020* (pp. 1466-1467).

- Sadeghipour Roudsari, M., Pak, M. (2013). Ladybug: a parametric environmental plugin for grasshopper to help designers create an environmentally-conscious design. In *13th Conference of International Building Performance Simulation Association, BS2013* (pp. 3128-3135).
- Sobol, I.M., Levitan, Y.L. (1999). A pseudo-random number generator for personal computers. *Computers & Mathematics with Applications*, 37(4-5), 33-40.
[https://doi.org/10.1016/S0898-1221\(99\)00057-7](https://doi.org/10.1016/S0898-1221(99)00057-7).
- Schubert, G. (2021). *Interaction forms for digital design: a concept and prototype for a computer-aided design platform for urban architectural design scenarios*. Dissertation. Technical University of Munich, Munich. <https://dx.doi.org/10.14459/2021md1610329>.

AD-BASED SURROGATE MODELS FOR SIMULATION AND OPTIMIZATION OF LARGE URBAN AREAS

GONÇALO ARAÚJO¹, LUÍS SANTOS², ANTÓNIO LEITÃO³ and RICARDO GOMES⁴

^{1,4} *IN+, Técnico Lisboa*

² *Dept. of Architecture, Design and Media Technology, Aalborg Un.*

³ *INESC-ID, Técnico Lisboa*

¹*goncalo.r.araujo@tecnico.ulisboa.pt, 0000-0002-0643-8113*

²*lfds@create.aau.dk, 0000-0002-2664-4301*

³*antonio.menezes.leitao@tecnico.ulisboa.pt, 0000-0001-7216-4934*

⁴*ricardo.a.gomes@tecnico.ulisboa.pt, 0000-0003-2180-2339*

Abstract. Urban Building Energy Model (UBEM) approaches help analyze the energy performance of urban areas and predict the impact of different retrofit strategies. However, UBEM approaches require a high level of expertise and entail time-consuming simulations. These limitations hinder their successful application in designing and planning urban areas and supporting the city policy-making sector. Hence, it is necessary to investigate alternatives that are easy-to-use, automated, and fast. Surrogate models have been recently used to address UBEM limitations; however, they are case-specific and only work properly within specific parameter boundaries. We propose a new surrogate modeling approach to predict the energy performance of urban areas by integrating Algorithmic Design, UBEM, and Machine Learning. Our approach can automatically model and simulate thousands of building archetypes and create a broad surrogate model capable of quickly predicting annual energy profiles of large urban areas. We evaluated our approach by applying it to a case study located in Lisbon, Portugal, where we compare its use in model-based optimization routines against conventional UBEM approaches. Results show that our approach delivers predictions with acceptable accuracy at a much faster rate.

Keywords. Urban Building Energy Modelling; Algorithmic Design; Machine Learning in Architecture; Optimization of Urban Areas; SDG 7; SDG 12; SDG 13.

1. Introduction

To face the challenges and threats posed by climate change, large efforts and funds are being deployed to reduce carbon emissions and energy consumption worldwide (United Nations, 2020). The operation of a large part of the building stock is still

energy-intensive and a cause of anthropogenic carbon emissions that actively contribute to climate change (United Nations, 2018). This motivates building retrofits in consolidated urban territories to meet the sustainable development goals set by the current political agenda (European Commission, 2020). Particularly, to reduce the energy consumption of our building stock, we need to assess its performance through building energy simulation. However, these typically require expertise and become slow when analyzing numerous buildings. These limitations hinder the analysis of large urban areas that is critical to support the design and planning of cities, and the city policy-making sector (Reinhart & Cerezo Davila, 2016).

Current practices use Urban Building Energy Modeling (UBEM) approaches to address this pressing issue (Ferrando et al., 2020). However, these approaches still require a high level of expertise and the process is still time-consuming, error-prone, and tiresome (Chen et al., 2017). Thus, it is crucial to make these approaches simple-to-use, more automated, and faster.

Previous attempts to reduce the computational cost of large numbers of simulations involved surrogate models developed with machine learning techniques. A surrogate model is constructed using data-driven approaches and reproduces the behavior of a simulation model while being computationally cheaper to evaluate. Such models have been used to predict building simulation outputs such as building carbon emissions (Thrampoulidis et al., 2021), energy consumption (Bamdad et al., 2020), and daylighting (Wortmann et al., 2015). They are trained with a simulated case study dataset and substantially improve simulation run-time, deliver faster and accurate results, and promote a smoother integration with current digital design workflows. However, such models are usually case-specific and can present errors when applied to cases that are outside the boundaries of the training data. Such limitation can cause problems while using the surrogate to analyze large urban areas with a diverse building stock (Thrampoulidis et al., 2021).

To address these limitations, we propose the integration of Algorithmic Design and Analysis (ADA) (Aguiar et al., 2017) in the creation of more versatile surrogate models for urban analyses. We use algorithmically modeled building archetypes based on city-specific building properties rather than context-specific data commonly used in UBEM surrogates. This approach allows a broader use of surrogate models for larger urban areas and mitigates the case-specific limitations in the usage of such approaches.

Algorithmic Design (AD) allows us to generate buildings through algorithms (Caetano et al., 2020) and when combined with simulation analysis - ADA - we can automatically model and simulate thousands of design variations. Thus, our approach used ADA to generate and simulate many instances of parametric building archetypes. With the results, we compile a training set and test multiple regression models to build a surrogate that promptly predicts the performance of different urban settings depending on simpler inputs such as building geometry and constructions, and its accuracy and speed can be compared against conventional UBEM approaches.

2. Methodology

The core tool used in our approach was Khepri (Aguiar et al., 2017), a multi-platform AD tool that allows us to seamlessly integrate five different steps involved in the development and validation of our approach (Figure 1). The five steps are as follows: (1) import of the GIS dataset into a CAD platform; (2) model the defined building archetypes for the database and simulate them using EnergyPlus; (3) using the generated dataset to test multiple regression models available in the machine-learning library Sci-Kit Learn; (4) select the best-performant surrogate model to predict energy consumption; (5) apply it in a Multi-Objective Optimization (MOO) routine. To test the surrogate model approach in the optimization of large-scale urban retrofit scenarios, we compare its accuracy and speed with a model-based optimization supported by conventional UBEM simulations.

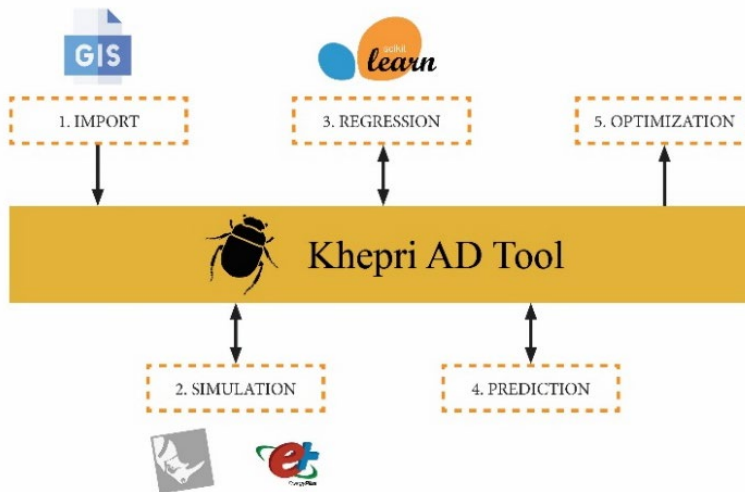


Figure 1. Workflow diagram illustrating the sequential stages of the research's methodology

2.1. CASE STUDY - IMPORT GIS DATASET

Through the analysis of a case study, we can define the domain of our surrogate model parameters and validate our approach. Figure 2 shows our building database, which contains data relative to 2193 residential buildings in Lisbon, Portugal. The city's residential buildings are characterized in Table 1 by 10 periods of construction, each with corresponding material (Santos & Matias, 2006) and retrofit solutions. Available information regarding the urban area, such as building implantation polygon, construction periods, floors, area, glazing ratio, and typology are all imported into our AD tool, and then automatically simulated in the simulation platform. This seamless integration allows us to automate all the subsequent steps of our approach.



Figure 2. Lisbon residential buildings from the dataset.

Table 1. U-values for each construction period in Lisbon.

Construction period	Wall U_Value (kWh/m ²)	Roof U_Value (W/m ² .°C)	Floor U_Value (W/m ² .°C)	Window U_Value (W/m ² .°C)	Wall retrofit U-value (W/m ² .°C)	Roof retrofit U-value (W/m ² .°C)
<1919	2.78	1.99	1.80	2.69	0.61	0.63
1919-1945	2.78	1.99	1.80	2.69	0.61	0.63
1946-1960	1.49	1.99	1.80	2.69	0.57	0.63
1961-1970	1.08	1.99	3.03	2.69	0.49	0.63
1971-1980	1.26	1.99	3.03	2.69	0.53	0.63
1981-1990	0.50	1.99	3.03	2.69	0.32	0.63
1991-1995	0.49	1.99	3.03	2.69	0.32	0.63
1996-2000	0.46	1.99	2.31	2.69	0.29	0.63
2001-2005	0.25	1.99	2.31	2.69	0.19	0.63
>2006	0.25	1.99	2.31	2.69	0.19	0.63

2.2. MODEL AND SIMULATION

In this step, we generate and simulate both the surrogate model and our UBEEM test dataset. With ADA, we set the inputs for the case study's building archetypes, which include multiple construction solutions and their possible retrofits. These archetypes represent our surrogate model's discrete parameters. In this case, we include all the construction periods and their possible retrofits (Table 1).

All the building archetypes are then modeled according to uniformly divided parameter domains such as the number of floors (from 2 to 11, step size = 3), rectangular proportion (from 1 to 5, step size = 2), orientation (from 0 to 180 degrees, where 0 is East, step size = $\pi/4$), glazing ratio (from 0 to 0.7, step size = 0.35), and floor area (from 50 to 800 m², step size = 75 m²). Figure 3 exemplifies some values of different parameters of one building archetype.

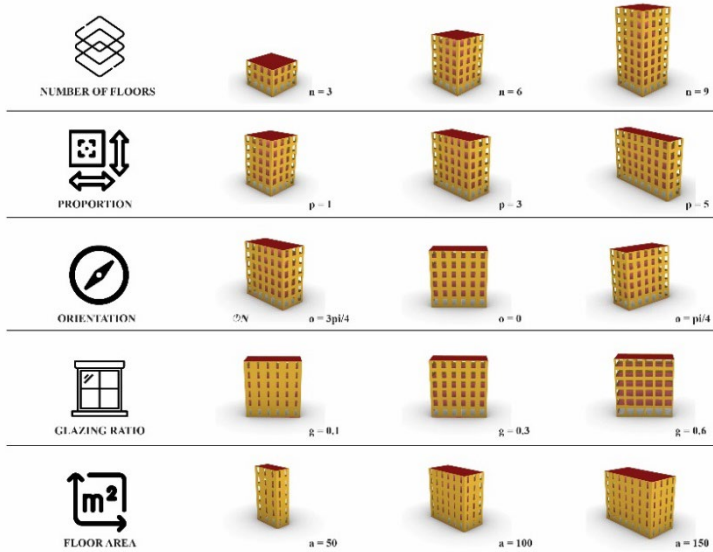


Figure 3. Parameters of a building archetype.

With all the parameters defined, we simulated our surrogate model, which due to the combination of values from different parameter domains, comprises more than 55000 different buildings. Table 2 describes the simulation settings used. The selected output was the required heating and cooling annual load (kWh/m^2).

Table 2. Simulation settings.

Timestep	ShadowCal	SolarDist/Reflex	Output timestep	Output	Context geo.
1	Polygon Clipping	Full exterior	Monthly	Annual loads	None

2.3. REGRESSION MODELS

In this stage, we extract simulation results from the AD tool to generate our training dataset. The dataset used to train our surrogate model comprises the simulation inputs and outputs of all the above-mentioned parameters.

The prediction of energy consumption in a building is a regression problem. Thus, we used different supervised learning models from the Sci-Kit learn package for Julia. From those, to find the most suitable model, we must (1) understand how the parameters affect energy consumption in a building (Araújo et al., 2021), and (2) test multiple models (Wolpert & Macready, 1997). Figure 4 shows interpolations of the energy needs (z-axis) according to our discrete (layers) and continuous (x- and y-axis) parameters step sizes. Since the interpolation graphs in Figure 4 show a polynomial behavior, we selected two linear models with polynomial features (Fan et al., 1995) of degree 3: Linear Regression, and Ridge. Additionally, we tested two ensemble regressors: RandomForest and ExtraTrees (Mendes-Moreira et al., 2012), which are also adequate for such regression problems.

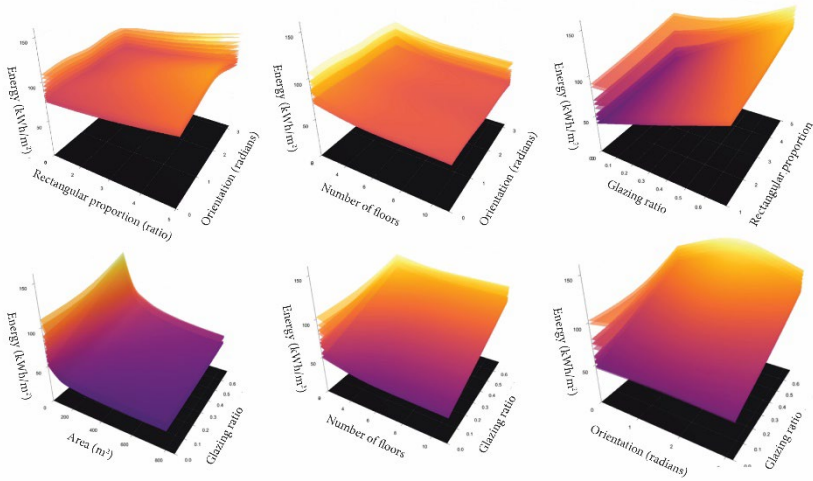


Figure 4. Heating and cooling needs (z-axis) of all the discrete parameters (represented as layers) for different continuous parameters in our dataset (x- and y-axis).

2.4. PREDICTION

After selecting our regression models, we fit them with the simulated dataset and compare our case study's UBEW with the predictions of the surrogate model. Figure 5 shows a histogram of the error, which measures the relative deviation of the surrogate's prediction from the simulated result for each building. From the figure, the best performing model appears to be the *Extra Trees regressor*, which presented the smaller error distribution of ± 10 kWh/m². However, the *Linear Regression* and *Ridge* models also show errors within the same interval. Thus to complement the error analysis, we used the statistical indexes presented in Table 3. They show that the Extra Trees regressor model is the most accurate, showing the best error results.

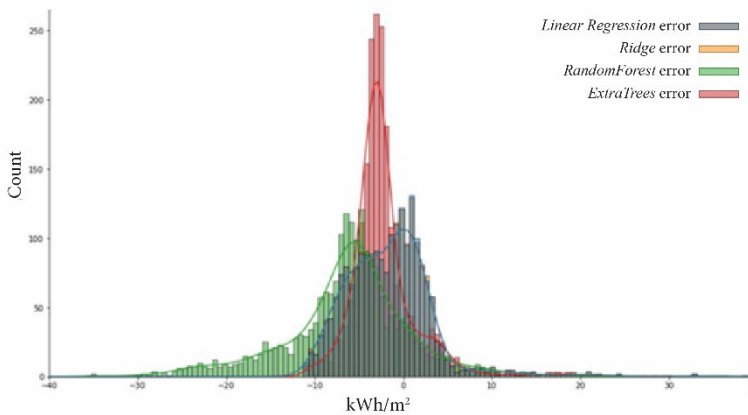


Figure 5. Histogram of the predictions error for each model.

Table 3. Regression model evaluation metrics

	Linear Regression	Ridge	Random Forest	Extra Trees
Mean Error (kWh/m ²)	15.85	15.79	-6.06	-2.21
Root Mean Squared Error (kWh/m ²)	15.40	15.40	9.88	5.44
R ² score	0.64	0.64	0.85	0.95

2.5. OPTIMIZATION

After selecting the *Extra Trees* regression model with the best score, we tested our surrogate approach in a MOO process on a subset of the case study; a block of 21 buildings illustrated in Figure 6. For the MOO we use the Pareto Genetic Algorithm NSGA-II, which analyzed 800 solutions spread out through 40 generations.

The goals were to find (1) the cheapest and (2) fairest retrofit solution for all buildings that (3) minimized annual heating and cooling loads, i.e.,

$$(1) \min \sum_{i=1}^n Cost_i, (2) \min \sigma(\text{annual loads}_i), (3) \min \sum_{i=1}^n \text{annual loads}_i,$$

Each building is represented as a variable with 4 options for its corresponding construction period: (1) no retrofit, (2) wall retrofit, (3) roof retrofit, and (4) wall and roof retrofit (Table 1). The defined objective functions for the optimization are intended to minimize annual loads (kWh/m²), cost (€), and standard deviation (σ) to ensure some homogeneity of performance among all buildings (Araújo et al., 2021).

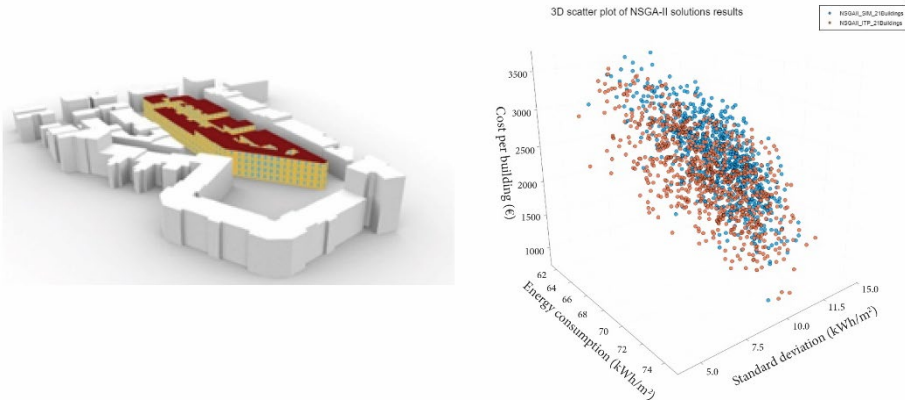


Figure 6. Building subset for optimization (left). Scatter plots of the solutions found in the optimization process (right), blue - conventional, orange - surrogate model optimization.

This MOO experiment used two methods: (1) a simulation-based approach that fully simulates each building block in each MOO evaluation, and (2) using our

surrogate model. The goal was to test the effectiveness of using our surrogate approach. The scatter plot in Figure 6 shows the existing trade-offs between the different objectives. One easily seen is that solutions that are more homogenous and have smaller energy consumptions entail more expensive renovations. Additionally, to validate the surrogate model in a MOO process, we computed the cosine similarity between each objective's results for both approaches. This is illustrated in table 4, showing high values of similarity, with the least similar being the cost objective with 0.96.

Table 4: Cosine similarity for each approach's objective.

	Energy Consumption	Standard deviation	Cost per building
Cosine similarity (-1 to 1)	0.99	0.98	0.96

3. Discussion

Table 3 and Figure 5 show high levels of accuracy for the simulation of the original case study in Lisbon of 2193 residential buildings (Figure 2). The model has shown a root mean squared error (RMSE) of 5.44 kWh/m², and a coefficient of determination (R²) score of 0.95, which explains the target results variance. Additionally, the larger error values come from extrapolations that the prediction model made outside the parameters' domain (e.g., areas of 2000 m² caused most of the outliers since the maximum simulated area for all archetypes was 800 m²). We can assert that the prediction is very accurate for buildings within the domain of the continuous parameters of our trained surrogate model.

Besides evaluating our model's accuracy, we performed a MOO process with both the surrogate and model-based approaches. Table 4 shows high levels of spatial similarity among the objectives of both approaches MOO process, while Table 5 compares both processes by showing the elapsed time for the simulation of our original case study in Lisbon, and for the MOO process with the 21 building subset from the case study.

Table 5: Elapsed time and obtained results for the full case study simulation and 21 building optimization processes. Simulations were performed using a CPU Intel I7-10700K.

	elapsed time (seconds)	
	Dataset simulation	Optimization
Surrogate model	0.08	791.99
Simulation	5820.00	67516.70

Table 5 shows that the surrogate model largely outperforms the simulation approach and the benefits obtained from model deployment with increased speed and low error rates among simulations. However, the time comparisons made in table 5, comprise only the end-user time to perform the simulation. Thus, it does not consider the time it took to prepare the dataset and train the model, nor the time to set up both

approaches. Admittedly, it takes more time to build the surrogate model than performing a simulation, but this time is quickly recovered when the surrogate is used to support numerous analyses.

Nevertheless, our approach bears some limitations. The simulation of the building archetypes does not account for shading and context geometry, which can hinder simulated and predicted results. Additionally, a low number of retrofits were added as discrete parameters, with only one retrofit for each wall and roof. In a situation where one must test multiple construction solutions, the surrogate model would take many discrete parameters, resulting in hundreds of thousands of buildings that need to be modeled and simulated, which would be highly time-consuming.

4. Conclusion

This paper presents a new surrogate model approach to quickly predict the annual heating and cooling loads of large numbers of buildings. The development and validation of our approach imparted five stages. First, we created parametric archetypal building energy models for a case study in Lisbon, Portugal. Then, we automatically modeled and simulated thousands of building archetypes. Subsequently, we utilized the simulation results to create a dataset used to fit regression models to predict simulation outputs according to the discrete and continuous parameters that defined the parametric archetypes. We select the best-performant regression model by testing its accuracy against the simulation results of our original case study in Lisbon with 2193 residential buildings. Finally, we test the effectiveness of our surrogate in a MOO that aimed to find the best retrofit solutions for a residential building block within the dataset. To that end, we compared optimization run-time of the same MOO process using our surrogate and simulation approaches. Results showed a significant decrease in optimization time for the developed surrogate. Thus, we conclude that developing surrogate models based on parametric archetypal buildings avoids the need of running expensive energy simulations and allows the surrogate model to easily adapt to other urban scenarios, opposed to those developed for specific urban areas.

Future improvements to the proposed approach will focus on outputs, accuracy, and user experience. Regarding outputs, we plan to test new metrics such as daylighting and thermal comfort. In terms of accuracy, we aim to extend the capabilities of our parametric building archetypes by including context shading, retrofit solution suites, building typologies (including commercial and office buildings), and different window types. Finally, to improve user experience, we plan to implement an easy-to-use Graphical User Interfaces (GUI) for practitioners, policy-makers, and homeowners to facilitate different urban energy analyzes.

Acknowledgments

This work was supported by international funds through Fundo Europeu de Desenvolvimento Regional (FEDER) with references POCI-01-0247-FEDER-045919, national funds through Fundação para a Ciência e a Tecnologia (FCT) with references UIDB/50021/2020, and PTDC/ART-DAQ/31061/2017, and PhD grant under contract of FCT 2021.04849.BD.

References

- Aguiar, R., Cardoso, C., & Leitão, A. (2017). Algorithmic design and analysis fusing disciplines. *Disciplines and Disruption - Proceedings Catalog of the 37th Annual Conference of the Association for Computer-Aided Design in Architecture, ACADIA 2017*, pp. 28–37.
- Araújo, G., Pereira, I., Leitão, A., & Correia Guedes, M. (2021). Conflicts in passive building performance: Retrofit and regulation of informal neighbourhoods. *Frontiers of Architectural Research*. <https://doi.org/10.1016/j.foar.2021.02.007>
- Bamdad, K., Cholette, M. E., & Bell, J. (2020). Building energy optimization using surrogate model and active sampling. *Journal of Building Performance Simulation*, 13(6), 760–776. <https://doi.org/10.1080/19401493.2020.1821094>
- Caetano, I., Santos, L., & Leitão, A. (2020). Computational design in architecture: Defining parametric, generative, and algorithmic design. *Frontiers of Architectural Research*, 9(2), 287–300. <https://doi.org/10.1016/j.foar.2019.12.008>
- Chen, Y., Hong, T., & Piette, M. A. (2017). Automatic generation and simulation of urban building energy models based on city datasets for city-scale building retrofit analysis. *Applied Energy*, 205(April), 323–335. <https://doi.org/10.1016/j.apenergy.2017.07.128>
- European Commission. (2020). *Proposed Mission: 100 Climate-neutral Cities by 2030 – by and for the Citizens*. <https://doi.org/10.2777/46063>
- Fan, J., Heckman, N. E., & Wand, M. P. (1995). Local polynomial kernel regression for generalized linear models and quasi-likelihood functions. *Journal of the American Statistical Association*, 90(429), 141–150. <https://doi.org/10.1080/01621459.1995.10476496>
- Ferrando, M., Causone, F., Hong, T., & Chen, Y. (2020). Urban building energy modeling (UBEM) tools: A state-of-the-art review of bottom-up physics-based approaches. *Sustainable Cities and Society*, 62, 102408. <https://doi.org/10.1016/j.scs.2020.102408>
- Mendes-Moreira, J., Soares, C., Jorge, A. M., & De Sousa, J. F. (2012). Ensemble approaches for regression: A survey. *ACM Computing Surveys*, 45(1). <https://doi.org/10.1145/2379776.2379786>
- Nations, U. (2020). *The Sustainable Development Goals*. In Design for Global Challenges and Goals. <https://doi.org/10.4324/9781003099680-3>
- Reinhart, C. F., & Cerezo Davila, C. (2016). Urban building energy modeling - A review of a nascent field. *Building and Environment*, 97, 196–202. <https://doi.org/10.1016/j.buildenv.2015.12.001>
- Santos, P. dos, & Matias, L. (2006). Coeficientes de Transmissão Térmica de Elementos da Envolvente dos Edifícios.
- Thrapoulidis, E., Mavromatidis, G., Lucchi, A., & Orehounig, K. (2021). A machine learning-based surrogate model to approximate optimal building retrofit solutions. *Applied Energy*, 281, 116024. <https://doi.org/10.1016/j.apenergy.2020.116024>
- United Nations. (2018). *The World's Cities in 2018*. In *The World's Cities in 2018 - Data Booklet (ST/ESA/SER.A/417)*. https://www.un.org/en/development/desa/population/publications/pdf/urbanization/the_worlds_cities_in_2018_data_booklet.pdf
- Wolpert, D. H., & Macready, W. G. (1997). No free lunch theorems for optimization. *IEEE Transactions on Evolutionary Computation*, 1(1), 67–82.
- Wortmann, T., Costa, A., Nannicini, G., & Schroepfer, T. (2015). Advantages of surrogate models for architectural design optimization. *Artificial Intelligence for Engineering Design, Analysis, and Manufacturing*, 29(4), 471–481. <https://doi.org/10.1017/S0890060415000451>

CLIMATE-DRIVEN ARCHITECTURAL DESIGN OPTIMIZATION AND EXPLORATION

A Reverse Passive Building Design Approach

TONG SHAO¹, LIKAI WANG² and GUOHUA JI³

^{1,3}*Nanjing University.*

²*National University of Singapore.*

¹*mg20360016@smail.nju.edu.cn, 0000-0002-5646-3376*

³*jgh@nju.edu.com, 0000-0003-3237-1263*

²*wang.likai@outlook.com, 0000-0003-4054-649X*

Abstract. This paper presents a reverse passive building design approach for sustainable architectural design based on the use of performance-based design optimization. The approach considers building massing and orientation, both of which are of great importance in passive building design, and combines the two factors in a design generation and optimization workflow in Rhino-Grasshopper. A case study based on SDE4 building in Singapore is conducted to demonstrate its capability of providing solutions and information about the trade-offs and interrelation between building massing and orientation with respect to the consideration of passive cooling and natural daylighting. The result shows that the approach can systematically explore a variety of building massing designs with different orientations and identify high-performing designs that outperform the existing one regarding the two performance objectives. The paper concludes by discussing its relevance in connecting performance-based design optimization research and architecture professionals.

Keywords. Passive Design; Performance-based Design; Building Massing; Orientation; Design Optimization; EvoMass; SDG 11.

1. Introduction

Passive design is an important topic in architecture, which has great potential in achieving sustainable and net-zero building design. In the book, *Design with Climate*, V. Olgyay (1963) emphasizes that the building design should begin with the climatic condition, utilizing passive methods to maximize the use of climatic and environmental resources and reduce the energy consumption of buildings. At the same time, there are many remarkable examples of applying passive strategies to building design, such as the Commerzbank tower designed by Norman Foster and Menara Mesiniaga by Ken Yeang. However, when designing a passive energy-saving building, most architects still primarily rely on empirical experience and conventional performance simulations,

which is insufficient to support a systematic design optimization and exploration. Thus, due to the technical and expertise barrier, it remains challenging for many architects to exploit the full potential of passive energy-saving strategies in architectural design.

In recent years, with the advance in computational design optimization, many studies have applied it to building design incorporating passive strategies, aiming to maximize the performance benefit of passive design. On the one hand, passive design problems related to materials and HVAC systems have been extensively investigated by many studies (Tian et al., 2018). Nevertheless, these design issues are mainly considered by mechanic engineers at later design stages and are hard to be integrated into the architectural form-finding or conceptual development process. On the other hand, there is, nevertheless, a great potential of using computational optimization in early-stage architectural design in terms of building forms and envelopes. For example, Caldas (2002) used computational optimization focusing on energy-saving in the design of Patio Houses. Wang et al. (2019) applied computational design to optimize and explore the shape of the courtyard for the enhancement of daylight accessibility.

When using computational design optimization in passive building design, the architect has to first decide the passive design strategy, such as courtyards and solar-envelope, and conduct the parametric modeling to encode the design strategy prior to the optimization is undertaken. Therefore, the optimization process often simply becomes a refinement of the selected design strategy, which is unlikely to help architects explore unknown design solutions beyond those encoded in the parametric model. Moreover, the optimization result could also be influenced by the designers' personal preferences, experiences, or design fixation.

Considering these limitations, a more systematic and comprehensive design exploration for passive design strategies can be a critical step in obtaining a more progressive building performance improvement. In response, we propose a reverse passive building design approach, which is based on EvoMass, a building massing design generation and optimization tool, and Ladybug in Rhino-Grasshopper. This approach leverages design generation and optimization capabilities in EvoMass to generate high-performing and site-specific building designs, which can reveal different passive design strategies related to passive cooling, natural daylighting, etc. Hence, the architect only needs to extract the architectural implications related to passive design strategies, such as courtyard, self-shading, and solar-envelope, and synthesize the strategy into the design. To demonstrate the efficacy of this design approach, this study presents a real-world example as a case study. The results show that this approach can provide architects with solutions and design information associated with passive design in the early design stage and help them make performance-informed decisions.

2. Method

The proposed reverse passive design approach is based on the use of computational design optimization. A similar *reverse design approach* has been proposed by Luca et al. (2021), which focuses on solar envelope buildings. Luca's approach, nevertheless, is developed for a specific type of passive building typologies, which limits its applicability for general passive building design. In response, this paper aims to provide a more flexible approach to passive building design by utilizing parametric design and computational optimization for finding suitable passive design strategies in various

specific design considerations.

The proposed design approach is based on the use of EvoMass, which can produce optimization results with diverse solutions that best satisfy the performance objective. The capability of generating diverse building massing forms makes EvoMass an ideal form-finding tool for performance-based building massing design optimization (Chen et al., 2022; Wang, Chen, et al., 2020b). In regards to passive design, building massing and orientation are two critical components that must be considered. This highlights a limitation in EvoMass: the orientation of the building massing generated by it cannot be changed. In this regard, this study emphasizes the combination of orientation and building massing in performance-based design optimization.

Unlike the common design optimization process, the reverse passive design approach does not require the architect to determine a specific passive design strategy before the optimization. The approach leverages the "genericity" in building massing design generation in EvoMass, which can produce solutions that reflect specific architectural implications related to the design condition and building performance objectives (Wang, Chen, et al., 2020a). More importantly, most of these implications are recognizable from the perspective of passive building design. By combining the change in orientation, the proposed design approach can help architects make informed design decisions about passive strategies at the early design stage. Figure 1 illustrates the design optimization workflow for the reverse passive design approach, which includes three components: design generation, evaluation, and optimization.

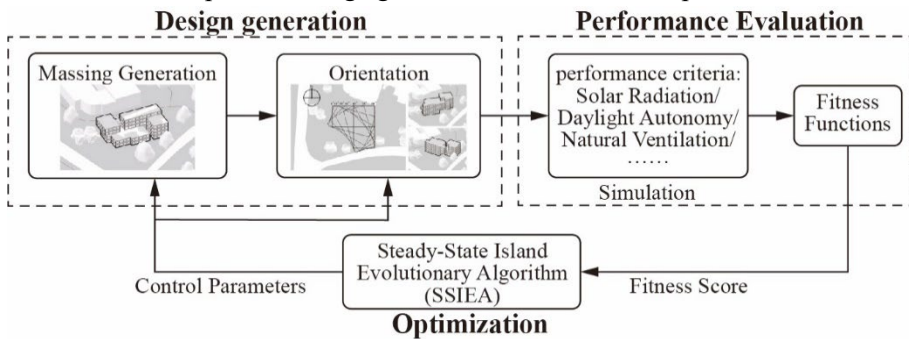


Figure 1. The proposed design generation and optimization workflow

First, the building massing is generated using the generative component in EvoMass. Evomass has two generative components, each generating building massing following the principle of subtractive or additive form generation (Wang, Chen, et al., 2020a). The building massing generated by the two components displays different formal characteristics. On the one hand, the additive component generates building massing by accumulating several mass elements. Thus, it tends to produce building massing with flexible topological configurations. On the other hand, the subtractive component generates building massing by removing several parts from a predefined volume, which can maintain the basic geometric volume in terms of the building form. EvoMass provides a set of user-defined parameters that allow the designer to adapt the generative component to different design conditions. These parameters include the size and number of the column-grid system, the floor numbers, etc. Hence, for the proposed

design approach, the designer only needs to define these parameters, and no additional programming or parametric modeling for building massing design is required.

As stated above, orientation is an important factor affecting building performance. Thus, the orientation is included as an additional parameter to the optimization workflow by rotating the building massing design generated by EvoMass. The rotation ranges and approaches can be tailored to the specific building site. In this study, the rotation step size is set at 15 degrees in order to reduce the search range. Additionally, to ensure the rotated building massing can stay within the plot boundary, different rotation strategies can be used. Figure 2 illustrates two approaches. The first approach rotates the building massing while keeping it aligning with the two boundary edges. In contrast, the second rotates the building massing based on its center point.

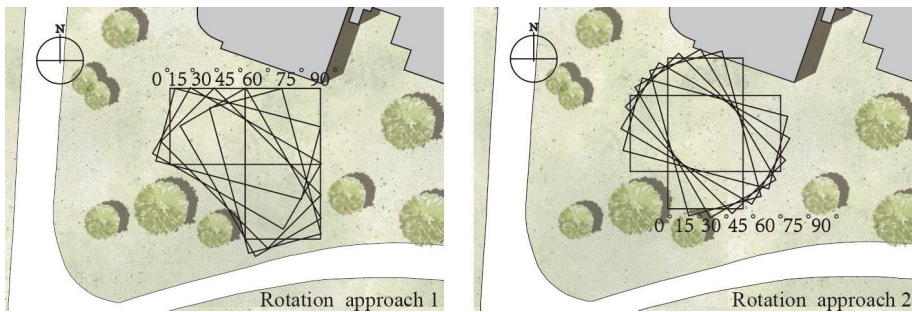


Figure 2. Two different rotation approaches to adjusting building orientation

The second step is the evaluation of the performance of the generated design, and according to the climatic condition of the given design task, different evaluation metrics can be connected to the design optimization workflow. For example, solar radiation can be used for passive heating, daylight autonomy for daylighting accessibility, natural ventilation for passive cooling, etc. In addition, as the proposed design approach is intended to provide clear information about passive design strategies, it is advisable to optimize only one or two performance factors. Otherwise, including too many factors could result in a mixture of design implications, making it difficult to distinguish the strategy in response to each of the performance factors.

The third and final step is optimization. After the simulation has been completed, a fitness score indicating the overall performance of the design is sent to the optimization algorithm, which will inform the creation of new control parameters in the subsequent optimization process. EvoMass provides an optimization algorithm called Steady-State Island Evolutionary Algorithm (SSIEA). SSIEA adopts a multi-island approach to subdivide the design population into several subpopulations and guides each subpopulation to focus on different regions in the design space, which prevents optimization from being stuck in a single region (Wang, Janssen, et al., 2020). Thus, SSIEA is able to provide optimization results with higher design diversity, thereby enhancing the design information feedback.

3. Case Study

To demonstrate the application of the reverse passive building design approach, a case

study is conducted where the SDE4 building in Singapore is selected as a reference, which is known for its energy efficiency (Zhou, 2019). By re-designing SDE4 using the proposed design approach, the existing building is used as a benchmark for evaluating the efficacy of the design approach (Figure 3).

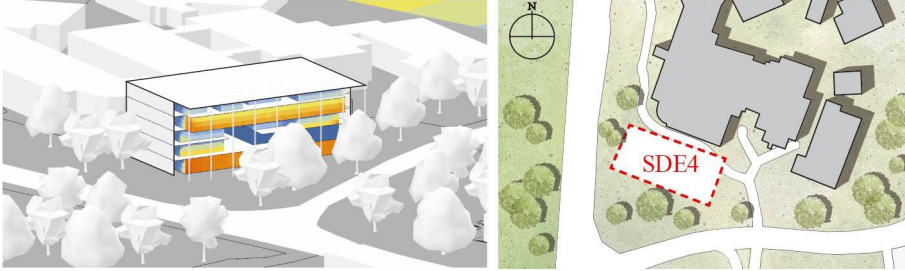


Figure 3. Case study design settings

Located in southeast Asia, Singapore has a tropical climate, which results in heavy annual cooling loads for buildings due to the intense solar exposure. SDE4 is an excellent example for tackling the overheating issue and is the first net-zero energy building in Singapore. Its design features a large overhanging roof and sunshades on the facades to protect the indoor space from excessive sunlight exposure (Zhou, 2019).

Considering the climatic condition, we first define the design objective to minimize the annual solar radiation (ASR) received by the facade surface of the building, which is simulated by Ladybug. However, minimizing solar heat gain can also decrease daylight accessibility. Hence, the spatial daylight autonomy (sDA) is also included in the optimization, which is simulated by ClimateStudio. Based on these two metrics, we first measure the performance of the SDE4 building, and the two corresponding values are 384,551 kWh (ASR) and 0.76 (sDA).

3.1. BUILDING DESIGN GENERATION AND OPTIMIZATION

The building massing design is created by the additive generative model in EvoMass. All parameters are set according to the dimensions of the SDE4 building. The major user-defined parameters are set as follows: 7 additive mass units, an 8 by 4 column-grid system in X and Y directions with an 8-meter column spacing, 7-floor levels with a 4-meter floor height, and a target area of 7500 meter². For the building orientation, we use the first rotation approach shown in Figure 2, since it has no collision with the preserved trees and other surrounding buildings. In addition, based on the selected rotation approach in Figure 2, we set the starting angle at 15 degrees, and the rotation ends at 90 degrees because 0 degrees is too close to one of the surrounding buildings.

The optimization objective includes minimizing the amount of ASR received by the surface of the building massing volume and maximizing daylight accessibility using sDA as the indicator. With these two objectives, Pareto optimization is used in this case study. The application of Pareto optimization is aimed to investigate the trade-off between the two design objectives. At the same time, as the Pareto approach will simultaneously optimize the two objectives, it is easier to understand how each design reflects these two aspects of performance.

In addition to the building performance, the gross floor area (GFA) of the generated building design is also included in the optimization as a soft constraint to guarantee that the design in the optimization result can meet the functional requirement. The additive generative model can automatically increase or decrease the overall volume of the generated building massing to make the actual GFA close to the target GFA, but this function may fail in certain extreme cases if the initial GFA difference is too significant. Thus, we formulate a penalty function for the soft constraint of GFA, which proportionally scales up the ASR value and scales down the sDA value. The final fitness evaluation functions for the two objectives are defined as follows:

$$Fitness_{sDA} = sDA \times \left(1 - \left| \frac{GFA_{actual} - GFA_{target}}{GFA_{target}} \right| \right)$$

$$Fitness_{ASR} = ASR \times \left(1 + \left| \frac{GFA_{actual} - GFA_{target}}{GFA_{target}} \right| \right)$$

where GFA_{actual} and GFA_{target} indicate the actual GFA of the generated building design and the target GFA.

For the setting of SSIEA, five subpopulations (islands) are set for the optimization process, each having 15 individuals. 80 generations are set as the termination criteria, and, finally, there are 2475 iterations of design generations and evaluations, which ensures that the design is sufficiently evolved.

4. Result

4.1. OPTIMIZED DESIGNS

Figure 4 shows the scatter diagram and histogram produced by using all the design individuals in the last generation, and we use the scatter diagram to represent the two-dimensional objective space. In comparison, most of the designs in the optimization result can outperform the existing one with respect to both performance objectives. Nevertheless, in real-world design projects, there are many other factors and constraints beyond daylighting and passive cooling that need to be taken into account. Thus, we acknowledged that the existing SDE4 building design may outperform the design in the optimization result in other aspects.

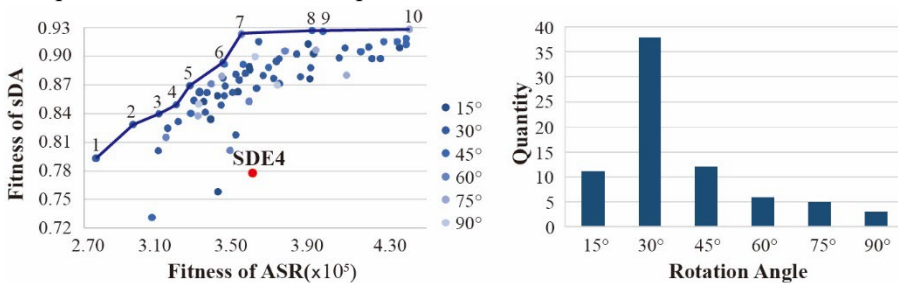


Figure 4. Analysis of the optimization result

The result also shows that orientation plays a critical role in determining the performance of the design. First, for buildings with 45-degree or 75-degree orientation, most of these designs are distributed in the upper-right region of the (performance)

objective space. This implies that the buildings with these two orientations are more conducive to achieving better daylight accessibility. Second, for buildings with a 60-degree orientation, most of them lie in the bottom-left of the objective space, implying that these designs are more capable of reducing solar radiation but incapable of achieving good daylighting quality. Third, 30-degree oriented designs are distributed across all parts of the objective space, indicating that the 30-degree orientation can incorporate different strategies that perform well when there is a need for good daylighting or lower solar radiation.

The histogram in Figure 4 shows the number of individuals with different orientations in the last generation. It is noticeable that about 50% of the designs are orientated at 30 degrees. Together with the fact that most of the 30-degree oriented designs are distributed across the Pareto front, it highlights that 30-degree is the most viable building orientation for this case study, and different passive design strategies can be incorporated to achieve various trade-offs between the two objectives.

Figure 5 presents all the designs on the Pareto front. These designs reflect the different passive strategies according to the trade-offs between the two objectives. As seen on the lower left of the Pareto front (the first row of Figure 5), the building massing is typically long and features large overhanging self-shading blocks to reduce the solar heat gain. For the upper right of the Pareto front (the second row of Figure 5), the daylight accessibility (sDA) of the design gradually increases, nevertheless, along with the increase in solar heat gain. As a result, the self-shading feature is replaced by narrow floor plans, sparse volumes, stepped/cascaded roofs, and courtyards to maximize daylight accessibility. In addition, it can also be noted that most of the building design keeps a certain distance away from the preserved tree to avoid context shading.

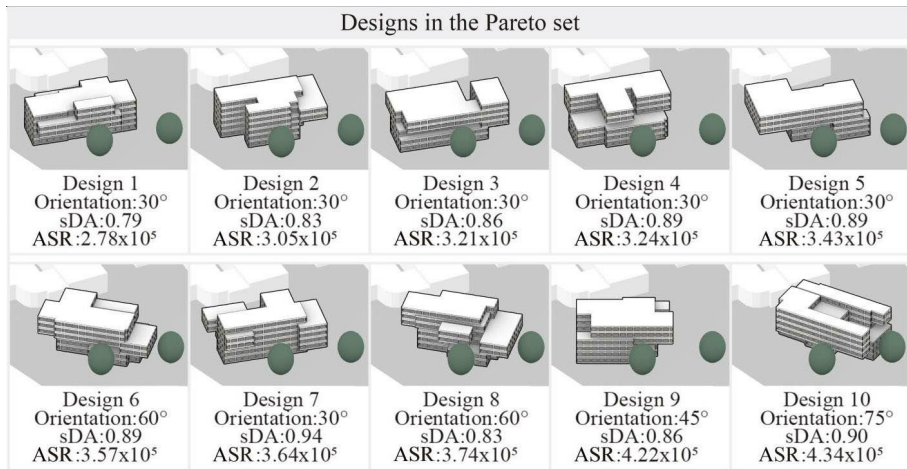


Figure 5. Designs in the Pareto set

4.2. FEATURES OF BUILDINGS WITH DIFFERENT ORIENTATIONS

To further investigate the interrelationship between building performance and the formal features of passive design strategies appearing in building designs with different orientations, we select five representative building designs with better performance

from the optimization results based on each orientation (Figure 6). By comparing the average ASR and sDA of the building in each direction, the building with a 30-degree orientation can achieve good compromise on both reducing ASR and increasing sDA, which further corroborates the conclusion drawn from the optimization result. In terms of daylight accessibility, the 45-degree oriented designs stand out, while it comes with an extremely high ASR.

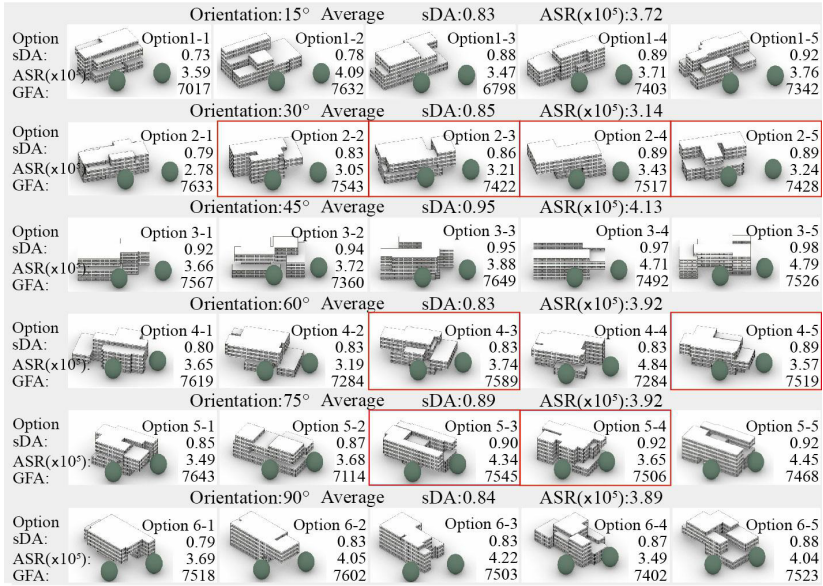


Figure 6. Selected designs with a high-fitness value (red boxes indicates the building design on the Pareto front)

For buildings with 15 and 30 and 60-degree orientations, a shared feature, as well as the underlying passive design strategy, is self-shading. First, building massings with 15 and 60-degree orientations typically consist of several small volumes, and the self-shading is mostly visible in the lower parts of the building. Hence, the effect of reducing ASR is trivial. Second, the building with a 30-degree orientation has a large overhanging roof, which has a better capability of reducing ASR than other designs do. At the same time, it can be noted that the design tends to have self-shading on its northwest and east sides. It is because the preserved tree in the south is close to the building, which helps reduce a certain amount of ASR on the south facade.

Buildings with 45-degree orientation are conducive to achieving better daylighting by incorporating two passive design strategies including narrow floor plans and large central courtyards. However, the additional facade area of the courtyard makes these designs typically have a higher ASR compared with those without a courtyard.

For buildings with 75-degree orientation, there are two major passive design strategies. The first strategy is the building design typically featuring a compact building massing volume, which results in a small facade surface area and shallow floor plan depth. With this strategy, the building can achieve lower ASR and higher sDA (Options 5-1 and 5-4). The second strategy is that the building massing elongates

along with its long axis. For this strategy, Options 5-3 and 5-5 display a wider depth in terms of the overall volume, with a central courtyard and stepped roofs, which increase daylight accessibility but are inefficient when it comes to reducing solar heat gain. In contrast, Option 5-2 has a narrow overall building massing volume in the short axis, which incorporates overhanging block to further decrease solar heat gain, but it is at the cost of relatively inferior daylighting.

For the 90-degree orientated building, there are also two different strategies appearing in these designs. The first one displays several small volumes, which enhances the daylight accessibility by increasing the façade surface area. The design with this strategy typically does not incorporate self-shading features, while due to the relatively small overall facade surface area, the solar heat gain tends to remain low (Options 6-4 and 6-5). The second strategy has a more solid and compact building massing volume and accompanies by a large self-shading block or a stilt ground floor, which results in a lower ASR but inferior daylighting (Options 6-1 and 6-2).

5. Conclusion and Discussion

The paper proposes a reverse passive design approach, which is intended to bridge the gap between the research of performance-based design optimization and architecture professionals. Based on our observation, despite the rapid development of performance-based design optimization over the past decade, there has been still little incentive for architects to apply this technique to routine design tasks. One reason accounting for this could be the lack of a connection between optimization and architects' design processes. The simple proof-of-concept building design displayed in many studies may hinder architects from fully understanding how this technique can be applied to more complex and ill-defined real-world design tasks and recognizing its potential in stimulating design creativity and innovation. Hence, using passive design to connect the two ends, this study offers architects a new opportunity to re-evaluate the potential of performance-based design optimization in architectural design, especially for sustainable and passive building design.

With the case study, the effectiveness of the proposed reverse passive design approach is demonstrated. By combining the variation of building massing design and orientations, the approach can provide architects with a rich diversity of task- and site-specific references for passive building design, which facilitates architects to understand the trade-off and interrelationship between passive design strategies and building orientations. More importantly, the approach also enables architects to perform a systematic exploration of passive building design, which can also effectively reduce human error and bias during the building design process. However, it should be highlighted that the proposed design approach only offers a set of preliminary building designs. Therefore, the approach is not intended to provide a solid and specific design solution or to replace architects' roles in design ideation and synthesis.

In regards to the utility of the approach, its application aims to encourage architects to leverage it in the early-stage design and synthesize the passive design strategy found in the optimization result in the process of design ideation and conceptual development. For example, architects can synthesize the passive design strategy with curved building shapes, which can not only make the final design more visually appealing but also can further strengthen the effectiveness of the passive design strategy (Wang et al., 2019).

In addition, the passive design strategy revealed by the optimization can also inform the design of other building elements, such as façades and spatial configurations. For instance, the self-shading feature can be transformed as external shading devices, while the optimization result can also inform architects' decisions about the type and disposition of shading devices.

Acknowledgements

This study is funded by China Postdoctoral Science Foundation (2021M701664) and National Natural Science Foundation of China (52178017).

References

- Caldas, L. G., & Norford, L. K. (2002). A design optimization tool based on a genetic algorithm. *Automation in Construction*, 11(2), 173–184. [https://doi.org/10.1016/S0926-5805\(00\)00096-0](https://doi.org/10.1016/S0926-5805(00)00096-0)
- Chen, Y., Lu, Y., Gu, T., Bian, Z., B. L. W., & Tong, Z. (2022). From Separation to Incorporation - A Full-Circle Application of Computational Approaches to Performance-Based Architectural Design. *Proceedings of the 2021 DigitalFUTURES* (pp. 189–198). <https://doi.org/10.1007/978-981-16-5983-6>
- Luca, F. De, Dogan, T., & Sepúlveda, A. (2021). Reverse solar envelope method . A new building form-finding method that can take regulatory frameworks into account. *Automation in Construction*, 123, 103518. <https://doi.org/10.1016/j.autcon.2020.103518>
- Olgay, V. (1963). Design with climate--bioclimatic approach to architectural regionalism: some chapters based on cooperative research with Aladar Olgay. *Princeton University*, Princeton.
- Tian, Z., Zhang, X., Jin, X., Zhou, X., Si, B., & Shi, X. (2018). Towards adoption of building energy simulation and optimization for passive building design: A survey and a review. *Energy and Buildings*, 158, 1306–1316. <https://doi.org/10.1016/j.enbuild.2017.11.022>
- Wang, L., Chen, K. W., Janssen, P., & Ji, G. (2020a). Algorithmic generation of architectural massing models for building design optimisation: Parametric modelling using subtractive and additive form generation principles. *RE: Anthropocene, Design in the Age of Humans - Proceedings of the 25th International Conference on Computer-Aided Architectural Design Research in Asia, CAADRIA 2020* (pp. 385–394).
- Wang, L., Chen, K. W., Janssen, P., & Ji, G. (2020b). Enabling optimisation-based exploration for building massing design: A coding-free evolutionary building massing design toolkit in rhino-grasshopper. *RE: Anthropocene, Design in the Age of Humans - Proceedings of the 25th International Conference on Computer-Aided Architectural Design Research in Asia, CAADRIA 2020* (pp. 255–264).
- Wang, L., Janssen, P., & Ji, G. (2020). SSIEA: a hybrid evolutionary algorithm for supporting conceptual architectural design. *Artificial Intelligence for Engineering Design, Analysis and Manufacturing*, 34(4), 458–476. <https://doi.org/10.1017/S0890060420000281>
- Wang, L., Janssen, P., & Ji, G. (2019). Progressive modelling for parametric design optimization. In T. F. M. Haeusler, M. A. Schnabel (Ed.), *Intelligent and Informed - Proceedings of the 24th International Conference on Computer-Aided Architectural Design Research in Asia, CAADRIA 2019* (pp. 383–392).
- Zhou, J. (2019). The challenges and opportunities to shift from Net Zero Energy Building to Net Zero Emission Building in a hot tropical climate in Singapore. *In Norwegian University of Science and Technology*, 5.

TACTILE OCEANS

Enabling Inclusive Access to Ocean Pools for Blind and Low Vision Communities

DAGMAR REINHARDT¹, LEONA HOLLOWAY², SUE SILVEIRA³
and NICOLE LARKIN⁴

¹The University of Sydney, ²Monash University, ³Macquarie University, ⁴Larkin Design

¹dagmar.reinhardt@sydney.edu.au, 0000-0003-0477-492X

²leona.holloway@monash.edu.au, 0000-0001-9200-5164

³sue.silveira@email.com, 0000-0003-3830-0140

⁴nlarkindesign@gmail.com, 0000-0001-5023-6650

Abstract. This research explores implementing computation to enhance access to ocean pool and marine landscapes for the inclusion of people who are blind or have low vision (BLV). Constructing reliable representations, explanations and descriptions can support interactions with objects and participation in activities, particularly in these ocean environments. We discuss the adoption of a series of computational design strategies to leverage the impact of recent scanning technologies in information transfer. The paper introduces a background to touch access and universal design. It presents a case study of aerial photogrammetry for an ocean pool in NSW, Australia, and presents multi-scalar workflows and processes across computational design and advanced fabrication methods, including a) photogrammetry through drone-flight on a macro-scale and 3D-scanning to establish data-sets; b) parametric design and scale adaptations; and c) 3D printing and robotic milling for touch access.

Keywords. Blind; Universal Design; Touch Access; Photogrammetry; 3D Printing; SDG 3; SDG 10; SDG 14.

1. Introduction

There are well over half a million people in Australia with vision loss, including over 65,000 who are blind (Vision 2020 Australia, 2010). With most vision loss related to age and an ageing population (Tong et al., 2015), the number of Australians who are blind or have low vision (BLV) is expected to grow rapidly in the coming years (Taylor et al., 2005). Blindness and low vision encompass a wide range of abilities and experiences, from total blindness to some usable vision; congenital blindness (from birth) compared with acquired blindness after gaining some visual experiences; photosensitivity versus the need for bright lighting; and tunnel vision versus peripheral vision. The commonalities are the barriers faced in accessing visual media, and

specifically any environment, including public and open places, spaces and landscapes.

Marine coastlines hold strong significance and value in many cultures, and a celebration of iconic beaches and landscapes lies at the heart of Australia's national beach culture. The coastal beaches, bays, rockpools and man-made ocean pools are natural resources and community assets that provide for individual recreation and health, and collective inhabitation and interaction (figure 1). However, environmental conditions such as temperatures, wind and tides, topographical changes, uneven walkways and other site-specific characteristics can make coastal landscapes and foreshores difficult to navigate for people with varying sets of abilities, including children or older adults. Specifically, BLV audiences require a different set of communication through braille and relief diagrams, which are rare in open public or natural environments. With better access description, equitable access to the open ocean could be provided. We argue that readily available computational data capture and digital fabrication methods enable multi-scale prototypes that provide information and narratives for diverse audiences. This aims to support integration and inclusion, and increasing knowledge for the dynamic coastal environments, in alignment with the UN Sustainable Development Goals (SDGs) for education (SDG 3), reduced inequality (SDG 10) and understanding of oceans (SDG 14).

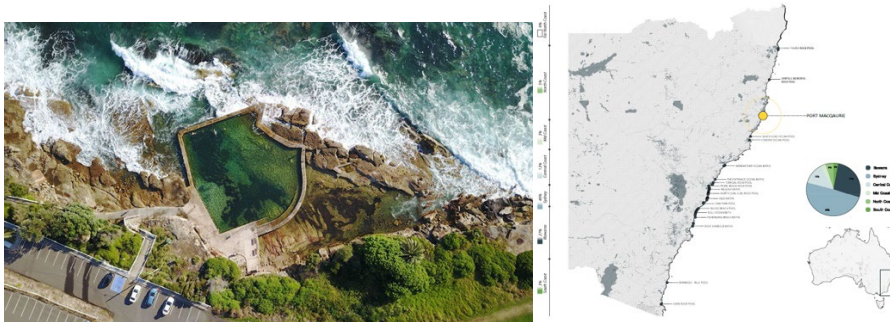


Figure 1. An aerial view of Malabar, NSW (left) and geographical distribution of ocean pools (right).

Constructing reliable representations, explanations and descriptions can support interactions with objects and participating in activities (Holloway, Butler and Marriott, 2018; Reinhardt, Sonne-Frederiksen & Christensen, 2019). Consequently, this research proposes an approach of multi-scalar methods to ocean pools for touch access and inclusion of BLV people and as engagement for all others. Based on a background to universal design, ocean pools and touch access, this paper provides a case study with development of workflows and processes across computational methods, including a) photogrammetry through drone-flight on a macro-scale and 3D-scanning to establish datasets; b) parametric and digital design; and c) 3D printing and robotic milling. The paper discusses results and concludes with an outlook towards future research.

1.1. UNIVERSAL ACCESS AND TOUCH ACCESS

In accordance with the UN Convention on the Rights for People with Disabilities (UN-DESA, 2006), the Australian Disability Discrimination Act states that 'a person with

disability has a right to have access to places used by the public' (Australian Human Rights Commission (AHRC), n.d.) and failing to provide such desired access is unlawful. However, people with BLV often face barriers to enjoying these experiences in an equitable way. Access to information and independent travel are amongst their greatest challenges. They may be excluded due to a lack of information on physical access or indirectly excluded from public open spaces (Siu, 2013). In contrast, Universal Access includes access to services, information and premises to encompass a complete experience (AHRC, n.d.). In this context, multimodal socio-technical systems and environments that situate tactile media as a fundamental mode of presentation can help overcome experiential barriers.

BLV audiences experience the world primarily through touch and sound, a first-hand experience that is invaluable in building up concepts of the world (Sapp, 2017). This provides a much richer and engaging experience than description alone. In particular, access by touch is essential for an understanding of spatial relationships (Millar, 1994) and material properties. However, touch access is limited to that which is within reach, is of an appropriate scale, and can be handled safely. The BLV person must also know that the object is available and where to find it (Siu, 2013).

While in infancy and school, BLV children are supported in concept development and tactile literacy through provision of story boxes, tactile graphics (also known as raised line drawings), and a variety of other tactually rich experiences. However, the same support is rarely extended to the workplace or public spaces. A notable exception is art galleries and museums, where new technologies are being harnessed to create tactile and multi-media artefacts for inclusion. As part of this work, researchers have created physical artefacts that are a suitable scale and safe to touch using new fabrication technologies such as 3D scanning, 3D printing, robotic milling and laser cutting (Reichinger et al., 2012; Scopignio et al., 2017). Similar strategies are required to provide accessibility by touch for other realms of culture and society, including the natural environment.

1.2. TACTILE MAPS AND 3D MEDIA

In providing accessibility measures for the natural environment, the ability to physically access the space is paramount. Tactile maps are of particular importance for independently building up a cognitive map of an area before visiting it, gaining an understanding of what is available, and where these features are located. Creation of 3D models is useful for tactile mapping, as 3D maps and maps with 3D icons have been found to be easier to understand than tactile graphics. Lastly, touch access begins to overcome the visual centrality that naturally exists while benefiting increased sensorial experiences for all users, including people who are fully sighted.

Meaningful touch access requires an appropriate scale that can be 'read' by a hand. Consequently, the research focuses on photogrammetry and 3D scanning for advanced manufacturing and fabrication, thus extending methods for image processing of landscapes (Arima and Sato, 1994), photogrammetry for heritage (Datta 2005) and other public databases (Lowe et al 2011), or texture maps to reconstruct real-world geometry (Alawadhi and Yan, 2018). Our research focus tests data to output, with comparison of fabrication processes (3D printing/CNC and robotic milling), with

future research investigating the details of the tools used in the research, libraries, image processing and scanning processes, and potential computing interfaces.

2. Methodology: Case Study, Ocean Pool and Coastline, NSW, Australia

Natural landscapes such as the NSW coastal line and ocean pools present environments that are complex and multi-layered. The research explores Malabar Ocean Pool as a case study using aerial photogrammetry. A prototype scale model is then created using computational design and fabrication for tactually communicating scale and spatial data and importantly, how to convey the rich and dynamic nature of coastal landscapes through touch.

2.1. LANDSCAPE SCALE: COASTAL TOPOGRAPHY

The geomorphology of coastal landscapes is shaped by natural processes and forces, often characterised by wandering rock platforms, spectacular headland formations and shifting sandy beaches. Tangible representations can provide effective information; however, this is not a matter of simple diagrams but requires mapping the landscape accurately and in a format that can be interpreted by designers, integrated in digital fabrication workflows, and reproduced through digital fabrication and manufacturing.

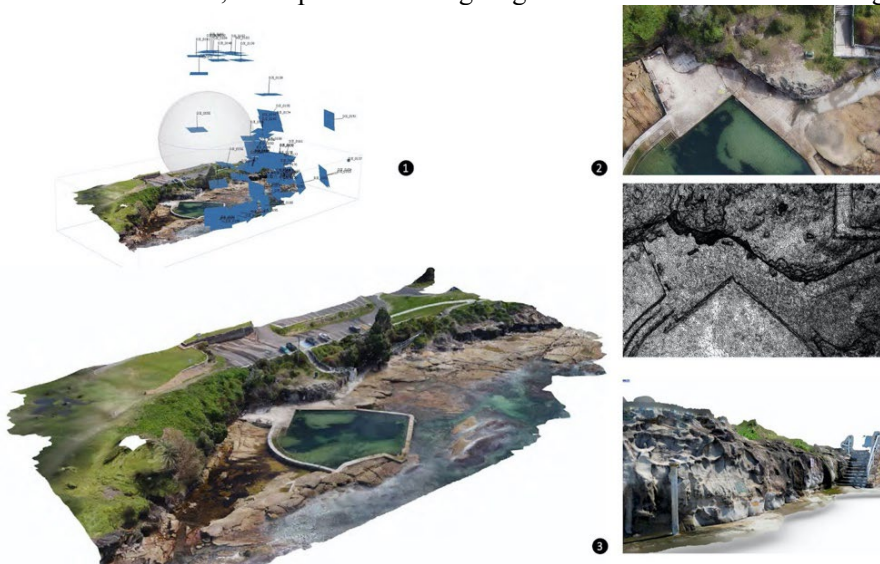


Figure 2. Data capture 2: Scans on environment-based scale. Aerial photogrammetry (drones, 1), overview of photo-based imagery and 3D mesh (2) and detail of rock surface (3).

Capturing such complex geometry through traditional, line of sight or laser-based survey methods would be challenging. This research therefore adopts aerial photogrammetry to efficiently retrieve data for a digital 3D model (figure 2) with photographs taken in a grid pattern, using UAV (DJI Mavic Pro) and software (Pix4D). Each image includes camera angle, GPS location and height, which supports triangulating points in space for mesh surface creation. While water movement and

light reflections pose a challenge to photogrammetry methods as they disturb data capture, calm surface conditions and sun position (oblique angle) allow capture of the pool and surrounding seabed. The resulting data are geospatially located and map immediate survey areas while also locating within broader regions, thus enabling practitioners to understand spatial information at micro and macro scales. The method accuracy captures a high level of detail including rock platforms, cliff under-crofts headland, beach, or surrounding context. The data and geospatial coordinate system were shared as an open-source platform (The Wild Edge).

Initial 3D prints were made (figure 3) but due to maximum dimensions accommodated by the 3D printer, the size and scale of the models limited their ability to communicate sufficient information to users, as touch offers far less resolution than vision (Grunwald, 2008; Hatwell, Streri and Gentaz, 2003). The limitation on size imposed by 3D printers innately reduces the information that a tactile map can convey as deviations, bumps and changes in texture are reduced in scale and less evident to the touch.



Figure 3. Malabar Ocean Pool | CNC milled timber model with benches and 3D prints (PVC)

A second prototype was CNC milled in timber (figure 3), which enabled a wider range of achievable finishes based on cutting tools but more importantly, fabrication at larger scale and higher level of detail. A ‘stepped’ or benched cutting method was adopted to permit users to run their hands continuously along edges, like contours on a map. Areas of the tactile map with many benches signal steep areas. A scale bar was designed to allow BLV users to identify lengths to measure distances and lengths with their hands. Further improvements could be made by enabling scale associations with recognizable objects (such as a car) and introducing secondary materials to distinguish key features (balustrades, hazards and water surface) through material differentiation (metal, ceramic or resin).

2.2. OBJECT SCALE: GEOGRAPHICAL STRATA AND PLANT SPECIES

Consecutively, the research moved from aerial photogrammetry on environment scale to an object scale, using an EinScan 3D scanner with structured light technology that casts light patterns onto an object. By analysing the edges of each line in the pattern, the distance from the scanner to the object’s surface is registered as a digital representation of the physical object by combining single dimension scans that are

captured at different angles. These scanning workflows and fabrication processes were shared with a group of designers for co-design of touch access objects and maps. In adopting 3D scanning and printing techniques, advanced CNC manufacturing and robotic fabrication for milled patterns and 3D upscaled prototypes, the research generated multi-scale prototypes, a tactile pattern archive and touch access objects including 3D objects, reliefs and mixed media tableaux that provide information and narratives for diverse audiences for inclusion and increasing awareness of the dynamic coastal environment.

Initially, different scripts enable a computational workflow from design data to manufacturing protocols. This included control over dot grids (as a braille translator); pixel grids and bitmap (for image conversion); and line tracing (for boundaries and shapes for direct use of scripted pattern description to tooling path) (figure 4). Different classes of scripts were developed in Grasshopper (GH, a visual scripting software) and robot programming in KUKA|prc (robot toolpath simulation) for a standard six-axis industrial robot arm. These supported the fabrication of test samples in beech, and the production of visual and tactile surfaces.

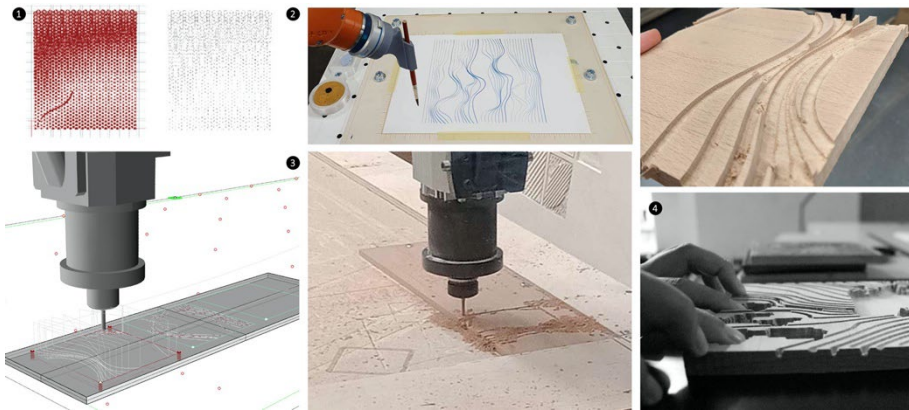


Figure 4. Script with pixilation for image conversion (1), trial of robotic milling path based on line codes through drawing (2) and transfer to milling (3), with manual testing of tactile proficiency (4).

A set of scripts controls the robotic toolpath, tool angle and standard industrial tools adopted for manufacturing (Dremel and router, with variability in tool dimension from 1.5-6-10mm drill bits). Codes are structured with sections pertaining to the generation of the robot targets, sections for creation and optimization of the robotic toolpath, and a final code section for export to robot fabrication and local database. Previous studies developed a pre-set scripts for the implementation of braille script into the robotic milling process (Reinhardt, Sonne-Frederiksen and Christensen, 2019), with a script translating braille text to uncontracted braille in accordance with Australian standards (Australian Braille Authority, 2020). The script integrated a common braille font into GH, so that text is directly translated into points that reference braille standards for cell and character, and a per line approach to situate words within a robotically milled surface with cavities where variable dimensions of ball bearings are inserted as raised braille dots. The workflow from scan to data to robotic fabrication was explored as a

series of scripts that derive meshes from a 3D scan, and then zoom into topographical lines of the upscaled object to convert this to a robot milling path. Figure 5 shows the first approach with robotic milling for touch access, with variability of pattern orientation and geometries, pattern types (module or path), grading and densities subtractive fabrication. The preliminary testing of the tactile plates clearly indicated that plates were more successful depending on the following factors: a) fine line engravings are readable only when drill lines correspond to finger dimensions; b) the higher the percentage of milled surface, the better the experience of touch, where higher contrasts in densities and height are better, and larger areas are better; and c) combined 3D prints (additive) and robotic milled (subtractive) techniques work best, as these produce recognizable changes in material, higher contrast, more detail and increased depth of the plate.



Figure 5 Sample collection of patterned texture that communicate botanical, geographical or marine data for touch access, including hybrid objects (subtractive/additive manufacturing coupled).

In a second development, the research investigation focused on the scale-up of details and zones, as opposed to the aerial photography model where scale is decreased to make the vast landscape tangible (figure 6). Studies included geographical strata of the cliff face, marine specimen including shells and fish species, and botanical samples with a high degree of detail (Banksia). Areas within the scanned objects' geometry were selected, enlarged and 3D printed relative to a hand scale, with testing in various sizes and positive or negative surface. The most successful prototypes were a) adequate in dimension to the fingertip; b) positive instead of negative, as cavities could not always be fully explored, and c) distinct in pattern as a repetition or high contrast. A cross section of models was distributed in Thingiverse for open sharing.

The engraved, deep patterns, embedded objects and tactile objects deliver information beyond simplified diagrams or pictorials of images, but convey physical phenomena, growth processes and dynamic formations that are an integral part of the landscape and natural environment, and thus form a detailed counterpart to the landscape topography discussed in the previous section. 'Hyper-artifacts' (Fuller and Watkins, 2010) is a term used to describe the integration of touch with an interpretive

information or underlying thematic. These hyper-artifacts are designed to be touched and handled by the audience and bring together people who are experts in vision (a common public) and experts in touch (BLV) so that they can together ‘decode’ or read data and information: as an inclusive design approach for multi-functional furniture that carries narratives in the form of images and text (braille), with the aim to provide shared objects for communities so that places we use become accessible and users with different abilities are comfortable, inspired and ‘feel’ a place that belongs to them.

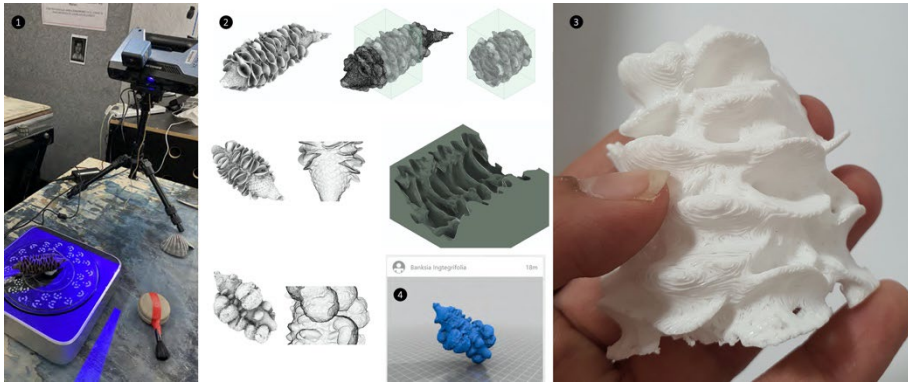


Figure 6. 3D scanning work process with botanical precedents (1), with conversion to pattern area selection and upscale (2), a 3D print of detailed area (3) and sharing the model in open platform (4)

3. Discussion

The prototypes discussed here highlight that 3D data can be successfully adopted across a range of subtractive and additive advanced manufacturing media (and combinations thereof) to provide tactile representations and information. The scalability of data is hereby of importance: as a readily available resource for designers to adapt prototypes to the size of a hand, making them tangible. As the case studies show, objects, signs and explanatory maps can be produced with relatively low effort, with commonly available media (3D print, CNC, robotic milling), in a direct workflow from aerial photogrammetry data or laser scan to fabrication. For this reason, designers used 3D data directly in McNeel Rhino, rather than image processing. Simplification via removal of redundant details is one of the basic design principles for effective tactile graphics (Edman, 1992). When using methods such as photogrammetry to produce 3D modelling, significant post-processing is required to remove 'noise' as a result of the modelling process and unwanted detail such as detailed vegetation on maps. As direct user feedback had been prevented by ongoing pandemic restrictions, future research will engage with BLV participants to further refine tactile content in the 3D objects.

With a focus on touch access, spatial mapping and access to environment, this work has been primarily aimed at people who are blind. While they may not use touch as their primary means of accessing information, people with low vision can also benefit from artefacts designed for touch access, as indeed can people who are fully sighted - this has been a common finding in studies of museums providing touch access. Nevertheless, future work should consider the addition of high contrast visual

enhancements on the touch models for greater ease of use by people with low vision.

The research explores the UN SDGs across several dimensions. In providing access for people with BLV in desirable and unique Australian marine environments, it contributes to SDG3 - 'Ensuring healthy lives and promote well-being for all at all ages' and SDG10 - 'Reducing inequalities and ensuring no one is left behind'. And for a wider population, it equally contributes with information to a better understanding of the resources of the natural environment, thus addressing a mixture of SDG4 – Education and SDG14: Oceans, enhancing an understanding thereof.

4. Conclusion and Future Work

The main contribution of this research is the adoption of data capturing and advanced manufacturing methods to enable touch access for BLV communities, with inclusion in and access to natural environments. The research has reported on leveraging aerial photogrammetry and 3D scans for computational data collection, design and advanced and robotic fabrication. Multi-scalar data and tactile representations of pathways, boundaries, marine and botanical information and narratives for audience engagement enable BLV communities to better inhabit and understand the inter-tidal landscape, and thus promote inclusion and sustainability for all communities.

The provision of tactile graphics has remained a domain of transcribers using a limited number of specialised techniques such as swell paper and braille embossers. This project demonstrates the potential of new modelling and fabrication technologies to greatly expand the tactile offerings available for people who are BLV, both in terms of richer materials and models, and provision beyond the classroom and into the natural environment. This project has been the impetus for specialists in fabrication technologies, vision impairment and accessible formats to share knowledge and collaborate. Future research will further explore digital scan and fabrication methods for access to the environment for people who are BLV and expand and implement research findings in real world applications to make practical contributions to accessibility, well-being and appreciation of natural environments.

Acknowledgements

This research has been developed in discussion with Nextsense, with Master students at the University of Sydney, and was produced at DMAf, USYD.

References

- Ah Tong, B., Duff, G., Mullen, G., and O'Neill, M. (2015). A snapshot of blindness and low vision services in Australia. In *Sydney: Vision 2020 and Australian Blindness Forum*.
- Alawadhi, M. and Yan, W. (2018) Geometry from 3D photogrammetry for building energy modeling. In *SIGraDi 2018*.
- Arima, T. and Sato, S. (1994). Form characteristics of landscape images: a landscape research by computer image processing. Second Design and Decision Support Systems, *Architecture & Urban Planning*, Vaals, the Netherlands
- Australian Braille Authority. (2020). *Physical specifications for braille*. Retrieved December 2021 from, <https://brailleaustralia.org/about-braille/physical-specifications-for-braille/>.

- Australian Human Rights Commission, (n.d.). *A brief guide to the Disability Discrimination Act*. Retrieved January 2022 from, <https://humanrights.gov.au/our-work/disability-rights/brief-guide-disability-discrimination-act>.
- Datta, S. (2005) On recovering the surface geometry of temple superstructures. In *Digital Opportunities: Proceedings of the 10th International Conference on Computer-Aided Architectural Design Research in Asia* (pp. 253-258). CAADRIA. New Delhi: Architexturez Imprints.
- Edman, P. K. (1992) *Tactile graphics*. Arlington, VA, USA: AFB Press.
- Fuller, R. and Watkins, W. (2010). Research on effective use of tactile exhibits with touch activated audio description for BLV. Bloomington, IN: Indiana University.
- Grunwald, M. (ed.) (2008) *Human haptic perception: Basics and applications*. Basel, Switzerland: Birkhäuser Verlag.
- Hatwell, Y, Streri, A. and Gentaz, E. (eds.), *Touching for knowing: cognitive psychology of haptic manual exploration*. Amsterdam: John Benjamins Publishing Company.
- Holloway, L., Butler, M., and Marriott, K. (2018) Accessible maps for the blind: comparing 3D printed models with tactile graphics. In *2018 CHI Conference on Human Factors in Computing Systems, Montréal, QC, Canada*.
- Lowe, R., Cromarty, J. and Goodwin, R. (2011) Real time modelling: a solution for accurate, updatable and real-time 3D modelling of as-built architecture. In *the Association for Computer-Aided Architectural Design Research in Asia*.
- Millar, S. (1994) *Understanding and representing space: Theory and evidence from studies with blind and sighted children*. New York, NY, USA: Clarendon Press.
- Reichinger, A., Neumuller, M., Rist, F., Maierhofer, S., and Purgathofer, W. (2012) 'Computer-aided design of tactile models', *International Conference on Computers Helping People with Special Needs*, Linz, Austria.
- Reinhardt, D., Sonne-Frederiksen, P. and Christensen, B. (2019) 'Robotic braille, Space and digital reality', 11.Sept 2019, *TAB19 Tallinn Biennale*, Estonia.
- Rowell, J., and Ungar, S. (2005) Feeling our way: tactile map user requirements - a survey, *ICA2005*, Coruña, Spain.
- Quero, L.C., Bartolomé, J.I., and Cho, J. (2021) Accessible visual artworks for blind and visually impaired people: comparing a multimodal approach with tactile graphics. *Electronics*, 10, 297.
- Sapp, W. (2017) Concept development in R. L. Pogrund, R.L. and Griffin-Shirley, N. (eds.), *Partners in O&M: supporting orientation and mobility for students*. New York, NY, USA: AFB Press, American Foundation for the Blind.
- Scopigno, R., Cignoni, P., Pietroni, N., Callieri, M. and Dellepiane, M. (2017) Digital fabrication for cultural heritage: a survey, *Computer Graphics Forum*, 36(1), 6-21.
- Siu, K.W.M. (2013) Accessible park environments and facilities for the visually impaired, *Facilities*, 31(13/14), 590-609.
- Taylor, H.R., Keeffe, J.E., Vu, H.T.V., Wang, J.J., Rochtchina, E., Pezzullo, M. and Mitchell, P. (2005) Vision loss in Australia. *The Medical Journal of Australia*, 182(11), p565-568.
- Ungar, S., Blades, M. and Spencer, C. (1993). The role of tactile maps in mobility training. *British Journal of Visual Impairment*, 11(2), 59-61.
- United Nations Department of Economic and Social Affairs (UN-DESA) (2006) Convention on the rights of persons with disabilities.
- Vision 2020 Australia (2010) *Clear focus: the economic impact of vision loss in Australia in 2009*. Melbourne, Australia
- Wright, T. S., Harris, B., and Sticken, E. (2010) A best evidence synthesis of research on orientation and mobility involving tactile maps and models. *Journal of Visual Impairment*, 104(2), 95-105.

QUANTIFICATION OF THE THERMAL ENVIRONMENTAL VALUE OF URBAN PORES

A Case Study of Nanjing

ZIHAO WU¹, YUNSONG ZHANG² and ZIYU TONG³

^{1,2,3}*School of Architecture and Urban Planning, Nanjing University.*

¹*zihawu1997@foxmail.com, 0000-0002-4951-5529*

²*1253167018@qq.com, 0000-0001-5246-6521*

³*tzy@nju.edu.cn, 0000-0002-5872-0890*

Abstract. The term “Urban pores” refers to the space formed by the enclosure of buildings, which have great value for regulating the microclimate. Many previous studies have focused only on a single urban pore section, ignoring the spatial distribution at the urban scale. In this study, the openness of urban pores in Nanjing was quantified and grouped, and then the spatial distribution characteristics of each openness group were further calculated. Based on this, the study combined the spatial distribution characteristics of urban pores with urban thermal environment data and an LCZ urban form classification model to analyse the impact of urban pores on the urban thermal environment. The results show that 1) the impact of urban pores is greater in summer and autumn, where its spatial agglomeration has a higher cooling value for the urban thermal environment, while this is not significant in winter; 2) the spatial agglomeration of urban pores in the high openness group, mid-high openness group and mid-low openness group have a higher cooling effect, which mainly corresponds to water, open spaces or parks and urban roads. These spaces should be given more attention when developing urban design strategies. The results can provide some references for urban development.

Keywords. Urban Pores; Openness; Spatial Distribution; Urban Thermal Environment; Local Climate Zone (LCZ); SDG 11; SDG 13.

1. Introduction

According to the IPCC’s Sixth Assessment Report, the global average land surface temperature has increased by approximately 1 °C over the past 100 years, and it is found that the temperature increase is expected to reach or exceed 1.5 °C in terms of the average temperature over the next 20 years. As the areas with the highest concentration of human activity, cities are facing a serious climate change challenge.

It is time to build a good urban microclimate environment through the construction of urban form to meet this challenge. In particular, the optimization of the thermal

environment will help improve people's comfort in the city and reduce the energy consumption of buildings. These efforts will further contribute to the achievement of the UN Sustainable Development Goals (SDGs), particularly SDG 11: Sustainable Cities and Communities and SDG 13: Climate Action.

A prerequisite for achieving this goal is to understand the impacts of the urban form on the thermal environment, which has been the focus of many previous studies (Guo et al., 2019, Yang et al., 2021). Among them, the urban pores formed by the enclosure of buildings are one of its most important components. At the neighbourhood scale, they are often referred to as street canyons or external spaces (Figure. 1.1 & 1.2). At the urban scale, urban pores can be approximated as a cluster of highly open external spaces (Figure. 1.3). Although there have been many studies analysing the impact of urban pores on regulating the microclimate at the neighbourhood scale (Lai et al., 2019), these are limited to the single urban pore section. Few studies have measured the impact of their spatial distribution on the thermal environment at the urban scale. It has proven that the distribution of urban pores, such as water, vegetation or forests (which can also actually be considered a type of urban pores) is quite important, since these pores' distribution have great cooling effects (Wang et al., 2019, Jiang et al., 2021). Based on this, it is also assumed that the overall spatial distribution of other types of urban pores, such as open spaces, parks or urban roads, will also impact the urban thermal environment. Therefore, this study aims to prove this idea through experiments, hoping to provide rational suggestions for urban design and further contribute to the achievement of the UN SDGs in our cities.



Figure 1. Schematic of Urban Pores

2. Methodology

This study aims to investigate the impact of the spatial distribution of urban pores on the urban thermal environment. Six key steps must be taken into consideration to achieve the objectives of the study. The first is to calculate urban pores' openness and group them in a certain way based on these data. After that, it is also important to describe the distribution of the different types of urban pores, which together serve as the basis for the quantitative model. Another important role is the characterization of the thermal environment, where we use the land surface temperature as the representative. Once these are established, we can construct a regression model to explain the effects of urban pores. Additionally, it is worth noting that we conjecture that this effect varies across urban form types, so we also need to construct an urban form classification model to explore this difference further. Figure. 2 illustrates the methodological framework of the research process.

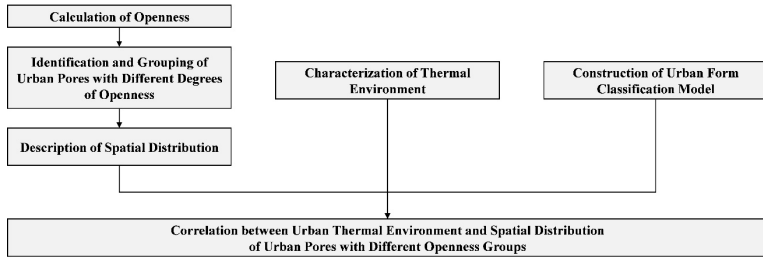


Figure 2. Methodological Framework

2.1. CALCULATION OF OPENNESS AND GROUPING

The openness of urban pores was calculated by the method (Tong et al., 2020), which mainly consists of two steps. First, a certain number of observation points were evenly distributed in the study area, and those inside the buildings were excluded. Second, section lines in 8 directions were generated at these observation points, thus forming a multidirectional section group. The building groups were rotate-sectioned to consider the sections in all directions. For the obtained sections, the study further calculated their width-to-height ratio and then took its average value as a variable to describe the openness of the urban pores at the location of the point.

Furthermore, to identify the impact of urban pores with different degrees of openness, this study used natural breaks (Jenks) to classify them into five groups, named the low openness group, mid-low openness group, mid openness group, mid-high openness group and high openness group.

2.2. DESCRIPTION OF SPATIAL DISTRIBUTION

Agglomeration was used to represent the spatial distribution characteristics of urban pores, and its value was calculated by kernel density analysis. This method uses kernel functions to calculate the density of the analysed elements in their surrounding neighbourhoods and outputs the results as continuous raster image elements.

2.3. CHARACTERIZATION OF THE THERMAL ENVIRONMENT

Land surface temperature (LST) was used to characterize the thermal environment. The data source is Landsat 8 TIRS, whose band 10 is the shortwave infrared band, and it can be used for the inversion of LST. Based on this, the study used the atmospheric correction method (radiative transfer equation) for the inversion of LST. To consider the variability of the urban thermal environment in different seasons, the LSTs of 4 seasons (spring, summer, autumn and winter) were all included in this study.

2.4. CONSTRUCTION OF URBAN FORM CLASSIFICATION MODEL

To further investigate the impact in different urban form types, it is necessary to construct a detailed and thermal-environment-related urban form classification model. The local climate zone (LCZ) is an urban form classification framework proposed for the urban heat island effect that can effectively differentiate urban from thermal

environments. Each zone type has similar urban form indicators, ground cover, building materials and human activities related to the thermal environment (Stewart et al., 2012).

Therefore, this study adopts the LCZ classification framework based on the World Urban Database Access Portal Tools (WUDAPT) to construct an urban form classification model (Bechtel et al., 2019). Landsat 8 OLI bands 1-6 in summer and available network information were used as the data sources, and the resolution was set as 300 m*300 m.

2.5. CONSTRUCTION OF REGRESSION MODELS

A classical linear regression model was used to analyse the impact of the spatial distribution of urban pores on the thermal environment. It contained 4 seasonal groups for interpretation, namely, spring, summer, autumn and winter. The independent variables were set as the results of kernel density for each openness group, reflecting the spatial agglomeration of urban pores, while the dependent variable was LST.

Furthermore, to investigate the differences in urban forms, the study took the LCZ model as a basis and classified the sample into multiple groups for regression analysis.

3. Case Study

3.1. STUDY AREA

This study took Nanjing, China, as an example. Nanjing is the capital of Jiangsu Province and one of the important cities in the Yangtze River basin. Over the past 40 years, Nanjing has experienced a rapid urbanization process with rich and complex internal urban forms, making it one of the typical high-density cities in China. In terms of climatic conditions, Nanjing has four distinct seasons, abundant rainfall, short spring and autumn, long summer and winter. It has an average temperature of 2.7 °C (January) to 28.1 °C (July), with significant subtropical monsoon climate characteristics, which can represent the common situation of cities in hot summer and cold winter zones.

Specifically, the study area (Figure. 3) was a square of 6 km*6 km, and due to the error in the edge area, we also created a buffer zone of 500 m outside each side of the square. The overall area was a 7 km*7 km square. To better illustrate the situation of the study area, we divided it into 25 small areas and classified the small areas as follows: 1-5 indicates the position of rows and A-E indicates the position of columns. For example, B-4 represents the 2nd column of the 4th row.

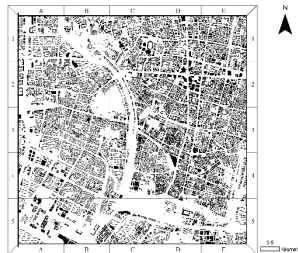


Figure 3. Study Area (6 km*6 km)

3.2. RESULTS OF OPENNESS CALCULATION AND GROUPING

The study used the method in Section 2.1 with 161 rows and 161 columns, with 25,921 observation points (17,689 observation points in the effective range). Among them, there are 19,498 valid calculation points (14,254 valid calculation points in the effective range). On this basis, they were further classified into 5 groups: urban pores with openness ranging from 0.125 to 4.500 were named the low openness group; urban pores with openness ranging from 4.500 to 9.125 were named the mid-low openness group; urban pores with openness ranging from 9.125 to 14.375 were named the mid openness group; urban pores with openness ranging from 14.375 to 20.625 were named the mid-high openness group; and urban pores with openness above 20.625 were named the high openness group. The values are shown in Figure. 4, and the distribution states in space are shown in Figure. 5.

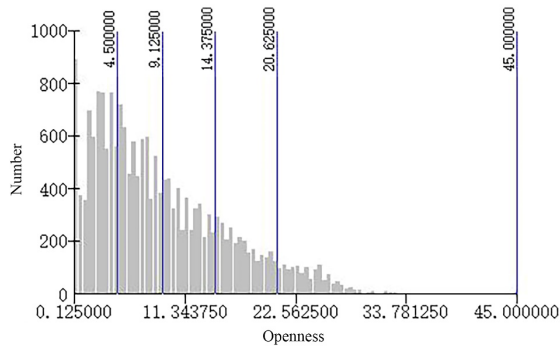


Figure 4. Distribution of Openness Values

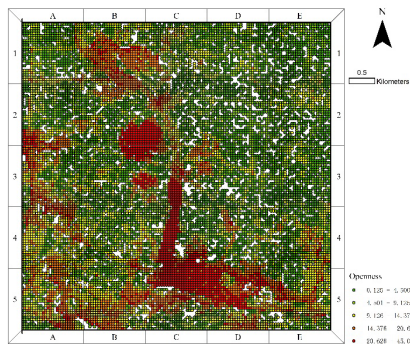


Figure 5. Calculation Results of Openness of Observation Points

Figure. 4 shows that most urban pores belonged to the low openness group and the mid-low openness group. Combined with Figure. 5, it can be seen that the urban pores forming the low openness group were mainly the external spaces among the high-density buildings, which were mainly distributed in D2, E1 and E3. The mid-low openness group was also dominated by urban roads, whose sections along the road direction have a higher width-to-height ratio. At the same time, others are also constrained by the mid-high density buildings, finally showing an overall mid-low

degree of openness. They were mainly located in A1, B4 and D1. The mid openness group included some roads and public green space between low-density buildings. Although the height of the buildings increased, the density was lower, and the building spacing was greater, resulting in an increase in openness, mainly in A4, B5 and E5. The mid-high openness group included open spaces or parks with fewer buildings; thus, the openness was higher, mainly in B1 and B5. The high openness group was mainly composed of rivers, which were kept at a certain distance from buildings, mainly in B2 and C5.

3.3. SPATIAL DISTRIBUTION OF URBAN PORES

Kernel density analysis was used to describe the agglomeration characteristics of the urban pores. In this study, the bandwidth was set to 500 m, and the results are shown in Figure. 6. The urban pores of the low openness group, mid-low openness group and mid openness group formed multiple agglomeration cores, and the distribution among these cores showed a certain continuity and uniformity. In contrast, the urban pores of the mid-high openness group and high openness group formed fewer agglomeration cores. The continuity and uniformity among the cores were not strong, and most of the study areas can be recognized as weak-agglomeration areas.

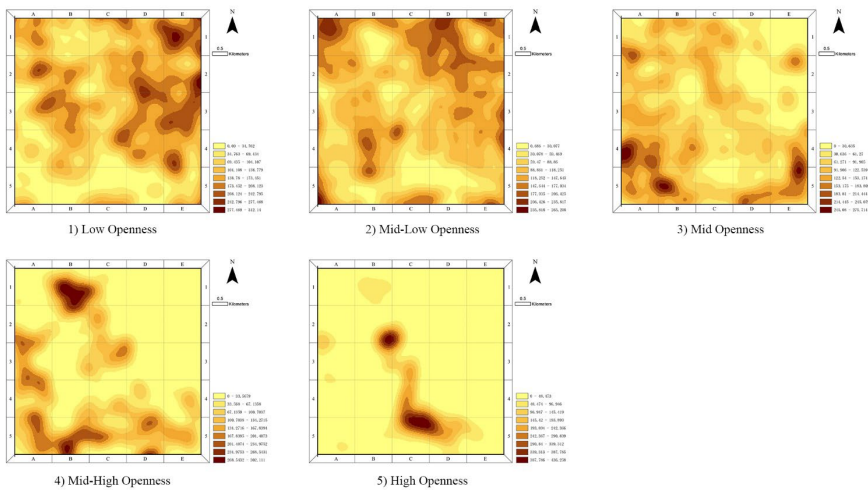


Figure 6. Nuclear Density Analysis for Each Openness Group

3.4. CHARACTERISTICS OF THE THERMAL ENVIRONMENT

Figure. 7 shows the distribution of LST in the four seasons. The range of LST was 22 °C-38 °C in spring, 30 °C-48 °C in summer, 20 °C-32 °C in autumn, and 9 °C-18 °C in winter. It presented higher values than the observed temperatures at the weather station. The areas of high LST were mainly distributed in B5, C1 and D4, while the areas of low LST overlapped with the natural environment, such as vegetation and water.

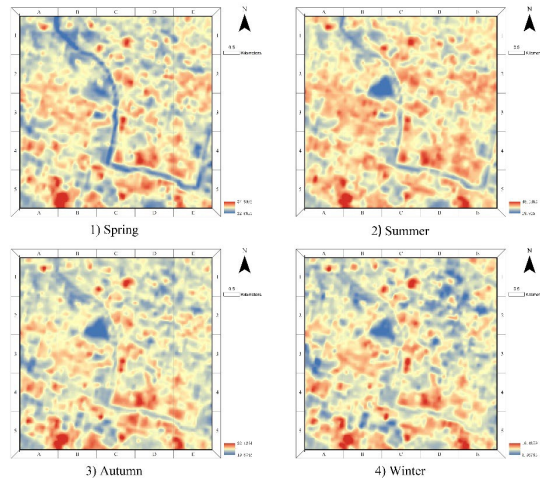


Figure 7. LST Distribution in Four Seasons

3.5. CONSTRUCTION OF URBAN FORM CLASSIFICATION MODEL

The study used the LCZ method to construct an urban form classification model. Based on the 17 types of LCZ, this study considered the actual situation of Nanjing and further grouped them into five categories: high-rise buildings (LCZ 1+LCZ 4), mid-rise buildings (LCZ 2+LCZ 5), low-rise buildings (LCZ 3+LCZ 6+LCZ 7+LCZ 8+ LCZ 9+LCZ 10), vegetation (LCZ A+LCZ B+LCZ C+LCZ D+LCZ E+LCZ F) and water (LCZ G). The LCZ samples are shown in Figure. 8, and the LCZ mapping results are shown in Figure. 9. The classification of urban form is used as an important basis for the grouping of the regression model below.

As seen in Figure. 8, the study area was dominated by mid-rise buildings, followed by high-rise and low-rise buildings, which were distributed in a more fragmented way. A river ran through the middle of the area, with some vegetation cover in the upper left and lower right of the area.

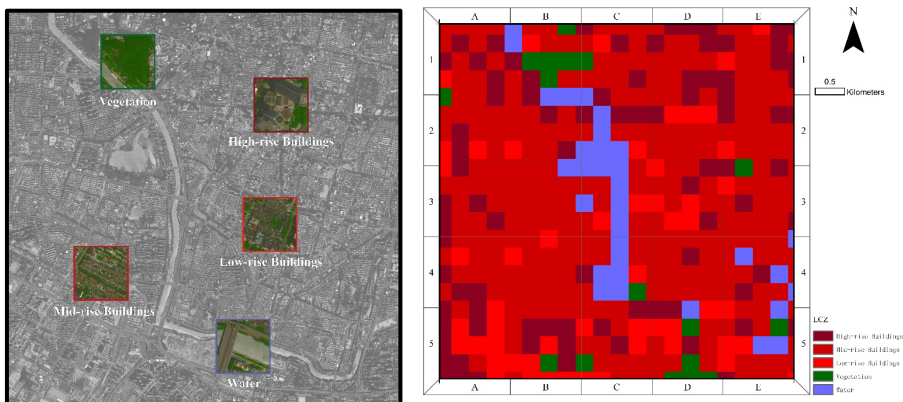


Figure 8. LCZ Samples (Left) Figure 9. LCZ Mapping (Right)

3.6. REGRESSION MODEL RESULTS

3.6.1. Preliminary Results of Regression Models

Figure 10 shows the preliminary regression model results for 4 seasonal and 6 LCZ groups (24 models in total). The overall coefficients ranged from 5% to 20% in terms of adjusted R². Comparing the adjusted R² of the LCZ groups in different seasons, three LCZ models (including the overall, same below) supported that summer has the best fit results, two LCZ groups supported autumn and one supported spring. This indicated that the spatial distribution of urban pores has a greater impact on the urban thermal environment, mainly in summer and autumn. Similarly, the five LCZ groups supported the worst fit in winter, indicating that the thermal environment value of urban pores was not significant in winter. By comparing the adjusted R² of different LCZ groups in the same season, it can be found that the adjusted R² after grouping was better than the overall R² in most of the groups, indicating that the grouping operation had a better explanatory effect.

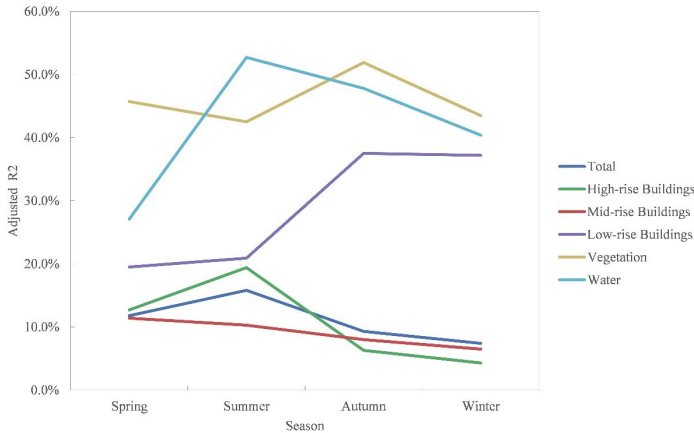


Figure 10. Adjusted R² of Four Seasonal Regression Models

3.6.2. Results of Grouped Regression Models in Summer

The study selected the model in summer to carry out further analysis, as it had the best explanatory effect. Table 1 shows the results of the regression models for each group. From an overall perspective, all coefficients were negative, indicating that the agglomeration of urban pores can produce a certain cooling effect regardless of the degree of openness. In particular, the spatial agglomeration of urban pores in the high openness group, mid-high openness group and mid-low openness group had a significant cooling effect on the urban thermal environment, while the effect of the medium openness group was the weakest. From the analysis results in Section 3.2, it is clear that the urban pores in the high openness group are mainly composed of water. The mid-high openness group is mainly composed of open spaces or parks, and the mid-low openness group is mainly composed of urban roads. These factors have a strong cooling value for the urban thermal environment. In particular, the distribution

of the mid-low openness group (urban roads) is an often overlooked but worthwhile type in the built environment.

Further comparing the coefficient differences in each LCZ group, it can be found that similar to the overall one, the spatial agglomeration in the high openness group, mid-high openness group and mid-low openness group still showed high regression coefficients for the urban thermal environment, while the mid openness group also presented the lowest regression coefficients in the built environment. The difference is that the spatial agglomeration of the low openness group had a lower regression coefficient in the natural environment (vegetation, water) than the mid openness group, which corresponds mainly to the external space among high-rise buildings.

It is also worth noting that the distribution of the regression coefficient values did not show a linear trend with the openness group. We speculate that this may be due to the presence of other factors that impact it, such as the complex heat transfer in the street canyons, the proportion of impervious surfaces, or the effects of vegetation and water.

Table 1. Results of Regression Model of Summer

	Total	High-rise Buildings	Mid-rise Buildings	Low-rise Buildings	Vegetation	Water
Adjusted R2	15.80%	19.40%	10.30%	20.90%	42.50%	52.70%
Low Openness	-0.698**	-0.698**	-0.367**	-1.032**	-0.778**	-0.763**
Mid-low Openness	-0.864**	-0.971**	-0.643**	-0.767**	-1.209**	-0.878**
Mid Openness	-0.448**	-0.491**	-0.276**	-0.244**	-1.264**	-1.191**
Mid-high Openness	-0.838**	-0.864**	-0.529**	-0.878**	-2.043**	-1.334**
High Openness	-0.954**	-1.027**	-0.457**	-0.846**	-1.253**	-2.857**

Notes: 1) Regression coefficients are all subject to normalization.

2) ** represents coefficients significant at the 0.01 level.

4. Conclusion and Discussion

In this study, we quantified the openness of urban pores in Nanjing, grouped them, and calculated the spatial distribution characteristics of each openness group. Based on this, this study combined the spatial distribution characteristics of urban pores with urban thermal environment data and an LCZ urban form classification model to analyse the impact of urban pores on the urban thermal environment. The results show that the spatial agglomeration of urban pores has a high cooling value for the urban thermal environment in summer and autumn, while it is not significant in winter.

Further analysis of the summer samples shows that the spatial agglomeration of urban pores has a higher cooling effect mainly in the high openness group, mid-high

openness group and mid-low openness group, which mainly correspond to water, open spaces or parks and urban roads. The mid openness group has the weakest effect in the built environment, and the low openness group has the weakest effect in the natural environment.

Therefore, priority will be given to enclosing urban forms with high cooling effects in future urban design. In combination with these areas, abundant public facilities should be installed to attract people to gather and to create a vibrant urban cold island. Meanwhile, in urban renewal, the cooling effect of pores with insignificant cooling effects can be enhanced by planting vegetation or increasing permeable ground.

At the same time, there are certain shortcomings in this study. This study explored the thermal environmental value of urban pores only from the perspective of openness. However, there is a lack of research regarding whether this cooling effect is brought about by high openness or the results of other elements that constitute urban pores (e.g., ventilation efficiency). The calculation method of openness also needs to be further updated to discuss the variability due to different ventilation, sunlight, and sightline conditions. Therefore, in the future, this issue will be further explored in depth by combining ideal models and simulations.

Acknowledgements

This research was supported by National Natural Science Foundation of China (51578277).

References

- Bechtel, B., Alexander, P. J., Beck, C., J Böhner., & Yong, X. (2018). Generating WUDAPT Level 0 data – Current status of production and evaluation. *Urban Climate*, 27, 24-45. <https://doi.org/10.1016/j.uclim.2018.10.001>.
- Guo, C., Riccardo, B., & Gao, Z. (2019). Characterizing the morphology of real street models and modeling its effect on thermal environment. *Energy and Buildings*, 203, 109433. <https://doi.org/10.1016/j.enbuild.2019.109433>.
- Jiang, Y.F, Huang, J., Shi, T.M., & Wang, H.X. (2021). Interaction of Urban Rivers and Green Space Morphology to Mitigate the Urban Heat Island Effect: Case-Based Comparative Analysis. *International Journal of Environmental Research and Public Health*, 18(21),11404. <https://doi.org/10.3390/ijerph182111404>.
- Lai, D., Liu, W., Gan, T., Liu, K., & Chen, Q. (2019). A review of mitigating strategies to improve the thermal environment and thermal comfort in urban outdoor spaces. *Science of The Total Environment*, 661. <https://doi.org/10.1016/j.scitotenv.2019.01.062>.
- Stewart, I.D., & Oke, T.R. (2012). Local climate zones for urban temperature studies. *Bulletin of the American Meteorological Society*, 93(12), 1879-1900. <https://doi.org/10.1175/BAMS-D-11-00019.1>.
- Tong, Z.Y., Yang, H.W., Liu, C., Xu, T.T., & Xu, S. (2020). Quantification of the openness of urban external space through urban section. *Geo-spatial Information Science*, 23(4), 316-326. <https://doi.org/10.1080/10095020.2020.1846464>.
- Wang, Y.S., Zhan, Q.M., & Ouyang, W.L. (2019). How to quantify the relationship between spatial distribution of urban waterbodies and land surface temperature? *Science of The Total Environment*, 671(JUN.25), 1-9. <https://doi.org/10.1016/j.scitotenv.2019.03.377>.
- Yang, J., Yang, Y.X., Sun, D.Q., Jin, C., & Xiao, X.M. (2021). Influence of urban morphological characteristics on thermal environment. *Sustainable Cities and Society*, 72, 103045. <https://doi.org/10.1016/j.scs.2021.103045>.

OUTDOOR THERMAL ENVIRONMENT ASSESSMENT OF EXISTING RESIDENTIAL AREAS SUPPORTED BY UAV THERMAL INFRARED AND 3D RECONSTRUCTION TECHNOLOGY

YONGJIE PAN¹ and TONG ZHANG²

^{1,2}*School of Architecture, Southeast University, Nanjing, China*

¹*youngee@seu.edu.cn, 0000-0002-7497-5682*

²*hytong@seu.edu.cn*

Abstract. The underlying surface temperature is an effective evaluation index to study the urban micro-scale thermal environment. For surface temperature acquisition, the thermal infrared camera mounted on a unmanned aerial vehicle (UAV) can reduce field work intensity, improve data collection efficiency, and ensure high accuracy at low cost. In order to convert the 2D thermal image into a more intuitive 3D thermal model, the UAV-based thermal infrared 3D reconstruction is adopted. The key element of thermal infrared 3D model reconstruction lies in the processing of thermal infrared images with low resolution and different temperature scales. In order to improve the quality of the final thermal 3D model, this paper proposes the reconstruction of the detailed 3D mesh using visible images (higher resolution), and map then mapping thermal textures onto the mesh using thermal images (low resolution). In addition, absolute temperature values are extracted from thermal images with different temperature ranges to ensure consistence between color and temperature values in the reconstructed thermal 3D model. The thermal 3D model generated for an existing residential area in Nanjing successfully displays the temperature distribution of the underlying surface and provides a valuable basis for outdoor thermal environment assessment.

Keywords. Thermal Image; UAV; 3D Reconstruction; Residential Outdoor Space; Underlying Surface Temperature; SDG 3; SDG 11.

1. Introduction

The development of urbanization brings large-scale construction which has significantly changed the urban pattern. Furthermore, the urban thermal environment has deteriorated, and this results in a reduction in the quality of the environment for urban residents. The comfort of the outdoor thermal environment has a direct bearing on the timing and frequency of outdoor activities. This is emphasized by the closed community management policy adopted in many locations after the outbreak of COVID-19. A healthy and comfortable outdoor thermal environment is necessary for residents to take part in outdoor activities.

It has been shown that the change in the underlying surface property caused by urban expansion has a significant impact on the urban thermal environment (Liu et al., 2021). The spatial distribution pattern and degree of coverage of urban vegetation confirm this (Huang et al., 2019). When examining current renovation of existing residential areas, an understanding of the impact of various underlying surface materials on the outdoor thermal environment can provide a scientific basis to determine the greening layout, tree species configuration and underlying material design for residential area renewal.

From the perspective of the residential thermal environment itself, various meteorological elements related to the site thermal environment are usually taken as evaluation indices. These include temperature, humidity, wind speed, solar radiation, etc. At present, these site thermal environment meteorological indicators are obtained from site meteorological measurements, software simulation and thermal infrared imaging technology. Although site meteorological measurements are very accurate, they require considerable manpower and expensive instrumentation for mobile observations in urban residential areas with strong internal environmental heterogeneity. Moreover, the observation point data cannot completely show the thermal environment in the space. Site models constructed using computer numerical simulation can have considerable differences from the actual site environment, as they do not consider the influence of regional microclimate on human thermal perception. These models do not provide sufficient guidance for precise design of small-scale outdoor environments. Thermal infrared technology converts the thermal infrared signals from ground objects into visually distinguishable images, and calculates temperature values to reflect the surface temperature distribution. At present, the surface temperature distribution map obtained by this technology is the most intuitive method commonly used in urban research to reflect the regional thermal environment (Wu et al., 2016; Zhao et al., 2020).

In recent years, lightweight thermal infrared products mounted on small UAV platforms have provided an efficient low-cost solution to obtain surface temperature (Tian et al., 2019; Rakha and Gorodetsky, 2018). Surface temperatures can be calculated from the color rendering of the thermal infrared images collected. However, the underlying surface temperature obtained in this way can only be displayed as a two-dimensional thermal infrared image. There is still a lack of effective methods for three-dimensional visualization analysis of the spatial distribution of surface temperature in the environment. In addition, due to the small viewing angle and the low resolution, the current two-dimensional thermal images do not meet the requirements for large-scale research areas.

To tackle this shortcoming, this study proposes a method to produce a 3D thermal infrared model by combining UAV thermal infrared images and 3D reconstruction technology. The proposed method converts the 2D thermal image into a more intuitive 3D thermal model. It can not only visualize the surface temperature distribution in space but also simply output temperature data at selected points for further analysis. This model can be used to evaluate the thermal environment in existing urban residential areas with complex spatial characteristics. This method is then adopted to build a 3D thermal model of an existing residential area in Nanjing. The results showed that the proposed method has good precision and efficiency. The heat gain difference

and internal mechanism of various surface underlying surfaces in existing residential areas revealed in the study can provide a scientific basis for outdoor environmental design in residential renewal.

2. Methodology

The methodology for the outdoor thermal environment assessment of existing residential areas using UAV thermal infrared data and 3D reconstruction technology consists of the following steps: data acquisition, 3D reconstruction and temperature analysis. These are shown in flowchart form in Figure 1.

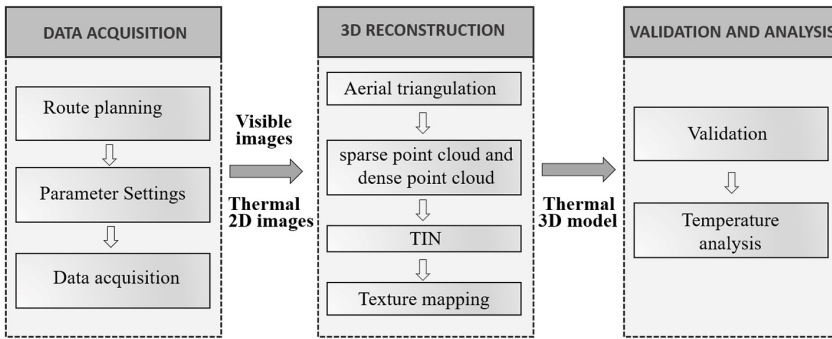


Figure 1. Methodology

2.1. DATA ACQUISITION

Data acquisition refers to the collection of visible and thermal infrared images of the study area using a camera on a UAV. In order to ensure the quality of data acquisition, it is necessary to plan the flight path of the UAV to ensure that the image data can be collected on this predetermined flight path whilst avoiding the risks and errors of manual data collection. The main parameters for route planning are the altitude, speed, camera angle and photo overlap rate, according to the scope and accuracy requirements of the research area. These parameters are used to generate the flight path for the UAV.

Before each take-off, it is necessary to input the real-time atmospheric temperature, humidity, emissivity and other parameters defining the prevailing weather conditions to improve the accuracy of temperature observation. Each data acquisition run is completed within a five-minute period to ensure that temperature data for different pictures in the run is unlikely to change much.

2.2. 3D RECONSTRUCTION

Similar to the three-dimensional reconstruction process for visible images, the recognition of feature points in thermal infrared images is the key to the success of three-dimensional reconstruction. Before starting the 3D reconstruction process, it is necessary to eliminate images that could influence feature point recognition due to color imbalance and blur.

The image resolution of a thermal infrared camera is usually much lower than that of an RGB camera, so the quality of the reconstructed 3D model is inferior to that of

the visible 3D model. In order to improve the quality of the final thermal 3D model, this study reconstructs a detailed 3D mesh using higher resolution visible images and then maps thermal textures onto this mesh. The specific process is defined as follows. The visible and thermal infrared images collected over one data acquisition period are imported into a 3D reconstruction software, Pix4Dmapper. Aerial triangulation is carried out by using the precise positional data from each visible and thermal infrared image, and the results of this aerial triangulation serve as a reference for the three-dimensional fusion of the two different image types. Feature point detection algorithms (SIFT, Scale-invariant Feature Transform) and feature point matching algorithms (SFM, Structure-from-Motion) are used to identify the same location points in each image and derive their 3D positions, so as to complete the sparse point cloud reconstruction. PMVS (Patch-Based Multi-View Stereo Software) technology is used to generate the dense point cloud. The Delaunay triangulation algorithm can then be used to construct an irregular triangulation network (TIN, Triangulated Irregular Network) from the dense point cloud. The thermal 3D model with thermal infrared texture is generated by mapping the thermal infrared image texture onto the TIN model.

2.3. VALIDATION AND ANALYSIS

It has been shown that the accuracy of temperature measurement by thermal infrared cameras is related to the shooting angle and the shooting distance. The thermal infrared camera mounted on a UAV experiences variable shooting angles and distances when acquiring thermal infrared images at high altitude due to variations in the flight altitude and pitching angle. In order to verify the accuracy of the temperature data obtained by the UAV thermal infrared camera, the surface temperature data for different positions at different camera heights and angles is obtained by means of control variables. Regression analysis is conducted. In order to verify that the same underlying surface does not show excessive temperature change within five minutes, the temperature data is analyzed to compare the readings before and after the five-minute period.

In order to obtain more accurate surface temperatures for different underlying surfaces, multiple sample points are selected for temperature measurement at different positions for each underlying surface in the study area. This eliminates potential errors that could be caused by single samples.

3. Case Study

3.1. STUDY AREA

A residential area in the Xuanwu District of Nanjing (Latitude 32.1 N, Longitude 118.8 E) is selected as the study area (Figure 2a).

Built in the 1990s, the residential area epitomized many old residential areas in Nanjing that are facing renovation and upgrading. Against the current background of urban renewal, research and analysis of the thermal environment characteristics of this area can be significant when formulating a renewal and transformation strategy for this and other residential areas of the same area. The size of the study area is approximately 165 m by 140m, with a homogenous base environment, including green space, water, buildings, hard pavement and other underlying surface types (Figure 2b).

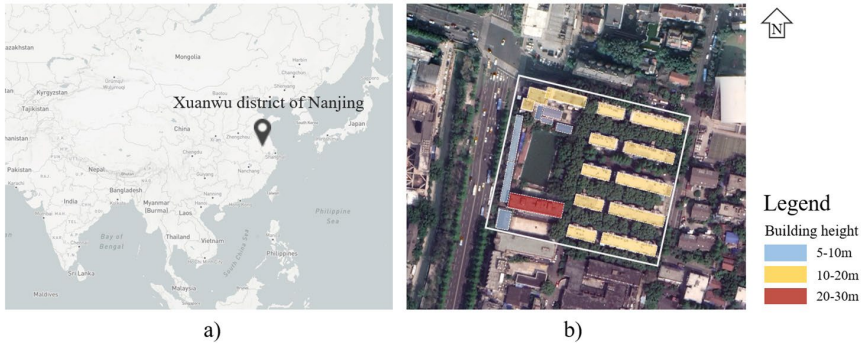



Figure 2. Location (a) and building layout (b) of the study area

3.2. DESCRIPTION OF DEVICE CONFIGURATIONS

The DJI Mavic 2 Enterprise Advanced (M2EA) is used for the acquisition of visible image and thermal infrared image data. The M2EA is equipped with advanced dual-light cameras, including a 640×512 resolution thermal infrared camera and a 48-megapixel visible camera using a 1/2 inch CMOS sensor (Table1). The onboard RTK module enables the M2EA to accurately locate, ensuring that visible and thermal images acquired simultaneously have similar external orientation parameters.

Table1 Main characteristics of the employed cameras

Characteristics	Thermal	Visible	Photo
Focal length	38mm	24mm	
Image size	640*512	8000*6000	
Image format	DJI R-JPEG	JPEG	
Range	-40-150℃	—	

3.3. ROUTE PLANNING AND DATA ACQUISITION

Before formal data acquisition, the UAV is tested, and the relevant shooting parameters are set. The meteorological parameters required for thermal infrared camera correction are obtained from the values taken at the handheld weather station at the operation point. The emissivity is uniformly set to 0.95, and the color bar is set to iron red.

Route planning is done using the specific software DJI poilt V2.3 configured for the M2EA. The route coverage area is defined to as the study area. In the relevant interface, the route type is created as oblique photography, and the relevant route parameters set at the same time. Existing studies have found that the effect of 3D reconstruction is optimum when the route height is twice the height of the photographed object (Han et al., 2019). In this exercise, the route height is set at 60 meters. The flight overlap rate and the side overlap rate are both set to 70%, and the camera angle for oblique flight is -60° (Figure 3). After the first route setting, it was verified that there were no overlaps between the planned route and high buildings in

the surroundings, so as to avoid risk of collision during the process of data acquisition.

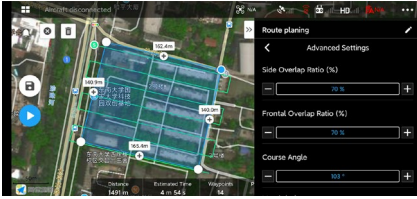


Figure 3. Route planning layout

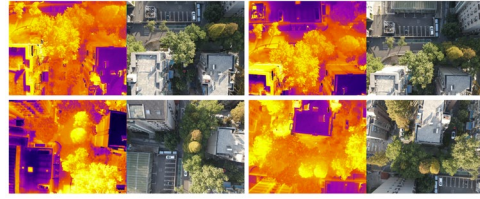


Figure 4. Visible and thermal infrared images

In order to effectively observe temperature change in the underlying surface for the existing residential area, data acquisition was carried out on November 14, 2021. The M2EA took off every hour between 8:00 and 17:00 throughout the day to complete the mission and obtain the corresponding visible and thermal infrared images. Since the focus was on the surface temperature of the underlying material and to ensure that the flight time did not exceed five minutes, the planned route consisted of only a single orthographic route. For verification of the 3D reconstruction, all planning routes were carried out at 12:00. About 150 visible and thermal infrared images were obtained for each mission at each time point (Figure 4). An additional 370 photos were obtained for the planning route mission at 12:00.

3.4. DATA PREPROCESSING AND 3D IMAGING

The data acquisition steps obtained several original thermal infrared images with location information and temperature information. The temperature data in these JPG files can only be used in the DJI Thermal Analysis Tool V2 for simple temperature measurement, and cannot be recognized by other software. In order to utilize the temperature data in the reconstruction process, it is necessary to convert the original picture file into an R-jpg file that can be recognized by FLIR or pix4d mapper to extract the data. The ThermoConverter software is used for conversion, and batch processing made this a quick process.

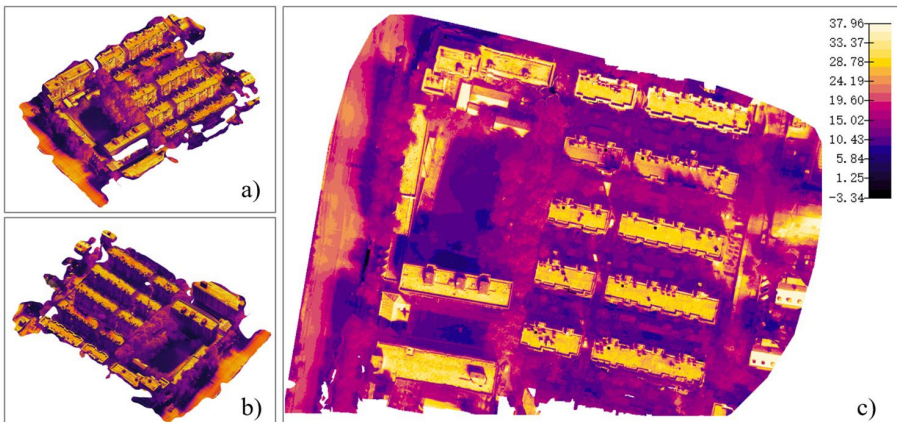


Figure 5. Thermal 3D model (a, b) and thermal ortho map (c) of study area

The processed data is imported into the pix4D Mapper software one by one for each time period, and the single reconstruction process is rapidly completed. Thermal infrared texture mapping on the visible 3D model is realized by combining the initial processing results from the two reconstruction projects (visible image and thermal infrared image project). After merging the projects, in the advanced settings for the projects, the point cloud group is selected as the visible image, and the mesh texture is checked as the thermal infrared image. The reconstructed thermal 3D model is shown in Figure 5(a, b).

The reconstructed ortho map can display the temperature information through the relevant settings, by generating the index map through the index calculator (Figure 5c). The temperature data can be obtained by clicking the mouse, and the numerical information (exponential value) is shown at the lower right of the software interface.

4. Results and Discussion

4.1. THE ACCURACY OF 2D THERMAL IMAGES

Existing studies have discussed the relationship between flight altitude and thermal infrared temperature measurement accuracy (Tian et al., 2019). In this case study, the temperature measurement data of the same underlying surface at two flight altitudes of 10m and 60m are obtained at the same time for analysis. The results show little difference in the surface temperature measurements taken at different flight altitudes, and the error is within the allowable range after calibration of the thermal infrared camera.

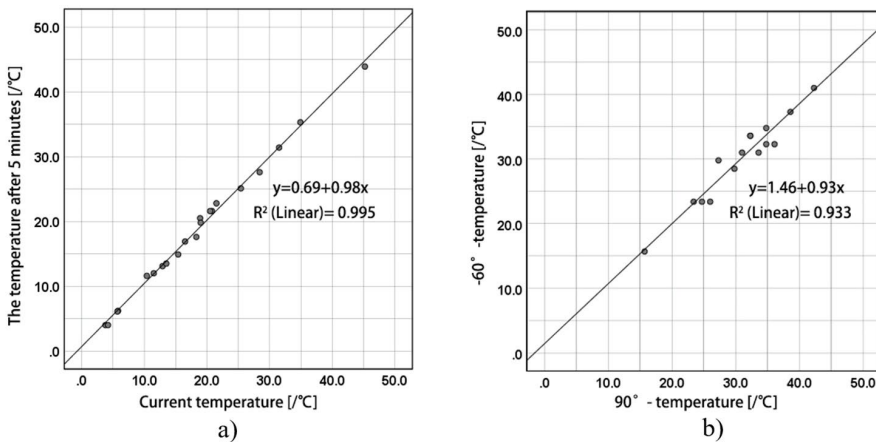


Figure 6. Linear regression plot of temperature before and after the time interval(a), Linear regression plot of temperature at two different shooting angles(b)

The temperature data at different locations before and after five-minute intervals are obtained by thermal infrared temperature measurement, and regression analysis is carried out (Figure 6a). The analysis shows that the surface temperature changes little during this time interval. Therefore, it is feasible to select images within five-minute intervals for 3D reconstruction when extracting surface temperatures for different

underlying surfaces.

Since 3D reconstruction requires the fusion of thermal infrared images from different shooting angles, it is necessary to verify the correlation between temperature values at different shooting angles. The results show that the temperature values at two different shooting angles (60° and 90°) have a high degree of fit, with a Pearson correlation coefficient of 99.6%, which is significant at the 0.01 level (Figure 6b). This analysis shows that it is feasible to select thermal infrared images from different shooting angles for 3D reconstruction.

4.2. THE EFFICIENCY OF THE THERMAL INFRARED 3D MODEL

In a similar manner to three-dimensional reconstruction of visible images, the efficiency of thermal 3D model reconstruction is closely related to altitude and image overlap. With the same image overlap, the lower the UAV altitude, the higher the corresponding ground resolution. This results in better resolution of the reconstructed model, but also a correspondingly longer software processing time. In addition, it becomes necessary to increase the flight time to obtain sufficient images to meet the set overlap rate, and this has a negative effect on the time-sensitive thermal infrared temperature measurement.

With the 70% overlap rate adopted in this case study, the ground resolution of the thermal infrared image is 7.79 cm / 3.07 in. The time-related statistics for the whole stage are shown in the Table 2. It can be seen that all external and internal steps can be completed in a relatively short time to obtain a thermal 3D model for the study area. When compared with traditional field weather measurement, this approach using UAV thermal infrared technology is more efficient and obtains temperature data over a large area in a short time.

Table 2 The time consuming statistics of the whole stage

	Steps	Time consuming
External	Route planning	2min
	Data acquisition	5min+4*6min
	Image convert	10min
	Initial Processing	6min (Thermal)+38min (Visible)
Internal	Point Cloud Densification	50min56s
	3D Textured Mesh Generation	12min21s
	Index map generation	1min19s
Total		150min

4.3. THE INFLUENCE FACTORS OF UNDERLYING SURFACE TEMPERATURE

In this study, measurements are taken for different underlying surface types in the region. These consist of four kinds of artificial underlying surface, namely concrete, asphalt, square brick (brick1) and floor brick (brick2), and three kinds of natural

underlying surfaces, water, grass and shrubs. The daytime variation characteristics of the surface temperatures for the different types of underlying surfaces are analyzed, as shown in Figure 7.

During the observation period, the daytime variation curve for the seven underlying surfaces showed a single trend, rising from 08:00, reaching a peak around 14:00, and then decreasing. The rate of increase and decrease of the artificial underlying surfaces is significantly higher than that of the natural surfaces. The daily maximum temperature of the constructed surfaces is generally about 15°C above that of the natural underlying surfaces.

Among the three kinds of natural underlying surfaces, the temperature changes in grassland were the most drastic. The temperature variations for the water and shrubs are low, showing good temperature stability. Water has a high specific heat capacity and strong heat absorption capacity, and solar radiation does not have much effect on the water surface temperature. In addition, water evaporation keeps the temperature stable. The important factors affecting vegetation surface temperature are solar radiation and vegetation transpiration. However, the grass in the study area is short and not shaded, and transpiration of vegetation was not obvious when receiving solar radiation, so the cooling effect was not as effective as that of shrubs.

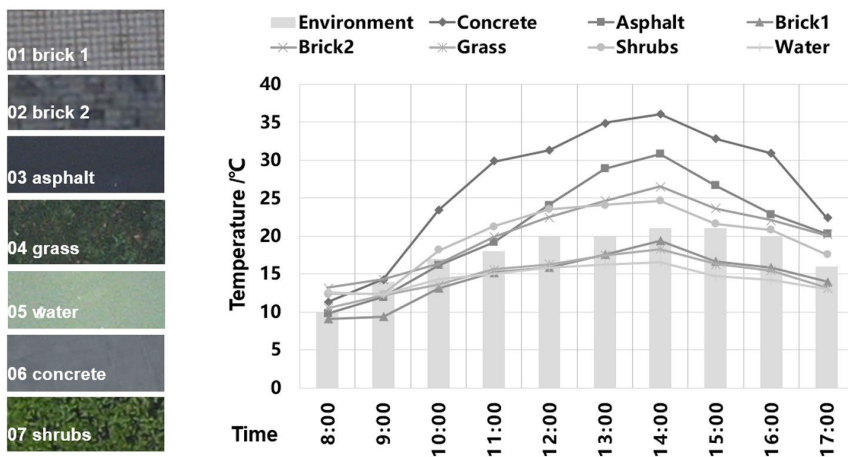


Figure 7. The daytime variation in temperature for different types of underlying surface

Amongst the four kinds of artificial underlying surfaces, the temperature changes in a day differ due to the different absorption and radiation characteristics of the materials. Concrete has the highest heat absorption and the most drastic temperature change, followed by the asphalt pavements. This shows that concrete and asphalt have the greatest impact on the thermal environment in residential areas.

5. Conclusions

This paper introduces the use of UAV-mounted thermal infrared cameras and 3D reconstruction technology to analyze and evaluate the mechanisms by which underlying surface materials influence the outdoor thermal environment. The major

findings follow.

The mapping texture of thermal infrared images onto a visible 3D model can produce a high quality thermal 3D model. The extraction and application of absolute temperature values in thermal images of different temperature ranges can ensure the consistency of color and temperature values in reconstructed thermal 3D models. Verification and data analysis indicate that this thermal 3D model has high accuracy and efficiency. In addition, the model can effectively display the surface temperature distribution at any point in the research area.

In the case study, the underlying surface temperature of a typical residential area in Nanjing is investigated in detail. The statistical analysis of temperature is used to determine the heat gain in different underlying surfaces during daytime. Solar radiation has a significant effect on the heat gain of the underlying surfaces, and the shielding of buildings or tall trees can obviously reduce the heat gain. The temperature of the natural underlying surfaces is clearly lower than that of the constructed surfaces. In the renovation design of outdoor spaces in existing residential areas, the outdoor thermal environment can be improved through the use of green layouts, tree species configurations and underlying surface material design.

Acknowledgements

The authors would like to acknowledge that this paper was financially supported by the National Natural Science Foundation of China (Grant No. 52178007), and the Postgraduate Research & Practice Innovation Program of Jiangsu Province (KYCX21_0109).

References

- Han, Y., Pan, Y., Zhao, T., Wang, C., & Sun, C. (2019). Use of UAV Photogrammetry to Estimate the Solar Energy Potential of Residential Buildings in Severe Cold Region. In *24th International Conference on Computer-Aided Architectural Design Research in Asia: Intelligent and Informed, CAADRIA 2019* (pp. 613-622). The Association for Computer-Aided Architectural Design Research in Asia (CAADRIA).
- Huang, M., Li, J., & He, X. A. (2019). The influence of underlying surface on land surface temperature -- a case study of urban green space in harbin. *Energy Procedia*, 157, 746-751.
- Liu, H., Huang, B., Gao, S., Wang, J., Yang, C., & Li, R. (2021). Impacts of the evolving urban development on intra-urban surface thermal environment: Evidence from 323 Chinese cities. *Science of The Total Environment*, 771, 144810.
- Rakha, T., & Gorodetsky, A. (2018). Review of Unmanned Aerial System (UAS) applications in the built environment: Towards automated building inspection procedures using drones. *Automation in Construction*, 93, 252-264.
- Tian, H., Li, F., Zhao, M., Song, G., & Dong, J. (2019). Analysis of Meticulous Features of Urban Surface Temperature based on UAV Thermal Thermography. *Remote Sensing Technology and Application*, 34(3), 553-563.
- Wu, Z., Wang, Y., Kong, F., Sun, R., Chen, L., & Zhan, W. (2016). Analysis of the thermal characteristics of selected urban surfaces in a typical residential area based on infrared thermography. *Acta Ecologica Sinica*, 36, 5421-5431.
- Zhao, X., Luo, Y., & He, J. (2020). Analysis of the thermal environment in pedestrian space using 3D thermal imaging. *Energies*, 13(14), 3674.

DESIGNING OUT HEAT – DEVELOPING A COMPUTER-AIDED STREET LAYOUT TOOL TO ADDRESS URBAN HEAT IN STREETS AND SUBURBS.

DANIEL YU¹, MATTHIAS IRGER², ALEX TOHIDI³ and M. HANK HAEUSLER⁴

^{1,2,4}UNSW / Computational Design. ²Cox Architecture.

¹d.yu@unsw.edu.au, 0000-0002-7788-548X

²m.irger@cox.com, 0000-0002-8158-9704

³a.tohidi@unsw.edu.au, 0000-0003-1335-4943

⁴m.haeusler@unsw.edu.au, 0000-0002-8405-0819

Abstract. As cities are getting hotter, the urban heat islands effect will become an increased concern for cities. While urban heat migration strategies are well researched and understood, some strategies of implementing urban heat mitigation focus on private land - thus depend on the owner's uptake. This research shifts mitigation strategies to the public land where governments have legislative control over the corridor between privately owned cadastral – the street corridor. This paper asks the question how a computational tool could assist councils in redesigning streets to mitigate urban heat. Literature review confirmed a direct relationship between the magnitude of urban heat and street layout, vegetation and materials used, position of street to sun and wind direction - yet no tool that assists a designer exists - the focus of the research. We present first findings and the iterative development of our street design tool. Via our tool one can alter variables such as vegetation type, materials or street configuration until urban heat mitigation is optimized. This is a significant step towards cooling our cities as designers now have a process that translates expert knowledge on urban heat into a tool that lets them design as well as evaluate their design.

Keywords. Urban Heat Island; Heat Mitigation; Landscape Architecture; Urban Design; Street Design; Traffic Engineering; Computational Tools; SDG 11.

1. Introduction and research background

Temperature records around the world are being broken at an increasing rate because of accelerating climate change (IPCC, 2021; WMO, 2021; Climate Council, 2019). This upwards trend is particularly severe in cities, where temperatures are generally higher than in rural areas due to the urban heat island phenomena (Oke, 1988b; Gartland, 2008). In January 2021, the city of Penrith in Western Sydney was the hottest place on earth with a new record of 48.9°C, while six months later Lytton in Canada

experienced 49.6°C and Nuwaiseeb in Kuwait 53.2°C. Global warming will continue to increase the severity and length of these extreme heat events as well as their frequency (WMO, 2021; Climate Council, 2019). In Australian cities, the number of days per year above 35°C, when most people experience moderate or great heat stress, are projected to grow significantly by 2050 compared to their historical long-term average: in Western Sydney from 11 to 24 days per year, in Western Adelaide from 18 to 34, in Brisbane from 2 to 14, and in Darwin from 22 to 187, respectively (WMO 2021). Higher temperatures not only drive-up energy consumption of air conditioners, cause damage to buildings and infrastructure, diminish productivity and make people feel uncomfortable (Hart and de Dear, 2004; Kolokotroni et al., 2006; Watkins et al., 2007), but increasingly reach extreme levels dangerous for human health. With more hot days people are increasingly confined indoors, while physical labour outside, active transport and outdoor recreation cease and a walk to the shops or doctor becomes a health risk, particularly for the elderly. Consequently, managing and mitigating urban heat is fast becoming an issue of great concern for cities who seek to protect their citizens from the adverse impacts on human health and wellbeing, liveability, productivity, and overall carbon emissions. The fact that urban areas are significantly warmer than their rural surroundings, a phenomenon called the Urban Heat Island effect, has been well documented and understood (Stewart and Mills, 2021; Stewart, 2011; Gartland, 2008). It is caused by the replacement of natural ground cover with impervious, dark coloured surfaces, such as roads and buildings, which absorb, store and re-emit more radiation (Akbari, 2009; Gartland, 2008). The lack of trees and other vegetation reduces evapotranspiration and shade, which exposes more ground surface to the sun, thus increasing surface temperatures and enabling more thermal storage (Akbari, 2009; Kuttler, 2011). Wide, suburban streets with single storey buildings expose more road surfaces to the sun to heat up, while relatively narrow inner-city streets with tall buildings experience less solar exposure at street level over the day, but also prevent more energy from escaping to the sky (Oke, 1988a; 1988b). Unsurprisingly, precincts that experience the highest maximum temperatures are low-rise developments dominated by dark roads and roofs, and a distinct lack of shade trees and soft landscaping. Several studies have shown that urban temperatures can vary more than 10°C within a city depending on the urban form of a precinct including its building density, vegetation content and surface materials of roofs and the ground (Irger, 2014). Strategies to mitigate urban heat involve increasing tree canopy and natural ground cover, reducing impervious surfaces and rainwater runoff, and the use of lighter-coloured and reflective materials for roofs, roads, and paving (Gartland, 2012; Akbari, 2009; Muller et al., 2014). Trees not only shade the ground and prevent surfaces with high thermal mass such as roads from heating up, but they also protect pedestrians from solar radiation and further heat stress on hot days (Akbari, 2002; Kuttler, 2012). According to recent research, choosing light-coloured materials for all roofs could reduce the ambient temperature in Sydney by an average of 2.4°C (Mohammed et al., 2021), while urban reforestation could provide 1-5°C of cooling (Kurn et al., 1994; McPherson et al., 2005). A comprehensive uptake of heat mitigation strategies in architecture, urban design and planning is vital as we progressively redesign our cities to cope with rising temperatures, thus directly addressing SDG 11 - making cities and human settlements inclusive, safe, resilient, and sustainable.

Mandating white roofs, trees on site or for a portion of land to be unsealed may be

achievable strategies for new developments, but they are challenging to apply to the existing built environment. Private landowners may be reluctant to invest in changing a functioning roof, dislike the aesthetics or glare. Secondly, buildings on recent suburban developments or inner-city blocks often cover the majority if not all the site, leaving no physical space for trees. As the opportunity to implement wide-spread heat mitigation policies on private land is largely tied to the rate of redevelopment or refurbishment, changing the existing building stock will be slow, incremental and a long-term effort. On public land on the other hand, which is in local or state government control such as streets, parks, plazas and other public landholdings, mitigation strategies could be implemented relatively quickly.

It is argued that a focus on streets should be a priority in mitigating urban heat for the following reasons:

Firstly, generally exposed to the sun, roads are often the hottest surface in a precinct and store a large amount of energy and are therefore a major contributor to the urban heat island effect at day and night (Gartland, 2008). This is particularly severe during a heat wave, when roads push already high temperatures to extreme levels considered dangerous to human health.

Secondly, streets are vital to public life and the economy. They exist to facilitate movement for people of all ages and abilities and are used by choice or necessity for access, work, or leisure. More frequent and severe extreme heat events as predicted impede on or outright prevent these activities, which presents a major and growing threat to the functioning of a city, its citizens and economy.

Thirdly, with about one fifth of urban areas in Australia allocated to streets and other public open spaces, they represent a large portion of land in a city that is under direct local or state government control. At this scale, rethinking streets with heat in mind would significantly improve the temperature profile of a city and make a meaningful difference to the experience of its residents.

The most important strategy to reduce temperatures in streets and improve the thermal comfort of pedestrians is the provision of shade by maximising tree canopy cover to protect people and surfaces such as roads and walkways from solar radiation. Other measures include introducing more pervious areas such as porous paving and soft landscaping, planted verges and bio swells, and choosing light coloured paving for footpaths and concrete over dark asphalt for transit lanes (Akbari, 2009; Gartland, 2012; Kuttler, 2012). Cities are also increasingly prioritizing active transport over vehicular traffic and replacing transit lanes with bike lanes, wider footpaths, and vegetation, thereby reducing anthropogenic heat and air pollution, too. While aforementioned measures could relatively easily be incorporated in the design and planning of streets, implementation is not yet widespread. Despite an increasing awareness of the mechanisms driving heat in cities as evidenced by recent publications of guidelines and policies by governments and other stakeholders, there is currently no tool available to assist urban design and planning professionals with the optimization of spatial arrangements to mitigate urban heat in a street.

Consequently, our research focused on the development of a computer-aided street design tool to address urban heat in streets and precincts presented in this paper.

2. Research hypothesis, question, objectives, and outcomes

In this research we aim to investigate the shape of the built environment by focusing on one part of the built environment - the street. The research proposes the hypothesis that **streets** - in their layout (road type / bicycle lane / trees / parking / etc.) and design (arrangement of the previous and the choice of materials, vegetation, etc.) - **are within the jurisdiction of a council, state or federal government and thus offer opportunities to address the shape of the built environment** and therefore urban heat. This hypothesis extends to both alterations in existing streets (grey / brown field optimisation) as well as designing new streets (green field developments) and counter urban heat aggravation as above by developing computational methods and tools to address the research problem. Our hypothesis extends further to:

- Tool would expedite street design / allow fast optioneering / testing
- Tool would allow to estimate impact of design on urban heat
- Tool would allow optimisation / testing of performance of new precinct layout
- Tool would support optimization of existing streets
- Tool would help optimize street design for heat and improve local microclimate / people's comfort / health / energy bills.

All to ask the core research question (I):

“What can computational design with its methods and tools offer to reduce heat at the urban scale when concentrating on street layout and design?”

With the sub question of (II):

“How can these computationally enabled changes in street layout and design towards reducing heat be verified by visualising the difference in air temperature via voxel display?”

And a follow up question of (III):

“How can the investigated and proposed computational tool be made accessible to design professionals in practice and government via web-based processes?”

With these research questions the *research objectives*, as a specific result that can be achieve within a time frame and with available resources, are:

- To study and understand urban heat island occurrence specifically to reduce heat at the urban scale. In particular: Physical principles that underpin heat at the urban scale. Literature on heat at the urban scale.
- To research and apply street layout and design principles. In particular: Literature that links street layout and design principles with heat at the urban scale. Street layout and design principles in an Australian (NSW) context using Sydney and in particular Western Sydney as case study.
- To investigate computational design methods and tools appropriate to address the

research question. In particular: Literature on computational methods and tools addressing sustainable issues. Tools and computing processes that allow the interaction, presentation, and visualisation on a browser (web application).

The *research outcomes*, as a detailed description of what will be produced at the conclusion of our work are a set of computational method(s) and/or tool(s) named ‘street layout planner’ - addressing Research question (I) and (III).

- For grey / brown field optimisation. Understand and inspect via computational methods and tools existing street layouts and the ‘material types’ - geometry of a material with a specific albedo value - they are made from. Understand and compute the absorption and conversion into heat by each ‘material tile’ - geometry of a material with a specific albedo value. Understand and replace existing ‘material tiles’ with new low albedo ‘material tiles.’ Alter, change or improve via selection of vegetation.
- For green field development. Plan and design streets from scratch that are optimised towards: urban canyon geometry, direction of street towards prevailing wind, and optimised choice for materials.

This paper presents in the following *Chapter heading 5 ‘Development of Street Design (SDT) Tool’* the agile development of first steps towards this ‘street layout planner’ tool. As part of an ongoing yet to be published research, a further, second, computational method(s) and/or tool(s) named ‘Voxel air temperature tool’ - addressing research question (II) and (III) will be developed.

- For grey / brown field optimisation as well as green field development. Calculate reflection and emission of long and shortwave radiation. Calculate and incorporate wind. Calculate and incorporate anthropogenic heat (cars, air conditioner). Representing above as air temperature via a voxel grid (volumetric pixel). Allow interaction and evaluation of urban design via voxel visualisation.

The first early steps of this development are shown in Figure 3.

3. Research Methodology

Exploring the problems and opportunities associated with emerging digital technologies in an applied and pragmatic context towards researching “*What can computational design with its methods and tools offer to reduce heat at the urban scale when concentrating on street layout and design?*”, is well-suited to an immersive and participatory approach that engages users as well as researchers. As argued by Hamilton et al. (2020), Action Research (AR) is the overarching methodological framework for this research project. Consequently, the research has followed the spiral of steps typical to the AR process of ‘*plan*’, ‘*action*’, ‘*observe*’ and ‘*reflect*’ (Kemmis 2009). The useability of the Action Research methodology investigating the opportunities offered by computational design for urban heat has been subject of and argued for in the 2019 paper ‘*Designing out Urban Heat*’ (Green et al), when optimising footpath materials with different albedo values through evolutionary algorithms to address the urban heat island effect. Green et al argued in the paper with O’Brian (2001) that Action Research as an iterative process was the chosen

methodology due to its effective and practical uses, and further argued with Avison (1999) who points out that action research is unique in the fact that it combines the results and processes of theory and practice synergistically, and “*research informs practice and practice informs research.*” As outlined in Action Research literature, the planning phase for this research consisted of researching relevant resources and performing literature reviews. Here the research was informed by research in three fields:

- First, understanding what an Urban Heat Island effect is, and what it is impacting. From this understanding the core research question was identified.
- Secondly, research has identified algorithms, equations, and tools that have been prior used to solve similar problems and translate this understanding to the field of enquiry. Here GH, Python or C-languages or web-based languages will assist.
- Lastly, from understanding of voxelization of information as a means to spatial temporal display as chromatophoric architecture to address research question (III).

The computationally assessing, reducing, and designing out heat at the urban scale while focusing on streets workflow method for understanding ‘*What can computational design with its methods and tools offer to reduce heat at the urban scale when concentrating on street layout and design*’ will be iteratively developed, deployed and assessed through cycles of action and reflection in this research.

4. Literature review specific to Street Design Tool (SDT) development

In general, streets can be categorized into different typologies according to their function, traffic carrying capacity and transport mode mix, surrounding land use and immediate context. As streets have traditionally been designed to facilitate vehicular traffic, common classifications are based on traffic volumes and speed providing minimum requirements for transit, parking and bicycle lanes, and footpaths (Austroads, 2021). While recent guidelines indicate a shift towards people-oriented design (Gehl, 2013), none mentions heat mitigation or thermal comfort.

Roadcorridor geometry guidelines - Best practice

Road Type	MAX AADT (av. cars/day)	MAX Speed (km/h)	MIN Footpath width (m)	MAX Footpath width (m)	MIN Lighting zone (m)	MAX Lighting zone (m)	MIN Bicycle lane (m)	MAX Bicycle lane (m)	MIN Green infrastructure (m)	MIN Travel lane width (m)	MAX Travel lane width (m)
Laneways / Local service road	1000.0	30.0	1.2	1.8	0.3	0.6	0.0	0.0	0.0	2.7	3.5
Pedestrian-only streets	0.0	15.0	3.5	7.5	0.3	0.6	0.0	0.0	1.5	0.0	0.0
Shared streets - residential	1000.0	30.0	1.8	2.4	0.3	0.6	0.0	0.0	1.5	2.7	3.5
Urban Local access road	1000.0	50.0	1.8	2.4	0.3	0.6	1.2	2.5	1.5	2.7	3.5
Shared streets - commercial	8000.0	30.0	2.4	7.5	0.3	0.9	0.0	0.0	1.5	2.7	3.5
Urban Local collector road	8000.0	60.0	2.4	3.0	0.6	0.9	1.8	2.5	1.5	3.0	3.5
Neighbourhood Main street	8000.0	50.0	2.4	7.5	0.6	0.9	1.8	2.5	1.5	3.0	3.5
Urban arterial road - single carriageway	14000.0	70.0	2.4	4.5	0.6	0.9	2.0	2.7	3.0	3.0	3.5
Urban arterial road - divided carriageway	30000.0	80.0	2.4	4.5	0.6	0.9	2.4	3.6	3.0	3.5	4.2

Table 1. Range of dimensions for each street typology and component according to international best practice

For the purpose of this research, the following nine street typologies has been identified as universally applicable, capturing vehicular capacity and traffic modes as well as the prevailing land-use context and urban setting: laneways or local service roads, pedestrian-only streets, shared streets - residential, urban local access roads, shared streets - commercial, urban local collector roads, neighbourhood main streets, Urban arterial roads - single carriageway, and Urban arterial roads - divided carriageway.

These typologies entail associated spatial requirements of street components such as footpaths, bicycle lanes, lighting zones, parking and transit lanes, green infrastructure and public transport corridors. Table 1 shows a range of dimensions according to international best practice (GSDG 2016, Gehl 2013).

Following a systematic review of computerized and computational tools we can safely assume that currently no street design tool that features parametric design capability and supports spatial, urban heat specific optimization exists. While there are street design tools examples within platforms such as Test Fit.io, Giraffe.build or urban design and evaluation tools in GH such as Urbano or Decoding Spaces Toolbox, these do not allow an integration of different materials (albedo) or vegetation (shadow).

5. Development of Street Design Tool (STD)

Prior to scripting we set up the program architecture as we aimed to have the 'Street Design Tool' as a 'backbone' that allow a later addition of various yet to be determinate 'plugins', such as a simulation of tree growth over time to calculate shade and potential cooling. We have categorised these into the following groups:

- **Usability and compatibility.** Works with current street typology conventions. Easy to access and operate. Compatible with common database formats (csv.). Allows the user to choose street typology and select components. Assists the user by suggesting dimensions for street components based on best international practice but allows the user to modify these values according to specific design requirements. Works parametrically to allow real-time optioneering.
- **Road features.** Assists to Minimise Road space and maximise space allocated to green infrastructure. Uses Cadastral data to establish the road corridor width and design boundary, centre line. Allows 3d data/city model as model input.
- **Vegetation.** Optimizes tree positioning and selection to maximise shade. Simulates tree growth over time.
- **Environmental.** Calculated sun exposure for any location. Calculated wind exposure for any location.

The Street Design Tool was developed using Rhino3D, Grasshopper & Python. The SDT has four major components:

- **Centreline. Linear** infrastructure is identified by its centreline. User of the system is to provide the associated centreline of the road.
- **User Interface.** As part of the UI development, a collection of components was developed in Grasshopper using Python. These components served as a data entry point to the system. User input are captured and stored in a self-explanatory *.JSON Data Format. By utilising this data structure, the system became scalable. It also allows for future integration of the tool into a later proposed web-based applications, using languages such as JavaScript. Additionally, some descriptive metadata can be captured from the user. (See Figure 1 - below).
- **Stack Of Elements.** All collected data from users are captured and stored in a sorted list. Each element in list describes an individual component of the road (see Table

computational landscape architecture publications (White et al., 2020) for the 'tree component' to visualise simulated plant growth. Other components such as materials will follow. This research is a significant step as it allows a user to design streets with a computer-aided tool that contains knowledge on the various elements of a street.

7. Conclusion

The tool in its current iteration has its limits. It is yet not able to work on intersections nor can one segment the street into smaller elements that are all designed individually, i.e. the street in front of each cadastre looks different due to driveways or above ground and below ground services that would not allow i.e. large trees - nor has it been tested.

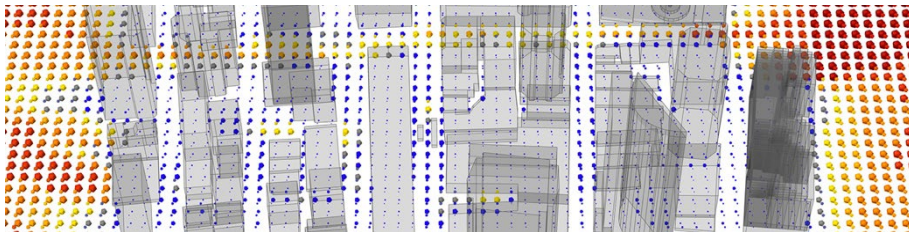


Figure 3. 'Next Steps - Development of a voxel-based air temperature calculation tool'.

These are features that we aim to develop and address in the tools next iteration as future research as well as building up each 'component' to a greater level of detail. While we argue that the research up to this stage could demonstrate first steps towards answering the first research question of 'What can computational design with its methods and tools offer to reduce heat at the urban scale when concentrating on street layout and design?' one important question (Research Sub Question 2) has not yet been answered with the tool - 'How can these computationally enabled changes in street layout and design towards reducing heat be verified by visualising the difference in air temperature via voxel display?' In parallel we are working on the development of a voxel-based air temperature calculation tool (see Figure 3) to address this question.

References

- Akbari, H. (2002). Shade trees reduce building energy use and CO2 emissions from power plants, *Environmental Pollution*, 116(1), 119-126.
- Akbari, H. (2009). *Cooling our Communities: A Guidebook on Tree Planting and Light-Coloured Surfacing*. USEPA.
- Austrroads (2021). *Guide to Road Design*, ISBN 978-1-922382-48-, Austrroads Ltd.
- Avison, D. (1999). Action Research, *Communications of the ACM*, 42(1), 94-97
- Climate Council (2019). *The angriest summer*. Retrieved December 3, 2021, from <https://www.climatecouncil.org.au/wp-content/uploads/2019/03/Climate-council-angriest-summer-report.pdf>
- Gartland, L. (2008). *Heat Islands*. Washington, Earthscan.
- Gartland, L. (2012). *Understanding and Mitigating Heat in Urban Areas.*, Earthscan.
- Gehl, J. (2013). *Cities for people*. Islandpress.
- Green, S., King, G., Fabbri, A., Gardner, N., Haeusler M.H., and Zavoleas, Y. (2019). *Designing Out Urban Heat Islands - Optimisation of footpath materials with different*

- albedo value through evolutionary algorithms to address urban heat island effect. In: M. Haeusler, M. A. Schnabel, T. Fukuda (eds.), *Intelligent & Informed - Proceedings of the 24th CAADRIA Conference - Volume 2*, pp. 603-612.
- Hamilton, W., Butler, A., Gardner, N., Haeusler, M.H., Ramos, C. and Zavoleas, Y. (2020). Keeping up with the Code - Communicating the Decision-Making History of Architectural Scripts. In: Werner, L and Koering, D (eds.), *Anthropologic: Architecture and Fabrication in the cognitive age - Proceedings of the 38th eCAADe Conference - Volume 1*, pp. 633-642.
- Hart, M. and de Dear, R. (2004). Weather sensitivity in household appliance energy end-use. *Energy and Buildings* 36(2): 161-174.
- IPCC (2021). *Climate Change 2021*. Retrieved December 3, 2021, from <https://www.ipcc.ch/report/ar6/wg1/>
- Irger, M. (2014). *The Effect of Urban Form on Urban Microclimate*, PhD Thesis, Built Environment, Faculty of Built Environment, UNSW
- Kemmis, S. (2009). Action research as a practice-based practice, *Educational Action Research*, 17(3), pp. 463-474
- Kolokotroni, M., Giannitsaris, I. (2006). The effect of the London urban heat island on building summer cooling demand and night ventilation strategies. *Solar Energy*, 80(4), 383-392.
- Kuttler, W. (2011). Climate change in urban areas, Part 1, Effects. *Environmental Sciences Europe*, 23(1): 11.
- Kuttler, W. (2012). *Climate Change on the Urban Scale – Effects and Countermeasures in Central Europe*. Human and Social Dimensions of Climate Change. N. Chhetri.
- Kurn, D., S. Bretz, B. Huang, and H. Akbari. (1994). The Potential for Reducing Urban Air Temperatures and Energy Consumption through Vegetative Cooling, *ACEEE Summer Study on Energy Efficiency in Buildings*, American Council for an Energy Efficient Economy. Pacific Grove, California.
- O’Brian, R. (2001). An Overview of the Methodological Approach of Action Research. Available from Roberto Richardson (Ed.) *Theory and Practice of Action Research*, João Pessoa, Brazil: Universidade Federal da Paraíba. (English version)
- Oke, T. R. (1988a). Street design and urban canopy layer climate. *Energy and Buildings*, 11(1-3): 103-113.
- Oke, T. R. (1988b). The Urban Energy Balance. *Progr. in Phys. Geography*, 12(4): 471-508.
- McPherson, E.G., J. R. Simpson, P. J. Peper, S. E. Maco, and Q. Xiao. (2005). Municipal forest benefits and costs in five US cities. *Journal of Forestry*, 103(8), 411–416.
- Mohammed, A., Khan, A., Santamouris, M. (2021). On the mitigation potential and climatic impact of modified urban albedo on a subtropical desert city, *Building and Environment*, 202, Elsevier.
- Müller, N., Kuttler, W., & Barlag, A.-B. (2014). Counteracting urban climate change: Adaptation measures and their effect on thermal comfort. *Theoretical and Applied Climatology*, 115(1-2), 243–257.
- Stewart, I. & Mills, G. (2021). *The Urban Heat Island*, Elsevier Publications
- Watkins, R., J. Palmer, et al. (2007). Increased Temperature and Intensification of the Urban Heat Island: Implications for Human Comfort and Urban Design. *Built Environment*, 33(1): 85-96.
- White, M; Haeusler, M.H, Zavoleas, Y (2020). Simulation of Plant-Agent Interaction in a Landscape Information Model, *Journal of Digital Landscape Architecture*, 5(2020), 188-197.
- WMO (2021) *State of Global Climate*. Retrieved December 3, 2021, from <https://public.wmo.int/en/media/press-release/state-of-climate-2021-extreme-events-and-major-impacts>

BUILDING RESILIENCE

Using Parametric Modelling and Gaming Engines to Simulate the Impacts of Secondary Structures in Bushfire Events

ANASTASIA GLOBAL¹, DAGMAR REINHARDT², ADRIENNE KEANE³ and PETER DAVIES⁴

^{1,2,3} *The University of Sydney, School of Architecture, Design and Planning.* ⁴*Macquarie University, Faculty of Science and Engineering*

¹ *anastasia.globa@sydney.edu.au, 0000-0002-4749-5675*

² *dagmar.reinhardt@sydney.edu.au, 0000-0003-0477-492X*

³ *adrienne.keane@sydney.edu.au, 0000-0002-6991-8528*

⁴ *peter.davies@mq.edu.au, 0000-0002-2711-891X*

Abstract. Bushfires are a global phenomenon, closely connected to climate change and safety, resilience and sustainability of cities and human settlements. Government agencies, architects and researchers across institutions are committed to improving Australia's resilience to bushfires yet grappling with ways to further mitigate risks. 'Build back better' is the often-used phrase to support bushfire resilience, yet there remains a limited understanding of how secondary structures, such as storage sheds, garages, and fences contribute to or mitigate fire loss. These secondary structures are integral to properties yet fall, largely, outside land use planning approval processes and other regulations. Computational modelling can be adapted to deliver visualisations that increase awareness. We developed several simulation approaches which addressed distances, relationship to and the construction materials of secondary structures, terrain slopes and environmental forces. We conclude that gaming engines may offer the optimal immersive opportunity for residents and others to visualise fire risks related to secondary structures to increase awareness and improve bushfire readiness behaviours.

Keywords. Bushfire; Simulation; Game Engine; Visualisation; SDG 11.

1. Introduction

Bushfires are a global phenomenon, closely connected to climate change, rising temperatures, and dry vegetation (Van Oldenborgh, et al. 2021). The 2019/20 Black Summer bushfires devastated communities throughout NSW (Australia) with over 3000 homes lost (Australian Institute for Disaster Resilience, 2022). Reflecting the aims of Sustainable Development Goal 11 government agencies, councils, architect

chapters, and researchers across institutions are committed to improving Australia's resilience to bushfires yet are grappling with ways to further mitigate future disasters and ask better questions to address risk and rebuild in a way that offers safeguards against environmental and structural damage in the future.

To build back better, understanding the resilience of structures affected by bushfires is critical. Bushfire resistance of buildings, including construction, typologies, materials, and siting has been subject to extensive research and consequent changes to building codes. However, less is known about the behaviour of secondary or auxiliary structures and outbuildings, collectively referred to in this paper as secondary structures. These are inclusive of Class 10 structures, defined by the National Construction Code, Volume 1 (Australian Building Codes Board 2019), which are structures subject to state policies where no development application or approval is required, such as "ancillary" or exempt development provisions of the NSW planning system, or which are simply unregulated in terms of their location on a lot and construction quality. These range from permanent to semi-permanent structures such as storage sheds, garages, and fences, but also include temporal assemblies which can play a significant role in elevating fire risks such as wood stacks, garden furniture or domestic debris.

Numerous studies have reported that these structures can serve to protect or contribute to the loss of houses as a source of heat and ember attack. Consequently, this research focuses on the impact of secondary structures (Brown 2018) and user habits/adaptations of plots that may or may not fall outside of land use planning regulations on their fire promotion or resilience in bushfire prone areas. We focus also on distances, relationship to and construction of secondary structures, materials, terrains and environmental forces that can contribute to fire progression and consequent loss of habitable structures through ember attack, radiant heat or direct flame.

There are various ways in which fire behaviour can be simulated digitally, including parametric modelling, use of game engines, or dynamic simulations. Phoenix Rapidfire was developed in 2014 as a Bushfire Simulator (2014). Recent visualisation of a bushfire spread simulation adopts SPARK software developed by CSIRO using the Workspace workflow engine. In this study we focus on the development of a simulation and interface that deploys critical aspects of secondary structures by using Grasshopper3D and game engine Unity3D. Figure 1 illustrates the workflow, input, and output parameters of both approaches that were adopted in this study, further detailed in sections 3.2.1 and 3.2.2.

In the following, the paper provides a background to the phenomenon of bushfire and gaps in legislative framework for structures. Methodologies and simulation approaches are introduced and discussed as a first pilot study into best practice for visualisations through parametric modelling that increase understanding for the impacts of secondary structure placements in bushfire prone areas. The paper concludes with an evaluation of results and an outlook to future research.

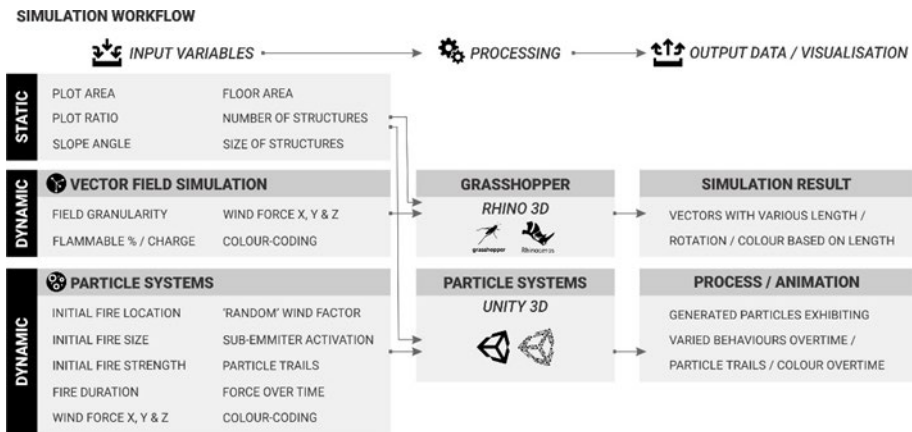


Figure 1. Simulation workflow: input / Processing / output for 2 tested approaches.

2. Background

Bushfires destroy houses and have significant environmental, social and economic impacts (Stephenson et al. 2013). They are becoming more frequent, larger and fiercer (Canadell et al. 2021). Research into the impacts of bushfires on houses has mostly identified the proximity of houses with bushland or vegetation as being the major factor for bushfire destruction. For instance, Crompton et al (2010) in their analysis of building damage and fatalities as part of the 2009 Black Saturday fires identified 25% of building damage occurred to properties located within a bushland setting and 60% of losses were less than 10m from the adjoining bushland. Such findings have supported various policies such as the 10:50 vegetation clearing policies, in effect giving the ability of a landholder to clear vegetation within 10m of a structure without consent from an authority, with some restrictions (Salgo and Gillespie 2018). Bushfire induced property loss and proximity to bushland has also been confirmed in studies in Europe and North America (Ganteaume et al. 2021; Masoudvaziri et al. 2021).

As cities grow and the need for housing people intensifies, planners are faced with the dilemma of where new housing should be located. Driven by economic and social pressures, some city responses include growing cities at their fringes and in the interface with bushland while cognisant that these areas are more vulnerable to bushfires. Increasingly these subdivisions and developments therein are the subject of increasing standards and regulations to manage bushfire risks reflecting policy gaps of the past (Ganteaume 2021). In NSW the cornerstone is provided by the Planning for Bushfire Protection guideline that links together planning and bushfire laws with building and construction standards, property to bush firefighting operational and maintenance requirements, and vegetation clearing maintenance among other elements. From a building perspective, the new standards are prospective and do not cover the extent of risks that may arise from secondary structures.

Research into the cause of bushfire destruction of homes has demonstrated that fire damage is magnified by the proximity of buildings and secondary structures, whereby fires, through ember attack, radiant heat or flame, can travel from one structure to

another (Blanchi and Leonard 2005). Given the complexities that relate to property loss associated with bushfires, few studies offer any clear statistical relationship between the inter-structure proximity and loss (Costin 2021) while greater research attention has focused on the proximity of a structure and bushland. Roberts et al. (2021) modelled the effects of embers on property loss. In developing their risk calculations, they note that the risk will be influenced by many variables that relate to the natural and built environments. For the purpose of impact on buildings, this includes a range of considerations such as choice of building materials, the shape and orientation of homes and other structures (Syphard et al. 2012), the distance between structures, and the presence of shade sails, decks, and pergolas. From a risk mitigation perspective, the direction of the prevailing wind, thus ember attack, can have a significant impact on mitigating bushfire loss. To reduce the risk of short-range embers, for example, the construction of non-flammable structures, such as high metal fences, water tanks, sheds constructed to bushfire standards upwind of a house may reduce ember attack.

3. Method and Simulation approaches

Simulation models have been applied to understand fire behaviour (Garcia 2003), fire progression (Ohgai et al., 2005), firefighting activities, building evacuation (Jabi et al., 2019) and fire management. While this research has focused on primary dwellings and largely fire progression, our aim is to increase the understanding of and investigate the impact of secondary and auxiliary structures in bushfire-prone areas. A criteria framework has been developed and explores the use of algorithmic modelling tools and gaming engines to simulate the impacts of auxiliary structures in bushfire events. This leverages the affordances of computation and simulation tools that enable the rapid visualisation of various scenarios, controlling crucial parameters related to both environmental forces and urban conditions.

It should be acknowledged that the aim of this study is not to predict the spread of fire with full accuracy. Precise fire simulations are extremely hard to achieve because they involve many fluctuating variables and uncertainties (Cox 1994). Instead, this study aims to simulate and effectively communicate via visualisations the fundamental inter-dependencies of the fire-spread probability. The overarching goal is to make these visualisation methods available to a range of stakeholders, including urban planners, architects, legislators, and dwellers themselves, and to communicate the importance and potential impact of secondary structures within a lot on the spread of fire.

Initial investigation into the parameters of typical dwelling configurations in the context of Australia has revealed that in recent years the relationship between the size of a house and the size of a land plot has shifted dramatically (Hall, 2010). Comparing between 2005-2006 and 2019-2020 (for newly built houses) across five capital cities, the sizes of plots are shrinking while the sizes of houses (floor area) are growing. When calculating a *combined average land area for the 'unbuilt' spaces (plot area minus house floor area), in 2006 this measured 368m² and in 2020 was reduced to 219m². This means that the average 'unbuilt' area surrounding the main dwelling has reduced by 42% over 15 years. This highlights two bushfire risks: greater urban densities and a consequent lessening of space between houses; and the reduced available distance between various secondary structures and the primary dwelling.

3.1. CRITERIA FRAMEWORK

The primary setup for our multi-criteria parametric model has considered a range of conditions to describe and explore the impact of auxiliary structures. Data from a 2020 survey on the average sizes of house plots and dwellings were used as a reference point for a range of context iterations, testing for both smaller and larger than average scenarios. The average plot size considered was 467m², with a floor area of 248m², slope angle of <5 degrees and a plot width-to-length ratio as 1x2. Twenty-four iterations of static input variables (Figure 2) were explored in this generative study including: plot area, plot ratio, slope angle, house floor area, number of secondary structures and their size that were used as the ‘static context’ or ‘base scenarios’ to test two simulation approaches adopted in this study.

As illustrated in figure 1 the test criteria were split into two distinct groups: 1) static input variables and conditions that relate to the attributes of ‘solid’ structures, surfaces and objects in the system; and 2) dynamic input variables that relate to the internal or external ‘forces’ such as wind strength and direction and flammable potential ‘charge’ of elements in the system, that could fluctuate due to humidity or temperature. Static variables have informed the experimental set-up: dimensions and configurations of the house and the land plot; location of the main dwelling and secondary structures, with distances/ proximity to dwelling or themselves; size and number of secondary elements; volume and dimensions of the main dwelling and terrain (flat / slightly or lot sloped). The dynamic input variables included: flammable / non-flammable materials, and buildings addressed as conductors (the ‘charge’: stop or propagate fire); and the location, strength and directional force (wind) direction and force of ‘fire’ propagation.

3.2. ALGORITHMIC MODEL AND GAME ENGINE IMPLEMENTATION

We compared two fire spread probability methods, examining their affordances and limitations. Firstly, a series of parametric models using Grasshopper3D; and secondly, using a gaming engine - Unity3D. Due to major differences in algorithmic logic of the developed simulation approaches and the limitations of software functionality the dynamic input variables were slightly different between the approaches (Figure 1), however static input variables remained the same for both test groups.

3.2.1. Vector Field Visualisation in Grasshopper3D

Visual programming in Grasshopper3D allows for development of sophisticated algorithms that can generate various forms, forces, and conditions in three dimensions. Several Grasshopper plugins were considered to be adopted for this study, including agent-based modelling in Physarealm plugin, utilising the shortest-path logic and allowing to introduce obstacle-objects within the constructed system; and RhinoCFD plugin, that uses computational fluid dynamics. The initial testing revealed these plugins were not the best match for the intended simulation scenario, being too restrictive and limited in their capacity to accommodate our established simulation objectives. For example, in the proposed scenario secondary structures should act as secondary sources of fire instead of merely being obstacles. Therefore, it was decided to develop algorithmic definitions bypassing any additional plugins and focus on a visualisation of a Vector field, applied to all 24 context configurations to illustrate the

variety of results depending on the input parameters.

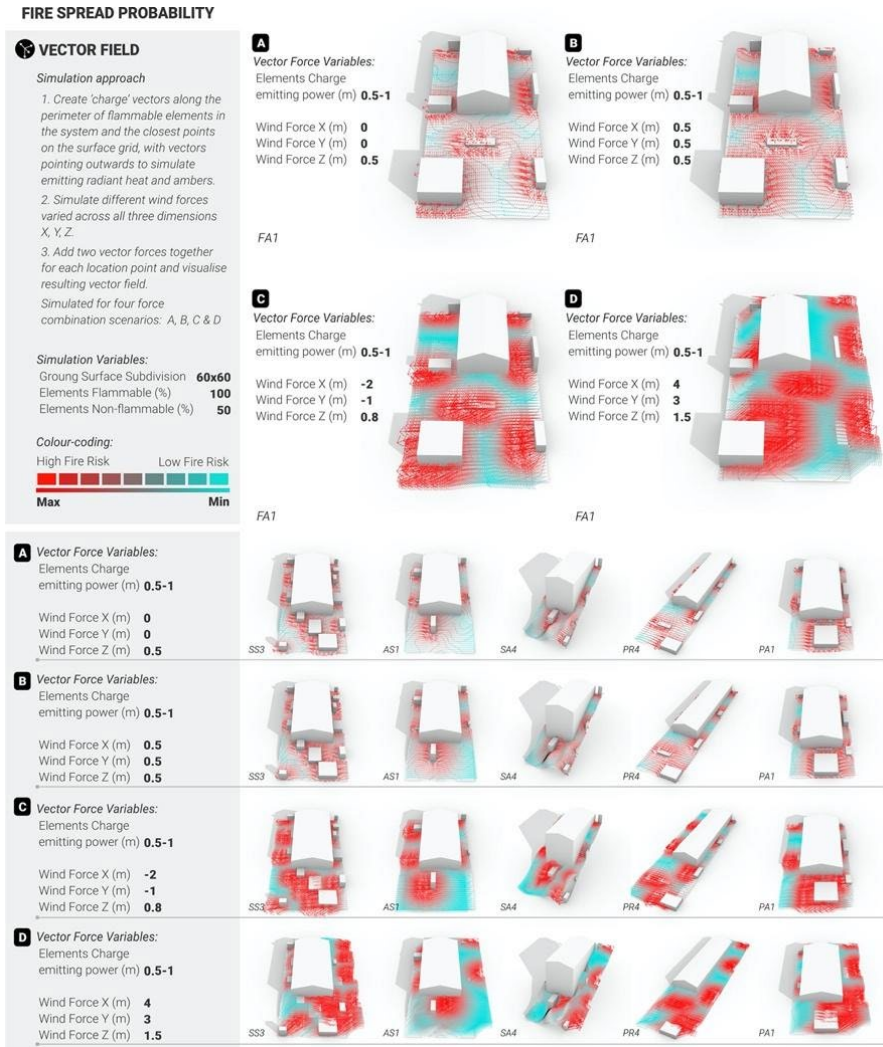


Figure 2. Vector Field visualisation approach using Grasshopper3D

The Vector Field approach was developed to simulate the effect of environmental forces - wind strength and direction in particular. This approach assumes that different elements in the system will have different directional fire potential / vector 'charges' (Figure 2). The algorithmic logic of this visualisation method progressed as follows: 1) secondary structures were assigned outward-facing 'positive charges'; 2) these charges were used to generate a vector field on the land-surface, with vectors located closest to the flammable objects facing perpendicular to the source objects and being longest and then becoming progressively shorter and cancelling each other out; 3) an external force

was created, affecting the length and direction of all initial vectors - representing the wind. The resulting vector field was colour-coded based on the length of each vector, with red representing high fire risk areas and blue representing low fire risk areas.

3.2.2. Particle Systems in Unity3D

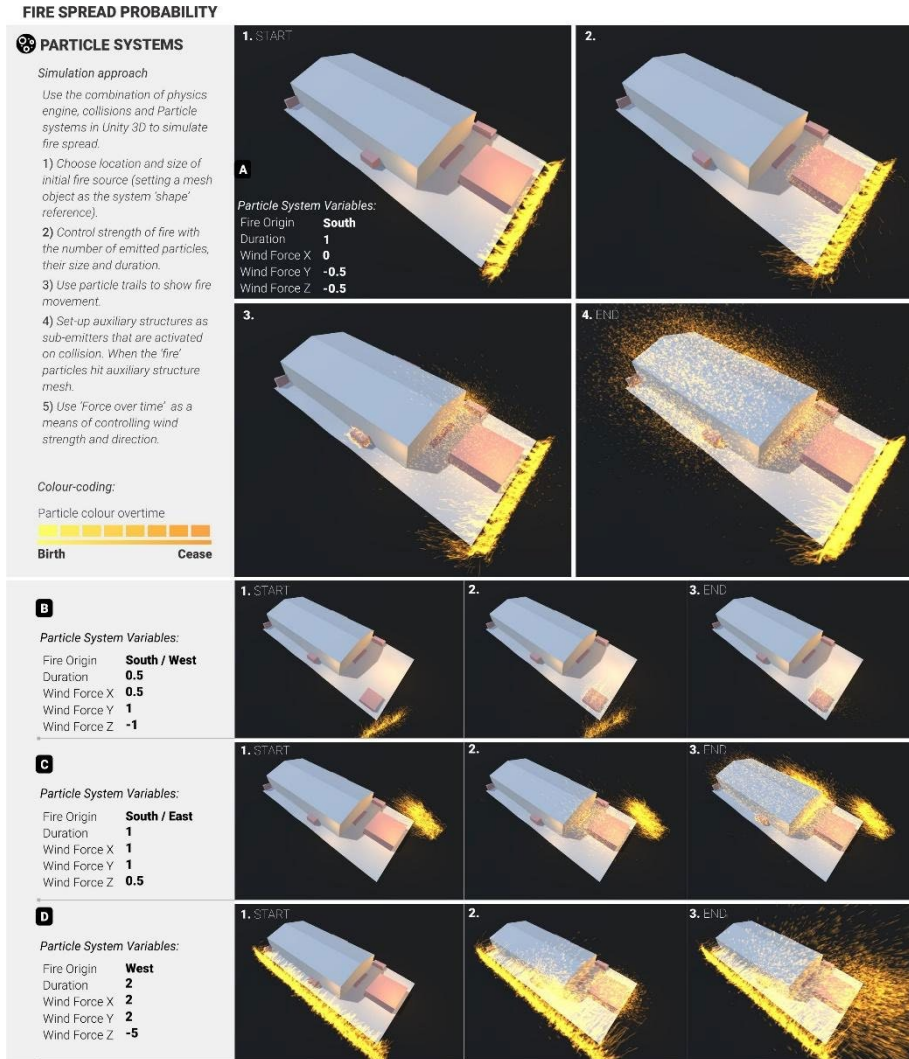


Figure 3. Particle Systems visualisation approach using Unity3D

A second stage of the fire-spread visualisations was implemented using advanced simulation capabilities of a game development platform - Unity3D. Unity3D is a powerful tool that has in-built Physics and Particle systems packages and can be

customised and adapted to simulate complex particle or agent behaviours, such as fire spread. For the Particle System visualisation approach our initial static 'design context' or setup, which included the land plot, main dwelling, and secondary structures, were imported to Unity directly from Rhino as solid /collidable mesh geometries via FBX files. A particle system was introduced into the scene to simulate the fire spread that determined multi-criteria fire/particle behaviour (Figure 3).

The prototype of the fire spread particle system was developed from the KriptoFX Mesh Effect 6 prefab. The input parameters for the resulting system included: 1) the location, shape and size of the fire origin was set as initial particle-emission source; 2) intensity of fire was regulated by the number, size and lifetime of particles; 3) environmental forces such as wind were simulated using the 'force overtime' function; 4) fire particles' paths and movement were visualised using particle 'trails'; 5) colour-coding was set as time-dependent, where at birth particles were bright yellow but gradually changed colour to orange closer to their end-of-life; 6) secondary structure geometries were set as customisable sub-emitters to be triggered at collision. Several scenarios were tested for varied fire locations and wind forces (direction and strength). Particle systems allowed the incorporation of 'random direction' movement criteria for particles, which helped to simulate different wind changes and gusts.

4. Discussion

Reducing the risks of natural disasters and their impacts on urban settlements remains a core element to meeting the SDG 11 sustainable cities and communities. While this research has focused on secondary structures, this is significant as urban developments are projected to increase their spread into the present peri-urban and often bushland areas and increase in density that is likely to increase bush fire risk. While research on the impact of secondary structures as a contributory factor to fire risk is nascent, past major bushfires in Australia point to the importance of structures from a risk and loss perspective.

We suggest visualisation tools can support individuals in their decision making yet there is a porosity of this research for fire risk from a behavioural perspective. Our study has developed and compared visualisations from different fire spread probability methods. Both developed simulation approaches have high potential of bringing new insights and rising awareness among key stakeholders (such as homeowners, designers, builders and legislators) regarding the role of auxiliary structures in relation to the potential spread of fire. The simulation results suggest that the particle animation (Figure 3) is successful as a visualisation due to highly appealing graphics and simpler user navigation. As the Unity software supporting this approach uses a gaming engine, this further has the potential for fire simulations as immersive first-person VR or AR applications. This communication and engagement tool may offer individuals a wider range of sensory experiences and support fire awareness and thus preventive behaviours. Specifically, the impact of secondary structures (which may otherwise bypass land use planning assessment processes as they are not subject to fire rating construction standards) may be better understood as users relate to, configure, and use spaces within the lot. Care however needs to be undertaken when interpreting these results as the modelling does not purport to model fire behaviour.

Achieving change in how secondary structures are considered as a bushfire risk will

require a concerted effort involving interdisciplinary approaches across architecture, planning, construction, modelling and community engagement. Our fundamental goal is to inform and influence behaviour (Brown 2018) to manage bushfire risks from those structures and activities that are left unregulated.

5. Conclusion and Future Research

This research illustrates alternative visualisation methods to enable users to better understand the consequences of decisions in relation to what and the placement of secondary structures in bushfire-prone areas. The aim of this empirical study has been to explore approaches and frameworks for bushfire risk visualisation.

Future research will further develop the utility of 3D data and simulation packages towards predictive modelling and pilot the output of the modelling with residents in a bushfire affected area to test its ability to inform and manage household-level risks associated with secondary structures. Future iterations of this study will involve further development of additional and more advanced simulation approaches and testing their implementation with potential stakeholders. The testing will include both comparative studies, evaluating the effectiveness of approaches separately and testing them as a complementary set of visualisations. Through benchmark testing, collaborations with councils and stakeholders on open-access data resources, we aim to provide crucial information on structural resilience and guide and support individuals one step closer to future proofing their house and local communities.

References

- Australian Building Codes Board (2019). National Construction Code, Volume One. Canberra, Australian Building Codes Board.
- Australian Institute for Disaster Resilience. (2022). Bushfires - Black Summer. Australian Disaster Resilience Knowledge Hub, <https://knowledge.aidr.org.au/resources/black-summer-bushfires-nsw-2019-20/>
- Blanchi, R., & Leonard, L. (2005). Investigation of bushfire attack mechanisms resulting in house loss in the ACT bushfire 2003. *Bushfire CRC*. Highgett, Victoria.
- Brown, D.N. (2018). Domestic Architecture and the Perception of Risk in Bushfire-Prone Areas, The University of Sydney. Unpublished PhD thesis.
- Canadell, J. G., Meyer, C.P, Cook, G D, Dowdy, A, Briggs, P.R, Knauer, J, Pepler, A., & Haverd, V, (2021). Multi-decadal increase of forest burned area in Australia is linked to climate change. *Nature Communications* 12(1): 6921.
- Costin, G. P. (2021). Bushfire: Retrofitting Rural and Urban Fringe Structures—Implications of Current Engineering Data. *Energies (Basel)* 14(12): 3526.
- Ganteaume, A., Barbero, R, Jappiot, M and Maillé, E, (2021). Understanding future changes to fires in southern Europe and their impacts on the wildland-urban interface. *Journal of Safety Science and Resilience* 2(1): 20-29.
- Garcia, R. (2003). Feeling the Heat - Exploring the Impact of Fire in Architectural Structures though Multimodal Interaction. *10th International Conference on Computer Aided Architectural Design Futures*. Taiwan.
- Hall, T. (2010). Goodbye to the Backyard? -The Minimisation of Private Open Space in the Australian Outer-Suburban Estate. *Urban Policy and Research* 28(4): 411-433.
- Jabi, W., Chatzivasileiadi, A, Wardhana, M. M., Lannon, S., and Aish, R. (2019). The synergy of non-manifold topology and reinforcement learning for fire egress. *Architecture in the Age of the 4th Industrial Revolution - Proceedings of the 37th eCAADe and 23rd*

- SIGraDi Conference*. J. Sousa, J. Xavier and G. Castro Henriques. Porto, Portugal, University of Porto. 2: 85-94.
- Masoudvaziri, N., Szasdi Bardales, F., Keskin, O.K., Sarreshtehdari, A., Su, K., and Elhami-Khorasani, N., (2021). Streamlined wildland-urban interface fire tracing (SWUIFT): Modeling wildfire spread in communities. *Environmental Modelling & Software* 143: 105097.
- NSW Government, N. (2008). State Environmental Planning Policy (Exempt and Complying Development Codes) 2008. NSW Government.
- NSW Rural Fire Service (2019). Planning for Bush Fire Protection, NSW Government.
- Ohgai, A., Gohnai, Y., Ikaruga, S., Murakami M., and Watanabe K., (2005). Japan Cellular Automata Modeling for Fire Spreading as a Tool to Aid Community Based Planning for Disaster Mitigation. *Recent Advances in Design & Decision Support Systems in Architecture and Urban Planning* J. P. van Leeuwen and H. Timmermans, J.P. Dordrecht, Kluwer Academic Publishers: pp. 193-209.
- Roberts, M. E., Rawlinson, A.A., and Wang, Z., (2021). Ember risk modelling for improved wildfire risk management in the peri-urban fringes. *Environmental modelling & software: with environment data news* 138: 104956.
- Stephenson, C., Handmer, J., and Betts, R (2013). Estimating the economic, social and environmental impacts of wildfires in Australia. *Environmental hazards* 12(2): 93-111.
- Syphard, A. D., Keeley, J. E., Massada, A. B., Brennan, T. J., & Radeloff, V. C. (2012). Housing arrangement and location determine the likelihood of housing loss due to wildfire. *PloS one*, 7(3), e33954.
- Van Oldenborgh, J., Krieken, G., Lewis, S., Leach, N.J, Lehner, F., Saunders, K.R., Haustein, K., Sparrow, S., and Arrighi, J., (2021). Attribution of the Australian bushfire risk to anthropogenic climate change. *Natural hazards and earth system sciences* 21(3): 941-960)

DECENTRALISED SOLAR ECONOMY: UNATTENDED AND SMART SOLAR ENERGY URBAN SYSTEM (UNSSEUS)

PROVIDES NG¹, DAVID DORIA², and ALBERTO FERNANDEZ³

¹ *The Chinese University of Hong Kong*

^{2,3} *Bartlett School of Architecture, UCL.*

^{1,2,3} *rationalenergyarchitects@gmail.com*

¹ *0000-0001-6975-4642*

² *0000-0001-5152-0098*

³ *0000-0002-1411-1284*

Abstract. Planners often go out of the city when planting large-scale solar farms due to requirements for huge, flat surface areas. This reduces urban proximity to renewable energy sources, causing dissipation during energy transfer and a waste in solar energy unused within urban areas. This paper aims at understanding the prospect and challenges in transforming buildings from passively consuming energy to actively generating energy for cities. As every building has a different renewable energy capacity, how may we re-distribute power amongst a network of users, forming a socio-economy around distributed power generation? This paper first presents its theoretical approach learning from fields of biology and information theory as a source of inspiration for its design methodology. It then presents a context study of Hong Kong and its Feed-in Tariff scheme that incentivizes distributed power generation, and identifies the challenges. Afterwards, it defines ‘Unattended and Smart Solar Energy Urban System’ and proposes the parameters which the system should comprehend on its dashboard for demand-side management of energy. Finally, preliminary results of using a sudoku algorithm in distributing time and pricing factors of energy exchange are presented. This on-going research project aims at SDG goals 7 and 11.

Keywords. Distributed Power Generation; Sudoku Gameplay; Unattended and Smart, Solar Energy; Urban System; SDG 7; SDG 11.

1. Introduction

Distributed generation is ‘electrical generation and storage performed by a variety of small, grid-connected or distribution system-connected devices’ (VirginiaTech, 2007). In particular, distributed solar power generation may enable individuals to supply and trade energy they harvested locally with photovoltaic (PV) elements. In densely populated urban environments, emerging smart materials such as thin-film and perovskite that are semi-transparent, flexible and economical in construction enables

light-harvesting on facades and other building surfaces (MacDonald et.al, 2019). With computational advancements in generative and predictive methods, novel networking strategies may enhance efficiency in energy exchanges and self-organisations. Information systems that feedback between a distributed network of users requires the design of mass sensing, actuating, and controlling components - a smart system. This highlights distributed generation not merely as a problem of technical engineering, but also socioeconomic engineering - a decentralised solar economy. This paper aims at discussing the significance of distributed generation in formulating unattended and smart solar energy urban systems (UnSSEUS) .

2. An Info-biological Approach to Solar Design

There is an increasing amount of research that looks at organisms and their interactions with information theory, which enables socio-biological processes to be captured computationally. Krakauer's (2020) Information Theory of Individuality (ITI) and Friston's (2019) Free Energy Principles (FEP) are two leading theories that relate entropy and prediction with scaled self-organisations. In particular, to understand energy exchanges in organisms through how information is acquired, disseminated, and used amongst individuals; this information can be inherited or inferred - from DNA topology to natural languages. The study of ITI and FEP may help us to map the limit to growth, networking between individuals, and a scaled measure of energy sustainability.

These info-biological theories aim at identifying an individual from its environment, providing philosophical and technical approaches towards understanding 'intelligence' (Krakauer, 2020). Within rapid socio-biological exchanges, the boundaries that set one individual apart from another becomes less apparent, where we may have common assumptions on individuality, with diverging views on its definition (Ng, Odaibat, Doria, 2020). When applied in data analysis of a dynamic environment, statistical boundaries may be mapped from input data, with no definite means to setting apart anomalies in a discriminative model. This illustrates why the identification of an individual might be crucial in dealing with mass exchange processes; with which we may begin to gain insights towards how one interacts with another, and how to enhance energy and information exchanges.

ITI and FEP both follow an entropy approach in identifying an individual within a complex system. In FEP, Friston (2019) stated that an individual is one that maintains equilibrium using an internal generative model to predict incoming sensory data and minimise entropy (i.e. surprises or disorder in information) towards its immediate environment - a form of active inference. Thus, intelligence is negentropic (i.e. negative entropy). The measure of entropy change over time within a dynamic system provides us with information towards the future evolution of the system, and act as a guide towards how much available energy a system should have in doing useful work (i.e. second law of thermodynamics)

(Ben-Naim, 2010). In ITI, West and Brown (2005) stated that living organisms tend to minimise energy consumption by a quarter everytime it doubles in size, as the pace of life becomes slower (e.g. lower heart rate) - nonlinear power scaling. Currently, our cities generally consume 15% more energy everytime it doubles in size (West, 2014). The exponential power-scaling of urban organisation in contrast to quarter power-

scaling of biological organisation shows us an entropy limit that may help to guide our solar strategies. An entropy limit captures the loss in energy ‘over the range of motion of the working body’; meaning, our current urban organisations have to reach a higher level of negentropic capacity (~40%) for it to be efficient within the Earth’s energy chains (Krakauer, 2020).

From distributed communication of ants, regulatory systems of cells, to feedback dynamics of neural nets, ITI and FEP define quantitative measures for networking within self-organisations. The study of which may help in tackling scalability issues - efficiency in synchronising information - which defines the limit to growth and resist the tendency to disorder (Friston, 2009). Networks can be captured and described using topologies and simulated through combinatorial games (Xu, 2001). The former is the arrangement of nodes and their connections in a communication network, and may be depicted physically or logically; logical topology determines how data flows in a network using system protocols (Groth & Skandier, 2005; Wynkoop, 2003). The latter is a branch of game theory and theoretical computer science that ‘draws tools from combinatorics, algebra and number theory to generate results for itself’ (Fraenkel, 1996). This paper will later focus on applying sudoku - a one-player combinatorial puzzle - in simulating energy networking between architectural components.

3. Context Study - Hong Kong

Hong Kong (HK) is one of the most densely populated cities, implying a high level of concentrated energy consumption. In 2019, HK launched a ‘Feed-in Tariff’ (FiT) scheme, where electricity generated with solar power can be sold back to electricity companies up to 5 times higher than normal electricity tariff rate (HKSAR, 2020). There are many FiT initiatives worldwide, HK’s FiT goal is to incentivise private sectors (mainly low-rise buildings like village houses) to install PV systems to compensate for HK’s modest renewable energy potential due to natural and geographical constraints.

Table 1: Ballpark parameters of a typical village house in HK for PV systems (HKSAR, 2019)

Number of village houses in HK	~ 30,000
Average roof area	~ 700 square feet
Annual electricity consumption	~ 4560 kW (380 units x 12 months)
Annual electricity generation by PV	~ 7000 kW
PV construction / installation cost	~ HK\$210k - 350k
Payback period	~ 4-7 years (based on a FiT rate at HK\$5 per kW)

It can be expected that most village houses are likely to generate much more electricity than the household would consume if they fully utilise their rooftops. On the other hand, emerging smart materials may help in utilising building facades and even bringing PV elements to the interior (Papakonstantinou, 2021). This makes the need for a localised energy distribution strategy, where adjacent buildings can collaboratively generate and consume solar power.

4. Unattended and Smart Solar Energy Urban System (UnSSEUS)

Table 2: Objectives for an Unattended and Smart Solar Energy Urban System (UnSSEUS)

Unattended	Any system that can be left unattended for its self-sufficient network that harvest energy from renewable sources; a system that ‘intelligently manages energy transfer for perpetual operation without human intervention or servicing’ (Jiang, et al., 2005).
Smart	A network of sensing, actuating, and controlling components, ‘making decisions based on available data in a predictive and adaptive manner’ (Rodrigues, 2020).
Solar Energy	Solar energy is a renewable energy source, generating electricity with PV elements.
Urban	Instead of transporting solar energy from afar locations, more organic designs can help to embed solar devices in urban structures. Also, to prevent the loss of solar energy in cities from direct and indirect sources (e.g. reflections from buildings and reflective surfaces, corners unused, large open spaces at public areas like universities, etc.).
System	A network strategy that does not promote congestion due to differences in protocols and varying development rates across urban fabrics. This would require collaborative dynamics between adjacent buildings, and across various building scales: Micro (building components and their formal organisations) Intermediate (components ensembles into local feedback groups at the building scale) Macro (building and infrastructural populations adapt, change, and grow)

Almost every city has relative proximity to solar energy with potential for decentralisation - light harvested in an area can be localised and used without having to be transmitted back and forth to central power stations (e.g. charging your phone directly from light harvested on a plaza bench). The immediate advantage would be a reduction in energy absorption by the power grid, which is often sustained using fossil fuel, thus becoming environmentally friendly (Miozzo, 2014). Primary batteries ‘do not scale up well for long term installations. Instead, energy harvesting methods must be used’ (Kimball, et al., 2009). Within rigorous energy and information feedback between a network of buildings, UnSSEUS can help in self-organisation and maintaining equilibrium between different parts and components of the city’s power grid - demand-side management (DSM). It is ‘the planning, implementation, and monitoring of those utility activities designed to influence customer use of electricity [...] changes in the time pattern and magnitude of a utility’s load’ (Smith & Parmenter, 2016). Any city-wide DSM would require control rooms that give access to urban data and enable real-time coordination; within which, urban dashboards (UD) gravitate the coordination.

4.1. URBAN DASHBOARD (UD)

UD is a ‘visual display of the most important information needed to achieve one or more objectives; consolidated and arranged on a single screen so the information can

be monitored at a glance' (Mattern, 2017). UD may assist coordination amongst the following issues:

1. Grid integration - PV devices would be 'built at locations close to the end users to fulfil their own electricity needs, or supplement part of their electricity needs', and 'can be designed either as standalone systems or grid-connected systems' (HKSAR, 2020). UD helps to analyse energy generation data, integrate grids, locally distribute energy, and balance between PV and conventional fossil supplies. Within such 'complex, decentralised systems with bi-directional electricity flow', UD can also help prevent grid congestion between a delivery network of substations, cable, and overhead lines (Mortier, 2020).

2. Weather forecast - Before the rise of smart systems, weather forecasts were based on weather models that do not comprehend microclimatic data which most affect PV performance; HK Observatory (2020) has recently formulated a deep learning model for nowcasting, increasing forecast abilities from a few days up to hours ahead. When paired with diversified PV designs (silicon, dye sensitised, Perovskite, carbon nanotube, etc.) that are good at working under different light conditions, UD can help activate and shut down various PV systems according to forecast data to decrease operational costs and solar power curtailment.

3. Minimise internal system load - Conventional silicon-based PV designs are ideal for the sun's electromagnetic spectrum, especially within the red bands, but they do not work so well on cloudy days (MacDonald, et.al, 2019). To perform sun tracking, they generally have to install motors, which implies an internal system load. UD's ability in coordinating diverse devices working from high to low lighting decreases start / shutdown costs of motors and conventional generators.

4. Local feedback group - Electricity generated from an area is best consumed locally to minimise energy dissipation. This implies grouping problems of how electricity circulates within an area; generation and load data are not static but have a statistical boundary. Bi-directional current helps in formulating an iterative approach to adapt to the everchanging supply and demand. A more organic management system can help in meeting the quarter power scaling goal between local feedback groups to minimise absorption by the power grid.

5. Asset management - Energy leakage and health of devices are important factors that sustain the life cycle of UnSSEUS. Algorithms that 'can learn to distinguish and precisely categorise normal operating data from defined system malfunctions' may be utilised to minimise disruption and lost-production costs for the industry (Mortier, 2020).

6. Intelligent storage - As FiT users can choose between a standalone or grid-connected scheme, UD can help in the management of a network of batteries within standalone systems, where only solar generation data is synchronised without having to connect to the power grid. In prediction of a peak during hours of the day, batteries can be activated quickly to maintain system equilibrium, relieve grid congestion, and reduce back-up use from fossil generators.

7. Policy design - data gathered and analysed provides a good guide during policy design processes. Take FiT as an example, an economy of scale was implied - the more electricity you generate, the cheaper it sells to utility companies. On what

basis do we set these financial standards as incentivisation? What secondary effect would it bring? UD helps in visualising data derivatives to comparatively analyse the effects of different technical tools and financial instruments.

4.2. DEMAND-SIDE MANAGEMENT (DSM)

UD provides centrality to operations, UnSSEUS can be technically distributed but socioeconomically decentralised, supporting a DSM. Within any large-scale information system, data direct and derivatives are useful functions in tackling information overload problems. Data direct can take forms of personalisation, where specific information is directed to users in need, and is a technique that social media use in collaborative filtering of information (Kalinski, 2019). Energy supply and demand can be analysed to tailor more suited energy plans to each individual, exploring new service models (e.g. to-go plans), and users can manage their monthly/weekly consumption under a certain margin. This not only helps users to manage energy use, but also informs them of their consumption. For instance, participating in peak energy hours contribute to larger operational costs and loads in the power grid, if users can be informed, they might wish to turn on their dish washer at other hours to help save energy.

Personalisation may also help local PV devices to manage system 'heating and cooling at the correct times' as part of a regional distribution strategy (Mortier, 2020). As such, it performs two major negentropic functions: minimise disorder in information and reduce internal energy entropy. Prediction-based actions and real-time communication would assist a network of users to make decisions at the appropriate time - design beyond traditional personalisation (suggestions are made after your decision) to hyper-personalisation (suggestions are made before your decision). In this sense, UnSSEUS aims at exploring algorithms that are light-weight to relieve runtime and scalability issues. Attention should also be paid to statistical boundaries with time components. During festive holidays or large-scale international events, hyper-personalisation may coordinate a network of batteries and activate them in advance to relieve consumption from backup energy in diesel generators (Mortier, 2020).

5. Personalised Information Feedback System with Sudoku Gameplay

In applying such research on the building level of architecture, UnSSEUS sought to investigate information feedback strategies to solve energy-sharing problems. Particularly, this test looked into predicting and preempting supply and demand to optimise energy logistic operations. This is a response to the PV units distribution requirements within a building tower context, a thriving green economic sector that can be hindered by traditional energy distribution because it needs responsive measures to manage the scattered and rapid exchanges from PV units to each compartment and interconnected towers. In this context, a prediction algorithm could assist in the negotiation between different actors - a network of users and IoT devices, minimising information entropy and addressing the data overload problem.

The strategy is based on Sudoku, a combinatorial game based on a 9-by-9 grid that can be populated by 9 distinct items (fig. 1). This same grid was used to discretize and encode energy exchanges into an architectural system, each computationally associated with a number from 1 to 9. Our initial experiment was based on a building tower that is equally distributed into 9 units, but such formulation can be altered to adapt to diverse building topologies.

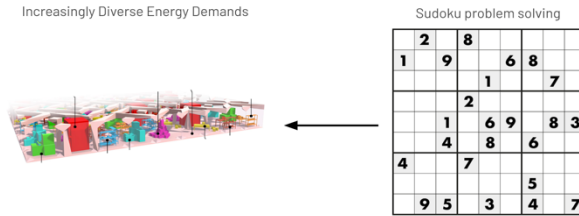


Figure 1. Applying sudoku - a combinatorial game strategy in energy distribution.

The computational game-playing strategy can then be used to solve the organisation of energy by finding optimal solutions for the games that are created and modified through informational feedback. Thereby, the system is able to consider energy as time and pricing factors between the 9 units to define different organisational solutions for different games and states (fig. 2).

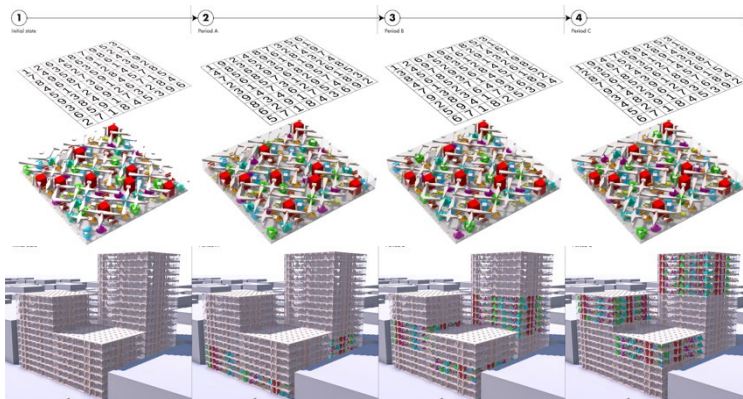


Figure 2. Solar supply and demand data cascade up interconnected buildings using sudoku.

The initial stage sensed changes in energy consumption from the ground floor, Period A redistributed pricing factors between the units on ground floor, which then cascaded up each floor until equilibrium. The state to which each game has been solved is the negentropic stage in the energy system, which feedback to the initial stage. As opposed to identifying users / units that consume the most, the combinatorial game simulates changes in pricing factor, revealing energy demands at different times of the day / year - the events that consume the most. Such awareness may help to prevent energy surge, which is one of the main challenges in renewables. Users can arrange their schedule according to these pricing factors that is determined by the amount of

light-harvested during the day and local energy demands.

This has potential to go beyond the 9x9 grid through fractal strategies (fig. 3). It can be applied to a wider spectrum of spatial configuration problems for agility beyond residential contexts, like warehouses, vehicle charging, and office spaces. During times of pandemics, individual work units are constrained by distancing parameters, users can rent units according to changes in schedule by week, and matchmake individual energy consumption to prevent excessive load.

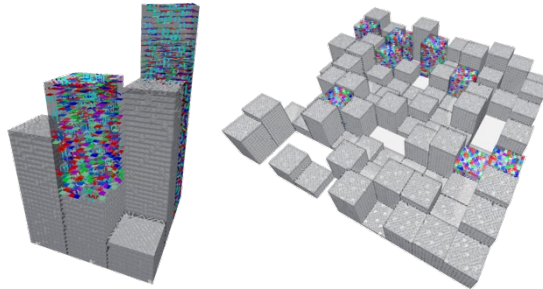


Figure 3. Preliminary results from phase two where the sudoku grid had been expanded to 9×9^{10} to accommodate a larger spectrum of urban distribution problems.

6. Discussion

Distributed generation is still being developed and far from being exploited in its full capacity. In the interim, the key is to understand the dynamics of development. How to incentivise participation in public and private sectors? What are the different kinds of participatory models, and how we might visualise the process to communicate progress?

Take HK's FiT program as an example, the paradox lies in the fact that rural areas have larger roof footprint to harvest energy; at the same time, these areas are less developed in infrastructural support. This contributes to grid congestion, where most users are unable to connect to the grid to transmit and share their generated solar power. Inevitably, infrastructural investment is needed, but the immediate return is not apparent enough for businesses, as the area is relatively sparsely populated. To start building up local infrastructure capacities, instead of having every house to connect to the main grid individually, which adds up to a larger cost, smaller local webs may be built between adjacent buildings to exchange with one another and accumulate momentum for the area - a decentralised topology. The energy and information chain can be two separate but parallel chains; energy circulates locally, but they complete their accounting profile using the FiT scheme. Once the regional participation adds up to an incremental level, it can branch out to meet with other regional groups, just as how slime moulds grow, for a more organic development strategy. The immediate advantage is agility and resilience during development stages, but this can only be achieved through standardisation of protocols (i.e. physical/logical topology, soft/hard wares) to ensure compatibility within public-private-partnerships.

Another way to stimulate participation would be to utilise media platforms. AMG (advanced micro grid) 'optimises the bidding of energy assets in wholesale markets using AI software', incorporating an intelligent battery system to automate the trade

(AMS, 2020). For instance, Tesla is developing a real-time trade platform with Hornsdale Power Reserve (HPR) in South Australia adding competition to drive down energy prices. This further illustrates the algorithmic need for personalisation, especially during the development stage, to organically incentivise participation and balancing out energy markets owned by diesel generators with PV systems.

Current PV strategies largely try to come up with a uniformed solution that is scalable in solving energy problems. This is analogical to thinking that a singular cell, if it is to scale, will produce the same ratio of value of effort to result. In reality, most organisms require diverse cells in order to minimise entropy. A biological system is more than a singular organism working independently, but a collective of all organisms that sustain a system to become self-sufficient. This is where our current energy systems fall short because the amount of energy we can produce and our operational costs multiplies simultaneously. This provides a different perspective to our current industrial practises, where the idea of an economy of scale is deeply embedded: the more we produce using the same method the cheaper it is. But it has been forgotten that we live in a complex environment with ever changing solar dynamics. A singular approach to PV will not win over diverse solar vectors, thus, would not result in a solar economy of scale. In contrast, scaling should promote diversity.

7. Conclusion

This paper translates concepts interdisciplinary from engineering to design, including 'Unattended', 'Smart', 'Solar Energy', and 'Urban System' (UnSSEUS). It first introduces emerging info-biological theories in complexity sciences with the aim of translating existing models in nature. From these theoretical approaches, this paper exemplifies its arguments with a design research UnSSEUS, and discusses its potentials in implementation by looking at the existing renewable energy challenges in one of the most densely populated cities - Hong Kong.

The study analysed the relationship between a singular unit and its larger structure, considering efficiency not as the amount of energy needed to overcome the disadvantages by scaling a singular solution, but to distribute power generation, and decentralise their exchange and communication, aggregating the effort of the many. The key is designing towards compatibility and standardisation of protocols.

References

- AMS. (2020). *Home*. Retrieved January 24, 2021, <https://www.advancedmicrogridsolutions.com/>
- Ben-Naim, A. (2010). *Discover entropy and the second law of thermodynamics: A playful way of discovering a law of nature*. Hackensack, NJ: World Scientific.
- CLP. (2020). *Power Grid*. Retrieved January 24, 2021, from <https://www.clp.com.hk/en/about-clp/media/resources/photos/power-grid>
- Fraenkel, A. S. (1996). Combinatorial Game Theory Foundations Applied to Digraph Kernels. *The Electronic Journal of Combinatorics*, 4(2).
- Friston, K. (2009). The free-energy principle: a rough guide to the brain?. *Trends in cognitive sciences*, 13(7), 293-301.
- Friston, K. (2019). A free energy principle for a particular physics. *arXiv:1906.10184*.
- Groth, D; Skandier, T., (2005). *Network+, Fourth Edition*. Sybex, Inc. ISBN 0-7821-4406-3.

- HKobservatory. (2020). *From machine learning to nowcasting*. Retrieved January 24, 2021, from <https://www.hko.gov.hk/en/education/weather/data-and-technology>
- HKSAR. (2019). *Feed-in Tariff (FiT) Scheme*. Retrieved January 24, 2021, from <https://www.hkelectric.com/en/smart-power-services/feed-in-tariff-scheme>
- HKSAR. (2020). *GovHK: Feed-in Tariff*. Retrieved January 24, 2021, from <https://www.gov.hk/en/residents/environment/renewable/feedintariff.htm>
- Jiang, X., Polastre, J., & Culler, D. (2005, April). Perpetual environmentally powered sensor networks. In *IPSN 2005. Fourth International Symposium on Information Processing in Sensor Networks, 2005* (pp. 463-468). IEEE.
- Kalinski, A. (2019, December 17). *Personalization using machine learning*. Retrieved from <https://medium.com/booking-product/personalization-using-machine-learning-from-data-science-to-user-experience-3b1ef5d23ced>
- Kimball, J. W., Kuhn, B. T., & Balog, R. S. (2009). A system design approach for unattended solar energy harvesting supply. *IEEE Transactions on Power Electronics*, 24(4), 952-962.
- Krakauer, D., Bertschinger, N., Olbrich, E., Flack, J. C., & Ay, N. (2020). The information theory of individuality. *Theory in Biosciences*, 139(2), 209-223.
- Miozzo, M., Zordan, D., Dini, P., & Rossi, M. (2014, May). SolarStat: Modeling photovoltaic sources through stochastic Markov processes. In *2014 IEEE International Energy Conference (ENERGYCON)* (pp. 688-695). IEEE.
- Macdonald, T. J., Batmunkh, M., Lin, C. T., Kim, J., Tune, D. D., Ambroz, F., ... & Durrant, J. R. (2019). *Origin of Performance Enhancement in TiO₂-Carbon Nanotube Composite Perovskite Solar Cells*. *Small Methods*, 3(10), 1900164
- Mattern, S. (2017). Urban dashboards. In Kitchin, R., Lauriault, (Eds.), *Understanding spatial media* (pp. 74-83). SAGE Publications Ltd, <https://www.doi.org/10.4135/9781526425850>
- Mortier, T. (2020, November 24). Why artificial intelligence is a game-changer for renewable energy. https://www.ey.com/en_ps/power-utilities
- Ng, P., Odaibat, B., & Doria, D. (2020). An Information Theory Application to Bio-design in Architecture. *1st CCBDT Conference*. Nanjing, China.
- Papakonstantinou, I., Portnoi, M., & Debije, M. G. (2021). The hidden potential of luminescent solar concentrators. *Advanced Energy Materials*, 11(3), 2002883.
- Rodrigues, J. M., Cardoso, P. J., Monteiro, J., & Ramos, C. M. (2020). Augmented intelligence: Leverage smart systems. In *Smart Systems Design, Applications, and Challenges* (pp. 1-22). IGI Global.
- Smith, C.B., Parmenter, K. E. (2016) in *Energy Management Principles* (Second Edition). Access: <https://www.sciencedirect.com/topics/engineering/energy-demand-management>
- Virginia Tech. (2007). *Introduction to Distributed Generation*. Retrieved from <https://www.dg.history.vt.edu/ch1/introduction.html>
- West, G. (2014, October 31). *Scaling: The surprising mathematics of life and civilization*. Retrieved from <https://medium.com/sfi-30-foundations-frontiers>
- West, G. B., & Brown, J. H. (2005). The origin of allometric scaling laws in biology from genomes to ecosystems: towards a quantitative unifying theory of biological structure and organization. *Journal of experimental biology*, 208(9), 1575-1592.
- Wynekoop, J. (2003). Local Area Networks. *Encyclopedia of Information Systems*, 91-102. doi:10.1016/b0-12-227240-4/00106-4
- Xu, J. M. (2001). *Topological Structure and Analysis of Interconnection Networks*. Kluwer Academic Publishers, October. Access: <http://staff.ustc.edu.cn/~xujm/courses61.htm>

INDEX OF AUTHORS

A

Akbar, Zuardin 1-393
 Alani, Mostafa 1-151
 Althoff, Klaus-Dieter 1-323,
 1-403, 2-435
 Alva, Pradeep 1-525
 Aman, Jayedi 1-595
 Amtsberg, Felix 2-141
 Anifowose, Hassan 2-547
 Antonio, Rishan 1-435
 An, Yudi 1-605
 Araujo, Goncalo 2-689
 Ataman, Cem 1-383

B

Bae, Jiyoona 2-121
 Balaban, Özgün 1-69
 Banihashemi, Farzan 2-629, 2-679
 Bao, Ding Wen 1-121
 Bao, Dingwen 2-71
 Barath, Shany 1-171
 Barton, Jack 1-687
 Bedarf, Patrick 2-61
 Beebe, Aaron G. 1-39
 Belek Fialho Teixeira, Müge 2-21
 Bidgoli, Ardavan 1-373
 Bielski, Jessica 1-323,
 1-403, 2-435
 Boim, Anna 1-223
 Bolojan, Daniel 1-353, 1-363
 Brown, Nathan 1-111
 Bui, Do Phuong Tung 2-495
 Burden, Alan 2-21
 Byrne, Daragh 1-333

C

Cai, Chengzhi 2-233
 Caldwell, Glenda 2-21
 Cao, Chufan 1-565
 Cao, Qingning 2-233
 Cao, Xiaoyu 2-233
 Carta, Silvio 1-615

Cattaneo, Tiziano 1-717
 Chadzynski, Arkadiusz 1-555
 Chai, Hua 2-41
 Chang, Teng-Wen 2-201
 Chavan, Tejas 1-313, 1-435
 Cheddadi, Aqil 1-585
 Chen, Chun-Yen 2-201
 Chen, Fukai 1-757
 Cheng, Cesar 1-313, 1-435
 Cheng, Chung-Chieh 2-213
 Cheng, Nancy 2-345
 Cheng, Sifan 1-495
 Chen, Guoyi 1-161
 Chen, Hao 1-89
 Chen, Jielin 2-385
 Chen, Kian Wee 1-415
 Chen, Lei 2-517
 Chen, Pei 1-181
 Chen, Qinchuan 1-19
 Chen, Shi Yu 1-505
 Chen, Ting-Chia 2-243
 Chen, Yao 1-757
 Chen, Yulong 1-625
 Cheung, Ling Kit 1-181
 Choi, Seungcheol 1-161
 Choo, Seungyeon 2-597
 Chowdhury, Shuva 2-465
 Chronis, Angelos 1-273,
 1-545, 2-577

Cole, Laura 2-455
 Cui, Qiang 2-101, 2-171
 Cui, Qinyu 1-515
 Cui, Weiwen 2-567

D

Dai, Sida 1-151
 Danahy, Patrick 1-131
 Davies, Peter 2-749
 Davis, Felecia 1-111
 De Wolf, Catherine 2-577
 Dengel, Andreas 1-323,
 1-403, 2-435
 Deshpande, Rutvik 1-313, 1-435

- | | | | |
|--------------------------|------------------------------|-------------------------|----------------------------------|
| Dias Guimaraes, Gabriela | 2-587 | Gramazio, Fabio | 2-111 |
| Dillenburg, Benjamin | 2-61 | Grisiute, Ayda | 1-555 |
| Ding, Xinyue | 2-425 | Grobman, Jacob | 1-283 |
| Dixit, Manish | 2-547 | Grugni, Francesco | 1-717 |
| Dong, Zhiyong | 1-213, 1-263 | Gu, Hyeongmo | 2-597 |
| Donovan, Jared | 2-21 | Guida, George | 2-485 |
| Doria, David | 2-759 | Gu, Ning | 2-527, 2-587 |
| Dortheimer, Jonathan | 1-223 | Guo, Xiangmin | 2-223, 2-425 |
| Dritsas, Stylianos | 2-263 | Guo, Yefei | 2-233 |
| Duering, Serjoscha | 1-545 | Guo, Yiyao | 2-91 |
| Dunn, Kate | 1-687 | Guo, Yuchen | 2-233 |
| Duran, Ayca | 2-669 | Guo, Zhe | 1-747, 2-233 |
| Düring, Serjoscha | 1-273 | Guo, Zhixian | 2-41 |
| E | | Gursel Dino, Ipek | 2-669 |
| Eisenstadt, Viktor | 1-323,
1-403, 2-435 | H | |
| Eshaghi, Sarvin | 1-69 | Haeusler, Matthias Hank | 1-253,
1-273,
1-687, 2-739 |
| F | | Hanegraaf, Johan | 2-465 |
| Fang, Yu-Cyuan | 2-201 | Hao, Qi | 1-425 |
| Farr, Marcus | 2-293 | Helmreich, Matthias | 2-111 |
| Feng, Jiajia | 1-425 | He, Mengxi | 2-171 |
| Feng, Xiqiao | 2-101 | Herthogs, Pieter | 1-555 |
| Fernandez, Alberto | 2-759 | Heusi, Alex | 2-61 |
| Fernandez, Javier | 2-263 | Hirano, Yuji | 2-131 |
| Fingrut, Adam | 2-11 | Holloway, Leona | 2-709 |
| Fink, Theresa | 1-545 | Hong, Soonmin | 2-597 |
| Förster, Nick | 1-635 | Hoo, Jian Li | 2-263 |
| Fujii, Haruyuki | 2-475 | Hotta, Akito | 1-303 |
| Fuji, Takaaki | 1-303 | Hotta, Kensuke | 1-303, 2-131 |
| Fukuda, Tomohiro | 1-89, 1-737,
2-395, 2-607 | Hou, June-Hao | 1-99, 1-667,
2-445 |
| G | | Hsiao, Chi-Fu | 2-201 |
| Gamerro, Julien | 2-325 | Huang, Chenyu | 1-141,
1-233,
1-455, 1-645 |
| García del Castillo y | 1-505, | | |
| López, Jose Luis | 2-283, 2-485 | Huang, Ching-Wen | 2-243 |
| Gardner, Nicole | 1-1, 1-253,
1-687, 2-1 | Huang, Jeffrey | 1-727 |
| Gero, John S. | 2-315 | Huang, Jie | 2-567 |
| Globa, Anastasia | 2-649, 2-749 | Huang, Shuyi | 1-475 |
| Goel, Abhimanyu | 2-365 | Huang, Tracy | 1-687 |
| Gomes da Silva, Vanessa | 2-587 | Huang, Xiaoran | 1-455,
1-645, 1-707 |
| Gomes, Ricardo | 2-689 | | |
| Gong, Lei | 2-273 | Huang, Yiting | 1-515 |
| Gong, Pixín | 1-455, 1-645 | Hu, Huiyao | 2-495 |
| Gough, Phillip | 2-649 | Hyun, Kyung Hoon | 1-1, 1-59, |

	2-1	Kuroki, Mitsuhiro	2-111
I			
Ikeda, Yasushi	1-585, 2-31, 2-131		
Inaba, Tooru	2-131		
Irger, Matthias	2-739		
Iseri, Orcun Koral	2-669		
Ito, Koki	2-131		
Ito, Nao	1-737		
J			
Jahn, Gwyllim	2-191		
Janssen, Patrick	1-415, 2-495, 2-505		
Jaramillo Pazmino, Pablo	2-181		
Isaac			
Jeong, Joowon	1-19		
Ji, Guohua	2-699		
Johansson, Mikael	1-29		
K			
Kahlon, Yuval	2-475		
Kaljevic, Sofija	1-677		
Kalkan, Sinan	2-669		
Karastathi, Nikoletta	2-759		
Kawakami, Takuma	2-131		
Keane, Adrienne	2-749		
Khajehee, Arastoo	2-31, 2-131		
Khean, Nariddh	1-273		
Kiesewetter, Laura	1-393		
Kikuchi, Naoki	2-607		
Kikuzato, Naoto	1-303		
Kim, Dongyun	2-485		
Kim, Frederick Chando	1-727		
Kim, Hwan	1-59		
Kim, Jong Bum	1-595, 2-455		
Kim, Ki	2-587		
Kim, Nayeon	1-19		
Kim, Taehoon	2-597		
Kleiss, Michael	1-151		
Kocaturk, Tuba	1-677		
Koch, Ethan	1-655		
Koh, Immanuel	1-465		
Kohler, Matthias	2-111		
König, Reinhard	1-273, 1-545		
Krezlik, Adrian	2-619		
Krishnamurti, Ramesh	1-333		
L			
Ladron de Guevara, Manuel	1-333, 1-373		
Langenhan, Christoph	1-323, 1-403, 2-435		
Lang, Werner	2-629, 2-679		
Larkin, Nicole	2-709		
Latteur, Pierre	2-151		
Lee, Alric	2-131		
Lee, Ching-Han	2-201		
Lee, Hyunsoo	1-19		
Leitão, António	2-689		
Leong, Siew Leng	2-505		
Leung, Carson Ka Shut	1-293, 1-495, 2-11		
Li, Andre	2-567		
Liang, Yuebing	1-425		
Li, Biao	1-625		
Li, Ce	1-747, 2-233		
Li, Cong	2-233		
Li, Haimiao	1-565		
Li, Kan	1-757		
Lim, Chor-Kheng	1-445		
Lin, Alexander	2-365		
Lin, Han-Ting	1-667		
Lin, Jinru	1-213		
Lin, Yinshan	1-79		
Lin, Yuxin	1-343		
Li, Shuyang	1-79		
Liu, Jia	2-31		
Liu, Liquan	1-757		
Liu, Nuozhi	1-465		
Liu, Sijie	2-405		
Liu, Xiao	1-213		
Liu, Xinyu	1-485		
Li, Wenjing	1-243, 1-565		
Li, Yuanyuan	1-141		
Li, Yuke	1-435		
Li, Zhixian	1-707		
Li, Ziyang	2-71		
Lo, Chun-Yu	1-99		
Lok, Leslie	2-121		
Lopez Rodriguez, Alvaro	2-181		
Lo, Tian Tian	1-757, 2-223, 2-425		

- Luo, Dan 1-1, 1-243,
1-565,
1-595, 2-1,
2-161
- Luo, Yang 2-91
- Lu, Xuanyu 2-31
- Lu, Yen-Cheng 2-243
- Lv, Xueyuan 2-517
- M**
- Makki, Mohammed 1-161,
1-181, 1-655
- Marengo, Mathilde 2-577
- Markopoulou, Areti 2-577
- Marsatyasti, Naya 2-475
- Marschall, Max 2-639
- Mathers, Jordan 1-161
- Matisziw, Timothy C 1-595
- Mayer, Hannes 2-111
- Mayer, Wolfgang 2-587
- May, Kieran 2-527
- Mazza, Domenico 1-677
- McMeel, Dermott 2-415
- Menges, Achim 1-393, 2-41,
2-81, 2-141
- Meng, Leo Lin 1-253
- Meral Akgul, Cagla 2-669
- Mete, Burak 1-323
- Miao, Junyi 2-233
- Miller, Clayton 1-525
- Milovanovic, Julie 2-315
- Min, Deedee 1-201
- Miyaguchi, Mikita 2-131
- Mondal, Tushar 2-253
- Moscovitz, Or 1-171
- Mosteiro-Romero, Martin 1-525
- Mo, Yichen 1-625
- Murata, Ryo 2-475
- N**
- Naboni, Roberto 2-375
- Nagakura, Takehiko 1-69
- Nagamachi, Shiho 1-737
- Nakajima, Tadahiro 2-111
- Nakamura, Hoki 1-737
- Nanasca, James 1-39
- Napier, Ilaena Mariam 2-303
- Narahara, Taro 1-11
- Neri, Iacopo 2-577
- Newnham, Cameron 2-191
- Ng, Provides 2-759
- Nguyen-Tran, Khang 2-475
- Nguyen, Tommy Bao 1-243
- Nghi
- Ni, Eryu 2-161
- Nisztuk, Maciej 1-313, 1-435
- O**
- Ochoa Paniagua, Jorge 2-587
- Odaibat, Baha 2-759
- Oghazian, Farzaneh 1-111
- Oki, Takuya 2-475
- Onishi, Ryo 2-395
- Oprean, Danielle 2-455
- Ortner, F. Peter 1-191
- P**
- Pacher, Matteo 2-111
- Pantic, Igor 2-181
- Panya, David Stephen 2-597
- Pan, Yongjie 2-729
- Park, Hyejin 2-597
- Park, Hyoung-June 1-697
- Patel, Sayjel Vijay 1-313, 1-435
- Pawar, Siddharth Suhas 2-101, 2-171
- Pebryani, Nyoman 1-151
- Perrault, Simon 1-383
- Perry, Gabriella 2-283
- Petrovic, Emina K. 2-415
- Petzold, Frank 1-635,
2-435, 2-557
- Pintacuda, Luigi 1-615
- Poranne, Roi 1-49
- Q**
- Qiu, Song 2-101
- Qiu, Waishan 1-243,
1-425, 1-565
- R**
- Raanan, Noam 1-283
- Raghu, Deepika 2-577
- Raja, Twisha 2-51
- Rameezdeen, Rameez 2-587
- Reinhardt, Dagmar 2-649,
2-709, 2-749
- Reitberger, Roland 2-629, 2-679

- Rezaei Rad, Aryan 2-151
 Rhee, Jinmo 1-373
 Ricafort, Kim 1-655
 Riggio, Mariapaola 2-345
 Robinson, Richard 1-697
 Rogeau, Nicolas 2-151
 Roupé, Mattias 1-29
 Rust, Romana 1-49
 Ruszczewski, Szymon 1-707
- S**
 Sakai, Yasushi 1-585
 Santos, Luis 2-689
 Sateei, Shahin 1-29
 Schmidiger, Robin 1-49
 Schneidman, Alexander 1-333
 Schubert, Gerhard 1-635
 Schumann, Kyle 2-355
 Schwinn, Tobias 2-81
 Sepulveda, Pablo 2-639
 Settimi, Andrea 2-325
 Shao, Tong 2-699
 Sheng, Yu-Ting 2-213
 Sheth, Urvi 1-1
 Shibuya, Masako 2-131
 Shimizu, Shunta 1-737
 Shi, Xing 2-537
 Shi, Zhongming 1-555
 Silveira, Sue 2-709
 Silvennoinen, Heidi 1-555
 Singh, Mayank 2-659
 Skoury, Lior 2-141
 Smith, Ross 2-527
 Someya, Syunsuke 2-131
 Sopher, Hadas 2-315
 Sprecher, Aaron 1-223
 Stark, Tim 2-41
 Stieler, David 2-81
 Stouffs, Rudi 1-525, 2-385
 Stuart-Smith, Robert 1-131
 Subramanian, Ramanathan 1-313, 1-435
 Sukegawa, Chika 2-131
 Sun, Chengyu 1-79
 Sun, Ke Nan 2-223
 Szabo, Anna 2-61
- T**
 Tabi, Salma 1-585
 Taima, Masahiro 1-585
 Tang, Chongyi 2-161
 Tang, Ming 1-575
 Tang, Peng 1-625
 Tang, Sheng Kai 2-445
 Tan, Ying Yi 2-91
 Tay, Jing Zhi 1-191
 Thomas, Bruce 2-527
 Tian, Jing 1-575
 Tohidi, Alex 2-739
 Tong, Ziyu 2-719
 Toohey, Gabrielle 1-243
 Tracy, Kenneth 2-91
 Tsai, Tsung-Han 2-243
 Tsubata, Shinya 2-111
 Tunçer, Bige 1-383
 Tung, Nguyen 1-585
 Turchi, Tommaso 1-615
- V**
 Vaez Afshar, Sepehr 1-69
 Vaidhyanathan, Vishal 2-51
 van Ameijde, Jeroen 1-1, 1-293, 1-485, 1-495, 2-1
 van den Berg, Nick 2-191
 Varinlioglu, Guzden 1-69
 Veloso, Pedro 1-373
 Vermisso, Emmanouil 1-353, 2-335
 Vestartas, Petras 2-151, 2-325
 Vilppola, Ritva 1-243
 Voltolina, Marco 1-717
 von Richthofen, Aurel 1-555
- W**
 Wagner, Hans Jakob 2-41, 2-141
 Walsh, James 2-527
 Wang, Hanmo 2-365
 Wang, Julian 1-575
 Wang, Ke 2-425
 Wang, Likai 1-415, 2-699
 Wang, Qiang 2-131
 Wang, Shih-Yuan 2-213, 2-243
 Wang, Sihan 2-91
 Wang, Sining 2-405
 Wang, Siqi 1-213

- | | | | |
|--------------------|-----------------------|------------------------|-----------------------------|
| Wang, Tsung-Hsien | 1-535 | Yoffe, Hatzav | 1-283 |
| Wang, Xiang | 2-517 | Yousif, Shermeen | 1-353,
1-363, 2-335 |
| Watanabe, Yoshiaki | 2-131 | Yuan, Philip F. | 2-41, 2-71,
2-273, 2-517 |
| Weijenberg, Camiel | 1-313, 1-435 | Yu, Chuan | 2-101, 2-171 |
| Weinand, Yves | 2-151, 2-325 | Yu, Daniel | 1-253,
1-687, 2-739 |
| Wei, Ziru | 2-405 | Yu, Junah | 1-201 |
| White, Marcus | 1-455, 1-645 | Z | |
| Won, Junghye | 2-597 | Zahedi, Ata | 2-557 |
| Wood, Dylan | 1-393 | Zangori, Laura | 2-455 |
| Wortmann, Thomas | 1-393 | Zanini, Michele | 2-61 |
| Wu, Hao | 2-71 | Zhang, Garry Hangge | 1-253 |
| Wu, Jinxuan | 2-223 | Zhang, Gengjia | 1-141, 1-233 |
| Wu, Wanling | 2-233 | Zhang, Hong | 2-567 |
| Wu, Xinyu | 2-71 | Zhang, Huikai | 2-101 |
| Wu, Zihao | 2-719 | Zhang, Qiyan | 1-625 |
| X | | Zhang, Shuyu | 1-515 |
| Xiang, Rufeng | 1-757 | Zhang, Tong | 2-729 |
| Xiao, Yahan | 1-303 | Zhang, Yunsong | 2-719 |
| Xin, Zhuoyang | 2-161 | Zhang, Zihuan | 1-747 |
| Xu, Hang | 1-535 | Zhao, Yucheng | 1-121 |
| Xu, Jiaqi | 1-213 | Zheng, Hao | 1-475 |
| Xu, Ke | 1-425 | Zheng, Lang | 2-273 |
| Xu, Yijia | 1-213 | Zheng, Zifei | 2-233 |
| Xu, Zhitao | 1-181 | Zhou, Margaret Z. | 1-505 |
| Xu, Zhiyan | 2-233 | Zhou, Xinjie | 2-71 |
| Y | | Zhou, Xinyan | 2-233 |
| Yabe, Taisei | 2-31 | Zhou, Xinyi | 1-757 |
| Yabuki, Nobuyoshi | 1-89, 2-395,
2-607 | Zhou, Yifan | 2-273 |
| Yamauchi, Yuji | 1-737 | Zhou, Ziqi | 2-517 |
| Yang, Qing | 1-565 | Zhuang, Dian | 2-537 |
| Yang, Xiliu | 2-141 | Zhu, Guanqi | 2-161 |
| Yang, Xuyou | 1-121 | Ziegler, Christoph | 1-403, 2-435 |
| Yan, Wei | 2-547 | Zomparelli, Alessandro | 2-375 |
| Yan, Xin | 1-121 | | |
| Yao, Jiawei | 1-141, 1-233 | | |
| Yin, Minggang | 1-233 | | |